NAS 1.9/4:25/1

VOLUME 25 / NUMBER 1
JANUARY 8, 1987
ACC. NOS. N87-10001 TO N87-10827

TECHNOLOGY AND SCIENCE
DETROIT PUBLIC LIBRARY

STAR

AN ABSTRACT JOURNAL

Scientific and Technical Aerospace Reports

PRODUCED BY THE
SCIENTIFIC AND TECHNICAL
INFORMATION
BRANCH

NASA

NATIONAL AERONAUTICS AND SPACE ADMINISTRATION

WHAT YOU CAN DO FOR *STAR*

All users of this abstract service are urged to forward reports to be considered for announcement in *STAR*. This will aid NASA in its efforts to provide the fullest possible coverage of all scientific and technical publications that might support aeronautics and space research and development. If you have prepared relevant reports (other than those that you will transmit to NASA, DoD, or DOE through the usual contract- or grant-reporting channels), please send them for consideration to the NASA Scientific and Technical Information Facility, P.O. Box 8757, B.W.I. Airport, Maryland 21240.

Reprints of journal articles, book chapters, and conference papers are also welcome. These will be considered for announcement in *STAR's* companion journal, *International Aerospace Abstracts.*

You may specify a particular source to be included in a report announcement if you wish; otherwise the report will be placed on public sale at the National Technical Information Service. Copyrighted publications will be announced but not distributed or sold.

PURCHASE OF *STAR*

The semimonthly issues are available for sale by the Superintendent of Documents, U.S. Government Printing Office, Washington, D.C. 20402.

PUBLISHED BY:

UNITED STATES GOVERNMENT
NATIONAL AERONAUTICS AND SPACE ADMINISTRATION
SCIENTIFIC AND TECHNICAL INFORMATION BRANCH
Scientific and Technical Aerospace Reports, Volume 25, is prepared by the NASA Scientific and Technical Information Facility operated for the National Aeronautics and Space Administration by RMS Associates.

The Administrator of the National Aeronautics and Space Administration has determined that the publication of this periodical is necessary in the transaction of the public business required by law of this Agency. Use of funds for printing this periodical has been approved by the Director of the Office of Management and Budget through March 22, 1988.

US ISSN 0036-8741

INTRODUCTION

Scientific and Technical Aerospace Reports (STAR) is a major component of a comprehensive National Aeronautics and Space Administration information system covering aeronautics, space, and supporting disciplines. *STAR* is issued on the 8th and 23rd of each month and announces current publications of the following types:

- NASA, NASA contractor, and NASA grantee reports
- Reports issued by other U.S. Government Agencies, domestic and foreign institutions, universities, and private firms
- Translations in report form
- NASA-owned patents and patent applications
- Dissertations and theses

Journal, book, and conference literature, cover-to-cover journal translations, and certain foreign dissertations are announced in a companion journal, *International Aerospace Abstracts (IAA)*, available on subscription from the American Institute of Aeronautics and Astronautics, Technical Information Service, 555 West 57th Street, 12th Floor, New York, New York 10019.

SUBJECT SCOPE

Subject scope of *STAR*, and *IAA* includes all aspects of aeronautics and space research and development, supporting basic and applied research, and applications. Aerospace aspects of earth resources, energy development, conservation, oceanography, environmental protection, urban transportation, and other topics of high national priority are also covered.

OTHER NASA PUBLICATIONS

Other NASA publications and information services are described in the publication, *The NASA Scientific and Technical Information System ... and How to Use It*, available without charge from the NASA Scientific and Technical Information Facility, P.O. Box 8757, B.W.I. Airport, Maryland 21240.

HOW TO USE *STAR* SUBJECT CATEGORIES

STAR is categorized by 10 major subject divisions divided into 76 specific subject categories and one general category/division. The major subject divisions are listed in the Table of Contents, together with a note for each that defines its scope and provides any cross-references. For example:

AERONAUTICS

Includes aeronautics (general); aerodynamics; air transportation and safety; aircraft communications and navigation; aircraft design, testing and performance; aircraft instrumentation; aircraft propulsion and power; aircraft stability and control; and research and support facilities (air).

For related information see also *Astronautics*.

Detroit Public Library
JAN - 2 1987
Depository Document

Each major division is further divided into as many as nine specific categories, which are identified by category numbers.

Abstracts in *STAR* are grouped by specific category, the categories appearing in sequential order. Category breaks in the abstract section are identified by the category number and title, and a scope note. Cross-references to other categories are provided as appropriate. For example:

> **02 AERODYNAMICS**
>
> Includes aerodynamics of bodies, combinations, wings, rotors, and control surfaces; and internal flow in ducts and turbomachinery.
>
> For related information see also *34 Fluid Mechanics and Heat Transfer.*

CROSS-REFERENCES

Individual *STAR* abstracts are not ordinarily cross-referenced, except for certain conference reports or book translations that have had separate abstracts written for their component papers or chapters. Citations and abstracts of the components follow immediately after those of the parent document. When the subject content of a component differs sufficiently from the general content of the parent, a cross-reference citation also is printed at the end of the category to which it normally would have been assigned if it were independent.

DOCUMENTS ON MICROFICHE

Documents on microfiche(1) are designated by a pound sign (#) following the accession number. The pound sign is used without regard to the source or quality of the microfiche.

AVAILABILITIES

One or more sources from which a document announced in *STAR* is available to the public is given in each citation. The most commonly indicated sources and their acronyms or abbreviations are listed below. If the publication is available from a source other than those listed, the publisher and his address will be displayed on the availability line or in combination with the corporate source line.

Avail: NTIS. Sold by the National Technical Information Service. Prices for hard copy (HC) and microfiche (MF) are indicated by a price code following the letters HC or MF in the *STAR* citation. Current values for the price codes are given in the tables on page vii.

Initially distributed microfiche under the NTIS SRIM (Selected Research in Microfiche) is available at greatly reduced unit prices. For this service and for information concerning subscription to NASA printed reports, consult the NTIS Subscription Section, Springfield, Va. 22161.

NOTE ON ORDERING DOCUMENTS: When ordering NASA publications (those followed by the * symbol), use the N accession number. NASA patent applications (only the specifications are offered) should be ordered by the US-Patent-Appl-SN number. Non-NASA publications (no asterisk) should be ordered by the AD, PB, or other *report* number shown on the last line of the citation, not by the N accession number. It is also advisable to cite the title and other bibliographic identification.

Avail: SOD (or GPO). Sold by the Superintendent of Documents, U.S. Government Printing Office, in hard copy. The current price and order number are given following the availability line. (NTIS will fill microfiche requests, as indicated above, for those documents identified by a # symbol.)

---

(1) A microfiche is a transparent sheet of film, 105 by 148 mm in size, containing as many as 60 to 98 pages of information reduced to micro images (not to exceed 26:1 reduction).

Avail: BLL (formerly NLL): British Library Lending Division, Boston Spa, Wetherby, Yorkshire, England. Photocopies available from this organization at the price shown. (If none is given, inquiry should be addressed to the BLL.)

Avail: DOE Depository Libraries. Organizations in U.S. cities and abroad that maintain collections of Department of Energy reports, usually in microfiche form, are listed in *Energy Research Abstracts*. Services available from the DOE and its depositories are described in a booklet, *DOE Technical Information Center - Its Functions and Services* (TID-4660), which may be obtained without charge from the DOE Technical Information Center.

Avail: ESDU. Pricing information on specific data, computer programs, and details on ESDU topic categories can be obtained from ESDU International Ltd. Requesters in North America should use the Virginia address while all other requesters should use the London address, both of which are on page vi.

Avail: Fachinformationszentrum, Karlsruhe. Sold by the Fachinformationszentrum Energie, Physik, Mathematik GMBH, Eggenstein Leopoldshafen, Federal Republic of Germany, at the price shown in deutschmarks (DM).

Avail: HMSO. Publications of Her Majesty's Stationery Office are sold in the U.S. by Pendragon House, Inc. (PHI), Redwood City, California. The U.S. price (including a service and mailing charge) is given, or a conversion table may be obtained from PHI.

Avail: NASA Public Document Rooms. Documents so indicated may be examined at or purchased from the National Aeronautics and Space Administration, Public Documents Room (Room 126), 600 Independence Ave., S.W., Washington, D.C. 20546, or public document rooms located at each of the NASA research centers, the NASA Space Technology Laboratories, and the NASA Pasadena Office at the Jet Propulsion Laboratory.

Avail: Univ. Microfilms. Documents so indicated are dissertations selected from *Dissertation Abstracts* and are sold by University Microfilms as xerographic copy (HC) and microfilm. All requests should cite the author and the Order Number as they appear in the citation.

Avail: US Patent and Trademark Office. Sold by Commissioner of Patents and Trademarks, U.S. Patent and Trademark Office, at the standard price of $1.50 each, postage free. (See discussion of NASA patents and patent applications below.)

Avail: (US Sales Only). These foreign documents are available to users within the United States from the National Technical Information Service (NTIS). They are available to users outside the United States through the International Nuclear Information Service (INIS) representative in their country, or by applying directly to the issuing organization.

Avail: USGS. Originals of many reports from the U.S. Geological Survey, which may contain color illustrations, or otherwise may not have the quality of illustrations preserved in the microfiche or facsimile reproduction, may be examined by the public at the libraries of the USGS field offices whose addresses are listed in this Introduction. The libraries may be queried concerning the availability of specific documents and the possible utilization of local copying services, such as color reproduction.

Avail: Issuing Activity, or Corporate Author, or no indication of availability. Inquiries as to the availability of these documents should be addressed to the organization shown in the citation as the corporate author of the document.

NASA PATENTS AND PATENT APPLICATIONS

Patents and patent applications owned by NASA are announced in *STAR* under appropriate subject categories and are referenced in the *STAR* indexes. In the Report/Accession Number Index, patents are indexed by the NASA Case Number (which appears in lieu of the report number in other indexes), the U.S. Patent Number, the U.S. Patent Application Serial Number, and the U.S. Patent Class. Patent applications for which patents have not yet been issued are indexed by the NASA Case Number and the U.S. Patent Application Serial Number.

NASA *patent application specifications* are sold in paper copy by the National Technical Information Service at price code A02. Microfiche are sold at price code A01. The US-Patent-Appl-SN- number should be used in ordering either paper copy or microfiche from NTIS. Printed copies of *patents* (which are not microfiched) are available for purchase at $1.50 per copy from:

Commissioner of Patents and Trademarks
U.S. Patent and Trademark Office
Washington, D.C. 20231

When ordering patents, the U.S. Patent Number should be used, and payment must be remitted in advance, preferably by money order or check payable to the Commissioner of Patents and Trademarks. Prepaid purchase coupons for ordering are also available from the Patent and Trademark Office. The patents and patent applications announced in *STAR* are owned by NASA and are available for royalty-free licensing. Requests for licensing terms and further information should be addressed to:

Assistant General Counsel for Patent Matters/Code GP
National Aeronautics and Space Administration
Washington, D.C. 20546

ELIGIBILITY AND REGISTRATION FOR NASA INFORMATION PRODUCTS AND SERVICES

A variety of services is available to organizations of the following types that have registered with NASA to receive specific services or products:

1. NASA offices, research centers, contractors, subcontractors, grantees, and consultants;
2. Other U.S. Government agencies and their contractors;
3. Libraries in the United States that have arrangements with NASA to maintain collections of NASA documents for public reference;
4. Other organizations in the United States having a need for NASA documents in work related to aeronautics and space research;
5. Organizations abroad that have established reciprocal document exchange arrangements with NASA.

Only the central service points or central points of document acquisition and control within qualified organizations are eligible to register for NASA products and services. Domestic organizations that may be eligible to receive various classes of NASA publications and services should address their requests for registration or for further information to:

NASA Scientific and Technical Information Facility
ATTN: Registration Activity
P.O. Box 8757
B.W.I. Airport, Maryland 21240

Organizations abroad should direct requests to the same address, but to the attention of: International Exchange Program.

AVAILABILITY OF *STAR* ABSTRACTS ON MICROFICHE

Microfiche of the abstract sections of this issue and other issues of *STAR* are available on annual subscription from NTIS, Attn: Subscriptions, 5285 Port Royal Road, Springfield, Virginia 22161. Annual subscription rates are $70.00 North America; $140.00 foreign. Abstract sections for previous years retroactive to 1964 are available at the current rates. Microfiche for individual *STAR* issue abstract sections are not available.

PUBLIC COLLECTIONS OF NASA DOCUMENTS

DOMESTIC: NASA and NASA-sponsored documents and a large number of aerospace publications are available to the public for reference purposes at the library maintained by the American Institute of Aeronautics and Astronautics, Technical Information Service, 555 West 57th Street, 12th Floor, New York, New York 10019

EUROPEAN: An extensive collection of NASA and NASA-sponsored publications is maintained by the British Library Lending Division, Boston Spa, Wetherby, Yorkshire, England for public access. The British Library Lending Division also has available many of the non-NASA publications cited in *STAR*. European requesters may purchase facsimile copy or microfiche of NASA and NASA-sponsored documents, those identified by both the symbols # and * from ESA - Information Retrieval Service European Space Agency, 8-10 rue Mario-Nikis, 75738 Paris CEDEX 15, France.

FEDERAL DEPOSITORY LIBRARY PROGRAM

In order to provide the general public with greater access to U.S. Government publications, Congress established the Federal Depository Library Program under the Government Printing Office (GPO), with 50 regional depositories responsible for permanent retention of material, inter-library loan, and reference services. At least one copy of nearly every NASA and NASA-sponsored publication, either in printed or microfiche format, is received and retained by the 50 regional depositories. A list of the regional GPO libraries, arranged alphabetically by state, appears on the inside back cover. These libraries are *not* sales outlets. A local library can contact a Regional Depository to help locate specific reports, or direct contact may be made by an individual.

ADDRESSES OF ORGANIZATIONS

American Institute of Aeronautics and
Astronautics
Technical Information Service
555 West 57th Street, 12th Floor
New York, New York 10019

British Library Lending Division,
Boston Spa, Wetherby, Yorkshire,
England

Commissioner of Patents and
Trademarks
U.S. Patent and Trademark Office
Washington, D.C. 20231

Department of Energy
Technical Information Center
P.O. Box 62
Oak Ridge, Tennessee 37830

ESA-Information Retrieval Service
ESRIN
Via Galileo Galilei
00044 Frascati (Rome) Italy

ESDU International, Ltd.
1495 Chain Bridge Road
McLean, Virginia 22101

ESDU International, Ltd.
251-259 Regent Street
London, W1R 7AD, England

Fachinformationszentrum Energie, Physik,
Mathematik GMBH
7514 Eggenstein Leopoldshafen
Federal Republic of Germany

Her Majesty's Stationery Office
P.O. Box 569, S.E. 1
London, England

NASA Scientific and Technical Information
Facility
P.O. Box 8757
B.W.I. Airport, Maryland 21240

National Aeronautics and Space
Administration
Scientific and Technical Information
Branch (NTT-1)
Washington, D.C. 20546

National Technical Information Service
5285 Port Royal Road
Springfield, Virginia 22161

Pendragon House, Inc.
899 Broadway Avenue
Redwood City, California 94063

Superintendent of Documents
U.S. Government Printing Office
Washington, D.C. 20402

University Microfilms
A Xerox Company
300 North Zeeb Road
Ann Arbor, Michigan 48106

University Microfilms, Ltd.
Tylers Green
London, England

U.S. Geological Survey Library
National Center - MS 950
12201 Sunrise Valley Drive
Reston, Virginia 22092

U.S. Geological Survey Library
2255 North Gemini Drive
Flagstaff, Arizona 86001

U.S. Geological Survey
345 Middlefield Road
Menlo Park, California 94025

U.S. Geological Survey Library
Box 25046
Denver Federal Center, MS914
Denver, Colorado 80225

NTIS PRICE SCHEDULES

(Effective January 1, 1987)

Schedule A
STANDARD PRICE DOCUMENTS AND MICROFICHE

PRICE CODE	PAGE RANGE	NORTH AMERICAN PRICE	FOREIGN PRICE
A01	Microfiche	$ 6.50	$13.00
A02	001-025	9.95	19.90
A03	026-050	11.95	23.90
A04-A05	051-100	13.95	27.90
A06-A09	101-200	18.95	37.90
A10-A13	201-300	24.95	49.90
A14-A17	301-400	30.95	61.90
A18-A21	401-500	36.95	73.90
A22-A25	501-600	42.95	85.90
A99	601-up	*	*
NO1		45.00	80.00
NO2		48.00	80.00

Schedule E
EXCEPTION PRICE DOCUMENTS AND MICROFICHE

PRICE CODE	NORTH AMERICAN PRICE	FOREIGN PRICE
E01	$ 7.50	15.00
E02	10.00	20.00
E03	11.00	22.00
E04	13.50	27.00
E05	15.50	31.00
E06	18.00	36.00
E07	20.50	41.00
E08	23.00	46.00
E09	25.50	51.00
E10	28.00	56.00
E11	30.50	61.00
E12	33.00	66.00
E13	35.50	71.00
E14	38.50	77.00
E15	42.00	84.00
E16	46.00	92.00
E17	50.00	100.00
E18	54.00	108.00
E19	60.00	120.00
E20	70.00	140.00
E99	*	*

*Contact NTIS for price quote.

IMPORTANT NOTICE

NTIS Shipping and Handling Charges
U.S., Canada, Mexico — ADD $3.00 per TOTAL ORDER
All Other Countries — ADD $4.00 per TOTAL ORDER

Exceptions — Does NOT apply to:
ORDERS REQUESTING NTIS RUSH HANDLING
ORDERS FOR SUBSCRIPTION OR STANDING ORDER PRODUCTS *ONLY*

NOTE: Each additional delivery address on an order
requires a separate shipping and handling charge.

VOLUME 25 NUMBER 1 / JANUARY 8, 1987

TABLE OF CONTENTS

AERONAUTICS

Includes aeronautics (general); aerodynamics; air transportation and safety; aircraft communications and navigation; aircraft design, testing and performance; aircraft instrumentation; aircraft propulsion and power; aircraft stability and control; and research and support facilities (air).

For related information see also *Astronautics.*

01 AERONAUTICS (GENERAL) 1

02 AERODYNAMICS 1

Includes aerodynamics of bodies, combinations, wings, rotors, and control surfaces; and internal flow in ducts and turbomachinery.

For related information see also *34 Fluid Mechanics and Heat Transfer*

03 AIR TRANSPORTATION AND SAFETY 9

Includes passenger and cargo air transport operations; and aircraft accidents.

For related information see also *16 Space Transportation* and *85 Urban Technology and Transportation.*

04 AIRCRAFT COMMUNICATIONS AND NAVIGATION 10

Includes digital and voice communication with aircraft; air navigation systems (satellite and ground based); and air traffic control.

For related information see also *17 Space Communications, Spacecraft Communications, Command and Tracking* and *32 Communications and Radar.*

05 AIRCRAFT DESIGN, TESTING AND PERFORMANCE 10

Includes aircraft simulation technology.

For related information see also *18 Spacecraft Design, Testing and Performance* and *39 Structural Mechanics.* For land transportation vehicles see *85 Urban Technology and Transportation.*

06 AIRCRAFT INSTRUMENTATION 13

Includes cockpit and cabin display devices; and flight instruments.

For related information see also *19 Spacecraft Instrumentation* and *35 Instrumentation and Photography.*

07 AIRCRAFT PROPULSION AND POWER 16

Includes prime propulsion systems and systems components, e.g., gas turbine engines and compressors; and onboard auxiliary power plants for aircraft.

For related information see also *20 Spacecraft Propulsion and Power, 28 Propellants and Fuels,* and *44 Energy Production and Conversion.*

08 AIRCRAFT STABILITY AND CONTROL 17

Includes aircraft handling qualities; piloting; flight controls; and autopilots.

For related information see also *05 Aircraft Design, Testing and Performance.*

09 RESEARCH AND SUPPORT FACILITIES (AIR) 17

Includes airports, hangars and runways; aircraft repair and overhaul facilities; wind tunnels; shock tubes; and aircraft engine test stands.

For related information see also *14 Ground Support Systems and Facilities (Space).*

ASTRONAUTICS

Includes astronautics (general); astrodynamics; ground support systems and facilities (space); launch vehicles and space vehicles; space transportation; space communications, spacecraft communications, command and tracking; spacecraft design, testing and performance; spacecraft instrumentation; and spacecraft propulsion and power.

For related information see also *Aeronautics*

12 ASTRONAUTICS (GENERAL) 18

For extraterrestrial exploration see *91 Lunar and Planetary Exploration.*

13 ASTRODYNAMICS 18

Includes powered and free-flight trajectories; and orbital and launching dynamics.

14 GROUND SUPPORT SYSTEMS AND FACILITIES (SPACE) 20

Includes launch complexes, research and production facilities; ground support equipment, e.g., mobile transporters; and simulators.

For related information see also *09 Research and Support Facilities (Air).*

15 LAUNCH VEHICLES AND SPACE VEHICLES N.A.

Includes boosters; operating problems of launch/space vehicle systems; and reusable vehicles.

For related information see also *20 Spacecraft Propulsion and Power.*

16 SPACE TRANSPORTATION N.A.

Includes passenger and cargo space transportation, e.g., shuttle operations; and space rescue techniques.

For related information see also *03 Air Transportation and Safety* and *18 Spacecraft Design, Testing and Performance.* For space suits see *54 Man/System Technology and Life Support.*

17 SPACE COMMUNICATIONS, SPACECRAFT COMMUNICATIONS, COMMAND AND TRACKING 20

Includes telemetry; space communications networks; astronavigation and guidance; and radio blackout.

For related information see also *04 Aircraft Communications and Navigation* and *32 Communications and Radar.*

18 SPACECRAFT DESIGN, TESTING AND PERFORMANCE 21

Includes satellites; space platforms; space stations; spacecraft systems and components such as thermal and environmental controls; and attitude controls.

For life support systems see *54 Man/System Technology and Life Support.* For related information see also *05 Aircraft Design, Testing and Performance, 39 Structural Mechanics,* and *16 Space Transportation.*

19 SPACECRAFT INSTRUMENTATION N.A.

For related information see also *06 Aircraft Instrumentation* and *35 Instrumentation and Photography.*

20 SPACECRAFT PROPULSION AND POWER 29

Includes main propulsion systems and components, e.g. rocket engines; and spacecraft auxiliary power sources.

For related information see also *07 Aircraft Propulsion and Power, 28 Propellants and Fuels, 44 Energy Production and Conversion,* and *15 Launch Vehicles and Space Vehicles.*

CHEMISTRY AND MATERIALS

Includes chemistry and materials (general); composite materials; inorganic and physical chemistry; metallic materials; nonmetallic materials; propellants and fuels; and materials processing.

23 CHEMISTRY AND MATERIALS (GENERAL) 30

24 COMPOSITE MATERIALS 30

Includes physical, chemical, and mechanical properties of laminates and other composite materials.

For ceramic materials see *27 Nonmetallic Materials.*

25 INORGANIC AND PHYSICAL CHEMISTRY 32

Includes chemical analysis, e.g., chromatography; combustion theory; electrochemistry; and photochemistry.

For related information see also *77 Thermodynamics and Statistical Physics.*

26 METALLIC MATERIALS 33

Includes physical, chemical, and mechanical properties of metals, e.g., corrosion; and metallurgy.

27 NONMETALLIC MATERIALS 35

Includes physical, chemical, and mechanical properties of plastics, elastomers, lubricants, polymers, textiles, adhesives, and ceramic materials.

For composite materials see *24 Composite Materials.*

28 PROPELLANTS AND FUELS 36

Includes rocket propellants, igniters and oxidizers; their storage and handling procedures; and aircraft fuels.

For related information see also *07 Aircraft Propulsion and Power, 20 Spacecraft Propulsion and Power,* and *44 Energy Production and Conversion.*

29 MATERIALS PROCESSING N.A.

Includes space-based development of products and processes for commercial application.

For biological materials see *55 Space Biology.*

ENGINEERING

Includes engineering (general); communications and radar; electronics and electrical engineering; fluid mechanics and heat transfer; instrumentation and photography; lasers and masers; mechanical engineering; quality assurance and reliability; and structural mechanics.

For related information see also *Physics.*

31 ENGINEERING (GENERAL) N.A.

Includes vacuum technology; control engineering; display engineering; cryogenics; and fire prevention.

32 COMMUNICATIONS AND RADAR 38

Includes radar; land and global communications; communications theory; and optical communications.

For related information see also *04 Aircraft Communications and Navigation* and *17 Space Communications, Spacecraft Communications, Command and Tracking.* For search and rescue see *03 Air Transportation and Safety,* and *16 Space Transportation.*

33 ELECTRONICS AND ELECTRICAL ENGINEERING 43

Includes test equipment and maintainability; components, e.g., tunnel diodes and transistors; microminiaturization; and integrated circuitry.

For related information see also *60 Computer Operations and Hardware* and *76 Solid-State Physics.*

34 FLUID MECHANICS AND HEAT TRANSFER 45

Includes boundary layers; hydrodynamics; fluidics; mass transfer and ablation cooling.

For related information see also *02 Aerodynamics* and *77 Thermodynamics and Statistical Physics.*

35 INSTRUMENTATION AND PHOTOGRAPHY 50

Includes remote sensors; measuring instruments and gages; detectors; cameras and photographic supplies; and holography.

For aerial photography see *43 Earth Resources and Remote Sensing.* For related information see also *06 Aircraft Instrumentation* and *19 Spacecraft Instrumentation.*

36 LASERS AND MASERS 69

Includes parametric amplifiers.

For related information see also *76 Solid-State Physics.*

37 MECHANICAL ENGINEERING 72

Includes auxiliary systems (nonpower); machine elements and processes; and mechanical equipment.

38 QUALITY ASSURANCE AND RELIABILITY 73

Includes product sampling procedures and techniques; and quality control.

39 STRUCTURAL MECHANICS 74

Includes structural element design and weight analysis; fatigue; and thermal stress.

For applications see *05 Aircraft Design, Testing and Performance* and *18 Spacecraft Design, Testing and Performance.*

GEOSCIENCES

Includes geosciences (general); earth resources and remote sensing; energy production and conversion; environment pollution; geophysics; meteorology and climatology; and oceanography.

For related information see also *Space Sciences.*

42 GEOSCIENCES (GENERAL) 77

43 EARTH RESOURCES AND REMOTE SENSING 95

Includes remote sensing of earth resources by aircraft and spacecraft; photogrammetry; and aerial photography.

For instrumentation see *35 Instrumentation and Photography.*

44 ENERGY PRODUCTION AND CONVERSION 96

Includes specific energy conversion systems, e.g., fuel cells; global sources of energy; geophysical conversion; and windpower.

For related information see also *07 Aircraft Propulsion and Power, 20 Spacecraft Propulsion and Power,* and *28 Propellants and Fuels.*

45 ENVIRONMENT POLLUTION 98

Includes atmospheric, noise, thermal, and water pollution.

46 GEOPHYSICS 99

Includes aeronomy; upper and lower atmosphere studies; ionospheric and magnetospheric physics; and geomagnetism.

For space radiation see *93 Space Radiation.*

47 METEOROLOGY AND CLIMATOLOGY 119

Includes weather forecasting and modification.

48 OCEANOGRAPHY 127

Includes biological, dynamic, and physical oceanography; and marine resources.

For related information see also *43 Earth Resources and Remote Sensing.*

LIFE SCIENCES

Includes life sciences (general); aerospace medicine; behavioral sciences; man/system technology and life support; and space biology.

51 LIFE SCIENCES (GENERAL) 128

52 AEROSPACE MEDICINE 129

Includes physiological factors; biological effects of radiation; and effects of weightlessness on man and animals.

53 BEHAVIORAL SCIENCES N.A.

Includes psychological factors; individual and group behavior; crew training and evaluation; and psychiatric research.

54 MAN/SYSTEM TECHNOLOGY AND LIFE SUPPORT 135

Includes human engineering; biotechnology; and space suits and protective clothing.

For related information see also *16 Space Transportation.*

55 SPACE BIOLOGY N.A.

Includes exobiology; planetary biology; and extraterrestrial life.

MATHEMATICAL AND COMPUTER SCIENCES

Includes mathematical and computer sciences (general); computer operations and hardware; computer programming and software; computer systems; cybernetics; numerical analysis; statistics and probability; systems analysis; and theoretical mathematics.

59 MATHEMATICAL AND COMPUTER SCIENCES (GENERAL) N.A.

60 COMPUTER OPERATIONS AND HARDWARE 135

Includes hardware for computer graphics, firmware, and data processing.

For components see *33 Electronics and Electrical Engineering.*

61 COMPUTER PROGRAMMING AND SOFTWARE 135

Includes computer programs, routines, algorithms, and specific applications, e.g., CAD/CAM.

62 COMPUTER SYSTEMS 138

Includes computer networks and special application computer systems.

63 CYBERNETICS 138

Includes feedback and control theory, artificial intelligence, robotics and expert systems.

For related information see also *54 Man/System Technology and Life Support.*

64 NUMERICAL ANALYSIS 139

Includes iteration, difference equations, and numerical approximation.

65 STATISTICS AND PROBABILITY N.A.

Includes data sampling and smoothing; Monte Carlo method; and stochastic processes.

66 SYSTEMS ANALYSIS N.A.

Includes mathematical modeling; network analysis; and operations research.

67 THEORETICAL MATHEMATICS N.A.

Includes topology and number theory.

PHYSICS

Includes physics (general); acoustics; atomic and molecular physics; nuclear and high-energy physics; optics; plasma physics; solid-state physics; and thermodynamics and statistical physics.

For related information see also *Engineering.*

70 PHYSICS (GENERAL) 141

For precision time and time interval (PTTI) see *35 Instrumentation and Photography;* for geophysics, astrophysics or solar physics see *46 Geophysics, 90 Astrophysics,* or *92 Solar Physics.*

71 ACOUSTICS 141

Includes sound generation, transmission, and attenuation.

For noise pollution see *45 Environment Pollution.*

72 ATOMIC AND MOLECULAR PHYSICS 142

Includes atomic structure, electron properties, and molecular spectra.

73 NUCLEAR AND HIGH-ENERGY PHYSICS 142

Includes elementary and nuclear particles; and reactor theory.

For space radiation see *93 Space Radiation.*

74 OPTICS 142

Includes light phenomena and optical devices.

For lasers see *36 Lasers and Masers.*

75 PLASMA PHYSICS 143

Includes magnetohydrodynamics and plasma fusion.

For ionospheric plasmas see *46 Geophysics.* For space plasmas see *90 Astrophysics.*

76 SOLID-STATE PHYSICS 144

Includes superconductivity.

For related information see also *33 Electronics and Electrical Engineering* and *36 Lasers and Masers.*

77 THERMODYNAMICS AND STATISTICAL PHYSICS 145

Includes quantum mechanics; theoretical physics; and Bose and Fermi statistics.

For related information see also *25 Inorganic and Physical Chemistry* and *34 Fluid Mechanics and Heat Transfer.*

SOCIAL SCIENCES

Includes social sciences (general); administration and management; documentation and information science; economics and cost analysis; law, political science, and space policy; and urban technology and transportation.

80 SOCIAL SCIENCES (GENERAL) N.A.

Includes educational matters.

81 ADMINISTRATION AND MANAGEMENT N.A.

Includes management planning and research.

82 DOCUMENTATION AND INFORMATION SCIENCE 145

Includes information management; information storage and retrieval technology; technical writing; graphic arts; and micrography.

For computer documentation see *61 Computer Programming and Software.*

83 ECONOMICS AND COST ANALYSIS N.A.

Includes cost effectiveness studies.

84 LAW, POLITICAL SCIENCE AND SPACE POLICY 146

Includes NASA appropriation hearings; aviation law; space law and policy; international law; international cooperation; and patent policy.

85 URBAN TECHNOLOGY AND TRANSPORTATION 146

Includes applications of space technology to urban problems; technology transfer; technology assessment; and surface and mass transportation.

For related information see *03 Air Transportation and Safety, 16 Space Transportation,* and *44 Energy Production and Conversion.*

SPACE SCIENCES

Includes space sciences (general); astronomy; astrophysics; lunar and planetary exploration; solar physics; and space radiation.

For related information see also *Geosciences.*

88 SPACE SCIENCES (GENERAL) N.A.

89 ASTRONOMY 148

Includes radio, gamma-ray, and infrared astronomy; and astrometry.

90 ASTROPHYSICS 150

Includes cosmology; celestial mechanics; space plasmas; and interstellar and interplanetary gases and dust.

For related information see also *75 Plasma Physics.*

91 LUNAR AND PLANETARY EXPLORATION 153

Includes planetology; and manned and unmanned flights.

For spacecraft design or space stations see *18 Spacecraft Design, Testing and Performance.*

92 SOLAR PHYSICS 154

Includes solar activity, solar flares, solar radiation and sunspots.

For related information see *93 Space Radiation.*

93 SPACE RADIATION 154

Includes cosmic radiation; and inner and outer earth's radiation belts.

For biological effects of radiation see *52 Aerospace Medicine.* For theory see *73 Nuclear and High-Energy Physics.*

GENERAL

Includes aeronautical, astronautical, and space science related histories, biographies, and pertinent reports too broad for categorization; histories or broad overviews of NASA programs.

99 GENERAL 156

Note: N.A. means that no abstracts were assigned to this category for this issue.

SUBJECT INDEX I-1
PERSONAL AUTHOR INDEX I-45
CORPORATE SOURCE INDEX I-53
CONTRACT NUMBER INDEX I-63
REPORT/ACCESSION NUMBER INDEX I-65

TYPICAL CITATIONS AND ABSTRACTS

NASA SPONSORED ↓

ON MICROFICHE ↓

ACCESSION NUMBER → **N87-10065*#** General Dynamics Corp., Fort Worth, Tex. ← **CORPORATE SOURCE**

TITLE → **DESIGN AND FABRICATION OF THE NASA DECOUPLER PYLON FOR THE F-16 AIRCRAFT Final Report, Jan. 1982 - Aug. 1983**

AUTHORS → J. D. Clayton, R. L. Haller, and J. M. Hassler, Jr. Jan. 1985 ← **PUBLICATION DATE**
204 p

CONTRACT OR GRANT → (Contract NAS1-16879)

REPORT NUMBER → (NASA-CR-172354; NAS 1.26:172354) Avail: NTIS ← **AVAILABILITY SOURCE**

PRICE CODE → HC A10/MF A01 CSCL 01C ← **COSATI CODE**

The NASA Decoupler Pylon is a passive means of suppressing wing-store flutter. The feasibility of demonstrating this concept on the F-16 aircraft was established through model wind tunnel tests and analyses. As a result of these tests and studies a ship set of Decoupler Pylons was designed and fabricated for a flight test demonstration on the F-16 aircraft. Basic design criteria were developed during the analysis study pertaining to pylon pitch stiffness, alignment system requirements, and damping requirements. A design was developed which utilized an electrical motor for the pylon alignment system. The design uses a four pin, two link pivot design which results in a remote pivot located at the center of gravity of the store when the store is in the aligned position. The pitch spring was fabricated from a tapered constant stress cantilevered beam. The pylon has the same external lines as the existing production pylon and is designed to use a MAU-12 ejection rack which is the same as the one used with the production pylon. The detailed design and fabrication was supported with a complete ground test of the pylon prior to shipment to NASA.

Author

VOLUME 25 NUMBER 1 / JANUARY 8, 1987

Scientific and Technical Aerospace Reports

A Semimonthly Publication of the National Aeronautics and Space Administration

01 AERONAUTICS (GENERAL)

N87-10001* National Aeronautics and Space Administration, Washington, D.C.
AEROSPACE MEDICINE AND BIOLOGY: A CONTINUING BIBLIOGRAPHY WITH INDEXES (SUPPLEMENT 287)
Aug. 1986 107 p
(NASA-SP-7011(287); NAS 1.21:7011(287)) Avail: NTIS HC A06 CSCL 01A

This bibliography lists 346 reports, articles and other documents introduced into the NASA scientific and technical information system in July 1986. Author

N87-10002# Federal Aviation Administration, Atlantic City, N.J. Technical Center.
HELICOPTER MLS FLIGHT INSPECTION PROJECT Final Report
Scott B. Shollenberger and Barry R. Billmann Apr. 1986 251 p
(DOT/FAA/CT-86/14) Avail: NTIS HC A12/MF A01

The results of tests designed to formalize microwave landing system (MLS) heliport flight inspection procedures are described. The tests, conducted in November 1985, demonstrated the feasibility of using a helicopter to perform some portion of the flight inspection of the MLS at heliports. Significant findings included the fact that radio theodolite techniques could be used for tracking a helicopter not equipped with stability augmentation equipment. Constituent parts of a portable flight inspection package were also identified and tested. Author

N87-10003*# Nielsen Engineering and Research, Inc., Mountain View, Calif.
DEVELOPMENT OF A TURBOMACHINERY DESIGN OPTIMIZATION PROCEDURE USING A MULTIPLE-PARAMETER NONLINEAR PERTURBATION METHOD Final Report
Stephen S. Stahara Sep. 1984 260 p
(Contract NAS3-20836)
(NASA-CR-3831; NAS 1.26:3831; NEAR-TR-295) Avail: NTIS HC A12/MF A01 CSCL 01B

An investigation was carried out to complete the preliminary development of a combined perturbation/optimization procedure and associated computational code for designing optimized blade-to-blade profiles of turbomachinery blades. The overall purpose of the procedures developed is to provide demonstration of a rapid nonlinear perturbation method for minimizing the computational requirements associated with parametric design studies of turbomachinery flows. The method combines the multiple parameter nonlinear perturbation method, successfully developed in previous phases of this study, with the NASA TSONIC blade-to-blade turbomachinery flow solver, and the COPES-CONMIN optimization procedure into a user's code for designing optimized blade-to-blade surface profiles of turbomachinery blades. Results of several design applications and a documented version of the code together with a user's manual are provided. Author

N87-10004# Air Force Systems Command, Wright-Patterson AFB, Ohio. Foreign Technology Div.
ACTA AERONAUTICA ET ASTRONAUTICA SINICA (SELECTED ARTICLES)
Hanxin Zhang, Shilu Chen, Xingjian Chen, Hengyuan Yan, and Xiufang Huo 9 May 1986 94 p Transl. into ENGLISH from Hangkong Xuebao (China), v. 6, no. 4, 1985 p 301-312; 321-334; 362-370; 379-384; 393-404
(AD-A167918; FTD-ID(RS)T-0109-86) Avail: NTIS HC A05/MF A01 CSCL 20/4

The following articles are from Acta Aeronautica et Astronautica Sinica, vol.6, no. 4, 1985: Advances in the Study of Separated Flows; Longitudinal Stability Analysis of Elastic Vehicles; Numerical Computation of Two Phase Turbulent Combustion Processes; Gust Alleviation Using Combined Control Laws; Calculation of Supersonic Flows around a Three-dimensional Wing and a Waisted Body with Characteristic Method in Stream Surface Coordinates; and Thermodynamic Analysis of Turbofan Engines. GRA

02 AERODYNAMICS

Includes aerodynamics of bodies, combinations, wings, rotors, and control surfaces; and internal flow in ducts and turbomachinery.

For related information see also *34 Fluid Mechanics and Heat Transfer.*

N87-10005 Georgia Inst. of Tech., Atlanta.
NUMERICAL SOLUTION OF THE 3-DIMENSIONAL BOUNDARY LAYER EQUATIONS IN THE INVERSE MODE USING FINITE DIFFERENCES Ph.D. Thesis
Samir Farid Radwan 1985 248 p
Avail: Univ. Microfilms Order No. DA8604015

A numerical formulation that uses a finite-difference method has been developed to solve the full three-dimensional boundary layer equations in inverse and direct modes. It is a implicit scheme and uses central differences in the direction normal to the wall, and weighted upwinding with three points in the plane parallel to the wall. The developed method has the following new features: (1) the formulation is done for non-orthogonal curvilinear coordinates; and (2) the developed scheme uses variable grid step size along all coordinates, and it preserves second-order accuracy if needed. The accuracy in the marching direction parallel to the wall can be of any order between first and second through input control. This makes the scheme stable and robust in the reversed flow regions. These features make the present numerical method more general and flexible than any of previous methods. The capability of the method in the inverse mode to march into the flow regions inaccessible to the direct mode calculations has been demonstrated for the following cases; (1) separated two-dimensional turbulent flow; (2) separated turbulent flow over an infinite swept wing and (3) laminar and turbulent flows over a prolate spheroid at low incidence. The principal achievement is the demonstration of the validity of the developed numerical inverse mode method to march into the regions of reversed flow which are inaccessible to the direct mode procedures. Dissert. Abstr.

N87-10006 Virginia Polytechnic Inst. and State Univ., Blacksburg.
ANALYSIS OF THE VORTICAL FLOW AROUND A 60 DEG DELTA WING WITH VORTEX FLAP Ph.D. Thesis
Bongzoo Sung 1985 260 p
Avail: Univ. Microfilms Order No. DA8605468

Subsonic wind tunnel investigations were conducted on a 60 deg. swept, flat plate, delta wing with a leading edge vortex flap. The pressure distributions were measured over a range of angles of attack starting from zero to 40 deg. to 5 deg. interval and flap deflection angles from zero to 45 deg. with 5 deg. increments at a Reynolds number of about 2.14 x 1 million based on the root chord. The flow visualization experiments were performed from zero degree to the stall angle, with ten different flap defection angles at the same Reynolds number. The mean flow field was measured at angles of attack 10 deg. and 15 deg. with the flap deflection angles of 10 deg. and 30 deg. at a Reynolds number of about 1.50 x 1 million. The experimental results show that the leading edge vortex flap is an effective means to control the vortex flow over a delta wing. The optimimum flap deflection angles were found where the primary vortex was confined to the leading edge vortex flap, thus producing a thrust on the flap. It was found that flap deflection could be used to restore a vortex flow from burst vortex condition. A non-linear vortex lattice code with a new velocity jump formula was developed to predict the aerodynamic characteristics of plain and vortex flapped delta wings including the pressure distributions. Dissert. Abstr.

N87-10007 Virginia Polytechnic Inst. and State Univ., Blacksburg.
THE EFFECT OF FREE STREAM DISTURBANCES AND CONTROL SURFACE DEFLECTIONS ON THE PERFORMANCE OF THE WORTMANN AIRFOIL AT LOW REYNOLDS NUMBERS Ph.D. Thesis
V. Sumantran 1985 249 p
Avail: Univ. Microfilms Order No. DA8605467

A wing with a Wortmann FX-63-137-ESM airfoil section has been used to study some unique problems encountered in wing aerodynamics in the range of Reynolds numbers between 50,000 and 500,000. The wind-tunnel testing conducted in the 6' x 6' Stability tunnel included strain-gauge data, pressure data and flow-visualization studies. The laminar separation bubble which frequently occurs on the upper surface of the wing is found to dominate its performance and gives rise to a hysteresis loop for lift and drag. Changes in airfoil performance due to positive flap or control surface deflections resemble changes witnessed at higher Reynolds numbers. Negative deflections are seen to considerably change the stall behavior and the flow over the airfoil. This is due to the considerably greater effect on the separation bubble for negative flap deflections. The structure and mechanism of the laminar separation bubble can also be altered by the introduction of selected acoustic disturbances and increased free-stream turbulence. The wind-tunnel test-section environment is, therefore, capable of considerably altering wing performance in this regime. Dissert. Abstr.

N87-10008 Virginia Polytechnic Inst. and State Univ., Blacksburg.
SEPARATION AND WAKES OVER 3-DIMENSIONAL BODIES Ph.D. Thesis
Christopher E. Costis 1985 163 p
Avail: Univ. Microfilms Order No. DA8605437

The laminar flow over a prolate spheroid was investigated via flow visualization and Laser-Doppler Velocimetry. Experiments were conducted in a water tunnel and the flow was visualized with dyes. The measurement of three-dimensional boundary layers required a special design of the laser optics. Attention was focused in the neighborhood of three-dimensional separation. The Vortex-Lattice method was employed to calculate the inviscid flow and the development of separated vortex sheets over a prolate spheroid. An approximate-method based on the assumption of local similarity was used to solve the boundary layer equations and calculate the line of open separation. A condition of vortex shedding along separation is proposed. The two schemes, viscous and inviscid, interact through the line of separation which is allowed to displace as the wake grows. Results are compared with flow visualization data for laminar separation and pressure data for turbulent separation. Dissert. Abstr.

N87-10009 Tennessee Univ., Knoxville.
A STUDY OF THE FLOW FIELD ABOUT AN UPPER SURFACE BLOWN WING AND ITS EFFECTS ON LONGITUDINAL STATIC STABILITY OF A SMALL JET AIRPLANE Ph.D. Thesis
Uwe Peter Solies 1985 149 p
Avail: Univ. Microfilms Order No. DA8608294

The effects of powered lift technology on the longitudinal stability characteristics of an upper surface blown (USB) jet-flapped aircraft have been studied. Both theoretical and experimental methods were employed to investigate the flow field in the vicinity of the lifting wing and its influence on pitching moments of the aircraft in motion. A nonlinear vortex-lattice theory was used to model the lift induced airflow in the near flow field about the wing. Comparison with literature data showed excellent agreement, giving confidence in the method used. Flight tests were conducted with the Ball-Bartoe Jetwing technology demonstration aircraft to visualize flow angles on the fuselage surface and at selected points in the flow field near the horizontal tail. To save cost, simple data acquiring techniques were used. Also, the theoretical flow computations were restricted to a simplified Jetwing model with a relatively small number of panels. Still, there was fair agreement between theoretically and experimentally determined flow angles at the tail of the Jetwing aircraft. The vortex-lattice routine was then used for a parametrical study of flow angles and longitudinal stability parameters. The results show that the powered lift strongly affects the flow field about the wing. Dissert. Abstr.

N87-10010 Colorado Univ., Boulder.
AN ASYMPTOTIC THEORY OF SUPERSONIC TURBULENT INTERACTIONS IN A COMPRESSION CORNER Ph.D. Thesis
Rodney Lee Cusic 1985 146 p
Avail: Univ. Microfilms Order No. DA8608595

The shock-boundary layer interaction is a phenomenon which occurs in a wide range of aerodynamic flows of practical importance. When a supersonic turbulent boundary layer encounters a compression corner, a continuous band of compressions is generated that coalesce into a shock wave. The undisturbed sonic height and the shock formation process occur deep inside the boundary layer on a scale typically two or three orders of magnitude smaller than one boundary layer thickness. The interaction flow field is determined by both the boundary layer profile and the compression corner angle. The inner region boundary value problem is scaled by sonic height, includes nonlinear transonic effects and must be solved by a conservative finite difference numerical scheme that captures the upstream influence, shock formation process, and abrupt pressure rise upstream of the vertex. The outer limit of the inner region solution is asymptotically matched to the inner limit of the existing outer region solution in some intermediate region. The result is a composite solution valid in both regions, which is analyzed by comparison to experimental data. Dissert. Abstr.

N87-10011# Tokyo Univ. (Japan). Inst. of Space and Astronautical Science.
PROCEEDINGS OF THE SYMPOSIUM ON MECHANICS FOR SPACE FLIGHT, 1985
Minoru Oda 1985 266 p The 15th Symposium was held in Tokyo, Japan, 7-8 Nov. 1985
(ISAS-SP-4) Avail: NTIS HC A12/MF A01

This 15th symposium was held on November 7 and 8, 1985 at the Japanese Institute of Space and Astronautical Science. The symposium program consisted of seven oral sessions: Vortical Flow; Flow around Flight Vehicles; Computational Fluid

Dynamics; Space Environment Control; Elementary Processes in Heat Pipes; Analysis of Heat Pipe Systems; Applications of Heat Pipes; and one panel discussion on Research and Development of Total Energy Systems for Space. During the Computational Fluid Dynamics Session, a report on the International Symposium on Computational Fluid Dynamics in Tokyo was presented. Eighteen papers of the 30 presented are included. For individual titles, see N87-10012 through N87-10038.

N87-10012# Tokyo Univ. (Japan).
THEORETICAL STUDY OF STRONG INTERACTION OF VORTEX FILAMENTS
Ryuji Takaki and A. K. M. F. Hussain *In its* Proceedings of the Symposium on Mechanics for Space Flight, 1985 1985 8 p Sponsored by Japan Society for the Promotion of Science (For primary document see N87-10011 01-02)
Avail: NTIS HC A12/MF A01

The recent analysis on the recombination of two vortex filaments in a viscous incompressible fluid is reported. The analysis is confined to a local flow field where this interaction occurs, and is based on the vorticity equation with the viscous term along with several assumptions, including fluid impulse conservation and spatial symmetry of the flow field. The flow field is expanded into polynomials of coordinates and the coefficient, which are functions of time, are obtained by substituting the expansions into the vorticity equation. It is proved that this process is completed within a short time t*=0(sigma sq. 2/gamma), where sigma and gamma are the size and the circulation of the vortex filaments respectively, and that the viscous effect is necessary for occurrence of the process. Author

N87-10013# Tokyo Univ. (Japan).
STUDIES ON VORTEX MOTION BASED ON THE DIVIDING VORTON MODEL
Sinzi Kuwabara *In its* Proceedings of the Symposium on Mechanics for Space Flight, 1985 1985 11 p (For primary document see N87-10011 01-02)
Avail: NTIS HC A12/MF A01

The basic equations and the division condition for dividing vortons in the incompressible, inviscid fluid are derived. Numerical analysis based on the dividing vorton model is applied to the evolution of the linked two vortex rings. The deformation of the rings at different times and the enstrophy, helicity, energy, momentum etc. of this system vs. time are calculated. Numerical results show that the invariance of the constants of motion of this system, the energy, momentum, angular momentum and total vorticity, except helicity, is satisfactory, and the helicity is constant in the initial stage but oscillates thereafter. As the two rings go close to each other and the interaction between them becomes stronger, the forms of vortex lines are so complicated, that they seem to develop to fractal curves. Author

N87-10014# Mitsubishi Heavy-Industries Ltd., Tokyo (Japan).
A DESCRIPTION OF A TURBULENT FLOW PAST A CIRCULAR CYLINDER BY A DISCRETE VORTEX METHOD
Hiroshi Nakajima and Yoshimasa Yoshizawa (Tsukuba Univ. (Japan).) *In* Tokyo Univ. Proceedings of the Symposium on Mechanics for Space Flighy, 1985 1985 10 p (For primary document see N87-10011 01-02)
Avail: NTIS HC A12/MF A01

Discrete vortex methods were often used to describe unsteady incompressible flows at high Reynolds numbers. Most studies already existing are concerned with large scale structures of the interested flows and integrated properties, that is, lift and drag coefficients of bodies. In order to examine potential abilities of the vortex methods in describing more detailed information, a correlation function in a wake of a circular cylinder is measured by a discrete vortex method and also an experiment of an actual flow. Comparisons between them show that turbulent structures also could be well described by the discrete vortex method. Author

N87-10015# Tokyo Univ. (Japan). Dept. of Physics.
ACOUSTIC WAVES EMITTED BY VORTEX-BODY INTERACTION c71
T. Kambe, T. Minota (Kyushu Univ., Fukuoka (Japan).), and Y. Ikushima *In its* Proceedings of the Symposium on Mechanics for Space Flight, 1985 1985 9 p (For primary document see N87-10011 01-02)
Avail: NTIS HC A12/MF A01

Acoustic emission by a vortex ring moving near a solid body is investigated both experimentally and theoreticly for three typical configurations of the vortex-body system. In the first case, a vortex ring passes near by a circular clinder whose axis is set at right angles to the vortex motion. In the remaining two cases, a vortex ring passes by a sharp edge of a flat plate, its width being comparable with the vortex size for the one case and semi-infinite for the others. A basis of comparison between the observations and the theoretical predictions is presented. Author

N87-10016# Tokyo Univ. (Japan). Inst. of Space and Astronautical Science.
STUDY OF THREE-DIMENSIONAL SEPARATION ON A SPHEROID AT INCIDENCE c34
Yoshio Ishu and Yuko Oshima (Ochanomizu Women's Univ., Tokyo (Japan).) *In its* Proceedings of the Symposium on Mechanics for Space Flight, 1985 1985 9 p (For primary document see N87-10011 01-02)
Avail: NTIS HC A12/MF A01

Experimental observation of flow separation on a spheroid at various angles of attack was carried out in low Reynolds number flow using a water channel by flow visualization method. Color oil method was adapted to make the surface separation pattern visible, and hydrogen bubble method was effective for visualization of the flow field around the model. The results support the three-dimensional separation criteria proposed by Maskell, Wang, and Han and Patel, and mechanism of the flow interaction with the longitudinal vortices along the body surface is made clear. Author

N87-10017# Chiba Univ. (Japan). Faculty of Engineering.
IMAGES OF THREE DIMENSIONAL FLOWS IN COMPUTER GRAPHICS c61
Nobuhide Nishikawa, Akira Suzuki, and Satoshi Akiyama *In* Tokyo Univ. Proceedings of the Symposium on Mechanics for Space Flight, 1985 1985 11 p (For primary document see N87-10011 01-02)
Avail: NTIS HC A12/MF A01

The numerical results are shown in graphic images for three dimensional boundary-layer flows. It is shown that the presentation of images, especially in solid model graphics, allows the utilization of the widest band width sense in an effective manner to create physical or geometrical models and to understand their behavior in simulated environments. As the results, external streamlines and limiting streamlines obtained with finite difference calculations are given for paraboloid, and for the front half region of wing-ellipsoid combination. Author

N87-10018# Yamagata Univ. (Japan). Faculty of Engineering.
ON ACCURATE NUMERICAL SOLUTIONS OF FALKNER-SKAN EQUATION c34
Masakazu Katagiri *In* Tokyo Univ. Proceedings of the Symposium on Mechanics for Space Flight, 1985 1985 6 p (For primary document see N87-10011 01-02)
Avail: NTIS HC A12/MF A01

Accurate numerical solutions of the Falkner-Skan equation are obtained by a numerical method of quasi-linear approximation. For various values of a parameter which measures the pressure gradient, solutions of ten decimal accuracy are obtained. For the case of a boundary layer flow along a semi-infinite flat plate, twelve decimal accuracy can be obtained. Author

N87-10019# IBM Japan. Science Inst.
NUMERICAL STUDY OF THE ENTRANCE FLOW AND ITS TRANSITION OF A CIRCULAR PIPE c34
H. Kanda and K. Oshima *In* Tokyo Univ. Proceedings of the

Symposium on Mechanics for Space Flight, 1985 1985 17 p (For primary document see N87-10011 01-02)
Avail: NTIS HC A12/MF A01

The dimensional, time-dependent computational scheme was devised for determining the flow development and the corresponding pressure drop in the entrance region of a circular pipe at the Reynolds numbers based on the pipe diameter of 10, 100, 2000, and 10000. An iterative, stream function-vorticity formulation was applied, utilizing a mesh system in which the axial grid size is nearly proportional to the Reynolds number. The velocity field, the pressure drop, and the convective and the viscous terms are compared with the experimental results and also with the previous analysis. Moreover, the effects of the Reynolds number and the superposed disturbances on the transition from laminar to turbulent flow were numerically simulated. Author

N87-10020# Kyoto Univ. (Japan). Dept. of Aeronautical Engineering.
NUMERICAL SIMULATION OF TWO-DIMENSIONAL FREEJET FLOW-FIELDS **c34**
Koji Teshima and Hiroyuki Nakatsuji *In* Tokyo Univ. Proceedings of the Symposium on Mechanics for Space Flight, 1985 1985 7 p Sponsored in part by the Data Processing Center (For primary document see N87-10011 01-02)
Avail: NTIS HC A12/MF A01

Supersonic jet flow fields from a two dimensional sonic nozzle are computed using the piecewise linear method. The sonic radius for a two dimensional source flow is estimated using the numerical results. It is shown that the flow properties on the jet axis can be approximated by the two dimensional source flow at large distances from the nozzle. The distance of the normal shock from the nozzle increases with the stagnation to ambient pressure ratio, but is somewhat larger than experiments. Author

N87-10021# Tokyo Univ. (Japan).
TECHNICAL OVERVIEW OF PLUME RADIATION FROM A SOLID ROCKET MOTOR **c20**
Yasushi Sakurai and Hiroshi Kimura *In its* Proceedings of the Symposium on Mechanics for Space Flight, 1985 1985 14 p (For primary document see N87-10011 01-02)
Avail: NTIS HC A12/MF A01

Current technology for calculation of plume radiation from a solid rocket motor is overviewed and a useful engineering model is reviewed and recommended for design purposes. A solid rocket motor plume is a conical cloud which contains cold scattering particles and hot emitting-absorbing particles. Radiation to aft-end equipment of spacecraft is a major concern of thermal design engineers. Radiative properties of the plume totally depends on the particle behavior in the flow field and the analysis requires numerious efforts. A simple Bobco model which starts without flow field analysis, is discussed. Author

N87-10022# Tokyo Univ. (Japan).
TWO DIMENSIONAL ANALYSIS OF HIGH VOLTAGE SOLAR ARRAY INTERFERING WITH IONOSPHERIC PLASMA **c44**
Hitoshi Kuninaka and Kyoichi Kuriki *In its* Proceedings of the Symposium on Mechanics for Space Flight, 1985 1985 10 p (For primary document see N87-10011 01-02)
Avail: NTIS HC A12/MF A01

The spacecraft which flies in Low Earth Orbit being biased at high voltage is affected by undesirable interference with the ionospheric plasma. Two dimensional analysis was performed about the solar array which has 10 m span and is biased at 1 kV. For the standard ionospheric conditions the drain power assumes about 0.25% of the generated power, which is rather insignificant. On the other hand, the ion drag amounts to about 130% of the neutral particles collision drag, which represents drastic increase of the satellite drag. Author

N87-10023# Miyazaki Univ. (Japan). Dept. of Applied Physics.
ANALYSIS ON GRAVITATIONAL EFFECT TO NONLINEAR DIFFUSION SYSTEM OF VAPOR MOLECULES IN A HEAT PIPE **c34**
Kanji Etori *In* Tokyo Univ. Proceedings of the Symposium on Mechanics for Space Flight, 1985 1985 12 p (For primary document see N87-10011 01-02)
Avail: NTIS HC A12/MF A01

A nonlinear diffusion equation with a diffusion coefficient depending on number density of diffusing particles affected by gravity is approximately solved in a steady state. Characteristic properties of vapor molecules in a heat pipe are analyzed as a diffusion process of Brownian particles. In order to explain the nonlinear shifts from a linear diffusion system in conventional theories, the expectation values and the variance of number density of vapor molecules are calculated by using the theory of stochastic processes. As a result, a diffusion thermal resistance of a heat flow in a heat pipe is estimated by taking an average value of the diffusion coefficient in a nonlinear system. Author

N87-10024# Nippon Inst. of Tech. (Japan).
EFFECT OF SURPLUS STANDING LIQUID ON HEAT TRANSFER RESISTANCE IN THE HEAT PIPE (WITH MESH WICK IN A HORIZONTAL MODE) **c34**
Makoto Kamata and Yoshio Ikeda *In* Tokyo Univ. Proceedings of the Symposium on Mechanics for Space Flight, 1985 1985 10 p (For primary document see N87-10011 01-02)
Avail: NTIS HC A12/MF A01

It is an engineering practice to fill a heat pipe with working fluid of a quantity a little larger than the clearance volume of the screen wick as the most desirable volume of working fluid is unknown. However, it is foreseeable that excessive volume of working fluid deteriorates the performance of the heat pipe. A new method is discussed of computation for heat flow and temperature distribution in a heat pipe with the assumptions that the depth of working fluid in the heat pipe can be calculated from the pressure losses in the evaporation and condensation zones, that surplus fluid adheres to the inner wall of the screen wick forming a cylindrical layer of liquid, and that the heat transfer resistance of the container, screen wick and cylindrical layer of working fluid are connected in series. To validate the computation, experiments were performed and good agreement was obtained. Author

N87-10025# Osaka Univ. (Japan). Dept. of Aeronautical Engineering.
DYNAMIC HEAT TRANSFER MECHANISM OF TWO-PHASE CLOSED THERMOSYPHON **c34**
Kanji Negishi, Ken-ichi Kaneko, and Fusao Kusumoto *In* Tokyo Univ. Proceedings of the Symposium on Mechanics for Space Flight, 1985 1985 9 p (For primary document see N87-10011 01-02)
Avail: NTIS HC A12/MF A01

The heat transfer mechanism of a two phase closed thermosyphon was dynamically analysed in the periodically motive behavior of working fluid with boiling. It is an important problem in order to obtain high heat transfer performance, how the liquid film of the working fluid can be held for longer time on the wider area of the evaporator heating wall, and how the active evaporation can be kept there. Author

N87-10026# National Research Inst. for Pollution and Resources, Tokyo (Japan).
A TRIAL ON PERFORMANCE TEST METHOD FOR Cu-WATER HEAT PIPE **c34**
Yoshio Tanaka and Tadashi Yamamoto *In* Tokyo Univ. Proceedings of the Symposium on Mechanics for Space Flight, 1985 1985 8 p (For primary document see N87-10011 01-02)
Avail: NTIS HC A12/MF A01

Because of the increase demand for heat pipes, the establishment of standard methods for the performance test and the performance expression of the heat pipe was requested. Generally, the measurement method for the heat transfer rate of heat pipes is divided into two categories. That is, the heat transfer rate of heat pipe is measured by heat input to the evaporator surface or the quantity of heat removed from the condenser zone. The heat loss to each method described must be determined by circulating some kind of fluid such as water in same size pipe located in the heating unit instead of the heat pipe under actual operating condition before use. The heat transfer rate of Cu-Water heat pipe is measured by means of the measurement method based on the principle of bomb calorimeter. The obtained measuring accuracy may be lower. E.R.

N87-10027# Toshiba Corp., Tokyo (Japan).

HIGH CAPACITY HEAT PIPE WITH AXIAL GROOVES c34

Yoshiro Miyazaki and Yuji Ido *In* Tokyo Univ. Proceedings of the Symposium on Mechanics for Space Flight, 1985 1985 5 p (For primary document see N87-10011 01-02)

Avail: NTIS HC A12/MF A01

A new type of high capacity heat pipe for spacecraft use was fabricated and tested. The heat pipe consists of an outer pipe and an inner pipe. The outer pipe is a container and it has two channels, one for liquid and one for vapor. The inner pipe is provided with axial grooves and circumferential slits, and it is inserted into the vapor channel of the outer pipe. The circumferential slits connect the liquid channel and the axial grooves. Preliminary test results for the first 1 m long development model are presented and discussed, relating to its heat transport capacity. Author

N87-10028# Tokyo Electric Power Co., Inc. (Japan).

OPERATING CHARACTERISTICS OF COOLING UNDERGROUND POWER CABLES USING UP SLOPED LONG HEAT PIPES IN CONDUIT c34

Keisuke Oka, Hachiro Tsuchihashi, Yoichi Nishimura, Tsuneaki Mohtai (Fujikura Ltd., Sakura (Japan).), Masataka Mochizuki, Koichi Mashiko, and Hiroshi Yamanouchi *In* Tokyo Univ. Proceedings of the Symposium on Mechanics for Space Flight, 1985 1985 10 p (For primary document see N87-10011 01-02)

Avail: NTIS HC A12/MF A01

Long heat pipes for cooling electric power cables in conduit pipe are required to operate not only in the down slope but also in the up slope. The stable operation of the heat pipe is attained by separating the vapor flow path and the liquid flow path completely, and returning the working fluid condensed by the radiator to the evaporation section end by utilizing a difference in the pressure head. Evaporating section consisting of corrugated metallic pipes and carbon fiber wicks were employed for liquid film evaporation and holding liquid uniformly along an axial length of the pipe. Long heat pipes with a length 100 m, outside diameter 70 mm, and up slope 1/100 were made experimentally and tested. They operated in the normal heat pipe mode, carrying heat 9kW. Further the heat pipes were layed in some cable conduits providing adequate cooling effect. Author

N87-10029# Tokyo Univ. (Japan). Inst. of Space and Astronautical Science.

REPORT OF THE INTERNATIONAL SYMPOSIUM ON COMPUTATIONAL FLUID DYNAMICS, TOKYO c34

Koichi Oshima *In its* Proceedings of the Symposium on Mechanics for Space Flight, 1985 1985 8 p (For primary document see N87-10011 01-02)

Avail: NTIS HC A12/MF A01

The International Symposium on Computational Fluid Dynamics-Tokyo was held on Sept. 9 thru 12, 1985 at Kenchiku Kaikan of Tokyo. Based on the recommendation given by the International Advisory Committee Members a few distinguished CFD scientists were asked to present a review paper on each specialized field, and 23 out of them were able to accept the invitation. They were noted as INVITED on the Program. Total of 97 abstracts of contributed papers were submitted, and, based on referee reports made by all the International Advisory Committee Members, 75 of them were accepted for presentation. Out of these 98 papers including the invited ones, 35 came from USA, 28 from Japan and 35 from rest of the world. All of these papers are listed. E.R.

N87-10030# Academy of Sciences (USSR), Moscow. Computing Center.

COMPUTATIONAL AERODYNAMICS OF SUPERSONIC LIFTING VEHICLES

P. I. Chushkin and G. P. Voskresensky *In* Tokyo Univ. Proceedings of the Symposium on Mechanics for Space Flight, 1985 1985 13 p (For primary document see N87-10011 01-02)

Avail: NTIS HC A12/MF A01

A review of investigations on numerical modelling of supersonic three dimensional steady flows about lifting vehicles and their elements carried out in the Soviet Union during the last five years is given. An inviscid gas, both perfect and high-temperature, is considered. A number of characteristic examples are presented. Author

N87-10031# Akademiya Nauk SSSR, Novosibirsk. Inst. of Theoretifcal and Applied Mechanics.

NUMERICAL MODELING OF SPATIAL FLOWS ON THE BASIS OF SPLITTING UP METHOD c34

V. M. Kovenya, G. A. Tarnavsky, and S. G. Cherny *In* Tokyo Univ. Proceedings of the Symposium on Mechanics for Space Flight, 1985 1985 10 p (For primary document see N87-10011 01-02)

Avail: NTIS HC A12/MF A01

The study of flows near the bodies of three dimensional, spatial configuration is one of the problems of paramount importance in computational aerodynamics. The difficulties of studying the spatial flows are conditioned by the presence of zones of sharp inhomogeneities of the shock wave type, boundary layer, separation regions and of other peculiarities in the field near a body and in the wake behind it, parallel with the regions of a smooth flow. The study requires the application of different physico-mathematical models which are valid for description of flows in different subregions. The stationary supersonic flows of a viscous gas near the bodies in the approximation of complete and simplified Navier-Stokes equations are examined. The parabolic approximation of Navier-Stokes equations (PNS) was taken as a simplified model. The PNS model is obtained by elimination from the complete equations of the second derivatives (repreated or repeated and mixed) along the one coordinate (marching) direction. It incorporates the models of viscous and thin shock wave and holds for description of the flows with the presence of transversal separations. A wide application of the PNS model is conditioned by a decrease in the problem dimension as well as in the possibility of finding the stationary solution by the marching method for supersonic flows. At the same time a class of problems for which the PNS approximation holds is wide enough. E.R.

N87-10032# Academy of Sciences (USSR), Moscow. Computing Center.

THE THIRD ORDER COMPACT SCHEMES FOR FLUID DYNAMIC PROBLEMS c34

A. I. Tolstykh *In* Tokyo Univ. Proceedings of the Symposium on Mechnics for Space Flight, 1985 1985 7 p (For primary document see N87-10011 01-02)

Avail: NTIS HC A12/MF A01

The algorithms for viscous flows computations should meet higher requirements to such kinds of properties as stability, the absence of scheme oscillations, etc. The first of these properties makes preferable implict schemes, the second one leads to the odd order of approximation. Computational practice has shown that from this point of view the three-point (compact) third order schemes proposed and investigated are efficient. Those are actually high accuracy schemes when supplemented with grid points condensing in the computational regions with strong gradients. The discription of the third order compact schemes and of some of their applications to fluid dynamic problems is given. Author

N87-10033# Academy of Sciences (USSR), Moscow. Inst. of Applied Mathematics.

SUPERSONIC FLOW AROUND TIP SIDES OF WINGS

G. P. Voskresensky *In* Tokyo Univ. Proceedings of the Symposium on Mechanics for Space Flight, 1985 1985 7 p (For primary document see N87-10011 01-02)

Avail: NTIS HC A12/MF A01

The problem of supersonic flow around the tip sides of wings with swept or unswept leading edges and an attached shock wave is presented. The solution of the problem is based on the assumption that the surface of a rounded tip side of a wing is conical and the flow around it is self-similar. This fact makes it possible to use the self-similar stationing principle for the solution of the problem. The realization of this principle is carried out with the help of the finite-difference second-order algorithm. Author

N87-10034# Technical Univ. of Opole (Poland).
AN IMPROVED PSI-CELL METHOD FOR TURBULENT MULTIPHASE FLOWS c34
B. Dobrowolski and Z. Kabza *In* Tokyo Univ. Proceedings of the Symposium on Mechanics for Space Flight 1985 6 p (For primary document see N87-10011 01-02)
Avail: NTIS HC A12/MF A01

The rapidly increasing capability of computers has led to the development of numerical models for two-phase flows. There are basically two schemes that have been used in literature to model two-dimensional subsonic gas-particle or gas-droplet flows; the two fluid methods and the trajectory method. The average equations which treat the conveying gas and the particle cloud as two interactive fluids are the basis of the two-fluid method. The other apporach to modelling gas particle flows is the trajectory approach. This approach, called PSI cell model is based on treating the droplets or particles as sources of mass, momentum and energy to the gaseous phase. The presented modifications of the PSI-cell method allows the computation, in an economic way, of complicated turbulent polydispersive(polyphase) flows. Some additional terms in the turbulence model equations are introduced in a theoretical manner. The results of numerical calculations point at the dissipative character of turbulent interphase interactions and the considerable dependence of macrostructure of the two-phase stream on the structure of turbulence. E.R.

N87-10035# Bulgarian Academy of Science, Sofia. Inst. of Mechanics and Biomechanics.
HYDRODYNAMIC AND THERMAL INTERACTION BETWEEN TWO SPHERES IN A STEADY VISCOUS FLOW c34
Z. D. Zapryanov and E. T. Toshev *In* Tokyo Univ. Proceedings of the Symposium on Mechanics for Space Flight, 1985 1985 7 p (For primary document see N87-10011 01-02)
Avail: NTIS HC A12/MF A01

The investigation of the hydrodynamic and thermal interaction between two spheres moving in a viscous fluid is very important from a practical and fundamental point of view. This problem is topical in modeling of suspensions, emulsions and many chemical technologies. An extension of the method of fractional steps to study the hydrodynamic and thermal interaction between two spherical particles in a steady viscous flow is presented. This numerical method yields good results from low to reasonably high Reynolds and Prandtl numbers. Author

N87-10036# Academy of Sciences (USSR), Moscow. Inst. of Applied Mathematics.
MATHEMATICAL AND COMPUTATIONAL MODELS OF PLASMA FLOWS c75
K. V. Brushlinsky *In* Tokyo Univ. Proceedings of the Symposium on Mechanics for Space Flight, 1985 1985 9 p (For primary document see N87-10011 01-02)
Avail: NTIS HC A12/MF A01

Investigations of plasma flows are of interest, firstly, due to numerous applications, and secondly, because of their general principles, which form a special branch of physics: the plasma dynamics. Numerical simulation and computation, together with theoretic and experimental methods, play an important part in these investigations. Speaking on flows, a relatively dense plasma is mentioned, so its mathematical models appertain to the fluid mechanics, i.e., they are based on the magnetohydrodynamic description of plasma. Time dependent two dimensional models of plasma flows of two wide-spread types are considered: the flows across the magnetic field and those in the magnetic field plane. Author

N87-10037# Academy of Sciences (USSR), Moscow. Computing Center.
THE NUMERICAL METHOD OF CALCULATION OF TWO-DIMENSIONAL STATIONARY ELECTRO-GASDYNAMIC INTERNAL FLOWS c34
V. V. Zhurin and A. V. Shipilin *In* Tokyo Univ. Proceedings of the Symposium on Mechanics for Space Flight, 1985 1985 7 p (For primary document see N87-10011 01-02)
Avail: NTIS HC A12/MF A01

The suggested numerical method is meant for computations of two dimensional stationary internal nonviscous gas flows in a presence of a heat supply at expense of Joule heating. Such flows and processes take place in the plasma thrusters and in the working regions of the electro-ionizing lasers. The numerical solution of the Euler equations for subsonic and transonic regimes are considered. For computations of supersonic internal flows the method of characteristics is a very effective method. The method suggested allows an easy connection with the method of characteristics. Author

N87-10038# Academy of Sciences (USSR), Moscow.
COMPUTER SIMULATION IN ENGINEERING HYDRODYNAMICS c61
A. A. Samarskh, B. P. Gerasimov, T. G. Elizarova, I. S. Kalachinskaya, A. B. Karagichev, A. V. Lesunovsky, S. A. Semushin, B. I. Chetversushkin, and A. G. Churbanov *In* Tokyo Univ. Proceedings of the Symposium on Mechanics for Space Flight, 1985 1985 4 p (For primary document see N87-10011 01-02)
Avail: NTIS HC A12/MF A01

Computer simulation becomes a major research tool in science and technology. The fluid flow is the most common transport mechanism in technical devices and technological processes. It gave rise to a new scientific field-computational engineering hydrodynamics, which implies special demands to the computer simulation software. Appropriate applied code packages (ACP) involve comprehensive physical and mathematical models, while allowing their implementation and modification by various users who do not specialize in computational mathematics. This is possible due to the modular standard structure of codes, simplicity and reliability of numerical techniques involved. The program complexes, NEPTUN and EOL, cover a wide subject area of engineering hydrodynamics. Experience gained in exploitation of these codes showed that it takes only 2 to 3 months to master them. Additional modules developed by users are included in ACP and become available to others. Such an approach considerably enhances the labor efficiency of mathematicians, programmers and users. Author

N87-10039*# National Aeronautics and Space Administration. Langley Research Center, Hampton, Va.
WIND-TUNNEL INVESTIGATION OF THE FLIGHT CHARACTERISTICS OF A CANARD GENERAL-AVIATION AIRPLANE CONFIGURATION
Dale R. Satran Oct. 1986 60 p
(NASA-TP-2623; L-15929; NAS 1.60:2623) Avail: NTIS HC A04/MF A01 CSCL 01A

A 0.36-scale model of a canard general-aviation airplane with a single pusher propeller and winglets was tested in the Langley 30- by 60-Foot Wind Tunnel to determine the static and dynamic stability and control and free-flight behavior of the configuration. Model variables made testing of the model possible with the canard in high and low positions, with increased winglet area, with outboard wing leading-edge droop, with fuselage-mounted vertical fin and rudder, with enlarged rudders, with dual deflecting rudders, and with ailerons mounted closer to the wing tips. The basic model exhibited generally good longitudinal and lateral stability and control characteristics. The removal of an outboard leading-edge droop degraded roll damping and produced lightly damped roll (wing rock) oscillations. In general, the model exhibited very stable dihedral effect but weak directional stability. Rudder and aileron control power were sufficiently adequate for control of most flight conditions, but appeared to be relatively weak for maneuvering

compared with those of more conventionally configured models.
Author

N87-10040*# Cincinnati Univ., Ohio. Dept. of Aerospace Engineering and Engineering Mec
ANALYSIS OF TWO-DIMENSIONAL INCOMPRESSIBLE FLOW PAST AIRFOILS USING UNSTEADY NAVIER-STOKES EQUATIONS
K. N. Ghia, G. A. Osswald, and U. Ghia 1986 15 p Previously announced in IAA as A85-42975
(Grants NAG1-465; AF-AFOSR-0160-80)
(NASA-CR-179823; NAS 1.26:179823) Avail: NTIS HC A02/MF A01 CSCL 01A

The conservative form of the unsteady Navier-Stokes equations in terms of vorticity and stream function in generalized curvilinear coordinates are used to analyze the flow structure of steady separation and unsteady flow with massive separation. The numerical method solves the discretized equations using an ADI-BGE method. The method is applied to a symmetric 12 percent thick Joukowski airfoil. A conformal clustered grid is generated; several 1-D stretching transformations are used to obtain a grid that attempts to resolve many of the multiple scales of the unsteady flow with massive separation, while maintaining the transformation metrics to be smooth and continuous in the entire flow field. Detailed numerical results are obtained for three flow configurations (1) Re = 1000, alpha = 5 deg., (2) Re =1000, alpha = 15 deg., (3) Re = 10,000, alpha = 5 deg. No artificial dissipation was added; however, lack of a fine grid in the normal direction has presently led to results which are considered qualitative, especially for case (3).
Author

N87-10041*# National Aeronautics and Space Administration. Langley Research Center, Hampton, Va.
SPIN-TUNNEL INVESTIGATION OF A 1/25-SCALE MODEL OF THE GENERAL DYNAMICS F-16XL AIRPLANE
Raymond D. Whipple and William L. White Oct. 1984 51 p
(NASA-TM-85660; L-15616; NAS 1.15:85660) Avail: NTIS HC A04/MF A01 CSCL 01A

A spin-tunnel investigation of the spin and recovery characteristics of a 1/25-scale model to the General Dynamics F-16XL aircraft was conducted in the Langley Spin Tunnel. Tests included erect and inverted spins at various symmetric and asymmetric loading conditions. The required size of an emergency spin-recovery parachute was determined.
Author

N87-10042*# National Aeronautics and Space Administration. Langley Research Center, Hampton, Va.
SUPERSONIC, NONLINEAR, ATTACHED-FLOW WING DESIGN FOR HIGH LIFT WITH EXPERIMENTAL VALIDATION
James L. Pittman, David S. Miller, and William H. Mason (Grumman Aerospace Corp., Bethpage, N.Y.) Aug. 1984 221 p
(NASA-TP-2336; L-15787; NAS 1.60:2336) Avail: NTIS HC A10/MF A01 CSCL 01A

Results of the experimental validation are presented for the three dimensional cambered wing which was designed to achieve attached supercritical cross flow for lifting conditions typical of supersonic maneuver. The design point was a lift coefficient of 0.4 at Mach 1.62 and 12 deg angle of attack. Results from the nonlinear full potential method are presented to show the validity of the design process along with results from linear theory codes. Longitudinal force and moment data and static pressure data were obtained in the Langley Unitary Plan Wind Tunnel at Mach numbers of 1.58, 1.62, 1.66, 1.70, and 2.00 over an angle of attack range of 0 to 14 deg at a Reynolds number of 2.0 x 10 to the 6th power per foot. Oil flow photographs of the upper surface were obtained at M = 1.62 for alpha approx. = 8, 10, 12, and 14 deg.
E.R.

N87-10043*# Grumman Aerospace Corp., Bethpage, N.Y.
VISCOUS WING THEORY DEVELOPMENT. VOLUME 1: ANALYSIS, METHOD AND RESULTS Final Report
R. R. Chow, R. E. Melnik, F. Marconi, and J. Steinhoff Oct. 1986 127 p
(Contract NAS1-16858)
(NASA-CR-178156; NAS 1.26:178156; RE-725-Vol-1) Avail: NTIS HC A07/MF A01 CSCL 01A

Viscous transonic flows at large Reynolds numbers over 3-D wings were analyzed using a zonal viscid-inviscid interaction approach. A new numerical AFZ scheme was developed in conjunction with the finite volume formulation for the solution of the inviscid full-potential equation. A special far-field asymptotic boundary condition was developed and a second-order artificial viscosity included for an improved inviscid solution methodology. The integral method was used for the laminar/turbulent boundary layer and 3-D viscous wake calculation. The interaction calculation included the coupling conditions of the source flux due to the wing surface boundary layer, the flux jump due to the viscous wake, and the wake curvature effect. A method was also devised incorporating the 2-D trailing edge strong interaction solution for the normal pressure correction near the trailing edge region. A fully automated computer program was developed to perform the proposed method with one scalar version to be used on an IBM-3081 and two vectorized versions on Cray-1 and Cyber-205 computers.

N87-10044*# Grumman Aerospace Corp., Bethpage, N.Y.
VISCOUS WING THEORY DEVELOPMENT. VOLUME 2: GRUMWING COMPUTER PROGRAM USER'S MANUAL Final Report
R. R. Chow and P. L. Ogilvie Oct. 1986 117 p
(Contract NAS1-16858)
(NASA-CR-178157; NAS 1.26:178157; RE-726-Vol-2) Avail: NTIS HC A06/MF A01 CSCL 01A

This report is a user's manual which describes the operation of the computer program, GRUMWING. The program computes the viscous transonic flow over three-dimensional wings using a boundary layer type viscid-inviscid interaction approach. The inviscid solution is obtained by an approximate factorization (AFZ)method for the full potential equation. The boundary layer solution is based on integral entrainment methods.
Author

N87-10045# Goldschmied (Fabio R.), Monroeville, Pa.
WIND TUNNEL TEST OF THE MODIFIED GOLDSCHMIED MODEL WITH PROPULSION AND EMPENNAGE: ANALYSIS OF TEST RESULTS Final Report, 3 Mar. 1981 - 30 Nov. 1982
Fabio R. Goldschmied 1 Feb. 1986 115 p
(Contract N00167-81-C-0075)
(AD-A167360; FRG-82-1; DTNSRDC/ASED-CR-02-86) Avail: NTIS HC A06/MF A01 CSCL 20/4

An extensive test program was carried out in DTNSRDC's 8x10 low-speed wind-tunnel for experimental verification of the integrated hull boundary-layer control/propulsion lighter-than-air design. The 1957 Goldschmied wind-tunnel model was overhauled with a new suction-slot inlet configuration, a suction/propulsion fan, a new aftbody and a tailboom/empennage assembly. The fan air power coefficient of the operational model with empennage ranged in steady flight from 0.0130 (free transition) to 0.0155 (transition tripped at 10% length) at the volume Reynolds number of two millions. Considerable excess thrust could be generated with an average incremental propulsive efficiency of 72%. As compared to wind-tunnel tests of conventional streamlined bodies with empennage at exactly the same volume Reynolds number, the integrated design offers 50% less equivalent drag for both free and tripped transitions. The empennage provided neutral static stability over the complete test range of 8 degrees; the ratio of total fin planform over volume equivalent was 0.404. It was found that efficient and stable BLC could be achieved only by the combination of Ringloeb cusp at the slot's leading-edge with suction flow and with the presence of the tailboom. The fan (or pump) design is an essential part of the system design: a procedure was developed for determining the optimum fan design parameters from the vehicle's wind-tunnel test data.
GRA

N87-10046# Air Force Inst. of Tech., Wright-Patterson AFB, Ohio.
APPLICATION OF BIFURCATION AND CATASTROPHE THEORIES TO NEAR STALL FLIGHT MECHANICS M.S. Thesis

Carl A. Hawkins 1985 247 p
(AD-A167697; AFIT/CI/NR-86-54T) Avail: NTIS HC A11/MF A01 CSCL 01/1

This thesis sought to develop nonlinear systems analysis techniques capable of analyzing and predicting the complex behavior found in high-angle-of-attack flight. The primary research method involved calculation of equilibrium surfaces where the time rate of change of each of the state variables is set to zero in the aircraft equations of motion, and the states that will satisfy that condition are found for various control deflections. The equilibrium surfaces were calculated numerically through use of continuation methods. An equilibrium trajectory analysis of a fifth order model of the aircraft showed significant adverse yaw problems at high AOA as well as the presence of roll coupling. Bifurcational behavior was found in the same fifth order model and verified by previous research. A mechanism for transfer of kinetic energy during the catastrophic behavior shown is hypothesized. A spin equilibrium surface for the aircraft was determined from an eighth order model and, from that surface, possible control deflections for recovery from the spin were obtained. GRA

N87-10047# Nielsen Engineering and Research, Inc., Mountain View, Calif.
PREDICTION OF GUST LOADINGS AND ALLEVIATION AT TRANSONIC SPEEDS Final Report, 20 Sep. 1983 - 20 Jul. 1985
David Nixon and Keh L. Tzuoo Mar. 1986 43 p
(Contract N00167-83-C-0114)
(AD-A167748; NEAR-TR-352; DTNSRDC/ASED-CR-01-86) Avail: NTIS HC A03/MF A01 CSCL 20/4

The transonic indicial theory is used to predict the effect of a gust on an airfoil at transonic speeds. The effect of operating two control surfaces is also modeled by the indicial method. The transonic indicial method is linear in a strained coordinate system and superposition can be used. This allows the effects of an arbitrary gust and control surface deflection to be modeled simply if the indicial responses for the gust and each control surface are known. The computation time is small and, therefore, an optimization technique can be used to determine the best control surface deflections to alleviate the gust loading. GRA

N87-10048# Max-Planck-Institut fuer Stroemungsforschung, Goettingen (West Germany).
VORTEX SHEDDING OF A SQUARE CYLINDER IN FRONT OF A SLENDER AIRFOIL AT HIGH REYNOLDS NUMBERS. PART 1: SPACING EFFECT
Takeo Nakagawa, Gerd E. A. Meier, Rainer Timm, and Hans-M. Lent Oct. 1985 34 p Sponsored by Minna-James-Heinemann Foundation, Hannover, West Germany
(MPIS-23/1985; ISSN-0436-1199; ETN-86-98221) Avail: NTIS HC A03/MF A01; Fachinformationszentrum, Karlsruhe, West Germany DM 22

The spacing effect on vortex shedding of a square cylinder in front of a NACA 0018 airfoil at high Reynolds numbers was visualized in wind tunnel tests. When the free stream velocity is constant, the amplitude of the pressure fluctuations at a point in the test section is of comparable order irrespective of the spacing between a square cylinder and an airfoil. When the separating shear layers from the upstream square cylinder reattach to the downstream airfoil, the pressure signal is most regular and the vortex shedding frequency is minimum. The airfoil can stabilize the vortex shedding process behind the upstream square cylinder. The Strouhal number of the square cylinder depends upon the nondimensional spacing normalized by the characteristic length of the cylinder. Once the spacing between the square cylinder and the airfoil becomes greater than the critical value, the airfoil does not provide any significant effect on the vortex shedding process behind the upstream cylinder. ESA

N87-10049 Syracuse Univ., N. Y.
FAR FIELD NOISE STUDIES OF CONTOURED AND SOLID/POROUS CONICAL PLUG-NOZZLE JET FLOWS Ph.D. Thesis
Indu Shekher Das 1985 215 p
Avail: Univ. Microfilms Order No. DA8603754

The effectiveness of short porous/nonporous plug-nozzles in shock noise suppression of supersonic jet flows was examined. Experimental investigations of the far field noise characteristics are reported for model baseline convergent nozzle, contoured plug-nozzle and solid/porous conical plug-nozzles. Extensive shadowgraphic recordings of the jet flows are also presented to help understand the shock associated noise generation and suppression mechanisms in solid/porous plug-nozzle jets. The contoured plug-nozzle has been designed to give a shockless flow at the design Mach number 1.5. Noise suppression characteristics of such a contoured plug-nozzle presented herein, provide an ideal to be approached through the use of an optimised short conical plug-nozzle with/without porosity of the plug surface. Noise studies of such optimised solid/porous conical plug-nozzles are reported. All the test plug-nozzles have the same annual radius ratio 0.43 and the same throat area. Porosity of 10% distributed over the whole surface and porosity of 4% distributed over the middle-third of the conical plug surface have been investigated. Shadowgraphic records of the jet flows indicate that the presence of a solid contoured/conical plug results in favorable modifications of the repetitive shock structures in an otherwise convergent nozzle jet flow, and the porosity of the plug surface results in further weakening of the shock structure in the solid conical plug-nozzle jet flow. Dissert. Abstr.

N87-10050 Stanford Univ., Calif.
EXPERIMENTAL AND THEORETICAL INVESTIGATIONS OF THE FLOW FIELD OF AN AIRFOIL WITH A DEFLECTED SPOILER Ph.D. Thesis
Chyang Sheng Johnson Lee 1985 140 p
Avail: Univ. Microfilms Order No. DA8602499

Experimental and theoretical investigations were undertaken in the Stanford low-speed wind tunnel to study the flow fields of an airfoil with a deflected spoiler. The numerical simulations were performed by the two dimensional vortex tracing method. Surface pressure distributions, boundary layer and wake profiles were measured systematically to evaluate the effects of the airfoil incidence and spoiler deflection on the means and fluctuating quantities of the flow fields. The development of the wake with airfoil incidence is hypothesized by the variation of the base pressure. The location of the hinge bubble depends on the boundary layer characteristics. The wake is self-preserved if a virtual origin is introduced. A modified vortex tracing method is developed to simulate this unsteady flow field. The surface pressure distributions, mean velocity profiles and turbulent stresses in the wake, and Strouhal number are calculated and compared with the experimental results for various angles of attack and spoiler deflections. Good agreement between the computational predictions and experimental results is found for large spoiler deflections. However, the agreement is not as good for small spoiler deflections. The reason for this deviation is believed to be the strong viscous interaction of the counter rotating vortices in the near wake, which is not included in the present model. Dissert. Abstr.

N87-10051 Texas Univ., Austin.
UNSTEADY FLOW OVER AN AIRFOIL INSIDE A WIND TUNNEL WITH AND WITHOUT TRANSPIRATION Ph.D. Thesis
William John Tedeschi 1985 205 p
Avail: Univ. Microfilms Order No. DA8609435

This research uses the viscous/inviscid interaction model to calculate the lift and drag characteristics of a two-dimensional airfoil inside two types of wind tunnels. The first is a conventional solid-wall wind tunnel with an airfoil oscilllating transversely to the freestream. In the second wind tunnel, an unsteady transverse flow field is produced by a time-varying fluid transpiration of the wind tunnel walls. Subsonic flows in the one to five million Reynolds number range are considered. A computer code based on the theoretical model formulated in this study is used to predict the unsteady flow field around the airfoil. The nonlinear inviscid flow problem is solved analytically for the disturbance velocity potential using a unqiue for Fourier transform method. The bounded influence coefficients which explicitly contain the airfoil thickness distribution and wind tunnel geometry provide an advantage over traditional Panel methods. The viscous flow problem utilizes a finite-difference numerical formulation to solve the unsteady boundary layer equations. Dissert. Abstr.

N87-10052 Notre Dame Univ., Ind.
EXPERIMENTAL STUDY OF THE BOUNDARY LAYER ON A LOW REYNOLDS NUMBER AIRFOIL IN STEADY AND UNSTEADY FLOW Ph.D. Thesis
Michael Brendel 1986 413 p
Avail: Univ. Microfilms Order No. DA8612989

An experimental study of the boundary layer on a Wortman FX63-137 airfoil at a Reynolds number of 100,000 and several angles of attack was conducted for steady and unsteady incompressibile flow. Pressure distributions and single-element hot-wire boundary layer surveys were obtained. A significant portion of the work consisted of the design, fabrication, and testing of an unsteady flow facility. Additionally, the design of data acquisition and data processing techniques for unsteady flow experiments were investigated. A benchmark test was conducted to validate the techniques and the test facility by studying the response of a laminar boundary layer to a periodic unsteady freestream. Results were found to agree with existing analytical and experimental data. The same techniques were then employed in the study of the airfoil boundary layer. Characteristics of the pressure distributions, boundary layer velocity profiles, integrated boundary layer thicknesses, and shape parameters were documented. Criteria for locating laminar separation, transition, and reattachment were developed and compared with flow visualization. These criteria were used to study the behavior of the separation bubble in unsteady flow. Dissert. Abstr.

N87-10330*# Deutsche Forschungs- und Versuchsanstalt fuer Luft- und Raumfahrt, Wesseling (West Germany).
EXPERIMENTAL AND THEORETICAL DOPPLER-LIDAR SIGNATURES OF AIRCRAFT WAKE VORTICES
F. Koepp and W. A. Krichbaumer *In* NASA. Langley Research Center 13th International Laser Radar Conference Aug. 1986 3 p (For primary document see N87-10263 01-35)
Avail: NTIS HC A15/MF A01 CSCL 01A

03 AIR TRANSPORTATION AND SAFETY

Includes passenger and cargo air transport operations; and aircraft accidents.

For related information see also *16 Space Transportation* and *85 Urban Technology and Transportation.*

N87-10053# National Transportation Safety Board, Washington, D. C.
AIRCRAFT ACCIDENT REEPORT, DELTA AIR LINES, INC., LOCKHEED L-1011-385-1, N726DA, DALLAS/FORT WORTH INTERNATIONAL AIRPORT, TEXAS, AUGUST 2, 1985 Aircraft Accident Report, 2 Aug. 1985
15 Aug. 1986 169 p
(PB86-910406; NTSB/AAR-86/05) Avail: NTIS HC A08/MF A01

On August 2, 1985, at 1805:52 central daylight time, Delta Air Lines flight 191, a Lockheed L-1011-385-1, N726DA, crashed while approaching to land on runway 17L at the Dallas Fort Worth International Airport, Texas. While passing through the rain shaft beneath a thunderstorm flight 191 entered a microburst which the pilot was unable to traverse successfully. The airplane struck the ground about 6,300 feet north of the approach end of runway 17L, hit a car on a highway north of the runway killing the driver, struck two water tanks on the airport, and broke apart. Except for a section of the airplane containing the aft fuselage and empennage, the remainder of the airplane disintegrated during the impact sequence, and a severe fire erupted immediately. Of the 163 persons aboard, 134 passengers and crewmembers were killed, 24 passengers and 3 cabin attendants survived. The National Transportation Safety Board determines that the probable causes of the accident were the flightcrew's decision to initiate and continue the approach into a cumulonimbus cloud which they observed to contain visible lightning; the lack of specific guidelines, procedures, and training for avoiding and escaping from low-altitude wind shear; and the lack of definitive, real-time wind shear hazard information. This resulted in the aircraft's encounter at low altitude with a microburst-induced, severe wind shear from a rapidly developing thunderstorm located on the final approach course. Author

N87-10054*# National Aeronautics and Space Administration. Langley Research Center, Hampton, Va.
DOPPLER RADAR DETECTION OF WIND SHEAR
V. E. Delnore, Comp. (PRC Kentron, Inc., Hampton, Va.) and V. A. McClellan (Research Triangle Inst., Research Triangle Park, N.C.) Sep. 1985 118 p Presented at a Meeting, Hampton, Va., 24-25 Sep., 1985; sponsored in part by FAA
(NASA-CP-2435; NAS 1.55:2435; FAA/PM-86/31) Avail: NTIS HC A06/MF A01 CSCL 01C

In response to the Nation's needs for decreasing the threat of violent weather phenomena to aviation, a two-day meeting was held. This meeting, which brought together representatives from NASA, the Federal Aviation Administration, and the avionics industry, focused on the applicability of Doppler radar techniques to the detection of low-level wind shear. B.G.

N87-10055# Federal Aviation Administration, Atlantic City, N.J.
CRASHWORTHINESS EXPERIMENT SUMMARY FULL-SCALE TRANSPORT CONTROLLED IMPACT DEMONSTRATION PROGRAM Final Report
D. Johnson and L. Garodz Jun. 1986 629 p
(DOT/FAA/CT-85/20) Avail: NTIS HC A99/MF A01

On December 1, 1984, the Federal Aviation Adminstration (FAA), and NASA, conducted an air-to-ground impact test demonstration with a remotely piloted jet transport category aircraft. This demonstration, identified as the Full-Scale Transport Controlled Impact Demonstration (CID) Program, was the culmination of four years of effort by the two agencies. The major FAA objectives included the demonstration of antimisting fuel and a series of fire safety and structural type crashworthiness experiments. The NASA demonstrated objectives also extended to the crashworthiness experiment area. A summary of the FAA structural experiments is provided which included an instrumented fuselage structure and an associated analytical KRASH model, on-board seat/cabin restraint and flight data recorder system installations, and a post-impact accident investigation exercise. The summary contains a description of each experiment, related pre and post test activities, and resulting data. Author

N87-10056# National Transportation Safety Board, Washington, D. C. Bureau of Field Operations.
AIRCRAFT ACCIDENT REPORTS: BRIEF FORMAT US CIVIL AND FOREIGN AVIATION, ISSUE NUMBER 2 OF 1985 ACCIDENTS
7 May 1986 404 p
(PB86-916916; NTSB/AAB-86/16) Avail: NTIS HC A18/MF A01; also available on subscription, North American Continent HC $185.00/year; all others write for quote CSCL 01B

The publication contains selected aircraft accident reports in brief format occurring in U. S. civil and foreign aviation operations during calendar year 1985. Approximately 200 general aviatiion and air carrier accidents contained in the publication represent a random selection. The publication is issued irregularly, normally eighteen times each year. The brief format represents the facts, conditions, circumstances and probable cause(s) for each accident. GRA

04 AIRCRAFT COMMUNICATIONS AND NAVIGATION

Includes digital and voice communication with aircraft; air navigation systems (satellite and ground based); and air traffic control.

For related information see also *17 Space Communications, Spacecraft Communications, Command and Tracking* and *32 Communications and Radar.*

N87-10057 Southern Methodist Univ., Dallas, Tex.
A DECENTRALIZED FAULT-TOLERANT APPROACH TO ESTIMATION IN MULTI-SENSOR NAVIGATION SYSTEMS Ph.D. Thesis
Brian David Brumback 1985 139 p
Avail: Univ. Microfilms Order No. DA8604722

This investigation considers the problem of designing estimation algorithms for aided-inertial navigation in which both global accuracy and reliability in the presence of soft sensor failures is required. The approach is to correlate subsets of available sensor data to create multiple estimates of the aircraft navigation state. A two-ellipsoid overlap test is used to determine which local estimates agree and which disagree. Knowledge of the underlying sensor set then provides information to determine which estimates are correct, and which sensors have failed. The estimates that are based on the unfailed sensors are then combined to obtain the global estimate. Monte Carlo simulation results are presented for a system composed of two inertial navigation systems and a Doppler radar. The soft failure considered in this application is an accelerometer bias shift. False alarm and detection probabilities, mean detection-time, and the estimation error of the fault-tolerant system are determined numerically. It is shown that the fault-tolerant approach yields improved performance, compared to a global filter, in the presence of the soft failure. Dissert. Abstr.

N87-10058# Defense Mapping Agency Hydrographic and Topographic Center, Washington, D.C.
DMAHTC (DEFENSE MAPPING AGENCY HYDROGRAPHIC/TOPOGRAPHIC CENTER) GPS POINT POSITIONING SOFTWARE: INITIAL RESULTS Final Report
Theodore E. Meyer, George T. Tennis, James A. Slater, and Barbara J. DeNoyer 28 Apr. 1986 18 p Presented at the 4th International Geodetic Symposium on Satellite Positioning, Austin, Tex., 28 Apr. - 2 May 1986
(AD-A167566) Avail: NTIS HC A02/MF A01 CSCL 17/7

Absolute positioning software written at the Defense Mapping Agency Hydrographic/Topographic Center (DMAHTC) was designed to process Texas Instruments 4100 (TI 4100) geodetic receiver phase and range observations. This paper describes absolute positioning solutions obtained by processing data collected during the Spring 1985 High Precision Baseline Test. The positioning software can accept phase or range observations and treat them as either pseudoranges or range differences, thus allowing four different processing modes. The software estimates receiver position, scaling for the tropospheric correction, clock bias, drift, and aging parameters, and biases to the scaled phase measurement. Data from the Spring Baseline Test have been reduced and position offsets relative to given reference positions have been tabulated. Comparisons have been made between solutions computed using different ephemerides, processing methods, observation types, clock treatments, and initial station offsets. Means and standard deviations of the differences between the position solutions and the reference positions are presented. Results show that the positioning software is computationally stable but that significant day to day variations of the solution are present due to the data. Author (GRA)

N87-10059# Transportation Systems Center, Cambridge, Mass.
TERRESTRIAL EVALUATION OF THE GLOBAL POSITIONING SYSTEM (GPS) STANDARD POSITIONING SERVICE (SPS) Final Report, Jan. - Aug. 1985
F. W. Mooney, J. A. Stickler, R. Depaolis, and A. D. Frost Apr. 1986 64 p
(PB86-219599; DOT-TSC-RSPA-86-1) Avail: NTIS HC A04/MF A01 CSCL 17G

The results of static and navigation tests conducted in the Boston, Massachusetts area during the period of January through April 1985 and also in August 1985 were summarized. The objective of these tests was to gather data to determine the viability of the Global Positioning System (GPS), and Standard Positioning Service (SPS) as a stand alone terrestrial radionavigation reference. Companion LORAN-C data were obtained to provide an evaluation of comparative system performance. The study concludes the GPS cannot serve as a stand alone radionavigation system in urban environments characterized by multiple highrise buildings. In less hostile environments, GPS was observed to be an effective radionavigation system with position accuracies exceeding those obtained with LORAN-C. GRA

05 AIRCRAFT DESIGN, TESTING AND PERFORMANCE

Includes aircraft simulation technology.

For related information see also *18 Spacecraft Design, Testing and Performance* and *39 Structural Mechanics.* For land transportation vehicles see *85 Urban Technology and Transportation.*

N87-10060 Maryland Univ., College Park.
AEROELASTIC STABILITY OF COMPOSITE ROTOR BLADES IN HOVER Ph.D. Thesis
Chang Ho Hong 1985 144 p
Avail: Univ. Microfilms Order No. DA8608813

The aeroelastic stability of flap bending, lead-lag bending, and torsion of hingeless and bearingless composite blades in hover are investigated using a finite element theory based on Hamilton's principle. The hingeless blade is treated as a single cell laminated shell beam. Bearingless blade configuration is assumed as the one consisting of a single flexbeam with a wrap-around type torque tube and the pitch links located at the leading edge and the trailing edge of the torque tube. For analysis, the outboard main blade and the torque tube are assumed to be made of metals (isotroic materials), and the flexbeam is assumed to be a laminated I-section beam. The energy expressions and governing differential equations are derived for moderately large deflections. Quasisteady strip theory is used to evaluate the aerodynamic forces and the unsteady aerodynamic effects are introduced approximately through dynamic inflow modeling. Numerical results are calculated for the selected various hingeless and bearingless blade configurations, categorized as symmetric and antisymmetric, based on the lay-up in the laminates. For both the hingeless and bearingless blade configurations, systematic studies are made to identify the importance of the stiffness coupling terms on blade stability with changing fibers orientation and for different configurations. Dissert. Abstr.

N87-10061# Aeronautical Research Labs., Melbourne (Australia).
ANALYSIS OF THE VIBRATION OF THE INPUT BEVEL PINION IN RAN WESSEX HELICOPTER MAIN ROTOR GEARBOX WAK143 PRIOR TO FAILURE
P. D. McFadden Sep. 1985 51 p
(ARL-AERO-PROP-R-169; AR-004-049) Avail: NTIS HC A04/MF A01

Following the crash of an RAN Wessex helicopter caused by the catastrophic fatigue failure of the input spiral bevel pinion in the main rotor gearbox, routine recordings of the gearbox vibration have been analyzed by ARL. It has been shown that conventional spectral analysis of the vibration is unable to give adequate indication of the presence of the fatigue crack but that an alternative technique of vibration analysis called signal averaging can give warning of the crack 42 hours before failure. Enhancement of the signal average using a computer enables detection of the crack as early as 103 hours before failure. Author

N87-10062# National Aeronautical Lab., Bangalore (India). Systems Engineering Div.
EFFECTS OF FLAP POSITION ON LONGITUDINAL PARAMETERS OF HFB-320
R. V. Jategaonkar and S. Balakrishna Feb. 1986 77 p
(NAL-TM-SE-8602) Avail: NTIS HC A05/MF A01

Parameter estimation results to evaluate the effects of small changes in flap position on the longitudinal derivatives of HFB-320 aircraft are presented. Maximum likelihood estimation procedure is used for kinematic consistency checking of flight test data and also for estimation of aerodynamic derivatives. Linear and nonlinear models are used to estimate dimensional and non-dimensional derivatives directly. Author

N87-10063*# Florida Atlantic Univ., Boca Raton. Dept. of Mechanical Engineering.
TOWARD COMPARING EXPERIMENT AND THEORY FOR CORROBORATIVE RESEARCH ON HINGELESS ROTOR STABILITY IN FORWARD FLIGHT (AN EXPERIMENTAL AND ANALYTICAL INVESTIGATION OF ISOLATED ROTOR-FLAP-LAG STABILITY IN FORWARD FLIGHT) Annual Report
G. Gaonkar Aug. 1986 33 p Prepared for Army Aviation Research and Development Command, Moffett Field, Calif.
(Contract NCC2-361)
(NASA-CR-179711; NAS 1.26:179711) Avail: NTIS HC A03/MF A01 CSCL 01C

For flap-lag stability of isolated rotors, experimental and analytical investigations are conducted in hover and forward flight on the adequacy of a linear quasisteady aerodynamics theory with dynamic inflow. Forward flight effects on lag regressing mode are emphasized. Accordingly, a soft inplane hingeless rotor with three blades is tested at advance ratios as high as 0.55 and at shaft angles as high as 20 degrees. The 1.62 m model rotor is untrimmed with an essentially unrestricted tilt of the tip path plane. In combination with lag natural frequencies, collective pitch settings and flap-lag coupling parameters, the data base comprises nearly 1200 test points (damping and frequency) in forward flight and 200 test points in hover. By computerized symbolic manipulation, a linear analytical model is developed in substall to predict stability margins with mode identificaton. To help explain the correlation between theory and data it also predicts substall and stall regions of the rotor disk from equilibrium values. The correlation shows both the strengthts and weaknesses of the theory in substall. Author

N87-10064# Army Aviation Systems Command, St. Louis, Mo.
SUMMARY OF ARTIFICIAL AND NATURAL ICING TESTS CONDUCTED ON US ARMY AIRCRAFT FROM 1974 TO 1985 Final Report
Harry W. Chambers and John Y. Adams Jul. 1986 223 p
(Contract DTFA03-80-A-00199)
(FAA/CT-85/26; TR-85-F-11) Avail: NTIS HC A10/MF A01

The U.S. Army Aviation Systems Command conducts airworthiness qualification testing on aircraft under artificial and natural icing conditions. A JCH-47C helicopter with a Helicopter Icing Spray System (HISS) installed is used for generating a simulated natural icing environment. The artificial icing tests are followed by natural icing tests to assure a wide variety of flight conditions are tested and to verify artificial icing test results. Also discussed is the use of deice and anti-ice systems; the impact of ice accretion and shedding characteristics, performance considerations, stability and control, and vibration characteristics; and the cloud parameters measurement equipment and test aircraft instrumentation used for documenting test data. The test methodology and requirements used for qualifying aircraft for flight into icing conditions, instrumentation, and special equipment are summarized, and the details for tests conducted are contained in the references. The report documents in part 14 years of U.S. Army experience in conducting inflight aircraft icing tests and is provided to the FAA under interagency agreement in the preparation of manuals and other documents relative to the certification of civil aircraft as appropriate. Author

N87-10065*# General Dynamics Corp., Fort Worth, Tex.
DESIGN AND FABRICATION OF THE NASA DECOUPLER PYLON FOR THE F-16 AIRCRAFT Final Report, Jan. 1982 - Aug. 1983
J. D. Clayton, R. L. Haller, and J. M. Hassler, Jr. Jan. 1985 204 p
(Contract NAS1-16879)
(NASA-CR-172354; NAS 1.26:172354) Avail: NTIS HC A10/MF A01 CSCL 01C

The NASA Decoupler Pylon is a passive means of suppressing wing-store flutter. The feasibility of demonstrating this concept on the F-16 aircraft was established through model wind tunnel tests and analyses. As a result of these tests and studies a ship set of Decoupler Pylons was designed and fabricated for a flight test demonstration on the F-16 aircraft. Basic design criteria were developed during the analysis study pertaining to pylon pitch stiffness, alignment system requirements, and damping requirements. A design was developed which utilized an electrical motor for the pylon alignment system. The design uses a four pin, two link pivot design which results in a remote pivot located at the center of gravity of the store when the store is in the aligned position. The pitch spring was fabricated from a tapered constant stress cantilevered beam. The pylon has the same external lines as the existing production pylon and is designed to use a MAU-12 ejection rack which is the same as the one used with the production pylon. The detailed design and fabrication was supported with a complete ground test of the pylon prior to shipment to NASA. Author

N87-10066# Boeing Military Airplane Development, Seattle, Wash.
VULNERABILITY METHODOLOGY AND PROTECTIVE MEASURES FOR AIRCRAFT FIRE AND EXPLOSION HAZARDS. VOLUME 3: ON-BOARD INERT GAS GENERATOR SYSTEM (OBIGGS) STUDIES. PART 1: OBIGGS GROUND PERFORMANCE TESTS Final Report, Aug. 1982 -Jul. 1984
C. L. Anderson Jan. 1986 200 p
(Contract F33615-78-C-2063)
(AD-A167357; D180-28862-Vol-3-Pt-1; AFWAL-TR-85-2060-V-3-Pt-1) Avail: NTIS HC A09/MF A01 CSCL 01/3

Results of performance evaluation tests of a molecular sieve (MSIGG) and a permeable membrane inert gas generator (PMIGG) system for airplane fuel tank inerting are presented. The IGG units, sized to inert the wing tanks of a KC-135, and the test facilities at Wright-Patterson AFB are described. Steady state performance envelope, endurance, and KC-135 mission simulation tests are conducted. The weight and fuel penalties of the MSIGG and the PMIGG installed in a KC-135 are compared. GRA

N87-10067# Advisory Group for Aerospace Research and Development, Neuilly-Sur-Seine (France). Propulsion and Energetics Panel.
ENGINE-AIRFRAME INTEGRATION FOR ROTORCRAFT
Loughton, England May 1986 154 p Lecture Series held in St. Louis, Mo., 2-3 Jun. 1986, in Rome, Italy, 9-10 Jun. 1986, and in Marseilles, France, 12-13 Jun. 1986
(AGARD-LS-148; ISBN-92-835-1529-3) Avail: NTIS HC A08/MF A01

Topics addressed include numerous airframe integration aspects relating to rotor wing aircraft. Various areas of engine airframe integration, including the impact of advanced engine design variables to specific propulsion subsystems, will be discussed. Other propulsion system integration aspects such as engine/rotor/drive system torsional stability and transient response will also be discussed. Additional areas considering the specification and qualification requirements of propulsion items will be examined. For individual titles, see N87-10068 through N87-10074.

N87-10068# Sikorsky Aircraft, Stratford, Conn. Propulsion Systems.
ENGINE-AIRFRAME INTEGRATION CONSIDERATIONS FOR PRELIMINARY AIR VEHICLE PERFORMANCE ANALYSIS
R. C. Frawley and H. N. Shohet *In* AGARD Engine-Airframe

Integration for Rotorcraft May 1986 21 p (For primary document see N87-10067 01-05)
Avail: NTIS HC A08/MF A01

Helicopter engine/airframe integration issues are examined from a preliminary design viewpoint with emphasis on those areas where an impact on aircraft power available and/or aerodynamics is involved. The areas of the helicopter propulsion system specifically addressed include: the engine air induction system considering aerodynamic performance, anti-icing, exhaust gas re-ingestion, and inlet particle separation; the engine exhaust system considering aerodynamic performance, engine compartment cooling, and exhaust ejector system; and lastly, engine bleed air extraction as it relates to environmental control systems and the trade studies associated with same. These subsystems are discussed in terms of basic design guidelines, interaction with other helicopter subsystems, system trade studies, and first order analytical design approaches adequate for preliminary design purposes. Author

N87-10069# Pisa Univ. (Italy). Dipt. de Energetica.
ENGINE-TRANSMISSION-STRUCTURAL AIRFRAME MEMBERS COMPATIBILITY
Dino Dini *In* AGARD Engine-Airframe Integration for Rotorcraft May 1986 33 p (For primary document see N87-10067 01-05)
Avail: NTIS HC A08/MF A01

The sophistication of current turbine-powered helicopters have introduced many new problems involving the compatibility of the major multidegree of freedom systems: rotor, control, airframe, drive train, and powerplant. The solutions to the various problems were obtained from the application of basic engineering principles. Engine installation is described in the helicopter, particularly the A-129, i.e., power plant attachment, oil cooling system, engine control and monitoring, electric starting system, location of components and leading particulars, and anti-vibration devices. The design of the transmission system is dictated by the configuration of the helicopter. An aerodynamic analysis is conducted on the helicopter mission in order to obtain complete spectra of the rotor loads and moments as well as the maneuver loads and transient for maximum transmission reliability. The application of fiber reinforced resin composites to selected areas of the helicopter drive system will produce weight and cost savings as well as improvements in reliability and safety. These improvements which were demonstrated in airframe applications can be transferred to structural components in the drive system, with high weight saving. Author

N87-10070# Rolls-Royce Ltd., Watford (England).
IMPACT OF IPS AND IRS CONFIGURATIONS ON ENGINE INSTALLATION DESIGN
J. R. Ballard *In* AGARD Engine-Airframe Integration for Rotorcraft May 1986 14 p (For primary document see N87-10067 01-05)
Avail: NTIS HC A08/MF A01

Helicopters operate in a variety of roles many of which pose severe problems to the engine due to ingestion of sand, ice, salt, and other foreign objects. It is possible to design a compromise engine intake which combats all these hazards to a limited degree. Engine design should be coordinated with both engine and airframe mounted separator performance characteristics to ensure that optimized designs can be offered to customers with very different operational requirements. A design method was outlined which would allow the erosion reduction characteristics of engine and airframe Intake Protection System (IPS) designs to be taken into account during engine design. The Infrared Suppression (IRS) designs can be integrated with IPS scavenge requirements to produce a low signature engine installation. B.G.

N87-10071# Army Aviation Systems Command, St. Louis, Mo. Engineering Dept.
ENGINE-AIRFRAME INTEGRATION FOR ROTORCRAFT: COMPONENT SPECIFICATIONS AND QUALIFICATION
James A. Ray *In* AGARD Engine-Airframe Integration for Rotorcraft May 1986 10 p (For primary document see N87-10067 01-05)
Avail: NTIS HC A08/MF A01

Both past history and current principles associated with engine-airframe integration for rotorcraft are provided as related to component specification requirements and their individual qualification assurance. Component specification and qualification requirements have tended to be generic and standardized without consideration of actual usage, location, and exposure. As such, overall requirements have had problems of being overly restrictive in some cases and not exacting enough in others. The current trend in tailoring for specific applications as well as insuring system performance requirements by conducting early component/bench level tests will be discussed along with lessons learned from past efforts. Components involved in the overall engine-airframe integration effort such as pumps, fans, starter, valves, sensors, infrared suppressors, inlet particle separators, and fuel cells will be discussed. Author

N87-10072# Garrett Turbine Engine Co., Phoenix, Ariz.
INFLUENCE OF ENGINE VARIABLES ON FUTURE HELICOPTER SYSTEMS
Michael L. Early and Peter K. Zeiner *In* AGARD Engine-Airframe Integration for Rotorcraft May 1986 24 p (For primary document see N87-10067 01-05)
Avail: NTIS HC A08/MF A01

A helicopter system defined for the year 2000 must make numerous assumptions about future technology and system requirements. In the case of propulsion system options, the required 5 to 15 year development cycle (from preliminary engine cycle studies through engine development to production) complicates the process of optimizing the engine/rotorcraft system. A well-disciplined approach to engine definiton studies to yield engine candidates that best use emerging technologies is illustrated. An advanced, single-engine helicopter requiring a 2000-shp powerplant was used a a base-line vehicle. Both simple and heat-recovery cycles were evaluated, using trade factors to establish engine effects on helicopter direct operating cost (DOC), the optimization parameter assumed for purposes of illustration. Author

N87-10073# Societe Nationale Industrielle Aerospatiale, Marignane (France). Helicopter Div.
HELICOPTER AIR INTAKE PROTECTION SYSTEMS
X. DelaServette and P. Cabrit *In* AGARD Engine-Airframe Integration for Rotorcraft May 1986 20 p (For primary document see N87-10067 01-05)
Avail: NTIS HC A08/MF A01

The primary function of an engine air intake is to provide air supply with minimum pressure drop and distortion. Static or dynamic air intakes are selected according to both the type of engine air intake and the helicopter missions envisaged. The other function of an engine air intake is to protect the engine against foreign object ingestion, sand erosion, and the various atmospheric agents such as rain, snow, and ice. As a general rule, the air intake protection systems are all the more penalizing as regards performance as they are efficient. The best tradeoff is therefore between both functions. The dimensioning and test criteria for each function of an air intake is examined and then the various development stages are given for the SA 366 G1 Dauphin air intake as an example. Author

N87-10074# Army Aviation Systems Command, St. Louis, Mo. Engineering Dept.
ENGINE-AIRFRAME INTEGRATION FOR ROTORCRAFT: SYSTEM SPECIFICATIONS AND QUALIFICATION
James A. Ray *In* AGARD Engine-Airframe Integration for Rotorcraft May 1986 10 p (For primary document see N87-10067 01-05)
Avail: NTIS HC A08/MF A01

Both past history and current principles associated with engine-airframe integration for rotorcraft are provided as related to system specification requirements and the resulting qualification assurance. System specification requirements have evolved through periods of few details and lack of definitive requirements to the opposite extreme of exacting details and extremely specific requirements. The current trend of performance related specifications is intended to enhance the freedom of design while meeting the essential mission related requirements. This has required a revised qualification program effort to insure essential requirements are being met throughout the develpment effort. Lessons learned in this evaluation as well as current methods will be discussed for overall engine-airframe integration system requirement. In particular, system qualification will be addressed for such areas as adverse environment requirements for icing, cold/hot temperatures and sand/dust; mission related requirements for engine response, infrared signature reduction, and crashworthiness; and basic engine integration requirements for torsional stability, vibration, and cooling. Author

06 AIRCRAFT INSTRUMENTATION

Includes cockpit and cabin display devices; and flight instruments.

For related information see also *19 Spacecraft Instrumentation* and *35 Instrumentation and Photography.*

N87-10075# Deutsche Forschungs- und Versuchsanstalt fuer Luft- und Raumfahrt, Brunswick (West Germany). Inst. fuer Flugfuehrung.

PROCEEDINGS OF THE 13TH SYMPOSIUM ON AIRCRAFT INTEGRATED DATA SYSTEMS

Feb. 1986 586 p Symposium held in Hamburg, West Germany, 17-19 Sep. 1985
(DFVLR-Mitt-86-04; ISSN-0176-7739; ETN-86-98176) Avail: NTIS HC A25/MF A01; DFVLR, Cologne, West Germany, DM 150

The application of aircraft integrated data systems for monitoring and recording flight and aircraft condition and performance, to improve safety, reliability, and economy of aircraft operation was discussed. For individual titles, see N87-10076 through N87-10099.

N87-10076# Messerschmitt-Boelkow-Blohm G.m.b.H., Hamburg (West Germany).

A-310 AIRCRAFT INTEGRATED DATA SYSTEMS (AIDS) DESIGN PHILOSOPHY

H. Kalbe *In* DFVLR Proceedings of the 13th Symposium on Aircraft Integrated Data Systems Feb. 1986 p 9-28 (For primary document see N87-10075 01-06)
Avail: NTIS HC A25/MF A01; DFVLR, Cologne, West Germany, DM 150

The A-310 air data system customer requirements and integration problems were examined. The repercussions of these aspects on the system architecture are discussed, and a solution which covers the problems is presented. ESA

N87-10077# Hamilton Standard, Farmington, Conn.

AIRCRAFT INTEGRATED DATA SYSTEMS (AIDS): EVOLUTION AND REVOLUTION

C. F. Bukowski *In* DFVLR Proceedings of the 13th Symposium on Aircraft Integrated Data Systems Feb. 1986 p 29-45 (For primary document see N87-10075 01-06)
Avail: NTIS HC A25/MF A01; DFVLR, Cologne, West Germany, DM 150

Development of aircraft integrated data systems (AIDS) from 1970 to the present is discussed. User desirable features are considered. Present and perceived AIDS integration/relationships with other aircraft systems, and the tools and resources necessary for implementation are treated. ESA

N87-10078# Nord-Micro Elektronic Feinmechanik G.m.b.H., Frankfort (West Germany).

MODERN AIRCRAFT INTEGRATED DATA SYSTEMS (AIDS) TECHNOLOGY EXEMPLIFIED ON THE A-320

D. Waldmann and K. Wnuk *In* DFVLR Proceedings of the 13th Symposium on Aircraft Integrated Data Systems Feb. 1986 p 47-74 (For primary document see N87-10075 01-06)
Avail: NTIS HC A25/MF A01; DFVLR, Cologne, West Germany, DM 150

The hardware design, software organization, and data processing of the flight data interface unit (FDIU) and the data management unit (DMU) for the A-320 aircraft are described. The DMU and FDIU provide high flexibility and expansion capability to keep pace with airline requirements. For example, the units are equipped with EEPROM's of size 8 k by 8, but footprint, wiring, and memory management are provided for memory chips with higher capacity. In the DMU prewired spare board slots are provided for future air data system applications as there is the supervision of the structural health of aircraft components. Technologies like gate arrays and surface mounted devices are used so that the equipment shows important reduction in physical size, weight, and power consumption compared to the predecessor. ESA

N87-10079# Messerschmitt-Boelkow-Blohm G.m.b.H., Ottobrunn (West Germany).

EXPERIENCE WITH THE ONBOARD CHECKOUT AND MONITORING SYSTEM (OCAMS) OF A MILITARY AIRCRAFT RESULTING IMPROVEMENTS AND THE CONSEQUENCE FOR FUTURE DESIGN

K. Numberger and K. Probst *In* DFVLR Proceedings of the 13th Symposium on Aircraft Integrated Data Systems Feb. 1986 p 75-92 (For primary document see N87-10075 01-06)
Avail: NTIS HC A25/MF A01; DFVLR, Cologne, West Germany, DM 150

The Onboard Checkout and Monitoring System was designed to provide for test and diagnosis of defects to avionic and certain nonavionic equipments. Experience showed what could be improved. Engine and structure monitoring must be improved, still more information would be useful to store, and it was realized that the high sensitivity of the BIT detected also very transient faults. In order to cover these problems, the data acquisition unit of the crash recorder system will be extended with an engine and structural life monitoring system. Using the opportunity of introducing a data communication bus into the avionic system, facilities for data collection, correlation, and event monitoring will be initiated. Based on this the principal structure of the monitoring and test systems of future aircraft can be designed. ESA

N87-10080# Plessey Co. Ltd., Havant (England).

INTEGRATED MONITORING SYSTEMS FOR TACTICAL AIRCRAFT

P. J. D. Bristowe and R. L. Thompson *In* DFVLR Proceedings of the 13th Symposium on Aircraft Integrated Data Systems Feb. 1986 p 93-124 (For primary document see N87-10075 01-06)
Avail: NTIS HC A25/MF A01; DFVLR, Cologne, West Germany, DM 150

An aircraft integrated monitoring system integrating previously stand alone avionic boxes in military aircraft, with consequent savings in equipment cost, weight, and volume is described. The crash-protected accident data recorder combines digital data recordings with 3 channels of voice. The data acquisition and processing unit combines the acquisition of accident data, and engine and structural parameters with the real-time implementation of engine and structural algorithms to determine component fatigue life. Other facilities include parameter exceedance monitoring, trend monitoring and event snapshots with simple latched displays for maintenance purposes. ESA

N87-10081# Civil Aviation Authority, Redhill (England). Airworthiness Div.

APPLICATION OF OPERATIONAL FLIGHT RECORDING TO HELICOPTERS

H. D. Ruben *In* DFVLR Proceedings of the 13th Symposium on Aircraft Integrated Data Systems Feb. 1986 p 125-138 (For primary document see N87-10075 01-06)
Avail: NTIS HC A25/MF A01; DFVLR, Cologne, West Germany, DM 150

Operational flight data recording tests were carried using helicopters. One helicopter carries a data recorder running continuously, and a second helicopter of a different type is being similarly equipped. The objective of the exercise is to establish real time utilization of the helicopter so that design assumptions, particularly with respect to fatigue, can be validated. It is too early to draw conclusions. ESA

N87-10082# Societe de Fabrication d'Instruments de Mesure, Massy (France).

THE AIRBORNE INTEGRATED DATA SYSTEM (AIDS) FOR THE AIRBUS A-310 ENGINE CONDITION MONITORING

C. Jouvenot *In* DFVLR Proceedings of the 13th Symposium on Aircraft Integrated Data Systems Feb. 1986 p 139-160 (For primary document see N87-10075 01-06)

Avail: NTIS HC A25/MF A01; DFVLR, Cologne, West Germany, DM 150

The A-310 aircraft integrated data system (AIDS) is developed in a single six modular common unit combining flight data acquisition unit and Data Management Unit (DMU) with no possible interaction between the two units. The system is controlled through a Central Data Unit (CDU) and programmed through a removable electrical module plugged in the CDU. A mass memory stores the data for immediate use after the flight. Outputs of DMU are to printer and digital AIDS recorder. Long term analysis reports for engine monitoring are engine cruise, and engine take-off trend reports as well as auxiliary power unit report. Short term analysis is done through engine real time, engine gas path limit exceedance, engine stall, engine divergence, engine start, and engine mechanical limit exceedance report. A prehistory of the data is printed or recorded after the report of the exceeded limit. ESA

N87-10083# British Airways, Heathrow (England).

CHOOSING AIRCRAFT INTEGRATED DATA SYSTEMS (AIDS) ARCHITECTURE SUITABLE FOR ENGINE HEALTH MONITORING (EHM) ON FUTURE GENERATION ENGINES

Donald E. Foxley *In* DFVLR Proceedings of the 13 Symposium on Aircraft Integrated Data Systems Feb. 1986 p 161-176 (For primary document see N87-10075 01-06)

Avail: NTIS HC A25/MF A01; DFVLR, Cologne, West Germany, DM 150

Airborne engine monitoring system architectures including air and ground elements are assessed. It is very desirable to perform the analysis function in the airborne computer, but it requires considerable effort to achieve, and it is probably unrealistic to expect an engine manufacturer to provide such a system to a diversity of airlines, many of whom do not wish to utilize it. What is important is that what they provide should not preclude incorporating it in an airborne computer. The approach for the V2500 engine is to provide only an analysis module and a plot module, leaving the airline to embed these into their system, whether it be a mainframe or dedicated one. Important interfaces such as file structure have not yet been defined. Even so, it is clear their system will need a mainframe or large minicomputer to run on, so perhaps the ultimate in transportable software will have to wait for another generation of equipment. ESA

N87-10084# Deutsche Lufthansa A.G., Hamburg (West Germany). Power Plant Engineering Div.

LUFTHANSA'S AIRCRAFT INTEGRATED DATA SYSTEMS (AIDS) BASED A-310 ENGINE CONDITION MONITORING SYSTEM: PROGRESS ACHIEVED BETWEEN THE 12TH AND 13TH AIDS SYMPOSIUMS

G. Dienger *In* DFVLR Proceedings of the 13th Symposium on Aircraft Integrated Data Systems Feb. 1986 p 177-205 (For primary document see N87-10075 01-06)

Avail: NTIS HC A25/MF A01; DFVLR, Cologne, West Germany, DM 150

The A-310 aircraft integrated data system which acquires, monitors, records, and prints data for aircraft/engine condition monitoring and trouble shooting is discussed. The data is fed-in and processed on-line by a comprehensive ground based diagnosis information system. Operational experience based on regular and ad hoc system reports, and development status are described. ESA

N87-10085# Philips Zentrallaboratorium G.m.b.H., Hamburg (West Germany).

A SYSTEM THEORETICAL BASED METHOD FOR MODULE FAILURE DIAGNOSTIC OF TURBINE ENGINES c07

M. Roesnick *In* DFVLR Proceedings of the 13th Symposium on Aircraft Integrated Data Systems Feb. 1986 p 207-233 (For primary document see N87-10075 01-06)

Avail: NTIS HC A25/MF A01; DFVLR, Cologne, West Germany, DM 150

A method for module failure diagnostic of turbine engines based on gas path analysis is presented. An effective failure diagnostic of all main modules is possible by a system theoretical based method. The basis of the method is a reduced model, gained by a degree of observability. The application of the state estimation and analytical redundancy guarantees that the failure diagnostic method is applicable even if the measurements are disturbed by random and systematic errors. Simulation results of the JT9D engine are presented. ESA

N87-10086# Technische Hochschule, Aachen (West Germany). Dept. of Aerospace Engineering.

WIND SHEAR MEASUREMENT ON BOARD A MORANE 893

H. Nelles *In* DFVLR Proceedings of the 13th Symposium on Aircraft Integrated Data Systems Feb. 1986 p 235-266 (For primary document see N87-10075 01-06)

Avail: NTIS HC A25/MF A01; DFVLR, Cologne, West Germany, DM 150

To investigate wind shear during flight, a pneumatic sensing device was developed and installed on board a single engine light aircraft. The device measures the difference in total pressure between two positions vertically displaced from the airplane. The mass flow rate created by the difference in pressure is measured by a hot-wire probe. The signal of this probe is a function of the wind shear. Results collected by this system compare favorably with those of a ground based sensing system and of a research aircraft. ESA

N87-10087# Deutsche Forschungs- und Versuchsanstalt fuer Luft- und Raumfahrt, Brunswick (West Germany). Forschungszentrum.

PERFORMANCE MONITORING OF SENSORS IN HIGH RELIABLE FLIGHT CONTROL SYSTEMS USING DETERMINISTIC OBSERVERS

Norbert Stuckenberg *In its* Proceedings of the 13th Symposium on Aircraft Integrated Data Systems Feb. 1986 p 261-284 (For primary document see N87-10075 01-06)

Avail: NTIS HC A25/MF A01; DFVLR, Cologne, West Germany, DM 150

The output vector of a sensor set used in a flight control system of a transport aircraft was monitored by an observer. Since the observer includes a mathematical model of the aircraft, dynamic deviations in the sensor performance due to failures can be detected. This idea is used in a sensor concept which achieves a high reliability with less sensor hardware than conventional redundancy concepts. Flight test results show the feasibility of the concept under the constraint of disturbances and model inaccuracies. ESA

N87-10088# Flight Data Co., London (England).

THE IMPACT OF FLIGHT DATA ON AN AIRLINE: A CASE STUDY

P. Waller *In* DFVLR Proceedings of the 13th Symposium on Aircraft Integrated Data Systems Feb. 1986 p 285-307 (For primary document see N87-10075 01-06)

Avail: NTIS HC A25/MF A01; DFVLR, Cologne, West Germany, DM 150

A medium size airline acquired a flight data recorder playback and analysis facility for three aircraft fleets. The effects on the user department are examined in relation to system accessibility. Analysis program developments resulting from the user becoming more aware of the possibilities are presented. Comparisons between this new user airline and others that have exploited flight recorder data over many years are drawn. ESA

N87-10089# Sundstrand Data Control, Inc., Redmond, Wash. Avionics System Div.
DATA RECOVERY TECHNIQUES, AN UPDATE
G. S. L. Benn *In* DFVLR Proceedings of the 13th Symposium on Aircraft Integrated Data Systems Feb. 1986 p 309-328 (For primary document see N87-10075 01-06)
Avail: NTIS HC A25/MF A01; DFVLR, Cologne, West Germany, DM 150

Innovations in flight data recovery techniques are reviewed. Data presentation methods designed to offer the data specialist rapid acess and greater understanding of data are included. Hardware used to manipulate data, and use of personal computers to access and examine flight recorded information are described. Techniques resulting from improvements in flight and ground hardware and application software are proposed, including the use of artificial intelligence and three dimensional display technology. ESA

N87-10090# Deutsche Lufthansa Aktiengesellschaft, Frankfurt am Main (West Germany). Abteilung Flugbetriebstechnik.
SOFTWARE FOR FLIGHT RECORDER DATA PROCESSING DEVELOPED BY LUFTHANSA
Hans-Armin Kaiser *In* DFVLR Proceedings of the 13th Symposium on Aircraft Integrated Data Systems Feb. 1986 p 329-348 (For primary document see N87-10075 01-06)
Avail: NTIS HC A25/MF A01; DFVLR, Cologne, West Germany, DM 150

Computer software to evaluate flight recorder data is described. Software to transcribe raw data to magnetic tape, to perform quality checks of the recorded data, to evaluate selectable parameters and their subsequent graphical display, and to display aircraft movement three dimensionally is available. ESA

N87-10091# Eurocontrol Agency, Brussels (Belgium).
THE AIR/GROUND TRANSFER OF AIRCRAFT INTEGRATED DATA SYSTEMS (AIDS) FOR AIR TRAFFIC CONTROL (ATC) PURPOSES: PRESENT EXPERIMENTS AND POSSIBLE FUTURE INTENTIONS
M. E. Cox *In* DFVLR Proceedings of the 13th Symposium on Aircraft Integrated Data Systems Feb. 1986 p 349-372 (For primary document see N87-10075 01-06)
Avail: NTIS HC A25/MF A01; DFVLR, Cologne, West Germany, DM 150

Use of SSR Mode S links for air traffic control (ATC) is discussed. Experiments indicate that data derived from aircraft in real time via the Mode S link can be very helpful in ATC related applications, including the enhancement of short-term meteorological forecast data. The work shows that digital aircraft can provide a range of potentially useful parameters that can be accessed via an ARINC 429 data port associated with the flight data acquisition system. It is believed that European ATC system requirements for aircraft data will expand rapidly with the implementation of Mode S, in the mid 1990's. By that date, however, there are likely to be applications which have yet to be evaluated to support dependent surveillance and approach and departure control. There may also be air/ground data channels, e.g., ACARS, ASDAR plus other satellite systems stemming from the PROSAT experiments. ESA

N87-10092# Trans World Airlines, Inc., Kansas City, Mo.
AIRLINE DATA ACQUISITION IN AN ACARS ENVIRONMENT
Todd R. Degner *In* DFVLR Proceedings of te 13th Symposium on Aircraft Integrated Data Systems Feb. 1986 p 373-390 (For primary document see N87-10075 01-06)
Avail: NTIS HC A25/MF A01; DFVLR, Cologne, West Germany, DM 150

The data acquisition system on TWA aircraft is described. It combines a tape-based system and an ACARS-based system. The tape-based system is plagued by low reliability, large data volume, long delays between events and analysis, and poor flexibility. An ACARS only system will allow removal of the airborne tape recorders and ground tape transmission units. The ACARS-based system allows real-time on-line data collection. This provides the user with a high-integrity system with great flexibility. The system design is being driven by user needs and the expected benefits. ESA

N87-10093# National Transportation Safety Board, Washington, D. C.
FLIGHT RECORDERS: NEW US REGULATIONS AND NEW INTERNATIONAL CIVIL AVIATION ORGANIZATION (ICAO) STANDARDS
C. A. Roberts and D. R. Grossi *In* DFVLR Proceedings of the 13th Symposium on Aircraft Integrated Data Systems Feb. 1986 p 391-417 (For primary document see N87-10075 01-06)
Avail: NTIS HC A25/MF A01; DFVLR, Cologne, West Germany, DM 150

On January 8, 1985, the U.S. Federal Aviation Administration issued a Notice of Proposed Rulemaking regarding improved flight recorders. It called for: expanded-parameter digital recorders on new air carrier airplanes manufactured 2 yr after the rule is adopted, regardless of the date of original type certificate; digital recorders to replace foil recorders within 2 yr of the rule change, and 5 additional parameters within 7 yr; and voice recorders on certain commuter airplanes. The International Civil Aviation Organization (ICAO) recorder amendments were adopted in March 1985, and became effective on July 29, 1985. The upgraded U.S. recorder requirements and the ICAO amendments are assessed. ESA

N87-10094# Lear Siegler, Inc., Grand Rapids, Mich. Instrument Div.
DATA COMPRESSION TECHNIQUES FOR MULTIFUNCTION FLIGHT DATA RECORDERS
F. Saggio, III *In* DFVLR Proceedings of the 13th Symposium on Aircraft Integrated Data Systems Feb. 1986 p 419-443 (For primary document see N87-10075 01-06)
Avail: NTIS HC A25/MF A01; DFVLR, Cologne, West Germany, DM 150

Basic principles of data compression systems are discussed, emphasizing multifunction flight data recording applications. The categorization of data compression methods is discussed, and reversible and irreversible compression techniques are described. Algorithm selection and development, and optimization of data labeling and formatting techniques are considered. Data decompression principles are introduced, and multifunction flight data recording applications which embody data compression techniques are highlighted. By using the spare computing capability of the onboard microprocessor, more functions may be added, or new applications may be possible. ESA

N87-10095# Fairchild Weston Systems, Inc., Sarasota, Fla.
THE FAIRCHILD CVDR: A NEW COMBINATION VOICE AND DATA RECORDER
Hans F. Napfel and Barry J. Hawkins *In* DFVLR Proceedings of the 13th Symposium on Aircraft Integrated Data Systems Feb. 1986 p 445-474 (For primary document see N87-10075 01-06)
Avail: NTIS HC A25/MF A01; DFVLR, Cologne, West Germany, DM 150

The Fairchild cockpit voice and data recorder developed to meet the SAE Aerospace Standard 8039 for Type 3 recorders for general aviation is described. It is designed to meet or exceed TSO C-51a and DO160B environment and survivability requirements. It records data and voice simultaneously. Calibration data and time are stored on recording medium for life for later data verification. Microprocessor circuitry provides exceptional flexibility and reliability of data storage. It features automatic test of voice recorder function at power-up and continuous verification of flight data recording function during operation. No manual testing is required. It uses internal GMT for data/voice correlation. The tape stops automatically after detection of nonflying status. It has complete ARINC 542 and ARINC 542 expanded parameter compatibility. It records last 33 min of each flight for voice and data, and last 8 hr of excerpted data for previous flight correlation. ESA

N87-10096# Federal Aviation Administration, Atlantic City, N.J.
THE BOEING B 720 AIRCRAFT CONTROLLED IMPACT DEMONSTRATION (CID): FLIGHT DATA RECORDER/COCKPIT VOICE RECORDER EXPERIMENT
Leo J. Garodz and Graham G. LeRoy (Lockheed Aircraft Service, Inc., Ontario, Calif.) *In* DFVLR Proceedings of the 13th Symposium on Aircraft Integrated Data Systems Feb. 1986 p 475-507 (For primary document see N87-10075 01-06)
(Contract DOT/FAA/CT-85/28P)
Avail: NTIS HC A25/MF A01; DFVLR, Cologne, West Germany, DM 150

A controlled crash was used to evaluate the adequacy and usefulness of state-of-the-art Flight Data Recorder (FDR) and Cockpit Voice Recorder (CVR) recorded data in postcrash aircraft accident investigation and analysis, particularly in human factors/crashworthiness. The crash shows a gross design deficiency in TSO-C51a specification, regarding recorder performance when recording data under relatively low g-loads, well within human tolerance limits, which may be experienced in unusual attitude flight. The experiment reveals that sampling rates are too low for certain aircraft performance parameter signals, particularly aircraft linear accelerations and pitch and roll attitude. Either the sampling rates should be increased or the attitude information pitch rate and roll-rate signals should be recorded. It is proved that a separate power supply (battery pack and static inverter) can properly operate an FDAU and three DFDR's even after basic aircraft electrical power is no longer available. ESA

N87-10097# Naval Air Test Center, Patuxent River, Md.
UNITED STATES NAVY - CANADIAN FORCES SOLID STATE FLIGHT DATA RECORDER/CRASH POSITION LOCATOR EXPERIMENT ON THE B-720 CONTROLLED IMPACT DEMONSTRATION
D. M. Watters *In* DFVLR Proceedings of the 13th Symposium on Aircraft Integrated Data Systems Feb. 1986 p 509-530 (For primary document see N87-10075 01-06)
Avail: NTIS HC A25/MF A01; DFVLR, Cologne, West Germany, DM 150

A solid state flight data recorder/crash position locator (SSFDR/CPL) was developed, configured for and crash tested in the FAA/NASA Boeing B-720. The SSFDR/CPL system contains nonvolatile memory and a CPL radio beacon airfoil. The CPL/RBA provides a selectable overt and covert locating capability. The SSFDR/CPL was ejected from the B-720 upon crash and radiated the overt emergency signals for 5 to 10 sec before silenced by a fuel induced short in the transmitter. The SSFDR was subjected to the worst case fuel fire from the crash, but no data were lost. ESA

N87-10098# Deutsche Forschungs- und Versuchsanstalt fuer Luft- und Raumfahrt, Brunswick (West Germany). Inst. fuer Flugmechanik.
COMPARATIVE EVALUATION OF REDUNDANT FLIGHT DATA RECORDED BY A DIGITAL AIRCRAFT INTEGRATED DATA SYSTEM RECORDER (DAR) ON BOARD AN AIRBUS A-310 AIRCRAFT
O. Weber and G. Rosenau *In its* Proceedings of the 13th Symposium on Aircraft Integrated Data Systems Feb. 1986 p 531-567 (For primary document see N87-10075 01-06)
Avail: NTIS HC A25/MF A01; DFVLR, Cologne, West Germany, DM 150

Flight data collected during two A-310 flights by a digital AIDS recorder were analyzed. Sixty-four standard data words and 137 data words which could be selected from the ARINC 429 bus as desired were recorded per second. From a flight-mechanical standpoint, redundant data from different sources are analyzed for take-off, landing, and en route. The characteristics of the standard A-310 AIDS are compared to those of the A-300 AIDS and the potential benefit of additional data to a reliable reconstruction of a flight is shown. The reconstruction of the motion state of the aircraft is more complete than with the older equipment; a completely satisfactory reconstruction of the flying motion, however, is not possible in cases where measured values of the flow angles are required. ESA

N87-10099# Technische Univ., Brunswick (West Germany).
INVESTIGATIONS ON A DIGITAL BIT SYNCHRONIZER FOR A DETAILED FLIGHT DATA RECOVERY
H.-D. vonLaue *In* DFVLR Proceedings of the 13th Symposium on Aircraft Integrated Data Systems Feb. 1986 p 569-584 (For primary document see N87-10075 01-06)
Avail: NTIS HC A25/MF A01; DFVLR, Cologne, West Germany, DM 150

A flight recorder digital bit synchronizer to process (with cross correlation considering several bits) even distorted signals as occur after aircraft crashes, was developed. Reliability of the recovered bits was measured. Results show that bit synchronization based on correlation permits a more reliable bit recognition in critical cases than previous procedures. One disadvantage of the procedure is the large amount of calculation involved. The hardware developed, however, achieves a processing speed of 20 k baud. ESA

07 AIRCRAFT PROPULSION AND POWER

Includes prime propulsion systems and systems components, e.g., gas turbine engines and compressors; and onboard auxiliary power plants for aircraft.

For related information see also *20 Spacecraft Propulsion and Power, 28 Propellants and Fuels,* and *44 Energy Production and Conversion.*

N87-10100*# National Aeronautics and Space Administration. Lewis Research Center, Cleveland, Ohio.
RESPONSE OF A SMALL-TURBOSHAFT-ENGINE COMPRESSION SYSTEM TO INLET TEMPERATURE DISTORTION
Thomas J. Biesiadny, Gary A. Klann (Army Research and Technology Labs., Cleveland, Ohio.), and Jeffery K. Little Sep. 1984 28 p
(NASA-TM-83765; E-2198; NAS 1.26:83765; USAAVSCOM-TR-84-C-13) Avail: NTIS HC A03/MF A01 CSCL 21E

An experimental investigation was conducted into the response of a small-turboshaft-engine compression system to steady-state and transient inlet temperature distortions. Transient temperature ramps range from less than 100 K/sec to above 610 K/sec and generated instantaneous temperatures to 420 K above ambient. Steady-state temperature distortion levels were limited by the engine hardware temperature list. Simple analysis of the steady-state distortion data indicated that a particle separator at the engine inlet permitted higher levels of temperature distortion before onset of compressor surge than would be expected without the separator. Author

N87-10085# Philips Zentrallaboratorium G.m.b.H., Hamburg (West Germany).
A SYSTEM THEORETICAL BASED METHOD FOR MODULE FAILURE DIAGNOSTIC OF TURBINE ENGINES
M. Roesnick *In* DFVLR Proceedings of the 13th Symposium on Aircraft Integrated Data Systems Feb. 1986 p 207-233 (For primary document see N87-10075 01-06)
Avail: NTIS HC A25/MF A01; DFVLR, Cologne, West Germany, DM 150

08 AIRCRAFT STABILITY AND CONTROL

Includes aircraft handling qualities; piloting; flight controls; and autopilots.

For related information see also *05 Aircraft Design, Testing and Performance.*

N87-10101*# National Aeronautics and Space Administration. Langley Research Center, Hampton, Va.

SUMMARY OF LONGITUDINAL STABILITY AND CONTROL PARAMETERS AS DETERMINED FROM SPACE SHUTTLE COLUMBIA FLIGHT TEST DATA

William T. Suit Aug. 1986 25 p

(NASA-TM-87768; NAS 1.15:87768) Avail: NTIS HC A02/MF A01 CSCL 01C

Extensive wind tunnel tests were conducted to establish the preflight aerodynamics of the Shuttle vehicle. This paper presents the longitudinal, short-period aerodynamics of the space shuttle Columbia as determined from flight test data. These flight-determined results are compared with the preflight predictions, and areas of agreement or disagreement are noted. In addition to the short-period aerodynamics, the pitch RCS effectiveness was determined. Author

N87-10102*# Textron, Inc., Irvine, Calif.

TECHNOLOGY REVIEW OF FLIGHT CRUCIAL FLIGHT CONTROL SYSTEMS (APPLICATION OF OPTICAL TECHNOLOGY)

H. A. Rediess and E. C. Buckley Sep. 1984 48 p

(Contract NAS1-17403)

(NASA-CR-172332; NAS 1.26:172332) Avail: NTIS HC A03/MF A01 CSCL 01C

The survery covers the various optical elements that are considered in a fly-by-light flight control system including optical sensors and transducers, optical data links, so-called optical actuators, and optical/electro-optical processing. It also addresses airframe installation, maintenance, and repair issues. Rather than an in-depth treatment of optical technology, the survey concentrates on technology readiness and the potential advantages/disadvantages of applying the technology. The information was assembeld from open literature, personal interviews, and responses to a questionnaire distributed specifically for this survey. Not all of the information obtained was consistent, particularly with respect to technology readiness. The synthesis of information into the perception of the state-of-technology is presented. Author

N87-10103*# National Aeronautics and Space Administration. Ames Research Center, Moffett Field, Calif.

IN-FLIGHT TOTAL FORCES, MOMENTS AND STATIC AEROELASTIC CHARACTERISTICS OF AN OBLIQUE-WING RESEARCH AIRPLANE

Robert E. Curry and Alex G. Sim Oct. 1984 30 p

(NASA-TP-2224; H-1181; NAS 1.60:2224) Avail: NTIS HC A03/MF A01 CSCL 01C

A low-speed flight investigation has provided total force and moment coefficients and aeroelastic effects for the AD-1 oblique-wing research airplane. The results were interpreted and compared with predictions that were based on wind tunnel data. An assessment has been made of the aeroelastic wing bending design criteria. Lateral-directional trim requirements caused by asymmetry were determined. At angles of attack near stall, flow visualization indicated viscous flow separation and spanwise vortex flow. These effects were also apparent in the force and moment data. Author

09 RESEARCH AND SUPPORT FACILITIES (AIR)

Includes airports, hangars and runways; aircraft repair and overhaul facilities; wind tunnels; shock tubes; and aircraft engine test stands.

For related information see also *14 Ground Support Systems and Facilities (Space).*

N87-10104# National Aeronautical Lab., Bangalore (India). Aerodynamics Div.

TUNNEL INTERFERENCE FROM PRESSURE MEASUREMENTS ON CONTROL SURFACES

R. Gopinath Aug. 1983 27 p

(AE-TM-8-83) Avail: NTIS HC A03/MF A01

Interference due to tunnel walls has been evaluated from pressure measurements on control surfaces by a method due to Capelier, Chevallier and Bouniod, using a simple exponential type of decay for extrapolating the pressure coefficients beyond the measurement stations to + or - infinity, respectively. The method has been validated against data presented at an AGARD meeting on Transonic Test Sections at NASA Langley, which discussed the merits of the various methods for evaluating the wall interference from pressure measurements. Author

N87-10105# Naval Ocean Systems Center, San Diego, Calif.

PRESSURE-RESISTANT PLANE DISC VIEWPORTS FROM ALLYL DIGLYCOL CARBONATE PLASTIC FOR HYPERBARIC CHAMBERS Research Report, Oct. 1984 - Sep. 1985

J. D. Stachiw Sep. 1985 81 p

(AD-A168007; NOSC/TR-1080) Avail: NTIS HC A05/MF A01 CSCL 11/9

Acrylic plastic viewports have been used for over 40 years in pressure vessels for human occupancy without any catastrophic failure resulting in a loss of life. However, there are special applications, such as hyperbaric chambers for medical purposes, in which the susceptibility of flex-stressed acrylic plastic to surface crazing and cracking in the presence of common organic solvents contained in antibacterial sprays is a distinct disadvantage. To solve this problem, a search has been initiated for transparent plastics that are not attacked by organic solvents and can be cast economically in thick sections. Allyl diglycol carbonate plastic appears not only to satisfy the above requirement, but also to provide better resistance to abrasion, pitting, and X-ray or gamma irradiation than acrylic plastic. Short-term, long-term, and cyclic pressure testing has been conducted on over one hundred allyl diglycol carbonate plane disc viewports with t/d sub o ratio in the 0.06 to 0.4 range and at temperatures in the +40 to +125 F range. It appears that plane discs cast from allyl diglycol carbonate plastic can perform safely as pressure-resistant viewports in pressure vessels for human occupancy. GRA

N87-10106 Stanford Univ., Calif.

ENERGY DELIVERY PROCESSES IN SHOCK TUBES Ph.D. Thesis

Dan Omry 1986 275 p

Avail: Univ. Microfilms Order No. DA8608202

Gas accleration in a shock tube is analyzed. Three topics are discussed: a general review of shock tube basic principles and an extensive survey of the state of the art; a methodology for comparative analysis of the impact of energy delivery configuration on shock tube performance and its application; and a mathematical model of a specific energy delivery process (Joule heating) in a particular geometric configuration (flowing gas heater). Understanding the inherent limitations can be gained by means of comparative analysis. The process of energy transfer is separated into states. The efficiency of each stage indiates the system's performance at that stage. A study of the pre-heated gas driver (energy is deposited in the driver gas prior to the initiation of the shock wave) and the flowing gas heater (energy transfer process starts simultaneously with shock initiation and the energy is deposited in the gas already in motion) shows the latter to be inherently more

efficient in energy delivery when maximum driver temperatures are comparable. A mathematical model of the latter configuration, for the specific case where the energy depostion is Joule heating, is constructed by a synthesis of approximate ideal processes.
Dissert. Abstr.

12 ASTRONAUTICS (GENERAL)

For extraterrestrial exploration see *91 Lunar and Planetary Exploration.*

N87-10107# General Accounting Office, Washington, D. C. National Security and International Affairs Div.
STRATEGIC DEFENSE INITIATIVE PROGRAM: STATUS OF AIRBORNE OPTICAL ADJUNCT AND TERMINAL IMAGING RADAR
Jun. 1986 24 p
(PB6-221132; GAO/NSIAD-86-153; B-223094) Avail: NTIS HC A02/MF A01 CSCL 15C

Information on the status of the Strategic Defence Initiative Organization's technology validation experiments on the Airborne Optical Adjunct (AOA) and Terminal Imaging Radar (TIR) is provided. These experiments, being managed by the Army's Strategic Defense Command, are designed to demonstrate that technology is available to develop effective sensors for a terminal phase ballistic missile defense system. The AOA consists of a Boeing 767 airplane, a long wave infrared sensor with a signal processor, data processor, and other components. GRA

13 ASTRODYNAMICS

Includes powered and free-flight trajectories; and orbital and launching dynamics.

N87-10108# Defense Mapping Agency Hydrographic and Topographic Center, Washington, D.C.
DMA (DEFENSE MAPPING AGENCY) ORBIT DETERMINATION FOR TRANSIT SATELLITES: 1985 Final Report
Jesse K. Murphy and Patrick J. Fell 30 Apr. 1986 15 p Presented at the 4th International Geodetic Symposium on Satellite Positioning, Austin, Tex., 28 Apr. - 2 May 1986
(AD-A167567) Avail: NTIS HC A02/MF A01 CSCL 22/3

Since 1975, the Defense Mapping Agency (DMA) has been computing precise orbits for the Navy navigation satellites, OSCAR series. In mid-1981, DMA began computing precise orbits for the NOVA-1 satellite and, in early 1985, for the NOVA-3 satellite. Currently, DMA determines precise orbits for the three OSCAR and two NOVA satellites which comprise the TRANSIT System. This paper presents a comparison of computational results for these satellites with regard to orbit accuracy, time (oscillator) stability, and polar motion. The comparison is made for results obtained for 1985. Author (GRA)

N87-10109# Sandia National Labs., Albuquerque, N. Mex.
TRAJECTORY SCORING IN GEODETIC COORDINATES USING TRANSPONDER-INTERROGATOR RANGE DATA
T. E. Owen Mar. 1986 75 p
(Contract DE-AC04-76DP-00789)
(DE86-009554; SAND-85-2360) Avail: NTIS HC A04/MF A01

Range measurements taken from a transponder-interrogator ranging system are processed via an extended Kalman filter to provide an accurate time-position history of a vehicle's trajectory by estimating the errors in the vehicle's inertial navigation system. The range and Kalman filter equations are derived in geodetic coordinates to allow for coverage over a large geographic area. The equations are then verified by processing data from flight tests at Edwards Air Force Base, producing position accuracies of 3 to 4 meters 1sigma. DOE

N87-10114 European Space Agency. European Space Research and Technology Center, ESTEC, Noordwijk (Netherlands).
TRANSFER ORBIT OPTIMIZATION FOR DUAL LAUNCHES
A. G. Bird, D. Plummer (British Aerospace Dynamics Group, Stevenage (England).), and M. J. Smalley *In* CNES Proceedings of an International Conference on Space Dynamics for Geostationary Satellites 1986 p 17-35 (For primary document see N87-10113 01-18)
Avail: CEPADUES-Editions, 111 rue Nicolas-Vauquelin, 31100 Toulouse, France

N87-10115 Arianespace, Evry (France).
ANALYSIS OF THE PROBLEM OF SATELLITE LAUNCH WINDOWS FOR ARIANE DUAL LAUNCHES [ANALYSE DU PROBLEME DES FENETRES DE LANCEMENT SATELLITE POUR LES LANCEMENTS DOUBLES SUR ARIANE]
Philippe Boland *In* CNES Proceedings of an International Conference on Space Dynamics for Geostationary Satellites 1986 p 37-52 In FRENCH; ENGLISH summary (For primary document see N87-10113 01-18)
Avail: CEPADUES-Editions, 111 rue Nicolas-Vauquelin, 31100 Toulouse, France

N87-10116 Communications Satellite Corp., Washington, D.C.
ORBIT GEOMETRY FOR CALIBRATION AND LAUNCH OPERATIONS OF A THREE-AXIS CONTROLLED SATELLITE WITH INERTIAL REFERENCE
David R. Brown *In* CNES Proceedings of an International Conference on Space Dynamics for Geostationary Satellites 1986 p 53-70 (For primary document see N87-10113 01-18)
Avail: CEPADUES-Editions, 111 rue Nicolas-Vauquelin, 31100 Toulouse, France

N87-10117 Telesat Canada, Ottawa (Ontario).
OPTIMAL TRANSFER TO INCLINED GEOSYNCHRONOUS ORBITS
J. Kerry Skipper *In* CNES Proceedings of an International Conference on Space Dynamics for Geostationary Satellites 1986 p 71-81 (For primary document see N87-10113 01-18)
Avail: CEPADUES-Editions, 111 rue Nicolas-Vauquelin, 31100 Toulouse, France

N87-10118 Rome Univ. (Italy). Dept. of Aerospace.
AN INVESTIGATION ON PASSIVELY CONTROLLED GEOSYNCHRONOUS ORBITS
C. Ulivieri, A. Agneni, A. Foni (Consiglio Nazionale delle Ricerche, Pisa (Italy).), and S. Trumpy *In* CNES Proceedings of an International Conference on Space Dynamics for Geostationary Satellites 1986 p 85-92 (For primary document see N87-10113 01-18)
Avail: CEPADUES-Editions, 111 rue Nicolas-Vauquelin, 31100 Toulouse, France

N87-10120 Escuela Tecnica Superior de Ingenieros Aeronauticos, Madrid (Spain).
OPTIMAL TRACKING STRATEGY DETERMINATION
J. J. Martinez-Garcia, C. Bachmaier, T. Prieto, S. Pallaschke (European Space Agency. European Space Operations Center, Darmstadt (West Germany).), and W. Peterhaensel (Mathematischer Beratungs- und Programmierungsdienst G.m.b.H. Dortmund (West Germany).) *In* CNES Proceedings of an International Conference on Space Dynamics for Geostationary Satellites 1986 p 101-118 (For primary document see N87-10113 01-18)
Avail: CEPADUES-Editions, 111 rue Nicolas-Vauquelin, 31100 Toulouse, France

N87-10121 Centre National d'Etudes Spatiales, Toulouse (France).
ACCURACY OF GOESTATIONARY ORBIT DETERMINATION [PRECISION DE LA RESTITUTION D'UNE ORBITE GEOSTATIONNAIRE]
O. Zarrouati *In its* Proceedings of an International Conference on Space Dynamics for Geostationary Satellites 1986 p 119-147 In FRENCH; ENGLISH summary (For primary document see N87-10113 01-18)

Avail: CEPADUES-Editions, 111 rue Nicolas-Vauquelin, 31100 Toulouse, France

N87-10123 National Aeronautics and Space Administration. Goddard Space Flight Center, Greenbelt, Md.
GEOSTATIONARY OPERATIONAL ENVIRONMENTAL SATELLITE (GOES) MISSION PROFILE
William C. Bryant, Robert L. DeFazio, and Judith A. Sauter *In* CNES Proceedings of an International Conference on Space Dynamics for Geostationary Satellites 1986 p 169-193 (For primary document see N87-10113 01-18)
Avail: CEPADUES-Editions, 111 rue Nicolas-Vauquelin, 31100 Toulouse, France

N87-10124 National Space Development Agency, Ibaraki (Japan). Tsukuba Space Center.
ATTITUDE DETERMINATIONS FOR GEOSTATIONARY SATELLITES OF THE NATIONAL SPACE DEVELOPMENT AGENCY (NASDA)
M. Horii *In* CNES Proceedings of an International Conference on Space Dynamics for Geostationary Satellites 1986 p 197-206 (For primary document see N87-10113 01-18)
Avail: CEPADUES-Editions, 111 rue Nicolas-Vauquelin, 31100 Toulouse, France

N87-10127 Indian Space Research Organization, Bangalore.
PRELIMINARY ORBIT DETERMINATION BY STATIC MULTIVARIATE SEARCH
P. RajendraPrasad, N. S. Gopinath, and R. S. Bhat *In* CNES Proceedings of an International Conference on Space Dynamics for Geostationary Satellites 1986 p 229-247 (For primary document see N87-10113 01-18)
Avail: CEPADUES-Editions, 111 rue Nicolas-Vauquelin, 31100 Toulouse, France

N87-10128 European Space Agency. European Space Operations Center, Darmstadt (West Germany).
EARLY ORBIT DETERMINATION
S. Pallaschke *In* CNES Proceedings of an International Conference on Space Dynamics for Geostationary Satellites 1986 p 249-261 (For primary document see N87-10113 01-18)
Avail: CEPADUES-Editions, 111 rue Nicolas-Vauquelin, 31100 Toulouse, France

N87-10129 National Space Development Agency, Tokyo (Japan). Satellite Development Dept.
STATE/ORBIT ESTIMATION FROM REAL DOPPLER DATA FOR SOLID APOGEE MOTOR BURNING PHASE OF GEOSTATIONARY SATELLITE
Shuji Ono *In* CNES Proceedings of an International Conference on Space Dynamics for Geostationary Satellites 1986 p 263-288 (For primary document see N87-10113 01-18)
Avail: CEPADUES-Editions, 111 rue Nicolas-Vauquelin, 31100 Toulouse, France

N87-10130 Centre National d'Etudes Spatiales, Toulouse (France).
REAL TIME ORBIT DETERMINATION DURING APOGEE MANEUVERS
B. Belon *In its* Proceedings of an International Conference on Space Dynamics for Geostationary Satellites 1986 p 289-300 In FRENCH; ENGLISH summary (For primary document see N87-10113 01-18)
Avail: CEPADUES-Editions, 111 rue Nicolas-Vauquelin, 31100 Toulouse, France

N87-10131 Porto Univ. (Portugal). Observatorio Astronomico.
INITIAL ORBIT DETERMINATION FOR GEOSTATIONARY SATELLITES
I. Couto and J. Osorio *In* CNES Proceedings of an International Conference on Space Dynamics for Geostationary Satellites 1986 p 301-313 (For primary document see N87-10113 01-18)
Avail: CEPADUES-Editions, 111 rue Nicolas-Vauquelin, 31100 Toulouse, France

N87-10132 Indian Space Research Organization, Bangalore.
REAL TIME ORBIT AND DYNAMIC SEARCH ZONE COMPUTATIONS TO AID SATELLITE ACQUISITION IN S-BAND DURING THE LAUNCH PHASE OF GEOSYNCHRONOUS TRANSFER ORBIT (GTO)
V. S. Iyengar and P. Soma *In* CNES Proceedings of an International Conference on Space Dynamics for Geostationary Satellites 1986 p 315-340 (For primary document see N87-10113 01-18)
Avail: CEPADUES-Editions, 111 rue Nicolas-Vauquelin, 31100 Toulouse, France

N87-10134 Consiglio Nazionale delle Ricerche, Pisa (Italy).
OPTICAL TRACKING OF THE SIRIO SATELLITE
L. Anselmo and S. Trumpy *In* CNES Proceedings of an International Conference on Space Dynamics for Geostationary Satellites 1986 p 353-361 (For primary document see N87-10113 01-18)
Avail: CEPADUES-Editions, 111 rue Nicolas-Vauquelin, 31100 Toulouse, France

N87-10135 Centre National d'Etudes Spatiales, Toulouse (France).
VERY FIRST ORBIT DETERMINATION AFTER LAUNCH OR MAIN MANEUVERS. APPLICATIONS TO GEOSTATIONARY TELECOM 1A AND 1B
F. Nouel, P. Broca, A. Guitart, R. Mesnard, and D. Zobler *In its* Proceedings of an International Conference on Space Dynamics for Geostationary Satellites 1986 p 363-374 (For primary document see N87-10113 01-18)
Avail: CEPADUES-Editions, 111 rue Nicolas-Vauquelin, 31100 Toulouse, France

N87-10137 Centre National d'Etudes Spatiales, Toulouse (France).
SYNCHRONOUS TRANSFER ORBIT OPERATION UNDER THREE-AXIS CONTROL
John V. Brown *In its* Proceedings of an International Conference on Space Dynamics for Geostationary Satellites 1986 p 395-403 (For primary document see N87-10113 01-18)
Avail: CEPADUES-Editions, 111 rue Nicolas-Vauquelin, 31100 Toulouse, France

N87-10148 European Space Agency. European Space Operations Center, Darmstadt (West Germany).
OPERATIONAL IMPLEMENTATION OF DEORBITING MANEUVERS
Jozef vanderHa *In* CNES Proceedings of an International Conference on Space Dynamics for Geostationary Satellites 1986 p 553-562 (For primary document see N87-10113 01-18)
Avail: CEPADUES-Editions, 111 rue Nicolas-Vauquelin, 31100 Toulouse, France

N87-10149 Centre National d'Etudes Spatiales, Toulouse (France).
APPLICATION OF LINEAR PROGRAMMING TO FINAL POSITIONING (DRIFT ORBIT) OF A GEOSTATIONARY SATELLITE [APPLICATION DE LA PROGRAMMATION LINEAIRE A LA MISE A POSTE FINALE (ORBITE DE DERIVE) D'UN SATELLITE GEOSTATIONNAIRE]
D. Blumstein *In* CNES Proceedings of an International Conference on Space Dynamics for Geostationary Satellites 1986 p 563-572 In FRENCH; ENGLISH summary (For primary document see N87-10113 01-18)
Avail: CEPADUES-Editions, 111 rue Nicolas-Vauquelin, 31100 Toulouse, France

N87-10162 Centre d'Etudes et de Recherches Geodynamiques et Astronomiques, Grasse (France).
CONSTRAINTS IMPOSED BY AN INTERSATELLITE COMMUNICATION LINK UPON STATIONKEEPING OF TWO CLOSE GEOSTATIONARY SATELLITES
V. Guermonprez *In* CNES Proceedings of an International Conference on Space Dynamics for Geostationary Satellites 1986 p 811-823 In FRENCH; ENGLISH summary (For primary document see N87-10113 01-18)
Avail: CEPADUES-Editions, 111 rue Nicolas-Vauquelin, 31100 Toulouse, France

14 GROUND SUPPORT SYSTEMS AND FACILITIES (SPACE)

Includes launch complexes, research and production facilities; ground support equipment, e.g., mobile transporters; and simulators.

For related information see also *09 Research and Support Facilities (Air).*

N87-10110*# Boeing Aerospace Co., Kennedy Space Center, Fla.
ORBITAL TRANSFER VEHICLE LAUNCH OPERATIONS STUDY. VOLUME 1: EXECUTIVE SUMMARY Final Report
7 Mar. 1986 12 p
(Contract NAS10-11165)
(NASA-CR-179701; NAS 1.26:179701) Avail: NTIS HC A02/MF A01 CSCL 22D

The purpose was to use the operational experience at the launch site to identify, describe and quantify the operational impacts of the various configurations on the Kennedy Space Center (KSC) and/or space station launch sites. Orbital Transfer Vehicle (OTV) configurations are being developed/defined by contractor teams. Lacking an approved configuration, the KSC Study Team defined a Reference Configuration to be used for this study. This configuration then become the baseline for the identification of the facilities, personnel and crew skills required for processing the OTV in a realistic manner that would help NASA achieve the lowest possible OTV life cycle costs. As the study progressed, researchers' initial apraisal that the vehicle, when delivered, would be a sophisticated, state-of-the-art vehicle was reinforced. It would be recovered and reused many times so the primary savings to be gained would be in the recurring-cycle of the vehicle operations--even to the point where it would be beneficial to break from tradition and make a significant expenditure in the development of processing facilities at the beginning of the program. Author

N87-10111*# Boeing Aerospace Co., Kennedy Space Center, Fla.
ORBITAL TRANSFER VEHICLE LAUNCH OPERATIONS STUDY. VOLUME 2: DETAILED SUMMARY
7 Mar. 1986 181 p
(Contract NAS10-11165)
(NASA-CR-179791; NAS 1.26:179791) Avail: NTIS HC A09/MF A01 CSCL 22D

A series of Operational Design Drivers were identified. Several of these could have significant impact(s) on program costs. These recommendations, for example, include such items as: complete factory assembly and checkout prior to shipment to the ground launch site to make significant reductions in time required at the launch site as well as overall manpower required to do this work; minimize use of nonstandard equipment when orbiter provided equipment is available; and require commonality (or interchangeability) of subsystem equipment elements that are common to the space station, Orbit Maneuvering Vehicles, and/or Orbit Transfer Vehicles. Several additional items were identified that will require a significant amount of management attention (and direction) to resolve. Key elements of the space based processing plans are discussed. B.G.

N87-10498*# Uppsala Ionospheric Observatory (Sweden).
HISCAT: A PROPOSED NEW SCATTER FACILITY IN NORTHERN SCANDINAVIA
R. Bostrom and B. Thide *In* International Council of Scientific Unions, Middle Atmosphere Program. Handbook for MAP, Vol. 20 Jun. 1986 1 p (For primary document see N87-10419 01-42)
Avail: NTIS HC A22/MF A01; also available from SCOSTEP Secretariat, Illinois Univ., 1406 West Green Street, Urbana, Ill. 61801 CSCL 14B

N87-10133 Aerospace Corp., El Segundo, Calif.
ORBIT DETERMINATION OF GEOSTATIONARY SATELLITES USING THE GLOBAL POSITIONING SYSTEM
M. P. Ananda and P. S. Jorgensen *In* CNES Proceedings of an International Conference on Space Dynamics for Geostationary Satellites 1986 p 341-352 (For primary document see N87-10113 01-18)
Avail: CEPADUES-Editions, 111 rue Nicolas-Vauquelin, 31100 Toulouse, France

15 LAUNCH VEHICLES AND SPACE VEHICLES

Includes boosters; operating problems of launch/space vehicle systems; and reusable vehicles.

For related information see also *20 Spacecraft Propulsion and Power.*

No abstracts in this category.

16 SPACE TRANSPORTATION

Includes passenger and cargo space transportation, e.g., shuttle operations; and space rescue techniques.

For related information see also *03 Air Transportation and Safety* and *18 Spacecraft Design, Testing and Performance.* For space suits see *54 Man/System Technology and Life Support.*

No abstracts in this category.

17 SPACE COMM., SPACECRAFT COMM., COMMAND & TRACKING

Includes telemetry; space communications networks; astronavigation and guidance; and radio blackout.

For related information see also *04 Aircraft Communications and Navigation* and *32 Communications and Radar.*

N87-10112# Eidgenoessische Technische Hochschule, Zurich (Switzerland). Inst. fuer Fernmeldetechnik.
METHODS AND STANDARDS FOR ENCRYPTION OF SPACECRAFT TELEMETRY AND TELECOMMAND LINKS Final Report
R. A. Rueppel and H. P. Bader Paris ESA Mar. 1985 253 p
Prepared in cooperation with Borer Electronics AG
(Contract ESTEC-5815/84-NL-BI(SC))
(RPT/ENC/62359/BO; ESA-CR(P)-2194; ETN-86-97794) Avail: NTIS HC A12/MF A01

Spacecraft telemetry and telecommand link transmission requirements were analyzed in order to define the best encryption technique. Implementation feasibility of the proposed telecommand authentication system was analyzed. The authentication system was simulated on a computer to verify the predicted system characteristics. A draft encryption guideline was produced. ESA

18 SPACECRAFT DESIGN, TESTING AND PERFORMANCE

Includes satellites; space platforms; space stations; spacecraft systems and components such as thermal and environmental controls; and attitude controls.

For life support systems see *54 Man/System Technology and Life Support.* For related information see also *05 Aircraft Design, Testing and Performance, 39 Structural Mechanics,* and *16 Space Transportation.*

N87-10113 Centre National d'Etudes Spatiales, Toulouse (France).
PROCEEDINGS OF AN INTERNATIONAL CONFERENCE ON SPACE DYNAMICS FOR GEOSTATIONARY SATELLITES
1986 869 p In ENGLISH and FRENCH Conference held in Toulouse, France, Oct. 1985
(ISBN-2-85428-149-7; ETN-86-98079) Copyright. Avail: CEPADUES-Editions, 111 rue Nicolas-Vauquelin, 31100 Toulouse, France

Geostationary satellite mission analysis, attitude determination, orbit determination, (onboard technology, low-thrust techniques, station acquisition, stationkeeping) ground segments, and future developments were discussed. For individual titles, see N87-10114 through N87-10165.

N87-10114 European Space Agency. European Space Research and Technology Center, ESTEC, Noordwijk (Netherlands).
TRANSFER ORBIT OPTIMIZATION FOR DUAL LAUNCHES c13
A. G. Bird, D. Plummer (British Aerospace Dynamics Group, Stevenage (England).), and M. J. Smalley *In* CNES Proceedings of an International Conference on Space Dynamics for Geostationary Satellites 1986 p 17-35 (For primary document see N87-10113 01-18)
Avail: CEPADUES-Editions, 111 rue Nicolas-Vauquelin, 31100 Toulouse, France

The dual launch configuration is shown to have design implications for missions with inclined geosynchronous orbits. Design objectives with respect to propellant tank and apogee boost motor size, launch mass, and launch window may be affected. Propellant requirements are a function of launch window, and it is advantageous to base the mission on minimum launch window requirements. It appears that considerable propellant savings can be made for dual launches, if the transfer orbit is optimized under the constraints of both missions. The combined optimization also tends to extend the launch window. To be effective, however, there must either be some commonality of mission requirements or additional launcher potential made available. ESA

N87-10115 Arianespace, Evry (France).
ANALYSIS OF THE PROBLEM OF SATELLITE LAUNCH WINDOWS FOR ARIANE DUAL LAUNCHES [ANALYSE DU PROBLEME DES FENETRES DE LANCEMENT SATELLITE POUR LES LANCEMENTS DOUBLES SUR ARIANE] c13
Philippe Boland *In* CNES Proceedings of an International Conference on Space Dynamics for Geostationary Satellites 1986 p 37-52 In FRENCH; ENGLISH summary (For primary document see N87-10113 01-18)
Avail: CEPADUES-Editions, 111 rue Nicolas-Vauquelin, 31100 Toulouse, France

Determination of launch windows for Ariane dual launches of geostationary satellites is described. First, the present situation is presented on the basis of the information provided by satellite projects. Then, solutions to reduce window incompatibilities are examined, such as: choice of compatible copassengers, relaxation of satellite constraints, extra satellite propellant consumption, and modification of satellite flight operations in transfer orbit. Finally, a universal launch window is proposed, the definition of which is independent of the launch vehicle trajectory. This launch window may be introduced in the short term in the Ariane User's Manual. ESA

N87-10116 Communications Satellite Corp., Washington, D.C.
ORBIT GEOMETRY FOR CALIBRATION AND LAUNCH OPERATIONS OF A THREE-AXIS CONTROLLED SATELLITE WITH INERTIAL REFERENCE c13
David R. Brown *In* CNES Proceedings of an International Conference on Space Dynamics for Geostationary Satellites 1986 p 53-70 (For primary document see N87-10113 01-18)
Avail: CEPADUES-Editions, 111 rue Nicolas-Vauquelin, 31100 Toulouse, France

A method for determining the spacecraft, Sun, Earth geometry for a three-axis controlled satellite with inertial reference in transfer orbit is presented. Using the spacecraft as the origin of the reference system, two orientation modes are considered: the Sun-Earth plane mode, in which the X axis is pointed along the sunline, the Z axis lies in the Sun-Earth plane, and the Y axis completes the right-hand triad; and the orbit plane mode, in which X is pointed along the projection of the Sun vector in the orbit plane, Z lies in the orbit plane, and Y completes the right-hand triad. The method is applied to key events, while the spacecraft is under Earth sensor control, leading up to apogee-motor-fire to determine control parameters. Flight results from the Arabsat program are presented. The dependence of window durations on spacecraft characteristics (e.g., Earth sensor field of view) and orbital characteristics (e.g., injection time within the launch window and orbit parameters) are discussed. A method to handle real-time changes that can occur due to launch delays and delays in the launch operations timeline is outlined. ESA

N87-10117 Telesat Canada, Ottawa (Ontario).
OPTIMAL TRANSFER TO INCLINED GEOSYNCHRONOUS ORBITS c13
J. Kerry Skipper *In* CNES Proceedings of an International Conference on Space Dynamics for Geostationary Satellites 1986 p 71-81 (For primary document see N87-10113 01-18)
Avail: CEPADUES-Editions, 111 rue Nicolas-Vauquelin, 31100 Toulouse, France

The concept of placing a communication satellite in an inclined geosynchronous orbit, or storage orbit, is introduced. The target orbit is determined by analyzing the secular motion of the orbit normal vector. The optimal transfer is obtained by modifying the generalized Hohmann ellipse (the optimal transfer between circular noncoplanar orbits) to account for the effects of perturbations and mission constraints. Maneuvers are planned by locating the impulses, and determining the resulting transfer orbit. The results of the analysis are applied to missions in which Canadian satellites were placed in 2 and 3 yr storage orbits. ESA

N87-10118 Rome Univ. (Italy). Dept. of Aerospace.
AN INVESTIGATION ON PASSIVELY CONTROLLED GEOSYNCHRONOUS ORBITS c13
C. Ulivieri, A. Agneni, A. Foni (Consiglio Nazionale delle Ricerche, Pisa (Italy).), and S. Trumpy *In* CNES Proceedings of an International Conference on Space Dynamics for Geostationary Satellites 1986 p 85-92 (For primary document see N87-10113 01-18)
Avail: CEPADUES-Editions, 111 rue Nicolas-Vauquelin, 31100 Toulouse, France

The long-term orbital pole evolution for geosynchronous circular uncontrolled satellites was analyzed to identify the initial conditions which allow the orbital plane to remain within a given tolerance, without any active control over the estimated lifetime of the satellite. A mission target compatible with a 7 yr spacecraft operational life and a tolerance of 0.3 deg with respect to the initial orbit inclination value was selected. Apogee motor requirements for positioning a satellite in an orbit having these characteristics were compared with requirements for the geostationary orbit. The fuel budget for the target mission was computed for 2 different satellites by assuming Ariane 44p and STS-PAM-D2 launch vehicles. The peculiarity of the orbit selected with respect to the geostationary one is discussed. ESA

N87-10119 National Space Development Agency, Ibaraki (Japan). Tsukuba Space Center.
OPERATIONAL CRITERIA FOR GEOSTATIONARY SATELLITES

IN NATIONAL SPACE DEVELOPMENT AGENCY (NASDA)
A. Tanaka, M. Utashima, M. Yambe (Fujitsu Ltd., Tokyo (Japan).), and M. Hasegawa *In* CNES Proceedings of an International Conference on Space Dynamics for Geostationary Satellites 1986 p 93-100 (For primary document see N87-10113 01-18)
Avail: CEPADUES-Editions, 111 rue Nicolas-Vauquelin, 31100 Toulouse, France

The criteria of orbit and attitude maneuver strategies during transfer orbit and near-synchronous orbit phase operations adopted by the National Space Development Agency of Japan (NASDA) are introduced. Following the criteria adopted by NASDA, attitude maneuvers are planned in the beginning of each revolution. In order to keep to the station acquisition maneuver schedule, a set of basic station acquisition maneuvers is divided into several small ones, and a strategy is prepared so that a precedent maneuver error can be compensated by the following ones without any change of maneuver time. Such a strategy contains a few small maneuvers to calibrate the thruster performance data, and maneuver magnitudes are equalized to get better calibration results. ESA

N87-10120 Escuela Tecnica Superior de Ingenieros Aeronauticos, Madrid (Spain).
OPTIMAL TRACKING STRATEGY DETERMINATION c13
J. J. Martinez-Garcia, C. Bachmaier, T. Prieto, S. Pallaschke (European Space Agency. European Space Operations Center, Darmstadt (West Germany).), and W. Peterhaensel (Mathematischer Beratungs- und Programmierungsdienst G.m.b.H. Dortmund (West Germany).) *In* CNES Proceedings of an International Conference on Space Dynamics for Geostationary Satellites 1986 p 101-118 (For primary document see N87-10113 01-18)
Avail: CEPADUES-Editions, 111 rue Nicolas-Vauquelin, 31100 Toulouse, France

A satellite tracking method is outlined. The approach consists in selecting a tracking sequence from a given set of possible measurement instants so as to minimize a given linear function of the covariance matrix of the error in the final satellite state. The estimated covariance matrix on the final error is obtained through a Kalman-Bucy or Kalman-Schmidt filter algorithm. Bias terms in the observations and in the dynamic parameters can be handled. By introducing a control variable associated to each measurement which can take the binary values 0 or 1 (1 means to consider that observation, 0 to ignore it) the task is formulated as a constrained binary parameter optimization problem. An algorithm to determine a subset of given possible measurement instants and which constitutes the optimal tracking strategy to be used was derived. A computer program consisting of a data generator computing the required input data such as observations, partials, and statistics of observations and system noise, and an optimization program using the data to solve the problem considered was written. Results for geostationary orbits are presented. ESA

N87-10121 Centre National d'Etudes Spatiales, Toulouse (France).
ACCURACY OF GOESTATIONARY ORBIT DETERMINATION [PRECISION DE LA RESTITUTION D'UNE ORBITE GEOSTATIONNAIRE] c13
O. Zarrouati *In its* Proceedings of an International Conference on Space Dynamics for Geostationary Satellites 1986 p 119-147 In FRENCH; ENGLISH summary (For primary document see N87-10113 01-18)
Avail: CEPADUES-Editions, 111 rue Nicolas-Vauquelin, 31100 Toulouse, France

A method to evaluate the performance of a global network for the localization of a geosynchronous satellite, given the distribution over the world of a set of ground stations and the individual performance of each ground station (distance or angular measurements) is outlined. Under very realistic assumptions, an analytical formulation of the errors in the computation of the satellite position is obtained. The shape and size of the error domain are discussed with observability arguments. The method can be very helpful in mission analysis for the optimal dimensionning of a radiolocalization system. ESA

N87-10122 RCA Astro-Electronics Div., Princeton, N. J.
ORBIT ACHIEVEMENT OF RCA COMMUNICATION SATELLITES
S. Parvez and S. Fox *In* CNES Proceedings of an International Conference on Space Dynamics for Geostationary Satellites 1986 p 149-168 (For primary document see N87-10113 01-18)
Avail: CEPADUES-Editions, 111 rue Nicolas-Vauquelin, 31100 Toulouse, France

Attitude determination and control techniques for 12 satellites are treated. Post-flight analyses to verify the ABM pointing and performance are presented. Targeting strategies for Ariane, Delta, and STS launches are compared. The extra complexity of planning for STS launches is discussed. Statistics (predicted vs actual) of transfer orbit parameters and station acquisition propellant requirements are included. In the transfer orbit, the spacecraft are spin stabilized. Attitude data provided by a Sun sensor and an Earth horizon sensor are used to determine the inertial attitude of the satellite spin axis. The orientation of the satellite is changed through a series of precession maneuvers to point the thrust vector of the ABM to the target attitude. The orbit determination, attitude determination, and attitude control provide all 12 satellites with an expected mission lifetime that meets or exceeds prelaunch nominal values. ESA

N87-10123 National Aeronautics and Space Administration. Goddard Space Flight Center, Greenbelt, Md.
GEOSTATIONARY OPERATIONAL ENVIRONMENTAL SATELLITE (GOES) MISSION PROFILE c13
William C. Bryant, Robert L. DeFazio, and Judith A. Sauter *In* CNES Proceedings of an International Conference on Space Dynamics for Geostationary Satellites 1986 p 169-193 (For primary document see N87-10113 01-18)
Avail: CEPADUES-Editions, 111 rue Nicolas-Vauquelin, 31100 Toulouse, France

The GOES mission profile used to achieve geostationary orbit following separation from the Delta launch vehicle is described. The mission profile was constrained by the solid-propellant apogee kick motor which was undersized relative to the spacecraft weight. The resulting deficiency in delivered delta-V had to be made up by the spacecraft hydrazine propulsion system. The mission profile which best utilizes the on-board hydrazine requires that the transfer orbit apogee height be biased 13,800 km above geosynchronous altitude. This maximizes the effectiveness of the apogee motor in performing the plane change necessary to achieve near-equatorial orbit. The highly eccentric drift orbit which results from the apogee motor firing has an average drift rate of 60 deg/day. Circularizing this orbit requires maneuvers designed to achieve geostationary position within a tightly constrained hydrazine allocation. The sequence takes advantage of the orbit changes resulting from attitude maneuvers and combined inplane/out-of-plane maneuvers to achieve hydrazine savings. ESA

N87-10124 National Space Development Agency, Ibaraki (Japan). Tsukuba Space Center.
ATTITUDE DETERMINATIONS FOR GEOSTATIONARY SATELLITES OF THE NATIONAL SPACE DEVELOPMENT AGENCY (NASDA) c13
M. Horii *In* CNES Proceedings of an International Conference on Space Dynamics for Geostationary Satellites 1986 p 197-206 (For primary document see N87-10113 01-18)
Avail: CEPADUES-Editions, 111 rue Nicolas-Vauquelin, 31100 Toulouse, France

The attitude determination for the final attitude maneuver planning to establish apogee motor firing of Japanese spacecraft in transfer orbit was scheduled using the horizon sensor data of a full orbital revolution. The software system is connected to the worldwide telemetry on-line system, and it can estimate the attitude in semi real time. The attitude estimation procedure and the software system work well. ESA

N87-10125 European Space Agency. European Space Operations Center, Darmstadt (West Germany).
COVERAGE TRANSITION TIMES OF IR PENCIL BEAM

SENSORS c19
W. Meyer, L. Fraiture, and N. Wiengarn *In* CNES Proceedings of an International Conference on Space Dynamics for Geostationary Satellites 1986 p 207-218 (For primary document see N87-10113 01-18)
Avail: CEPADUES-Editions, 111 rue Nicolas-Vauquelin, 31100 Toulouse, France

It is shown that coverage start and stop events of IR-pencil beam sensors (OG, SODERN) show repeatable biases. They are equivalent to augmentations delta rho to be added to the apparent Earth radius of an oblate Earth. The SODERN augmentations are: delta rho = 0.065 deg at start of coverage, and 0.205 deg at end of coverage; for OG devices delta rho = 0.514 deg at start and stop of coverage, all valid for sensing above 25000 km distance from the Earth center. The accuracy of the delta rho's is better than 0.1 deg (worst case). Results at low altitude were only obtained for OG-sensors. For the latter, larger dispersions are observed. It is best not to utilize start and stop of coverage for attitude reconstitution with perigee data for which the error context is usually not favorable. ESA

N87-10126 VEGA Space Systems Engineering, Saint-Albans (England).
APPLICATION OF SIMPLIFIED SPIN AXIS ATTITUDE DETERMINATION TECHNIQUES TO ESA TELECOM SATELLITES
A. S. Fagg and L. vanHoltz (European Space Agency. European Space Research and Technology Center, ESTEC, Noordwijk (Netherlands).) *In* CNES Proceedings of an International Conference on Space Dynamics for Geostationary Satellites 1986 p 219-226 (For primary document see N87-10113 01-18)
Avail: CEPADUES-Editions, 111 rue Nicolas-Vauquelin, 31100 Toulouse, France

Simplified spin axis attitude determination techniques for satellites in the spin phase in geostationary transfer orbit were developed. The techniques are applicable to cases when geometric solutions to the spherical triangle equations are sufficiently accurate, and no hardware failures prevent the use of both pencil beams of the infrared Earth elevation sensors. On all ESA telecommunication spacecraft launched to-date, these conditions were always met, and satisfactory results obtained. ESA

N87-10127 Indian Space Research Organization, Bangalore.
PRELIMINARY ORBIT DETERMINATION BY STATIC MULTIVARIATE SEARCH c13
P. RajendraPrasad, N. S. Gopinath, and R. S. Bhat *In* CNES Proceedings of an International Conference on Space Dynamics for Geostationary Satellites 1986 p 229-247 (For primary document see N87-10113 01-18)
Avail: CEPADUES-Editions, 111 rue Nicolas-Vauquelin, 31100 Toulouse, France

A static multivariate search algorithm based on the Gram-Schmidt method is used for the problem of preliminary orbit determination using tracking data covering a very short arc of the orbit and very approximate initial estimate. The method is based on orthogonalization to find the primary and secondary search directions. No partial derivatives are needed. The extremum is found by parabolic extrapolation or interpolation of the function values. The suitability and effectiveness of the method for the problem of preliminary orbit determination is demonstrated. The approach yields desirable accuracies in simulated tracking data and application to actual tracking data of Indian satellites BHASKARA-2 APPLE and INSAT 1-A. ESA

N87-10128 European Space Agency. European Space Operations Center, Darmstadt (West Germany).
EARLY ORBIT DETERMINATION c13
S. Pallaschke *In* CNES Proceedings of an International Conference on Space Dynamics for Geostationary Satellites 1986 p 249-261 (For primary document see N87-10113 01-18)
Avail: CEPADUES-Editions, 111 rue Nicolas-Vauquelin, 31100 Toulouse, France

Orbit determination for near real time monitoring of satellite movement based on limited observations is discussed. For geostationary satellites this early orbit determination requirement arises after injection into geostationary transfer orbit, apogee motor firing, and larger orbit maneuvers during the on-station phase. Early orbit determination is hampered by the limited amount of data caused by nonavailability of the tracking system. Experience with the injection of nine satellites was used to derive procedures for observation scheduling, orbit determination, and estimation of achieved orbit determination accuracy. Orbit determination is performed after each new measurement in order to obtain a series of solutions which can be checked for convergence. The mode of operations is illustrated using ECS-2 tracking data. ESA

N87-10129 National Space Development Agency, Tokyo (Japan). Satellite Development Dept.
STATE/ORBIT ESTIMATION FROM REAL DOPPLER DATA FOR SOLID APOGEE MOTOR BURNING PHASE OF GEOSTATIONARY SATELLITE c13
Shuji Ono *In* CNES Proceedings of an International Conference on Space Dynamics for Geostationary Satellites 1986 p 263-288 (For primary document see N87-10113 01-18)
Avail: CEPADUES-Editions, 111 rue Nicolas-Vauquelin, 31100 Toulouse, France

Methods for the state/orbit sequential estimation from real Doppler data for the solid ABM burning phase are presented. The estimations were performed for Engineering Test Satellite 2, and for 2 satellites which both failed during this ABM phase. The state estimations were performed by deterministic and stochastic methods using real Doppler data intermittently acquired at the neighboring tracking stations. The deterministic method conquers this intermittence and estimates well the motor acceleration, but the attitude change is strongly influenced by the neighboring geometry. The stochastic Kalman sequential filter, constructed with spin dynamics considerations, conquers the intermittence and the neighboring geometry and excellently estimates the acceleration and the attitude drift due to an unbalance with reasonably converging variances. The estimated state/orbit at ABM burn out agrees well with the drift orbit and the attitude independently determined by the batch method. ESA

N87-10130 Centre National d'Etudes Spatiales, Toulouse (France).
REAL TIME ORBIT DETERMINATION DURING APOGEE MANEUVERS c13
B. Belon *In its* Proceedings of an International Conference on Space Dynamics for Geostationary Satellites 1986 p 289-300 In FRENCH; ENGLISH summary (For primary document see N87-10113 01-18)
Avail: CEPADUES-Editions, 111 rue Nicolas-Vauquelin, 31100 Toulouse, France

The use of bi-propellant thrusters, of low thrust level, for apogee boost maneuvers to determine, in real time during the thrust, the instantaneously obtained orbits is described. The accuracy of the orbit determination is sufficient to predict the optimum date of the cut off of the thruster, in order to minimize errors due to the thrust inaccuracy. The expected accuracy of such a procedure could simplify greatly the station acquisition phase, by shorter station acquisition duration; and all the maneuvers could be achieved in sight of the same stations, so the number of necessary stations could be reduced. ESA

N87-10131 Porto Univ. (Portugal). Observatorio Astronomico.
INITIAL ORBIT DETERMINATION FOR GEOSTATIONARY SATELLITES c13
I. Couto and J. Osorio *In* CNES Proceedings of an International Conference on Space Dynamics for Geostationary Satellites 1986 p 301-313 (For primary document see N87-10113 01-18)
Avail: CEPADUES-Editions, 111 rue Nicolas-Vauquelin, 31100 Toulouse, France

The efficiency of Laplace and Gauss methods for initial orbit determination is analyzed. To avoid errors in the observed directions, fictitious observational data are used and the corresponding orbit generation procedure is described. ESA

N87-10132 Indian Space Research Organization, Bangalore.
REAL TIME ORBIT AND DYNAMIC SEARCH ZONE COMPUTATIONS TO AID SATELLITE ACQUISITION IN S-BAND DURING THE LAUNCH PHASE OF GEOSYNCHRONOUS TRANSFER ORBIT (GTO) c13
V. S. Iyengar and P. Soma *In* CNES Proceedings of an International Conference on Space Dynamics for Geostationary Satellites 1986 p 315-340 (For primary document see N87-10113 01-18)
Avail: CEPADUES-Editions, 111 rue Nicolas-Vauquelin, 31100 Toulouse, France

Software for an orbit and search zone generator embedded in the antenna controller of ground stations to aid real time tracking was developed. The orbit generator was synthesized from the Unified System of Orbit Computation developed at ESOC. The search zone for the spacecraft is obtained by propagating the error covariance at initial epoch by computing the partial derivatives for a Kepler orbit. Results show that the technique is suitable for all elliptic orbits. ESA

N87-10133 Aerospace Corp., El Segundo, Calif.
ORBIT DETERMINATION OF GEOSTATIONARY SATELLITES USING THE GLOBAL POSITIONING SYSTEM c14
M. P. Ananda and P. S. Jorgensen *In* CNES Proceedings of an International Conference on Space Dynamics for Geostationary Satellites 1986 p 341-352 (For primary document see N87-10113 01-18)
Avail: CEPADUES-Editions, 111 rue Nicolas-Vauquelin, 31100 Toulouse, France

Analyses showing how the Navstar Global Positioning System (GPS) can be used to achieve accurate orbit determination of geostationary satellites are presented. Since Block 2 satellites radiate the PRN radio signals towards the Earth, for a geostationary satellite which is above the GPS satellite altitude, the GPS satellites are visible only when they are on the opposite side of the Earth. For this reason, the geostationary satellites can track only one or two GPS satellites, and on rare occasions three. Analysis show that the GPS signal, even with significant transmission loss, can be acquired with a relatively simple antenna placed on the geostationary satellite. Navigation accuracy analysis shows that the orbit determination accuracy (rms position accuracy) is in the range 100 m with 2 days of tracking. Position accuracy improves to 20 m if the geostationary satellite has a rubidium atomic clock. ESA

N87-10134 Consiglio Nazionale delle Ricerche, Pisa (Italy).
OPTICAL TRACKING OF THE SIRIO SATELLITE c13
L. Anselmo and S. Trumpy *In* CNES Proceedings of an International Conference on Space Dynamics for Geostationary Satellites 1986 p 353-361 (For primary document see N87-10113 01-18)
Avail: CEPADUES-Editions, 111 rue Nicolas-Vauquelin, 31100 Toulouse, France

The possibility to obtain a useful orbit determination for SIRIO geosynchronous satellite by optical tracking was analyzed. Accuracy achievable with one or more observatories, depending on observation precision, number, and time distribution was studied. More interesting results are attainable with optical observations massed around the equinoxes, when the Sun-Earth-spacecraft geometry allows the observation of SIRIO in reflected light, and not in diffused light as in the rest of the year. It is shown that an orbit determination accuracy comparable with that obtained during the operative life of the spacecraft is possible with a cheap observation strategy. ESA

N87-10135 Centre National d'Etudes Spatiales, Toulouse (France).
VERY FIRST ORBIT DETERMINATION AFTER LAUNCH OR MAIN MANEUVERS. APPLICATIONS TO GEOSTATIONARY TELECOM 1A AND 1B c13
F. Nouel, P. Broca, A. Guitart, R. Mesnard, and D. Zobler *In its* Proceedings of an International Conference on Space Dynamics for Geostationary Satellites 1986 p 363-374 (For primary document see N87-10113 01-18)
Avail: CEPADUES-Editions, 111 rue Nicolas-Vauquelin, 31100 Toulouse, France

The strategies adopted for estimating Telecom 1A and 1B orbit, and the accuracy reached at different epochs with various models are described. Correlations between orbit determination anomalies and events in the satellite life are shown. Results indicate that the S-band network can provide distance measurements of a precision within 10 m. But, in operation, strategies cannot be set up for reaching such a precision. A posteriori evaluations can come to that level, but after a few guesses. The needs, when operating, are not difficult to reach, given good data sets. It is always safe to rely on comparisons when estimates have to be made during the operations. ESA

N87-10136 National Aeronautics and Space Administration. Goddard Space Flight Center, Greenbelt, Md.
TRACKING AND DATA RELAY SATELLITE (TDRS) TRACKING AND ORBIT DETERMINATION
J. Teles, M. Samii, and Y. Nakai *In* CNES Proceedings of an International Conference on Space Dynamics for Geostationary Satellites 1986 p 375-391 (For primary document see N87-10113 01-18)
Avail: CEPADUES-Editions, 111 rue Nicolas-Vauquelin, 31100 Toulouse, France

Analysis results were derived using the Goddard Trajectory Determination System to determine the orbit of TDRS-East. A batch weighted least-squares algorithm is used to fit the Bilateration Ranging Transponder system tracking measurements. Six state parameters (position and velocity components) and the solar radiation pressure coefficient are estimated. The solutions are obtained by fitting the data over 34 hr arcs that overlap by 10 hr. Ephemerides are generated over the 34 hr arcs and then compared over the overlapping regions. The position differences indicate the consistency of the solutions and give a measure of their accuracy. The effect of the modeling of perturbative forces (solar radiation pressure, nonspherical geopotential field) on these results are studied. Error analysis is performed using the ORAN program to estimate the effect of force-model errors and measurement-related errors on the TDRS-East ephemeris. ESA

N87-10137 Centre National d'Etudes Spatiales, Toulouse (France).
SYNCHRONOUS TRANSFER ORBIT OPERATION UNDER THREE-AXIS CONTROL c13
John V. Brown *In its* Proceedings of an International Conference on Space Dynamics for Geostationary Satellites 1986 p 395-403 (For primary document see N87-10113 01-18)
Avail: CEPADUES-Editions, 111 rue Nicolas-Vauquelin, 31100 Toulouse, France

A mode of attitude control during the transfer orbit phase of a synchronous satellite mission was successfully demonstrated on the INSAT-1 and Arabsat missions. Three-axis attitude control during the transfer orbit and integral bipropellant propulsion were flight proven. Design considerations that lead to the approach, the sequence of events, and experience gained during the missions are described. ESA

N87-10138 Instituto de Pesquisas Espaciais, Sao Jose dos Campos (Brazil).
PARAMETER OPTIMIZATION AND ATTITUDE STABILIZATION OF A FLEXIBLE SPACECRAFT
Decio Castilho Ceballos *In* CNES Proceedings of an International Conference on Space Dynamics for Geostationary Satellites 1986 p 405-412 (For primary document see N87-10113 01-18)
Avail: CEPADUES-Editions, 111 rue Nicolas-Vauquelin, 31100 Toulouse, France

The synthesis and analysis of a control law for a flexible spacecraft are described. The control law is considered a simple proportional, integral, and derivative law together with a second order structural filter. Parameter optimization is applied for finding the controller parameters, to optimize behavior when applied to the high order model. Frequency and Laplace domain analysis which indicate the satisfactory behavior of the proposed controller are shown. ESA

N87-10139 MATRA Espace, Paris-Velizy (France).
A NEW THREE-AXIS CONTROL SYSTEM FOR A GEOSYNCHRONOUS SATELLITE IN TRANSFER ORBIT
A. Benoit *In* CNES Proceedings of an International Conference on Space Dynamics for Geostationary Satellites 1986 p 413-421 In FRENCH; ENGLISH summary (For primary document see N87-10113 01-18)
Avail: CEPADUES-Editions, 111 rue Nicolas-Vauquelin, 31100 Toulouse, France

A strategy for apogee motor reorientation maneuvers was developed for Italsat. It produced an attractive attitude and orbit control system configuration: to the operational 2-axis Earth sensor and yaw rate integrating gyrometer are only added a roll gyrometer and a 2-axis digital Sun sensor. No calibration of the gyro scale factors is required but only the compensation of their drifts, achieved through an algorithm which is presented. ESA

N87-10140 National Space Development Agency, Tokyo (Japan). Satellite Development Dept.
SPIN DYNAMICS WITH SLOSHING EFFECTS FOR SOLID MOTOR BURNING PHASE
Shuji Ono *In* CNES Proceedings of an International Conference on Space Dynamics for Geostationary Satellites 1986 p 423-443 (For primary document see N87-10113 01-18)
Avail: CEPADUES-Editions, 111 rue Nicolas-Vauquelin, 31100 Toulouse, France

The dynamics of a spinning satellite during a solid motor burn including the sloshing effects of liquid fuel within spherical tanks on board is discussed. A general equation of motion for this unsteady nonlinear phase was formulated, assuming a spherical pendulum as a sloshing model, from the development of Thomson's equation with jet damping of combustion gases. The simulated motion of the spherical pendulum shows a reasonable swirling, conjectured for the liquid motion under these circumstances. Simulations show that bad effects are non-negligible and remarkable against the spin stability and the orbit injection, in a case of moment of inertia ratio close to 1.0. ESA

N87-10141 British Aerospace Dynamics Group, Stevenage (England). Space and Communications Div.
OPERATIONAL STRATEGIES FOR MULTI-BURN APOGEE MANEUVERS OF GEOSTATIONARY SPACECRAFT
J. J. Pocha and M. C. Webber *In* CNES Proceedings of an International Conference on Space Dynamics for Geostationary Satellites 1986 p 447-455 (For primary document see N87-10113 01-18)
Avail: CEPADUES-Editions, 111 rue Nicolas-Vauquelin, 31100 Toulouse, France

Sensitivity of the apogee burn optimization strategy to launch vehicle injection dispersions; sensitivity of the design of subsequent burns to the execution errors of previous burns; and target orbits to be used for maneuver optimization are discussed. Simulations of operational scenarios indicate that the ground control center must reoptimize each maneuver in the light of on-orbit conditions to achieve the maximum spacecraft beginning-of-life mass. ESA

N87-10142 MATRA Espace, Toulouse (France).
GEOSTATIONARY SATELLITE POSITIONING WITH A RESTARTABLE MOTOR
J. Boissieres *In* CNES Proceedings of an International Conference on Space Dynamics for Geostationary Satellites 1986 p 457-474 In FRENCH; ENGLISH summary (For primary document see N87-10113 01-18)
Avail: CEPADUES-Editions, 111 rue Nicolas-Vauquelin, 31100 Toulouse, France

The positioning of a geostationary satellite with a biliquid motor is examined in a simplified manner using the impulsive approximation whose validity for the utilized low thrust level is checked. The simplified study allows the consideration of operational constraints. The obtained solution is used to initialize a numerical optimization which improves the solution locally. Optimization is done with a second order method allowing the dispersion computation around the optimal solution by covariance matrices propagation. ESA

N87-10143 European Space Agency. European Space Operations Center, Darmstadt (West Germany).
OLYMPUS: APOGEE ENGINE FIRING
R. Mugellesi and W. Flury *In* CNES Proceedings of an International Conference on Space Dynamics for Geostationary Satellites 1986 p 475-491 (For primary document see N87-10113 01-18)
Avail: CEPADUES-Editions, 111 rue Nicolas-Vauquelin, 31100 Toulouse, France

The apogee engine firing of OLYMPUS is analyzed taking into account the positioning at the on-station longitude in the geostationary orbit. One and two-burn strategies are considered for two thrust steering policies: inertially fixed thrust direction, and constant rotation of the thrust vector around a fixed axis. It is shown that the mass loss with two burns stays below 0.06% (reference = impulsive transfer). Constant rotation of the thrust vector leads to a slightly better performance than an inertially fixed thrust direction. ESA

N87-10144 Deutsche Forschungs- und Versuchsanstalt fuer Luft- und Raumfahrt, Oberpfaffenhofen (West Germany).
OPTIMAL INJECTION OF TV SAT WITH MULTI-IMPULSE APOGEE MANEUVERS WITH MISSION CONSTRAINTS AND THRUST UNCERTAINTIES
C. K. Rajasingh and A. F. Leibold *In* CNES Proceedings of an International Conference on Space Dynamics for Geostationary Satellites 1986 p 493-510 (For primary document see N87-10113 01-18)
Avail: CEPADUES-Editions, 111 rue Nicolas-Vauquelin, 31100 Toulouse, France

The method of injecting TV-SAT from an elliptical transfer orbit into a near-synchronous orbit by a liquid fuel apogee boost motor is presented. The apogee maneuver is split into three, in order to satisfy solar constraints, to reduce the long arc burning losses, and to minimize the fuel required to compensate the thrust errors (magnitude and direction). The optimal thrust direction and firing times are computed taking into consideration the finite burning times and mission constraints. The orbit resulting from the execution of three impulses, even with execution errors in thrust magnitude and direction, must lie in the optimal acquisition range, defined by a combination of deviations in longitude, apogee height and perigee heights, which require minimum fuel for fine correction maneuvers. The problem is formulated as a nonlinear optimization problem with equality and inequality constraints, and solved by a standard nonlinear parameter optimization algorithm. ESA

N87-10145 Centre National d'Etudes Spatiales, Toulouse (France).
DEFINITION OF A STRUCTURE FOR THE APOGEE THRUSTS FOR GEOSTATIONARY SATELLITE POSITIONING: APPLICATION TO TDF-1 [DEFINITION D'UNE STRUCTURE POUR LES POUSSEES D'APOGEE D'UNE MISE A POSTE D'UN SATELLITE GEOSTATIONNAIRE: APPLICATION A TDF1]
Ph. Escudier *In its* Proceedings of an International Conference on Space Dynamics for Geostationary Satellites 1986 p 511-522 In FRENCH; ENGLISH summary (For primary document see N87-10113 01-18)
Avail: CEPADUES-Editions, 111 rue Nicolas-Vauquelin, 31100 Toulouse, France

A simplified analytical formulation of the propellant cost associated with a strategy of maneuver for the station acquisition phase of a geostationary satellite is presented. This is used to select the minimum cost strategy which satisfies every possible constraint on the satellite or ground network. ESA

N87-10146 Communications Satellite Corp., Washington, D.C.
TARGETING MULTIBURN, LONG DURATION APOGEE BURST MANEUVERS
Peter C. Kammeyer *In* CNES Proceedings of an International Conference on Space Dynamics for Geostationary Satellites 1986 p 523-531 (For primary document see N87-10113 01-18)
Avail: CEPADUES-Editions, 111 rue Nicolas-Vauquelin, 31100 Toulouse, France

A method for targeting multiburn, long duration apogee boost maneuvers used during the launch of Arabsat spacecraft and proposed for spin-stabilized spacecraft is discussed. Apogee boost equations of motion give the derivatives of position, velocity, unit thrust vector, spacecraft weight, and time with respect to a function of energy. Given a starting trajectory and a firing time, the method determines a single impulse apogee boost resulting in a specified drift rate and a velocity vector with zero radial component, lying in the plane of a circular synchronous target orbit. The time and the unit thrust vector at the start of a burn are calculated by integrating backwards from the position, unit thrust vector, and time of the single impulse apogee boost originating on the preburn trajectory. Burn duration is determined by integrating forward, from the position, velocity, and weight at the starting time on the preburn trajectory, until the drift rate equals a specified value. Test cases demonstrate the effectiveness of the method. ESA

N87-10147 Centre National d'Etudes Spatiales, Toulouse (France).
ORBIT AND ATTITUDE OPERATIONS DURING THE TELECOM 1B TRANSFER PHASE
B. Belon, J. C. Berges, G. Campan, H. Donat, J. Foliard, and P. Legendre *In its* Proceedings of an International Conference on Space Dynamics for Geostationary Satellites 1986 p 535-551 In FRENCH; ENGLISH summary (For primary document see N87-10113 01-18)
Avail: CEPADUES-Editions, 111 rue Nicolas-Vauquelin, 31100 Toulouse, France

Orbit and attitude operations performed by the Maneuver Determination Center during the transfer phase of TELECOM 1-B station acquisition are summarized. Improvements for future missions, especially for TELECOM 1-C station acquisition are suggested. ESA

N87-10148 European Space Agency. European Space Operations Center, Darmstadt (West Germany).
OPERATIONAL IMPLEMENTATION OF DEORBITING MANEUVERS c13
Jozef vanderHa *In* CNES Proceedings of an International Conference on Space Dynamics for Geostationary Satellites 1986 p 553-562 (For primary document see N87-10113 01-18)
Avail: CEPADUES-Editions, 111 rue Nicolas-Vauquelin, 31100 Toulouse, France

The problem of determining the number and timing of GEOS-2 deorbiting maneuvers is addressed. Assessment of worst-case spin rate and attitude changes during the thrust periods, and the consequences thereof are stressed. Results of a semianalytical model for the long-term orbit drift motion after deorbiting are presented. ESA

N87-10149 Centre National d'Etudes Spatiales, Toulouse (France).
APPLICATION OF LINEAR PROGRAMMING TO FINAL POSITIONING (DRIFT ORBIT) OF A GEOSTATIONARY SATELLITE [APPLICATION DE LA PROGRAMMATION LINEAIRE A LA MISE A POSTE FINALE (ORBITE DE DERIVE) D'UN SATELLITE GEOSTATIONNAIRE] c13
D. Blumstein *In* CNES Proceedings of an International Conference on Space Dynamics for Geostationary Satellites 1986 p 563-572 In FRENCH; ENGLISH summary (For primary document see N87-10113 01-18)
Avail: CEPADUES-Editions, 111 rue Nicolas-Vauquelin, 31100 Toulouse, France

Utilization of linear programming to optimize the fuel consumption of station acquisition while taking sensor visibilities into account is illustrated using TDF-1. The satellite uses solar measurement during orbit maneuvers which forbids thrust at some periods (sensor visibility). Linear programming allows changes in one type of constraint to be taken into account by modifying a general algorithm which describes all possible corrections. This flexibility has no effect on rapidity of calculation. ESA

N87-10150 Instituto de Pesquisas Espaciais, Sao Jose dos Campos (Brazil).
TV-SAT FINAL ORBIT ACQUISITION OPTIMIZATION STRATEGY
Valder MatosdeMedeiros *In* CNES Proceedings of an International Conference on Space Dynamics for Geostationary Satellites 1986 p 573-586 (For primary document see N87-10113 01-18)
Avail: CEPADUES-Editions, 111 rue Nicolas-Vauquelin, 31100 Toulouse, France

A strategy for the final station acquisition for three-axis stabilized geostationary satellites with solar constraints, that affect the allowed regions where maneuvers might be performed is described. Linear programming methods to compute optimal velocity increments, times, and true longitudes for a prescribed maximum number of impulses outside the forbidden regions were developed. A strategy to get initial guesses for the position of the maneuvers is outlined. Results obtained for TV-SAT simulation are included. ESA

N87-10151 Communications Satellite Corp., Washington, D.C.
EFFICIENCY ECCENTRICITY CONTROL USING CONTINUOUS, VECTORED THRUSTING FOR SATELLITES WITH LARGE AREA/MASS RATIOS
Victor J. Slabinski *In* CNES Proceedings of an International Conference on Space Dynamics for Geostationary Satellites 1986 p 589-613 (For primary document see N87-10113 01-18)
Avail: CEPADUES-Editions, 111 rue Nicolas-Vauquelin, 31100 Toulouse, France

It is shown that varying geostationary satellite thrust direction so as to counteract only the secular perturbations from the force can reduce the impulse requirement by 6.6%. For thrusting in the orbit plane, an analytic calculus-of-variations minimization shows that the thrust direction should vary + or 19.5 deg at twice the orbit frequency, about the Sun's projection onto the orbit plane. The thrust direction then lies between the Sun's projection and the orbit tangent at the satellite. If the thrust can be vectored out of the orbit plane, the secular rotation of the orbit plane due to Sun and Moon gravity can also be countered. Minimization for this case shows that the thrust direction must oscillate approximatively + or - 26 deg about the orbit plane with the orbit frequency, in addition to the in-plane oscillation. The impulse must also be increased by a m/sec/yr, but this eliminates the need for 46 m/sec/yr of separate thrusting normal to the orbit plane for orbit plane control. ESA

N87-10152 Messerschmitt-Boelkow-Blohm G.m.b.H., Bremen (West Germany).
STATIONKEEPING FOR DFS-KOPERNIKUS
H. Klotz and R. Prigge *In* CNES Proceedings of an International Conference on Space Dynamics for Geostationary Satellites 1986 p 615-630 (For primary document see N87-10113 01-18)
Avail: CEPADUES-Editions, 111 rue Nicolas-Vauquelin, 31100 Toulouse, France

The DFS-Kopernikus satellite's mission and the attitude and orbit control sybsystem (AOCS) are described, particularly constraints imposed by the AOCS hardware on orbit correction maneuvers. The perturbation analysis includes external disturbances as well as coupling effects from north-south (NS) maneuvers into the east-west (EW) direction. Strategies are developed separately for NS and EW stationkeeping. It is shown that for DFS a one-impulse strategy can be applied for EW station keeping. The overall maneuver sequence is based on a weekly control cycle for EW maneuver and a bi-weekly cycle for NS correction. ESA

N87-10153 Deutsche Forschungs- und Versuchsanstalt fuer Luft- und Raumfahrt, Oberpfaffenhofen (West Germany).
STATIONKEEPING STRATEGY TEST, DESIGN AND OPTIMIZATION BY COMPUTER SIMULATION
M. C. Eckstein *In* CNES Proceedings of an International Conference on Space Dynamics for Geostationary Satellites 1986 p 631-677 (For primary document see N87-10113 01-18)
Avail: CEPADUES-Editions, 111 rue Nicolas-Vauquelin, 31100 Toulouse, France

A computer simulation method of stationkeeping strategy design and optimization in which orbital motion, orbital maneuvers, and all significant error types are approximated by simplified models and random generation for the entire lifetime of the satellite is described. Certain strategy parameters are iteratively optimized. Thus the simulation program allows realistic testing and optimization of proposed stationkeeping strategies. Simulation examples and results are presented. ESA

N87-10154 Centre National d'Etudes Spatiales, Toulouse (France).
STATIONKEEPING STRATEGY FOR TDF 1 SATELLITE
Fernand Alby *In its* Proceedings of an International Conference on Space Dynamics for Geostationary Satellites 1986 p 679-691 In FRENCH; ENGLISH summary (For primary document see N87-10113 01-18)
Avail: CEPADUES-Editions, 111 rue Nicolas-Vauquelin, 31100 Toulouse, France

The method used to keep TDF-1 in a + or - 0.1 deg window around the stationkeeping point located at 19 deg West longitude for 7 yr is described. Main characteristics of the satellite and constraints; tracking data; expected orbit determination accuracy; North-South stationkeeping strategy; East-West stationkeeping strategy; and cycles organization are described. ESA

N87-10155 Telesat Canada, Ottawa (Ontario).
ECCENTRICITY CONTROL STRATEGY FOR GEOSYNCHRONOUS COMMUNICATIONS SATELLITES
Dale J. Gantous *In* CNES Proceedings of an International Conference on Space Dynamics for Geostationary Satellites 1986 p 693-706 (For primary document see N87-10113 01-18)
Avail: CEPADUES-Editions, 111 rue Nicolas-Vauquelin, 31100 Toulouse, France

A method of defining a complete eccentricity control strategy for a geosynchronous communications satellite is presented. Factors affecting satellite longitude stationkeeping are defined, and eccentricity control requirements are derived. Long-term eccentricity vector motion is analyzed. The inputs required for the control strategy development are specified, including spacecraft dependent parameters, celestial forces, and their interaction. The control strategy parameters are defined, and their effects on satellite stationkeeping are illustrated. For satellites with large steady-state eccentricity motion, sun-synchronous strategy is amended to control secular growth of the eccentricity vector as well. For satellites with relatively small steady-state eccentricity motion, a separate strategy is recommended. ESA

N87-10156 Communications Satellite Corp., Washington, D.C.
LONGITUDINAL ORBIT CONTROL FROM INTELSAT 5 INCLINATION STATIONKEEPING MANEUVERS
M. P. Arluk and L. Virdee (International Telecommunications Satellite Organization, Washington, D. C.) *In* CNES Proceedings of an International Conference on Space Dynamics for Geostationary Satellites 1986 p 707-735 (For primary document see N87-10113 01-18)
Avail: CEPADUES-Editions, 111 rue Nicolas-Vauquelin, 31100 Toulouse, France

A strategy for the geosynchronous three-axis stabilized INTELSAT 5 satellite whereby the pitch attitude control thruster firings during inclination stationkeeping maneuvers are used for East-West orbit control was developed. Utilizing this strategy, longitudinal drift rate changes introduced by roll attitude control thruster firings, thruster plume impingement forces, and yaw attitude errors can be overcome to permit sufficient time for proper evaluation of the inclination maneuver before an East-West stationkeeping maneuver is required. In many instances one can achieve a significant portion of an East-West stationkeeping maneuver with these firings and decrease the number of explicit East-West stationkeeping maneuvers required for the satellite. Sources contributing to the drift rate change, the manner in which the attitude control system is configured to obtain East-West orbit control, considerations in determining the velocity change to be introduced by the attitude control thrusters, and results on INTELSAT 5 satellites are described. ESA

N87-10157 Aeroformation Blagnac (France).
ORBITOGRAPHY COURSE FOR GROUND OPERATORS
M. F. Beaudet *In* CNES Proceedings of an International Conference on Space Dynamics for Geostationary Satellites 1986 p 739-742 In FRENCH; ENGLISH summary (For primary document see N87-10113 01-18)
Avail: CEPADUES-Editions, 111 rue Nicolas-Vauquelin, 31100 Toulouse, France

The need for computer assisted instruction of geostationary satellite ground controllers is outlined. ESA

N87-10158 Centre National d'Etudes Spatiales, Toulouse (France).
OPERATIONAL PERFORMANCE OF THE INTELSAT 5 ATTITUDE DETERMINATION AND CONTROL SYSTEM
L. Virdee *In its* Proceedings of an International Conference on Space Dynamics for Geostationary Satellites 1986 p 743-764 (For primary document see N87-10113 01-18)
Avail: CEPADUES-Editions, 111 rue Nicolas-Vauquelin, 31100 Toulouse, France

The operational aspects of INTELSAT 5 attitude determination and control subsystem are presented using in-flight data obtained during the launch, the postlaunch checkout, and in-orbit phases of the mission. The in-flight data is compared with the prelaunch prediction and design data. The subsystem performs to or exceeds the requirements on all spacecraft during the transfer and geostationary operations. Significant improvements were made in the launch operations and operational on-orbit phases, where multipart stationkeeping operations are routinely carried out. ESA

N87-10159 Deutsche Forschungs- und Versuchsanstalt fuer Luft- und Raumfahrt, Oberpfaffenhofen (West Germany).
UPDATES TO OPERATIONAL PROCEDURES AS A RESULT OF IN-ORBIT EXPERIENCE WITH SYMPHONIE SPACECRAFT
H. Wobbe, P. Brittinger, and S. Arnold *In* CNES Proceedings of an International Conference on Space Dynamics for Geostationary Satellites 1986 p 765-779 (For primary document see N87-10113 01-18)
Avail: CEPADUES-Editions, 111 rue Nicolas-Vauquelin, 31100 Toulouse, France

Attitude and orbit control of SYMPHONIE satellites is described. Stability and control around the pitch axis was achieved by a fixed momentum wheel with a momentum vector parallel to the pitch axis which was the main axis of moments of inertia. A hot gas system with seven 10N thrusters (H1 to H7) was used for orbit control, H1-H4 for inclination and H5, H6 for East-West corrections. Both cold and hot gas systems consisted of 2 separate branches for redundancy purposes (H7 was only used for positioning phase). Two redundant static infrared sensors with a linear range of + or - 0.75 deg were used for nominal attitude reference measurements in roll and pitch. Three Sun sensors with + or - 60 deg field of view provided yaw reference during stationkeeping maneuvers as well as roll/yaw information in case of loss of attitude. ESA

N87-10160 MATRA Espace, Toulouse (France).
TELECOM-1 DYNAMIC SIMULATOR [SIMULATEUR DYNAMIQUE TELECOM 1]
G. Mace *In* CNES Proceedings of an International Conference on Space Dynamics for Geostationary Satellites 1986 p 781-797 In FRENCH (For primary document see N87-10113 01-18)
Avail: CEPADUES-Editions, 111 rue Nicolas-Vauquelin, 31100 Toulouse, France

The role of satellite dynamic simulators during the various stages of the satellite's life are recalled. While the benefits in terms of flight safety and personnel training are difficult to quantify, it is clear that simulation activities constitute a considerable part of satellite program budgets. It is therefore essential to ensure that the simulator chosen meets needs as regards training in procedures, understanding of operations, and validation of operations. ESA

N87-10161 MATRA Espace, Toulouse (France).
SEAGOS: A PROTOTYPE EXPERT SYSTEM TO AID GROUND OPERATORS IN SATELLITE COMMAND AND CONTROL TASKS
J. M. Darroy and C. Tessier (Office National d'Etudes et de

Recherches Aerospatiales, Toulouse (France).) *In* CNES Proceedings of an International Conference on Space Dynamics for Geostationary Satellites 1986 p 799-808 In FRENCH; ENGLISH summary (For primary document see N87-10113 01-18)
Avail: CEPADUES-Editions, 111 rue Nicolas-Vauquelin, 31100 Toulouse, France

A prototype expert system, called SEAGOS was designed to help in the management of the operational life of a geostationary telecommunication satellite TELECOM 1. A second generation SEAGOS system is under development to improve knowledge transfer from the expert designers to the satellite operators. ESA

N87-10162 Centre d'Etudes et de Recherches Geodynamiques et Astronomiques, Grasse (France).
CONSTRAINTS IMPOSED BY AN INTERSATELLITE COMMUNICATION LINK UPON STATIONKEEPING OF TWO CLOSE GEOSTATIONARY SATELLITES c13
V. Guermonprez *In* CNES Proceedings of an International Conference on Space Dynamics for Geostationary Satellites 1986 p 811-823 In FRENCH; ENGLISH summary (For primary document see N87-10113 01-18)
Avail: CEPADUES-Editions, 111 rue Nicolas-Vauquelin, 31100 Toulouse, France

Stationkeeping by two satellites located at a mean distance of 50 km from each other, with linkage antenna or telescope angular moves within + or - 11 deg maximum is examined. Procedures implemented in this particular case could be used in the resolution of other clusters. The procedures involve the translation of the constraints imposed by the intersatellite link into terms of acceptable deltas between orbital elements; and the determination of stationkeeping cycles with implementation inaccuracies staying within the acceptable deltas. ESA

N87-10163 MATRA Espace, Paris-Velizy (France).
COMPARISON OF DIFFERENT AUTONOMOUS STATIONKEEPING SYSTEMS FOR GEOSTATIONARY SATELLITES
P. Riant *In* CNES Proceedings of an International Conference on Space Dynamics for Geostationary Satellites 1986 p 825-836 In FRENCH; ENGLISH summary (For primary document see N87-10113 01-18)
Avail: CEPADUES-Editions, 111 rue Nicolas-Vauquelin, 31100 Toulouse, France

Systems for autonomous stationkeeping of geosynchronous satellites are evaluated in terms of orbit estimation accuracy, autonomy duration, and complexity of hardware and software. The navigation system uses a Kalman filter updated by optical measurements. The onboard control laws can use conventional or suboptimal station keeping strategies according to the estimation accuracy of orbital parameters. An accuracy of 10 to 20 km can be obtained simply, using a classical infrared Earth sensor and measurement of other celestial objects. The simplest solution of this type allows the estimation of the longitude only, and thus the autonomy duration is limited. To allow stationkeeping within 0.1 deg tolerance, and to control the eccentricity to a constant value of 0.0003, estimation accuracy must be reduced to a few kilometers. Two solutions are proposed. The first analyzes the whole image of the Earth. The other measures the refraction angle of light coming from known stars, and crossing Earth atmosphere. This is a more accurate way of sensing the Earth horizon. ESA

N87-10164 Societe Nationale Industrielle Aerospatiale, Cannes (France).
GEOSTATIONARY SATELLITES AUTONOMOUS STATIONKEEPING
P. Maute and F. Porte *In* CNES Proceedings of an International Conference on Space Dynamics for Geostationary Satellites 1986 p 837-862 (For primary document see N87-10113 01-18)
Avail: CEPADUES-Editions, 111 rue Nicolas-Vauquelin, 31100 Toulouse, France

Stationkeeping of a three axis stabilized satellite with conventional thrusters is described. Hardware consists of one Earth sensor, four Sun sensors, one polaris sensor, and on-board clock and computer. Software comprises one orbit determination module and a maneuver execution module. Orbit determination is performed by Kalman filtering of sensor data. The measurement vector consists of two navigation angles: Sun-S/C Earth angle (in plane information) and polaris-S/C earth angle (out of plane information). The state vector comprises the six orbit parameters and three bias parameters which need to be identified during a ground assisted calibration phase for system good performance. A control strategy to maintain the satellite within a 0.05 deg deadband was defined. Realistic execution maneuvers and orbit determination errors were considered. System performance was assessed in simulations consisting of a numerical integration orbit program generating the actual orbit and of a sensor measurements generator. ESA

N87-10165 Centre National d'Etudes Spatiales, Toulouse (France).
GEOSTATIONARY SATELLITES: THEIR MARKET, THEIR EVOLUTION IN THE 1990S [LES SATELLITES GEOSTATIONNAIRES: LEUR MARCHE, LEUR EVOLUTION DANS LA DECENNIE 90]
M. Clautrier *In its* Proceedings of an International Conference on Space Dynamics for Geostationary Satellites 1986 p 863-869 In FRENCH (For primary document see N87-10113 01-18)
Avail: CEPADUES-Editions, 111 rue Nicolas-Vauquelin, 31100 Toulouse, France

The trend towards more sophisticated geostationary satellites, e.g., featuring increased use of onboard data processing is noted. Key dates for geostationary satellite users in the 1990's, such as the introduction of new telemetry standards and the advent of Ariane 5 and the replacement for STS are discussed. The impact of fiber optics on the satellite communication market is assessed. The outlook remains optimistic, in spite of increasing competition and the worsening economic climate. ESA

N87-10166 Virginia Polytechnic Inst. and State Univ., Blacksburg.
MANEUVER AND CONTROL OF FLEXIBLE SPACECRAFT Ph.D. Thesis
Roger Dennis Quinn 1985 171 p
Avail: Univ. Microfilms Order No. DA8605456

The problem of slewing large flexible structures in space and simultaneously suppressing vibrations is considered. The equations of motion for a three-dimensional spacecraft undergoing large rigid-body maneuvers are derived. The elastic motions are assumed to remain in the linear range. A method of substructures synthesis is presented which spatially discretizes the equations of motion. A perturbation approach is used to solve the equations of motion. The zero-order equations describing the rigid-body maneuver are independent of the first-order vibration problem which includes small rigid-body motions. The vibrational problem is described by linear nonself-adjoint equations with time dependent coefficients. Minimum-time, single-axis rotational maneuvers are considered. The axis of rotation is not necessarily a principal axis. The optimal maneuver force distribution is proportional to the corresponding rigid-body modes with the mass acting as the control gain. The premaneuver eigenvectors are used as admissible vectors to reduce the degree of freedom describing the vibration of the spacecraft during the maneuver. Natural control and uniform damping control are used to suppress the vibrations during the maneuver. Actuator dynamics cause a degradation of control performance. The inclusion of the actuator dynamics in the control formulation partially offsets this effect. The performance of these control techniques is adversely affected by actuator saturation but they remain effective. Numerical results are presented for a spacecraft in orbit and in an earth-based laboratory. Dissert. Abstr.

N87-10167*# Massachusetts Inst. of Tech., Cambridge. Dept. of Aeronautics and Astronautics.
RELIABILITY ISSUES IN ACTIVE CONTROL OF LARGE FLEXIBLE SPACE STRUCTURES Semiannual Status Report, 16 May - 15 Nov. 1984
W. E. VanderVelde 15 Nov. 1984 12 p
(Grant NAG1-126)
(NASA-CR-179785; NAS 1.26:179785) Avail: NTIS

HC A02/MF A01 CSCL 22B

Progress in robust failure detection and isolation, control system reconfiguration, and performance evaluation of systems having redundancy management features is briefly summarized. B.G.

N87-10168*# Massachusetts Inst. of Tech., Cambridge. Dept. of Aeronautics and Astronautics.
CONTROL OF LARGE FLEXIBLE SPACE STRUCTURES Semiannual Status Report, 16 Nov. 1985 - 15 May 1986
W. E. VanderVelde 23 Jul. 1986 11 p
(Grant NAG1-126)
(NASA-CR-177063; NAS 1.26:177063) Avail: NTIS HC A02/MF A01 CSCL 22B

Progress in robust design of generalized parity relations, design of failure sensitive observers using the geometric system theory of Wonham, computational techniques for evaluation of the performance of control systems with fault tolerance and redundancy management features, and the design and evaluation od control systems for structures having nonlinear joints are described. B.G.

N87-10169*# Energy Science Labs., Inc., San Diego, Calif.
GUIDEBOOK FOR ANALYSIS OF TETHER APPLICATIONS Final Report
Joseph A. Carroll Mar. 1985 47 p
(Contract NAS8-35499)
(NASA-CR-178904; NAS 1.26:178904) Avail: NTIS HC A03/MF A01 CSCL 22A

This guidebook is intended as a tool to facilitate initial analyses of proposed tether applications in space. The guiding philosophy is that a brief analysis of all the common problem areas is far more useful than a detailed study in any one area. Such analyses can minimize the waste of resources on elegant but fatally flawed concepts, and can identify the areas where more effort is needed on concepts which do survive the initial analyses. The simplified formulas, approximations, and analytical tools included should be used only for preliminary analyses. For detailed analyses, the references with each topic and in the bibliography may be useful. B.G.

N87-10170*# National Aeronautics and Space Administration. Langley Research Center, Hampton, Va.
A SPACE STATION STRUCTURES AND ASSEMBLY VERIFICATION EXPERIMENT, SAVE
Richard A. Russell, J. P. Raney, and L. J. DeRyder Aug. 1986 376 p
(NASA-TM-89004; NAS 1.15:89004) Avail: NTIS HC A17/MF A01 CSCL 22B

The Space Station structure has been baselined to be a 5 M (16.4 ft) erectable truss. This structure will provide the overall framework to attach laboratory modules and other systems, subsystems and utilities. The assembly of this structure represents a formidable EVA challenge. To validate this capability the Space Station Structures/Dynamics Technical Integration Panel (TIP) met to develop the necessary data for an integrated STS structures flight experiment. As a result of this meeting, the Langley Research Center initiated a joint Langley/Boeing Aerospace Company study which supported the structures/dynamics TIP in developing the preliminary definition and design of a 5 M erectable space station truss and the resources required for a proposed flight experiment. The purpose of the study was to: (1) devise methods of truss assembly by astronauts; (2) define a specific test matrix for dynamic characterization; (3) identify instrumentation and data system requirements; (4) determine the power, propulsion and control requirements for the truss on-orbit for 3 years; (5) study the packaging of the experiment in the orbiter cargo bay; (6) prepare a preliminary cost estimate and schedule for the experiment; and (7) provide a list of potential follow-on experiments using the structure as a free flyer. The results of this three month study are presented. M.G.

N87-10171*# National Aeronautics and Space Administration, Washington, D.C.
THE NEW SPACE NETWORK: THE TRACKING AND DATA RELAY SATELLITE SYSTEM
Walter Froehlich 1986 32 p Original contains color illustrations
(NASA-EP-251; NAS 1.19:251) Avail: NTIS HC A03/MF A01 CSCL 22B

When the Tracking and Data Relay Satellite System (TDRSS) is completed, the system, together with its various NASA support elements will be known simply as the Space Networks. It will substantially increase information exchanges between low-orbiting spacecraft and the ground. The structural design, functions, earth-based links, and present and future use are discussed. B.G.

N87-10172*# Virginia Polytechnic Inst. and State Univ., Blacksburg. Dept. of Engineering Science and Mechancis.
IDENTIFICATION AND CONTROL OF STRUCTURES IN SPACE Progress Report, 1 Jul. - 31 Dec. 1985
Leonard Meirovitch 1985 42 p
(Grant NAG1-225)
(NASA-CR-179811; NAS 1.26:179811) Avail: NTIS HC A03/MF A01 CSCL 22B

Work during the period July 1 - December 31, 1985, has concentrated on the application of the equations derived in the preceding period to the maneuvering and vibration suppression of the Spacecraft Control Laboratory Experiment (SCOLE) model. Two different situations have been considered: (1) a space environment and (2) a laboratory environment. This report covers the first case and consists of a paper entitled Maneuvering and Vibration Control of Flexible Spacecraft, presented at the Workshop on Structural Dynamics and Control Interaction of Flexible Structures, Marshall Space Flight Center, Huntsville, AL, April 22 to 24, 1986. The second case will be covered in the report for the next period. Author

19 SPACECRAFT INSTRUMENTATION

For related information see also *06 Aircraft Instrumentation* and *35 Instrumentation and Photography.*

N87-10125 European Space Agency. European Space Operations Center, Darmstadt (West Germany).
COVERAGE TRANSITION TIMES OF IR PENCIL BEAM SENSORS
W. Meyer, L. Fraiture, and N. Wiengarn *In* CNES Proceedings of an International Conference on Space Dynamics for Geostationary Satellites 1986 p 207-218 (For primary document see N87-10113 01-18)
Avail: CEPADUES-Editions, 111 rue Nicolas-Vauquelin, 31100 Toulouse, France

20 SPACECRAFT PROPULSION AND POWER

Includes main propulsion systems and components, e.g., rocket engines; and spacecraft auxiliary power sources.

For related information see also *07 Aircraft Propulsion and Power, 28 Propellants and Fuels, 44 Energy Production and Conversion,* and *15 Launch Vehicles and Space Vehicles.*

N87-10173 Virginia Polytechnic Inst. and State Univ., Blacksburg.
MODELING AND ANALYSIS OF SPACECRAFT POWER SYSTEMS Ph.D. Thesis
Bo Hyung Cho 1985 187 p
Avail: Univ. Microfilms Order No. DA8605436

A Comprehensive large-scale power system modeling is developed to facilitate the design and analysis of present and future spacecraft power systems. A two-port coupling method is utilized to provide a modularity in model building and analysis of the system. The modular approach allows the model to be flexible, verifiable and computationally efficient. A methodology for the system level analysis is presented with the ability to focus on the performance characteristics of an arbitrary component or subsystem. The system performance parameters are derived explicitly in terms of the two-port hybrid g-parameter representation of the component or system, and impedances of its terminating subsystems. For this, the stability of the system is analytically determined and the subsystem interaction criteria is observed. Also presented is a model development from the empirical data employing the curve fitting technique. The technique is especially powerful for large scale system modeling and analysis where certain components and subsystems are viewed as black boxes with measurable terminal characteristics. The technique can also be used to realize a reduced order model of a complex subsystem. The Direct Energy Transfer (DET) spacecraft power system is modeled to demonstrate the versatility of the comprehensive system model by performing various D.C. small-signal and large-signal analyses. Dissert. Abstr.

N87-10174*# National Aeronautics and Space Administration. Lewis Research Center, Cleveland, Ohio.
COAXIAL TUBE TETHER/TRANSMISSION LINE FOR MANNED NUCLEAR SPACE POWER Patent Application
David J. Bents, inventor (to NASA) Filed 18 Aug. 1986 15 p
(NASA-Case-LEW-14338-1; US-Patent-Appl-SN-897239) Avail: NTIS HC A02/MF A01 CSCL 10B

A spacecraft comprising a platform, a power system and a power transmission line adapted to transmitting high voltage electrical power in a space environment is disclosed. The transmission power line tethers the suborbiting platform to the power system located in a superorbital position relative to the platform. NASA

N87-10175*# Aerojet Techsystems Co., Sacramento, Calif.
MAIN CHAMBER COMBUSTION AND COOLING TECHNOLOGY STUDY Monthly Progress Report, 3 Mar. - 6 Apr. 1986
J. VanKleeck Apr. 1986 45 p
(Contract NAS8-36167)
(NASA-CR-178853; NAS 1.26:178853; MPR-1370-M-9) Avail: NTIS HC A03/MF A01 CSCL 21H

The general objective is to evaluate and extend technology relating to the Main Combustion Assembly (MCA) of a high pressure staged combustion rocket engine operating with O2/H2 propellants. Three specific technology areas are addressed: main injector chamber improvements, main chamber blanching, and combustion stability rating techniques. B.G.

N87-10176*# Rockwell International Corp., Canoga Park, Calif. Rocketdyne Div.
COMPOSITE LOAD SPECTRA FOR SELECT SPACE PROPULSION STRUCTURAL COMPONENTS Annual Report
J. F. Newell, R. E. Kurth, and H. Ho Mar. 1986 365 p
(Contract NAS3-24382)
(NASA-CR-179496; NAS 1.26:179496; RI/RD86-123; AR-1) Avail: NTIS HC A16/MF A01 CSCL 21H

A multiyear program is performed with the objective to develop generic load models with multiple levels of progressive sophistication to simulate the composite (combined) load spectra that are induced in space propulsion system components, representative of Space Shuttle Main Engines (SSME), such as transfer ducts, turbine blades, and liquid oxygen (LOX) posts. Progress of the first year's effort includes completion of a sufficient portion of each task -- probabilistic models, code development, validation, and an initial operational code. This code has from its inception an expert system philosophy that could be added to throughout the program and in the future. The initial operational code is only applicable to turbine blade type loadings. The probabilistic model included in the operational code has fitting routines for loads that utilize a modified Discrete Probabilistic Distribution termed RASCAL, a barrier crossing method and a Monte Carlo method. An initial load model was developed by Battelle that is currently used for the slowly varying duty cycle type loading. The intent is to use the model and related codes essentially in the current form for all loads that are based on measured or calculated data that have followed a slowly varying profile. Author

N87-10021# Tokyo Univ. (Japan).
TECHNICAL OVERVIEW OF PLUME RADIATION FROM A SOLID ROCKET MOTOR
Yasushi Sakurai and Hiroshi Kimura *In its* Proceedings of the Symposium on Mechanics for Space Flight, 1985 1985 14 p
(For primary document see N87-10011 01-02)
Avail: NTIS HC A12/MF A01

23 CHEMISTRY AND MATERIALS (GENERAL)

N87-10177*# National Aeronautics and Space Administration. Lewis Research Center, Cleveland, Ohio.
BLACK-AND-WHITE PHOTOGRAPHIC CHEMISTRY: A REFERENCE
Ernie D. Walker, comp. Jun. 1986 164 p
(NASA-TM-87296; E-3006; NAS 1.15:87296) Avail: NTIS HC A08/MF A01 CSCL 14E

This work is intended as a reference of black-and-white photographic chemistry. Included is a basic history of the photographic processes and a complete description of all chemicals used, formulas for the development and fixation process, and associated formulas such as cleaners, hardeners, and toners. The work contains a complete glossary of photographic terms, a troubleshooting section listing causes and effects regarding photographic film and papers, and various conversion charts. Author

N87-10178# Lawrence Livermore National Lab., Calif.
CHEMISTRY RESEARCH RESOURCE Progress Report, Mar. 1986
Apr. 1986 87 p
(Contract W-7405-eng-48)
(DE86-009891; UCID-20622-86-3) Avail: NTIS HC A05/MF A01

Summaries are presented of projects in the following areas: synthesis of new materials, development of analytical techniques, chemical kinetics and transport processes, cryogenic and other physical properties of H isotopes, artificial intelligence, development of characterization techniques, materials modeling analysis, mechanical properties of polymers, physical metallurgy (mechanical properties, phase transformations), surface modification and surface studies, and new materials development and properties. DOE

24 COMPOSITE MATERIALS

Includes physical, chemical, and mechanical properties of laminates and other composite materials.
For ceramic materials see *27 Nonmetallic Materials.*

N87-10179*# National Aeronautics and Space Administration. Lewis Research Center, Cleveland, Ohio.
CARBIDE/FLUORIDE/SILVER SELF-LUBRICATING COMPOSITE Patent Application
Harold E. Sliney, inventor (to NASA) Filed 5 May 1986 12 p
(NASA-Case-LEW-14196-1; US-Patent-Appl-SN-859688) Avail: NTIS HC A02/MF A01 CSCL 11D

This invention relates to a self-lubricating, friction and wear reducing composite material for use over a wide temperature spectrum from cryogenic temperature to about 900 C in a chemically reactive environment. The composites are comprised of silver, barium fluoride/calcium fluoride eutectic, and bonded chromium carbide. NASA

N87-10180# British Aerospace Aircraft Group, Weybridge (England).
INVESTIGATION INTO THE ATTENUATION AND VELOCITY OF ACOUSTIC EMISSIONS IN CARBON FIBER COMPOSITE AIR-

CRAFT STRUCTURES
R. F. C. Hall Sep. 1985 99 p
(Contract A93B/1362)
(BAe-KGT-R-GEN-01349; BR97843; ETN-86-97947) Avail: NTIS HC A05/MF A01

The attenuation and propagation velocity of acoustic emission signals in carbon fiber composite honeycomb, monolithic multispar, and integral stringer type constructions were investigated. Very high attenuations are found. Variations in velocity depend on ply orientation, and the substructure arrangement. Metal substructures reduce the measured velocity compared with carbon fiber substructures. Studies which introduced a pointed brass probe used as a source of simulated emission result in a considerable decrease in the overall velocities measured. This phenomenon applies particularly to the flat plate specimens and, to a lesser extent, to the honeycomb type of structure. ESA

N87-10181# Virginia Polytechnic Inst. and State Univ., Blacksburg.
STRUCTURAL OPTIMIZATION FOR CONTROL OF STIFFENED LAMINATED COMPOSITE PLATES USING NONLINEAR MIXED INTEGER PROGRAMMING Ph.D. Thesis
Luis Clemente Mesquita 1985 150 p
Avail: Univ. Microfilms Order No. DA8605352

The effect of structural optimization on control of stiffened laminated composite structures is considered, i.e., the maximization of structural frequencies subject to maximum weight and frequency separation constraints and an upper bound on weight. The number of plies with a given orientation and the stiffener areas form the two sets of design variables. As the number of plies is restricted to integer values, the optimization problem considered belongs to the class of nonlinear mixed integer problems (NMIP). Several efficiency measures are proposed to reduce the computational cost for solution of the optimization problem. Savings in computer time is discussed. The control problem is solved using independent modal space control techniques. The latter greatly simplifies the evaluation of the sensitivity of the performance index with respect to the individual frequencies. The effect of different optimization schemes on control performance is considered. To reduce the probability that conclusions drawn from numerical results are purely coincidental, a large number of cases has been studied. Control performance improvement can be achieved via structural optimization.

N87-10182*# Sikorsky Aircraft, Stratford, Conn.
FLIGHT SERVICE EVALUATION OF COMPOSITE HELICOPTER COMPONENTS Annual Report, Oct. 1983 - Dec. 1985
George H. Mardoian and Maureen B. Ezzo Sep. 1986 66 p
(NASA-CR-178149; NAS 1.26:178149; SER-510237; AR-3) Avail: NTIS HC A04/MF A01 CSCL 11D

This report presents an assessment of composite helicopter tail rotor spars and horizontal stabilizers, exposed to the effects of the environment, after up to five and a half years of commercial service. This evaluation is supported by test results of helicopter components and panels which have been exposed to outdoor environmental effects since September 1979. Full scale static and fatigue tests have been conducted on graphite/epoxy and Kevlar/epoxy composite components obtained from Sikorsky Model S-76 helicopters in commercial operations in the Gulf Coast region of Louisiana. Small scale static and fatigue tests are being conducted on coupons obtained from panels under exposure to outdoor conditions in Stratford, Connecticut and West Palm, Florida. The panel layups are representative of the S-76 components. Additionally, this report discusses the results of moisture absorption evaluations and strength tests on the S-76 components and composite panels with up to five years of outdoor exposure. Author

N87-10183*# Virginia Polytechnic Inst. and State Univ., Blacksburg. Materials Response Group.
FATIGUE RESPONSE OF NOTCHED LAMINATES SUBJECTED TO TENSION-COMPRESSION CYCLIC LOADS Interim Report
C. E. Bakis and W. W. Stinchcomb Jun. 1986 201 p
(Grant NAG1-343)
(NASA-CR-179804; NAS 1.26:179804; CCMS-86-04) Avail: NTIS HC A10/MF A01 CSCL 11D

The fatigue response of a ((0/45/90/-45)(sub s))(sub 4) T300-5208 graphite-epoxy laminate with a drilled center-hole subjected to various components of tensile and compressive cyclic loads was investigated. Damage evaluation techniques such as stiffness monitoring, penetrant-enhanced X-ray radiography, C-scan, laminate deply and residual strength measurement were used to establish the mechanisms of damage development as well as the effect of such damage on the laminate strength, stiffness and life. Damage modes consisted of transverse matrix cracks, initiating at the hole, in all plies, followed by delamination between plies of different orientation. A characteristic stiffness repsonse during cyclic loading at two load levels was identified and utilized a more reliable indicator of material and residual properties than accumulated cycles. For the load ratios of tension-compression loading, residual tensile strength increased significantly above the virgin strength early in the fatigue life and remained approximately constant to near the end of life. A technique developed for predicting delamination initiation sites along the hole boundary correlated well with experimental evidence. Author

N87-10184*# National Aeronautics and Space Administration. Langley Research Center, Hampton, Va.
EFFECTS OF THERMAL CYCLING ON GRAPHIE-FIBER-REINFORCED 6061 ALUMINUM
Gregory A. Dries (PRC Kentron, Inc., Hampton, Va.) and Stephen S. Tompkins Oct. 1986 29 p
(NASA-TP-2612; L-16139; NAS 1.60:2612) Avail: NTIS HC A03/MF A01 CSCL 11D

Graphite-reinforced aluminum alloy metal-matrix composites are among materials being considered for structural components in dimensionally stable space structures. This application requires materials with low values of thermal expansions and high specific stiffnesses. They must remain stable during exposures to the space environment for periods extending to 20 years. The effects of thermal cycling on the thermal expansion behavior and mechanical properties of Thornel P100 graphite 6061 aluminum composites, as fabricated and after thermal processing to eliminate thermal strain hysteresis, have been investigated. Two groups of composites were studied: one was fabricated by hot roll bonding and the other by diffusion bonding. Processing significantly reduced strain hysteresis during thermal cycling in both groups and improved the ultimate tensile strength and modulus in the diffusion-bonded composites. Thermal cycling stabilized the as-fabricated composites by reducing the residual fabrication stress and increased the matrix strength by metallurgical aging. Thermal expansion behavior of both groups after processing was insensitive to thermal cycling. Data scatter was too large to determine effects of thermal cycling on the mechanical properties. The primary effects of processing and thermal cycling can be attributed to changes in the metallurgical condition and stress state of the matrix. Author

N87-10185# Sabbagh Associates, Inc., Bloomington, Ind.
AN EDDY-CURRENT MODEL FOR THREE-DIMENSIONAL NONDESTRUCTIVE EVALUATION OF ADVANCED COMPOSITES Final Report, 28 Nov. 1984 - 28 Jul. 1985
Harold A. Sabbagh, L. David Sabbagh, and Thomas M. Roberts 28 Jul. 1985 64 p
(Contract N60921-85-C-0046)
(AD-A167688; SA/TR-1/85; NSWC-TR-85-304) Avail: NTIS HC A04/MF A01 CSCL 11/4

The research problem is to devlop a model and an inversion algorithm suitable for the three-dimensional quantitative nondestructive evaluation (NDE) of advanced composite materials by using eddy currents. The technical objectives are to determine the feasibility of using multifrequencies for this job, to determine in localized regions the fiber-resin ratio in graphite epoxy, and to determine more precisely the types of anomalies, whether flaws, delaminations, broken fibers, etc., that can be reconstructed by the inversion method. These objectives are met by: (1) applying rigorous electromagnetic theory to determine a Green's function for a slab of anisotropic composite material, (2) determining the integral relations for the direct and inverse problems using the Green's function just derived, (3) determining suitable numerical algorithms for solving the inverse problem, and (4) writing a computer program to execute the model. These objectives have been met; in addition we illustrate some interesting electromagnetic phenomena in composite materials. GRA

N87-10186# Naval Postgraduate School, Monterey, Calif.
EXPERIMENTAL PROCEDURE FOR LIFETIME TESTING OF GRAPHITE BUNDLES UNDER CONSTANT LOAD M.S. Thesis
Fred D. Carozzo, Jr. Mar. 1986 50 p
(AD-A167714) Avail: NTIS HC A03/MF A01 CSCL 11/4

An experimental procedure is presented for lifetime testing of graphite bundles under constant load. The attributes of the experiment are expedience in implementation and a substantial accumulation of information equivalent to a large number of single filament tests. To achieve the objectives of the experiment a specially adapted Instron machine was used with a digital process/controller. Two trial experiments were conducted using Hercules high strength graphite. The preliminary results are presented and the effects of inter-fiber friction evaluated. GRA

25 INORGANIC AND PHYSICAL CHEMISTRY

Includes chemical analysis, e.g., chromatography; combustion theory; electrochemistry; and photochemistry.

For related information see also *77 Thermodynamics and Statistical Physics.*

N87-10187*# Old Dominion Univ., Norfolk, Va. Dept. of Mechanical Engineering.
NUMERICAL STUDY OF HYDROGEN-AIR SUPERSONIC COMBUSTION BY USING ELLIPTIC AND PARABOLIZED EQUATIONS Progress Report, 1 Dec. 1985 - 31 May 1986
31 May 1986
Tawit Chitsomboon and Surendra N. Tiwari Aug. 1986 115 p
(Grant NAG1-423)
(NASA-CR-179800; NAS 1.26:179800) Avail: NTIS HC A06/MF A01 CSCL 21B

The two-dimensional Navier-Stokes and species continuity equations are used to investigate supersonic chemically reacting flow problems which are related to scramjet-engine configurations. A global two-step finite-rate chemistry model is employed to represent the hydrogen-air combustion in the flow. An algebraic turbulent model is adopted for turbulent flow calculations. The explicit unsplit MacCormack finite-difference algorithm is used to develop a computer program suitable for a vector processing computer. The computer program developed is then used to integrate the system of the governing equations in time until convergence is attained. The chemistry source terms in the species continuity equations are evaluated implicitly to alleviate stiffness associated with fast chemical reactions. The problems solved by the elliptic code are re-investigated by using a set of two-dimensional parabolized Navier-Stokes and species equations. A linearized fully-coupled fully-implicit finite difference algorithm is used to develop a second computer code which solves the governing equations by marching in spce rather than time, resulting in a considerable saving in computer resources. Results obtained by using the parabolized formulation are compared with the results obtained by using the fully-elliptic equations. The comparisons indicate fairly good agreement of the results of the two formulations. Author

N87-10188# Los Alamos National Lab., N. Mex.
DEVELOPING SIMPLIFIED MODELS OF COMBUSTION CHEMISTRY BY SIMULATION WITH DETAILED CHEMICAL KINETICS MODELS
J. R. Creighton 13 Mar. 1986 9 p Presented at the Summer Computer Simulation Conference, Reno, Nev., 28 Jul. 1986
(Contract W-7405-eng-48)
(DE86-008381; UCRL-93614; CONF-860729-2) Avail: NTIS HC A02/MF A01

Simulations with detailed chemical kinetics mechanisms were used to develop simplified models for the oxidation of simple fuels, with emphasis on methane. The first simplification was based on the observation that the concentrations of several radical species were in steady state so that they formed a radical pool where the concentrations of pool species track one another. During the induction period these concentrations grow exponentially. Simulations showed that as concentrations grow, non-linear terms due to specific reaction steps bring the entire radical pool to steady state and that thereafter the radical pool concentration is determined by the temperature. Simulations also show that all reactions with the same initial reactant concentrations reach the same steady state regardless of initial temperature or initial radical concentration. Because the rate of heat release is a function of the radical pool concentration, the rate of temperature increase during this steady state is a function only of temperature with initial reactant concentrations as parameters. A model based on these simplifications reproduces much of the behavior of the detailed kinetics model in simulations of explosions and flames. DOE

N87-10189# Sandia National Labs., Albuquerque, N. Mex.
NUMERICAL MODEL OF THE THERMAL PROCESSES LEADING TO IGNITION IN A PYROTECHNIC DEVICE
K. G. Pierce and J. R. Leith 1986 14 p Presented at the 11th International Pyrotechnics Seminar, Vail, Colo., 7 Jul. 1986 Prepared in cooperation with New Mexico Univ., Albuquerque.
(Contract DE-AC04-76DP-00789)
(DE86-009626; SAND-85-2798C; CONF-860739-2) Avail: NTIS HC A02/MF A01

The predicted ignition behavior of a hot-wire initiated pyrotechnic device, as obtained from simple numerical models, is presented. The models are based on the heat diffusion equation with temperature dependent properties. The predictions of the model for the short-term responses of a specific pyrotechnic device are consistent with experimental results. The predictions of the long-term response differ significantly from experimental data. The causes of this difference are discussed, and a parametric study of the variables which have an effect on the ignition process is presented. DOE

N87-10190# Mississippi State Univ., Mississippi State. MHD Energy Center.
DIFFERENTIAL OPTICAL ABSORPTION TECHNIQUES FOR DIAGNOSTICS OF FOSSIL FUEL COMBUSTION Final Report, Oct. 1982 - Mar. 1986
Mar. 1986 18 p
(Contract DE-AC21-82MC-19314)
(DE86-010084; DOE/MC-19314/2046) Avail: NTIS HC A02/MF A01

The application of differential optical absorption (DOA) techniques for the in-situ determination of the chemical composition of fossil fuel combustion streams is investigated. Absorption spectra of relevant molecular species and the temperature and pressure effects on DOA-determined spectral characteristics of these species will be determined and catalogued. A system will be configured, assembled, and tested. DOE

N87-10191# Lawrence Livermore National Lab., Calif.
MICRO-TOMOGRAPHY USING SYNCHROTRON RADIATION
Q. C. Johnson, J. H. Kinney, U. Bonse, M. C. Nichols, R. Nusshardt, and J. M. Brase Apr. 1986 8 p Presented at the Materials Research Society Spring Meeting, Palo Alto, Calif., 15 Apr. 1986 Prepared in cooperation with Dortmund Univ., West Germany and Sandia National Labs., Livermore, Calif.
(Contract W-7405-eng-48)
(DE86-010982; UCRL-93538; CONF-860445-13) Avail: NTIS HC A02/MF A01

This paper discusses the results of recent experiments at Stanford Synchrotron Radiation Laboratory (SSRL) and Hamburger Synchrotronstrahlungslabor (HASYLAB) which were designed to explore the feasibility of using synchrotron radiation in high-resolution, computerized, critical-absorption tomography. The results demonstrate that it is possible, using absorption-edge differencing, to identify adjacent elements in the periodic table with high sensitivity. Furthermore, by using the fine structure in the absorption spectra, it is possible to distinguish between regions of different chemical states. Methods of using synchrotron radiation for high-resolution, three-dimensional chemical-state mapping in small samples are discussed. DOE

26 METALLIC MATERIALS

Includes physical, chemical, and mechanical properties of metals, e.g., corrosion; and metallurgy.

N87-10192*# National Aeronautics and Space Administration. Lewis Research Center, Cleveland, Ohio.
CASTABLE HOT CORROSION RESISTANT ALLOY Patent Application
Charles A. Barrett, inventor (to NASA) and William H. Holt, inventor (to NASA) Filed 30 Jul. 1986 8 p
(NASA-Case-LEW-14134-1; US-Patent-Appl-SN-890584) Avail: NTIS HC A02/MF A01 CSCL 11F

About ten weight percent nickel is added to a Fe-base ferritic alloy to improve the high temperature castability and crack resistance while about 0.2 weight percent zirconium is added for improved high temperature cyclic oxidation and corrosion resistance. The basic material is a high temperature FeCrAl heater alloy, and the addition provides a material suitable for burner rig nozzles. NASA

N87-10193# Amalgamated Technologies, Inc., Scottsdale, Ariz.
SURFACE ATTACK ON METALS IN THE PRESENCE OF LIQUID METALS Final Report
Roy E. Beal 10 Apr. 1986 132 p
(Contract N00014-85-C-0848)
(AD-A167403) Avail: NTIS HC A07/MF A01 CSCL 11/6

A study has been undertaken to evaluate liquid metals as electrical collectors in contact with solid metal alloys. Surface attack of the liquid metal on the solid metal is expected to be a major challenge to the development of a credible system. Low melting temperature metals and alloys of the fusible type are to be utilized for a collector that will operate in the 200-500 F range, with emphasis towards the lower end. Solid metals have been selected for experimental work based on their electrical properties and minimal potential reaction with the candidate liquid metal alloys. Material properties of both liquid and solid metals were reviewed to identify initial material combinations for evaluation. Thorough literature searches were conducted to obtain as much pertinent physical property and metallurgical data as possible, prior to actual experimental work. Process and material modelling was adopted to select candidate materials for both solids and liquids. Consideration of practical requirements for the eventual collectors is an integral part of the study. Work effort has concentrated on apparatus construction, evaluation and a program of testing to obtain screening data on materials selected and the chosen test method. Results have identified limitations of the test unit design and maximum current loads under test conditions with experimental current collectors. Candidate electrode materials have been exposed in low melting fusible alloys for direct dissolution data. GRA

N87-10194# TRW Materials and Mfg. Center, Euclid, Ohio.
DEVELOPMENT OF IRON ALUMINIDES Final Report, Sep. 1 981 - Nov. 1985
G. C. Culbertson and C. S. Kortovich Mar. 1986 186 p Prepared in cooperation with Systems Research Labs
(Contract F33615-81-C-5155)
(AD-A168578; ER-8215-6; AFWAL-TR-85-4155) Avail: NTIS HC A09/MF A01 CSCL 11/6

A program was conducted to develop improved iron-aluminide alloys with higher elevated temperature strength and room temperature ductility compared to the baseline Fe3Al alloy. The technical approach involved the screening evaluation of two experimental series of alloys which then formed the basis for the selection of a single alloy composition for more complete properties testing. The screening studies involved the evaluation of precipitation strengthening as well as solid solution strengthening alloy additions to the Fe3Al system. The most optimum of the precipitation strengthened alloys contained 2 a/o Nb and in the fully solution heat treated and aged condition exhibited 4 times the 600 C (1112 F) yield strength of Fe3Al, with about 60% the room temperature elongation. A negative feature of the two-phase alloys, however, was the occurrence of quench cracking, discovered during heat treatment of isothermally forged material. The most optimum of the solid solution strengthened alloys contained 3.5 Cr + 0.5 Mo (atomic percent) and exhibited 1.3 times the 600 C (1112 F) yield strength of Fe3Al, with equivalent room temperature ductility (4.8 percent elongation). Additional positive features of all the alloys were the attractive oxidation resistance compared to the Fe3Al baseline and the high degree of workability demonstrated during upset isothermal forging studies. Final alloy evaluation was conducted on Fe-35Al-4Cr-2Mo. GRA

N87-10195# Pacific Northwest Labs., Richland, Wash.
GRAIN BOUNDARY SEGREGATION AND ENVIRONMENTALLY-INDUCED FRACTURE OF MATERIALS
R. H. Jones Aug. 1985 24 p Presented at the 115th American Institute of Minining, Metallurgical and Petroleum Engineers Annual Meeting, New Orleans, La., 2 Mar. 1986
(Contract DE-AC06-76RL-01830)
(DE86-010219; PNL-SA-13067; CONF-860340-4) Avail: NTIS HC A02/MF A01

Segregation of metalloid impurities such as S, P, and Sb to grain boundaries can induce hydrogen embrittlement (HE) and intergranular stress corrosion cracking (IGSCC) of materials. Hydrogen-induced intergranular subcritical crack growth is affected by metalloid segregation with a combined impurity-hydrogen effect which follows the embrittling trend for impurity segregation in the absence of hydrogen. In Fe, S is more effective than Sb which is more effective than P. A similar relationship has been demonstrated for Ni. The role of metalloid impurity segregation in IGSCC may differ significantly from HE such that an impurity which has a small effect in HE can have a large effect in IGSCC. Sulfur and P in Ni are examples where this role reversal is observed. DOE

N87-10196# Pacific Northwest Labs., Richland, Wash.
REVIEW OF EMBRITTLEMENT MECHANISMS IN TUNGSTEN HEAVY ALLOYS
W. E. Gurwell Apr. 1986 24 p Presented at the Annual Powder Metallurgy Conference and Exhibition, Boston, Mss., 18 May 1986
(Contract DE-AC06-76RL-01830)
(DE86-011114; PNL-SA-13645; CONF-8605116-1) Avail: NTIS HC A02/MF A01

Tungsten heavy alloys compete directly with depleted uranium for applications requiring a high-density material. In some applications, such as armor-piercing projectiles, where high toughness is required, tungsten heavy alloys are perceived to suffer from generally low or inconsistent toughness. Commercial tungsten heavy alloys containing 90% to 97% tungsten are therefore liquid-phase sintered in hydrogen to full density and then annealed to reduce hydrogen embrittlement. This paper reviews published investigations of the embrittling mechanisms responsible for toughness variations in W-Ni-Fe alloys. These mechanisms include: (1) incomplete oxide reduction, (2) residual porosity, (3) increased contiguity, (4) hydrogen embrittlement, (5) impurity segregation, (6) variation in ductile-to-brittle transition temperature, (7) tungsten precipitation in the matrix, and (8) mechanical working and annealing. The general properties and fracture behavior of the alloys are outlined. Published information on embrittling mechanisms is then reviewed and integrated into a single picture. DOE

N87-10197# Sandia National Labs., Livermore, Calif.
COMPOSITIONAL AND MICROSTRUCTURAL EFFECTS ON HYDROGEN EMBRITTLEMENT OF ASTM GRADE 12 TITANIUM

(Ti 0.3 Mo - 0.8 Ni)
N. R. Moody and S. L. Robinson May 1986 41 p
(Contract DE-AC04-76DR-00789)
(DE86-011379; SAND-85-8247) Avail: NTIS HC A03/MF A01

This study characterized the effects of alloy composition, microstructure, and hydrogen on ASTM grade 12 titanium tensile properties and fracture. The effect of alloy composition on the tensile properties agreed with previous studies. Mo, Fe, and O each increased the yield and ultimate tensile strengths and the fracture stress in all heats studied. Ni had little effect on the yield and ultimate strengths but decreased the fracture stress. Mo and Fe increased ductility, whereas, Ni and O decreased it. In contrast, hydrogen increased the ultimate tensile strength but decreased the yield strength, fracture stress and ductility. The decrease in properties was independent of alloy composition. However, the amount of hydrogen-induced secondary cracking exhibited significant heat-to-heat variation which was directly related to the microstructure. These results showed that grade 12 titanium used for high-level nuclear waste storage applications should have the lowest total concentration of alloying elements required to provide adequate toughness and corrosion resistance. The alloy should also be fully annealed. The low concentration of alloying elements and a full anneal will reduce susceptibility to hydrogen embrittlement. DOE

N87-10198# Sandia National Labs., Albuquerque, N. Mex.
TRANSFORMATIONS AND NEW PHACOMP ANALYSIS IN WELD METAL OF HASTELLOY C-TYPE ALLOYS
M. J. Cieslak, T. J. Headley, and A. D. Romig, Jr. 1986 7 p
Presented at the ASM International Trends in Welding Research Meeting, Gatlinburg, Tenn., 18 May 1986
(Contract DE-AC04-76DP-00789)
(DE86-011422; SAND-85-1586C; CONF-860594-5) Avail: NTIS HC A02/MF A01

The sequence of phase transformations occurring during solidification and cooling of weld metals in the Hastelloy C family (C-4, C-22, C-276) has been determined. An equivalent component chemistry model has been defined for these alloys which allows existing Ni-Cr-Mo ternary phase diagrams to be used to predict the transformation sequence (both liquid solid and solid solid) in these complex alloys. In the cases of Alloys C-22 and C-276, the solidification events terminate with the formation of a constituent containing a topologically-close-packed (TCP) phase (sigma in C-22; P in C-276). The New PHACOMP formalism developed by Morinaga et al. for predicting TCP phase precipitation by solid state transformation in superalloys is applied for the first time to measured weld solidification segregation profiles. This formalism correctly predicts the occurrence of terminal solidification TCP phases in Alloys C-22 and C-276 and correctly predicts the absence of such phases as terminal solidification products in Alloy C-4. Implications to analysis of other nickel alloy weld metals are suggested. DOE

N87-10199# Oak Ridge National Lab., Tenn.
WELDABILITY OF AN NIAI ALLOY
M. L. Santella, S. A. David, and J. A. Horton 1986 16 p Presented at the ASM International Trends in Welding Research Meeting, Gatlinburg, Tenn., 18 May 1986
(Contract DE-AC05-84OR-21400)
(DE86-011510; CONF-860594-4) Avail: NTIS HC A02/MF A01

Since joining by conventional welding processes is an important means of fabricating structural components, weldability has become a key issue in the development of these new Ni/Al alloys. Results of an initial evaluation of the weldability of Ni/Al containing 0.1 at. % B and 0.5 at. % Hf are reported. Plates were prepared by conventional methods and used to make full penetration electron beam and gas tungsten arc welds. Initial results indicate that hafnium improves the weldability of Ni/Al alloys, although they are still susceptible to cracking. Examination of microstructures indicated that a distinct microsegregation pattern developed in the welds and affected the ordering behavior of fusion zones. Room temperature tensile testing suggested that welds can have strength and ductility values comparable to base materials, and that postweld heat treatment can improve tensile properties. DOE

N87-10200# Rheinisch Westfaelische Elektrizitaetswerke A.G., Essen (West Germany).
PROCESS FOR PREPARING NICKEL COATINGS IN CONDUCTING, POROUS BODIES, ESPECIALLY FOR BATTERY ELECTRODES
P. Faber 1986 9 p
(DE86-901439; NP-tr-6901439) Avail: NTIS HC A02/MF A01

This patent pertains to a process for preparing nickel coatings in conducting, porous bodies, especially for battery electrodes. In the process, a nickel layer is first galvanically applied on the body, characterized in that the body with its galvanic nickel layer is heated to a temperature above 200 C on the inside and a temperature below 200 C in peripheral zones by ohmic heat in a carbon monoxide atmosphere, whereby nickel is introduced as a coating from the nickel layer into the body. An electrical current is sent through the body for the ohmic heating in the direction of a longitudinal axis or a thickness axis. The body is heated under pressure. The carbon monoxide atmosphere is pressed through the body. Up to 50% hydrogen is mixed into the carbon monoxide atmosphere. Up to 10% nickel tetracarbonyl is mixed into the carbon monoxide atmosphere. DOE

N87-10201# Oak Ridge National Lab., Tenn.
DEFORMATION BEHAVIOR OF POWDER METALLURGY NI Al-Hf-B
V. K. Sikka and E. A. Loria 1986 25 p Presented at the 25th Annual Conference on Metallurgists, Toronto, Ontario, 17 Aug. |986
(Contract DE-AC05-84OR-21400)
(DE86-011508; CONF-860876-1) Avail: NTIS HC A02/MF A01

Boron-doped NiAl-Hf processed by powder metallurgy technology exhibits superplastic behavior within certain strain rates of isothermal tension and compression. A fine, equiaxed grain size provided the optimum conditions. In this investigation, that grain size was 6 m in as-extruded bar stock. The strain rate dependence of flow stress in tensile testing at 950 to 1150°C confirmed the limitations for hot working as opposed to cold working. As in other products, the P/M product shows intergranular fracture and limited ductility above 800°C under conventional strain rates. However, the results on the P/M product exhibit superplasticity (greater than 100%) in tensile testing at strain rates below 10^{-4}/s. These results provided the opportunity for fabrication by hot isothermal forging. In two different press operations, isothermal forging of small cylinders cut from as-extruded bar stock revealed no peripheral cracking via 60% compression tests at strain rates of 0.5 and 0.1/min at 1100°C. In some tests, the cylinders were compressed without cracking at a strain rate of 2 x 10-3/s, one order of magnitude faster than the optimum strain rate in tensile testing. Even though isothermal forging is possible at a strain rate as high as 1.0/min at 1100°C, both forging sources prefer a strain rate of 0.5/min for overall performance on a commercial-scale press. DOE

N87-10202# Oak Ridge National Lab., Tenn.
MODIFICATION OF THE GRAIN BOUNDARY MICROSTRUCTURE OF THE AUSTENITIC PCA STAINLESS STEEL TO IMPROVE HELIUM EMBRITTLEMENT RESISTANCE
P. J. Maziasz and D. N. Braski 1986 16 p Presented at the 2nd International Conference on Fusion Reactor Materials (ICFRM-2), Chicago, Ill., 13 Apr. 1986
(Contract DE-AC05-84OR-21400)
(DE86-010396; CONF-860421-31) Avail: NTIS HC A02/MF A01

Grain boundary MC precipitation was produced by a modified thermal-mechanical pretreatment in 25% cold worked (CW) austenitic prime candidate alloy (PCA) stainless steel prior to HFIR irradiation. Postirradiation tensile results and fracture analysis showed that the modified material (B3) resisted helium embrittlement better than either solution annealed (SA) or 25% CW PCA irradiated at 500 to 600(0)C to approx. 21 dpa and 1370 at. ppM He. PCA SA and 25% CW were not embrittled at 300 to 400(0)C.

Grain boundary MC survives in PCA-B3 during HFIR irradiation at 500(0)C but dissolves at 600(0)C; it does not form in either SA or 25% CW PCA during similar irradiation. The grain boundary MC appears to play an important role in the helium embrittlement resistance of PCA-B3. DOE

N87-10203# Maschinenfabrik Augsburg-Nuernberg A.G., Munich (West Germany). Abteilung EGT 2.
INVESTIGATIONS ON THE PARAMETERS FOR LASER SURFACE TREATMENT BY CLADDING AND ALLOYING Final Report, Dec. 1983
Welf Amende Bonn Bundesministerium fuer Forschung und Technologie Dec. 1985 85 p In GERMAN; ENGLISH summary Sponsored by Bundesministerium fuer Forschung und Technologie
(BMFT-FB-T-85-183; ISSN-0340-7608; ETN-86-97842) Avail: NTIS HC A05/MF A01; Fachinformationszentrum, Karlsruhe, West Germany DM 18

Processing of metallic surfaces with a laser beam with a power up to 5 kW was investigated. By remelting of technical alloys a remarkable grain refining is achieved. With adding alloying elements such as chromium or nickel, dense alloyed layers which are strongly connected with the bulk material are produced. At cladding the component is coated with a nonidentical material. The results for the remelting and alloying of steels, gray cast iron and aluminum are described. The cladding was performed mainly with satellite alloys. The maximum thickness of the layers is 1 mm. Special components for beam handling were developed. The technology is considered suitable for application in production lines. ESA

N87-10204*# National Academy of Sciences - National Research Council, Washington, D. C.
MICROGRAVITY SCIENCE AND APPLICATIONS Final Report
Feb. 1986 292 p Workshop held at Pasadena, Calif., 3-4 Dec. 1984 Sponsored by NASA
(Grant NSF DMR-81-19500)
(NASA-CR-179793; NAS 1.26:179793; PB86-202736) Avail: NTIS HC A13/MF A01 CSCL 11F

The report presents fifteen papers from a workshop on microgravity science and applications held at the Jet Propulsion Laboratory in Pasadena, California, on December 3 to 4, 1984. The workshop and panel were formed by the Solid State Sciences Committee of the Board on Physics and Astronomy of the National Research Council in response to a request from the Office of Science and Technology Policy. The goal was to review the microgravity science and applications (MSA) program of NASA and to evaluate the quality of the program. The topics for the papers are metals and alloys, electronic materials, ceramics and glasses, biotechnology, combustion science, and fluid dynamics. GRA

27 NONMETALLIC MATERIALS

Includes physical, chemical, and mechanical properties of plastics, elastomers, lubricants, polymers, textiles, adhesives, and ceramic materials.

For composite materials see *24 Composite Materials.*

N87-10205*# National Aeronautics and Space Administration. Ames Research Center, Moffett Field, Calif.
BORON-CONTAINING ORGANOSILANE POLYMERS AND CERAMIC MATERIALS THEREOF Patent Application
Salvatore R. Riccitiello, inventor (to NASA), Ming-ta S. Hsu, inventor (to NASA) (Chem (H. C.) Research and Service Corp., San Jose, Calif.), and Timothy S. Chan, inventor (to NASA) Filed 30 Jul. 1986 20 p
(NASA-Case-ARC-11649-1-SB; US-Patent-Appl-SN-890577) Avail: NTIS HC A02/MF A01 CSCL 11B

The present invention relates to organic silicon-boron polymers which upon pyrolysis produce high-temperature ceramic materials. More particularly, it relates to the polyorganoborosilanes containing -Si-B- bonds which generate high-temperature ceramic materials (e.g., SiC, SiB4, SiB6, B3C) upon thermal degradation. The processs for preparing these organic silicon-boron polymer precursors are also a part of this invention. M.G.

N87-10206*# National Aeronautics and Space Administration. Langley Research Center, Hampton, Va.
A METHOD OF ESTIMATING THE MOLECULAR WEIGHT OF POLYMERIC MATERIALS Patent Application
James R. Tyeryar, inventor (to NASA), Brian J. Jensen, inventor (to NASA), and Robert L. Fox, inventor (to NASA) Filed 22 Aug. 1986 14 p
(NASA-Case-LAR-13212-1; US-Patent-Appl-SN-898986) Avail: NTIS HC A02/MF A01 CSCL 11B

A rapid method to estimate the molecular weight of polymers by forming a film from the polymeric material and subjecting the newly formed film to a crease test to estimate molecular weight is disclosed. An induction heating apparatus, essentially as disclosed in U.S. Patent No. 4,521,659, is mounted in a hydraulic press. The polymeric material to be tested is placed between two sheets of high-temperature release film, which is placed between two conductive plates, which is placed between two layers of insulation to form a sandwich specimen fixture. Heat is applied rapidly to the fixture by the induction heating apparatus until a temperature above the melting point of the polymer is reached, while pressure is applied simultaneously by means of the hydraulic press. The temperature of the fixture is held constant for between one and five minutes, after which the fixture is cooled to a temperature below the glass transition temperature of the polymer, and the pressure is then released. The newly formed film is then subjected to a crease test. If the film is creaseable and not brittle, the polymer is determined to be of sufficiently high molecular weight. NASA

N87-10207# Army Natick Labs., Mass.
THE FUNGAL RESISTANCE OR SUSCEPTIBILITY OF RESINS, PLASTICIZERS, AND OTHER CONSTITUENTS OF ADHESIVE FORMULATIONS Final Report, Oct. 1983 - Sep. 1985
B. J. Wiley, D. L. Kaplan, and A. M. Kaplan Oct. 1985 52 p
(AD-A166930; NATICK/TR-86/023) Avail: NTIS HC A04/MF A01 CSCL 11/1

Studies were performed to develop a database for the microbial resistance or susceptibility of adhesives used by the military. Commercial and GSA formulations and bases were evaluated by plate testing, and this report identifies those adhesives and constituents that were resistant or susceptible within the categories that were used to classify these materials. Adhesive components were identified by the type of resin used, that is, elastomeric, thermoplastic or thermosetting, natural, etc., or as a constituent such as a plasticizer or filler, etc. Additionally, a list of biocides used for adhesives has been provided. GRA

N87-10208# Materials Research Labs., Ascot Vale (Australia).
COMPUTER ASSISTED GAS CHROMATOGRAPHY FOR THERMODYNAMIC MEASUREMENTS OF POLYMER SURFACES
P. J. C. Chappell Dec. 1985 33 p
(AD-A167450; MRL-R-982) Avail: NTIS HC A03/MF A01 CSCL 07/4

Accurate measurement of the surface thermodynamics of polymers is essential if one is to understand how polymeric fibers such as Kevlar interact with the matrix in fiber reinforced composites. The term surface thermodynamics includes quantities such as enthalpies of adsorption, entropies of absorption, absorption isotherms, surface areas and spreading pressures. Gas chromatography lends itself to the determination of these quantities because it can be carried out at low concentrations of absorbate (the infinite dilution regime), it does not need to be carried out under a vacuum, and its accuracy is as good as, or better than, the accuracy of alternate methods, e.g., calorimetry. This report documents the development of a system, based on an existing gas chromatograph and multichannel analyser, for digital acquisition and analysis of chromatographic data. A brief outline of the theory is followed by a section detailing specific requirements. The bulk of the report, describing the development of the system, follows with some results illustrating its capabilities. Finally, an extensive set of appendices gives technical details. GRA

N87-10209# Products Research and Chemical Corp., Glendale, Calif. Research and Development Lab.
POLYMER SYSTEMS FOR RAPID SEALING OF AIRCRAFT STRUCTURES AT LOW TEMPERATURE Final Report, Sep. 1981 - Aug. 1983
Lester Morris, Morris Williams, and Nicholas Champlin 1 Nov. 1985 40 p
(Contract N62269-81-C-0741; F61-542)
(AD-A167667; NADC-85158-60) Avail: NTIS HC A03/MF A01 CSCL 11/1

Materials examined for low temperature, rapid curing, fuel and water resistant sealants included hot melts, UV activated, moisture curing, and anaerobic polymers. Two component polymers utilizing urethane cures, oxidation, and mercaptan-epoxy additions were evaluated. Epoxy cures of mercaptan terminated polythioethers gave excellent low temperature cures along with practical application times. Physical and chemical properties were examined and found to essentially meet requirements of MIL-S-85420 (AS). Storage stability was excellent. GRA

N87-10210# Oak Ridge Gaseous Diffusion Plant, Tenn.
SYNTHETIC CARBON PRECURSOR MATERIALS
B. J. Frame Mar. 1986 28 p
(Contract DE-AC05-84OT-21400)
(DE86-011584; K/TS-11-796) Avail: NTIS HC A03/MF A01

Synthetic carbon precursor systems offer advantages over natural petroleum and coal-tar pitch precursors in that they can reproducibly provide a material with a known and uniform composition. They also permit controlled modifications of the derived carbon's properties through variations in the precursor's properties and processing conditions. Extensive research efforts at Oak Ridge have been directed toward the production and characterization of synthetic carbon precursors and the correlations that exist between carbon precursor properties and the properties of the ultimate carbon. This report describes how synthetic carbon precursors can be used to tailor and develop reproducible carbon structures for advanced materials applications. The potential and capability for performing carbon material development at Oak Ridge is also described. DOE

N87-10211# Midwest Research Inst., Golden, Colo. Solar Energy Research Inst.
POLYMER REFLECTORS RESEARCH DURING FISCAL YEAR 1985
P. Schissel, H. H. Neidlinger, and A. W. Czanderna May 1986 113 p
(Contract DE-AC02-83CH-10093)
(DE86-010697; SERI/PR-255-2835) Avail: NTIS HC A06/MF A01

The long-term objective of the Silvered Polymer Reflectors subtask within the SERI Solar Thermal Program is to develop silvered polymers that have a high specular reflectance, and to develop modifications of polymers that will protect the silver and maintain the reflectance in outdoor service environments for many years. The specific goals for FY 1985 were to achieve 90% specular reflectance within 7 mrad acceptance angle and to achieve ultraviolet radiation resistance that prevents detectable degradation during short-term accelerated laboratory tests. These goals set as intermediate checkpoints have been accomplished toward the long-term targets of a solar-weighted hemispherical reflectance of at least 90%, a specularity resulting 90% of the solar flux being contained within a cone angle of 4 to 10 mrad, and a useful life of at least 5 years. This document reports the progress accomplished during FY 1985. DOE

N87-10212# Missouri Univ., Kansas City.
THEORETICAL STUDIES ON THE STRUCTURES OF INSULATING AND METALLIC GLASSES Annual Progress Report, 1 Jul. 1985 - 30 Jun. 1986
W. Y. Ching Jan. 1986 14 p
(Contract DE-FG02-84ER-45170)
(DE86-011484; DOE/ER-45170/T1) Avail: NTIS HC A02/MF A01

This is the second year of a three-year project to study the electronic and structural properties of glassy systems by means of large scale theoretical calculations. The major accomplishments covered in this report are: completion of study of electronic structures of Ni sub x P sub 1-x metallic glasses; completion of the construction of periodic structural models for (NaO)(SiO) insulating glass; construction of the cannonical potentials for all the metallic elements in the periodic table with atomic number Z up to 55; initiation of electronic and magnetic property studies of some intermetallic compounds with complex structures; and implementation of a newly developed orbital-charge self-consistent procedure into the OLCAO calculation and the successful extension of the OLCAO codes to f-electron systems. DOE

N87-10213# Brookhaven National Lab., Upton, N. Y.
CHEMISORPTION MECHANISM AND EFFECT OF POLYACRYLIC ACID ON THE IMPROVEMENT IN BOND DURABILITY OF ZINC PHOSPHATE-TO-POLYMER ADHESIVE JOINTS
T. Sugama, L. E. Kukacka, N. Carciello, and J. B. Warren Jan. 1986 46 p
(Contract DE-AC02-76CH-00016)
(DE86-011535; BNL-37808) Avail: NTIS HC A03/MF A01

It has been found that the outermost surface sites of polyacrylic acid-complexed crystalline Zn x Ph layers precipitated on cold-rolled steel surfaces act significantly to promote interfacial adhesive bonding to polymeric topcoats. This is the result of electrostatic internal diffusion and segmental chemisorption mechanisms of polyelectrolyte macromolecules either on newly precipitated crystal nuclei or on crystal growth sites during the primary zinc phosphate (Zn x Ph) conversion process. The nature of the polymer-to-polymer chemical bond produced at the polymer-to-complex Zn x Ph precoat interfacial joints plays the key role in the achievement of long-term bond durability upon exposure to chemically corrosive environments. The locus of adhesive loss at the polymer-to-complex Zn x Ph joints after exposure to a hot acid solution was clearly identified to be cohesive failure in the crystalline precoat layers. A stable bond resulted from the formation of an interfacially produced hydrophobic structure by interactions between the polymer and the functional organic species existing on the complex precoat surfaces. The chemisorbed polyelectrolytes also served to chemically couple the organic coating and the inorganic Zn x Ph conversion layer. DOE

28 PROPELLANTS AND FUELS

Includes rocket propellants, igniters, and oxidizers; their storage and handling procedures; and aircraft fuels.

For related information see also *07 Aircraft Propulsion and Power, 20 Spacecraft Propulsion and Power,* and *44 Energy Production and Conversion.*

N87-10214# Naval Surface Weapons Center, Silver Spring, Md.
SYNTHESIS OF ENERGETIC MATERIALS Anual Progress Report, 1 Jan. - 31 Dec. 1985
H. G. Adolph, M. Chaykovsky, J. M. Goldwasser, and W. M. Koppes 31 Mar. 1986 48 p
(AD-A167787) Avail: NTIS HC A03/MF A01 CSCL 07/3

Investigation of the synthesis of polyformals from several nitro- and fluorodiols was continued. A new fluoropolyformal derived from 2,4,4,5,5,6,6-heptafluoro 2-trifluoromethyl 3-oxaheptane 1,7-diol was obtained. Formation of the homopolyformal of 4,4-dinitroheptane 1,7-diol was studied to assess effects of changing reaction parameters on molecular weight. Copolyformal formation was studied for several monomer (diol) pairs, especially DINOL/4,4-dinitroheptane 1,7-diol, and was demonstrated by GPC and H NMR analysis of the polymer products. Effects of varying reaction parameters and monomer ratios were investigated qualitatively.

The synthesis of the trifluoromethyl stabilized ring system of bicyclo-HMX (2,4,5,8-tetraza-bicyclooctane) was investigated and the di-, tri-, and tetranitro derivatives were prepared and characterized. The chemistry of the 2,6-diazabicyclooctane ring system was studied toward the synthesis of tetra- and hexa-substituted nitro derivatives. Several dinitro derivatives were prepared. A new reduction of nitroamides to nitramino alcohols was discovered.
Author (GRA)

N87-10215# Oak Ridge National Lab., Tenn.
PHOTOSYNTHETIC WATER SPLITTING Annual Report, 1 Mar. 1985 - 28 Feb. 1986
E. Greenbaum May 1986 27 p
(Contract DE-AC05-84OR-21400)
(DE86-010269; ORNL/TM-10018; GRI-86/0087) Avail: NTIS HC A03/MF A01

This document is an annual report prepared for the Gas Research Institute dealing with two key advances which have been made during the current reporting period. First, net thermodynamic efficiencies of the conversion of light energy into a gaseous fuel via photobiological water splitting have been measured. Based on the Gibbs free energy of hydrogen production by intact microalgae, conversion efficiencies of approx.10% have been measured in the linear, low-intensity region of the light saturation curve of photosynthesis. These are, by far, the highest conversion efficiencies reported for photobiological hydrogen production. Success in this measurement was based, in part, on a recognition of the physiological state of the algae with respect to the number of monolayers used for the measurement. Second, a key advance in biotechnology methodology has been made in the area of rapid assay and screening techniques for gaseous fuel synthesis of microalgae. Working with isolated colonies cultured on specially formulated, optically black, solid-growth media, hydrogen production by individual colonies of algae irradiated with an X-Y translatable helium-neon laser has been quantitatively measured. It is believed that this newly developed methodology represents an important instrumentational advance for applying modern techniques of genetics and molecular biology to the problem of gaseous fuel synthesis from renewable inorganic resources via microalgal water splitting. DOE

N87-10216# Los Alamos National Lab., N. Mex.
RE-EXAMINATION OF THE NEPTUNIUM-HYDROGEN SYSTEM
J. W. Ward, W. Bartscher, and J. Rebizant 1986 15 p Presented at the Properties and Applications of Metal Hydrides, Maubuisson, France, 25 May 1986 Prepared in cooperation with Commission of the European Communities, Karlsruhe, West Germany
(Contract W-7405-eng-36)
(DE86-010197; LA-UR-86-1401; CONF-8605114-1) Avail: NTIS HC A02/MF A01

New P-C-T studies have been made on the Np + H system, using ultrapure double-electrorefined metal. Measurements were carried out over six orders of magnitude in pressure, from 0.0005 to 70 bar. The solubility of hydrogen was found to be very low. Metal-dihydride plateaus were flat, the two-phase boundary extremely sharp; this occurred at the unusual value H/Np approx. = 2.13. The dihydride lattice expanded upon addition of hydrogen, also in contrast to other trivalent rare-earth and actinide hydrides. A rather narrow cubic/hexagonal two-phase region was found (only on dehydriding), together with an even narrower hexagonal phase region. The effect of the beta-gamma transition at 576°C could be seen both in the curvature of the phase boundary and the partial molal enthalpy values. Entropies of formation were found to be nearly constant. The data below 576°C can be described by the equation ln P(bar) = 13.297 - 13233/T(K), giving values, adjusted for the reaction 0.93 Np + H = 0.93 NpH/sub 2.13/: H/sub f/(NpH/sub 2.13/) = 118.3 kJ/mol (28.27 kcal/mol), and S/sub f/(NpH/sub 2.13/) = 118.4 J/mol-K (28.3 cal/mol/-K). Integral heats and entropies are calculated for the entire system, and the unusual phase behavior is discussed in terms of the electronic structure. DOE

N87-10217# Sandia National Labs., Albuquerque, N. Mex.
PERCUSSION PRIMER/DDT DETONATOR
M. R. Kopczewski and R. R. Weinmaster 1986 16 p Presented at the 11th International Pyrotechnics Seminar, Vail, Colo., 7 Jul. 1986
(Contract DE-AC04-76DP-00789)
(DE86-010477; SAND-85-2864C; CONF-860739-4) Avail: NTIS HC A02/MF A01

A detonator has been designed and tested using a commercial percussion primer as the input stimulus. The detonator uses a secondary DDT explosive to provide a detonation output. The detonator can be tailored to initiate with a range of mechanical input levels. DOE

N87-10218# Sandia National Labs., Albuquerque, N. Mex.
TITANIUM OXIDATION KINETICS AND THE MECHANISM FOR THERMAL IGNITION OF TITANIUM-BASED PYROTECHNICS
K. L. Erickson, J. W. Rogers, Jr., and S. J. Ward 1986 19 p Presented at the 11th International Pyrotechnics Seminar, Vail, Colo., 7 Jul. 1986
(Contract DE-AC04-76DP-00789)
(DE86-010987; SAND-85-2872C; CONF-860739-6) Avail: NTIS HC A02/MF A01

Previously published experimental studies proposed that thermal ignition of titanium-based pyrotechnics is controlled by the rate at which an initial oxide coating dissolves into the bulk metal as a result of molecular diffusion. The proposed dissolution mechanism was based primarily on the exotherms and ignition temperatures, which were about 793°K, observed using differential thermal methods involving heating rates of 0.33 K/s. Data from a more recent investigation of titanium oxidation kinetics at temperatures between 473 and 773°K showed that, for time scales on the order of minutes and temperatures near 773°K, pyrotechnic ignition are determined by diffusion-controlled growth of a TiO (rutile) layer adjacent to the gas-solid interface. They are not controlled by oxygen dissolution into the bulk metal. This result was based primarily on Auger depth profiles from isothermally oxidized titanium single crystals. It is further supported by the present work, in which a model for pyrotechnic response during differential thermal analysis experiments was derived using an oxidation rate expression based on growth of a TiO layer. The model predicts exotherms which are consistent with those reported in the previously published experimental studies. DOE

N87-10219# Sandia National Labs., Albuquerque, N. Mex.
CP DDT DETONATORS. 5: OUTPUT PERFORMANCE AND ANALYSIS OF MULTIPLE-OUT DEVICES
M. L. Lieberman, R. L. Hughes, and L. E. Hearnes 1986 22 p Presented at the 11th International Pyrotechnics Seminar, Vail, Colo., 7 Jul. 1986
(Contract DE-AC04-76DP-00789)
(DE86-010995; SAND-85-2814C; CONF-860739-7) Avail: NTIS HC A02/MF A01

The effects on device output of corner turning in pre- and post-detonation conditions have been evaluated via several experimental and analytical procedures for CP-loaded devices. The results imply that multiple-output detonators with designed differences in output and/or relative timing can be achieved. It has also been established that corner turning in the pre-detonation condition can be implemented in detonator designs. DOE

N87-10220# Lawrence Livermore National Lab., Calif.
CHEMISTRY AND SHOCK INITIATION OF INTERMETALLIC REACTIONS
A. P. Hardt (Lockheed Missiles and Space Co., Palo Alto, Calif.), S. L. McHugh, and S. L. Weinland 27 Mar. 1986 24 p Presented at the 11th International Pyrotechnics Seminar, Vail, Colo., 7 Jul. 1986 Prepared in cooperation with Lockheed Palo Alto Research Labs., CA.
(Contract W-7405-eng-48)
(DE86-009694; UCRL-94351; CONF-860739-3) Avail: NTIS HC A02/MF A01

Shock initiation of pyrotechnic mixtures is a relatively new discipline. In earlier studies, the estimation of the Hugoniots of porous mixtures had been described and application of experimental results to pyrotechnic mixtures was reported. In this investigation the shocked reaction mixture was recovered in order to determine whether or not reaction took place. The mixture hafnium-platinum was chosen for its low thermal initiation threshold and highly exothermic reaction. Specimens were subjected to shock in a gas gun using aluminum fliers. The product was recovered from a steel catcher and examined by metallography. The initiation threshold in terms of flier velocity was predicted from the Herrmann P- model and the initiation enthalpy. Whereas there was a distinct difference between reacted and unreacted material, it was not possible to observe a narrow initiation threshold. The reaction product was characterized by spherical micropores. DOE

N87-10221# Lawrence Livermore National Lab., Calif.

CHEMISTRY AND SHOCK INITIATION OF INTERMETALLIC REACTIONS

A. P. Hardt (Lockheed Missiles and Space Co., Palo Alto, Calif.), S. L. McHugh, and S. L. Weinland 22 Apr. 1986 22 p Presented at the 11th International Pyrotechnics Seminar, Vail, Colo., 7 Jul. 1986 Prepared in cooperation with Lawrence Livermore National Lab., CA.

(Contract W-7405-eng-48)

(DE86-010549; UCRL-94351-Rev-1; CONF-860739-3-Rev-1) Avail: NTIS HC A02/MF A01

Shock initiation of pyrotechnic mixtures is a relatively new discipline. In earlier studies, the estimation of the Hugoniots of porous mixtures had been described and application of experimental results to pyrotechnic mixtures was reported. In this investigation, the shocked reaction mixture was recovered in order to demonstrate that reaction took place. The mixture hafnium-platinum was chosen for its low thermal initiation threshold and highly exothermic reaction. Specimens were subjected to shock in a gas gun using aluminum fliers. The product was recovered from a steel catcher and examined by metallography. The initiation threshold in terms of flier velocity was predicted from the Herrmann P- model and the initiation enthalpy. Although reacted material was clearly identified, the initiation threshold was not bracketed. The reaction product, Pt Hf, was characterized by density and metallography. Although shock was shown to compact the starting mixture, the product, after melting, contained a uniform distribution of micropores. DOE

29 MATERIALS PROCESSING

Includes space-based development of products and processes for commercial applications.

For biological materials see *55 Space Biology.*

No abstracts in this category.

31 ENGINEERING (GENERAL)

Includes vacuum technology; control engineering; display engineering; cryogenics; and fire prevention.

No abstracts in this category.

32 COMMUNICATIONS AND RADAR

Includes radar; land and global communications; communications theory; and optical communications.

For related information see also *04 Aircraft Communications and Navigation* and *17 Space Communications, Spacecraft Communications, Command and Tracking.* For search and rescue see *03 Air Transportation and Safety,* and *16 Space Transportation.*

N87-10222 British Broadcasting Corp., Kingswood (England). Engineering Div.

VSB 2-PSK: A MODULATION SYSTEM FOR DIGITAL SOUND WITH TELEVISION

P. Shelswell, A. P. Robinson, R. P. Ritchie, and P. R. Durrant Aug. 1986 22 p

(BBC-RD-1986/7) Avail: BBC, Kingswood Warren, Tadworth, Surrey, Engl.

The VSB2-PSK, a modulation system suitable for the transmission of digital sound and data associated with a television signal is described. This modulation system shows good spectral efficiency and little sensitivity to the type of channel imperfections associated with typical television transmission channels. Author

N87-10223 British Broadcasting Corp., Kingswood (England). Engineering Div.

REVIEW OF VHF BAND 1 FIELD STRENGTH PREDICTION

R. S. Sandell, R. W. Lee, and J. Malcolm-Coe Jun. 1986 25 p

(BBC-RD-1986/4) Avail: BBC, Kingswood Warren, Tadworth, Surrey, England

The results of a review of Very High Frequency (VHF) Band I field strength measurements and prediction methods are described. Most of the measurements were made by the British Broadcasting Company (BBC) and many were used in the early 1960s to prepare CCIR propagation curves. Modern computational methods have permitted a fuller analysis of the data than was possible previously. This led to conculsions about the accuracy of the CCIR prediction method, how it should best be used, and the extent of discrepancies in the existing procedures. In addition, this review examines the BBC's more detailed path loss computerized prediction method. This has the potential to give more accurate results than the CCIR curves, although the program is not yet developed for operations at Band I frequencies. Finally the report makes proposals for future improvements to these prediction techniques, and considers the possibility of developing a harmonized approach. Author

N87-10224# Atomic Weapons Research Establishment, Aldermaston (England).

THEORY OF WIRE-GRID MODELLING: CRITERIA FOR HIGHLY CONDUCTING SURFACES

J. Moore Apr. 1986 36 p

(AWRE-O-20/85; BR99172; ETN-86-97997) Avail: NTIS HC A03/MF A01

The simulation of a plane solid highly conducting surface by a wire grid or mesh is considered for scattering of an electromagnetic plane wave. Mathematical conditions for equivalence are derived. Analysis relevance to the modeling of solid surfaces in any wire grid method-of-moments treatment is emphasized. ESA

N87-10225*# Illinois Univ., Urbana-Champaign. Electromagnetics Lab.

THE STUDY OF MICROSTRIP ANTENNA ARRAYS AND RELATED PROBLEMS Semiannual Report, 20 May 1985 - 25 Sep. 1986

Y. T. Lo 3 Oct. 1986 61 p

(Grant NAG3-418)

(NASA-CR-179714; NAS 1.26:179714) Avail: NTIS HC A04/MF A01 CSCL 20N

In February, an initial computer program to be used in analyzing the four-element array module was completed. This program performs the analysis of modules composed of four rectangular patches which are corporately fed by a microstrip line network terminated in four identical load impedances. Currently, a rigorous full-wave analysis of various types of microstrip line feed structures and patches is being performed. These tests include the microstrip line feed between layers of different electrical parameters. A method of moments was implemented for the case of a single dielectric layer and microstrip line fed rectangular patches in which the primary source is assumed to be a magnetic current ribbon across the line some distance from the patch. Measured values are compared with those computed by the program. B.G.

N87-10226# Martin Marietta Aerospace, Orlando, Fla. Technical Computational Center.
MODTEQ (MODULATION TECHNIQUES), AN/FRC-170(V), EQUALIZATION, AND CHANNEL MEDIUM SIMULATIONS Interim Report, 1 Dec. 1984 - 1 Dec. 1985
C. R. Gardner, Jerome J. Viviano, Randall Walker, Constance Norris, and Vince Costanza Jan. 1986 186 p
(Grant DCA100-81-G-0001)
(AD-A167965) Avail: NTIS HC A09/MF A01 CSCL 17/2

This report documents the hybrid simulations of LOS Selective Fading Channel Model, AN/FRC-170(V), Modulation Techniques and Hybrid Equalization, designed and maintained by Martin Marietta Aerospace in Orlando, Florida. Areas of special interest to this report are tasks 1 through 4 outlined in statement of work R220-85-011 as part of contract number DCA 100-81 G-0001. Those tasks include maintenance and modification to the existing hybrid simulation of the AN/FRC-170(V) DRAMA radio, modifications, additions, and enhancements to the Advanced Modulation Techniques simulation study, and development of software systems to control and monitor the various simulation models. GRA

N87-10227# Massachusetts Inst. of Tech., Lexington. Lincoln Lab.
CRAMER-RAO BOUND ANALYSIS FOR FREQUENCY ESTIMATION OF SINUSOIDS IN NOISE
Joy M. Skon 24 Mar. 1986 24 p
(Contract F19628-85-C-0002)
(AD-A167992; TR-727; ESD-TR-85-323) Avail: NTIS HC A02/MF A01 CSCL 09/3

The Cramer-Rao inequality is used to determine a lower bound on the variance with which a sinusoidal frequency can be estimated in the presence of Gaussian white noise. A parametric study has elucidated the influence of number of samples (N), sampling frequency (1/delta), phase (phi), and signal to noise ratio on the Cramer-Rao bound. A closed form expression for the asymptotic level to which the Cramer-Rao bound decays is characterized and, for low frequencies, the bound is determined analytically and graphically. The form of the Cramer-Rao bound is linked to resolution in the sampling problem. Identification of trade-offs characterizing the sensitivity of the bound and parameters associated with it are discussed. GRA

N87-10228# Los Alamos National Lab., N. Mex.
DIFFUSION APPROXIMATION FOR MODELING OF 3-D RADIATION DISTRIBUTIONS
A. Zardecki, S. A.W. Gerstl, and R. E. DeKinder, Jr. 1985 10 p Presented at the CRDC Conference, Aberdeen, Md., 17 Jun. 1985
(Contract W-7405-eng-36)
(DE86-000810; LA-UR-85-3347; CONF-8506217-2) Avail: NTIS HC A02/MF A01

A three-dimensional transport code DIF3D, based on the diffusion approximation, is used to model the spatial distribution of radiation energy arising from volumetric isotropic sources. Future work will be concerned with the determination of irradiances and modeling of realistic scenarios, relevant to the battlefield conditions. DOE

N87-10229# Oak Ridge National Lab., Tenn.
NEW SOLUTION OF THE PROBLEM OF EMP COUPLING ON CABLES OVER GROUND OF FINITE CONDUCTIVITY
D. C. Agouridis 1986 5 p Presented at the 23rd Annual Conference on Nuclear and Space Radiation Effects, Providence, R.I., 20 Jul. 1986
(Contract DE-AC05-84OR-21400)
(DE86-006078; CONF-860706-2) Avail: NTIS HC A02/MF A01

This new solution replaces Dawson's Integral, in the old solution, by an infinite series. For typical EMP parameters, the solution is approximated by a double exponential function whose numerical constants are derived. Both forms of the new solution are convenient for the calculation of the transient. DOE

N87-10230# Forschungsinstitut der Deutschen Bundespost, Darmstadt (West Germany).
HIGH SPEED DIGITAL SIGNAL TRANSMISSION OVER COAXIAL PAIRS BETWEEN NETWORK TERMINATION AND SEVERAL TERMINALS WITHOUT VARIABLE EQUALIZATION
Manfred Bertelsmeier Sep. 1985 46 p In GERMAN; ENGLISH summary
(FI-44-TBr-101; ETN-86-97825) Avail: NTIS HC A03/MF A01

It is analyzed how digital signals with a bit rate of the order of 140 Mbit/sec can be transmitted over coaxial pair cables at the subscriber's premises between the network termination and several terminals. It is assumed that variable linear filters which can be adapted to the effective line length cannot be used. This is important for a simple passive bus system. It is shown that if a receive eye opening loss of 50% is tolerated it is possible to transit 140 Mbit/sec over CCITT small coaxial pairs of lengths from 0 to 228 m. As it can be important for channel access control, the detection of superimposed pulses from different transmitters which arrive at a receiver simultaneously is also analyzed. It is proposed to lower momentarily the bit rate of the time division multiplex signal and to transmit ternary pulses. ESA

N87-10274*# Ludwig-Maximilians-Universitaet, Munich (West Germany). Meteorological Inst.
THE USEFULNESS OF KLETT'S INVERSION ALGORTHMS TO SIMULATED SATELLITE LIDAR RETURNS
M. Kastner and H. Quenzel *In* NASA. Langley Research Center 13th International Laser Radar Conference Aug. 1986 4 p (For primary document see N87-10263 01-35)
Avail: NTIS HC A15/MF A01 CSCL 17I

N87-10275*# National Aeronautics and Space Administration. Langley Research Center, Hampton, Va.
WAVELENGTH DEPENDENCE OF AEROSOL BACKSCATTER COEFFICIENTS OBTAINED BY MULTIPLE WAVELENGTH LIDAR MEASUREMENTS
Yasuhiro Sasano (Old Dominion Univ., Norfolk, Va.) and Edward V. Browell *In its* 13th International Laser Radar Conference Aug. 1986 4 p (For primary document see N87-10263 01-35)
Avail: NTIS HC A15/MF A01 CSCL 17I

N87-10276*# Research Inst. of National Defence, Linkoeping (Sweden).
EXTINCTION AND VISIBILITY MEASUREMENTS IN THE LOWER ATMOSPHERE WITH UV-YAG-LIDAR
Arne Hagard *In* NASA. Langley Research Center 13th International Laser Radar Conference Aug. 1986 2 p (For primary document see N87-10263 01-35)
Avail: NTIS HC A15/MF A01 CSCL 17I

N87-10277*# Defence Research Establishment Valcartier (Quebec).
SENSITIVITY OF THE LIDAR RATIO TO CHANGES IN SIZE DISTRIBUTION AND INDEX OF REFRACTION
B. T. N. Evans *In* NASA. Langley Research Center 13th International Laser Radar Conference Aug. 1986 3 p (For primary document see N87-10263 01-35)
Avail: NTIS HC A15/MF A01 CSCL 17I

N87-10287*# National Aeronautics and Space Administration. Langley Research Center, Hampton, Va.
INFLUENCE OF RAYLEIGH-DOPPLER BROADENING ON THE SELECTION OF H2O DIAL SYSTEM PARAMETERS
Syed Ismail and Edward V. Browell *In its* 13th International Laser

Radar Conference Aug. 1986 5 p (For primary document see N87-10263 01-35)
Avail: NTIS HC A15/MF A01 CSCL 20N

N87-10288*# Max-Planck-Inst. fuer Meteorologie, Hamburg (West Germany).
CORRECTION OF DOPPLER-BROADENED RAYLEIGH BACKSCATTERING EFFECTS IN H2O DIAL MEASUREMENTS
A. Ansmann and J. Bosenberg *In* NASA. Langley Research Center 13th International Laser Radar Conference Aug. 1986 3 p (For primary document see N87-10263 01-35)
Avail: NTIS HC A15/MF A01 CSCL 20N

N87-10294*# Atmospheric Sciences Lab., White Sands Missile Range, N. Mex.
EFFECT OF BACKSCATTER-TO-EXTINCTION RATIO ON LIDAR INVERSIONS
Edward M. Measure *In* NASA. Langley Research Center 13th International Laser Radar Conference Aug. 1986 6 p (For primary document see N87-10263 01-35)
Avail: NTIS HC A15/MF A01 CSCL 20N

N87-10295*# Optech, Inc., Downsview (Ontario).
LABORATORY MEASUREMENTS OF FORWARD AND BACKWARD SCATTERING OF LASER BEAMS IN WATER DROPLET CLOUDS
R. B. Smith, J. D. Houston, A. Ulitsky, and A. I. Carswell (York Univ., Downsview (Ontario).) *In* NASA. Langley Research Center 13th International Laser Radar Conference Aug. 1986 2 p (For primary document see N87-10263 01-35)
Avail: NTIS HC A15/MF A01 CSCL 20N

N87-10296*# National Aeronautics and Space Administration. Goddard Space Flight Center, Greenbelt, Md.
REAL-TIME ATMOSPHERIC ABSORPTION SPECTRA FOR IN-FLIGHT TUNING OF AN AIRBORNE DIAL SYSTEM
M. Dombrowski, H. Walden, G. K. Schwemmer, J. Milrod, and C. L. Korb *In* NASA. Langley Research Center 13th International Laser Radar Conference Aug. 1986 1 p (For primary document see N87-10263 01-35)
Avail: NTIS HC A15/MF A01 CSCL 20N

N87-10310*# Fraunhofer-Inst. fuer Atmosphaerische Umweltforschung, Garmisch-Partenkirchen (West Germany).
IMPROVED SOLUTION OF THE LIDAR EQUATION UTILIZING PARTICLE COUNTER MEASUREMENTS
H. Jaeger, M. Littfass, D. J. Hofmann (Wyoming Univ., Laramie.), and J. M. Rosen *In* NASA. Langley Research Center 13th International Laser Radar Conference Aug. 1986 2 p (For primary document see N87-10263 01-35)
Avail: NTIS HC A15/MF A01 CSCL 20N

N87-10315*# Florence Univ. (Italy). Dept. of Physics.
MULTIPLE SCATTERING MEASUREMENTS IN LABORATORY AND FOGGY ATMOSPHERE
P. Bruscaglioni, E. Battistelli, P. Pili, and C. Zaccanti *In* NASA. Langley Research Center 13th International Laser Radar Conference Aug. 1986 4 p (For primary document see N87-10263 01-35)
Avail: NTIS HC A15/MF A01 CSCL 20N

N87-10316*# Los Alamos National Lab., N. Mex.
MULTIPLE SCATTERING OF LASER BEAMS IN DENSE HYDROSOLS
A. Zardecki, S. A. W. Gerstl, Wesley P. Unruh, Grant H. Stokes, David M. Stupin, Norman E. Elliott, and J. A. Weinman (Wisconsin Univ., Madison.) *In* NASA. Langley Research Center 13th International Laser Radar Conference Aug. 1986 3 p (For primary document see N87-10263 01-35)
Avail: NTIS HC A15/MF A01 CSCL 20N

N87-10328*# Israel Atomic Energy Commission, Yavneh. Dept. of Atmospheric Optics.
THE EFFECT OF TURBULENCE ON LIDAR BACKSCATTERED SIGNAL FLUCTUATIONS
S. Fastig and A. Choen *In* NASA. Langley Research Center 13th International Laser Radar Conference Aug. 1986 1 p (For primary document see N87-10263 01-35)
Avail: NTIS HC A15/MF A01 CSCL 20N

N87-10350*# Utah Univ., Salt Lake City. Dept. of Meteorology.
MULTIPLE SCATTERING DEPOLARIZATION IN MARINE STRATUS CLOUDS: LIDAR EXPERIMENTS
Kenneth Sassen and Richard L. Petrilla *In* NASA. Langley Research Center 13th International Laser Radar Conference Aug. 1986 1 p (For primary document see N87-10263 01-35)
Avail: NTIS HC A15/MF A01 CSCL 20N

N87-10351*# Harry Diamond Labs., Adelphi, Md.
NEAR-IR EXTINCTION AND BACKSCATTER COEFFICIENT MEASUREMENTS IN LOW- AND MID-ALTITUDE CLOUDS
Z. G. Sztankay *In* NASA. Langley Research Center 13th International Laser Radar Conference Aug. 1986 6 p (For primary document see N87-10263 01-35)
Avail: NTIS HC A15/MF A01 CSCL 20N

N87-10352*# University Coll., Galway (Ireland). Dept. of Experimental Physics.
BACKSCATTER AND EXTINCTION MEASUREMENTS IN CLOUD AND DRIZZLE AT CO2 LASER WAVELENGTHS
S. G. Jennings *In* NASA. Langley Research Center 13th International Laser Radar Conference Aug. 1986 4 p (For primary document see N87-10263 01-35)
Avail: NTIS HC A15/MF A01 CSCL 20N

N87-10370*# National Aeronautics and Space Administration. Langley Research Center, Hampton, Va.
LINEWIDTH CHARACTERISTICS OF RAMAN-SHIFTED DYE LASER OUTPUT AT 720 AND 940 nm
B. E. Grossman, U. N. Singh (Maryland Univ. College Park), N. S. Higdon, L. J. Cotnoir, T. D. Wilkerson, and E. V. Browell *In its* 13th International Laser Radar Conference Aug. 1986 5 p (For primary document see N87-10263 01-35)
Avail: NTIS HC A15/MF A01 CSCL 20N

N87-10482*# National Oceanic and Atmospheric Administration, Boulder, Colo. Aeronomy Lab.
THE PROPOSED FLATLAND RADAR
J. L. Green, K. S. Gage, T. E. VanZandt, and G. D. Nastrom *In* International Council of Scientific Unions, Middle Atmosphere Program. Handbook for MAP, Vol. 20 Jun. 1986 5 p (For primary document see N87-10419 01-42)
Avail: NTIS HC A22/MF A01; also available from SCOSTEP Secretariat, Illinois Univ., 1406 West Green Street, Urbana, Ill. 61801 CSCL 17I

N87-10483*# National Oceanic and Atmospheric Administration, Boulder, Colo. Aeronomy Lab.
CURRENT STATUS OF THE POKER FLAT MST RADAR
B. B. Balsley *In* International Council of Scientific Unions, Middle Atmosphere Program. Handbook for MAP, Vol. 20 Jun. 1986 1 p (For primary document see N87-10419 01-42)
Avail: NTIS HC A22/MF A01; also available from SCOSTEP Secretariat, Illinois Univ., 1406 West Green Street, Urbana, Ill. 61801 CSCL 17I

N87-10485*# Illinois Univ., Urbana. Aeronomy Lab.
RECENT PROGRESS IN THE URBANA MST RADAR
S. A. Bowhill *In* International Council of Scientific Unions, Middle Atmosphere Program. Handbook for MAP, Vol. 20 Jun. 1986 1 p (For primary document see N87-10419 01-42)
Avail: NTIS HC A22/MF A01; also available from SCOSTEP Secretariat, Illinois Univ., 1406 West Green Street, Urbana, Ill. 61801 CSCL 17I

N87-10489*# Pennsylvania State Univ., University Park. Dept. of Meteorology.
THE PENN STATE DOPPLER NETWORK PROGRESS REPORT

S. R. Williams and R. Peters *In* International Council of Scientific Unions, Middle Atmosphere Program. Handbook for MAP, Vol. 20 Jun. 1986 3 p (For primary document see N87-10419 01-42)
Avail: NTIS HC A22/MF A01; also available from SCOSTEP Secretariat, Illinois Univ., 1406 West Green Street, Urbana, Ill. 61801 CSCL 17I

N87-10490*# Adelaide Univ. (Australia). Dept. of Physics.
THE ADELAIDE MF PARTIAL-REFLECTION RADAR AND VHF ST RADAR Progress Report
R. A. Vincent *In* International Council of Scientific Unions, Middle Atmosphere Program. Handbook for MAP, Vol. 20 Jun. 1986 1 p (For primary document see N87-10419 01-42)
Avail: NTIS HC A22/MF A01; also available from SCOSTEP Secretariat, Illinois Univ., 1406 West Green Street, Urbana, Ill. 61801 CSCL 17I

N87-10491*# Centre de Recherches en Physique de l'Environnement, Saint Maur des Fosses (France).
THE PROUST RADAR
F. Bertin, M. Glass, R. Ney, and M. Petitdidier *In* International Council of Scientific Unions, Middle Atmosphere Program. Handbook for MAP, Vol. 20 Jun. 1986 3 p (For primary document see N87-10419 01-42)
Avail: NTIS HC A22/MF A01; also available from SCOSTEP Secretariat, Illinois Univ., 1406 West Green Street, Urbana, Ill. 61801 CSCL 17I

N87-10492*# Toulon Univ. (France). Lab. de Sondages Electromagnetiques.
THE PROVENCE ST RADAR
M. Crochet *In* International Council of Scientific Unions, Middle Atmosphere Program. Handbook for MAP, Vol. 20 Jun. 1986 1 p (For primary document see N87-10419 01-42)
Avail: NTIS HC A22/MF A01; also available from SCOSTEP Secretariat, Illinois Univ., 1406 West Green Street, Urbana, Ill. 61801 CSCL 17I

N87-10493*# CNRM, Toulouse (France).
THE INSU AND DMN NETWORK OF ST RADARS
M. Petitdidier (Centre de Recherches en Physique de l'Environnement, Saint Maur des Fosses, France), V. Klaus, F. Baudin (Centre de Recherches en Physique de l'Environnement, Issy-les-Moulineaux, France), M. Crochet (Toulon Univ., France), G. Penazzi (Centre de Recherches en Physique de l'Environnement, Saint Maur des Fosses, France), and P. Quinty *In* International Council of Scientific Unions, Middle Atmosphere Program. Handbook for MAP, Vol. 20 Jun. 1986 2 p (For primary document see N87-10419 01-42)
Avail: NTIS HC A22/MF A01; also available from SCOSTEP Secretariat, Illinois Univ., 1406 West Green Street, Urbana, Ill. 61801 CSCL 17I

N87-10495*# National Central Univ., Chung-Li (Taiwan).
THE FIRST OPERATION AND RESULTS OF THE CHUNG-LI VHF RADAR
J. K. Chao, F. S. Kuo, Y. S. Chu, I. J. Fu, J. Rottger (Arecibo Ionospheric Observatory, Puerto Rico), and C. H. Liu (Illinois Univ., Urbana) *In* International Council of Scientific Unions, Middle Atmosphere Program. Handbook for MAP, Vol. 20 Jun. 1986 5 p (For primary document see N87-10419 01-42)
Avail: NTIS HC A22/MF A01; also available from SCOSTEP Secretariat, Illinois Univ., 1406 West Green Street, Urbana, Ill. 61801 CSCL 17I

N87-10496*# Saskatchewan Univ., Saskatoon. Dept. of Physics.
PROGRESS IN THE MF RADAR SYSTEM AT SASKATOON
C. E. Meek and A. H. Manson *In* International Council of Scientific Unions, Middle Atmosphere Program. Handbook for MAP, Vol. 20 Jun. 1986 4 p (For primary document see N87-10419 01-42)
Avail: NTIS HC A22/MF A01; also available from SCOSTEP Secretariat, Illinois Univ., 1406 West Green Street, Urbana, Ill. 61801 CSCL 17I

N87-10497*# Indian Space Research Organization, Bangalore.
SYSTEM ASPECTS OF THE INDIAN MST RADAR FACILITY
G. Viswanathan *In* International Council of Scientific Unions, Middle Atmosphere Program. Handbook for MAP, Vol. 20 Jun. 1986 6 p (For primary document see N87-10419 01-42)
Avail: NTIS HC A22/MF A01; also available from SCOSTEP Secretariat, Illinois Univ., 1406 West Green Street, Urbana, Ill. 61801 CSCL 17I

N87-10499*# National Oceanic and Atmospheric Administration, Boulder, Colo. Aeronomy Lab.
PHASED-ARRAY DESIGN FOR MST AND ST RADARS
W. L. Ecklund *In* International Council of Scientific Unions, Middle Atmosphere Program. Handbook for MAP, Vol. 20 Jun. 1986 2 p (For primary document see N87-10419 01-42)
Avail: NTIS HC A22/MF A01; also available from SCOSTEP Secretariat, Illinois Univ., 1406 West Green Street, Urbana, Ill. 61801 CSCL 17I

N87-10500*# National Oceanic and Atmospheric Administration, Boulder, Colo. Aeronomy Lab.
THE NOAA TOGA ANTENNA ARRAY
W. L. Ecklund, D. A. Carter, and B. B. Balsley *In* International Council of Scientific Unions, Middle Atmosphere Program. Handbook for MAP, Vol. 20 Jun. 1986 2 p (For primary document see N87-10419 01-42)
Avail: NTIS HC A22/MF A01; also available from SCOSTEP Secretariat, Illinois Univ., 1406 West Green Street, Urbana, Ill. 61801 CSCL 17I

N87-10501*# Illinois Univ., Urbana. Dept. of Electrical and Computer Engineering.
BEAM STEERING SYSTEM
S. A. Bowhill and K. O. Merewether *In* International Council of Scientific Unions, Middle Atmosphere Program. Handbook for MAP, Vol. 20 Jun. 1986 4 p (For primary document see N87-10419 01-42)
Avail: NTIS HC A22/MF A01; also available from SCOSTEP Secretariat, Illinois Univ., 1406 West Green Street, Urbana, Ill. 61801 CSCL 17I

N87-10503*# National Oceanic and Atmospheric Administration, Boulder, Colo. Wave Propagation Lab.
A 405-MHz, 5-BEAM PHASED ARRAY ANTENNA
Daniel C. Law *In* International Council of Scientific Unions, Middle Atmosphere Program. Handbook for MAP, Vol. 20 Jun. 1986 5 p (For primary document see N87-10419 01-42)
Avail: NTIS HC A22/MF A01; also available from SCOSTEP Secretariat, Illinois Univ., 1406 West Green Street, Urbana, Ill. 61801 CSCL 17I

N87-10504*# National Oceanic and Atmospheric Administration, Boulder, Colo. Aeronomy Lab.
LOW-ALTITUDE COVERAGE OF ST RADARS
W. L. Ecklund *In* International Council of Scientific Unions, Middle Atmosphere Program. Handbook for MAP, Vol. 20 Jun. 1986 1 p (For primary document see N87-10419 01-42)
Avail: NTIS HC A22/MF A01; also available from SCOSTEP Secretariat, Illinois Univ., 1406 West Green Street, Urbana, Ill. 61801 CSCL 17I

N87-10505*# National Oceanic and Atmospheric Administration, Boulder, Colo. Aeronomy Lab.
THE GRID ARRAY ANTENNA
W. L. Ecklund *In* International Council of Scientific Unions, Middle Atmosphere Program. Handbook for MAP, Vol. 20 Jun. 1986 1 p (For primary document see N87-10419 01-42)
Avail: NTIS HC A22/MF A01; also available from SCOSTEP Secretariat, Illinois Univ., 1406 West Green Street, Urbana, Ill. 61801 CSCL 17I

N87-10507*# Adelaide Univ. (Australia). Dept. of Physics.
MEASUREMENTS OF ANTENNA POLAR DIAGRAMS AND EFFICIENCIES USING A PHASE-SWITCHED INTERFEROME-

describing the development of the system, follows with some results illustrating its capabilities. Finally, an extensive set of appendices gives technical details. GRA

N87-10209# Products Research and Chemical Corp., Glendale, Calif. Research and Development Lab.
POLYMER SYSTEMS FOR RAPID SEALING OF AIRCRAFT STRUCTURES AT LOW TEMPERATURE Final Report, Sep. 1981 - Aug. 1983
Lester Morris, Morris Williams, and Nicholas Champlin 1 Nov. 1985 40 p
(Contract N62269-81-C-0741; F61-542)
(AD-A167667; NADC-85158-60) Avail: NTIS HC A03/MF A01 CSCL 11/1

Materials examined for low temperature, rapid curing, fuel and water resistant sealants included hot melts, UV activated, moisture curing, and anaerobic polymers. Two component polymers utilizing urethane cures, oxidation, and mercaptan-epoxy additions were evaluated. Epoxy cures of mercaptan terminated polythioethers gave excellent low temperature cures along with practical application times. Physical and chemical properties were examined and found to essentially meet requirements of MIL-S-85420 (AS). Storage stability was excellent. GRA

N87-10210# Oak Ridge Gaseous Diffusion Plant, Tenn.
SYNTHETIC CARBON PRECURSOR MATERIALS
B. J. Frame Mar. 1986 28 p
(Contract DE-AC05-84OT-21400)
(DE86-011584; K/TS-11-796) Avail: NTIS HC A03/MF A01

Synthetic carbon precursor systems offer advantages over natural petroleum and coal-tar pitch precursors in that they can reproducibly provide a material with a known and uniform composition. They also permit controlled modifications of the derived carbon's properties through variations in the precursor's properties and processing conditions. Extensive research efforts at Oak Ridge have been directed toward the production and characterization of synthetic carbon precursors and the correlations that exist between carbon precursor properties and the properties of the ultimate carbon. This report describes how synthetic carbon precursors can be used to tailor and develop reproducible carbon structures for advanced materials applications. The potential and capability for performing carbon material development at Oak Ridge is also described. DOE

N87-10211# Midwest Research Inst., Golden, Colo. Solar Energy Research Inst.
POLYMER REFLECTORS RESEARCH DURING FISCAL YEAR 1985
P. Schissel, H. H. Neidlinger, and A. W. Czanderna May 1986 113 p
(Contract DE-AC02-83CH-10093)
(DE86-010697; SERI/PR-255-2835) Avail: NTIS HC A06/MF A01

The long-term objective of the Silvered Polymer Reflectors subtask within the SERI Solar Thermal Program is to develop silvered polymers that have a high specular reflectance, and to develop modifications of polymers that will protect the silver and maintain the reflectance in outdoor service environments for many years. The specific goals for FY 1985 were to achieve 90% specular reflectance within 7 mrad acceptance angle and to achieve ultraviolet radiation resistance that prevents detectable degradation during short-term accelerated laboratory tests. These goals set as intermediate checkpoints have been accomplished toward the long-term targets of a solar-weighted hemispherical reflectance of at least 90%, a specularity resulting 90% of the solar flux being contained within a cone angle of 4 to 10 mrad, and a useful life of at least 5 years. This document reports the progress accomplished during FY 1985. DOE

N87-10212# Missouri Univ., Kansas City.
THEORETICAL STUDIES ON THE STRUCTURES OF INSULATING AND METALLIC GLASSES Annual Progress Report, 1 Jul. 1985 - 30 Jun. 1986
W. Y. Ching Jan. 1986 14 p
(Contract DE-FG02-84ER-45170)
(DE86-011484; DOE/ER-45170/T1) Avail: NTIS HC A02/MF A01

This is the second year of a three-year project to study the electronic and structural properties of glassy systems by means of large scale theoretical calculations. The major accomplishments covered in this report are: completion of study of electronic structures of Ni sub x P sub 1-x metallic glasses; completion of the construction of periodic structural models for (NaO)(SiO) insulating glass; construction of the cannonical potentials for all the metallic elements in the periodic table with atomic number Z up to 55; initiation of electronic and magnetic property studies of some intermetallic compounds with complex structures; and implementation of a newly developed orbital-charge self-consistent procedure into the OLCAO calculation and the successful extension of the OLCAO codes to f-electron systems. DOE

N87-10213# Brookhaven National Lab., Upton, N. Y.
CHEMISORPTION MECHANISM AND EFFECT OF POLYACRYLIC ACID ON THE IMPROVEMENT IN BOND DURABILITY OF ZINC PHOSPHATE-TO-POLYMER ADHESIVE JOINTS
T. Sugama, L. E. Kukacka, N. Carciello, and J. B. Warren Jan. 1986 46 p
(Contract DE-AC02-76CH-00016)
(DE86-011535; BNL-37808) Avail: NTIS HC A03/MF A01

It has been found that the outermost surface sites of polyacrylic acid-complexed crystalline Zn x Ph layers precipitated on cold-rolled steel surfaces act significantly to promote interfacial adhesive bonding to polymeric topcoats. This is the result of electrostatic internal diffusion and segmental chemisorption mechanisms of polyelectrolyte macromolecules either on newly precipitated crystal nuclei or on crystal growth sites during the primary zinc phosphate (Zn x Ph) conversion process. The nature of the polymer-to-polymer chemical bond produced at the polymer-to-complex Zn x Ph precoat interfacial joints plays the key role in the achievement of long-term bond durability upon exposure to chemically corrosive environments. The locus of adhesive loss at the polymer-to-complex Zn x Ph joints after exposure to a hot acid solution was clearly identified to be cohesive failure in the crystalline precoat layers. A stable bond resulted from the formation of an interfacially produced hydrophobic structure by interactions between the polymer and the functional organic species existing on the complex precoat surfaces. The chemisorbed polyelectrolytes also served to chemically couple the organic coating and the inorganic Zn x Ph conversion layer. DOE

28 PROPELLANTS AND FUELS

Includes rocket propellants, igniters, and oxidizers; their storage and handling procedures; and aircraft fuels.

For related information see also *07 Aircraft Propulsion and Power, 20 Spacecraft Propulsion and Power,* and *44 Energy Production and Conversion.*

N87-10214# Naval Surface Weapons Center, Silver Spring, Md.
SYNTHESIS OF ENERGETIC MATERIALS Anual Progress Report, 1 Jan. - 31 Dec. 1985
H. G. Adolph, M. Chaykovsky, J. M. Goldwasser, and W. M. Koppes 31 Mar. 1986 48 p
(AD-A167787) Avail: NTIS HC A03/MF A01 CSCL 07/3

Investigation of the synthesis of polyformals from several nitro- and fluorodiols was continued. A new fluoropolyformal derived from 2,4,4,5,5,6,6-heptafluoro 2-trifluoromethyl 3-oxaheptane 1,7-diol was obtained. Formation of the homopolyformal of 4,4-dinitroheptane 1,7-diol was studied to assess effects of changing reaction parameters on molecular weight. Copolyformal formation was studied for several monomer (diol) pairs, especially DINOL/4,4-dinitroheptane 1,7-diol, and was demonstrated by GPC and H NMR analysis of the polymer products. Effects of varying reaction parameters and monomer ratios were investigated qualitatively.

The synthesis of the trifluoromethyl stabilized ring system of bicyclo-HMX (2,4,5,8-tetraza-bicyclooctane) was investigated and the di-, tri-, and tetranitro derivatives were prepared and characterized. The chemistry of the 2,6-diazabicyclooctane ring system was studied toward the synthesis of tetra- and hexa-substituted nitro derivatives. Several dinitro derivatives were prepared. A new reduction of nitroamides to nitramino alcohols was discovered.
Author (GRA)

N87-10215# Oak Ridge National Lab., Tenn.
PHOTOSYNTHETIC WATER SPLITTING Annual Report, 1 Mar. 1985 - 28 Feb. 1986
E. Greenbaum May 1986 27 p
(Contract DE-AC05-84OR-21400)
(DE86-010269; ORNL/TM-10018; GRI-86/0087) Avail: NTIS HC A03/MF A01

This document is an annual report prepared for the Gas Research Institute dealing with two key advances which have been made during the current reporting period. First, net thermodynamic efficiencies of the conversion of light energy into a gaseous fuel via photobiological water splitting have been measured. Based on the Gibbs free energy of hydrogen production by intact microalgae, conversion efficiencies of approx.10% have been measured in the linear, low-intensity region of the light saturation curve of photosynthesis. These are, by far, the highest conversion efficiencies reported for photobiological hydrogen production. Success in this measurement was based, in part, on a recognition of the physiological state of the algae with respect to the number of monolayers used for the measurement. Second, a key advance in biotechnology methodology has been made in the area of rapid assay and screening techniques for gaseous fuel synthesis of microalgae. Working with isolated colonies cultured on specially formulated, optically black, solid-growth media, hydrogen production by individual colonies of algae irradiated with an X-Y translatable helium-neon laser has been quantitatively measured. It is believed that this newly developed methodology represents an important instrumentational advance for applying modern techniques of genetics and molecular biology to the problem of gaseous fuel synthesis from renewable inorganic resources via microalgal water splitting. DOE

N87-10216# Los Alamos National Lab., N. Mex.
RE-EXAMINATION OF THE NEPTUNIUM-HYDROGEN SYSTEM
J. W. Ward, W. Bartscher, and J. Rebizant 1986 15 p Presented at the Properties and Applications of Metal Hydrides, Maubuisson, France, 25 May 1986 Prepared in cooperation with Commission of the European Communities, Karlsruhe, West Germany
(Contract W-7405-eng-36)
(DE86-010197; LA-UR-86-1401; CONF-8605114-1) Avail: NTIS HC A02/MF A01

New P-C-T studies have been made on the Np + H system, using ultrapure double-electrorefined metal. Measurements were carried out over six orders of magnitude in pressure, from 0.0005 to 70 bar. The solubility of hydrogen was found to be very low. Metal-dihydride plateaus were flat, the two-phase boundary extremely sharp; this occurred at the unusual value H/Np approx. = 2.13. The dihydride lattice expanded upon addition of hydrogen, also in contrast to other trivalent rare-earth and actinide hydrides. A rather narrow cubic/hexagonal two-phase region was found (only on dehydriding), together with an even narrower hexagonal phase region. The effect of the beta-gamma transition at 576°C could be seen both in the curvature of the phase boundary and the partial molal enthalpy values. Entropies of formation were found to be nearly constant. The data below 576°C can be described by the equation ln P(bar) = 13.297 - 13233/T(K), giving values, adjusted for the reaction 0.93 Np + H = 0.93 NpH/sub 2.13/: H/sub f/(NpH/sub 2.13/) = 118.3 kJ/mol (28.27 kcal/mol), and S/sub f/(NpH/sub 2.13/) = 118.4 J/mol-K (28.3 cal/mol/-K). Integral heats and entropies are calculated for the entire system, and the unusual phase behavior is discussed in terms of the electronic structure. DOE

N87-10217# Sandia National Labs., Albuquerque, N. Mex.
PERCUSSION PRIMER/DDT DETONATOR
M. R. Kopczewski and R. R. Weinmaster 1986 16 p Presented at the 11th International Pyrotechnics Seminar, Vail, Colo., 7 Jul. 1986
(Contract DE-AC04-76DP-00789)
(DE86-010477; SAND-85-2864C; CONF-860739-4) Avail: NTIS HC A02/MF A01

A detonator has been designed and tested using a commercial percussion primer as the input stimulus. The detonator uses a secondary DDT explosive to provide a detonation output. The detonator can be tailored to initiate with a range of mechanical input levels. DOE

N87-10218# Sandia National Labs., Albuquerque, N. Mex.
TITANIUM OXIDATION KINETICS AND THE MECHANISM FOR THERMAL IGNITION OF TITANIUM-BASED PYROTECHNICS
K. L. Erickson, J. W. Rogers, Jr., and S. J. Ward 1986 19 p Presented at the 11th International Pyrotechnics Seminar, Vail, Colo., 7 Jul. 1986
(Contract DE-AC04-76DP-00789)
(DE86-010987; SAND-85-2872C; CONF-860739-6) Avail: NTIS HC A02/MF A01

Previously published experimental studies proposed that thermal ignition of titanium-based pyrotechnics is controlled by the rate at which an initial oxide coating dissolves into the bulk metal as a result of molecular diffusion. The proposed dissolution mechanism was based primarily on the exotherms and ignition temperatures, which were about 793°K, observed using differential thermal methods involving heating rates of 0.33 K/s. Data from a more recent investigation of titanium oxidation kinetics at temperatures between 473 and 773°K showed that, for time scales on the order of minutes and temperatures near 773°K, pyrotechnic ignition are determined by diffusion-controlled growth of a TiO (rutile) layer adjacent to the gas-solid interface. They are not controlled by oxygen dissolution into the bulk metal. This result was based primarily on Auger depth profiles from isothermally oxidized titanium single crystals. It is further supported by the present work, in which a model for pyrotechnic response during differential thermal analysis experiments was derived using an oxidation rate expression based on growth of a TiO layer. The model predicts exotherms which are consistent with those reported in the previously published experimental studies. DOE

N87-10219# Sandia National Labs., Albuquerque, N. Mex.
CP DDT DETONATORS. 5: OUTPUT PERFORMANCE AND ANALYSIS OF MULTIPLE-OUT DEVICES
M. L. Lieberman, R. L. Hughes, and L. E. Heames 1986 22 p Presented at the 11th International Pyrotechnics Seminar, Vail, Colo., 7 Jul. 1986
(Contract DE-AC04-76DP-00789)
(DE86-010995; SAND-85-2814C; CONF-860739-7) Avail: NTIS HC A02/MF A01

The effects on device output of corner turning in pre- and post-detonation conditions have been evaluated via several experimental and analytical procedures for CP-loaded devices. The results imply that multiple-output detonators with designed differences in output and/or relative timing can be achieved. It has also been established that corner turning in the pre-detonation condition can be implemented in detonator designs. DOE

N87-10220# Lawrence Livermore National Lab., Calif.
CHEMISTRY AND SHOCK INITIATION OF INTERMETALLIC REACTIONS
A. P. Hardt (Lockheed Missiles and Space Co., Palo Alto, Calif.), S. L. McHugh, and S. L. Weinland 27 Mar. 1986 24 p Presented at the 11th International Pyrotechnics Seminar, Vail, Colo., 7 Jul. 1986 Prepared in cooperation with Lockheed Palo Alto Research Labs., CA.
(Contract W-7405-eng-48)
(DE86-009694; UCRL-94351; CONF-860739-3) Avail: NTIS HC A02/MF A01

Shock initiation of pyrotechnic mixtures is a relatively new discipline. In earlier studies, the estimation of the Hugoniots of porous mixtures had been described and application of experimental results to pyrotechnic mixtures was reported. In this investigation the shocked reaction mixture was recovered in order to determine whether or not reaction took place. The mixture hafnium-platinum was chosen for its low thermal initiation threshold and highly exothermic reaction. Specimens were subjected to shock in a gas gun using aluminum fliers. The product was recovered from a steel catcher and examined by metallography. The initiation threshold in terms of flier velocity was predicted from the Herrmann P- model and the initiation enthalpy. Whereas there was a distinct difference between reacted and unreacted material, it was not possible to observe a narrow initiation threshold. The reaction product was characterized by spherical micropores. DOE

N87-10221# Lawrence Livermore National Lab., Calif.
CHEMISTRY AND SHOCK INITIATION OF INTERMETALLIC REACTIONS
A. P. Hardt (Lockheed Missiles and Space Co., Palo Alto, Calif.), S. L. McHugh, and S. L. Weinland 22 Apr. 1986 22 p Presented at the 11th International Pyrotechnics Seminar, Vail, Colo., 7 Jul. 1986 Prepared in cooperation with Lawrence Livermore National Lab., CA.
(Contract W-7405-eng-48)
(DE86-010549; UCRL-94351-Rev-1; CONF-860739-3-Rev-1) Avail: NTIS HC A02/MF A01

Shock initiation of pyrotechnic mixtures is a relatively new discipline. In earlier studies, the estimation of the Hugoniots of porous mixtures had been described and application of experimental results to pyrotechnic mixtures was reported. In this investigation, the shocked reaction mixture was recovered in order to demonstrate that reaction took place. The mixture hafnium-platinum was chosen for its low thermal initiation threshold and highly exothermic reaction. Specimens were subjected to shock in a gas gun using aluminum fliers. The product was recovered from a steel catcher and examined by metallography. The initiation threshold in terms of flier velocity was predicted from the Herrmann P- model and the initiation enthalpy. Although reacted material was clearly identified, the initiation threshold was not bracketed. The reaction product, Pt Hf, was characterized by density and metallography. Although shock was shown to compact the starting mixture, the product, after melting, contained a uniform distribution of micropores. DOE

29 MATERIALS PROCESSING

Includes space-based development of products and processes for commercial applications.

For biological materials see *55 Space Biology.*

No abstracts in this category.

31 ENGINEERING (GENERAL)

Includes vacuum technology; control engineering; display engineering; cryogenics; and fire prevention.

No abstracts in this category.

32 COMMUNICATIONS AND RADAR

Includes radar; land and global communications; communications theory; and optical communications.

For related information see also *04 Aircraft Communications and Navigation* and *17 Space Communications, Spacecraft Communications, Command and Tracking.* For search and rescue see *03 Air Transportation and Safety,* and *16 Space Transportation.*

N87-10222 British Broadcasting Corp., Kingswood (England). Engineering Div.
VSB 2-PSK: A MODULATION SYSTEM FOR DIGITAL SOUND WITH TELEVISION
P. Shelswell, A. P. Robinson, R. P. Ritchie, and P. R. Durrant Aug. 1986 22 p
(BBC-RD-1986/7) Avail: BBC, Kingswood Warren, Tadworth, Surrey, Engl.

The VSB2-PSK, a modulation system suitable for the transmission of digital sound and data associated with a television signal is described. This modulation system shows good spectral efficiency and little sensitivity to the type of channel imperfections associated with typical television transmission channels. Author

N87-10223 British Broadcasting Corp., Kingswood (England). Engineering Div.
REVIEW OF VHF BAND 1 FIELD STRENGTH PREDICTION
R. S. Sandell, R. W. Lee, and J. Malcolm-Coe Jun. 1986 25 p
(BBC-RD-1986/4) Avail: BBC, Kingswood Warren, Tadworth, Surrey, England

The results of a review of Very High Frequency (VHF) Band I field strength measurements and prediction methods are described. Most of the measurements were made by the British Broadcasting Company (BBC) and many were used in the early 1960s to prepare CCIR propagation curves. Modern computational methods have permitted a fuller analysis of the data than was possible previously. This led to conclusions about the accuracy of the CCIR prediction method, how it should best be used, and the extent of discrepancies in the existing procedures. In addition, this review examines the BBC's more detailed path loss computerized prediction method. This has the potential to give more accurate results than the CCIR curves, although the program is not yet developed for operations at Band I frequencies. Finally the report makes proposals for future improvements to these prediction techniques, and considers the possibility of developing a harmonized approach. Author

N87-10224# Atomic Weapons Research Establishment, Aldermaston (England).
THEORY OF WIRE-GRID MODELLING: CRITERIA FOR HIGHLY CONDUCTING SURFACES
J. Moore Apr. 1986 36 p
(AWRE-O-20/85; BR99172; ETN-86-97997) Avail: NTIS HC A03/MF A01

The simulation of a plane solid highly conducting surface by a wire grid or mesh is considered for scattering of an electromagnetic plane wave. Mathematical conditions for equivalence are derived. Analysis relevance to the modeling of solid surfaces in any wire grid method-of-moments treatment is emphasized. ESA

N87-10225*# Illinois Univ., Urbana-Champaign. Electromagnetics Lab.
THE STUDY OF MICROSTRIP ANTENNA ARRAYS AND RELATED PROBLEMS Semiannual Report, 20 May 1985 - 25 Sep. 1986
Y. T. Lo 3 Oct. 1986 61 p
(Grant NAG3-418)
(NASA-CR-179714; NAS 1.26:179714) Avail: NTIS HC A04/MF A01 CSCL 20N

In February, an initial computer program to be used in analyzing the four-element array module was completed. This program performs the analysis of modules composed of four rectangular patches which are corporately fed by a microstrip line network terminated in four identical load impedances. Currently, a rigorous full-wave analysis of various types of microstrip line feed structures and patches is being performed. These tests include the microstrip line feed between layers of different electrical parameters. A method of moments was implemented for the case of a single dielectric layer and microstrip line fed rectangular patches in which the primary source is assumed to be a magnetic current ribbon across the line some distance from the patch. Measured values are compared with those computed by the program. B.G.

N87-10226# Martin Marietta Aerospace, Orlando, Fla. Technical Computational Center.
MODTEQ (MODULATION TECHNIQUES), AN/FRC-170(V), EQUALIZATION, AND CHANNEL MEDIUM SIMULATIONS Interim Report, 1 Dec. 1984 - 1 Dec. 1985
C. R. Gardner, Jerome J. Viviano, Randall Walker, Constance Norris, and Vince Costanza Jan. 1986 186 p
(Grant DCA100-81-G-0001)
(AD-A167965) Avail: NTIS HC A09/MF A01 CSCL 17/2

This report documents the hybrid simulations of LOS Selective Fading Channel Model, AN/FRC-170(V), Modulation Techniques and Hybrid Equalization, designed and maintained by Martin Marietta Aerospace in Orlando, Florida. Areas of special interest to this report are tasks 1 through 4 outlined in statement of work R220-85-011 as part of contract number DCA 100-81 G-0001. Those tasks include maintenance and modification to the existing hybrid simulation of the AN/FRC-170(V) DRAMA radio, modifications, additions, and enhancements to the Advanced Modulation Techniques simulation study, and development of software systems to control and monitor the various simulation models. GRA

N87-10227# Massachusetts Inst. of Tech., Lexington. Lincoln Lab.
CRAMER-RAO BOUND ANALYSIS FOR FREQUENCY ESTIMATION OF SINUSOIDS IN NOISE
Joy M. Skon 24 Mar. 1986 24 p
(Contract F19628-85-C-0002)
(AD-A167992; TR-727; ESD-TR-85-323) Avail: NTIS HC A02/MF A01 CSCL 09/3

The Cramer-Rao inequality is used to determine a lower bound on the variance with which a sinusoidal frequency can be estimated in the presence of Gaussian white noise. A parametric study has elucidated the influence of number of samples (N), sampling frequency (1/delta), phase (phi), and signal to noise ratio on the Cramer-Rao bound. A closed form expression for the asymptotic level to which the Cramer-Rao bound decays is characterized and, for low frequencies, the bound is determined analytically and graphically. The form of the Cramer-Rao bound is linked to resolution in the sampling problem. Identification of trade-offs characterizing the sensitivity of the bound and parameters associated with it are discussed. GRA

N87-10228# Los Alamos National Lab., N. Mex.
DIFFUSION APPROXIMATION FOR MODELING OF 3-D RADIATION DISTRIBUTIONS
A. Zardecki, S. A.W. Gerstl, and R. E. DeKinder, Jr. 1985 10 p Presented at the CRDC Conference, Aberdeen, Md., 17 Jun. 1985
(Contract W-7405-eng-36)
(DE86-000810; LA-UR-85-3347; CONF-8506217-2) Avail: NTIS HC A02/MF A01

A three-dimensional transport code DIF3D, based on the diffusion approximation, is used to model the spatial distribution of radiation energy arising from volumetric isotropic sources. Future work will be concerned with the determination of irradiances and modeling of realistic scenarios, relevant to the battlefield conditions. DOE

N87-10229# Oak Ridge National Lab., Tenn.
NEW SOLUTION OF THE PROBLEM OF EMP COUPLING ON CABLES OVER GROUND OF FINITE CONDUCTIVITY
D. C. Agouridis 1986 5 p Presented at the 23rd Annual Conference on Nuclear and Space Radiation Effects, Providence, R.I., 20 Jul. 1986
(Contract DE-AC05-84OR-21400)
(DE86-006078; CONF-860706-2) Avail: NTIS HC A02/MF A01

This new solution replaces Dawson's Integral, in the old solution, by an infinite series. For typical EMP parameters, the solution is approximated by a double exponential function whose numerical constants are derived. Both forms of the new solution are convenient for the calculation of the transient. DOE

N87-10230# Forschungsinstitut der Deutschen Bundespost, Darmstadt (West Germany).
HIGH SPEED DIGITAL SIGNAL TRANSMISSION OVER COAXIAL PAIRS BETWEEN NETWORK TERMINATION AND SEVERAL TERMINALS WITHOUT VARIABLE EQUALIZATION
Manfred Bertelsmeier Sep. 1985 46 p In GERMAN; ENGLISH summary
(FI-44-TBr-101; ETN-86-97825) Avail: NTIS HC A03/MF A01

It is analyzed how digital signals with a bit rate of the order of 140 Mbit/sec can be transmitted over coaxial pair cables at the subscriber's premises between the network termination and several terminals. It is assumed that variable linear filters which can be adapted to the effective line length cannot be used. This is important for a simple passive bus system. It is shown that if a receive eye opening loss of 50% is tolerated it is possible to transit 140 Mbit/sec over CCITT small coaxial pairs of lengths from 0 to 228 m. As it can be important for channel access control, the detection of superimposed pulses from different transmitters which arrive at a receiver simultaneously is also analyzed. It is proposed to lower momentarily the bit rate of the time division multiplex signal and to transmit ternary pulses. ESA

N87-10274*# Ludwig-Maximilians-Universitaet, Munich (West Germany). Meteorological Inst.
THE USEFULNESS OF KLETT'S INVERSION ALGORTHMS TO SIMULATED SATELLITE LIDAR RETURNS
M. Kastner and H. Quenzel *In* NASA. Langley Research Center 13th International Laser Radar Conference Aug. 1986 4 p (For primary document see N87-10263 01-35)
Avail: NTIS HC A15/MF A01 CSCL 17I

N87-10275*# National Aeronautics and Space Administration. Langley Research Center, Hampton, Va.
WAVELENGTH DEPENDENCE OF AEROSOL BACKSCATTER COEFFICIENTS OBTAINED BY MULTIPLE WAVELENGTH LIDAR MEASUREMENTS
Yasuhiro Sasano (Old Dominion Univ., Norfolk, Va.) and Edward V. Browell *In its* 13th International Laser Radar Conference Aug. 1986 4 p (For primary document see N87-10263 01-35)
Avail: NTIS HC A15/MF A01 CSCL 17I

N87-10276*# Research Inst. of National Defence, Linkoeping (Sweden).
EXTINCTION AND VISIBILITY MEASUREMENTS IN THE LOWER ATMOSPHERE WITH UV-YAG-LIDAR
Arne Hagard *In* NASA. Langley Research Center 13th International Laser Radar Conference Aug. 1986 2 p (For primary document see N87-10263 01-35)
Avail: NTIS HC A15/MF A01 CSCL 17I

N87-10277*# Defence Research Establishment Valcartier (Quebec).
SENSITIVITY OF THE LIDAR RATIO TO CHANGES IN SIZE DISTRIBUTION AND INDEX OF REFRACTION
B. T. N. Evans *In* NASA. Langley Research Center 13th International Laser Radar Conference Aug. 1986 3 p (For primary document see N87-10263 01-35)
Avail: NTIS HC A15/MF A01 CSCL 17I

N87-10287*# National Aeronautics and Space Administration. Langley Research Center, Hampton, Va.
INFLUENCE OF RAYLEIGH-DOPPLER BROADENING ON THE SELECTION OF H2O DIAL SYSTEM PARAMETERS
Syed Ismail and Edward V. Browell *In its* 13th International Laser

Radar Conference Aug. 1986 5 p (For primary document see N87-10263 01-35)
Avail: NTIS HC A15/MF A01 CSCL 20N

N87-10288*# Max-Planck-Inst. fuer Meteorologie, Hamburg (West Germany).
CORRECTION OF DOPPLER-BROADENED RAYLEIGH BACKSCATTERING EFFECTS IN H2O DIAL MEASUREMENTS
A. Ansmann and J. Bosenberg *In* NASA. Langley Research Center 13th International Laser Radar Conference Aug. 1986 3 p (For primary document see N87-10263 01-35)
Avail: NTIS HC A15/MF A01 CSCL 20N

N87-10294*# Atmospheric Sciences Lab., White Sands Missile Range, N. Mex.
EFFECT OF BACKSCATTER-TO-EXTINCTION RATIO ON LIDAR INVERSIONS
Edward M. Measure *In* NASA. Langley Research Center 13th International Laser Radar Conference Aug. 1986 6 p (For primary document see N87-10263 01-35)
Avail: NTIS HC A15/MF A01 CSCL 20N

N87-10295*# Optech, Inc., Downsview (Ontario).
LABORATORY MEASUREMENTS OF FORWARD AND BACKWARD SCATTERING OF LASER BEAMS IN WATER DROPLET CLOUDS
R. B. Smith, J. D. Houston, A. Ulitsky, and A. I. Carswell (York Univ., Downsview (Ontario).) *In* NASA. Langley Research Center 13th International Laser Radar Conference Aug. 1986 2 p (For primary document see N87-10263 01-35)
Avail: NTIS HC A15/MF A01 CSCL 20N

N87-10296*# National Aeronautics and Space Administration. Goddard Space Flight Center, Greenbelt, Md.
REAL-TIME ATMOSPHERIC ABSORPTION SPECTRA FOR IN-FLIGHT TUNING OF AN AIRBORNE DIAL SYSTEM
M. Dombrowski, H. Walden, G. K. Schwemmer, J. Milrod, and C. L. Korb *In* NASA. Langley Research Center 13th International Laser Radar Conference Aug. 1986 1 p (For primary document see N87-10263 01-35)
Avail: NTIS HC A15/MF A01 CSCL 20N

N87-10310*# Fraunhofer-Inst. fuer Atmosphaerische Umweltforschung, Garmisch-Partenkirchen (West Germany).
IMPROVED SOLUTION OF THE LIDAR EQUATION UTILIZING PARTICLE COUNTER MEASUREMENTS
H. Jaeger, M. Littfass, D. J. Hofmann (Wyoming Univ., Laramie.), and J. M. Rosen *In* NASA. Langley Research Center 13th International Laser Radar Conference Aug. 1986 2 p (For primary document see N87-10263 01-35)
Avail: NTIS HC A15/MF A01 CSCL 20N

N87-10315*# Florence Univ. (Italy). Dept. of Physics.
MULTIPLE SCATTERING MEASUREMENTS IN LABORATORY AND FOGGY ATMOSPHERE
P. Bruscaglioni, E. Battistelli, P. Pili, and C. Zaccanti *In* NASA. Langley Research Center 13th International Laser Radar Conference Aug. 1986 4 p (For primary document see N87-10263 01-35)
Avail: NTIS HC A15/MF A01 CSCL 20N

N87-10316*# Los Alamos National Lab., N. Mex.
MULTIPLE SCATTERING OF LASER BEAMS IN DENSE HYDROSOLS
A. Zardecki, S. A. W. Gerstl, Wesley P. Unruh, Grant H. Stokes, David M. Stupin, Norman E. Elliott, and J. A. Weinman (Wisconsin Univ., Madison.) *In* NASA. Langley Research Center 13th International Laser Radar Conference Aug. 1986 3 p (For primary document see N87-10263 01-35)
Avail: NTIS HC A15/MF A01 CSCL 20N

N87-10328*# Israel Atomic Energy Commission, Yavneh. Dept. of Atmospheric Optics.
THE EFFECT OF TURBULENCE ON LIDAR BACKSCATTERED SIGNAL FLUCTUATIONS
S. Fastig and A. Choen *In* NASA. Langley Research Center 13th International Laser Radar Conference Aug. 1986 1 p (For primary document see N87-10263 01-35)
Avail: NTIS HC A15/MF A01 CSCL 20N

N87-10350*# Utah Univ., Salt Lake City. Dept. of Meteorology.
MULTIPLE SCATTERING DEPOLARIZATION IN MARINE STRATUS CLOUDS: LIDAR EXPERIMENTS
Kenneth Sassen and Richard L. Petrilla *In* NASA. Langley Research Center 13th International Laser Radar Conference Aug. 1986 1 p (For primary document see N87-10263 01-35)
Avail: NTIS HC A15/MF A01 CSCL 20N

N87-10351*# Harry Diamond Labs., Adelphi, Md.
NEAR-IR EXTINCTION AND BACKSCATTER COEFFICIENT MEASUREMENTS IN LOW- AND MID-ALTITUDE CLOUDS
Z. G. Sztankay *In* NASA. Langley Research Center 13th International Laser Radar Conference Aug. 1986 6 p (For primary document see N87-10263 01-35)
Avail: NTIS HC A15/MF A01 CSCL 20N

N87-10352*# University Coll., Galway (Ireland). Dept. of Experimental Physics.
BACKSCATTER AND EXTINCTION MEASUREMENTS IN CLOUD AND DRIZZLE AT CO2 LASER WAVELENGTHS
S. G. Jennings *In* NASA. Langley Research Center 13th International Laser Radar Conference Aug. 1986 4 p (For primary document see N87-10263 01-35)
Avail: NTIS HC A15/MF A01 CSCL 20N

N87-10370*# National Aeronautics and Space Administration. Langley Research Center, Hampton, Va.
LINEWIDTH CHARACTERISTICS OF RAMAN-SHIFTED DYE LASER OUTPUT AT 720 AND 940 nm
B. E. Grossman, U. N. Singh (Maryland Univ. College Park), N. S. Higdon, L. J. Cotnoir, T. D. Wilkerson, and E. V. Browell *In its* 13th International Laser Radar Conference Aug. 1986 5 p (For primary document see N87-10263 01-35)
Avail: NTIS HC A15/MF A01 CSCL 20N

N87-10482*# National Oceanic and Atmospheric Administration, Boulder, Colo. Aeronomy Lab.
THE PROPOSED FLATLAND RADAR
J. L. Green, K. S. Gage, T. E. VanZandt, and G. D. Nastrom *In* International Council of Scientific Unions, Middle Atmosphere Program. Handbook for MAP, Vol. 20 Jun. 1986 5 p (For primary document see N87-10419 01-42)
Avail: NTIS HC A22/MF A01; also available from SCOSTEP Secretariat, Illinois Univ., 1406 West Green Street, Urbana, Ill. 61801 CSCL 17I

N87-10483*# National Oceanic and Atmospheric Administration, Boulder, Colo. Aeronomy Lab.
CURRENT STATUS OF THE POKER FLAT MST RADAR
B. B. Balsley *In* International Council of Scientific Unions, Middle Atmosphere Program. Handbook for MAP, Vol. 20 Jun. 1986 1 p (For primary document see N87-10419 01-42)
Avail: NTIS HC A22/MF A01; also available from SCOSTEP Secretariat, Illinois Univ., 1406 West Green Street, Urbana, Ill. 61801 CSCL 17I

N87-10485*# Illinois Univ., Urbana. Aeronomy Lab.
RECENT PROGRESS IN THE URBANA MST RADAR
S. A. Bowhill *In* International Council of Scientific Unions, Middle Atmosphere Program. Handbook for MAP, Vol. 20 Jun. 1986 1 p (For primary document see N87-10419 01-42)
Avail: NTIS HC A22/MF A01; also available from SCOSTEP Secretariat, Illinois Univ., 1406 West Green Street, Urbana, Ill. 61801 CSCL 17I

N87-10489*# Pennsylvania State Univ., University Park. Dept. of Meteorology.
THE PENN STATE DOPPLER NETWORK PROGRESS REPORT

S. R. Williams and R. Peters *In* International Council of Scientific Unions, Middle Atmosphere Program. Handbook for MAP, Vol. 20 Jun. 1986 3 p (For primary document see N87-10419 01-42)
Avail: NTIS HC A22/MF A01; also available from SCOSTEP Secretariat, Illinois Univ., 1406 West Green Street, Urbana, Ill. 61801 CSCL 17I

N87-10490*# Adelaide Univ. (Australia). Dept. of Physics.
THE ADELAIDE MF PARTIAL-REFLECTION RADAR AND VHF ST RADAR Progress Report
R. A. Vincent *In* International Council of Scientific Unions, Middle Atmosphere Program. Handbook for MAP, Vol. 20 Jun. 1986 1 p (For primary document see N87-10419 01-42)
Avail: NTIS HC A22/MF A01; also available from SCOSTEP Secretariat, Illinois Univ., 1406 West Green Street, Urbana, Ill. 61801 CSCL 17I

N87-10491*# Centre de Recherches en Physique de l'Environnement, Saint Maur des Fosses (France).
THE PROUST RADAR
F. Bertin, M. Glass, R. Ney, and M. Petitdidier *In* International Council of Scientific Unions, Middle Atmosphere Program. Handbook for MAP, Vol. 20 Jun. 1986 3 p (For primary document see N87-10419 01-42)
Avail: NTIS HC A22/MF A01; also available from SCOSTEP Secretariat, Illinois Univ., 1406 West Green Street, Urbana, Ill. 61801 CSCL 17I

N87-10492*# Toulon Univ. (France). Lab. de Sondages Electromagnetiques.
THE PROVENCE ST RADAR
M. Crochet *In* International Council of Scientific Unions, Middle Atmosphere Program. Handbook for MAP, Vol. 20 Jun. 1986 1 p (For primary document see N87-10419 01-42)
Avail: NTIS HC A22/MF A01; also available from SCOSTEP Secretariat, Illinois Univ., 1406 West Green Street, Urbana, Ill. 61801 CSCL 17I

N87-10493*# CNRM, Toulouse (France).
THE INSU AND DMN NETWORK OF ST RADARS
M. Petitdidier (Centre de Recherches en Physique de l'Environnement, Saint Maur des Fosses, France), V. Klaus, F. Baudin (Centre de Recherches en Physique de l'Environnement, Issy-les-Moulineaux, France), M. Crochet (Toulon Univ., France), G. Penazzi (Centre de Recherches en Physique de l'Environnement, Saint Maur des Fosses, France), and P. Quinty *In* International Council of Scientific Unions, Middle Atmosphere Program. Handbook for MAP, Vol. 20 Jun. 1986 2 p (For primary document see N87-10419 01-42)
Avail: NTIS HC A22/MF A01; also available from SCOSTEP Secretariat, Illinois Univ., 1406 West Green Street, Urbana, Ill. 61801 CSCL 17I

N87-10495*# National Central Univ., Chung-Li (Taiwan).
THE FIRST OPERATION AND RESULTS OF THE CHUNG-LI VHF RADAR
J. K. Chao, F. S. Kuo, Y. S. Chu, I. J. Fu, J. Rottger (Arecibo Ionospheric Observatory, Puerto Rico), and C. H. Liu (Illinois Univ., Urbana) *In* International Council of Scientific Unions, Middle Atmosphere Program. Handbook for MAP, Vol. 20 Jun. 1986 5 p (For primary document see N87-10419 01-42)
Avail: NTIS HC A22/MF A01; also available from SCOSTEP Secretariat, Illinois Univ., 1406 West Green Street, Urbana, Ill. 61801 CSCL 17I

N87-10496*# Saskatchewan Univ., Saskatoon. Dept. of Physics.
PROGRESS IN THE MF RADAR SYSTEM AT SASKATOON
C. E. Meek and A. H. Manson *In* International Council of Scientific Unions, Middle Atmosphere Program. Handbook for MAP, Vol. 20 Jun. 1986 4 p (For primary document see N87-10419 01-42)
Avail: NTIS HC A22/MF A01; also available from SCOSTEP Secretariat, Illinois Univ., 1406 West Green Street, Urbana, Ill. 61801 CSCL 17I

N87-10497*# Indian Space Research Organization, Bangalore.
SYSTEM ASPECTS OF THE INDIAN MST RADAR FACILITY
G. Viswanathan *In* International Council of Scientific Unions, Middle Atmosphere Program. Handbook for MAP, Vol. 20 Jun. 1986 6 p (For primary document see N87-10419 01-42)
Avail: NTIS HC A22/MF A01; also available from SCOSTEP Secretariat, Illinois Univ., 1406 West Green Street, Urbana, Ill. 61801 CSCL 17I

N87-10499*# National Oceanic and Atmospheric Administration, Boulder, Colo. Aeronomy Lab.
PHASED-ARRAY DESIGN FOR MST AND ST RADARS
W. L. Ecklund *In* International Council of Scientific Unions, Middle Atmosphere Program. Handbook for MAP, Vol. 20 Jun. 1986 2 p (For primary document see N87-10419 01-42)
Avail: NTIS HC A22/MF A01; also available from SCOSTEP Secretariat, Illinois Univ., 1406 West Green Street, Urbana, Ill. 61801 CSCL 17I

N87-10500*# National Oceanic and Atmospheric Administration, Boulder, Colo. Aeronomy Lab.
THE NOAA TOGA ANTENNA ARRAY
W. L. Ecklund, D. A. Carter, and B. B. Balsley *In* International Council of Scientific Unions, Middle Atmosphere Program. Handbook for MAP, Vol. 20 Jun. 1986 2 p (For primary document see N87-10419 01-42)
Avail: NTIS HC A22/MF A01; also available from SCOSTEP Secretariat, Illinois Univ., 1406 West Green Street, Urbana, Ill. 61801 CSCL 17I

N87-10501*# Illinois Univ., Urbana. Dept. of Electrical and Computer Engineering.
BEAM STEERING SYSTEM
S. A. Bowhill and K. O. Merewether *In* International Council of Scientific Unions, Middle Atmosphere Program. Handbook for MAP, Vol. 20 Jun. 1986 4 p (For primary document see N87-10419 01-42)
Avail: NTIS HC A22/MF A01; also available from SCOSTEP Secretariat, Illinois Univ., 1406 West Green Street, Urbana, Ill. 61801 CSCL 17I

N87-10503*# National Oceanic and Atmospheric Administration, Boulder, Colo. Wave Propagation Lab.
A 405-MHz, 5-BEAM PHASED ARRAY ANTENNA
Daniel C. Law *In* International Council of Scientific Unions, Middle Atmosphere Program. Handbook for MAP, Vol. 20 Jun. 1986 5 p (For primary document see N87-10419 01-42)
Avail: NTIS HC A22/MF A01; also available from SCOSTEP Secretariat, Illinois Univ., 1406 West Green Street, Urbana, Ill. 61801 CSCL 17I

N87-10504*# National Oceanic and Atmospheric Administration, Boulder, Colo. Aeronomy Lab.
LOW-ALTITUDE COVERAGE OF ST RADARS
W. L. Ecklund *In* International Council of Scientific Unions, Middle Atmosphere Program. Handbook for MAP, Vol. 20 Jun. 1986 1 p (For primary document see N87-10419 01-42)
Avail: NTIS HC A22/MF A01; also available from SCOSTEP Secretariat, Illinois Univ., 1406 West Green Street, Urbana, Ill. 61801 CSCL 17I

N87-10505*# National Oceanic and Atmospheric Administration, Boulder, Colo. Aeronomy Lab.
THE GRID ARRAY ANTENNA
W. L. Ecklund *In* International Council of Scientific Unions, Middle Atmosphere Program. Handbook for MAP, Vol. 20 Jun. 1986 1 p (For primary document see N87-10419 01-42)
Avail: NTIS HC A22/MF A01; also available from SCOSTEP Secretariat, Illinois Univ., 1406 West Green Street, Urbana, Ill. 61801 CSCL 17I

N87-10507*# Adelaide Univ. (Australia). Dept. of Physics.
MEASUREMENTS OF ANTENNA POLAR DIAGRAMS AND EFFICIENCIES USING A PHASE-SWITCHED INTERFEROME-

TER
R. A. Vincent, B. Candy, and B. H. Briggs *In* International Council of Scientific Unions, Middle Atmosphere Program. Handbook for MAP, Vol. 20 Jun. 1986 1 p (For primary document see N87-10419 01-42)
Avail: NTIS HC A22/MF A01; also available from SCOSTEP Secretariat, Illinois Univ., 1406 West Green Street, Urbana, Ill. 61801 CSCL 17I

N87-10508*# Colorado Univ., Boulder. Cooperative Inst. for Research in Environ. Sci.
USE OF THE SUN TO DETERMINE POINTING OF ST RADAR BEAMS
A. C. Riddle *In* International Council of Scientific Unions, Middle Atmosphere Program. Handbook for MAP, Vol. 20 Jun. 1986 4 p (For primary document see N87-10419 01-42)
Avail: NTIS HC A22/MF A01; also available from SCOSTEP Secretariat, Illinois Univ., 1406 West Green Street, Urbana, Ill. 61801 CSCL 17I

N87-10509*# Kyoto Univ., Uji (Japan). Radio Atmospheric Science Center.
MONITORING OF THE MU RADAR ANTENNA PATTERN BY SATELLITE OHZORA (EXOS-C)
Toru Sato, Yasuhiro Inooka, Shoichiro Fukao (Kyoto Univ., Japan), and Susumu Kato *In* International Council of Scientific Unions, Middle Atmosphere Program. Handbook for MAP, Vol. 20 Jun. 1986 5 p (For primary document see N87-10419 01-42)
Avail: NTIS HC A22/MF A01; also available from SCOSTEP Secretariat, Illinois Univ., 1406 West Green Street, Urbana, Ill. 61801 CSCL 17I

N87-10510*# Arecibo Ionospheric Observatory, Puerto Rico.
METHOD TO DETERMINE THE OPTIMAL PARAMETERS OF THE ARECIBO 46.8-MHz ANTENNA SYSTEM
H. M. Ierkic, J. Rottger, J. B. Hagen, and R. K. Zimmerman *In* International Council of Scientific Unions, Middle Atmosphere Program. Handbook for MAP, Vol. 20 Jun. 1986 5 p (For primary document see N87-10419 01-42)
Avail: NTIS HC A22/MF A01; also available from SCOSTEP Secretariat, Illinois Univ., 1406 West Green Street, Urbana, Ill. 61801 CSCL 17I

N87-10511*# National Oceanic and Atmospheric Administration, Boulder, Colo. Aeronomy Lab.
THE ELIMINATION OF A CLASS OF PSEUDO ECHOES BY AN IMPROVED T/R SWITCH TECHNIQUE
J. L. Green and W. L. Ecklund *In* International Council of Scientific Unions, Middle Atmosphere Program. Handbook for MAP, Vol. 20 Jun. 1986 6 p (For primary document see N87-10419 01-42)
Avail: NTIS HC A22/MF A01; also available from SCOSTEP Secretariat, Illinois Univ., 1406 West Green Street, Urbana, Ill. 61801 CSCL 17I

N87-10512*# Case Western Reserve Univ., Cleveland, Ohio. Dept. of Electrical Engineering and Appl. Physics.
AN OVERVIEW OF DATA ACQUISITION, SIGNAL CODING AND DATA ANALYSIS TECHNIQUES FOR MST RADARS
P. K. Rastogi *In* International Council of Scientific Unions, Middle Atmosphere Program. Handbook for MAP, Vol. 20 Jun. 1986 10 p (For primary document see N87-10419 01-42)
Avail: NTIS HC A22/MF A01; also available from SCOSTEP Secretariat, Illinois Univ., 1406 West Green Street, Urbana, Ill. 61801 CSCL 17I

N87-10513*# Arecibo Ionospheric Observatory, Puerto Rico.
OPTIMUM CODING TECHNIQUES FOR MST RADARS
Michael P. Sulzer and Ronald F. Woodman (Instituto Geofisico del Peru, Lima) *In* International Council of Scientific Unions, Middle Atmosphere Program. Handbook for MAP, Vol. 20 Jun. 1986 7 p (For primary document see N87-10419 01-42)
Avail: NTIS HC A22/MF A01; also available from SCOSTEP Secretariat, Illinois Univ., 1406 West Green Street, Urbana, Ill. 61801 CSCL 17I

N87-10514*# Illinois Univ., Urbana. Aeronomy Lab.
IMPROVING RANGE RESOLUTION WITH A FREQUENCY-HOPPING TECHNIQUE
G. R. Stitt and S. A. Bowhill *In* International Council of Scientific Unions, Middle Atmosphere Program. Handbook for MAP, Vol. 20 Jun. 1986 10 p (For primary document see N87-10419 01-42)
Avail: NTIS HC A22/MF A01; also available from SCOSTEP Secretariat, Illinois Univ., 1406 West Green Street, Urbana, Ill. 61801 CSCL 17I

N87-10518*# National Oceanic and Atmospheric Administration, Boulder, Colo. Wave Propagation Lab.
A MICROPROGRAMMABLE RADAR CONTROLLER
Daniel C. Law *In* International Council of Scientific Unions, Middle Atmosphere Program. Handbook for MAP, Vol. 20 Jun. 1986 3 p (For primary document see N87-10419 01-42)
Avail: NTIS HC A22/MF A01; also available from SCOSTEP Secretariat, Illinois Univ., 1406 West Green Street, Urbana, Ill. 61801 CSCL 17I

N87-10520*# Case Western Reserve Univ., Cleveland, Ohio. Electrical Engineering and Applied Physics.
INTERFERENCE DETECTION AND CORRECTION APPLIED TO INCOHERENT-SCATTER RADAR POWER SPECTRUM MEASUREMENT
W. P. Ying, J. D. Mathews, and P. K. Rastogi *In* International Council of Scientific Unions, Middle Atmosphere Program. Handbook for MAP, Vol. 20 Jun. 1986 10 p (For primary document see N87-10419 01-42)
Avail: NTIS HC A22/MF A01; also available from SCOSTEP Secretariat, Illinois Univ., 1406 West Green Street, Urbana, Ill. 61801 CSCL 17I

N87-10521*# Illinois Univ., Urbana. Aeronomy Lab.
THE TUKEY ALGORITHM FOR ENHANCING MST RADAR DATA
S. A. Bowhill *In* International Council of Scientific Unions, Middle Atmosphere Program. Handbook for MAP, Vol. 20 Jun. 1986 3 p (For primary document see N87-10419 01-42)
Avail: NTIS HC A22/MF A01; also available from SCOSTEP Secretariat, Illinois Univ., 1406 West Green Street, Urbana, Ill. 61801 CSCL 17I

N87-10523*# Pennsylvania State Univ., University Park. Dept. of Meteorology.
DATA COMMUNICATIONS AND MONITOR FOR THE PENN STATE UNIVERSITY PROFILER NETWORK
Robert M. Peters *In* International Council of Scientific Unions, Middle Atmosphere Program. Handbook for MAP, Vol. 20 Jun. 1986 2 p (For primary document see N87-10419 01-42)
Avail: NTIS HC A22/MF A01; also available from SCOSTEP Secretariat, Illinois Univ., 1406 West Green Street, Urbana, Ill. 61801 CSCL 17I

N87-10524*# Colorado Univ., Boulder. Cooperative Inst. for Res. in the Environ. Sci.
ARCHIVAL OF POKER FLAT MST RADAR DATA
A. C. Riddle, B. B. Balsley (National Oceanic and Atmospheric Administration, Boulder, Colo.), and K. S. Gage *In* International Council of Scientific Unions, Middle Atmosphere Program. Handbook for MAP, Vol. 20 Jun. 1986 3 p (For primary document see N87-10419 01-42)
Avail: NTIS HC A22/MF A01; also available from SCOSTEP Secretariat, Illinois Univ., 1406 West Green Street, Urbana, Ill. 61801 CSCL 17I

N87-10525*# National Center for Atmospheric Research, Boulder, Colo.
MST DATA EXCHANGE THROUGH THE NCAR INCOHERENT-SCATTER RADAR DATA BASE
A. D. Richmond *In* International Council of Scientific Unions, Middle

Atmosphere Program. Handbook for MAP, Vol. 20 Jun. 1986 2 p (For primary document see N87-10419 01-42)
Avail: NTIS HC A22/MF A01; also available from SCOSTEP Secretariat, Illinois Univ., 1406 West Green Street, Urbana, Ill. 61801 CSCL 17I

N87-10570 Centre National de la Recherche Scientifique, Orleans (France). Lab. de Physique et Chimie de l'Environnement.
ATTENUATION BANDS AND CUT-OFF FREQUENCIES FOR ELF ELECTROMAGNETIC WAVES
J. L. Rauch, J. C. Cerisier (Centre de Recherches en Physique de l'Environnement, Saint Maur des Fosses France), J. J. Berthelier, F. Lefeuvre, N. Boudko (Academy of Sciences (USSR), Moscow), G. Michailova, and O. Kapustina *In* CNES Results of the ARCAD 3 Project and of Recent Programs in Magnetospheric and Ionospheric Physics 1985 p 465-484 (For primary document see N87-10541 01-46)
Avail: CEPADUES, Toulouse

N87-10571 Academy of Sciences (USSR), Moscow.
POLARIZATION OF ELECTROMAGNETIC WAVES RECORDED ON BOARD THE AUREOL-3 SATELLITE
F. Lefeuvre (Centre National de la Recherche Scientifique, Orleans, France), J. L. Rauch, L. V. Volkomiskaya, and B. Lundin *In* CNES Results of the ARCAD 3 Project and of Recent Programs in Magnetospheric and Ionospheric Physics 1985 p 485-498 (For primary document see N87-10541 01-46)
Avail: CEPADUES, Toulouse

N87-10572 Nagoya Univ., Toyokawa (Japan). Research Inst. of Atmospherics.
THE DIRECTION FINDING ABOARD AUREOL-3 OF ELF WAVES AT FREQUENCY ABOVE AND BELOW THE PROTON GYROFREQUENCY
M. Hayakawa, F. Lefeuvre (Centre National de la Recherche Scientifique, Orleans, France), and J. L. Rauch *In* CNES Results of the ARCAD 3 Project and of Recent Programs in Magnetospheric and Ionospheric Physics 1985 p 499-507 (For primary document see N87-10541 01-46)
Avail: CEPADUES, Toulouse

N87-10573 Centre de Recherches en Physique de l'Environnement, Saint Maur des Fosses (France).
DENSITY GRADIENT INSTABILITY IN THE HIGH LATITUDE IONOSPHERE. RELATION WITH THE ELECTROSTATIC TURBULENCE AND CONVECTION
J. C. Cerisier, J. J. Berthelier, C. Beghin (Centre National de la Recherche Scientifique, Orleans, France), and D. Roux *In* CNES Results of the ARCAD 3 Project and of Recent Programs in Magnetospheric and Ionospheric Physics 1985 p 509-516 (For primary document see N87-10541 01-46)
Avail: CEPADUES, Toulouse

N87-10575 Poitiers Univ. (France). Lab. de Physique de la Haute Atmosphere.
VERY LOW FREQUENCY SAUCERS WITH ATTENUATION BANDS
Y. Corcuff and M. Tixier *In* CNES Results of the ARCAD 3 Project and of Recent Programs in Magnetospheric and Ionospheric Physics 1985 p 529-535 Sponsored by Administration du Territoire des Terres Australes et Antarctique Francaises (For primary document see N87-10541 01-46)
Avail: CEPADUES, Toulouse

N87-10577 Ecole Polytechnique, Palaiseau (France). Centre de Physique Theorique.
SCENARIOS FOR THE GENERATION OF AURORAL KILOMETRIC RADIATION
D. LeQueau, R. Pellat, and A. Roux (Centre de Recherches en Physique de l'Environnement, Issy-les-Moulineaux, France) *In* CNES Results of the ARCAD 3 Project and of Recent Programs in Magnetospheric and Ionospheric Physics 1985 p 547-557 (For primary document see N87-10541 01-46)
Avail: CEPADUES, Toulouse

N87-10578 Maryland Univ., College Park. Inst. for Physical Science and Technology.
THE CYCLOTRON MASER THEORY OF AKR AND Z-MODE RADIATION
C. S. Wu *In* CNES Results of the ARCAD 3 Project and of Recent Programs in Magnetospheric and Ionospheric Physics 1985 p 559-570 (For primary document see N87-10541 01-46)
(Grant NGL-21-002-005)
Avail: CEPADUES, Toulouse

N87-10579 British Antarctic Survey, Cambridge (England). Space Plasma Physics Section.
NONTHERMAL CONTINUUM-TERRESTRIAL MYRIAMETRIC RADIATION NARROWBAND ELECTROMAGNETIC EMISSION
Dyfrig Jones *In* CNES Results of the ARCAD 3 Project and of Recent Programs in Magnetospheric and Ionospheric Physics 1985 p 571-577 (For primary document see N87-10541 01-46)
Avail: CEPADUES, Toulouse

N87-10580 Academy of Sciences (USSR), Troitsk.
MECHANISM OF LOW-FREQUENCY WAVE PROPAGATION IN THE MAGNETOSPHERE
O. A. Molchanov, O. A. Maltseva (Rostov State Univ., Rostov-on-Don, USSR), and E. E. Titova *In* CNES Results of the ARCAD 3 Project and of Recent Programs in Magnetospheric and Ionospheric Physics 1985 p 579-598 (For primary document see N87-10541 01-46)
Avail: CEPADUES, Toulouse

N87-10583 Nagoya Univ., Toyokawa (Japan). Research Inst. of Atmospherics.
STUDY OF THE MIDDLE LATITUDE BROADENING OF THE SPECTRUM OF THE WAVES EMITTED FROM GROUND
Y. Tanaka, M. Hayakawa, D. Lagoutte (Centre National de la Recherche Scientifique, Orleans, France), and F. Lefeuvre *In* CNES Results of the ARCAD 3 Project and of Recent Programs in Magnetospheric and Ionospheric Physics 1985 p 621-626 (For primary document see N87-10541 01-46)
Avail: CEPADUES, Toulouse

N87-10584 Academy of Sciences (USSR), Apatity. Polar Geophysical Inst.
ON THE SPECTRAL BROADENING OF THE GROUND-BASED VLF TRANSMITTER SIGNALS IN THE HIGH-LATITUDE IONOSPHERE OBSERVED FROM INTERCOSMOS-19 AND AUREOL-3 SATELLITES
E. E. Titova, A. M. Perlikov, V. E. Yurov, I. V. Lychkina, O. M. Raspopov, V. Yu. Trakhtengertz, O. A. Molchanov, O. A. Maltseve (Rostov State Univ., Rostov-on-Don, USSR), and Yu. I. Galperin *In* CNES Results of the ARCAD 3 Project and of Recent Programs in Magnetospheric and Ionospheric Physics 1985 p 627-644 (For primary document see N87-10541 01-46)
Avail: CEPADUES, Toulouse

N87-10586 Stanford Univ., Palo Alto, Calif. STAR Lab.
DE-1/SIPLE VLF WAVE-INJECTION EXPERIMENTS
U. S. Inan *In* CNES Results of the ARCAD 3 Project and of Recent Programs in Magnetospheric and Ionospheric Physics 1985 p 655-659 (For primary document see N87-10541 01-46)
(Contract NAS5-25688; Grants DPP80-22282; DPP80-22540)
Avail: CEPADUES, Toulouse

33 ELECTRONICS AND ELECTRICAL ENGINEERING

Includes test equipment and maintainability; components, e.g., tunnel diodes and transistors; microminiaturization; and integrated circuitry.

For related information see also *60 Computer Operations and Hardware* and *76 Solid-State Physics.*

N87-10231*# National Aeronautics and Space Administration. Pasadena Office, Calif.

CROSS-CONTACT CHAIN Patent Application
Udo Lieneweg, inventor (to NASA) Filed 26 Jun. 1986 16 p
(Contract NAS7-918)
(NASA-Case-NPO-16784-1; US-Patent-Appl-SN-879757) Avail: NTIS HC A02/MF A01 CSCL 09A

A system is provided for use with wafers that include multiple integrated circuits that include two conductive layers in contact at multiple interfaces. Contact chains are formed beside the integrated circuits, each contact chain formed of the same two layers as the circuits, in the form of conductive segments alternating between the upper and lower layers and with the ends of the segments connected in series through interfaces. A current source passes a current through the series-connected segments, by way of a pair of current tabs connected to opposite ends of the series of segments. While the current flows, voltage measurements are taken between each of a plurality of pairs of voltage tabs, the two tabs of each pair connected to opposite ends of an interface that lies along the series-connected segments. A plot of interface conductances on normal probability chart enables prediction of the yield of good integrated circuits from the wafer. NASA

N87-10232*# National Aeronautics and Space Administration. Lewis Research Center, Cleveland, Ohio.
OPTICALLY CONTROLLED GaAs DUAL-GATE MESFET AND PERMEABLE BASE TRANSISTORS
R. N. Simons and K. B. Bhasin 1986 7 p Presented at the Conference on Lasers and Electro-Optics (CLEO), San Francisco, Calif., 9-13 Jun. 1986; sponsored by IEEE and Optical Society of America
(NASA-TM-88823; E-3183-1; NAS 1.15:88823) Avail: NTIS HC A02/MF A01 CSCL 09A

Optically induced voltage and dc characteristics of the GaAs Dual-gate MESFET and the Permeable Base Transistor (PBT) with optical illumination at wavelength below 0.87 microns were obtained and compared with GaAs MESFET. It was observed that PBT can handle higher current density when illuminated. Author

N87-10233 Defence Research Information Centre, Orpington (England).
AN ALGORITHM FOR THE DETECTION OF SIGNALS BY COLOUR CONTRAST ON THE SCREEN OF A COLOUR CATHODE RAY TUBE (COLOUR DISPLAY)
S. I. Pozdnyak, P. A. Pozin, and A. K. Senatorov Jan. 1986 12 p Transl. into ENGLISH from Izvestiya Vuzov SSSR: Radioelektronika (USSR), v. 17, no. 10, 1974 p 37-40
(DRIC-T-7655; BR99447; ETN-86-97992) Avail: NTIS HC A02/MF A01

A rule for decision taking in signal detection by color contrast is formulated on the basis of MacAdam's uniform chromaticity diagram taking into account the threshold sensitivity of the operator's eye. Two and three-color displays are considered. ESA

N87-10234# Atomic Weapons Research Establishment, Aldermaston (England).
EXTENSION OF THE ELECTROMAGNETIC METHOD OF MOMENTS CODE CHAOS TO TREAT CONFIGURATIONS OF DIELECTRIC-COATED WIRES
J. Moore Feb. 1986 19 p
(AWRE-O-18/85; BR98864; ETN-86-97995) Avail: NTIS HC A02/MF A01

The development and use of CHAOS 6, an extension of the method of moments code CHAOS (5), to calculate radiation and scattering by an arbitrary configuration of dielectric-coated wires, assumed thin, and either joined or unjoined are described. Radar cross sections of coated dipoles and the current distribution on a coated monopole calculated by the code are compared with experimental data. It is shown how magnetic-coated wires and wires having mixed coatings can be transformed to purely dielectric-coated wires for treatment by the program. There is excellent agreement between the predictions of the code and experimental data for glass-coated copper dipoles. ESA

N87-10235# Atomic Weapons Research Establishment, Aldermaston (England).
WIRE DIPOLES AND ANTENNAS WITH DIELECTRIC OR MAGNETIC COATINGS
J. Moore and Alison C. Scrimgeour Mar. 1980 25 p
(AWRE-O-19/85; BR99171; ETN-86-97996) Avail: NTIS HC A02/MF A01

A prescription which enables any theoretical formulation for scattering and radiation by an arbitrary bare wire antenna of circular cross section to be extended to antennas having a thin coating of dielectric or magnetic material is derived. The prescription is applied to the Harrison and Heinz (1963) treatment of a bare half-wave dipole to extend that theory to treat dielectric-coated dipoles. There is excellent agreement between the resulting theoretical predictions and measurements for the radar cross section of glass-coated copper dipoles. ESA

N87-10236*# Stanford Univ., Calif. Center for Space Science and Astrophysics.
THE DEVELOPMENT AND TEST OF MULTI-ANODE MICROCHANNEL ARRAY DETECTOR SYSTEMS. PART 2: SOFT X-RAY DETECTORS Progress Report, 1 Feb. - 31 Jul. 1986
J. G. Timothy Jul. 1986 18 p
(Grant NAG5-622)
(NASA-CR-177066; NAS 1.26:177066) Avail: NTIS HC A02/MF A01 CSCL 09A

Multi-Anode Microchannel Array (MAMA) detector systems with formats of 256 x 1024 pixels and active areas of 6 x 26 square mm are now under evaluation at visible, ultraviolet and soft x-ray wavelengths. Very-large-format versions of the MAMA detectors with formats of 2048 x 2048 pixels and active areas of 52 x 52 square mm are under development for use in the NASA Goddard Space Flight Center's Space Telescope Imaging Spectrograph (STIS). Open-structure versions of these detectors with CsI photocathodes can provide a high-resolution imaging capability at extreme ultraviolet (EUV) and soft x-ray wavelengths and can deliver a maximum count rate from each array in excess of 1 million counts s-1. In addition, these detector systems have the unique capability to determine the arrival time of a detected photon to an accuracy of 100 ns or better. The construction, mode-of-operation and performance characteristics of the MAMA detectors are described and the program for the development of the very-large-format detectors is outlined. Author

N87-10237*# Watkins-Johnson Co., Palo Alto, Calif.
DESIGN, CONSTRUCTION AND LONG LIFE ENDURANCE TESTING OF CATHODE ASSEMBLIES FOR USE IN MICROWAVE HIGH-POWER TRANSMITTING TUBES Final Report
R. Batra and D. Marino Sep. 1986 99 p
(Contract NAS3-23346)
(NASA-CR-175116; NAS 1.26:175116) Avail: NTIS HC A05/MF A01 CSCL 09A

The cathode life test program sponsored by NASA Lewis Research Center at Watkins-Johnson Company has been in continuous operation since 1972. Its primary objective has been to evaluate the long life capability of barium dispenser cathodes to produce emission current densities of 2 A sq. cm. or more in an operational environment simulating that of a highpower microwave tube. The life test vehicles were equipped with convergent flow electron guns, drift space tubes with solenoid magnets for electron beam confinement and water-cooled depressed collectors. A variety of cathode types has been tested, including GE Tungstate, Litton Impregnated, Philips Type B and M, Semicon types S and M, and Spectra-Mat Type M. Recent emphasis has been on monitoring the performance of Philips Type M cathodes at 2 A sq. cm. and Sprectra-Mat and Semicon Type M cathodes at 4 A sq. cm. These cathodes have been operated at a constant current of 616 mA and a cathode anode voltage on the order of 10 kV. Cathode temperatures were maintained at

1010 C true as measured from black body holes in the backs of the cathodes. This report presents results of the cathode life test program from July 1982 through April 1986. The results include hours of operation and performance data in the form of normalized emission current density versus temperature curves (Miram plots). NASA

N87-10238# California Univ., Berkeley. Lawrence Berkeley Lab.
RELATIONSHIP BETWEEN CRITICAL CURRENT AND MICROSTRUCTURE OF INTERNAL TIN WIRE
D. R. Dietderich, W. V. Hassenzahl, and J. W. Morris, Jr. Aug. 1985 14 p Presented at the Cryogenic Engineering Conference and International Cryogenic Materials Conference, Boston, Mass., 12 Aug. 1985
(Contract DE-AC03-76SF-00098)
(DE86-009922; LBL-19406; CONF-850814-39) Avail: NTIS HC A02/MF A01

Prior work on internal tin wire has shown that an increase in critical current results when the Nb3Sn reaction temperatures (650 to 730 C) are preceded by low temperature diffusion heat treatments that distribute the tin. These heat treatments produce a more uniform tin distribution through the niobium filament array before substantial Nb3Sn formation has occurred. Heat treatments as long as 19 days have been proposed as the optimal heat treatment for the conductor. However, it is possible to substantially reduce the low temperature heat treatment time while retaining the same high critical current. The success of shortened heat treatments may be interpreted on the basis of the Cu-Sn reaction, diffusion kinetics and the Nb3Sn growth kinetics. DOE

N87-10239# Los Alamos National Lab., N. Mex.
THERMIONIC INTEGRATED CIRCUITS
M. MacRoberts, D. R. Brown, R. Dooley, R. Lemons, D. Lynn, B. McCormick, C. Mombourquette, and D. Sinah 1986 5 p Presented at the 23d Annual Conference on Nuclear and Space Radiation Effects, Providence, R.I., 20 Jul. 1986
(Contract W-7405-eng-36)
(DE86-005849; LA-UR-86-428; CONF-860706-1) Avail: NTIS HC A02/MF A01

Thermionic integrated circuits combine vacuum-tube technology with integrated-circuit techniques to form integrated vacuum circuits. These circuits are capable of extended operation in both high-temperature and high-radiation environments. DOE

N87-10240# Wisconsin Univ., Madison.
ELECTRICAL CIRCUIT MODELING OF CONDUCTORS WITH SKIN EFFECT
D. W. Kerst and J. C. Sprott Mar. 1986 40 p
(Contract DE-FG02-85ER-53198)
(DE86-011085; DOE/ER-53198/90) Avail: NTIS HC A03/MF A01

The electrical impedance of a lossy conductor is a complicated function of time (or frequency) because of the skin effect. By solving the diffusion equation for magnetic fields in conductors of several prototypical shapes, the impedance can be calculated as a function of time for a step function of current. The solution suggests an electrical circuit representation that allows calculation of time-dependent voltages and currents of arbitrary waveforms. A technique using an operational amplifier to determine the current in such a conductor by measuring some external voltage is described. Useful analytical approximations to the results are derived. DOE

N87-10241# Lawrence Livermore National Lab., Calif.
ELECTRONICS ENGINEERING DEPARTMENT TECHNICAL REVIEW
Apr. 1986 41 p
(Contract W-7405-eng-48)
(DE86-011371; UCRL-50025-86-1) Avail: NTIS HC A03/MF A01

The EE Technical Review has two purposes - to inform readers of various activities within the Electronics Engineering Department and to promote the exchange of ideas. The articles, by design, are brief summaries of EE work. For further details on a subject covered, please contact one of the authors. The authors are primarily responsible for the content of their articles. Inasmuch as most projects are the result of the cooperative efforts of many individuals, the person you contact will either provide the requested information directly or refer you to the appropriate person to answer your question. DOE

N87-10242# Office of Technology Assessment, Washington, D.C.
MICROELECTRONICS RESEARCH AND DEVELOPMENT BACKGROUND PAPER
Mar. 1986 47 p
(PB86-205200; OTA-BP-CIT-40) Avail: NTIS HC A03/MF A01 CSCL 09C

Microelectronics has progressed at a tremendous rate over the last few decades and has become a vital part of US commerce and defense. Federal participation in microelectronic research and development is two fold: the government directly funds a significant fraction of the activities and several Federal policies indirectly affect private support of research and development. GRA

N87-10515*# Illinois Univ., Urbana. Aeronomy Lab.
A VARIABLE-FREQUENCY LOCAL OSCILLATOR FOR THE FREQUENCY-HOPPING TECHNIQUE
G. R. Stitt and L. J. Johnson *In* International Council of Scientific Unions, Middle Atmosphere Program. Handbook for MAP, Vol. 20 Jun. 1986 3 p (For primary document see N87-10419 01-42)
Avail: NTIS HC A22/MF A01; also available from SCOSTEP Secretariat, Illinois Univ., 1406 West Green Street, Urbana, Ill. 61801 CSCL 09C

N87-10517*# National Oceanic and Atmospheric Administration, Boulder, Colo. Aeronomy Lab.
A SINGLE-BOARD PREPROCESSOR AND PULSE GENERATOR
D. A. Carter, A. E. Ayers, and R. P. Schneider *In* International Council of Scientific Unions, Middle Atmosphere Program. Handbook for MAP, Vol. 20 Jun. 1986 3 p (For primary document see N87-10419 01-42)
Avail: NTIS HC A22/MF A01; also available from SCOSTEP Secretariat, Illinois Univ., 1406 West Green Street, Urbana, Ill. 61801 CSCL 09A

N87-10519*# National Oceanic and Atmospheric Administration, Boulder, Colo. Aeronomy Lab.
AN EXAMPLE OF SCALING MST DOPPLER SPECTRA USING MEDIAN SPECTRA, SPECTRAL SMOOTHING, AND VELOCITY TRACING
J. L. Green *In* International Council of Scientific Unions, Middle Atmosphere Program. Handbook for MAP, Vol. 20 Jun. 1986 4 p (For primary document see N87-10419 01-42)
Avail: NTIS HC A22/MF A01; also available from SCOSTEP Secretariat, Illinois Univ., 1406 West Green Street, Urbana, Ill. 61801 CSCL 09C

34 FLUID MECHANICS AND HEAT TRANSFER

Includes boundary layers; hydrodynamics; fluidics; mass transfer; and ablation cooling.

For related information see also *02 Aerodynamics* and *77 Thermodynamics and Statistical Physics.*

N87-10243 Michigan Univ., Ann Arbor.
NUMERICAL STUDIES OF A TUBULENT JET IN CROSSFLOW Ph.D. Thesis
Pei Yuan Tzeng 1985 110 p
Avail: Univ. Microfilms Order No. DA8600562

The application of an improved finite-difference solution procedure to the analysis of the flow field due to a turbulent jet in crossflow is presented. The governing time-averaged differential equations are solved by means of an efficient SIMPLEC algorithm. Two difference schemes, namely, power law and second order upwind, for approximating the convection terms are used and compared. Reynolds stresses are calculated by solving the modelled transport equations for the turbulent kinetic energy and its viscous rate of dissipation. Attention is focused on the cases of high and moderate jet-to-crossflow velocity ratio R. This range of conditions is of direct relevance to the studies of VSTOL in transition flight and the dilution zone mixing in gas turbine combustors. Two-dimensional computations of the plane jet case are performed for the flow geometry corresponding to the experiment of Stek and Brandt (1976). The reattachment length and streamline patterns obtained from the calculations agree very well with the experimental data. Three-dimensional computations of the round jet case are made for the flow geometry associated with the recent measurement of Andropoulos and Rodi (1984). The calculated results are presented with the aid of computer graphics. Flow patterns emerging from various profile, contour, and vector plots indicate that the general features of this complex flow situation are well predicted by the present numerical method. The possible causes of quantitiave discrepancies between computed and measured data are discussed. It appears that further refinements of the turbulence model and grid system are most desirable. Dissert. Abstr.

N87-10244 Pennsylvania State Univ., University Park.
AN EXPERIMENTAL INVESTIGATION OF END-WALL FLOWFIELD OF A COMPRESSOR ROTOR Ph.D. Thesis
K. N. SachidanandaMurthy 1985 266 p
Avail: Univ. Microfilms Order No. DA8606379

An investigation of the end-wall flowfield in a single-stage compressor rotor is presented. The main emphasis of the investigation was to measure the flowfield in detail in a low-speed compressor rotor. A single-channel laser Doppler velocimeter (LDV) was used to measure the flowfield in the tip clearance region. The investigation was carried out for two tip clearances (clearance/chord = 1.78 and 3.4 percent). In addition, the relative stagnation pressure field, corresponding to a tip clearance of 1.78 percent, was also measured using a Kiel probe to supplement the LDV measurement. The measurements showed that the leakage flow originated at about one-quarter-chord location. Past quarter-chord location, the inteaction between the leakage flow and the annulus-wall boundary layer resulted in unconventional and skewed boundary layer profiles. Inside the rotor passage, the leakage flow effects were augmented by the leakage flow emanating from the entire blade chord length. Downstream of the rotor, the interaction between the leakage flow and the rotor wake resulted in rapid wake decay at higher radii. The leakage flow which was intense at larger clearance might have rapidly smoothed the irregularities downstream of the rotor. Dissert. Abstr.

N87-10245 Georgia Inst. of Tech., Atlanta.
ORDERED AND RANDOM STRUCTURES IN PULSATILE FLOW THROUGH CONSTRICTED TUBES Ph.D. Thesis
Baruch Barry Lieber 1985 185 p
Avail: Univ. Microfilms Order No. DA8605427

The poststenotic flow field in a rigid tube was investigated under pulsatile conditions. The waveform employed in the present experiment was sinusoidal and three contoured constrictions with 50, 75, and 90% area reduction were investigated. The fluid dynamic similarity parameters were chosen to represent conditions found in large arteries of humans and of experimental animals, using a Reynolds number range of 200 to 1000 and a frequency parameter value of 5.3. The analysis techniques of autoregressive modeling, correlation methods, and phase-shift averaging were employed in order to extract the maximum information about flow behavior. Analysis focuses on identification and representation of coherent flow disturbances, and examination of the influence of core flow behavior on the cyclic wall shear stress. Dissert. Abstr.

N87-10246 Virginia Polytechnic Inst. and State Univ., Blacksburg.
TRANSIENT BEHAVIOR OF LIQUID JETS INJECTED NORMAL TO A HIGH VELOCITY GAS STREAM Ph.D. Thesis
David Matthew Less 1985 222 p
Avail: Univ. Microfilms Order No. DA8605348

The transient effects of the breakup and atomization of liquid jets in a crossflow on the size of droplets within the spray plume was experimentally determined. Water and water/methanol mixtures were injected normal to a high velocity air stream at Mach numbers of 0.48 and 3.0 with ambient stagnation temperature and respective stagnation pressures of 1.4 and 4.3 atm. The liquids were injected at liquid-to-gas momentum flux ratios ranging from 4 to 12. Droplet size distributions were obtained using a Fraunhofer diffraction technique at sampling rates of up to 9 kHz. Liquid mass flow rates were inferred from measurements of the extinction of a laser beam traversing the plume. The droplet sizes were found to fluctuate with frequencies of the order of 1 to 10 kHz. The fluctuations were characterized by a sudden and relatively brief increase in the mean diameter of the droplets caused by the passage of fractured clumps through the spray plume. Also evident in the droplet size distributions was the very small size of the droplets that had been sheared off the windward surfaces of the jet. The jet fracture frequency was related to the frequency of waves propagating along the initial jet column. The column waves are postulated to have been caused by jet perturbations created by vortices in the air flow around the jet column. Dissert. Abstr.

N87-10247 Cincinnati Univ., Ohio.
GLOBAL PRESSURE RELAXATION PROCEDURE WITH APPLICATION TO VISCOUS AND INVISCID FLOWS Ph.D. Thesis
Hien The Lai 1985 201 p
Avail: Univ. Microfilms Order No. DA8605502

Compressible, mostly transonic, flows involving strong viscous-inviscid interactions at high Reynolds numbers were studied. The governing equations employed are known as the Reduced Navier-Stokes (RNS) equations. The RNS equations are formulated to include the inviscid normal momentum equation, and an unknown streamwise pressure gradient term. This single RNS system is valid in both the viscous layer and the inviscid flow field. The numerical method follows the global pressure relaxation procedure. Extension to transonic flows with the global procedure is presented. Applications to the RNS as well as Euler equations are considered. All Shock waves are captured. Computed results are presented for a number of complex flow field structures in the transonic regime. These flows include shock-wave/boundary-layer interaction flow fields, large recirculation regions (base flows) and mixing shear layers (jet flows). Laminar and turbulent flows are considered for axisymmetric bodies. Simple algebraic models are employed in the turbulence computations. Inviscid solutions in subsonic, transonic, and supersonic regimes are investigated in two dimensional and axisymmetric cases. Inviscid and turbulent results are compared with data obtained from other numerical methods or experiments. Global convergence behavior is also assessed. Dissert. Abstr.

N87-10248*# Continuum, Inc., Huntsville, Ala.
COMPUTATIONAL FLUID MECHANICS UTILIZING THE VARIATIONAL PRINCIPLE OF MODELING DAMPING SEALS Final Report
J. Michael Abernathy 1 May 1986 35 p
(Contract NAS8-35508)
(NASA-CR-178902; NAS 1.26:178902; CI-FR-0088) Avail: NTIS HC A03/MF A01 CSCL 20D

A computational fluid dynamics code for application to traditional incompressible flow problems has been developed. The method is actually a slight compressibility approach which takes advantage of the bulk modulus and finite sound speed of all real fluids. The finite element numerical analog uses a dynamic differencing scheme based, in part, on a variational principle for computational fluid dynamics. The code was developed in order to study the feasibility of damping seals for high speed turbomachinery. Preliminary seal analyses have been performed. Author

N87-10249*# University of Southern California, Los Angeles.
NEAR FIELD PRESSURE FLUCTUATIONS IN A CIRCULAR JET

Final Report, 4 Nov. 1983 - 3 Nov. 1985
Chih-Ming Ho 1985 16 p
(Grant NAG1-420)
(NASA-CR-179847; NAS 1.26:179847) Avail: NTIS HC A02/MF A01 CSCL 20D

The vortical structures in shear layers govern many dynamic aspects of the jet, including entrainment of mass, transfer of momentum and noise generation. These structures develop from instability waves and undergo a merging process. Vortex merging reduces the time scale and increases the length scale of the shear layer. At the same time pressure fluctuations are induced by the unsteady motion. These pressure perturbations can exert high level dynamic loading on nearby structures, and radiate to the far field as noise. In this study, the generation mechanism of the pressure fluctuations and the radiation process are examined. Author

N87-10250# Naval Postgraduate School, Monterey, Calif.
AN ANALYSIS OF THE PERFORMANCE OF A VERTICALLY ORIENTED, GAS LOADED, VARIABLE CONDUCTANCE HEAT PIPE M.S. Thesis
Grey A. Glover, Sr. Mar. 1986 54 p
(AD-A167874) Avail: NTIS HC A04/MF A01 CSCL 20/13

An analysis of steady state operation of a vertically oriented, variable conductance heat pipe is presented. The effects of binary mass diffusion, axial pipe wall conduction, and gravitational effects, caused by the difference in molecular weight of the non-condensible gas and the working fluid are incorporated. Analytical expressions for the conservation of mass, momentum, and energy are combined along with equations of state to describe steady state operation of the heat pipe. These expressions are combined to form a system of three differential equations with three unknowns; working fluid vapor velocity, mass fraction, and temperature. These equations are nondimensionalized and an iteration scheme for numerical solution of the equations is presented. GRA

N87-10251# Michigan Technological Univ., Houghton. Dept. of Chemistry and Chemical Engineering.
FREE SURFACE TURBULENCE Annual Report, 1 Mar. 1985 - 28 Feb. 1986
D. W. Hubbard and G. Trevino 28 Feb. 1986 49 p
(Contract N00014-85-K-0236)
(AD-A168013) Avail: NTIS HC A03/MF A01 CSCL 20/4

When turbulent jets or wakes interact with a free surface, the turbulent eddies are apparently damped in the vertical direction and extended in the horizontal direction. Turbulent velocities are being measured for this zone of interaction to enable verifying turbulence modelling techniques. A two-dimensional jet is formed by pumping water through a rectangular slit into a channel filled with still water. Hot-film anemometry techniques measure velocity fluctuations in the jet and in the immediate neighborhood outside the jet. Some effects of jet flow rate and jet submergence have been studied. The raw data are sampled time records of the anemometer output voltages obtained at different positions in the jet. These time records together with the sensor calibration information are analyzed using digital signal processing techniques. The mean velocities, turbulence intensities, and velocity correlation functions are being calculated, and the results used to develop a two-point closure scheme and a mathematical model for jet flow turbulence. GRA

N87-10252# Argonne National Lab., Ill.
ANALYSIS OF HEAT-PIPE ABSORBERS IN EVACUATED-TUBE SOLAR COLLECTORS
J. R. Hull, W. W. Schertz, and J. W. Allen Feb. 1986 46 p
(Contract W-31-109-eng-38)
(DE86-010764; ANL-86-16) Avail: NTIS HC A03/MF A01

Heat transfer in evacuated-tube solar collectors with heat-pipe absorbers is compared with that for similar collectors with flow-through absorbers. In systems that produce hot water or other heated fluids, the heat-pipe absorber suffers a heat transfer penalty compared with the flow-through absorber, but in many cases the penalty can be minimized by proper design at the heat-pipe condenser and system manifold. The heat transfer penalty decreases with decreasing collector heat loss coefficient, suggesting that evacuated tubes with optical concentration are more appropriate for use with heat pipes than evacuated or nonevacuated flat-plate collectors. When the solar collector is used to drive an absorption chiller, the heat-pipe absorber has better heat transfer characteristics than the flow-through absorbers. DOE

N87-10253# Sandia National Labs., Albuquerque, N. Mex.
NONREACTING TURBULENT MIXING FLOWS: A LITERATURE SURVEY AND DATA BASE
R. W. Schefer, S. C. Johnston, R. W. Dibble, F. C. Gouldin, and W. Kollmann Apr. 1986 222 p Prepared in cooperation with Cornell Univ., Ithaca, N.Y. and California Univ., Davis
(Contract DE-AC04-76DR-00789)
(DE86-010864; SAND-86-8217) Avail: NTIS HC A10/MF A01

The objective of this report is to provide a comprehensive review of available data on turbulent nonreacting flows. This review is limited to parabolic, stationary shear flows with well defined boundary conditions; these flows have many of the characteristics found in combustion devices and are typical of laboratory flames for which model evaluation data are most likely to be available. This report is an outgrowth of a more extensive study conducted under the direction of the Air Force Office of Scientific Research. A bound volume containing the results of that study will be available in the near future. Our purpose in compiling the data presented here is to provide a more comprehensive tabulation of nonreacting flow measurements than was possible to include in the Air Force report. DOE

N87-10254# Oak Ridge Y-12 Plant, Tenn.
PERMEATION MEMBRANE-TYPE DISTILLER
K. Fujita 1986 8 p Transl. into ENGLISH of Japanese Patent Application No. 60-187305, 24 Sep. 1985
(Contract DE-AC05-84OS-21400)
(DE86-011153; Y/TR-86/3) Avail: NTIS HC A02/MF A01

The permeation membrane-type distiller is characterized by and is comprised of a condensed liquid channel positioned parallel to and between a permeation membrane that borders a high-temperature raw liquid channel and a condensed heat transfer plate that borders a cooling liquid channel, wherein said condensed heat transfer plate has a wavelike cross section whose ridges come close to said permeation membrane and, at the same time, a screen is positioned between said condensed heat transfer plate and said permeation membrane in such a way that it comes in contact with said membrane. DOE

N87-10255# Oak Ridge Gaseous Diffusion Plant, Tenn.
THERMOPERVAPORATION DEVICE
Takashi Kimura, Takeshi Nomura (Tokyo Univ. (Japan).), Shunichi Shimatani, and Atsunari Yoshimura 1986 9 p Transl. into ENGLISH of Japanese Patent Application No. 60-118205 (25 Jun. 1985) Prepared in cooperation with Nitto Electric Industrial Co. Ltd., Ibaraki, Osaka (Japan).
(Contract DE-AC05-84OS-21400)
(DE86-011151; Y/TR-86/4) Avail: NTIS HC A02/MF A01

A thermopervaporation device consists of (1) a shell and (2) one or more tubular membranes, which are made of polymer-porous membranes, which allow liquid vapor to permeate, but does not allow the liquid itself to permeate, and which are contained in the above-mentioned shell and form a liquid channel between themselves and the shell. The characteristic feature of the thermopervaporation apparatus is that it allows high-temperature liquid to flow through the above tubular membrane of the liquid channel, while low-temperature liquid passes through the other, then the vapor which is produced from the high-temperature liquid and permeates the tubular membrane will be cooled and condensed by the low-temperature liquid and then will be collected in the low-temperature liquid. DOE

N87-10256# Technion - Israel Inst. of Tech., Haifa.
ABSORPTION HEAT PUMP SIMULATION AND STUDIES: A MODULAR COMPUTER SIMULATION OF ABSORPTION SYS-

TEMS Final Report
G. Grossman and E. Michelson Apr. 1986 83 p
(Contract DE-AC05-84OR-21400)
(DE86-011206; ORNL/Sub-83-43337/2) Avail: NTIS HC A05/MF A01

A computer simulation program for absorption systems has been developed in a flexible and modular form, which makes it possible to simulate various configurations with different working fluids. The user supplies input containing information about given flow rates and temperatures, as well as characteristics of the various subunits of the system. In addition, the user must convey to the computer an image of the cycle in question. The program calculates the temperature, composition, flow rate, and pressure at each state point of the system and the heat quantities at each unit, from which the coefficient of performance may be determined. The program has been tested on single- and double-stage absorption heat pumps and heat transformers with lithium bromide-water and water-ammonia as the working fluids. Results have been compared with experimental data from tests of a lithium bromide-water heat transformer, giving good agreement. DOE

N87-10257# Costello (Frederick A.), Inc., Herndon, Va.
DETAILED TRANSIENT MODEL OF A LIQUID-METAL HEAT PIPE
Frederick A. Costello, A. F. Montague, and M. A. Merrigan 1986 6 p Presented at the 4th AIAA/ASME Thermophysics and Heat Transfer Conference, Boston, Mass., 2 Jun. 1986 Prepared in cooperation with Los Alamos National Lab., NM.; General Electric Co., Philadelphia, PA.
(Contract W-7405-eng-36)
(DE86-011212; LA-UR-86-1707; CONF-860612-7) Avail: NTIS HC A02/MF A01

A detailed transient model of a liquid-metal heat pipe is being developed. The model includes start from the frozen state, with provision for free-molecule flow, and proceeds through the steady-state operating conditions. The KACHINA method was selected for simulating the compressible flow in the core. The SIMPLER method was selected for simulating the liquid flow in the wicks and grooves. The computational methods have been demonstrated on a Compaq Deskpro II. The FORTRAN cove is currently being converted to the IBM 3033 and Cray I. Based on the ratio of Cray to Compaq speeds, the Cray computation times are estimated to be 30 minutes per hour simulated. DOE

N87-10258# Little (Arthur D.), Inc., Cambridge, Mass.
SUMMARY AND EVALUATION OF FIELD PERFORMANCE DATA ON UNITARY HEAT PUMPS
J. C. Burke, K. F. Fitzgerald, and L. Frantzis Apr. 1986 126 p
(Contract DE-AC05-84OR-21400)
(DE86-011289; ORNL/Sub-85-00219/1) Avail: NTIS HC A07/MF A01

Thirty-eight programs involving over 700 heat pump units were categorized in three levels: Level I programs measured energy input normally using utility load research methods, to obtain semi-quantitative performance information and hands on operating experience. In Level II programs (almost 150 units) both energy input and output were obtained allowing estimation of HSPF. Level III programs involved measurement of input, output and at least some isolation of dynamic losses due to part load cycling and frost/defrost. Energy input data is abundant and frequently reliable but the results are seldom either statically valid or easily generalized. A considerable amount of HSPF (and much less SEER) data is also available. Certain comparisons of these experimental performance factors with ARI 240-81 predictions have indicated good apparent agreement. Dynamic losses can degrade seasonal performance by over 20% in some instances. Unresolved experimental problems include optimization of flip-flop techniques, practical field measurement of cooling load and means of detecting performance degradation Also very few programs presented error analyses. DOE

N87-10259# Kentucky Univ., Lexington. Dept. of Mechanical Engineering.
TRANSIENT HEAT TRANSFER ANALYSIS AND RADIATIVE PROPERTIES MEASUREMENTS OF POROUS THERMAL INSULATION
T. W. Tong May 1986 83 p
(Contract DE-AC05-84OR-21400)
(DE86-011296; ORNL/Sub-84-43366/2) Avail: NTIS HC A05/MF A01

A combined radiative and conductive heat transfer model that uses the two-flux equations for radiation exchange has been applied to analyze the transient heat transfer data obtained with the flat-screen tester at ORNL. The data included those for the National Bureau of Standards (NBS) transfer standard and the NBS 1450b fiberglass board. Predictions that deviated by no more than 0.2°C of the measured screen temperature rise were obtained. Results indicate that the model can be used in conjunction with the transient data to determine the thermophysical properties of porous insulations. Transient heat transfer through porous insulations with one diurnal temperature boundary condition has been investigated using the same combined heat transfer model. By comparing the accumulated heat flow at the boundaries to those predicted using a purely conductive model, differences as large as 40% were found for some conditions. Results for a thermal resistance defined in terms of time-integrated quantities were also obtained and compared with that defined for steady-state conditions. Radiative properties for the NBS transfer standard, NBS 1450b, Cab-O-Sil S-17 and the Degussa R-974 have been measured. Properties reported included the extinction coefficient, single scattering albedo and the back-scattered fraction for the former two materials and the extinction coefficient for the latter two materials. DOE

N87-10260# Laboratorio de Computacao Cientifica, Rio de Janeiro (Brazil).
MODELLING OF THE FILLING UP OF A POROUS PLATE
R. Sampaio and R. M. S. da Gama 1985 7 p In POLISH
(DE86-702033; LCC-021/85) Avail: NTIS (US Sales Only) HC A02/MF A01

A generalization of Darcy's law is constructed using mixture theory to describe the transient flow of an incompressible fluid through a rigid solid porous matrix. The model is used to study the process of filling-up of an one dimensional unsaturated porous medium that is mathematically described by a system of nonlinear hyperbolic equations which is nonhomogeneous due to the drag force between the fluid and the solid matrix. The system is analysed throughly and solved numerically using the Glimm-Chorin method with a splitting to treat the non-homogeneous term. The results are discussed and shown to describe well the filling-up process. DOE

N87-10261# Laboratorio de Computacao Cientifica, Rio de Janeiro (Brazil).
CONSTITUTIVE RELATIONS FOR FLOW OF A NON-NEWTONIAN FLUID THROUGH SATURATED POROUS MEDIA
R. M. S. daGama and R. Sampaio 1985 16 p In POLISH
(DE86-702035; LCC-023/85) Avail: NTIS (US Sales Only) HC A02/MF A01

The behavior of two types of non-newtonian incompressible fluids, flowing through a porous medium which is assumed to be composed by several plane plates separated by a constant distance, is analysed. With the obtained results, constitutive relations are proposed for calculating the solid-fluid interaction force, that appears in the equations of the Continuum Theory of Mixtures, when the fluid and the solid (porous medium) are assumed continuous constituents of a binary mixture. DOE

N87-10262 Iowa State Univ. of Science and Technology, Ames.
APPLICATION OF A POTENTIAL CODE TO GENERAL STEADY FLOWS IN THREE DIMENSIONS Ph.D. Thesis
Akil Abbas Rangwalla 1986 88 p
Avail: Univ. Microfilms Order No. DA8615078

A low order panel method is described for the calculation of incompressible unsteady inviscid flow over general configurations. The numerical method is based upon piecewise constant doublet and source distributions. The wake and the geometry of the body are made to evolve with time. The unperturbed flow is chosen as the internal Dirichlet boundary condition and the source distribution is determined by the external Neumann boundary condition. The application of the Kutta condition for this formulation is straightforward. Two cases are examined. One is the impulsive start of a finite rectangular wing and the other is the interference between a propeller and a wing. The development of the circulation near the root for the first case is compared with the theoretical solution of an impulsively started two dimensional flat plate. The numerical results are very well behaved. The results for the interference between a propeller and a wing did conform with physical expectations. Also, this case is sufficiently general and has many aerodynamic features that either have not been solved or were solved for special cases. Dissert. Abstr.

N87-10016# Tokyo Univ. (Japan). Inst. of Space and Astronautical Science.
STUDY OF THREE-DIMENSIONAL SEPARATION ON A SPHEROID AT INCIDENCE
Yoshio Ishu and Yuko Oshima (Ochanomizu Women's Univ., Tokyo (Japan).) *In its* Proceedings of the Symposium on Mechanics for Space Flight, 1985 1985 9 p (For primary document see N87-10011 01-02)
Avail: NTIS HC A12/MF A01

N87-10018# Yamagata Univ. (Japan). Faculty of Engineering.
ON ACCURATE NUMERICAL SOLUTIONS OF FALKNER-SKAN EQUATION
Masakazu Katagiri *In* Tokyo Univ. Proceedings of the Symposium on Mechanics for Space Flight, 1985 1985 6 p (For primary document see N87-10011 01-02)
Avail: NTIS HC A12/MF A01

N87-10019# IBM Japan. Science Inst.
NUMERICAL STUDY OF THE ENTRANCE FLOW AND ITS TRANSITION OF A CIRCULAR PIPE
H. Kanda and K. Oshima *In* Tokyo Univ. Proceedings of the Symposium on Mechanics for Space Flight, 1985 1985 17 p (For primary document see N87-10011 01-02)
Avail: NTIS HC A12/MF A01

N87-10020# Kyoto Univ. (Japan). Dept. of Aeronautical Engineering.
NUMERICAL SIMULATION OF TWO-DIMENSIONAL FREEJET FLOW-FIELDS
Koji Teshima and Hiroyuki Nakatsuji *In* Tokyo Univ. Proceedings of the Symposium on Mechanics for Space Flight, 1985 1985 7 p Sponsored in part by the Data Processing Center (For primary document see N87-10011 01-02)
Avail: NTIS HC A12/MF A01

N87-10023# Miyazaki Univ. (Japan). Dept. of Applied Physics.
ANALYSIS ON GRAVITATIONAL EFFECT TO NONLINEAR DIFFUSION SYSTEM OF VAPOR MOLECULES IN A HEAT PIPE
Kanji Etori *In* Tokyo Univ. Proceedings of the Symposium on Mechanics for Space Flight, 1985 1985 12 p (For primary document see N87-10011 01-02)
Avail: NTIS HC A12/MF A01

N87-10024# Nippon Inst. of Tech. (Japan).
EFFECT OF SURPLUS STANDING LIQUID ON HEAT TRANSFER RESISTANCE IN THE HEAT PIPE (WITH MESH WICK IN A HORIZONTAL MODE)
Makoto Kamata and Yoshio Ikeda *In* Tokyo Univ. Proceedings of the Symposium on Mechanics for Space Flight, 1985 1985 10 p (For primary document see N87-10011 01-02)
Avail: NTIS HC A12/MF A01

N87-10025# Osaka Univ. (Japan). Dept. of Aeronautical Engineering.
DYNAMIC HEAT TRANSFER MECHANISM OF TWO-PHASE CLOSED THERMOSYPHON
Kanji Negishi, Ken-ichi Kaneko, and Fusao Kusumoto *In* Tokyo Univ. Proceedings of the Symposium on Mechanics for Space Flight, 1985 1985 9 p (For primary document see N87-10011 01-02)
Avail: NTIS HC A12/MF A01

N87-10026# National Research Inst. for Pollution and Resources, Tokyo (Japan).
A TRIAL ON PERFORMANCE TEST METHOD FOR Cu-WATER HEAT PIPE
Yoshio Tanaka and Tadashi Yamamoto *In* Tokyo Univ. Proceedings of the Symposium on Mechanics for Space Flight, 1985 1985 8 p (For primary document see N87-10011 01-02)
Avail: NTIS HC A12/MF A01

N87-10027# Toshiba Corp., Tokyo (Japan).
HIGH CAPACITY HEAT PIPE WITH AXIAL GROOVES
Yoshiro Miyazaki and Yuji Ido *In* Tokyo Univ. Proceedings of the Symposium on Mechanics for Space Flight, 1985 1985 5 p (For primary document see N87-10011 01-02)
Avail: NTIS HC A12/MF A01

N87-10028# Tokyo Electric Power Co., Inc. (Japan).
OPERATING CHARACTERISTICS OF COOLING UNDERGROUND POWER CABLES USING UP SLOPED LONG HEAT PIPES IN CONDUIT
Keisuke Oka, Hachiro Tsuchihashi, Yoichi Nishimura, Tsuneaki Mohtai (Fujikura Ltd., Sakura (Japan).), Masataka Mochizuki, Koichi Mashiko, and Hiroshi Yamanouchi *In* Tokyo Univ. Proceedings of the Symposium on Mechanics for Space Flight, 1985 1985 10 p (For primary document see N87-10011 01-02)
Avail: NTIS HC A12/MF A01

N87-10029# Tokyo Univ. (Japan). Inst. of Space and Astronautical Science.
REPORT OF THE INTERNATIONAL SYMPOSIUM ON COMPUTATIONAL FLUID DYNAMICS, TOKYO
Koichi Oshima *In its* Proceedings of the Symposium on Mechanics for Space Flight, 1985 1985 8 p (For primary document see N87-10011 01-02)
Avail: NTIS HC A12/MF A01

N87-10031# Akademiya Nauk SSSR, Novosibirsk. Inst. of Theoretifcal and Applied Mechanics.
NUMERICAL MODELING OF SPATIAL FLOWS ON THE BASIS OF SPLITTING UP METHOD
V. M. Kovenya, G. A. Tarnavsky, and S. G. Cherny *In* Tokyo Univ. Proceedings of the Symposium on Mechanics for Space Flight, 1985 1985 10 p (For primary document see N87-10011 01-02)
Avail: NTIS HC A12/MF A01

N87-10032# Academy of Sciences (USSR), Moscow. Computing Center.
THE THIRD ORDER COMPACT SCHEMES FOR FLUID DYNAMIC PROBLEMS
A. I. Tolstykh *In* Tokyo Univ. Proceedings of the Symposium on Mechnics for Space Flight, 1985 1985 7 p (For primary document see N87-10011 01-02)
Avail: NTIS HC A12/MF A01

N87-10034# Technical Univ. of Opole (Poland).
AN IMPROVED PSI-CELL METHOD FOR TURBULENT MULTIPHASE FLOWS
B. Dobrowolski and Z. Kabza *In* Tokyo Univ. Proceedings of the Symposium on Mechanics for Space Flight 1985 6 p (For primary document see N87-10011 01-02)
Avail: NTIS HC A12/MF A01

N87-10035# Bulgarian Academy of Science, Sofia. Inst. of Mechanics and Biomechanics.
HYDRODYNAMIC AND THERMAL INTERACTION BETWEEN TWO SPHERES IN A STEADY VISCOUS FLOW
Z. D. Zapryanov and E. T. Toshev *In* Tokyo Univ. Proceedings of the Symposium on Mechanics for Space Flight, 1985 1985 7 p

(For primary document see N87-10011 01-02)
Avail: NTIS HC A12/MF A01

N87-10037# Academy of Sciences (USSR), Moscow. Computing Center.
THE NUMERICAL METHOD OF CALCULATION OF TWO-DIMENSIONAL STATIONARY ELECTRO-GASDYNAMIC INTERNAL FLOWS
V. V. Zhurin and A. V. Shipilin *In* Tokyo Univ. Proceedings of the Symposium on Mechanics for Space Flight, 1985 1985 7 p (For primary document see N87-10011 01-02)
Avail: NTIS HC A12/MF A01

35 INSTRUMENTATION AND PHOTOGRAPHY

Includes remote sensors; measuring instruments and gages; detectors; cameras and photographic supplies; and holography.

For aerial photography see *43 Earth Resources and Remote Sensing*. For related information see also *06 Aircraft Instrumentation*, and *19 Spacecraft Instrumentation*.

N87-10263*# National Aeronautics and Space Administration. Langley Research Center, Hampton, Va.
THIRTEENTH INTERNATIONAL LASER RADAR CONFERENCE
Aug. 1986 335 p Conference held in Toronto, Ontario, 11-15 Aug. 1986; sponsored by NASA, Washington, D.C., Atmospheric Environment Service, and York Univ.
(NASA-CP-2431; L-16201; NAS 1.55:2431) Avail: NTIS HC A15/MF A01 CSCL 20E

One hundred fifteen papers were presented in both oral and poster sessions. The topics of the conference sessions were: spaceborne lidar applications; extinction/visibility; differential absorption lidar; winds and tropospheric studies; middle atmosphere; clouds and multiple scattering; pollution studies; and new systems. For individual titles, see N87-10264 through N87-10375.

N87-10264*# European Space Agency. European Space Research and Technology Center, ESTEC, Noordwijk (Netherlands).
ESA ACTIVITIES IN SPACE LASER SOUNDING AND RANGING c36
H. Lutz *In* NASA. Langley Research Center 13th International Laser Radar Conference Aug. 1986 1 p (For primary document see N87-10263 01-35)
Avail: NTIS HC A15/MF A01 CSCL 20E

Laser remote sensing from space is undoubtedly one of the most promising means to obtain essential atmospheric and geophysical parameters on a global scale. Efforts including feasibility assessments, technology developments, and mission definition studies are in progress at the European Space Agency (ESA) to prepare for the prospective use of laser remote sensing systems in space. An overview of the programs under way is presented and the perspectives of laser remote sensing in the context of ESA's Long-Term European Space Plan are discussed. Author

N87-10265*# National Aeronautics and Space Administration, Washington, D.C.
LIDAR REMOTE SENSING FROM SPACE: NASA'S PLANS IN THE EARTH SCIENCES c43
Robert J. Curran *In* NASA. Langley Research Center 13th International Laser Radar Conference Aug. 1986 1 p (For primary document see N87-10263 01-35)
Avail: NTIS HC A15/MF A01 CSCL 20E

A multidisciplinary study of the Earth System to provide a better understanding of the complex interrelated processes involved in the system, the Earth Observing System (EOS), is being developed. Capabilities of the Space Station, both the polar orbiting platform and the lower inclination platforms, will be used to accommodate a number of large active and/or passive sensors. Two lidar instruments being considered as part of the Eos payload are the Lidar Atmospheric Sounder and Altimeter (LASA) and the Laser Atmospheric Wind Sounder (LAWS). The LASA instrument is separable into two portions: the atmospheric sounder component and the retroranging component. The LASA atmospheric sounder will sample the spatial distribution of several atmospheric parameters. The retroranging component will be used to determine the precise three-dimensional position of specifically placed retroreflectors and to sense how these retro-reflectors change position over monthly to yearly time periods. The LAWS utilizes a lidar system capable of measuring the Doppler shift in the backscattered intensity to determine the wind velocity profile. B.G.

N87-10266*# National Aeronautics and Space Administration. Langley Research Center, Hampton, Va.
TUNABLE SOLID-STATE LASER TECHNOLOGY FOR APPLICATIONS TO SCIENTIFIC AND TECHNOLOGICAL EXPERIMENTS FROM SPACE c36
F. Allario and L. V. Taylor *In its* 13th International Laser Radar Conferance Aug. 1986 1 p (For primary document see N87-10263 01-35)
Avail: NTIS HC A15/MF A01 CSCL 20E

Current plans for the Earth Observing System (EOS) include development of a lidar facility to conduct scientific experiments from a polar orbiting platforms. A recommended set of experiments were scoped, which includes techniques of atmospheric backscatter (Lidar), Differential Absorption Lidar (DIAL), altimetry, and retroranging. Preliminary assessments of the resources (power, weight, volume) required by the Eos Lidar Facility were conducted. A research program in tunable solid state laser technology was developed, which includes laser materials development, modeling and experiments on the physics of solid state laser materials, and development of solid state laser transmitters with a strong focus on Eos scientific investigations. Some of the system studies that were conducted which highlight the payoff of solid state laser technology for the Eos scientific investigations will be discussed. Additionally, a summary of some promising research results which have recently emerged from the research program will be presented. B.G.

N87-10267*# Coherent Technologies, Inc., Boulder, Colo.
COHERENT LIDAR TECHNOLOGY FOR GLOBAL WIND PROFILING c47
R. Milton Huffaker *In* NASA. Langley Research center 13th International Laser Radar Conference Aug. 1986 2 p (For primary document see N87-10263 01-35)
Avail: NTIS HC A15/MF A01 CSCL 04B

Current lidar systems are proven sensors for atmospheric wind measurement. Ground-based and airborne continuous wave and pulsed CO2 systems were developed and applied to several wind measuring applications. Analytical and hardware feasibility studies indicte the feasibility of measuring the global wind field from a space splatform. A Global Backscater Experiment is planned by NASA to develop a global model of aerosol backscatter using a CO2 laser. Ground-based aerosol backscatter profiles will also be obtained using a ruby and a pulsed CO2 lidar. B.G.

N87-10268*# National Aeronautics and Space Administration. Langley Research Center, Hampton, Va.
DEVELOPMENT OF A HIGH-ALTITUDE AIRBORNE DIAL SYSTEM: THE LIDAR ATMOSPHERIC SENSING EXPERIMENT (LASE) c46
E. V. Browell, W. R. Vaughan, W. M. Hall, J. J. Degnan, R. D. Averill, J. G. Wells, D. E. Hinton, and J. H. Goad *In its* 13th International Laser Radar Conference Aug. 1986 4 p (For primary document see N87-10263 01-35)
Avail: NTIS HC A15/MF A01 CSCL 04A

The ability of a Differential Absorption Lidar (DIAL) system to measure vertical profiles of H2O in the lower atmosphere was demonstrated both in ground-based and airborne experiments. In these experiments, tunable lasers were used that required real-time experimenter control to locate and lock onto the atmospheric H2O absorption line for the DIAL measurements. The Lidar Atmospheric Sensing Experiment (LASE) is the first step in a long-range effort to develop and demonstrate an autonomous DIAL system for airborne and spaceborne flight experiments. The LASE instrument is being developed to measure H2O, aerosol, and cloud profiles from a high-altitude ER-2 (extended range U-2) aircraft. The science of the LASE program, the LASE system design, and the expected measurement capability of the system are discussed. Author

N87-10269*# Deutsche Forschungs- und Versuchsanstalt fuer Luft- und Raumfahrt, Wesseling (West Germany). Inst. for Atmospheric Physics.
MIE LIDAR PROPOSED FOR THE GERMAN SPACE SHUTTLE MISSION D2 c36
W. Renger, M. Endemann (Battelle Inst., Frankfurt am Main (West Germany).), H. Quenzel (Ludwig-Maximilians-Universitaet, Munich (West Germany).), and Ch. Werner *In* NASA. Langley Research center 13th International Laser Radar Conference Aug. 1986 4 p (For primary document see N87-10263 01-35)
Avail: NTIS HC A15/MF A01 CSCL 20E

Firm plans for a second German Spacelab mission (D2-mission), originally scheduled for late 1988 is basically a zero-g mission, but will also include earth observation experiments. On board the D2-facility will allow performance of a number of different measurements with the goal to obtain performance data (cloud top heights, height of the planetary boundary layer, optical thickness, and cloud base height of thin and medium thick clouds, ice/water phase discriminatin for clouds, tropopause height, tropaspheric height, tropospheric aerosols, and stratospheric aerosols. B.G.

N87-10270*# National Aeronautics and Space Administration. Langley Research Center, Hampton, Va.
THE LIDAR IN-SPACE TECHNOLOGY EXPERIMENT (LITE) c36
M. P. McCormick *In its* 13th International Laser Radar Conference Aug. 1986 1 p (For primary document see N87-10263 01-35)
Avail: NTIS HC A15/MF A01 CSCL 20E

A spaceborne lidar system is presently being constructed for flight aboard the U. S. Space Shuttle in early 1991. The experiment, Lidar In Space Technology Experiment (LITE), utilizes a neodymium: YAG laser and 0.85 meter effective diameter Cassegranian-configured telescope receiver for making elastic backscatter measurements. The laser will be frequency doubled and tripled simulataneously producing a 10 Hz rate of 200 mJ at 1064 nm, 400 mJ at 532 nm, and 150 mJ at 355 nm. The technological objectives of LITE are to evaluate lidar system operations in space, lidar techniques in space, and to provide a test bed for new lidar technologies in later flights. The measurement objectives include the determination of cloud top and planetary boundary layer heights, the measurement of tropospheric and stratospheric aerosols, and the measurement of temperature and density between 10 to 40 km altitude. Detailed simulations will be presented showing the errors associated with each of these measurement objectives. In addition, the experiment scenario will be described including measurement times, data flow, processing and archival, and initial plans for validation of the LITE data set with correlative measurements. B.G.

N87-10271*# University of Western Australia, Perth. School of Physics and Geoscience.
AEROSOL STUDIES IN MID-LATITUDE COASTAL ENVIRONMENTS IN AUSTRALIA c45
S. A. Young, D. Cutten (Electronics Research Lab., Adelaide (Australia).), M. J. Lynch, and J. E. Davies *In* NASA. Langley Research Center 13th International Laser Radar Conference Aug. 1986 4 p (For primary document see N87-10263 01-35)
Avail: NTIS HC A15/MF A01 CSCL 13B

The results of the evaluation of several inversion procedures that were used to select one which provides the most accurate atmospheric extinction profiles for small aerosol extinction coefficients (that often predominate in the maritime airmass) are presented. Height profiles of atmospheric extinction calculated by a two component atmospheric solution to the LIDAR equation will be compared with corresponding in-situ extinction profiles based on the size distribution profiles obtained in Western Australia. Values of the aerosol backscatter to extinction ratio obtained from multi-angle LIDAR measurements will be used in this solution. B.G.

N87-10272*# Atmospheric Sciences Lab., White Sands Missile Range, N. Mex.
VISIBILITY RELATED TO BACKSCATTER AT 1.54 MICRON c45
T. L. Barber and D. R. Larson (New Mexico State Univ., Las Cruces.) *In* NASA. Langley Research Center 13th International Laser Radar Conference Aug. 1986 2 p (For primary document see N87-10263 01-35)
Avail: NTIS HC A15/MF A01 CSCL 13B

The lidar process was shown to have the necessary potential to fulfill the need for a remote measurement of visibility. Visibility can be inferred from a lidar return optical extinction. The wavelength 1.54 micron was chosen, being near the visible wavelength region and having a high eye safety threshol, 200,000 times higher than 1.06 micron; 1.54 is the erbium laser wavelength. This research utilized 105 measured height profiles of natural droplet size distributions data, taken in clouds, fog, and haze. These profiles were examined to determine the completeness of the droplet counting data. It was found that the particle spectrometer data were incomplete in the very light ford and haze so this portion of the data was eliminated. Utilizing the Mie theory, these droplet size distribution profiles were converted to backscatter at 1.54 micron and extinction in the visible region, 0.55 micron. Using Koschmeider's relationship, the extinction profiles were converted to visibility. The visibility and backscatter profiles were compared to develop a relationship between visibility and backscatter at 1.54 micron. B.G.

N87-10273*# York Univ., Downsview (Ontario). Dept. of Physics.
INVERSION OF 2 WAVELENGTH LIDAR DATA FOR CLOUD PROPERTIES c47
S. R. Pal and A. I. Carswell *In* NASA. Langley Research Center 13th International Laser Radar Conference Aug. 1986 2 p (For primary document see N87-10263 01-35)
Avail: NTIS HC A15/MF A01 CSCL 04B

The inversion of the lidar equation to derive quantitative properties of the atmosphere has continued to present considerable difficulty. The results of a study in which Klett's procedure was utilized for the analysis of cloud backscatter measurements made simulataneously at two ruby lidar wavelengths (694nm,347nmm) are presented. With one lidar system a cloud is probed at the two wavelength and the backscatter measured simulataneously by separate receivers. As a result two sigma profiles which should differ only because the wavlength dependence of the scattering. Experimental data presented to demonstrate the effects and the implications of the applications of the inversion method will be discussed. B.G.

N87-10274*# Ludwig-Maximilians-Universitaet, Munich (West Germany). Meteorological Inst.
THE USEFULNESS OF KLETT'S INVERSION ALGORTHMS TO SIMULATED SATELLITE LIDAR RETURNS c32
M. Kastner and H. Quenzel *In* NASA. Langley Research Center 13th International Laser Radar Conference Aug. 1986 4 p (For primary document see N87-10263 01-35)
Avail: NTIS HC A15/MF A01 CSCL 17I

The lidar equation is a special form of the radiative transport equation in single scattering approximation and describes the return signal of a lidar. Klett's algorithm for retrieving the total extinction coefficient profile was developed for application to ground-based lidar returns by a backward integration from the far end to the near end, the range where the incident and backscattered pulse overlap totally. The applicability of Klett's algorithm to satellite backscatter lidar returns was assessed. The simulated data of a

1 J Alexandrite laser operated at about 0.7 micron and at a satellite flight level of 840 km. B.G.

N87-10275*# National Aeronautics and Space Administration. Langley Research Center, Hampton, Va.
WAVELENGTH DEPENDENCE OF AEROSOL BACKSCATTER COEFFICIENTS OBTAINED BY MULTIPLE WAVELENGTH LIDAR MEASUREMENTS c32
Yasuhiro Sasano (Old Dominion Univ., Norfolk, Va.) and Edward V. Browell *In its* 13th International Laser Radar Conference Aug. 1986 4 p (For primary document see N87-10263 01-35)
Avail: NTIS HC A15/MF A01 CSCL 17I

Aerosols are often classified into several general types according to their origins and composition, such as maritime, continental, and stratospheric aerosols, and these aerosol types generally have different characteristics in chemical and physical properties. The present study aims at demonstrating the potential for distinguishing these aerosol types by the wavelength dependence of their backscatter coefficients obtained from quantitative analyses of multiple wavelength lidar signals. Data from the NASA Airborne Differential Abosrption lidar (DIAL) S ystems, which can measure aerosol backscatter profiles at wavelenghts of 300, 600, and 1064 nm and ozone profiles of backscatter coefficients for these three wavelength were derived from the observations of aerosols of different types. Observations were performed over the Atlantic Ocean, the Southwestern United States, and French Guyana. B.G.

N87-10276*# Research Inst. of National Defence, Linkoeping (Sweden).
EXTINCTION AND VISIBILITY MEASUREMENTS IN THE LOWER ATMOSPHERE WITH UV-YAG-LIDAR c32
Arne Hagard *In* NASA. Langley Research Center 13th International Laser Radar Conference Aug. 1986 2 p (For primary document see N87-10263 01-35)
Avail: NTIS HC A15/MF A01 CSCL 17I

With the intention to investigate methods for slant path visibiltiy measurements and to develop information for modelling of extinction profiles in the atmospheric boundary layer, measurements were performed with a lidar based on a YAG-laser. The third harmonic at 355 nm in the ultraviolet was used and thus eye safety problems are avoided. At this wavelength the lens of the human eye is not transparent and the safety distance for the laser is a 50 meters as compared to several km for a corresponding green laser. The lidar is a coaxial system with a turnable mirror system for beam steering. The extinction coefficient at both 355 and 532 nm was measured and the ratio determined. Provided that the wavelength dependence of the aerosol extinction is range independent, the measured extinction profile at 355 nm can be converted to a corresponding profile at 532 nm, which is more relevant for visibility. In order to calculate the extinction profile the lidar equation is inverted by a method, which is based on Klett's method. B.G.

N87-10277*# Defence Research Establishment Valcartier (Quebec).
SENSITIVITY OF THE LIDAR RATIO TO CHANGES IN SIZE DISTRIBUTION AND INDEX OF REFRACTION c32
B. T. N. Evans *In* NASA. Langley Research Center 13th International Laser Radar Conference Aug. 1986 3 p (For primary document see N87-10263 01-35)
Avail: NTIS HC A15/MF A01 CSCL 17I

In order to invert lidar signals to obtain reliable extinction coefficients, sigma, a relationship between sigma and the backscatter coefficient, beta, must be given. These two coefficients are linearly related if the complex index of refraction, m, particle shape size distribution, N, does not change along the path illuminated by the laser beam. This, however, is generally not the case. An extensive Mie computation of the lidar ratio R = beta/sigma and the sensitivity of R to the changes in a parametric space defined by N and m were examined. B.G.

N87-10278*# Academy of Sciences (USSR), Tomsk. Inst. of Atmospheric Optics.
LIDAR MEASUREMENTS OF SLANT VISUAL RANGE c36
Yu. S. Balin, S. I. Kavkyanov, G. M. Krekov, and I. A. Razenkov *In* NASA. Langley Research Center 13th International Laser Radar Conference Aug. 1986 3 p (For primary document see N87-10263 01-35)
Avail: NTIS HC A15/MF A01 CSCL 20E

When converting the lidar equation relative to the extinction coefficient and, correspondingly, the visual range, the instability of the solution at the increase of the optical density of the sounding path is encountered. The search for a stable solution has resulted in the appearance of a set of inversion algorithms differing mainly in the manner of assigning the a priori information on the profile sought. A stable algorithm of inversion is suggested and a comparative analysis and experimental verification of some methods of processing the signals at sounding the optically dense atmospheric formations are given. B.G.

N87-10279*# National Inst. for Environmental Studies, Tsukuba (Japan).
VISIBILITY AND AEROSOL MEASUREMENT BY DIODE-LASER RANDOM-MODULATION CW LIDAR c36
N. Takeuchi, H. Baba (Tokyo Univ. (Japan).), K. Sakurai, T. Ueno (Chiba Univ. (Japan).), and N. Ishikawa *In* NASA. Langley Research Center 13th International Laser Radar Conference Aug. 1986 4 p (For primary document see N87-10263 01-35)
Avail: NTIS HC A15/MF A01 CSCL 20E

Examples of diode laser (DL) random-modulation continuous wave (RM-CW) lidar measurements are reported. The ability of the measurement of the visibility, vertical aerosol profile, and the cloud ceiling height is demonstrated. Although the data shown here were all measured at night time, the daytime measurement is, of course, possible. For that purpose, accurate control of the laser frequency to the center frequency of a narrow band filter is required. Now a new system with a frequency control is under construction. B.G.

N87-10280*# Arizona Univ., Tucson. Inst. of Atmospheric Physics.
CORRECTION FUNCTION IN THE LIDAR EQUATION AND THE SOLUTION TECHNIQUES FOR CO2 LIDAR DATE REDUCTION c36
Yanzeng Zhao, Ting Kaung Lea, and Richard M. Schotland *In* NASA. Langley Research Center 13th International Laser Radar Conference Aug. 1986 4 p (For primary document see N87-10263 01-35)
Avail: NTIS HC A15/MF A01 CSCL 20E

For lidar systems with long laser pulses the unusual behavior of the near-range signals causes serious difficulties and large errors in reduction. The commonly used lidar equation is no longer applicable since the convolution of the laser pulse with the atmospheric parameter distributions should be taken into account. It is important to give more insight into this problem and find the solution techniques. Starting from the original equation, a general form is suggested for the single scattering lidar equation where a correction function Cr is introduced. The correction Function Cr(R) derived from the original equation indicates the departure from the normal lidar equation. Examples of Cr(R) for a coaxial CO2 lidar system are presented. The Differential Absorption Lidar (DIAL) errors caused by the differences of Cr(R) for H2O measurements are plotted against height. B.G.

N87-10281*# National Aeronautics and Space Administration. Langley Research Center, Hampton, Va.
ASSESSMENT OF DIAL DATA COLLECTION AND ANALYSIS TECHNIQUES c36
E. V. Browell and P. T. Woods (National Physical Lab., Teddington (England).) *In its* 13th International Laser Radar Conference Aug. 1986 3 p (For primary document see N87-10263 01-35)
Avail: NTIS HC A15/MF A01 CSCL 20E

The key issues in all areas of Differential Absorption Lidar (DIAL) data collection and analysis techniques were examined.

This included consideration of the practical and theoretical limitations of DIAL and the range of possible DIAL measurements. B.G.

N87-10282*# National Aeronautics and Space Administration. Goddard Space Flight Center, Greenbelt, Md.
AIRBORNE LIDAR MEASUREMENTS OF THE ATMOSPHERIC PRESSURE PROFILE WITH TUNABLE ALEXANDRITE LASERS c36
C. L. Korb, G. K. Schwemmer, M. Dombrowski, J. Milrod, and H. Walden *In* NASA. Langley Research Center 13th International Laser Radar Conference Aug. 1986 3 p (For primary document see N87-10263 01-35)
Avail: NTIS HC A15/MF A01 CSCL 20E

The first remote measurements of the atmospheric pressure profile made from an airborne platform are described. The measurements utilize a differential absorption lidar and tunable solid state Alexandrite lasers. The pressure measurement technique uses a high resolution oxygen A band where the absorption is highly pressure sensitive due to collision broadening. Absorption troughs and regions of minimum absorption were used between pairs of stongly absorption lines for these measurements. The trough technique allows the measurement to be greatly desensitized to the effects of laser frequency instabilities. The lidar system was set up to measure pressure with the on-line laser tuned to the absorption trough at 13147.3/cm and with the reference laser tuned to a nonabsorbing frequency near 13170.0/cm. The lidar signal returns were sampled with a 200 range gate (30 vertical resoltion) and averaged over 100 shots. B.G.

N87-10283*# National Aeronautics and Space Administration. Langley Research Center, Hampton, Va.
MEASUREMENTS OF THE EFFECT OF HORIZONTAL VARIABILITY OF ATMOSPHERIC BACKSCATTER ON DIAL MEASUREMENTS c46
G. K. Schwemmer, C. L. Korb, M. Dombrowski, and C. Y. Weng (Science Systems and Applications, Inc., Seabrook, Md.) *In its* 13th International Laser Radar Conference Aug. 1986 2 p (For primary document see N87-10263 01-35)
Avail: NTIS HC A15/MF A01 CSCL 04A

The horizontal variability of atmospheric backscatter may have a substantial effect on how Differential Absorption Lidar (DIAL) data must be taken and analyzed. To minimize errors, lidar pulse pairs are taken with time separations which are short compared to the time scales associated with variations in atmospheric backscatter. To assess the atmospheric variability for time scales which are long compared to the lidar pulse repetition rate, the variance of the lidar return signal in a given channel can be computed. The variances of the on-line, off-line, and ration of the on-line to off-line signals at given altitudes obtained with the dual solid-state Alexandrite laser system were calculated. These evaluations were made for both down-looking aircraft and up-looking ground-based lidar data. Data were taken with 200 microsecond separation between on-line and off-line laser pulses, 30 m altitude resolution, 5 Hz repetition rate, and the signal were normalized for outgoing laser energy. B.G.

N87-10284*# Radio Research Labs., Tokyo (Japan). Ministry of Posts and Telecommunications.
FLIGHT TESTS OF A RANGE-RESOLVED AIRBORNE DIAL WITH TWO MIN-TEA CO2 LASERS c36
T. Itabe, M. Ishizu, T. Aruga, T. Igarashi, and K. Asai (Tohoku Univ., Sendai (Japan).) *In* NASA. Langley Research Center 13th International Laser Radar Conference Aug. 1986 2 p (For primary document see N87-10263 01-35)
Avail: NTIS HC A15/MF A01 CSCL 20E

It is important to measure regional distributions of ozone concentrations in a short time for understanding a mechanism of photo-chemical smog development. An airborne Differential Absorption Lidar (DIAL) system with two low-power mini-TEA CO2 lasers was developed for measuring three-dimensional distributions of ozone in the lower troposphere. The CO2 DIAL is a nadir-looking system and is designed to measure ozone profiles between ground and airplane by using atmospheric aerosols as a distributed radar target. First flight test with a single laser were conducted in February 1985 over the Tokyo area. The system was operated at an altitude of 5000 ft. Results of the first flight tests show that the height profiles of the received power in the boundary layer were different between over land and ocean. The received power has to be inverted to an expression of a single optical parameter to see real aerosol distributions. Inversion of the lidar signal to the aerosol extinction was performed by using Klett's solution. B.G.

N87-10285*# RCA Astro-Electronics Div., Princeton, N. J.
Nd:GLASS-RAMAN LASER FOR WATER VAPOR DIAL c36
R. H. Kagann, J. C. Petheram, and A. Rosenberg *In* NASA. Langley Research Center 13th International Laser Radar Conference Aug. 1986 2 p (For primary document see N87-10263 01-35)
Avail: NTIS HC A15/MF A01 CSCL 20E

A tunable solid-state Raman shifted laser which was used in a water vapor Differential Absorption Lidar (DIAL) system at 9400 A is described. The DIAL transmitter is based on a tunable glass laser operating at 1.06 microns, a hydrogen Raman cell to shift the radiation to 1.88 microns, and a frequency doubling crystal. The results of measurements which characterize the output of the laser with respect to optimization of optical configuration and of Raman parameters were reported. The DIAL system was also described and preliminary atmospheric returns shown. B.G.

N87-10286*# Electricite de France, Chatou.
A METEOROLOGICAL (HUMIDITY, TEMPERATURE, AEROSOLS)) MOBILE DIAL SYSTEM: CONCEPTS AND DESIGN c47
Cl. Cahen, J. L. Lesne, J. Benard, and P. Ponsardin *In* NASA. Langley Research Center 13th International Laser Radar Conference Aug. 1986 4 p (For primary document see N87-10263 01-35)
Avail: NTIS HC A15/MF A01 CSCL 04B

Since 1982 a program was conducted to develop a mobile meteorological (humidity, temperature, aerosols) Differential Absorption Lidar (DIAL) devoted to the studies of the nuclear power plant atmospheric surroundings. The measurement objectives are defined according to the user needs and the lidar feasibility. The concepts and design adopted to meet both the requirement and the measurement objectives are described. Each sub-system is addressed sequentially: transmitting system, receiving system, detection system, and post detection. B.G.

N87-10287*# National Aeronautics and Space Administration. Langley Research Center, Hampton, Va.
INFLUENCE OF RAYLEIGH-DOPPLER BROADENING ON THE SELECTION OF H2O DIAL SYSTEM PARAMETERS c32
Syed Ismail and Edward V. Browell *In its* 13th International Laser Radar Conference Aug. 1986 5 p (For primary document see N87-10263 01-35)
Avail: NTIS HC A15/MF A01 CSCL 20N

Computer simulations have enabled the performance of a H2O Differential Absorption Lidar (DIAL) system to be studied by spectrally analyzing the forward propagating and backscattered laser energy. The simulations were done for a high altitude (21 km) DIAL system operating in a nadir-viewing mode. The influence of Rayleigh Doppler broadening on DIAL measurement accuracies were evaluated and show that the Rayleigh broadening influence, which can be corrected to first order in regions free of large aerosol gradients, reduces the sensitivity of DIAL H2O measurement errors in the upper tropospheric region. The ability to correct the Rayleigh broadening and the selection of H2O DIAL parameters when all the systematic effects are combined, were discussed. B.G.

N87-10288*# Max-Planck-Inst. fuer Meteorologie, Hamburg (West Germany).
CORRECTION OF DOPPLER-BROADENED RAYLEIGH BACKSCATTERING EFFECTS IN H2O DIAL MEASUREMENTS c32
A. Ansmann and J. Bosenberg *In* NASA. Langley Research Center

13th International Laser Radar Conference Aug. 1986 3 p (For primary document see N87-10263 01-35)
Avail: NTIS HC A15/MF A01 CSCL 20N

A general method of solutions for treating effects of Doppler-broadened Rayleigh backscattering in H2O Differential Absorption Lidar (DIAL) measurements are described and discussed. Errors in vertical DIAL measurements caused by this laser line broadening effect can be very large and, therefore, this effect has to be accounted for accurately. To analyze and correct effects of Doppler-broadened Rayleigh backscattering in DIAL experiments, a generalized DIAL approximation was derived starting from a lidar equation, which includes Doppler broadening. To evaluate the accuracy of H2O DIAL measurements, computer simulations were performed. It was concluded that correction of Doppler broadened Rayleigh backscattering is possible with good accuracy in most cases of tropospheric H2O DIAL measurements, but great care has to be taken when layers with steep gradients of Mie backscattering like clouds or inversion layers are present. B.G.

N87-10289*# National Physical Lab., Teddington (England). Div. of Quantum Metrology.

ATMOSPHERIC CONTRIBUTIONS TO THE COLUMN VARIANCE IN DIRECT-DETECTION DIAL **c36**

M. J. T. Milton and P. T. Woods *In* NASA. Langley Research Center 13th International Laser Radar Conference Aug. 1986 3 p (For primary document see N87-10263 01-35)
Avail: NTIS HC A15/MF A01 CSCL 20E

One of the most important parameters of a Differential Absorption Lidar (DIAL) system is the delay time between the on and off resonant pulses. It is important that this delay time is sufficiently small to ensure that the atmosphere is effectively frozen between the pulses. Therefore, most Dial systems were designed with two lasers firing alternately less than 1 msec apart. Despite the importance of this parameter in the design of DIAL systems and its contribution to the overall error of a column measurement, very little is known about the size of the error for the case of a direct-detection system using atmospheric backscatter. The ultraviolet DIAL system uses two independent YAG/dye lasers and is therefore suitable for measuring the effects of different pulse delays on the variance of column measurements for a variety of atmospheric conditions. A set of DIAL returns were acquired with the two lasers tuned to the same wavelength and with a range of pulse delay times between 250 microseconds and several minutes. This data set was recorded in full on a computer and was used both to test different averaging techniques and also to evaluate atmospheric contributions to DIAL columns. B.G.

N87-10290*# Maryland Univ., College Park. Inst. for Physical Science.

HIGH SPECTRAL PURITY, NARROW LINEWIDTH LASER TRANSMITTER FOR DIAL MEASUREMENTS **c36**

U. N. Singh and P. H. Flamant (Laboratoire de Meteorologie Dynamique du CNRS, Palaiseau (France).) *In* NASA. Langley Research Center 13th International Laser Radar Conference Aug. 1986 4 p (For primary document see N87-10263 01-35)
Avail: NTIS HC A15/MF A01 CSCL 20E

A laser transmission with very high degree of spectral purity was described. Amplified Spontaneous Emission (ASE) dependence on the oscillator energy and the detuning away from the gain curve center are demonstrated. The effects of both finite laser linewidth and spectral purity on humidity measurements are experimentally demonstrated. B.G.

N87-10291*# National Aeronautics and Space Administration. Goddard Space Flight Center, Greenbelt, Md.

ON THE MEASUREMENT OF ATMOSPHERIC DENSITY USING DIAL IN THE O2 A-BAND (770 nm) **c46**

T. D. Wilkerson (Maryland Univ., College Park.), G. K. Schwemmer, L. J. Cotnoir, and U. N. Singh *In* NASA. Langley Research Center 13th International Laser Radar Conference Aug. 1986 4 p (For primary document see N87-10263 01-35)
(Contracts NCC1-25; DAAG29-81-D-0100; Grant NA83-AA-A-00036)
Avail: NTIS HC A15/MF A01 CSCL 04A

Differential Absorption Lidar (DIAL) measurements in the A-band of molecular oxygen were suggested as a means of profiling atmospheric density. Progress towards this capability is reported. B.G.

N87-10292*# Naval Research Lab., Washington, D.C. Atmospheric Physics Branch.

USING A LASER AUREOLE TO INVERT LIDAR RETURN **c36**

William P. Hooper and H. Gerber *In* NASA. Langley Research Center 13th International Laser Radar Conference Aug. 1986 1 p (For primary document see N87-10263 01-35)
Avail: NTIS HC A15/MF A01 CSCL 20E

An aureole generated by a laser beam was studied. The strength of the signal redirected towards a sensor high above the surface by a combination of one scattering event in the marine boundary layer (mbl) and one single reflection event from the ocean surface was estimated. A model of mbl aerosol size distributions was used to estimate Mie scattering for a wide range of meteorolocial conditions. The sea surface reflection was determined from a Gaussian model of the wave slopes. These laser aureoles which were estimated over the wide range of conditions and were normalized by the reflected laser light were found to be highly correlated with the optical depth of the boundary layer. By estimating optical depth from the aureole, the Bernoulli-Riccati inversion of lidar return could be constrained and the inversion accuracy improved. A Monte Carlo program was developed to study the laser aureole generated by up to 8 orders of reflection and scattering. The aureole was generated by a narrow, 10 nsec laser pulse at 1.06 microns and measured by a receiver 10 km above the ocean surface. The original theoretical computation compared well with the Monte Carlo method. When multiple scattereffects were included, the normalized aureole was still highly correlated with the mbl optical depth over the range of conditions. B.G.

N87-10293*# York Univ., Downsview (Ontario). Dept. of Physics.

DETERMINATION OF CLOUD MICROPHYSICAL PROPERTIES BY LASER BACKSCATTERING AND EXTINCTION MEASUREMENTS **c47**

R. N. Dubinsky, A. I. Carswell, and S. R. Pal *In* NASA. Langley Research Center 13th International Laser Radar Conference Aug. 1986 1 p (For primary document see N87-10263 01-35)
Avail: NTIS HC A15/MF A01 CSCL 04B

The extinction and backscattering of 514 nm laser radiation in polydisperse water droplet clouds was studied in the laboratory. Three cloud size distributions with modal diameters of 0.02, 5.0, and 12.0 microns were investigated. The relationships between the cloud optical parameters (attentuation coefficient, sigma and volume backscattering coefficient, Beta (sub pi)) and the cloud water content, C, were measured for each size distribution. It was found that a linear relationship exists between sigma and C and between beta (sub pi) and C for cloud water content values up to 3gm/cubic m. The linear relationships obtained, however, have slopes which depend on the droplet size distribution. For a given water content both sigma and beta (sub pi) increase as the modal diameter decreases. The measured data are compared with existing theoretical analyses and discussed in terms of thie application to lidar measurements of atmospheric clouds. It is concluded that the empirical information obtained can serve as a basis for quantitative lidar measurements. Author

N87-10294*# Atmospheric Sciences Lab., White Sands Missile Range, N. Mex.

EFFECT OF BACKSCATTER-TO-EXTINCTION RATIO ON LIDAR INVERSIONS **c32**

Edward M. Measure *In* NASA. Langley Research Center 13th International Laser Radar Conference Aug. 1986 6 p (For primary document see N87-10263 01-35)
Avail: NTIS HC A15/MF A01 CSCL 20N

One way of deriving the atmospheric extinction coefficient from lidar measurements is to start from the single scattering lidar equation. Simulations of lidar experiments and extinction coefficient calculation were conducted and the resulting errors examined. In order to make the simulation realistic, the volume backscatter coefficients and extinction coefficients used in the simulation were based on measured particle distributions, in this case on the particle size distributions measured in Meppen, Germany in the fall of 1980. In that experiment particle size distributions were measured with a balloon-borne particle spectrometer during balloon descents from about 600 meters above ground to the surface. Each particle spectrum represented a layer of at most a few meter thickness, so an altitude resolved profile of particle size spectra is measured. A Mie code was used to compute linear extinction coefficient and volume backscatter coefficient profiles from the particle size spectra for each balloon sounding. B.G.

N87-10295*# Optech, Inc., Downsview (Ontario).
LABORATORY MEASUREMENTS OF FORWARD AND BACKWARD SCATTERING OF LASER BEAMS IN WATER DROPLET CLOUDS c32
R. B. Smith, J. D. Houston, A. Ulitsky, and A. I. Carswell (York Univ., Downsview (Ontario).) *In* NASA. Langley Research Center 13th International Laser Radar Conference Aug. 1986 2 p (For primary document see N87-10263 01-35)
Avail: NTIS HC A15/MF A01 CSCL 20N

Many aspects of the forward and backward scattering in dense water droplet clouds were studied using a laboratory scattering facility. This system is configured in a lidar geometry to facilitate comparison of the laboratory results to current lidar oriented theory and measurements. The backscatter measurements are supported with simultaneous measurements of the optical density, mass concentration, and droplet size distribution of the clouds. Measurements of the extinction and backscatter coefficients at several important laser wavelength have provided data on the relationship between these quantities for laboratory clouds at .633, 1.06, and 10.6 microns. The polarization characteristics of the backscatter of 1.06 microns were studied using several different types of clouds. More recently, the laboratory facility was modified to allow range-resolved backscatter measurements at 1.06 microns. Clouds made up of 3 layers, each with its own density, can be constructed. This allows the study of the effect of cloud inhomogeneity on the forward and backscatter. B.G.

N87-10296*# National Aeronautics and Space Administration. Goddard Space Flight Center, Greenbelt, Md.
REAL-TIME ATMOSPHERIC ABSORPTION SPECTRA FOR IN-FLIGHT TUNING OF AN AIRBORNE DIAL SYSTEM c32
M. Dombrowski, H. Walden, G. K. Schwemmer, J. Milrod, and C. L. Korb *In* NASA. Langley Research Center 13th International Laser Radar Conference Aug. 1986 1 p (For primary document see N87-10263 01-35)
Avail: NTIS HC A15/MF A01 CSCL 20N

Real-time measurements of atmospheric absorption spectra are displayed and used to precisely calibrate and fix the frequency of an Alexandrite laser to specific oxygen absorption features for airborne Differential Absorption Lidar (DIAL) measurements of atmospheric pressure and temperature. The DIAL system used contains two narrowband tunable Alexandrite lasers: one is electronically scanned to tune to oxygen absorption features for on-line signals while the second is used to obtain off-line (nonabsorbed) atmospheric return signals. The lidar operator may select the number of shots to be averaged, the altitude, and altitude interval over which the signals are averaged using single key stroke commands. The operator also determines exactly which oxygen absorption lines are scanned by comparing the line spacings and relative strengths with known line parameters, thus calibrating the laser wavelength readout. The system was used successfully to measure the atmospheric pressure profile on the first flights of this lidar, November 20, and December 9, 1985, aboard the NASA Wallops Electra aircraft. B.G.

N87-10297*# Kyushu Univ., Fukuoka (Japan). Dept. of Electrical Engineering.
OBSERVATION OF ATMOSPHERIC OZONE BY DIAL WITH RAMAN LASERS PUMPED BY A KrF LASER c46
M. Maeda and T. Shibata *In* NASA. Langley Research Center 13th International Laser Radar Conference Aug. 1986 3 p (For primary document see N87-10263 01-35)
Avail: NTIS HC A15/MF A01 CSCL 04A

Since the XeCl excimer laser (308 nm) was first used in Differential Absorption Lidar (DIAL) for stratospheric ozone detection, the XeCl ozone lidar became a useful tool for the monitoring of the stratospheric ozone concentration. Shorter wavelength lasers are needed for the observation of ozone in the troposphere where the ozone concentration is about one order of magnitude smaller than in the stratosphere. In 1983, tropospheric ozone was observed with the combination of the second Stokes line (290.4 nm) of stimulated Raman scattering from methane pumped by a KrF laser and the XeCl laser line. The measurement of the ozone distribution from ground to 30 km was reported, using three Stokes lines of Raman lasers pumped by a KrF laser. At wavelengths shorter than 295 nm, the background solar radiation is effectively suppressed by atmospheric ozone. Such a solar-blind effect can be expected when two wavelengths 277 and 290.4 nm are used for DIAL ozone detection. A preliminary measurement of the day time ozone distribution in the troposphere is presented using these wavelengths generated by a KrF laser with a Raman shifter. Analysis using the lidar equation predicts the maximum detectable range is 7 km. B.G.

N87-10298*# Maryland Univ., College Park. Inst. for Physical Science and Technology.
STRENGTH, WIDTH, AND PRESSURE SHIFT MEASUREMENTS OF 54 LINES IN THE OXYGEN A-BAND c46
K. J. Ritter and T. D. Wilkerson *In* NASA. Langley Research Center 13th International Laser Radar Conference Aug. 1986 4 p (For primary document see N87-10263 01-35)
Avail: NTIS HC A15/MF A01 CSCL 04A

The absorption band of molecular oxygen, centered at 760 nm, is the atmospheric absorber for the Differential Absorption Lidar (DIAL) systems used to measure atmospheric temperature, pressure, and density. To provide accurate line parameters for such systems, a careful spectroscopic study was made of the A-band, with measurements of line strengths, widths, pressure-induced frequency shifts, and collisional narrowing effects. The width and shift parameters were measured over a temperature range of -20 to 100 C so that the temperature dependence of these parameters can also be determined. To analyze the results, a least-squares fiting routine was written to fit standard line profiles to the observed profiles. These measurements, which include the first observations of pressure shifts and collisional narrowing in the band, are an important contribution to lidar system utilizing the A-band. B.G.

N87-10299*# National Oceanic and Atmospheric Administration, Washington, D. C.
AN ALL-PURPOSE COMPUTER PROGRAM FOR LIDAR SIMULATIONS AND REDUCTION OF LIDAR DATA c61
Charles Braun *In* NASA. Langley Research Center 13th International Laser Radar Conference Aug. 1986 2 p (For primary document see N87-10263 01-35)
Avail: NTIS HC A15/MF A01 CSCL 09B

A general computer program was written for the dual purpose of simulating lidar return signals and extracting H2O vapor and temperature (T) profiles from actual lidar returns. This program will be used to retrieve H2O vapor and T profiles from data obtained with the University of Maryland ground-based lidar systems. The program is designed to simulate and to analyze lidar returns from a monostatic system for two cases: when the output laser pulse is monochromatic, and when the pulse has a known wavelength spectrum. The simulation part of the program has several model H2O vapor, T, and aerosol profiles which can be combined to form different model atmospheres. The simulation program also permits the testing of different methods of numerical filtering to suppress noise, and testing the accuracy of different methods of numerical integration. B.G.

N87-10300*# National Aeronautics and Space Administration. Goddard Space Flight Center, Greenbelt, Md.

CONVECTIVE STRUCTURE OF THE PLANETARY BOUNDARY LAYER OF THE OCEAN DURING GALE **c46**

S. H. Melfi and R. Boers *In* NASA. Langley Research Center 13th International Laser Radar Conference Aug. 1986 1 p (For primary document see N87-10263 01-35)

Avail: NTIS HC A15/MF A01 CSCL 04A

The structure of the Planetary Boundary Layer (PBL) was measured, using an airborne lidar, over the Atlantic Ocean during several intensive observation periods of the Genesis of Atlantic Lows Experiment (GALE). Primary emphasis is on the understanding of the convective structure within the PBL during cold air outbreaks. Cold outbreaks generally occur in between the development of coastal storms; and behind a cold front sweeping down from Canada out across the Atlantic. As the cold dry air moves over the relatively warm ocean, it is heated and moistened. The transfer of latent and sensible heat during these events accounts for most of the heat transfer between the ocean and atmosphere during winter. Moistening of the PBL during these eventsis believed to be an important factor in determining the strength of development of the storm system which follows. In general, the more PBL moisture available as latent heat the higher the probability the storm will intensify. The major mechanism for vertical mixing of heat and mositure within the PBL is cellular convection. Knowlede of the organization and structure of the convection is important for understanding the process. Author

N87-10301*# Academy of Sciences (USSR), Tomsk. Inst. of Atmospheric Optics.

METHODS FOR ESTIMATING THE OPTICAL CONSTANTS OF ATMOSPHERIC HAZES BASED ON COMPLEX OPTICAL MEASUREMENTS **c74**

V. E. Zuev, B. S. Kostin, and I. E. Naats *In* NASA. Langley Research Center 13th International Laser Radar Conference Aug. 1986 3 p (For primary document see N87-10263 01-35)

Avail: NTIS HC A15/MF A01 CSCL 20F

The methods of multifrequency laser sounding (MLS) are the most effective remote methods for investigating the atmospheric aerosols, since it is possible to obtain complete information on aerosol microstructure and the effective methods for estimating the aerosol optical constants can be developed. The MLS data interpretation consists in the solution of the set of equations containing those of laser sounding and equations for polydispersed optical characteristics. As a rule, the laser sounding equation is written in the approximation of single scattering and the equations for optical characteristics are written assuming that the atmospheric aerosol is formed by spherical and homogeneous particles. To remove the indeterminacy of equations, the method of optical sounding of atmospheric aerosol, consisting in a joint use of a mutifrequency lidar and a spectral photometer in common geometrical scheme of the optical experiment was suggested. The method is used for investigating aerosols in the cases when absorption by particles is small and indicates the minimum necessary for interpretation of a series of measurements. B.G.

N87-10302*# Academy of Sciences (USSR), Tomsk.

MULTIFREQUENCY DIAL SENSING OF THE ATMOSPHERIC GASEOUS CONSTITUENTS USING THE FIRST AND SECOND HARMONICS OF A TUNABLE CO2 LASER RADIATION **c46**

V. E. Zuev, Yu. M. Andreev, V. G. Voevodin, A. I. Gribenyukov, V. A. Kapitanov, A. V. Sosnin, G. A. Stuchebrov, and G. S. Khmelnitskii *In* NASA. Langley Research Center 13th International Laser Radar Conference Aug. 1986 3 p (For primary document see N87-10263 01-35)

Avail: NTIS HC A15/MF A01 CSCL 04A

The results of field measurements of concentration of some gaseous components of the atmosphere along the paths, in Sofia, Bulgaria, using a gas analyzer based on the use of a CO2 laser radiation frequency-doubled with ZnGeP2 monocrystals are presented. The gas analyzer is a traditional long path absorption meter. Radiation from the tunable CO2 laser of low pressure and from an additional He-Ne laser is directed to a colliminating hundredfold Gregori telescope with a 300 mm diameter of the principal mirror. The dimensions of the mirrors of a retroreflector 500 x 500 mm and a receiving telescope allow one to totally intercept the beam passed through the atmospheric layer under study and back. B.G.

N87-10303*# Academy of Sciences (USSR), Tomsk. Inst. of Atmospheric Optics.

REMOTE EXPRESS ANALYSIS OF GROUND-LAYER AEROSOL BASED ON LASER-INDUCED SPARK SPECTRA **c46**

V. E. Zuev, Yu. D. Kopytin, V. A. Korolkov, M. E. Levitskii, M. F. Nebolsin, B. G. Sidorov, and N. P. Soldatkin *In* NASA. Langley Research Center 13th International Laser Radar Conference Aug. 1986 2 p (For primary document see N87-10263 01-35)

Avail: NTIS HC A15/MF A01 CSCL 04A

The creation of high-power pulsed CO2 and Nd-glass lasers enables the realization of the method for remote spectrochemical analysis of atmospheric aerosols based on excitation of the emission spectrum of the aerosol particle atoms. A description of construction and characteristics of a spectrochemical lidar based on both Nd-glass and CO2 lasers is presented. B.G.

N87-10304*# Academy of Sciences (USSR), Tomsk. Inst. of Atmospheric Optics.

LASER SOUNDING OF INSTANTANEOUS AND MEAN SPEED OF WIND USING CORRELATION METHOD **c47**

V. E. Zuev, I. V. Samokhvalov, G. G. Matvienko, I. N. Kolev (Academy of Sciences, Sofia (Bulgaria).), and O. P. Prvanov *In* NASA. Langley Research Center 13th International Laser Radar Conference Aug. 1986 4 p (For primary document see N87-10263 01-35)

Avail: NTIS HC A15/MF A01 CSCL 04B

The correlation methods for laser sounding of wind speed are based on mutual processing of lidar signals scattered from several spatially separated volumes at each altitude investigated. The time of atmospheric aerosol transport between the scattering volumes estimated by the position of maximum of the mutual correlation function is the measure of corresponding wind speed. In this case the distance between the scattering volumes (the measuring base), defining the time of aerosol movement through the measuring base also determines the lidar possibilities for measuring the instantaneous (during the time interval of several seconds) or the mean wind speed (some minutes). Based on the experimental investigations performed using two lidars, these possibilites are analyzed. B.G.

N87-10305*# Academy of Sciences (USSR), Tomsk. Inst. of Atmospheric Optics.

OPTIMAL FILTRATION OF THE ATMOSPHERIC PARAMETERS PROFILES **c46**

V. E. Zuev, G. N. Glazov, and G. M. Igonin *In* NASA. Langley Research Center 13th International Laser Radar Conference Aug. 1986 2 p (For primary document see N87-10263 01-35)

Avail: NTIS HC A15/MF A01 CSCL 04A

The idea of optimal Marcovian filtration of fluctuating profiles from lidar signals is developed but as applied to a double-frequency sounding which allows the use of large cross sections of elastic scattering and correct separation of the contributions due to aerosol and Rayleigh scatterings from the total lidar return. The filtration efficiency is shown under different conditions of sounding using a computer model. The accuracy of restituted profiles (temperature, pressure, density) is determined by the elements of a posteriori matrix K. The results obtained allow the determination of the lidar power required for providing the necessary accuracy of restitution of the atmospheric parameter profiles at chosen wavelengths of sounding in the ultraviolet and visible range. B.G.

N87-10306*# Academy of Sciences (USSR), Tomsk. Inst. of Atmospheric Optics.

OPTICAL MODELS OF THE MOLECULAR ATMOSPHERE **c46**

V. E. Zuev, Yu. S. Makushkin, A. A. Mitsel, Yu. N. Ponomarev, V. P. Rudenko, and K. M. Firsov *In* NASA. Langley Research Center 13th International Laser Radar Conference Aug. 1986 3 p (For

primary document see N87-10263 01-35)
Avail: NTIS HC A15/MF A01 CSCL 04A

The use of optical and laser methods for performing atmospheric investigations has stimulated the development of the optical models of the atmosphere. The principles of constructing the optical models of molecular atmosphere for radiation with different spectral composition (wideband, narrowband, and monochromatic) are considered in the case of linear and nonlinear absorptions. The example of the development of a system which provides for the modeling of the processes of optical-wave energy transfer in the atmosphere is presented. Its physical foundations, structure, programming software, and functioning were considered. B.G.

N87-10307*# Academy of Sciences (USSR), Tomsk. Inst. of Atmospheric Optics.
THE INFLURENCE OF AN OPTICAL RECEIVING SYSTEM ON STATISTICAL CHARACTERISTICS OF A LIDAR SIGNAL c36
A. E. Zuev, V. A. Banakh, and V. L. Mironov *In* NASA. Langley Research Center 13th International Laser Radar Conference Aug. 1986 3 p (For primary document see N87-10263 01-35)
Avail: NTIS HC A15/MF A01 CSCL 20E

The effects connected with correlation of direct and backward waves propagating through the same randomly inhomogeneous media can be observed along the path with refection in a turbulent atmosphere. In particular, the mean intensity of the reflected wave can increase in comparison with the wave propagating in the forward direction at a doubled distance; the intensity fluctuations can become stronger. These effects depend on the strength of optical turbulence, as well as on the diffraction sizes of the exit apertures of the source and the reflector. However, the focusing of radiation reflected with a receiving telescope leads, in some cases, to the fact that the dependence of amplification effects on the parameters becomes essentially different. This should be taken into account when alayzing the lidar signals. The effect of backscattering amplification and amplification of the intensity fluctuations is discussed. B.G.

N87-10308*# Academy of Sciences (USSR), Tomsk. Inst. of Atmospheric Optics.
COHERENT LIDARS BASED ON INTRACAVITY HETERODYNING OF ECHO SIGNALS c36
V. E. Zuev, S. D. Burakov, A. P. Godlevskii, Yu. D. Kopytin, S. V. Lazarev, S. A. Ostanin, and P. O. Sharin *In* NASA. Langley Research Center 13th International Laser Radar Conference Aug. 1986 1 p (For primary document see N87-10263 01-35)
Avail: NTIS HC A15/MF A01 CSCL 20E

The development and technical realization of the method of laser sounding of the atmosphere based on the effects of mixing of reference and external fields of scattering inside a laser cavity are presented. An approximate theory of the method was developed on the basis of the investigations using the model of a three-mirror laser. The nonlinear effect of a wideband laser on frequency-dependent external influences of the atmosphere was investigated. The field measurements of gaseous composition of the atmosphere were performed on the basis of a given method of coherent reception using a tunable CO2 laser. B.G.

N87-10309*# Academy of Sciences (USSR), Tomsk. Inst. of Atmospheric Optics
THE INFLUENCE OF SCATTERING PARTICLES MORPHOLOGY ON THE CHARACTERISTICS OF LIDAR SIGNALS c36
V. E. Zuev, I. E. Naats, and A. A. Popov *In* NASA. Langley Research Center 13th International Laser Radar Conference Aug. 1986 2 p (For primary document see N87-10263 01-35)
Avail: NTIS HC A15/MF A01 CSCL 20E

The characteristics of light scattering by a separate spherical particle are used as a priori information when interpreting the data on laser sounding of atmospheric aerosols. Analogously, it is necessary to have a priori information on the characteristics of light scattering by a single crystals in order to restitute the microstructure of crystal formation in the atmosphere. In contrast to the aerosol particles the crystals are of different shapes. On the one hand, this complicates the solution of electrodynamic problems on light scattering by such crystals. On the other hand, if obtaining such a solution is possible, one can determine the morphology of scattering particles accoring to the sounding data and this enables additonal information to be obtained on such meteorological parameters as temperature, pressure, and humidity. Using the geometric-wave approach the problem of scattering of plane electromagnetic wave on convex polyhedrons of arbitrary form was solved. As a result, the expressions were obtained for electric field components of perpendicular and parallel polarizations scattered in any given direction. B.G.

N87-10310*# Fraunhofer-Inst. fuer Atmosphaerische Umweltforschung, Garmisch-Partenkirchen (West Germany).
IMPROVED SOLUTION OF THE LIDAR EQUATION UTILIZING PARTICLE COUNTER MEASUREMENTS c32
H. Jaeger, M. Littfass, D. J. Hofmann (Wyoming Univ., Laramie.), and J. M. Rosen *In* NASA. Langley Research Center 13th International Laser Radar Conference Aug. 1986 2 p (For primary document see N87-10263 01-35)
Avail: NTIS HC A15/MF A01 CSCL 20N

The extraction of particle backscattering from incoherent lidar measurements poses some problems. In the case of measurements of the stratospheric aerosol layer the solution of the lidar equation is based on two assumptions which are necessary to normalize the measured signal and to correct it with the two-way transmission of the laser pulse. Normalization and transmission are tackled by adding the information contained in aerosol particle counter measurements of the University of Wyoming to the ruby lidar measurements at Garmisch-Partenkirchen. Calculated backscattering from height levels above 25 km for the El Chichon period will be compared with lidar measurements and necessary corrections. The calculated backscatter-to-extinction ratios are compared to those, which were derived from a comparison of published extinction values to measured lidar backscattering at Garmisch. These ratios were used to calculate the Garmisch lidar returns. For the period 4 to 12 months after the El Chichon eruption a backscater-to-extinction ratio of 0.026 1/sr was applied with smaller values before and after that time. B.G.

N87-10311*# National Aeronautics and Space Administration. Goddard Space Flight Center, Greenbelt, Md.
IMPROVEMENTS IN THE GODDARD BALLOON-BORNE LIDAR c36
William S. Heaps *In* NASA. Langley Research Center 13th International Laser Radar Conference Aug. 1986 1 p (For primary document see N87-10263 01-35)
Avail: NTIS HC A15/MF A01 CSCL 20E

The Goddard balloon-borne lidar system for the measurement of stratospheric ozone and the hydroxyl radical has made three additional flights since the last laser radar conference. On September 27, 1984, a flight was made from Palestine, Texas obtaining a measurement of hydroxyl diurnal variation at 36 km. These data are presented on the plot which shows hydroxyl concentration as a function of GMT for the range cell closest to the instrument. Local noon corresponds to 18 hours on the plot. The rapid drop in concentration after noon is not predicted by models of stratospheric chemistry. It may represent the effects of contamination of the sample volume by hydrocarbons outgassed from the balloon. The more recent flights on June 30, 1985, and December 6, 1985, focussed on measurements of concentration in the lower stratosphere (less than 30 km). The June flight succeeded in obtaining an average concentration measurement (1.8 + or - 0.0000018 molecules/cubic cm) over the altitude range 21 to 26 km. The December flight obtained measurements down to 24 km with a better signal-to-noise ratio than that obtained in June. Prospects for further improvement in sensitivity and absolute calibration will be discussed. Author

N87-10312*# National Oceanic and Atmospheric Administration, Boulder, Colo.
FEATURES OF STRATOSPHERIC AEROSOL LIDAR OBSERVATIONS AT MAUNA LOA, 1974 - 1985 c46
J. J. DeLusi, T. DeFoor, and D. U. Longenecker *In* NASA. Langley

Research Center 13th International Laser Radar Conference Aug. 1986 1 p (For primary document see N87-10263 01-35)
Avail: NTIS HC A15/MF A01 CSCL 04A

Lidar observations of the stratospheric aerosol over Mauna Loa were begun in the fall of 1974 and have continued to the present. An analysis of these observations has yielded interesting features of the stratospheric aerosol profile that change according to perturbed (from volcanic activity) and quiescent conditions. In the Mauna Loa lidar record there are two major perturbations that are contrasted, Fuego and El Chichon. The variations in relative aerosol cloud thickness, altitude of the maximum concentration and nonsymmetry are compared for the quiescent and perturbed time periods. Also, a climatology of annual average aerosol profiles is descrbied. A brief description will be given of procedures used to validate the lidar optical thickness information. Author

N87-10313*# Kyushu Univ., Fukuoka (Japan). Dept. of Physics.
EL CHICHON AEROSOLS IN THE STRATOSPHERE: ANALYSES OF LIDAR DATA AND CALCULATIONS OF RADIATION BUDGET **c46**
M. Fujiwara, H. Akiyoshi, and N. Otsuka *In* NASA. Langley Research Center 13th International Laser Radar Conference Aug. 1986 1 p (For primary document see N87-10263 01-35)
Avail: NTIS HC A15/MF A01 CSCL 04A

Lidar observation at Fukuoka has provided over four years the data of ElChichon aerosols in the stratosphere. Analyses of the data show that an enormous amount of volcanic aerosols has continuously decreased since the beginning of 1983 with significant fluctuations. These fluctuations reveal themselves as a seasonal variation of aerosol content with a maximum in winter-spring and a minimum in summer. The vertical structure of the aerosol layer also shows the seasonal variation. Although the height of a peak around 18 km in the vertical profile of scattering ratio show littel variation, the higher second peak appears frequently from late fall and the lower third peak from late winter to late spring just as two and more tropopauses appear in these periods. The mechanism which causes the seasonal variation will be discussed in terms of the transport by the atmospheric circulation and the removal through the tropopause gap. Radiation budget in the atmosphere was calculated taking into account the large amount of aerosols observed in the early stages of the El Chichon event. The heating rate of the atmosphere is more than 1 K in the bottom region of the stratosphere even in the nighttime. The possible effect of the volcanic aerosols on the other geophysical phenomena will be discussed using the calculated values of the heating rate. Author

N87-10314*# Nagoya Univ. (Japan). Water Research Inst.
LIDAR MEASUREMENT OF STRATOSPHERIC AEROSOL AT SYOWA STATION, ANTARCTICA **c46**
Y. Iwasaka, T. Hirasawa (National Inst. of Polar Research, Tokyo (Japan).), H. Fukunishi, T. Ono, and A. Nomura *In* NASA. Langley Research Center 13th International Laser Radar Conference Aug. 1986 4 p (For primary document see N87-10263 01-35)
Avail: NTIS HC A15/MF A01 CSCL 04A

Lidar measurement on Antarctic aerosols were made during the Antarctic Middle Atmosphere (AMA) period, 1983 to 1985, at Syowa Station. Topics measured are winter enhancement aerosol layer and volcanic effect of El Chichon on the Antarctic stratosphere aerosols. The large depolarization ratio (maximum value was about 0.8) seems to support sublimation growth of ice crystals. The lidar measurements showed a meaningful time lag between aerosol content increase and depolarization ratio increase. Considering the balloon observations made in early winter, it was speculated that an increase in large particle number concentration also contributed to the winter enhancement. The El Chichon cloud spread to the Antarctic region by the beginning of 1983. The temporal change of integrated backscatter coefficient shows a clear decay pattern, although strong winter enhancement superposes. B.G.

N87-10315*# Florence Univ. (Italy). Dept. of Physics.
MULTIPLE SCATTERING MEASUREMENTS IN LABORATORY AND FOGGY ATMOSPHERE **c32**
P. Bruscaglioni, E. Battistelli, P. Pili, and C. Zaccanti *In* NASA. Langley Research Center 13th International Laser Radar Conference Aug. 1986 4 p (For primary document see N87-10263 01-35)
Avail: NTIS HC A15/MF A01 CSCL 20N

Multiple scattering affects propagation of light beams in turbid media. Backscattering or forward scattering based measurements of atmospheric parameters are influenced by this effect. Although largely studied theoretically, the effect needs measurements in control of situations due to the large variety of situations of practical importance. The results of laboratory measurements pertaining to the transmission of a collimated light beam (Helium-Neon souce, 10 mW) through suspensions of latex spheres in water are presented and a comparison was made with the predictions of calculation in a foggy atmosphere will also be presented. B.G.

N87-10316*# Los Alamos National Lab., N. Mex.
MULTIPLE SCATTERING OF LASER BEAMS IN DENSE HYDROSOLS **c32**
A. Zardecki, S. A. W. Gerstl, Wesley P. Unruh, Grant H. Stokes, David M. Stupin, Norman E. Elliott, and J. A. Weinman (Wisconsin Univ., Madison.) *In* NASA. Langley Research Center 13th International Laser Radar Conference Aug. 1986 3 p (For primary document see N87-10263 01-35)
Avail: NTIS HC A15/MF A01 CSCL 20N

The multiple scattering of laser beams is usually described within the framework of small-angle scattering theory. The validity of this approximation as well as improvements due to the incorporation of diffusion theory in the calculations were studied. B.G.

N87-10317*# Centro Informazioni Studi Esperienze, Milan (Italy).
TIME-RESOLVED LIDAR FLUOROSENSOR FOR SEA POLLUTION DETECTION **c45**
A. Ferrario, P. L. Pizzolati, and E. Zanzottera *In* NASA. Langley Research Center 13th International Laser Radar Conference Aug. 1986 2 p (For primary document see N87-10263 01-35)
Avail: NTIS HC A15/MF A01 CSCL 13B

A contemporary time and spectral analysis of oil fluorescence is useful for the detection and the characterization of oil spills on the sea surface. Nevertheless the fluorosensor lidars, which were realized up to now, have only partial capability to perform this double analysis. The main difficulties are the high resolution required (of the order of 1 nanosecond) and the complexity of the detection system for the recording of a two-dimensional matrix of data for each laser pulse. An airborne system whose major specifications were: time range, 30 to 75 ns; time resolution, 1 ns; spectral range, 350 to 700 nm; and spectral resolution, 10 nm was designed and constructed. The designed system of a short pulse ultraviolet laser source and a streak camera based detector are described. B.G.

N87-10318*# Lund Inst. of Tech. (Sweden). Dept. of Physics.
VARIATION OF THE URBAN NO2 CONCENTRATION DURING A GROUND INVERSION SITUATION **c45**
A. Sunesson, W. Wendt, and B. Galle (Swedish Water and Air Pollution Research Lab., Goeteborg.) *In* NASA. Langley Research Center 13th International Laser Radar Conference Aug. 1986 3 p (For primary document see N87-10263 01-35)
Avail: NTIS HC A15/MF A01 CSCL 13B

In February 1985 the NO2 concentration over Goeteborg, a major Swedish city, was monitored during two inversion situations. The differential absorption technique was employed and the results show the build-up of the concentration. In this experiment the laser beam was scanned horizontally over Goeteborg. The results were presented as maps over the NO2 concentration distribution. For security reasons the beam was not parallel to the ground, which gives a height gradient in some measurements. During the measurement period the NO2 concentration variation build-up from the morning to the afternoon was monitored. Great concentration variations were seen. Later the mixing below the inversion layer, resulting in a more uniform, high concentration was seen. The breakdown of the inversion when stronger winds start was also seen. Comparisons with a traditional point-measuring chemiluminiscence instrument and an optical method DOAS (Differential Optical Absorption Spectroscopy), were made. The results are discussed. Strong spatial concentration variations are shown by the lidar measurements. For a point-measuring system, the instrument must be very carefully placed since its location will strongly influence the values it gives. B.G.

N87-10319*# Keio Univ., Yokahama (Japan). Dept. of Physics.
AN INTENSITY-MODULATED DUAL-WAVELENGTH He-Ne LASER FOR REMOTE SENSING OF METHANE c45
Kiyoji Uehara and Fujitaka Taguchi (Tokyo Gas Co. Ltd. (Japan).) *In* NASA. Langley Research Center 13th International Laser Radar Conference Aug. 1986 4 p -CP-2431 (For primary document see N87-10263 01-35)
Avail: NTIS HC A15/MF A01 CSCL 13B

A new type of dual wavelength He-Ne laser is described in which the output power at each of the two wavelengths is modulated with equal amplitude and opposite phase to each other. This laser source can greatly simplify the setup and improve the sensitivity of the differential absorption measurements for the methane detection, as verified by a preliminary experiment. A simple scheme to measure the concentration of methane is also proposed. E.R.

N87-10320*# Israel Inst. for Biological Research, Ness-Ziona.
LIDAR MAPPING OF A MIXTURE OF AEROSOL CONCENTRATIONS IN A VARYING ATMOSPHERE c45
Moshe Kleiman, Smadar Egert, and Ariel Cohen *In* NASA. Langley Research Center 13th International Laser Radar Conference Aug. 1986 3 p (For primary document see N87-10263 01-35)
Avail: NTIS HC A15/MF A01 CSCL 13B

In several recent applications dealing with lidar measurement of atmospheric pollution, two basic assumptions are made: (1)The investigated aerosol layer is the only particulate material within the scattering volume; and (2)The contribution of the gaseous atmosphere to the lidar backscattering signals can be estimated and deducted from the total backscattering measurements. In the method discussed a generalized method which allows the elimination of the above mentioned assumptions was developed using multiparameter lidar measurements. The different parameters can be several wavelengths, polarization of the scattered light, scattering angles, or any combination of these parameters. The basic requirements are given. The detailed derivations are presented and discussed. E.R.

N87-10321*# National Oceanic and Atmospheric Administration, Boulder, Colo. Wave Propagation Lab.
THREE ATMOSPHERIC DISPERSION EXPERIMENTS INVOLVING OIL FOG PLUMES MEASURED BY LIDAR c46
W. L. Eberhard, G. T. McNice, and S. W. Troxel *In* NASA. Langley Research Center 13th International Laser Radar Conference Aug. 1986 4 p (For primary document see N87-10263 01-35)
Avail: NTIS HC A15/MF A01 CSCL 04A

The Wave Propagation Lab. participated with the U.S. Environmental Protection Agency in a series of experiments with the goal of developing and validating dispersion models that perform substantially better that models currently available. The lidar systems deployed and the data processing procedures used in these experiments are briefly described. Highlights are presented of conclusions drawn thus far from the lidar data. E.R.

N87-10322*# Joint Research Centre of the European Communities, Ispra (Italy).
FEASIBILITY EXPERIMENTS ON TIME-RESOLVED FLUOROSENSING APPLIED TO OIL SLICKS c45
P. Camagni, G. Colombo, C. Koechler, A. Pedrini, N. Omenetto, and G. Rossi *In* NASA. Langley Research Center 13th International Laser Radar Conference Aug. 1986 5 p (For primary document see N87-10263 01-35)
Avail: NTIS HC A15/MF A01 CSCL 13B

The introduction of time resolved observations can provide a very penetrating tool in the practice of laser fluorosensing. The investigations have demonstrated a relevance of multispectral, time resolved analysis for oil fingerprinting. By comparative studies on a variety of crude oils and their most significant fractions, it was found that the process of time decay in a composite oil is characterized by a few steps, which are associated with specific components in the medium light range. The average decay times of these pure fractions are markedly differentiated as to absolute values and spectral spread; as a consequence, the corresponding parameters in the resultant crude are quite sensitive to the particular mixture of these components. Measurements of the time response give then a finer discrimination between oil classes, depending on the relative content of certain fractions. Experiments were pursued with an improved fluorosensor facility, in order to test the application of time resolved fluorosensing to remote samples on water. E.R.

N87-10323*# National Aeronautics and Space Administration. Goddard Space Flight Center, Greenbelt, Md.
ROTATIONALLY RESOLVED COLLISIONAL TRANSFER RATES IN OH c36
Thomas J. McGee, James Butler, John Burris, and William Heaps *In* NASA. Langley Research Center 13th International Laser Radar Conference Aug. 1986 1 p (For primary document see N87-10263 01-35)
Avail: NTIS HC A15/MF A01 CSCL 20E

Fluorescence lidar measurements of the hydroxyl radical require detailed information concerning collision induced processes in order to deduce the radical number density from a lidar return. The Goddard SFC OH lidar currently utilizes a broadband detector which precludes the necessity of fully understanding collisional redistribution of rotational energy within the excited state. Numerous advantages result however from the inclusion of a detector with a bandpass only slightly larger that the Doppler width of a rotational line. This however places more stringent requirements on the spectroscopy. Measurements were accordingly made of rotationally resolved quenching rates for collisions with O2, N2, and H2O. Rotational transfer rates were also measured for the same colliders. Quenching rates were measured using a Nd-YAG pumped Rh6G dye laser doubled into the UV. The OH lifetimes were measured as a function of pressure of quenching gas at total pressures of between 50 and 250 microns. Rotational transfer rates were measured by recording the emission spectrum on an intensified diode array and integrating over 10.000 laser shots. E.R.

N87-10324*# Okayama Univ. (Japan).
TIME-DOMAIN SENSITIVITY ENHANCEMENT IN PULSED Pb-TDL GAS MONITORS c36
R. Koga, M. Kosaka, and H. Sano *In* NASA. Langley Research Center 13th International Laser Radar Conference Aug. 1986 4 p (For primary document see N87-10263 01-35)
Avail: NTIS HC A15/MF A01 CSCL 20E

A Pb-salt tunable diode laser (TDL) has found many applications in the field of atmospheric gas analysis. Its continuous tunablility and fine spectral purity in the mid infrared region are outstanding from other lasers. The only shortcoming is that it requires cryogenic operating temperatures, though, it is improved year by year towards the room temperature operation. A repeated pulse operation of Pb salt diode lasers is possible with a thermoelectric cooling device, which allows an instrument a portable geometry disusing a heavy, bulky and power consuming mechanical refrigerator. A derivative spectrometry was exploiting the quick tunability of Pb salt diode lasers, though they are continuous wave (cw) operated with refrigerator or liquid nitrogen so far. A new system for derivative spectrometry with a pulsed diode laser will extend its field of applications because of reduced weights and size of measuring instruments. A preliminary results is shown that demonstrates the feasibility of an attempt to implement the derivative spectrometry with repeatedly pulse driven diode lasers. Atmospheric methane was measured with 8 ppm/m sensitivity. Further results of parametric optimization for the best signal to noise ratios under any given device characteristics as well as for available real devices is given. E.R.

N87-10325*# University of the West Indies, Mona (Jamaica). Dept. of Physics.
PERFORMANCE TESTING OF LIDAR RECEIVERS **c36**
M. Y. Shams *In* NASA. Langley Research Center 13th International Laser Radar Conference Aug. 1986 2 p (For primary document see N87-10263 01-35)
Avail: NTIS HC A15/MF A01 CSCL 20E

In addition to the considerations about the different types of noise sources, dynamic range, and linearity of a lidar receiver, one requires information about the pulse shape retaining capabilities of the receiver. For this purpose, relatively precise information about the height resolution as well as the recovery time of the receiver, due both to large transients and to fast changes in the received signal, is required. As more and more analog receivers using fast analog to digital converters and transient recorders will be used in the future lidar systems, methods to test these devices are essential. The method proposed for this purpose is shown. Tests were carried out using LCW-10, LT-20, and FTVR-2 as optical parts of the optical pulse generator circuits. A commercial optical receiver, LNOR, and a transient recorder, VK 220-4, were parts of the receiver system. E.R.

N87-10326*# Royal Signals and Radar Establishment, Malvern (England).
PROGRESS IN COHERENT LASER RADAR **c36**
J. M. Vaughan *In* NASA. Langley Research Center 13th International Laser Radar Conference Aug. 1986 2 p (For primary document see N87-10263 01-35)
Avail: NTIS HC A15/MF A01 CSCL 20E

Considerable progress with coherent laser radar has been made over the last few years, most notably perhaps in the available range of high performance devices and components and the confidence with which systems may now be taken into the field for prolonged periods of operation. Some of this increasing maturity was evident at the 3rd Topical Meeting on Coherent Laser Radar: Technology and Applications. Topics included in discussions were: mesoscale wind fields, nocturnal valley drainage and clear air down bursts; airborne Doppler lidar studies and comparison of ground and airborne wind measurement; wind measurement over the sea for comparison with satellite borne microwave sensors; transport of wake vortices at airfield; coherent DIAL methods; a newly assembled Nd-YAG coherent lidar system; backscatter profiles in the atmosphere and wavelength dependence over the 9 to 11 micrometer region; beam propagation; rock and soil classification with an airborne 4-laser system; technology of a global wind profiling system; target calibration; ranging and imaging with coherent pulsed and CW system; signal fluctuations and speckle. Some of these activities are briefly reviewed. E.R.

N87-10327*# National Oceanic and Atmospheric Administration, Boulder, Colo.
DOPPLER LIDAR STUDIES OF ATMOSPHERIC WIND FIELD DYNAMICS **c47**
R. M. Hardesty, M. J. Post, T. R. Lawrence, and F. F. Hall, Jr. *In* NASA. Langley Research Center 13th International Laser Radar Conference Aug. 1986 4 p (For primary document see N87-10263 01-35)
Avail: NTIS HC A15/MF A01 CSCL 04B

For the past 5 years the Wave Propagation Lab. has operated a pulsed CO2 Doppler lidar system to evaluate coherent laser radar technology and to investigate applications of the technique in atmospheric research. The capability of the system to provide measurements of atmospheric winds, backscatter, and water vapor has been extensively studied over this period. Because Doppler lidar can measure atmospheric wind structure in the clear air without degradation by terrain features, it offers a unique capability as a research tool for studies of many transient or local scale atmospheric events. This capability was demonstrated in recent field experiments near Boulder, Colo. and Midland, Tex., in which the lidar clearly depicted the wind field structure associated with several types of phenomena, including thunderstorm microbursts, valley drainage flow, and passage of a dryline front. To improve sensitivity during the periods of low aerosol backscatter, the system has recently been upgraded with new transmitter/receiver hardware. The upgraded system, which transmit 2 J per pulse of output energy at a rate of 50 Hz and incorporates computer control for automated operation, underwent calibration testing during the spring of 1986. E.R.

N87-10328*# Israel Atomic Energy Commission, Yavneh. Dept. of Atmospheric Optics.
THE EFFECT OF TURBULENCE ON LIDAR BACKSCATTERED SIGNAL FLUCTUATIONS **c32**
S. Fastig and A. Choen *In* NASA. Langley Research Center 13th International Laser Radar Conference Aug. 1986 1 p (For primary document see N87-10263 01-35)
Avail: NTIS HC A15/MF A01 CSCL 20N

CO2 lidar measurements being subjected to uncertainties caused by strong fluctuations were explained to appear primarily due to speckle effects whereas turbulence was to be negligible. Spectral cross correlation measurements performed in the near IR and in the visible show that the main contribution to the fluctuation for the above lidar wavelengths originates from the atmospheric turbulence. The standard deviation of the fluctuation signal was measured for the two wavelengths simultaneously. A typical curve representing mid-summer day changes in the value of sigma as a function of time is shown. The results, indicating the strong dependence on the turbulence, is analyzed and discussed. Author

N87-10329*# Oregon Graduate Center for Study and Research, Beaverton. Dept. of Applied Physics and Electrical Engineering.
REMOTE SENSING OF ATMOSPHERIC WINDS USING A COHERENT, CW LIDAR AND SPECKLE-TURBULENCE INTERACTION **c47**
J. Fred Holmes, Farzin Amzajerdian, V. S. Rao Gudimetla, and John M. Hunt *In* NASA. Langley Research Center 13th International Laser Radar Conference Aug. 1986 4 p (For primary document see N87-10263 01-35)
Avail: NTIS HC A15/MF A01 CSCL 04B

Speckle turbulence interaction has the potential for allowing single ended remote sensing of the path averaged vector crosswind in a plane perpendicular to the line of sight to a target. If a laser transmitter is used to illuminate a target, the resultant speckle field generated by the target is randomly perturbed by the atmospheric turbulence as it propagates back to the location of the transmitter-receiver. When a cross wind is present, this scintillation pattern will move with time across the receiver. A continuous wave (cw) laser transmitter of modest power level in conjunction with optical heterodyne detection was used to exploit the speckel turbulence interaction and measure the crosswind. The use of a cw transmitter at 10.6 microns and optical heterodyne detection has many advantages over direct detection and a double pulsed source in the visible or near infrared. These advantages include the availability of compact, reliable and inexpensive transmitters, better penetration of smoke, dust and fog; stable output power; low beam pointing jitter; and considerably reduced complexity in the receiver electronics. E.R.

N87-10330*# Deutsche Forschungs- und Versuchsanstalt fuer Luft- und Raumfahrt, Wesseling (West Germany).
EXPERIMENTAL AND THEORETICAL DOPPLER-LIDAR SIGNATURES OF AIRCRAFT WAKE VORTICES **c02**
F. Koepp and W. A. Krichbaumer *In* NASA. Langley Research Center 13th International Laser Radar Conference Aug. 1986 3 p (For primary document see N87-10263 01-35)
Avail: NTIS HC A15/MF A01 CSCL 01A

The DFVLR laser Doppler anemometer is a CO2 continuous wave homodyne system designed for boundary layer wind measurements. During the last three years, it was mainly used in the wake-vortex program at Frankfurt airport for determination of vortex strength, transport, and lifetime. The strategy for that special type of measurement was previously reported in detail along with single experimental results. Therefore, herein is given a short summary of the data concerning questions of air traffic control. In addition to the experimental activities a computer model describing wake-vortex behavior was installed. It allows the comparison of the measured data with the hydrodynamically predicted quantities. On the other hand, it leads to an improved procedure for future wake-vortex measurements. E.R.

N87-10331*# National Aeronautics and Space Administration. Goddard Space Flight Center, Greenbelt, Md.
LOWER ATMOSPHERIC TEMPERATURE PROFILE MEASUREMENTS USING A RAMAN LIDAR **c47**
S. H. Melfi and D. Whiteman *In* NASA. Langley Research Center 13th International Laser Radar Conference Aug. 1986 1 p (For primary document see N87-10263 01-35)
Avail: NTIS HC A15/MF A01 CSCL 04B

A Raman lidar system was used to measure the temperature profile of the upper troposphere and lower stratosphere. The system consists of a tripled Nd-YAG laser and a 1.5 meter diameter telescope. Two photomultipliers are used at the output of the telescope to allow for measurements at both the laser wavelength and at the Raman shifted wavelength due to atmospheric nitrogen. The signal from the photomultipliers is recorded as photon counts in 1 microsec bins. The results of a number of laser shots are summed together to provide atmospheric returns which have acceptable signal to noise characteristics. Measurements of the Raman nitrogen return were acquired up to an altitude in excess of 20 km. Temperature profiles were retrieved from the attenuation corrected Raman nitrogen return assuming the atmosphere to be in hydrostatic equilibrium and using the ideal gas law. Retrieved temperature profiles are shown compared with independent temperature measurements. Author

N87-10332*# Academy of Sciences (USSR), Tomsk. Inst. of Atmospheric Optica.
A COMBINED RAMAN LIDAR FOR LOW TROPOSPHERIC STUDIES **c46**
Yu. F. Arshinov, S. M. Bobrovnikov, V. E. Zuev, A. I. Nadeev, and K. D. Shelevoy *In* NASA. Langley Research Center 13th International Laser Radar Conference Aug. 1986 3 p (For primary document see N87-10263 01-35)
Avail: NTIS HC A15/MF A01 CSCL 04A

One of the main goals of laser sensing of the atmosphere was the development of techniques and facilities for remote determination of atmospheric meteorological and optical parameters. Of lidar techniques known at present the Raman-lidar technique occupies a specific place. On the one hand Raman lidar returns due to scattering on different molecular species are very simple for interpretation and for extracting the information on the atmospheric parameters sought, but, on the other hand, the performance of these techniques in a lidar facility is overburdened with some serious technical difficulties due to extremely low cross sections of Raman effect. Some results of investigations into this problem is presented which enables the construction of a combined Raman lidar capable of acquiring simultaneously the profiles of atmospheric temperature, humidity, and some optical characteristics in the ground atmospheric layer up to 1 km height. The operation of this system is briefly discussed. E.R.

N87-10333*# Naval Air Development Center, Warminster, Pa.
INTERCOMPARISONS OF HIGH-RESOLUTION SOLAR BLIND RAMAN LIDAR ATMOSPHERIC PROFILES OF WATER VAPOR WITH RADIOSONDES AND KYTOON **c46**
K. Petri, A. Salik, and J. Cooney (Drexel Univ., Philadelphia, Pa.) *In* NASA. Langley Research Center 13th International Laser Radar Conference Aug. 1986 1 p (For primary document see N87-10263 01-35)
Avail: NTIS HC A15/MF A01 CSCL 04A

A report is given of measurements of atmospheric profiles of water vapor in the boundary layer by use of solar blind Raman lidar. These measurement episodes, occuring twice a day over a two week period, were accompanied by a dense net of supporting measurements. The support included two radiosonde launches per measurement episodes as well as a kytoon support measurement of water vapor using a wet bulb-dry bulb instrument. The kytoon strategy included ten minute stops at strategic altitudes. Additional kytoon measurements included ozone profiles and nephelometric extinction profiles in the visible. Typically, six or seven 1000 shot lidar profile averages were collected during a measurement episode. Overall performance comparisons are provided and intercomparisons between auxiliary measurement devices are presented. Data on the accuracy of the lidar water vapor profiles are presented. Author

N87-10334*# Drexel Univ., Philadelphia, Pa. Dept. of Physics and Atmospheric Sciences.
LIDAR METHOD OF MEASUREMENT OF ATMOSPHERIC EXTINCTION AND OZONE PROFILES **c46**
John A. Cooney *In* NASA. Langley Research Center 13th International Laser Radar Conference Aug. 1986 1 p (For primary document see N87-10263 01-35)
Avail: NTIS HC A15/MF A01 CSCL 04A

A description of a method of measurement of atmospheric extinction and of ozone profiles by use of the backscatter signal from a monostatic lidar is given. The central feature of the procedure involves a measurement of the ratio of the Raman backscatter returns of both the oxygen and nitrogen atmospheric content. Because the ratio of the number density of both species is known to high accuracy, the measurement itself becomes a measure of the ratio of two transmissions to altitude along with a ratio of the two system constants. The calibration measurement for determining the value of the ratio of the two system constants or electro-optical conversion constants is accomplished by a lidar measurement of identical atmospheric targets while at the same time interchanging the two optical filters in the two optical channels of the receiver. More details of the procedure are discussed. Factoring this calibrated value into the measured O2/N2 profile ratio provides a measured value of the ratio of the two transmissions. Or equivalently, it provides a measurement of the difference of the two extinction coefficients at the O2 and N2 Raman wavelengths as a function of the height. E.R.

N87-10335*# Atmospheric Environment Service, Downsview (Ontario).
VERTICAL STRUCTURE OF ARCTIC HAZE OBSERVED BY LIDAR **c47**
R. M. Hoff *In* NASA. Langley Research Center 13th International Laser Radar Conference Aug. 1986 3 p (For primary document see N87-10263 01-35)
Avail: NTIS HC A15/MF A01 CSCL 04B

In the study of the Arctic Haze phenomenon, understanding the vertical structure of the haze aerosol is crucial in defining mechanisms of haze transport. Questions have also arisen concerning the representativeness of surface observations of Arctic Haze. Due to the strongly stratified nature of the Arctic troposphere, the mechanisms which transport aerosol to the surface from the transport altitudes of the lower troposphere are not obvious. In order to examine these questions, a Mie scattering lidar was installed at Alert, NWT, Canada. Lidar observes atmospheric aerosols and hydrymeteors as they appear in nature, unmodified by sampling effects. As such the results obtained are more realistic of the light scattering characteristics of the in situ aerosol than are those obtained by integrating nephelometers, for example, which heat the aerosol and dry it before measurement. With this lidar, a pulse was transmitted vetically through an evacuated tube in the roof of a building at Alert. The receiver consisted of a 20cm diameter Fresnel telescope, neutral density and polarizing filters, and RCA C31000A PMT, Analog Modules LA-90-P logarithmic amplifier and a Lecroy TR8827 32 MHz digitizer. The lidar equation was solved for the backscattering coefficient of the aerosol assuming no two way transmission losses in the signal. The lidar results have shown that intercomparison between lidar obtained visibilities and observer visibilities are in much better agreement than for other optical or aerosol monitors. Three new effects were identified in the lidar profiles which contribute to the vertical transport of haze. These effects are briefly discussed. E.R.

N87-10336*# National Aeronautics and Space Administration. Goddard Space Flight Center, Greenbelt, Md.

LIDAR OBSERVATIONS AND MODELING OF COLD AIR OUTBREAKS DURING MASEX AND GALE c47
R. Boers and S. H. Melfi *In* NASA. Langley Research Center 13th International Laser Radar Conference Aug. 1986 4 p (For primary document see N87-10263 01-35)
Avail: NTIS HC A15/MF A01 CSCL 04B

As part of MASEX and GALE a number of research flights were carried out over the Marine Boundary Layer (MBL) during periods when extremely cold and dry continental air was flowing out over the warm coastal waters at the east coast of the U.S. Such periods, which are named cold air outbreaks are characterized by massive warming and moistening of the MBL resulting in rapid entrainment conditions. As the MBL deepens as a function of fetch over the ocean, clouds develop. The line of cloud formation typically follows the coast line closely as has been observed many times from satellite imagery. The backscatter data from the NASA Goddard airborne lidar, which was used to measure the depth of the MBL in great detail, is ideally suited to verify parametrized models of boundary layer growth rate. The data indicates that the deepening MBL gradually develops clouds at its top. Those clouds form an integral part of the MBL and exercise an important influence on the energy cycle within the MBL. It is suggested that the rapid entrainment observed during overcast conditions represent an increase in efficiency of conversion of available turbulence kinetic energy into entrainment energy. E.R.

N87-10337*# National Aeronautics and Space Administration. Langley Research Center, Hampton, Va.
THE APPLICATION OF LIDAR TO STRATOSPHERIC AEROSOL STUDIES c46
M. P. McCormick *In* NASA. Langley Research Center 13th International Laser Radar Conference Aug. 1986 2 p (For primary document see N87-10263 01-35)
Avail: NTIS HC A15/MF A01 CSCL 04A

The global climatology and understanding of stratospheric aerosols evolving primarily from lidar and satellite measurements is presented. The importance of validation of these remotely sensed data with in situ measurements is also discussed. The advantage of lidar for providing high vertical and horizontal resolution and its independence from a remote source for measurement will become evident with examples of long term lidar data sets at fixed sites and the use of lidar on airborne platforms. Volcanic impacts of the last 20 years are described with emphasis on the last 8 years where satellite data are available. With satellite and high resolution lidar measurements, an understanding of the global circulation of volcanic material is attempted along with the temporal change of aerosol physical parameters and the stratospheric cleansing or decay times associated with these eruptions. E.R.

N87-10338*# National Inst. for Environmental Studies, Tsukuba (Japan).
VOLCANIC ERUPTIONS AND THE INCREASES IN THE STRATOSPHERIC AEROSOL CONTENT: LIDAR MEASUREMENTS FROM 1982 TO 1986 c46
S. Hayashida, Y. Iikura, H. Shimizu, Y. Sasano, H. Nakane, N. Sugimoto, I. Matsui, and N. Takeuchi *In* NASA. Langley Research Center 13th International Laser Radar Conference Aug. 1986 4 p (For primary document see N87-10263 01-35)
Avail: NTIS HC A15/MF A01 CSCL 04A

The results of the observation for stratospheric aerosols which were carried out since the autumn of 1982 by using the NIES large lidar are described. Specifications of the lidar system are shown. The lidar has two wavelenghts of 1.06 and 0.53 micrometers. The 0.53 micrometer is mainly used for the stratospheric aerosols, because the PMT for 0.53 micrometers has higher sensitivity that that for 1.06 micrometers and the total efficiency is higher in the former. A switching circuit is used to control the PMT gain for avoiding signal induced noise in PMT. For the last four years, the stratospheric aerosol layer which was significantly perturbed by the El Chichon volcanic eruption was observed. The scattering ratio profiles observed from 1982 through 1983 are given. E.R.

N87-10339*# University Coll. of Wales, Aberystwyth.
OBSERVATIONS OF STRATOSPHERIC AEROSOLS ASSOCIATED WITH THE EL CHICHON ERUPTION c46
L. Thomas, G. Vaughan, D. B. Jenkins, D. Wareing, and M. Farrington *In* NASA. Langley Research Center 13th International Laser Radar Conference Aug. 1986 1 p (For primary document see N87-10263 01-35)
Avail: NTIS HC A15/MF A01 CSCL 04A

Lidar observations of aerosols were carried out at Aberystwyth between Nov. 1982 and Dec. 1985 using a frequency doubled and frequency tripled Nd/Yag laser and a receiver incorporating a 1 m diameter in a Newtonian telescope configuration. In analyses of the experimental data attention is paid to the magnitude of the coefficient relating extinction and backscatter, the choice being related to the possible presence of aerosols in the upper troposphere and the atmospheric densities employed in the normalisation procedure. The aerosol loading showed marked day to day changes in early months and an overall decay was apparent only after April 1983, this decay being consistent with an e sup -1 time of about 7 months. The general decay was accompanied by a lowering of the layer but layers of aerosols were shown intermittently at heights above the main layer in winter months. The height variations of photon counts corrected for range, or of aerosol backscatter ratio, showed clear signatures of the tropopause. A strong correlation was found between the heights of the tropopause identified from the lidar measurements and from radiosonde-borne temperature measurements. A notable feature of the observations is the appearance of very sharp height gradients of backscatter ratio which seem to be produced by differential advection. Author

N87-10340*# Fraunhofer-Inst. fuer Atmosphaerische Umweltforschung, Garmisch-Partenkirchen (West Germany).
LIDAR OBSERVATIONS OF THE DECLINE OF THE EL CHICHON STRATOSPHERIC LOAD c46
H. Jaeger and W. Carnuth *In* NASA. Langley Research Center 13th International Laser Radar Conference Aug. 1986 2 p (For primary document see N87-10263 01-35)
Avail: NTIS HC A15/MF A01 CSCL 04A

The eruption of the Mexican volcano El Chichon in Apr. 1982 enhanced the stratospheric aerosol load to a level which so far has not been observed by remote sensing techniques. The ruby lidar system at Garmisch-Partenkirchen recorded an increase of about two orders of magnitude above the background level of the years 1977/78. At northern midlatitudes backscattering was peaking in Jan./Feb. 1983, as illustrated. The decline of the El Chichon stratospheric perturbation is discussed. The decay of the El Chichon stratospheric cloud is characterized by an overall 1/e lifetime of about 12 months. The El Chichon decay is further characterized by seasonal variations of the integral backscattering coefficient, which exhibit a winter maximum and a summer minimum. These variations are inversely correlated with the seasonal mean movement of the tropopause height indicating transport processes. E.R.

N87-10341*# National Aeronautics and Space Administration. Langley Research Center, Hampton, Va.
AIRBORNE LIDAR OBSERVATIONS OF ARCTIC POLAR STRATOSPHERIC CLOUDS c46
L. R. Poole and G. S. Kent *In* NASA. Langley Research Center 13th International Laser Radar Conference Aug. 1986 1 p (For primary document see N87-10263 01-35)
Avail: NTIS HC A15/MF A01 CSCL 04A

Polar stratospheric clouds (PSC's) have been detected repeatedly during Arctic and Antarctic winters since 1978/1979 by the SAM II (Stratospheric Aerosol Measurement II) instrument aboard the NIMBUS-7 satellite. PSC's are believed to form when supercooled sulfuric acid droplets freeze, and subsequently grow by deposition of ambient water vapor as the local stratospheric temperature falls below the frost point. In order to study the characteristics of PSC's at higher spatial and temporal resolution than that possible from the satellite observations, aircraft missions were conducted within the Arctic polar night vortex in Jan. 1984 and Jan. 1986 using the NASA Langley Research Center airborne dual polarization ruby lidar system. A synopsis of the 1984 and 1986 PSC observations is presented illustrating short range spatial changes in cloud structure, the variation of backscatter ratio with temperature, and the depolarization charactecrics of cloud layers. Implications are noted with regard to PSC particle characteristics and the physical process by which the clouds are thougth to form. Author

N87-10342*# Kyushu Univ., Fukuoka (Japan). Dept. of Electronical Engineering.
XeF LIDAR MEASUREMENTS OF DENSITY AND TEMPERATURE IN THE MIDDLE ATMOSPHERE c47
T. Shibata and M. Maeda *In* NASA. Langley Research Center 13th International Laser Radar Conference Aug. 1986 3 p (For primary document see N87-10263 01-35)
Avail: NTIS HC A15/MF A01 CSCL 04B

In recent years, it has been widely recognized that vertically propagating internal gravity waves in the middle atmosphere play an important role in determining the large scale wind field by their momentum transport and deposition. However, very little is known about them in the upper stratosphere and lower mesosphere because of the lack of adequate techinques to observe small scale motions. A XeF excimer laser was used for the Rayleigh lidar observation. The characteristics of the XeF lidar system are given. The wavelength of the XeF laser is in the region that is ozone absorption free, and the Rayleigh scattering cross section is 5 times larger than in 532 nm. The advantages of using the XeF laser as against the YAG laser have been discussed in detail. The density and temperature profiles between the altitude range of 30 and 70 km measured with this lidar system are illustrated. The accuracy is less than + or - 3% and 10k at 60 km for an observation time of 15 min. The results on the gravity waves by the observation through about one year since Apr. 1985 is presented. E.R.

N87-10343*# University Coll. of Wales, Aberystwyth. Dept. of Physics.
LIDAR MEASUREMENTS OF THERMAL STRUCTURE c46
D. B. Jenkins, D. P. Wareing, L. Thomas, and G. Vaughan *In* NASA. Langley Research Center 13th International Laser Radar Conference Aug. 1986 1 p (For primary document see N87-10263 01-35)
Avail: NTIS HC A15/MF A01 CSCL 04A

Rayleigh backscatter observations at 532 nm and 355 nm of relative atmospheric density above Aberystwyth on a total of 93 nights between Dec. 1982 and Feb. 1985 were used to derive the height variation of temperature in the upper stratosphere and mesosphere. Preliminary results for height up to about 25 km were also obtained from observations of Raman backscattering from nitrogen molecules. Comparisons were carried out for stratospheric heights with satellite borne measurements; good agreement was found between equivalent black body temperatures derived from the lidar observations and those obtained from nadir measurements in three channels of the stratosphere sounder units on NOAA satellites; the lidar based atmospheric temperatures have shown general agreement with but a greater degree of structure than the limb sounding measurements obtained using the SAMS experiment on the NOAA-7 satellite. In summer, stratospheric and mesospheric temperatures showed a smooth height variation similar to that of the CIRA model atmosphere. In contrast, the winter data showed a great variability with height, and marked temperature changes both from night to night and within a given night. Author

N87-10344*# Centre National de la Recherche Scientifique, Verrieres-Le Buisson (France).
LIDAR STRATOSPHERIC OZONE MEASUREMENTS AT THE OBSERVATOIRE DE HAUTE PROVENCE (FRANCE) c46
S. Godin, J. Pelon, and G. Megie *In* NASA. Langley Research Center 13th International Laser Radar Conference Aug. 1986 4 p (For primary document see N87-10263 01-35)
Avail: NTIS HC A15/MF A01 CSCL 04A

Strastospheric ozone monitoring is of particular importance to confirm present day theories predicting a maximal ozone depletion, due to chlorofluorocarbon emission, in the 35 to 45 km altitude range. Measurements presently rely on both ground based and satellite-borne passive experiments. Such systems have been recently shown to have intrinsic limitations mainly due to atmospheric aerosol presence and calibration problems. During the last few years, active lidar profiling of the ozone vertical distribution by the Differential Absorption Laser technique (DIAL) in the UV wavelength range has been developed using two different laser sources: a Nd-YAG pumped dye laser which enables a large tuning range of the UV emitted wavelengths; and exciplex laser sources using xenon chloride as an active medium and emitting at 308 nm, the off wavelength being usually generated by Raman shifting techniques. Advantages and limitations of using both of these systems are briefly discussed. E.R.

N87-10345*# Shinshu Univ., Nagano (Japan). Faculty of Engineering.
LIDAR OBSERVATION OF THE MESOSPHERIC SODIUM LAYER IN ANTARCTICA c46
A. Nomura, Y. Iwasaka (Nagoya Univ. (Japan).), H. Fukunishi (National Inst. of Polar Research, Tokyo (Japan).), T. Hirasawa, S. Kawaguchi (Nagoya Univ. (Japan).), and T. Kano (Shinshu Univ., Nagano (Japan).) *In* NASA. Langley Research Center 13th International Laser Radar Conference Aug. 1986 3 p (For primary document see N87-10263 01-35)
Avail: NTIS HC A15/MF A01 CSCL 04A

The mesospheric sodium layer has been observed at Syowa Station in Antarctica during the wintering period of the 26th Japanese Antarctic Research Expedition. A lidar observation of the polar middle atmosphere at the station has been performed as a part of the Middle Atmosphere Program since 1983. At first stratospheric aerosols have been observed by the system based on a ruby laser. In 1985 a new transmitting system consisting of a tunable dye laser was added to that system to observe the sodium layer, too. The characteristics of the lidar system are given. The results of the mesospheric sodium layer observed on 42 nights during the period from March to October, 1985 are also given. Author

N87-10346*# Centre National de la Recherche Scientifique, Verrieres-Le Buisson (France).
LIDAR DETECTION OF METALLIC SPECIES AT THE MESOPAUSE LEVEL c46
C. Granier, J. P. Jegou, and G. Megie *In* NASA. Langley Research Center 13th International Laser Radar Conference Aug. 1986 4 p (For primary document see N87-10263 01-35)
Avail: NTIS HC A15/MF A01 CSCL 04A

The measurement alkali species present in the atomic form at the mesopause level has been performed by lidar for more than ten years. Atomic and ionic calcium density profiles are obtained for 3 years by the same technique in the visible range, at 423 nm for atomic calcium, and 393 nm for ionic calcium Ca(+). The experimental set-up and the preliminary results have been presented elsewhere. The 423 nm wavelength is directly obtained by the emission of a dye laser pumped by the third harmonic of a Nd-YAG laser. For the generation of the 393 nm wavelength, frequency mixing was used: the emission at 624 nm of a dye laser pumped by the 2nd harmonic of a Nd-Yag laser is mixed with the fundamental infrared emission (remaining after frequency doubling), in a non-linear KDP crystal, which gives the 393 nm emission. The behavior of the two atomic species, calcium and sodium, which are in the same altitude range are compared. For 45% of the observations, no ionic calcium was detected: the ionic calcium abundance was thus below the detection threshold. Contrasting with the density profiles of the atomic species, sodium and calcium, the ionic calcium profile present important variations on small time scales. The main characteristics of theatomic and ionic calcium behaviors that can be deduced from the measurements made are given. Author

N87-10347*# Illinois Univ., Urbana.
DAYTIME LIDAR MEASUREMENTS OF TIDAL WINDS IN THE

MESOSPHERIC SODIUM LAYER AT URBANA, ILLINOIS c46
K. H. Kwon, D. C. Senft, C. S. Gardner, D. G. Voelz, C. F. Sechrist, Jr., and F. L. Roesler (Wisconsin Univ., Madison.) *In* NASA. Langley Research Center 13th International Laser Radar Conference Aug. 1986 4 p (For primary document see N87-10263 01-35)
Avail: NTIS HC A15/MF A01 CSCL 04A

For more than 15 years lidar systems have been used to study the chemistry and dynamics of the mesospheric sodium layer. Because the layer is an excellent tracer of atmospheric wave motions, sodium lidar has proven to be particularly useful for studying the influence of gravity waves and tides on mesospheric dynamics. These waves, which originate in the troposphere and stratosphere, propagate through the mesosphere and dissipate their energy near the mesopause making important contributions to the momentum and turbulence budget in this region of the atmosphere. Recently, the sodium lidar was modified for daytime operation so that wave phenomena and chemical effects could be monitored throughout the complete diurnal cycle. The results of continuous 24 hour lidar observations of the sodium layer structure are presented alond with measurement of the semidiurnal tidal winds. Author

N87-10348*# National Aeronautics and Space Administration. Goddard Space Flight Center, Greenbelt, Md.
LIDAR STUDY OF STORM TOPS c47
J. D. Spinhirne and W. D. Hart *In* NASA. Langley Research Center 13th International Laser Radar Conference Aug. 1986 3 p (For primary document see N87-10263 01-35)
Avail: NTIS HC A15/MF A01 CSCL 04B

Satellite thermal and visible observations are routinely used for storm tracking and diagnostics. In recent years attempts have also been made to apply satellite measurements to the study of evolutional factors for storms such as divergence and subsidence mechanisms. These studies involve analysis of the thermal height structure of the storm tops as obtained from the satellite observations. An outstanding problem is the importance of emissivity effects for the interpretation of the storm top thermal radiance measurements. In part to understand the correct interpretation of satellite observations, a storm top observation experiment involving advanced instrumentation on board a high altitude NASA aircraft has been in progress. A downlooking lidar system is an important part of the instrument complement. A combined analysis of the lidar return data and thermal radiance measurements was developed to study cloud top emissivity effects and their relation to satellite observations. Some preliminary conclusions are given. Author

N87-10349*# Academy of Sciences, Sofia (Bulgaria). Inst. of Electronics.
INVESTIGATION OF CLOUDS SPATIAL DISTRIBUTION USING GROUND-BASED LIDAR c47
I. N. Kolev, O. P. Parvanov, B. K. Kaprielov, and I. K. Ilev *In* NASA. Langley Research Center 13th International Laser Radar Conference Aug. 1986 4 p (For primary document see N87-10263 01-35)
Avail: NTIS HC A15/MF A01 CSCL 04B

Certain investigations of spatial distribution of clouds by employing ground based lidar are presented. The great changeability is one of the main properties of the clouds in the boundary layer. As a result, their optical properties change rapidly which complicates the modeling of cloud evolution. Suitable equipped lidars are widely used for diagnostics of the clouds via a number of scattering and absorption processes. In particular, lidar can provide information on the distribution of meteorological parameters and of the other important cloud characteristics both in vertical and horizontal directions. Herein the time and spatial distribution of the aerosol backscattering coefficient of S sub t and S sub c type clouds are investigated by means of a correlation analysis of the lidar obtained data provided from several arbitrary directions and heights. Author

N87-10350*# Utah Univ., Salt Lake City. Dept. of Meteorology.
MULTIPLE SCATTERING DEPOLARIZATION IN MARINE STRATUS CLOUDS: LIDAR EXPERIMENTS c32
Kenneth Sassen and Richard L. Petrilla *In* NASA. Langley Research Center 13th International Laser Radar Conference Aug. 1986 1 p (For primary document see N87-10263 01-35)
Avail: NTIS HC A15/MF A01 CSCL 20N

The depolarization of ruby lidar backscattering caused by multiple scattering in marine stratus clouds was examined systematically from a field site on the southern California coast. Investigated were the effects on the linear depolarization (delta) of lidar receiver field of view (FOV), elevation angle and laser beam pointing errors. An approximately linear increase in maximum delta values was observed with increasing receiver FOV, and the importance of accurate transmitter/receiver beam alignment was demonstrated during experiments in which the laser axis was deliberately misaligned. An elevation angle dependence to the delta values was observed as a consequence of the natural vertical inhomogeneity of water cloud content above the cloud base. Time histories of the depolarization characteristics of dissipating stratus clouds revealed significant spatial and temporal variability in delta values attributed to cloud composition variations. Employing a 1 mrad transmitter FOV, maximum delta values of 0.21 nd 0.33 were observed with 1 and 3 mrad receiver FOVs, respectively, from the low stratus clouds. The fundamental causes and effects on the lidar equation of multiple scattering are also discussed. Author

N87-10351*# Harry Diamond Labs., Adelphi, Md.
NEAR-IR EXTINCTION AND BACKSCATTER COEFFICIENT MEASUREMENTS IN LOW- AND MID-ALTITUDE CLOUDS c32
Z. G. Sztankay *In* NASA. Langley Research Center 13th International Laser Radar Conference Aug. 1986 6 p (For primary document see N87-10263 01-35)
Avail: NTIS HC A15/MF A01 CSCL 20N

Knowledge of the attenuation and backscattering properties of clouds is required to high resolution for several types of optical sensing systems. Such data was obtained in about 15 hours of flights through clouds in the vicinity of Washington, D.C. The flights were mainly through stratocumulus, altocumulus, stratus, and stratus fractus clouds and covered an altitude and temperature range of 300 to 3200 m and -13 to 17 C. Two instruments were flown, each of which measured the backscatter from close range in two range bins to independently determine both the extinction and backscatter coefficients. The extinction and backscatter coefficients can be obtained from the signals in the two channels of each instrument, provided that the aerosol is uniform over the measurement region. When this assumptions holds, the extinction coefficient is derived basically from the ratio of the signal in the two channels; the backscatter coefficient can then be obtained from the signal in either channel. E.R.

N87-10352*# University Coll., Galway (Ireland). Dept. of Experimental Physics.
BACKSCATTER AND EXTINCTION MEASUREMENTS IN CLOUD AND DRIZZLE AT CO2 LASER WAVELENGTHS c32
S. G. Jennings *In* NASA. Langley Research Center 13th International Laser Radar Conference Aug. 1986 4 p (For primary document see N87-10263 01-35)
Avail: NTIS HC A15/MF A01 CSCL 20N

The backscatter and extinction of laboratory generated cloud and drizzle sized water drops were measured at carbon dioxide laser wavelengths (predominately at lambda = 10.591 micrometers). Two distinctly different drop size regimes were studied: one which covers the range normally encompassed by natural cloud droplets and the other representative of mist or drizzle sized drops. The derivation and verification of the relation between extinction and backscatter at carbon dioxide laser wavelengths should allow the determination of large cloud drop and drizzle extinction coefficient solely from a lidar return signal without requiring knowledge of the drop size distribution. This result will also apply to precipitation sized drops so long as they are spherical. Author

N87-10353*# Naval Postgraduate School, Monterey, Calif. Dept. of Physics.
CLOUD DETECTION BY LIDAR EXTINCTION CALCULATIONS

c47

W. J. Lentz *In* NASA. Langley Research Center 13th International Laser Radar Conference Aug. 1986 3 p (For primary document see N87-10263 01-35)

Avail: NTIS HC A15/MF A01 CSCL 04B

A new lidar method of measuring cloud ceiling height using the Klett solution to the lidar equation was developed. This simple technique will find cloud ceiling height for clouds that rangefinder-like lidars cannot theoretically detect. In addition, the noise signals that do not correspond to clouds removed by using the convergence of the Klett solution to discriminate between signal changes and broader signal changes due to clouds. Clouds above rain or light fog can be detected without error, and it is possible to discriminate against haze layers by the magnitude of their maximum extinction. Author

N87-10354*# Tohoku Univ., Sendai (Japan). Research Inst. of Electrical Communication.

WIDE-AREA REMOTE-SENSING SYSTEM OF POLLUTION AND GAS DISPERSAL BY NEAR-INFRARED ABSORPTION BASED ON LOW-LOSS OPTICAL FIBER NETWORK c45

Humio Inaba *In* NASA. Langley Research Center 13th International Laser Radar Conference Aug. 1986 4 p (For primary document see N87-10263 01-35)

Avail: NTIS HC A15/MF A01 CSCL 13B

An all optical remote sensing system utilizing long distance, ultralow loss optical fiber networks is studied and discussed for near infrared absorption measurements of combustible and/or explosive gases such as CH4 and C3H8 in our environment, including experimental results achieved in a diameter more than 20 km. The use of a near infrared wavelength range is emphasized. Author

N87-10355*# Lund Inst. of Tech. (Sweden). Dept. of Physics.

A MOBILE SYSTEM FOR ACTIVE OTPICAL POLLUTION MONITORING c45

A. Sunesson, H. Edner, S. Svanberg, L. Uneus, W. Wendt, and K. Fredriksson (National Swedish Environment Protection Board, Stockholm.) *In* NASA. Langley Research Center 13th International Laser Radar Conference Aug. 1986 3 p (For primary document see N87-10263 01-35)

Avail: NTIS HC A15/MF A01 CSCL 13B

The remote monitoring of atmospheric pollutants can now be performed in several ways. Laser radar techniques have proven their ability to reveal the spatial distribution of different species or particles. Classical optical techniques can also be used, but yield the average concentration over a given path and hence no range resolution. One such technique is Differential Optical Absorption Spectroscopy, DOAS. Such schemes can be used to monitor paths that a preliminary lidar investigation has shown to be of interest. Having previously had access to a mobile lidar system, a new system has been completed. The construction builds on experience from using the other system and it is meant to be more of a mobile optical laboratory than just a lidar system. A complete system description is given along with some preliminary usage. Future uses are contemplated. E.R.

N87-10356*# Centro Informazioni Studi Esperienze, Milan (Italy).

GAS CORRELATION LIDAR FOR METHANE DETECTION c46

E. Galletti, E. Zanzottera, S. Draghi, M. Garbi, and R. Petroni *In* NASA. Langley Research Center 13th International Laser Radar Conference Aug. 1986 1 p (For primary document see N87-10263 01-35)

Avail: NTIS HC A15/MF A01 CSCL 04A

A new type of DIAL system for the detection of methane in the atmosphere is being developed. The main feature of this lidar is the use of a gas correlation technique to obtain the reference signal by means of a single laser pulse, instead of two shots at different wavelengths. This fact is useful to make measurements on fast moving platforms. To meet the infrared absorption band of methane an optical parametric oscillator (OPO) was used with a LiNbO3 crystal as active element, and a tuning range between 1.5 divided by 4 microns. As known, the major problem to overcome in parametric oscillators are the pump beam quality and the difficulty in reducing the linewidth. The first requirement is met by using, as a pump, a Nd-YAG laser based on a new type of resonator cavity, named SFUR (Self Filtering Unstable Resonator). The laser emits, with high efficiency, near diffraction limited pulsed beams of about 250 mJ of energy, 20 ns of duration at 10 pps of frequency repetition rate. On the other hand, the gas correlation technique allows the operation with a bandwidth as large as 1/cm, which is obtainable using only a diffraction grating as a dispersive element in the OPO cavity. Author

N87-10357*# Academia Sinica, Beijing (China). Inst. of Atmospheric Physics.

DETECTION OF NO SUB X,C2H4 CONCENTRATIONS BY USING CO AND CO2 LASERS c46

Wang Gengchen and Kong Qinxin *In* NASA. Langley Research Center 13th International Laser Radar Conference Aug. 1986 4 p (For primary document see N87-10263 01-35)

Avail: NTIS HC A15/MF A01 CSCL 04A

A laser, especially the infrared line tunable laser, opens up a new way to monitor the atmospheric environment, and already has gotten effective practical application. One of the most serious problems in open path remote measurement at atmospheric pressure is the broadening effect which leads to increased linewidths, spectral interferences, and, as a result, tends to reduce detection sensitivity, so measuring laser wavelengths should be selected carefully, and interaction between the measuring wavelength and gas to be measured must be known very well. Therefore, N2O, No, NO2, CH4, NH3 and C2H4 absorption properties at some lines of CO and CO2 line tunable lasers were studied. The absorption coefficients of NO, NO2, and C2H4; some results on detection of NO sub x, C2H4 concentrations in both laboratory and field; and selection of measuring wavelengths and error analysis are discussed. Author

N87-10358*# Jet Propulsion Lab., California Inst. of Tech., Pasadena.

MAPM: A COHERENT DUAL CO2 LASER DIAL SYSTEM c46

William B. Grant and James R. Bogan *In* NASA. Langley Research Center 13th International Laser Radar Conference Aug. 1986 1 p Sponsored in part by AF (For primary document see N87-10263 01-35)

Avail: NTIS HC A15/MF A01 CSCL 04A

The Mobile Atmospheric Pollutant Mapping System (MAPM) is a dual CO2 laser DIAL system with heterodyne detection that is being developed for large distance range resolved measurement of organic solvent vapors and aerosol clouds. The components have been chosen to allow measurements to be made to distances of 6 to 7 km in a period of 20 to 30 s. The major components of the system are listed. MAPM is being integrated into a system and will be tested with several organic solvent gases and vapors in a remotely positioned sample chamber and with a free release of ethylene. Experimental results and system performance are discussed. Author

N87-10359*# National Physical Lab., New Delhi (India). Radio Science Div.

LASER HETERODYNE SYSTEM FOR OBTAINING HEIGHT PROFILES OF MINOR SPECIES IN THE ATMOSPHERE c46

S. L. Jain and A. K. Saha *In* NASA. Langley Research Center 13th International Laser Radar Conference Aug. 1986 1 p (For primary document see N87-10263 01-35)

Avail: NTIS HC A15/MF A01 CSCL 04A

An infrared laser heterodyne system for obtaining height profiles of minor constituents of the atmosphere was developed and erected. A brief discription of the system is given. The system consists of a tunable CO2 waveguide laser in the 9 to 11 micrometer band, that is used as a local oscillator and a heliostat that follows the sun and brings in solar radiation, that is mixed with the laser beam in a high speed liquid nitrogen cooled mercury cadmium telluride detector. The detected signal is analysed in a RF spectrum analyser that allows tracing absorption line profiles. Absorption lines of a number of minor constituents in the troposphere and stratosphere, such as O3, NH3, H2O, SO2, ClO, N2O, are in the 9 to 11 micrometer band and overlap with that of CO2 laser range. The experimental system has been made operational and trial observations taken. Current measurements are limited to ozone height profiles. Results are presented. Author

N87-10360*# Arizona Univ., Tucson.
COHERENT LIDAR SIGNAL FLUCTUATION REDUCTION BY MEANS OF FREQUENCY DIVERSITY TECHNIQUE c36
R. M. Schotland, P. Vujkovic Cvijin, and Yan-Zeng Zhao *In* NASA. Langley Research Center 13th International Laser Radar Conference Aug. 1986 3 p (For primary document see N87-10263 01-35)
Avail: NTIS HC A15/MF A01 CSCL 20E

The atmospheric return measured by a coherent lidar is typically characterized by rapid and deep fluctuations in signal strength. These fluctuations result from the interference of the fields backscattered to the lidar from randomly located aerosol particles which move relative to the lidar pulse. In many applications, it is necessary to determine the average value of the lidar signal intensity at some range. A new method utilizes frequency diversity initially suggested by Goldstein and subsequently studied in the microwave radar domain by others. It is expected that the application of the frequency diversity method in the coherent lidar domain will eventually provide greater efficiency and speed in the return signal averaging needed to obtain accurate intensity estimates. The frequency diversity method recognizes that the transmitted lidar pulse is very long compared to a wavelength and consequently a given phase, theta sub i, is repeated many times within the pulse. In order to test this concept, a fairly simple laboratory experiment was designed which simulates scattering of a lidar pulse from atmospheric aerosol. The testing of the frequency diversity method is discussed. E.R.

N87-10361*# Coherent Technologies, Inc., Boulder, Colo.
WAVELENGTH DEPENDENCE OF COHERENT AND INCOHERENT SATELLITE-BASED LIDAR MEASUREMENTS OF WIND VELOCITY AND AEROSOL BACKSCATTER c47
Michael J. Kavaya and R. Milton Huffaker *In* NASA. Langley Research Center 13th International Laser Radar Conference Aug. 1986 4 p (For primary document see N87-10263 01-35)
Avail: NTIS HC A15/MF A01 CSCL 04B

The results are presented of a capability study of Earth orbiting lidar systems, at various wavelengths from 1.06 to 10.6 microns, for the measurement of wind velocity and aerosol backscatter, and for the detection of clouds. Both coherent and incoherent lidar systems were modeled and compared for the aerosol backscatter and cloud detection applications. E.R.

N87-10362*# National Center for Atmospheric Research, Boulder, Colo. Research Aviation Facility.
THE NCAR AIRBORNE INFRARED LIDAR SYSTEM (NAILS) c36
R. L. Schwiesow and P. A. Lightsey *In* NASA. Langley Research Center 13th International Laser Radar Conference Aug. 1986 3 p (For primary document see N87-10263 01-35)
Avail: NTIS HC A15/MF A01 CSCL 20E

A planned airborne lidar system is presented which is intended to provide a remote sensing facility for a variety of applications. The eventual goal of the system development is a Doppler wind measurement capability for boundary layer dynamics and cloud physics applications. The first stage of development is focused initially on a direct detection lidar to measure aerosol profiles and depolarization from cloud backscatter. Because of the Doppler goal, interest in larger particles to define the top of the mixed layer, and eye safety, the first stage of the system is based on a pulsed CO2 laser. A compact, relatively simple and inexpensive system that achieves flexibility to meet the data requirements of a variety of investigators by being easily modified rather than having many different capabilities built in is the goal. Although the direct detection sensitivity is less than that for heterodyne detection, the simpler system allows the achievement of useful scientific results and operating experience towards more complex lidars while staying within budget and time constraints. Author

N87-10363*# Jet Propulsion Lab., California Inst. of Tech., Pasadena.
ATMOSPHERIC CORRELATION TIME MEASUREMENTS USING COHERENT CO2 LIDAR c46
G. M. Ancellet and R. T. Menzies *In* NASA. Langley Research Center 13th International Laser Radar Conference Aug. 1986 4 p (For primary document see N87-10263 01-35)
Avail: NTIS HC A15/MF A01 CSCL 04A

A pulsed TEA-CO2 lidar with coherent detection was used to measure the correlation time of backscatter from an ensemble of atmospheric aerosol particles which are illuminated by the pulsed radiation. The correlation time of the backscatter return signal is important in studies of atmospheric turbulence and its effects on optical propagation and backscatter. If the temporal coherence of the pulse is large enough, then the temporal coherence of the return signal is dominated by the turbulence and shear for a variety of interesting atmospheric conditions. Various techniques for correlation time measurement are discussed and evaluated. Author

N87-10364*# Centre National de la Recherche Scientifique, Verrieres-Le Buisson (France).
PULSED MONONODE DYE LASER DEVELOPED FOR A GEOPHYSICAL APPLICATION c36
J. P. Jegou, T. Pain, and G. Megie *In* NASA. Langley Research Center 13th International Laser Radar Conference Aug. 1986 3 p (For primary document see N87-10263 01-35)
Avail: NTIS HC A15/MF A01 CSCL 20E

Following the extension of the lidar technique in the study of the atmosphere, the necessity of having a high power pulsed laser beam with a narrowed bandwidth and the possibility of selecting a particular wavelength within a certain spectral region arises. With the collaboration of others, a laser cavity using the multiwave Fizeau wedge (MWFW) was developed. Using the classical method of beam amplification with the aid of different stages, a new pulsed dye laser device was designed. The originality resides in the use of reflecting properties of the MFWF. Locally a plan wave coming with a particular angular incidence is reflected with a greater than unity coefficient; this is the consequence of the wedge angle which doubles the participation of every ray in the interferometric process. This dye laser operation and advantages are discussed. The feasibility of different geophysical applications envisageable with this laser is discussed. Author

N87-10365*# RCA Astro-Electronics Div., Princeton, N. J.
CALIBRATION AND ANALYSIS FOR A 0.53 MICRON INCOHERENT DOPPLER LIDAR c36
J. Sroga and A. Rosenberg *In* NASA. Langley Research Center 13th International Laser Radar Conference Aug. 1986 4 p (For primary document see N87-10263 01-35)
Avail: NTIS HC A15/MF A01 CSCL 20E

A ground based, prototype Doppler lidar is being developed to demonstrate the feasibility of an incoherent detection technique to remotely measure winds in the atmosphere. This prototype system consists of a narrow band, single frequency laser transmitter, a high resolution, Fabry-Perot Interferometer utilizing a multichannel image plane detector and a data acquisition system. A description of the prototype Doppler lidar hardware is given in Rosenberg and Sroga, 1985. The calibration and analysis procedures for this system is described. Preliminary results from data obtained with the system pointed vertically is presented. Author

N87-10366*# European Nuclear Energy Agency, Frascati (Italy). Div. Fisica Applicata.
CO2 LIDAR SYSTEM FOR ATMOSPHERIC STUDIES c46
R. Barbini, A. Ghigo, M. Giorgi, K. N. Iyer, A. Palucci, and S. Ribezzo *In* NASA. Langley Research Center 13th International Laser Radar Conference Aug. 1986 4 p (For primary document see N87-10263 01-35)
Avail: NTIS HC A15/MF A01 CSCL 04A

A lidar facility using a TEA CO2 laser source is being developed at the ENEA Laboratories for Atmospheric Studies. The different subsystems and the proposed experimental activities are described. Author

N87-10367*# Wisconsin Univ., Madison. Dept. of Meteorology.
GENERATION OF ATTENUATION CORRECTED IMAGES FROM LIDAR DATA
Edwin W. Eloranta and Daniel K. Forrest *In* NASA. Langley Research Center 13th International Laser Radar Conference Aug. 1986 4 p (For primary document see N87-10263 01-35)
Avail: NTIS HC A15/MF A01 CSCL 05B

The interpretation of data generated by aerosol backscatter lidars is often facilitated by presentation of RHI and PPI images. These pictures are especially useful in studies of atmospheric boundary layer structure where convective elements, stratifications and aerosol laden plumes can be easily delineated. Procedures used at the University of Wisconsin to generate lidar images on a color enhanced raster scan display are described. Author

N87-10368*# Optech, Inc., Downsview (Ontario).
GAS DISPERSION MEASUREMENTS USING A MOBILE RAMAN LIDAR SYSTEM **c43**
J. D. Houston and D. R. Brown *In* NASA. Langley Research Center 13th International Laser Radar Conference Aug. 1986 3 p (For primary document see N87-10263 01-35)
Avail: NTIS HC A15/MF A01 CSCL 13B

The exploitation of natural gas resources to supply energy demands has resulted in the need to engineer pipelines and plants capable of handling extremely high pressures and throughputs. Consequently, more attention has been directed to evaluating the consequences of releases of material whether accidental or deliberate in nature. An important aspect of assessing the consequences of a release is an understanding of how gas disperses in the atmosphere over a wide range of release and atmospheric conditions. The most cost effective way of providing such information is through the development and use of reliable theoretical prediction methods. The need for some form of remote sensing device was identified. The various possibilities studied led to the conclusion that LIDAR (Light Detection And Ranging) offered the most suitable method. The system designed and built is described, and its recent use in monitoring operational ventings from a high pressure transmission system is discussed. E.R.

N87-10369*# Academy of Sciences (USSR), Tomsk. Inst. of Atmospheric Optics.
SPECTROSCOPIC ASPECTS OF DIFFERENTIAL METHOD FOR SOUNDING GAS COMPOSITION OF THE ATMOSPHERE **c46**
V. V. Zuev, I. I. Ippolitov, and Yu. N. Ponomarev *In* NASA. Langley Research Center 13th International Laser Radar Conference Aug. 1986 2 p (For primary document see N87-10263 01-35)
Avail: NTIS HC A15/MF A01 CSCL 04A

The problems concerning the dynamics of populations of the sounded atmospheric gas molecule levels taking into account the nonmonochromatic character of radiation, durations of exciting and sounding pulses, rates of relaxation of excited vibration-rotation states population along different channels in a natural multicomponent mixture of gases and air were investigated. The problems of spectroscopic software, completeness and accuracy of the initial spectroscopic information, information on channels and rates of relaxation from the viewpoint of developing specific schemes of sounding are discussed. The values of deviations of vibration-rotation level populations of some atmospheric molecules from their equilibrium value at simultaneous action of double frequency radiation on the sounding path and the corresponding dynamic variation of lidar return amplitude were estimated. The importance of nonlinear spectrosopic effects in the lidar return value variation at sounding radiation frequency equaling the resonance frequency of vibration-rotation transition in the problem on sounding the humidity profiles and concentrations of gaseous pollutants was also estimated. Author

N87-10370*# National Aeronautics and Space Administration. Langley Research Center, Hampton, Va.
LINEWIDTH CHARACTERISTICS OF RAMAN-SHIFTED DYE LASER OUTPUT AT 720 AND 940 nm **c32**
B. E. Grossmann, U. N. Singh (Maryland Univ., College Park.), N. S. Higdon, L. J. Cotnoir, T. D. Wilkerson, and E. V. Browell *In its* 13th International Laser Radar Conference Aug. 1986 5 p (For primary document see N87-10263 01-35)
Avail: NTIS HC A15/MF A01 CSCL 20N

Existing DIAL systems for water vapor measurements in the troposphere operate at wavelengths near 720 nm. The use of stronger water vapor absorption lines in the range 930 to 960 nm will significantly improve DIAL measurements in the upper troposphere and lower stratosphere where water vapor concentrations are low. The generation of light at 940 nm using a frequency doubled Nd:YAG pumped dye laser is inefficient due to the small absorption if infrared dyes at the pump wavelength. However, 940 nm generation utilizing stimulated Raman scattering of dye lasers is attractive because of a potentially high conversion efficiency plus the possibility of retaining the narrow linewidth available from some dye lasers. The Raman conversion efficiency and line broadening are presented for first Stokes operation at 720 and 940 nm using hydrogen and deuterium as the Raman media. E.R.

N87-10371*# National Aeronautics and Space Administration. Goddard Space Flight Center, Greenbelt, Md.
THE GSFC GOUND-BASED LIDAR FOR THE MEASUREMENT OF STRATOSPHERIC OZONE **c46**
Thomas J. McGee *In* NASA. Langley Research Center 13th International Laser Radar Conference Aug. 1986 1 p (For primary document see N87-10263 01-35)
Avail: NTIS HC A15/MF A01 CSCL 04A

Concern has risen over the last decade concerning the release of gases into the atmosphere which when photolyzed in the stratosphere can catalyze the destruction of ozone. Although the expected change is only on the order of 5%, significant changes in the vertical profile are anticipated. Predictions at 40 km run as high as a 60% change in the next 50 to 100 years. Because of the importance of ozone in the thermal budget of the atmosphere, such a change will have a direct impact on the earth's climate. Long term monitoring of stratospheric ozone is required to validate the predictions and Differential Absorption Lidar is particularly well suited to this measurement. GSFC is currently constructing a mobile lidar system based on a high powered XeCl excimer laser. The system is expected to be operating by fall 1986 and a campaign to compare the lidar results with a series of ROCOZ flights is planned. Author

N87-10372*# National Aeronautics and Space Administration. Langley Research Center, Hampton, Va.
LINEWIDTH CHARACTERISTICS OF RAMAN-SHIFTED DYE LASER OUTPUT AT 720 AND 940 nm **c36**
B. E. Grossmann, U. N. Singh (Maryland Univ., College Park.), N. S. Higdon, L. J. Cotnoir, T. D. Wilkerson, and E. V. Browell *In* NASA. Langley Research Center 13th International Laser Radar Conference Aug. 1986 5 p (For primary document see N87-10263 01-35)
(Contract NCCI-32)
Avail: NTIS HC A15/MF A01 CSCL 20E

A compact and simple simultaneous multi-wavelength dye laser cavity was developed for a differential absorption technique. Dielectric multilayer interference filters were inserted inside the cavities as tuning elements, and two types of a DIAL system were constucted by using the dye laser tuned with dielectric multilayer filters to measure NO2 concentration. The usefulness of this dye laser was clarified for the differential absorption technique in outdoor experiments. Some basic designs of the laser cavity with these filters to get simultaneously multi-wavelength output are summarized. E.R.

N87-10373*# Centre National de la Recherche Scientifique, Verrieres-Le Buisson (France).

ALEXANDRITE LASER SOURCE FOR ATMOSPHERIC LIDAR MEASUREMENTS c36
J. Pelon, C. Loth, P. Flamant, and G. Megie *In* NASA. Langley Research Center 13th International Laser Radar Conference Aug. 1986 4 p (For primary document see N87-10263 01-35)
Avail: NTIS HC A15/MF A01 CSCL 20E

During the past years, there has been a marked increase in interest in the applications of vibronic solid state lasers to meteorology and atmospheric physics. Two airborne lidar programs are now under development in France. The differential absorption lidar (DIAL) method with vibronic solid state lasers is very attractive for water vapor, temperature and pressure measurements. Alexandrite laser and titanium-sapphire are both suitable for these applications. However, only alexandrite rods are commercially available. The requirements on the laser source for airborne dial applications are two fold: (1) a restriction on laser linewidth and a requirement on stability and tunability with a good spectral purity; and (2) a requirement on the time separation between the two pulses. These constraints are summarized. Author

N87-10374*# National Inst. for Environmental Studies, Tsukuba (Japan).
THE TFP AND A PULSED LD: NEW LIDAR COMPONENTS c36
Hiroshi Shimizu, Ichiro Matsui, and Kazuhiro Asai (Tohoku Univ., Sendai (Japan).) *In* NASA. Langley Research Center 13th International Laser Radar Conference Aug. 1986 4 p (For primary document see N87-10263 01-35)
Avail: NTIS HC A15/MF A01 CSCL 20E

One of the large problems of lidar in practical use is that the price and the weight of a laser and a receiving telescope is too high. To solve this problem, many trials have been made. The system with the TFP (thin film paraboloid) for a receiving telescope and a pulsed LD (laser diode) for a laser source is proposed. It is hoped that as a consequence the lidar system will become very lightweight and inexpensive. Author

N87-10375*# Army Chemical Research and Development Center, Aberdeen Proving Ground, Md.
CHEMICAL CONTAMINATION REMOTE SENSING c45
John P. Carrico, Kirkman R. Phelps, Ernest N. Webb, Raymond A. Mackay, and E. R. Murray (SRI International Corp., Menlo Park, Calif.) *In* NASA. Langley Research Center 13th International Laser Radar Conference Aug. 1986 1 p (For primary document see N87-10263 01-35)
Avail: NTIS HC A15/MF A01 CSCL 13B

A ground mobile laser test bed system was assembled to assess the feasibility of detection of various types of chemical contamination using Differential Scattering (DISC) and Differential Absorption (DIAL) Lidar techniques. Field experiments with the test bed system using chemical simulants were performed. Topographic reflection and range resolved DIAL detection of vapors as well as DISC detection of aerosols and surface contamination were achieved. Review of detection principles, design of the test bed system, and results of the experiments are discussed. Author

N87-10376*# Smithsonian Astrophysical Observatory, Cambridge, Mass.
RESEARCH RELATIVE TO HIGH RESOLUTION CAMERA ON THE ADVANCED X-RAY ASTROPHYSICS FACILITY Final Report, 13 May 1985 - 15 Mar. 1986
Sep. 1986 14 p
(Grant NAG8-527)
(NASA-CR-179757; NAS 1.26:179757) Avail: NTIS HC A02/MF A01 CSCL 14E

The HRC (High Resolution Camera) is a photon counting instrument to be flown on the Advanced X-Ray Astrophysics Facility (AXAF). It is a large field of view, high angular resolution, detector for the x-ray telescope. The HRC consists of a CsI coated microchannel plate (MCP) acting as a soft x-ray photocathode, followed by a second MCP for high electronic gain. The MCPs are readout by a crossed grid of resistively coupled wires to provide high spatial resolution along with timing and pulse height data. The instrument will be used in two modes, as a direct imaging detector with a limiting sensitivity of 10 to the -15 ergs sq cm sec in a 10 to the 5th second exposure, and as a readout for an objective transmission grating providing spectral resolution of several hundreds to thousands. Author

N87-10377*# United Technologies Corp., East Hartford, Conn.
DEMONSTRATION OF LASER SPECKLE SYSTEM ON BURNER LINER CYCLIC RIG Final Report
Karl A. Stetson Jun. 1986 28 p
(Contract NAS3-24615)
(NASA-CR-179509; NAS 1.26:179509; R86-927298-10) Avail: NTIS HC A03/MF A01 CSCL 14B

A demonstration test was conducted to apply speckle photogrammetry to the measurement of strains on a sample of combustor liner material in a cyclic fatigue rig. A system for recording specklegrams was assembled and shipped to the NASA Lewis Research Center, where it was set up and operated during rig tests. Data in the form of recorded specklegrams were sent back to United Technologies Research Center for processing to extract strains. Difficulties were found in the form of warping and bowing of the sample during the tests which degraded the data. Steps were taken by NASA personnel to correct this problem and further tests were run. Final data processing indicated erratic patterns of strain on the burner liner sample. Author

N87-10378# Massachusetts Inst. of Tech., Lexington. Lincoln Lab.
INTEGRATED-OPTICAL COMPONENTS FOR FIBER GYROSCOPES
Leonard M. Johnson 1985 4 p
(Contract F19628-80-C-0002)
(AD-A167624; MS-6890; ESD-TR-86-011) Avail: NTIS HC A02/MF A01 CSCL 14/2

Progress in developing a fiber-gyroscope integrated-optical chip is reviewed. Two LiNbO3 channel-waveguide components are described. Excess insertion loss as low as 5.5 dB has been obtained in a double-Y branch and 40 dB sideband suppression has been achieved in a serrodyne frequency translator. Integrated optical circuits which can perform the function of a combination of bulk optical components are of considerable interest for fiber-gyroscope systems. These circuits could be utilized to reduce both system size and complexity as well as to improve system performance. Integrated-optical circuits could include components such as beam splitters, polarizers, intensity modulators, phase modulators and frequency shifters. Here we review recent progress in realizing a fiber-gyroscope integrated-optical chip, including the design and performance of two LiNb03 channel-waveguide components, a double-Y branch and a serrodyne frequency translator. GRA

N87-10379# Los Alamos National Lab., N. Mex.
ATTEMPTS TO CHARACTERIZE MICROBALLOON SENSORS FOR SHOCK VELOCITY AND MATERIAL MOTION STUDIES
H. W. Kruse, L. D. Looney, R. C. Taylor, R. S. Medina, J. S. Baumgart (Edgerton, Germeshausen and Grier, Inc., Los Alamos, N. Mex.), G. T. Baca, and D. E. Dominguez 1986 15 p Presented at the 11th International Pyrotechnics Seminar, Vail, Colo, 7 Jul. 1986
(Contract W-7405-eng-36)
(DE86-011210; LA-UR-86-1704; CONF-860739-12) Avail: NTIS HC A02/MF A01

Optimization of performance of gas filled microballoons mounted on optical fibers as sensors for shock and material motion studies, was attempted by variation of several parameters. In some cases, results were not predictable and, in general, results were not as reproductible as desired. Change of some parameters caused little effect but effects of the sleeve size and sleeve material seem to be significant. Recorded shape of optical spectra match black-body temperature of 8000 K when argon filled balloons were impacted with projectiles with velocity of 1 km/s, in close agreement with expected values based on ideal gas calculations. DOE

N87-10474*# Saskatchewan Univ., Saskatoon. Inst. of Space and Atmospheric Studies.

COMPARISON OF MEDIUM FREQUENCY PULSED RADAR INTERFEROMETER AND CORRELATION ANALYSIS WINDS, PART 1

C. E. Meek, I. M. Reid, and A. H. Manson *In* International Council of Scientific Unions, Middle Atmosphere Program. Handbook for MAP, Vol. 20 Jun. 1986 6 p (For primary document see N87-10419 01-42)

Avail: NTIS HC A22/MF A01; also available from SCOSTEP Secretariat, Illinois Univ., 1406 West Green Street, Urbana, Ill. 61801 CSCL 14B

N87-10475*# Saskatchewan Univ., Saskatoon. Inst. of Space and Atmospheric Studies.

COMPARISON OF MEDIUM FREQUENCY PULSED RADAR INTERFEROMETER AND CORRELATION ANALYSIS WINDS, PART 2

C. E. Meek, I. M. Reid, and A. H. Manson *In* International Council of Scientific Unions, Middle Atmosphere Program. Handbook for MAP, Vol. 20 Jun. 1986 4 p (For primary document see N87-10419 01-42)

Avail: NTIS HC A22/MF A01; also available from SCOSTEP Secretariat, Illinois Univ., 1406 West Green Street, Urbana, Ill. 61801 CSCL 14B

36 LASERS AND MASERS

Includes parametric amplifiers.
For related information see also *76 Solid-State Physics.*

N87-10380# Brookhaven National Lab., Upton, N. Y.

TRANSVERSE CORRELATIONS IN START-UP OF A FREE ELECTRON LASER FROM NOISE

L. H. Yu and S. Krinsky Mar. 1986 12 p Presented at the Topical Meeting on Short Wavelength Coherent Radiation, Monterey, Calif., 24 Mar. 1986
(Contract DE-AC02-76CH-00016)
(DE86-009917; BNL-37898; CONF-860316-4) Avail: NTIS HC A02/MF A01

Linearized Vlasov-Maxwell equations are used to derive a partial differential equation determining the 3-dimensional slowly varying envelope function of the radiated electric field. The equation is solved analytically. From the correlation function <E(z,r,t) E*(z',r',t)> of the electric field averaged over the stochastic ensemble describing the initial shot noise in the beam, the longitudinal and transverse correlation lengths sigma(sub L) and sigma(sub T) are computed. The radiated power S per unit cross-sectional area of the the electron beam is determined. Our analysis is applicable for wiggler length L = N(sub w)lambda(sub w) long enough for the exponential regime to be researched, but short enough so that L sigma(sub theta) is less than or equal to a, the electron beam radius. DOE

N87-10381# Northwestern Univ., Evanston, Ill. Dept. of Physics and Astronomy.

POSSIBILITY OF OBTAINING COHERENT SHORT WAVE RADIATION FROM A SOLID STATE FREE ELECTRON LASER

S. A. Bogacz and J. B. Ketterson Mar. 1986 9 p Presented at the Topical Meeting on Short Wavelength Coherent Radiation, Monterey, Calif., 24 Mar. 1986 Prepared in cooperation with Argonne National Lab., Ill.
(Contract W-31-109-eng-38)
(DE86-010525; CONF-860316-7) Avail: NTIS HC A02/MF A01

The idea of using a crystal lattice or a superlattice as an undulator for a free electron laser is explored. A purely classical treatment of relativistic positrons channeling through the proposed structure involving a self consistent solution of the wave equation for the radiating electromagnetic field and the kinetic equation for the positron distribution function leads to a positive gain coefficient for a forward radiating field. Matching the Kumakhov resonance to the undulator frequency further enhances the gain. This result, combined with a feedback mechanism arising from Bragg diffraction within the basic crystal lattice, leads to an instability of the radiation inside the crystal. Finally a numerical estimate of the Kumakhov-enhanced gain coefficient is made for the (110) planar channeling in a strain modulated Si superlattice. DOE

N87-10382# Rochester Univ., N. Y. Inst. of Optics.

NONLINEAR OPTICS WITH BROAD-BAND LASERS Progress Report, 15 Jul. 1985 - Jul. 1986

M. G. Raymer Mar. 1986 9 p
(Contract DE-AC02-81ER-10979)
(DE86-011286; DOE/ER-10979/12) Avail: NTIS HC A02/MF A01

Progress has been made in the studies of both stimulated Raman scattering (SRS) with pulsed broad-band lasers and the statistical behavior of multimode cw dye lasers. It has been observed that in pumping SRS by a broad-band dye laser intensity fluctuations in the pump laser are transferred to some extent to the generated Stokes light. The intensity cross-correlation function between the pump and Stokes were directly measured and its form was found to be influenced by the medium's relaxation time. The statistical properties of a cw dye laser are being studied by observing its intensity autocorrelation function and corresponding power spectrum. DOE

N87-10383# Los Alamos National Lab., N. Mex.

OVERTONE PRODUCTION OF SOFT X-RAYS WITH FREE-ELECTRON LASERS

M. J. Schmitt, C. J. Elliott, K. Lee, and B. D. McVey 1986 8 p Presented at the Topical Meeting on Short Wavelength Coherent Radiation, Monterey, Calif., 24 Mar. 1986
(Contract W-7405-eng-36)
(DE86-011248; LA-UR-86-1682; CONF-860316-8) Avail: NTIS HC A02/MF A01

Two one-dimensional free-electron laser codes have recently been written that include harmonic generation. A comparison of the results of these codes shows that a self-consistent treatment of the harmonic interaction is not required in the presence of a strong fundamental field. Use of these codes to predict the effects of emittance on harmonic production have been conducted. The effects of wiggler-field amplitude fluctuations and odd-harmonic wiggler-field components on the harmonic-radiation production are also discussed. DOE

N87-10384# Los Alamos National Lab., N. Mex.

LONG-PULSE EXCIMER LASERS FOR MATERIALS PROCESSING AND MEDICAL APPLICATIONS

Robert Chia-Ting Sze 1986 17 p Presented at the OPTO '86 Conference, Paris, France, 13 May 1986
(Contract W-7405-eng-36)
(DE86-011267; LA-UR-86-1525; CONF-8605110-2) Avail: NTIS HC A02/MF A01

This report discusses a passive stabilization technique that not only allows long pulse laser operation, but allows for a much slower charging circuit as well as a factor of 10 gain in pulse repetition rate per given gas flow compared with more conventional excimer laser systems. The slower charging circuit greatly eases the stress on the pulse power components such as thyrations and capacitors and should be an important factor contributing to dependable industrial excimer laser systems. The gain of a factor of 10 in pulse repetition rate per unit gas flow results in extremely high pulse repetition rate laser systems in a very compact package; such lasers should find a place in a number of industrial and medical applications. DOE

N87-10385# Chicago Univ., Ill.

LASER INDUCED CHEMICAL REACTIONS AND LASER-COLLISION PROCESSES Final Technical Report, 1 May 1978 - 30 Apr. 1986

J. C. Light May 1986 5 p
(Contract DE-AC02-78ER-04908)
(DE86-011459; DOE/ER-04908/T1) Avail: NTIS

HC A02/MF A01

Theoretical investigations into the dynamics of atoms and molecules in strong radiation (laser) fields and under electron impact have been carried out. The studies were carried out using quantum mechanics and new approaches were developed for six major areas. First, a new and much more efficient method of solving the time independent quantum scattering equations was developed (VIVAS) and has been disseminated. Second, laser-collision processes were investigated and a negative result was determined. Only under very special circumstances and very strong laser fields can the field affect the course of a collision process (versus affecting the states of reactants before collisions). Third, methods for calculating multiphoton absorption by diatomic and polyatomic molecules were developed and applied. Fourth, methods of calculating the final states from single photon photodissociation of triatomic molecules were developed and applied. Analogous methods were developed and applied to electron-molecule collisions which result in either vibrational excitation or dissociative attachment. The first accurate calculations of dissociative-attachment of a triatomic molecule (CO) were made. Finally, the distributed Gaussian basis was developed as a general basis for the quantum calculations of vibrational states of polyatomic molecules. DOE

N87-10386# Los Alamos National Lab., N. Mex.

SCATTERED RADIATION FIELD OF A LASER BEAM PROPAGATING THROUGH TURBID MEDIA

S. A. W. Gerstl, S. M. Chitanvis, and A. Zardecki 1986 9 p Presented at the 10th Smoke-Obscurants Symposium, Adelphi, Md., 22 Apr. 1986
(Contract W-7405-eng-36)
(DE86-010188; LA-UR-86-1332; CONF-8604181-1) Avail: NTIS HC A02/MF A01

A combination of the small-angle approximation and the diffusion approximation is used to study the propagation of laser beams through dense scattering media. DOE

N87-10387# Los Alamos National Lab., N. Mex.

SUBPICOSECOND HIGH-BRIGHTNESS UV LASER SYSTEM

R. B. Gibson 1986 5 p Presented at the Society of Photo-Optical Instrumentation Engineers International Symposium: Topics in Optical and Optoelectronic Applied Sciences and Engineering, Quebec City, Canada, 2 Jun. 1986
(Contract W-7405-eng-36)
(DE86-011271; LA-UR-86-1499; CONF-860620-3) Avail: NTIS HC A02/MF A01

A laser system that produces intense subpicosecond pulses of 248 nm light is under development. Ultrashort pulses are generated in the visible in a synchronously-pumped mode-locked dye oscillator, heterodyned into the uv by two KDP crystals, and amplified in a chain of KrF* amplifiers. Front end output of 5 micro-J is amplified to 20 mJ and focused to peak intensities of order 10 to the 17th power W/cm. Additional amplification is expected to permit experiments at intensities >10 to the 20th power W/cm. DOE

N87-10388# Los Alamos National Lab., N. Mex.

LASER-INITIATED CHAIN REACTIONS IN THE PARTIAL OXIDATION OF METHANE

S. L. Baughcum, R. C. Oldenborg, W. C. Danen, G. E. Streit, and C. Rofer 1986 28 p Presented at the Society of Photo-Optical Instrumentation Engineers International Symposium: Topics in Optical and Optoelectronic Applied Sciences and Engineering, Quebec City, Canada, 2 Jun. 1986
(Contract W-7405-eng-36)
(DE86-011272; LA-UR-86-1483; CONF-860620-4) Avail: NTIS HC A03/MF A01

Using laser photolysis of suitable precursor molecules to produce gas-phase free radicals, we have been studying important kinetic processes in the partial oxidation of methane. Prompt production of a relatively high concentration of free radicals via laser photolysis makes it possible to separate the thermal initiation step from the subsequent chain propagation steps. Since the conditions (temperature, pressure, and mixture composition) for rapid thermal initiation and optimum production may differ, this provides an exciting potential application for laser-induced chemistry where the laser acts as the initiation source. We report our results on the partial oxidation of methane by oxygen at moderate temperatures. A trace amount of acetone is photolyzed at 193 nm a prompt source of methyl radicals in methane-oxygen mixtures. Details of the proposed mechanism are discussed as well as application of the technique to technologies for methane conversion to transportable fuels such as methanol. DOE

N87-10389# Virginia Univ., Charlottesville.

HIGH PRECISION ABSOLUTE LASER POWER MEASUREMENTS USING A MAGNETICALLY SUSPENDED ROTOR

G. T. Gillies and S. W. Allison 1985 3 p Presented at the International Laser Science Conference, Dallas, Tex., 18 Nov. 1985 Prepared in cooperation with Oak Ridge Gaseous Diffusion Plant, Tenn.
(Contract DE-AC05-84OT-21400)
(DE86-011585; K/TS-11-704; CONF-851185-20) Avail: NTIS HC A02/MF A01

Improvements to a torsion pendulum technique for making radiation pressure based measurements of laser power absolutely are presented. By replacing torsion fiber suspensions with magnetic suspensions, increases in sensitivity and reduced systematic drift are possible. DOE

N87-10264*# European Space Agency. European Space Research and Technology Center, ESTEC, Noordwijk (Netherlands).

ESA ACTIVITIES IN SPACE LASER SOUNDING AND RANGING

H. Lutz *In* NASA. Langley Research Center 13th International Laser Radar Conference Aug. 1986 1 p (For primary document see N87-10263 01-35)
Avail: NTIS HC A15/MF A01 CSCL 20E

N87-10266*# National Aeronautics and Space Administration. Langley Research Center, Hampton, Va.

TUNABLE SOLID-STATE LASER TECHNOLOGY FOR APPLICATIONS TO SCIENTIFIC AND TECHNOLOGICAL EXPERIMENTS FROM SPACE

F. Allario and L. V. Taylor *In its* 13th International Laser Radar Conferance Aug. 1986 1 p (For primary document see N87-10263 01-35)
Avail: NTIS HC A15/MF A01 CSCL 20E

N87-10269*# Deutsche Forschungs- und Versuchsanstalt fuer Luft- und Raumfahrt, Wesseling (West Germany). Inst. for Atmospheric Physics.

MIE LIDAR PROPOSED FOR THE GERMAN SPACE SHUTTLE MISSION D2

W. Renger, M. Endemann (Battelle Inst., Frankfurt am Main (West Germany).), H. Quenzel (Ludwig-Maximilians-Universitaet, Munich (West Germany).), and Ch. Werner *In* NASA. Langley Research center 13th International Laser Radar Conference Aug. 1986 4 p (For primary document see N87-10263 01-35)
Avail: NTIS HC A15/MF A01 CSCL 20E

N87-10270*# National Aeronautics and Space Administration. Langley Research Center, Hampton, Va.

THE LIDAR IN-SPACE TECHNOLOGY EXPERIMENT (LITE)

M. P. McCormick *In its* 13th International Laser Radar Conference Aug. 1986 1 p (For primary document see N87-10263 01-35)
Avail: NTIS HC A15/MF A01 CSCL 20E

N87-10278*# Academy of Sciences (USSR), Tomsk. Inst. of Atmospheric Optics.

LIDAR MEASUREMENTS OF SLANT VISUAL RANGE

Yu. S. Balin, S. I. Kavkyanov, G. M. Krekov, and I. A. Razenkov *In* NASA. Langley Research Center 13th International Laser Radar Conference Aug. 1986 3 p (For primary document see N87-10263 01-35)
Avail: NTIS HC A15/MF A01 CSCL 20E

N87-10279*# National Inst. for Environmental Studies, Tsukuba (Japan).
VISIBILITY AND AEROSOL MEASUREMENT BY DIODE-LASER RANDOM-MODULATION CW LIDAR
N. Takeuchi, H. Baba (Tokyo Univ. (Japan).), K. Sakurai, T. Ueno (Chiba Univ. (Japan).), and N. Ishikawa *In* NASA. Langley Research Center 13th International Laser Radar Conference Aug. 1986 4 p (For primary document see N87-10263 01-35)
Avail: NTIS HC A15/MF A01 CSCL 20E

N87-10280*# Arizona Univ., Tucson. Inst. of Atmospheric Physics.
CORRECTION FUNCTION IN THE LIDAR EQUATION AND THE SOLUTION TECHNIQUES FOR CO2 LIDAR DATE REDUCTION
Yanzeng Zhao, Ting Kaung Lea, and Richard M. Schotland *In* NASA. Langley Research Center 13th International Laser Radar Conference Aug. 1986 4 p (For primary document see N87-10263 01-35)
Avail: NTIS HC A15/MF A01 CSCL 20E

N87-10281*# National Aeronautics and Space Administration. Langley Research Center, Hampton, Va.
ASSESSMENT OF DIAL DATA COLLECTION AND ANALYSIS TECHNIQUES
E. V. Browell and P. T. Woods (National Physical Lab., Teddington (England).) *In its* 13th International Laser Radar Conference Aug. 1986 3 p (For primary document see N87-10263 01-35)
Avail: NTIS HC A15/MF A01 CSCL 20E

N87-10282*# National Aeronautics and Space Administration. Goddard Space Flight Center, Greenbelt, Md.
AIRBORNE LIDAR MEASUREMENTS OF THE ATMOSPHERIC PRESSURE PROFILE WITH TUNABLE ALEXANDRITE LASERS
C. L. Korb, G. K. Schwemmer, M. Dombrowski, J. Milrod, and H. Walden *In* NASA. Langley Research Center 13th International Laser Radar Conference Aug. 1986 3 p (For primary document see N87-10263 01-35)
Avail: NTIS HC A15/MF A01 CSCL 20E

N87-10284*# Radio Research Labs., Tokyo (Japan). Ministry of Posts and Telecommunications.
FLIGHT TESTS OF A RANGE-RESOLVED AIRBORNE DIAL WITH TWO MIN-TEA CO2 LASERS
T. Itabe, M. Ishizu, T. Aruga, T. Igarashi, and K. Asai (Tohoku Univ., Sendai (Japan).) *In* NASA. Langley Research Center 13th International Laser Radar Conference Aug. 1986 2 p (For primary document see N87-10263 01-35)
Avail: NTIS HC A15/MF A01 CSCL 20E

N87-10285*# RCA Astro-Electronics Div., Princeton, N. J.
Nd:GLASS-RAMAN LASER FOR WATER VAPOR DIAL
R. H. Kagann, J. C. Petheram, and A. Rosenberg *In* NASA. Langley Research Center 13th International Laser Radar Conference Aug. 1986 2 p (For primary document see N87-10263 01-35)
Avail: NTIS HC A15/MF A01 CSCL 20E

N87-10289*# National Physical Lab., Teddington (England). Div. of Quantum Metrology.
ATMOSPHERIC CONTRIBUTIONS TO THE COLUMN VARIANCE IN DIRECT-DETECTION DIAL
M. J. T. Milton and P. T. Woods *In* NASA. Langley Research Center 13th International Laser Radar Conference Aug. 1986 3 p (For primary document see N87-10263 01-35)
Avail: NTIS HC A15/MF A01 CSCL 20E

N87-10290*# Maryland Univ., College Park. Inst. for Physical Science.
HIGH SPECTRAL PURITY, NARROW LINEWIDTH LASER TRANSMITTER FOR DIAL MEASUREMENTS
U. N. Singh and P. H. Flamant (Laboratoire de Meteorologie Dynamique du CNRS, Palaiseau (France).) *In* NASA. Langley Research Center 13th International Laser Radar Conference Aug. 1986 4 p (For primary document see N87-10263 01-35)
Avail: NTIS HC A15/MF A01 CSCL 20E

N87-10292*# Naval Research Lab., Washington, D. C. Atmospheric Physics Branch.
USING A LASER AUREOLE TO INVERT LIDAR RETURN
William P. Hooper and H. Gerber *In* NASA. Langley Research Center 13th International Laser Radar Conference Aug. 1986 1 p (For primary document see N87-10263 01-35)
Avail: NTIS HC A15/MF A01 CSCL 20E

N87-10307*# Academy of Sciences (USSR), Tomsk. Inst. of Atmospheric Optics.
THE INFLUENCE OF AN OPTICAL RECEIVING SYSTEM ON STATISTICAL CHARACTERISTICS OF A LIDAR SIGNAL
A. E. Zuev, V. A. Banakh, and V. L. Mironov *In* NASA. Langley Research Center 13th International Laser Radar Conference Aug. 1986 3 p (For primary document see N87-10263 01-35)
Avail: NTIS HC A15/MF A01 CSCL 20E

N87-10308*# Academy of Sciences (USSR), Tomsk. Inst. of Atmospheric Optics.
COHERENT LIDARS BASED ON INTRACAVITY HETERODYNING OF ECHO SIGNALS
V. E. Zuev, S. D. Burakov, A. P. Godlevskii, Yu. D. Kopytin, S. V. Lazarev, S. A. Ostanin, and P. O. Sharin *In* NASA. Langley Research Center 13th International Laser Radar Conference Aug. 1986 1 p (For primary document see N87-10263 01-35)
Avail: NTIS HC A15/MF A01 CSCL 20E

N87-10309*# Academy of Sciences (USSR), Tomsk. Inst. of Atmospheric Optics
THE INFLUENCE OF SCATTERING PARTICLES MORPHOLOGY ON THE CHARACTERISTICS OF LIDAR SIGNALS
V. E. Zuev, I. E. Naats, and A. A. Popov *In* NASA. Langley Research Center 13th International Laser Radar Conference Aug. 1986 2 p (For primary document see N87-10263 01-35)
Avail: NTIS HC A15/MF A01 CSCL 20E

N87-10311*# National Aeronautics and Space Administration. Goddard Space Flight Center, Greenbelt, Md.
IMPROVEMENTS IN THE GODDARD BALLOON-BORNE LIDAR
William S. Heaps *In* NASA. Langley Research Center 13th International Laser Radar Conference Aug. 1986 1 p (For primary document see N87-10263 01-35)
Avail: NTIS HC A15/MF A01 CSCL 20E

N87-10323*# National Aeronautics and Space Administration. Goddard Space Flight Center, Greenbelt, Md.
ROTATIONALLY RESOLVED COLLISIONAL TRANSFER RATES IN OH
Thomas J. McGee, James Butler, John Burris, and William Heaps *In* NASA. Langley Research Center 13th International Laser Radar Conference Aug. 1986 1 p (For primary document see N87-10263 01-35)
Avail: NTIS HC A15/MF A01 CSCL 20E

N87-10324*# Okayama Univ. (Japan).
TIME-DOMAIN SENSITIVITY ENHANCEMENT IN PULSED Pb-TDL GAS MONITORS
R. Koga, M. Kosaka, and H. Sano *In* NASA. Langley Research Center 13th International Laser Radar Conference Aug. 1986 4 p (For primary document see N87-10263 01-35)
Avail: NTIS HC A15/MF A01 CSCL 20E

N87-10325*# University of the West Indies, Mona (Jamaica). Dept. of Physics.
PERFORMANCE TESTING OF LIDAR RECEIVERS
M. Y. Shams *In* NASA. Langley Research Center 13th International Laser Radar Conference Aug. 1986 2 p (For primary document see N87-10263 01-35)
Avail: NTIS HC A15/MF A01 CSCL 20E

N87-10326*# Royal Signals and Radar Establishment, Malvern (England).

PROGRESS IN COHERENT LASER RADAR

J. M. Vaughan *In* NASA. Langley Research Center 13th International Laser Radar Conference Aug. 1986 2 p (For primary document see N87-10263 01-35)

Avail: NTIS HC A15/MF A01 CSCL 20E

N87-10360*# Arizona Univ., Tucson.

COHERENT LIDAR SIGNAL FLUCTUATION REDUCTION BY MEANS OF FREQUENCY DIVERSITY TECHNIQUE

R. M. Schotland, P. Vujkovic Cvijin, and Yan-Zeng Zhao *In* NASA. Langley Research Center 13th International Laser Radar Conference Aug. 1986 3 p (For primary document see N87-10263 01-35)

Avail: NTIS HC A15/MF A01 CSCL 20E

N87-10362*# National Center for Atmospheric Research, Boulder, Colo. Research Aviation Facility.

THE NCAR AIRBORNE INFRARED LIDAR SYSTEM (NAILS)

R. L. Schwiesow and P. A. Lightsey *In* NASA. Langley Research Center 13th International Laser Radar Conference Aug. 1986 3 p (For primary document see N87-10263 01-35)

Avail: NTIS HC A15/MF A01 CSCL 20E

N87-10364*# Centre National de la Recherche Scientifique, Verrieres-Le Buisson (France).

PULSED MONONODE DYE LASER DEVELOPED FOR A GEOPHYSICAL APPLICATION

J. P. Jegou, T. Pain, and G. Megie *In* NASA. Langley Research Center 13th International Laser Radar Conference Aug. 1986 3 p (For primary document see N87-10263 01-35)

Avail: NTIS HC A15/MF A01 CSCL 20E

N87-10365*# RCA Astro-Electronics Div., Princeton, N. J.

CALIBRATION AND ANALYSIS FOR A 0.53 MICRON INCOHERENT DOPPLER LIDAR

J. Sroga and A. Rosenberg *In* NASA. Langley Research Center 13th International Laser Radar Conference Aug. 1986 4 p (For primary document see N87-10263 01-35)

Avail: NTIS HC A15/MF A01 CSCL 20E

N87-10372*# National Aeronautics and Space Administration. Langley Research Center, Hampton, Va.

LINEWIDTH CHARACTERISTICS OF RAMAN-SHIFTED DYE LASER OUTPUT AT 720 AND 940 nm

B. E. Grossmann, U. N. Singh (Maryland Univ., College Park.), N. S. Higdon, L. J. Cotnoir, T. D. Wilkerson, and E. V. Browell *In* NASA. Langley Research Center 13th International Laser Radar Conference Aug. 1986 5 p (For primary document see N87-10263 01-35)

(Contract NCCI-32)

Avail: NTIS HC A15/MF A01 CSCL 20E

N87-10373*# Centre National de la Recherche Scientifique, Verrieres-Le Buisson (France).

ALEXANDRITE LASER SOURCE FOR ATMOSPHERIC LIDAR MEASUREMENTS

J. Pelon, C. Loth, P. Flamant, and G. Megie *In* NASA. Langley Research Center 13th International Laser Radar Conference Aug. 1986 4 p (For primary document see N87-10263 01-35)

Avail: NTIS HC A15/MF A01 CSCL 20E

N87-10374*# National Inst. for Environmental Studies, Tsukuba (Japan).

THE TFP AND A PULSED LD: NEW LIDAR COMPONENTS

Hiroshi Shimizu, Ichiro Matsui, and Kazuhiro Asai (Tohoku Univ., Sendai (Japan).) *In* NASA. Langley Research Center 13th International Laser Radar Conference Aug. 1986 4 p (For primary document see N87-10263 01-35)

Avail: NTIS HC A15/MF A01 CSCL 20E

37 MECHANICAL ENGINEERING

Includes auxiliary systems (nonpower); machine elements and processes; and mechanical equipment.

N87-10390 Carnegie-Mellon Univ., Pittsburgh, Pa.

DYNAMIC MODELING AND CONTROL OF ROBOTIC MANIPULATORS Ph.D. Thesis

Vassilios Dimitrios Tourassis 1985 255 p

Avail: Univ. Microfilms Order No. DA8601197

The objective of this dissertation is to advance the state of the art in the dynamic modeling and feedback control robotic manipulators with rigid links. The dissertation revolves around three complementary themes: robot dynamics, discrete-time dynamic robot modeling, and nonlinear feedback robot control. Controller design for manipulators requires a fundamental physical understanding of the properties and structure of robot dynamics. Robot dynamics are embedded in the mathematical foundations of classical mechanics to introduce novel physical interpretations and structural characteristics of the closed-form dynamic robot model. This approach reinforces the need to integrate the mechanical and controller designs of robotic manipulators. An inherently discrete-time dynamic robot model, which is compact and designed for computer-control of robots, is then introduced. The model guarantees conservation of energy (and momentum, if appropriate) over each sampling period. This discrete-time dynamic robot model is acceleration-free and is attractive for both forward and inverse dynamics applications in trajectory planning and dynamic feedback control. A review of the fundamental principles of nonlinear feedback robot control algorithms leads to an outline of the practical problems introduced by modeling inaccuracies, unmodeled dynamics and parameter errors. The alpha-computed-torque nonlinear feedback control algorithm, which is robust in the presence of these modeling errors is then introduced. Dissert. Abstr.

N87-10391*# National Aeronautics and Space Administration. Lewis Research Center, Cleveland, Ohio.

TESTING OF UH-60A HELICOPTER TRANSMISSION IN NASA LEWIS 2240-kW (3000-HP) FACILITY

Andrew M. Mitchell, Fred B. Oswald, and Harold H. Coe Aug. 1986 30 p

(NASA-TP-2626; E-2941; NAS 1.60:2626) Avail: NTIS HC A03/MF A01 CSCL 13I

The U.S. Army's UH-60A Black Hawk 2240-kW (3000-hp) class, twin-engine helicopter transmission was tested at the NASA Lewis Research Center. The vibration and efficiency test results will be used to enhance the data base for similar-class helicopters. Most of the data were obtained for a matrix of test conditions of 50 to 100 percent of rated rotor speed and 20 to 100 percent of rated input power. The transmission's mechanical efficiency at 100 percent of rated power was 97.3 and 97.5 percent with its inlet oil maintained at 355 and 372 K (180 and 210 F), respectively. The highest vibration reading was 72 g's rms at the upper housing side wall. Other vibration levels measured near the gear meshes are reported. Author

N87-10392# Helsinki Univ. Technology, Otaniemi (Finland). Internal Combustion Engine Lab.

COLD-START TESTS WITH SPEED DIESEL ENGINES USING ALCOHOL AS MAIN FUEL

J. Laurikko and J. Pitkaenen 1985 72 p In FINNISH

(DE86-751651; TKK-KO/PM-49) Avail: NTIS (US Sales Only) HC A04/MF A01

This report describes the cold-startability of alcohol powered diesel engines and the results of tests carried out on two test engines based on different application methods. In cold-start tests carried out under laboratory conditions two direct injection alcohol powered diesel engines based on different application methods were evaluated. On the other engine alcohol mixture with ignition improving additive was used as main fuel and the other was equipped with two separate fuel systems using pure alcohol as main fuel and ordinary diesel oil as ignition fuel. The aim was to determine the temperature limit of cold-startability and find the methods and devices which guarantee adequate startability. Test were made within the temperature range of +20 deg C to -30 deg C and during the start-up the engine speed, cylinder pressure, intake air and exhaust gas temperatures plus needle lift of fuel injectors in the dual-fuel engine were recorded in addition to the test conditions. In the tests the startability of the alcohol mixture engine was found superior to the dual-fuel engine. The startability of the mixture-fuel engine was satisfactory until -15 deg C without any auxiliary devices but with the dual-fuel engine intake air preheating was necessary already at 0 deg C. Using intake air p reheating both engines could be started at -30 deg. DOE

N87-10393# Oak Ridge National Lab., Tenn.
DESIGN RULE FOR FATIGUE OF WELDED JOINTS IN ELEVATED-TEMPERATURE NUCLEAR COMPONENTS
D. G. OConnor and J. M. Corum 1986 21 p Presented at the ASME Pressure Vessel and Piping Conference and Exhibit, Chicago, Ill., 20 Jul. 1986
(Contract DE-AC05-84OR-21400)
(DE86-007569; CONF-860722-6) Avail: NTIS HC A02/MF A01

Elevated-temperature weldment fatigue failures have occurred in several operating liquid-metal reactor plants. Yet, ASME Code Case N-47, which governs the design of such plants in the United States, does not currently address the Code Subgroup on Elevated Temperature Design recently proposed a fatigue strength reduction factor for austenitic and ferritic steel weldments. The factor is based on a variety of weld metal and weldment fatigue data generated in the United States, Europe, and Japan. This paper describes the factor and its bases, and it presents the results of confirmatory fatigue tests conducted at Oak Ridge National Laboratory on 316 stainless steel tubes with axial and circumferential welds of 16-8-2 filler metal. These test results confirm the suitability of the design factor, and they support the premise that the metallurgical notch effect produced by yield strength variations across a weldment is largely responsible for the observed elevated-temperature fatigue strength reduction. DOE

N87-10394# Comissao Nacional de Energia Nuclear de Brasil, Rio de Janeiro.
STUDY ABOUT THE STRUCTURAL BEHAVIOR OF WStE-36N STEEL
M. dosSantosPinto and M. B. Trindade 1985 89 p In POLISH
(DE86-702011; CNEN-DR-130/85) Avail: NTIS (US Sales Only) HC A05/MF A01

The influence of a stress relaxation heat treatment in welding done by submerged arc welding is studied. This influence was studied in a structural steel, WStE-36N, niobium alloy, made in Brazil, through Charpy V test, hardness measurements, microstructural aspects and X ray diffraction. DOE

N87-10395# Kernforschungszentrum, Karlsruhe (West Germany).
PROCESS CONTROL IN ARC WELDING
P. Drews and K. Mages Feb. 1986 147 p In GERMAN; ENGLISH summary Sponsored by Bundesministerium fuer Forschung und Technologie
(KfK-PFT-105; ETN-86-97838) Avail: NTIS HC A07/MF A01

Improvement of the automation of arc welding processes is discussed. Controlable and programmable welding power sources were developed. An inverter power source which, based on its transfer frequency, is distinguished by economy and less noise emission at the work place was realized. For the reproducability of the process parameters, preprogramming units were developed, which are integrated in the power source, and control the power source externally by developed interfaces. Production welding multiple-axis handling units with electrical and hydraulic motors were built and strategies for seam-tracking were developed. For the supervision of welding processes a measurement unit which enables a comprehensive, flexible and intelligent supervision and documentation was built. Opto-electronic sensors which guarantee an exact seam-tracking and positioning of the torch at the beginning of the joint as well as the analysis of the joint geometry were developed. ESA

N87-10396# Kernforschungszentrum, Karlsruhe (West Germany).
PROGRAMMING OF SENSOR BASED ASSEMBLY ROBOTS
C. Blume, B. Frommherz, and K. Hoermann Feb. 1986 42 p In GERMAN; ENGLISH summary Sponsored by Bundesministerium fuer Forschung und Technologie
(KfK-PFT-120; ETN-86-97840) Avail: NTIS HC A03/MF A01

Research developments of the AL and SRL Robot Programming systems are reviewed. Based on experience with the AL-System, SRL-System was designed and implemented. The language SRL incorporates most of the concepts of robot programming and concepts of structured computer programming languages. The components of these programming systems are treated. ESA

N87-10397 California Univ., Berkeley.
EXPERIMENTAL IDENTIFICATION AND CONTROL OF THE TIP POSITION OF A FLEXIBLE, SINGLE LINK MANIPULATOR Ph.D. Thesis
Srinivasan Ramakrishnan 1985 160 p
Avail: Univ. Microfilms Order No. DA8610175

Vibration control of light, flexible links is important for the design of fast and precise robots. A closed loop control system for damping such vibrations is studied. The objective of this study is defined as follows: Consider a beam of finite flexibility and unknown parameters, with one end fixed to the shaft of a motor with finite torque capability. Assume that the beam is free to rotate in the horizontal plane only, with no torsional or vertical plane deflection. The objective is to control the position of the free end of the beam in any horizontal trajectory within the range of motion of the system, while minimizing the time integral of the sum of the square of the deviations of the tip position from the reference and the weighted square of the control effort. An anlytical model is derived for the flexible beam and motor system, and validated by experiment using a new sensor developed for tip postion measurement. The model is then used to simulate adaptive tip position control. The system parameters are estimeted using a model reference adaptive scheme. The estimated parameters are used to design an optimal controller, and tip position control of the flexible beam and motor system is demonstrated. It is shown that the closed loop scheme increases the speed of response and reduces the steady state error compared to an open loop sheme. Dissert. Abstr.

N87-10398 Stanford Univ., Calif.
RAPID PRECISE END POINT CONTROL OF A WRIST CARRIED BY A FLEXIBLE MANIPULATOR Ph.D. Thesis
Wen-Wei Chiang 1986 141 p
Avail: Univ. Microfilms Order No. DA8612724

The speed and accuracy of a robot manipulator can be increased by using end-point sensors for motion measurement and control, along with an accurate dynamic model of the mechanical system in the control algorithm. However, the closed-loop control bandwidth of a robot manipulator is still physically limited ultimately by its structural flexibility, since the end effector and the actuator are separated. Analyses were performed to study the dynamic interaction between the motion of a mini-manipulator and the structural flexibility of the main robot arm. A plane-motion mechanical system was built to demonstrate several fast maneuvers of such a mini-macro manipulator system. A frequency identification scheme was also developed and implemented successfully in a closed-loop adaptive control on a separate mechanical laboratory system consisting of two inertia disks connected by a torsional rod. It is believed that the same frequency identification scheme can be used to improve further the performance of the mini-macro manipulator system when adaptive control is employed. Dissert. Abstr.

38 QUALITY ASSURANCE AND RELIABILITY

Includes product sampling procedures and techniques; and quality control.

N87-10399*# National Aeronautics and Space Administration. Lewis Research Center, Cleveland, Ohio.

ULTRASONIC DETERMINATION OF RECRYSTALLIZATION
Edward R. Generazio 1986 15 p Presented at the Review of Progress in Quantitative NDE, La Jolla, Calif. 3-8 Aug. 1986; sponsored by Ames Lab. and Iowa State Univ.
(NASA-TM-88855; E-3248; NAS 1.15:88855) Avail: NTIS HC A02/MF A01 CSCL 14D

Ultrasonic attenuation was measured for cold worked Nickel 200 samples annealed at increasing temperatures. Localized dislocation density variations, crystalline order and colume percent of recrystallized phase were determined over the anneal temperature range using transmission electron microscopy, X-ray diffraction, and metallurgy. The exponent of the frequency dependence of the attenuation was found to be a key variable relating ultrasonic attenuation to the thermal kinetics of the recrystallization process. Identification of this key variable allows for the ultrasonic determination of onset, degree, and completion of recrystallization. B.G.

N87-10400*# Boeing Commercial Airplane Co., Seattle, Wash.
FAULT TOLERANT CONTROL LAWS Final Report
Uy-Loi Ly and John K. Ho 1986 113 p
(Contract NAS1-17635)
(NASA-CR-178094; NAS 1.26:178094) Avail: NTIS HC A06/MF A01 CSCL 14D

A systematic procedure for the synthesis of fault tolerant control laws to actuator failure has been presented. Two design methods were used to synthesize fault tolerant controllers: the conventional LQ design method and a direct feedback controller design method SANDY. The latter method is used primarily to streamline the full-state Q feedback design into a practical implementable output feedback controller structure. To achieve robustness to control actuator failure, the redundant surfaces are properly balanced according to their control effectiveness. A simple gain schedule based on the landing gear up/down logic involving only three gains was developed to handle three design flight conditions: Mach .25 and Mach .60 at 5000 ft and Mach .90 at 20,000 ft. The fault tolerant control law developed in this study provides good stability augmentation and performance for the relaxed static stability aircraft. The augmented aircraft responses are found to be invariant to the presence of a failure. Furthermore, single-loop stability margins of +6 dB in gain and +30 deg in phase were achieved along with -40 dB/decade rolloff at high frequency. Author

39 STRUCTURAL MECHANICS

Includes structural element design and weight analysis; fatigue; and thermal stress.

For applications see *05 Aircraft Design, Testing and Performance* and *18 Spacecraft Design, Testing and Performance.*

N87-10401 Purdue Univ., West Lafayette, Ind.
GEOMETRIC AND MATERIAL NONLINEAR DYNAMIC ANALYSIS OF COMPLEX SHELLS Ph.D. Thesis
Sunil Saigal 1985 169 p
Avail: Univ. Microfilms Order No. DA8606610

A 48 degree-of-freedom doubly curved quadrilateral thin shell element, including the effect of both material and geometric nonlinearities, is formulated and appropriate numerical procedures are adopted for the development of a systematic and efficient approach for static and dynamic nonlinear analysis of general shell structures. The Cartesian displacement functions are described by bicubic Hermitian polynomials in curvilinear coordinates. The geometry of the shell surface is modeled using variable-order polynomials. This may allow the stiffness formulation of the shell element to be linked to the geometric data bases created by the computer aided design systems. The geometric formulations employ the Lagrangian mode for description of motion. A systematic choice of examples is solved and compared with available solutions to evaluate the formulations and procedures recommended. As an application of the present element, a detailed study of the static contact of an inflated radial automotive tire with rigid surface is conducted. An inflation analysis of the tire is first performed and then the results for footprint areas at different stages of contact; and the resulting redistribution of stress and moments resultants, all of practical significance to the tire industry are obtained. Dissert. Abstr.

N87-10402 Purdue Univ., West Lafayette, Ind.
DYNAMIC DELAMINATION CRACK PROPAGATION IN A GRAPHITE/EPOXY LAMINATE Ph.D. Thesis
Joseph Edward Grady 1985 165 p
Avail: Univ. Microfilms Order No. DA8606544

Impact tests of (90/0) sub 5 s T-300/934 graphite/epoxy laminates of beam-like dimension with embedded delamination cracks were conducted. High speed photography (16000 frames/sec) was used to record the impact response and subsequent crack propagation. From the photographic data, impact characteristics such as the contact duration and the dynamic response of the impact specimen were measured. In addition, the time of initiation of crack propagation and measurements of the subsequent crack length versus time were obtained. By changing the location of the embedded delamination in the specimens relative to the impact point, additional results were obtained on the variation of the threshold impact velocity necessary to cause crack propagation in the different specimen configurations. A further series of impact tests with instrumented targets was used to characterize the dynamic force history resulting from the high speed impact of a rubber ball. A finite element analysis was performed to calculate the dynamic strain energy release rate prior to the onset of delamination. The critical value of the strain energy release rate necessary to initate propagation of a delamination in this material was investigated. Dissert. Abstr.

N87-10403 Delaware Univ., Newark.
SHORT-WAVELENGTH BUCKLING AND SHEAR FAILURES FOR COMPRESSION-LOADED COMPOSITE LAMINATES
Mark James Shuart 1985 231 p
Avail: Univ. Microfilms Order No. DA8609058

This investigation studies the short-wavelength buckling (or the microbuckling) and the interlaminar and inplane shear failures of multi-directional composite laminates loaded in uniaxial compression. A laminate model is presented that idealizes each lamina. The fibers in the lamina are modeled as a plate, and the matrix in the lamina is modeled as an elastic foundation. The out-of-plane w displacement for each plate is expressed as a trigonometric series in the half-wavelength of the mode shape for laminate short-wavelength buckling. Nonlinear strain-displacement ralations are used. The model is applied to symmetric laminates having linear material behavior. The laminates are loaded in uniform end shortening and are simply supported. A linear analysis is used to determine the laminate stress strain, and mode shape when short-wavelength buckling occurs. The equations for the laminate compressive stress at short-wavelength buckling are dominated by matrix contributions. The effects of fiber volume fraction on the compressive stress at short-wavelength buckling is reported for a laminate with any stacking sequence and any thickness. The laminate mode shape at short-wavelength buckling is discussed. A nonlinear analysis for laminae with initial imperfections is used to determine laminate stresses and interlaminar strains.

N87-10404# National Aeronautical Lab., Bangalore (India). Structures Div.
EFFECT OF STATIC INPLANE LOADS AND BOUNDARY CONDITIONS ON THE FLUTTER OF FLAT RECTANGULAR PANELS
A. Joshi and B. R. Somashekar Feb. 1986 38 p
(NAL-TM-ST-8604) Avail: NTIS HC A03/MF A01

Presented are investigations of the problem of flutter of initially stressed rectangular panels having various types of boundary conditions including the elastic end restraint. Using the Galerkins modal analysis technique the solutions are obtained for various cases of panel aspect ratio, thickness ratio, and elastic stiffness of the support. The results show that the flutter mode is primarily determined by the first and the second vibration modes. The results also show that the effect of elastic end can be reasonably accurately modelled by simple closed form analytical expressions. Author

N87-10405# British Aerospace Aircraft Group, Weybridge (England). Structures Dept.
THE EFFECTS OF TEMPERATURE AND LOADING RATE ON R-CURVES USING THE CLWL TECHNIQUES
S. Nowak Jul. 1985 66 p
(Contract A93B/1391)
(BAe-MSM-R-GEN-0544; BR97093; ETN-86-97946) Avail: NTIS HC A04/MF A01

The effects on crack growth resistance curves of typical aircraft temperature and loading rate variations were investigated. The crack line wedge loaded specimen was used and 2 aluminum alloys, specifications 7475T761 and BSL72 were considered. It is found that at low temperature or high strain rates the resistance to crack growth of 7475T61 is considerably reduced, whereas that of BSL72 benefits slightly. The combined effect of low temperature and high strain rates is shown to further increase the difference between the two alloys. ESA

N87-10406*# Old Dominion Univ., Norfolk, Va. Dept. of Mechanical Engineering and Mechanics.
A TAYLOR-GALERKIN FINITE ELEMENT ALGORITHM FOR TRANSIENT NONLINEAR THERMAL-STRUCTURAL ANALYSIS Progress Report, period ending 1 Jan. 1986
Earl A. Thornton and Pramote Dechaumphai Apr. 1986 12 p
Previously announced in IAA as A86-38823
(Grant NsG-1321)
(NASA-CR-177064; NAS 1.26:177064) Avail: NTIS HC A02/MF A01 CSCL 20K

A Taylor-Galerkin finite element method for solving large, nonlinear thermal-structural problems is presented. The algorithm is formulated for coupled transient and uncoupled quasistatic thermal-structural problems. Vectorizing strategies ensure computational efficiency. Two applications demonstrate the validity of the approach for analyzing transient and quasistatic thermal-structural problems. Author

N87-10407*# Auburn Univ., Ala. Dept. of Computer Science and Engineering.
NONLINEAR ROTORDYNAMICS ANALYSIS Progress Report, 1 Jun. 1985 - 15 Jun. 1986
William B. Day and Richard A. Zalik 1986 66 p
(Contract NAS8-36475)
(NASA-CR-178931; NAS 1.26:178931) Avail: NTIS HC A04/MF A01 CSCL 20K

Three analytic consequences of the nonlinear Jeffcott equations are examined. The primary application of these analyses is directed toward understanding the excessive vibrations recorded in the Liquid Oxygen (LOX) pump of the Space Shuttle Main Engine (SSME) during hot firing ground testing. The first task is to provide bounds on the coefficients of the equations which delimit the two cases of numerical solution as a circle or an annulus. The second task examines the mathematical generalization to multiple forcing functions, which includes the special problems of mass imbalance, side force, rubbing, and combination of these forces. Finally, stability and boundedness of the steady-state solutions is discussed and related to the corresponding linear problem. Author

N87-10408*# Drexel Univ., Philadelphia, Pa. Dept. of Mechanical Engineering and Mechanics.
CONTROLLER DESIGN VIA STRUCTURAL REDUCED MODELING BY FETM Semiannual Report
Ajmal Yousuff 13 Oct. 1986 25 p
(Grant NAG1-622)
(NASA-CR-179838; NAS 1.26:179838) Avail: NTIS HC A02/MF A01 CSCL 20K

The Finite Element - Transfer Matrix (FETM) method has been developed to reduce the computations involved in analysis of structures. This widely accepted method, however, has certain limitations, and does not directly produce reduced models for control design. To overcome these shortcomings, a modification of FETM method has been developed. The modified FETM method easily produces reduced models that are tailored toward subsequent control design. Other features of this method are its ability to: (1) extract open loop frequencies and mode shapes with less computations, (2) overcome limitations of the original FETM method, and (3) simplify the procedures for output feedback, constrained compensation, and decentralized control. This semi annual report presents the development of the modified FETM, and through an example, illustrates its applicability to an output feedback and a decentralized control design. Author

N87-10409*# Tuskegee Inst., Ala. School of Engineering and Architecture.
MODE 1 DELAMINATION GROWTH IN ADHESIVELY BONDED JOINTS UNDER STATIC AND FATIGUE LOADS Semiannual Report
Subodh C. Biswas and Shaik Jeelani 1986 17 p
(Grant NAG1-447)
(NASA-CR-179812; NAS 1.26:179812) Avail: NTIS HC A02/MF A01 CSCL 20K

The objective of this investigation was to characterize the pure mode 1 delamination growth in metal to metal adhesively bonded joints under static and fatigue loading conditions, using FM 73 adhesive. Double cantilever beam specimens (DCB) were used for pure mode 1 tests. Aluminum 2024-T3 adherends were bonded with FM 73 adhesive. Delamination was introduced during fabrication by inserting a Teflon film between the two adherends. The mode 1 strain energy release rate G sub I sub c was obtained directly from static DCB tests conducted in accordance with the ASTM designation D1876-12. Constant amplitude fatigue tests on DCB specimens were conducted to determine the relationship between delamination growth rate da/dN and strain energy release rate G sub I sub c for a pure mode 1 delamination growth. It is found that the debond propagation rate in adhesive joints using FM 73 is more sensitive to errors in design load than is typical crack growth rate in metallic structures. Author

N87-10410*# North Carolina Agricultural and Technical State Univ., Greensboro.
DYNAMICS AND CONTROL OF ORBITING GRID AND THE SYNCHRONOUSLY DEPLOYABLE BEAM Semiannual Report
Elias G. Abu-Saba Jul. 1985 19 p
(Grant NAG1-405)
(NASA-CR-179808; NAS 1.26:179808) Avail: NTIS HC A02/MF A01 CSCL 20K

The dynamic analysis of a grid structure hung from the ceiling by two steel wires is described. The method of approach uses the discrete mass model system. The concept of the bifilar pendulum is used in writing the equation of motion. Assumptions are made with regard to the bar stiffnesses in the vertical and horizontal planes. The discrete mases are assumed to be connected by inextensible massless strings that do not provide any torsion or bending. The modal frequencies obtained by this method are compared with those obtained from the finite element model. Author

N87-10411# Alabama Univ., University.
FOUNDATION INTERACTION PROBLEMS INVOLVING AN ELASTIC HALF-PLANE Final Report
Howard B. Wilson and Louis H. Turcotte Mar. 1986 76 p
(Contract DACW39-83-M-2630)
(AD-A167925; BER-319-241; WES/TR/ATC-86-1) Avail: NTIS HC A05/MF A01 CSCL 13/13

Stress analysis problems involving interaction between a structure and its foundation often lead to extensive computational effort. This fact becomes obvious when finite-element methods are used to study problems where the foundation is idealized as an infinite elastic half-plane. Attempts to represent the half-plane by a finite size structure using many elements entail solving large systems of simultaneous equations at a considerable computational cost. This report presents a more computationally efficient procedure which employs the exact solution of the equations of elasticity for an elastic half-plane subjected to arbitrary surface loading. Complex variable formulations are shown to yield a compact solution for the stresses and displacements in a half-plane supporting several concentrated loads. This solution is also employed to compute flexibility and stiffness matrices relating the concentrated loads and the displacements at the points of application of the loads. The stiffness matrix derived in this manner is then employed to investigate a simple type of interaction problem where an Euler beam rests on an elastic half-plane and is subjected to external loading. The foundation interaction forces, as well as other quantities such as beam shear and moment, are also computed. GRA

N87-10412# Ballistic Research Labs., Aberdeen Proving Ground, Md.

FURTHER RESULTS ON THE INITIATION AND GROWTH OF ADIABATIC SHEAR BANDS

Thomas W. Wright and Romesh C. Batra Apr. 1986 30 p
(AD-A168012; BRL-MR-3508) Avail: NTIS HC A03/MF A01 CSCL 20/11

Growth of perturbations in the simple shearing deformation of a softening thermo-visco-plastic solid have been examined by means of a finite element technique. It has been found that very small perturbations grow slowly at first, even though the underlying homogeneous stress strain response has passed peak stress, but that eventually explosive growth occurs. During the slow growth phase, the stress follows the homogeneous response quite closely, but in the explosive phase, the stress drops precipitously. Large perturbations grow at a larger initial rate, and accelerate rapidly even before peak homogeneous stress. Inclusion of a dipolar plastic effect appears to be stabilizing. GRA

N87-10413# Northwestern Univ., Evanston, Ill. Structural Mechanics Lab.

CRACK-TIP FIELDS IN A VISCOPLASTIC MATERIAL Interim Report

J. D. Achenbach, N. Nishimura, and J. C. Sung Apr. 1986 41 p
(Contract N00014-76-C-0063)
(AD-A168014; NU-SML-TR-86-1) Avail: NTIS HC A03/MF A01 CSCL 20/11

An integral representation for the particle velocity in terms of a Green's function and certain linear combinations of the inelastic strain rates was used in this study, both for a numerical method to compute full field solutions and to develop unequivocal asymptotic expressions for the near-tip fields. Specific results have been obtained for a stationary crack in a solid whose constitutive behavior is represented by the Bodner Partom model. It is shown that the leading term of the near-tip particle velocity is of order r to the 1/2 power, and the higher-order terms are of the forms r logr and r. Expressions were derived for the angular variations and for the multiplying time-dependent intensity factors. The r logr term is absent for the Mode-II case. Two questions were addressed in further detail: the dependence of the multiplying terms on time and the importance of the higher-order terms. The numerical results show a stress intensity factor which decays with time. At a small distance from the crack tip the numerically computed normalized opening stress was compared with a one-term asymptotic representation. The two curves diverge at very small values of time. Inclusion of a second term in the asymptotic expression for the stress gives very acceptable agreement as time increases. GRA

N87-10414# Los Alamos National Lab., N. Mex.

SIMPLE BLAST MODEL FOR STRUCTURAL DESIGN

T. R. Neal 1985 7 p Presented at the International Symposium on Intense Dynamic Loading and its Effects, Beijing, China, 3 Jun. 1986
(Contract W-7405-eng-36)
(DE86-000802; LA-UR-85-3420; CONF-860616-3) Avail: NTIS HC A02/MF A01

Structures capable of either containing or surviving nearby detonating explosive are useful research tools for investigating properties of materials. Our particular interest is in spherical steel vessels that are only stressed elastically. Although there is a large amount of data describing blast waves in air, it is mostly for the farfield region $R > 1$ where R is the reduced radius - that is, the distance from the charge center divided by the cube root of the change mass - expressed here in m/kg/(1)/(3). Our region of investigation was the range $0.3 < R < 0.7$. For these distances the blast effect is mainly impulsive, and normally less than 1% of the explosive energy is coupled into kinetic energy of the vessel. The response of vessels to spherical changes of the HMX-based explosive PBX 9501 has been investigated both for vessels filled with ambient air and evacuated. A simple scaling model is used to correlate the data for various size vessels and to describe the impulse on structures. This model is then applied to one test of the TATB-based explosive PBX 9502. Finally, the immediate residual pressure in the vessels was measured to show the degree of short-term overpressure in evacuated structures. DOE

N87-10415# Sandia National Labs., Albuquerque, N. Mex.

RESPONSE OF A 3-LAYERED RING TO AN AXISYMMETRIC IMPULSE

M. J. Sagartz May 1986 35 p
(Contract DE-AC04-76DP-00789)
(DE86-011016; SAND-85-2403) Avail: NTIS HC A03/MF A01

A modal solution for the axisymmetric response of a three-layered shell to an impulse load is derived. The outer and inner layers are each assumed to be thin and are separated by a relatively soft middle or core layer. Elasticity theory is used to treat the core layer while the inner and outer layers are governed by shell theory. Formulas for the circumferential stresses in the inner and outer layers and for the radial stress in the core are presented. A limited parameter study is included to demonstrate the use of the solution. Comments about the convergence of the series solution and its range of applicability are included. A listing of a computer program used to evaluate the series solutions is included in an Appendix. DOE

N87-10416# Brown Univ., Providence, R. I. Div. of Engineering.

GROWTH OF CRACKS UNDER FAR-FIELD CYCLIC COMPRESSIVE LOADS: NUMERICAL AND EXPERIMENTAL RESULTS

D. K. Holm, A. F. Blom, and S. Suresh Jun. 1985 26 p Prepared in cooperation with Royal Inst. of Tech., Stockholm, Sweden and Aeronautical Research Inst. of Sweden, Bromma
(Contract DE-FG02-84ER-45167)
(DE86-010279; DOE/ER-45167/3) Avail: NTIS HC A03/MF A01

Crack growth from a notch-tip, under the influence of fully compressive far-field cyclic loads, is investigated both numerically and experimentally in notched specimens of a lower strength steel and an aluminum alloy. Such cracks, emanating from the root of the notch, progressively decelerate until complete crack arrest occurs. Analyses of the stress state along the crack plane indicate that while the extent of the residual tensile stress field diminishes with an increase in crack length, there is a progressive increase in crack closure during crack advance. Approximate numerical calculations of the crack closure loads are in reasonable agreement with experimental results. DOE

N87-10417# Kernforschungszentrum, Karlsruhe (West Germany). Inst. fuer Reaktorentwicklung.

CONCENTRATIONS OF PLASTIC STRAINS IN THE CLAMPING REGION OF CYLINDRICAL SHELLS UNDER EXCESSIVE LOADING Thesis - Karlsruhe University, West Germany

M. Geiss Feb. 1986 94 p In GERMAN; ENGLISH summary
(KfK-3915; ISSN-0303-4003; ETN-86-97833) Avail: NTIS HC A05/MF A01

The behavior of cylindrical shells under overload is investigated. Different clamping conditions and variations of the material behavior are considered. Plastic strain concentrations at the shell clamping are determined. The analyses were carried out with a finite-element code. The results show that only minor plastic strain concentrations have to be expected for a rigidly clamped shell loaded by internal pressure. Considerable plastic strain concentrations have to be expected at a flange type clamping loaded by axial stresses in the shell. Comparison of these analyses with standard stress analysis procedures shows that these procedures are conservative. The structural integrity of the core barrel clamping of a pressurized water reactor under blowdown loading was assessed. Even in case of a sudden and complete pipe break the structure can withstand blowdown loading. ESA

N87-10418 Iowa State Univ. of Science and Technology, Ames.

APPLICATION OF GRAPH THEORY TO THE NONLINEAR ANALYSIS OF LARGE SPACE STRUCTURES Ph.D. Thesis

Magdy Ibrahim Hindawy 1986 100 p
Avail: Univ. Microfilms Order No. DA8615055

A new graph representation of nonlinear large space structures is introduced. During the loading process the structural graph changes its levels as the nonlinear regions in the large space structure change configuration. This variable structured graph is used to order the nodes and members of the discretized nonlinear structural model. A new algorithm is used to change the established order of the nonlinear model and updates the condensed nonlinear stiffness matrix equation for the structure. In addition to accounting for structural nonlinearities the algorithm can take into consideration plastic hinge formation and fracture of members in large space structures. Dissert. Abstr.

42 GEOSCIENCES (GENERAL)

N87-10419*# International Council of Scientific Unions, Urbana, Ill.

MIDDLE ATMOSPHERE PROGRAM. HANDBOOK FOR MAP, VOLUME 20

S. A. Bowhill, ed. and Belva Edwards, ed. Jun. 1986 519 p Presented at the URSI/SCOSTEP Workshop on Technical and Scientific Aspects of MST Radar, Aguadilla, Puerto Rico, 21-25 Oct. 1985 Sponsored by NASA and UNESCO
(NASA-CR-176882; NAS 1.26:176882; MAP-HANDBOOK-20)
Avail: NTIS HC A22/MF A01; also available from SCOSTEP Secretariat, Illinois Univ., 1406 West Green Street, Urbana, Ill. 61801 CSCL 04A

Various topics related to investigations of the middle atmosphere are discussed. Numerical weather prediction, performance characteristics of weather profiling radars, determination of gravity wave and turbulence parameters, case studies of gravity-wave propagation, turbulence and diffusion due to gravity waves, the climatology of gravity waves, mesosphere-stratosphere-troposphere radar, antenna arrays, and data management techniques are among the topics discussed. For individual titles, see N87-10420 through N87-10525.

N87-10420*# National Meteorological Center, Washington, D.C.

ON THE POTENTIAL USE OF RADAR-DERIVED INFORMATION IN OPERATIONAL NUMERICAL WEATHER PREDICTION c47

Ronald D. McPherson *In* International Council of Scientific Unions, Middle Atmosphere Program. Handbook for MAP, Vol. 20 Jun. 1986 4 p (For primary document see N87-10419 01-42)
Avail: NTIS HC A22/MF A01; also available from SCOSTEP Secretariat, Illinois Univ., 1406 West Green Street, Urbana, Ill. 61801 CSCL 04B

Estimates of requirements likely to be levied on a new observing system for mesoscale meteonology are given. Potential observing systems for mesoscale numerical weather prediction are discussed. Thermodynamic profiler radiometers, infrared radiometer atmospheric sounders, Doppler radar wind profilers and surveillance radar, and moisture profilers are among the instruments described. R.J.F.

N87-10421*# Oklahoma Univ., Norman. School of Meteorology.

A THEORY FOR THE RETRIEVAL OF VIRTUAL TEMPERATURE FROM WINDS, RADIANCES AND THE EQUATIONS OF FLUID DYNAMICS c47

Gal-Chen Tzvi *In* International Council of Scientific Unions, Middle Atmosphere Program. Handbook for MAP, Vol. 20 Jun. 1986 12 p (For primary document see N87-10419 01-42)
Avail: NTIS HC A22/MF A01; also available from SCOSTEP Secretariat, Illinois Univ., 1406 West Green Street, Urbana, Ill. 61801 CSCL 04B

A technique to deduce the virtual temperature from the combined use of the equations of fluid dynamics, observed wind and observed radiances is described. The wind information could come from ground-based sensitivity very high frequency (VHF) Doppler radars and/or from space-borne Doppler lidars. The radiometers are also assumed to be either space-borne and/or ground-based. From traditional radiometric techniques the vertical structure of the temperature can be estimated only crudely. While it has been known for quite some time that the virtual temperature could be deduced from wind information only, such techniques had to assume the infallibility of certain diagnostic relations. The proposed technique is an extension of the Gal-Chen technique. It is assumed that due to modeling uncertainties the equations of fluid dynamics are satisfied only in the least square sense. The retrieved temperature, however, is constrained to reproduce the observed radiances. It is shown that the combined use of the three sources of information (wind, radiances and fluid dynamical equations) can result in a unique determination of the vertical temperature structure with spatial and temporal resolution comparable to that of the observed wind.

N87-10422*# Pennsylvania State Univ., University Park. Dept. of Meteorology.

EXAMPLES OF MESOSCALE STRUCTURES AND SHORT-TERM WIND VARIATIONS DETECTED BY VHF DOPPLER RADAR c47

G. S. Forbes *In* International Council of Scientific Unions, Middle Atmosphere Program. Handbook for MAP, Vol. 20 Jun. 1986 13 p (For primary document see N87-10419 01-42)
Avail: NTIS HC A22/MF A01; also available from SCOSTEP Secretariat, Illinois Univ., 1406 West Green Street, Urbana, Ill. 61801 CSCL 04B

The first of three wind profilers planned for operation in central and western Pennsylvania began full-time, high-quality operation during July 1985. It is located about 20 km south-southeast of University Park and operates at 50 MHz. Another 50-MHz radar and a 400-MHz radar are to be installed over the next few months, to complete a mesoscale triangle with sides of 120 to 160 km. During the period since early July, a number of weather systems have passed over the wind profiler. Those accompanied by thunderstorms caused data losses either because the Department computer system lost power or because power went out at the profiler site. A backup power supply and an automatic re-start program will be added to the profiler system to minimize such future losses. Data have normally been averaged over a one-hour period, although there have been some investigations of shorter-period averaging. In each case, preliminary examinations reveal that the profiler winds are indicative of meteorological phenomena. The only occasions of bad or missing data are obtained when airplane noise is occasionally experienced and when the returned power is nearly at the noise level, at the upper few gates, where a consensus wind cannot be determined. Jets streams, clouds, and diurnal variations of winds are discussed. Author

N87-10423*# National Center for Atmospheric Research, Boulder, Colo.

WIND PROFILER DATA IN A MESOSCALE EXPERIMENT FROM A METEOROLOGICAL PERSPECTIVE c47

Edward J. Zipser, John Augustine (National Oceanic and Atmospheric Administration, Boulder, Colo.), and John Cunning *In* International Council of Scientific Unions, Middle Atmosphere Program. Handbook for MAP, Vol. 20 Jun. 1986 5 p Sponsored in part by NSF (For primary document see N87-10419 01-42)
Avail: NTIS HC A22/MF A01; also available from SCOSTEP Secretariat, Illinois Univ., 1406 West Green Street, Urbana, Ill. 61801 CSCL 04B

During May and June of 1985, the Oklahoma-Kansas Preliminary Regional Experiment of STORM-Central (OK PRE-STORM) was carried out, with the major objectives of learning more about mesoscale convective systems (MCSs) and gaining experience in the use of new sensing systems and measurement strategies that will improve the design of STORM-Central. Three 50-MHz wind profilers were employed in a triangular array with sides about 275 km. It is far too soon to report any results of this effort, for it has barely begun. The purpose here is to show some examples of the data, some of the surrounding conventional data, and to discuss some of the issues important to meteorologists in evaluating the contribution of the profiler data. The case of 10 to 11 June 1985, featuring a major squall line system which crossed the dense observing network from northwest to southeast, passing the Liberal site about 2230 GMT/10 June, the McPherson site about 0100 GMT/11 June, and Wichita about 0300 GMT/11 June is discussed. Radar and satellite data show that the system was growing rapidly when it passed Liberal, and was large and mature when it passed through McPherson and Wichita. The radar depiction of the system during this stage is given, with the McPherson site in the intense convective echoes near the leading edge at 01 GMT and in the stratiform precipitation at 03 GMT. The profiler wind data for a 9-hour period encompassing the squall line passage at each site are given. Author

N87-10424*# Clemson Univ., S.C. Dept. of Physics.
OBSERVATIONS OF MESOSCALE VERTICAL VELOCITIES AROUND FRONTAL ZONES c47
T. S. Dennis, M. F. Larsen, and J. Rottger (Arecibo Ionospheric Observatory, Puerto Rico) *In* International Council of Scientific Unions, Middle Atmosphere Program. Handbook for MAP, Vol. 20 Jun. 1986 9 p (For primary document see N87-10419 01-42)
Avail: NTIS HC A22/MF A01; also available from SCOSTEP Secretariat, Illinois Univ., 1406 West Green Street, Urbana, Ill. 61801 CSCL 04B

Vertical velocity and reflectivity data obtained with a VHF Doppler radar over a 15-day period in October and November of 1981 are analyzed. Standard radiosonde data and surface observations were used to locate two occluded fronts, two warm fronts, and a cold front that passed the radar site. These fronts are also evident in the radar reflectivity data. Most studies of the vertical circulation patterns associated with mososcale systems have used precipitation and cloud formations as tracers. Unlike other observational techniques, the VHF radar permits the continuous measurement of the three-dimensional air velocity vector in time and height from a fixed location. With the beam in a vertically pointing position, signals are scattered from turbulent variations in the refractive index with half the scale of the radar wavelength and by regions with sudden changes in the refractive index associated with horizontally stratified layers. Generally, the strongest echoes occur at the maximum in the vertical gradient of refractivity, usually at the base of a temperature inversion, such as the tropopause. VHF radars can also be used to locate atmospheric fronts, which are characterized by static stability, large horizontal temperature gradients, large vorticities, and vertical wind shears. These radars can provide the velocity field data needed to study wave motions associated with fronts and compare the actual vertical circulation to theoretical predictions. Author

N87-10425*# Clemson Univ., S.C. Dept. of Physics and Astronomy.
COMPARISON OF VERTICAL VELOCITIES ANALYZED BY A NUMERICAL MODEL AND MEASURED BY A VHF WIND PROFILER c47
M. F. Larsen, J. Rottger (Arecibo Ionospheric Observatory, Puerto Rico), and T. S. Dennis *In* International Council of Scientific Unions, Middle Atmosphere Program. Handbook for MAP, Vol. 20 Jun. 1986 4 p (For primary document see N87-10419 01-42)
Avail: NTIS HC A22/MF A01; also available from SCOSTEP Secretariat, Illinois Univ., 1406 West Green Street, Urbana, Ill. 61801 CSCL 04B

The use of wind profilers for measuring vertical velocities in the troposphere and lower stratosphere is potentially of great interest for verification of forecasts, diagnosis of mesoscale circulations, and studies of wave motions. The studies of profiler vertical velocities to date have shown that the observed patterns of ascent and subsidence are reasonable when compared to the synoptic conditions. However, difficulties arise when a direct verification of the profiler vertical winds is sought. Since no other technique can measure the vertical velocities over the same height range and with the same claimed accuracy as the profilers, direct comparisons are impossible. The only alternative is to compare the measurements to analyzed vertical velocity fields. Here, researchers compare vertical measurements made with the SOUSY VHF radar over a period of 11 days at the beginning of November 1981 to the analyzed vertical velocities produced by the European Center for Medium-range Weather Forecasting (ECMWF) model for grid points near the radar site. Author

N87-10426*# Kyoto Inst. of Tech. (Japan). Dept. of Electrical Engineering.
MEASUREMENTS OF PRECIPITATING ATMOSPHERE BY THE MU RADAR c47
Koichiro Wakasugi, Shoichiro Fukao (Kyoto Univ., Japan), and Susumu Kato *In* International Council of Scientific Unions, Middle Atmosphere Program. Handbook for MAP, Vol. 20 Jun. 1986 5 p (For primary document see N87-10419 01-42)
Avail: NTIS HC A22/MF A01; also available from SCOSTEP Secretariat, Illinois Univ., 1406 West Green Street, Urbana, Ill. 61801 CSCL 04B

Sensitive VHF Doppler radars have the capability to detect echoes from precipitation particles as well as refractive index irregularities. Researchers used the middle and upper (MU) atmosphere radar at Shigaraki, Japan for tropospheric observations of precipitating atmosphere. They detected precipitation motions simultaneously with the ambient air motion and showed the capabilities of the MU radar in investigating mesoscale structures of meteorological phenomena such as air precipitation motions within a cold frontal system. More recently, a direct method for deducing the drop size distribution of precipitation particles was developed using Doppler spectra of the MU radar. This method is free from errors inherent in conventional measurements using microwave Doppler spectra. Meteorological microwave radar data are also utilized for monitoring vertical and horizontal structures of precipitation. Author

N87-10427*# National Oceanic and Atmospheric Administration, Boulder, Colo.
THE REAL-TIME USE OF WIND PROFILERS IN NOWCASTING c47
Tracy Lorraine Smith and Thomas W. Schlatter *In* International Council of Scientific Unions, Middle Atmosphere Program. Handbook for MAP, Vol. 20 Jun. 1986 7 p (For primary document see N87-10419 01-42)
Avail: NTIS HC A22/MF A01; also available from SCOSTEP Secretariat, Illinois Univ., 1406 West Green Street, Urbana, Ill. 61801 CSCL 04B

The program for Regional Observing and Forecasting Services (PROFS) has been using wind profile data in experimental forecast applications for over two years, mostly in the form of real-time color displays on the PROFS forecast workstation. The most ambitious test of the workstation to date, the 1985 PROFS Real-Time Experiment (RT-85), ran from 15 May to 23 August, 1985. The use of wind profiler products during this and previous experiments is described. Data from the experimental profiler network in Colorado and from the profiler in Oklahoma are in the form of hourly averages. Arriving data frequently contain errors whose origins range from interference by aircraft in the beams to highway truck traffic. Most of the irregularities are apparent through visual inspection of profiler wind observations plotted on a time-height cross section, but this method of quality control is inadequate if the intended uses of the data involve numerical calculations. Author

N87-10428*# Arecibo Ionospheric Observatory, Puerto Rico.
THE INFLUENCE OF VELOCITY VARIABILITY ON THE DETERMINATION OF WIND PROFILES c47
Jurgen Rottger *In* International Council of Scientific Unions, Middle

Atmosphere Program. Handbook for MAP, Vol. 20 Jun. 1986 5 p (For primary document see N87-10419 01-42)
Avail: NTIS HC A22/MF A01; also available from SCOSTEP Secretariat, Illinois Univ., 1406 West Green Street, Urbana, Ill. 61801 CSCL 04B

High sensitivity radars allow the determination of velocity estimates at time resolutions down to one minute or better. Because of the variability introduced to the mean wind due to turbulence and waves, the high resolution profiles may not be too useful for forecasting applications, although they yield the most realistic estimate of the instantaneous wind profile. Profiles of wind speed and direction, vertical velocity and echo power, which were deduced in real-time on 23 August 1981 with the spaced antenna drift mode of the SOUSY-VHF-Radar are shown. Whereas these profiles were measured within 1 minute, the operating routine allowed the selection of variable (longer) measuring periods, and one has to search for the optimum duration of the data averaging period. A high time resolution wind vector diagram is given which gives an idea of the temporal variability. The data were obtained with the spaced antenna technique, which allows a good estimate of the horizontal wind without having to correct for the vertical velocity component. The wind vectors specifically indicate a quasi-periodic variation in direction. This is assumed to be due to gravity waves since the vertical velocity also shows periodical variations with the same period. The consistency of these spaced-antenna VHF radar results along with the radiosonde data convinced researchers that the method is quite suitable for wind profiling applications.
Author

N87-10429*# National Oceanic and Atmospheric Administration, Boulder, Colo.
PERFORMANCE CHARACTERISTICS OF WIND PROFILING RADARS c47
R. G. Strauch, A. S. Frisch, and B. L. Weber *In* International Council of Scientific Unions, Middle Atmosphere Program. Handbook for MAP, Vol. 20 Jun. 1986 7 p (For primary document see N87-10419 01-42)
Avail: NTIS HC A22/MF A01; also available from SCOSTEP Secretariat, Illinois Univ., 1406 West Green Street, Urbana, Ill. 61801 CSCL 04B

Doppler radars used to measure winds in the troposphere and lower stratosphere for weather analysis and forecasting are lower-sensitivity versions of mesosphere-stratosphere-troposphere radars widely used for research. The term wind profiler is used to denote these radars because measurements of vertical profiles of horizontal and vertical wind are their primary function. It is clear that wind profilers will be in widespread use within five years: procurement of a network of 30 wind profilers is underway. The Wave Propagation Laboratory (WPL) has operated a small research network of radar wind profilers in Colorado for about two and one-half years. The transmitted power and antenna aperture for these radars is given. Data archiving procedures have been in place for about one year, and this data base is used to evaluate the performance of the radars. One of the prime concerns of potential wind profilers users is how often and how long wind measurements are lacking at a given height. Since these outages constitute an important part of the performance of the wind profilers, they are calculated at three radar frequencies, 50-, 405-, and 915-MHz, (wavelengths of 6-, 0.74-, and 0.33-m) at monthly intervals to determine both the number of outages at each frequency and annual variations in outages. Author

N87-10430*# National Severe Storms Lab., Norman, Okla.
A LOOK AT PROFILER PERFORMANCE c47
Edwin Kessler, Michael Eilts, and Kevin Thomas (Oklahoma Univ., Norman) *In* International Council of Scientific Unions, Middle Atmosphere Program. Handbook for MAP, Vol. 20 Jun. 1986 13 p (For primary document see N87-10419 01-42)
Avail: NTIS HC A22/MF A01; also available from SCOSTEP Secretariat, Illinois Univ., 1406 West Green Street, Urbana, Ill. 61801 CSCL 04B

Since about 1974, Doppler radars operating in UHF and VHF ranges have been used increasingly to study atmospheric winds. Historically, large systems capable of obtaining data from high altitudes have focused attention on the mesosphere and stratosphere, rather than on the troposphere wherein abides most of the weather considered by most meteorologists. Research address some questions the meteorologist must logically ask first, viz., what is the actual performance capability of these systems, how accurate is the wind data of interest to meteorologists, and from what altitudes in the troposphere are the data reliably obtained.
Author

N87-10431*# Adelaide Univ. (Australia). Dept. of Physics.
HARDWARE REQUIREMENTS: A NEW GENERATION PARTIAL REFLECTION RADAR FOR STUDIES OF THE EQUATORIAL MESOSPHERE c47
R. A. Vincent *In* International Council of Scientific Unions, Middle Atmosphere Program. Handbook for MAP, Vol. 20 Jun. 1986 1 p (For primary document see N87-10419 01-42)
Avail: NTIS HC A22/MF A01; also available from SCOSTEP Secretariat, Illinois Univ., 1406 West Green Street, Urbana, Ill. 61801 CSCL 04B

A new partial reflection (PR) radar is being developed for operation at the proposed Equatorial Observatory. The system is being designed to make maximum use of recent advances in solid-state technology in order to minimize the power requirements. In particular, it is planned to use a solid-state transmitter in place of the tube transmitters previously used in PR systems. Solid-state transmitters have the advantages that they do not need high voltage supplies, they do not require cathode heaters with a corresponding saving in power consumption and parts are readily available and inexpensive. It should be possible to achieve 15 kW peak powers with recently announced fast switching transistors. Since high mean powers are desirable for obtaining good signal-to-noise ratios, it is also planned to phase code the transmitted pulses and decode after coherent integration. All decoding and signal processing will be carried out in dedicated microprocessors before the signals are passed to a microcomputer for on-line analysis. Recent tests have shown that an Olivetti M24 micro (an IBM compatible) running an 8-MHz clock with a 8087 coprocessor can analyze data at least as fast as the minicomputers presently being used with the Adelaide PR radar and at a significantly lower cost. The processed winds data will be stored in nonvolatile CMOS RAM modules; about 0.5 to 1 Mbyte is required to store one week's information.
Author

N87-10432*# Arecibo Ionospheric Observatory, Puerto Rico.
NEED FOR A SUBTROPICAL WIND PROFILING SYSTEM c47
J. Rottger, M. F. Larsen (Clemson Univ., S.C.), H. M. Ierkic, and T. Hagfors *In* International Council of Scientific Unions, Middle Atmosphere Program. Handbook for MAP, Vol. 20 Jun. 1986 4 p (For primary document see N87-10419 01-42)
Avail: NTIS HC A22/MF A01; also available from SCOSTEP Secretariat, Illinois Univ., 1406 West Green Street, Urbana, Ill. 61801 CSCL 04B

The purpose is to point out the need for, and the benefit that can be derived from, a national wind profiling facility located in the subtropics. At present no such facility exists. There are several advantages associated with a low-latitude location. The first is that wave motions and large-scale circulations unique to the tropics can be studied. The second is that the relatively steady mean flows in the subtropical belt may provide a cleaner environment for studies of waves common at all latitudes. Researchers suggest the Arecibo Observatory as an ideal site for a wind profiling facility since the land and much of the computing, technical, and scientific support is already available. Author

N87-10433*# Alaska Univ., Fairbanks. Geophysical Inst.
GRAVITY WAVES IN THE MIDDLE ATMOSPHERE: RECENT PROGRESS AND NEEDED STUDIES c46
David C. Fritts *In* International Council of Scientific Unions, Middle Atmosphere Program. Handbook for MAP, Vol. 20 Jun. 1986 6 p (For primary document see N87-10419 01-42)
Avail: NTIS HC A22/MF A01; also available from SCOSTEP Secretariat, Illinois Univ., 1406 West Green Street, Urbana, Ill.

61801 CSCL 04A

The recent recognition of the important role played by gravity waves in the large-scale circulation and thermal structure of the mesosphere and lower thermosphere has stimulated considerable research on their properties and their middle atmosphere effects. For example, these studies have begun to provide important information on gravity wave scales, propagation, filtering, and the processes responsible for saturation and turbulent diffusion. There remain, however, many areas in which our current understanding of middle atmosphere gravity waves is deficient. The purpose here is to review the progress that has been made to date and to suggest areas in which additional studies are most needed. Gravity wave scales, gravity wave saturation mechanisms, turbulence production and turbulent diffusion, and distribution of gravity wave energies and momentum fluxes with height and time are discussed. Author

N87-10434*# National Oceanic and Atmospheric Administration, Boulder, Colo.

A MODEL FOR GRAVITY-WAVE SPECTRA OBSERVED BY DOPPLER SOUNDING SYSTEMS c46

T. E. VanZandt *In* International Council of Scientific Unions, Middle Atmosphere Program. Handbook for MAP, Vol. 20 Jun. 1986 1 p (For primary document see N87-10419 01-42)

Avail: NTIS HC A22/MF A01; also available from SCOSTEP Secretariat, Illinois Univ., 1406 West Green Street, Urbana, Ill. 61801 CSCL 04A

A model for Mesosphere - Stratosphere - Troposphere (MST) radar spectra is developed following the formalism presented by Pinkel (1981). Expressions for the one-dimensional spectra of radial velocity versus frequency and versus radial wave number are presented. Their dependence on the parameters of the gravity-wave spectrum and on the experimental parameters, radar zenith angle and averaging time are described and the conditions for critical tests of the gravity-wave hypothesis are discussed. The model spectra is compared with spectra observed in the Arctic summer mesosphere by the Poker Flat radar. This model applies to any monostatic Doppler sounding system, including MST radar, Doppler lidar and Doppler sonar in the atmosphere, and Doppler sonar in the ocean. Author

N87-10435*# Arecibo Ionospheric Observatory, Puerto Rico.

HALF-DAY AND FOUR-DAY WAVES IN THE STATOSPHERE c46

Jurgen Rottger *In* International Council of Scientific Unions, Middle Atmosphere Program. Handbook for MAP, Vol. 20 Jun. 1986 2 p (For primary document see N87-10419 01-42)

Avail: NTIS HC A22/MF A01; also available from SCOSTEP Secretariat, Illinois Univ., 1406 West Green Street, Urbana, Ill. 61801 CSCL 04A

Further analysis of spaced-antenna measurements of 3-dimensional velocity in the stratosphere was performed over a period of 10 days and compared with meteorological observations. A quasi-four-day wave in the lower stratosphere can be shown to originate in planetary wave/synoptic scale disturbances in the troposphere. Its phase propagates downwards and its amplitude decreases strongly with height in the lower stratosphere. The wave features are most pronounced in the meridional wind component, but they show up also in the vertical component. A 12-h oscillation with downward phase progression and about 1.5 ms-1 velocity amplitude is also detected in the meridional component above 18 km, but there is no comparable feature seen in the troposphere. Author

N87-10436*# Kyoto Univ., Uji (Japan). Radio Atmospheric Science Center.

TROPOSPHERIC TURBULENCE PARAMETERS MEASURED BY USING THE MU RADAR c46

Toru Sato, Hiromasa Matsumoto (Kyoto Univ., Japan), Shoichiro Fukao, and Susumu Kato *In* International Council of Scientific Unions, Middle Atmosphere Program. Handbook for MAP, Vol. 20 Jun. 1986 4 p (For primary document see N87-10419 01-42)

Avail: NTIS HC A22/MF A01; also available from SCOSTEP Secretariat, Illinois Univ., 1406 West Green Street, Urbana, Ill. 61801 CSCL 04A

The spectral width of the Doppler radar echo has been used to estimate the atmospheric turbulence parameters because it is directly related to the kinetic energy contained in the turbulence. However, sufficient care must be taken in deriving the turbulence parameters since the measured spectral width can be easily affected by undesired factors such as beam broadening, shear broadening, and the temporal variation of the wind field. Here researchers examine these factors in the case of the MU radar observation of the upper troposphere, and present preliminary results. Author

N87-10437*# Case Western Reserve Univ., Cleveland, Ohio.

SIMULTANEOUS VHF AND UHF RADAR OBSERVATION OF THE MESOSPHERE AT ARECIBO DURING A SOLAR FLARE: A CHECK ON THE GRADIENT-MIXING HYPOTHESIS c46

P. K. Rastogi, J. D. Mathews, and J. Rottger (Arecibo Ionospheric Observatory, Puerto Rico) *In* International Council of Scientific Unions, Middle Atmosphere Program. Handbook for MAP, Vol. 20 Jun. 1986 8 p (For primary document see N87-10419 01-42)

Avail: NTIS HC A22/MF A01; also available from SCOSTEP Secretariat, Illinois Univ., 1406 West Green Street, Urbana, Ill. 61801 CSCL 04A

The results of a two wavelength (VHF and UHF) mesosphere experiment performed at the Arecibo Observatory on January 5, 1981 are discussed. The 46.8-MHz VHF radar (3.21 m Bragg scale) was operated to provide spectral measurements of signals scattered from refractivity fluctuations due to turbulence. Other physical parameters such as radial velocities, scattered signal power, and Doppler spread due to turbulence can be derived from signal spectra. The 430-MHz UHF radar (0.36 m Bragg scale) was used for D-region electron-density measurements using the incoherent scatter technique with a comparable height resolution. The radars were pointed symmetrically about the vertical with a beam spacing of 5.5 degree in the meridional plane. Occurrence of a type 4 solar flare during the experiment produced enhanced D-region electron-density gradients. This was a unique circumstance that provided the possibility of testing the basic premises of the turbulent gradient-mixing hypothesis. Author

N87-10438*# Air Force Geophysics Lab., Hanscom AFB, Mass.

EVIDENCE OF ATMOSPHERIC GRAVITY WAVE PERTURBATIONS OF THE BRUNT-VAISALA FREQUENCY IN THE ATMOSPHERE c46

R. E. Good, R. W. Beland, J. H. Brown, and E. M. Dewan *In* International Council of Scientific Unions, Middle Atmosphere Program. Handbook for MAP, Vol. 20 Jun. 1986 7 p (For primary document see N87-10419 01-42)

Avail: NTIS HC A22/MF A01; also available from SCOSTEP Secretariat, Illinois Univ., 1406 West Green Street, Urbana, Ill. 61801 CSCL 04A

A series of high altitude, medium resolution, measurements of temperature, pressure and turbulence have been performed by the Air Force Geophysics Laboratory. These measurements were conducted using the VIZ Manufacturing Co. microsondes with attached micro-thermal probes measuring the temperature structure coefficient. A typical atmospheric temperature measurement is given. Several small temperature inversions are evident in the troposphere. The stratosphere is marked with numerous fluctuations in the temperature profile. Microsondes provide temperature and pressure measurements every 4 seconds up to a maximum altitude of 30 km (MSL). Since the average ascent rate is 5 m/s, the altitude interval between the measurement reports is 20 m. The potential temperature is calculated from the temperature and pressure. Spectral analysis of atmospheric Brunt-Vaisala frequencies reveal spectra similiar to the velocity spectra of Dewan et al. (1984), Daniels (1982), and Endlich and Singleton (1969). The Brunt-Vaisala spectra indicate the existence of separate, distinguishable wave modes. R.J.F.

N87-10439*# Air Force Geophysics Lab., Hanscom AFB, Mass.

ATMOSPHERIC WAVES AND THE NATURE OF BUOYANCY

TURBULENCE IN THE CONTEXT OF THE WAVES VS 2D-TURBULENCE DEBATE **c46**
Edmond M. Dewan *In* International Council of Scientific Unions, Middle Atmosphere Program. Handbook for MAP, Vol. 20 Jun. 1986 4 p (For primary document see N87-10419 01-42)
Avail: NTIS HC A22/MF A01; also available from SCOSTEP Secretariat, Illinois Univ., 1406 West Green Street, Urbana, Ill. 61801 CSCL 04A

The problem of how to empirically distinguish between velocity fluctuations due to turbulence and those due to atmospheric waves is addressed. The physical differences between waves and turbulence are reviewed. New theoretical ideas on the subject of bouyancy range turbulence are presented. A unique scale K sub B is given that allows one to differentiate between waves and turbulence for the special case of theta = 0 (i.e., horizontal propagating waves). R.J.F.

N87-10440*# Air Force Geophysics Lab., Hanscom AFB, Mass.
A PROPOSED EXPERIMENTAL TEST TO DISTINGUISH WAVES FROM 2-D TURBULENCE **c46**
Edmond M. Dewan *In* International Council of Scientific Unions, Middle Atmosphere Program. Handbook for MAP, Vol. 20 Jun. 1986 3 p (For primary document see N87-10419 01-42)
Avail: NTIS HC A22/MF A01; also available from SCOSTEP Secretariat, Illinois Univ., 1406 West Green Street, Urbana, Ill. 61801 CSCL 04A

A theory of buoyancy range turbulence that leads to a unique scale, K sub B, that allows one to differentiate between waves and turbulence for the special case of theta = 0 (i.e., horizontally propagating waves) is discussed. The theory does not seem to lead to a practical empirical distinction for the general situation. This is due to the fact that, as theta is increased, one has the ever-increasing presence of BRT for longer wavelengths. The fact that the numerical values of epsilon prime are not yet available compounds the difficulty. In addition, it does not appear possible to encompass true 2-D turbulence in the theory. We are thus driven to a test which circumvents all these difficulties. A proposed test is based on the idea that waves are coherent and propagate, while in turbulence we have the opposite situation. In particular, the test is suggested by the following quotation from MULLER (1984), on the nature of such turbulence: The turbulence in each horizontal plane is independent from the turbulence in the other planes. If this statement were to be taken literally, it would imply that the temporal coherence between horizontal speeds, separated only in altitude, would be zero. Any vertical separation would be forced to take into account the effects of viscosity: that is to say, a specific finite vertical separation would be needed to destroy coherence. In order to estimate this distance, L, one can use L = C(v/S) (1/2) were v is the kinematic viscosity, S is the shear scale, and C is a constant of order unity. Author

N87-10441*# Illinois Univ., Urbana. Dept. of Electrical and Computer Engineering.
PROPAGATING TIDES IN THE MESOSPHERE **c46**
S. A. Bowhill and K. O. Merewether *In* International Council of Scientific Unions, Middle Atmosphere Program. Handbook for MAP, Vol. 20 Jun. 1986 1 p (For primary document see N87-10419 01-42)
Avail: NTIS HC A22/MF A01; also available from SCOSTEP Secretariat, Illinois Univ., 1406 West Green Street, Urbana, Ill. 61801 CSCL 04A

A preliminary search has begun for evidence of tides in the 1-hr average line-of-sight mesospheric velocity data from the Urbana radar in the period 1978 to 1982, inclusive. Observations are restricted to the southeasterly component of those velocities. Since observations are only available for a fraction of a day due to the absence of night-time ionization in the Urbana mesosphere, it was decided to adopt an unusual procedure in the search; namely, to perform a Fourier analysis in the vertical direction and look for rotation in phase of vectors representing spatial frequency components. Propagating tidal modes would then show as vectors with a net rotation corresponding to their downward phase velocity. Five year monthly averages of hourly mean horizontal velocities inferred from the Urbana data are given. Consistent diurnal variation is seen for a number of months. These data were analyzed for vertical spatial periods of 3, 4.5, 6, 9, 12, and 24 km. When plotted as a function of time of day, many of the phasors tended to show a net rotation. The sense of rotation of a spinning vector in the complex plane can be determined objectively by computing the signed area swept out by the vector in saving from point to point. This calculation, indicated downward motion in 8 out of 12 months for the 9-km component and in 11 out of 12 months for the 24-km component. A comparison of the magnitudes of the 6 modes showed that the primary component was the 24-km component, a result confirmed by the tidal models of Forbes. Author

N87-10442*# Illinois Univ., Urbana. Aeronomy Lab.
GRAVITY WAVES IN SEVERE WEATHER **c46**
S. A. Bowhill and S. Gnanalingam *In* International Council of Scientific Unions, Middle Atmosphere Program. Handbook for MAP, Vol. 20 Jun. 1986 8 p (For primary document see N87-10419 01-42)
Avail: NTIS HC A22/MF A01; also available from SCOSTEP Secretariat, Illinois Univ., 1406 West Green Street, Urbana, Ill. 61801 CSCL 04A

With a view to determining the role of severe weather in producing gravity waves, two tests were made. In the first, the wind speed measured at two nearby radiosonde stations, Peoria and Salem, was correlated with the stratosphere gravity-wave intensity at Urbana. Although the gravity-wave intensity fluctuated greatly from day to day, these is little if any correlation with the stratospheric wind speed. This suggests that orographic forcing is not a factor in generating gravity waves in Urbana. On the other hand, a clear correlation is found between cloud to heights exceeding 20,000 ft and an increased gravity-wave amplitude in the stratosphere. Author

N87-10443*# Alaska Univ., Fairbanks. Dept. of Physics.
SIMULTANEOUS ROCKET AND MST RADAR OBSERVATION OF AN INTERNAL GRAVITY WAVE BREAKING IN THE MESOSPHERE **c46**
Steven A. Smith, David C. Fritts, Ben B. Balsley (National Oceanic and Atmospheric Administration, Boulder, Colo.), and C. Russell Philbrick (Air Force Geophysics Lab., Hanscom AFB, Mass.) *In* International Council of Scientific Unions, Middle Atmosphere Program. Handbook for MAP, Vol. 20 Jun. 1986 11 p (For primary document see N87-10419 01-42)
Avail: NTIS HC A22/MF A01; also available from SCOSTEP Secretariat, Illinois Univ., 1406 West Green Street, Urbana, Ill. 61801 CSCL 04A

In June, 1983, the Structure and Atmospheric Turbulence Environment (STATE) rocket and Poker Flat Mesosphere-Stratosphere-Troposphere radar campaign was conducted to measure the interaction between turbulence, electron density and electron density gradient that has produced unusually strong MST radar echoes from the summer mesosphere over Poker Flat, Alaska. Analysis or radar wind measurements and a concurrent wind and temperature profile obtained from a rocket probe carrying a three-axis accelerometer are given. The two data sets provide a fairly complete (and in some cases, redundant) picture of the breaking (or more correctly, the saturation) of a large-amplitude, low-frequency, long-wavelength internal gravity wave. The data show that small-scale turbulence and small-scale wave intensity is greatest at those altitudes where the large-scale wave-induced temperature lapse rate is most negative or most nearly unstable, but the wind shear due to the large-scale wave is a minimum. A brief review of linear gravity-wave theory is presented as an aid to the identification of the gravity-wave signature in the radar and rocket data. Analysis of the time and height cross sections of wind speed and turbulence intensity observed by the Poker Flat MST radar follows. Then, the vertical profile of temperature and winds measured by a rocket probe examined. Finally, the use of the independent data sets provided by the rocket and the radar are discussed and implications for theories of wave saturation are presented. Author

N87-10444*# Clemson Univ., S.C. Dept. of Physics and Astronomy.
OBSERVATIONS OF THUNDER WITH THE ARECIBO VHF RADAR c46
D. N. Holden and M. F. Larsen *In* International Council of Scientific Unions, Middle Atmosphere Program. Handbook for MAP, Vol. 20 Jun. 1986 6 p (For primary document see N87-10419 01-42)
Avail: NTIS HC A22/MF A01; also available from SCOSTEP Secretariat, Illinois Univ., 1406 West Green Street, Urbana, Ill. 61801 CSCL 04A

An experiment was carried out at the Arecibo Observatory in Puerto Rico in August 1985 to study Doppler velocities in a thunderstorm environment with a beam pointed 2.5 degrees off-vertical. Researchers detected two types of echoes associated with lightning. The first was associated with scattering from the lightning channel itself and had characteristics similar to those observed previously with meteorological radars. The second appeared to be due to scattering from the turbulence organized by phase fronts of an acoustic wave generated by lightning. The observations were consistent with a wave traveling at a velocity near the speed of sound and having a vertical phase velocity component of 40 m/s. Author

N87-10445*# Centre National d'Etudes des Telecommunications, Saint Maur des Fosses (France).
THE PROUST RADAR: FIRST RESULTS c47
F. Bertin, A. Cremieu, M. Glass, M. Massebeuf, and M. Petitdidier *In* International Council of Scientific Unions, Middle Atmosphere Program. Handbook for MAP, Vol. 20 Jun. 1986 4 p (For primary document see N87-10419 01-42)
Avail: NTIS HC A22/MF A01; also available from SCOSTEP Secretariat, Illinois Univ., 1406 West Green Street, Urbana, Ill. 61801 CSCL 04B

Two campaigns took place in 1984 with the PROUST Radar operating in a bistatic mode, the transmitting antenna pointing at the vertical and the receiving one, 1 deg. off the vertical axis. The antenna beam intersection covers an altitude range between 3 and 9 km. The first of these campaigns are analyzed. The results analyzed show the capability of the PROUST Radar to measure the turbulent parameters and study the turbulence-wave interaction. In its present configuration (bistatic mode and 600 m vertical resolution), it has been necessary to make some assumptions that are known not to be truly fulfilled: homogeneous turbulence and constant vertical wind intensity over a 600-m thickness. It is clear that a more detailed study of the interaction between wave and turbulence will be possible with the next version of PROUST Radar (30-m altitude resolution and monostatic mode) that will soon be achieved. Author

N87-10446*# Centre National d'Etudes des Telecommunications, Saint Maur des Fosses (France).
SIMULTANEOUS FINE STRUCTURE OBSERVATION OF WIND AND TEMPERATURE PROFILES BY THE ARECIBO 430-MHz RADAR AND IN SITU MEASUREMENTS c47
D. Thomas, F. Bertin, M. Petitdidier, H. Teitelbaum (Ecole Polytechnique, Palaiseau, France), and R. F. Woodman (Instituto Geofisico del Peru, Lima) *In* International Council of Scientific Unions, Middle Atmosphere Program. Handbook for MAP, Vol. 20 Jun. 1986 3 p (For primary document see N87-10419 01-42)
Avail: NTIS HC A22/MF A01; also available from SCOSTEP Secretariat, Illinois Univ., 1406 West Green Street, Urbana, Ill. 61801 CSCL 04B

A simultaneous campaign of balloon and radar measurements took place on March 14 to 16, 1984, above the Arecibo 430-MHz radar. This radar was operating with a vertical resolution of 150 m following two antenna beam directions: 15 deg. from the zenith, respectively, in the N-S and E-W directions. The main results concerning the comparison between the flight and simultaneous radar measurements obtained on March 15, 1984 are analyzed. The radar return power profile (S/N ratio in dB) exhibits maxima which are generally well correlated with step-like structures in the potential temperature profile. These structures are generally considered as the consequence of the mixing processes induced by the turbulence. A good correlation appears in the altitude range 12.5 to 19 km between wind shears induced by a wave structure observed in the meridional wind and the radar echo power maxima. This wave structure is characterized by a vertical wavelength of about 2.5 km, and a period in the range 30 to 40 hours. These characteristics are deduced from the twice daily rawinsonde data launched from the San Juan Airport by the National Weather Service. These results pointed out an example of the interaction between wave and turbulence in the upper troposphere and lower stratosphere. Turbulent layers are observed at locations where wind shears related to an internal inertia-gravity wave are maxima. Author

N87-10447*# Centre National de la Recherche Scientifique, Verrieres-Le Buisson (France).
COMPARISON BETWEEN S. T. RADAR AND IN SITU BALLOON MEASUREMENTS c46
F. Dalaudier, J. Barat, F. Bertin (Centre National d'Etudes des Telecommunications, Saint Maur des Fosses, France), E. Brun (Toulon Univ., France), M. Crochet, and F. Cuq *In* International Council of Scientific Unions, Middle Atmosphere Program. Handbook for MAP, Vol. 20 Jun. 1986 6 p (For primary document see N87-10419 01-42)
Avail: NTIS HC A22/MF A01; also available from SCOSTEP Secretariat, Illinois Univ., 1406 West Green Street, Urbana, Ill. 61801 CSCL 04A

A campaign for simultaneous in situ and remote observation of both troposphere and stratosphere took place near Aire-sur-l'Adour (in southeastern France) on May 4, 1984. The aim of this campaign was a better understanding of the physics of radar echoes. The backscattered signal obtained with a stratosphere-troposphere radar both at the vertical and 15 deg. off vertical is compared with the velocity and temperature measurements made in the same region (about 10 km north of the radar site) by balloon-borne ionic anenometers and temperature sensors. In situ measurements clearly indicate that the temperature fluctuations are not always consistent with the standard turbulent theory. Nevertheless, the assumptions generally made (isotropy and turbulent field in k) and the classical formulation so derived for radar reflectivity are able to reproduce the shape of the radar return power profiles in oblique directions. Another significant result is the confirmation of the role played by the atmospheric stratification in the vertical echo power. It is important to develop these simultaneous in situ and remote experiments for a better description of the dynamical and thermal structure of the atmosphere and for a better understanding of the mechanisms governing clear-air radar reflectivity. Author

N87-10448*# National Oceanic and Atmospheric Administration, Boulder, Colo. Aeronomy Lab.
A STATISTICAL MODEL TO ESTIMATE REFRACTIVITY TURBULENCE STRUCTURE CONSTANT C SUB n SUP 2 IN THE FREE ATMOSPHERE c46
J. M. Warnock and T. E. VanZandt *In* International Council of Scientific Unions, Middle Atmosphere Program. Handbook for MAP, Vol. 20 Jun. 1986 2 p (For primary document see N87-10419 01-42)
Avail: NTIS HC A22/MF A01; also available from SCOSTEP Secretariat, Illinois Univ., 1406 West Green Street, Urbana, Ill. 61801 CSCL 04A

A computer program has been tested and documented (Warnock and VanZandt, 1985) that estimates mean values of the refractivity turbulence structure constant in the stable free atmosphere from standard National Weather Service balloon data or an equivalent data set. The program is based on the statistical model for the occurrence of turbulence developed by VanZandt et al. (1981). Height profiles of the estimated refractivity turbulence structure constant agree well with profiles measured by the Sunset radar with a height resolution of about 1 km. The program also estimates the energy dissipation rate (epsilon), but because of the lack of suitable observations of epsilon, the model for epsilon has not yet been evaluated sufficiently to be used in routine applications. Vertical profiles of the refractivity turbulence structure constant were compared with profiles measured by both radar and optical remote sensors and good agreement was found. However, at times the scintillometer measurements were less than both the radar and model values. Author

N87-10449*# Arecibo Ionospheric Observatory, Puerto Rico. Arecibo Observatory.

DETERMINATION OF THE BRUNT-VAISALA FREQUENCY FROM VERTICAL VELOCITY SPECTRA **c46**

Jurgen Rottger *In* International Council of Scientific Unions, Middle Atmosphere Program. Handbook for MAP, Vol. 20 Jun. 1986 5 p (For primary document see N87-10419 01-42)

Avail: NTIS HC A22/MF A01; also available from SCOSTEP Secretariat, Illinois Univ., 1406 West Green Street, Urbana, Ill. 61801 CSCL 04A

Recent work on the spectra of vertical velocity oscillations due to gravity waves in the troposphere, stratosphere and the mesosphere has revealed a typical feature which we call the Brunt-Vaisala cutoff. Several observers noticed a spectral peak near the Brunt-Vaisala frequency. This peak often is characterized by a very steep slope at the high frequency part, but a fairly shallow slope towards lower frequencies. Some example spectra of stratosphere observations are given. This distinct spectral shape (most clear at the upper height 22.5 km) can be explained by the fact that the vertical velocity amplitudes of atmospheric gravity waves increase with frequency up to their natural cutoff at the Brunt-Vaisala frequency. The measurement of the frequency of the peak in a vertical velocity spectrum was found to yield most directly the Brunt-Vaisala-frequency profile. Knowing the Brunt-Vaisala frequency profile, one can deduce the potential temperature profile, if one has a calibration temperature at one height. However, even the uncalibrated profile will be quite useful, e.g., to determine fronts (defined by temperature inversions) and the tropopause height. This method fails for superadiabatic lapse rates when the Brunt-Viasala frequency is imaginary. The application of this method will also be difficult when the wind velocity is too high, causing the Doppler effect to smear out the total spectrum and blur the Brunt-Vaisala cutoff. A similar deficiency will also appear if the gravity-wave distribution has a maximum in wind direction. Author

N87-10450*# Arecibo Ionospheric Observatory, Puerto Rico.

THE USE OF THE EXPERIMENTALLY DEDUCED BRUNT-VAISALA FREQUENCY AND TURBULENT VELOCITY FLUCTUATIONS TO ESTIMATE THE EDDY DIFFUSION COEFFICIENT **c46**

Jurgen Rottger *In* International Council of Scientific Unions, Middle Atmosphere Program. Handbook for MAP, Vol. 20 Jun. 1986 6 p (For primary document see N87-10419 01-42)

Avail: NTIS HC A22/MF A01; also available from SCOSTEP Secretariat, Illinois Univ., 1406 West Green Street, Urbana, Ill. 61801 CSCL 04A

The determination of the turbulent energy dissipation rate or the eddy diffusion coefficient from radar observations can be done through the turbulence refractive index structure constant, deduced from calibrated echo power measurements, or through the turbulent velocity fluctuations, deduced from the echo spectrum width. Besides the radar parameters, power and spectrum width, the first approach needs knowledge of profiles of temperature and electron density in the mesosphere and the fraction of the radar volume filled with turbulence. The latter approach needs knowledge of the temperature profile, namely, the Brunt-Vaisala frequency. The use of this latter approach is demonstrated. Author

N87-10451*# Arecibo Ionospheric Observatory, Puerto Rico.

THE RELATION OF GRAVITY WAVES AND TURBULENCE IN THE MESOSPHERE **c46**

Jurgen Rottger *In* International Council of Scientific Unions, Middle Atmosphere Program. Handbook for MAP, Vol. 20 Jun. 1986 5 p (For primary document see N87-10419 01-42)

Avail: NTIS HC A22/MF A01; also available from SCOSTEP Secretariat, Illinois Univ., 1406 West Green Street, Urbana, Ill. 61801 CSCL 04A

Since researchers couldn't prove that the mesospheric turbulence layers are generated by the simultaneously existing short-period gravity waves, they invoked other generation mechanisms than wave breaking. Possible mechanisms like lateral convection (Rottger 1980a), quasi-geostrophic flows at mesoscales (Lilly, 1983) or vortical modes of motion as seen in the ocean (Muller and Pujalet, 1984) could be candidates. Researchers are inclined to see a connection of these layers or laminae with very-long-period internal waves because of the periodicity in their vertical structure and their long mean persistency. Rottger (1980b) had proposed that such structures are due the modulation of the me an temperature and wind profiles by internal waves. The superposition of random or short-term wave-induced wind and temperature fluctuations with the background profile, modulated by very-long-period waves (quasi-inertia waves) then would yield the observed effects, and could explain the vertical periodicity, the long-term mean persistency as well as some short-term variability of their intensity. Author

N87-10452*# National Oceanic and Atmospheric Administration, Boulder, Colo. Aeronomy Lab.

CAN STOCHASTIC, DISSIPATIVE WAVE FIELDS BE TREATED AS RANDOM WALK GENERATORS **c46**

J. Weinstock *In* International Council of Scientific Unions, Middle Atmosphere Program. Handbook for MAP, Vol. 20 Jun. 1986 3 p (For primary document see N87-10419 01-42)

Avail: NTIS HC A22/MF A01; also available from SCOSTEP Secretariat, Illinois Univ., 1406 West Green Street, Urbana, Ill. 61801 CSCL 04A

A suggestion by Meek et al. (1985) that the gravity wave field be viewed as stochastic, with significant nonlinearities, is applied to calculate diffusivities. The purpose here is to calculate the diffusivity for stochastic wave model and compare it with previous diffusivity estimates. The researchers do this for an idealized case in which the wind velocity changes but slowly, and for which saturation is the principal mechanism by which wave energy is lost. A related calculation was given in a very brief way (Weinstock, 1976), but the approximations were not fully justified, nor were the physical pre-suppositions clearly explained. The observations of Meek et al. (1985) have clarified the pre-suppositions for the researchers and provided a rationalization and improvement of the approximations employed. Author

N87-10453*# Alaska Univ., Fairbanks. Geophysical Inst.

OBSERVATIONS AND A MODEL OF GRAVITY-WAVE VARIABILITY IN THE MIDDLE ATMOSPHERE **c46**

David C. Fritts and Robert A. Vincent (Adelaide Univ., Australia) *In* International Council of Scientific Unions, Middle Atmosphere Program. Handbook for MAP, Vol. 20 Jun. 1986 4 p (For primary document see N87-10419 01-42)

Avail: NTIS HC A22/MF A01; also available from SCOSTEP Secretariat, Illinois Univ., 1406 West Green Street, Urbana, Ill. 61801 CSCL 04A

A major goal was to determine what portion of the gravity-wave frequency spectrum accounted for the majority of the momentum flux and divergence, as this has important implications for the middle atmosphere response. It was found that approx. 70% of the total flux and divergence was due to wave motions with observed periods less than 1 hour, consistent with expectations based on the shape of the observed gravity-wave spectrum (Fritts, 1984). This dominance of the momentum flux and divergence by high-frequency motions implies a potential for the modulation of those quantities by large-amplitude motions at lower frequencies. A second, striking aspect of the velocity and momentum flux data is its dramatic diurnal variability, particularly at certain levels. This variability is illustrated with the momentum flux, computed in 8-hr blocks. The dominant contributions here are due to waves with periods less than 1 hr. The variability with height and size of the mean square velocity in the west beam and the momentum flux, energed over the 3-day period. A detailed analysis of the various tidal motions present during this data interval was performed, and it was determined that variations in the zontal wind profile imposed by the diurnal tidal motion are probably responsible for the modulation of the gravity-wave amplitudes and momentum fluxes. Author

N87-10454*# National Oceanic and Atmospheric Administration, Boulder, Colo. Aeronomy Lab.

CLIMATOLOGY OF GRAVITY WAVES OVER POKER FLAT, ALASKA FOR 1983 **c47**

Ben B. Balsley and Rene Garello (Ecole Nationale Superieure de Techniques Avancees, Paris, France) *In* International Council of Scientific Unions, Middle Atmosphere Program. Handbook for MAP, Vol. 20 Jun. 1986 2 p (For primary document see N87-10419 01-42)

Avail: NTIS HC A22/MF A01; also available from SCOSTEP Secretariat, Illinois Univ., 1406 West Green Street, Urbana, Ill. 61801 CSCL 04B

An analysis of short-period wind fluctuations over Poker Flat, Alaska, obtained using the Poker Flat mesosphere-stratosphere-troposphere radar is presented. Results are shown for the troposphere and lower stratosphere as well as for the upper mesosphere and lower thermosphere. Contours depict various levels of wind variance (m2s-2). These results pertain only to wind fluctuation periods lying between one and six hours. These particular fluctuations are generally considered to arise primarily from atmospheric gravity waves. Insofar as this is true, the figure thus describes a general climatology of gravity waves at high latitudes. Author

N87-10455*# National Oceanic and Atmospheric Administration, Boulder, Colo. Aeronomy Lab.

CLIMATOLOGY OF TROPOSPHERIC VERTICAL VELOCITY SPECTRA **c47**

W. L. Ecklund, K. S. Gage, B. B. Balsley, and D. A. Carter *In* International Council of Scientific Unions, Middle Atmosphere Program. Handbook for MAP, Vol. 20 Jun. 1986 2 p (For primary document see N87-10419 01-42)

Avail: NTIS HC A22/MF A01; also available from SCOSTEP Secretariat, Illinois Univ., 1406 West Green Street, Urbana, Ill. 61801 CSCL 04B

Vertical velocity power spectra obtained from Poker Flat, Alaska; Platteville, Colorado; Rhone Delta, France; and Ponape, East Caroline Islands using 50-MHz clear-air radars with vertical beams are given. The spectra were obtained by analyzing the quietest periods from the one-minute-resolution time series for each site. The lengths of available vertical records ranged from as long as 6 months at Poker Flat to about 1 month at Platteville. The quiet-time vertical velocity spectra are shown. Spectral period ranging from 2 minutes to 4 hours is shown on the abscissa and power spectral density is given on the ordinate. The Brunt-Vaisala (B-V) periods (determined from nearby sounding balloons) are indicated. All spectra (except the one from Platteville) exhibit a peak at periods slightly longer than the B-V period, are flat at longer periods, and fall rapidly at periods less than the B-V period. This behavior is expected for a spectrum of internal waves and is very similar to what is observed in the ocean (Eriksen, 1978). The spectral amplitudes vary by only a factor of 2 or 3 about the mean, and show that under quiet conditions vertical velocity spectra from the troposphere are very similar at widely different locations. Author

N87-10456*# Adelaide Univ. (Australia). Dept. of Physics

MESOSPHERIC GRAVITY-WAVE CLIMATOLOGY AT ADELAIDE **c46**

R. A. Vincent *In* International Council of Scientific Unions, Middle Atmosphere Program. Handbook for MAP, Vol. 20 Jun. 1986 1 p (For primary document see N87-10419 01-42)

Avail: NTIS HC A22/MF A01; also available from SCOSTEP Secretariat, Illinois Univ., 1406 West Green Street, Urbana, Ill. 61801 CSCL 04A

The MF Adelaide partial-reflection radar has been operating continuously since November 1983. This has enabled a climatology of gravity-wave activity to be constructed for the mesosphere. The data have been analyzed for a medium-period range of 1 to 8 hr. and a longer period range between 8 and 24 hr. covering the inertio-period waves. The tidal motions have been filtered out prior to analysis. For the data analyses so far (Nov. 1983 to Dec. 1984), a number of interesting features emerged. Firstly, the wave activity at heights above 80 km shows a small seimannual variation with season with the activity being strongest in summer and winter. At heights below 80 km however, there is a similar but more marked variation with the weakest amplitudes occurring at the time of the changeovers in the prevailing circulation. If breaking gravity waves are responsible for much of the turbulence in the mesosphere, then the periods March to April and September to October might also be expected to be periods of weak turbulence. The wave field appears to be partially polarized. The meridional amplitudes are larger than the zonal amplitudes, especially in water. It is found that the degree of polarization is about 15% in summer and 30% in winter. The polarized component is found to propagate in the opposite direction to the background flow in the stratosphere, which suggests that the polarization arises through directional filtering of the waves as they propagate up from below. Author

N87-10457*# Cologne Univ. (West Germany). Inst. for Geophysik und Meteorologie.

HORIZONTAL WIND PERTURBATIONS AND THEIR RELATION TO TRANSIENT INTERNAL GRAVITY WAVES **c46**

A. Ebel, A. H. Manson (Saskatchewan Univ., Saskatoon), and C. E. Meek *In* International Council of Scientific Unions, Middle Atmosphere Program. Handbook for MAP, Vol. 20 Jun. 1986 5 p (For primary document see N87-10419 01-42)

Avail: NTIS HC A22/MF A01; also available from SCOSTEP Secretariat, Illinois Univ., 1406 West Green Street, Urbana, Ill. 61801 CSCL 04A

Horizontal winds as measured with the Saskatoon MF radar exhibit wind fluctuations which have preferred directions toward north or south in the period range 0 to 60 min at heights between about 60 and 110 km. Longer period perturbations (approx 1-6 h) tend to have an additional maximum of direction frequencies in the E-W sector.The polarization effect analyzed for more than 6 years shows regular changes with season. The main features of the seasonal variations of the direction distributions can be explained by directional filtering of vertically propagating nonstationary gravity waves and appropriate changes of the wave source strength and position in the troposphere. The N-S polarization of the gravity-wave field appears to result in meridional wind reversals with height above the mesopause. Author

N87-10458*# Illinois Univ., Urbana-Champaign. Dept. of Electrical and Computer Engineering.

POSSIBILITY OF MEASURING GRAVITY-WAVE MOMENTUM FLUX BY SINGLE BEAM OBSERVATION OF MST RADAR **c46**

C. H. Liu *In* International Council of Scientific Unions, Middle Atmosphere Program. Handbook for MAP, Vol. 20 Jun. 1986 3 p (For primary document see N87-10419 01-42)

Avail: NTIS HC A22/MF A01; also available from SCOSTEP Secretariat, Illinois Univ., 1406 West Green Street, Urbana, Ill. 61801 CSCL 04A

Vincent and Reid (1983) proposed a technique to measure gravity-wave momentum fluxes in the atmosphere by mesosphere-stratosphere-troposphere (MST) radars using two or more radar beams. Since the vertical momentum fluxes are assumed to be due to gravity waves, it appears possible to make use of the dispersion and polarization relations for gravity waves in extracting useful information from the radar data. In particular, for an oblique radar beam, information about both the vertical and the horizontal velocities associated with the waves are contained in the measured Doppler data. Therefore, it should be possible to extract both V sub Z and V sub h from a single beam observational configuration. A procedure is proposed to perform such an analysis. The basic assumptions are: the measured velocity fluctuations are due to gravity waves and a separable model gravity-wave spectrum of the Garrett-Munk type that is statistically homogeneous in the horizontal plane. Analytical expressions can be derived that relate the observed velocity fluctuations to the wave momentum flux at each range gate. In practice, the uncertainties related to the model parameters and measurement accuracy will affect the results. A MST radar configuration is considered. Author

N87-10459*# Control Data Corp., Minneapolis, Minn.
PRELIMINARY ESTIMATES OF VERTICAL MOMENTUM FLUX **c46**
G. D. Nastrom and J. L. Green (National Oceanic and Atmospheric Administration, Boulder, Colo.) *In* International Council of Scientific Unions, Middle Atmosphere Program. Handbook for MAP, Vol. 20 Jun. 1986 5 p (For primary document see N87-10419 01-42)
Avail: NTIS HC A22/MF A01; also available from SCOSTEP Secretariat, Illinois Univ., 1406 West Green Street, Urbana, Ill. 61801 CSCL 04A

Preliminary results of themomentum flux and flux divergence during a transient episode, as a jet stream moved over the radar are given. The zonal and meridional momentum flux and flux divergences displayed remarkable continuity with altitude in time, increasing in intensity as lee waves and other gravity-wave activity developed while the jet stream approached. The momentum flux values observed compare favorably with aircraft measurements made over similar topography, at least during the early part of the day. The accelerations due to the momentum flux divergence seem rather large at first glance, especially for the late part of the day. However, there may be compensating forces due to effects not considered here, such as transverse circulations or, scales of motion to small to be resolved by these data. Author

N87-10460*# Illinois Univ., Urbana-Champaign. Dept. of Electrical and Computer Engineering.
EFFECTS OF ANISOTROPY ON THE FREQUENCY SPECTRUM OF GRAVITY WAVES OBSERVED BY MST RADAR **c46**
C. H. Liu *In* International Council of Scientific Unions, Middle Atmosphere Program. Handbook for MAP, Vol. 20 Jun. 1986 2 p (For primary document see N87-10419 01-42)
Avail: NTIS HC A22/MF A01; also available from SCOSTEP Secretariat, Illinois Univ., 1406 West Green Street, Urbana, Ill. 61801 CSCL 04A

In the investigation of gravity waves using mesosphere-stratosphere-troposphere radar data, model gravity-wave spectra have been used. In these model spectra, one usually assumes azimuthal symmetry. The effect of spectral anisotropy on the observed spectrum is studied here. It is shown that for a general Garrett-Munk-type spectrum, the anisotropy does not affect the frequency spectrum observed by the vertically beamed radar. For the oblique beam, however, the observed frequency spectrum is changed. A general gravity wave spectrum including azimuthal anisotropy is considered. Author

N87-10461*# Control Data Corp., Minneapolis, Minn.
THE FREQUENCY SPECTRUM OF C SUB n SUP 2 FROM MST RADAR DATA **c46**
G. D. Nastrom *In* International Council of Scientific Unions, Middle Atmosphere Program. Handbook for MAP, Vol. 20 Jun. 1986 5 p (For primary document see N87-10419 01-42)
Avail: NTIS HC A22/MF A01; also available from SCOSTEP Secretariat, Illinois Univ., 1406 West Green Street, Urbana, Ill. 61801 CSCL 04A

In a recent study (Nastrom et al., 1986), the variability of the refractivity turbulence structure constant, C sub n(2), was examined using observations from the stratosphere troposphere/mesosphere stratosphere troposphere (ST/MST) radar at Poker Flat, Alaska, and Platteville, Colorado. Variations of C2 with height, season, and weather conditions were examined. Also, the autocorrelation function and the frequency distribution of C sub n(2) were studied, and it was shown that C sub n(2), follows a log-normal frequency distribution. One of the more tentative results given in that paper is a first look at the spectrum of log C sub n(2), as a function of frequency at Poker Flat. This spectrum appears to obey a power law relation with frequency, P(F) approx. F(k), with k near -5/3 at periods between about 4 hours and 6 days, and with k near -1 at shorter periods. Power law behavior of a spectrum often helps us to infer the underlying dynamics which give rise to this spectrum, and it is thus of some concern to establish further confidence in the spectral shape. The purpose here is to address these questions. Author

N87-10462*# Case Western Reserve Univ., Cleveland, Ohio. Dept. of Elec. Engineering and Applied Physics.
A STUDY OF GRAVITY-WAVE SPECTRA IN THE TROPOSPHERE AND STRATOSPHERE AT 5-MIN TO 5-DAY PERIODS WITH THE POKER FLAT MST RADAR **c46**
R. S. Bemra, P. K. Rastogi, and B. B. Balsley (National Oceanic and Atmospheric Administration, Boulder, Colo.) *In* International Council of Scientific Unions, Middle Atmosphere Program. Handbook for MAP, Vol. 20 Jun. 1986 9 p (For primary document see N87-10419 01-42)
Avail: NTIS HC A22/MF A01; also available from SCOSTEP Secretariat, Illinois Univ., 1406 West Green Street, Urbana, Ill. 61801 CSCL 04A

An analysis of frequency spectra at periods of about 5 days to 5 min from two 20-day sets of velocity measurements in the stratosphere and troposphere region obtained with the Poker Flat mesosphere-stratosphere-troposphere (MST) radar during January and June, 1984 is presented. A technique based on median filtering and averaged order statistics for automatic editing, smoothing and spectral analysis of velocity time series contaminated with spurious data points or outliers is outlined. The validity of this technique and its effects on the inferred spectral index was tested through simulation. Spectra obtained with this technique are discussed. The measured spectral indices show variability with season and height, especially across the tropopause. The discussion briefly outlines the need for obtaining better climatologies of velocity spectra and for the refinements of the existing theories to explain their behavior. Author

N87-10463*# Arecibo Ionospheric Observatory, Puerto Rico.
ON THE VARYING SLOPE OF VELOCITY SPECTRA **c46**
Jurgen Rottger *In* International Council of Scientific Unions, Middle Atmosphere Program. Handbook for MAP, Vol. 20 Jun. 1986 3 p (For primary document see N87-10419 01-42)
Avail: NTIS HC A22/MF A01; also available from SCOSTEP Secretariat, Illinois Univ., 1406 West Green Street, Urbana, Ill. 61801 CSCL 04A

Spectra of zonal, meridional and vertical wind velocity, measured during a 24 hour period with the spaced-antenna technique indicate quite a variable slope as a function of height. It is found that the spectral slope (1h to 24h) of all three components correlates with the mean horizontal wind velocity. A possible conclusion is that the frequency dependence of power density of horizontal and vertical fluctuation component apparently depends on the mean wind velocity. However, the vertical spectra at periods larger than about 1 hour can also be influenced by spillover (due to finite radar antenna beam width) from the horizontal fluctuation component or by a Doppler shift. Author

N87-10464*# Illinois Univ., Urbana. Dept. of Electrical and Computer Engineering.
DOPPLER EFFECTS ON VELOCITY SPECTRA OBSERVED BY MST RADARS **c46**
A. O. Scheffler and C. H. Liu *In* International Council of Scientific Unions, Middle Atmosphere Program. Handbook for MAP, Vol. 20 Jun. 1986 3 p (For primary document see N87-10419 01-42)
Avail: NTIS HC A22/MF A01; also available from SCOSTEP Secretariat, Illinois Univ., 1406 West Green Street, Urbana, Ill. 61801 CSCL 04A

Recently, wind data from mesosphere-stratosphere-troposphere (MST) radars have been used to study the spectra of gravity waves in the atmosphere (Scheffler and Liu, 1985; VanZandt et al., 1985). Since MST radar measures the line-of-sight Doppler velocities, it senses the components of the wave-associated velocities along its beam directions. These components are related through the polarization relations which depend on the frequency and wave number of the wave. Therfore, the radar-observed velocity spectrum will be different from the original gravity-wave spectrum. Their relationship depends on the frequency and wave number of the wave as well as the propagation geometry.

This relation can be used to interpret the observed data. It can also be used to test the assumption of gravity-wave spectrum (Scheffler and Liu, 1985). In deriving this relation, the background atmosphere has been assumed to be motionless. Obviously, the Doppler shift due to the background wind will change the shape of the gravity-wave power spectrum as well as its relation with the radar-observed spectrum. Here, researcher's investigate these changes. Author

N87-10465*# Clemson Univ., S.C. Dept. of Physics and Astronomy.
OBSERVATIONS OF VERTICAL VELOCITY POWER SPECTRA WITH THE SOUSY VHF RADAR **c46**
M. F. Larsen, J. Rottger, and D. N. Holden *In* International Council of Scientific Unions, Middle Atmosphere Program. Handbook for MAP, Vol. 20 Jun. 1986 5 p (For primary document see N87-10419 01-42)
Avail: NTIS HC A22/MF A01; also available from SCOSTEP Secretariat, Illinois Univ., 1406 West Green Street, Urbana, Ill. 61801 CSCL 04A

A data set taken with the SOUSY VHF radar from October 28 to November 13, 1981 was used to calculate the power spectrum of the vertical velocities directly from the vertical beam measurements. The spectral slopes for the frequency spectra have been determined out to periods of several days and have been found to have values near -1 in the troposphere and shallower slopes in the lower stratosphere. The value of -1 is in agreement with the value found by Larsen et al. (1985) and Balsley and Carter (1982) in the range from a few minutes to 1 hr. Author

N87-10466*# Alaska Univ., Fairbanks. Geophysical Inst.
MESOSPHERIC WAVE NUMBER SPECTRA FROM POKER FLAT MST RADAR MEASUREMENTS COMPARED WITH GRAVITY-WAVE MODEL **c46**
Steven A. Smith, David C. Fritts, and Thomas E. VanZandt (National Oceanic and Atmospheric Administration, Boulder, Colo.) *In* International Council of Scientific Unions, Middle Atmosphere Program. Handbook for MAP, Vol. 20 Jun. 1986 8 p (For primary document see N87-10419 01-42)
Avail: NTIS HC A22/MF A01; also available from SCOSTEP Secretariat, Illinois Univ., 1406 West Green Street, Urbana, Ill. 61801 CSCL 04A

The results of a comparison of mesospheric wind fluctuation spectra computed from radial wind velocity estimates made by the Poker Flat mesosphere-stratosphere-troposphere (MST) radar are compared with a gravity-wave model developed by VanZandt (1982, 1985). The principal conclusion of this comparison is that gravity waves can account for 80% of the mesospheric power spectral density. Author

N87-10467*# Alaska Univ., Fairbanks. Geophysical Inst.
EVIDENCE OF A SATURATED GRAVITY-WAVE SPECTRUM THROUGHOUT THE ATMOSPHERE **c46**
David C. Fritts and Steven A. Smith (National Oceanic and Atmospheric Administration, Boulder, Colo.) *In* International Council of Scientific Unions, Middle Atmosphere Program. Handbook for MAP, Vol. 20 Jun. 1986 5 p (For primary document see N87-10419 01-42)
Avail: NTIS HC A22/MF A01; also available from SCOSTEP Secretariat, Illinois Univ., 1406 West Green Street, Urbana, Ill. 61801 CSCL 04A

The view adapted here is that the dominant mesoscale motions are due to internal gravity waves and show that previous and new vertical wave number spectra of horizontal winds are consistent with the notion of a saturation limit on wave amplitudes. It is also proposed that, at any height, only those vertical wave numbers m less than m sub asterisk are at saturation amplitudes, where m sub asterisk is the vertical wave number of the dominant energy-containing scale. Wave numbers m less than m sub asterisk are unsaturated, but experience growth with height due to the decrease of atmospheric density. The result is a saturated spectrum of gravity waves with both m sub asterisk decreasing and wave energy increasing with height. This saturation theory is consistent with a variety of atmospheric spectral observations and provides a basis for the notion of a universal spectrum of atmospheric gravity waves. Author

N87-10468*# Adelaide Univ. (Australia). Dept. of Physics.
INTERCOMPARISON AND CALIBRATION OF WIND AND WAVE MEASUREMENTS AT VARIOUS FREQUENCIES **c47**
R. A. Vincent *In* International Council of Scientific Unions, Middle Atmosphere Program. Handbook for MAP, Vol. 20 Jun. 1986 7 p (For primary document see N87-10419 01-42)
Avail: NTIS HC A22/MF A01; also available from SCOSTEP Secretariat, Illinois Univ., 1406 West Green Street, Urbana, Ill. 61801 CSCL 04B

Radars are increasingly being used for determinations of the small-scale wave and turbulence fields of the atmosphere. It is important to understand as fully as possible the likely sources of error or bias in radar velocity determinations. This is especially true for the determination of wave and turbulence parameters which often rely on the measurement of first or second order deviations from the prevailing wind and therefore require better precision and time resolution than is usually required for measurements of the mean winds alone. The intercomparison of velocity measurements made with different techniques (e.g., radar and balloon) can be expected to help determine not only the relative effectiveness of the different methods, but also the degree of reliability. Author

N87-10469*# Pennsylvania State Univ., University Park. Dept. of Meteorology.
AN EVALUATION OF ERRORS OBSERVED IN THE MEASUREMENT OF LOW WIND VELOCITIES **c47**
S. R. Williams and D. W. Thomson *In* International Council of Scientific Unions, Middle Atmosphere Program. Handbook for MAP, Vol. 20 Jun. 1986 7 p (For primary document see N87-10419 01-42)
Avail: NTIS HC A22/MF A01; also available from SCOSTEP Secretariat, Illinois Univ., 1406 West Green Street, Urbana, Ill. 61801 CSCL 04B

Measurements of low wind velocities (the absolute value of V sub H is approx. equal to 6 m/s) with a VHF wind profiler can be difficult if ground clutter or other biases in the system dominate in altering the position of the perceived peak in the calculated power spectrum. A variety of methods for ground clutter suppression are used in profiler systems today (Cornish, 1983). An editing method called zero suppression takes the spectral value of selectable number of points (N) on each side of 0 velocity (one point on either side, in this study) and sets them equal to the mean value of the points exterior to the specified N points on either side of 0. Analysis done with the PSU VHF(1) radar, shows that this zero-suppression method can systematically bias horizontal wings V sub H below 6 m/s. With the zero suppression, an artificial increase in absolute wind velocities occurs when the spectral peaks fall within the plus or minus N points of the FFT (personal communication, Strauch, 1985). It was also established that the method artificially decreases the absolute wind velocities inferred from spectral peaks that are outside but near the suppressed region. Comparisons of wind profiles observed with and without zero suppression are given. The range of the biased velocities extends to about plus or minus 6 m/s. Biases have been deduced to be as much as 2 m/s, but more commonly they are on the order of 1.0 m/s. Author

N87-10470*# National Oceanic and Atmospheric Administration, Boulder, Colo. Aeronomy Lab.
A COMPARISON OF VERTICAL VELOCITIES MEASURED FROM SPECULAR AND NONSPECULAR ECHOES BY A VHF RADAR **c46**
J. L. Green, W. L. Clark, J. M. Warnock, and G. D. Nastrom (Control Data Corp., Minneapolis, Minn.) *In* International Council of Scientific Unions, Middle Atmosphere Program. Handbook for MAP, Vol. 20 Jun. 1986 10 p (For primary document see N87-10419 01-42)
Avail: NTIS HC A22/MF A01; also available from SCOSTEP

Secretariat, Illinois Univ., 1406 West Green Street, Urbana, Ill. 61801 CSCL 04A

For a number of years, there have been doubts about the accuracy of vertical wind velocities measured with quasi-specular reflections from mesosphere-stratosphere-troposphere (MST) radar. The concern has been that the layers producing the quasi-specular reflection process this hypothetical tilt. Because of the quasi-specular reflection process, this hypothetical tilt would control the effective zenith angle of the radar antenna beam so that a small component of the horizontal velocity would be included in what was assumed to be a truly vertical beam. The purpose here is to test the hypothesis that there is an effect on the wind velocities measured on a vertical antenna beam due to a long-term tilting of the stable atmospheric layers that cause quasi-specular reflection. Gravity waves have been observed to cause short-term tilting of turbulent layers and specularly reflecting layers. In both cases, the effect was a wave-like deformation atmospheric layers with a period of a few minutes. This geometry is shown. Because of this influence of gravity waves, it was expected that there would be short-term variations in the vertical velocity. Author

N87-10471*# National Oceanic and Atmospheric Administration, Boulder, Colo.

METHODS FOR VERIFYING THE ACCURACY OF WIND PROFILES c47

R. C. Strauch *In* International Council of Scientific Unions, Middle Atmosphere Program. Handbook for MAP, Vol. 20 Jun. 1986 6 p (For primary document see N87-10419 01-42)

Avail: NTIS HC A22/MF A01; also available from SCOSTEP Secretariat, Illinois Univ., 1406 West Green Street, Urbana, Ill. 61801 CSCL 04B

Comparisons of radar-measured winds have been made with several types of measurements not only to verify radar data but also to seek a satisfactory comparison method. Three of the comparisons that have been made with Colorado Profiler radars are summarized. Radar measurements were compared with radiosonde measurements. Infrared lidar and 915 MHz radar were compared with radiosondes. A brief radar/radar comparison was made using the 50-MHz radar and a 3-cm wavelength meteorological Doppler radar during precipitation. R.J.F.

N87-10472*# Clemson Univ., S.C. Dept. of Physics and Astronomy.

A COMPARISON OF THUNDERSTORM REFLECTIVITIES MEASURED AT THE VHF AND UHF c47

M. F. Larsen and J. Rottger *In* International Council of Scientific Unions, Middle Atmosphere Program. Handbook for MAP, Vol. 20 Jun. 1986 9 p (For primary document see N87-10419 01-42)

Avail: NTIS HC A22/MF A01; also available from SCOSTEP Secretariat, Illinois Univ., 1406 West Green Street, Urbana, Ill. 61801 CSCL 04B

Observations of thunderstorms made with two radars operating at different wavelengths of 70 cm and 5.67 m are compared. The first set of observations was made with the UHF radar at the Arecibo Observatory in Puerto Rico, and the second set was made with the Max-Planck-Institut fur Aeronomie VHF radar in the Harz Mountains in West Germany. Both sets of observations show large echo strengths in the convective region above the -10 C isothem. At UHF, there appears to be a contribution from both the precipitation echoes and the normal echoes due to scatter from turbulent variations in the refractive index. Author

N87-10473*# Clemson Univ., S.C. Dept. of Physics and Astronomy.

UHF AND VHF RADAR OBSERVATIONS OF THUNDERSTORMS c47

D. N. Holden, C. W. Ulbrich, M. F. Larsen, J. Rottger (Arecibo Ionospheric Observatory, Puerto Rico), H. M. Ierkic, and W. Swartz (Cornell Univ., Ithaca, N.Y.) *In* International Council of Scientific Unions, Middle Atmosphere Program. Handbook for MAP, Vol. 20 Jun. 1986 5 p (For primary document see N87-10419 01-42)

Avail: NTIS HC A22/MF A01; also available from SCOSTEP Secretariat, Illinois Univ., 1406 West Green Street, Urbana, Ill. 61801 CSCL 04B

A study of thunderstorms was made in the Summer of 1985 with the 430-MHz and 50-MHz radars at the Arecibo Observatory in Puerto Rico. Both radars use the 300-meter dish, which gives a beam width of less than 2 degrees even at these long wavelengths. Though the radars are steerable, only vertical beams were used in this experiment. The height resolution was 300 and 150 meters for the UHF and VHF, respectively. Lightning echoes, as well as returns from precipitation and clear-air turbulence were detected with both wavelengths. Large increases in the returned power were found to be coincident with increasing downward vertical velocities at UHF, whereas at VHF the total power returned was relatively constant during the life of a storm. This was attributed to the fact that the VHF is more sensitive to scattering from the turbulence-induced inhomogeneities in the refractive index and less sensitive to scatter from precipitation particles. On occasion, the shape of the Doppler spectra was observed to change with the occurrence of a lightning discharge in the pulse volume. Though the total power and mean reflectivity weighted Doppler velocity changed little during these events, the power is Doppler frequency bins near that corresponding to the updraft did increase substantially within a fraction of a second after a discharge was detected in the beam. This suggests some interaction between precipitation and lightning. Author

N87-10474*# Saskatchewan Univ., Saskatoon. Inst. of Space and Atmospheric Studies.

COMPARISON OF MEDIUM FREQUENCY PULSED RADAR INTERFEROMETER AND CORRELATION ANALYSIS WINDS, PART 1 c35

C. E. Meek, I. M. Reid, and A. H. Manson *In* International Council of Scientific Unions, Middle Atmosphere Program. Handbook for MAP, Vol. 20 Jun. 1986 6 p (For primary document see N87-10419 01-42)

Avail: NTIS HC A22/MF A01; also available from SCOSTEP Secretariat, Illinois Univ., 1406 West Green Street, Urbana, Ill. 61801 CSCL 14B

In principle, the interferometer analysis determines the radial velocity and direction of single scatterers provided that each has a sufficiently different Doppler frequency to permit separation by spectral analysis. In fact, scatterers will not have constant radial velocity, and their Doppler frequencies as well as their directions will be modulated by their horizontal motion. Thus, there is a tradeoff between the poorer resolution but less smeared scatterers on shorter records and the higher resolution (longer) records. Three or more non-collinear scatterers are sufficient to determine the wind. It appears that the velocity found from the combined interferometer peaks agrees well with the apparent velocity from correlation methods, but the true velocity is a factor of 2 smaller. This difference might be resolved by searching for scatters showing regular movement between adjacent records. Author

N87-10475*# Saskatchewan Univ., Saskatoon. Inst. of Space and Atmospheric Studies.

COMPARISON OF MEDIUM FREQUENCY PULSED RADAR INTERFEROMETER AND CORRELATION ANALYSIS WINDS, PART 2 c35

C. E. Meek, I. M. Reid, and A. H. Manson *In* International Council of Scientific Unions, Middle Atmosphere Program. Handbook for MAP, Vol. 20 Jun. 1986 4 p (For primary document see N87-10419 01-42)

Avail: NTIS HC A22/MF A01; also available from SCOSTEP Secretariat, Illinois Univ., 1406 West Green Street, Urbana, Ill. 61801 CSCL 14B

In order to test whether the chosen Doppler peaks represent localized scatters in motion, as opposed to some sort of integrated composite, an attempt was made to determine the change in position of single scatterers over a series of sequential records. A four-antenna system was employed which had 1 degree of freedom in phase. Due to limitations N-S linear transmission and E-W linear reception were used. The Doppler frequency peak selection criteria were that at least two of the four power spectra should have a local peak, and that normalized phase discrepancy, should be less than 0.3. The lack of success in tracking individual scatters seems to suggest a short lifetime. If this is the case, then the present experiment is not able to resolve the difference found between the correlation analysis true velocity and the interferometer value. On the other hand, it appears that the interferometer may be of some use in tracking waves. B.G.

N87-10476*# Utah State Univ., Logan. Center for Atmospheric and Space Sciences.
MESOSPHERIC WIND MEASUREMENTS USING A MEDIUM-FREQUENCY IMAGING DOPPLER INTERFEROMETER c46
G. W. Adams and J. W. Brosnahan (Tycho Technology, Inc., Boulder, Colo.) *In* International Council of Scientific Unions, Middle Atmosphere Program. Handbook for MAP, Vol. 20 Jun. 1986 4 p (For primary document see N87-10419 01-42)
Avail: NTIS HC A22/MF A01; also available from SCOSTEP Secretariat, Illinois Univ., 1406 West Green Street, Urbana, Ill. 61801 CSCL 04A

Wind results from a medium-frequency radar operated as an imaging Doppler interferometer are presented. Ten independent antennas, together with mesospheric wind motions, were used to Doppler-sort and then echo-locate individual scattering points. The three-dimensional location and radial velocity of each discrete scattering point was determined. Mean winds were then determined by a least squares fit to the radial velocities of the ensemble of scatterers. B.G.

N87-10477*# Arecibo Ionospheric Observatory, Puerto Rico.
COMPARISON OF REFLECTIVITY AND WIND PROFILES MEASURED ON 46.8 MHz AND 430 MHz AT THE ARECIBO OBSERVATORY c47
Jurgen Rottger *In* International Council of Scientific Unions, Middle Atmosphere Program. Handbook for MAP, Vol. 20 Jun. 1986 2 p (For primary document see N87-10419 01-42)
Avail: NTIS HC A22/MF A01; also available from SCOSTEP Secretariat, Illinois Univ., 1406 West Green Street, Urbana, Ill. 61801 CSCL 04B

Comparisons of troposphere and stratosphere radar experiments at ultrahigh frequency (UHF) and very high frequency (VHF) were done at the Arecibo Observatory in April 1980 with the 430 MHz and 46.8 MHz radar. The velocity profiles measured on both frequencies with the Doppler beam swinging mode were compared. In general, the velocity profiles were equivalent. The VHF profile, however, shows more fluctuations with height than the UHF profile, although the latter was recorded with 150 m resolution instead of 300 m resolution on VHF. B.G.

N87-10478*# Arecibo Ionospheric Observatory, Puerto Rico.
MST RADAR NETWORKS AND CAMPAIGNS SESSION SUMMARY AND RECOMMENDATIONS c46
Jurgen Rottger *In* International Council of Scientific Unions, Middle Atmosphere Program. Handbook for MAP, Vol. 20 Jun. 1986 1 p (For primary document see N87-10419 01-42)
Avail: NTIS HC A22/MF A01; also available from SCOSTEP Secretariat, Illinois Univ., 1406 West Green Street, Urbana, Ill. 61801 CSCL 04A

Topics addressed included: determination of sources of propagation and dissipation of atmospheric disturbances and waves; measurement parameters; comparison of different method and instruments; suitable combinations of instruments; information exchange; and training courses. B.G.

N87-10479*# Illinois Univ., Urbana. Dept. of Electrical and Computer Engineering.
AN ANALYSIS AT MESOSPHERIC COHERENT-SCATTER POWER ENHANCEMENTS DURING SOLAR FLARE EVENTS c92
J. Parker and S. A. Bowhill *In* International Council of Scientific Unions, Middle Atmosphere Program. Handbook for MAP, Vol. 20 Jun. 1986 7 p (For primary document see N87-10419 01-42)
Avail: NTIS HC A22/MF A01; also available from SCOSTEP Secretariat, Illinois Univ., 1406 West Green Street, Urbana, Ill. 61801 CSCL 03B

Solar flares produce increases in coherent-scatter power from the mesosphere due to the increase in free electrons produced by X-ray photoionization. Thirteen such power enhancements were observed at Urbana. When such an enhancement occurs at an altitude containing a turbulence layer with constant strength, the relative enhancement of electon density is estimated from the enhancement in power. Such estimates of enchanced electron density are compared with estimates of the X-ray photoionization at that altitude, deduced from geostationary satellite measurements. It is found that possible types ion-chemical reaction scheme may be distinguished, and the nonflare ion-pair production function may be estimated. The type of ion-chemical scheme and the nonflare ion-production function are shown to depend on the solar zenith angle. Author

N87-10480*# Centre National d'Etudes des Telecommunications, Saint Maur des Fosses (France).
SCIENTIFIC REASONS FOR A NETWORK OF ST RADARS AND COOPERATIVE CAMPAIGNS c46
M. Petitdidier and M. Crochet (Toulon Univ., France) *In* International Council of Scientific Unions, Middle Atmosphere Program. Handbook for MAP, Vol. 20 Jun. 1986 6 p (For primary document see N87-10419 01-42)
Avail: NTIS HC A22/MF A01; also available from SCOSTEP Secretariat, Illinois Univ., 1406 West Green Street, Urbana, Ill. 61801 CSCL 04A

Due to their capabilities of measuring wind profiles in the troposphere and stratosphere with good time and height resolution, whatever the weather conditions, stratosphere-troposphere (ST) radars are well adapted to carry out atmospheric research in many fields as well as to fulfill the meteorological forecasting needs. Examples are presented from previous and future national or international campaigns planned in France. The ST radars were used first by themselves with the adjunction of radiosonde data. Then networks were built and used to get horizontal parameters. It appears that ST radar networks should naturally be included in cooperative campaigns. B.G.

N87-10481*# National Oceanic and Atmospheric Administration, Boulder, Colo.
PROGRESS IN EXISTING AND PLANNED MST RADARS c46
T. E. VanZandt *In* International Council of Scientific Unions, Middle Atmosphere Program. Handbook for MAP, Vol. 20 Jun. 1986 3 p (For primary document see N87-10419 01-42)
Avail: NTIS HC A22/MF A01; also available from SCOSTEP Secretariat, Illinois Univ., 1406 West Green Street, Urbana, Ill. 61801 CSCL 04A

Radar systems are described which use two different wind measuring techniques: the partial-reflection drift technique and the mesosphere-stratosphere-troposphere (MST) or Doppler beam-swing radar technique. The advantages and disadvantages of each technique are discussed. B.G.

N87-10482*# National Oceanic and Atmospheric Administration, Boulder, Colo. Aeronomy Lab.
THE PROPOSED FLATLAND RADAR c32
J. L. Green, K. S. Gage, T. E. VanZandt, and G. D. Nastrom *In* International Council of Scientific Unions, Middle Atmosphere Program. Handbook for MAP, Vol. 20 Jun. 1986 5 p (For primary document see N87-10419 01-42)
Avail: NTIS HC A22/MF A01; also available from SCOSTEP Secretariat, Illinois Univ., 1406 West Green Street, Urbana, Ill. 61801 CSCL 17I

A flexible very high frequency (VHF) stratosphere-troposphere (ST) radar configured for meteorological research is to be constructed near Urbana, Illinois. Measurement of small vertical velocities associated with synoptic-scale meteorology can be performed. A large Doppler microwave radar (CHILL) is located a few km from the site of the proposed ST radar. Since the microwave radar can measure the location and velocity of hydrometeors and the VHF ST radar can measure clear (or cloudy) air velocities, simultaneous observations by these two radars of stratiform or convective weather systems would provide valuable meteorological information. B.G.

N87-10483*# National Oceanic and Atmospheric Administration, Boulder, Colo. Aeronomy Lab.
CURRENT STATUS OF THE POKER FLAT MST RADAR c32
B. B. Balsley *In* International Council of Scientific Unions, Middle Atmosphere Program. Handbook for MAP, Vol. 20 Jun. 1986 1 p (For primary document see N87-10419 01-42)
Avail: NTIS HC A22/MF A01; also available from SCOSTEP Secretariat, Illinois Univ., 1406 West Green Street, Urbana, Ill. 61801 CSCL 17I

The change of the Poker Flat, Alaska, Mesosphere-Stratosphere (MST) radar to a configuration to measure gravity-wave momentum flux is discussed. B.G.

N87-10484*# National Oceanic and Atmospheric Administration, Boulder, Colo. Aeronomy Lab.
CONTINUOUS WIND MEASUREMENT IN THE TROPICAL PACIFIC USING VHF RADARS c47
B. B. Balsley, W. L. Ecklund, and D. A. Carter *In* International Council of Scientific Unions, Middle Atmosphere Program. Handbook for MAP, Vol. 20 Jun. 1986 1 p (For primary document see N87-10419 01-42)
Avail: NTIS HC A22/MF A01; also available from SCOSTEP Secretariat, Illinois Univ., 1406 West Green Street, Urbana, Ill. 61801 CSCL 04B

Very High Frequency (VHF) Radar Wind Profilers are being installed on Ponape, East Caroline Islands and Christmas Island, Republic of Kiribati to continuously monitor winds aloft. The purpose of this experiment is to study wind fluctuations on time scales between minutes and days, to determine the longitudinal character of these fluctuations, and to examine their relationship to climate variability. Six-hourly wind profiles will be provided via satellite to the scientific community for Project TOGA (Tropical Ocean Global Atmosphere). B.G.

N87-10485*# Illinois Univ., Urbana. Aeronomy Lab.
RECENT PROGRESS IN THE URBANA MST RADAR c32
S. A. Bowhill *In* International Council of Scientific Unions, Middle Atmosphere Program. Handbook for MAP, Vol. 20 Jun. 1986 1 p (For primary document see N87-10419 01-42)
Avail: NTIS HC A22/MF A01; also available from SCOSTEP Secretariat, Illinois Univ., 1406 West Green Street, Urbana, Ill. 61801 CSCL 17I

The Urbana radar, which operates at 40.92 MHz with a peak power of about 1.2 MW into a 100 x 120 m phased array antenna was improved. An accelerated data-acquisition system, a beam-steering system, and a transmit/receive switch were installed. With these changes, the radar is in regular operations for two hours every day around local noon gathering stratospheric and mesospheric data. Special campaigns are mounted in addition under severe weather conditions. B.G.

N87-10486*# National Oceanic and Atmospheric Administration, Boulder, Colo.
COLORADO WIND PROFILERS c47
R. G. Strauch *In* International Council of Scientific Unions, Middle Atmosphere Program. Handbook for MAP, Vol. 20 Jun. 1986 2 p (For primary document see N87-10419 01-42)
Avail: NTIS HC A22/MF A01; also available from SCOSTEP Secretariat, Illinois Univ., 1406 West Green Street, Urbana, Ill. 61801 CSCL 04B

The Wave Propagation Laboratory (WPL) has operated a network of wind profiling radars in Colorado. The current configuration of the network is described. All radars operate continuously and unattended to supply hourly-averaged wind profiles to a central computer in Boulder in real time. The hardware and software changes made to improve reliability are discussed. This research network will continue to be used to provide wind profiles for operational and research meteorologists and the performance of various wavelength systems will be evaluated. B.G.

N87-10487*# National Oceanic and Atmospheric Administration, Boulder, Colo.
WIND PROFILER DEMONSTRATION SYSTEM c47
R. B. Chadwick *In* International Council of Scientific Unions, Middle Atmosphere Program. Handbook for MAP, Vol. 20 Jun. 1986 2 p (For primary document see N87-10419 01-42)
Avail: NTIS HC A22/MF A01; also available from SCOSTEP Secretariat, Illinois Univ., 1406 West Green Street, Urbana, Ill. 61801 CSCL 04B

The National Oceanic and Atmospheric Administration (NOAA) has started procurement of a 30-station demonstration network of Doppler radar wind profilers to be deployed in the central United States by 1989. The purposes of this demonstration network are: (1) to assess the impact of a large wind profiler network on meteorological forecasting; (2) to test wind profiler hardware designed specifically for commercial production and widespread deployment; and (3) to provide wind data for research programs involving weather phenomena in the central United States. B.G.

N87-10488*# Radio Research Labs., Tokyo (Japan).
REMOTE TEMPERATURE PROFILING IN THE TROPOSPHERE AND STRATOSPHERE BY THE RADIO-ACOUSTIC SOUNDING TECHNIQUE c46
Nobuo Matuura, Yoshihisa Masuda, and Hisao Inuki *In* International Council of Scientific Unions, Middle Atmosphere Program. Handbook for MAP, Vol. 20 Jun. 1986 1 p (For primary document see N87-10419 01-42)
Avail: NTIS HC A22/MF A01; also available from SCOSTEP Secretariat, Illinois Univ., 1406 West Green Street, Urbana, Ill. 61801 CSCL 04A

Radar application of the radio-acoustic sounding technique uses the Doppler frequency shift of radar echoes returning from the atmospheric wave structure, in association with a traveling acoustic pulse transmitted from the ground, to determine the speed of sound, and hence the atmospheric temperature, as a function of altitude. Temperature measurement in the troposphere and stratosphere were determined using the radio-acoustic sounding technique with the Radio-Acoustic Sounding System (RASS). Successful experiments were performed in March 1985, and in August 1985. B.G.

N87-10489*# Pennsylvania State Univ., University Park. Dept. of Meteorology.
THE PENN STATE DOPPLER NETWORK PROGRESS REPORT c32
S. R. Williams and R. Peters *In* International Council of Scientific Unions, Middle Atmosphere Program. Handbook for MAP, Vol. 20 Jun. 1986 3 p (For primary document see N87-10419 01-42)
Avail: NTIS HC A22/MF A01; also available from SCOSTEP Secretariat, Illinois Univ., 1406 West Green Street, Urbana, Ill. 61801 CSCL 17I

The software and hardware implementation for the Penn State University network were discussed. Delayed delivery of radio frequency equipment and signal processing components resulted in modification of the original timetables. It was determined that the best approach for implementing the second very high frequency (VHF) would be when the VHF radar was in reliable and unattended operation. A short summary of the specifications for the three radars is presented. B.G.

N87-10490*# Adelaide Univ. (Australia). Dept. of Physics.
THE ADELAIDE MF PARTIAL-REFLECTION RADAR AND VHF ST RADAR Progress Report c32
R. A. Vincent *In* International Council of Scientific Unions, Middle Atmosphere Program. Handbook for MAP, Vol. 20 Jun. 1986 1 p (For primary document see N87-10419 01-42)
Avail: NTIS HC A22/MF A01; also available from SCOSTEP Secretariat, Illinois Univ., 1406 West Green Street, Urbana, Ill. 61801 CSCL 17I

The microwave frequency (MF) partial-reflection radar ran continuously since November 1983, with data being analyzed in real time. The spaced antenna technique was used routinely to produce a climatology of the mean circulation, atmospheric tides, and gravity waves. Since the beginning of 1985, the system was also used as a Doppler radar to measure the spectral widths of the mesospheric echoes. This has enabled the turbulence dissipation rates to be determined. The Stratosphere-Troposphere (ST) radar was operated in the spaced antenna mode to measure winds in November 1984, in conjunction with a cooperative campaign to study the propagation of cold fronts across SE Australia. Observations were also performed to study the structure of the more intense and deeper cold fronts, which occur in late winter. B.G.

N87-10491*# Centre de Recherches en Physique de l'Environnement, Saint Maur des Fosses (France).
THE PROUST RADAR **c32**
F. Bertin, M. Glass, R. Ney, and M. Petitdidier *In* International Council of Scientific Unions, Middle Atmosphere Program. Handbook for MAP, Vol. 20 Jun. 1986 3 p (For primary document see N87-10419 01-42)
Avail: NTIS HC A22/MF A01; also available from SCOSTEP Secretariat, Illinois Univ., 1406 West Green Street, Urbana, Ill. 61801 CSCL 17I

The Stratosphere-Troposphere (ST) radar called PROUST works at 935 MHz using the same klystron and antenna as the coherent-scatter radar. The use of this equipment for ST work has required some important modifications of the transmitting system and the development of receiving, data processing and acquisition (1984,1985) equipment. The modifications are discussed. B.G.

N87-10492*# Toulon Univ. (France). Lab. de Sondages Electromagnetiques.
THE PROVENCE ST RADAR **c32**
M. Crochet *In* International Council of Scientific Unions, Middle Atmosphere Program. Handbook for MAP, Vol. 20 Jun. 1986 1 p (For primary document see N87-10419 01-42)
Avail: NTIS HC A22/MF A01; also available from SCOSTEP Secretariat, Illinois Univ., 1406 West Green Street, Urbana, Ill. 61801 CSCL 17I

Since the Alpex Campaign, when 3 Stratosphere-Troposphere (ST) radar operated in Camarque as a cooperative effort of the Aeronomy Laboratory of NOAA, CO, and LSEET from Toulon, a 50 MHz Very High Frequency (VHF) ST radar was developed, improved, and tested. The operating characteristics, main objectives, preliminary results, and future experiment costs of the VHF ST radar are discussed. B.G.

N87-10493*# CNRM, Toulouse (France).
THE INSU AND DMN NETWORK OF ST RADARS **c32**
M. Petitdidier (Centre de Recherches en Physique de l'Environnement, Saint Maur des Fosses, France), V. Klaus, F. Baudin (Centre de Recherches en Physique de l'Environnement, Issy-les-Moulineaux, France), M. Crochet (Toulon Univ., France), G. Penazzi (Centre de Recherches en Physique de l'Environnement, Saint Maur des Fosses, France), and P. Quinty *In* International Council of Scientific Unions, Middle Atmosphere Program. Handbook for MAP, Vol. 20 Jun. 1986 2 p (For primary document see N87-10419 01-42)
Avail: NTIS HC A22/MF A01; also available from SCOSTEP Secretariat, Illinois Univ., 1406 West Green Street, Urbana, Ill. 61801 CSCL 17I

Due to their capabilities of measuring wind profiles with good time and height resolution, Stratosphere-Troposphere (ST) are well adapted to carry out atmospheric research. In France, a Very High Frequency (VHF) and an Ultrahigh Frequency (UHF) ST radar are working for research purposes. The INSU (Institut National des Sciences de l'Univers) and the DMN (Direction de la Meteorologie Nationale) networks are discussed. B.G.

N87-10494*# Arecibo Ionospheric Observatory, Puerto Rico.
INVESTIGATIONS OF THE LOWER AND MIDDLE ATMOSPHERE AT THE ARECIBO OBSERVATORY AND A DESCRIPTION OF THE NEW VHF RADAR PROJECT **c46**
J. Rottger, H. M. Ierkic, R. K. Zimmerman, and J. Hagen *In* International Council of Scientific Unions, Middle Atmosphere Program. Handbook for MAP, Vol. 20 Jun. 1986 10 p (For primary document see N87-10419 01-42)
Avail: NTIS HC A22/MF A01; also available from SCOSTEP Secretariat, Illinois Univ., 1406 West Green Street, Urbana, Ill. 61801 CSCL 04A

The atmospheric science research at the Arecibo Observatory is performed by means of (active) radar methods and (passive) optical methods. The active methods utilize the 430 NHz radar, the S-band radar on 2380 MHz, and a recently constructed Very High Frequency (VHF) radar. The passive methods include measurements of the mesopause temperature by observing the rotational emissions from OH-bands. The VHF radar design is discussed. B.G.

N87-10495*# National Central Univ., Chung-Li (Taiwan).
THE FIRST OPERATION AND RESULTS OF THE CHUNG-LI VHF RADAR **c32**
J. K. Chao, F. S. Kuo, Y. S. Chu, I. J. Fu, J. Rottger (Arecibo Ionospheric Observatory, Puerto Rico), and C. H. Liu (Illinois Univ., Urbana) *In* International Council of Scientific Unions, Middle Atmosphere Program. Handbook for MAP, Vol. 20 Jun. 1986 5 p (For primary document see N87-10419 01-42)
Avail: NTIS HC A22/MF A01; also available from SCOSTEP Secretariat, Illinois Univ., 1406 West Green Street, Urbana, Ill. 61801 CSCL 17I

The Chung-Li Very High Frequency (VHF) radar is used in the dual-mode operations, applying Doppler beam-swinging as well as the spaced-antenna-drift method. The design of the VHF radar is examined. Results of performance tests are discussed. B.G.

N87-10496*# Saskatchewan Univ., Saskatoon. Dept. of Physics.
PROGRESS IN THE MF RADAR SYSTEM AT SASKATOON **c32**
C. E. Meek and A. H. Manson *In* International Council of Scientific Unions, Middle Atmosphere Program. Handbook for MAP, Vol. 20 Jun. 1986 4 p (For primary document see N87-10419 01-42)
Avail: NTIS HC A22/MF A01; also available from SCOSTEP Secretariat, Illinois Univ., 1406 West Green Street, Urbana, Ill. 61801 CSCL 17I

Two improvements were made to the radar system in the last year, one was the addition of O/X mode capability to the full antenna array used in the real-time wind system, and the other was the development of a coherent receiver. The design of the transmitter antenna is examined. The proposed coherent real-time wind system is also discussed. B.G.

N87-10497*# Indian Space Research Organization, Bangalore.
SYSTEM ASPECTS OF THE INDIAN MST RADAR FACILITY **c32**
G. Viswanathan *In* International Council of Scientific Unions, Middle Atmosphere Program. Handbook for MAP, Vol. 20 Jun. 1986 6 p (For primary document see N87-10419 01-42)
Avail: NTIS HC A22/MF A01; also available from SCOSTEP Secretariat, Illinois Univ., 1406 West Green Street, Urbana, Ill. 61801 CSCL 17I

One of the major objectives of the Indian Middle Atmosphere Program is to investigate the motions of the middle atmosphere on temporal and spatial scales and the interaction between the three height regions of the middle atmosphere. Realizing the fact that radar technique has proven to be a very powerful tool for the study of Earth atmosphere, the Indian Middle Atmosphere Program has recommended establishing a mesosphere-stratosphere-troposphere (MST) radar as a national facility for atmospheric research. The major landmarks in this attempt to setup the MST radar as a national facility are described. Author

N87-10498*# Uppsala Ionospheric Observatory (Sweden).
HISCAT: A PROPOSED NEW SCATTER FACILITY IN NORTHERN SCANDINAVIA **c14**
R. Bostrom and B. Thide *In* International Council of Scientific

Unions, Middle Atmosphere Program. Handbook for MAP, Vol. 20 Jun. 1986 1 p (For primary document see N87-10419 01-42)
Avail: NTIS HC A22/MF A01; also available from SCOSTEP Secretariat, Illinois Univ., 1406 West Green Street, Urbana, Ill. 61801 CSCL 14B

It is proposed that a new versatile ionospheric and atmospheric scatter radar be constructed in northern Scandavia through a multinational collaborative effort. The new facility tentatively named HISCAT (High frequency, High power, High latitude, Heating and Ionospheric Scatter facility), should be used for scientific investigations of: the physics of the neutral (middle) atmosphere; fundamental plasma phenomena, natural or artificially induced in the ionosphere; electrodynamic conditions at high altitudes above the auroral region and in the polar cap ionosphere; plasma waves in the solar atmosphere. The system should thus be able to operate as a mesosphere-stratosphere-troposphere (MST) radar, a so-called ionospheric modification facility, incoherent-scatter radar, coherent-scatter radar, and solar radar. Basically, the new facility should be a device that can operate simultaneously on several frequencies in the frequency range 5 to 50 MHz not covered by other instruments. It should comprise: powerful transmitters, capable of delivering a total average power of several megawatts; an advanced phased antenna array of high gain forming one or two steerable and well collimated beams; and an advanced data collection and analysis system. Author

N87-10499*# National Oceanic and Atmospheric Administration, Boulder, Colo. Aeronomy Lab.
PHASED-ARRAY DESIGN FOR MST AND ST RADARS c32
W. L. Ecklund *In* International Council of Scientific Unions, Middle Atmosphere Program. Handbook for MAP, Vol. 20 Jun. 1986 2 p (For primary document see N87-10419 01-42)
Avail: NTIS HC A22/MF A01; also available from SCOSTEP Secretariat, Illinois Univ., 1406 West Green Street, Urbana, Ill. 61801 CSCL 17I

All of the existing radar systems fully dedicated to clear-air radar studies use some type of phased-array antennas. The effects of beam-steering techniques including feed networks and phase shifters; sidelobe control; ground-clutter suppression; low altitude coverage; arrays with integrated radiating elements and feed networks; analysis of coaxial-collinear antennas; use of arrays with multiple beams; and array testing and measure on structural design of the antenna are discussed. B.G.

N87-10500*# National Oceanic and Atmospheric Administration, Boulder, Colo. Aeronomy Lab.
THE NOAA TOGA ANTENNA ARRAY c32
W. L. Ecklund, D. A. Carter, and B. B. Balsley *In* International Council of Scientific Unions, Middle Atmosphere Program. Handbook for MAP, Vol. 20 Jun. 1986 2 p (For primary document see N87-10419 01-42)
Avail: NTIS HC A22/MF A01; also available from SCOSTEP Secretariat, Illinois Univ., 1406 West Green Street, Urbana, Ill. 61801 CSCL 17I

The Aeronomy Laboratory recently installed a 100 x 100 meter array antenna with limited beam steering on Christmas Island as a part of the TOGA (Tropical Ocean and Global Atmosphere) program. The array and the associated beam steering and indicating hardware are described. Author

N87-10501*# Illinois Univ., Urbana. Dept. of Electrical and Computer Engineering.
BEAM STEERING SYSTEM c32
S. A. Bowhill and K. O. Merewether *In* International Council of Scientific Unions, Middle Atmosphere Program. Handbook for MAP, Vol. 20 Jun. 1986 4 p (For primary document see N87-10419 01-42)
Avail: NTIS HC A22/MF A01; also available from SCOSTEP Secretariat, Illinois Univ., 1406 West Green Street, Urbana, Ill. 61801 CSCL 17I

A simple technique for steering the beam of a multimodule phased array MST (mesosphere, stratosphere, troposphere) radar antenna is described. It is desirable to be able to point the antenna in multiple directions, so as to derive all components of the horizontal velocity. This was done on an experimental basis by adding parallel wire line to the feed and achieving a southward tilt of the antenna. It is proved possible to steer the beam through most of the available range without adversely affecting the VSWR seen from the transmitter. Calibrating the antenna direction can be accomplished by observing radio sources, though there are an inadequate number to cover all directions. For various assumed values of the aspect sensitivity in dB/deg, and the calculated antenna pattern, it is possible to calculate the effective pointing angle of the antenna, defined as that angle which would give an identical location for the centroid of the power spectrum if aspect sensitivity were absent. Using averaged apparent steering directions, eastward and northward winds were calculated for special radar runs simultaneous with 14 balloon launches at Peoria and results are presented. E.R.

N87-10502*# National Oceanic and Atmospheric Administration, Boulder, Colo. Aeronomy Lab.
DETERMINATION OF U, V, AND W FROM SINGLE STATION DOPPLER RADAR RADIAL VELOCITIES c47
W. L. Clark, J. L. Green, and J. M. Warnock *In* International Council of Scientific Unions, Middle Atmosphere Program. Handbook for MAP, Vol. 20 Jun. 1986 8 p (For primary document see N87-10419 01-42)
Avail: NTIS HC A22/MF A01; also available from SCOSTEP Secretariat, Illinois Univ., 1406 West Green Street, Urbana, Ill. 61801 CSCL 04B

The ST/MST (stratosphere troposphere/mesosphere stratosphere troposphere) clear air Doppler radar, or wind profiler, is an important tool in observational meteorology because of its capability to remote observe dynamic parameters of the atmosphere. There are difficulties in transforming the observed radial velocities into meteorological wind components. How this problem has been treated in the past is reviewed, and some of the analysis is recast to a form more suited to the high diagnostic abilities of a number of fixed beam configurations with reference to a linear wind field. The results, in conjunction with other works which treats problems such as the effects of finite sample volumes in the presence of nonhomogeneous atmospheric reflectivity, have implications important to the design of both individual MST/ST radars and MST/ST radar networks. The key parameters to uncoupling terms in the scaling equations are w sub x and w sub y. Whenever the stratiform condition, which states that these two parameters are negligible, is satisfied, a five beam ST radar may determine unbiased values of u, v, and w for sample volumes directly above the radar. The divergence and partial deformation of the flow may also be determined. Three beam systems can determine w and w sub z, but are unable to obtain u and v wind components uncontaminated by vertical sheer terms, even when the stratiform condition is satisfied. E.R.

N87-10503*# National Oceanic and Atmospheric Administration, Boulder, Colo. Wave Propagation Lab.
A 405-MHz, 5-BEAM PHASED ARRAY ANTENNA c32
Daniel C. Law *In* International Council of Scientific Unions, Middle Atmosphere Program. Handbook for MAP, Vol. 20 Jun. 1986 5 p (For primary document see N87-10419 01-42)
Avail: NTIS HC A22/MF A01; also available from SCOSTEP Secretariat, Illinois Univ., 1406 West Green Street, Urbana, Ill. 61801 CSCL 17I

The Wave Propagation Lab. has completed the design and construction of a phased array antenna for use at 405.25 MHz for atmospheric wind profiling. The steering geometry of the sequentially switched beam is shown. The Yagi-Uda antenna elements are arranged on a square grid whose axes are 45 deg with respect to the cardinal directions. By constraining the phase difference between rows of identically phased elements to an even, integral submultiple of 360 deg, symmetries appear in the phasing maps which reduce the switching hardware. The vertical beam is generated by switching around the four beam circuitry which results in identical phasing on all of the elements. After the 18 signals are synthesized they are split and distributed about the array while maintaining proper phasing because of the symmetries. Computer simulations were employed in the design process. E.R.

N87-10504*# National Oceanic and Atmospheric Administration, Boulder, Colo. Aeronomy Lab.
LOW-ALTITUDE COVERAGE OF ST RADARS c32
W. L. Ecklund *In* International Council of Scientific Unions, Middle Atmosphere Program. Handbook for MAP, Vol. 20 Jun. 1986 1 p (For primary document see N87-10419 01-42)
Avail: NTIS HC A22/MF A01; also available from SCOSTEP Secretariat, Illinois Univ., 1406 West Green Street, Urbana, Ill. 61801 CSCL 17I

Clear air ST (stratosphere troposphere) radars are now widely used for atmospheric research and wind profiling. Most attention to date has been directed toward extending the altitude coverage as high as possible. It is also desirable to extend the coverage as low as possible. Any improvement in the low altitude coverage of existing wind profiling radars would be useful. The approximate lower limits of some existing ST radars are listed and what set these limits are briefly examined. E.R.

N87-10505*# National Oceanic and Atmospheric Administration, Boulder, Colo. Aeronomy Lab.
THE GRID ARRAY ANTENNA c32
W. L. Ecklund *In* International Council of Scientific Unions, Middle Atmosphere Program. Handbook for MAP, Vol. 20 Jun. 1986 1 p (For primary document see N87-10419 01-42)
Avail: NTIS HC A22/MF A01; also available from SCOSTEP Secretariat, Illinois Univ., 1406 West Green Street, Urbana, Ill. 61801 CSCL 17I

Attention is called to the grid array as a possible useful antenna design for UHF clear air radars. This type of antenna integrates radiating elements and the feed network into a single structure so that a fairly large array can be driven from a single feed point. Figures are given which demonstrate the basic principle of the grid array, which are adapted from Conti et al. (1981). Conductors are arranged above a ground plane in a repeating, staggered array of connected rectangles. Each rectangular element is approximately one by one-half wavelength in size. The currents on the conductors at resonance is indicated. The grid array illustrated can be expanded in both vertical and horizontal directions about the feed point by adding additional rectangular conductors. The design eliminates the feed network and would provide a thin, panel-like antenna that could be easily built and transported. E.R.

N87-10506*# Toulon Univ. (France).
SIMULTANEOUS MULTIBEAM SOUNDING OF WIND AND TURBULENCE c47
E. Brun, M. Crochet, and W. L. Ecklund (National Oceanic and Atmospheric Administration, Boulder, Colo.) *In* International Council of Scientific Unions, Middle Atmosphere Program. Handbook for MAP, Vol. 20 Jun. 1986 7 p (For primary document see N87-10419 01-42)
Avail: NTIS HC A22/MF A01; also available from SCOSTEP Secretariat, Illinois Univ., 1406 West Green Street, Urbana, Ill. 61801 CSCL 04B

Most clear air radars use an antenna with either a few fixed beam positions or one that can be steered to a number of beam positions, one position at a time. For spatial studies of parameters that can change rapidly these conventional radar may be severely limited. The problem is that the fixed beam radars do not cover enough positions and the steerable radars may not be able to cover the entire field of interest in a short enough time period. Preliminary results are presented from a brief experiment that suggests a way to overcome some of these space-time problems in clear air radar research. A typical clear air radar antenna located in France was modified in a simple way to produce a number of beam simultaneouly. The radar, the modifications and the resulting beam patterns are described. Spectra is then shown obtained with the multibeam array and some results are presented on the spatial variations of reflectivity. Both the positive and negative aspects of using a multibeam antenna array for clear air radar studies are summarized. E.R.

N87-10507*# Adelaide Univ. (Australia). Dept. of Physics.
MEASUREMENTS OF ANTENNA POLAR DIAGRAMS AND EFFICIENCIES USING A PHASE-SWITCHED INTERFEROMETER c32
R. A. Vincent, B. Candy, and B. H. Briggs *In* International Council of Scientific Unions, Middle Atmosphere Program. Handbook for MAP, Vol. 20 Jun. 1986 1 p (For primary document see N87-10419 01-42)
Avail: NTIS HC A22/MF A01; also available from SCOSTEP Secretariat, Illinois Univ., 1406 West Green Street, Urbana, Ill. 61801 CSCL 17I

It is desirable to know antenna polar patterns and efficiencies accurately. In the past, calibration measurements have been made using balloons and aircraft and more recently satellites. These techniques are usually very expensive. It is shown that under certain circumstances it is possible to use a simpler and inexpensive technique by connecting together the antenna under test with another antenna to form a phase switched interferometer as first described by Ryle (1952). The technique does require a suitable radio source which gives measurable powers when using small antennas and since dipoles have broad patterns, radio sources with similar right ascensions but different declinations to the primary source can be a problem. These problems can partly be overcome by filtering the interference pattern. E.R.

N87-10508*# Colorado Univ., Boulder. Cooperative Inst. for Research in Environ. Sci.
USE OF THE SUN TO DETERMINE POINTING OF ST RADAR BEAMS c32
A. C. Riddle *In* International Council of Scientific Unions, Middle Atmosphere Program. Handbook for MAP, Vol. 20 Jun. 1986 4 p (For primary document see N87-10419 01-42)
Avail: NTIS HC A22/MF A01; also available from SCOSTEP Secretariat, Illinois Univ., 1406 West Green Street, Urbana, Ill. 61801 CSCL 17I

Verification of the beam pointing direction for ST (stratosphere troposphere) radars is a technically difficult problem. Consequently it is not usually done. For measurement of horizontal wind, the lack of precise knowledge of the beam pointing direction is usually of little consequence as any errors cause only a small uncertainty in the measured velocity. However, instantaneous vertical velocities are typically more than an order of magnitude less than horizontal velocities and average vertical velocities are more than two orders of magnitude less than average horizontal velocities. Hence small pointing errors for vertical beams can result in large errors due to contamination by horizontal winds. Experimental confirmation of pointing accuracy using the measured winds is difficult but has been achieved where horizontal and vertical winds are measured at the same site. Using the techniques described by Balsley and Riddle, 1984 and Riddle and Balsley, 1985, pointing accuracy was measured at Ponape, Federated States of Micronesia. The experiment is described in detail. E.R.

N87-10509*# Kyoto Univ., Uji (Japan). Radio Atmospheric Science Center.
MONITORING OF THE MU RADAR ANTENNA PATTERN BY SATELLITE OHZORA (EXOS-C) c32
Toru Sato, Yasuhiro Inooka, Shoichiro Fukao (Kyoto Univ., Japan), and Susumu Kato *In* International Council of Scientific Unions, Middle Atmosphere Program. Handbook for MAP, Vol. 20 Jun. 1986 5 p (For primary document see N87-10419 01-42)
Avail: NTIS HC A22/MF A01; also available from SCOSTEP Secretariat, Illinois Univ., 1406 West Green Street, Urbana, Ill. 61801 CSCL 17I

As the first attempt among MST (mesosphere stratosphere troposphere) type radars, the MU (middle and upper atmosphere) radar features an active phased array system. Unlike the conventional large VHF radars, in which output power of a large vacuum tube is distributed to individual antenna elements, each of 475 solid state power amplifier feeds each antenna element. This system configuration enables very fast beam steering as well as various flexible operations by dividing the antenna into independent subarrays, because phase shift and signal division/combination are performed at a low signal level using electronic devices under control of a computer network. The antenna beam can be switched within 10 microsec to any direction within the zenith angle of 30 deg. Since a precise phase alignment of each element is crucial to realize the excellent performance of this system, careful calibration of the output phase of each power amplifier and antenna element was carried out. Among various aircraft which may be used for this purpose artificial satellites have an advantage of being able to make a long term monitoring with the same system. An antenna pattern monitoring system for the MU radar was developed using the scientific satellite OHZORA (EXOS-C). A receiver named MUM (MU radar antenna Monitor) on board the satellite measures a CW signal of 100 to 400 watts transmitted from the MU radar. The principle of the measurement and results are discussed. E.R.

N87-10510*# Arecibo Ionospheric Observatory, Puerto Rico.

METHOD TO DETERMINE THE OPTIMAL PARAMETERS OF THE ARECIBO 46.8-MHz ANTENNA SYSTEM c32

H. M. Ierkic, J. Rottger, J. B. Hagen, and R. K. Zimmerman *In* International Council of Scientific Unions, Middle Atmosphere Program. Handbook for MAP, Vol. 20 Jun. 1986 5 p (For primary document see N87-10419 01-42)

Avail: NTIS HC A22/MF A01; also available from SCOSTEP Secretariat, Illinois Univ., 1406 West Green Street, Urbana, Ill. 61801 CSCL 17I

The spherical reflector at the Arecibo Observatory (AO) offers great advantages for the design of simple and inexpensive high performance steerable antennas at VHF. Light and small feeds have the added benefit that they can be quickly installed in the Arecibo platform. It is important to evaluate the performance of any given feed including the effects of the spherical reflector. The optimization is emphasized of two parameters, namely, the distance below the focal point of the reflector and the beam width of a point feed. For the design of the feed at 46.8 MHz at the AO there were other requirements independent of MST (mesosphere stratosphere troposphere) work. The design of the primary array is discussed along with its performance with the AO spherical reflector. E.R.

N87-10511*# National Oceanic and Atmospheric Administration, Boulder, Colo. Aeronomy Lab.

THE ELIMINATION OF A CLASS OF PSEUDO ECHOES BY AN IMPROVED T/R SWITCH TECHNIQUE c32

J. L. Green and W. L. Ecklund *In* International Council of Scientific Unions, Middle Atmosphere Program. Handbook for MAP, Vol. 20 Jun. 1986 6 p (For primary document see N87-10419 01-42)

Avail: NTIS HC A22/MF A01; also available from SCOSTEP Secretariat, Illinois Univ., 1406 West Green Street, Urbana, Ill. 61801 CSCL 17I

An annoying class of pseudo echoes are described that evidently occur occasionally in a number of ST (stratosphere troposphere) radars. The origin of these signals are located in the output circuitry of the radar transmitter. Two methods for the elimination of the radar echoes are suggested and briefly described. E.R.

N87-10512*# Case Western Reserve Univ., Cleveland, Ohio. Dept. of Electrical Engineering and Appl. Physics.

AN OVERVIEW OF DATA ACQUISITION, SIGNAL CODING AND DATA ANALYSIS TECHNIQUES FOR MST RADARS c32

P. K. Rastogi *In* International Council of Scientific Unions, Middle Atmosphere Program. Handbook for MAP, Vol. 20 Jun. 1986 10 p (For primary document see N87-10419 01-42)

Avail: NTIS HC A22/MF A01; also available from SCOSTEP Secretariat, Illinois Univ., 1406 West Green Street, Urbana, Ill. 61801 CSCL 17I

An overview is given of the data acquisition, signal processing, and data analysis techniques that are currently in use with high power MST/ST (mesosphere stratosphere troposphere/ stratosphere troposphere) radars. This review supplements the works of Rastogi (1983) and Farley (1984) presented at previous MAP workshops. A general description is given of data acquisition and signal processing operations and they are characterized on the basis of their disparate time scales. Then signal coding, a brief description of frequently used codes, and their limitations are discussed, and finally, several aspects of statistical data processing such as signal statistics, power spectrum and autocovariance analysis, outlier removal techniques are discussed. E.R.

N87-10513*# Arecibo Ionospheric Observatory, Puerto Rico.

OPTIMUM CODING TECHNIQUES FOR MST RADARS c32

Michael P. Sulzer and Ronald F. Woodman (Instituto Geofisico del Peru, Lima) *In* International Council of Scientific Unions, Middle Atmosphere Program. Handbook for MAP, Vol. 20 Jun. 1986 7 p (For primary document see N87-10419 01-42)

Avail: NTIS HC A22/MF A01; also available from SCOSTEP Secretariat, Illinois Univ., 1406 West Green Street, Urbana, Ill. 61801 CSCL 17I

The optimum coding technique for MST (mesosphere stratosphere troposphere) radars is that which gives the lowest possible sidelobes in practice and can be implemented without too much computing power. Coding techniques are described in Farley (1985). A technique mentioned briefly there but not fully developed and not in general use is discussed here. This is decoding by means of a filter which is not matched to the transmitted waveform, in order to reduce sidelobes below the level obtained with a matched filter. This is the first part of the technique discussed here; the second part consists of measuring the transmitted waveform and using it as the basis for the decoding filter, thus reducing errors due to imperfections in the transmitter. There are two limitations to this technique. The first is a small loss in signal to noise ratio (SNR), which usually is not significant. The second problem is related to incomplete information received at the lowest ranges. An appendix shows a technique for handling this problem. Finally, it is shown that the use of complementary codes on transmission and nonmatched decoding gives the lowest possible sidelobe level and the minimum loss in SNR due to mismatch. E.R.

N87-10514*# Illinois Univ., Urbana. Aeronomy Lab.

IMPROVING RANGE RESOLUTION WITH A FREQUENCY-HOPPING TECHNIQUE c32

G. R. Stitt and S. A. Bowhill *In* International Council of Scientific Unions, Middle Atmosphere Program. Handbook for MAP, Vol. 20 Jun. 1986 10 p (For primary document see N87-10419 01-42)

Avail: NTIS HC A22/MF A01; also available from SCOSTEP Secretariat, Illinois Univ., 1406 West Green Street, Urbana, Ill. 61801 CSCL 17I

Range resolution of a conventional pulsed Doppler radar is determined by the scattering volume defined by the transmitted pulse shape. To increase the resolution, the length of the pulse must be reduced. Reducing the pulse length also reduces the transmitted power and hense the signal to noise ratio unless the peak power capability of the transmitter is greatly increased. Improved range resolution may also be attained through the use of various pulse coding methods, but such methods are sometimes difficult to implement from a hardware standpoint. The frequency-hopping (F-H) technique described increases the range resolution of pulse Doppler MST (mesosphere stratosphere troposphere) radar without the need for extensive modifications to the radar transmitter. This technique consists of sending a repeated sequence of pulses, each pulse in the sequence being transmitted at a unique radio frequency that is under the control of a microcomputer. This technique is discussed along with other radar parameters. E.R.

N87-10515*# Illinois Univ., Urbana. Aeronomy Lab.

A VARIABLE-FREQUENCY LOCAL OSCILLATOR FOR THE FREQUENCY-HOPPING TECHNIQUE c33

G. R. Stitt and L. J. Johnson *In* International Council of Scientific Unions, Middle Atmosphere Program. Handbook for MAP, Vol. 20 Jun. 1986 3 p (For primary document see N87-10419 01-42)

Avail: NTIS HC A22/MF A01; also available from SCOSTEP Secretariat, Illinois Univ., 1406 West Green Street, Urbana, Ill. 61801 CSCL 09C

The frequency hopping technique described elsewhere requires the use of a local oscillator whose output frequency may be rapidly and accurately changed by a fixed frequency increment. Such a device, capable of producing 16 different frequencies separated by 50 kHz over the range of 35.02 to 35.77 MHz, has been built for the Urbana MST (mesosphere stratosphere troposphere) radar facility. The design and construction of that device is described and illustrated. E.R.

N87-10516*# Illinois Univ., Urbana. Dept. of Electrical and Computer Engineering.
AN ACCELERATED FORTH DATA-ACQUISITION SYSTEM c82
S. A. Bowhill and A. D. Rennier *In* International Council of Scientific Unions, Middle Atmosphere Program. Handbook for MAP, Vol. 20 Jun. 1986 2 p (For primary document see N87-10419 01-42)
Avail: NTIS HC A22/MF A01; also available from SCOSTEP Secretariat, Illinois Univ., 1406 West Green Street, Urbana, Ill. 61801 CSCL 05B

A new data acquisition system was put into operation at Urbana in August 1984. It uses a standard Apple 2 microcomputer with 48 k RAM and a standard 5 1/4 inch floppy disk. Design criteria for the system is given. The system was implemented using fig-FORTH, a threaded interpretive language which permits easy interfacing to machine code. The throughput of this system is better by a factor of 6 than the PDP-15 minicomputer system previously used, and it has the real time display feature and provides the data in much more convenient form. The features which contribute to this improved performance is listed. E.R.

N87-10517*# National Oceanic and Atmospheric Administration, Boulder, Colo. Aeronomy Lab.
A SINGLE-BOARD PREPROCESSOR AND PULSE GENERATOR c33
D. A. Carter, A. E. Ayers, and R. P. Schneider *In* International Council of Scientific Unions, Middle Atmosphere Program. Handbook for MAP, Vol. 20 Jun. 1986 3 p (For primary document see N87-10419 01-42)
Avail: NTIS HC A22/MF A01; also available from SCOSTEP Secretariat, Illinois Univ., 1406 West Green Street, Urbana, Ill. 61801 CSCL 09A

The Aeronomy Lab. of NOAA has designed and built a single board, programmable radar controller for use with VHF ST (stratosphere troposphere) radars. The controller consists of a coherent integrator preprocessor and a radar pulse generator, both of which are described, as well as interfaces to an antenna beam switch and a receiver bandwidth switch. The controller occupies a single slot in a Data General Nova of Eclipse computer. The integrator and pulse generator take advantage of high density, dual port FIFO chips such as the 512 x 9 Mostek MK 4501. These FIFOs have separate input and output ports and independent read and write cycles with cycle times of less than 200 ns, making them very fast and easy to interface. A simple block diagram of the coherent integrator is shown. The integrator is designed to handle inputs from one receiver (2 channels) with 1 sec sample spacing. The pulse generator is based on controllers designed by R. F. Woodman for the Arecibo and SOUSY radars us a recirculating memory scheme. E.R.

N87-10518*# National Oceanic and Atmospheric Administration, Boulder, Colo. Wave Propagation Lab.
A MICROPROGRAMMABLE RADAR CONTROLLER c32
Daniel C. Law *In* International Council of Scientific Unions, Middle Atmosphere Program. Handbook for MAP, Vol. 20 Jun. 1986 3 p (For primary document see N87-10419 01-42)
Avail: NTIS HC A22/MF A01; also available from SCOSTEP Secretariat, Illinois Univ., 1406 West Green Street, Urbana, Ill. 61801 CSCL 17I

The Wave Propagation Lab. has completed the design and construction of a microprogrammable radar controller for atmospheric wind profiling. Unlike some radar controllers using state machines or hardwired logic for radar timing, this design is a high speed programmable sequencer with signal processing resources. A block diagram of the device is shown. The device is a single 8 1/2 inch by 10 1/2 inch printed circuit board and consists of three main subsections: (1) the host computer interface; (2) the microprogram sequencer; and (3) the signal processing circuitry. Each of these subsections are described in detail. E.R.

N87-10519*# National Oceanic and Atmospheric Administration, Boulder, Colo. Aeronomy Lab.
AN EXAMPLE OF SCALING MST DOPPLER SPECTRA USING MEDIAN SPECTRA, SPECTRAL SMOOTHING, AND VELOCITY TRACING c33
J. L. Green *In* International Council of Scientific Unions, Middle Atmosphere Program. Handbook for MAP, Vol. 20 Jun. 1986 4 p (For primary document see N87-10419 01-42)
Avail: NTIS HC A22/MF A01; also available from SCOSTEP Secretariat, Illinois Univ., 1406 West Green Street, Urbana, Ill. 61801 CSCL 09C

Although automatic, computer scaling methods appeared at the start of the MST (mesosphere stratosphere troposphere) radar technique, there is a continuing need for scaling algorithms that perform editing functions and increase the sensitivity of radar by post processing. The scaling method presented is an adaptation of the method of scaling MST Doppler spectra presented by Rastogi (1984). A brief overview of this method is as follows: a median spectrum is calculated from several sequential spectra; the median noise value is subtracted from this derived spectrum; the median spectrum is smoothed; the detection/nondetection decision is made by comparing the smoothed spectrum to the variance of the smoothed noise; and if a signal is detected, then the half-power points of the smoothed echo spectrum are used to place limits on the evaluation of the first two moments of the unsmoothed median spectrum. In all of the above steps, the algorithm is guided by tracing the expected velocity range upward from the lowest range as far as possible. The method is discussed in more detail. E.R.

N87-10520*# Case Western Reserve Univ., Cleveland, Ohio. Electrical Engineering and Applied Physics.
INTERFERENCE DETECTION AND CORRECTION APPLIED TO INCOHERENT-SCATTER RADAR POWER SPECTRUM MEASUREMENT c32
W. P. Ying, J. D. Mathews, and P. K. Rastogi *In* International Council of Scientific Unions, Middle Atmosphere Program. Handbook for MAP, Vol. 20 Jun. 1986 10 p (For primary document see N87-10419 01-42)
Avail: NTIS HC A22/MF A01; also available from SCOSTEP Secretariat, Illinois Univ., 1406 West Green Street, Urbana, Ill. 61801 CSCL 17I

A median filter based interference detection and correction technique is evaluated and the method applied to the Arecibo incoherent scatter radar D-region ionospheric power spectrum is discussed. The method can be extended to other kinds of data when the statistics involved in the process are still valid. Author

N87-10521*# Illinois Univ., Urbana. Aeronomy Lab.
THE TUKEY ALGORITHM FOR ENHANCING MST RADAR DATA c32
S. A. Bowhill *In* International Council of Scientific Unions, Middle Atmosphere Program. Handbook for MAP, Vol. 20 Jun. 1986 3 p (For primary document see N87-10419 01-42)
Avail: NTIS HC A22/MF A01; also available from SCOSTEP Secretariat, Illinois Univ., 1406 West Green Street, Urbana, Ill. 61801 CSCL 17I

One of the most troublesome features in MSR (mesosphere stratosphere troposphere) velocity measurements is the determination of unwanted scatterer whose velocity is different from that of the surrounding atmosphere. Aircraft seen in the sidelobes of the antenna are the principal problem. Because coherent integration essentially eliminates echoes with line of sight velocities greater than 10 or 20 m/s, aircraft are seen only when their flight path is almost perpendicular to the line of sight. Then, they give large returns whose velocities may be positive or negative, and certainly different from that of the surrounding air. The glitches in the minute by minute velocity records are quite troublesome in that they may distort the statistics of the velocity. An objective way is therefore needed to remove sporadic points of this kind. For this purpose, the Tukey algorithm is appropriate and has some advantages over averaging. The Tukey algorithm, applied to a data array, uses for each data point the median of it and the two points surrounding it. If the three points form a monotonically increasing or decreasing sequence, the original point is copied with change. However, if the central point is remote from the other two, it is replaced by whichever of the two surrounding points is closest in value. The greatest effect of the Tukey algorithm is on data where the successive points are uncorrelated. Examples are given. E.R.

N87-10522*# Arecibo Ionospheric Observatory, Puerto Rico.
ON THE USE OF COLOUR REFLECTIVITY PLOTS TO MONITOR THE STRUCTURE OF THE TROPOSPHERE AND STRATOSPHERE c46
J. Rottger, I. J. Fu (National Central Univ., Chung-Li Taiwan), F. S. Kuo, C. H. Liu (Illinois Univ., Urbana), and J. K. Chao (National Central Univ., Chung-Li Taiwan) *In* International Council of Scientific Unions, Middle Atmosphere Program. Handbook for MAP, Vol. 20 Jun. 1986 2 p (For primary document see N87-10419 01-42)
Avail: NTIS HC A22/MF A01; also available from SCOSTEP Secretariat, Illinois Univ., 1406 West Green Street, Urbana, Ill. 61801 CSCL 04A

The radar reflectivity, defined as the range squared corrected power of VHF radar echoes, can be used to monitor and study the temporal development of inversion layer, frontal boundaries and convective turbulence. From typical featurs of upward or downward motion of reflectivity structures, the advection/convection of cold and warm air can be predicted. High resolution color plots appear to be useful to trace and to study the life history of these structures, particularly their persistency, descent and ascent. These displays allow an immediate determination of the tropopause height as well as the determination of the tropopause structure. The life history of warm fronts, cold fronts, and occlusions can be traced, and these reflectivity plots allow detection of even very weak events which cannot be seen in the traditional meteorological data sets. The life history of convective turbulence, particular evolving from the planetary boundary layer, can be tracked quite easily. Its development into strong convection reaching the middle troposphere can be followed and predicted. E.R.

N87-10523*# Pennsylvania State Univ., University Park. Dept. of Meteorology.
DATA COMMUNICATIONS AND MONITOR FOR THE PENN STATE UNIVERSITY PROFILER NETWORK c32
Robert M. Peters *In* International Council of Scientific Unions, Middle Atmosphere Program. Handbook for MAP, Vol. 20 Jun. 1986 2 p (For primary document see N87-10419 01-42)
Avail: NTIS HC A22/MF A01; also available from SCOSTEP Secretariat, Illinois Univ., 1406 West Green Street, Urbana, Ill. 61801 CSCL 17I

The profiler network installed by the Department of Meteorology at Penn State University utilizes a microcomputer for network monitoring and control. The network consists of two VHF and one UHF wind profiling Doppler radars. Additional measurement systems added to the network include temperature and humidity profiling radiometers, sodar for boundary layer wind profiling and selected surface based baseline systems. Remote diagnostic capabilities were also implemented in the Penn State network. It is possible to remotely analyze many specific malfunctions of the transmitter or signal processor. E.R.

N87-10524*# Colorado Univ., Boulder. Cooperative Inst. for Res. in the Environ. Sci.
ARCHIVAL OF POKER FLAT MST RADAR DATA c32
A. C. Riddle, B. B. Balsley (National Oceanic and Atmospheric Administration, Boulder, Colo.), and K. S. Gage *In* International Council of Scientific Unions, Middle Atmosphere Program. Handbook for MAP, Vol. 20 Jun. 1986 3 p (For primary document see N87-10419 01-42)
Avail: NTIS HC A22/MF A01; also available from SCOSTEP Secretariat, Illinois Univ., 1406 West Green Street, Urbana, Ill. 61801 CSCL 17I

The Poker Flat MST (mesosphere stratosphere troposphere) radar has operated from early 1979 to 1985. The data recorded during that time resides on some 1100 magnetic tapes. A second set containing only the derived parameters of velocity, width and signal to noise of the primary echo at each height, plus the noise spectra, occupies another 250 tapes. While processing to generate the compressed data set does correct some known errors, no attempt has been made to identify or remove spurious echoes. Because the Poker Flat data set is such a unique and valuable resource, a proposal is made to archive the data in forms more useful for analysis. The archived data set would contain only the parameters for significant echoes with contamination from airplanes, unwanted ionospheric returns, frequently aliased Doppler signals and other sources removed. The archived set should be as good or better than the example shown and may occupy only 25 to 50 tapes. E.R.

N87-10525*# National Center for Atmospheric Research, Boulder, Colo.
MST DATA EXCHANGE THROUGH THE NCAR INCOHERENT-SCATTER RADAR DATA BASE c32
A. D. Richmond *In* International Council of Scientific Unions, Middle Atmosphere Program. Handbook for MAP, Vol. 20 Jun. 1986 2 p (For primary document see N87-10419 01-42)
Avail: NTIS HC A22/MF A01; also available from SCOSTEP Secretariat, Illinois Univ., 1406 West Green Street, Urbana, Ill. 61801 CSCL 17I

One means of making MST (mesosphere stratosphere troposphere) radar data more easily accessible for scientific research by the general scientific community is through a centralized data base. Such a data base can be designed to readily provide information on data availability and quality, and to provide copies of data from any radar in a common format to the user. The ionospheric incoherent scatter community has established a centralized data base at NCAR that may serve not only as a model for a possible MST data base, but also as a catalyst for getting an MST data base started. (Some key elements of the NCAR data base are given.) The NCAR data base can include MST data in the same framework with relatively little extra effort. They are willing to handle MST data on a limited basis in order to permit assessment of community interest and in order to provide some experience with a centralized data base for MST data. E.R.

43 EARTH RESOURCES AND REMOTE SENSING

Includes remote sensing of earth resources by aircraft and spacecraft; photogrammetry; and aerial photography.

For instrumentation see *35 Instrumentation and Photography.*

N87-10526*# Lunar and Planetary Inst., Houston, Tex.
LANDSAT IMAGERY OF THE CENTRAL ANDES Progress Report, 22 Oct. 1986
Catherine A. Korner and Paul Morgan 29 Aug. 1986 1 p (Contract NASw-4066)
(NASA-CR-179852; NAS 1.26:179852) Avail: NTIS HC A02/MF A01 CSCL 08B

The central Andes of South America extend from approximately 14 deg. S to 28 deg. S as an unbroken chain of mountains and volcanoes over 2000 km long. It is here that the Nazca plate dives under the South American plate at angles varying from 10 deg to 30 deg. Very little is known about the volcanoes comprising this classic, subduction-type plate margin. A catalogue of the volcanoes in the central Andes is being prepared by Dr. P.W. Francis and Dr. C.A. Wood at the NASA Lunar and Planetary Institute. At present, more than 800 volcanoes of Cenozoic age have been recognized in the chain, with an estimated 75-80 major, active Quarternary volcanoes. Approximately one hundred 1536 x

1536 pixel color composite Optronics positives were produced from six full LANDSAT Thermatic Mapper scenes and three partial TM scenes. These positives cover a large portion of the central Andes. The positives were produced from LANDSAT data using the VAX imaging package, LIPS. The scenes were first transferred from magnetic tape to disk. The LIPS package was then used to select volcanically interesting areas which were then electronically enhanced. Finally, the selected areas were transferred back to tape and printed on the Optronics equipment. The pictures are color composites using LANDSAT TM bands 7,4, and 2 in the red, green, and blue filters, respectively. Author

N87-10527# Defense Mapping Agency Aerospace Center, St. Louis, Mo.
WORLD GEODETIC SYSTEM 1984
B. L. Decker Apr. 1986 27 p Presented at the 4th International Geodetic Symposium on Satellite Positioning, Austin, Tex., 28 Apr. - 2 May 1986
(AD-A167570) Avail: NTIS HC A03/MF A01 CSCL 08/5

The Defense Mapping Agency (DMA) has developed World Geodetic System 1984 (WGS 84) as a replacement for WGS 72. The defining parameters and reference frame orientation of the WGS 84 Ellipsoid, and the WGS 84 ellipsoidal gravity formula, are those of the internationally-sanctioned Geodetic Reference System 1980. The WGS 84 Earth Gravitational Model (EGM), complete through degree (n) and order (m) 180, was developed using various types of data. The low degree and order portion of the WGS 84 EBM (through n=m=41) was developed from a weighted least squares solution based on use of surface gravity data, satellite radar altimetry, laser and Doppler satellite tracking data, range difference data (from NAVASTAR satellites), and lumped coefficient data. The WGS 84 EGM coefficients above n=m=41 were determined from a spherical harmonic analysis of a worldwide residual 1 deg x 1 deg mean free-air gravity anomaly field from which the effect of the coefficients through n=m=41 had been removed. The WGS 84 Geoid was formed using a spherical harmonic expansion and the WGS 84 EGM (through n=m=180). Local Geodetic System-to-WGS 84 datum shifts are available for converting geodetic coordinates of approximately 80 local geodetic systems to WGS 84. GRA

N87-10528# Defense Mapping Agency, Washington, D.C.
DIGITAL MAPPING: FACT OR FICTION Final Report
Dennis P. Franklin Apr. 1986 11 p
(AD-A167571) Avail: NTIS HC A02/MF A01 CSCL 08/2

The Defense Mapping Agency has passed the point where we provide only the traditional paper maps and charts used by the Armed Forces. Many of the traditional, manual, labor intensive production processes currently in use are no longer cost effective in supporting present readiness requirements. DMA is now heavily into the production of digital data to support the navigation and guidance requirements of new advanced systems. To meet the ever increasing sophistication of these new systems, as well as updating our capability to support our traditional products, DMA is in the midst of the most ambitious modernization in the history of cartography. While the all digital softcopy production system is today still a fiction, the Defense Mapping Agency has committed itself to make this fiction a fact by the early 1990's. GRA

N87-10529# Technische Univ., Clausthal-Zellerfeld (West Germany). Inst. fuer Geologie und Palaeontologie.
SPACE IMAGING RADAR FOR REMOTE SENSING OF THE EARTH: AN EVALUATION Final Report, Dec. 1984
Peter Kronberg and Barbara Theilen-Willige Bonn Bundesministerium fuer Forschung und Technologie Dec. 1985 131 p In GERMAN; ENGLISH summary Sponsored by Bundesministerium fuer Forschung und Technologie
(BMFT-FB-W-85-024; ISSN-0170-1339; ETN-86-97843) Avail: NTIS HC A07/MF A01; Fachinformationszentrum, Karlsruhe, West Germany DM 27.50

The usefulness of SIR A-type imagery for thematic inventories and mapping of land use, geomorphology, hydrology, and geology was evaluated by comparing data contents of SIR A, LANDSAT MSS, and Metric Camera imagery from test sites in various parts of the world. Results indicate that spaceborne SAR (synthetic aperture radar) sensors (as well as spaceborne optical sensors) provide useful information only under specific surface conditions (morphology, surface cover, geological setting, climate). Possibilities and limitations in the use of spaceborne SAR-imagery for inventories and mapping projects are discussed. Correlative evaluations of spaceborne SAR and optical sensor imagery (providing surface roughness and spectral reflectance information for the area covered) are recommended. ESA

N87-10530 Arizona Univ., Tucson.
IN-FLIGHT ABSOLUTE RADIOMETRIC CALIBRATION OF THE LANDSAT THEMATIC MAPPER Ph.D. Thesis
Carol Jane Kastner 1985 212 p
Avail: Univ. Microfilms Order No. DA8603342

The inflight absolute radiometric calibration of the Thematic Mapper (TM) is being conducted using the results of field measurements at White Sands, New Mexico. These measurements are made to characterize the ground and atmosphere at the time the TM is acquiring an image of White Sands. The data are used as input to a radiative transfer code that computes the radiance at the entrance pupil of the TM. The calibration is obtained by comparing the digital counts associated with the TM image of the measured ground site with the radiative transfer code result. The calibrations discussed here are for the first four visible and near-infrared band of the TM. Dissert. Abstr.

N87-10265*# National Aeronautics and Space Administration, Washington, D.C.
LIDAR REMOTE SENSING FROM SPACE: NASA'S PLANS IN THE EARTH SCIENCES
Robert J. Curran *In* NASA. Langley Research Center 13th International Laser Radar Conference Aug. 1986 1 p (For primary document see N87-10263 01-35)
Avail: NTIS HC A15/MF A01 CSCL 20E

N87-10368*# Optech, Inc., Downsview (Ontario).
GAS DISPERSION MEASUREMENTS USING A MOBILE RAMAN LIDAR SYSTEM
J. D. Houston and D. R. Brown *In* NASA. Langley Research Center 13th International Laser Radar Conference Aug. 1986 3 p (For primary document see N87-10263 01-35)
Avail: NTIS HC A15/MF A01 CSCL 13B

44 ENERGY PRODUCTION AND CONVERSION

Includes specific energy conversion systems, e.g., fuel cells; global sources of energy; geophysical conversion; and windpower.

For related information see also *07 Aircraft Propulsion and Power, 20 Spacecraft Propulsion and Power,* and *28 Propellants and Fuels.*

N87-10531*# Paragon Pacific, Inc., Torrance, Calif.
WEST-3 WIND TURBINE SIMULATOR DEVELOPMENT. VOLUME 2: VERIFICATION Final Report
S. Sridhar Jul. 1985 31 p
(Contracts DEN3-247; DE-AI01-76ET-20320)
(NASA-CR-174982; DOE/NASA-0247/2; NAS 1.26:174982; PPI-FID-300102-Vol-2) Avail: NTIS HC A03/MF A01 CSCL 10A

The details of a study to validate WEST-3, a new time wind turbine simulator developed by Paragib Pacific Inc., are presented in this report. For the validation, the MOD-0 wind turbine was simulated on WEST-3. The simulation results were compared with those obtained from previous MOD-0 simulations, and with test data measured during MOD-0 operations. The study was successful in achieving the major objective of proving that WEST-3 yields results which can be used to support a wind turbine development process. The blade bending moments, peak and cyclic, from the WEST-3 simulation correlated reasonably well with the available MOD-0 data. The simulation was also able to predict the resonance phenomena observed during MOD-0 operations. Also presented in the report is a description and solution of a serious numerical instability problem encountered during the study. The problem was caused by the coupling of the rotor and the power train models. The results of the study indicate that some parts of the existing WEST-3 simulation model may have to be refined for future work; specifically, the aerodynamics and procedure used to couple the rotor model with the tower and the power train models. Author

N87-10532# Solarex Corp., Gaithersburg, Md. Aerospace Div.
VERTICAL JUNCTION SOLAR CELLS Final Report
20 Dec. 1985 64 p
(Contract N00014-83-C-2340)
(AD-A167757) Avail: NTIS HC A04/MF A01 CSCL 10/2

The goal of this program was to develop and evaluate an acceptable coversliding technology for vertical junction solar cells. The technical program was divided into the following sub-tasks: 1.0. to fabricate 80 vertical junction cells of most recent configuration for evaluation as individual samples and for test module assembly. 2.1. to develop a satisfactory method for coversliding V.J. cells to withstand deep thermal cycle in space. 2.2. to establish welding parameters for V.J. cells and evaluate their weldability. 3.0. Using techniques from 2.1 and 2.2 four modules (4 cell each) to be fabricated and thermal cycled in dry nitrogen (115 c to +125 c 25 cycles) and thermal vacuum tested at 135 c. 4.0. based on results of tasks 2 and 3, two six cell modules to be designed: 1 soldered, 1 welded, and design to be discussed with COTR prior to finalization, and 5.0. final design to be fabricated subjected to a thermal vacuum test at +135 c, thermal cycled -115 c to + 125 c, and characterized by I-V measurements and delivered to NRL for testing and evaluation. GRA

N87-10533# Ashrae, Inc., Atlanta, Ga.
METHODS OF TESTING TO DETERMINE THE THERMAL PERFORMANCE OF SOLAR COLLECTORS
1985 93 p
(Contract DE-FG03-81SF-08392)
(DE86-009311; DOE/SF-08392/T1) Avail: NTIS HC A05/MF A01

This Standard has been prepared by a committee drawn primarily from the membership of ASHRAE. The Committee's objective was to formulate a test procedure whereby solar energy collectors can be tested both indoors and outdoors, to rate the collectors in accordance with their thermal performance, and to determine their time constant and the variation of their efficiency with changes in the angle of incidence between the Sun's direct rays and the normal to the collector aperture. DOE

N87-10534# Naval Weapons Support Center, Crane, Ind.
EVALUATION OF A NEW TYPE STABLE NICKEL-ZINC BATTERY FOR ELECTRIC VEHICLE APPLICATION Final Report
26 Jul. 1985 23 p
(Contract DE-AI01-83CE-90038)
(DE86-010895; DOE/CE-90038/T1) Avail: NTIS HC A02/MF A01

This report describes discharge-recharge cycle testing of 14 nickel-zinc storage battery cells of a proprietary design. This testing was to obtain performance data on new types of stabilized nickel-zinc battery cells for possible electric vehicle applications. The test sample cells were manufactured by Electrochimica Corporation (ELCA) in two sizes (15 ampere-hours and 225 ampere-hours) with a total of seven different internal combinations. The cells completed up to 470 cycles when testing was halted due to funding limitations. Near the end of testing, the cells were providing 40% of nominal capacity when discharged to 1.2 volts and 58 to 73% when discharged in two steps to 1.0 volt. DOE

N87-10535# Sandia National Labs., Albuquerque, N. Mex.
EXPERIENCE WITH THE APPLICATION OF PHOTOVOLTAICS DEVICES
G. J. Jones 1986 15 p Presented at the American Solar Energy Society Annual Meeting and at the 11th National Passive Solar Conference, Boulder, Colo., 8 Jun. 1986
(Contract DE-AC04-76DP-00789)
(DE86-010472; SAND-86-2034C; CONF-860655-10) Avail: NTIS HC A02/MF A01

Photovoltaic systems have been the subject of a large research and development activity for the last decade. Hundreds of studies have addressed the question of optimal system and subsystem design. Field experiments have tested the resulting concepts and verified the reliability of the technology. As a result of these efforts, system design has reached a state of maturity in all application classes. Configurations are simple, with the photovoltaic system viewed as an electricity source. This paper reviews the evolution of system understanding to the present and provides a summary of the current design approach for each of the application types. DOE

N87-10536# Midwest Research Inst., Golden, Colo. Solar Energy Research Inst.
ADVANCED DESICCANT MATERIALS RESEARCH
A. W. Czanderna and T. M. Thomas May 1986 38 p
(Contract DE-AC02-83CH-10093)
(DE86-010695; SERI/PR-255-2887) Avail: NTIS HC A03/MF A01

The long-range goal of this task is to understand the role of surface phenomena in desiccant cooling materials. The background information includes a brief introduction to desiccant cooling systems (DCS) and the role of the desiccant as a system component. The purpose, background, rationale, and long-term technical approach for studying advanced desiccant materials are then treated. Experimental methods for measuring water vapor sorption by desiccants are described, and the rationale is then given for choosing a quartz crystal microbalance (QCM) for measuring sorption isotherms, rates, and cyclic stability. Background information is given about the QCM, including the quartz crystal resonator itself, the support structure for the quartz crystal, and the advantages and limitations of a QCM. The apparatus assembled and placed into operation during CY 1985 is described. The functions of the principal components of the equipment, i.e., the QCM, vacuum system, pressure gauges, residual gas analyzer, constant temperature bath, and data acquisition system, are described as they relate to the water vapor sorption measurements now under way. The criteria for narrowing the potential candidates as advanced desiccant materials for the initial studies are given. Also given is a list of 20 principal candidate materials identified based on the criteria and data available in the literature. DOE

N87-10537# Pacific Northwest Labs., Richland, Wash.
REVIEW OF STORAGE BATTERY SYSTEM COST ESTIMATES
D. R. Brown and J. A. Russell Apr. 1986 175 p
(Contract DE-AC06-76RL-01830)
(DE86-011182; PNL-5741) Avail: NTIS HC A08/MF A01

Cost analyses for zinc bromine, sodium sulfur, and lead acid batteries were reviewed. Zinc bromine and sodium sulfur batteries were selected because of their advanced design nature and the high level of interest in these two technologies. Lead acid batteries were included to establish a baseline representative of a more mature technology. DOE

N87-10022# Tokyo Univ. (Japan).
TWO DIMENSIONAL ANALYSIS OF HIGH VOLTAGE SOLAR ARRAY INTERFERING WITH IONOSPHERIC PLASMA
Hitoshi Kuninaka and Kyoichi Kuriki *In its* Proceedings of the Symposium on Mechanics for Space Flight, 1985 1985 10 p
(For primary document see N87-10011 01-02)
Avail: NTIS HC A12/MF A01

45 ENVIRONMENT POLLUTION

Includes atmospheric, noise, thermal, and water pollution.

N87-10538 Prins Maurits Lab. TNO, Rijswijk (Netherlands).
LABORATORY EVALUATION OF THREE PASSIVE CO CONCENTRATION MONITORS [LABORATORIUM-EVALUATIE VAN 3 PASSIEVE KOOLMONOXIDE-CONCENTRATIEMETERS]
A. Kaaijk Jan. 1985 22 p In DUTCH; ENGLISH summary
(Contract A82/KL/118)
(PML-1985-13; TDCK-93539; ETN-86-98044) Copyright. Avail: Issuing Activity

The precision of commercial CO monitors was determined. The effects of air velocity and interfering compounds were analyzed. The response time (1 to 3 min) and the recovery time (3 to 12 min) are long and can cause errors in case of fast fluctuating CO-concentrations. Accuracy is within 5%. ESA

N87-10539# Argonne National Lab., Ill.
BIOCONVERSION: A NEW TECHNOLOGY FOR WASTE AND SLUDGE DISPOSAL. WORKSHOP PROCEEDINGS
C. Brooks, comp. Feb. 1986 117 p Workshop held at Fort Lauderdale, Fla., 22 May 1985
(Contract W-31-109-eng-38)
(DE86-009668; ANL/CNSV-TM-174; CONF-850539) Avail: NTIS HC A06/MF A01

Anaerobic digestion of biomass offers a solution to the disposal of sewage sludge, municipal wastes, and other organic materials (agricultural and industrial residue, as well as terrestrial and marine energy crops) and produces a methane-rich gas. These proceedings are the result of a bioconversion workshop that was held to introduce the technology that results in bioconversion of these wastes to gas. The technology is based on bacterial decomposition of organic material into simpler compounds. The principal products of this process are methane and carbon dioxide. The workshop agenda included discussions of the anaerobic technology and presentations of operating data and economic forecasts developed at RefCoM (refuse conversion to methane), an experimental plant operating in Pompano Beach, Florida. DOE

N87-10540# California State Dept. of Transportation, Sacramento. Office of Transportation Lab.
DEVELOPMENT OF WORST CASE METEOROLOGY CRITERIA Final Report
W. A. Nokes and P. E. Benson Nov. 1985 90 p Sponsored by Federal Highway Administration
(PB86-215993; TL-604196; FHWA/CA/TL-85/14) Avail: NTIS HC A05/MF A01 CSCL 13B

A meteorological severity index (MSI) representing the relationship between meteorological paramenters that contribute to worst case carbon monoxide concentrations near roadways is described. The MSI is based on sensitivity studies of the California Lines Source Dispersion Model, CALINE4. Meteorological data collected at several monitoring sites throughout California are described. Probabilistic analysis of the monitoring data (stratified by geography and time-of-day) is combined with the MSI to develop worst case meteorology inputs for estimation 1-hour CO levels using CALINE4. Guidelines are presented to help CALINE4 users develop or estimate an appropriate persistent factor for a project location. The probabilistic method described can be used to establish new worst case meteorology criteria in the event of changes in the number of exceedances allowed by the National Ambient Air Quality Standards. The variety of locations studied in California should make results of the study useable by other states. GRA

N87-10271*# University of Western Australia, Perth. School of Physics and Geoscience.
AEROSOL STUDIES IN MID-LATITUDE COASTAL ENVIRONMENTS IN AUSTRALIA
S. A. Young, D. Cutten (Electronics Research Lab., Adelaide (Australia).), M. J. Lynch, and J. E. Davies *In* NASA. Langley Research Center 13th International Laser Radar Conference Aug. 1986 4 p (For primary document see N87-10263 01-35)
Avail: NTIS HC A15/MF A01 CSCL 13B

N87-10272*# Atmospheric Sciences Lab., White Sands Missile Range, N. Mex.
VISIBILITY RELATED TO BACKSCATTER AT 1.54 MICRON
T. L. Barber and D. R. Larson (New Mexico State Univ., Las Cruces.) *In* NASA. Langley Research Center 13th International Laser Radar Conference Aug. 1986 2 p (For primary document see N87-10263 01-35)
Avail: NTIS HC A15/MF A01 CSCL 13B

N87-10317*# Centro Informazioni Studi Esperienze, Milan (Italy).
TIME-RESOLVED LIDAR FLUOROSENSOR FOR SEA POLLUTION DETECTION
A. Ferrario, P. L. Pizzolati, and E. Zanzottera *In* NASA. Langley Research Center 13th International Laser Radar Conference Aug. 1986 2 p (For primary document see N87-10263 01-35)
Avail: NTIS HC A15/MF A01 CSCL 13B

N87-10318*# Lund Inst. of Tech. (Sweden). Dept. of Physics.
VARIATION OF THE URBAN NO2 CONCENTRATION DURING A GROUND INVERSION SITUATION
A. Sunesson, W. Wendt, and B. Galle (Swedish Water and Air Pollution Research Lab., Goeteborg.) *In* NASA. Langley Research Center 13th International Laser Radar Conference Aug. 1986 3 p (For primary document see N87-10263 01-35)
Avail: NTIS HC A15/MF A01 CSCL 13B

N87-10319*# Keio Univ., Yokahama (Japan). Dept. of Physics.
AN INTENSITY-MODULATED DUAL-WAVELENGTH He-Ne LASER FOR REMOTE SENSING OF METHANE
Kiyoji Uehara and Fujitaka Taguchi (Tokyo Gas Co. Ltd. (Japan).) *In* NASA. Langley Research Center 13th International Laser Radar Conference Aug. 1986 4 p -CP-2431 (For primary document see N87-10263 01-35)
Avail: NTIS HC A15/MF A01 CSCL 13B

N87-10320*# Israel Inst. for Biological Research, Ness-Ziona.
LIDAR MAPPING OF A MIXTURE OF AEROSOL CONCENTRATIONS IN A VARYING ATMOSPHERE
Moshe Kleiman, Smadar Egert, and Ariel Cohen *In* NASA. Langley Research Center 13th International Laser Radar Conference Aug. 1986 3 p (For primary document see N87-10263 01-35)
Avail: NTIS HC A15/MF A01 CSCL 13B

N87-10322*# Joint Research Centre of the European Communities, Ispra (Italy).
FEASIBILITY EXPERIMENTS ON TIME-RESOLVED FLUOROSENSING APPLIED TO OIL SLICKS
P. Camagni, G. Colombo, C. Koechler, A. Pedrini, N. Omenetto, and G. Rossi *In* NASA. Langley Research Center 13th International Laser Radar Conference Aug. 1986 5 p (For primary document see N87-10263 01-35)
Avail: NTIS HC A15/MF A01 CSCL 13B

N87-10354*# Tohoku Univ., Sendai (Japan). Research Inst. of Electrical Communication.
WIDE-AREA REMOTE-SENSING SYSTEM OF POLLUTION AND GAS DISPERSAL BY NEAR-INFRARED ABSORPTION BASED ON LOW-LOSS OPTICAL FIBER NETWORK
Humio Inaba *In* NASA. Langley Research Center 13th International Laser Radar Conference Aug. 1986 4 p (For primary document see N87-10263 01-35)
Avail: NTIS HC A15/MF A01 CSCL 13B

N87-10355*# Lund Inst. of Tech. (Sweden). Dept. of Physics.
A MOBILE SYSTEM FOR ACTIVE OTPICAL POLLUTION MONITORING
A. Sunesson, H. Edner, S. Svanberg, L. Uneus, W. Wendt, and K. Fredriksson (National Swedish Environment Protection Board, Stockholm.) *In* NASA. Langley Research Center 13th International Laser Radar Conference Aug. 1986 3 p (For primary document

see N87-10263 01-35)
Avail: NTIS HC A15/MF A01 CSCL 13B

N87-10375*# Army Chemical Research and Development Center, Aberdeen Proving Ground, Md.
CHEMICAL CONTAMINATION REMOTE SENSING
John P. Carrico, Kirkman R. Phelps, Ernest N. Webb, Raymond A. Mackay, and E. R. Murray (SRI International Corp., Menlo Park, Calif.) *In* NASA. Langley Research Center 13th International Laser Radar Conference Aug. 1986 1 p (For primary document see N87-10263 01-35)
Avail: NTIS HC A15/MF A01 CSCL 13B

N87-10639# Tsukuba Univ. (Japan). Inst. of Geoscience.
AIR QUALITY IN TROPICAL CITIES
T. Kawamura *In* WMO Proceedings of the Technical Conference on Urban Climatology and its Applications with Special Regard to Tropical Areas 1986 p 46-62 (For primary document see N87-10636 01-47)
Avail: NTIS MF A01; print copy available at WMO, Geneva, Switzerland

46 GEOPHYSICS

Includes aeronomy; upper and lower atmosphere studies; ionospheric and magnetospheric physics; and geomagnetism.

For space radiation see *93 Space Radiation.*

N87-10541 Centre National d'Etudes Spatiales, Toulouse (France).
RESULTS OF THE ARCAD 3 PROJECT AND OF RECENT PROGRAMS IN MAGNETOSPHERIC AND IONOSPHERIC PHYSICS
1985 976 p International Conference held in Toulouse, France, May 1984
(ISBN-2-85428-126-8; ETN-86-94737) Copyright. Avail: CEPADUES, Toulouse

Magnetosphere-ionosphere coupling; auroral electrodynamics; particle precipitation; high latitude ionosphere; interplanetary magnetic field; wave generation; ionospheric and magnetospheric instabilities; active experiments; and coordinated measurements were discussed. For individual titles, see N87-10542 through N87-10607.

N87-10542 California Univ., Berkeley. Space Sciences Lab.
MAGNETIC FIELD-ALIGNED PARTICLE PRECIPITATION
Charles W. Carlson *In* CNES Results of the ARCAD 3 Project and of Recent Programs in Magnetospheric and Ionospheric Physics 1985 p 37-48 (For primary document see N87-10541 01-46)
(Grant NAG6-10)
Avail: CEPADUES, Toulouse

Magnetic field-aligned auroral particle fluxes are discussed. Precipitating field-aligned electrons are seen in the vicinity of auroral arcs as suprathermal bursts, as well as superimposed on the more isotropic inverted V electron precipitation. Electron distribution functions reveal two distinct source populations for the inverted V and field-aligned electron components, and suggest possible acceleration mechanisms. The inverted V electrons are a hot, boundary plasma sheet population that gains the full parallel acceleration. The field-aligned component appears to originate from cold ionospheric electrons that may be distributed throughout the acceleration region. A turbulent parallel field might explain the apparent lifetime of cold electrons in the acceleration region. ESA

N87-10543 Centre d'Etude Spatiale des Rayonnements, Toulouse (France).
STATISTICAL STUDY OF AURORAL ELECTRON PRECIPITATION STRUCTURES DETECTED BY THE AUREOL-3 SATELLITE
J. M. Bosqued, C. Maurel, J. A. Sauvaud, R. A. Kovrazhkin (Academy of Sciences (USSR), Moscow), and Yu. I. Galperin *In* CNES Results of the ARCAD 3 Project and of Recent Programs in Magnetospheric and Ionospheric Physics 1985 p 49-59 (For primary document see N87-10541 01-46)
Avail: CEPADUES, Toulouse

The distribution of the inverted-V electron precipitation detected in the 500 to 2000 km altitude range aboard the AUREOL-3 satellite was studied. Structured precipitations are statistically observed inside the auroral oval with a maximum occurrence in the evening-midnight sector. They correspond to primary electron fluxes peaked at energies of less than 10 keV and precipitating in large-scale structures (50 to 100 km in latitudinal width). It is shown that, as predicted by collisionless kinetic theories, most inverted-V structures present a clear relationship between the field-aligned current density carried by the 1 to 20 keV primary electrons and the potential drop inferred from particle distribution functions. The study demonstrates the existence of strong electron heating inside the acceleration region. ESA

N87-10544 Centre National de la Recherche Scientifique, Orleans (France). Lab. de Physique et Chimie de l'Environnement.
SIMULTANEOUS MEASUREMENTS OF THERMAL ELECTRON DENSITY-TEMPERATURE AND LOW ENERGY PRECIPITATING ELECTRON FLUXES IN TOPSIDE IONOSPHERE
C. Beghin, J. M. Bosqued (Toulon Univ., France).), R. A. Kovrazhkin (Academy of Sciences (USSR), Moscow), J. A. Sauvaud (Toulon Univ., France), C. Maurel, N. V. Jorjio (Academy of Sciences (USSR), Moscow), and R. Debrie *In* CNES Results of the ARCAD 3 Project and of Recent Programs in Magnetospheric and Ionospheric Physics 1985 p 61-75 (For primary document see N87-10541 01-46)
Avail: CEPADUES, Toulouse

Topside F-region nearly horizontal profiles of electron density and temperature, as measured on board AUREOL 3 satellite by the mutual impedance probes, at different local times from the plasmasphere latitudes up to the polar cap, for scales ranging from thousands of km down to a few tens of meters are presented. Simultaneous measurements of low energy precipitating electron fluxes with good time resolution show that one to one correlations in space between those fluxes and electron density and temperature structures are rare. When they occur, if they are not pure accident, they are thought to correspond with very stable, steady arcs. Data support ideas on production, lifetime, and convection-type transport of the topside F-region electron density irregularities. ESA

N87-10545 California Univ., Berkeley. Space Sciences Lab.
MAGNETIC FIELD-ALIGNED POTENTIAL DROPS
Michael A. Temerin *In* CNES Results of the ARCAD 3 Project and of Recent Programs in Magnetospheric and Ionospheric Physics 1985 p 77-92 (For primary document see N87-10541 01-46)
(Contract N00014-81-C-0006)
Avail: CEPADUES, Toulouse

Discrete aurora genesis is discussed. Regions of large field-aligned potential drops can occur without electrostatic shocks, and regions of small parallel field-aligned potential drops usually occur without such shocks. This suggests that a varying portion of the magnetic field-aligned potential drop is widely distributed along the magnetic field line. Some of this potential may be confined to a series of small-scale, small-amplitude double layers. Such double layers typically occur along with electrostatic ion cyclotron waves in regions of upflowing ion beams. While the potential through each double layer is only a few volts, a series of such double layers along the magnetic field line can produce potential drops of several hundred volts. Some of the potential drop may be more continuously distributed along the magnetic field line. This small, continuously distributed electric field is the most difficult to measure and its contribution to the total potential drop along auroral magnetic field lines is unclear. ESA

N87-10546 Centre de Recherches en Physique de l'Environnement, Saint Maur des Fosses (France).
SMALL SCALE AND INTENSE FIELD-ALIGNED CURRENTS

DETECTED BY THEIR MAGNETIC SIGNATURE
C. Machard, A. Berthelier, J. J. Berthelier, J. C. Cerisier, Y. I. Galperin (Academy of Sciences (USSR), Moscow), and M. M. Mogilevsky *In* CNES Results of the ARCAD 3 Project and of Recent Programs in Magnetospheric and Ionospheric Physics 1985 p 93-97 (For primary document see N87-10541 01-46)
Avail: CEPADUES, Toulouse

From the simultaneous measurements of three components of the magnetic field, DC and in the ELF range, on board the satellite AUREOL-3, small scale field aligned currents with a horizontal scale ranging from a few hundred meters to a few km were deduced. The intensity can be as large as 100 micro A/sqm or more. The currents, which are a frequent feature of the high latitude ionosphere, are mainly observed in the evening and morning sectors, but also in the polar cusps. ESA

N87-10547 Centre d'Etude Spatiale des Rayonnements, Toulouse (France).
POSITIVE ION DISTRIBUTIONS IN THE MORNING AURORAL ZONE: LOCAL ACCELERATION AND DRIFT EFFECTS
J. A. Sauvaud, J. M. Bosqued, R. A. Kovrazhkin (Academy of Sciences (USSR), Moscow), J. J. Berthelier (Centre de Recherches en Physique de l'Environnement, Saint Maur des Fosses France), A. Berthelier, and Yu. I. Galperin (Academy of Sciences (USSR), Moscow) *In* CNES Results of the ARCAD 3 Project and of Recent Programs in Magnetospheric and Ionospheric Physics 1985 p 99-105 (For primary document see N87-10541 01-46)
Avail: CEPADUES, Toulouse

The structure of the large scale ion precipitation and field aligned currents in the morning sector of the auroral zone is discussed, using data obtained during near radial passes of the AUREOL-3 satellite. Poleward, the latitudinal variation of the average energy of precipitated ions (H+) indicates that they are adiabatically accelerated in the outer magnetosphere. This high energy precipitation is associated with a low energy upward flowing component. Near the boundary between discrete and diffuse electron aurorae the flux of energetic precipitated H(+) ions is sharply reduced, due to formation of Alfven layers. Intense fluxes of precipitated ions with energies of less than 2 keV are observed equatorward of the Alfven layers, in coincidence with the diffuse aurora. As the characteristic convection and bounce times of the energy upward flowing heavy ion component are comparable, the precipitation of ionospheric ions inside the diffuse aurora may result from convection and corotation of the ions accelerated to suprathermal energies at higher latitudes. Low energy H(+) precipitation is due to a solar and an ionospheric source. ESA

N87-10548 European Space Agency. European Space Research and Technology Center, ESTEC, Noordwijk (Netherlands). Space Science Dept.
PLASMA SHEET BOUNDARY ELECTRIC FIELDS DURING SUBSTORMS c75
Arne Pedersen *In* CNES Results of the ARCAD 3 Project and of Recent Programs in Magnetospheric and Ionospheric Physics 1985 p 107-121 (For primary document see N87-10541 01-46)
Avail: CEPADUES, Toulouse

Electric field data from the ISEE-1 and GEOS-2 satellites on substorms when ISEE-1 was in the magnetotail and GEOS-2 in the afternoon/evening sector of the geostationary orbit are discussed. In one case GEOS-2, in the afternoon sector, detected an increase of the dawn-to-dusk electric field during plasma sheet thinning 10 min prior to a substorm expansion. At the time of this expansion ISEE-1 was near an X-line, on the Earthward side and detected Earthward E x B velocities greater than 500 km/sec. Once ISEE-1 was near an X-line, on the tailward side, and observed tailward E x B velocities, which were followed 5 to 20 min later, by characteristic oscillating electric fields on GEOS-2. Such signatures are connected with observations of westward traveling surges. The ISEE-1 observations of large dawn-to-dusk electric fields were concentrated on the outer boundary of the plasma sheet, and for the westward traveling surge, GEOS-2 was at the inner, Earthward edge of the sheet. Time delays between ISEE-1 and GEOS-2 indicate a propagation velocity comparable to the E x B velocity. ESA

N87-10549 Alaska Univ., Fairbanks. Inst. of Geophysics.
CONSEQUENCES OF IMPERFECT MAGNETOSPHERE-IONOSPHERE COUPLING
J. R. Kan *In* CNES Results of the ARCAD 3 Project and of Recent Programs in Magnetospheric and Ionospheric Physics 1985 p 123-142 (For primary document see N87-10541 01-46)
(Grant NSF ATM-83-17456)
Avail: CEPADUES, Toulouse

Imperfect magnetosphere-ionosphere coupling, defined by the existence of an aurora-producing electric potential drop along field lines, is used as a theoretical framework for the substorm phenomena. The source of the field-aligned potential is believed to be the enhanced convection electric field in the plasma sheet being partially short-circuited by the conducting ionosphere. The mechanism which maintains the auroral potential and the process which controls its field-aligned scale-length are summarized. In addition to causing the brightening of discrete auroras, the imperfect magnetosphere-ionosphere coupling also leads to the Pi2 magnetic pulsations and the westward traveling surge which are manifestations of a substorm. The generation of Pi2 pulsations and the distortion of the convection pattern associated with the westward traveling surge are shown to result from the transient ionospheric response to an enhanced magnetospheric convection. Conductivity enhancement due to auroral electron precipitation is shown to play a crucial role in all aspects of substorm phenomena. ESA

N87-10550 Max-Planck-Inst. fuer Aeronomie, Katlenburg-Lindau (West Germany).
MAGNETOSPHERIC-IONOSPHERIC COUPLING DEDUCED FROM MEASUREMENTS ABOVE A DISCRETE AURORAL ARC
K. Broening and C. K. Goertz (Iowa Univ., Iowa City) *In* CNES Results of the ARCAD 3 Project and of Recent Programs in Magnetospheric and Ionospheric Physics 1985 p 145-151 (For primary document see N87-10541 01-46)
Avail: CEPADUES, Toulouse

The perpendicular electric field, the height integrated conductivities, and the field-aligned currents above and at the edge of a discrete auroral arc in the local post midnight sector were deduced from rocket measurements. Above the arc, an upward field-aligned current is carried by energetic electrons. At the edge of the arc, stronger field-aligned currents flow. Above the arc, a polarization electric field is generated. At the edge of the arc, the strong enhancement of the perpendicular electric field generated in the magnetosphere and propagated to the ionosphere, creates a strong field-aligned current. Above the arc, the results of j'(V') and for n, T0, B1/B0 agree with the stationary model of single particle description. At the edge of the arc, these descriptions work only if the electron density increases by a factor of 10. Above the arc, equilibrium between the electric field in the magnetosphere and ionosphere has time to establish itself. Therefore the stationary model is reasonable. At the edge of a moving arc, this equilibrium is not reached. ESA

N87-10551 Academy of Sciences (USSR), Moscow. Inst. of Space Science.
MODELS OF ELECTRIC POTENTIAL AND CURRENT DISTRIBUTION IN STABLE DISCRETE AURORAL FORMS
Yu. I. Galperin, E. E. Timofeev, M. A. Volkov, and A. V. Volosevich *In* CNES Results of the ARCAD 3 Project and of Recent Programs in Magnetospheric and Ionospheric Physics 1985 p 153-175 (For primary document see N87-10541 01-46)
Avail: CEPADUES, Toulouse

A simplified stationary model for calculations of magnetospheric Alfven layer effects on the auroral ionosphere is described. The model computes the profile of particle density across the L-shells at ionospheric level. The model for a generation of the V-shaped potential structure takes into account the mirror force, and the nonadiabatic cross-L motion of ionospheric ions in a sharply inhomogeneous electric field. With very low current density it is shown to be significant for scales of an arc as providing a partial closure when integrated along the field tube. Examples of calculations are given for L0=7. The model results can be fitted to agree with data for a sharp jump of plasma density radial profile from 1.0/cc on one side to 0.4/cc on the other side of an Alfven layer inside the main (closed) equatorial nightside plasmasheet, giving the scale = 10 km at ionospheric altitudes. ESA

N87-10552 Kiruna Geophysical Inst. (Sweden).
THE HOT ION COMPOSITION IN THE MAGNETOSPHERE
Bengt Hultqvist *In* CNES Results of the ARCAD 3 Project and of Recent Programs in Magnetospheric and Ionospheric Physics 1985 p 177-217 (For primary document see N87-10541 01-46)
Avail: CEPADUES, Toulouse

Hot ion composition measurements on board S3-3, GEOS-1, 2, ISEE-1, PROGNOZ-7, SCATHA, and Dynamics Explorer-1 in the low and high latitude boundary layers, the lobes, plasma sheet, and ring current regions are discussed. Observations of individual flow vectors of different ion species in the low latitude boundary layer are described. The PROGNOZ-7 measurements in the mantle are reviewed. Results of DE-1 observations in the lobes and ISEE-1 data in the plasma sheet and in the ring current region are presented. The GEOS-1, 2 and PROGNOZ-7 measurements of ring current ions are summarized. ESA

N87-10553 Centre d'Etude Spatiale des Rayonnements, Toulouse (France).
INJECTION OF LOW-ENERGY IONS DURING GEOMAGNETIC STORMS
J. M. Bosqued, D. Delcourt, C. Beghin (Centre National de la Recherche Scientifique, Orleans, France), R. A. Kovrazhkin (Academy of Sciences (USSR), Moscow), V. L. Khalipov, J. J. Berthelier (Centre de Recherches en Physique de l'Environnement, Saint Maur des Fosses, France), H. Reme, and V. D. Maslov (Academy of Sciences (USSR), Moscow) *In* CNES Results of the ARCAD 3 Project and of Recent Programs in Magnetospheric and Ionospheric Physics 1985 p 219-232 (For primary document see N87-10541 01-46)
(Grant CNES-84-1212)
Avail: CEPADUES, Toulouse

Suprathermal ion composition measurements as a function of latitude and local time taken at ionospheric altitudes by the ion spectrometers aboard the AUREOL-3 satellite during magnetically disturbed periods are presented. Although H(+) is the most abundant ion during quiet periods, the hot plasma ion composition is variable and depends strongly on magnetic activity. The importance of the low-altitude ionospheric source is stressed particularly at low latitudes (L = 3 to 4) in the outer plasmasphere when upflowing 0(+) ion fluxes appear over large regions during the magnetic storm recovery phase. These low-energy intense fluxes can contribute after a period of enhanced activity to the refilling of the depleted plasmasphere. ESA

N87-10554 Academy of Sciences (USSR), Moscow. Inst. of Space Research.
DETECTION OF SUPRATHERMAL O(+) IONS INSIDE THE PLASMASPHERE
N. V. Jorjio, J. M. Bosqued (Centre d'Etude Spatiale des Rayonnements, Toulouse, France), J. A. Sauvaud, D. Delcourt, R. A. Kovrazhkin, M. Monchant, V. D. Maslov, V. M. Pokras, M. M. Mogilevsky, C. Beghin (Centre National de la Recherche Scientifique, Orleans, France) et al *In* CNES Results of the ARCAD 3 Project and of Recent Programs in Magnetospheric and Ionospheric Physics 1985 p 233-237 (For primary document see N87-10541 01-46)
Avail: CEPADUES, Toulouse

The plasma diagnostic experiments on the AUREOL-3 satellite revealed flows of low energy O(+) ions deep inside the night plasmasphere during a large substorm. Flux gradients of the O(+) ions were accompanied by enhancements of ELF electric field noise. The appearance of suprathermal ions at L = 2.5 to 3 is interpreted in the framework of electrostatic ion-cyclotron acceleration of ionospheric ions in the diffuse auroral zone followed by a radial displacement of these ions inside the plasmasphere driven by azimuthal electric fields during substorm activity. Electrostatic oscillations observed inside the plasmasphere are associated with gradient instability at the sharp boundaries of suprathermal ion flows. ESA

N87-10555 Institut d'Aeronomie Spatiale de Belgique, Brussels.
FORMATION AND DEFORMATION OF THE PLASMAPAUSE DURING A SUBSTORM EVENT c75
J. Lemaire *In* CNES Results of the ARCAD 3 Project and of Recent Programs in Magnetospheric and Ionospheric Physics 1985 p 239-260 (For primary document see N87-10541 01-46)
Avail: CEPADUES, Toulouse

Plasmapause deformation during a magnetic storm was observed and simulated. When the electric field varies in time with the geomagnetic activity index, the plasmapause deforms and reforms in the midnight sector at decreasing distances where the convection electric field is important. It is shown that the formation of multiple plasmapauses is the result of the filling in of the intermediary region between an old plasmapause and a new one being formed after a reduction of the geomagnetic activity. It is shown that the quick decrease (in a few hours) of the density gradient at the plasmapause is a consequence of the plasma element exchange under the influence of the gravitational force. ESA

N87-10556 Academy of Sciences (USSR), Moscow. Inst. of Space Research.
OBSERVATIONS OF LOW INTENSITY PARTICLE FLUXES INSIDE THE REGION OF THE IONOSPHERIC MAIN TROUGH AND THEIR VARIABILITY
Yu. V. Lissakov, N. V. Jorjio, L. M. Nikolaenko, and M. R. Ainbund *In* CNES Results of the ARCAD 3 Project and of Recent Programs in Magnetospheric and Ionospheric Physics 1985 p 261-274 (For primary document see N87-10541 01-46)
Avail: CEPADUES, Toulouse

The AUREOL-3 satellite spectrometer recorded very weak intensities of precipitating electrons during ionospheric disturbances at latitudes corresponding to main ionospheric F-region trough (MIT) minimum. The precipitations are detected at the equator by a sharp jump of the electron intensity at soft electron boundary (SEB). The electron fluxes lead to weak ionization enhancements in the F and E-regions, and to decrease of MIT depth. With increased geomagnetic activity level, the SEB displaces equatorward, filling the region of previous low-intensity precipitation of low energy electrons; electron intensity profile and MIT polar wall can become stepped. Dynamics of the form of the latitudinal profile of precipitating electron intensity under increased perturbation can be explained by the diffusive mechanism of low-energy electron penetration through the plasmapause into the plasmasphere via small-scale nonstationary electric fields at this boundary, and proves the convection boundary nature of the SEB. ESA

N87-10557 California Univ., San Diego. Dept. of Physics.
EQUATORIAL MAGNETOSPHERIC PARTICLES AND AURORAL PRECIPITATIONS
C. E. McIlwain *In* CNES Results of the ARCAD 3 Project and of Recent Programs in Magnetospheric and Ionospheric Physics 1985 p 275-280 (For primary document see N87-10541 01-46)
(Grants NGL-05-005-007; NSF INT-8119963)
Avail: CEPADUES, Toulouse

The injection boundary beyond which fresh hot plasma appears each magnetospheric substorm is generalized and extended to circle the Earth. The concept of an auroral shell representing the inner limit of active auroral processes is introduced. It is proposed that at low altitudes, this shell marks the equatorward edge of the auroral ovals, and that at high altitudes, it marks the injection boundary. The auroral ring is defined as the intersection of the auroral shell with the magnetic equator. A simple equation for computing the expected location of the auroral ring as a function of local time and magnetic disturbance level is obtained. Tests indicate that the model is valid and reasonably accurate. ESA

N87-10558 Texas Univ. at Dallas, Richardson. Center for Space Sciences.

THE DISTANT MAGNETOTAIL

Walter J. Heikkila and J.-P. Treilhou (Centre d'Etude Spatiale des Rayonnements, Toulouse, France) *In* CNES Results of the ARCAD 3 Project and of Recent Programs in Magnetospheric and Ionospheric Physics 1985 p 281-288 (For primary document see N87-10541 01-46)
(Grants NsG-5085; CNES-73-212)
Avail: CEPADUES, Toulouse

Satellite, balloon, aircraft, and ground-based data for a night when variations in the interplanetary magnetic field caused a series of small substorms are presented. The data indicate that a series of small plasmoids was formed in the magnetotail, travelled tailward rubbing on closed field lines, and produced poleward traveling auroral features as the ionospheric footprint of the plasmoids. When the plasmoids cross the X-line and magnetopause onto interplanetary magnetic field lines, they lose connection with the Earth and the auroral features disappear. In this instance, the closed field line portion reached up to 80 deg geomagnetic latitude, over 10 deg poleward from the auroral oval. ESA

N87-10559 Johns Hopkins Univ., Laurel, Md. Applied Physics Lab.

DYNAMIC VARIATIONS OF THE AURORAL PRECIPITATION AND THE POLAR CAP

Ching-I. Meng *In* CNES Results of the ARCAD 3 Project and of Recent Programs in Magnetospheric and Ionospheric Physics 1985 p 289-309 (For primary document see N87-10541 01-46)
Avail: CEPADUES, Toulouse

Satellite observations of polar region precipitations are discussed. The morphology of auroral electron precipitation and its variations with the interplanetary magnetic field (IMF) and substorm activity are presented. Implications for magnetospheric configuration and solar-terrestrial interaction are considered. Results indicate that the unusually high latitude of the precipitation poleward boundary is due to a very small number of geomagnetic flux lines interconnected with the IMF during a northward IMF condition. The size of the polar cap is inversely controlled by the magnitude of the northward Bz component. The insensitivity of the equatorward precipitation boundary to the northward IMF Bz means that its dynamics is dominated by internal magnetospheric processes and not by direct solar-magnetospheric interactions. The dawn-dusk and noon-midnight dimensions of the polar cap vary in harmony with the AE index. ESA

N87-10560 Academy of Sciences (USSR), Moscow. Inst. of Space Research.

POLAR CAP PARTICLE PRECIPITATION AS MEASURED BY THE AUREOL-3 AND INTERCOSMOS-19 SATELLITES

F. K. Shuiskaya, A. D. Boljunova, J. M. Bosqued (Centre d'Etude Spatiale des Rayonnements, Toulouse, France), H. Reme, and J. Cuvilo *In* CNES Results of the ARCAD 3 Project and of Recent Programs in Magnetospheric and Ionospheric Physics 1985 p 313-329 (For primary document see N87-10541 01-46)
Avail: CEPADUES, Toulouse

Polar cap measurements of low energy charged particles by AUREOL-3 and Intercosmos-19 satellites are discussed. Polar cap arcs are detected by the plasma experiments at latitudes greater than 78 deg during periods of moderate geomagnetic activity and northward directed interplanetary magnetic field Bz component. They correspond to intense electron precipitation with energies less than 0.5 to 1 kev with Maxwellian distributions. Analysis of anticorrelations between electron and ion precipitation fluxes and the detection of energy-peaked distributions can indicate electron acceleration by a field-aligned potential drop. During the recovery phase of a substorm, precipitating electrons were recorded with energies of 5 kev with intensity of 10 million el/sqcm/s sr kev at 87 deg. ESA

N87-10561 Centre d'Etude Spatiale des Rayonnements, Toulouse (France).

EVIDENCE FOR ION ENERGY DISPERSION IN THE POLAR CUSP RELATED TO A NORTHWARD DIRECTED INTERPLANETARY MAGNETIC FIELD (IMF)

J. M. Bosqued, J. A. Sauvaud, H. Reme, J. Crasnier, D. Roux (Centre de Recherches en Physique de l'Environnement, Saint Maur des Fosses France), Yu. I. Galperin (Academy of Sciences (USSR), Moscow), T. M. Muliarchik, and V. A. Gladyshev *In* CNES Results of the ARCAD 3 Project and of Recent Programs in Magnetospheric and Ionospheric Physics 1985 p 331-341 (For primary document see N87-10541 01-46)
(Grant CNES-212)
Avail: CEPADUES, Toulouse

Mechanisms of energy, momentum, and particle transfer from the solar wind to the Earth magnetosphere are discussed. Data from the particle experiment aboard the AUREOL-3 polar satellite show that 30% of the summer cusp crossings are characterized by a clear latitudinal energy dispersion of the solar wind ions. This energy-latitude correlation is observed at very high latitudes (80 deg to 85 deg) near the polar boundary of the cusp, as an increase of the ion average energy with latitude. These structures have a typical latitude extent of 1 to 2 deg at ionospheric heights and correspond to a northward-directed interplanetary magnetic field. The observations are consistent with a sunward convection of the foot of the magnetic flux tubes recently merged with a northward directed interplanetary magnetic field. ESA

N87-10562 Danish Meteorological Inst., Copenhagen. Div. of Geophysics.

POLAR CAP/POLAR CUSP STUDIES USING INCOHERENT SCATTER RADAR FACILITIES

T. S. Joergensen *In* CNES Results of the ARCAD 3 Project and of Recent Programs in Magnetospheric and Ionospheric Physics 1985 p 343-351 (For primary document see N87-10541 01-46)
Avail: CEPADUES, Toulouse

The application of incoherent scatter radar for polar cap and cusp studies is discussed and investigations of plasma convection in the very high latitude ionosphere are reported. Results show that the sunward convection at auroral latitudes turns antisunward toward high polar latitudes over a considerable range of local time around noon, and that there is little evidence of a narrow throat through which the bulk of sunward plasma convection is channeled into the polar cusp. It is found that the predominant east-west convection poleward of the dayside convection reversal region depends on the interplanetary magnetic field (IMF) By component, and that the IMF Bz component affects convection in a wide latitude range in all local time sectors. The time lag between the occurrence of an IMF change at the front of the magnetopause and the corresponding change in the convection is at the most 15 to 20 min. ESA

N87-10563 SRI International Corp., Menlo Park, Calif.

OBSERVATIONS OF POLAR-CAP IONOSPHERIC SIGNATURES OF POLAR WIND/MAGNETOSPHERE COUPLING

O. delaBeujardiere, V. B. Wickwar, and J. D. Kelly *In* CNES Results of the ARCAD 3 Project and of Recent Programs in Magnetospheric and Ionospheric Physics 1985 p 353-365 (For primary document see N87-10541 01-46)
(Grants NSF ATM-80-24889; NSF ATM-81-21671)
Avail: CEPADUES, Toulouse

The influence of the interplanetary magnetic field (IMF) on plasma convection, density, and temperature was examined using 24 hr incoherent scatter radar observations. While the radar was in the noon sector the IMF Bz was north and the By component changed direction around local noon. The convection reversal from sunward to antisunward occurred along a latitude that smoothly increased on either side of noon. The F-region densities were the largest in the westward drifting part of the afternoon convection cell. At 1900 MLT (2100 UT) the IMF direction reversed and its magnitude increased. The plasma convection pattern became sunward within the entire radar field of view. This sunward convection, in the polar cap, persisted as long as By remained positive, regardless of the sign of Bz. The observations indicate that the By component is significant in controlling ion drift, even in the night side of the convection. ESA

N87-10564 Centre d'Etude Spatiale des Rayonnements, Toulouse (France).

EVIDENCE FOR HIGH LATITUDE IONOSPHERIC ION ACCELERATION

H. Reme, J. M. Bosqued, J. A. Sauvaud, D. Roux (Centre de Recherches en Physique de l'Environnement, Saint Maur des Fosses France), R. A. Kovrazhkin (Academy of Sciences (USSR), Moscow), and F. K. Shuiskaya *In* CNES Results of the ARCAD 3 Project and of Recent Programs in Magnetospheric and Ionospheric Physics 1985 p 367-379 (For primary document see N87-10541 01-46)

Avail: CEPADUES, Toulouse

The SPECTRO experiment energetic ion composition spectrometers on AUREOL-3 satellite measured ion features in the ranges 0.01 to 14 keV/Q and 1 to 32 amu. At high latitude the spectrometers analyzed upflowing and downflowing nearly transverse ion streams. Inside the auroral oval, transversely accelerated ions (TAI) associated with electron precipitation are relatively frequent. Above the polar cap, TAI are observed at AUREOL-3 altitudes. The ions are mainly O(+), observed in all MLT sectors and in the 400 to 2000 km altitude range of the satellite, showing that the acceleration mechanisms are efficient at very low altitude and can operate on a broad scale. In the auroral region TAI are interpreted as the result of a strong heating by electrostatic ion cyclotron waves. Ionospheric ions accelerated above the polar cap with an energy between 10 and 200 eV are not consistent with predictions and observations of polar wind composition. All the ions constitute an important source of energetic magnetospheric plasma. ESA

N87-10565 Centre de Recherches en Physique de l'Environnement, Saint Maur des Fosses (France).

VERTICAL TRANSPORT OF O(+) IONS AT HIGH LATITUDES

D. Roux, J. J. Berthelier, V. A. Gladyshev (Academy of Sciences (USSR), Moscow), L. V. Zinnie, V. D. Maslov, and Pivovarov *In* CNES Results of the ARCAD 3 Project and of Recent Programs in Magnetospheric and Ionospheric Physics 1985 p 381-390 (For primary document see N87-10541 01-46)

Avail: CEPADUES, Toulouse

The ion mass spectrometer on AUREOL-3 measured the angular and energy distribution for each thermal ion species in order to determine ion concentration, temperature, and three dimensional velocity vector. Data obtained in the auroral zones and polar cap reveal a significant component along the magnetic field lines. A downward flow of O(+) in the noon sector of the polar cap, and a reversal of the O(+) flow along B from upward to downward, associated with changes in the structure and intensity of energetic electron precipitations are discussed. The first observation agrees with a model proposed by Whitteker (1977) to determine the ionospheric perturbations induced by soft particle precipitations. The second indicates that heating processes act with different time constants upon the vertical velocity and temperature of ionospheric ions. ESA

N87-10566 Academy of Sciences (USSR), Moscow. Inst. of Space Research.

NONSTATIONARY FIELD-ALIGNED FLUXES OF THERMAL IONS O(+) AND H(+) OUTSIDE THE PLASMAPAUSE: REFINEMENT OF THE POLAR WIND THEORY

L. V. Zinin, Yu. I. Galperin, K. S. Latyshev (Kalingrad State Univ., USSR), and S. A. Grigoriev *In* CNES Results of the ARCAD 3 Project and of Recent Programs in Magnetospheric and Ionospheric Physics 1985 p 391-408 (For primary document see N87-10541 01-46)

Avail: CEPADUES, Toulouse

A nonstationary model of polar wind was constructed for the night-latitude ionosphere, consisting of ions O(+), H(+), O2(+) and NO(+). Calculations show that for an initial O(+) density altitude profile which sufficiently differs from a stationary profile, the O(+) ion velocities can reach 2 km/sec in the magnetosphere. The stationary O(+) altitude profile restores density in 1 to 1.5 hr, and velocity in 2.0 to 2.5 hr. This suggests that altitude distributions of thermal ions convecting across the polar cap have no time to reach an equilibrium distribution. Hence in the polar upper ionosphere the considerable velocities of field-aligned motions of O(+) ions are expected at high altitudes, and increase at dayside cusp and at polar cap boundary where auroral heating and ionization disturb altitude profiles of the thermal plasma. ESA

N87-10567 Academy of Sciences (USSR), Moscow. Inst. of Space Research.

FIELD-ALIGNED MOTIONS OF O(+) AND H(+) THERMAL IONS IN A MAGNETIC FIELD TUBE CONVECTED ACROSS THE DAYSIDE POLAR CUSP: MODEL CALCULATIONS

L. V. Zinin, Yu. I. Galperin, and K. S. Latyshev (Kalingrad State Univ., USSR) *In* CNES Results of the ARCAD 3 Project and of Recent Programs in Magnetospheric and Ionospheric Physics 1985 p 409-416 (For primary document see N87-10541 01-46)

Avail: CEPADUES, Toulouse

A nonstationary hydrodynamic model of thermal ion motion and density in the magnetospheric field tube shows that ion heating and ionization in the polar cusp strongly affect the field-aligned velocities of O(+) ions, while H(+) velocities reach equilibrium much faster and so are less sensitive to disturbances experienced by a tube during cusp crossing. Differential fluxes of O(+) ions become 10 times greater than for the stationary profile. The total escape ion flux after cusp crossing by a field tube is greater than 50% O(+) ions. The O(+) velocity at great altitudes in a tube which crossed the cusp reaches 3 km/sec. The O(+) ions are predominant in density in all the altitude range and their flux to the magnetosphere is a very important source of magnetospheric ions during quiet times. At disturbed times, the integral flux of O(+) ions greatly increases. ESA

N87-10568 Academy of Sciences (USSR), Moscow. Inst. of Space Research.

FINE STRUCTURE OF FIELDS AND PLASMA IN THE FIELD-ALIGNED CURRENT REGION ON THE INTERCOSMOS-BULGARIA-1300 SATELLITE DATA

V. M. Balebanov, E. M. Dubinin, and I. M. Podgorny *In* CNES Results of the ARCAD 3 Project and of Recent Programs in Magnetospheric and Ionospheric Physics 1985 p 422-446 (For primary document see N87-10541 01-46)

Avail: CEPADUES, Toulouse

Electric and magnetic field fine structures, plasma density and velocity, and precipitating particle fluxes in electromagnetic shocks in the auroral regions at altitude 850 km observed by the Intercosmos-1300 satellite are discussed. Typical values of the transverse electric field component are 200 mV/m. Field aligned current densities reach hundreds micro A/sqm. The strong plasma density fluctuations of several tens percent are usually observed in the microstructures. The data are discussed in terms of electromagnetic models with effects of anomalous resistivity. ESA

N87-10569 Academy of Sciences (USSR), Apatity. Polar Geophysical Inst.

SMALL SCALE STRUCTURES OF ELECTRIC FIELD VARIATIONS AND PARTICLE PRECIPITATIONS AS OBSERVED ONBOARD AUREOL-3 SATELLITE

E. E. Titova, V. E. Yurov, M. M. Mogilevsky, O. A. Molchanov, I. G. Shibaev, A. A. Galeev, Yu. I. Galperin, N. V. Jorjio, R. A. Kovrazhkin, V. V. Krasnoselskikh et al *In* CNES Results of the ARCAD 3 Project and of Recent Programs in Magnetospheric and Ionospheric Physics 1985 p 447-464 (For primary document see N87-10541 01-46)

Avail: CEPADUES, Toulouse

From AUREOL-3 satellite VLF-measurements in the multicomponent waveform VLF-data transmission mode, strong low-frequency electric field variations with amplitudes up to 50 to 200 mV/m are studied. The variations can have bipolar impulses with duration less than or = 0.1 sec, but usually have more complex and/or short duration waveforms. In the second case the frequency spectrum decreases at frequencies less than 50 to 200 Hz. The ratio of the field aligned to the perpendicular component is variable, but with statistical predominance of perpendicular component. The regions of such electric field variations and energetic particle fluxes are well correlated, but their detailed correspondence is not always present. The electric field variations can be generated as a result of an initial nonstationarity of particle fluxes, in the nonlinear stage of the ion-cyclotron instability, or due to current-driven instability of downward hot electron beams and upward cold (or suprathermal) ion fluxes. ESA

N87-10570 Centre National de la Recherche Scientifique, Orleans (France). Lab. de Physique et Chimie de l'Environnement.

ATTENUATION BANDS AND CUT-OFF FREQUENCIES FOR ELF ELECTROMAGNETIC WAVES c32

J. L. Rauch, J. C. Cerisier (Centre de Recherches en Physique de l'Environnement, Saint Maur des Fosses France), J. J. Berthelier, F. Lefeuvre, N. Boudko (Academy of Sciences (USSR), Moscow), G. Michailova, and O. Kapustina *In* CNES Results of the ARCAD 3 Project and of Recent Programs in Magnetospheric and Ionospheric Physics 1985 p 465-484 (For primary document see N87-10541 01-46)
Avail: CEPADUES, Toulouse

The propagation characteristic of ELF (10 to 1500 Hz) electromagnetic waves observed on ARCAD 3, in 3 different zones: low L value (L less than 4), medium L values (4 less than L less than 6) and high L values (L less than 6) are discussed. Unambiguous determinations of the wave normal directions are obtained from the interpretations of the measurements of four (three magnetic, one electric) wave field components. The analysis is based on the Means method for highly polarized waves and on the Storey and Lefeuvre method in the other cases. The propagation characteristics of the waves in a multiple ion plasma, and the cut-off frequencies at and below the local proton gyrofrequency are discussed. ESA

N87-10571 Academy of Sciences (USSR), Moscow.

POLARIZATION OF ELECTROMAGNETIC WAVES RECORDED ON BOARD THE AUREOL-3 SATELLITE c32

F. Lefeuvre (Centre National de la Recherche Scientifique, Orleans, France), J. L. Rauch, L. V. Volkomiskaya, and B. Lundin *In* CNES Results of the ARCAD 3 Project and of Recent Programs in Magnetospheric and Ionospheric Physics 1985 p 485-498 (For primary document see N87-10541 01-46)
Avail: CEPADUES, Toulouse

The detection, on board AUREOL-3 satellite, of left magnetoplasma waves in a frequency range where only right waves are predicted by the magnetoionic theory is discussed. The validity of the methods used to determine the sense of polarization of electromagnetic emissions, which assume that the wave is a plane wave, is questioned. A method based on the sign of the imaginary part of the cross-spectrum between two magnetic wave field components is discussed. It is valid for non-plane waves as well as for plane waves. Abnormal polarizations are shown to be correlated with scintillations in the telemetry signal. ESA

N87-10572 Nagoya Univ., Toyokawa (Japan). Research Inst. of Atmospherics.

THE DIRECTION FINDING ABOARD AUREOL-3 OF ELF WAVES AT FREQUENCY ABOVE AND BELOW THE PROTON GYROFREQUENCY c32

M. Hayakawa, F. Lefeuvre (Centre National de la Recherche Scientifique, Orleans, France), and J. L. Rauch *In* CNES Results of the ARCAD 3 Project and of Recent Programs in Magnetospheric and Ionospheric Physics 1985 p 499-507 (For primary document see N87-10541 01-46)
Avail: CEPADUES, Toulouse

The systematic direction finding system developed for the analyses of the ELF waves (mode C1) on the AUREOL-3 satellite is described. It is based on the use of one and two plane wave models. Sensor outputs are fast Fourier transformed every 80 msec with a frequency resolution of 12.5 Hz. Averaged spectral matrices are estimated at 120 frequencies, using 9 successive spectral matrices over the period of 0.72 sec (=80 msec x 9). The averaged spectral matrices are used to estimate the frequency dependence of the degree of polarization of the coherence function and of the refractive index deduced from the wave data. For simplicity, direction finding is done at 8 specific frequencies only (175 to 1275 Hz) lower frequencies falling below the local proton gyrofrequency, fH (H+). Direction finding for the frequency above fH (H+) with only one whistler mode, and below fH (H+) where two modes are possible are covered. ESA

N87-10573 Centre de Recherches en Physique de l'Environnement, Saint Maur des Fosses (France).

DENSITY GRADIENT INSTABILITY IN THE HIGH LATITUDE IONOSPHERE. RELATION WITH THE ELECTROSTATIC TURBULENCE AND CONVECTION c32

J. C. Cerisier, J. J. Berthelier, C. Beghin (Centre National de la Recherche Scientifique, Orleans, France), and D. Roux *In* CNES Results of the ARCAD 3 Project and of Recent Programs in Magnetospheric and Ionospheric Physics 1985 p 509-516 (For primary document see N87-10541 01-46)
Avail: CEPADUES, Toulouse

Electron density irregularities at medium scale (from a few to a few tens of kilometers) observed in the high latitude topside ionosphere by the satellite AUREOL-3 are described. The irregularities are characterized by a large extension along the magnetic field, revealed by their ducting effect on the ELF down-going hiss; and an asymmetrical structure in the direction perpendicular to the magnetic field. On one side of the density enhancement, an intense electrostatic turbulence is observed, the other side is steeper and appears stable. The observations suggest that the density irregularities are convected by the DC electric field and that the instabilities are of the gradient drift type. ESA

N87-10574 Centre National de la Recherche Scientifique, Orleans (France). Lab. de Physique et Chimie de l'Environnement.

EXPERIMENTAL EVIDENCE OF FIELD-ALIGNED ELF PLASMA DUCTS IN THE IONOSPHERIC TROUGH AND IN THE AURORAL ZONE c75

C. Beghin, J. C. Cerisier (Centre de Recherches en Physique de l'Environnement, Saint Maur des Fosses, France), J. L. Rauch, J. J. Berthelier, F. Lefeuvre, R. Debrie, O. A. Maltseva (Rostov State Univ., Rostov-on-Don, USSR), and N. I. Massevitch (Academy of Sciences (USSR), Moscow) *In* CNES Results of the ARCAD 3 Project and of Recent Programs in Magnetospheric and Ionospheric Physics 1985 p 517-527 (For primary document see N87-10541 01-46)
Avail: CEPADUES, Toulouse

The fine structure of the topside F-region electron density and the ELF hiss wave characteristics were measured simultaneously by the AUREOL/ARCAD 3 satellite. They suggest an efficient ducting mechanism by crests of ionization. Typical horizontal size of the plasma ducts lies in a range 5 to 50 km. The shape of the density structures and wave propagation characteristics exhibit a well marked difference between the inner and outer sides of the equatorward boundary of the midlatitude ionospheric through. Observation of small scale plasma instabilities and electrostatic turbulence occurring usually on the flanks of density enhancements strongly suggests that the ducts are convecting structures, assumed to be created in the auroral zone. ESA

N87-10575 Poitiers Univ. (France). Lab. de Physique de la Haute Atmosphere.

VERY LOW FREQUENCY SAUCERS WITH ATTENUATION BANDS c32

Y. Corcuff and M. Tixier *In* CNES Results of the ARCAD 3 Project and of Recent Programs in Magnetospheric and Ionospheric Physics 1985 p 529-535 Sponsored by Administration du Territoire des Terres Australes et Antarctique Francaises (For primary document see N87-10541 01-46)
Avail: CEPADUES, Toulouse

Forty-three VLF saucers exhibiting attenuation bands related to the proton gyrofrequency were observed on the ISIS satellites over the Antarctic in local winter. It is deduced that the generation/interaction region is located very near the satellite at distances often less than 50 km, either below or above it. It is found that saucers with attenuation bands are observed in the 2000 to 0500 local time sector, between 60 and 70 deg geomagnetic latitude, in an auroral region closely correlated to the plasmapause.

It is inferred that the equatorward edges of the saucers region and the plasma sheet are closely related. ESA

N87-10576 Centre National de la Recherche Scientifique, Orleans (France). Lab. de Physique et Chimie de l'Environnement.
INSTABILITIES ASSOCIATED WITH THE EQUATORIAL SPREAD-F PHENOMENON AND THEIR NORTH-SOUTH ASYMMETRY
C. Beghin, R. Pandey (Indian Space Research Organization, Ahmedabad), and D. Roux (Centre de Recherches en Physique de l'Environnement, Saint Maur des Fosses, France) *In* CNES Results of the ARCAD 3 Project and of Recent Programs in Magnetospheric and Ionospheric Physics 1985 p 537-546 (For primary document see N87-10541 01-46)
Avail: CEPADUES, Toulouse

Six north to south passes of AUREOL/ARCAD 3 satellite through the equatorial electron density depletion at variable altitude between 400 and 550 km, at night, during a 2 wk period are discussed. They exhibit a similar feature in plasma density irregularities thought to be associated with spread F phenomenon. The irregularities are found to be quasi-sinusoidal with a scale size of 2 km along the satellite trajectory and occur only on the northern edge of the equatorial electron density depletion. This implies a violation of the principle of conjugate mapping for those wavelengths. The observations are analyzed in terms of generation mechanisms. ESA

N87-10577 Ecole Polytechnique, Palaiseau (France). Centre de Physique Theorique.
SCENARIOS FOR THE GENERATION OF AURORAL KILOMETRIC RADIATION c32
D. LeQueau, R. Pellat, and A. Roux (Centre de Recherches en Physique de l'Environnement, Issy-les-Moulineaux, France) *In* CNES Results of the ARCAD 3 Project and of Recent Programs in Magnetospheric and Ionospheric Physics 1985 p 547-557 (For primary document see N87-10541 01-46)
Avail: CEPADUES, Toulouse

The maser synchrotron instability process is used to model auroral kilometric radiation (AKR) generation. The role of inhomogeneities in or near the source region is emphasized. The strong inhomogeneity of the geomagnetic field allows a description of the sources, a determination of the emission beam, and an explanation of observed AKR features (spectral bandwidth structures of the dynamical spectrum including the presence of harmonic emission). This inhomogeneous theory also predicts necessary conditions for the generation of the fundamental emission, that could be of observational significance and lead to experimental test of the theory. The role of density gradients is discussed. Nonlinear mechanisms leading to a limitation of the emitted intensity are presented. ESA

N87-10578 Maryland Univ., College Park. Inst. for Physical Science and Technology.
THE CYCLOTRON MASER THEORY OF AKR AND Z-MODE RADIATION c32
C. S. Wu *In* CNES Results of the ARCAD 3 Project and of Recent Programs in Magnetospheric and Ionospheric Physics 1985 p 559-570 (For primary document see N87-10541 01-46)
(Grant NGL-21-002-005)
Avail: CEPADUES, Toulouse

The cyclotron maser mechanism which may be responsible for the generation of auroral kilometric radiation and Z-mode radiation is discussed. The relativistic effect of the cyclotron resonance is considered. A computer simulation which elucidates the nonlinear saturation of the maser instability is summarized. ESA

N87-10579 British Antarctic Survey, Cambridge (England). Space Plasma Physics Section.
NONTHERMAL CONTINUUM-TERRESTRIAL MYRIAMETRIC RADIATION NARROWBAND ELECTROMAGNETIC EMISSION c32
Dyfrig Jones *In* CNES Results of the ARCAD 3 Project and of Recent Programs in Magnetospheric and Ionospheric Physics 1985 p 571-577 (For primary document see N87-10541 01-46)
Avail: CEPADUES, Toulouse

Theories for the generation of terrestrial myriametric radiation are reviewed. Gyrosynchrotron emission, linear mode-conversion of upper-hybrid to L-O mode waves, and nonlinear interaction of upper-hybrid and lower-hybrid waves are considered. Observations support best the linear mode-conversion theory where the L-O radiation is emitted in a density gradient at frequencies near the plasma frequency. Thus the emission is inherently narrow-banded. The continuum is formed by multiple reflections within the magnetospheric cavity of radiation of different frequencies from different sources. Observations of narrowband emissions from density gradients at the plasmapause and magnetosheath and of analogous radiation from the Io plasma torus and magnetosheath at Jupiter support the linear theory. No observational evidence for the coexistence in source regions of upper hybrid and lower hybrid waves as required by the nonlinear theory is reported. ESA

N87-10580 Academy of Sciences (USSR), Troitsk.
MECHANISM OF LOW-FREQUENCY WAVE PROPAGATION IN THE MAGNETOSPHERE c32
O. A. Molchanov, O. A. Maltseva (Rostov State Univ., Rostov-on-Don, USSR), and E. E. Titova *In* CNES Results of the ARCAD 3 Project and of Recent Programs in Magnetospheric and Ionospheric Physics 1985 p 579-598 (For primary document see N87-10541 01-46)
Avail: CEPADUES, Toulouse

Resonant scattering and channeling of VLF waves due to the small-scale plasma density irregularities caused by ion cyclotron waves near the equatorial plane is considered. This process leads to simultaneous existence of quasi-longitudinal and of quasi-resonant propagation modes and to diffusion of wave vector directions. It is shown that resonant scattering by wave irregularities is similar to optical scattering by diffraction gratings. ESA

N87-10581 Stanford Univ., Palo Alto, Calif. STAR Lab.
ACTIVE EXPERIMENTS FROM GROUND
U. S. Inan and R. A. Helliwell *In* CNES Results of the ARCAD 3 Project and of Recent Programs in Magnetospheric and Ionospheric Physics 1985 p 599-607 (For primary document see N87-10541 01-46)
(Contract NAS5-25688; Grant NGL-05-020-008; Contract N00014-82-K-0489; Grants DPP80-22282; DPP80-22540)
Avail: CEPADUES, Toulouse

Active experiments using ground based wave sources to study ionospheric and magnetospheric phenomena are summarized. Amplification of and emission generation by coherent ducted whistler mode signals in the magnetosphere; precipitation of radiation belt particles by controled injection of VLF waves from ground based sources; spectral broadening of VLF transmitter signals during transionospheric propagation; and generation of ELF/VLF signals by HF heating of the auroral electrojet are discussed. ESA

N87-10582 Centre National de la Recherche Scientifique, Orleans (France). Lab. de Physique et Chimie de l'Environnement.
DETECTION FROM AUREOL-3 OF THE MODULATION OF AURORAL ELECTROJET BY HF-HEATING FROM ELF SIGNALS IN THE UPPER IONOSPHERE ABOVE TROMSOE (NORWAY)
F. Lefeuvre, J. L. Rauch, V. I. Dee (Academy of Sciences (USSR), Apatity), E. E. Titova, V. E. Yurov, O. A. Molchanov (Academy of Sciences (USSR), Troitsk), M. M. Mogilevsky, O. A. Maltseva (Rostov State Univ., Rostov-on-Don USSR), L. V. Zinin (Academy of Sciences (USSR), Moscow) 10(Max-Planck-Inst. fuer Aeronomie, Katlenburg-Lindau, West Germany), H. Kopka et al *In* CNES Results of the ARCAD 3 Project and of Recent Programs in Magnetospheric and Ionospheric Physics 1985 p 609-619 (For primary document see N87-10541 01-46)
Avail: CEPADUES, Toulouse

Extremely low frequency waves generated by artificial modulation of the auroral electrojet were detected on the AUREOL-3 satellite. The emission is seen on the EH electric antenna at all the modulation frequencies (525, 825, 1125, 1425 Hz) except at 15 Hz where the level of the natural emissions is too high. The amplitude, which increases with the frequency, reaches 5 microV/m at 1425 Hz. From time to time, a weak signal (0.1 mgamma) is detected on the magnetic BX and BZ antennas. The region of observations is very localized, but is 3 deg south of the L shell that crosses the expected heating zone. ESA

N87-10583 Nagoya Univ., Toyokawa (Japan). Research Inst. of Atmospherics.
STUDY OF THE MIDDLE LATITUDE BROADENING OF THE SPECTRUM OF THE WAVES EMITTED FROM GROUND c32
Y. Tanaka, M. Hayakawa, D. Lagoutte (Centre National de la Recherche Scientifique, Orleans, France), and F. Lefeuvre *In* CNES Results of the ARCAD 3 Project and of Recent Programs in Magnetospheric and Ionospheric Physics 1985 p 621-626 (For primary document see N87-10541 01-46)
Avail: CEPADUES, Toulouse

Spectral broadening in VLF wave field data acquired on AUREOL 3 satellite at middle latitudes is discussed. Broadening can be as high as 10% of the transmitter frequency, and it occurs only in ionospheric disturbed conditions. Spectrally broadened components are observed on EH antenna. The broadening may be interpreted as a doppler shift effect on the satellite in which the transmitter signals scatter from field-aligned irregularities in the F region and couple into quasi-electrostatic modes of small group velocity. Spectral broadening phenomena show side bands at a frequency interval centered on transmitter frequency. Bicoherence calculations demonstrate that they result from a nonlinear wave interaction between the transmitter signal and a natural emission occurring just above the local proton gyrofrequency. ESA

N87-10584 Academy of Sciences (USSR), Apatity. Polar Geophysical Inst.
ON THE SPECTRAL BROADENING OF THE GROUND-BASED VLF TRANSMITTER SIGNALS IN THE HIGH-LATITUDE IONOSPHERE OBSERVED FROM INTERCOSMOS-19 AND AUREOL-3 SATELLITES c32
E. E. Titova, A. M. Perlikov, V. E. Yurov, I. V. Lychkina, O. M. Raspopov, V. Yu. Trakhtengertz, O. A. Molchanov, O. A. Maltseve (Rostov State Univ., Rostov-on-Don, USSR), and Yu. I. Galperin *In* CNES Results of the ARCAD 3 Project and of Recent Programs in Magnetospheric and Ionospheric Physics 1985 p 627-644 (For primary document see N87-10541 01-46)
Avail: CEPADUES, Toulouse

The effect of spectral broadening of VLF signals propagating through the turbulent polar ionosphere (300 to 500 Hz) is discussed. Two-satellite observation results show that the electric component prevails in a broadened signal (BS); the effect is independent of transmitter power; and BS is in a good correlation with the appearance of ELF electrostatic noise. Digital processing of BS reveals 20 to 50 msec temporal variations and harmonic components at 30 to 40 recurrence frequency. At altitudes greater than 700 km the characteristic rate of frequency variation is 3000 to 30,000/sec/sec. Results indicate scattering of whistler waves by ion cyclotron turbulence near the oxygen ion gyrofrequency involving the transformation of an initial wave into the electrostatic plasma mode in the upper ionosphere. ESA

N87-10585 Academy of Sciences (USSR), Moscow. Inst. of Space Research.
PRECIPITATION OF ELECTRONS AND PROTONS IN THE SUBAURORAL ZONE STIMULATED BY GROUND-BASED VLF EMITTER
R. A. Kovrazhkin, M. M. Mogilevsky, O. A. Molchanov, Yu. I. Galperin, N. V. Jorjio, Yu. V. Lisakov, J. M. Bosqued, and H. Reme (Centre d'Etude Spatiale des Rayonnements, Toulouse, France) *In* CNES Results of the ARCAD 3 Project and of Recent Programs in Magnetospheric and Ionospheric Physics 1985 p 645-653 (For primary document see N87-10541 01-46)
Avail: CEPADUES, Toulouse

Electron and proton precipitation artificially stimulated by a groundbased VLF-emitter (F = 19.1 kHz, L = 4.0), were detected in the subauroral zone by the AUREOL-3 satellite at altitudes of 1500 to 2000 km in the MLT morning sector. The precipitation zone corresponds to the projection on the ionosphere of the ring current region (L = 2.8 to 3.6) and shifts equatorward with respect to the location of the VLF transmitter. The intensities of the artificial 0.1 to 2 keV electron fluxes range from 10,000 to 100,000 (sqcm sec ster/keV) those of the 60 to 220 keV protons from 1 to 100 (sqcm sec ster/keV). The 1.8 keV electron bursts are delayed by 1 sec with respect to the VLF pulses, and the 110 keV proton fluxes by 3 to 5 sec. Comparison of experimental results with theoretical estimates shows that Cerenkov and cyclotron interaction mechanisms between ring current particles and VLF waves can account for the precipitating particles. ESA

N87-10586 Stanford Univ., Palo Alto, Calif. STAR Lab.
DE-1/SIPLE VLF WAVE-INJECTION EXPERIMENTS c32
U. S. Inan *In* CNES Results of the ARCAD 3 Project and of Recent Programs in Magnetospheric and Ionospheric Physics 1985 p 655-659 (For primary document see N87-10541 01-46)
(Contract NAS5-25688; Grants DPP80-22282; DPP80-22540)
Avail: CEPADUES, Toulouse

Very low frequency (1 to 6 kHz) waves from Siple (Antarctica) were detected by the Dynamics Explorer 1 satellite in an almost field aligned orbit with apogee (4.6 Re) close to the geomagnetic equator. Results indicate that the injected signals, while propagating in the magnetosphere in the nonducted mode, are amplified, generate sidebands, and trigger VLF emissions. The propagation paths include direct nonducted paths and reflected modes involving propagation initially in a duct followed by a reflected nonducted path up to the satellite. Calibrated measurements of the wave magnetic and electric intensities are used to estimate the local refractive index. ESA

N87-10587 Academy of Sciences (USSR), Moscow. Inst. of Space Research.
VERY LOW FREQUENCY AND ELF EFFECTS IN THE UPPER IONOSPHERE CAUSED BY LARGE-SCALE ACOUSTIC WAVES IN THE LOWER IONOSPHERE OBSERVED FROM AUREOL-3 SATELLITE
Yu. I. Galperin, V. A. Gladyshev, N. V. Jorjio, R. A. Kovrazhkin, Yu. V. Lissakov, V. D. Maslov, L. M. Nikolaenko, R. Z. Sagdeev, O. A. Molchanov, M. M. Mogilevsky et al *In* CNES Results of the ARCAD 3 Project and of Recent Programs in Magnetospheric and Ionospheric Physics 1985 p 661-684 (For primary document see N87-10541 01-46)
Avail: CEPADUES, Toulouse

The active MASSA experiment studied the effects generated in the upper atmosphere and in the magnetosphere by a large-scale acoustic wave from a chemical explosion reaching ionospheric altitudes. The AUREOL-3 satellite crossed the corresponding magnetic force tubes by the time of the development of the electromagnetic processes expected in the lower ionosphere E-region above the explosion. Measurements reveal electromagnetic effects in the ionospheric and magnetospheric plasmas. Effects include nearly electrostatic ELF and VLF noises in the magnetic force tube based on the E-layer ionosphere above the explosion. Their area expands with a velocity of 0.6 km/sec, i.e., as of an acoustic wave in the lower ionosphere. An intense MHD wave is detected at L = 1.31, equatorwards from the explosion L-shell (L = 1.5). ESA

N87-10588 Academy of Sciences (USSR), Moscow. Inst. of Space Research.
EARTHQUAKE EFFECTS IN THE IONOSPHERE ACCORDING TO INTERCOSMOS-19 AND AUREOL-3 SATELLITE DATA
V. I. Larkina, V. V. Migulin, M. M. Mogilevsky, O. A. Molchanov, Yu. I. Galperin, N. V. Jorjio, M. B. Gokhberg, and F. Lefeuvre (Centre National de la Recherche Scientifique, Orleans, France) *In* CNES Results of the ARCAD 3 Project and of Recent Programs in Magnetospheric and Ionospheric Physics 1985 p 685-699 (For primary document see N87-10541 01-46)

Avail: CEPADUES, Toulouse

During low frequency electromagnetic noise observations from the Intercosmos-19 and OGO-6 satellites, bursts of ELF and VLF noises were found on passes nearly above the epicenters of earthquakes during the preseismic phase (up to several hours before the main shock) and also after the main shocks. Bursts of VLF noise are registered in a wide band centered on the L-shell of the future earthquake epicenter. A tendency for an activation of the VLF and ELF emissions with the approaching main shock is suggested by the data samples and by a change in the characteristics of the VLF emissions after an earthquake main shock. Probably the source of the VLF emissions connected with the earthquakes lies in the magnetosphere. ESA

N87-10589 Centre National de la Recherche Scientifique, Orleans (France). Lab. de Physique et Chimie de l'Environnement.

STUDY OF VLF EMISSIONS APPARENTLY ASSOCIATED WITH EARTHQUAKES FROM GROUND-BASED AND GEOS SATELLITES DATA

M. Parrot and F. Lefeuvre *In* CNES Results of the ARCAD 3 Project and of Recent Programs in Magnetospheric and Ionospheric Physics 1985 p 701-711 (For primary document see N87-10541 01-46)

Avail: CEPADUES, Toulouse

Very low frequency emissions associated with earthquakes were independently observed at the Kerguelen station and on the GEOS-1 and GEOS-2 satellites, at frequencies less than 10 kHz. Kerguelen observations were made on magnetic antennas, in a period when earthquakes of moderate intensity (M = 4.7) took place near the station. The GEOS observations were made from magnetic and electric antennas. The analysis used cases for which intense earthquakes (M greater than 5) occurred in regions close to the satellite longitude (GEOS-2 is geostationary and its geographical longitude is 22 E) with the satellite operating in a VLF mode. Methods of distinguishing between correlations and coincidences are discussed. ESA

N87-10590 Minnesota Univ., Minneapolis. School of Physics and Astronomy.

OBJECTIVES AND DESIGN OF THE ECHO 6 ELECTRON BEAM EXPERIMENT: LARGE IONOSPHERIC PERTURBATIONS AND ENERGETIC PARTICLE PATTERNS

J. R. Winckler, J. E. Steffen, P. R. Malcolm, K. N. Erickson, Y. Abe, and R. L. Swanson *In* CNES Results of the ARCAD 3 Project and of Recent Programs in Magnetospheric and Ionospheric Physics 1985 p 713-727 Sponsored by Minnesota Univ. Graduate Research Fund (For primary document see N87-10541 01-46) (Grant NsG-5088)

Avail: CEPADUES, Toulouse

The ECHO 6 sounding rocket was launched to detect and analyze conjugate electron echoes using duplex accelerators on the main payload and throwaway detectors separated in a pattern to cover the echo region. Although the system operated as expected, model calculations show that the absence of echoes is due to a greatly extended tail field, which increased bounce times and placed the echoes out of range. Electron beam interactions with the ionospheric plasma were studied. Electron gun pulses produced large electric probe signals covering the entire frequency range between DC and the system Nyquist frequency of 1250 Hz. A signal driven at the 1 kHz gun frequency and a naturally occurring resonance at 840 Hz near the 799 Hz proton gyrofrequency were studied. The 1 kHz signal response confirms that pulsed electron beams may serve as ELF wave sources in space. ESA

N87-10591 Centre de Recherches en Physique de l'Environnement, Saint Maur des Fosses (France).

ARTIFICIAL ION BEAM INTERACTION WITH THE AURORAL PLASMA

R. Pottelette, R. Treumann (Max-Planck-Inst. fuer Extraterrestrische Physik, Garching, West Germany), O. H. Bauer, and J. P. Lebreton (European Space Agency. European Space Research and Technology Center, ESTEC, Noordwijk Netherlands) *In* CNES Results of the ARCAD 3 Project and of Recent Programs in Magnetospheric and Ionospheric Physics 1985 p 729-734 Sponsored by CNES (For primary document see N87-10541 01-46)

Avail: CEPADUES, Toulouse

Results obtained during the PORCUPINE experiment on the interaction of an artificial conical beam with the background auroral plasma are presented. The results are compared to the measurements performed by the S3-3 satellite when natural ion conics are present. The comparison shows that conical ion beams can induce the same kind of electrostatic shocks and electrostatic turbulences as those recorded by S3-3. ESA

N87-10592 Bulgarian Academy of Science, Sofia. Central Lab. for Space Research.

INTERCOSMOS-BULGARIA-1300 SATELLITE: LARGE-SCALE STRUCTURE AND DYNAMICS OF THE POLAR IONOSPHERE DURING GEOMAGNETIC STORMS

K. Serafimov and I. Kutiev *In* CNES Results of the ARCAD 3 Project and of Recent Programs in Magnetospheric and Ionospheric Physics 1985 p 735-745 (For primary document see N87-10541 01-46)

Avail: CEPADUES, Toulouse

To analyze the auroral F-region dynamics during a geomagnetic storm, data from simultaneous measurements of electron precipitation fluxes in the energy range 0.2 to 15 kev, emission intensity of 6300 A, 5577 A and 4278 A, field aligned currents, ion drift, and density and temperature of the cold plasma around the midnight sector of the auroral oval, and data from ground based magnetometers were used. It is shown that the main structure characteristics have different inertia to the changes of the intensity of the auroral electrojet. ESA

N87-10593 Academy of Sciences (USSR), Moscow. Inst. of Space Research.

SOME RESULTS OF SCANNER SPECTROPHOTOMETRIC MEASUREMENTS OF AURORA AND AIRGLOW FROM IK-BULGARIA-1300 SATELLITE AND PROSPECTS OF SIMILAR MEASUREMENTS

V. M. Balebanov, A. K. Kuzmin, M. M. Gogoshev (Bulgarian Academy of Science, Sofia), Ts. N. Gogosheva, N. P. Petkov, and K. Kinev *In* CNES Results of the ARCAD 3 Project and of Recent Programs in Magnetospheric and Ionospheric Physics 1985 p 747-764 (For primary document see N87-10541 01-46)

Avail: CEPADUES, Toulouse

Magnetosphere-ionosphere scanner photometric observations from Intercosmos 1300 satellite are considered. For the onboard plasma measurement analysis continuous onboard spectrophotometric measurements of aurora and airglow in the subsatellite area are performed simultaneously with the measurements of the plasma characteristics on the satellite. Delineation of the physical processes in the underlying ionosphere is facilitated by combined analysis of the scanner data and the fixed vertical direction multifilter intensity-latitude profiles of the main auroral emissions. Study of small-scale auroral discrete forms from near-Earth satellites with imagers is discussed. ESA

N87-10594 Max-Planck-Inst. fuer Aeronomie, Katlenburg-Lindau (West Germany).

CONNECTION BETWEEN PARTICLE PRECIPITATIONS AND THE PLASMA SHEET DURING SUBSTORMS

G. Kremser *In* CNES Results of the ARCAD 3 Project and of Recent Programs in Magnetospheric and Ionospheric Physics 1985 p 765-774 (For primary document see N87-10541 01-46)

Avail: CEPADUES, Toulouse

The relationship between particle precipitation and the plasma sheet was studied using simultaneous measurements from balloons and a geostationary satellite during a substorm. Impulsive precipitation of electrons near earthward moving injection fronts, and interaction of hot unstably distributed plasma sheet electrons with whistler mode electromagnetic waves are directly related to plasma sheet dynamics. Impulsive precipitation is related to field aligned electron beams generated by local acceleration by magnetic field aligned electric fields. Electron distribution during wave particle interaction can be described by a bi-Maxwellian distribution function at energies between 3 and 70 keV and a power law function at higher energies. Both components are anisotropically distributed. Numerical calculations of the anisotropy and the wave growth rate agree with wave observations. Wave particle interaction generates strong pitch angle diffusion responsible for the precipitation. ESA

N87-10595 Centre d'Etude Spatiale des Rayonnements, Toulouse (France).

A MULTIPOINT STUDY OF A SUBSTORM ON 4 MARCH 1979

J. A. Sauvaud, J. P. Treilhou, A. Saint-Marc, H. Reme, J. Dandouras, A. Korth (Max-Planck-Inst. fuer Aeronomie, Katlenburg-Lindau West Germany), G. Kremser, G. K. Parks (Washington Univ., Seattle), A. N. Zaitzev (Academy of Sciences (USSR), Troitsk), V. Petrov et al *In* CNES Results of the ARCAD 3 Project and of Recent Programs in Magnetospheric and Ionospheric Physics 1985 p 775-796 (For primary document see N87-10541 01-46)
Avail: CEPADUES, Toulouse

Coordinated measurements performed in the solar wind (ISEE-3, IMP-8), at geostationary orbit (GEOS-2), in the tail (ISEE-1 and 2), at ionospheric level (SAMBO-79), and on the ground were used to study the magnetospheric response to a southward turning of the interplanetary magnetic field (IMF). The change of the IMF is immediately associated with an increase of the eastward and westward electrojets and the beginning of a tail-like deformation of the B-field geometry at geostationary orbit near midnight. After IMF reversal and before main substorm onset, the electrojets move southward in the night and day sectors. Results indicate that the bulk of the energy dissipated inside the magnetosphere during the 2 hr of southward IMF is directly extracted from the solar wind. Explosive energy release during the two last substorms is problematical. Storage of excess energy during the southward IMF episode cannot be excluded. Results support a model in which there is simultaneous storage and dissipation of the incoming energy. ESA

N87-10596 Kiruna Geophysical Inst. (Sweden).

OBSERVATIONS OF AURORAL ELECTRONS WITH SOUNDING ROCKETS AND THE GEOS-2 GEOSTATIONARY SATELLITE

Lars Eliasson, Ingrid Sandahl, and Rickard Lundin *In* CNES Results of the ARCAD 3 Project and of Recent Programs in Magnetospheric and Ionospheric Physics 1985 p 797-802 (For primary document see N87-10541 01-46)
Avail: CEPADUES, Toulouse

Electron energy distributions observed during sounding rocket campaigns are presented. Many properties of the distributions during discrete auroral events can be explained if an electric field parallel to the magnetic field lines exists. A discrete arc constitutes a temperature and density boundary in the magnetosphere. The acceleration region is calculated to have its lower border at 0.5 to 2 Re. During discrete auroras in the evening local time sector the Birkeland current can be carried by the energetic electrons. In that case the parallel electric field is a consequence of a magnetospheric dynamo requiring a current to flow along the magnetic field lines. ESA

N87-10597 European Space Agency. European Space Research and Technology Center, ESTEC, Noordwijk (Netherlands). Space Science Dept.

SIMULTANEOUS OBSERVATIONS OF Pc4 AND Pc5 ELECTRIC FIELDS IN THE NOON SECTOR WITH GEOS-1 AND GEOS-2

Rejean Grard and John Matthews *In* CNES Results of the ARCAD 3 Project and of Recent Programs in Magnetospheric and Ionospheric Physics 1985 p 803-816 (For primary document see N87-10541 01-46)
Avail: CEPADUES, Toulouse

Hydromagnetic oscillations were observed simultaneously by GEOS-1 and 2, with GEOS-1 at apogee close to GEOS-2, and identical double probe electric field detectors in operation on both spacecraft. Two periods of wave activity with markedly different characteristics are compared. The first period is a second harmonic resonance of the local geomagnetic field line. A magnetic oscillation with a typical rms amplitude of 2 nT and an electric field node are observed near the geomagnetic equator, but an electric field of the order of 2 mV/m is measured at geomagnetic latitude minus 12 deg. The average frequency of the wave is 10 mHz. The second event is an odd harmonic because the transverse wave magnetic field is vanishingly small near the equator while the electric field remains finite; electric field magnitude is comparable at larger magnetic latitude. This 5 mHz oscillation can be associated with the fundamental mode. Neither source is monochromatic. ESA

N87-10598 Centre de Recherches en Physique de l'Environnement, Issy-les-Moulineaux (France).

ENERGY SPECTRA OF ELECTRONS PRECIPITATING ABOVE THE EISCAT AREA. COMPARISON WITH ARCAD MEASUREMENTS

S. Perraut, D. Fontaine, N. Cornilleau-Wehrlin, J. M. Bosqued (Centre d'Etude Spatiale des Rayonnements, Toulouse, France), D. Alcayde, R. A. Kovrazhkin (Academy of Sciences (USSR), Moscow), A. Korth (Max-Planck-Inst. fuer Aeronomie, Katlenburg-Lindau West Germany), G. Kremser, and W. Kofman (Grenoble Univ., France) *In* CNES Results of the ARCAD 3 Project and of Recent Programs in Magnetospheric and Ionospheric Physics 1985 p 819-829 (For primary document see N87-10541 01-46)
Avail: CEPADUES, Toulouse

The energy distribution function of precipitating electrons directly measured by ARCAD 3 was computed from EISCAT measurements by the UNTANGLE method, which inverts a height profile of the ionospheric electron density into an incident energy spectrum, using a library of ionization production profiles for monoenergetic electrons. The excellent agreement confirms the validity of the method in the energy range from 1 to 10 keV. Results show that in the morning sector the spectra are very flat with an important high energy component; in the evening sector this component is absent. Energy peaks around 3 keV are observed during short time intervals. The results differentiate auroral forms: diffuse auroras or intense localized structures. ESA

N87-10599 Hydrometeorological Service of the USSR.

THE E REGION INSTABILITIES IN THE POLAR IONOSPHERE

Cl. Renard (Institut Univ. de Technologie, Bourges, France), S. I. Avdiuchine, and A. A. Pokhunkov *In* CNES Results of the ARCAD 3 Project and of Recent Programs in Magnetospheric and Ionospheric Physics 1985 p 831-840 (For primary document see N87-10541 01-46)
Avail: CEPADUES, Toulouse

Polar ionospheric electron density profiles obtained by sounding rockets are presented. Instabilities in horizontal and vertical density gradients are analyzed. ESA

N87-10600 Toulon Univ., La Garde (France).

THE ARCAD 3-SAFARI COORDINATED STUDY OF AURORAL AND POLAR F-REGION IONOSPHERIC IRREGULARITIES

J. P. Villain, C. Beghin (Centre National de la Recherche Scientifique, Orleans, France), and C. Hanuise *In* CNES Results of the ARCAD 3 Project and of Recent Programs in Magnetospheric and Ionospheric Physics 1985 p 841-853 Sponsored by Inst. National d'Astronomie et de Geophysique (For primary document see N87-10541 01-46)
(Contract CNRS-ERA-668)
Avail: CEPADUES, Toulouse

Ionospheric F-region irregularities were observed simultaneously with the SAFARI ground based HF radars and the ISOPROBE experiment on the AUREOL-3 satellite. Spectral power of electron density variations was calculated for wavelengths between 20 m and 1 km from ISOPROBE high time resolution thermal plasma measurements. One spectrum is obtained every 1.2 sec (= 10 km along the satellite trajectory). The SAFARI radars are sensitive to F-region ionospheric irregularities of 10 m wavelength in the polar and auroral ionosphere. The phase velocity of the irregularities obtained from the Doppler spectrum is related to the ambient plasma drift. Echoes observed with SAFARI are compared with the spectral power of electron density variations deduced from the ISOPROBE measurements. Good agreement is found, and a numerical value of the spectral power corresponding to detection of echoes by the radar is given. The event is interpreted according to theories on plasma irregularities. ESA

N87-10601 Academy of Sciences (USSR), Moscow. Inst. of Space Research.

TWO-DIMENSIONAL SNAPSHOTS OF ELECTRON DENSITY IN THE MAIN TROUGH AND DIFFUSE AURORAL ZONE FROM A CLOSE NETWORK OF IONOSONDES: COMPARISON WITH MEASUREMENTS FROM AUREOL-3 SATELLITE

N. P. Benkova, E. F. Kozlov, N. I. Samorokin, Yu. I. Galperin, and C. Beghin (Centre National de la Recherche Scientifique, Orleans, France) *In* CNES Results of the ARCAD 3 Project and of Recent Programs in Magnetospheric and Ionospheric Physics 1985 p 855-884 (For primary document see N87-10541 01-46)

Avail: CEPADUES, Toulouse

Coordinated ground and satellite F-region observations are used to construct two-dimensional height-latitude plots using the N-h profiles deduced from subauroral ionograms. Results show that oblique reflections from sharp latitudinal density gradients (and/or from curtains of inhomogeneities at these density gradients) constitute the main part of strong traces on the ionograms. The soft electron precipitation boundary (SEB) oval shape and positions agree with a quantitative SEB-position model as a function of Kp and MLT. As well as the main SEB, which marks the transition to high precipitation intensity in the diffuse auroral zone, one or more smaller steps at much lower particle intensities are observed at lower latitudes, inside the nightside main trough. ESA

N87-10602 National Aeronautics and Space Administration. Marshall Space Flight Center, Huntsville, Ala.

COMPARATIVE MAGNETOSPHERIC/IONOSPHERIC STUDIES USING DYNAMICS EXPLORER SPACECRAFT AND GROUND-BASED RADARS

James L. Green, M. O. Chandler, and C. R. Chappell *In* CNES Results of the ARCAD 3 Project and of Recent Programs in Magnetospheric and Ionospheric Physics 1985 p 884-894 Sponsored by NASA Office of Space Science and Applications and SPAN Pilot Project (For primary document see N87-10541 01-46)

Avail: CEPADUES, Toulouse

Coincident magnetosphere-ionosphere observations between the Dynamics Explorer 1 and 2 spacecraft with ground-based radar are reviewed. Ionospheric-magnetospheric coupling processes in the plasmasphere, main trough, auroral zone, and polar cap are inferred from the density, temperature, composition, and angular distributions of the low-energy plasma observed from the E-region ionosphere out into the magnetosphere to an altitude of 2.5 Re. From the polar cap to the inner plasmasphere, parallel and perpendicular electric fields, polar wind flow, and equilibrium diffusion appear to be involved in the ionospheric-magnetospheric coupling of the low energy plasma. ESA

N87-10603 Academy of Sciences (USSR), Yakutsk. Inst. of Cosmophysical Research and Aeronomy.

STEP-LIKE PROFILES OF ELECTRON DENSITY IN THE SUB-AURORAL LOWER F-REGION IN THE MORNING SECTOR AND POSSIBLE MECHANISMS OF THEIR FORMATION DURING SUBSTORMS: THE COMPARISON OF DATA OF GROUND-BASED IONOSONDES WITH THE AUREOL-3 SATELLITE MEASUREMENTS

V. L. Khalipov, L. D. Sivtseva, V. M. Filippov, L. M. Nikolaenko, A. E. Stepanov, J. M. Bosqued (Centre d'Etude Spatiale des Rayonnements, Toulouse, France), and C. Beghin (Centre National de la Recherche Scientifique, Orleans, France) *In* CNES Results of the ARCAD 3 Project and of Recent Programs in Magnetospheric and Ionospheric Physics 1985 p 895-916 (For primary document see N87-10541 01-46)

Avail: CEPADUES, Toulouse

Latitudinal profiles of electron density in the subauroral lower F-region are considered for the morning sector, from the data of a meridional chain of vertical and oblique sounding ionosphere stations. It is shown that during substorms the electron density on the polar wall of the main ionosphere trough can attain a step-like structure. Step-like density profiles at the polar edge of the ionospheric main trough were compared with simultaneous measurements of soft electron precipitations from the AUREOL satellites. It is shown that in the morning sector during a substorm the most equatorward step of the electron density increase, at the trough polar edge, coincides with the equatorial boundary of precipitations of soft electrons. In the morning sector it is displaced equatorward in respect to the soft auroral diffuse boundary. ESA

N87-10604 Kiruna Geophysical Inst. (Sweden).

GROWING ELECTROSTATIC WAVES WITH A WAVELENGTH OF 67 cm IN THE UPPER IONOSPHERE

Bengt Hultqvist *In* CNES Results of the ARCAD 3 Project and of Recent Programs in Magnetospheric and Ionospheric Physics 1985 p 917-936 (For primary document see N87-10541 01-46)

Avail: CEPADUES, Toulouse

Electrostatic waves of wavelength half of that of the EISCAT VHF radar (67 cm) generated by auroral electrons precipitating into the auroral zone ionosphere were studied. Wave frequency, growth rate, and beam flow velocity are estimated as function of propagation direction, beam density, and temperature and ionospheric density for situations in and near the auroral zone. Results show only a small dependence on propagation angle less than 80 deg of field line direction. Growth rate is proportional to beam density, except where it goes negative. Flow velocity can be well above 10,000 km/sec. ESA

N87-10605 Goettingen Univ. (West Germany). Inst. fuer Geophysik.

GENERATION OF Pc2 PULSATIONS BY ENERGETIC O(+) IONS

B. Inhester, U. Wedeken, A. Korth (Max-Planck-Inst. fuer Aeronomie, Katlenburg-Lindau, West Germany), S. Perraut (Centre de Recherches en Physique de l'Environnement, Issy-les-Moulineaux, France), and M. Stokholm (Bern Univ., Switzerland) *In* CNES Results of the ARCAD 3 Project and of Recent Programs in Magnetospheric and Ionospheric Physics 1985 p 937-942 (For primary document see N87-10541 01-46)

Avail: CEPADUES, Toulouse

Observational evidence that Pc2 pulsations with an amplitude of several nT on the ground are destabilized by energetic O(+) ions in the magnetospheric equatorial plane is presented. The Pc1 pulsations simultaneously observed on board GEOS-2 were not detected on the ground, which indicates that heavy ions were also present in the cold magnetospheric plasma. ESA

N87-10606 Max-Planck-Inst. fuer Aeronomie, Katlenburg-Lindau (West Germany).

SELF-CONSISTENT ANALYSIS OF HIGH DRIFT VELOCITY MEASUREMENTS WITH THE SCANDINAVIAN TWIN AURORAL RADAR EXPERIMENT (STARE) SYSTEM

L. A. Reinleitner and E. Nielsen *In* CNES Results of the ARCAD 3 Project and of Recent Programs in Magnetospheric and Ionospheric Physics 1985 p 943-947 (For primary document see N87-10541 01-46)

Avail: CEPADUES, Toulouse

The use of the STARE and SABRE coherent radar systems in geophysical research with the superimposed grid point method is discussed. The method permits an analysis of E-layer plasma irregularity phase velocity versus flow angle utilizing only STARE or SABRE data. Analysis confirms that the cosine law assumption breaks down for velocities near and exceeding the local ion acoustic velocities. The method improves understanding of naturally-occurring plasma irregularities in the E-layer. ESA

N87-10607 Academy of Sciences (USSR), Moscow. Inst. of Space Research.

COORDINATED DATA ON AURORAL ELECTRODYNAMICS FROM GROUND BASED RADAR DIAGNOSTICS AND AUREOL-3 SATELLITE

E. E. Timofeev, V. M. Smyshliaev, N. V. Jorjio, Yu. I. Galperin, J. M. Bosqued, J. J. Berthelier, M. K. Vallinkoski, and R. J. Pellinen

In CNES Results of the ARCAD 3 Project and of Recent Programs in Magnetospheric and Ionospheric Physics 1985 p 949-971
(For primary document see N87-10541 01-46)
Avail: CEPADUES, Toulouse

Coordinated ground-satellite measurements of VHF radar arcs, magnetic variations, and all-sky auroral imagery were performed with particle and field measurements from AUREOL-3 satellite. Analysis of two satellite passes in the evening (midnight) MLT sector in the conditions of predominantly northward (westward) ionospheric electric field show that inverted V-associated electrodynamical pattern is the same in both events. Model calculations show that meridional ionospheric (Hall-Pedersen) closing current direction is a decisive factor controling the direction of currents in the meridianal Birkeland current loop of the inverted V. An interpretative scheme of the hierarchy of meridional Birkeland current loops is proposed: zone 2 / zone 1 large-scale current loop, inverted V current loops, and auroral arc-associated current loops, all with the same direction of the ionospheric closing current, northward in the evening and southward in the morning. ESA

N87-10608 North Carolina State Univ., Raleigh.
A MODEL FOR THE EVOLVING STABLY STRATIFIED NOCTURNAL BOUNDARY LAYER BASED ON THE TURBULENT KINETIC ENERGY EQUATION Ph.D. Thesis
Avraham Lacser 1985 249 p
Avail: Univ. Microfilms Order No. DA8529444

A numerical and observational study of the nocturnal boundary layer (NBL) overlying a relatively flat terrain is described. The numerical model is one-dimensional (1-D), based on the equations of mean momentum, thermodynamic energy and turbulent kinetic energy with a mixing length closure scheme, and includes a predictive equation for the surface temperature and in-situ longwave radiational cooling. A large number of mixing length formulations were examined and compared for their effects on the predicted mean profiles as well as on the turbulent flux profiles. It was found that different mixing length schemes produce much greater differences in the profiles of the turbulent variances and covariances than in those of mean wind and temperature. A detailed comparison of model predictions and the Cabauw data (few nights) shows that the Delage (1974) mixing length formulation with the appropriate choice of the empirical constant beta predicted the vertical turbulent flux profiles and their temporal evolutions better than the other mixing length schemes. The recommended mixing length scheme predicts the Monin-Obukhov surface layer similarity functions in good agreement with their observed form. The turbulent fluxes can be represented well by scaling them with surface values and scaling the height with the NBL height. The ability of a 1-D model to predict some features in the real NBL was shown, but counter-gradient heat fluxes and full advection effects cannot be predicted by the current model. Dissert. Abstr.

N87-10609 Stanford Univ., Calif.
CRYOGENIC RESONANT-MASS GRAVITATIONAL WAVE DETECTORS Ph.D. Thesis
Massimo Bassan 1985 176 p
Avail: Univ. Microfilms Order No. DA8602453

Gravitational radiation was postulated by Einstein in 1916 as a direct consequence of general relativity. It is generated by dramatic astrophysical events, and the information it carries might have paramount astrophysical relevance. The effect of such waves on matter can be represented with a tidal force; however this effect on the Earth is so small that no direct experimental evidence of their discovery has yet been produced. Twenty five years after J. Weber's pioneering experiments, as many as 14 groups around the world are developing more and more sensitive detectors for gravitational waves. Many, including the one at Standard University, use Weber's original approach of a resonant mass antenna. The state of the art of this program is reviewed, with particular attention to experimental problems involved and the best strategies available today to overcome them. An analysis of the problem of sensitivity and bandwidth of resonant antennae is then given and an explicit algorithm is presented. A detailed description of the Standard detector is given. Improvements and modifications done after the last period of operation are described, as well as the calibration procedures used. Some preliminary data are reported about the current observation with the antenna, which is now operating with a noise temperature for pulse detection of 20 milliKelvin. Dissert. Abstr.

N87-10610 California Univ., Santa Barbara.
A COMPONENT DECOMPOSITION MODEL FOR EVALUATING ATMOSPHERIC EFFECTS IN REMOTE SENSING Ph.D. Thesis
Shusun Li 1985 151 p
Avail: Univ. Microfilms Order No. DA8609703

A radiance value of a target pixel recorded by a remote sensor can be decomposed into three components: attenuated target signature, pure atmospheric radiation, and the contribution made by the ground through the atmospheric scattering process. Given the meteorological and optical parameters of a layer-structured atmosphere, its transmittance and radiance distribution can be accurately calculated with a plane-parallel radiative transfer model. By applying the component decomposition model in an atmosphere with an underlying homogeneous Lambertian surface, the band-averaged pure atmospheric radiance and the downward and upward direct, diffuse, and total transmittances are calculated for the six reflective wavelength bands of the LANDSAT Thematic Mapper. By applying the component decomposition model in an atmosphere-snow system, the band-averaged upward atmospheric transmittances from an anisotropic snow surface are calculated and compared with their counterparts for Lambertian surfaces of the same albedo. Knowing the pattern of the surface anisotropic reflectance factor, an adjusted band-averaged point spread function can be calculated and be used to retrieve the upwelling radiance from an inhomogeneous surface with a stable anisotropic reflectance pattern. Dissert. Abstr.

N87-10611 California Univ., Davis.
A HIGH RESOLUTION ENTRAINMENT MODEL FOR THE CONVECTIVE PLANETARY BOUNDARY LAYER Ph.D. Thesis
Ray Francis Kamada 1985 193 p
Avail: Univ. Microfilms Order No. DA8607596

A theory for a high resolution model day-time growth or entrainment of the convective planetary boundary layer is developed. It is similar to other entrainment models in that it is based upon a parameterized form of the turbulent kinetic energy equation. It differs from other models in that it takes an ensemble averaged view of the actual, convoluted, inversion interface which tops the well-mixed region, rather than a lower resolution, spatially averaged view of the capping inversion and/or mixed layer regions. The theory uses a fractal method to estimate the enhancement of the surface area for an irregularly convoluted, discontinuous interface, while a mixed Lagrangian-Eulerian technique (virtual particle analysis) is developed to determine the thickness. The outcome is a fractal interfacial entrainment (FIE) model which predicts the time evolutions of the mixed layer height, its vertically averaged potential temperature, and the magnitude of the temperature jump across the inversion. The resulting mixed layer growth predictions are consistent with measurements under convective conditions observed during day 33 of the Wangara experiment. Dissert. Abstr.

N87-10612*# National Aeronautics and Space Administration, Washington, D.C.
ATMOSPHERIC OZONE 1985. ASSESSMENT OF OUR UNDERSTANDING OF THE PROCESSES CONTROLLING ITS PRESENT DISTRIBUTION AND CHANGE, VOLUME 1 Global Ozone Research and Monitoring Project
1985 505 p Prepared in cooperation with FAA, Washington, D.C., NOAA, Washington, D.C., United Nations Environment Program, Nairobi, Kenya, WMO, Geneva, Switzerland, Commission of the European Communities, Brussels, Belgium, and BMFT, Bonn (West Germany) Original contains color illustrations
(NASA-TM-89237; NAS 1.15:89237; WMO-Rept-16-Vol-1) Avail: NASA, Goddard Space Flight Center, Code 610, Greenbelt, Md. 20770 HC free; NTIS HC A22/MF A01 CSCL 04A

Topics addressed include: stratospheric chemistry; tropospheric trace gas (sources, distributions, and trends); tropospheric chemistry (processes, controlling the ozone and hydroxyl radicals); stratosphere-troposphere exchange; dynamic processes; and radiative processes (solar and terrestrial). For individual titles, see N87-10613 through N87-10618.

N87-10613*# National Aeronautics and Space Administration, Washington, D.C.
STRATOSPHERIC CHEMISTRY
R. A. Cox, W. B. DeMore, E. E. Ferguson, R. Lesclaux, A. R. Ravishankara, S. P. Sander, N. D. Sze, and R. Zellner *In its* Atmospheric Ozone 1985. Assessment of our Understanding of the Processes Controlling its Present Distribution and Change, Volume 1 1985 32 p (For primary document see N87-10612 01-46)
Avail: NASA, Goddard Space Flight Center, Code 610, Greenbelt, Md. 20770 HC free; NTIS HC A22/MF A01 CSCL 04A

Recent improvements in the data base for the currently identified reactions describing the chemistry of the major families of trace gas species, HO(x), NO(x), ClO(x), and hydrocarbons are assessed. The important coupling reactions between the families are introduced progressively. Chemical aspects such as heterogeneous reactions and reactions of sodium species, the importance of which are not yet completely established, are discussed. Recent attempts to reconcile some of the more unexpected kinetic behavior which has emerged from the extensive experimental studies of key reactions with current reaction rate theory are also examined. The uncertainties in the current kinetic and photochemical data base is given. The prospects for improvement of data for known reactions of atmospheric importance as well as for the identification of gaps in the chemical description of the atmosphere. B.G.

N87-10614*# National Aeronautics and Space Administration, Washington, D.C.
TROPOSPHERIC TRACE GASES
R. Gammon, S. C. Wofsy, R. J. Cicerone, A. C. Delany, R. T. Harriss, M. A. K. Khalil, J. A. Logan, P. Midgley, and M. Prather *In its* Atmospheric Ozone 1985. Assessment of our Understanding of the Processes Controlling its Present Distribution and Change, Volume 1 1985 62 p (For primary document see N87-10612 01-46)
Avail: NASA, Goddard Space Flight Center, Code 610, Greenbelt, Md. 20770 HC free; NTIS HC A22/MF A01 CSCL 04A

Trace gas concentrations in the atmosphere reflect in part the overall metabolism of the biosphere, and in part the broad range of human activities such as agriculture, production of industrial chemicals, and combustion of fossil fuels and biomass. There is compelling evidence that the composition of the atmosphere is now changing. Observed trends in trace gas levels are reviewed and implications for the chemistry of the atmosphere are discussed. Throughout the discussion, particular emphasis is given to those species which are now increasing in the atmosphere. B.G.

N87-10615*# National Aeronautics and Space Administration, Washington, D.C.
TROPOSPHERIC CHEMISTRY
V. A. Mohnen, W. Chameides, K. L. Demerjian, D. H. Lenschow, J. A. Logan, R. J. McNeal, S. A. Penkett, U. Platt, U. Schurath, and P. daSilva Dias *In its* Atmospheric Ozone 1985. Assessment of our Understanding of the Processes Controlling its Present Distribution and Change, Volume 1 1985 36 p (For primary document see N87-10612 01-46)
Avail: NASA, Goddard Space Flight Center, Code 610, Greenbelt, Md. 20770 HC free; NTIS HC A22/MF A01 CSCL 04A

The chemistry of the background troposphere, the source region, and the transition regions are discussed. The troposphere is governed by heterogeneous chemistry far more so than the stratosphere. Heterogeneous processes of interest involve scavenging of trace gases by aerosols, cloud and precipitation elements leading to aqueous phase chemical reactions and to temporary and permanent removal of material from the gas phase. Dry deposition is a major removal process for ozone, as well as for other gases of importance in tropospheric photochemistry. These processes are also discussed. B.G.

N87-10616*# National Aeronautics and Space Administration, Washington, D.C.
STRAT-TROP EXCHANGE
A. F. Tuck, E. V. Browell, E. F. Danielsen, J. R. Holton, D. Kley, A. J. Krueger, G. Megie, R. E. Newell, G. Vaughan, B. J. Hoskins et al *In its* Atmospheric Ozone 1985. Assessment of our Understanding of the Processes Controlling its Present Distribution and Change, Volume 1 1985 92 p (For primary document see N87-10612 01-46)
Avail: NASA, Goddard Space Flight Center, Code 610, Greenbelt, Md. 20770 HC free; NTIS HC A22/MF A01 CSCL 04A

Exchange between the stratosphere and troposphere is important to the chemical composition of both regions. The export of ozone from the stratosphere provides the troposphere with a means of initiating photochemistry. The precursor molecules originating from the planetary surface provide the stratosphere with its chemical feedstock from which the ozone-controlling HO(x), NO(x), and Cl(x) photochemistries are driven. The tropopause is defined both statistically and in a local, synoptic sense by the value P(sub theta) = .000016 K sq m/kg/s, taken from an objective analysis of 8 years of zonal, temporal mean cross sections of potential temperature, wind and potential vorticity. B.G.

N87-10617*# National Aeronautics and Space Administration, Washington, D.C.
DYNAMICAL PROCESSES
R. A. Plumb, D. G. Andrews, M. A. Geller, W. L. Grose, A. ONeill, M. Salby, and R. A. Vincent *In its* Atmospheric Ozone 1985. Assessment of our Understanding of the Processes Controlling its Present Distribution and Change, Volume 1 1985 110 p (For primary document see N87-10612 01-46)
Avail: NASA, Goddard Space Flight Center, Code 610, Greenbelt, Md. 20770 HC free; NTIS HC A22/MF A01 CSCL 04A

The techniques used to observe the middle atmosphere; the zonally-averaged and eddy structure of the middle atmosphere; seasonal variations and interannual variability; theoretical understanding of the middle atmospheric circulation are discussed. Recent satellite-based observational studies of stratospheric transport process, as revealed by the behavior of constituents and of potential vorticity (a dynamical tracer) are reviewed. The theory of global transport and its representation in transport models is discussed. B.G.

N87-10618*# National Aeronautics and Space Administration, Washington, D.C.
RADIATIVE PROCESSES
J. E. Frederick, C. Leovy, D. E. Anderson, Jr., G. P. Anderson, R. E. Dickinson, S. R. Drayson, S. Fels, L. A. Hall, J. Kiehl, J. E. Mentall et al *In its* Atmospheric Ozone 1985. Assessment of our Understanding of the Processes Controlling its Present Distribution and Change, Volume 1 1985 46 p (For primary document see N87-10612 01-46)
Avail: NASA, Goddard Space Flight Center, Code 610, Greenbelt, Md. 20770 HC free; NTIS HC A22/MF A01 CSCL 04A

Solar radiation and the processes that control its deposition in the Earth atmosphere are considered. The published data obtained since 1978 define a reference solar spectral irradiance for use in atmospheric chemical and dynamical studies, while long term satellite measurements are now providing information on variations in the output of the Sun over a range of time scales. As concerns absorption of solar radiation in the atmosphere, new cross section data for molecular oxygen and ozone are now available. Line-by-line calculations used to predict infrared flux divergences, both as regards assumptions made in radiative transfer calculations and in the spectroscopic parameters used as inputs are examined. Also examined are the influence of radiative processes on planetary scale wave activity, photochemical acceleration of radiative damping, and the breakdown of local thermodynamic equilibrium at mesospheric altitudes. B.G.

N87-10619# Atomic Weapons Research Establishment, Aldermaston (England).
SOME SEISMIC RESULTS OF AN UNDERGROUND EXPLOSION AT THE MURUROA TEST SITE (SHOT REPORT NO. 6)
R. C. Stewart and Penelope J. Warburton Mar. 1986 20 p
(AWRE-O-17/85; BR99175; ETN-86-97994) Avail: NTIS HC A02/MF A01

Data from an underground explosion at the Pacific test site at Mururoa recorded by seismological arrays in Australia, Brazil, Canada, India, and the UK are presented. Data include SP and BB results. ESA

N87-10620*# National Aeronautics and Space Administration. Langley Research Center, Hampton, Va.
DIRECT COMPUTATION OF ORBITAL SUNRISE OR SUNSET EVENT PARAMETERS
James J. Buglia Oct. 1986 37 p
(NASA-TM-87717; L-16155; NAS 1.15:87717) Avail: NTIS HC A03/MF A01 CSCL 04A

An analytical method is developed for determining the geometrical parameters which are needed to describe the viewing angles of the Sun relative to an orbiting spacecraft when the Sun rises or sets with respect to the spacecraft. These equations are rigorous and are frequently used for parametric studies relative to mission planning and for determining instrument parameters. The text is wholly self-contained in that no external reference to ephemerides or other astronomical tables is needed. Equations are presented which allow the computation of Greenwich sidereal time and right ascension and declination of the Sun generally to within a few seconds of arc, or a few tenths of a second in time. Author

N87-10621# National Oceanic and Atmospheric Administration, Boulder, Colo. Space Environment Lab.
SPACE ENVIRONMENT LABORATORY, FY 1985 Annual Report, 1 Oct. 1984 - 30 Sep. 1985
H. Leinbach 1985 49 p
(PB86-218567) Avail: NTIS HC A03/MF A01 CSCL 04A

Topics covered include: space environment services (space environment products and services, projects, equipment, and systems); systems support (operational satellite instrumentation, Space Environment Laboratory Solar Imaging System, scientific workstation system); research (solar physics, interplanetary physics, magnetospheric physics, atmospheric-ionosphere-magnetosphere interactions); staff; publications; and talks. GRA

N87-10622# National Geophysical Data Center, Boulder, Colo.
SOLAR-GEOPHYSICAL DATA NUMBER 501, MAY 1986. PART 2: (COMPREHENSIVE REPORTS). DATA FOR NOVEMBER 1985 AND MISCELLANEA
H. E. Coffey, ed. May 1986 41 p
(PB86-218047; SGD-501-Pt-2) Avail: NTIS HC A03/MF A01 CSCL 03B

Topics covered include: detailed index for 1985 to 1986; data for November 1985 (Meudon carte synoptique, solar flares, solar radio bursts at fixed frequencies, solar X-ray radiation from GOES satellite, and active prominences and filaments); and miscellaneus data (IAU quarterly bulletin on solar activity, Meudon observatory carte sypnotiques de la chromosphere solaire et catalogues des filaments et des centres d'activite). GRA

N87-10623# National Geophysical Data Center, Boulder, Colo.
SOLAR-GEOPHYSICAL DATA NUMBER 501, MAY 1986. PART 1: (PROMPT REPORTS). DATA FOR APRIL 1986, MARCH 1986 AND LATE DATA
H. E. Coffey, ed. May 1986 143 p
(PB86-218039; SGD-501-Pt-1) Avail: NTIS HC A07/MF A01 CSCL 03B

Topics covered include: detailed index for 1985 to 1986; data for April 1986 (advance and worldwide IUWDS alert periods, solar activity indices, solar flares, solar radio emission, VOSTOK inferred interplanetary magnetic field polarity, Stanford mean solar magnetic field); data for March 1986 (solar active regions, sudden ionospheric disturbances, solar radio spectral observations, cosmic ray measurements by neutron monitor, geomagnetic indices, radio propagation indices); and late data (solar radio spectral observations Culgoora February 1986, geomagnetic indices, calcium plage data, and daily maps June to October 1985). GRA

N87-10624*# National Geophysical Data Center, Boulder, Colo.
SOLAR-GEOPHYSICAL DATA NUMBER 499, MARCH 1986, SUPPLEMENT
Mar. 1986 87 p
(NASA Order W-15519; Grant NSF ATM-83-18491)
(NASA-CR-179797; NAS 1.26:179797; PB86-196102; SGD-499-Suppl) Avail: NTIS HC A05/MF A01 CSCL 03B

This supplement contains the description and explanation of the data in the monthly publication Solar-Geophysical Data, compiled by the National Geophysical Data Center (NGDC) in Boulder, Colo., USA. Solar-Geophysical Data is intended to keep research workers informed on a timely schedule of the major events of solar activity and the associated interplanetary, ionospheric, radio propagation and other geophysical effects. GRA

N87-10625*# National Geophysical Data Center, Boulder, Colo.
SOLAR-GEOPHYSICAL DATA NUMBER 499, MARCH 1986. PART 2: (COMPREHENSIVE REPORTS). DATA FOR SEPTEMBER 1986 AND MISCELLANEA
H. E. Coffey, ed. Mar. 1986 36 p
(NASA Order W-15519; Grant NSF ATM-83-18491)
(NASA-CR-179796; NAS 1.26:179796; PB86-196094; SGD-499-Pt-2) Avail: NTIS HC A03/MF A01 CSCL 03B

Solar-Geophysical Data Number 499, March 1986, Part 2 (Comprehensive Reports); Data for September 1985, and Miscellanea, contains the following: Detailed index for 1985 to 1986; Data for September 1985--(Solar flares, Solar radio bursts at fixed frequencies; Solar X-ray radiation from GOES satellite; Mass ejections from the Sun; Active prominences and filaments); (Meudon carte synoptique 7 July - 26 September 1985, Solar irradiance). GRA

N87-10626*# National Geophysical Data Center, Boulder, Colo.
SOLAR-GEOPHYSICAL DATA NUMBER 499, MARCH 1986. PART 1: (PROMPT REPORTS). DATA FOR FEBRUARY 1986, JANUARY 1986 AND LATE DATA
H. E. Coffey, ed. Mar. 1986 175 p
(NASA Order W-15519; Grant NSF ATM-83-18491)
(NASA-CR-179795; NAS 1.26:179795; PB86-196086; SGD-499-Pt-1) Avail: NTIS HC A08/MF A01 CSCL 03B

Solar-Geophysical Data Number 499, March 1986, Part 1 (Prompt Reports); Data for February 1986, January 1986 and Late Data, contains the following: Detailed index for 1985 to 1986; Data for February 1986--(IUWDS alert periods (Advance and worldwide), Solar activity indices, Solar flares, Solar radio emission, Vostok inferred interplanetary magnetic field polarity, Stanford mean solar magnetic field); data for January 1986--(Solar active regions, Sudden ionospheric disturbances, Solar radio spectral observations, Cosmic ray measurements by neutron monitor, Geomagnetic indices, Radio propagation indices); Late data-(Solar active regions, Solar radio spectral observations Culgoora, Cosmic ray measurements by neutron monitor, Calcium plage data). GRA

N87-10627 Wisconsin Univ., Madison.
CASE STUDIES OF THE STRUCTURE OF THE ATMOSPHERIC BOUNDARY LAYER ENTRAINMENT ZONE Ph.D. Thesis
Timothy D. Crum 1985 267 p
Avail: Univ. Microfilms Order No. DA8524260

The structure of the atmospheric entrainment zone, an interfacial layer between the convective boundary layer and the stable air aloft, was studied using data obtained during the Boundary Layer Experiment 1983 in Oklahoma. Coincident high resolution aircraft and lidar observations provided a picture of the daytime continental entrainment zone. Fast-response Lyman alpha hygrometer output voltages from the aircraft were calculated to yield meteorological units of humidity. These humidity measurements compare well with those made by ground-based sensors. Selection of specific humidity as a conditional sampling criteria for surface layer air in the entrainment zone results from a comparison of coincident aircraft data traces and ground-based lidar range height indicator scans. Using these conditional sampling criteria, two approaches were taken to describe the humidity structure of the entrainment zone. The first uses the linear mixing character of specific humidity. The second approach models frequency distributions of three types of air in the entrainment zone: unmixed free atmosphere (dry); unmixed surface layer air (moist); and a mixture of these two. Dissert. Abstr.

N87-10628 Washington Univ., Seattle.
A PHOTOMETRIC AND IN SITU STUDY OF STABLE AURORAL RED ARCS Ph.D. Thesis
Donald Wayne Slater 1985 162 p
Avail: Univ. Microfilms Order No. DA8603126

A history of the study of Stable Auroral Red (SAR) Arc occurrences between 1967 and 1984 (including the period of the international Magnetospheric Study) reveals 383 features that are interpreted to be SAR arcs; a listing is presented. A strong correlation of SAR arc occurrence frequency with the solar cycle is demonstrated, though with a two to three year phase lag. The large number of events available to this study has confirmed the direct association of SAR are occurrences with enhanced ring current fluxes. Clear evidence has demonstrated the consistent presence of precipitating low energy electrons into SAR arc locations identified by the Battelle operated MASP network. A search for electric currents resulting from this precipitation revealed no magnetic field fluctuations as expected to be associated with these fluxes. For the first time, atmospheric composition within SAR arcs is reported. Although there is evidence of significant compositional perturbation, the region over which this occurs is found to be considerably more extensive than the SAR arc itself. Auroral precipitation may be the primary cause of this perturbation. Calculations of the expected 6300 A volume emission rates and energy loss rates from the heated ionospheric electrons for a variety of neutral atmospheric compositions demonstrate the importance of recognizing these compositional perturbations. It is shown that molecular nitrogen becomes increasingly important as an energy sink as exospheric temperature is increased.
Dissert. Abstr.

N87-10629 Harvard Univ., Cambridge, Mass.
MILLIMETER-WAVE SPECTROMETRY OF OZONE IN THE MIDDLE ATMOSPHERE Ph.D. Thesis
Brian Joseph Connor 1985 163 p
Avail: Univ. Microfilms Order No. DA8602204

Pressure broadened linewidths of the rotational transitions of ozone were measured, for the foreign gases N2 and O2, over a pressure range of 200 to 1000 mTorr. The temperature dependence of the broadening was measured over the range 195 to 320 K. The air broadened lindewidth of the 6 (sub15)-6 (sub06) transition, was measured at 294 K, and is readily calculated, for other temperatures and transitions, from the N2 and O2 results. The results are compared with recent theoretical calculations, and also with previous measurements, where these are available. The measurements have direct application to the interpretation of observations of microwave emission of middle atmosphere ozone. The results also serve as reference points for theoretical linewidth calculations applicable from the microwave to the infrared spectral regions. Dissert. Abstr.

N87-10630 Colorado State Univ., Fort Collins.
NUMERICAL STUDIES OF THERMALLY AND MECHANICALLY FORCED CIRCULATIONS OVER COMPLEX TERRAIN Ph.D. Thesis
Raymond W. Arritt 1985 215 p
Avail: Univ. Microfilms Order No. DA8607627

Thermally and mechanically forced circulations over complex terrain are studied using one and two dimensional numerical simulations. Particular emphasis is placed on nocturnal katabatic winds (slope flows) and on upstream blocking of stratified flow. These phenomena are first examined independently, and then are combined so that their interactions can be evaluated. Upstream blocking in the absence of thermal forcing is found to be reasonably well described for air quality assessment purposes by the critical dividing streamline hypothesis. It is found that the highest pollutant concentrations are obtained on the windward side of the topography for contaminant sources within the blocked region and on the lee side for sources above the blocked region. Sensitivity experiments indicate that nocturnal slope flows decrease in intensity as the ambient thermal stratification increases. It is also found that slope winds can lead to high pollutant concentrations on windward slopes even when the Froude number is well above the range where upstream blocking is expected. Reasons why this behavior was not observed in previous studies of tracer flow around small hills are discussed. Dissert. Abstr.

N87-10631 Alaska Univ., Fairbanks.
GRAVITY WAVE DYNAMICS NEAR THE MESOPAUSE OVER POKER FLAT, ALASKA Ph.D. Thesis
Steven Andrews Smith 1985 206 p
Avail: Univ. Microfilms Order No. DA8612264

The characteristics of mesospheric gravity waves are studied using rocket and radar soundings. The soundings are examined in two different approaches: identification of individual, nearly monochromatic waves, and through the statistical view offered by spectral analysis of wind velocity fluctuations. Simultaneous rocket and radar data have provided a complete overview of the saturation of a large scale inertio-gravity wave near the summer mesopause. A comparison of vertical wavenumber spectra, of high spatial resolution of radar measurements, with a gravity wave model demonstrates that gravity waves dominate the mesospheric wind spectrum. The mesospheric spectra agree in shape and amplitude with similar spectra obtained in the stratosphere and troposphere. It is concluded that small scale gravity waves are saturated throughout the lower and middle atmosphere. Observations of the growth of wave amplitudes with height as seen in frequency spectral studies are compatible with the conclusion that the small scale waves are saturated since the vertical wavelengths of the largest saturing wave increases with height. Dissert. Abstr.

N87-10632 Michigan Univ., Ann Arbor.
OBSERVATIONAL AND THEORETICAL INVESTIGATION OF STABLE AURORAL RED ARCS AND THEIR MAGNETOSPHERIC ENERGY SOURCE, VOLUMES 1 AND 2 Ph.D. Thesis
Janet Urbanski Kozyra 1986 484 p
Avail: Univ. Microfilms Order No. DA8612558

The Stable Auroral Red (SAR) arc's nearly monochromatic emission at 6300 A is the ionospheric signature of an energy transfer process spanning tens of thousands of kilometers (the energy source being in the equatorial plasmasphere and the ultimate energy sink being in the F region). Thirty one coordinated data sets were compiled during which Dynamics Explorer-1 was at high altitudes and Dynamics Explorer-2 was at the F region heights during traversals of SAR arc field lines on dates identified by ground based photometry. The conclusions drawn from theoretical and statistical investigations are discussed.
Dissert. Abstr.

N87-10268*# National Aeronautics and Space Administration. Langley Research Center, Hampton, Va.
DEVELOPMENT OF A HIGH-ALTITUDE AIRBORNE DIAL SYSTEM: THE LIDAR ATMOSPHERIC SENSING EXPERIMENT (LASE)
E. V. Browell, W. R. Vaughan, W. M. Hall, J. J. Degnan, R. D. Averill, J. G. Wells, D. E. Hinton, and J. H. Goad *In its* 13th International Laser Radar Conference Aug. 1986 4 p (For primary document see N87-10263 01-35)
Avail: NTIS HC A15/MF A01 CSCL 04A

N87-10283*# National Aeronautics and Space Administration. Langley Research Center, Hampton, Va.
MEASUREMENTS OF THE EFFECT OF HORIZONTAL VARIABILITY OF ATMOSPHERIC BACKSCATTER ON DIAL MEASURE-

MENTS
G. K. Schwemmer, C. L. Korb, M. Dombrowski, and C. Y. Weng (Science Systems and Applications, Inc., Seabrook, Md.) *In its* 13th International Laser Radar Conference Aug. 1986 2 p (For primary document see N87-10263 01-35)
Avail: NTIS HC A15/MF A01 CSCL 04A

N87-10291*# National Aeronautics and Space Administration. Goddard Space Flight Center, Greenbelt, Md.
ON THE MEASUREMENT OF ATMOSPHERIC DENSITY USING DIAL IN THE O2 A-BAND (770 nm)
T. D. Wilkerson (Maryland Univ., College Park.), G. K. Schwemmer, L. J. Cotnoir, and U. N. Singh *In* NASA. Langley Research Center 13th International Laser Radar Conference Aug. 1986 4 p (For primary document see N87-10263 01-35)
(Contracts NCC1-25; DAAG29-81-D-0100; Grant NA83-AA-A-00036)
Avail: NTIS HC A15/MF A01 CSCL 04A

N87-10297*# Kyushu Univ., Fukuoka (Japan). Dept. of Electrical Engineering.
OBSERVATION OF ATMOSPHERIC OZONE BY DIAL WITH RAMAN LASERS PUMPED BY A KrF LASER
M. Maeda and T. Shibata *In* NASA. Langley Research Center 13th International Laser Radar Conference Aug. 1986 3 p (For primary document see N87-10263 01-35)
Avail: NTIS HC A15/MF A01 CSCL 04A

N87-10298*# Maryland Univ., College Park. Inst. for Physical Science and Technology.
STRENGTH, WIDTH, AND PRESSURE SHIFT MEASUREMENTS OF 54 LINES IN THE OXYGEN A-BAND
K. J. Ritter and T. D. Wilkerson *In* NASA. Langley Research Center 13th International Laser Radar Conference Aug. 1986 4 p (For primary document see N87-10263 01-35)
Avail: NTIS HC A15/MF A01 CSCL 04A

N87-10300*# National Aeronautics and Space Administration. Goddard Space Flight Center, Greenbelt, Md.
CONVECTIVE STRUCTURE OF THE PLANETARY BOUNDARY LAYER OF THE OCEAN DURING GALE
S. H. Melfi and R. Boers *In* NASA. Langley Research Center 13th International Laser Radar Conference Aug. 1986 1 p (For primary document see N87-10263 01-35)
Avail: NTIS HC A15/MF A01 CSCL 04A

N87-10302*# Academy of Sciences (USSR), Tomsk.
MULTIFREQUENCY DIAL SENSING OF THE ATMOSPHERIC GASEOUS CONSTITUENTS USING THE FIRST AND SECOND HARMONICS OF A TUNABLE CO2 LASER RADIATION
V. E. Zuev, Yu. M. Andreev, V. G. Voevodin, A. I. Gribenyukov, V. A. Kapitanov, A. V. Sosnin, G. A. Stuchebrov, and G. S. Khmelnitskii *In* NASA. Langley Research Center 13th International Laser Radar Conference Aug. 1986 3 p (For primary document see N87-10263 01-35)
Avail: NTIS HC A15/MF A01 CSCL 04A

N87-10303*# Academy of Sciences (USSR), Tomsk. Inst. of Atmospheric Optics.
REMOTE EXPRESS ANALYSIS OF GROUND-LAYER AEROSOL BASED ON LASER-INDUCED SPARK SPECTRA
V. E. Zuev, Yu. D. Kopytin, V. A. Korolkov, M. E. Levitskii, M. F. Nebolsin, B. G. Sidorov, and N. P. Soldatkin *In* NASA. Langley Research Center 13th International Laser Radar Conference Aug. 1986 2 p (For primary document see N87-10263 01-35)
Avail: NTIS HC A15/MF A01 CSCL 04A

N87-10305*# Academy of Sciences (USSR), Tomsk. Inst. of Atmospheric Optics.
OPTIMAL FILTRATION OF THE ATMOSPHERIC PARAMETERS PROFILES
V. E. Zuev, G. N. Glazov, and G. M. Igonin *In* NASA. Langley Research Center 13th International Laser Radar Conference Aug. 1986 2 p (For primary document see N87-10263 01-35)
Avail: NTIS HC A15/MF A01 CSCL 04A

N87-10306*# Academy of Sciences (USSR), Tomsk. Inst. of Atmospheric Optics.
OPTICAL MODELS OF THE MOLECULAR ATMOSPHERE
V. E. Zuev, Yu. S. Makushkin, A. A. Mitsel, Yu. N. Ponomarev, V. P. Rudenko, and K. M. Firsov *In* NASA. Langley Research Center 13th International Laser Radar Conference Aug. 1986 3 p (For primary document see N87-10263 01-35)
Avail: NTIS HC A15/MF A01 CSCL 04A

N87-10312*# National Oceanic and Atmospheric Administration, Boulder, Colo.
FEATURES OF STRATOSPHERIC AEROSOL LIDAR OBSERVATIONS AT MAUNA LOA, 1974 - 1985
J. J. DeLusi, T. DeFoor, and D. U. Longenecker *In* NASA. Langley Research Center 13th International Laser Radar Conference Aug. 1986 1 p (For primary document see N87-10263 01-35)
Avail: NTIS HC A15/MF A01 CSCL 04A

N87-10313*# Kyushu Univ., Fukuoka (Japan). Dept. of Physics.
EL CHICHON AEROSOLS IN THE STRATOSPHERE: ANALYSES OF LIDAR DATA AND CALCULATIONS OF RADIATION BUDGET
M. Fujiwara, H. Akiyoshi, and N. Otsuka *In* NASA. Langley Research Center 13th International Laser Radar Conference Aug. 1986 1 p (For primary document see N87-10263 01-35)
Avail: NTIS HC A15/MF A01 CSCL 04A

N87-10314*# Nagoya Univ. (Japan). Water Research Inst.
LIDAR MEASUREMENT OF STRATOSPHERIC AEROSOL AT SYOWA STATION, ANTARCTICA
Y. Iwasaka, T. Hirasawa (National Inst. of Polar Research, Tokyo (Japan).), H. Fukunishi, T. Ono, and A. Nomura *In* NASA. Langley Research Center 13th International Laser Radar Conference Aug. 1986 4 p (For primary document see N87-10263 01-35)
Avail: NTIS HC A15/MF A01 CSCL 04A

N87-10321*# National Oceanic and Atmospheric Administration, Boulder, Colo. Wave Propagation Lab.
THREE ATMOSPHERIC DISPERSION EXPERIMENTS INVOLVING OIL FOG PLUMES MEASURED BY LIDAR
W. L. Eberhard, G. T. McNice, and S. W. Troxel *In* NASA. Langley Research Center 13th International Laser Radar Conference Aug. 1986 4 p (For primary document see N87-10263 01-35)
Avail: NTIS HC A15/MF A01 CSCL 04A

N87-10332*# Academy of Sciences (USSR), Tomsk. Inst. of Atmospheric Optica.
A COMBINED RAMAN LIDAR FOR LOW TROPOSPHERIC STUDIES
Yu. F. Arshinov, S. M. Bobrovnikov, V. E. Zuev, A. I. Nadeev, and K. D. Shelevoy *In* NASA. Langley Research Center 13th International Laser Radar Conference Aug. 1986 3 p (For primary document see N87-10263 01-35)
Avail: NTIS HC A15/MF A01 CSCL 04A

N87-10333*# Naval Air Development Center, Warminster, Pa.
INTERCOMPARISONS OF HIGH-RESOLUTION SOLAR BLIND RAMAN LIDAR ATMOSPHERIC PROFILES OF WATER VAPOR WITH RADIOSONDES AND KYTOON
K. Petri, A. Salik, and J. Cooney (Drexel Univ., Philadelphia, Pa.) *In* NASA. Langley Research Center 13th International Laser Radar Conference Aug. 1986 1 p (For primary document see N87-10263 01-35)
Avail: NTIS HC A15/MF A01 CSCL 04A

N87-10334*# Drexel Univ., Philadelphia, Pa. Dept. of Physics and Atmospheric Sciences.
LIDAR METHOD OF MEASUREMENT OF ATMOSPHERIC EXTINCTION AND OZONE PROFILES
John A. Cooney *In* NASA. Langley Research Center 13th

International Laser Radar Conference Aug. 1986 1 p (For primary document see N87-10263 01-35)
Avail: NTIS HC A15/MF A01 CSCL 04A

N87-10337*# National Aeronautics and Space Administration. Langley Research Center, Hampton, Va.
THE APPLICATION OF LIDAR TO STRATOSPHERIC AEROSOL STUDIES
M. P. McCormick *In* NASA. Langley Research Center 13th International Laser Radar Conference Aug. 1986 2 p (For primary document see N87-10263 01-35)
Avail: NTIS HC A15/MF A01 CSCL 04A

N87-10338*# National Inst. for Environmental Studies, Tsukuba (Japan).
VOLCANIC ERUPTIONS AND THE INCREASES IN THE STRATOSPHERIC AEROSOL CONTENT: LIDAR MEASUREMENTS FROM 1982 TO 1986
S. Hayashida, Y. Iikura, H. Shimizu, Y. Sasano, H. Nakane, N. Sugimoto, I. Matsui, and N. Takeuchi *In* NASA. Langley Research Center 13th International Laser Radar Conference Aug. 1986 4 p (For primary document see N87-10263 01-35)
Avail: NTIS HC A15/MF A01 CSCL 04A

N87-10339*# University Coll. of Wales, Aberystwyth.
OBSERVATIONS OF STRATOSPHERIC AEROSOLS ASSOCIATED WITH THE EL CHICHON ERUPTION
L. Thomas, G. Vaughan, D. B. Jenkins, D. Wareing, and M. Farrington *In* NASA. Langley Research Center 13th International Laser Radar Conference Aug. 1986 1 p (For primary document see N87-10263 01-35)
Avail: NTIS HC A15/MF A01 CSCL 04A

N87-10340*# Fraunhofer-Inst. fuer Atmosphaerische Umweltforschung, Garmisch-Partenkirchen (West Germany).
LIDAR OBSERVATIONS OF THE DECLINE OF THE EL CHICHON STRATOSPHERIC LOAD
H. Jaeger and W. Carnuth *In* NASA. Langley Research Center 13th International Laser Radar Conference Aug. 1986 2 p (For primary document see N87-10263 01-35)
Avail: NTIS HC A15/MF A01 CSCL 04A

N87-10341*# National Aeronautics and Space Administration. Langley Research Center, Hampton, Va.
AIRBORNE LIDAR OBSERVATIONS OF ARCTIC POLAR STRATOSPHERIC CLOUDS
L. R. Poole and G. S. Kent *In* NASA. Langley Research Center 13th International Laser Radar Conference Aug. 1986 1 p (For primary document see N87-10263 01-35)
Avail: NTIS HC A15/MF A01 CSCL 04A

N87-10343*# University Coll. of Wales, Aberystwyth. Dept. of Physics.
LIDAR MEASUREMENTS OF THERMAL STRUCTURE
D. B. Jenkins, D. P. Wareing, L. Thomas, and G. Vaughan *In* NASA. Langley Research Center 13th International Laser Radar Conference Aug. 1986 1 p (For primary document see N87-10263 01-35)
Avail: NTIS HC A15/MF A01 CSCL 04A

N87-10344*# Centre National de la Recherche Scientifique, Verrieres-Le Buisson (France).
LIDAR STRATOSPHERIC OZONE MEASUREMENTS AT THE OBSERVATOIRE DE HAUTE PROVENCE (FRANCE)
S. Godin, J. Pelon, and G. Megie *In* NASA. Langley Research Center 13th International Laser Radar Conference Aug. 1986 4 p (For primary document see N87-10263 01-35)
Avail: NTIS HC A15/MF A01 CSCL 04A

N87-10345*# Shinshu Univ., Nagano (Japan). Faculty of Engineering.
LIDAR OBSERVATION OF THE MESOSPHERIC SODIUM LAYER IN ANTARCTICA
A. Nomura, Y. Iwasaka (Nagoya Univ. (Japan).), H. Fukunishi (National Inst. of Polar Research, Tokyo (Japan).), T. Hirasawa, S. Kawaguchi (Nagoya Univ. (Japan).), and T. Kano (Shinshu Univ., Nagano (Japan).) *In* NASA. Langley Research Center 13th International Laser Radar Conference Aug. 1986 3 p (For primary document see N87-10263 01-35)
Avail: NTIS HC A15/MF A01 CSCL 04A

N87-10346*# Centre National de la Recherche Scientifique, Verrieres-Le Buisson (France).
LIDAR DETECTION OF METALLIC SPECIES AT THE MESOPAUSE LEVEL
C. Granier, J. P. Jegou, and G. Megie *In* NASA. Langley Research Center 13th International Laser Radar Conference Aug. 1986 4 p (For primary document see N87-10263 01-35)
Avail: NTIS HC A15/MF A01 CSCL 04A

N87-10347*# Illinois Univ., Urbana.
DAYTIME LIDAR MEASUREMENTS OF TIDAL WINDS IN THE MESOSPHERIC SODIUM LAYER AT URBANA, ILLINOIS
K. H. Kwon, D. C. Senft, C. S. Gardner, D. G. Voelz, C. F. Sechrist, Jr., and F. L. Roesler (Wisconsin Univ., Madison.) *In* NASA. Langley Research Center 13th International Laser Radar Conference Aug. 1986 4 p (For primary document see N87-10263 01-35)
Avail: NTIS HC A15/MF A01 CSCL 04A

N87-10356*# Centro Informazioni Studi Esperienze, Milan (Italy).
GAS CORRELATION LIDAR FOR METHANE DETECTION
E. Galletti, E. Zanzottera, S. Draghi, M. Garbi, and R. Petroni *In* NASA. Langley Research Center 13th International Laser Radar Conference Aug. 1986 1 p (For primary document see N87-10263 01-35)
Avail: NTIS HC A15/MF A01 CSCL 04A

N87-10357*# Academia Sinica, Beijing (China). Inst. of Atmospheric Physics.
DETECTION OF NO SUB X,C2H4 CONCENTRATIONS BY USING CO AND CO2 LASERS
Wang Gengchen and Kong Qinxin *In* NASA. Langley Research Center 13th International Laser Radar Conference Aug. 1986 4 p (For primary document see N87-10263 01-35)
Avail: NTIS HC A15/MF A01 CSCL 04A

N87-10358*# Jet Propulsion Lab., California Inst. of Tech., Pasadena.
MAPM: A COHERENT DUAL CO2 LASER DIAL SYSTEM
William B. Grant and James R. Bogan *In* NASA. Langley Research Center 13th International Laser Radar Conference Aug. 1986 1 p Sponsored in part by AF (For primary document see N87-10263 01-35)
Avail: NTIS HC A15/MF A01 CSCL 04A

N87-10359*# National Physical Lab., New Delhi (India). Radio Science Div.
LASER HETERODYNE SYSTEM FOR OBTAINING HEIGHT PROFILES OF MINOR SPECIES IN THE ATMOSPHERE
S. L. Jain and A. K. Saha *In* NASA. Langley Research Center 13th International Laser Radar Conference Aug. 1986 1 p (For primary document see N87-10263 01-35)
Avail: NTIS HC A15/MF A01 CSCL 04A

N87-10363*# Jet Propulsion Lab., California Inst. of Tech., Pasadena.
ATMOSPHERIC CORRELATION TIME MEASUREMENTS USING COHERENT CO2 LIDAR
G. M. Ancellet and R. T. Menzies *In* NASA. Langley Research Center 13th International Laser Radar Conference Aug. 1986 4 p (For primary document see N87-10263 01-35)
Avail: NTIS HC A15/MF A01 CSCL 04A

N87-10366*# European Nuclear Energy Agency, Frascati (Italy). Div. Fisica Applicata.
CO2 LIDAR SYSTEM FOR ATMOSPHERIC STUDIES
R. Barbini, A. Ghigo, M. Giorgi, K. N. Iyer, A. Palucci, and S. Ribezzo *In* NASA. Langley Research Center 13th International

Laser Radar Conference Aug. 1986 4 p (For primary document see N87-10263 01-35)
Avail: NTIS HC A15/MF A01 CSCL 04A

N87-10369*# Academy of Sciences (USSR), Tomsk. Inst. of Atmospheric Optics.
SPECTROSCOPIC ASPECTS OF DIFFERENTIAL METHOD FOR SOUNDING GAS COMPOSITION OF THE ATMOSPHERE
V. V. Zuev, I. I. Ippolitov, and Yu. N. Ponomarev *In* NASA. Langley Research Center 13th International Laser Radar Conference Aug. 1986 2 p (For primary document see N87-10263 01-35)
Avail: NTIS HC A15/MF A01 CSCL 04A

N87-10371*# National Aeronautics and Space Administration. Goddard Space Flight Center, Greenbelt, Md.
THE GSFC GOUND-BASED LIDAR FOR THE MEASUREMENT OF STRATOSPHERIC OZONE
Thomas J. McGee *In* NASA. Langley Research Center 13th International Laser Radar Conference Aug. 1986 1 p (For primary document see N87-10263 01-35)
Avail: NTIS HC A15/MF A01 CSCL 04A

N87-10433*# Alaska Univ., Fairbanks. Geophysical Inst.
GRAVITY WAVES IN THE MIDDLE ATMOSPHERE: RECENT PROGRESS AND NEEDED STUDIES
David C. Fritts *In* International Council of Scientific Unions, Middle Atmosphere Program. Handbook for MAP, Vol. 20 Jun. 1986 6 p (For primary document see N87-10419 01-42)
Avail: NTIS HC A22/MF A01; also available from SCOSTEP Secretariat, Illinois Univ., 1406 West Green Street, Urbana, Ill. 61801 CSCL 04A

N87-10434*# National Oceanic and Atmospheric Administration, Boulder, Colo.
A MODEL FOR GRAVITY-WAVE SPECTRA OBSERVED BY DOPPLER SOUNDING SYSTEMS
T. E. VanZandt *In* International Council of Scientific Unions, Middle Atmosphere Program. Handbook for MAP, Vol. 20 Jun. 1986 1 p (For primary document see N87-10419 01-42)
Avail: NTIS HC A22/MF A01; also available from SCOSTEP Secretariat, Illinois Univ., 1406 West Green Street, Urbana, Ill. 61801 CSCL 04A

N87-10435*# Arecibo Ionospheric Observatory, Puerto Rico.
HALF-DAY AND FOUR-DAY WAVES IN THE STATOSPHERE
Jurgen Rottger *In* International Council of Scientific Unions, Middle Atmosphere Program. Handbook for MAP, Vol. 20 Jun. 1986 2 p (For primary document see N87-10419 01-42)
Avail: NTIS HC A22/MF A01; also available from SCOSTEP Secretariat, Illinois Univ., 1406 West Green Street, Urbana, Ill. 61801 CSCL 04A

N87-10436*# Kyoto Univ., Uji (Japan). Radio Atmospheric Science Center.
TROPOSPHERIC TURBULENCE PARAMETERS MEASURED BY USING THE MU RADAR
Toru Sato, Hiromasa Matsumoto (Kyoto Univ., Japan), Shoichiro Fukao, and Susumu Kato *In* International Council of Scientific Unions, Middle Atmosphere Program. Handbook for MAP, Vol. 20 Jun. 1986 4 p (For primary document see N87-10419 01-42)
Avail: NTIS HC A22/MF A01; also available from SCOSTEP Secretariat, Illinois Univ., 1406 West Green Street, Urbana, Ill. 61801 CSCL 04A

N87-10437*# Case Western Reserve Univ., Cleveland, Ohio.
SIMULTANEOUS VHF AND UHF RADAR OBSERVATION OF THE MESOSPHERE AT ARECIBO DURING A SOLAR FLARE: A CHECK ON THE GRADIENT-MIXING HYPOTHESIS
P. K. Rastogi, J. D. Mathews, and J. Rottger (Arecibo Ionospheric Observatory, Puerto Rico) *In* International Council of Scientific Unions, Middle Atmosphere Program. Handbook for MAP, Vol. 20 Jun. 1986 8 p (For primary document see N87-10419 01-42)
Avail: NTIS HC A22/MF A01; also available from SCOSTEP Secretariat, Illinois Univ., 1406 West Green Street, Urbana, Ill. 61801 CSCL 04A

N87-10438*# Air Force Geophysics Lab., Hanscom AFB, Mass.
EVIDENCE OF ATMOSPHERIC GRAVITY WAVE PERTURBATIONS OF THE BRUNT-VAISALA FREQUENCY IN THE ATMOSPHERE
R. E. Good, R. W. Beland, J. H. Brown, and E. M. Dewan *In* International Council of Scientific Unions, Middle Atmosphere Program. Handbook for MAP, Vol. 20 Jun. 1986 7 p (For primary document see N87-10419 01-42)
Avail: NTIS HC A22/MF A01; also available from SCOSTEP Secretariat, Illinois Univ., 1406 West Green Street, Urbana, Ill. 61801 CSCL 04A

N87-10439*# Air Force Geophysics Lab., Hanscom AFB, Mass.
ATMOSPHERIC WAVES AND THE NATURE OF BUOYANCY TURBULENCE IN THE CONTEXT OF THE WAVES VS 2D-TURBULENCE DEBATE
Edmond M. Dewan *In* International Council of Scientific Unions, Middle Atmosphere Program. Handbook for MAP, Vol. 20 Jun. 1986 4 p (For primary document see N87-10419 01-42)
Avail: NTIS HC A22/MF A01; also available from SCOSTEP Secretariat, Illinois Univ., 1406 West Green Street, Urbana, Ill. 61801 CSCL 04A

N87-10440*# Air Force Geophysics Lab., Hanscom AFB, Mass.
A PROPOSED EXPERIMENTAL TEST TO DISTINGUISH WAVES FROM 2-D TURBULENCE
Edmond M. Dewan *In* International Council of Scientific Unions, Middle Atmosphere Program. Handbook for MAP, Vol. 20 Jun. 1986 3 p (For primary document see N87-10419 01-42)
Avail: NTIS HC A22/MF A01; also available from SCOSTEP Secretariat, Illinois Univ., 1406 West Green Street, Urbana, Ill. 61801 CSCL 04A

N87-10441*# Illinois Univ., Urbana. Dept. of Electrical and Computer Engineering.
PROPAGATING TIDES IN THE MESOSPHERE
S. A. Bowhill and K. O. Merewether *In* International Council of Scientific Unions, Middle Atmosphere Program. Handbook for MAP, Vol. 20 Jun. 1986 1 p (For primary document see N87-10419 01-42)
Avail: NTIS HC A22/MF A01; also available from SCOSTEP Secretariat, Illinois Univ., 1406 West Green Street, Urbana, Ill. 61801 CSCL 04A

N87-10442*# Illinois Univ., Urbana. Aeronomy Lab.
GRAVITY WAVES IN SEVERE WEATHER
S. A. Bowhill and S. Gnanalingam *In* International Council of Scientific Unions, Middle Atmosphere Program. Handbook for MAP, Vol. 20 Jun. 1986 8 p (For primary document see N87-10419 01-42)
Avail: NTIS HC A22/MF A01; also available from SCOSTEP Secretariat, Illinois Univ., 1406 West Green Street, Urbana, Ill. 61801 CSCL 04A

N87-10443*# Alaska Univ., Fairbanks. Dept. of Physics.
SIMULTANEOUS ROCKET AND MST RADAR OBSERVATION OF AN INTERNAL GRAVITY WAVE BREAKING IN THE MESOSPHERE
Steven A. Smith, David C. Fritts, Ben B. Balsley (National Oceanic and Atmospheric Administration, Boulder, Colo.), and C. Russell Philbrick (Air Force Geophysics Lab., Hanscom AFB, Mass.) *In* International Council of Scientific Unions, Middle Atmosphere Program. Handbook for MAP, Vol. 20 Jun. 1986 11 p (For primary document see N87-10419 01-42)
Avail: NTIS HC A22/MF A01; also available from SCOSTEP Secretariat, Illinois Univ., 1406 West Green Street, Urbana, Ill. 61801 CSCL 04A

N87-10444*# Clemson Univ., S.C. Dept. of Physics and Astronomy.
OBSERVATIONS OF THUNDER WITH THE ARECIBO VHF RADAR
D. N. Holden and M. F. Larsen *In* International Council of Scientific Unions, Middle Atmosphere Program. Handbook for MAP, Vol. 20

Jun. 1986 6 p (For primary document see N87-10419 01-42)
Avail: NTIS HC A22/MF A01; also available from SCOSTEP Secretariat, Illinois Univ., 1406 West Green Street, Urbana, Ill. 61801 CSCL 04A

N87-10447*# Centre National de la Recherche Scientifique, Verrieres-Le Buisson (France).
COMPARISON BETWEEN S. T. RADAR AND IN SITU BALLOON MEASUREMENTS
F. Dalaudier, J. Barat, F. Bertin (Centre National d'Etudes des Telecommunications, Saint Maur des Fosses, France), E. Brun (Toulon Univ., France), M. Crochet, and F. Cuq *In* International Council of Scientific Unions, Middle Atmosphere Program. Handbook for MAP, Vol. 20 Jun. 1986 6 p (For primary document see N87-10419 01-42)
Avail: NTIS HC A22/MF A01; also available from SCOSTEP Secretariat, Illinois Univ., 1406 West Green Street, Urbana, Ill. 61801 CSCL 04A

N87-10448*# National Oceanic and Atmospheric Administration, Boulder, Colo. Aeronomy Lab.
A STATISTICAL MODEL TO ESTIMATE REFRACTIVITY TURBULENCE STRUCTURE CONSTANT C SUB n SUP 2 IN THE FREE ATMOSPHERE
J. M. Warnock and T. E. VanZandt *In* International Council of Scientific Unions, Middle Atmosphere Program. Handbook for MAP, Vol. 20 Jun. 1986 2 p (For primary document see N87-10419 01-42)
Avail: NTIS HC A22/MF A01; also available from SCOSTEP Secretariat, Illinois Univ., 1406 West Green Street, Urbana, Ill. 61801 CSCL 04A

N87-10449*# Arecibo Ionospheric Observatory, Puerto Rico. Arecibo Observatory.
DETERMINATION OF THE BRUNT-VAISALA FREQUENCY FROM VERTICAL VELOCITY SPECTRA
Jurgen Rottger *In* International Council of Scientific Unions, Middle Atmosphere Program. Handbook for MAP, Vol. 20 Jun. 1986 5 p (For primary document see N87-10419 01-42)
Avail: NTIS HC A22/MF A01; also available from SCOSTEP Secretariat, Illinois Univ., 1406 West Green Street, Urbana, Ill. 61801 CSCL 04A

N87-10450*# Arecibo Ionospheric Observatory, Puerto Rico.
THE USE OF THE EXPERIMENTALLY DEDUCED BRUNT-VAISALA FREQUENCY AND TURBULENT VELOCITY FLUCTUATIONS TO ESTIMATE THE EDDY DIFFUSION COEFFICIENT
Jurgen Rottger *In* International Council of Scientific Unions, Middle Atmosphere Program. Handbook for MAP, Vol. 20 Jun. 1986 6 p (For primary document see N87-10419 01-42)
Avail: NTIS HC A22/MF A01; also available from SCOSTEP Secretariat, Illinois Univ., 1406 West Green Street, Urbana, Ill. 61801 CSCL 04A

N87-10451*# Arecibo Ionospheric Observatory, Puerto Rico.
THE RELATION OF GRAVITY WAVES AND TURBULENCE IN THE MESOSPHERE
Jurgen Rottger *In* International Council of Scientific Unions, Middle Atmosphere Program. Handbook for MAP, Vol. 20 Jun. 1986 5 p (For primary document see N87-10419 01-42)
Avail: NTIS HC A22/MF A01; also available from SCOSTEP Secretariat, Illinois Univ., 1406 West Green Street, Urbana, Ill. 61801 CSCL 04A

N87-10452*# National Oceanic and Atmospheric Administration, Boulder, Colo. Aeronomy Lab.
CAN STOCHASTIC, DISSIPATIVE WAVE FIELDS BE TREATED AS RANDOM WALK GENERATORS
J. Weinstock *In* International Council of Scientific Unions, Middle Atmosphere Program. Handbook for MAP, Vol. 20 Jun. 1986 3 p (For primary document see N87-10419 01-42)
Avail: NTIS HC A22/MF A01; also available from SCOSTEP Secretariat, Illinois Univ., 1406 West Green Street, Urbana, Ill. 61801 CSCL 04A

N87-10453*# Alaska Univ., Fairbanks. Geophysical Inst.
OBSERVATIONS AND A MODEL OF GRAVITY-WAVE VARIABILITY IN THE MIDDLE ATMOSPHERE
David C. Fritts and Robert A. Vincent (Adelaide Univ., Australia) *In* International Council of Scientific Unions, Middle Atmosphere Program. Handbook for MAP, Vol. 20 Jun. 1986 4 p (For primary document see N87-10419 01-42)
Avail: NTIS HC A22/MF A01; also available from SCOSTEP Secretariat, Illinois Univ., 1406 West Green Street, Urbana, Ill. 61801 CSCL 04A

N87-10456*# Adelaide Univ. (Australia). Dept. of Physics
MESOSPHERIC GRAVITY-WAVE CLIMATOLOGY AT ADELAIDE
R. A. Vincent *In* International Council of Scientific Unions, Middle Atmosphere Program. Handbook for MAP, Vol. 20 Jun. 1986 1 p (For primary document see N87-10419 01-42)
Avail: NTIS HC A22/MF A01; also available from SCOSTEP Secretariat, Illinois Univ., 1406 West Green Street, Urbana, Ill. 61801 CSCL 04A

N87-10457*# Cologne Univ. (West Germany). Inst. for Geophysik und Meteorologie.
HORIZONTAL WIND PERTURBATIONS AND THEIR RELATION TO TRANSIENT INTERNAL GRAVITY WAVES
A. Ebel, A. H. Manson (Saskatchewan Univ., Saskatoon), and C. E. Meek *In* International Council of Scientific Unions, Middle Atmosphere Program. Handbook for MAP, Vol. 20 Jun. 1986 5 p (For primary document see N87-10419 01-42)
Avail: NTIS HC A22/MF A01; also available from SCOSTEP Secretariat, Illinois Univ., 1406 West Green Street, Urbana, Ill. 61801 CSCL 04A

N87-10458*# Illinois Univ., Urbana-Champaign. Dept. of Electrical and Computer Engineering.
POSSIBILITY OF MEASURING GRAVITY-WAVE MOMENTUM FLUX BY SINGLE BEAM OBSERVATION OF MST RADAR
C. H. Liu *In* International Council of Scientific Unions, Middle Atmosphere Program. Handbook for MAP, Vol. 20 Jun. 1986 3 p (For primary document see N87-10419 01-42)
Avail: NTIS HC A22/MF A01; also available from SCOSTEP Secretariat, Illinois Univ., 1406 West Green Street, Urbana, Ill. 61801 CSCL 04A

N87-10459*# Control Data Corp., Minneapolis, Minn.
PRELIMINARY ESTIMATES OF VERTICAL MOMENTUM FLUX
G. D. Nastrom and J. L. Green (National Oceanic and Atmospheric Administration, Boulder, Colo.) *In* International Council of Scientific Unions, Middle Atmosphere Program. Handbook for MAP, Vol. 20 Jun. 1986 5 p (For primary document see N87-10419 01-42)
Avail: NTIS HC A22/MF A01; also available from SCOSTEP Secretariat, Illinois Univ., 1406 West Green Street, Urbana, Ill. 61801 CSCL 04A

N87-10460*# Illinois Univ., Urbana-Champaign. Dept. of Electrical and Computer Engineering.
EFFECTS OF ANISOTROPY ON THE FREQUENCY SPECTRUM OF GRAVITY WAVES OBSERVED BY MST RADAR
C. H. Liu *In* International Council of Scientific Unions, Middle Atmosphere Program. Handbook for MAP, Vol. 20 Jun. 1986 2 p (For primary document see N87-10419 01-42)
Avail: NTIS HC A22/MF A01; also available from SCOSTEP Secretariat, Illinois Univ., 1406 West Green Street, Urbana, Ill. 61801 CSCL 04A

N87-10461*# Control Data Corp., Minneapolis, Minn.
THE FREQUENCY SPECTRUM OF C SUB n SUP 2 FROM MST RADAR DATA
G. D. Nastrom *In* International Council of Scientific Unions, Middle Atmosphere Program. Handbook for MAP, Vol. 20 Jun. 1986 5 p (For primary document see N87-10419 01-42)

Avail: NTIS HC A22/MF A01; also available from SCOSTEP Secretariat, Illinois Univ., 1406 West Green Street, Urbana, Ill. 61801 CSCL 04A

N87-10462*# Case Western Reserve Univ., Cleveland, Ohio. Dept. of Elec. Engineering and Applied Physics.
A STUDY OF GRAVITY-WAVE SPECTRA IN THE TROPOSPHERE AND STRATOSPHERE AT 5-MIN TO 5-DAY PERIODS WITH THE POKER FLAT MST RADAR
R. S. Bemra, P. K. Rastogi, and B. B. Balsley (National Oceanic and Atmospheric Administration, Boulder, Colo.) *In* International Council of Scientific Unions, Middle Atmosphere Program. Handbook for MAP, Vol. 20 Jun. 1986 9 p (For primary document see N87-10419 01-42)
Avail: NTIS HC A22/MF A01; also available from SCOSTEP Secretariat, Illinois Univ., 1406 West Green Street, Urbana, Ill. 61801 CSCL 04A

N87-10463*# Arecibo Ionospheric Observatory, Puerto Rico.
ON THE VARYING SLOPE OF VELOCITY SPECTRA
Jurgen Rottger *In* International Council of Scientific Unions, Middle Atmosphere Program. Handbook for MAP, Vol. 20 Jun. 1986 3 p (For primary document see N87-10419 01-42)
Avail: NTIS HC A22/MF A01; also available from SCOSTEP Secretariat, Illinois Univ., 1406 West Green Street, Urbana, Ill. 61801 CSCL 04A

N87-10464*# Illinois Univ., Urbana. Dept. of Electrical and Computer Engineering.
DOPPLER EFFECTS ON VELOCITY SPECTRA OBSERVED BY MST RADARS
A. O. Scheffler and C. H. Liu *In* International Council of Scientific Unions, Middle Atmosphere Program. Handbook for MAP, Vol. 20 Jun. 1986 3 p (For primary document see N87-10419 01-42)
Avail: NTIS HC A22/MF A01; also available from SCOSTEP Secretariat, Illinois Univ., 1406 West Green Street, Urbana, Ill. 61801 CSCL 04A

N87-10465*# Clemson Univ., S.C. Dept. of Physics and Astronomy.
OBSERVATIONS OF VERTICAL VELOCITY POWER SPECTRA WITH THE SOUSY VHF RADAR
M. F. Larsen, J. Rottger, and D. N. Holden *In* International Council of Scientific Unions, Middle Atmosphere Program. Handbook for MAP, Vol. 20 Jun. 1986 5 p (For primary document see N87-10419 01-42)
Avail: NTIS HC A22/MF A01; also available from SCOSTEP Secretariat, Illinois Univ., 1406 West Green Street, Urbana, Ill. 61801 CSCL 04A

N87-10466*# Alaska Univ., Fairbanks. Geophysical Inst.
MESOSPHERIC WAVE NUMBER SPECTRA FROM POKER FLAT MST RADAR MEASUREMENTS COMPARED WITH GRAVITY-WAVE MODEL
Steven A. Smith, David C. Fritts, and Thomas E. VanZandt (National Oceanic and Atmospheric Administration, Boulder, Colo.) *In* International Council of Scientific Unions, Middle Atmosphere Program. Handbook for MAP, Vol. 20 Jun. 1986 8 p (For primary document see N87-10419 01-42)
Avail: NTIS HC A22/MF A01; also available from SCOSTEP Secretariat, Illinois Univ., 1406 West Green Street, Urbana, Ill. 61801 CSCL 04A

N87-10467*# Alaska Univ., Fairbanks. Geophysical Inst.
EVIDENCE OF A SATURATED GRAVITY-WAVE SPECTRUM THROUGHOUT THE ATMOSPHERE
David C. Fritts and Steven A. Smith (National Oceanic and Atmospheric Administration, Boulder, Colo.) *In* International Council of Scientific Unions, Middle Atmosphere Program. Handbook for MAP, Vol. 20 Jun. 1986 5 p (For primary document see N87-10419 01-42)
Avail: NTIS HC A22/MF A01; also available from SCOSTEP Secretariat, Illinois Univ., 1406 West Green Street, Urbana, Ill. 61801 CSCL 04A

N87-10470*# National Oceanic and Atmospheric Administration, Boulder, Colo. Aeronomy Lab.
A COMPARISON OF VERTICAL VELOCITIES MEASURED FROM SPECULAR AND NONSPECULAR ECHOES BY A VHF RADAR
J. L. Green, W. L. Clark, J. M. Warnock, and G. D. Nastrom (Control Data Corp., Minneapolis, Minn.) *In* International Council of Scientific Unions, Middle Atmosphere Program. Handbook for MAP, Vol. 20 Jun. 1986 10 p (For primary document see N87-10419 01-42)
Avail: NTIS HC A22/MF A01; also available from SCOSTEP Secretariat, Illinois Univ., 1406 West Green Street, Urbana, Ill. 61801 CSCL 04A

N87-10476*# Utah State Univ., Logan. Center for Atmospheric and Space Sciences.
MESOSPHERIC WIND MEASUREMENTS USING A MEDIUM-FREQUENCY IMAGING DOPPLER INTERFEROMETER
G. W. Adams and J. W. Brosnahan (Tycho Technology, Inc., Boulder, Colo.) *In* International Council of Scientific Unions, Middle Atmosphere Program. Handbook for MAP, Vol. 20 Jun. 1986 4 p (For primary document see N87-10419 01-42)
Avail: NTIS HC A22/MF A01; also available from SCOSTEP Secretariat, Illinois Univ., 1406 West Green Street, Urbana, Ill. 61801 CSCL 04A

N87-10478*# Arecibo Ionospheric Observatory, Puerto Rico.
MST RADAR NETWORKS AND CAMPAIGNS SESSION SUMMARY AND RECOMMENDATIONS
Jurgen Rottger *In* International Council of Scientific Unions, Middle Atmosphere Program. Handbook for MAP, Vol. 20 Jun. 1986 1 p (For primary document see N87-10419 01-42)
Avail: NTIS HC A22/MF A01; also available from SCOSTEP Secretariat, Illinois Univ., 1406 West Green Street, Urbana, Ill. 61801 CSCL 04A

N87-10480*# Centre National d'Etudes des Telecommunications, Saint Maur des Fosses (France).
SCIENTIFIC REASONS FOR A NETWORK OF ST RADARS AND COOPERATIVE CAMPAIGNS
M. Petitdidier and M. Crochet (Toulon Univ., France) *In* International Council of Scientific Unions, Middle Atmosphere Program. Handbook for MAP, Vol. 20 Jun. 1986 6 p (For primary document see N87-10419 01-42)
Avail: NTIS HC A22/MF A01; also available from SCOSTEP Secretariat, Illinois Univ., 1406 West Green Street, Urbana, Ill. 61801 CSCL 04A

N87-10481*# National Oceanic and Atmospheric Administration, Boulder, Colo.
PROGRESS IN EXISTING AND PLANNED MST RADARS
T. E. VanZandt *In* International Council of Scientific Unions, Middle Atmosphere Program. Handbook for MAP, Vol. 20 Jun. 1986 3 p (For primary document see N87-10419 01-42)
Avail: NTIS HC A22/MF A01; also available from SCOSTEP Secretariat, Illinois Univ., 1406 West Green Street, Urbana, Ill. 61801 CSCL 04A

N87-10488*# Radio Research Labs., Tokyo (Japan).
REMOTE TEMPERATURE PROFILING IN THE TROPOSPHERE AND STRATOSPHERE BY THE RADIO-ACOUSTIC SOUNDING TECHNIQUE
Nobuo Matuura, Yoshihisa Masuda, and Hisao Inuki *In* International Council of Scientific Unions, Middle Atmosphere Program. Handbook for MAP, Vol. 20 Jun. 1986 1 p (For primary document see N87-10419 01-42)
Avail: NTIS HC A22/MF A01; also available from SCOSTEP Secretariat, Illinois Univ., 1406 West Green Street, Urbana, Ill. 61801 CSCL 04A

N87-10494*# Arecibo Ionospheric Observatory, Puerto Rico.
INVESTIGATIONS OF THE LOWER AND MIDDLE ATMOSPHERE AT THE ARECIBO OBSERVATORY AND A DESCRIPTION OF THE NEW VHF RADAR PROJECT

J. Rottger, H. M. Ierkic, R. K. Zimmerman, and J. Hagen *In* International Council of Scientific Unions, Middle Atmosphere Program. Handbook for MAP, Vol. 20 Jun. 1986 10 p (For primary document see N87-10419 01-42)
Avail: NTIS HC A22/MF A01; also available from SCOSTEP Secretariat, Illinois Univ., 1406 West Green Street, Urbana, Ill. 61801 CSCL 04A

N87-10522*# Arecibo Ionospheric Observatory, Puerto Rico.
ON THE USE OF COLOUR REFLECTIVITY PLOTS TO MONITOR THE STRUCTURE OF THE TROPOSPHERE AND STRATOSPHERE
J. Rottger, I. J. Fu (National Central Univ., Chung-Li Taiwan), F. S. Kuo, C. H. Liu (Illinois Univ., Urbana), and J. K. Chao (National Central Univ., Chung-Li Taiwan) *In* International Council of Scientific Unions, Middle Atmosphere Program. Handbook for MAP, Vol. 20 Jun. 1986 2 p (For primary document see N87-10419 01-42)
Avail: NTIS HC A22/MF A01; also available from SCOSTEP Secretariat, Illinois Univ., 1406 West Green Street, Urbana, Ill. 61801 CSCL 04A

47 METEOROLOGY AND CLIMATOLOGY

Includes weather forecasting and modification.

N87-10633 Michigan Univ., Ann Arbor.
VERTICAL MODES AND ENERGETICS OF GRAVITATIONAL AND ROTATIONAL MODES IN A MULTILEVEL GLOBAL SPECTRAL MODEL Ph.D. Thesis
Shun Der Ko 1985 245 p
Avail: Univ. Microfilms Order No. DA8600474

The energetics analysis is made based on the NCAR Community Climate Model. As usual, the normal modes of the model are computed through the method of separation of variables. One difficulty, which is studied here for the first time, is that the discrete vertical structure equation is not unique. For some typical vertical profiles of temperature and pressure, the solutions of the discrete differential and integral vertical equations are compared. The difference between these solutions is smaller for lower baroclinic modes but larger for higher modes. Moreover, the eigenfrequencies of the gravity waves, and thus their energy, will be effected by the choice of different vertical equation. Available potential energy and divergent and nondivergent kinetic energy are investigated both globally and in the tropics. Gravity waves play a more important role in the tropics than globally. To retain the strength of tropical circulations in the forecast, researchers recommend that the gravity waves corresponding to the internal modes 3-5 and zonal wave numbers 1 to 6 with frequency lower than 1.07 x 0.0001 sec-1 (or period longer than 16 hr.) not be adjusted by the initialization. New concepts of the balanced energy (BE), transient energy (TE), and balanced gravitational energy (BGE) are introduced. Author

N87-10634 Illinois Univ., Urbana-Champaign.
OBSERVATIONAL STUDIES OF WAVE DISTURBANCES IN THE TROPICAL PACIFIC AND THEIR RELATIONSHIP WITH DEEP CLOUD ACTIVITY Ph.D. Thesis
King-Sheng Tai 1985 240 p
Avail: Univ. Microfilms Order No. DA8600329

First Global Atmospheric Research Program (GARP) Global Experiment, Level III-b data and the outgoing longwave radiation data are used to investigate relationships between deep cloud activity and large-scale meteorological fields from May to September in 1979. Discussion is focused on the situations in the eastern Pacific for the following reasons: (1) this is the area where strong deep convection frequently develops in the northern summer, (2) it is also an area which has been least explored meteorologically. A power spectrum analysis using Maximum Entropy Method is made for the meridional wind component at 850 mb from May through August. The waves with a period of 4 to 6 days are stronger in July and August than in other months, also they are active in the regions of 100 to 130 E and 130 to 160 E within the zone of 5 to 15 N. A cross-spectrum analysis between the deep cloud activity and the meridional wind indicates that deep convection occurs at or slightly behind the wave trough axis. The structure of easterly waves, obtained by a composite technique is similar to those of African waves observed in GATE (GARP Atlantic Tropical Experiment) Phase III and easterly waves in the western Pacific determined by Reed and Recker (1971). Author

N87-10635 Colorado State Univ., Fort Collins.
ENVIRONMENTAL INFLUENCES ON HURRICANE INTENSIFICATION Ph.D. Thesis
Robert T. Merrill 1985 158 p
Avail: Univ. Microfilms Order No. DA8607660

Though qualitatively similar in structure, different hurricanes can attain different peak intensities during their lifetimes. Forecasters and empiricists relate the intensity to the sea surface temperature and the effectiveness of the upper tropospheric outflow, but offer no clear explanation of how the latter operates. The observed upper tropospheric environment flow differences between hurricanes which intensify and those which fail to do so are examined and then combined with previously published empirical and modeling results into a general conceptual mode of environmental influences on hurricane intensification. Several observational and numerical tests for this conceptual model are then proposed. Dissert. Abstr.

N87-10636# World Meteorological Organization, Geneva (Switzerland).
PROCEEDINGS OF THE TECHNICAL CONFERENCE ON URBAN CLIMATOLOGY AND ITS APPLICATIONS WITH SPECIAL REGARD TO TROPICAL AREAS
T. R. Oke, ed. Geneva, Switzerland 1986 559 p Conference held in Mexico, 26-30 Nov. 1984; sponsored by WMO and WHO (WMO-652; ETN-86-97658) Avail: NTIS MF A01; print copy available at WMO, Geneva, Switzerland

Climate of tropical cities; air quality in tropical cities; regional planning; urban architectural and environmental design; human comfort; urban hydrology; life expectancy; and risk analysis were discussed. For individual titles, see N87-10637 through N87-10656.

N87-10637# British Columbia Univ., Vancouver. Dept. of Geography.
URBAN CLIMATOLOGY AND THE TROPICAL CITY: AN INTRODUCTION
T. R. Oke *In* WMO Proceedings of the Technical Conference on Urban Climatology and its Applications with Special Regard to Tropical Areas 1986 p 1-25 Sponsored by Canadian Natural Sciences and Engineering Research Council (For primary document see N87-10636 01-47)
Avail: NTIS MF A01; print copy available at WMO, Geneva, Switzerland

The role of urban climatology in tropical city planning is discussed and guidelines on practical procedures and applications are given. The sequence of decisions to be made by an urban planner when incorporating climatic information into a design are detailed. It is shown that urban population growth in 21st century tropical cities is going to be a major problem, and climatic studies are a valid contribution to anticipate aspects of the difficulties to be found. ESA

N87-10638# Universidad Nacional de Mexico, Mexico City. Inst. de Geografia.
TROPICAL URBAN CLIMATES: REVIEW AND ASSESSMENT
Ernesto Jauregui *In* WMO Proceedings of the Technical Conference on Urban Climatology and its Applications with Special Regard to Tropical Areas 1986 p 26-45 (For primary document see N87-10636 01-47)
Avail: NTIS MF A01; print copy available at WMO, Geneva, Switzerland

The main characteristics of the urban heat island effect are reviewed. The differences between midlatitude and tropical in regard to thermal inertia and the configuration of urban canyons are discussed. The seasonal variations of the heat island intensity are illustrated by data from Mexico and South America cities. The climatic factors which are affected by urbanization are examined. It is shown that surveys leading to description of features are necessary in tropical areas until sufficient knowledge is available for generalization. ESA

N87-10639# Tsukuba Univ. (Japan). Inst. of Geoscience.
AIR QUALITY IN TROPICAL CITIES **c45**
T. Kawamura *In* WMO Proceedings of the Technical Conference on Urban Climatology and its Applications with Special Regard to Tropical Areas 1986 p 46-62 (For primary document see N87-10636 01-47)
Avail: NTIS MF A01; print copy available at WMO, Geneva, Switzerland

The causes of urban air pollution in tropical cities are examined. Climatic factors such as inversions and pollution sources are discussed. It is shown that high temperature exerts an active photochemical role when nitrogen oxides and hydrocarbons are mixed. Schematic representations of the diurnal changes of local wind and the temporal changes in the concentration of oxidants around Tokyo are given. ESA

N87-10640# Universidad Nacional de Mexico, Mexico City. Inst. de Geografia.
THE URBAN CLIMATE OF MEXICO CITY
Ernesto Jauregui *In* WMO Proceedings of the Technical Conference on Urban Climatology and its Applications with Special Regard to Tropical Areas 1986 p 63-86 (For primary document see N87-10636 01-47)
Avail: NTIS MF A01; print copy available at WMO, Geneva, Switzerland

Empirical evidence concerning urban effects of Mexico City on the local climate of the valley where the city lies is presented, and physical examinations to account for the city's climatic regime particularities in comparison with those of midlatitude cities are offered. Detailed monthly variation data are presented. Heat island intensity, surface temperature inversions, and urban/rural temperature differences are discussed. It is shown that the cool island seems to be a characteristic daytime phenomenon and that the urban area of Mexico City enhances the intensity of afternoon showers downwind from the center of the city during the wet season. ESA

N87-10641# Shanghai Normal Univ. (China). Dept. of Geography.
SOME ASPECTS OF THE URBAN CLIMATE OF SHANGHAI
Shu Djen Chow *In* WMO Proceedings of the Technical Conference on Urban Climatology and its Applications with Special Regard to Tropical Areas 1986 p 87-109 (For primary document see N87-10636 01-47)
Avail: NTIS MF A01; print copy available at WMO, Geneva, Switzerland

The urban climate of Shanghai is discussed using meteorological data covering a period of 100 yr. The evolution of the population density from 1865 to 1982 is detailed. The annual temperature averages, minimum and maximum of urban center, urban areas, and rural areas are compared. Urban wind and humidity fields are described. It is concluded that the urban influence of Shanghai on temperature, wind, humidity, and precipitation are very pronounced. The long term trend of temperature is towards greater warmth, weaker winds and humidity decreases. ESA

N87-10642# Ibadan Univ. (Nigeria). Dept. of Geography.
SOME ASPECTS OF THE URBAN CLIMATES OF TROPICAL AFRICA
J. S. Oguntoyinbo *In* WMO Proceedings of the Technical Conference on Urban Climatology and its Applications with Special Regard to Tropical Areas 1986 p 110-135 (For primary document see N87-10636 01-47)
Avail: NTIS MF A01; print copy available at WMO, Geneva, Switzerland

African city case studies are presented in order to highlight urban climate characteristics, to outline the limitations of the studies already carried out, and to suggest areas of further research. The spatial and temporal variation of radiation, albedo, temperature, and pollutant concentration in the urban atmosphere are analyzed for Lagos, Ibadan, and Nairobi. The results show that the urban heat island phenomenon is well established but it is not as pronounced as in temperate latitude cities. There is no conclusive evidence to show the impact of the city on precipitation. ESA

N87-10643# Indian Meteorological Dept., New Delhi.
SOME ASPECTS OF THE URBAN CLIMATES OF INDIA
B. Padmanabhamurty *In* WMO Proceedings of the Technical Conference on Urban Climatology and its Applications with Special Regard to Tropical Areas 1986 p 136-165 (For primary document see N87-10636 01-47)
Avail: NTIS MF A01; print copy available at WMO, Geneva, Switzerland

The parameters which characterize the urban heat islands of several Indian cities are studied, including spatial and temporal distribution of temperature, dew point, relative humidity, wind speed and direction, cooling rates, and thermal radial emittance. The vertical structure of heat islands, air pollution, and water balance are also studied. It is concluded that urban complexes, even in the tropics, are likely to result in significant changes of meteorological parameters. ESA

N87-10644# Sao Paulo Univ. (Brazil). Dept. of Geography.
SOME ASPECTS OF THE URBAN CLIMATES OF TROPICAL SOUTH AMERICA: THE BRAZILIAN CONTRIBUTION
Carlos Augustos deFigueiredoMonteiro *In* WMO Proceedings of the Technical Conference on Urban Climatology and its Applications with Special Regard to Tropical Areas 1986 p 166-198 (For primary document see N87-10636 01-47)
Avail: NTIS MF A01; print copy available at WMO, Geneva, Switzerland

Information on the urban climates of Brazil is presented. The physical settings of the large metropolitan areas are described and heat island effects in large, medium, and small cities are examined. The application of urban climate knowledge in planning is discussed. It is shown that medium size cities, with a population between 150.000 and 200.000 inhabitants, present a clear heat island effect. The analysis indicates that the physical setting plays the leading role in determining the urban thermal structure. ESA

N87-10645# Swedish Meteorological and Hydrological Inst., Norkoeping.
URBAN CLIMATOLOGICAL METHODS AND DATA
Roger Taesler *In* WMO Proceedings of the Technical Conference on Urban Climatology and its Applications with Special Regard to Tropical Areas 1986 p 199-236 (For primary document see N87-10636 01-47)
Avail: NTIS MF A01; print copy available at WMO, Geneva, Switzerland

The methodology for quantitative assessments using input-output models incorporating the urban climate and the system affected by this climate is discussed. The analysis includes synoptic controls, scales associated with urban effects, conceptual models of the urban atmosphere, experimental methods, and model simulations and applications. It is shown that the basic challenge for urban climatology is to develop methods for accurate local predictions of climatic parameters, which are relevant to a particular planning aspect. ESA

N87-10646# San Jose State Univ., Calif. Dept. of Meteorology.
URBAN CLIMATE MODELS: NATURE, LIMITATIONS AND APPLICATIONS
R. D. Bornstein *In* WMO Proceedings of the Technical Conference on Urban Climatology and its Applications with Special Regard to Tropical Areas 1986 p 237-267 (For primary document see N87-10636 01-47)
(Grant RP-1630-13)
Avail: NTIS MF A01; print copy available at WMO, Geneva, Switzerland

Atmospheric models of the microscale climate within the urban canopy layer and the mesoscale variations within the urban boundary layer (above-roof level) are reviewed. The basic workings of each type of model are examined with respect to assumptions, equations, parameterizations, boundary conditions, mimerics, grids, and initial conditions. Outputs produced, evaluation techniques, and limitations associated with each type are also discussed. The role of such models in city planning is evaluated. Possible developments in urban climate modeling are explored. The most useful of the numerical urban models in increasing order of computer power requirements, are the advective integral power, one dimensional energy balance models, and the two and three dimensional dynamic differential models. ESA

N87-10647# Oxford Polytechnic (England). Dept. of Architecture.
THE PLANNING AND MAINTENANCE OF URBAN SETTLEMENTS TO RESIST EXTREME CLIMATIC FORCES c85
Ian R. Davis *In* WMO Proceedings of the Technical Conference on Urban Climatology and its Applications with Special Regard to Tropical Areas 1986 p 277-312 (For primary document see N87-10636 01-47)
Avail: NTIS MF A01; print copy available at WMO, Geneva, Switzerland

City planning to reduce vulnerability to high winds, flooding, and drought is discussed. The arms and sectors of mitigation planning are examined. The study of risk includes hazard mapping, vulnerability analysis, and risk assessment. A balanced protective strategy involving the raising of public awareness, legislation, training and education, and physical measures is suggested. Warning systems are also discussed. The establishment of a panel on risk reduction in hazard prone areas is shown to be an encouraging step towards international cooperation in this field. ESA

N87-10648# Zurich Univ. (Switzerland). Central Biological Lab.
LIFE EXPECTANCY IN TROPICAL CLIMATES AND URBANIZATION c54
W. H. Weihe *In* WMO Proceedings of the Technical Conference on Urban Climatology and its Applications with Special Regard to Tropical Areas 1986 p 313-353 (For primary document see N87-10636 01-47)
Avail: NTIS MF A01; print copy available at WMO, Geneva, Switzerland

Demographic data, mortality levels, and trends are studied analyzing urban-rural and latitudinal gradient situations. The distribution of the causes of death and its correlation with climatic factors are examined. Heat tolerance levels suggest tropical cities as death islands when they are too large, dense, with short distances between buildings, and little green land. The build-up of heat islands becomes a threat in tropical climates. ESA

N87-10649# World Meteorological Organization, Geneva (Switzerland).
HUMAN COMFORT IN THE URBAN TROPICS c54
Luis SanchezdeCarmona *In its* Proceedings of the Technical Conference on Urban Climatology and its Applications with Special Regard to Tropical Areas 1986 p 354-404 (For primary document see N87-10636 01-47)
Avail: NTIS MF A01; print copy available at WMO, Geneva, Switzerland

Factors dictating thermal and climatic well being in tropical regions are analyzed. Measurements are mainly made in cities outside the tropics but the findings may be applied to cities in the tropics by careful transposition. Environmental pollution is studied as a factor which threatens the well being of urban populations. Specific possibilities and measures for improving thermal comfort in the urban humid tropics are suggested. It is shown that the climate may be controlled using the elements of nature (wind, radiation, vegetation), thus avoiding the use of costly technology-intensive devices. ESA

N87-10650# Washington Univ., Seattle. Dept. of Geological Sciences.
URBAN HYDROLOGY IN THE TROPICS: PROBLEMS, SOLUTIONS, DATA COLLECTION AND ANALYSIS c85
Thomas Dunne *In* WMO Proceedings of the Technical Conference on Urban Climatology and its Applications with Special Regard to Tropical Areas 1986 p 405-434 (For primary document see N87-10636 01-47)
Avail: NTIS MF A01; print copy available at WMO, Geneva, Switzerland

The impact of urbanization on the type and magnitude of the runoff processes is discussed. The changes in speed and volume of flood discharge, pollutant washoff, soil water content, and evaporation are examined. Flood control solutions in small urban catchments are described. The probability analysis of floods, hydrographic measurement methods, and the prediction of storm runoff volume and timing are also discussed. It is shown that the usefulness of strategies for reducing or delaying storm runoff varies with local conditions. The basis of any plan for controlling urban storm runoff must be the obtaining of data on rainfall, runoff and the hydrologically relevant aspects of urban land use. ESA

N87-10651# Sheffield Univ. (England).
ENERGY RELATED ISSUES c85
John K. Page *In* WMO Proceedings of the Technical Conference on Urban Climatology and its Applications with Special Regard to Tropical Areas 1986 p 435-450 (For primary document see N87-10636 01-47)
Avail: NTIS MF A01; print copy available at WMO, Geneva, Switzerland

The patterns of energy consumption in tropical cities are examined in order to assess the potential contributions of energy issues to city planning. Bioclimatic analysis in urban energy studies, energy analysis of urban climates, natural climatic resources available to reduce fossil fuel demand, climatic planning, seasonal storage of coolness, transportation and energy use, and techniques of urban climatic energy analysis are treated. It is shown that significant energy savings and increased comfort can be achieved by climatic planning. ESA

N87-10652# Office for Chemical Analyses, Stuttgart (West Germany). Dept. of Climatology.
THE INTRODUCTION OF CLIMATOLOGY INTO THE ADMINISTRATION AND DEVELOPMENT OF PLANNING IN THE CITY OF STUTTGART c85
J. Baumueller *In* WMO Proceedings of the Technical Conference on Urban Climatology and its Applications with Special Regard to Tropical Areas 1986 p 451-460 (For primary document see N87-10636 01-47)
Avail: NTIS MF A01; print copy available at WMO, Geneva, Switzerland

The activities of the Stuttgart department of climatology are described pointing out the interactions with city planning activities and the study of air pollution over the city. The spatial and temporal variations of pollutants such as SO2, NO and O3 are discussed, giving the approximate empirical expressions and the results of wind tunnel simulations. It is shown that the fact that the urban climate of Stuttgart is acceptable is thanks to an order issued in 1951, that climatologists must be consulted by all agencies whose actions can affect the city's climate. ESA

N87-10653# Maryland Univ., College Park. Inst. for Physical Science and Technology.
PROBLEMS OF DESIGN FOR CITIES IN THE TROPICS c85
H. E. Landsberg *In* WMO Proceedings of the Technical Conference on Urban Climatology and its Applications with Special Regard to Tropical Areas 1986 p 461-472 (For primary document see N87-10636 01-47)
Avail: NTIS MF A01; print copy available at WMO, Geneva, Switzerland

The design problems found in planning tropical cities are discussed. Tropical urban climates are surveyed, including typical problems such as heat islands, air pollution, ventilation, and floods in the rainy zones. An ideal tropical city design is given. The energy aspects are highlighted, mainly the utilization of solar energy to cover electric or water supply needs and protection against excessive radiation absorption. It is shown that modern cities in many respects deviate from the ideal design. ESA

N87-10654# Murdoch Univ. (Australia). School of Environmental and Life Sciences.
CLIMATIC FACTORS IN THE SITING OF NEW TOWNS AND SPECIALIZED URBAN FACILITIES **c85**
T. J. Lyons *In* WMO Proceedings of the Technical Conference on Urban Climatology and its Applications with Special Regard to Tropical Areas 1986 p 473-486 (For primary document see N87-10636 01-47)
Avail: NTIS MF A01; print copy available at WMO, Geneva, Switzerland

The meteorological input to the city planning process is highlighted in terms of initial location, overall structure, and location of additional facilities within an existing city that may impact on air quality. The importance of relevant variables according to scale of interest and elevation of emission source is estimated. The typical applications of direct sensors are detailed. The development of air quality models using meteorological and on-site tracer experiments data is discussed. It is concluded that urban planners must be aware of climatic constraints on the siting of new towns, including energy and water requirements, mitigation of environmental hazards, and maintenance of urban air quality. ESA

N87-10655# Ben Gurion Univ. of the Negev, Sede Boqer (Israel). Blaustein Inst. for Desert Research.
DESIGN FOR CLIMATE IN HOT, DRY CITIES **c85**
Baruch Givoni *In* WMO Proceedings of the Technical Conference on Urban Climatology and its Applications with Special Regard to Tropical Areas 1986 p 487-513 (For primary document see N87-10636 01-47)
Avail: NTIS MF A01; print copy available at WMO, Geneva, Switzerland

Human thermal comfort requirements are analyzed showing the relationship between heat sensation and sensible perspiration. Daytime and night-time requirements and ventilation requirements are considered. The theoretical possibilities to reverse the heat island phenomenon, the relationship of building height to ventilation, urban solar control, reducing dust by proper planning, the vegetation as microclimate control, and building design guidelines are considered. It is shown that many options which imply the use of natural resources only are available to designers. ESA

N87-10656# World Meteorological Organization, Geneva (Switzerland).
DESIGN FOR CLIMATE IN HOT, HUMID CITIES **c85**
S. Nieuwolt *In its* Proceedings of the Technical Conference on Urban Climatology and its Applications with Special Regard to Tropical Areas 1986 p 514-534 (For primary document see N87-10636 01-47)
Avail: NTIS MF A01; print copy available at WMO, Geneva, Switzerland

Ways for urban planners and architects to reduce climatic discomfort in hot humid cities are indicated. Climatic information to be supplied, determination of the microclimate, prevention of floods, natural ventilation, protection from solar radiation, and architectural design factors are discussed. It is shown that high buildings, houses on stilts, continuous ventilation, better protection against solar radiation, and low heat storage capacity are design possibilities to increase human comfort. ESA

N87-10657# World Climate Programme, Geneva (Switzerland).
A PRELIMINARY CLOUDLESS STANDARD ATMOSPHERE FOR RADIATION COMPUTATION
Mar. 1986 65 p Presented at International Association for Meteorology and Atmospheric Physics Radiation Commission, Boulder, Colo., 1984
(WCP-112; WMO/TD-24; ETN-86-97807) Avail: NTIS MF A01; print copy available at WMO, Geneva, Switzerland

A cloudfree standard atmosphere to compute the radiation terms for sensitivity studies in climate research is presented. The models presented can be used in first approximation sensitivity studies. They cover atmospheric temperature and humidity, aerosols, and the vertical distribution of radiatively active trace gases. ESA

N87-10658*# National Aeronautics and Space Administration. Goddard Space Flight Center, Greenbelt, Md.
REVIEW OF MEASUREMENTS OF THE RF SPECTRUM OF RADIATION FROM LIGHTNING
David M. LeVine Mar. 1986 20 p
(NASA-TM-87788; NAS 1.15:87788) Avail: NTIS HC A02/MF A01 CSCL 04B

Measurements reported in the literature of the spectrum of electromagnetic radiation from lightning in the frequency range from 1 kHz to 1 GHz are reviewed. Measurements have been made either by monitoring the power received at individual frequencies using a narrow bandwidth recording device tuned to the frequencies under investigation or by recording the transient (time dependent) radiation with a wide bandwidth device and then Fourier transforming the waveform to obtain a spectrum. Measurements of the first type were made extensively in the 1950's and 1960's and several composite spectra have been deduced by normalizing the data of different investigators to common units of bandwidth and distance. The composite spectra tend to peak near 5 kHz and then decrease roughly as (frequency) to the -1, up to nearly 100 MHz where scatter in the data make the behavior uncertain. Measurements of the second type have been reported for return strokes, the stepped leader and for some intracloud processes. The spectrum of first return strokes obtained in this manner is very similar to the composite spectra obtained from the narrow-band measurements. M.G.

N87-10659*# National Aeronautics and Space Administration, Washington, D.C.
NASA AND FAA LAUNCH WIND SHEAR RESEARCH PROJECT
Debra J. Rahn 9 Oct. 1986 2 p
(NASA-News-Rel-86-143) Avail: NTIS HC A02 CSCL 04B

The National Aeronautics and Space Administration and the Federal Aviation Administration have signed a memorandum of agreement calling for a joint 5-year, $24 million research project to develop technology for airborne wind-shear detection and avoidance. The most dangerous type of wind shear, the microburst, is a small intense downdraft which, upon striking the ground, spreads out into a circular vortex radiating in all directions. When encountered at low levels on approach or takeoff, the pilot usually has little time to react correctly to maintain the desired flight path or even react enough to survive. Between 1964 and 1985, there were at least 26 accidents and 3 incidents involving 626 fatalities and 235 injuries where wind shear was the direct cause or a contributing factor. The NASA/FAA research project will cover five major areas: technology assessment, present position sensor integration, hazard characterization, pilot factors in wind shear and effects of heavy rain. This represents a consensus approach among the aviation community. Researchers will thoroughly assess the application of technologies such as Doppler and laser radar for airborne equipment to detect the wind-shear danger with the intent of avoiding it. They also will look at the current reactive systems that tell a pilot he is in wind shear and offer the crew guidance information to facilitate a safe exit from wind shear. Another goal is to develop a better understanding of the complex wind structure of a microburst. Author

N87-10660*# Oklahoma Univ., Norman. Cooperative Inst. for Mesoscale Meteorological Studies.
FURTHER STUDIES WITH DATA COLLECTED BY NASA'S AIRBORNE DOPPLER LIDAR IN OKLAHOMA IN 1981 Final Technical Report, Sep. 1985 - Aug. 1986
Howard B. Bluestein and Eugene W. McCaul, Jr. Oct. 1986 38 p
(NASA Order H-78746B)

(NASA-CR-179779; NAS 1.26:179779) Avail: NTIS HC A03/MF A01 CSCL 04B

Continued study of the lidar data collected in 1981 has resulted in significant new improvements in the analysis techniques reported by Bluestein et al. (1985) and McCaul (1985). Through comparison of fore- and aft-derived scalar fields of intensity and spectral width, the self-consistency of the lidar moment estimates was assessed. Reflectivity estimates were found to be quite stable and reliable, while spectral widths were prone to become noisy if signal to noise ratio (SNR) fell below 12 dB. In addition, spectral widths contained a significant component due to radial velocity gradients in areas along gust fronts, and these components were different along the fore and aft lines of sight. Significant improvement in agreement between the fore and aft fields of spectral width was obtained by estimating the radial velocity gradient component and then removing it from the raw measured widths to yield only the turbulent portion of the contribution to width. Additional analyses showed that lidar-derived vorticity estimates were consistent with several approximate models of vorticity growth along gust front zones, and with the hypothesis that Helmholtz instability could have been responsible for vortices seen along part of the gust front of 30 June 1981. Computations of divergence transverse to axes through an isolated cumulus congestus indicated that the strongest convergence tended to lie along an axis parallel to the congestus. This and the results of other additional analyses seem to suggest that the lidar winds do indeed accurately reflected the basic features of the real wind field. M.G.

N87-10661# Colorado State Univ., Fort Collins. Dept. of Atmospheric Science.

AN OBSERVATIONAL STUDY OF TROPICAL CLOUD CLUSTER EVOLUTION AND CYCLOGENESIS IN THE WESTERN NORTH PACIFIC

Cheng Shang Lee and William M. Gray Sep. 1986 261 p
(Grant NSF ATM-84-19116)
(CSU-ASP-403) Avail: NTIS HC A12/MF A01

A combination of rawinsonde composite and individual case analyses using First GARP Global Experiment (FGGE) III-b data was used to study the evolution of precyclone tropical cloud clusters and those prominent cloud clusters which do not develop into tropical cyclones in the western North Pacific. These two types of cloud clusters are defined as genesis and nongenesis cases. The individual FGGE analyses indicate three possible large scale surges: the cross-equatorial surges, trade wind surges, or summer monsoon surges within the North Indian Ocean. A convection burst and a low-level vorticity buildup are generally found to be associated with these surges. Tropical cyclone formation generally occurs when these surges reach the inner region of the pre-cyclone cloud cluster. The results also indicate large variations between different individual formation cases. Author

N87-10662*# Analytical Mechanics Associates, Inc., Hampton, Va.

SHUTTLE DERIVED ATMOSPHERIC DENSITY MODEL. PART 1: COMPARISONS OF THE VARIOUS AMBIENT ATMOSPHERIC SOURCE DATA WITH DERIVED PARAMETERS FROM THE FIRST TWELVE STS ENTRY FLIGHTS, A DATA PACKAGE FOR AOTV ATMOSPHERIC DEVELOPMENT Final Report

John T. Findlay, G. Mel Kelly, and Patrick A. Troutman Dec. 1984 51 p
(Contract NAS9-17158)
(NASA-CR-171824; NAS 1.26:171824; AMA-84-16) Avail: NTIS HC A04/MF A01 CSCL 04B

The ambient atmospheric parameter comparisons versus derived values from the first twelve Space Shuttle Orbiter entry flights are presented. Available flights, flight data products, and data sources utilized are reviewed. Comparisons are presented based on remote meteorological measurements as well as two comprehensive models which incorporate latitudinal and seasonal effects. These are the Air Force 1978 Reference Atmosphere and the Marshall Space Flight Center Global Reference Model (GRAM). Atmospheric structure sensible in the Shuttle flight data is shown and discussed. A model for consideration in Aero-assisted Orbital Transfer Vehicle (AOTV) trajectory analysis, proposed to modify the GRAM data to emulate Shuttle experiments. B.G.

N87-10663*# Analytical Mechanics Associates, Inc., Hampton, Va.

SHUTTLE DERIVED ATMOSPHERIC DENSITY MODEL. PART 2: STS ATMOSPHERIC IMPLICATIONS FOR AOTV TRAJECTORY ANALYSIS, A PROPOSED GRAM PERTURBATION DENSITY MODEL Final Report

John T. Findlay, G. Mel Kelly, and Patrick A. Troutman Dec. 1984 28 p
(Contract NAS9-17158)
(NASA-CR-171824; NAS 1.26:171824) Avail: NTIS HC A03/MF A01 CSCL 04B

A perturbation model to the Marshall Space Flight Center (MSFC) Global Reference Atmosphere Model (GRAM) was developed for use in the Aeroassist Orbital Transfer Vehicle (AOTV) trajectory and analysis. The model reflects NASA Space Shuttle experience over the first twelve entry flights. The GRAM was selected over the Air Force 1978 Reference Model because of its more general formulation and wider use throughout NASA. The add-on model, a simple scaling with altitude to reflect density structure encountered by the Shuttle Orbiter was selected principally to simplify implementation. Perturbations, by season, can be utilized to minimize the number of required simulations, however, exact Shuttle flight history can be exercised using the same model if desired. Such a perturbation model, though not meteorologically motivated, enables inclusion of High Resolution Accelerometer Package (HiRAP) results in the thermosphere. Provision is made to incorporate differing perturbations during the AOTV entry and exit phases of the aero-asist maneuver to account for trajectory displacement (geographic) along the ground track. Author

N87-10664# National Weather Service, Washington, D.C. Climate Analysis Center.

MONTHLY AND SEASONAL WEATHER OUTLOOK FOR MID-MAY TO MID-JUNE 1986, VOLUME 40, NUMBER 10, MAY 14, 1986

May 1986 10 p
(PB86-199825) Avail: NTIS HC A02/MF A01 CSCL 04B

This long range weather report gives temperature and precipitation probabilities for the Northern Hemisphere on a periodic and seasonal basis. GRA

N87-10665# National Oceanic and Atmospheric Administration, Boulder, Colo. Wave Propagation Lab.

SURFACE MEASUREMENTS OF GUST FRONTS AND MICROBURSTS DURING THE JAWS (JOINT AIRPORT WEATHER STUDIES) PROJECT: STATISTICAL RESULTS AND IMPLICATIONS FOR WIND SHEAR DETECTION, PREDICTION AND MODELING

A. J. Bedard and J. LeFebvre Apr. 1986 123 p
(PB86-200847; NOAA-TM-ERL-WPL-135) Avail: NTIS HC A06/MF A01 CSCL 04B

During the 1982 Joint Airport Weather Studies Project (JAWS), the authors identified 168 microbursts, 20 macrobursts, and 99 gust fronts using surface sensors in the vicinity of Denver's Stapleton Airport. The report reviews aspects of these measurements important to the problem of understanding and detecting wind shear hazardous to aircraft. GRA

N87-10666 Oklahoma Univ., Norman.

THE ASSESSMENT OF CLIMATOLOGICAL IMPACTS ON AGRICULTURAL PRODUCTION AND RESIDENTIAL ENERGY DEMAND Ph.D. Thesis

Ellen Jean Cooter 1985 552 p
Avail: Univ. Microfilms Order No. DA8603508

The assessment of climatological impacts on selected economic activities is presented as a multi-step, inter-disciplinary problem. The assessment process focuses on: (1) user identification, (2) direct impact model selection, (3) methodological development, (4) product development, and (5) product-communication. Two user groups of major economic importance were selected for study; agriculture and gas utilities. The broad agricultural sector is further defined as U.S.A. corn production. The general category of utilities is narrowed to Oklahoma residential gas heating demand. The CERES physiological growth model was selected as the process model for corn production. The statistical analysis for corn production suggests that: (1) although this is a statistically complex model, it can yield useful impact information, (2) as a result of output distributional biases, traditional statistical techniques are not adequate analytical tools, (3) the model yield distribution as a whole is probably non-Gaussian, and (4) there appears to be identifiable weekly patterns of forecasted yields throughout the growing season. The NBSLD energy load model was selected to represent residential gas heating consumption. A cursory statistical analysis suggests relationships among weather variables across the Oklahoma study sites. No linear trend in technology-free modeled energy demand or input weather variables which would correspond to that contained in observed state-level residential energy use was detected. Dissert. Abstr.

N87-10667 Washington Univ., Seattle.
TURBULENT MIXING, DROPLET SPECTRAL EVOLUTION AND DYNAMICS OF WARM CUMULUS CLOUDS Ph.D. Thesis
Jorgen Bjornevad Jensen 1985 212 p
Avail: Univ. Microfilms Order No. DA8603107

The microphysical and dynamical effects of turbulent mixing between a cumulus cloud and its environment are investigated experimentally and theoretically. Conservation principles are applied to determine the composition of the cloudy air, and to discuss microphysical properties in mixed parcels of cloud base air and entrained air using the properties of unmixed parcels as a reference. Comparison of theoretical predictions with observations are performed using 26 cumulus cloud (moderate congestus to supercell thunderstorms) observed during the 1981 Cooperative Convective Precipitation Experiment (CCOPE) in eastern Montana. The source of the entrained air is found by using Paluch's (1979) thermodynamical method on observations from three aircraft. The mixing between cloudy and clear air high above cloud base is investigated with a simple one-dimensional model of turbulent filiments near the interface separating the two air masses. The model incorporates: (1) turbulent deformation, (2) molecular diffusion across the interface, (3) sedimentation of droplets across the interface, and (4) droplet evaporation in the changing humidity field. The model is based on recent mechanical studies of turbulent mixing; it predicts droplet distributions after the homogenization of two air masses (cloudy and clear air). Dissert. Abstr.

N87-10668 Wisconsin Univ., Madison.
RELATIONSHIPS BETWEEN AVAILABLE POTENTIAL ENERGY, KINETIC ENERGY AND EXTRATROPICAL CYCLONES WITHIN LIMITED REGIONS OF THE NORTHERN HEMISPHERE DURING THE FGGE YEAR Ph.D. Thesis
John Victor Zapotocny 1985 176 p
Avail: Univ. Microfilms Order No. DA8524303

Interrelationships between available potential energy and kinetic energy associated with extratropical cyclones are examined for portions of the First GARP (Global Atmospheric Research Program) Global Experiment (FGGE) year. The study is confined to the cyclogenetically active regions encompassing the eastern coasts of Asia (ECA) and North America (NA). Calculations of twice daily regional total values of available potential energy and kinetic energy, and vertically integrated contributions to the totals by individual grid point subvolumes, are done using gridded isentropic data produced from the Level IIIa data set for an active late winter period and a relatively inactive summer period. Dissert. Abstr.

N87-10669 Georgia Inst. of Tech., Atlanta.
FLOW DYNAMICS AND STABILITY IN SEVERE RAINBANDS Ph.D. Thesis
George Basil Kallos 1985 136 p
Avail: Univ. Microfilms Order No. DA8605277

Cold frontal rainbands consist of a quasi-two-dimensional line of strong, but shallow, convection. A relatively cold air-mass at the ground moves through a region with a deep, almost saturated, boundary layer. The air at the inflow location above the saturated boundary layer is relatively dry. In this thesis, the flow dynamics and stability characteristics in a cold frontal rainband are presented. A two-dimensional steady-state model is developed to examine the mechanism by which the cold air-mass at the surface of a cold frontal rainband modifies local stability as it moves through the deep, almost saturated boundary layer. The potential instability evident in the moist stratification ahead of the system is activated by dynamic lifting of boundary-layer air. A dynamic or convective overturning is also observed in the mid-troposphere. This effect results from the intense lee-wave response of the flow in the mid-troposphere. The overturning appears to provide the forcing mechanism for severe convection, and defines the rainband's vertical extent. Cold frontal rainbands exhibit similar characteristics to some squall lines. Thus, the technique developed here would be appropriate to the flow in some squall-line cases. Dissert. Abstr.

N87-10670 Wisconsin Univ., Madison.
ADVECTIVE INFLUENCES ON STEADY AND TRANSIENT FORCED TROPICAL MOTIONS Ph.D. Thesis
Andrew Hugh VanTuyl 1986 184 p
Avail: Univ. Microfilms Order No. DA8605724

The nonlinear response to idealized low-latitude heating is examined and compared with the linear response using a spectral, equatorial Beta-plane shallow-water model for large scale motions. Here the linear solution contains no advections. The differential heating, which may be either steady state or periodic in time, is modeled by a mass source term. Three categories of forcing patterns are considered: wave-only forcing, wave plus latitudinally symmetric Hadley zonal forcing centered on the equator, and wave plus latitudinally antisymmetric monsoonal zonal forcing. The forced zonal wavenumber index may be M = 1, 2, 5, or 8; nonlinear effects scatter energy into harmonics 0 and 2M. Dissert. Abstr.

N87-10267*# Coherent Technologies, Inc., Boulder, Colo.
COHERENT LIDAR TECHNOLOGY FOR GLOBAL WIND PROFILING
R. Milton Huffaker *In* NASA. Langley Research center 13th International Laser Radar Conference Aug. 1986 2 p (For primary document see N87-10263 01-35)
Avail: NTIS HC A15/MF A01 CSCL 04B

N87-10273*# York Univ., Downsview (Ontario). Dept. of Physics.
INVERSION OF 2 WAVELENGTH LIDAR DATA FOR CLOUD PROPERTIES
S. R. Pal and A. I. Carswell *In* NASA. Langley Research Center 13th International Laser Radar Conference Aug. 1986 2 p (For primary document see N87-10263 01-35)
Avail: NTIS HC A15/MF A01 CSCL 04B

N87-10286*# Electricite de France, Chatou.
A METEOROLOGICAL (HUMIDITY, TEMPERATURE, AEROSOLS)) MOBILE DIAL SYSTEM: CONCEPTS AND DESIGN
Cl. Cahen, J. L. Lesne, J. Benard, and P. Ponsardin *In* NASA. Langley Research Center 13th International Laser Radar Conference Aug. 1986 4 p (For primary document see N87-10263 01-35)
Avail: NTIS HC A15/MF A01 CSCL 04B

N87-10293*# York Univ., Downsview (Ontario). Dept. of Physics.
DETERMINATION OF CLOUD MICROPHYSICAL PROPERTIES BY LASER BACKSCATTERING AND EXTINCTION MEASUREMENTS
R. N. Dubinsky, A. I. Carswell, and S. R. Pal *In* NASA. Langley Research Center 13th International Laser Radar Conference Aug. 1986 1 p (For primary document see N87-10263 01-35)
Avail: NTIS HC A15/MF A01 CSCL 04B

N87-10304*# Academy of Sciences (USSR), Tomsk. Inst. of Atmospheric Optics.
LASER SOUNDING OF INSTANTANEOUS AND MEAN SPEED OF WIND USING CORRELATION METHOD
V. E. Zuev, I. V. Samokhvalov, G. G. Matvienko, I. N. Kolev (Academy of Sciences, Sofia (Bulgaria).), and O. P. Prvanov *In* NASA. Langley Research Center 13th International Laser Radar Conference Aug. 1986 4 p (For primary document see N87-10263 01-35)
Avail: NTIS HC A15/MF A01 CSCL 04B

N87-10327*# National Oceanic and Atmospheric Administration, Boulder, Colo.
DOPPLER LIDAR STUDIES OF ATMOSPHERIC WIND FIELD DYNAMICS
R. M. Hardesty, M. J. Post, T. R. Lawrence, and F. F. Hall, Jr. *In* NASA. Langley Research Center 13th International Laser Radar Conference Aug. 1986 4 p (For primary document see N87-10263 01-35)
Avail: NTIS HC A15/MF A01 CSCL 04B

N87-10329*# Oregon Graduate Center for Study and Research, Beaverton. Dept. of Applied Physics and Electrical Engineering.
REMOTE SENSING OF ATMOSPHERIC WINDS USING A COHERENT, CW LIDAR AND SPECKLE-TURBULENCE INTERACTION
J. Fred Holmes, Farzin Amzajerdian, V. S. Rao Gudimetla, and John M. Hunt *In* NASA. Langley Research Center 13th International Laser Radar Conference Aug. 1986 4 p (For primary document see N87-10263 01-35)
Avail: NTIS HC A15/MF A01 CSCL 04B

N87-10331*# National Aeronautics and Space Administration. Goddard Space Flight Center, Greenbelt, Md.
LOWER ATMOSPHERIC TEMPERATURE PROFILE MEASUREMENTS USING A RAMAN LIDAR
S. H. Melfi and D. Whiteman *In* NASA. Langley Research Center 13th International Laser Radar Conference Aug. 1986 1 p (For primary document see N87-10263 01-35)
Avail: NTIS HC A15/MF A01 CSCL 04B

N87-10335*# Atmospheric Environment Service, Downsview (Ontario).
VERTICAL STRUCTURE OF ARCTIC HAZE OBSERVED BY LIDAR
R. M. Hoff *In* NASA. Langley Research Center 13th International Laser Radar Conference Aug. 1986 3 p (For primary document see N87-10263 01-35)
Avail: NTIS HC A15/MF A01 CSCL 04B

N87-10336*# National Aeronautics and Space Administration. Goddard Space Flight Center, Greenbelt, Md.
LIDAR OBSERVATIONS AND MODELING OF COLD AIR OUTBREAKS DURING MASEX AND GALE
R. Boers and S. H. Melfi *In* NASA. Langley Research Center 13th International Laser Radar Conference Aug. 1986 4 p (For primary document see N87-10263 01-35)
Avail: NTIS HC A15/MF A01 CSCL 04B

N87-10342*# Kyushu Univ., Fukuoka (Japan). Dept. of Electronical Engineering.
XeF LIDAR MEASUREMENTS OF DENSITY AND TEMPERATURE IN THE MIDDLE ATMOSPHERE
T. Shibata and M. Maeda *In* NASA. Langley Research Center 13th International Laser Radar Conference Aug. 1986 3 p (For primary document see N87-10263 01-35)
Avail: NTIS HC A15/MF A01 CSCL 04B

N87-10348*# National Aeronautics and Space Administration. Goddard Space Flight Center, Greenbelt, Md.
LIDAR STUDY OF STORM TOPS
J. D. Spinhirne and W. D. Hart *In* NASA. Langley Research Center 13th International Laser Radar Conference Aug. 1986 3 p (For primary document see N87-10263 01-35)
Avail: NTIS HC A15/MF A01 CSCL 04B

N87-10349*# Academy of Sciences, Sofia (Bulgaria). Inst. of Electronics.
INVESTIGATION OF CLOUDS SPATIAL DISTRIBUTION USING GROUND-BASED LIDAR
I. N. Kolev, O. P. Parvanov, B. K. Kaprielov, and I. K. Ilev *In* NASA. Langley Research Center 13th International Laser Radar Conference Aug. 1986 4 p (For primary document see N87-10263 01-35)
Avail: NTIS HC A15/MF A01 CSCL 04B

N87-10353*# Naval Postgraduate School, Monterey, Calif. Dept. of Physics.
CLOUD DETECTION BY LIDAR EXTINCTION CALCULATIONS
W. J. Lentz *In* NASA. Langley Research Center 13th International Laser Radar Conference Aug. 1986 3 p (For primary document see N87-10263 01-35)
Avail: NTIS HC A15/MF A01 CSCL 04B

N87-10361*# Coherent Technologies, Inc., Boulder, Colo.
WAVELENGTH DEPENDENCE OF COHERENT AND INCOHERENT SATELLITE-BASED LIDAR MEASUREMENTS OF WIND VELOCITY AND AEROSOL BACKSCATTER
Michael J. Kavaya and R. Milton Huffaker *In* NASA. Langley Research Center 13th International Laser Radar Conference Aug. 1986 4 p (For primary document see N87-10263 01-35)
Avail: NTIS HC A15/MF A01 CSCL 04B

N87-10420*# National Meteorological Center, Washington, D.C.
ON THE POTENTIAL USE OF RADAR-DERIVED INFORMATION IN OPERATIONAL NUMERICAL WEATHER PREDICTION
Ronald D. McPherson *In* International Council of Scientific Unions, Middle Atmosphere Program. Handbook for MAP, Vol. 20 Jun. 1986 4 p (For primary document see N87-10419 01-42)
Avail: NTIS HC A22/MF A01; also available from SCOSTEP Secretariat, Illinois Univ., 1406 West Green Street, Urbana, Ill. 61801 CSCL 04B

N87-10421*# Oklahoma Univ., Norman. School of Meteorology.
A THEORY FOR THE RETRIEVAL OF VIRTUAL TEMPERATURE FROM WINDS, RADIANCES AND THE EQUATIONS OF FLUID DYNAMICS
Gal-Chen Tzvi *In* International Council of Scientific Unions, Middle Atmosphere Program. Handbook for MAP, Vol. 20 Jun. 1986 12 p (For primary document see N87-10419 01-42)
Avail: NTIS HC A22/MF A01; also available from SCOSTEP Secretariat, Illinois Univ., 1406 West Green Street, Urbana, Ill. 61801 CSCL 04B

N87-10422*# Pennsylvania State Univ., University Park. Dept. of Meteorology.
EXAMPLES OF MESOSCALE STRUCTURES AND SHORT-TERM WIND VARIATIONS DETECTED BY VHF DOPPLER RADAR
G. S. Forbes *In* International Council of Scientific Unions, Middle Atmosphere Program. Handbook for MAP, Vol. 20 Jun. 1986 13 p (For primary document see N87-10419 01-42)
Avail: NTIS HC A22/MF A01; also available from SCOSTEP Secretariat, Illinois Univ., 1406 West Green Street, Urbana, Ill. 61801 CSCL 04B

N87-10423*# National Center for Atmospheric Research, Boulder, Colo.
WIND PROFILER DATA IN A MESOSCALE EXPERIMENT FROM A METEOROLOGICAL PERSPECTIVE
Edward J. Zipser, John Augustine (National Oceanic and Atmospheric Administration, Boulder, Colo.), and John Cunning *In* International Council of Scientific Unions, Middle Atmosphere Program. Handbook for MAP, Vol. 20 Jun. 1986 5 p Sponsored in part by NSF (For primary document see N87-10419 01-42)
Avail: NTIS HC A22/MF A01; also available from SCOSTEP

Secretariat, Illinois Univ., 1406 West Green Street, Urbana, Ill. 61801 CSCL 04B

N87-10424*# Clemson Univ., S.C. Dept. of Physics.
OBSERVATIONS OF MESOSCALE VERTICAL VELOCITIES AROUND FRONTAL ZONES
T. S. Dennis, M. F. Larsen, and J. Rottger (Arecibo Ionospheric Observatory, Puerto Rico) *In* International Council of Scientific Unions, Middle Atmosphere Program. Handbook for MAP, Vol. 20 Jun. 1986 9 p (For primary document see N87-10419 01-42)
Avail: NTIS HC A22/MF A01; also available from SCOSTEP Secretariat, Illinois Univ., 1406 West Green Street, Urbana, Ill. 61801 CSCL 04B

N87-10425*# Clemson Univ., S.C. Dept. of Physics and Astronomy.
COMPARISON OF VERTICAL VELOCITIES ANALYZED BY A NUMERICAL MODEL AND MEASURED BY A VHF WIND PROFILER
M. F. Larsen, J. Rottger (Arecibo Ionospheric Observatory, Puerto Rico), and T. S. Dennis *In* International Council of Scientific Unions, Middle Atmosphere Program. Handbook for MAP, Vol. 20 Jun. 1986 4 p (For primary document see N87-10419 01-42)
Avail: NTIS HC A22/MF A01; also available from SCOSTEP Secretariat, Illinois Univ., 1406 West Green Street, Urbana, Ill. 61801 CSCL 04B

N87-10426*# Kyoto Inst. of Tech. (Japan). Dept. of Electrical Engineering.
MEASUREMENTS OF PRECIPITATING ATMOSPHERE BY THE MU RADAR
Koichiro Wakasugi, Shoichiro Fukao (Kyoto Univ., Japan), and Susumu Kato *In* International Council of Scientific Unions, Middle Atmosphere Program. Handbook for MAP, Vol. 20 Jun. 1986 5 p (For primary document see N87-10419 01-42)
Avail: NTIS HC A22/MF A01; also available from SCOSTEP Secretariat, Illinois Univ., 1406 West Green Street, Urbana, Ill. 61801 CSCL 04B

N87-10427*# National Oceanic and Atmospheric Administration, Boulder, Colo.
THE REAL-TIME USE OF WIND PROFILERS IN NOWCASTING
Tracy Lorraine Smith and Thomas W. Schlatter *In* International Council of Scientific Unions, Middle Atmosphere Program. Handbook for MAP, Vol. 20 Jun. 1986 7 p (For primary document see N87-10419 01-42)
Avail: NTIS HC A22/MF A01; also available from SCOSTEP Secretariat, Illinois Univ., 1406 West Green Street, Urbana, Ill. 61801 CSCL 04B

N87-10428*# Arecibo Ionospheric Observatory, Puerto Rico.
THE INFLUENCE OF VELOCITY VARIABILITY ON THE DETERMINATION OF WIND PROFILES
Jurgen Rottger *In* International Council of Scientific Unions, Middle Atmosphere Program. Handbook for MAP, Vol. 20 Jun. 1986 5 p (For primary document see N87-10419 01-42)
Avail: NTIS HC A22/MF A01; also available from SCOSTEP Secretariat, Illinois Univ., 1406 West Green Street, Urbana, Ill. 61801 CSCL 04B

N87-10429*# National Oceanic and Atmospheric Administration, Boulder, Colo.
PERFORMANCE CHARACTERISTICS OF WIND PROFILING RADARS
R. G. Strauch, A. S. Frisch, and B. L. Weber *In* International Council of Scientific Unions, Middle Atmosphere Program. Handbook for MAP, Vol. 20 Jun. 1986 7 p (For primary document see N87-10419 01-42)
Avail: NTIS HC A22/MF A01; also available from SCOSTEP Secretariat, Illinois Univ., 1406 West Green Street, Urbana, Ill. 61801 CSCL 04B

N87-10430*# National Severe Storms Lab., Norman, Okla.
A LOOK AT PROFILER PERFORMANCE
Edwin Kessler, Michael Eilts, and Kevin Thomas (Oklahoma Univ., Norman) *In* International Council of Scientific Unions, Middle Atmosphere Program. Handbook for MAP, Vol. 20 Jun. 1986 13 p (For primary document see N87-10419 01-42)
Avail: NTIS HC A22/MF A01; also available from SCOSTEP Secretariat, Illinois Univ., 1406 West Green Street, Urbana, Ill. 61801 CSCL 04B

N87-10431*# Adelaide Univ. (Australia). Dept. of Physics.
HARDWARE REQUIREMENTS: A NEW GENERATION PARTIAL REFLECTION RADAR FOR STUDIES OF THE EQUATORIAL MESOSPHERE
R. A. Vincent *In* International Council of Scientific Unions, Middle Atmosphere Program. Handbook for MAP, Vol. 20 Jun. 1986 1 p (For primary document see N87-10419 01-42)
Avail: NTIS HC A22/MF A01; also available from SCOSTEP Secretariat, Illinois Univ., 1406 West Green Street, Urbana, Ill. 61801 CSCL 04B

N87-10432*# Arecibo Ionospheric Observatory, Puerto Rico.
NEED FOR A SUBTROPICAL WIND PROFILING SYSTEM
J. Rottger, M. F. Larsen (Clemson Univ., S.C.), H. M. Ierkic, and T. Hagfors *In* International Council of Scientific Unions, Middle Atmosphere Program. Handbook for MAP, Vol. 20 Jun. 1986 4 p (For primary document see N87-10419 01-42)
Avail: NTIS HC A22/MF A01; also available from SCOSTEP Secretariat, Illinois Univ., 1406 West Green Street, Urbana, Ill. 61801 CSCL 04B

N87-10445*# Centre National d'Etudes des Telecommunications, Saint Maur des Fosses (France).
THE PROUST RADAR: FIRST RESULTS
F. Bertin, A. Cremieu, M. Glass, M. Massebeuf, and M. Petitdidier *In* International Council of Scientific Unions, Middle Atmosphere Program. Handbook for MAP, Vol. 20 Jun. 1986 4 p (For primary document see N87-10419 01-42)
Avail: NTIS HC A22/MF A01; also available from SCOSTEP Secretariat, Illinois Univ., 1406 West Green Street, Urbana, Ill. 61801 CSCL 04B

N87-10446*# Centre National d'Etudes des Telecommunications, Saint Maur des Fosses (France).
SIMULTANEOUS FINE STRUCTURE OBSERVATION OF WIND AND TEMPERATURE PROFILES BY THE ARECIBO 430-MHz RADAR AND IN SITU MEASUREMENTS
D. Thomas, F. Bertin, M. Petitdidier, H. Teitelbaum (Ecole Polytechnique, Palaiseau, France), and R. F. Woodman (Instituto Geofisico del Peru, Lima) *In* International Council of Scientific Unions, Middle Atmosphere Program. Handbook for MAP, Vol. 20 Jun. 1986 3 p (For primary document see N87-10419 01-42)
Avail: NTIS HC A22/MF A01; also available from SCOSTEP Secretariat, Illinois Univ., 1406 West Green Street, Urbana, Ill. 61801 CSCL 04B

N87-10454*# National Oceanic and Atmospheric Administration, Boulder, Colo. Aeronomy Lab.
CLIMATOLOGY OF GRAVITY WAVES OVER POKER FLAT, ALASKA FOR 1983
Ben B. Balsley and Rene Garello (Ecole Nationale Superieure de Techniques Avancees, Paris, France) *In* International Council of Scientific Unions, Middle Atmosphere Program. Handbook for MAP, Vol. 20 Jun. 1986 2 p (For primary document see N87-10419 01-42)
Avail: NTIS HC A22/MF A01; also available from SCOSTEP Secretariat, Illinois Univ., 1406 West Green Street, Urbana, Ill. 61801 CSCL 04B

N87-10455*# National Oceanic and Atmospheric Administration, Boulder, Colo. Aeronomy Lab.
CLIMATOLOGY OF TROPOSPHERIC VERTICAL VELOCITY SPECTRA
W. L. Ecklund, K. S. Gage, B. B. Balsley, and D. A. Carter *In*

International Council of Scientific Unions, Middle Atmosphere Program. Handbook for MAP, Vol. 20 Jun. 1986 2 p (For primary document see N87-10419 01-42)
Avail: NTIS HC A22/MF A01; also available from SCOSTEP Secretariat, Illinois Univ., 1406 West Green Street, Urbana, Ill. 61801 CSCL 04B

N87-10468*# Adelaide Univ. (Australia). Dept. of Physics.
INTERCOMPARISON AND CALIBRATION OF WIND AND WAVE MEASUREMENTS AT VARIOUS FREQUENCIES
R. A. Vincent *In* International Council of Scientific Unions, Middle Atmosphere Program. Handbook for MAP, Vol. 20 Jun. 1986 7 p (For primary document see N87-10419 01-42)
Avail: NTIS HC A22/MF A01; also available from SCOSTEP Secretariat, Illinois Univ., 1406 West Green Street, Urbana, Ill. 61801 CSCL 04B

N87-10469*# Pennsylvania State Univ., University Park. Dept. of Meteorology.
AN EVALUATION OF ERRORS OBSERVED IN THE MEASUREMENT OF LOW WIND VELOCITIES
S. R. Williams and D. W. Thomson *In* International Council of Scientific Unions, Middle Atmosphere Program. Handbook for MAP, Vol. 20 Jun. 1986 7 p (For primary document see N87-10419 01-42)
Avail: NTIS HC A22/MF A01; also available from SCOSTEP Secretariat, Illinois Univ., 1406 West Green Street, Urbana, Ill. 61801 CSCL 04B

N87-10471*# National Oceanic and Atmospheric Administration, Boulder, Colo.
METHODS FOR VERIFYING THE ACCURACY OF WIND PROFILES
R. C. Strauch *In* International Council of Scientific Unions, Middle Atmosphere Program. Handbook for MAP, Vol. 20 Jun. 1986 6 p (For primary document see N87-10419 01-42)
Avail: NTIS HC A22/MF A01; also available from SCOSTEP Secretariat, Illinois Univ., 1406 West Green Street, Urbana, Ill. 61801 CSCL 04B

N87-10472*# Clemson Univ., S.C. Dept. of Physics and Astronomy.
A COMPARISON OF THUNDERSTORM REFLECTIVITIES MEASURED AT THE VHF AND UHF
M. F. Larsen and J. Rottger *In* International Council of Scientific Unions, Middle Atmosphere Program. Handbook for MAP, Vol. 20 Jun. 1986 9 p (For primary document see N87-10419 01-42)
Avail: NTIS HC A22/MF A01; also available from SCOSTEP Secretariat, Illinois Univ., 1406 West Green Street, Urbana, Ill. 61801 CSCL 04B

N87-10473*# Clemson Univ., S.C. Dept. of Physics and Astronomy.
UHF AND VHF RADAR OBSERVATIONS OF THUNDERSTORMS
D. N. Holden, C. W. Ulbrich, M. F. Larsen, J. Rottger (Arecibo Ionospheric Observatory, Puerto Rico), H. M. Ierkic, and W. Swartz (Cornell Univ., Ithaca, N.Y.) *In* International Council of Scientific Unions, Middle Atmosphere Program. Handbook for MAP, Vol. 20 Jun. 1986 5 p (For primary document see N87-10419 01-42)
Avail: NTIS HC A22/MF A01; also available from SCOSTEP Secretariat, Illinois Univ., 1406 West Green Street, Urbana, Ill. 61801 CSCL 04B

N87-10477*# Arecibo Ionospheric Observatory, Puerto Rico.
COMPARISON OF REFLECTIVITY AND WIND PROFILES MEASURED ON 46.8 MHz AND 430 MHz AT THE ARECIBO OBSERVATORY
Jurgen Rottger *In* International Council of Scientific Unions, Middle Atmosphere Program. Handbook for MAP, Vol. 20 Jun. 1986 2 p (For primary document see N87-10419 01-42)
Avail: NTIS HC A22/MF A01; also available from SCOSTEP Secretariat, Illinois Univ., 1406 West Green Street, Urbana, Ill. 61801 CSCL 04B

N87-10484*# National Oceanic and Atmospheric Administration, Boulder, Colo. Aeronomy Lab.
CONTINUOUS WIND MEASUREMENT IN THE TROPICAL PACIFIC USING VHF RADARS
B. B. Balsley, W. L. Ecklund, and D. A. Carter *In* International Council of Scientific Unions, Middle Atmosphere Program. Handbook for MAP, Vol. 20 Jun. 1986 1 p (For primary document see N87-10419 01-42)
Avail: NTIS HC A22/MF A01; also available from SCOSTEP Secretariat, Illinois Univ., 1406 West Green Street, Urbana, Ill. 61801 CSCL 04B

N87-10486*# National Oceanic and Atmospheric Administration, Boulder, Colo.
COLORADO WIND PROFILERS
R. G. Strauch *In* International Council of Scientific Unions, Middle Atmosphere Program. Handbook for MAP, Vol. 20 Jun. 1986 2 p (For primary document see N87-10419 01-42)
Avail: NTIS HC A22/MF A01; also available from SCOSTEP Secretariat, Illinois Univ., 1406 West Green Street, Urbana, Ill. 61801 CSCL 04B

N87-10487*# National Oceanic and Atmospheric Administration, Boulder, Colo.
WIND PROFILER DEMONSTRATION SYSTEM
R. B. Chadwick *In* International Council of Scientific Unions, Middle Atmosphere Program. Handbook for MAP, Vol. 20 Jun. 1986 2 p (For primary document see N87-10419 01-42)
Avail: NTIS HC A22/MF A01; also available from SCOSTEP Secretariat, Illinois Univ., 1406 West Green Street, Urbana, Ill. 61801 CSCL 04B

N87-10502*# National Oceanic and Atmospheric Administration, Boulder, Colo. Aeronomy Lab.
DETERMINATION OF U, V, AND W FROM SINGLE STATION DOPPLER RADAR RADIAL VELOCITIES
W. L. Clark, J. L. Green, and J. M. Warnock *In* International Council of Scientific Unions, Middle Atmosphere Program. Handbook for MAP, Vol. 20 Jun. 1986 8 p (For primary document see N87-10419 01-42)
Avail: NTIS HC A22/MF A01; also available from SCOSTEP Secretariat, Illinois Univ., 1406 West Green Street, Urbana, Ill. 61801 CSCL 04B

N87-10506*# Toulon Univ. (France).
SIMULTANEOUS MULTIBEAM SOUNDING OF WIND AND TURBULENCE
E. Brun, M. Crochet, and W. L. Ecklund (National Oceanic and Atmospheric Administration, Boulder, Colo.) *In* International Council of Scientific Unions, Middle Atmosphere Program. Handbook for MAP, Vol. 20 Jun. 1986 7 p (For primary document see N87-10419 01-42)
Avail: NTIS HC A22/MF A01; also available from SCOSTEP Secretariat, Illinois Univ., 1406 West Green Street, Urbana, Ill. 61801 CSCL 04B

48 OCEANOGRAPHY

Includes biological, dynamic, and physical oceanography; and marine resources.

For related information see also *43 Earth Resources and Remote Sensing.*

N87-10671*# Jet Propulsion Lab., California Inst. of Tech., Pasadena.
SCIENCE OPPORTUNITIES FROM THE TOPEX/POSEIDON MISSION
R. Stewart, L.-L. Fu, and M. Lefebvre 15 Jul. 1986 68 p
(Contract NAS7-918)
(NASA-CR-179752; JPL-Pub-86-18; NAS 1.26:179752) Avail: NTIS HC A04/MF A01 CSCL 08C

The U.S. National Aeronautics and Space Administration (NASA) and the French Centre National d'Etudes Spatiales (CNES) propose to conduct a Topex/Poseidon Mission for studying the global ocean circulation from space. The mission will use the techniques of satellite altimetry to make precise and accurate measurements of sea level for several years. The measurements will then be used by Principal Investigators (selected by NASA and CNES) and by the wider oceanographic community working closely with large international programs for observing the Earth, on studies leading to an improved understanding of global ocean dynamics and the interaction of the ocean with other processes influencing life on Earth. The major elements of the mission include a satellite carrying an altimetric system for measuring the height of the satellite above the sea surface; a precision orbit determination system for referring the altimetric measurements to geodetic coordinates; a data analysis and distribution system for processing the satellite data, verifying their accuracy, and making them available to the scientific community; and a principal investigator program for scientific studies based on the satellite observations. This document describes the satellite, its sensors, its orbit, the data analysis system, and plans for verifying and distributing the data. It then discusses the expected accuracy of the satellite's measurements and their usefulness to oceanographic, geophysical, and other scientific studies. Finally, it outlines the relationship of the Topex/Poseidon mission to other large programs, including the World Climate Research Program, the U.S. Navy's Remote Ocean Sensing System satellite program and the European Space Agency's ERS-1 satellite program. Author

N87-10672# Scripps Institution of Oceanography, La Jolla, Calif. Marine Physical Lab.
THE INTERNAL TIDE OFF SOUTHERN CALIFORNIA Summary Report
Robin G. Williams Jan. 1986 176 p
(Contract N00014-79-C-0472)
(AD-A167722; MPL-U-34/85; S10-REF-86-1) Avail: NTIS HC A09/MF A01 CSCL 08/10

The internal tide may well form an important link in the chain of events between the forcing of the surface tide and the eventual dissipation of internal waves by viscous forces. Two issues related to this chain of events are addressed. One is the directionality of the internal tide off the coast of California and the other is the widespread occurrence of semi-diurnal tidal harmonics in internal wave spectra. It is commonly accepted that the internal tide derives its energy from the forcing of isopycnal surfaces over topographic features by the surface tide. Accordingly, steep continental slopes like the Patton escarpment should be important generation regions. The directionality of the internal tide off California and hence the importance of the Patton escarpment as a source are assessed by analyzing data collected by the R/P FLIP. The results indicate that the direction of propagation of the internal tide is variable and that the majority of its energy does not appear to originate at the escarpment. GRA

N87-10673 North Carolina State Univ., Raleigh.
MODELING THE EFFECTS OF THE SPATIALLY VARYING SEA SURFACE TEMPERATURE ON THE MARINE ATMOSPHERIC BOUNDARY LAYER Ph.D. Thesis
Mickey Man-Kui Wai 1986 248 p
Avail: Univ. Microfilms Order No. DA8610713

A model for numerical simulation of the marine boundary layer was constructed. The model consists of three parts: a planetary boundary layer model using primitive equations with the Boussinesq approximation; a longwave thermal radiative transfer model using flux method and mixed emissivity; and a second-order turbulent closure model which allows water vapor condensation. In the one-dimensional case for the daytime convection boundary layer, the predicted mean fields agree well with the observations, and the turbulent fields are similar to those obtained by large-eddy simulation model and the third-order closure model. For the quasi-steady state of one-dimensional simulation for the marine stratocumulus-capped mixed layer, the turbulent warming effect approximately balances the radiative effects in the moist static energy equation. For the case with no background flow, the two-dimensional simulation of a cold anomaly reproduces symmetric direct circulation cells. For the case of a finite background flow, the cold anomaly sets up an asymmetric perturbation pressure which induces a system of horizontal divergence and convergence in the boundary layer which gives rise to vertical motion and the subsequent modification of thermal and moisture fields. Dissert. Abstr.

51 LIFE SCIENCES (GENERAL)

N87-10686# Institute of Biomedical Problems, Moscow (USSR).
FUNCTIONS OF SKELETAL MUSCLES OF RATS AND MONKEYS AFTER 5-DAY SPACE FLIGHT (ON COSMOS 1514)
V. S. Oganov, A. S. Rakhmanov, S. A. Skuratova, M. A. Shirvinskaya, and V. S. Magedov *In* ESA Proceedings of 2nd International Conference on Space Physiology Feb. 1986 p 89-93 (For primary document see N87-10675 01-52)
Avail: NTIS HC A12/MF A01

N87-10687# Centre National de la Recherche Scientifique, Lyon (France). Lab. de Physiologie.
HINDLIMB SUSPENSION EFFECTS ON RAT SKELETAL MUSCLE RESPONSE
D. Desplanches, M. H. Mayet, B. Sempore, M. Grandmontagne, J. Frutoso, and R. Flandrois *In* ESA Proceedings of 2nd International Conference on Space Physiology Feb. 1986 p 95-98 (For primary document see N87-10675 01-52)
Avail: NTIS HC A12/MF A01

N87-10704# National Aeronautics and Space Administration, Washington, D.C.
ANIMAL STUDIES ON SPACELAB-3
C. Schatte, R. Grindeland, P. Callahan, W. Berry, G. Funk (Management and Technical Services Co., Philadelphia, Pa.), and W. Lencki *In* ESA Proceedings of 2nd International Conference on Space Physiology Feb. 1986 p 233-244 Previously announced as N86-16889 (For primary document see N87-10675 01-52)
Avail: NTIS HC A12/MF A01

N87-10705# Centre d'Etudes et de Recherches de Medecine Aeronautique, Paris (France).
ANIMAL MODELS IN SPACE PHYSIOLOGY [MODELES ANIMAUX EN PHYSIOLOGIE SPATIALE]
C. L. Milhaud *In* ESA Proceedings of 2nd International Conference on Space Physiology Feb. 1986 p 203-209 In FRENCH (For primary document see N87-10675 01-52)
Avail: NTIS HC A12/MF A01

N87-10706# Centre d'Etudes et de Recherches de Medecine Aeronautique, Paris (France).
CONTRIBUTION OF ANIMAL MODELS TO THE INVESTIGATION OF BONE CHANGES IN WEIGHTLESSNESS
C. Nogues, C. Milhaud, P. Pesquies, and V. S. Oganov (Institute of Biomedical Problems, Moscow, USSR) *In* ESA Proceedings of 2nd International Conference on Space Physiology Feb. 1986 p 211-215 (For primary document see N87-10675 01-52)
Avail: NTIS HC A12/MF A01

N87-10707# Centre d'Etudes et de Recherches de Medecine Aeronautique, Paris (France).
COSMOS 1514 FLIGHT: STUDY OF RHESUS MONKEY ECG
R. Blostin, C. Milhaud, B. Cailler, P. Pesquies, V. Melnitchenko (Institute of Biomedical Problems, Moscow, USSR), B. Kulaev, V. Magedoc, and G. Tchamurliev *In* ESA Proceedings of 2nd International Conference on Space Physiology Feb. 1986 p 217-223 (For primary document see N87-10675 01-52)
Avail: NTIS HC A12/MF A01

N87-10708# Institute of Biomedical Problems, Moscow (USSR).
THE STATE OF BONES OF PREGNANT RATS DURING AN ACUTE STAGE OF ADAPTATION TO WEIGHTLESSNESS
A. V. Bakulin, E. A. Ilyan, V. S. Oganov, and V. I. Lebedev *In* ESA Proceedings of 2nd International Conference on Space Physiology Feb. 1986 p 225-228 (For primary document see N87-10675 01-52)
Avail: NTIS HC A12/MF A01

52 AEROSPACE MEDICINE

Includes physiological factors; biological effects of radiation; and effects of weightlessness on man and animals.

N87-10674* National Aeronautics and Space Administration, Washington, D.C.
AEROSPACE MEDICINE AND BIOLOGY: A CONTINUING BIBLIOGRAPHY WITH INDEXES
Oct. 1986 76 p
(NASA-SP-7011(289); NAS 1.21:7011(289)) Avail: Issuing Activity CSCL 06E

This bibliography lists 210 reports, articles and other documents introduced into the NASA scientific and information system in September 1986. Author

N87-10675# European Space Agency, Paris (France).
PROCEEDINGS OF 2ND INTERNATIONAL CONFERENCE ON SPACE PHYSIOLOGY
J. J. Hunt, ed. Feb. 1986 259 p Partly in ENGLISH and FRENCH Conference held in Toulouse, France, 20-22 Nov. 1985; sponsored by ESA and CNES
(ESA-SP-237; ISSN-0379-6566; ETN-86-97561) Avail: NTIS HC A12/MF A01

The effects of space flight on the cardiovascular system, fluid and electrolyte regulations, bones and muscles, neurovestibular system, and motion sickness were discussed. Ground based weightlessness simulation, animal models, and mathematical models were reviewed. For individual titles, see N87-10676 through N87-10709.

N87-10676# Copenhagen Univ. (Denmark). August Krogh Inst.
CARDIOVASCULAR MEASUREMENTS IN MICROGRAVITY
P. Norsk and F. Bonde-Petersen *In* ESA Proceedings of 2nd International Conference on Space Physiology Feb. 1986 p 9-12 (For primary document see N87-10675 01-52)
Avail: NTIS HC A12/MF A01

Skylab and Biosatellite 3 cardiovascular measurements are discussed. During microgravity the volume of the lower extremities decreases while the intrathoracic blood volume increases. This is indicated by the decrease in calf girth measured during the Skylab missions and the increase in central venous pressure measured in a monkey on Biosatellite 3 and in human subjects during short periods of microgravity in a parabolic flight. An increase in left ventricle diastolic volume, cardiac output, and stroke volume supports this. Probably due to this translocation of extracellular fluid, cardiovascular reflexes are elicited inducing increased peripheral blood flow and decreased venous compliance with a decrease in orthostatic tolerance. Changes in electrocardiographic measurements indicate a prolonged PR-interval and an increase in QRS maximum vector magnitude. ESA

N87-10677# Centre Hospitalier Univ. Rangueil, Toulouse (France). Service Neurologie.
CARDIOVASCULAR EXAMINATION DURING STS 51 G MISSION JUNE (1985)
L. Pourcelot (Hopital Bretonneau, Tours, France), Ph. Arbeille, J.-M. Pottier, L. Patat, M. Berson, A. Roncin, Ch. leToullec, A. Guell, and C. Gharib (Lyon-1 Univ., France) *In* ESA Proceedings of 2nd International Conference on Space Physiology Feb. 1986 p 13-17 (For primary document see N87-10675 01-52)
Avail: NTIS HC A12/MF A01

Cardiovascular examination was performed on two astronauts during STS 51 G. The ultrasound based device used for the study was designed for multimode operation: real time imaging, time-motion, Doppler, and duplex B-Doppler. Cardiac function and volume changes, blood flow volume in carotid and femoral arteries, transit time of pressure waves, and venous circulation were studied preflight, inflight and postflight. The dynamic response of the cardiovascular system was measured inflight and during ground simulation. Results show a decrease of cardiac output stroke volume and left ventricular diastolic volume; a decrease in cerebral circulatory resistance, and variations in peripheral resistance and vascular stiffness of the lower limbs in accordance with orthostatic disturbances during the recovery period. ESA

N87-10678# Centre d'Essais en Vol, Bretigny-sur-Orge (France). Lab. de Medecine Aerospatiale.
THE INTEREST OF CENTRIFUGE TESTS FOR THE SELECTION OF FRENCH COSMONAUTS [INTERET DES EPREUVES EN CENTRIFUGEUSE POUR LA SELECTION DES COSMONAUTES FRANCAIS]
J. M. Clere, B. Agin, Y. Guezennec, J. L. Poirier, and H. Vieillefond *In* ESA Proceedings of 2nd International Conference on Space Physiology Feb. 1986 p 21-27 In FRENCH (For primary document see N87-10675 01-52)
Avail: NTIS HC A12/MF A01

Human centrifuge tests for space flight crew selection are reviewed. The tests examine cardiovascular response to gravitational stresses equivalent to those encountered during launch and reentry. They include electrocardiograms, heart rate, blood pressure, central and peripheral vision, and arterial oxygen saturation. Results led to the elimination of 2 payload specialists (from 13 candidates) even though they have no functions to execute under hypergravity. ESA

N87-10679# National Aeronautics and Space Administration. Lyndon B. Johnson Space Center, Houston, Tex.
THE REGULATION OF FLUID AND ELECTROLYTE METABOLISM IN WEIGHTLESSNESS
C. S. Leach, P. C. Johnson, and N. M. Cintron *In* ESA Proceedings of 2nd International Conference on Space Physiology Feb. 1986 p 31-36 (For primary document see N87-10675 01-52)
Avail: NTIS HC A12/MF A01

Endocrine and biochemical changes in astronauts caused by weightlessness are discussed. Translocation of fluid from the extremities to the head and chest at the onset of weightlessness is thought to lead to the establishment of a lower blood volume as an adaptation to microgravity. Results of Skylab experiments indicate that several other regulatory systems have lower homeostatic set points during space flight. Inflight blood samples from three Spacelab flights show increased antidiuretic hormone throughout these short flights and decreased aldosterone and cortisol after 3 days. Results help to explain blood hypoosmolality and hyponatremia but do not explain what happens between the onset of weightlessness and hormone changes. Other factors such as natriuretic peptides and changes in renal function are being studied to elucidate the physiologic adaptation mechanisms. ESA

N87-10680# Hopital Lariboisiere, Paris (France).
ANTICORTISOL MONOCLONAL ANTIBODIES: CHARACTERIZATION OF THEIR SPECIFICITY [ANTICORPS MONOCLONAUX ANTI-CORTISOL: CARACTERISATION DE LEUR SPECIFICITE]
P. J. Birkui, Ph. Pouletty (CLONATEC, Paris, France), Ch. Rebollo, and M. Leroy (Hopital Saint Louis, Paris, France) *In* ESA Proceedings of 2nd International Conference on Space Physiology Feb. 1986 p 37-39 In FRENCH (For primary document see N87-10675 01-52)
Avail: NTIS HC A12/MF A01

Four anticortisol monoclonal antibodies from a group of nine developed by cell fusion were studied. Their constant of affinity was investigated by radioimmunological dosing in competition. Cross reactivity was evaluated on a panel of 10 structural analogs of cortisol by the same technique. The molar concentrations used for each analog corresponded to 5000 times (or more) the concentration of plasma in human physiology. The antibodies can be used to specify the structure/antigen relation of steroids and to fix a dose of cortisol by competition. ESA

N87-10681# Hopital Nord, Saint-Priest-en-Jarez (France). Lab. de Biologie du Tissu Osseux.
BONES AND WEIGHTLESSNESS [OS ET APESANTEUR]
C. Alexandre *In* ESA Proceedings of 2nd International Conference on Space Physiology Feb. 1986 p 45-52 In FRENCH (For primary document see N87-10675 01-52)
Avail: NTIS HC A12/MF A01

The effects of weightlessness on the phosphorus and calcium metabolisms and on bone remodeling are reviewed. The difficulties of extrapolating data from ground based studies to space conditions are discussed, and contradictions in results from space flights are noted. Weightlessness appears to affect load bearing and non load bearing bones differently. During the first two weeks in space, bone demineralization occurs, but the process stabilizes afterwards. The old bone ages through reduced turnover, while the new bone is immature and is quickly eliminated. These phenomena are completely reversible after a few weeks, but only partially reversible after two or three months. ESA

N87-10682# European Space Agency, Paris (France).
THE MUSCULAR SYSTEM IN WEIGHTLESSNESS [LE SYSTEME MUSCULAIRE EN APESANTEUR]
Yvonne Mounier *In* ESA Proceedings of 2nd International Conference on Space Physiology Feb. 1986 p 53-59 In FRENCH (For primary document see N87-10675 01-52)
Avail: NTIS HC A12/MF A01

Muscular atrophy, especially in the legs, after a period of weightlessness is discussed. The drop in muscular strength may be due to a decrease in the calcium affinity of the contractile proteins. The muscles acquire kinetic functions opposite those characteristic of the functions normally found on the ground. The proportions of slow and fast fibers of each muscle are modified. These phenomena can be interpretated via a purely muscular theory of molecular rearrangement and/or by considering changes in nerve control of muscle commands after a stay in space. ESA

N87-10683# Universite des Sciences et Techniques de Lille (France).
MICROGRAVITY EFFECTS ON THE CONTRACTILE PROTEINS OF RAT MUSCLES
X. Holy, Y. Mounier, and C. Goblet *In* ESA Proceedings of 2nd International Conference on Space Physiology Feb. 1986 p 61-64 (For primary document see N87-10675 01-52)
Avail: NTIS HC A12/MF A01

Tensions activated by calcium concentrations on chemically skinned fibers of rat muscles were used to study the effect of microgravity on contractile protein activity. Three muscles (gastrocnemius, plantaris, and diaphragm) and three groups (vivarium, synchronous, and flight rats) were tested. The muscle function criteria studied were the maximum mechanical activity, the cross-bridge cycling speed, and calcium binding affinity. Microgravity induces a decrease of maximum mechanical activity on gastrocnemius and plantaris; no modification is observed on diaphragm. Cross-bridge cycling speed and calcium binding affinity are reduced on gastrocnemius; plantaris muscle only exhibits a reduction in cross-bridge activity. ESA

N87-10684# Hopital Nord, Saint-Priest-en-Jarez (France). Lab. de Biologie du Tissu Osseux.
WEIGHTLESSNESS EFFECTS ON THE BONE TISSUE OF RATS AFTER A 5 DAY SPACE FLIGHT (COSMOS 1514) [EFFETS DE L'APESANTEUR SUR LE TISSU OSSEUX DE RAT APRES UN VOL SPATIAL DE CINQ JOURS (COSMOS 1514)]
L. Vico, D. Chappard, C. Alexandre, S. Palle, P. Minaire, G. Riffat, A. I. Grigoriev, and V. S. Oganov *In* ESA Proceedings of 2nd International Conference on Space Physiology Feb. 1986 p 67-78 In FRENCH (For primary document see N87-10675 01-52)
Avail: NTIS HC A12/MF A01

Five pregnant female rats (rapid growth phase) were exposed to weightlessness in a Cosmos satellite. Two other groups of five (vivarium, synchronous) were also studied. Histomorphometric analyses were performed to study: early effects on bone mass of load bearing (tibia-femur) and non load bearing bones (dorsal and lumbar vertebrae); and osteoblast and osteoclast activity. Short stays in weightlessness appear to have no effect on bone mass and bone structure. Vertebrate osteoblasts are also unaffected. Osteoclasts/cumm do not vary, but an increase per sqmm on the bone surface is noted. Bone formation of non bearers is unaffected after 5 days, but absorption increases. ESA

N87-10685# Hopital Nord, Saint-Priest-en-Jarez (France). Lab. de Biologie du Tissu Osseux.
BONE TISSUE AND MUSCULAR PERFORMANCE IN A POPULATION OF ELDERLY MEN AS A FUNCTION OF PHYSICAL EXERCISE [TISSU OSSEUX ET PERFORMANCES MUSCULAIRES DANS UNE POPULATION D'HOMMES SAINS AGES, EN FONCTION DE LEUR NIVEAU D'EXERCICE PHYSIQUE]
L. Vico, D. Chappard, C. Alexandre, S. Palle, J. C. Chatard, J. R. Lacour, and G. Riffat *In* ESA Proceedings of 2nd International Conference on Space Physiology Feb. 1986 p 79-88 In FRENCH (For primary document see N87-10675 01-52)
Avail: NTIS HC A12/MF A01

Muscular performance of 20 male volunteers aged between 61 and 77 (3 sedentary; 6 doing less than 3 hr sport/week; 5 doing 3 to 6 hr; 6 doing less than 6 hr) was studied. Results show that less than 6 hr sport/week maintains bone mass and stimulates bone cell activity. Over 6 hr, stimulated bone remodeling leads to thinning of the corticals. ESA

N87-10686# Institute of Biomedical Problems, Moscow (USSR).
FUNCTIONS OF SKELETAL MUSCLES OF RATS AND MONKEYS AFTER 5-DAY SPACE FLIGHT (ON COSMOS 1514) c51
V. S. Oganov, A. S. Rakhmanov, S. A. Skuratova, M. A. Shirvinskaya, and V. S. Magedov *In* ESA Proceedings of 2nd International Conference on Space Physiology Feb. 1986 p 89-93 (For primary document see N87-10675 01-52)
Avail: NTIS HC A12/MF A01

Contractile properties of skeletal muscles were investigated using glycerinated myofibers of pregnant rats. The soleus muscle of a rhesus monkey was examined using electromyograms and mechanograms of leg movements recorded in vivo. It is found that the contraction strength of myofibers of predominantly postural muscles of rats decrease. The decline of the electromechanical efficiency of the monkey soleus muscle can also be associated with a decrease of strength properties of motor units. It is assumed that mechanisms of regulation of muscle contraction in rats and monkeys may change at early flight stages. It is also assumed that the response of the monkey soleus muscle at that stage may reflect changes in the central components of movement coordination. ESA

N87-10687# Centre National de la Recherche Scientifique, Lyon (France). Lab. de Physiologie.
HINDLIMB SUSPENSION EFFECTS ON RAT SKELETAL MUSCLE RESPONSE c51
D. Desplanches, M. H. Mayet, B. Sempore, M. Grandmontagne, J. Frutoso, and R. Flandrois *In* ESA Proceedings of 2nd International Conference on Space Physiology Feb. 1986 p 95-98 (For primary document see N87-10675 01-52)
Avail: NTIS HC A12/MF A01

The effects of hindlimb tail suspension on histochemical and biochemical properties of rat skeletal muscle were evaluated. Five weeks of suspension result in a significant atrophy (60% and 19%) in soleus (SOL) and extensor digitorum longus (EDL) respectively. The myosine ATPase method reveals a significant change in fiber repartition with an increase of intermediate fiber subgroups (IAB, IB in soleus, IIAB in EDL). Citrate synthase and 3 hydroxyacyl CoA dehydrogenase activities decrease significantly in SOL but are not affected in EDL. Lactate dehydrogenase activity is unchanged in SOL and EDL. It appears that muscle response to hindlimb suspension is greater in slow twitch muscle than in fast twitch ones. ESA

N87-10688# Institute of Biomedical Problems, Moscow (USSR).
BONE EXAMINATION BY NONINVASIVE TECHNIQUES IN A 120-DAY HEAD-DOWN TILT TEST
A. I. Grigoriev, V. S. Oganov, A. S. Rakhmanov, B. V. Morukov, H. A. Janson (Polytechnic Inst., Riga, USSR), V. V. Dzenis, and V. E. Zaichick (Institute of Medical Radiology, Moscow, USSR) *In* ESA Proceedings of 2nd International Conference on Space Physiology Feb. 1986 p 99-103 (For primary document see N87-10675 01-52)
Avail: NTIS HC A12/MF A01

The effect of 120-day head-down tilt (-5 deg) on bones was investigated using gamma-photon absorptiometry, ultrasonic introscopy, and neutro-activation analyses. The study was carried out on 15 test subjects divided into a control group and 3 groups that used various countermeasures (drugs, exercises, or a combination of drugs and exercises). No strict correlation is established between the negative calcium balance and the variation of photon absorptiometry and neutron-activation data. The mineral content of leg bones is best in the drug groups. The noninvasive methods of mineral measurement and mechanical properties of bones are compared from the point of view of their diagnostic and prognostic significance. ESA

N87-10689# Hopital Nord, Saint-Priest-en-Jarez (France). Lab. de Biologie du Tissu Osseux.
HISTOMORPHOMETRIC STUDY OF BONE CELL MASS AND ACTIVITY IN MAN CAUSED BY A 120 DAY DECUBITUS. TEST OF PREVENTIVE PROTOCOLS [ETUDE HISTOMORPHOMETRIQUE DES MODIFICATIONS DE LA MASSE ET DES ACTIVITES CELLULAIRES OSSEUSES INDUITE PAR UN DECUBITUS DE 120 JOURS CHEZ L'HOMME. ESSAI DE PROTOCOLES PREVENTIFS]
L. Vico, D. Chappard, C. Alexandre, S. Palle, P. Minaire, and G. Riffat *In* ESA Proceedings of 2nd International Conference on Space Physiology Feb. 1986 p 105-114 In FRENCH (For primary document see N87-10675 01-52)
Avail: NTIS HC A12/MF A01

The effects of 120 days immobilization on bones was studied using 20 healthy male volunteers divided into: (1) 5 ambulant subjects (control); (2) 3 strictly immobilized; (3) 4 hypokinetic receiving a diphosphonate; (4) 4 hypokinetic taking exercise; and (5) 4 hypokinetic taking exercise plus diphosphonate. Results show that for (3) bone formation and absorption diminish; for (4) they increase; for (5) they diminish, but less than for (3). No bone loss is noted for (2). Results show the difficulties of extrapolating findings of weightlessness simulation to space conditions, although exercise seems to have the greatest effect in both cases. ESA

N87-10690# Hopital Nord, Saint-Priest-en-Jarez (France). Lab. de Biologie du Tissu Osseux.
AMPUTATION-INDUCED OSTEOPOROSIS: A NEW MODEL TO EXPLORE THE EFFECTS OF WEIGHTLESSNESS ON THE HUMAN SKELETON
D. Chappard, C. Alexandre, L. Vico, S. Palle, and G. Riffat *In* ESA Proceedings of 2nd International Conference on Space Physiology Feb. 1986 p 115-118 (For primary document see N87-10675 01-52)
Avail: NTIS HC A12/MF A01

Leg amputees were used to explore the absence of load bearing and muscle activity on the homolateral pelvis. Amputation induces a localized form of osteoporosis of the hemipelvis on the affected side. A histomorphometric analysis indicates that cortical and trabecular bones rarefy with a marked thinning of the trabeculae, while the trabecular number is less affected. Amputation realizes a unique form of microgravity with muscular ineffectiveness and provides a better human model than bed-rest immobilization of spinal injured patients since neurovascular changes are not present. ESA

N87-10691# Hopital Nord, Saint-Priest-en-Jarez (France). Lab. de Biologie du Tissu Osseux.
WEIGHTLESSNESS EFFECTS ON THE PHOSPHORUS-CALCIUM BALANCE AND ITS HORMONAL REGULATION IN MAN DURING STS FLIGHT 51-G [EFFETS DE L'APESANTEUR SUR LE BILAN PHOSPHO-CALCIQUE ET SA REGULATION HORMONALE CHEZ L'HOMME AU COURS DU VOL SPATIAL 51 G]
C. Alexandre, G. Pilonchery, C. Chapuy, and P. Delmas *In* ESA Proceedings of 2nd International Conference on Space Physiology Feb. 1986 p 119-124 In FRENCH (For primary document see N87-10675 01-52)
Avail: NTIS HC A12/MF A01

Blood and urine minerals were measured in STS 51-G astronauts (1 man, 1 woman) 30, 7, and 4 days preflight, on return, and 2 and 4 days postflight. Results confirm bone demineralization and bone matrix atrophy at the start of the flight. They are well correlated with osteoclast increases observed in rats during a 5 day flight. However, bone formation problems in rats after 20 days in space can be retarded in man. The variations do not depend on the hormone control system, and are an adaptation of the bone to weightlessness. ESA

N87-10692# Centre National de la Recherche Scientifique, Paris (France). Lab. de Physiologie Neurosensorielle.
PRELIMINARY RESULTS ON THE EQUILIBRIUM AND VERTIGO EXPERIMENT PERFORMED DURING STS 51-G SHUTTLE FLIGHT
G. Clement, T. Vieville, F. Lestienne, and A. Berthoz *In* ESA Proceedings of 2nd International Conference on Space Physiology Feb. 1986 p 129135 (For primary document see N87-10675 01-52)
Avail: NTIS HC A12/MF A01

The Equilibrium and Vertigo experiment on STS 51-G studied the motor strategies underlying the adaptation of sensorimotor systems to microgravity. Using data from Salyut-7 and Spacelab-1, interaction between posture and movement, role of vision in postural control, modifications of the optokinetic nystagmus, and the vestibulo-ocular reflex were investigated. Results suggest a general downward drive exerted by the otoliths on the first exposure to microgravity, and an upward drive on the first days of return. In microgravity the antigravity tonic influence exerted by the sacculus (which tends on Earth to lift upward the body, the limbs, and the eyeball) is suppressed in order to compensate for the downward pull of gravity. Downward eye movements and activity of flexor muscles are enhanced. On return, gravity is perceived as an upward linear acceleration, inducing an upward drive opposite to the downward inertial force vector. Consequently, upward eye movements and activity of extensor muscles are facilitated. ESA

N87-10693# National Aeronautics and Space Administration. Lyndon B. Johnson Space Center, Houston, Tex.
SPACE MOTION SICKNESS
J. M. Vanderploeg, D. F. Stewart, and J. R. Davis *In* ESA Proceedings of 2nd International Conference on Space Physiology Feb. 1986 p 137-142 (For primary document see N87-10675 01-52)
Avail: NTIS HC A12/MF A01

Space motion sickness clinical characteristics, time course, prediction of susceptibility, and effectiveness of countermeasures were evaluated. Although there is wide individual variability, there appear to be typical patterns of symptom development. The duration of symptoms ranges from several hours to four days with the majority of individuals being symptom free by the end of third day. The etiology of this malady remains uncertain but evidence points to reinterpretation of otolith inputs as being a key factor in the response of the neurovestibular system. Prediction of susceptibility and severity remains unsatisfactory. Countermeasures tried include medications, preflight adaptation, and autogenic feedback training. No countermeasure is entirely successful in eliminating or alleviating symptoms. ESA

N87-10694# Centre d'Essais en Vol, Bretigny-sur-Orge (France). Lab. de Medecine Aerospatiale.
VESTIBULAR TESTS IN COSMONAUT SELECTION AND TRAINING [LES TESTS VESTIBULAIRES DANS LA SELECTION ET L'ENTRAINEMENT DES COSMONAUTES]
A. Leger, D. Lejeune, F. Midy, and M. Kerguelen *In* ESA Proceedings of 2nd International Conference on Space Physiology

Feb. 1986 p 143-148 In FRENCH (For primary document see N87-10675 01-52)
Avail: NTIS HC A12/MF A01

Experiment designs used in cosmonaut selection vestibular tests are described. The tests include a questionnaire used for preselection and Coriolis acceleration tests at 90 and 180 deg/sec for 4 min. Differences between American and Soviet training methods are discussed. ESA

N87-10695# Centre National d'Etudes Spatiales, Toulouse (France).
INFRARED MEASUREMENT OF EYE MOVEMENT. PRESENTATION OF THE EYE MOVEMENT IN INFRARED AND ANGULAR TORSION (EMIRAT) EXPERIMENT [MESURE DU MOUVEMENT DE L'OEIL EN INFRAROUGE. PRESENTATION DE L'EXPERIENCE EMIRAT ET DES TRAITEMENTS TEMPS DIFFERE]
A. L. Camus *In* ESA Proceedings of 2nd International Conference on Space Physiology Feb. 1986 p 149-152 In FRENCH (For primary document see N87-10675 01-52)
Avail: NTIS HC A12/MF A01

A system to measure eye movements of subjects in weightlessness was flown on Spacelab D1 mission. A helmet mounted infrared camera films the eye at 60 frames/sec. The image signal is transmitted to the ground in digital form. Ground equipment calculates the horizontal and vertical position of the center of the pupil and torsion angle in real time. Complete data processing off-line reconstructs eye movement around the X, Y, and Z axes, and derives the stimulus-eye response correlation. ESA

N87-10696# Groupe d'Etude en Medecine et Physiologie Spatiales, Toulouse (France).
GROUND BASED SIMULATION TECHNIQUES FOR CARDIOVASCULAR AND HORMONAL CHANGES OBSERVED IN MAN IN WEIGHTLESSNESS [LES TECHNIQUES DE SIMULATION AU SOL DES MODIFICATIONS CARDIO-VASCULAIRES ET HORMONALES OBSERVEES CHEZ L'HOMME EN IMPESANTEUR]
A. Guell, Cl. Gharib, J. L. Mauroux, J. M. Pottier, Ph. Arbeille, L. Pourcelot, and A. Bes *In* ESA Proceedings of 2nd International Conference on Space Physiology Feb. 1986 p 157-162 (For primary document see N87-10675 01-52)
Avail: NTIS HC A12/MF A01

Immersion and bed rest techniques used to simulate weightlessness effects on body fluid flow, and thus cardiovascular and hormonal responses, are reviewed. Applications to spaceborne experiment design and to studies of microgravity adaptation are discussed. ESA

N87-10697# National Aeronautics and Space Administration. Lyndon B. Johnson Space Center, Houston, Tex.
THE USE OF DECOMPRESSION TO SIMULATE THE EFFECT OF EXTRAVEHICULAR ACTIVITY ON HUMAN LYMPHOCYTE TRANSFORMATION
R. T. Meehan (Texas A&M Univ., Galveston), U. Duncan, L. Neale, J. Waligora, and G. R. Taylor *In* ESA Proceedings of 2nd International Conference on Space Physiology Feb. 1986 p 163-166 (For primary document see N87-10675 01-52)
Avail: NTIS HC A12/MF A01

Lymphocytes from 35 subjects participating in a chamber study simulating extravehicular activity (EVA) conditions were studied. No significant differences in H3 thymidine uptake between pre chamber and post chamber response to any mitogens autologous plasma, or among circulating mononuclear cells by flow cytometry are observed. The studies could not identify the subjects who developed venous bubbles. Data from eight subjects suggests that acute stress associated with participating in the study augments in vitro lymphocyte proliferation. Results indicate EVA exposure does not greatly influence space-flight induced alterations in immune effector cell function. ESA

N87-10698# Institute of Biomedical Problems, Moscow (USSR).
METABOLIC CHANGES DURING PROLONGED ANTIORTHOSTATIC HYPOKINESIA
I. A. Popova, B. V. Morukov, and A. S. Ushakov *In* ESA Proceedings of 2nd International Conference on Space Physiology Feb. 1986 p 167-172 (For primary document see N87-10675 01-52)
Avail: NTIS HC A12/MF A01

Variations of biochemical parameters of blood and urine of the normal man during a 120-day head-down tilt test were studied. A test of 9 healthy male volunteers, aged 25 to 44, led to a negative balance of water and electrolytes with calcium losses of 5 g per month. Changes in the ionic composition of blood include a decrease of potassium and an increase of total calcium and its ionized fraction. Weight losses average 1.8 kg, primarily due to muscle losses responsible for changes in protein homeostasis. The content of free amino acids increases, total protein decreases (mainly due to the decrease of albumins), the content of nitrogen products of protein metabolism increases although their renal excretion remains unchanged. The prolonged antiorthostatic exposure changes the level of tissue metabolism as indicated by a change in the activity of blood enzymes. The isoenzymic specificity suggests that metabolic changes occur primarily in bones and muscles. ESA

N87-10699# Lyon-1 Univ. (France). Faculte de Medecine Grange Blanche.
LEVELS OF PLASMA ATRIAL NATRIURETIC FACTOR (ALPHA h ANF) DURING ACUTE SIMULATED WEIGHTLESSNESS
C. Gharib, G. Gauquelin, G. Geelin, M. Vincent, F. Ghaemmaghami, Ch. Grange, M. Cantin (Institut Recherches Cliniques, Montreal, Quebec), J. Gutkovska, and A. Guell (Centre Hospitalier Univ. Rangueil, Toulouose, France) *In* ESA Proceedings of 2nd International Conference on Space Physiology Feb. 1986 p 173-176 Sponsored by CNES (For primary document see N87-10675 01-52) (Grant DRET-50-85-26)
Avail: NTIS HC A12/MF A01

Head-down tilt at -9 deg (n = 3) and head-out water immersion (n = 2) were used to study the variations of the atrial natriuretic factor (alphahANF). Data show a rapid elevation of alphahANF during the first 60 min of head-down tilt, accompanied by a decrease in plasma renin activity (PRA) plasma osmolality and protein concentration. The same results along with a decrease in PRA and vasopressin are obtained for immersion, but the curve of alphahANF is blunted and the level of alphahANF remains increased during the 2 hr of the experiment. The known actions of ANF on GFR, FF, renin and aldosterone could explain data obtained during simulated weightlessness. ESA

N87-10700# Lyon-1 Univ. (France). Faculte de Medecine Grande Blanche.
VOLUME REGULATING HORMONES DURING A 5 HOUR HEAD-DOWN TILT AT -10 DEG. PART 1: EPINEPHRINE, NOREPINEPHRINE AND DOPAMINE
A. Guell (Centre Hospitalier Univ. Rangueil, Toulouse, France), J. M. Pequignot, G. Gauquelin, J. L. Bascands, G. Geelen, A. M. Allevard, G. Annat, L. Pourcelot (Hopital Bretonneau, Tours, France), L. Peyrin, A. Bes (Centre Hospitalier Univ. Rangueil, Toulouse, France) et al *In* ESA Proceedings of 2nd International Conference on Space Physiology Feb. 1986 p 177-179 Sponsored by CNES and DIGITAL France (For primary document see N87-10675 01-52)
(Grant DRET-50-85-26)
Avail: NTIS HC A12/MF A01

In order to determine the short term effects of weightlessness simulation on plasma catecholamines (epinephrine) (E), norepinephrine (NE) and dopamine (DA) and to compare the results with the supine position taken as control for simulation studies, 10 young healthy volunteers were submitted to 3 postural tests. Tests were: day 1: 7 hr sitting; day 2: 1 hr sitting, then 5 hr horizontal supine and 1 hr sitting; day 3: 1 hr sitting, then 5 hr head-down tilt -10 deg, and 1 hr sitting. The results show that a 5 hr head-down tilt or bed rest induce an early decrease in NE compared to the seated position; E decreases in head-down tilt only. During such maneuvers there is decrease in the sympathoadrenal activity which could explain the decrease in plasma renin activity. ESA

N87-10701# Institute of Biomedical Problems, Moscow (USSR).

RELATIONSHIP BETWEEN CARDIOVASCULAR FUNCTIONS AND FLUID-ELECTROLYTE METABOLISM DURING ANTI-ORTHOSTATIC HYPOKINESIA

A. A. Savilov, V. M. Mikkailov, and A. I. Grigoriev *In* ESA Proceedings of 2nd International Conference on Space Physiology Feb. 1986 p 181-186 (For primary document see N87-10675 01-52)

Avail: NTIS HC A12/MF A01

The cardiovascular function and fluid-electrolyte metabolism in healthy men exposed to head-down tilt tests of 7 days to 6 months were investigated. During the first hours and days of exposure the cardiovascular changes are associated with hemodynamic shifts typical of this simulation procedure, while fluid-electrolyte changes are manifestations of the compensatory-adaptive reactions aimed at maintaining an adequate circulatory homoestasis. As the exposure continued for several months, the cardiovascular changes, particularly cardiovascular deconditioning, are produced by the effect of hypokinesia as such. In this situation changes in fluid-electrolyte balance are one of the major factors responsible for cardiovascular disorders. Water-salt supplements combined with other countermeasures may help to decrease significantly the adverse effects of antiorthostatic hypokinesia and weightlessness on the human body. ESA

N87-10702# Erlangen-Nuremberg Univ. (West Germany). Med. Poliklinik.

EXERCISE-INDUCED MYOCARDIAL ISCHEMIA AT HIGH ALTITUDE SIMULATED IN A NEGATIVE PRESSURE CHAMBER

H. J. Deuber, A. Wortman, and K. Bachmann *In* ESA Proceedings of 2nd International Conference on Space Physiology Feb. 1986 p 187-190 (For primary document see N87-10675 01-52)

Avail: NTIS HC A12/MF A01

The influence of high altitude hypoxia on myocardial ischemia in 15 patients aged 48 to 73 with coronary heart disease was studied during rest and during bicycle ergometry at simulated altitudes of 1000 and 9000ft above sea level. At high altitude the working capacity is significantly reduced due to an earlier onset of angina pectoris and ST-segment depressions. Without labor there is no angina pectoris or ST-segment depression. ESA

N87-10703# Lyon-1 Univ. (France). Faculte de Medecine Grande Blanche.

VOLUME REGULATING HORMONES DURING A 5-HOUR HEAD-DOWN TILT AT -10 DEG. PART 2: PLASMA RENIN ACTIVITY AND ALDOSTERONE

G. Gauquelin, A. Guell (Centre Hospitalier Univ. Rangueil, Toulouse, France), J. L. Mauroux, G. Geelen, G. Annat, M. Vincent, A. M. Allevard, A. Sassolas, C. A. Bizollon, and C. Gharib *In* ESA Proceedings of 2nd International Conference on Space Physiology Feb. 1986 p 191-193 Sponsored by CNES and DIGITAL France (For primary document see N87-10675 01-52)
(Grant DRET-50-85-26)

Avail: NTIS HC A12/MF A01

Head-down tilt experiments were conducted to simulate the cardiovascular and hormonal modifications occurring during space flight. The short term effects of weightlessness simulations on the hormones controlling volume homoestasis were observed. Ten young healthy volunteers were submitted to 3 postural tests: day 1: 7 hr sitting; day 2: 1 hr sitting, then 5 hr horizontal supine and 1 hr sitting; day 3: 1 hr sitting, then 5 hr head down tilt, and 1 hr sitting. The results show that a 5 hour horizontal bed rest or head-down tilt induce an early and progressive decline of PRA and aldosterone which is comparable to that observed during immersion. The study also shows that posture during the control period is critical. ESA

N87-10704# National Aeronautics and Space Administration, Washington, D.C.

ANIMAL STUDIES ON SPACELAB-3 c51

C. Schatte, R. Grindeland, P. Callahan, W. Berry, G. Funk (Management and Technical Services Co., Philadelphia, Pa.), and W. Lencki *In* ESA Proceedings of 2nd International Conference on Space Physiology Feb. 1986 p 233-244 Previously announced as N86-16889 (For primary document see N87-10675 01-52)

Avail: NTIS HC A12/MF A01

Two squirrel monkeys and 24 rats were flown on Spacelab-3 to provide hands-on maintenance of animals in a laboratory environment. With few exceptions, the animals grew and behaved normally, were free of chronic stress, and differed from ground controls only for gravity-dependent parameters. One of the monkeys exhibited symptoms of space sickness similar to those observed in humans, which suggests squirrel monkeys may be good models for studying the space-adaptation syndrome. Among parameters measured in the rats, most notable is the dramatic loss of muscle mass and increased fragility of long bones. Other rat findings include suppressed interferon production by spleen cells, defective release of growth hormone by somatrophs, possible dissociation of circadian pacemakers, changes in hepatic lipid and carbohydrate metabolism, and hypersensitivity of marrow cells to erythropoietin. ESA

N87-10705# Centre d'Etudes et de Recherches de Medecine Aeronautique, Paris (France).

ANIMAL MODELS IN SPACE PHYSIOLOGY [MODELES ANIMAUX EN PHYSIOLOGIE SPATIALE] c51

C. L. Milhaud *In* ESA Proceedings of 2nd International Conference on Space Physiology Feb. 1986 p 203-209 In FRENCH (For primary document see N87-10675 01-52)

Avail: NTIS HC A12/MF A01

The moral, scientific, and operational reasons for animal experiments in space physiology are reviewed. Choice of animal is discussed. Bioinstrumentation and weightlessness simulation facilities are described. Space flight experiment design is considered. ESA

N87-10706# Centre d'Etudes et de Recherches de Medecine Aeronautique, Paris (France).

CONTRIBUTION OF ANIMAL MODELS TO THE INVESTIGATION OF BONE CHANGES IN WEIGHTLESSNESS c51

C. Nogues, C. Milhaud, P. Pesquies, and V. S. Oganov (Institute of Biomedical Problems, Moscow, USSR) *In* ESA Proceedings of 2nd International Conference on Space Physiology Feb. 1986 p 211-215 (For primary document see N87-10675 01-52)

Avail: NTIS HC A12/MF A01

Bone change space flight results obtained on rats and on a rhesus monkey are compared with those obtained in bedresting primates or hypokinetic rats. A change in cell systems responsible for bone remodeling is revealed by the morphometric method. Bed rest produces stress in the monkey and is not recommended. Hypokinesis can be used with rats. ESA

N87-10707# Centre d'Etudes et de Recherches de Medecine Aeronautique, Paris (France).

COSMOS 1514 FLIGHT: STUDY OF RHESUS MONKEY ECG c51

R. Blostin, C. Milhaud, B. Cailler, P. Pesquies, V. Melnitchenko (Institute of Biomedical Problems, Moscow, USSR), B. Kulaev, V. Magedoc, and G. Tchamurliev *In* ESA Proceedings of 2nd International Conference on Space Physiology Feb. 1986 p 217-223 (For primary document see N87-10675 01-52)

Avail: NTIS HC A12/MF A01

The electrocardiogram of 2 rhesus monkeys flown aboard Cosmos 1514 satellite (9 day flight) was analyzed in order to monitor the animals' health, and evaluate the validity of the rhesus monkey in cardiovascular physiology in space. The analysis of morphology long and short term changes in heart rate suggests that no serious pathological phenomenon occurred during flight. The neurovegetative reactivity of the rhesus model in space seems close to man's. ESA

N87-10708# Institute of Biomedical Problems, Moscow (USSR).

THE STATE OF BONES OF PREGNANT RATS DURING AN ACUTE STAGE OF ADAPTATION TO WEIGHTLESSNESS c51

A. V. Bakulin, E. A. Ilyan, V. S. Oganov, and V. I. Lebedev *In* ESA Proceedings of 2nd International Conference on Space

Physiology Feb. 1986 p 225-228 (For primary document see N87-10675 01-52)
Avail: NTIS HC A12/MF A01

Integrated mineralization parameters, biomechanical characteristics and elemental composition of spongy bones of the proximal epiphysis of the humerus in pregnant rats flown on Cosmos-1514 for 5 days were investigated. Results suggest that bone resorption is activated but does not lead to noticeable osteoporosis, probably due to the short flight duration, but could produce bone destructuring accompanied by deterioration of bone mechanical properties. This is paralleled by physico-chemical changes in the mineral component, responsible for a decline of the strength parameters of bones with their density remaining unaltered. It is suggested that bone variations in the weightless state may develop in a phaselike manner. ESA

N87-10709# National Aeronautics and Space Administration, Washington, D.C.

MATH MODELLING AS A COMPLEMENT TO THE SCIENTIFIC INQUIRY OF PHYSIOLOGICAL ADAPTATION TO SPACE FLIGHT: FLUID, ENDOCRINE AND CIRCULATORY REGULATION

J. I. Leonard (General Electric Co., Washington, D. C.), R. J. White, and J. A. Rummel (MAP, Inc., Houston, Tex.) *In* ESA Proceedings of 2nd International Conference on Space Physiology Feb. 1986 p 233-244 (For primary document see N87-10675 01-52)
(Contracts NAS9-15487; NAS9-16328; NAS9-15850; NAS9-17151)
Avail: NTIS HC A12/MF A01 CSCL 06P

The contribution of mathematical modeling and computer simulation to the understanding of problems arising during weightless space flight is reviewed. Examples from fluid, endocrine, and circulatory regulation are provided to illustrate the utility of modeling as an adjunct to the process of scientific inquiry, especially in the development and theoretical testing of hypotheses. The models were used to examine the acute and chronic phases of space flight. Paradoxial results appear when data obtained during chronic adaptation is interpreted using theories which pertain to acute adjustments. The modeling process provides a means of developing a theoretical basis for interpreting the chronic adaptive phase of flight. ESA

N87-10710# Army Research Inst. of Environmental Medicine, Natick, Mass.

UPPER AND LOWER BODY ANAEROBIC POWER COMPARISON BETWEEN BIATHLETES AND CONTROL SUBJECTS

J. F. Patton and A. Duggan Apr. 1986 21 p
(AD-A167636; USARIEM-M25/86) Avail: NTIS HC A02/MF A01 CSCL 06/16

This study compared power outputs (PO) from both the upper body (UB) and lower body (LB) Wingate tests of anaerobic power between biathletes and control subjects. Ten biathletes (B) selected by the British Ski Federation for potential assignment to the British team and 13 control (C) subjects cranked or pedalled the same Bodyguard ergometer at maximal RPM's for 30s against resistances of 2.94 and 4.41 joules/rev/kg body weight (BW), respectively. PO's were calculated in watts (W) and expressed as peak power (PP, highest 5s interval), mean power (MP, the mean for 30s), and power decrease (PD, difference between PP and lowest 5s PO divided by time). Absolute PP and MP for both UB and LB did not differ between groups. A comparison of PO's made relative to BW showed B to have higher values than C: 11.25 vs 10.25 W/kg for LB PP ($p<.01$) and 9.21 vs 7.96 W/kg for LB MP ($p<.001$). Similar PO relationships were found for the UB where PP and MP values were higher for B than C: 7.61 vs 6.76 W/kg ($p<.01$) and 6.07 vs 4.95 W/kg ($p<.001$), respectively. Concomitantly, PD was lower in B than C for both the UB ($p<.01$) and Lb ($p<.001$). These data show that significant differences exist in the anaerobic performance of aerobically trained athletes compared to subjects who are not highly trained and that these differences are reflected in the musculature of the Ub as well as the legs. GRA

N87-10711# School of Aerospace Medicine, Brooks AFB, Tex.

RADIATION DOSES FROM FLYING THROUGH NUCLEAR DEBRIS CLOUDS Final Report, 2-10 Jan. 1985

Peter M. VandenBosch and Arthur Woodrum Apr. 1986 20 p
(AD-A167959; USAFSAM-TR-85-86) Avail: NTIS HC A02/MF A01 CSCL 15/6

Taboada et al. have recently developed a computer model to predict gamma radiation doses to aircrews flying through nuclear debris clouds. Although the model has the advantages of taking a large number of parameters into account and using the benchmark DELFIC code to model cloud dynamics, it takes up to 20 min for a single run on a mainframe computer. Results from a number of runs have been generalized into empirical formulae. From these results it is possible to estimate worst case gamma radiation doses for complex scenarios using a hand calculator. GRA

N87-10712# Army Research Inst. of Environmental Medicine, Natick, Mass.

A SYSTEM FOR CONTROLLED PRESENTATION OF THE ARDEN CONTRAST SENSITIVITY TEST

John L. Kobrick, Harry I. Zeltzer, and Stephen Mullen Dec. 1985 14 p
(AD-A167969; USARIEM-T-3/86) Avail: NTIS HC A02/MF A01 CSCL 06/5

Contrast sensitivity has been identified as a significant index of visual function, and as an indicator of visual disorders. The Arden test of contrast sensitivity has been recognized as a simple and easily administered technique for measurement of this process. However, this test involves manual manipulation and considerable individual subjectivity. The instrument described in this report was designed and developed to eliminate variability in the testing procedure due to differences in individual testing techniques, and to standardize testing conditions, ambient illumination, viewing distance and presentation rates. GRA

N87-10713# Pacific Northwest Labs., Richland, Wash.

COMPARISON OF THE COUPLING OF GROUNDED AND UNGROUNDED HUMANS TO VERTICAL 60-Hz ELECTRIC FIELDS

W. T. Kaune, L. M. Kistler, and M. C. Miller Dec. 1985 26 p
Presented at the 24th Hanford Life Sciences Symposium on Health and Environmental Research on Complex Organic Mixtures, Richland, Wash., 21 Oct. 1985
(Contract DE-AC06-76RL-01830)
(DE86-011140; PNL-SA-13600; CONF-851027-11) Avail: NTIS HC A03/MF A01

Total induced currents and average induced axial current densities have been published in the literature for human models exposed to 60-Hz electric fields. The results of these studies have been quite useful, but they deal with a somewhat idealized exposure situation that ignores the insulating effects of most types of footwear. This paper describes a new laboratory technique for studying the relationship between grounded and ungrounded exposure of humans. A conducting model of the body 40-cm-tall man was electrically divided into seven segments. Wires connected to the conducting surfaces of these segments were routed horizontally through shielded cable to remote, battery-powered electronics. The common potential of the electronics was biased to the electric-field-induced potential of the model, allowing us to accurately measure the current induced in each body segment of the model. The method was tested by measuring the current induced in the upper hemisphere of a ungrounded sphere. Agreement between theory and measurement was excellent. Measurements were made with the human mod el located at 15 positions, ranging from touching ground to remote from ground (i.e., in free space). The ratios of free-space to grounded currents crossing horizontal sections through the body were: neck, 0.58; chest, 0.40; abdomen, 0.39; thigh, 0.36; ankle, 0.17. DOE

53 BEHAVIORAL SCIENCES

Includes psychological factors; individual and group behavior; crew training and evaluation; and psychiatric research.

No abstracts in this category.

54 MAN/SYSTEM TECHNOLOGY AND LIFE SUPPORT

Includes human engineering; biotechnology; and space suits and protective clothing.
For related information see also *16 Space Transportation.*

N87-10714# Anacapa Sciences, Inc., Fort Rucker, Ala.
HUMAN FACTORS RESEARCH IN AIRCREW PERFORMANCE AND TRAINING Annual Summary Report, 1 Sep. 1982 - 31 Aug. 1983
Kenneth D. Cross Dec. 1985 135 p
(Contracts MDA903-81-C-0504; DA Proj. 2Q2-63731-A-792; DA Proj. 2Q2-63731-A-793)
(AD-A167950; ASI-479-19-1; ARI-RN-85-104) Avail: NTIS HC A07/MF A01 CSCL 05/5

This report presents Human Factors Research in Aircrew Performance and Training for the Army Research Institute Field Unit at Fort Rucker, Ala. The report contains summary descriptions for each of the 19 projects on which the ASI personnel worked during the second contract year. Each summary description contains: (1) a background section that describes the rationale for the research need and the project objectives, (2) a research approach section that describes the tasks and activities required to fulfill the project objectives, and (3) a project status section that describes the work completed, preliminary findings (if available), and the anticipated project completion date. GRA

N87-10648# Zurich Univ. (Switzerland). Central Biological Lab.
LIFE EXPECTANCY IN TROPICAL CLIMATES AND URBANIZATION
W. H. Weihe *In* WMO Proceedings of the Technical Conference on Urban Climatology and its Applications with Special Regard to Tropical Areas 1986 p 313-353 (For primary document see N87-10636 01-47)
Avail: NTIS MF A01; print copy available at WMO, Geneva, Switzerland

N87-10649# World Meteorological Organization, Geneva (Switzerland).
HUMAN COMFORT IN THE URBAN TROPICS
Luis SanchezdeCarmona *In its* Proceedings of the Technical Conference on Urban Climatology and its Applications with Special Regard to Tropical Areas 1986 p 354-404 (For primary document see N87-10636 01-47)
Avail: NTIS MF A01; print copy available at WMO, Geneva, Switzerland

55 SPACE BIOLOGY

Includes exobiology; planetary biology; and extraterrestrial life.

No abstracts in this category.

59 MATHEMATICAL AND COMPUTER SCIENCES (GENERAL)

No abstracts in this category.

60 COMPUTER OPERATIONS AND HARDWARE

Includes hardware for computer graphics, firmware, and data processing.
For components see *33 Electronics and Electrical Engineering.*

N87-10715# Sandia National Labs., Albuquerque, N. Mex.
FACTORS CONTRIBUTING TO STATIC RAM CELL TRANSIENT UPSET
M. R. Ackermann and R. E. Mikawa 1986 5 p Presented at the 23rd Annual Conference on Nuclear and Space Radiation Effects, Providence, R.I., 20 Jul. 1986
(Contract DE-AC04-76DP-00789)
(DE86-007710; SAND-86-0341C; CONF-860706-9) Avail: NTIS HC A02/MF A01

Rail Span Collapse is proposed to be the dominant transient upset mechanism in CMOS static random access memories. This paper examines the many factors contributing to RAM cell upset and comments on the strengths and weaknesses of the rail span model. DOE

N87-10716*# Jet Propulsion Lab., California Inst. of Tech., Pasadena.
INTELLIGENT COMPUTER ASSISTED INSTRUCTION (ICAI): FORMATIVE EVALUATION OF TWO SYSTEMS Final Report, Apr. 1984 - Aug. 1985
Mar. 1986 356 p
(Contract NAS7-918; DA Proj. 2Q2-63743-A-794)
(NASA-CR-176873; NAS 1.26:176873; AD-A167910; ARI-RN-86-29) Avail: NTIS HC A16/MF A01 CSCL 09/2

This report reviews major components of an 18 month evaluation of Intelligent Computer Assisted Instruction (ICAI), and emerging field of Artificial Intelligence that draws on computer technologies and cognitive science in an attempt to build more powerful instructional programs. The primary goals of this effort were to develop an increased understanding of the state of the art of ICAI for the purposes of: (1) identifying strategies to enhance the general usefulness of ICAI technology for Army training problems, and (2) developing concepts for efficiently and effectively managing military ICAI projects. The approach taken to accomplish these goals was to intensively examine two selected ICAI systems using a formative evaluation methodology. The two systems selected were: (1) PROUST, a system designed by Soloway and Johnson for analyzing bugs in novice programmers' PASCAL programs, using a top-down approach which attempts to infer the intentions and plans of the programmer, and (2) WEST, a system designed by Burton and Brown to teach basic mathematics and strategic thinking skills, based on the premise that students can learn from their mistakes or bugs. GRA

61 COMPUTER PROGRAMMING AND SOFTWARE

Includes computer programs, routines, algorithms, and specific applications, e.g., CAD/CAM.

N87-10717*# Harvey Mudd Coll., Claremont, Calif.
FREE VIBRATION AND DYNAMIC RESPONSE ANALYSIS OF

SPINNING STRUCTURES Final Report
1986 11 p
(NASA-CR-179672; NAS 1.26:179672) Avail: NTIS HC A02/MF A01 CSCL 09B

The proposed effort involved development of numerical procedures for efficient solution of free vibration problems of spinning structures. An eigenproblem solution procedure, based on a Lanczos method employing complex arithmetic, was successfully developed. This task involved formulation of the numerical procedure, FORTRAN coding of the algorithm, checking and debugging of software, and implementation of the routine in the STARS program. A graphics package for the E/S PS 300 as well as for the Tektronix terminals was successfully generated and consists of the following special capabilities: (1) a dynamic response plot for the stresses and displacements as functions of time; and (2) a menu driven command module enabling input of data on an interactive basis. Finally, the STARS analysis capability was further improved by implementing the dynamic response analysis package that provides information on nodal deformations and element stresses as a function of time. A number of test cases were run utilizing the currently developed algorithm implemented in the STARS program and such results indicate that the newly generated solution technique is significantly more efficient than other existing similar procedures. M.G.

N87-10718# National Aeronautical Lab., Bangalore (India). Aerodynamics Div.
ADAPTATION OF TSFOIL FOR UNIVAC 1100/60H COMPUTER AT NAL, BANGALORE
R. Gopinath and V. Kanagarajan Sep. 1983 56 p
(AE-TB-9-83) Avail: NTIS HC A04/MF A01

The TSFOIL code has been adapted for operation on the Univac 1100/60-H computer at NAL, Bangalore. The code has been validated for the Free-Air case, for the Korn airfoil, for which results are available. Also three additional cases for which data is available have been analyzed using this code. Author

N87-10719*# National Aeronautics and Space Administration. Langley Research Center, Hampton, Va.
DYNAMIC REMAPPING DECISIONS IN MULTI-PHASE PARALLEL COMPUTATIONS Final Report
David M. Nicol and Paul F. Reynolds, Jr. Sep. 1986 48 p Submitted for publication
(Contracts NAS1-17070; NAS1-18107)
(NASA-CR-178174; NAS 1.26:178174; ICASE-86-58) Avail: NTIS HC A03/MF A01 CSCL 09B

The effectiveness of any given mapping of workload to processors in a parallel system is dependent on the stochastic behavior of the workload. Program behavior is often characterized by a sequence of phases, with phase changes occurring unpredictably. During a phase, the behavior is fairly stable, but may become quite different during the next phase. Thus a workload assignment generated for one phase may hinder performance during the next phase. We consider the problem of deciding whether to remap a paralled computation in the face of uncertainty in remapping's utility. Fundamentally, it is necessary to balance the expected remapping performance gain against the delay cost of remapping. This paper treats this problem formally by constructing a probabilistic model of a computation with at most two phases. We use stochastic dynamic programming to show that the remapping decision policy which minimizes the expected running time of the computation has an extremely simple structure: the optimal decision at any step is followed by comparing the probability of remapping gain against a threshold. This theoretical result stresses the importance of detecting a phase change, and assessing the possibility of gain from remapping. We also empirically study the sensitivity of optimal performance to imprecise decision threshold. Under a wide range of model parameter values, we find nearly optimal performance if remapping is chosen simply when the gain probability is high. These results strongly suggest that except in extreme cases, the remapping decision problem is essentially that of dynamically determining whether gain can be achieved by remapping after a phase change; precise quantification of the decision model parameters is not necessary. Author

N87-10720*# National Aeronautics and Space Administration. Goddard Space Flight Center, Greenbelt, Md.
PROCEEDINGS OF THE 5TH ANNUAL USERS' CONFERENCE
Martha Szczur, ed. and Elfrieda Harris, ed. 1985 400 p Conference held at Greenbelt, Md., 4-6 Jun. 1985
(NASA-CP-2399; NAS 1.55:2399) Avail: NTIS HC A17/MF A01 CSCL 09B

The Transportable Applications Executive (TAE) was conceived in 1979. It was proposed to be a general purpose software executive that could be applied in various systems. The success of this concept and of TAE was demonstrated. Topics included: TAE current status; TAE development; TAE applications; and UNIX emphasis. B.G.

N87-10721*# National Aeronautics and Space Administration. Goddard Space Flight Center, Greenbelt, Md.
A RULE BASED COMPUTER AIDED DESIGN SYSTEM
Timothy Premack Oct. 1986 59 p
(NASA-TM-86241; Rept-86B0078; NAS 1.15:86241) Avail: NTIS HC A04/MF A01 CSCL 09B

A Computer Aided Design (CAD) system is presented which supports the iterative process of design, the dimensional continuity between mating parts, and the hierarchical structure of the parts in their assembled configuration. Prolog, an interactive logic programming language, is used to represent and interpret the data base. The solid geometry representing the parts is defined in parameterized form using the swept volume method. The system is demonstrated with a design of a spring piston. Author

N87-10722# Sandia National Labs., Albuquerque, N. Mex.
GRAPH 3: A DIGITIZING AND GRAPH PLOTTING PROGRAM
C. B. Selleck Mar. 1986 59 p
(Contract DE-AC04-76DP-00789)
(DE86-010628; SAND-86-0525) Avail: NTIS HC A04/MF A01

GRAPH is an interactive program that allows the user to perform two functions. The first is to plot two dimensional graphs and the second is to digitize graphs or plots to create data files of points. The program is designed to allow the user to get results quickly and easily. It is written in RATIV (a FORTRAN preprocessor) and is currently in use at Sandia under VMS on a VAX computer and CTSS on a Cray supercomputer. The program provides graphical output through all of the Sandia Virtual Device Interface (VDI) graphics devices. DOE

N87-10723# Colorado Univ., Boulder.
INTEGRATED TESTING AND ANALYSIS OF MATHEMATICAL SOFTWARE TOOLS. SUMMARY OF RESEARCH ACTIVITIES, 1 AUGUST 1985-1 MAY 1986
L. Osterweil 1986 10 p
(Contract DE-FG02-84ER-13283)
(DE86-010882; DOE/ER-13283/4) Avail: NTIS HC A02/MF A01

Work in each of the three main thrusts which have been pursued during the past year is addressed: (1) the large scale integration of software tools into effective software environments, (2) the effective integration of debugging, testing and analysis tools and aids, and (3) the creation of effective user interfaces to testing, debugging and analysis tools exploiting high resolution interactive graphics workstations. DOE

N87-10724# Los Alamos National Lab., N. Mex.
DATABASE ALGORITHMS FOR MULTIPROCESSOR AND VERY LARGE MEMORY SYSTEMS
W. C. Thompson, III 18 Mar. 1986 26 p Presented at the Syracuse University Minnowbrook Workshop on Data Base Machines, Blue Mountain Lake, N.Y., 22 Jul. 1986
(Contract W-7405-eng-48)
(DE86-009406; UCRL-94333; CONF-860740-1) Avail: NTIS HC A03/MF A01

Many recent computer designs exhibit two features which have been too expensive to exploit previously. The first, very large main memories, may allow significant portions of databases to be kept in main memory. The second, parallel processing, provides multiple processors to speed the operations on databases in memory. A recent paper by DeWitt, et al discusses the effect of providing a very large main memory in a computer for database operations. This paper explores the algorithms appropriate for relational operations when large main memories and parallel processors are provided. DOE

N87-10725# Colorado Univ., Boulder. Dept. of Computer Science.
SOFTWARE PROCESS INTERPRETATION AND SOFTWARE ENVIRONMENTS
L. Osterweil Apr. 1986 58 p
(Contract DE-FG02-84ER-13283)
(DE86-010881; DOE/ER-13283/5; CU-CS-324-86) Avail: NTIS HC A04/MF A01

This paper suggests that software engineering must become the study of how to formalize, specify, and automate the complex processes by which software products are synthesized. The author believes that software systems are most profitably thought of as products of large and complex manufacturing and fabrication processes which can be described, automated, and controlled by familiar algorithmic programming techniques. Included in this paper are discussions of programming software engineering processes, the relations of the author's research to other computer science research areas, and the design of a software engineering language. DOE

N87-10726# Argonne National Lab., Ill.
PARALLEL LOGIC PROGRAMMING FOR NUMERIC APPLICATIONS
R. Butler, E. Lusk, W. McCune, and R. Overbeek Apr. 1986 18 p
(Contract W-31-109-eng-38)
(DE86-011004; ANL/MCS-TM-72) Avail: NTIS HC A02/MF A01

This paper reports on a series of experiments involving the use of various dialects of parallel logic programming to express and control parallelism. The central goal of these experiments was to explore the possibility of writing numeric code for multiprocessors while expressing the synchronization requirements using logic programming. Three dialects of parallel logic programming are considered: Parlog, Delta-Prolog, and Flat Concurrent Prolog. The experiments involved the formulation of a well-known, highly-parallel algorithm in each of the three languages. In one case (Parlog, semi-manually compiled code for an implementation of an extended Warren Abstract Machine), a comparison is made of the performance of the resulting program with that of the same problem expressed in C, with monitors as the added parallelism construct. Speedups obtained for the C and Parlog versions are presented. The experiments illustrate the effect of granularity size on attainable degrees of parallelism. Based on the limited evidence from these experiments, conclusions are offered on the suitability of logic programming languages for programming multiprocessors. DOE

N87-10727# Los Alamos National Lab., N. Mex.
PULSE FORMING NETWORK DESIGN PROGRAM FOR LINEAR AND TIME-VARYING LOADS FOR THE IBM PERSONAL COMPUTER
G. G. McDuff and B. D. Nelson 1986 4 p Presented at the 17th Power Modulator Symposium, Seattle, Wash., 23 Jun. 1986
(Contract W-7405-eng-36)
(DE86-011209; LA-UR-86-1703; CONF-860674-2) Avail: NTIS HC A02/MF A01

A design aid program written to perform pulse forming network calculations is described. The program will perform calculations for either linear, time-varying, or near linear loads. The program is described as user-friendly and is written in BASIC language for the IBM PC. DOE

N87-10728# Sandia National Labs., Albuquerque, N. Mex.
DESIGN GUIDELINES FOR HUMAN-COMPUTER DIALOGUES
B. P. Chao May 1986 40 p
(Contract DE-AC04-76DP-00789)
(DE86-011543; SAND-86-0259) Avail: NTIS HC A03/MF A01

This report presents a set of guidelines for designing human-computer dialogues. User requirements, dialogue modes, entry devices, error management and recovery, and data loss protection and disaster prevention are discussed, and a checklist for dialogue design is provided. DOE

N87-10729# Los Alamos National Lab., N. Mex.
IMPLEMENTATION AND OPTIMIZATION OF PORTABLE STANDARD LISP FOR THE CRAY
J. W. Anderson, R. R. Kessler (Utah Univ., Salt Lake City), and W. F. Galway 1986 10 p Presented at the European Conference on Artificial Intelligence, Brighton, England, 21 Jul. 1986 Prepared in cooperation with Utah Univ., Salt Lake City
(Contract W-7405-eng-36)
(DE86-008717; LA-UR-86-831; CONF-860733-1) Avail: NTIS HC A02/MF A01

Portable Standard LISP (PSL), a dialect of LISP developed at the University of Utah, has been implemented on the CRAY-1s and CRAY X-MPs at the Los Alamos National Laboratory and at the National Magnetic Fusion Energy Computer Center at Lawrence Livermore National Laboratory. This implementation was developed using a highly portable model and then tuned for the Cray architecture. The speed of the resulting system is quite impressive, and the environment is very good for symbolic processing. DOE

N87-10730# Bhabha Atomic Research Centre, Bombay (India).
PLOT 3D: A MULTIPURPOSE, INTERACTIVE PROGRAM FOR PLOTTING THREE DIMENSIONAL GRAPHS
B. Jayaswal 1985 56 p
(DE86-702101; BARC-1274) Avail: NTIS (US Sales Only) HC A04/MF A01

PLOT3D is a general purpose, interactive, three dimensional display and plotter program. Written in FORTRAN-77, it uses a two dimensional plotter software (PLOT-10) to draw orthographic axonometric projections of a three dimensional graph comprising a smooth surface or cubical histogram, in any desired orientation, magnification and window, employing throughout highly accurate hidden lines removal techniques. The figure, so generated, can optionally be clipped, smoothed by interpolation, or shaded selectively to distinguish among its different faces. The program accepts data from an external file, or generates them through built-in functions. It can be used for graphical representation of data such as neutron flux, theta(x,y) in form of smooth surface, even if available data are very few in number. It is also capable of drawing histograms of quantities such as fuel power in a reactor lattice. Listing of the program is given. DOE

N87-10017# Chiba Univ. (Japan). Faculty of Engineering.
IMAGES OF THREE DIMENSIONAL FLOWS IN COMPUTER GRAPHICS
Nobuhide Nishikawa, Akira Suzuki, and Satoshi Akiyama *In* Tokyo Univ. Proceedings of the Symposium on Mechanics for Space Flight, 1985 1985 11 p (For primary document see N87-10011 01-02)
Avail: NTIS HC A12/MF A01

N87-10038# Academy of Sciences (USSR), Moscow.
COMPUTER SIMULATION IN ENGINEERING HYDRODYNAMICS
A. A. Samarskh, B. P. Gerasimov, T. G. Elizarova, I. S. Kalachinskaya, A. B. Karagichev, A. V. Lesunovsky, S. A. Semushin, B. I. Chetversushkin, and A. G. Churbanov *In* Tokyo Univ. Proceedings of the Symposium on Mechanics for Space Flight, 1985 1985 4 p (For primary document see N87-10011 01-02)
Avail: NTIS HC A12/MF A01

N87-10299*# National Oceanic and Atmospheric Administration, Washington, D. C.

AN ALL-PURPOSE COMPUTER PROGRAM FOR LIDAR SIMULATIONS AND REDUCTION OF LIDAR DATA

Charles Braun *In* NASA. Langley Research Center 13th International Laser Radar Conference Aug. 1986 2 p (For primary document see N87-10263 01-35)
Avail: NTIS HC A15/MF A01 CSCL 09B

62 COMPUTER SYSTEMS

Includes computer networks and special application computer systems.

N87-10731*# National Aeronautics and Space Administration. Langley Research Center, Hampton, Va.

FTMP (FAULT TOLERANT MULTIPROCESSOR) PROGRAMMER'S MANUAL

Frank E. Feather, Carlos A. Liceaga, and Peter A. Padilla Sep. 1986 43 p
(NASA-TM-89015; NAS 1.15:89015) Avail: NTIS HC A03/MF A01 CSCL 09B

The Fault Tolerant Multiprocessor (FTMP) computer system was constructed using the Rockwell/Collins CAPS-6 processor. It is installed in the Avionics Integration Research Laboratory (AIRLAB) of NASA Langley Research Center. It is hosted by AIRLAB's System 10, a VAX 11/750, for the loading of programs and experimentation. The FTMP support software includes a cross compiler for a high level language called Automated Engineering Design (AED) System, an assembler for the CAPS-6 processor assembly language, and a linker. Access to this support software is through an automated remote access facility on the VAX which relieves the user of the burden of learning how to use the IBM 4381. This manual is a compilation of information about the FTMP support environment. It explains the FTMP software and support environment along many of the finer points of running programs on FTMP. This will be helpful to the researcher trying to run an experiment on FTMP and even to the person probing FTMP with fault injections. Much of the information in this manual can be found in other sources; we are only attempting to bring together the basic points in a single source. If the reader should need points clarified, there is a list of support documentation in the back of this manual. Author

N87-10732# Royal Signals and Radar Establishment, Malvern (England).

REMOTE CAPABILITIES IN COMPUTER NETWORKS

J. M. Foster and I. F. Currie 1986 21 p
(RSRE-3947; BR100129) Avail: NTIS HC A02/MF A01

System-wide types, capabilities and procedure values can be used in computer networks to improve control of access and flexibility. This paper describes a network system based on these ideas. They provide a standard, uniform way of referring to data and using procedures in remote computers, with control over access and system type-checking. A working experimental version of the system exists, implemented on Flex computers, which provide microcoded support of capabilities. The mechanisms are such that normal programs written in terms of procedures, even those using procedure parameters, can be converted into network services without change. A possible way of implementing a similar scheme on conventional hardware is discussed. Author

N87-10733*# Illinois Univ., Urbana-Champaign. Coordinated Science Lab.

FAULT AND ERROR LATENCY UNDER REAL WORKLOAD: AN EXPERIMENTAL STUDY Ph.D. Thesis

Ram Chillarege 1986 100 p
(Grant NAG1-613; Contract N00014-84-C-0149)
(NASA-CR-179802; NAS 1.26:179802; UILU-ENG-86-2230; CSG-55) Avail: NTIS HC A05/MF A01 CSCL 09B

A practical methodology for the study of fault and error latency is demonstrated under a real workload. This is the first study that measures and quantifies the latency under real workload and fills a major gap in the current understanding of workload-failure relationships. The methodology is based on low level data gathered on a VAX 11/780 during the normal workload conditions of the installation. Fault occurrence is simulated on the data, and the error generation and discovery process is reconstructed to determine latency. The analysis proceeds to combine the low level activity data with high level machine performance data to yield a better understanding of the phenomena. A strong relationship exists between latency and workload and that relationship is quantified. The sampling and reconstruction techniques used are also validated. Error latency in the memory where the operating system resides was studied using data on the physical memory access. Fault latency in the paged section of memory was determined using data from physical memory scans. Error latency in the microcontrol store was studied using data on the microcode access and usage. Author

63 CYBERNETICS

Includes feedback and control theory, artificial intelligence, robotics and expert systems.

For related information see also *54 Man/System Technology and Life Support.*

N87-10734# Illinois Univ., Urbana.

FORPS: A FORTH-BASED PRODUCTION SYSTEM AND ITS APPLICATION TO A REAL-TIME ROBOT CONTROL PROBLEM

C. J. Matheus and H. L. Martin (Oak Ridge National Lab., Tenn.) Jan. 1986 24 p Presented at the ASME Pressure Vessel and Piping Conference and Exhibit, Chicago, Ill., 20 Jul. 1986 Prepared in cooperation with Oak Ridge National Lab., Tenn.
(Contract DE-AC05-84OR-21400)
(DE86-005426; CONF-860722-14) Avail: NTIS HC A02/MF A01

A simple yet very powerful system has been developed that merges the artificial intelligence qualities of a production system with the real-time control capabilities of FORTH. FORPS (FORTH-based Production System) offers the advantages of intelligent, rule-based control in a small package offering high speed, extensibility, and simplicity. A practical example of the system is presented in the development of an obstacle avoidance program to aid in controlling an overhead manipulator transport system. Several other potential applications to the area of control are discussed. DOE

N87-10735# Edgerton, Germeshausen and Grier, Inc., Idaho Falls, Idaho.

ISSUES IN EXPERT SYSTEM AIDS FOR A LARGE ENGINEERING SIMULATION CODE

R. K. Fink, R. A. Callow, and V. H. Ransom 1986 6 p Presented at the Summer Computer Simulation Conference, Reno, Nev., 28 Jul. 1986
(Contract DE-AC07-76ID-01570)
(DE86-009098; EGG-M-29885; CONF-860729-5) Avail: NTIS HC A02/MF A01

Coupling expert systems with existing engineering analysis codes is a promising area for artificial intelligence applications. An expert system can provide ready access to a knowledge base larger than most individual analysts would possess and thus can provide for easier and less costly use of the code and also reduce the potential for code misuse. The functions appropriate for expert system assistance and some of the issues that arise in developing such systems that have been identified through experimentation with the ATHENA code, a large digital simulation code for analysis of thermal-hydraulic energy networks, are discussed. The use of an expert system as a front-end user interface to analysis codes is conceptually appealing and with obvious benefits. Expert systems can play a substantial role in the execution and output analysis phases of simulation code usage. The integration of these roles leads to the concept of an intelligent environment for simulation code usage. The knowledge specific to the particular system being modeled, including modeling abstraction decisions, and specific knowledge about the numerical solution methods of the code can be used for more effective code execution control and output diagnosis. Expected benefits are improved quality of results and/or reduced execution cost. The methods for using this knowledge in an intelligent environment are discussed, with applications to current codes as well as implications for architecture of future large engineering simulation codes. DOE

64 NUMERICAL ANALYSIS

Includes iteration, difference equations, and numerical approximation.

N87-10736# Universitaet der Bundeswehr, Neubiberg (West Germany).

SEMINAR ON FINITE ELEMENTS IN UNSTEADY PROBLEMS [SEMINAR UEBER FINITE ELEMENTE BEI INSTATIONAEREN PROBLEMEN]

K. J. Schwenzfeger, ed. Jan. 1986 92 p Partly in GERMAN and ENGLISH Seminar held in Neubiberg, West Germany, 1985 (ETN-86-97824) Avail: NTIS HC A05/MF A01

The influence of nonlinearities on the local convergence of Ritz and Galerkin approximation methods, and asymptotic error expansions of finite element solutions of parabolic equations are treated. The unsteady calculation of ground water problems using the finite element method; and the properties of adaptive finite element methods are discussed. Mixed finite element methods used in flow mechanics are reviewed. Hierarchical bases for the solution of plane elliptic boundary value problems are presented. For individual titles, see N87-10737 through N87-10742.

N87-10737# Universitaet der Bundeswehr, Neubiberg (West Germany).

THE LOCAL CONVERGENCE OF RITZ AND GALERKIN METHODS FOR NONLINEAR PROBLEMS [ZUR LOKALEN KONVERGENZ VON RITZ- UND GALERKIN-VERFAHREN BEI NICHTLINEAREN PROBLEMEN]

J. A. Nitsche *In its* Seminar on Finite Elements in Unsteady Problems Jan. 1986 p 1-12 In GERMAN (For primary document see N87-10736 01-64)

Avail: NTIS HC A05/MF A01

The influence of nonlinearities on the local convergence behavior of Ritz and Galerkin approximation methods is treated. The local convergence problem treatment using one-dimensional finite elements is explained. The local convergence of the approximation methods depends on the local regularity of the solution which has to be approximated, and on global characteristics of the problem. An irregularity at the boundary can decisively determine the local convergence. ESA

N87-10738# Bonn Univ. (West Germany).

ASYMPTOTIC ERROR EXPANSIONS OF FINITE ELEMENT SOLUTIONS OF PARABOLIC EQUATIONS [ASYMPTOTISCHE FEHLERENTWICKLUNGEN VON FINITE ELEMENTE LOESUNGEN PARABOLISCHER GLEICHUNGEN]

Hans-Peter Helfrich *In* Universitaet der Bundeswehr Seminar on Finite Elements in Unsteady Problems Jan. 1986 p 13-26 In GERMAN (For primary document see N87-10736 01-64)

Avail: NTIS HC A05/MF A01

Asymptotic error expansions for finite element solutions of linear initial and boundary value problems, assuming that such expansions are known for the corresponding stationary problems, are presented. Asymptotic expansions for a semidiscrete Galerkin method and for the implicit Euler method are given. The comparison of the results with numerical results for the one-dimensional heat transfer equation shows that the asymptotic expansion represents well the error behavior. ESA

N87-10739# Universitaet der Bundeswehr, Neubiberg (West Germany).

UNSTEADY CALCULATIONS OF GROUND WATER PROBLEMS [INSTATIONAERE BERECHNUNG VON GRUNDWASSERPROBLEMEN]

Casimir Katz *In its* Seminar on Finite Elements in Unsteady Problems Jan. 1986 p 28-40 In GERMAN (For primary document see N87-10736 01-64)

Avail: NTIS HC A05/MF A01

Models for ground water calculations using the finite element method were made. The basic laws, equations, and boundary conditions for ground water problems are presented. The soil-mechanical and mathematical assumptions for the application of the method are explained. Examples demonstrate the possibilities of the calculation using a large programming package. ESA

N87-10740# Technische Univ., Munich (West Germany). Fachgebiet Elektronisches Rechen im Konstruktiven Ingenieurbau.

ADAPTIVE FINITE ELEMENT METHODS [ADPATIVE FINITE-ELEMENT-VERFAHREN]

Ernst Rank *In* Universitaet der Bundeswehr Seminar on Finite Elements in Unsteady Problems Jan. 1986 p 41-59 In GERMAN (For primary document see N87-10736 01-64)

Avail: NTIS HC A05/MF A01

The a posteriori error estimates which allow statements about the magnitude and distribution of the global error in finite element (FE) meshes are presented. Knowledge of the error estimates is used to control an adaptive FE mesh adaptation, whereby there is an essential difference between the mesh refinement (h-version) and the local enhancement of the degree of the starting functions (p-version). Examples explain the properties of an adaptive FE program for potential and elasticity problems. It is shown that the results for stationary problems can also be applied to unsteady cases. ESA

N87-10741# Universitaet der Bundeswehr, Neubiberg (West Germany).

MIXED FINITE ELEMENT METHODS IN FLOW MECHANICS [GEMISCHTE FINITE ELEMENT VERFAHREN IN DER STROEMUNGSMECHANIK]

R. Verfuerth *In its* Seminar on Finite Elements in Unsteady Problems Jan. 1986 p 60-61 In GERMAN (For primary document see N87-10736 01-64)

Avail: NTIS HC A05/MF A01

Finite element methods used in flow mechanics are introduced via the finite element approximation of the Stokes problem. The results can be transferred to the stationary Navier-Stokes equations. Finite element spaces which fulfill the so-called inf-sup condition are presented. The simplest starting points for the Stokes problem are steady, piecewise linear functions for the velocity, and piecewise constant functions for the pressure. ESA

N87-10742# Technische Hochschule, Aachen (West Germany). Inst. fuer Geometrie und Praktische Mathematik.

HIERARCHICAL BASES FOR THE SOLUTION OF PLANE ELLIPTIC BOUNDARY VALUE PROBLEMS

Harry Yserentant *In* Universitaet der Bundeswehr Seminar on Finite Elements in Unsteady Problems Jan. 1986 p 73-86 (For primary document see N87-10736 01-64)

Avail: NTIS HC A05/MF A01

A method to solve the large systems of linear equations arising from the approximate solution of linear elliptic boundary value problems using finite element or finite difference methods is presented. The method has nearly the same optimal computational complexity as the conventional multigrid methods but is free of many of their restrictions. Especially its speed of convergence does not depend on the regularity properties of the boundary value problem to be solved. The method replaces the usual nodal bases of the finite element spaces by hierarchical bases which originate in a very natural way if one starts with a coarse initial triangulation of the considered domain and refines it several times to get to final triangulation. ESA

N87-10743*# Carnegie-Mellon Univ., Pittsburgh, Pa. Dept. of Electrical and Computer Engineering.

NOVEL PARALLEL ARCHITECTURES AND ALGORITHMS FOR

LINEAR ALGEBRA PROCESSING Semiannual Report
David Casasent Oct. 1986 12 p
(Grant NAG1-575)
(NASA-CR-179826; NAS 1.26:179826) Avail: NTIS HC A02/MF A01 CSCL 12A

Advanced problems in computational fluid dynamics, finite element structural analysis, and related areas require the solution of large partial differential equations and matrices of large size and dynamic range. This project considers an advanced parallel linear algebra processor and associated novel parallel algorithms for such applications. Research on system fabrication, quantitative performance evaluation and new parallel algorithms are described and considered. Case studies in structural mechanics, dynamics and nonlinear systems, finite element methods, computational fluid dynamics, and partial differential equations are included. The novel utilization of an optical processor for the processing of such problems is the major research given attention. Author

N87-10744*# Massachusetts Inst. of Tech., Cambridge. Dept. of Aeronautics and Astronautics.
FINITE VOLUME SOLUTION OF THE COMPRESSIBLE BOUNDARY-LAYER EQUATIONS
Bernard Loyd and Earll M. Murman Washington NASA Oct. 1986 81 p
(Grant NAG1-507)
(NASA-CR-4013; NAS 1.26:4013; CFDL-TR-86-1) Avail: NTIS HC A05/MF A01 CSCL 12A

A box-type finite volume discretization is applied to the integral form of the compressible boundary layer equations. Boundary layer scaling is introduced through the grid construction: streamwise grid lines follow eta = y/h = const., where y is the normal coordinate and h(x) is a scale factor proportional to the boundary layer thickness. With this grid, similarity can be applied explicity to calculate initial conditions. The finite volume method preserves the physical transparency of the integral equations in the discrete approximation. The resulting scheme is accurate, efficient, and conceptually simple. Computations for similar and non-similar flows show excellent agreement with tabulated results, solutions computed with Keller's Box scheme, and experimental data. Author

N87-10745*# National Aeronautics and Space Administration. Langley Research Center, Hampton, Va.
GLOBAL COLLOCATION METHODS FOR APPROXIMATION AND THE SOLUTION OF PARTIAL DIFFERENTIAL EQUATIONS Final Report
A. Solomonoff and E. Turkel Sep. 1986 68 p Submitted for publication
(Contracts NAS1-17070; NAS1-18107)
(NASA-CR-178179; ICASE-86-60; NAS 1.26:178179) Avail: NTIS HC A04/MF A01 CSCL 12A

Polynomial interpolation methods are applied both to the approximation of functions and to the numerical solutions of hyperbolic and elliptic partial differential equations. The derivative matrix for a general sequence of the collocation points is constructed. The approximate derivative is then found by a matrix times vector multiply. The effects of several factors on the performance of these methods including the effect of different collocation points are then explored. The resolution of the schemes for both smooth functions and functions with steep gradients or discontinuities in some derivative are also studied. The accuracy when the gradients occur both near the center of the region and in the vicinity of the boundary is investigated. The importance of the aliasing limit on the resolution of the approximation is investigated in detail. Also examined is the effect of boundary treatment on the stability and accuracy of the scheme. Author

N87-10746# Illinois Univ., Urbana. Dept. of Computer Science.
COMPUTATIONAL METHODS AND SOFTWARE FOR DIFFERENTIAL EQUATIONS AND THEIR APPLICATIONS Annual Report, 16 Nov. 1985 - 15 Nov. 1986
1986 23 p
(Contract DE-AC02-76ER-02383)
(DE86-010231; DOE/ER-02383/0122; COO-2383-0122) Avail: NTIS HC A02/MF A01

Research efforts in algorithms, numerical software, and support software are described. The theory and implementation of adaptive methods for differential equations in various forms have been studied. The use of iterative methods in this environment and parallel techniques for ordinary differential equations have also been investigated. An introduction to the design and development of three tools to aid in scientific software development are presented. These tools are Polylith, a system which permits rapid prototyping of interconnected software modules; Fred, a syntax-directed, screen-oriented editor that can be used for any textual objects (programs, documentation, etc.); and a mathematical expression editor which permits easy modification of expressions in graphic form while retaining an internal structure that permits translation of other useful forms such as a computer language. DOE

N87-10747# Purdue Univ., West Lafayette, Ind. Joint Highway Research Project.
USE OF FUZZY SETS MATHEMATICS TO ASSIST PAVEMENT EVALUATION AND MANAGEMENT (REVISED MARCH 18, 1986) Final Report
M. Andonyadis, A. G. Altschaeffl, and J. L. Chameau Jul. 1985 290 p Sponsored by FHWA and Indiana Dept. of Highways
(PB86-214798; JHRP-85-14-Rev; FHWA/IN/JHRP-85/14-Rev) Avail: NTIS HC A13/MF A01 CSCL 13B

The mathematics of fuzzy sets that was created in the companion Interim Report by Gunaratne are applied. The new scheme being suggested for pavement management is predicated on the presence of uncertainty at various stages in pavement management which requires that judgment be used in the process. The fuzzy sets mathematics can methodically combine subjective information and crisp measurement data. Fuzzy sets are used to represent the subjectivity in pavement serviceability ratings and distress surveys, and the variability in Roadmeter, Skid-Tester, and Dynaflect readings. The ranking of pavement is formulated using fuzzy multi-attribute decision-making concepts using an expert knowledge base. To use the new scheme required the one-time development of the knowledge base. GRA

65 STATISTICS AND PROBABILITY

Includes data sampling and smoothing; Monte Carlo method; and stochastic processes.

No abstracts in this category.

66 SYSTEMS ANALYSIS

Includes mathematical modeling; network analysis; and operations research.

No abstracts in this category.

67 THEORETICAL MATHEMATICS

Includes topology and number theory.

No abstracts in this category.

70 PHYSICS (GENERAL)

For precision time and time interval (PTTI) see *35 Instrumentation and Photography;* for geophysics, astrophysics or solar physics see *46 Geophysics, 90 Astrophysics,* or *92 Solar Physics.*

N87-10748# Tokyo Univ. (Japan). Inst. of Space and Astronautical Science.
NUMERICAL AND EXPERIMENTAL STUDY OF DYNAMICS OF TWO-DIMENSIONAL BODY
Naoki Izutsu Mar. 1986 67 p
(ISAS-619; ISSN-0285-6808) Avail: NTIS HC A04/MF A01

Autorotation of a two-dimensional elliptic cylinder around its spanwise axis fixed perpendicularly to a uniform flow was numerically simulated by means of a discrete vortex-blob method. The results were compared with those of the experiments by a wind tunnel and a water channel, which were carried out in both the autorotating state and the forced rotating state with constant angular velocities driven by a stepping motor. The behavior and the interaction of the vortices shed behind the rotating elliptic cylinder were studied, making use of visualization of the numerical simulation results. Moreover, animation of the displayed image was made to illustrate the vortex interaction processes. Based on the moment of inertia and the thickness ratio of the cylinder, the starting condition of the autorotation was determined based on the mechanism of the autorotation. The driving force is produced by eliminating the vortex created behind the retreating edge. By means of graphic simulation utilizing a color coded vorticity display and animation, processes of the merging, rearrangement, interaction and splitting of the vortices in the wake of the rotating wing were visualized making these processes clearly understandable.
Author

71 ACOUSTICS

Includes sound generation, transmission and attenuation. For noise pollution see *45 Environment Pollution.*

N87-10749*# Bionetics Corp., Hampton, Va.
THE HELMHOLTZ RESONANCE BEHAVIOR OF SINGLE AND MULTIPLE ROOMS
Harvey H. Hubbard and Kevin P. Shepherd Sep. 1986 27 p
(Contract NAS1-16978)
(NASA-CR-178173; NAS 1.26:178173) Avail: NTIS HC A03/MF A01 CSCL 20A

The results of exploratory measurements of the noise fields inside rooms which are excited to resonance either acoustically or mechanically are presented. The data illustrate the nature and extent of the sound pressure level enhancements in single rooms and also how multiple rooms may resonate by means of either acoustic or mechanical coupling. Sound pressure level enhancements of about 5 dB were measured during resonance of rooms having flexible walls. For such conditions the sound pressure levels in the room were essentially uniform and in phase. Variability of up to 20 dB was measured in a room hallway complex having significant acoustic interactions. Resonant frequency prediction methods which work well at model scale, give only fair results for rooms.
Author

N87-10750*# National Aeronautics and Space Administration. Langley Research Center, Hampton, Va.
PREDICTION OF HELICOPTER ROTOR DISCRETE FREQUENCY NOISE: A COMPUTER PROGRAM INCORPORATING REALISTIC BLADE MOTIONS AND ADVANCED ACOUSTIC FORMULATION
Kenneth S. Brentner Oct. 1986 94 p
(NASA-TM-87721; L-16130; NAS 1.15:87721) Avail: NTIS HC A05/MF A01 CSCL 20A

A computer program has been developed at the Langley Research Center to predict the discrete frequency noise of conventional and advanced helicopter rotors. The program, called WOPWOP, uses the most advanced subsonic formulation of Farassat that is less sensitive to errors and is valid for nearly all helicopter rotor geometries and flight conditions. A brief derivation of the acoustic formulation is presented along with a discussion of the numerical implementation of the formulation. The computer program uses realistic helicopter blade motion and aerodynamic loadings, input by the user, for noise calculation in the time domain. A detailed definition of all the input variables, default values, and output data is included. A comparison with experimental data shows good agreement between prediction and experiment; however, accurate aerodynamic loading is needed.
Author

N87-10751*# Missouri Univ., Rolla. Dept. of Mechanical and Aerospace Engineering.
FUNDAMENTAL INVESTIGATIONS OF THE FINITE ELEMENT SOLUTIONS FOR ACOUSTIC PROPAGATION IN DUCTS Final Report
N. J. Walkington, T. W. Wicks, and W. Eversman 1986 86 p
(Grant NAG1-198)
(NASA-CR-179845; NAS 1.26:179845) Avail: NTIS HC A05/MF A01 CSCL 20A

The question of convergence of three finite element algorithms for the modelling of acoustic transmission in ducts carrying a nonuniform mean flow is addressed. The details of each algorithm are stated and example calculations in uniform and nonuniform ducts are made and assessed for accuracy and convergence. The algorithm based on the assumption of irrotationality is found to be highly convergent. This algorithm is the one used in current turbo-fan inlet acoustic radiation codes. A theoretical analysis indicating convergence is supported by example calculations. Two additional algorithms which do not require irrotationality are found to be less convergent, and perhaps not convergent at all for certain severely sheared velocity profiles. No theoretical convergence criteria can presently be established for these algorithms and convergence difficulties are shown here by example. Included in this class of algorithms is the duct analysis program ADAM which is known to display apparently nonconvergent solutions in certain cases.
Author

N87-10752*# General Electric Co., Cincinnati, Ohio.
FREE JET FEASIBILITY STUDY OF A THERMAL ACOUSTIC SHIELD CONCEPT FOR AST/VCE APPLICATION: DUAL STREAM NOZZLES Final Report
B. A. Janardan, J. F. Brausch, and R. K. Majjigi Washington NASA Mar. 1985 203 p
(Contract NAS3-22137)
(NASA-CR-3867; E-2392; NAS 1.26:3867) Avail: NTIS HC A10/MF A01 CSCL 20A

The influence of selected geometric and aerodynamic flow variables of an unsuppressed coannular plug nozzle and a coannular plug nozzle with a 20-chute outer stream suppressor were experimentally determined. A total of 136 static and simulated flight acoustic test points were conducted with 9 scale model nozzles. Also, aerodynamic measurements of four selected plumes were made with a laser velocimeter. The presence of the 180 deg shield produced different mixing characteristics on the shield side compared to the unshield side because of the reduced mixing with ambient air on the shielded side. This resulted in a stretching of the jet, yielding a higher peak mean velocity up to a length of 10 equivalent diameters from the nozzle exit. The 180 deg shield in community orientation around the suppressed coannular plug nozzle yielded acoustic benefit at all observer angles for a simulated takeoff. While the effect of shield-to-outer stream velocity ratio was small at angles up to 120 deg, beyond this angle significant acoustic benefit was realized with a shield-to-outer stream velocity ratio of 0.64.
Author

N87-10753*# General Electric Co., Cincinnati, Ohio. Aircraft Engine Business Group.
FREE-JET ACOUSTIC INVESTIGATION OF HIGH-RADIUS-RATIO COANNULAR PLUG NOZZLES Final Report
P. R. Knott, B. A. Janardan, R. K. Majjigi, P. K. Bhutiani, and P.

G. Vogt Washington NASA Oct. 1984 218 p
(Contract NAS3-20619)
(NASA-CR-3818; E-2177; NAS 1.26:3818; R83AEB574) Avail: NTIS HC A10/MF A01 CSCL 20A

The experimental and analytical results of a scale model simulated flight acoustic exploratory investigation of high radius ratio coannular plug nozzles with inverted velocity and temperature profiles are summarized. Six coannular plug nozzle configurations and a baseline convergent conical nozzle were tested for simulated flight acoustic evaluation. The nozzles were tested over a range of test conditions that are typical of a Variable Cycle Engine for application to advanced high speed aircraft. It was found that in simulate flight, the high radius ratio coannular plug nozzles maintain their jet noise and shock noise reduction features previously observed in static testing. The presence of nozzle bypass struts will not significantly affect the acoustic noise reduction features of a General Electric type nozzle design. A unique coannular plug nozzle flight acoustic spectral prediction method was identified and found to predict the measured results quite well. Special laser velocimeter and acoustic measurements were performed which have given new insights into the jet and shock noise reduction mechanisms of coannular plug nozzles with regard to identifying further benificial research efforts. Author

N87-10015# Tokyo Univ. (Japan). Dept. of Physics.
ACOUSTIC WAVES EMITTED BY VORTEX-BODY INTERACTION
T. Kambe, T. Minota (Kyushu Univ., Fukuoka (Japan).), and Y. Ikushima *In its* Proceedings of the Symposium on Mechanics for Space Flight, 1985 1985 9 p (For primary document see N87-10011 01-02)
Avail: NTIS HC A12/MF A01

72 ATOMIC AND MOLECULAR PHYSICS

Includes atomic structure, electron properties, and molecular spectra.

N87-10754# Technische Hochschule, Aachen (West Germany). Physikalisches Inst.
PROMPT NEUTRINO PRODUCTION IN 400 GeV PROTON COPPER INTERACTIONS
H. Graessler, W. Droege (Bonn Univ., West Germany), U. Idschok, H. Kreutzmann, B. Nellen, B. Wuensch, A. M. Cooper-Sarkar (European Organization for Nuclear Research, Geneva, Switzerland), D. C. Cundy, H. Foeth, A. Grant et al Stockholm, Sweden Stockholm Univ. Feb. 1986 32 p Submitted for publication
(USIP-86-02; ETN-86-97232) Avail: NTIS HC A03/MF A01

The prompt electron neutrino and muon neutrino fluxes from proton copper interactions at 400 GeV/c proton momentum were measured. The asymmetry between the prompt electron (anti) neutrino and the prompt muon (anti)neutrino event rates above 20 GeV is 0.07 + or - 0.08 corresponding to an Ne/Nmn ratio of 1.14 (+0.19, -0.16). The cross section weighted charge asymmetry for electrons and muons combined is 0.15 + or - 0.08. The number of D(-)decays into nu(-)e or nu(-)mu is (4.1 + or - 0.9) times 0.0001 per incident proton. No evidence for nu/tan interactions is found. ESA

73 NUCLEAR AND HIGH-ENERGY PHYSICS

Includes elementary and nuclear particles; and reactor theory.
For space radiation see *93 Space Radiation.*

N87-10755# Naval Research Lab., Washington, D. C.
CURRENT ENHANCEMENT FOR HOSE-UNSTABLE ELECTRON BEAMS
R. F. Fernsler, R. F. Hubbard, B. Hui, G. Joyce, and M. Lampe 24 Apr. 1986 74 p
(AD-A167804; NRL-MR-5769) Avail: NTIS HC A04/MF A01 CSCL 20/7

An electron beam injected into a conducting medium produces inductive electric fields. These fields drive conduction currents which, for stable beams, oppose the beam current and thereby reduce the total (net) current. For unstable beams which undergo large transverse displacements, the inductive field can reverse direction and drive conduction current parallel to the beam current. An analytic and numerical treatment of the latter effect is presented to explain current enhancement as observed for electron beams propagating in gases at pressures above 10 torr. GRA

N87-10756# Lawrence Livermore National Lab., Calif.
ELECTRICAL MEASUREMENT TECHNIQUES FOR PULSED HIGH CURRENT ELECTRON BEAMS
K. W. Struve 1 Apr. 1986 10 p Presented at the Conference on Measurement of Electrical Quantities in Pulse Power Systems-2, Gaithersburg, Md., 5 Mar. 1986
(Contract W-7405-eng-48)
(DE86-010980; UCRL-93261; CONF-860384-8) Avail: NTIS HC A02/MF A01

The advent of high current (1 to 100 kA), moderate energy (greater than 10 MeV), short pulse (1 to 100 ns) electron accelerators used for charged particle beam research has motivated a need to complement standard diagnostics with development of new diagnostic techniques to measure electron beam parameters. A brief survey is given of the diagnostics for measuring beam current, position, size, energy, and emittance. While a broad scope of diagnostics will be discussed, this survey will emphasize diagnostics used on the Experimental Test Accelerator (ETA) and Advanced Test Accelerator (ATA). Focus is placed on diagnostics measuring beam current, position and size. Among the diagnostics discussed are resistive wall current monitors, B sub theta loops, Rogowski coils, Faraday cups, and X-ray wire diagnostics. Operation at higher current levels also increases radiation and electromagnetic pulse interference. These difficulties and methods for circumventing them are also discussed. DOE

N87-10757# Kernforschungszentrum, Karlsruhe (West Germany). Inst. fuer Reaktorbauelemente.
LINEARIZED MODEL FOR THE HYDRODYNAMIC STABILITY INVESTIGATION OF MOLTEN FUEL JETS INTO THE COOLANT OF A LIQUID METAL FAST BREEDER REACTOR (LMFBR)
Karel Hartel Feb. 1986 33 p In GERMAN; ENGLISH summary
(KfK-3978; ISSN-0303-4003; ETN-86-97834) Avail: NTIS HC A03/MF A01

The hydrodynamic stability of liquid jets in a liquid continuum, both characterized by low viscosity was analyzed. A linearized mathematical model was developed. This model enables the length necessary for fragmentation of a vertical, symmetric jet of molten fuel by hydraulic forces in the coolant of a liquid metal fast breeder reactor to be evaluated. On the basis of this model the FRAG code for numerical calculation of the hydrodynamic fragmentation mechanism was developed. ESA

74 OPTICS

Includes light phenomena; and optical devices.
For lasers see *36 Lasers and Masers.*

N87-10758*# California Univ., San Diego. Center for Astrophysics and Space Sciences.
[DESIGN SUPPORT OF THE BURST AND TRANSIENT SOURCE EXPERIMENT (BATSE) OF THE GAMMA RAY OBSERVATORY (GRO) MISSION] Final Technical Report
Edwin A. Stephan, Jr. 12 Sep. 1986 6 p
(Contract NAS8-35012)
(NASA-CR-178920; NAS 1.26:178920) Avail: NTIS

HC A02/MF A01 CSCL 20F

Engineering design specifications and development of the large area detector and photomultiplier tube assemblies for the Burst and Transient Source Experiment (BATSE) of the Gamma Ray Observatory (GRO) mission are examined. B.G.

N87-10759# Letterman Army Inst. of Research, San Francisco, Calif.

FLASH/CRAZING EFFECTS ON SIMULATOR PURSUIT TRACKING PERFORMANCE Final Report, Mar. - Sep. 1983

David A. Stamper, David J. Lund, Richard R. Levine, Jerome W. Molchany, and Paul Best Mar. 1986 26 p

(AD-A167689; LAIR-214) Avail: NTIS HC A03/MF A01 CSCL 19/5

Day sights which are purposefully or inadvertently irradiated with laser radiation may become nonfunctional due to cracking or crazing of the optical glass. The degree of performance degradation may be related to the amount of damage to the glass and possible flash blindness from reradiation. Thirty-two male enlisted men and officers tracked a scale model tank through a constant arc at a simulated distance of 1 km, using a laboratory constructed viscous-damped tracking device. There were four crazing groups (4 men/group) under bright and dim ambient light conditions for a total of eight groups. Each man tracked the target during three flash/crazing and three crazing only trials, which were randomly presented during 30 trials. The simulated countermeasure which included the flash and crazing had dramatic effects on tracking performance, even under daylight conditions. Under the most severe degree of crazing, tracking performance was not possible under either ambient light condition. The relatively small amounts of laser radiation used to craze the BK-7 glass used in this study, which lead to significant performance decrements, demonstrates the potential impact of flash/crazing effects on operators of day sights. GRA

N87-10760# Lawrence Livermore National Lab., Calif.

EXTREME ULTRAVIOLET EXPLORER: MIRROR OPTICAL TESTS AND RESULTS

C. H. Gillespie, D. F. Edwards, M. A. Nichols, and D. S. Finley (California Univ., Berkeley) 31 Mar. 1986 8 p Presented at the SPIE Technical Symposium on Applications of Artificial Intelligence, Orlando, Fla., 31 Mar. 1986

(Contract W-7405-eng-48)

(DE86-010560; UCRL-94362; CONF-860366-8) Avail: NTIS HC A02/MF A01

The optical tests described here were performed after each step in the fabrication process of three Extreme Ultraviolet Explorer (EUVE) Type 1 telescope mirrors. The surface finish and irregularity was determined by image analysis and the geometrical figure was tested interferometrically. Images of a collimated point source were relayed to obtain magnifications and photographic exposures were adjusted to include all the scattered light while still resolving the smallest bright image core. By linearizing film sensitivity and taking digitized lineouts of the photographed image, less than 1 arc second full width half maximum (FWHM) intensities were measured. The integrated energy density was measured photometrically, and diffraction limited curves of 5 arc second half energy widths (HEW) were obtained. The test purpose, instruments employed, alignment methods, and test results are detailed. DOE

N87-10761# California Univ., Berkeley. Lawrence Berkeley Lab.

OPTICAL SYSTEMS FOR SYNCHROTRON RADIATION. LECTURE 4: SOFT X-RAY IMAGING SYSTEMS

M. R. Howells Apr. 1986 32 p Presented at the Synchrotron Radiation Sources and their Applications Conference, Aberdeen, Scotland, 14 Sep. 1985

(Contract DE-AC03-76SF-00098)

(DE86-011567; LBL-21365; CONF-8509255-4) Avail: NTIS HC A03/MF A01

The history and present techniques of soft X-ray imaging are reviewed briefly. The physics of X-ray imaging is described, including the temporal and spatial coherence of X-ray sources. Particular technologies described are: contact X-ray microscopy, zone plate imaging, scanned image zone plate microscopy, scanned image reflection microscopy, and soft X-ray holography and diffraction. DOE

N87-10301*# Academy of Sciences (USSR), Tomsk. Inst. of Atmospheric Optics.

METHODS FOR ESTIMATING THE OPTICAL CONSTANTS OF ATMOSPHERIC HAZES BASED ON COMPLEX OPTICAL MEASUREMENTS

V. E. Zuev, B. S. Kostin, and I. E. Naats *In* NASA. Langley Research Center 13th International Laser Radar Conference Aug. 1986 3 p (For primary document see N87-10263 01-35)

Avail: NTIS HC A15/MF A01 CSCL 20F

75 PLASMA PHYSICS

Includes magnetohydrodynamics and plasma fusion.

For ionospheric plasmas see *46 Geophysics*. For space plasmas see *90 Astrophysics*.

N87-10762 Maryland Univ., College Park.

THE ONSET OF ALFVENIC TURBULENCE Ph.D. Thesis

Sanjoy Ghosh 1985 220 p

Avail: Univ. Microfilms Order No. DA8528974

The onset of turbulence in a magnetized plasma is of considerable importance in both the laboratory and in astrophysics. Recent theoretical work has focused on the turbulent behavior of high frequency Langmuir waves. This dissertation investigates how low frequency omega less than or equal to OMEGA sub i, magnetohydrodynamic (MHD) oscillations in a warm plasma may undergo a transition from a coherent state to one of turbulence. A nonlinear (DNLS) equation describing the evolution of Alfven and magnetosonic waves is derived from the fluid equations. Propagation angles slightly oblique to the ambient magnetic field are considered, and a linear operator which includes kinetic effects is incorporated. The time evolution of an arbitrary spectrum of waves is analyzed in the case where one k-mode is unstable, with the rest damped. Growth is due to the presence of a warm low-density ion beam. Landau effects from background ions provide the major source of damping. It is found that breathing solitons arise in the system from any arbitrary initial spectrum. The energy of the nonlinear wave can undergo a transition to turbulence when the growth rate of the unstable mode exceeds the average damping rate of the damped modes. The observed MHD turbulence upstream of the quasi-parallel region of the Earth's bow shock is modelled according to the above results. Shocklet formation and particle trapping effects as predicted by the driven/dissipative DNLS equation are also discussed. Dissert. Abstr.

N87-10763# Nagoya Univ. (Japan). Inst. of Plasma Physics.

PLASMA CONFINEMENT BY A RADIO FREQUENCY PLUGGING POTENTIAL IN AN AXISYMMETRIC MIRROR-CUSP DEVICE

R. Kumazawa, S. Okamura, K. Adati, T. Aoki, H. Fujita, K. Hattori, S. Hidekuma, T. Kawamoto, Y. Okubo, T. Sato et al Jul. 1986 20 p

(IPPJ-784; ISSN-0469-4732) Avail: NTIS HC A02/MF A01

The RFC-XX-M is a magnetohydrodynamic (MHD) stable and axisymmetric mirror-cusp device with radio frequency (RF) plugging. The plasma is produced by ion cyclotron resonant heating (ICRH) with gas puffing at the central mirror. The total ion energy confinement time including axial loss, electron drag, and charge exchange is improved by a factor of three by the RF plugging and reaches 1 ms. The energy confinement time due to axial particle loss is estimated to be 7.5 ms from a detailed analysis of ion energy loss channels. An RF plugging potential is measured from the energy analysis of the escaping ions. It is determined that the RF plugging potential is proportional to the square of an applied RF voltage and the maximum value reaches 250 V. This value agrees with a plugging potential deduced from the Pastuknov formula within a factor of 2. Author

N87-10764*# National Aeronautics and Space Administration. Langley Research Center, Hampton, Va.

LASER-POWERED MHD GENERATORS FOR SPACE APPLICATION

N. W. Jalufka Oct. 1986 15 p
(NASA-TP-2621; NAS 1.60:2621) Avail: NTIS HC A02/MF A01 CSCL 20I

Magnetohydrodynamic (MHD) energy conversion systems of the pulsed laser-supported detonation (LSD) wave, plasma MHD, and liquid-metal MHD (LMMHD) types are assessed for their potential as space-based laser-to-electrical power converters. These systems offer several advantages as energy converters relative to the present chemical, nuclear, and solar devices, including high conversion efficiency, simple design, high-temperature operation, high power density, and high reliability. Of these systems, the Brayton cycle liquid-metal MHD system appears to be the most attractive. The LMMHD technology base is well established for terrestrial applications, particularly with regard to the generator, mixer, and other system components. However, further research is required to extend this technology base to space applications and to establish the technology required to couple the laser energy into the system most efficiently. Continued research on each of the three system types is recommended. Author

N87-10036# Academy of Sciences (USSR), Moscow. Inst. of Applied Mathematics.

MATHEMATICAL AND COMPUTATIONAL MODELS OF PLASMA FLOWS

K. V. Brushlinsky *In* Tokyo Univ. Proceedings of the Symposium on Mechanics for Space Flight, 1985 1985 9 p (For primary document see N87-10011 01-02)
Avail: NTIS HC A12/MF A01

N87-10548 European Space Agency. European Space Research and Technology Center, ESTEC, Noordwijk (Netherlands). Space Science Dept.

PLASMA SHEET BOUNDARY ELECTRIC FIELDS DURING SUBSTORMS

Arne Pedersen *In* CNES Results of the ARCAD 3 Project and of Recent Programs in Magnetospheric and Ionospheric Physics 1985 p 107-121 (For primary document see N87-10541 01-46)
Avail: CEPADUES, Toulouse

N87-10555 Institut d'Aeronomie Spatiale de Belgique, Brussels.

FORMATION AND DEFORMATION OF THE PLASMAPAUSE DURING A SUBSTORM EVENT

J. Lemaire *In* CNES Results of the ARCAD 3 Project and of Recent Programs in Magnetospheric and Ionospheric Physics 1985 p 239-260 (For primary document see N87-10541 01-46)
Avail: CEPADUES, Toulouse

N87-10574 Centre National de la Recherche Scientifique, Orleans (France). Lab. de Physique et Chimie de l'Environnement.

EXPERIMENTAL EVIDENCE OF FIELD-ALIGNED ELF PLASMA DUCTS IN THE IONOSPHERIC TROUGH AND IN THE AURORAL ZONE

C. Beghin, J. C. Cerisier (Centre de Recherches en Physique de l'Environnement, Saint Maur des Fosses, France), J. L. Rauch, J. J. Berthelier, F. Lefeuvre, R. Debrie, O. A. Maltseva (Rostov State Univ., Rostov-on-Don, USSR), and N. I. Massevitch (Academy of Sciences (USSR), Moscow) *In* CNES Results of the ARCAD 3 Project and of Recent Programs in Magnetospheric and Ionospheric Physics 1985 p 517-527 (For primary document see N87-10541 01-46)
Avail: CEPADUES, Toulouse

76 SOLID-STATE PHYSICS

Includes superconductivity.

For related information, see also *33 Electronics and Electrical Engineering* and *36 Lasers and Masers.*

N87-10765*# Jet Propulsion Lab., California Inst. of Tech., Pasadena.

TOTAL-DOSE RADIATION EFFECTS DATA FOR SEMICONDUCTOR DEVICES. 1985 SUPPLEMENT. VOLUME 2, PART B

Keith E. Martin, Michael K. Gauthier, James R. Coss, Armando R. V. Dantas, and William E. Price 15 May 1986 421 p
(Contract NAS7-100)
(NASA-CR-179741; JPL-Pub-85-43-Vol-2-Pt-B; NAS 1.26:179741) Avail: NTIS HC A18/MF A01 CSCL 20L

Steady-state, total-dose radiation test data are provided in graphic format, for use by electronic designers and other personnel using semiconductor devices in a radiation environment. The data were generated by JPL for various NASA space programs. The document is in two volumes: Volume 1 provides data on diodes, bipolar transistors, field effect transistors, and miscellaneous semiconductor types, and Volume 2 (Parts A and B) provides data on integrated circuits. The data are presented in graphic, tabular, and/or narrative format, depending on the complexity of the integrated circuit. Most tests were done steady-state 2.5-MeV electron beam. However, some radiation exposures were made with a Cobalt-60 gamma ray source, the results of which should be regarded as only an approximate measure of the radiation damage that would be incurred by an equivalent electron dose. All data were generated in support of NASA space programs by the JPL Radiation Effects and Testing Group (514). Author

N87-10766*# Roberts Associates, Inc., Vienna, Va.

MATHEMATICAL MODEL FOR THE BRIDGMAN-STOCKBARGER CRYSTAL GROWING SYSTEM Final Report, 20 Aug. 1984 - 19 Sep. 1986

Glyn O. Roberts 19 Sep. 1986 200 p
(Contract NAS8-36190)
(NASA-CR-178921; NAS 1.26:178921; RAI-86-B-1) Avail: NTIS HC A09/MF A01 CSCL 20B

In a major technical breakthrough, a computer model for Bridgman-Stockbarger crystal growth was developed. The model includes melt convection, solute effects, thermal conduction in the ampule, melt, and crystal, and the determination of the curved moving crystal-melt interface. The key to the numerical method is the use of a nonuniform computational mesh which moves with the interface, so that the interface is a mesh surface. In addition, implicit methods are used for advection and diffusion of heat, concentration, and vorticity, for interface movement, and for internal gracity waves. This allows large time-steps without loss of stability or accuracy. Numerical results are presented for the interface shape, temperature distribution, and concentration distribution, in steady-state crystl growth. Solutions are presented for two test cases using water, with two different salts in solution. The two diffusivities differ by a factor of ten, and the concentrations differ by a factor of twenty. Author

N87-10767# State Univ. of New York, Stony Brook. Dept. of Materials Science.

INTERFACE PROPERTIES AND CRYSTAL-GROWTH MECHANISMS Progress Report, Jul. 1985 - Jan. 1986

J. Q. Broughton 13 Jan. 1986 5 p
(Contract DE-FG02-85ER-45218)
(DE86-010846; DOE/ER-45218/1) Avail: NTIS HC A02/MF A01

The pulsed heating of Si-vapor interfaces has been modelled for the close-packed (111) and open (100) faces. A Si (111)-melt interface has been quenched. Grain-boundary interfaces with melt have also been studied, along with properties of Si liquid. Pseudopotentials have been obtained for the electron-argon system. DOE

N87-10768# Argonne National Lab., Ill.

SULFUR-BASED SYNTHETIC METAL SUPERCONDUCTORS

J. M. Williams, M. A. Beno, K. D. Carlson, T. J. Emge, U. Geiser, A. J. Schultz, H. H. Wang, and M. H. Whangbo 1986 16 p
Presented at the Conference on Fine Chemicals for the Electronics Industry, London, England, 2 Apr. 1986 Prepared in cooperation with North Carolina State Univ., Raleigh
(Contract W-31-109-eng-38)

(DE86-010512; CONF-8604192-1) Avail: NTIS HC A02/MF A01

Although organic synthetic metals (synmetals) are composed of nonmetallic elements, they frequently exhibit novel electrical and magnetic properties. Their electrical conductivities range from insulating, to semiconducting, to even superconducting. Through imaginative synthetic organic chemistry, it should be possible to prepare a steadily rising number of systems with very high superconducting transition temperatures, T/sub c/. In fact, T/sub c/'s have risen from approx. 1 K in the early 1980's in the TMTSF systems to approx. 8 K in the ET (BEDT-TTF) materials, but T/sub c/'s still remain low. However, the steadily rising T/sub c/'s lend credence to the likelihood that higher values can be achieved. This paper summarizes the current status and findings regarding the ET based synmetal superconductors. Within a few years of the synthesis of the ET donor molecule, it was discovered that (ET)2(ClO4)(C2H3Cl3)/sub 0.5/ exhibited metallic conductivity down to 1.4 K, and then, that (ET)2ReO4 became superconducting (T/sub c/ approx. = 2 K) under an applied pressure of 4 kbar (1 kbar = 14,505 psi). Then, in early 1984, ambient pressure superconductivity was reported in Beta-(ET)2I3 (T/sub c/ approx. = 1.4 K), followed by Beta-(ET)2IBr2 (T/sub c/ approx. = 2.8 K) and Beta-(ET)2AuI2 (T/sub c/ approx. = 5 K), respectively. Results of our rf penetration depth studies of these 3 systems are summarized. Superconductivity at ambient pressure has also been reported for certain non-Beta phases. DOE

N87-10769# Kernforschungszentrum, Karlsruhe (West Germany). Inst. fuer Material- und Festkoerperforschung.
MICROSTRUCTURE, GRAIN BOUNDARIES AND PROPERTIES OF SINTERED AND ISOTATICALLY HOT PRESSED SIC MATERIALS Thesis - Karlsruhe University, West Germany
Rainer Hamminger Feb. 1986 141 p In GERMAN; ENGLISH summary
(KfK-4063; ISSN-0303-4003; ETN-86-97837) Avail: NTIS HC A07/MF A01

A microstructural characterization of pressureless sintered and isostatically hot pressed SiC-materials was elaborated by microchemical and microanalytical methods. Grain boundary analyses were conducted by high resolution Auger electron spectroscopy. The materials studied contain inclusions of the sintering additives and agglomerates of the impurity elements. Characteristic distinctions between the different types of materials occur mainly in the region of grain boundaries. It is proved that (Al, C)-doped materials produce Al-rich segregation films at the grain boundaries; (B,C)-doped materials are characterized by grain boundaries of high purity without any layers of doping or impurity elements. Grain boundary films rich in O, which occur in isostatically hot pressed SiC, are responsible for the pronounced time dependancy of strength of this material. The pure grain boundaries of (B,C)-doped materials have a positive impact on creep resistance, while the segregation films of (Al,C)-doped qualities result in a tendency of increasing creep rates. ESA

77 THERMODYNAMICS AND STATISTICAL PHYSICS

Includes quantum mechanics; theoretical physics; and Bose and Fermi statistics.

For related information see also *25 Inorganic and Physical Chemistry* and *34 Fluid Mechanics and Heat Transfer.*

N87-10770 North Carolina Univ., Chapel Hill.
NULL SURFACE DYNAMICS Ph.D. Thesis
Charles Gregory Torre 1985 138 p
Avail: Univ. Microfilms Order No. DA8527239

The dynamical structure of Einstein's theory of gravity is investigated using a time parameter whose level surfaces are null hypersurfaces in spacetime. A spacelike foliation of codimension two is used in order to give an invariant kinematic description. Dynamics are analyzed via a constrained Hamiltonian formalism. As preliminary examples the classical and quantum formulations of a self interacting scalar field and a genetic non-Abelian gauge theory are studied. In the gravitational case it is found that the Hamiltonian formulation includes both first and second class constraints. The first class constraints are associated with the invariance of the theory under diffeomorphisms of the null hypersurfaces. The second class constraints are direct consequences of the fact that the equal time surfaces are null. Our results suggest that the central dynamical role is played by the conformal 2-geometry of the null hypersurfaces, or equivalently, the shear of the null congruence which generates a given equal time surface. Dissert. Abstr.

80 SOCIAL SCIENCES (GENERAL)

Includes educational matters.

No abstracts in this category.

81 ADMINISTRATION AND MANAGEMENT

Includes management planning and research.

No abstracts in this category.

82 DOCUMENTATION AND INFORMATION SCIENCE

Includes information management; information storage and retrieval technology; technical writing; graphic arts; and micrography.

For computer documentation see *61 Computer Programming and Software.*

N87-10771# Oak Ridge National Lab., Tenn.
STUDY OF UNIX AND ITS SUITABILITY FOR THE AIR FORCE'S WWMCCS INFORMATION SYSTEM
R. S. Loffman Apr. 1986 22 p
(Contract DE-AC05-84OR-21400)
(DE86-011293; ORNL/TM-9901) Avail: NTIS HC A02/MF A01

The US Department of Defense is in the process of modernizing its Worldwide Military Command and Control System (WWMCCS) Automatic Data Processing (ADP) system. This modernization will include a new ADP system: WWMCCS Information System (WIS). The need for modernization results from a rapid growth in technology and an increased dependency on ADP support. The Air Force's role in this effort is the modernization of the Air Force WIS (AFWIS). The Air Force requested the assistance of Oak Ridge National Laboratory (ORNL) in investigating UNIX as a possible operating system for its new WIS ADP environment. ORNL reviewed and analyzed: (1) WWMCCS documentation for system requirements, (2) technical materials for information about UNIX, and (3) business sources for indications about UNIX's future in a commercial market. This analysis concluded that there are some features required by AFWIS that currently only UNIX can provide; however, its place in the future marketplace is still uncertain. DOE

N87-10772# Oak Ridge National Lab., Tenn.
COMPUTER SOFTWARE EVALUATION METHODOLOGY AND DATA BASE MANAGEMENT SYSTEM SELECTION
A. F. Huntley Apr. 1986 45 p
(Contract DE-AC05-84OR-21400)
(DE86-011343; ORNL-6260) Avail: NTIS HC A03/MF A01

This document presents a Data Base Management System (DBMS) evaluation methodology that has been developed under the sponsorship of the Department of the Navy, Naval Management Systems Support Office (NAVMASSO), Norfolk, Virginia. NAVMASSO has recognized the need for a DBMS to support the Shipboard Nontactical Automated Data Processing Program (SNAP) and has tasked Oak Ridge National Laboratory (ORNL) with evaluating DBMSes that are available for the SNAP-I computer system - a Honeywell DPS-6 minicomputer - and the SNAP-II computer system a Harris 300 minicomputer. In preparation for the SNAP-I/SNAP-II DBMS evaluation, ORNL has developed the DBMS evaluation methodology presented in this document. First, a discussion of the traditional computer software evaluation methodology is provided, with identification of aspects of the methodology that may cause the resulting evaluation to be deficient. A DBMS evaluation methodology that stresses the layered functionality of the software is then presented. The methodology requires a large amount of hands-on testing and allows evaluation team members to evaluate the software from the perspective of application developers and end-users who will use the system on a day-to-day basis. The document contains a discussion of several general considerations that must be evaluated. These are items that form a supportive environment and enhance the usability of the software, even though they may not affect the intrinsic functionality of the software. The technical facilities that define the limits of functionality of the software are then presented for evaluation. Areas where these facilities may not meet the desired functionality are identified. DOE

N87-10516*# Illinois Univ., Urbana. Dept. of Electrical and Computer Engineering.
AN ACCELERATED FORTH DATA-ACQUISITION SYSTEM
S. A. Bowhill and A. D. Rennier *In* International Council of Scientific Unions, Middle Atmosphere Program. Handbook for MAP, Vol. 20 Jun. 1986 2 p (For primary document see N87-10419 01-42)
Avail: NTIS HC A22/MF A01; also available from SCOSTEP Secretariat, Illinois Univ., 1406 West Green Street, Urbana, Ill. 61801 CSCL 05B

83 ECONOMICS AND COST ANALYSIS

Includes cost effectiveness studies.

No abstracts in this category.

84 LAW, POLITICAL SCIENCE AND SPACE POLICY

Includes NASA appropriation hearings; aviation law; space law and policy; international law; international cooperation; and patent policy.

N87-10773# Committee on Appropriations (U. S. Senate).
DEPARTMENT OF HOUSING AND URBAN DEVELOPMENT-INDEPENDENT AGENCIES APPROPRIATION BILL, 1987
J. Garn Washington GPO 1986 111 p Report to accompany H.R. 5313 presented by the Committee on Appropriations, 99th Congr., 2nd Sess., 25 Sep. 1986
(S-Rept-99-487) Avail: US Capitol, Senate Document Room

Appropriations for the Department of Housing and Urban Development, and for sundry agencies, boards, commissions, corporations, and offices were discussed for the fiscal year ending September 30, 1987. For individual titles, see N87-10774 through N87-10774.

N87-10774# Committee on Appropriations (U. S. Senate).
NATIONAL AERONAUTICS AND SPACE ADMINISTRATION
In its Department of Housing and Urban Development-Independent Agencies Appropriation Bill, 1987 1986 p 64-70 (For primary document see N87-10773 01-84)
Avail: US Capitol, Senate Document Room

The appropriations for research, development, and procurement activities of NASA are discussed. B.G.

N87-10775# Committee on Science and Technology (U. S. House).
NATIONAL AERONAUTICS AND SPACE ADMINISTRATION AUTHORIZATION ACT, 1987
Washington GPO 1986 37 p An act, H.R. 5495, referred to the Committee on Commerce, Science and Transportation, 99th Congress, 2d Session, 30 Sep. 1986
Avail: US Capitol, House Document Room

Appropriations are discussed for research and development; space flight, control, and data communication; construction of facilities; and research and program management by NASA. B.G.

85 URBAN TECHNOLOGY AND TRANSPORTATION

Includes applications of space technology to urban problems; technology transfer; technology assessment; and surface and mass transportation.

For related information see also *03 Air Transportation and Safety, 16 Space Transportation,* and *44 Energy Production and Conversion.*

N87-10776# National Physical Lab., Teddington (England).
[PROGRESS MADE DURING 1985 IN THE SCIENTIFIC AND TECHNICAL PROGRAM OF NATIONAL PHYSICAL LABORATORY'S DIVISION OF RADIATION SCIENCE AND ACOUSTICS]
Feb. 1986 81 p
Avail: NTIS HC A05/MF A01

The progress made during 1985 in the scientific and technical program of the Division of Radiation Science and Acoustics (DRSA) is discussed. Topics addressed include: dosimetry; radioactivity and neutron measurements; acoustical standards; noise and speech technology; and ultrasonics and underwater acoustical standards. B.G.

N87-10777*# Argonne National Lab., Ill.
ANL/RBC: A COMPUTER CODE FOR THE ANALYSIS OF RANKINE BOTTOMING CYCLES, INCLUDING SYSTEM COST EVALUATION AND OFF-DESIGN PERFORMANCE Final Report
G. A. McLennan May 1986 68 p
(NASA Order C-80002-E; Contract DE-AI01-86CE-50162)
(NASA-CR-179462; NAS 1.26:179462; DOE/NASA/80002-1; ANL/CT-86-3) Avail: NTIS HC A04/MF A01 CSCL 10B

This report describes, and is a User's Manual for, a computer code (ANL/RBC) which calculates cycle performance for Rankine bottoming cycles extracting heat from a specified source gas stream. The code calculates cycle power and efficiency and the sizes for the heat exchangers, using tabular input of the properties of the cycle working fluid. An option is provided to calculate the costs of system components from user defined input cost functions. These cost functions may be defined in equation form or by numerical tabular data. A variety of functional forms have been included for these functions and they may be combined to create very general cost functions. An optional calculation mode can be used to determine the off-design performance of a system when operated away from the design-point, using the heat exchanger areas calculated for the design-point. Author

N87-10778# Massachusetts Inst. of Tech., Cambridge.
RLE PROGRESS REPORT
J. Allen and R. Birgeneau Jan. 1986 287 p
(MIT-PR-128) Avail: NTIS HC A13/MF A01

Topics addressed include: submicron structures; kinetic phenomena in thin film electronic materials; focused ion beams; surface chemical reactions; quantum electronics; nonlinear optics;

X-ray diffused scattering; semiconductor surfaces; custom integrated circuits; speech communication; communications biophysics; physiology; molecule microscopy; quantum optics; atomic resonance and scattering; plasma dynamics; digital signal processing; information processing; microwave and quantum magnetics; radio astronomy; and electromagnetic wave theory. B.G.

N87-10779# Air Force Wright Aeronautical Labs., Wright-Patterson AFB, Ohio.
AIR FORCE TECHNICAL OBJECTIVE DOCUMENT FISCAL YEAR 1987
William E. Berner and Alan M. Salus Dec. 1985 77 p Supersedes AFWAL-TR-84-4000
(AD-A167324; AFWAL-TR-85-4000; AFWAL-TR-84-4000) Avail: NTIS HC A05/MF A01 CSCL 01/3

This technical objective document describes the technical program in materials to meet future Air Force operational needs. The technology program is divided into ten focal areas which encompass the full spectrum of materials capabilities required for future aircraft, missile, space and electronic systems. These ten areas are: Thermal Protection Materials and Structures; Metallic Structural Materials; Nonmetallic Structural Materials; Nondestructive Evaluation; Aerospace Propulsion Materials; Nonstructural Materials; Electromagnetic Windows and Electronic Materials; Laser Hardened Materials; Computer Aided Manufacturing/Manufacturing R&D; and Systems Support. GRA

N87-10780# Naval Postgraduate School, Monterey, Calif.
A SUMMARY OF THE FOUNDATION RESEARCH PROGRAM, FISCAL YEAR 1985 Summary Report, 1 Oct. 1984 - 30 Sep. 1985
G. T. Howard 12 May 1986 63 p
(AD-A168009; NPS-012-86-002PR) Avail: NTIS HC A04/MF A01 CSCL 05/1

Thirty projects of Independent Research/Independent Exploratory Development were funded by the Naval Postgraduate School Foundation Research Program. This research was in the areas of: Computer science, Administrative sciences, Operations research, National security affairs, Physics, Electrical and computer engineering, Meteorology, Aeronautics, Oceanography, and Mechanical engineering. A tabulation in the Appendix identifies the area of research and the investigator(s). Summaries of each project are provided together with a list of publications and theses. GRA

N87-10781# Bhabha Atomic Research Centre, Bombay (India). Spectroscopy Div.
[RESEARCH AND DEVELOPMENT ACTIVITIES OF THE SPECTROSCOPY DIVISION OF THE BHABHA ATOMIC RESEARCH CENTRE] Progress Report, Jan. 1983 - Dec. 1984
R. M. Dixit, ed. 1985 233 p
(DE86-702154; BARC-1269) Avail: (US Sales Only) NTIS HC A11/MF A01

The Research abd Development (R and D) activities of the Spectroscopy Division of the Bhabha Atomic Research Center, Bombay, during the period from January 1983 to December 1984 are reported. The main thrust of the activites of the Division is directed towards meeting the spectrochemical analytical requirements of the nuclear energy programs and the related R and D projects of the Department of Atomic Energy. These activities are described in the form of summaries grouped under the headings: (1) analyses by optical emission, X-ray fluorescence, X-ray excited optical luminescence and other techniques, (2) atomic, molecular, and solid state spectroscopy. (3) optics and thin films, and (4) electronic instrumentation. Two feature articles which are included in the report bring out the salient features of X-ray absorption fine structure spectroscopy (EXFAS) and laser spectroscopic techniques for trace analysis and describe the Division's efforts in setting up facilities to carry out work in these emerging fields. Other activities of the Division are teaching trainees and guiding research leading to M.Sc. and Ph.D. degrees. A list of papers published in journals and papers presented at conferences, symposia etc. by tge staff-members of the Division is given. A divisional staff chart is also given. DOE

N87-10782# California Univ., Berkeley. Lawrence Berkeley Lab.
LAWRENCE BERKELEY LABORATORY RECENT PAPERS SUBMITTED AND REPORTS ISSUED, FEBRUARY 1986
Feb. 1986 17 p
(Contract DE-AC03-76SF-00098)
(DE86-011319; LBL-PUB-445) Avail: NTIS HC A02/MF A01

One-hundred thirty-two references are arranged under the following headings: accelerator and fusion research, applied science, biology and medicine, Center for Advanced Materials, chemical biodynamics, earth sciences, engineering, materials and molecular research, nuclear science, and physics. DOE

N87-10647# Oxford Polytechnic (England). Dept. of Architecture.
THE PLANNING AND MAINTENANCE OF URBAN SETTLEMENTS TO RESIST EXTREME CLIMATIC FORCES
Ian R. Davis *In* WMO Proceedings of the Technical Conference on Urban Climatology and its Applications with Special Regard to Tropical Areas 1986 p 277-312 (For primary document see N87-10636 01-47)
Avail: NTIS MF A01; print copy available at WMO, Geneva, Switzerland

N87-10650# Washington Univ., Seattle. Dept. of Geological Sciences.
URBAN HYDROLOGY IN THE TROPICS: PROBLEMS, SOLUTIONS, DATA COLLECTION AND ANALYSIS
Thomas Dunne *In* WMO Proceedings of the Technical Conference on Urban Climatology and its Applications with Special Regard to Tropical Areas 1986 p 405-434 (For primary document see N87-10636 01-47)
Avail: NTIS MF A01; print copy available at WMO, Geneva, Switzerland

N87-10651# Sheffield Univ. (England).
ENERGY RELATED ISSUES
John K. Page *In* WMO Proceedings of the Technical Conference on Urban Climatology and its Applications with Special Regard to Tropical Areas 1986 p 435-450 (For primary document see N87-10636 01-47)
Avail: NTIS MF A01; print copy available at WMO, Geneva, Switzerland

N87-10652# Office for Chemical Analyses, Stuttgart (West Germany). Dept. of Climatology.
THE INTRODUCTION OF CLIMATOLOGY INTO THE ADMINISTRATION AND DEVELOPMENT OF PLANNING IN THE CITY OF STUTTGART
J. Baumueller *In* WMO Proceedings of the Technical Conference on Urban Climatology and its Applications with Special Regard to Tropical Areas 1986 p 451-460 (For primary document see N87-10636 01-47)
Avail: NTIS MF A01; print copy available at WMO, Geneva, Switzerland

N87-10653# Maryland Univ., College Park. Inst. for Physical Science and Technology.
PROBLEMS OF DESIGN FOR CITIES IN THE TROPICS
H. E. Landsberg *In* WMO Proceedings of the Technical Conference on Urban Climatology and its Applications with Special Regard to Tropical Areas 1986 p 461-472 (For primary document see N87-10636 01-47)
Avail: NTIS MF A01; print copy available at WMO, Geneva, Switzerland

N87-10654# Murdoch Univ. (Australia). School of Environmental and Life Sciences.
CLIMATIC FACTORS IN THE SITING OF NEW TOWNS AND SPECIALIZED URBAN FACILITIES
T. J. Lyons *In* WMO Proceedings of the Technical Conference on Urban Climatology and its Applications with Special Regard to Tropical Areas 1986 p 473-486 (For primary document see N87-10636 01-47)

Avail: NTIS MF A01; print copy available at WMO, Geneva, Switzerland

N87-10655# Ben Gurion Univ. of the Negev, Sede Boqer (Israel). Blaustein Inst. for Desert Research.
DESIGN FOR CLIMATE IN HOT, DRY CITIES
Baruch Givoni *In* WMO Proceedings of the Technical Conference on Urban Climatology and its Applications with Special Regard to Tropical Areas 1986 p 487-513 (For primary document see N87-10636 01-47)
Avail: NTIS MF A01; print copy available at WMO, Geneva, Switzerland

N87-10656# World Meteorological Organization, Geneva (Switzerland).
DESIGN FOR CLIMATE IN HOT, HUMID CITIES
S. Nieuwolt *In its* Proceedings of the Technical Conference on Urban Climatology and its Applications with Special Regard to Tropical Areas 1986 p 514-534 (For primary document see N87-10636 01-47)
Avail: NTIS MF A01; print copy available at WMO, Geneva, Switzerland

88 SPACE SCIENCES (GENERAL)

No abstracts in this category.

89 ASTRONOMY

Includes radio, gamma-ray, and infrared astronomy, and astrometry.

N87-10783 Dartmouth Coll., Hanover, N.H.
THE ULTRAVIOLET SPECTRA OF DA WHITE DWARFS Ph.D. Thesis
Edmund Paul Nelan 1985 213 p
Avail: Univ. Microfilms Order No. DA8601400

Using the International Ultraviolet Explorer (IUE) satellite, observations of cool to moderately warm DA white dwarfs have shown the presence of broad absorption features at wavelength 1400 and 1600. The wavelength 1600 feature is prominent for T (sub eff) is less than 13000 K and the wavelength 1400 feature is visible up to about T (sub eff) = 18000 K. It is proposed that the absorption in both cases is due to perturbations of the energy level structure of neutral hydrogen atoms undergoing collisions. Model atmospheres were constructed using the computer program LUCIFER assuming a pure hydrogen composition. With the addition of these Ly alpha satellite lines at 1400 and 1600 to the usual hydrogen continuum and line opacities, all of the observed spectral energy distributions of DA white dwarf stars can be explained. Further investigations have shown that the strength of these features is far more sensitive to gravity and temperature than the Balmer line profiles and continuum slopes; thus even at low resolution, the absorption at 1400 and 1600 promise to be an excellent indicator of these fundamental stellar parameters.
Dissert. Abstr.

N87-10784 Washington Univ., Seattle.
THE X-RAY PROPERTIES OF HIGH REDSHIFT, OPTICALLY SELECTED QSOS Ph.D. Thesis
Scott Frederick Anderson 1985 173 p
Avail: Univ. Microfilms Order No. DA8603097

In order to study the X-ray properties of high redshift QSOs, grism/grens plates covering 17 deg (2) of sky previously imaged to very sensitive X-ray flux levels with the Einstein Observatory were used. Following optical selection of the QSO, the archived X-ray image is examined to extract an X-ray flux detection or a sensitive upper limit. Two samples of grism/grens selected QSOs are emphasized. The first, sample C, is an approximately 80% complete sample of 37 QSOs with 1.8 less than or = z less than or = 3.0, and B less than or = 19.5. Using two statistical approaches that also incorporate information contained in X-ray non-detections, it is inferred from sample C data that such QSOs contribute less than 3% to the diffuse X-ray background (XRB). The contribution of all QSOs with B less than or = 19.5 to the XRB is found to be 21 +/- 8%. Through the use of complete samples, very few uncertain parameters or extrapolations are used in these determinations. The second sample, sample N, includes 78 QSOs that occupy a narrow region of redshift, z, and optical luminosity, L(opt), space. The X-ray to optical luminosity ratio is parameterized by a hypothetical power law slope, a(ox), connecting the two wavebands, and is thought to depend on L(opt) and/or z. Sample N occupies a sufficiently narrow region of L(opt)-Z space that ensemble mean parameters such as a(ox)eff can be directly determined without the need to correct for such dependences. For sample N QSOs it was found that a(ox)eff = 1.50 +/- 0.03 in excellent agreement with the model of Avni and Tananbaum (A-T) for the evolution of a(ox)eff. However, the width found here for the a(ox) distribution is narrower than that found by A-T.
Dissert. Abstr.

N87-10785 Arizona Univ., Tucson.
HIGH RESOLUTION SPECTROSCOPY OF QUASAR ABSORPTION LINES Ph.D. Thesis
Jill Eleanor Bechtold 1985 342 p
Avail: Univ. Microfilms Order No. DA8603142

This dissertation investigates the properties of the metal-containing absorption lines seen in quasar spectra which have Z(abs) much less then Z(em). These systems, which probably originate in the halos of galaxies at high redshift, are then compared to observations of the halo and interstellar medium of the Milky Way. Echelle spectra were obtained at the Multiple Mirror Telescope (MMT) of the Z = 1.79 absorption system of the quasar B2 1225 + 317. The velocity profiles showed complex structure which varied from ion to ion, with ionization and column densities varying from component to component. The relative columns were consistent with the expectations for approximately interstellar abundance, low density material, in equilibrium with the ultraviolet radiation field of a spiral galaxy for lambda greater than 912 A, and the integrated light from QSOs at Z = 1.79 for lambda less than 912 A. The aggregate C IV profile has a width of about 450 km/sec, larger than that expected for a single galaxy halo, however. With the MMT spectrograph and echellette grating, and MMT echelle, we studied the properties of three other redshift systems of B2 1225+317, which are optically thin at the Ly man limit, but have saturated Lyman alpha. We calculated the contribution of quasars to the UV radiation field as a function of redshift. The calculated field depends on a number of uncertain assumptions, which were varied in order to estimate their effect on the result. Finally, we discuss an important input into these calculations, the continuum spectral energy distribution for quasars, with particular attention to the extreme ultraviolet. Dissert. Abstr.

N87-10786*# National Aeronautics and Space Administration. Goddard Inst. for Space Studies, New York.
MOLECULAR CLOUDS IN THE CARINA ARM
David Andrew Grabelsky (Columbia Univ., New York.) Sep. 1986 358 p
(NASA-TM-87798; NAS 1.15:87798) Avail: NTIS HC A16/MF A01 CSCL 03A

Results from the first large-scale survey in the CO(J = 1 to 0) line of the Vela-Carina-Centaurus region of the Southern Milky Way are reported. The observations, made with the Columbia University 1.2 m millimeter-wave telescope at Cerro Tololo, were spaced every beamwidth (0.125 deg) in the range 270 deg is less than or = l is less than or = 300 deg and -1 deg less than or = b less then or = 1 deg, with latitude extensions to cover all Carina arm emission beyond absolute b = 1 deg. In a concurrent survey made with the same telescope, every half-degree in latitude and longitude was sampled. Both surveys had a spectral coverage of 330 km/s with a resolution of 1.3 km/s. The Carina arm is the dominant feature in the data. Its abrupt tangent at l is approx. = 280 deg and characteristic loop in the l,v diagram are unmistakable evidence for CO spiral structure. When the emission is integrated over velocity and latitude, the height of the step seen in the tangent direction suggests that the arm-interarm contrast is at least 13:1. Comparison of the CO and H I data shows close agreement between these two species in a segment of the arm lying outside the solar circle. The distribution of the molecular layer about the galactic plane in the outer Galaxy is determined. Between R = 10.5 and 12.5 kpc, the average CO midplane dips from z = -48 to -167 pc below the b = 0 deg plane, following a similar well-known warping of the H I layer. In the same range of radii the half-thickness of the CO layer increases from 112 to 182 pc. Between l = 270 deg and 300 deg, 27 molecular clouds are identified and cataloged along with heliocentric distances and masses. An additional 16 clouds beyond 300 deg are cataloged from an adjoining CO survey made with the same telescope. The average mass for the Carina arm clouds is 1.4x 10(6)M (solar), and the average intercloud spacing along the arm is 700 pc. Comparison of the distribution of the Carina arm clouds with that of similarly massive molecular clouds in the first and second quadrants strongly suggests that the Carina and Sagittarius arms form a single spiral arm approx. 40 kpc long wrapping two-thirds of the way around the Galaxy. Author

N87-10787*# National Aeronautics and Space Administration, Washington, D.C.

NASA STUDYING CONCEPT TO MEASURE DISTANCE BETWEEN STARS, GALAXIES

Jim Kukowski and Frank Bristow 15 Sep. 1986 3 p
(NASA-News-Rel-86-133) Avail: NTIS HC A02 CSCL 03A

NASA's Jet Propulsion Laboratory (JPL), Pasadena, Calif., is studying the possibility of sending a spacecraft millions of miles beyond the planets at speeds of more than a quarter million miles an hour to directly measure the distance to stars in our galaxy and to neighboring glaxies. The 21st Century project, Thousand Astronomical Units (TAU), was conceived by JPL Director Dr. Lew Allen. An astronomical unit (AU) is the average distance between the Earth and the Sun, or 93 million miles. The TAU voyage may signal the beginning of deep space exploration. The project would use a 50,000 pound, 131 feet long ion (electric) propulsion system to boost the 11,000 pound science spacecraft to about 225, 000 mph by the time it is twice the distance of Pluto, about 6 billion miles from Earth. Astronomy would begin during the voyage past the planets, using a 1.5 meter telescope. For instance, the spacecraft could return high resolution pictures of Saturn's rings and of the small planet Pluto with its moon Charon. About 10 years after launch, the spacecraft could begin taking measurements of star distances as far away as the center of our galaxy. One of TAU's astonomic objectives would be to do precision astrometry from a very long baseline, 1,000 AU. But before reaching that distance, TAU will have increased that baseline from the present 2 AU limitation of the Earth's orbit, and therefore, increased the ability to directly measure stellar distances while enroute. Author

N87-10788*# National Aeronautics and Space Administration, Washington, D.C.

NEW SPACE ASTRONOMY TECHNIQUE DEVELOPED TO STUDY CELESTIAL BODIES

Leon Perry and Franklin ODonnell 3 Oct. 1986 2 p
(NASA-News-Rel-86-140) Avail: NTIS HC A02

A new space radio-astronomy technique, using an orbiting satellite to study celestial objects, has been successfully tested by scientists at NASA'S Jet Propulsion Laboratory, Pasadena, Calif. An international team of scientists conducted experiments during July and August employing a new space technique called very long baseline interferometry (VLBI). They combined data from radio telescopes on the ground with data from an antenna on NASA's Tracking and Data Relay Satellite System (TDRSS) spacecraft. Investigators obtained better resolution of three quasars than is possible in ground-based radio studies at the same wavelength. Quasars, or quasi-stellar objects, are among the most distant objects known. The resolution obtained from the orbiting VLBI experiment was equivalent to that of a radio telescope with a size of 1.4 Earth diameters. The quasars studied are designated 1730-130, 1741-038 and 1510-089. For the first time, a VLBI experiment used an orbiting satellite as one of its radio telescopes. Previously, scientists linked widely separated antennae on the ground with VLBI techniques to produce high-resolution radio astronomy studies of celestial objects. Author

N87-10789*# Washington Univ., Seattle.

HIGH RESOLUTION CCD SPECTRA OF STARS IN GLOBULAR CLUSTERS. PART 2: METALS AND CNO IN M71

E. Myckky Leep, J. B. Oke, and George Wallerstein 1986 24 p
(Grants NGL05-002-134; NSF 84-15353)
(NASA-CR-179853; NAS 1.26:179853) Avail: NTIS HC A02/MF A01 CSCL 03A

Palomar coude CCD spectra of resolution 0.3 and 0.6 has been used to redetermine abundances in five stars of the relatively metal rich globular cluster M71. The (Fe/H) value is restricted to the limits of -0.6 to -1.0. The largest source of uncertainty is a systematic difference in f-values between those derived via the Holweger-Muller (1974) solar model and the Bell et al. (1976) solar model. If we use absolute f-values measured by the Oxford group (Blackwell et al. 1982) we find [Fe/H] to lie in the range of -0.6 to -0.75, i.e., as given by using the Bell et al. solar model. The relative abundances of the light elements, i.e., Na through Ca and probably including Ti show an average excess relative to iron of 0.4 dex. The effect of this difference on metal indices derived from broad- and narrow- band photometry is discussed. For three stars we find [O/H] = -0.6 using absolute f-values. For CN an analysis of individual rotational lines of the 2-0 band of the red system yields lines in the (C/H,N/H) plane that are consistent with either an original [C/Fe] = [N/Fe] = 0 or a modest increase in N relative to C due to CN burning and mixing. A search for C-13N was not successful and an uncertain lower limit of C-12/C-13 near 10 was obtained. Author

N87-10790*# California Inst. of Tech., Pasadena.

SPECTROSCOPY OF THE GLOBULAR CLUSTERS IN M87

J. R. Mould, J. B. Oke, and J. M. Nemec 18 Jul. 1986 26 p
(Grant NGL05-002-134)
(NASA-CR-179854; NAS 1.26:179854) Avail: NTIS HC A03/MF A01 CSCL 03A

With a velocity dispersion of 370 + or - 50 km/sec the globular cluster system of M87 is kinematically hotter than the stars in the giant elliptical itself. This is consistent with the clusters' shallower density distribution for isotropic orbits. The mean metallicity of the 27 clusters in the sample analyzed here is no more than a factor of 2 more metal rich than the cluster system of the Milky Way, but considerably more metal poowr than the integrated starlight in the field at a radius of 1' from the center of M87. There is no evidence for the existence of young clusters in the system. The mass-radius relation between 1' and 5' required to contain the globular clusters joins on to that required to contain the hot gas around M87. Author

N87-10791 Cornell Univ., Ithaca, N.Y.

INFRARED EMISSION LINES FROM PLANETARY NEBULAE Ph.D. Thesis

Mark Alan Shure 1985 156 p
Avail: Univ. Microfilms Order No. DA8525805

The ionic abundances and electron temperatures in the central regions of a number of planetary nebulae were determined using infrared fine-structure lines in the 15 to 40 micron range. The 91 cm telescope of the NASA Kuiper Airborne Observatory was used to measure the following lines: (S III) 18.71, (Ar III) 21.83, (Ne V) 24.28, (O IV) 25.87, (S III) 33.47, and Ne (III) 36.02 microns. Line emission was integrated over the entire emitting region in a total of twenty-two planetary nebulae, ranging from medium to high excitation. All except the (Ar III) line were detected at greater than 3 sigma. Although optical emission lines were used for decades to derive both abundances and temperatures, use of the infrared lines offer two distinct advantages over the optical lines: infrared line emission is insensitive to temperature; and the high excitation ions O(IV) and Ne(V) prove regions closer to the central star than do the bright optical lines. As a consequence, abundances derived from infrared lines do not require accurate temperatures for nebulae, in contrast to the case for temperature-sensitive optical lines. Infrared ionic abundances are therefore potentially much more accurate than the optical abundances. By comparing integrated radio free-free emissions to the infrared line fluxes, abundances were determined for nineteen nebulae. Dissert. Abstr.

N87-10792 Wyoming Univ., Laramie.
LIGHT SCATTERING IN RESONANCE REGION FROM POLYDISPERSE NON-SPHERICAL PARTICLES Ph.D. Thesis
Joseph Stanley Mentek 1985 205 p
Avail: Univ. Microfilms Order No. DA8606183

Angular light intensity scattering patterns for particles with equivalent sphere radii approximately equal to the wavelength of the light source have been investigated in both experimental and analytic senses. Experimental measurements of the Mie scattering matrix elements M sub 1 and M sub 2 were performed for polydisperse samples of high irregularly shaped particles of SiO2. Experiments show that, at backscattering angles, the Mie theory for equivalent spheres overestimates the scattered intensities for M sub 1 and M sub 2. A model was developed to attempt to remove the surface wave contribution to the backscattering. The least squares parameter estimation technique that was applied does provide a satisfactory backscatter correction while maintaining the use of the Mie calculation that is applicable to spheres. Dissert. Abstr.

N87-10793# Harvard Univ., Cambridge, Mass.
OBSERVATIONS OF NON-THERMAL RADIATION FROM LATE-TYPE STARS Ph.D. Thesis
Jay Aaron Bookbinder 1985 223 p
Avail: Univ. Microfilms Order No. DA8602193

The statistical properties of the X-ray and radio emission from the coronae of a sample of late-type stars are studied. The sample consists of a large, nearly volume-limited, population of K and M dwarfs. From these analyses we draw conclusions regarding stellar dynamos, the evolution of low-mass binary systems, and the nature of the coronal heating mechanism in low mass stars. We first examine the statistical behavior of the x-ray emission from the complete Einstein survey 243 late-type stars within 25 pc, focusing on the stellar age and color dependences. Optically selected, nearly volume limited subsamples which are reasonably free of known biases are used to show that, relative to the uoung disk stars, old disk stars have levels of coronal emission almost an order of magnitude smaller. There is also a steady, but small, decrease of coronal activity with decreasing mass. Furthermore, though we find that stars later than M5 are strongly under-represented in our X-ray survey, we are able to show that this is a direct result of their lower activity levels and cannot be due to a bias in the sample. A subset of these stars present in the X-ray survey was selected for observations at radio wavelengths. Combined with previously reported radio observations of M dwarfs and the X-ray date, it is shown that these observations can provide a new characterization of the coronal activity of late-type stars. The basic result is that the quiescent X-ray and radio emissions are strongly correlated, and that both show similar dependences on the stellar population. The high brightness temperatures inferred for the quiescent radio emission argues that a non-maxwellian distribution of electrons is responsible for the radio emission. Dissert. Abstr.

N87-10794 Wisconsin Univ., Madison.
OBSERVATIONS OF MOLECULAR CLOUDS IN THE DIRECTION OF GALACTIC AND EXTRAGALACTIV RADIO SOURCES Ph.D. Thesis
Ana Gomes Nash 1986 145 p
Avail: Univ. Microfilms Order No. DA8605704

The (1,1) and (2,2) inversion transitions of NH3 and the (1(sub 11)-1(sub 10)) K-doublet of H2CO were observed toward 3 extragalactic sources (NRA0150, 3C123, and 3C111) and 3 galactic H II regions (G24.8+0.1, G25.4-0.2, and G37.8-0.2). The OH absorption at 18 cm was observed toward NRA0150. The emission/absorption technique was employed in order to reduce the number of assumptions and, therefore, uncertainties involved in determining excitation temperature and optical depths. Kinetic temperatures were found from the NH3(1,1) and (2,2) data. A range in molecular hydrogen density was found from model curves of Stutzki and Winnewisser (1985). Dissert. Abstr.

N87-10795 California Univ., Berkeley.
SURFACE PHOTOMETRY OF EARLY-TYPE GALAXIES Ph.D. Thesis
Stanislav Bratislav Djorgovski 1985 635 p
Avail: Univ. Microfilms Order No. DA8609999

The results of a Charge Coupled Device (CCD) surface photometry survey of 262 elliptical and lenticular galaxies are presented. The original data set consists of some 720 CCD exposures of galaxies, and a large number of calibration exposures. All data were obtained in red bandpasses indigenous to Lick Observatory. The survey, the sample of galaxies covered, the methods of surface photometry, calibration procedures, and comparisons with other, published work by other authors are described. The survey results and some simple applications are then presented. The results are presented in the form of semimajor axis profiles of surface brightness, ellipticity, position angle, elliptical aperture magnitude, circular aperture magnitude, and residual Fourier amplitudes. Error-bars are evaluated for all quantities. Dissert. Abstr.

90 ASTROPHYSICS

Includes cosmology; celestial mechanics; space plasmas; and interstellar and interplanetary gases and dust.
For related information see also *75 Plasma Physics.*

N87-10796 Michigan Univ., Ann Arbor.
COMPUTATIONAL HYDRODYNAMICS IN ASTROPHYSICAL STUDIES: HIGHLY SHOCKED FLOWS IN 3 DIMENSIONS Ph.D. Thesis
Clifford Nicholas Arnold 1985 217 p
Avail: Univ. Microfilms Order No. DA8600402

A second order alternating direction implicit/explicit computer code (SADIE) was designed to model supersonic gas dynamics in one, two, or three dimensions. SADIE uses van Leer's Vector-Flux Splitting technique to track strong shocks accurately. On a Cyber 205, SADIE evolves 70,000 grid points per time step per second for three dimensional flows. Using this computational tool, several complicated flow problems were studied. The results of several test problems used to verify the code are reported. The simulation of a pressure matched supersonic jet (Mach 3 and Mach 6) propagating into a quiet medium was also presented. These simulations are done in hopes of gaining insight to some of the perplexing questions of extragalactic jets. Dissert. Abstr.

N87-10797 Pittsburgh Univ., Pa.
THE EFFECT OF A QUASI-STELLAR OBJECT ON ITS HOST GALAXY: DYNAMICAL AND PHYSICAL PROCESSES IN THE INTERSTELLAR MEDIUM AROUND A QSO Ph.D. Thesis
Chong-An Chang 1985 144 p
Avail: Univ. Microfilms Order No. DA8600621

The dynamical and physical processes in the interstellar medium around a quasi-stellar object (QSO) were calculated for the purpose of understanding the effects of QSO radiation on its host galaxy. Numerical hydrodynamical solutions were calculated for both one-dimensional and two-dimensional cases. Shock wave driven QSO radiation was simulated and followed under a MacCormmack differencing scheme to understand the density, pressure, temperature and velocity components of the gas. Physical processes and their effects on the dynamics are calculated, including the change of the size of a dust grain due to ion sputtering, ion-field emission, the change of dust grain surface charge, charge equilibrium, ionization equilibrium, thermal equilibrium and the coupling between the dust grain and the interstellar gas ions and atoms. Results are obtained under different initial conditions and different physical parameters. It is shown that dust grains play an important role in determining the dynamics of the ISM around a QSO. Since they are destroyed by ion-field emission and sputtering when the shock passes through that region. The electric potential on a grain surface can be as high as thousands of Volts near the QSO prior to grain destruction. However, a high voltage induces ion-field emission and rapid destruction of the grain. Dissert. Abstr.

N87-10798 Boston Univ., Mass.

ELECTRON-POSITRON PAIR PRODUCTION BY ULTRARELATIVISTIC ELECTRONS IN A SOFT PHOTON FIELD Ph.D. Thesis Ph.D. Thesis

Apostolos Mastichiadis 1985 92 p

Avail: Univ. Microfilms Order No. DA8601362

The fully differential cross section for photon-electron pair production is integrated numerically over phase space. Results were obtained for the astrophysically interesting case in which the interaction between an ultrarelativistic electron and a soft photon results in e-e+ pair production. The positron spectrum is a function of the energies of both the photon and the electron, as well as the angle of interaction. The energy at which the positron distribution peak is inversely proportional to the photon energy and independent of the electron energy. The positron spectrum is integrated once more over initial electron energies for a power law energy distribution depends linearly on the energy of the primary electron. Finally, semi-analytical expressions are obtained for the energy losses of the primary electrons. Dissert. Abstr.

N87-10799 Illinois Univ., Urbana-Champaign.

PULSE TIMING AND NEUTRON STAR STRUCTURE Ph.D. Thesis

Radha Nandkumar 1985 134 p

Avail: Univ. Microfilms Order No. DA8600274

Pulsar glitches, postglitch behavior, and timing noise are examined in terms of dynamical processes associated with the pinned crustal superfluid in neutron stars. The vortex creep theory satisfactorily explains the postglitch behaviour and pulsar glitches. Models for pulsar timing noise, which are based on the vortex creep theory, are considered. The noise power spectrum was evaluated in each case and compared to the theoretical models with the observed noise power spectra of some two dozen pulsars. The electrical and thermal conductivities and the shear viscosity are calculated. The effects of ionic correlations are taken into account by using the results of liquid structure factor of the one component plasma obtained from numerical simulations, as well as the effects of screening of the electron-ion interaction. Dissert. Abstr.

N87-10800 Washington Univ., Seattle.

GAS AND DUST IN REGIONS OF RECENT STAR FORMATION Ph.D. Thesis

Jason A. Cardelli 1985 305 p

Avail: Univ. Microfilms Order No. DA8529890

A variety of observations of gas and dust have been obtained in two regions of recent star formation for the purpose of determining basic physical properties. The analyses center on extinction and scattering in the Orion complex and extinction and atomic and molecular absorption near the center of rho Oph molecular cloud. In Orion, the visual extinction towards theta(1,2) Ori indicates that, for the grains responsible for the visual extinction, the average size has increased on the order of 20 to 30%. The subsequent increase in absolute visual extinction has resulted in an apparent lowering of the UV extinction via normalization in the visual. Analysis of small angle scattering in NGC 1999 in the UV indicates the phase function (g) changes from about 0.60 near lambda 4000 A to about 0.25 near lambda 1400 A. This seems to imply that the observed continua of H-H 1 and 2 cannot be the result of small angle scattering from imbedded T Tauri stars. For four lines of sight near the center of the rho Oph molecular cloud, the determined column densities of CH extend the relation N(CH) alpha N(H2)3 is extended to log N(H2) approx.=21. For three lines of sight with log N(H2) greater than 21, N(CN) falls well below this relation and consequently indicates that gas-phase reactions like C(+) + CH dominate over photodestruction at the higher densities appropriate for these three lines of sight. Depletions determined from atomic absorption lines are also discussed. Dissert. Abstr.

N87-10801# Fermi National Accelerator Lab., Batavia, Ill.

POSSIBLE SIGNIFICANCE OF A NEW DIMENSIONLESS RATIO IN COSMOLOGY

M. S. Turner and B. J. Carr May 1986 11 p Prepared in cooperation with Chicago Univ., Ill. and London Univ., England

(Contract DE-AC02-76CH-03000)

(DE86-011026; FNAL/Pub-86/66-A) Avail: NTIS HC A02/MF A01

Observations suggest that the mass density of the Universe is dominated, not by ordinary matter, but by exotic particles which are a relic of the Big Bang. In this case, a new dimensionless cosmological ratio arises, the ratio of the mass density in ordinary matter to that in exotic matter, whose value is about 0.1. A priori it might seem remarkable that this ratio should be so close to unity. However, we point out that, for many exotic dark matter candidates, the ratio is related to the fundamental scales of particle physics. A value of order unity arises naturally providing rather simple relationships exist between these scales. DOE

N87-10802# Delaware Univ., Newark. Research Foundation.

PARTICLE THEORY AND COSMOLOGY Final Report, 16 Jul. 1984 - 31 Mar. 1986

Q. Shafi 17 Apr. 1986 8 p

(Contract DE-FG02-84ER-40176)

(DE86-010366; DOE/ER-40176/02) Avail: NTIS HC A02/MF A01

The major thrust of the research reported was in the area of unified theories, in particular in grand unified and higher dimensional superstring theories. The problems that were addressed included: (1) the construction of realistic low energy (four dimensional) gauge models motivated from the ten-dimensional E8 x E8 superstring theory; (2) a study of the phenomenological and cosmological implications of such models; (3) implementation of the inflationary scenario in the context of higher dimensional theories of gravity; and (4) clarification of the role of extended structures such as strings, monopoles and domain walls in a cosmological setting, particularly in an inflationary cosmology. DOE

N87-10803 Wisconsin Univ., Madison.

CONDITIONS FOR THE FORMATION OF MASSIVE STARS Ph.D. Thesis

Mark Guy Wolfire 1985 184 p

Avail: Univ. Microfilms Order No. DA8601133

Upper limits on the masses of stars that can form are reinvestigated and models for the inflow of matter through cocoons around stars of 60, 100, and 100 solar mass are calculated. Radiative forces on dust play a crucial role in halting an accretion inflow. Rather general conditions that must hold at the inner and outer boundaries of a protostellar cocoon are considered. Limits are derived on the dust to gas ratios and mass inflow rates that will permit inflow onto very massive stars. It is found that the ISM dust mixture of Mathis, Rumpl, and Nordsieck would not allow an inflow to occur. It is necessary that the standard Galactic gas to dust ratio by reduced by a factor four or more and the larger graphite grains be missing from the dust size distribution function. The inflows also require mass accretion rates of about 10 to the-3 solar mass/yr or more for there to be sufficiently strong ram-pressure to overcome the strong radiative deceleration that occurs at the inner boundary of the shell. For the model calculations, radiative deceleration of grains and grain destruction processes are explicitly accounted for in an iterative solution of the radiation-hydrodynamic equations. Inflow can occur if intermediate sized grains (0.05-0.25 microns) are missing from the initial gas/dust mixture. Very small grains or very large grains greater than 100 microns allow infall to proceed. The existence of massive stars in certain locations in galaxies suggest that preconditioning of the interstellar medium by shocks or by turbulence is required for massive star formation. Dissert. Abstr.

N87-10804 Columbia Univ., New York.
BRIGHT GALACTIC X-RAY BINARY SOURCES: TEMPORAL AND SPECTRAL STUDIES Ph.D. Thesis
Saeqa Dil Vrtilek 1985 143 p
Avail: Univ. Microfilms Order No. DA8604685

A detailed analysis of the time-dependent X-ray spectra of five bright binary sources were performed: Cygnus X-2, GX9 + 9, 1820-30 (a globular cluster burst source), Serpens X-1 (also a burster), and Hercules X-1. The observations were taken with the Einstein Monitor Proportional Counter and Objective Grating Spectrometer. Dissert. Abstr.

N87-10805 Pennsylvania State Univ., University Park.
ON THE STABILITY OF ACCRETION DISKS AROUND BLACK HOLES Ph.D. Thesis
M. Randall McKee 1985 116 p
Avail: Univ. Microfilms Order No. DA8607186

A stability analysis of the accretion process around a black hole is presented within the context of a thin alpha-disk model. The analysis includes azimuthal as well as radial perturbations. All terms resulting from the dispersion relation are retained. For the purely radial analysis, a viscous and a thermal instability arise in the inner region of the accretion disk. A phase velocity is present over all radial perturbation wavelengths and pure standing waves do not result. The viscous instability is found to arise only in the purely radial mode. When azimuthal perturbations are included, the thermal instability behaves radially like a standing wave upon which is superposed an azimuthal mode with constant phase velocity. Hot spots may therefore develop, whose Keplerian rotation may account for the rapid fluctuations observed from accreting systems. Due to the inherent shearing of the hot spots, a duration time of the oscillations is predicted. The results are applied to several types of accreting objects where this analysis is thought to be relevant, such as the galactic black hole candidate source Cyg X-1, active galactic nuclei, and nonmagnetic neutron star systems. date source Cyg X-1, active galactic nuclei, and nonmagnetic neutron star systems. Dissert. Abstr.

N87-10806 California Univ., Berkeley.
A STUDY OF HIERARCHICAL CLUSTERING OF GALAXIES IN AN EXPANDING UNIVERSE Ph.D. Thesis
David Henry Porter 1985 152 p
Avail: Univ. Microfilms Order No. DA861173

The nonlinear hierarchical clustering of galaxies in an Einstein-deSitter (Omega = 1), initially white noise mass fluctuations (n = 0) model universe is investigated and shown to be in contradiction with previous results. The model is done in terms of an 11,000-body numerical simulation. The independent statics of 0.72 million particles are used to simulte the boundary conditions. A new method for integrating the Newtonian N-body gravity equations, which has controllable accuracy, incorporates a recursive center of mass reduction, and regularizes two body encounters is used to do the simulation. The coordinate system used here is well suited for the investigation of galaxy clustering, incorporating the independent positions and velocities of an arbitrary number of particles are used to simulate the boundary conditions. A new method for integrating the Newtonian N-body gravity equations, to map the independent statics of 0.72 million particles into just 4,000 particles. This method for simulating the boundary conditions also has controllable accuracy. Dissert. Abstr.

N87-10807 Michigan Univ., Ann Arbor.
EMISSION-LINE GALAXIES TOWARD THE BOOTES VOID Ph.D. Thesis
Joseph Ward Moody 1986 181 p
Avail: Univ. Microfilms Order No. DA8612585

Galaxies with strong emission are potentially useful as probes of the large-scale galaxian distribution. However, to serve as probes their relative frequency and clustering properties must be known. A study of these properties for field galaxies having (OIII)wavelength 5007 emission equivalent widths greater than 10 A and reports on a search for galaxies (OIII)wavelength 5007 in the direction of the Bootes void is presented. The study of field emission-line galaxies was done in two magnitude limited surveys consisting of 341 galaxies from both the north and south galactic caps having previously published red shifts and photometry. A search for emission-line galaxies toward the Bootes void was undertaken using the Burrell Schmidt telescope and and objective prism giving a reciprocal dispersion of 900 A/mm at H beta. A spectral survey was also done of galaxies from an independent, low-dispersion objective prism of the southern portion of the void. A comparison with previous work finds tentative but not conclusive evidence that emission-line galaxies have a higher relative abundance in voids that in the field. Dissert. Abstr.

N87-10808 California Univ., Berkeley.
PHYSICAL PROCESSES IN COLLAPSE DRIVEN SUPERNOVA Ph.D. Thesis
Ronald William Mayle 1985 233 p
Avail: Univ. Microfilms Order No. DA8610131

Supernova are believed to occur when a massive star, unable to continue burning nuclear fuel in its interior, collapses, and subsequently produces a spectacular explosion. The explosive mechanism relies on the fact that the central part of these massive stars evolve into neutron stars. Late time supernovae are examined. The method of neutrino transport being used in a numerical simulation is very important in the study of late time supernovae, as the explosive mechanism depends on neutrino heating of the material behind the shock. Neutrino transport is discussed, and results are presented that indicate flux limited neutrino transport does an adequate job of following neutrino evolution. An approximate method of incorporating convection is described, and some results of including convection in a computer model are presented. Another phenomena seen in computer simulations of supernovae are oscillations in the neutrino luminosity and mass accretion rate onto the proto-neutron star. An attempt is made to understand this oscillation by perturbation of the steady state solution to equations approximating the complex physical processes occurring in the late time supernovae. Dissert. Abstr.

N87-10809 Columbia Univ., New York.
MOLECULAR CLOUDS IN ORION AND MONOCEROS Ph.D. Thesis
Ronald Joseph Maddalena 1986 212 p
Avail: Univ. Microfilms Order No. DA8610791

About one-eighth of a well-sampled 850 square degree region of Orion and Monoceros, extending from the Taurus dark cloud complex to the CMa OB 1 association, shows emission at the frequency of the J =1 0 transition of CO coming from either local clouds (d < 1 kpc) lying as much as 25% from the galactic plane or from more distant objects located within a few degrees of the plane and well outside the solar circle. Cloud masses derived from CO luminosity are as reliable as others determined with more difficulty. Local giant molecular clouds associated with Orion A and B have enhanced temperatures and densities near their western edges possibly due to compression of molecular gas by a high pressure region created by the cumulative effects of approx. 10 supernovae that occurred in the Orion OB association. Another gain molecular cloud found to be associated with Mon R2 may be related to the Orion clouds. Two filamentary clouds (one possible 300 pc long but only 3- 10 pc wide) were found which may represent a new class of object. Magnetic fields probably play a role in confining these filaments. An expanding ring of clouds concentric with the H 11 region S 264 and its ionizing 08 star, Lambda Ori, was also investigated, and a possible evolutionary sequence for the ring is given in detail. The clouds probably constitute fragments of the original cloud from which lambda Ori formed. Dissert. Abstr.

N87-10810 California Univ., Berkeley.
ON THE TIDAL INTERACTION BETWEEN SPHERICAL GALAXIES Ph.D. Thesis
Luis Alberto Aguilar-Chiu 1985 96 p

Avail: Univ. Microfilms Order No. DA8609915

The effects of tidal forces on the internal structure of non-rotating spherical galaxies that undergo a hyperbolic encounter are investigated using the impulse approximation and N-body experiments. The simulations use models with King and de Vaucouleurs surface-density profiles and radial, tangential and isotropic velocity distributions. Dissert. Abstr.

91 LUNAR AND PLANETARY EXPLORATION

Includes planetology; and manned and unmanned flights. For spacecraft design or space stations see *18 Spacecraft Design, Testing and Performance.*

N87-10811*# Atmospheric and Environmental Research, Inc., Cambridge, Mass.

A MODELING ANALYSIS PROGRAM FOR THE JPL TABLE MOUNTAIN Io SODIUM CLOUD DATA Annual Report, 1 Jun. 1986 - 31 May 1986

William H. Smyth and Bruce A. Goldberg (Jet Propulsion Lab., California Inst. of Tech., Pasadena) Aug. 1986 77 p
(Contract NASw-3949)
(NASA-CR-179671; NAS 1.26:179671) Avail: NTIS HC A05/MF A01 CSCL 03B

Progress and achievements in the second year are discussed in three main areas: (1) data quality review of the 1981 Region B/C images; (2) data processing activities; and (3) modeling activities. The data quality review revealed that almost all 1981 Region B/C images are of sufficient quality to be valuable in the analyses of the JPL data set. In the second area, the major milestone reached was the successful development and application of complex image-processing software required to render the original image data suitable for modeling analysis studies. In the third area, the lifetime description of sodium atoms in the planet magnetosphere was improved in the model to include the offset dipole nature of the magnetic field as well as an east-west electric field. These improvements are important in properly representing the basic morphology as well as the east-west asymmetries of the sodium cloud. Author

N87-10812*# Jet Propulsion Lab., California Inst. of Tech., Pasadena.

THE CASE FOR MARS: CONCEPT DEVELOPMENT FOR A MARS RESEARCH STATION

S. M. Welch, ed. and C. R. Stoker, ed. 15 Apr. 1986 139 p
(Contract NAS7-918)
(NASA-CR-179753; JPL-Pub-86-28; NAS 1.26:179753) Avail: NTIS HC A07/MF A01 CSCL 03B

A program to establish a permanent scientific research base on Mars is described. A Mars base as the much needed long-term focus for the space program is presented. A permanent base was chosen rather than the more conventional concept of a series of individual missions to different sites because the permanent base offers much greater scientific return plus greater crew safety and the potential for eventual growth into a settlement. The Mars base will strive for self-sufficiency and autonomy from Earth. Martian resources will be used to provide life support materials and consumables. The Martian atmosphere will provide a convenient source of volatiles: CO2, N2, and water. Rocket propellant (for returning vehicles), fuels, breathable air, and fertilizers will be manufactured from Mars air. Food will be grown on Mars using Martian materials as plant nutrients. A permanent human presence will be maintained on Mars beginning with the first manned landing via a strategy of crew overlap. This permanent presence will ensure safety and reliability of systems through continuous tending, maintenance, and expansion of the base's equipment and systems. A permanent base will allow the development of a substantial facility on Mars for the same cost (in terms of Earth departure mass) as a series of temporary camps. A base equipped with surface rovers, airplanes, and the ability to manufacture consumables and return propellant will allow far more extensive planetary exploration over a given period of years than would approaches featuring a series of short exploration missions such as the Apollo Moon program. Author

N87-10813*# Iowa Univ., Iowa City.

PERIODIC AMPLITUDE VARIATIONS IN JOVIAN CONTINUUM RADIATION Progress Report, Period Ending Feb. 1986

W. S. Kurth, D. A. Gurnett, and F. L. Scarf (TRW Space Technology Labs., Redondo Beach, Calif.) 2 Apr. 1986 31 p Sponsored in part by NASA Prepared in cooperation with JPL
(Contract N00014-82-K-0183)
(NASA-CR-177070; NAS 1.26:177070; AD-A167923; U-of-Iowa-86-17) Avail: NTIS HC A03/MF A01 CSCL 03B

An analysis of periodic variations in the amplitude of continuum radiation trapped in the Jovian magnetosphere shows structure with periods near both five and ten hours. Contrary to a plausible initial idea, the continuum amplitudes are not organized by position of the observer relative to the dense plasma sheet. Instead, there seem to be preferred orientations of system III longitude with respect to the direction to the Sun which account for the peaks. This implies a clock-like modulation of the continuum radiation intensity as opposed to a searchlight effect. The importance of the dipole longitude-solar wind alignment to the amplitude of the continuum radiation implies the source region of the radiation is near the magnetopause and may tie the generation of the radio waves to the clock like modulation of energetic electron fluxes from Jupiter. GRA

N87-10814*# Jet Propulsion Lab., California Inst. of Tech., Pasadena.

PLASMA WAVE OBSERVATIONS AT URANUS FROM VOYAGER 2 Progress Report, period ending Feb. 1986

D. A. Gurnett (Iowa Univ., Iowa City), W. S. Kurth, F. L. Scarf (TRW Space Technology Labs., Redondo Beach, Calif.), and R. L. Poynter 26 Mar. 1986 21 p Sponsored by NASA
(Contract N00014-85-K-0404)
(NASA-CR-177069; NAS 1.26:177069; AD-A167924; U-OF-IOWA-86-16) Avail: NTIS HC A02/MF A01 CSCL 03B

Radio emissions from Uranus were detected by the Voyager 2 plasma wave instrument about 5 days before closest approach at frequencies of 31.1 and 56.2 khz. The bow shock was identified by an abrupt broadband burst of electrostatic turbulence about 10 hours before closest approach at a radial distance of 23.5 ru. Once inside of the magnetosphere strong whistler mode hiss and chorus emissions were observed at radial distances less than about 8 R sub u, in the same region where the energetic particle instruments detected intense fluxes of energetic electrons. A variety of other plasma waves, such as (f sub c) electron cyclotron waves, were also observed in this same region. At the ring plane crossing the plasma wave instrument detected a large number of impulsive events that are interpreted as impacts of micron sized dust particles on the spacecraft. The maximum impact rate was about 20 to 30 impacts/sec, and the north-south thickness of the impact region was about 4,000 km. This paper presents an overview of the principal results from the plasma wave instrument, starting with the first detection of radio emissions from Uranus, and ending a few days after closest approach. GRA

N87-10815 Michigan Univ., Ann Arbor.

CLOUDS AND METHANE PHOTOCHEMICAL HAZES ON THE OUTER PLANETS Ph.D. Thesis

Paul Nichols Romani 1986 208 p
Avail: Univ. Microfilms Order No. DA8612612

A numerical model which uses thermodynamic and hydrostatic equilibrium was developed to study the cloud structure of the outer planets: Jupiter, Saturn, Uranus, and Neptune. The model calculates cloud locations, cloud densities, the mixing ratio profiles of the condensates, and the thermal structure from the appropriate wet/dry adiabatic lapse rate. The effects of ortho-to-para H2 conversion (latent heat release and change in heat capacity of H2) are also considered. The outer planets are predicted to have a multilayered cloud structure consisting of one or more of the following clouds: NH3-H2O solution; H2O-ice; NH3-ice; NH4SH-solid; H2S-ice; or CH4-ice. Model predictions are compared to relevant observations. Dissert. Abstr.

92 SOLAR PHYSICS

Includes solar activity, solar flares, solar radiation and sunspots.

For related information see *93 Space Radiation.*

N87-10816*# Alaska Univ., Fairbanks.

A STUDY OF DISTURBED SOLAR WIND AND MAGNETOTAIL BASED ON ISEE-3 DATA Semiannual Status Report, 1 Jan. - 31 Jul. 1986

S.-I. Akasofu 1986 45 p

(Grant NAG5-571)

(NASA-CR-177060; NAS 1.26:177060) Avail: NTIS HC A03/MF A01 CSCL 03B

Images of auroral emissions observed with the Dynamics Explorer 1 are used to calculate ionospheric conductivities over the polar region. The combination of ground-based magnetometer data and the inferred conductivities enable the estimation on a global scale of the distributions of ionospheric electric fields and currents and field-aligned currents, as well as, the Joule heating production rate, with a time resolution of 12 min. Although the inference of the conductivity distribution requires further improvements, the following conclusions may be drawn: The westward electrojet is, in general, collocated with the region of high auroral luminoisty, while the region of relatively low luminosity in the evening section is collocated with the eastward electrojet. The upward field-aligned currents exist in the brightest auroral region on the poleward side of the evening auroral oval and on the equatorward side of the morning oval. A significant amount of ionospheric currents can flow in regions where there are no bright auroral emissions. The distribution of calculated field-aligned currents displays many localized structures which characterize the development of the substorm current system. Author

N87-10817# Midwest Research Inst., Golden, Colo. Solar Energy Research Inst.

WORKSHOP ON THE PHYSICS AND CHEMISTRY OF SOLAR-FLUX EFFECTS ON CONDENSED PHASE/GAS INTERFACES

G. E. Gross and H. Harris May 1986 36 p Workshop held in Golden, Colo., 30 Jul. 1985

(Contract DE-AC02-83CH-10093)

(DE86-004460; SERI/CP-255-2908; CONF-8507124-Summs) Avail: NTIS HC A03/MF A01

Notes transcribed from a workshop on effects of high intensity visible radiation (high solar flux) on materials are presented with comments by the workshop chairman and participants. Discussions presented include laser damage, photochemical effects, crystal defects, high temperature effects, and testing of materials in large solar concentrators. Contrasts are observed between highly concentrated solar radiation and equivalent power levels of coherent radiation from monochromatic lasers. The discussions suggest a lack of nonlinear or multiphoton optical effects to be expected from solar radiation even at the theoretical maximum of concentration (some 60,000 times normal sun light). DOE

N87-10818 Alaska Univ., Fairbanks.

THREE-DIMENSIONAL STRUCTURE OF THE HELIOSPHERE: QUIET-TIME AND DISTURBED PERIODS Ph.D. Thesis

Craig Daniel Fry 1985 371 p

Avail: Univ. Microfilms Order No. DA8612261

An improved kinematic method is used to perform simulation studies of temporal and spatial variations of solar wind speed and interplanetary magnetic field during periods when the sun is quiet and when it is active. The procedure of Hakamada and Akasofu (1982) is imporved and calibrated with a one-dimensional magnetohydrodynamic solution of solar wind flow. The solar-cycle evolution of solar wind velocity is studied using the data sets of King (1979,1983) and Hoeksema (1982,1983) for the period 1976 to 1982. The background solar wind velocity and magnetic field are simulated and compared to observations near the Earth. Three-dimensional representations ofthe heliospheric current sheet (HCS) are displayed out to 5 AU for idealized dipole and quadrupole cases, and for observed source field configurations. The propagation of solar wind disturbances in the solar equatorial plane to 30 Au is simulated. Two major disturbance event periods are simulated, and it is seen how a series of solar flares can greatly disrupt both the inner and outer heliosphere. Visual representations of the distorted HCS due to a series of hypothetical solar flares are presented. Dissert. Abstr.

N87-10479*# Illinois Univ., Urbana. Dept. of Electrical and Computer Engineering.

AN ANALYSIS AT MESOSPHERIC COHERENT-SCATTER POWER ENHANCEMENTS DURING SOLAR FLARE EVENTS

J. Parker and S. A. Bowhill *In* International Council of Scientific Unions, Middle Atmosphere Program. Handbook for MAP, Vol. 20 Jun. 1986 7 p (For primary document see N87-10419 01-42)

Avail: NTIS HC A22/MF A01; also available from SCOSTEP Secretariat, Illinois Univ., 1406 West Green Street, Urbana, Ill. 61801 CSCL 03B

93 SPACE RADIATION

Includes cosmic radiation; and inner and outer earth's radiation belts.

For biological effects of radiation see *52 Aerospace Medicine.* For theory see *73 Nuclear and High-Energy Physics.*

N87-10819# Aerospace Corp., El Segundo, Calif. Electronics Research Lab.

AMPLITUDE DISTRIBUTION OF COSMIC RAY EVENTS IN EXTRINSIC IR DETECTORS

L. Aukerman 15 Mar. 1986 23 p

(Contract F04701-85-C-0086)

(AD-A167692; TR-0086(6427-01)-1; SD-TR-86-17) Avail: NTIS HC A02/MF A01 CSCL 17/5

A method of calculating the amplitude distribution of cosmic ray events in IR detectors utilizing known range energy relationships for the various cosmic particles (mostly protons and helium nuclei) and published cosmic ray energy spectra is described. Good agreement is obtained between the calculated amplitude distribution and the spurious events observed in an extrinsic detector during a flight test. GRA

N87-10820# Los Alamos National Lab., N. Mex.

INTENSE SOFT X-RAYS FROM RS OPHIUCHI DURING THE 1985 OUTBURST

K. O. Mason, F. A. Cordova, M. F. Bode, and P. Barr 1985 11 p Presented at the Conference on RS Ophiuchi and the Recurrent Nova Phenomenon, Manchester, England, 1 Dec. 1985 Prepared in cooperation with Mullard Space Science Lab., Dorking, England, Preston Polytechnic, England European Space Agency European Space Operations Centre, Darmstadt, West Germany

(Contract W-7405-eng-36)

(DE86-010175; LA-UR-86-1216; CONF-851272-2) Avail: NTIS HC A02/MF A01

Intense soft X ray emission with a characteristic temperature of a few million degrees has been detected from the recurrent nova RS Oph approximately two months after its January 1985 optical outburst. This is the first detection of X rays from such a system at outburst. The X radiation is interpreted as emission from circumstellar gas that is shock heated by the passage of the blast wave from the nova explosion. The rapid decline of the X ray flux between about 60 and 90 days after the outburst probably occurs because the blast wave has reached the edge of the volume filled, between outbursts, by the stellar wind of the red giant component of the binary system. Residual X ray emission detected from RS Oph 250 days after the outburst is interpreted as coming from the surface of a white dwarf, at a temperature of approx 300,000K, where thermonuclear burning is persisting. DOE

N87-10821# Los Alamos National Lab., N. Mex.

NUCLIDE PRODUCTION BY PRIMARY COSMIC-RAY PROTONS

R. C. Reedy 1986 18 p Presented at the Lunar and Planetary Science Conference, Houston, Tex., 17 Mar. 1986
(Contract W-7405-eng-36)
(DE86-011268; LA-UR-86-1524; CONF-860375-2) Avail: NTIS HC A02/MF A01

The production rates of cosmogenic nuclides in the solar system and in interstellar space were calculated for the primary protons in the galactic and solar cosmic rays. At 1 AU, the long-term average fluxes of solar protons usually produce many more atoms of a cosmogenic nuclide than the primary protons in the galactic cosmic rays (GCR), the exceptions being nuclides made only by high-energy reactions (like ^{10}Be). Because the particle fluxes inside meteorites and other large objects in space include many secondary neutrons, the production rates are much higher. The production rates of cosmogenic nuclides are calculated to vary by about factors of 2.5 during at typical 11-year solar cycle, in agreement with measurements of short-lived radionuclides in recently fallen meteorites. The production of cosmogenic nuclides by the GCR particles outside the heliosphere is higher than that by the modulated GCR primaries normally in the solar system. However, there is considerable uncertainty in the fluxes of interstellar protons and, therefore, in the production rates of cosmogenic nuclides in interstellar space. Production rates and ratios for cosmogenic nuclides would be able to identify particles that were small in space or that were exposed to an unmodulated spectrum of GCR particles. DOE

N87-10822# Department of Energy, New York. Environmental Measurements Lab.

COSMIC-RAY HADRONS UNDERGROUND

K. OBrien Dec. 1985 20 p
(DE86-011334; EML-447) Avail: NTIS HC A02/MF A01

Hadron fluxes and star densities in volcanic material have been calculated down to a depth of 6000 g/cm to supply a data base for use in calculating cosmogenic isotopes production. It is hoped to be able to use these isotopes to determine the age of the volcanic material. Some curves of star density with depth and of hadron spectra for various depths in basalt are presented. DOE

N87-10823# Los Alamos National Lab., N. Mex.

INTERPRETATION OF EXTRAGALACTIC JETS

M. L. Norman 1985 16 p Presented at the International Astronomical Union (IAU) Colloquium, Copenhagen, Denmark, 11 Jun. 1985
(Contract W-7405-eng-36)
(DE86-011211; LA-UR-86-1705; CONF-8506205-4) Avail: NTIS HC A02/MF A01

The nature of extragalatic radio jets is modeled. The basic hypothesis of these models is that extragalatic jets are outflows of matter which can be described within the framework of fluid dynamics and that the outflows are essentially continuous. The discussion is limited to the interpretation of large-scale (i.e., kiloparsec-scale) jets. The central problem is to infer the physical parameters of the jets from observed distributions of total and polarized intensity and angle of polarization as a function of frequency. DOE

N87-10824 California Inst. of Tech., Pasadena.

INVESTIGATIONS OF RADIO JETS IN M87, 3C273 AND 3C345 Ph.D. Thesis

John Anthony Biretta 1986 155 p
Avail: Univ. Microfilms Order No. DA8605393

Observational studies of extra-galactic radio jets in M87,3C273, and 3C345 are presented. Observations of the M87 jet were made at 15 GHz with 0.12' resolution. All of the knots are clearly resolved both along and across the jet. Most of the knots are found to be smooth in appearance with no evidence of shocklike discontinuities. The brightest knot and the innermost knot are exceptions to this. The brightest knot (knot A) seems consistent with a shock caused by unsteady flow in the jet. Models for this feature are discussed. Combining our data with X-ray data suggests that the jet is neither freely expanding, thermally confined, nor ram pressure confined. The jet may, however, be magnetically confined. Observations of 3C273 at 10.7 GHz VLBI with high northsouth resolution are presented. A strong, non-monotonic curvature is found in the jet at projected radii less than or equal to 5 pc. It is unlikely that this curvature can be caused by precession. Measurements of the core size show that bulk relativistic motion in the core is not required for consistency with the observed X-ray flux. Dissert. Abstr.

N87-10825 Texas Univ., Austin.

GAUGE INVARIANT PERTURBATION THEORY PREDICTION OF THE SENSITIVITY REQUIRED FOR EXPERIMENTAL MEASUREMENT OF QUADRUPOLE AND HIGHER MOMENTS OF THE COSMIC MICROWAVE BACKGROUND RADIATION Ph.D. Thesis

Kenneth Earl Wilson 1985 429 p
Avail: Univ. Microfilms Order No. DA8609611

The temperature variation of the cosmic microwave background radiation is computed in a spherical harmonic expansion for a 4 million term sum of perturbations. Each term has a different direction and a randomly chosen path. The computation was performed by starting with the model for gauge invariant cosmological perturbations. This model does linear perturbatin theory against a background Friedmann-Robertson-Walker general relativistic cosmological model. The Bardeen model was recomputed for a cosmological-time metric, then solved for zero curvature and zero cosmological constant in the background for radiation and dust equations of state. The model was solved for zero curvature, cosmological constant, and pressure in perturbation order. These solution were used to compute the redshift equation, and then the temperature variation equation. Analytical equations are obtained for the temperature variation caused by an isothermal or adiabatic perturbatin of a single mode (amplitude, wavelength, phase, and direction). A Fourier series is formulated with short wavelength cutoff set by acoustic damping, and long wavelength cuttoff set by the perturbation assumption. The temperature variation was predicted for ten cases: adiabatic and isothermal perturbations with power law exponents of 0 through 4. Dissert. Abstr.

N87-10826 Iowa Univ., Iowa City.

A STUDY OF THE GROUND STATE HYDROXYL MASER EMISSIONS ASSOCIATED WITH ELEVEN REGIONS OF STAR FORMATION Ph.D. Thesis

Ralph A. Gaume, Jr. 1985 186 p
Avail: Univ. Microfilms Order No. DA8611089

Arcsecond resolution maps were obtained for the ground state hydroxyl maser and 15 GHz continuum emissions associated with eleven regions of star formation. Within these regions over 30 individual sites of maser emission were identified. Main line transitions occurred most frequently and were usually the strongest features. It was found that 20% of the maser clusters do not appear closely associated with 15 Ghz continuum sources. The data does not support the idea that hydroxyl masers are uniformly distributed in a thin or thick shell surrounding a central star, or that continuum background photons play a significant part in determining the output intensities of hydroxyl masers. Five of the continuum sources appear to be the cometary class of H II regions, whose structure suggest relative motion between the region and surrounding neutral material. In four of the five regions it is found that the strongest hydroxyl maser emission are projected onto the upstream leading edge of the ionized hydrogen regions, suggesting that the masers form in the interaction region between the neutral material and H II complex. The maser emission in four of the five regions exhibit velocity structure, indicating existence of ordered velocity fields. Dissert. Abstr.

99 GENERAL

N87-10827*# National Aeronautics and Space Administration, Washington, D.C.

AERONAUTICS AND SPACE REPORT OF THE PRESIDENT

1985 148 p

(NASA-TM-89239; NAS 1.15:89239; GPO-495-812) Avail: NTIS HC A07/MF A01 CSCL 05B

The achievements and activities of the United States aeronautics and space programs for 1985 are examined. The activities are listed by the sponsoring government agency. B.G.

SUBJECT INDEX

SCIENTIFIC AND TECHNICAL AEROSPACE REPORTS VOLUME 25 NUMBER 1

Typical Subject Index Listing

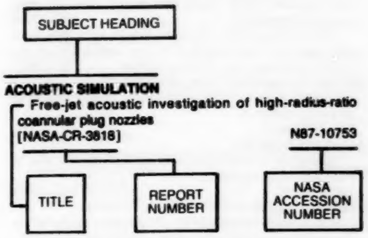

The subject heading is the key to the subject content of the document. Titles, report numbers, and accession numbers of pertinent documents are provided under each subject heading. When the title is insufficiently descriptive of the document content, a title extension has been added, separated from the title by three hyphens. The report number helps to indicate the type of document cited (e.g., NASA report, NASA translation, NASA contractor report). The NASA accession number is the number by which the document abstracts are arranged in this journal and by which the document is sold or requested. The titles, with title extensions if present, are arranged under each subject heading in ascending accession number order. The subject headings have been selected from the latest revision of the *NASA Thesaurus* (NASA SP-7053).

A

A-310 AIRCRAFT
A-310 Aircraft Integrated Data SystemS (AIDS) design philosophy N87-10076
The Airborne Integrated Data System (AIDS) for the Airbus A-310 engine condition monitoring N87-10082
Lufthansa's Aircraft Integrated Data Systems (AIDS) based A-310 engine condition monitoring system: Progress achieved between the 12th and 13th AIDS Symposiums N87-10084
Comparative evaluation of redundant flight data recorded by a digital aircraft integrated data system recorder (DAR) on board an Airbus A-310 aircraft N87-10098
A-320 AIRCRAFT
Modern Aircraft Integrated Data Systems (AIDS) technology exemplified on the A-320 N87-10078
ABSORBERS (MATERIALS)
Analysis of heat-pipe absorbers in evacuated-tube solar collectors
[DE86-010764] N87-10252
ABSORPTION COOLING
Analysis of heat-pipe absorbers in evacuated-tube solar collectors
[DE86-010764] N87-10252
ABSORPTION SPECTRA
On the measurement of atmospheric density using dial in the O2 A-band (770 nm) N87-10291
Real-time atmospheric absorption spectra for in-flight tuning of an airborne dial system N87-10296
Strength, width, and pressure shift measurements of 54 lines in the oxygen A-band N87-10298
Multifrequency dial sensing of the atmospheric gaseous constituents using the first and second harmonics of a tunable CO2 laser radiation N87-10302
Detection of NO sub x,C2H4 concentrations by using CO and CO2 lasers N87-10357
Laser heterodyne system for obtaining height profiles of minor species in the atmosphere N87-10359
Spectroscopic aspects of differential method for sounding gas composition of the atmosphere N87-10369
The GSFC gound-based lidar for the measurement of stratospheric ozone N87-10371
Linewidth characteristics of Raman-shifted dye laser output at 720 and 940 nm N87-10372
The ultraviolet spectra of DA white dwarfs N87-10783
High resolution spectroscopy of quasar absorption lines N87-10785
Gas and dust in regions of recent star formation N87-10800
ABSORPTION SPECTROSCOPY
Differential optical absorption techniques for diagnostics of fossil fuel combustion
[DE86-010084] N87-10190
ABUNDANCE
High resolution CCD spectra of stars in globular clusters. Part 2: Metals and CNO in M71
[NASA-CR-179853] N87-10789
Infrared emission lines from planetary nebulae N87-10791
Emission-line galaxies toward the Bootes void N87-10807
ACCELERATED LIFE TESTS
Experimental procedure for lifetime testing of graphite bundles under constant load
[AD-A167714] N87-10186
ACCELERATION (PHYSICS)
Energy delivery processes in shock tubes N87-10106
ACCELERATION TOLERANCE
The interest of centrifuge tests for the selection of French cosmonauts N87-10678
ACCESS CONTROL
Proceedings of the 5th Annual Users' Conference
[NASA-CP-2399] N87-10720
ACCRETION DISKS
On the stability of accretion disks around black holes N87-10805
ACOUSTIC ATTENUATION
Investigation into the attenuation and velocity of acoustic emissions in carbon fiber composite aircraft structures
[BAE-KGT-R-GEN-01349] N87-10180
ACOUSTIC EMISSION
Acoustic waves emitted by vortex-body interaction N87-10015
Investigation into the attenuation and velocity of acoustic emissions in carbon fiber composite aircraft structures
[BAE-KGT-R-GEN-01349] N87-10180
ACOUSTIC PROPAGATION
Fundamental investigations of the finite element solutions for acoustic propagation in ducts
[NASA-CR-179845] N87-10751
ACOUSTIC PROPERTIES
The Helmholtz resonance behavior of single and multiple rooms
[NASA-CR-178173] N87-10749
ACOUSTIC SIMULATION
Free-jet acoustic investigation of high-radius-ratio coannular plug nozzles
[NASA-CR-3818] N87-10753
ACOUSTIC SOUNDING
Remote temperature profiling in the troposphere and stratosphere by the radio-acoustic sounding technique N87-10488
ACOUSTIC VELOCITY
Investigation into the attenuation and velocity of acoustic emissions in carbon fiber composite aircraft structures
[BAE-KGT-R-GEN-01349] N87-10180
ACRYLIC RESINS
Pressure-resistant plane disc viewports from allyl diglycol carbonate plastic for hyperbaric chambers
[AD-A168007] N87-10105
Chemisorption mechanism and effect of polyacrylic acid on the improvement in bond durability of zinc phosphate-to-polymer adhesive joints
[DE86-011535] N87-10213
ADAPTATION
Preliminary results on the equilibrium and vertigo experiment performed during STS 51-G shuttle flight N87-10692
The state of bones of pregnant rats during an acute stage of adaptation to weightlessness N87-10708
Math modelling as a complement to the scientific inquiry of physiological adaptation to space flight: Fluid, endocrine and circulatory regulation N87-10709
ADAPTIVE CONTROL
Adaptive finite element methods — error estimates N87-10740
ADHESION
Chemisorption mechanism and effect of polyacrylic acid on the improvement in bond durability of zinc phosphate-to-polymer adhesive joints
[DE86-011535] N87-10213
ADHESIVE BONDING
Mode 1 delamination growth in adhesively bonded joints under static and fatigue loads
[NASA-CR-179812] N87-10409
ADHESIVES
The fungal resistance or susceptibility of resins, plasticizers, and other constituents of adhesive formulations
[AD-A166930] N87-10207
Chemisorption mechanism and effect of polyacrylic acid on the improvement in bond durability of zinc phosphate-to-polymer adhesive joints
[DE86-011535] N87-10213
ADIABATIC CONDITIONS
Further results on the initiation and growth of adiabatic shear bands
[AD-A168012] N87-10412
ADSORPTION
Absorption heat pump simulation and studies: a modular computer simulation of absorption systems
[DE86-011206] N87-10256
ADVECTION
Advective influences on steady and transient forced tropical motions N87-10670
AEROACOUSTICS
Prediction of helicopter rotor discrete frequency noise: A computer program incorporating realistic blade motions and advanced acoustic formulation
[NASA-TM-87721] N87-10750
AEROASSIST
Shuttle derived atmospheric density model. Part 1: Comparisons of the various ambient atmospheric source data with derived parameters from the first twelve STS entry flights, a data package for AOTV atmospheric development
[NASA-CR-171824] N87-10662
Shuttle derived atmospheric density model. Part 2: STS atmospheric implications for AOTV trajectory analysis, a proposed GRAM perturbation density model
[NASA-CR-171824] N87-10663
AERODYNAMIC CHARACTERISTICS
Prediction of gust loadings and alleviation at transonic speeds
[AD-A167748] N87-10047
Engine-airframe integration considerations for preliminary air vehicle performance analysis N87-10068
AERODYNAMIC COEFFICIENTS
Effects of flap position on longitudinal parameters of HFB-320
[NAL-TM-SE-8602] N87-10062
AERODYNAMIC DRAG
Wind tunnel test of the modified goldschmied model with propulsion and empennage: Analysis of test results
[AD-A167360] N87-10045
AERODYNAMIC INTERFERENCE
Tunnel interference from pressure measurements on control surfaces
[AE-TM-8-83] N87-10104
AERODYNAMIC LOADS
Aeroelastic stability of composite rotor blades in hover N87-10060
Effect of static inplane loads and boundary conditions on the flutter of flat rectangular panels
[NAL-TM-ST-8604] N87-10404

AERODYNAMIC NOISE
Effect of static inplane loads and boundary conditions on the flutter of flat rectangular panels [NAL-TM-ST-8604] N87-10404
AERODYNAMIC STABILITY
Acta Aeronautica et Astronautica Sinica (selected articles) [AD-A167918] N87-10004
Wind tunnel test of the modified goldschmied model with propulsion and empennage: Analysis of test results [AD-A167360] N87-10045
AERODYNAMIC STALLING
Application of bifurcation and catastrophe theories to near stall flight mechanics [AD-A167697] N87-10046
AEROELASTIC RESEARCH WINGS
In-flight total forces, moments and static aeroelastic characteristics of an oblique-wing research airplane [NASA-TP-2224] N87-10103
AEROELASTICITY
Aeroelastic stability of composite rotor blades in hover N87-10060
Design and fabrication of the NASA decoupler pylon for the F-16 aircraft [NASA-CR-172354] N87-10065
Effect of static inplane loads and boundary conditions on the flutter of flat rectangular panels [NAL-TM-ST-8604] N87-10404
AEROSOLS
Coherent lidar technology for global wind profiling N87-10267
Development of a high-altitude airborne dial system: The Lidar Atmospheric Sensing Experiment (LASE) N87-10268
The Lidar In-Space Technology Experiment (LITE) N87-10270
Aerosol studies in mid-latitude coastal environments in Australia N87-10271
Wavelength dependence of aerosol backscatter coefficients obtained by multiple wavelength Lidar measurements N87-10275
Extinction and visibility measurements in the lower atmosphere with UV-YAG-lidar N87-10276
Visibility and aerosol measurement by diode-laser random-modulation CW lidar N87-10279
Flight tests of a range-resolved airborne dial with two min-tea CO2 lasers N87-10284
Using a laser aureole to invert lidar return N87-10292
Methods for estimating the optical constants of atmospheric hazes based on complex optical measurements N87-10301
Remote express analysis of ground-layer aerosol based on laser-induced spark spectra N87-10303
Laser sounding of instantaneous and mean speed of wind using correlation method N87-10304
Optimal filtration of the atmospheric parameters profiles N87-10305
Improved solution of the lidar equation utilizing particle counter measurements N87-10310
Features of stratospheric aerosol lidar observations at Mauna Loa, 1974 - 1985 N87-10312
El Chichon aerosols in the stratosphere: Analyses of lidar data and calculations of radiation budget N87-10313
Lidar measurement of stratospheric aerosol at Syowa Station, Antarctica N87-10314
The application of lidar to stratospheric aerosol studies N87-10337
Volcanic eruptions and the increases in the stratospheric aerosol content: Lidar measurements from 1982 to 1986 N87-10338
Observations of stratospheric aerosols associated with the El Chichon eruption N87-10339
Lidar observations of the decline of the El Chichon stratospheric load N87-10340
Lidar stratospheric ozone measurements at the observatoire de Haute Provence (France) N87-10344
Wavelength dependence of coherent and incoherent satellite-based lidar measurements of wind velocity and aerosol backscatter N87-10361
Chemical contamination remote sensing N87-10375
Scattered radiation field of a laser beam propagating through turbid media [DE86-010188] N87-10386
Atmospheric Ozone 1985. Assessment of our understanding of the processes controlling its present distribution and change, volume 1 [NASA-TM-89237] N87-10612
Tropospheric trace gases N87-10614
Tropospheric chemistry N87-10615
AEROSPACE ENVIRONMENTS
Vertical junction solar cells [AD-A167757] N87-10532
Space Environment Laboratory, FY 1985 [PB86-218567] N87-10621
AEROSPACE MEDICINE
Aerospace medicine and biology: A continuing bibliography with indexes (supplement 287) [NASA-SP-7011(287)] N87-10001
Aerospace medicine and biology: A continuing bibliography with indexes [NASA-SP-7011(289)] N87-10674
Space motion sickness N87-10693
AEROSPACE SYSTEMS
Air Force technical objective document fiscal year 1987 [AD-A167324] N87-10779
AFRICA
Some aspects of the urban climates of tropical Africa N87-10642
AGRICULTURE
The assessment of climatological impacts on agricultural production and residential energy demand N87-10666
AIR
Diffusion approximation for modeling of 3-D radiation distributions [DE86-000810] N87-10228
Simple blast model for structural design [DE86-000802] N87-10414
AIR DATA SYSTEMS
Proceedings of the 13th Symposium on Aircraft Integrated Data Systems [DFVLR-MITT-86-04] N87-10075
A-310 Aircraft Integrated Data SystemS (AIDS) design philosophy N87-10076
Aircraft Integrated Data Systems (AIDS): Evolution and revolution N87-10077
Modern Aircraft Integrated Data Systems (AIDS) technology exemplified on the A-320 N87-10078
Experience with the Onboard Checkout And Monitoring System (OCAMS) of a military aircraft resulting improvements and the consequence for future design N87-10079
Integrated monitoring systems for tactical aircraft N87-10080
The Airborne Integrated Data System (AIDS) for the Airbus A-310 engine condition monitoring N87-10082
Choosing Aircraft Integrated Data Systems (AIDS) architecture suitable for Engine Health Monitoring (EHM) on future generation engines N87-10083
Lufthansa's Aircraft Integrated Data Systems (AIDS) based A-310 engine condition monitoring system: Progress achieved between the 12th and 13th AIDS Symposiums N87-10084
Data recovery techniques, an update — flight data N87-10089
The air/ground transfer of aircraft integrated data systems (AIDS) for Air Traffic Control (ATC) purposes: Present experiments and possible future intentions N87-10091
Airline data acquisition in an ACARS environment N87-10092
Comparative evaluation of redundant flight data recorded by a digital aircraft integrated data system recorder (DAR) on board an Airbus A-310 aircraft N87-10098
AIR LAW
Flight recorders: New US regulations and new International Civil Aviation Organization (ICAO) standards N87-10093
AIR POLLUTION
Lidar mapping of a mixture of aerosol concentrations in a varying atmosphere N87-10320
Three atmospheric dispersion experiments involving oil fog plumes measured by lidar N87-10321
Wide-area remote-sensing system of pollution and gas dispersal by near-infrared absorption based on low-loss optical fiber network N87-10354
A mobile system for active otpical pollution monitoring N87-10355
MAPM: A coherent dual CO2 laser DIAL system N87-10358
Laser heterodyne system for obtaining height profiles of minor species in the atmosphere N87-10359
AIR QUALITY
Variation of the urban NO2 concentration during a ground inversion situation N87-10318
Development of worst case meteorology criteria [PB86-215993] N87-10540
Air quality in tropical cities N87-10639
AIR TRAFFIC CONTROL
Helicopter MLS Flight Inspection Project [DOT/FAA/CT-86/14] N87-10002
The air/ground transfer of aircraft integrated data systems (AIDS) for Air Traffic Control (ATC) purposes: Present experiments and possible future intentions N87-10091
AIRBORNE EQUIPMENT
Strategic Defense Initiative Program: Status of airborne optical adjunct and terminal imaging radar [P86-221132] N87-10107
Aerosol studies in mid-latitude coastal environments in Australia N87-10271
AIRBORNE LASERS
Airborne lidar observations of Arctic polar stratospheric clouds N87-10341
The NCAR Airborne Infrared Lidar System (NAILS) N87-10362
AIRCRAFT ACCIDENT INVESTIGATION
Aircraft accident reports: Brief format US civil and foreign aviation, issue number 2 of 1985 accidents [PB86-916916] N87-10056
The Boeing B 720 aircraft Controlled Impact Demonstration (CID): Flight data recorder/cockpit voice recorder experiment N87-10096
United States Navy - Canadian Forces solid state flight data recorder/crash position locator experiment on the B-720 controlled impact demonstration N87-10097
AIRCRAFT CONSTRUCTION MATERIALS
Polymer systems for rapid sealing of aircraft structures at low temperature [AD-A167667] N87-10209
AIRCRAFT CONTROL
Application of bifurcation and catastrophe theories to near stall flight mechanics [AD-A167697] N87-10046
AIRCRAFT DESIGN
Spin-tunnel investigation of a 1/25-scale model of the General Dynamics F-16XL airplane [NASA-TM-85660] N87-10041
Engine-Airframe Integration for Rotorcraft [AGARD-LS-148] N87-10067
Engine-transmission-structural airframe members compatibility N87-10069
Response of a small-turboshaft-engine compression system to inlet temperature distortion [NASA-TM-83765] N87-10100
In-flight total forces, moments and static aeroelastic characteristics of an oblique-wing research airplane [NASA-TP-2224] N87-10103
AIRCRAFT ENGINES
Engine-Airframe Integration for Rotorcraft [AGARD-LS-148] N87-10067
Engine-airframe integration considerations for preliminary air vehicle performance analysis N87-10068
Engine-airframe integration for rotorcraft: Component specifications and qualification N87-10071
Influence of engine variables on future helicopter systems N87-10072
Helicopter air intake protection systems N87-10073
Engine-airframe integration for rotorcraft: System specifications and qualification N87-10074
Choosing Aircraft Integrated Data Systems (AIDS) architecture suitable for Engine Health Monitoring (EHM) on future generation engines N87-10083
AIRCRAFT EQUIPMENT
Air Force technical objective document fiscal year 1987 [AD-A167324] N87-10779
AIRCRAFT HAZARDS
Doppler Radar Detection of Wind Shear [NASA-CP-2435] N87-10054
Vulnerability methodology and protective measures for aircraft fire and explosion hazards. Volume 3: On-Board Inert Gas Generator System (OBIGGS) studies. Part 1: OBIGGS ground performance tests [AD-A167357] N87-10066
Surface measurements of gust fronts and microbursts during the JAWS (Joint Airport Weather Studies) Project: Statistical results and implications for wind shear detection, prediction and modeling [PB86-200847] N87-10665
AIRCRAFT MAINTENANCE
Polymer systems for rapid sealing of aircraft structures at low temperature [AD-A167667] N87-10209
AIRCRAFT MANEUVERS
Toward comparing experiment and theory for corroborative research on hingeless rotor stability in forward flight (an experimental and analytical investigation of isolated rotor-flap-lag stability in forward flight) [NASA-CR-179711] N87-10063
AIRCRAFT NOISE
Prediction of helicopter rotor discrete frequency noise: A computer program incorporating realistic blade motions and advanced acoustic formulation [NASA-TM-87721] N87-10750
AIRCRAFT RELIABILITY
Summary of artificial and natural icing tests conducted on US Army aircraft from 1974 to 1985 [FAA/CT-85/26] N87-10064
AIRCRAFT SAFETY
Summary of artificial and natural icing tests conducted on US Army aircraft from 1974 to 1985 [FAA/CT-85/26] N87-10064

Vulnerability methodology and protective measures for aircraft fire and explosion hazards. Volume 3: On-Board Inert Gas Generator System (OBIGGS) studies. Part 1: OBIGGS ground performance tests [AD-A167357] N87-10066
NASA and FAA launch wind shear research project [NASA-NEWS-REL-86-143] N87-10659
Surface measurements of gust fronts and microbursts during the JAWS (Joint Airport Weather Studies) Project: Statistical results and implications for wind shear detection, prediction and modeling [PB86-200847] N87-10665

AIRCRAFT STABILITY
Application of bifurcation and catastrophe theories to near stall flight mechanics [AD-A167697] N87-10046

AIRCRAFT STRUCTURES
Polymer systems for rapid sealing of aircraft structures at low temperature [AD-A167667] N87-10209

AIRCRAFT WAKES
Experimental and theoretical Doppler-lidar signatures of aircraft wake vortices N87-10330

AIRFOIL PROFILES
Development of a turbomachinery design optimization procedure using a multiple-parameter nonlinear perturbation method [NASA-CR-3831] N87-10003
Vortex shedding of a square cylinder in front of a slender airfoil at high Reynolds numbers. Part 1: Spacing effect [MPIS-23/1985] N87-10048

AIRFOILS
The effect of free stream disturbances and control surface deflections on the performance of the Wortmann airfoil at low Reynolds numbers N87-10007
Analysis of two-dimensional incompressible flow past airfoils using unsteady Navier-Stokes equations [NASA-CR-179823] N87-10040
Prediction of gust loadings and alleviation at transonic speeds [AD-A167748] N87-10047
Experimental and theoretical investigations of the flow field of an airfoil with a deflected spoiler N87-10050
Unsteady flow over an airfoil inside a wind tunnel with and without transpiration N87-10051
Experimental study of the boundary layer on a low Reynolds number airfoil in steady and unsteady flow N87-10052
Adaptation of TSFOIL for Univac 1100/60H computer at NAL, Bangalore [AE-TB-9-83] N87-10718

AIRFRAMES
Engine-Airframe Integration for Rotorcraft [AGARD-LS-148] N87-10067
Engine-airframe integration for rotorcraft: Component specifications and qualification N87-10071
Influence of engine variables on future helicopter systems N87-10072
Engine-airframe integration for rotorcraft: System specifications and qualification N87-10074

AIRGLOW
Some results of scanner spectrophotometric measurements of aurora and airglow from IK-Bulgaria-1300 satellite and prospects of similar measurements N87-10593

AIRLINE OPERATIONS
The impact of flight data on an airline: A case study N87-10088
Airline data acquisition in an ACARS environment N87-10092

AIRPORTS
Surface measurements of gust fronts and microbursts during the JAWS (Joint Airport Weather Studies) Project: Statistical results and implications for wind shear detection, prediction and modeling [PB86-200847] N87-10665

ALCOHOLS
Cold-start tests with speed diesel engines using alcohol as main fuel [DE86-751651] N87-10392

ALDOSTERONE
Volume regulating hormones during a 5-hour head-down tilt at -10 deg. Part 2: Plasma renin activity and aldosterone N87-10703

ALGEBRA
Novel parallel architectures and algorithms for linear algebra processing [NASA-CR-179826] N87-10743

ALGORITHMS
The third order compact schemes for fluid dynamic problems N87-10032
Preliminary orbit determination by static multivariate search N87-10127
An algorithm for the detection of signals by colour contrast on the screen of a colour cathode ray tube (colour display) — radarscopes [DRIC-T-7655] N87-10233
The usefulness of Klett's inversion algorithms to simulated satellite Lidar returns N87-10274
Lidar measurements of slant visual range N87-10278
Atmospheric contributions to the column variance in direct-detection dial N87-10289
Mesospheric wind measurements using a medium-frequency imaging Doppler interferometer N87-10476
The Tukey algorithm for enhancing MST radar data N87-10521
Database algorithms for multiprocessor and very large memory systems [DE86-009406] N87-10724
Novel parallel architectures and algorithms for linear algebra processing [NASA-CR-179826] N87-10743

ALLOYS
Surface attack on metals in the presence of liquid metals [AD-A167403] N87-10193

ALUMINATES
Development of iron aluminides [AD-A166578] N87-10194

ALUMINUM
Deformation behavior of powder metallurgy Ni Al-Hf-B [DE86-011508] N87-10201

ALUMINUM ALLOYS
Weldability of an NiAl alloy [DE86-011510] N87-10199
The effects of temperature and loading rate on R-curves using the CLWL techniques — crack growth resistance curve (R curve); crack line wedge load (CLWL) [BAE-MSM-R-GEN-0544] N87-10405

ALUMINUM GRAPHITE COMPOSITES
Effects of thermal cycling on graphie-fiber-reinforced 6061 aluminum [NASA-TP-2612] N87-10184

AMPLIFIERS
Subpicosecond high-brightness UV laser system [DE86-011271] N87-10387

AMPLITUDE DISTRIBUTION ANALYSIS
Amplitude distribution of cosmic ray events in extrinsic IR detectors [AD-A167692] N87-10819

AMPLITUDE MODULATION
MODTEQ (Modulation Techniques), AN/FRC-170(V), equalization, and channel medium simulations [AD-A167965] N87-10226

AMPLITUDES
Periodic amplitude variations in Jovian continuum radiation [NASA-CR-177070] N87-10813

ANALYSIS OF VARIANCE
Cramer-Rao bound analysis for frequency estimation of sinusoids in noise [AD-A167992] N87-10227
Fault and error latency under real workload: An experimental study [NASA-CR-179802] N87-10733

ANDES MOUNTAINS (SOUTH AMERICA)
LANDSAT imagery of the Central Andes [NASA-CR-179852] N87-10526

ANEMOMETERS
Free surface turbulence [AD-A168013] N87-10251

ANGINA PECTORIS
Exercise-induced myocardial ischemia at high altitude simulated in a negative pressure chamber N87-10702

ANGLE OF ATTACK
Application of bifurcation and catastrophe theories to near stall flight mechanics [AD-A167697] N87-10046

ANIMALS
Animal models in space physiology N87-10705

ANISOTROPY
Effects of anisotropy on the frequency spectrum of gravity waves observed by MST radar N87-10460

ANNUAL VARIATIONS
Shuttle derived atmospheric density model. Part 1: Comparisons of the various ambient atmospheric source data with derived parameters from the first twelve STS entry flights, a data package for AOTV atmospheric development [NASA-CR-171824] N87-10662

ANNULAR NOZZLES
Free jet feasibility study of a thermal acoustic shield concept for AST/VCE application: Dual stream nozzles [NASA-CR-3867] N87-10752
Free-jet acoustic investigation of high-radius-ratio coannular plug nozzles [NASA-CR-3818] N87-10753

ANOMALIES
Review of VHF Band 1 field strength prediction [BBC-RD-1986/4] N87-10223

ANTARCTIC REGIONS
Lidar measurement of stratospheric aerosol at Syowa Station, Antarctica N87-10314
Lidar observation of the mesospheric sodium layer in Antarctica N87-10345
Very low frequency saucers with attenuation bands N87-10575

ANTENNA ARRAYS
The study of microstrip antenna arrays and related problems [NASA-CR-179714] N87-10225
Comparison of medium frequency pulsed radar interferometer and correlation analysis winds, part 2 N87-10475
Phased-array design for MST and ST radars N87-10499
The NOAA TOGA antenna array N87-10500
Beam steering system N87-10501
A 405-MHz, 5-beam phased array antenna N87-10503
The grid array antenna N87-10505
Method to determine the optimal parameters of the Arecibo 46.8-MHz antenna system N87-10510

ANTENNA DESIGN
The study of microstrip antenna arrays and related problems [NASA-CR-179714] N87-10225
Phased-array design for MST and ST radars N87-10499
A 405-MHz, 5-beam phased array antenna N87-10503
The grid array antenna N87-10505
A variable-frequency local oscillator for the frequency-hopping technique N87-10515
Cryogenic resonant-mass gravitational wave detectors N87-10609

ANTENNA FEEDS
The grid array antenna N87-10505
Method to determine the optimal parameters of the Arecibo 46.8-MHz antenna system N87-10510

ANTENNA RADIATION PATTERNS
Wire dipoles and antennas with dielectric or magnetic coatings [AWRE-O-19/85] N87-10235
Beam steering system N87-10501
A 405-MHz, 5-beam phased array antenna N87-10503
Low-altitude coverage of ST radars N87-10504
Simultaneous multibeam sounding of wind and turbulence N87-10506
Measurements of antenna polar diagrams and efficiencies using a phase-switched interferometer N87-10507
Monitoring of the MU radar antenna pattern by Satellite Ohzora (EXOS-C) N87-10509

ANTIBODIES
Anticortisol monoclonal antibodies: Characterization of their specificity N87-10680

ANTIMISSILE DEFENSE
Strategic Defense Initiative Program: Status of airborne optical adjunct and terminal imaging radar [P86-221132] N87-10107

APOGEE BOOST MOTORS
Geostationary Operational Environmental Satellite (GOES) mission profile N87-10123
State/orbit estimation from real Doppler data for solid apogee motor burning phase of geostationary satellite N87-10129
Real time orbit determination during apogee maneuvers — satellite orbits N87-10130
Spin dynamics with sloshing effects for solid motor burning phase — satellite dynamics N87-10140
Operational strategies for multi-burn apogee maneuvers of geostationary spacecraft N87-10141
Olympus: Apogee engine firing N87-10143
Optimal injection of TV SAT with multi-impulse apogee maneuvers with mission constraints and thrust uncertainties N87-10144
Definition of a structure for the apogee thrusts for geostationary satellite positioning: Application to TDF-1 N87-10145
Targeting multiburn, long duration apogee burst maneuvers N87-10146

APPLICATIONS PROGRAMS (COMPUTERS)
Numerical study of hydrogen-air supersonic combustion by using elliptic and parabolized equations [NASA-CR-179800] N87-10187
The study of microstrip antenna arrays and related problems [NASA-CR-179714] N87-10225
An all-purpose computer program for lidar simulations and reduction of lidar data N87-10299

Pulse forming network design program for linear and time-varying loads for the IBM personal computer
[DE86-011209] N87-10727
Computational hydrodynamics in astrophysical studies: Highly shocked flows in 3 dimensions N87-10796

APPROPRIATIONS
Department of Housing and Urban Development-Independent Agencies Appropriation Bill, 1987
[S-REPT-99-487] N87-10773
National Aeronautics and Space Administration N87-10774
National Aeronautics and Space Administration Authorization Act, 1987 N87-10775

APPROXIMATION
On accurate numerical solutions of Falkner-Skan equation N87-10018
The third order compact schemes for fluid dynamic problems N87-10032
Diffusion approximation for modeling of 3-D radiation distributions
[DE86-000810] N87-10228
Laboratory measurements of forward and backward scattering of laser beams in water droplet clouds N87-10295
Methods for estimating the optical constants of atmospheric hazes based on complex optical measurements N87-10301
Multiple scattering of laser beams in dense hydrosols N87-10316
Global collocation methods for approximation and the solution of partial differential equations
[NASA-CR-178179] N87-10745

ARC WELDING
Process control in arc welding
[KFK-PFT-105] N87-10395

ARCHITECTURE
Design for climate in hot, humid cities N87-10656

ARCHITECTURE (COMPUTERS)
Choosing Aircraft Integrated Data Systems (AIDS) architecture suitable for Engine Health Monitoring (EHM) on future generation engines N87-10083
Integrated testing and analysis of mathematical software tools. Summary of research activities, 1 August 1985-1 May 1986
[DE86-010882] N87-10723
Novel parallel architectures and algorithms for linear algebra processing
[NASA-CR-179826] N87-10743

ARCTIC REGIONS
Vertical structure of Arctic haze observed by lidar N87-10335
Airborne lidar observations of Arctic polar stratospheric clouds N87-10341

ARIANE LAUNCH VEHICLE
Analysis of the problem of satellite launch windows for Ariane dual launches N87-10115

ARID LANDS
Design for climate in hot, dry cities N87-10655

ARMED FORCES (UNITED STATES)
Air Force technical objective document fiscal year 1987
[AD-A167324] N87-10779

ARTERIES
Ordered and random structures in pulsatile flow through constricted tubes N87-10245

ARTIFICIAL INTELLIGENCE
Chemistry research resource
[DE86-009891] N87-10178
Intelligent Computer Assisted Instruction (ICAI): Formative evaluation of two systems
[NASA-CR-176873] N87-10716
Software process interpretation and software environments
[DE86-010881] N87-10725
Implementation and optimization of portable standard LISP for the CRAY
[DE86-008717] N87-10729
FORPS: A FORTH-based production system and its application to a real-time robot control problem
[DE86-005426] N87-10734

ASTROMETRY
NASA studying concept to measure distance between stars, galaxies
[NASA-NEWS-REL-86-133] N87-10787

ASTRONOMICAL MODELS
The ultraviolet spectra of DA white dwarfs N87-10783
Observations of molecular clouds in the direction of galactic and extragalactiv radio sources N87-10794
Bright galactic X-ray binary sources: Temporal and spectral studies N87-10804
A study of hierarchical clustering of galaxies in an expanding universe N87-10806
A modeling analysis program for the JPL Table Mountain Io sodium cloud data
[NASA-CR-179671] N87-10811
Clouds and methane photochemical hazes on the outer planets N87-10815
Interpretation of extragalactic jets
[DE86-011211] N87-10823

ASTRONOMICAL SPECTROSCOPY
High resolution spectroscopy of quasar absorption lines N87-10785

ASTROPHYSICS
Computational hydrodynamics in astrophysical studies: Highly shocked flows in 3 dimensions N87-10796

ASYMPTOTIC METHODS
An asymptotic theory of supersonic turbulent interactions in a compression corner N87-10010

ASYMPTOTIC SERIES
Crack-tip fields in a viscoplastic material
[AD-A168014] N87-10413
Asymptotic error expansions of finite element solutions of parabolic equations N87-10738

ATMOSPHERIC BOUNDARY LAYER
Lidar observations and modeling of cold air outbreaks during MASEX and GALE N87-10336
Investigation of clouds spatial distribution using ground-based lidar N87-10349
Generation of attenuation corrected images from lidar data N87-10367
A model for the evolving stably stratified nocturnal boundary layer based on the turbulent kinetic energy equation N87-10606
Case studies of the structure of the atmospheric boundary layer entrainment zone N87-10627
Modeling the effects of the spatially varying sea surface temperature on the marine atmospheric boundary layer N87-10673

ATMOSPHERIC CHEMISTRY
Atmospheric Ozone 1985. Assessment of our understanding of the processes controlling its present distribution and change, volume 1
[NASA-TM-89237] N87-10612
Stratospheric chemistry N87-10613
Tropospheric trace gases N87-10614
Tropospheric chemistry N87-10615
Strat-trop exchange N87-10616
Radiative processes N87-10618

ATMOSPHERIC CIRCULATION
Doppler lidar studies of atmospheric wind field dynamics N87-10327
Remote sensing of atmospheric winds using a coherent, CW lidar and speckle-turbulence interaction N87-10329
The application of lidar to stratospheric aerosol studies N87-10337
Volcanic eruptions and the increases in the stratospheric aerosol content: Lidar measurements from 1982 to 1986 N87-10338
Observations of stratospheric aerosols associated with the El Chichon eruption N87-10339
Daytime lidar measurements of tidal winds in the mesospheric sodium layer at Urbana, Illinois N87-10347
Middle Atmosphere Program. Handbook for MAP, volume 20
[NASA-CR-176882] N87-10419
Examples of mesoscale structures and short-term wind variations detected by VHF Doppler radar N87-10422
Observations of mesoscale vertical velocities around frontal zones N87-10424
Comparison of vertical velocities analyzed by a numerical model and measured by a VHF wind profiler N87-10425
Measurements of precipitating atmosphere by the MU radar N87-10426
The real-time use of wind profilers in nowcasting N87-10427
Need for a subtropical wind profiling system N87-10432
Gravity waves in the middle atmosphere: Recent progress and needed studies N87-10433
Evidence of atmospheric gravity wave perturbations of the Brunt-Vaisala frequency in the atmosphere N87-10438
Evidence of a saturated gravity-wave spectrum throughout the atmosphere N87-10467
The Adelaide MF partial-reflection radar and VHF ST radar N87-10490
On the use of colour reflectivity plots to monitor the structure of the troposphere and stratosphere N87-10522
Atmospheric Ozone 1985. Assessment of our understanding of the processes controlling its present distribution and change, volume 1
[NASA-TM-89237] N87-10612
Tropospheric chemistry N87-10615
Strat-trop exchange N87-10616
Dynamical processes N87-10617
Numerical studies of thermally and mechanically forced circulations over complex terrain N87-10630
Vertical modes and energetics of gravitational and rotational modes in a multilevel global spectral model N87-10633
Further studies with data collected by NASA's airborne Doppler lidar in Oklahoma in 1981
[NASA-CR-179779] N87-10660
A study of disturbed solar wind and magnetotail based on ISEE-3 data
[NASA-CR-177060] N87-10816

ATMOSPHERIC COMPOSITION
Flight tests of a range-resolved airborne dial with two min-tea CO2 lasers N87-10284
Observation of atmospheric ozone by dial with Raman lasers pumped by a KrF laser N87-10297
Lidar mapping of a mixture of aerosol concentrations in a varying atmosphere N87-10320
Three atmospheric dispersion experiments involving oil fog plumes measured by lidar N87-10321
Time-domain sensitivity enhancement in pulsed Pb-TDL gas monitors N87-10324
Intercomparisons of high-resolution solar blind Raman lidar atmospheric profiles of water vapor with radiosondes and kytoon N87-10333
Lidar method of measurement of atmospheric extinction and ozone profiles N87-10334
Detection of NO sub x,C2H4 concentrations by using CO and CO2 lasers N87-10357
Laser heterodyne system for obtaining height profiles of minor species in the atmosphere N87-10359
Spectroscopic aspects of differential method for sounding gas composition of the atmosphere N87-10369
A photometric and in situ study of stable auroral red arcs N87-10628
Millimeter-wave spectrometry of ozone in the middle atmosphere N87-10629
Shuttle derived atmospheric density model. Part 1: Comparisons of the various ambient atmospheric source data with derived parameters from the first twelve STS entry flights, a data package for AOTV atmospheric development
[NASA-CR-171824] N87-10662
Clouds and methane photochemical hazes on the outer planets N87-10815

ATMOSPHERIC DENSITY
On the measurement of atmospheric density using dial in the O2 A-band (770 nm) N87-10291
XeF lidar measurements of density and temperature in the middle atmosphere N87-10342
Lidar measurements of thermal structure N87-10343
Lidar detection of metallic species at the mesopause level N87-10346
Atmospheric correlation time measurements using coherent CO2 lidar N87-10363

ATMOSPHERIC DIFFUSION
Comparison of reflectivity and wind profiles measured on 46.8 MHz and 430 MHz at the Arecibo Observatory N87-10477

ATMOSPHERIC EFFECTS
A component decomposition model for evaluating atmospheric effects in remote sensing N87-10610
Space Environment Laboratory, FY 1985
[PB86-218587] N87-10621

ATMOSPHERIC ENERGY SOURCES
Observational and theoretical investigation of stable auroral red arcs and their magnetospheric energy source, volumes 1 and 2 N87-10632

ATMOSPHERIC ENTRY
Shuttle derived atmospheric density model. Part 1: Comparisons of the various ambient atmospheric source data with derived parameters from the first twelve STS entry flights, a data package for AOTV atmospheric development
[NASA-CR-171824] N87-10662
Shuttle derived atmospheric density model. Part 2: STS atmospheric implications for AOTV trajectory analysis, a proposed GRAM perturbation density model
[NASA-CR-171824] N87-10663

ATMOSPHERIC HEATING
Advective influences on steady and transient forced tropical motions N87-10670

ATMOSPHERIC MODELS
Optical models of the molecular atmosphere N87-10306
Variation of the urban NO2 concentration during a ground inversion situation N87-10318
Can stochastic, dissipative wave fields be treated as random walk generators N87-10452
Observations and a model of gravity-wave variability in the middle atmosphere N87-10453
Models of electric potential and current distribution in stable discrete auroral forms N87-10551

Nonstationary field-aligned fluxes of thermal ions O(+) and H(+) outside the plasmapause: Refinement of the polar wind theory N87-10586
A model for the evolving stably stratified nocturnal boundary layer based on the turbulent kinetic energy equation N87-10608
A component decomposition model for evaluating atmospheric effects in remote sensing N87-10610
A high resolution entrainment model for the convective planetary boundary layer N87-10611
Strat-trop exchange N87-10616
Dynamical processes N87-10617
Case studies of the structure of the atmospheric boundary layer entrainment zone N87-10627
Environmental influences on hurricane intensification N87-10635
Urban climatological methods and data N87-10645
Urban climate models: Nature, limitations and applications N87-10646
A preliminary cloudless standard atmosphere for radiation computation
[WCP-112] N87-10657
Shuttle derived atmospheric density model. Part 2: STS atmospheric implications for AOTV trajectory analysis, a proposed GRAM perturbation density model
[NASA-CR-171824] N87-10663
Modeling the effects of the spatially varying sea surface temperature on the marine atmospheric boundary layer N87-10673
A study of disturbed solar wind and magnetotail based on ISEE-3 data
[NASA-CR-177060] N87-10816

ATMOSPHERIC PHYSICS
Alexandrite laser source for atmospheric lidar measurements N87-10373
HISCAT: A proposed new scatter facility in Northern Scandinavia N87-10498
A preliminary cloudless standard atmosphere for radiation computation
[WCP-112] N87-10657

ATMOSPHERIC PRESSURE
Airborne Lidar measurements of the atmospheric pressure profile with tunable Alexandrite lasers N87-10282
Nd:Glass-Raman laser for water vapor dial N87-10285
Evidence of atmospheric gravity wave perturbations of the Brunt-Vaisala frequency in the atmosphere N87-10438

ATMOSPHERIC RADIATION
A preliminary cloudless standard atmosphere for radiation computation
[WCP-112] N87-10657

ATMOSPHERIC SCATTERING
Measurements of the effect of horizontal variability of atmospheric backscatter on dial measurements N87-10283
An analysis at mesospheric coherent-scatter power enhancements during solar flare events N87-10479
HISCAT: A proposed new scatter facility in Northern Scandinavia N87-10498
Study of the middle latitude broadening of the spectrum of the waves emitted from ground N87-10583

ATMOSPHERIC SOUNDING
Methods for estimating the optical constants of atmospheric hazes based on complex optical measurements N87-10301
Laser sounding of instantaneous and mean speed of wind using correlation method N87-10304
Optimal filtration of the atmospheric parameters profiles N87-10305
Coherent lidars based on intracavity heterodyning of echo signals N87-10308
The influence of scattering particles morphology on the characteristics of lidar signals N87-10309
Lidar measurements of thermal structure N87-10343
Alexandrite laser source for atmospheric lidar measurements N87-10373
On the potential use of radar-derived information in operational numerical weather prediction N87-10420
A model for gravity-wave spectra observed by Doppler sounding systems N87-10434
Tropospheric turbulence parameters measured by using the MU radar N87-10436

ATMOSPHERIC STRATIFICATION
Lidar observation of the mesospheric sodium layer in Antarctica N87-10345
Comparison between S. T. radar and in situ balloon measurements N87-10447
A comparison of vertical velocities measured from specular and nonspecular echoes by a VHF radar N87-10470

ATMOSPHERIC TEMPERATURE
XeF lidar measurements of density and temperature in the middle atmosphere N87-10342
Lidar measurements of thermal structure N87-10343
Lidar study of storm tops N87-10348
A model for gravity-wave spectra observed by Doppler sounding systems N87-10434
Evidence of atmospheric gravity wave perturbations of the Brunt-Vaisala frequency in the atmosphere N87-10438

ATMOSPHERIC TIDES
Daytime lidar measurements of tidal winds in the mesospheric sodium layer at Urbana, Illinois N87-10347

ATMOSPHERIC TURBULENCE
Remote sensing of atmospheric winds using a coherent, CW lidar and speckle-turbulence interaction N87-10329
Lidar observations and modeling of cold air outbreaks during MASEX and GALE N87-10336
Middle Atmosphere Program. Handbook for MAP, volume 20
[NASA-CR-176882] N87-10419
Tropospheric turbulence parameters measured by using the MU radar N87-10436
Evidence of atmospheric gravity wave perturbations of the Brunt-Vaisala frequency in the atmosphere N87-10438
Atmospheric waves and the nature of buoyancy turbulence in the context of the waves VS 2D-turbulence debate N87-10439
A proposed experimental test to distinguish waves from 2-D turbulence N87-10440
Simultaneous rocket and MST radar observation of an internal gravity wave breaking in the mesosphere N87-10443
Observations of thunder with the Arecibo VHF radar N87-10444
The PROUST radar: First results N87-10445
Simultaneous fine structure observation of wind and temperature profiles by the Arecibo 430-MHz radar and in situ measurements N87-10446
A statistical model to estimate refractivity turbulence structure constant C sub n sup 2 in the free atmosphere N87-10448
The use of the experimentally deduced Brunt-Vaisala frequency and turbulent velocity fluctuations to estimate the eddy diffusion coefficient N87-10450
The relation of gravity waves and turbulence in the mesosphere N87-10451
Can stochastic, dissipative wave fields be treated as random walk generators N87-10452
Mesospheric gravity-wave climatology at Adelaide N87-10456
A comparison of vertical velocities measured from specular and nonspecular echoes by a VHF radar N87-10470
A comparison of thunderstorm reflectivities measured at the VHF and UHF N87-10472
UHF and VHF radar observations of thunderstorms N87-10473
MST radar networks and campaigns session summary and recommendations N87-10478
An analysis at mesospheric coherent-scatter power enhancements during solar flare events N87-10479
Density gradient instability in the high latitude ionosphere. Relation with the electrostatic turbulence and convection N87-10573
A model for the evolving stably stratified nocturnal boundary layer based on the turbulent kinetic energy equation N87-10608
Turbulent mixing, droplet spectral evolution and dynamics of warm cumulus clouds N87-10667

ATOMIZING
Transient behavior of liquid jets injected normal to a high velocity gas stream N87-10246

ATTACKING (ASSAULTING)
Surface attack on metals in the presence of liquid metals
[AD-A167403] N87-10193

ATTITUDE INDICATORS
Coverage transition times of IR pencil beam sensors — satellite attitude sensors N87-10125

AUDIO EQUIPMENT
The Fairchild CVDR: A new combination voice and data recorder — Cockpit Voice and Data Recorder (CVDR) N87-10095

AURORAL ABSORPTION
Attenuation bands and cut-off frequencies for ELF electromagnetic waves — high latitudes N87-10570
Very low frequency saucers with attenuation bands N87-10575

AURORAL ARCS
Magnetic field-aligned particle precipitation N87-10542
Statistical study of auroral electron precipitation structures detected by the AUREOL-3 Satellite N87-10543
Magnetospheric-ionospheric coupling deduced from measurements above a discrete auroral arc N87-10550
A photometric and in situ study of stable auroral red arcs N87-10628

AURORAL ELECTROJETS
Detection from AUREOL-3 of the modulation of auroral electrojet by HF-heating from ELF signals in the upper ionosphere above Tromsoe (Norway) N87-10582
Observations of auroral electrons with sounding rockets and the GEOS-2 geostationary satellite N87-10596

AURORAL IRRADIATION
Scenarios for the generation of auroral kilometric radiation N87-10577
The cyclotron maser theory of AKR and Z-mode radiation — Auroral Kilometric Radiation (AKR) N87-10578

AURORAL SPECTROSCOPY
A study of disturbed solar wind and magnetotail based on ISEE-3 data
[NASA-CR-177060] N87-10816

AURORAL ZONES
Results of the ARCAD 3 Project and of Recent Programs in Magnetospheric and Ionospheric Physics — conferences
[ISBN-2-85428-126-8] N87-10541
Positive ion distributions in the morning auroral zone: Local acceleration and drift effects N87-10547
Detection of suprathermal O(+) ions inside the plasmasphere N87-10554
Evidence for high latitude ionospheric ion acceleration N87-10564
Experimental evidence of field-aligned ELF plasma ducts in the ionospheric trough and in the auroral zone N87-10574
Precipitation of electrons and protons in the subauroral zone stimulated by ground-based VLF emitter N87-10585
The ARCAD 3-SAFARI coordinated study of auroral and polar F-region ionospheric irregularities N87-10600
Two-dimensional snapshots of electron density in the main trough and diffuse auroral zone from a close network of ionosondes: Comparison with measurements from AUREOL-3 satellite N87-10601
Step-like profiles of electron density in the subauroral lower F-region in the morning sector and possible mechanisms of their formation during substorms: The comparison of data of ground-based ionosondes with the AUREOL-3 satellite measurements N87-10603
Growing electrostatic waves with a wavelength of 67 cm in the upper ionosphere N87-10604

AURORAS
Magnetic field-aligned potential drops N87-10545
Models of electric potential and current distribution in stable discrete auroral forms N87-10551
Dynamic variations of the auroral precipitation and the polar cap N87-10559
Artificial ion beam interaction with the auroral plasma N87-10591
Some results of scanner spectrophotometric measurements of aurora and airglow from IK-Bulgaria-1300 satellite and prospects of similar measurements N87-10593
Energy spectra of electrons precipitating above the EISCAT area. Comparison with ARCAD measurements N87-10598
Coordinated data on auroral electrodynamics from ground based radar diagnostics and AUREOL-3 satellite N87-10607

AUSTENITIC STAINLESS STEELS
Modification of the grain boundary microstructure of the austenitic PCA stainless steel to improve helium embrittlement resistance
[DE86-010396] N87-10202

AUTOMATIC GAIN CONTROL
MODTEQ (Modulation Techniques), AN/FRC-170(V), equalization, and channel medium simulations
[AD-A167965] N87-10226

AUTOMATIC LANDING CONTROL
Helicopter MLS Flight Inspection Project
[DOT/FAA/CT-86/14] N87-10002

AUTOREGRESSIVE PROCESSES
Ordered and random structures in pulsatile flow through constricted tubes N87-10245

AUTOROTATION
Numerical and experimental study of dynamics of two-dimensional body
[ISAS-619] N87-10748

AVIONICS
Experience with the Onboard Checkout And Monitoring System (OCAMS) of a military aircraft resulting improvements and the consequence for future design N87-10079
Integrated monitoring systems for tactical aircraft N87-10080

AXIAL COMPRESSION LOADS
Concentrations of plastic strains in the clamping region of cylindrical shells under excessive loading
[KFK-3915] N87-10417

B

BACKGROUND RADIATION
Gauge invariant perturbation theory prediction of the sensitivity required for experimental measurement of quadrupole and higher moments of the cosmic microwave background radiation N87-10825
BACKSCATTERING
Coherent lidar technology for global wind profiling N87-10267
Visibility related to backscatter at 1.54 micron N87-10272
Inversion of 2 wavelength Lidar data for cloud properties N87-10273
The usefulness of Klett's inversion algorthms to simulated satellite Lidar returns N87-10274
Wavelength dependence of aerosol backscatter coefficients obtained by multiple wavelength Lidar measurements N87-10275
Extinction and visibility measurements in the lower atmosphere with UV-YAG-lidar N87-10276
Lidar measurements of slant visual range N87-10278
Airborne Lidar measurements of the atmospheric pressure profile with tunable Alexandrite lasers N87-10282
Measurements of the effect of horizontal variability of atmospheric backscatter on dial measurements N87-10283
Correction of Doppler-broadened Rayleigh backscattering effects in H2O dial measurements N87-10288
Determination of cloud microphysical properties by laser backscattering and extinction measurements N87-10293
Effect of backscatter-to-extinction ratio on lidar inversions N87-10294
Laboratory measurements of forward and backward scattering of laser beams in water droplet clouds N87-10295
Optimal filtration of the atmospheric parameters profiles N87-10305
The influrence of an optical receiving system on statistical characteristics of a lidar signal N87-10307
Coherent lidars based on intracavity heterodyning of echo signals N87-10308
Improved solution of the lidar equation utilizing particle counter measurements N87-10310
Investigation of clouds spatial distribution using ground-based lidar N87-10349
Near-IR extinction and backscatter coefficient measurements in low- and mid-altitude clouds N87-10351
Backscatter and extinction measurements in cloud and drizzle at CO2 laser wavelengths N87-10352
Coherent lidar signal fluctuation reduction by means of frequency diversity technique N87-10360
Wavelength dependence of coherent and incoherent satellite-based lidar measurements of wind velocity and aerosol backscatter N87-10361
Atmospheric correlation time measurements using coherent CO2 lidar N87-10363
Generation of attenuation corrected images from lidar data N87-10367
Simultaneous VHF and UHF radar observation of the mesosphere at Arecibo during a solar flare: A check on the gradient-mixing hypothesis N87-10437
Comparison between S. T. radar and in situ balloon measurements N87-10447
BALANCE
Preliminary results on the equilibrium and vertigo experiment performed during STS 51-G shuttle flight N87-10692
BALLOON-BORNE INSTRUMENTS
Simultaneous fine structure observation of wind and temperature profiles by the Arecibo 430-MHz radar and in situ measurements N87-10446
Comparison between S. T. radar and in situ balloon measurements N87-10447
A statistical model to estimate refractivity turbulence structure constant C sub n sup 2 in the free atmosphere N87-10448
Intercomparison and calibration of wind and wave measurements at various frequencies N87-10468
BANDPASS FILTERS
Surface photometry of early-type galaxies N87-10795
BARIUM FLUORIDES
Carbide/fluoride/silver self-lubricating composite [NASA-CASE-LEW-14196-1] N87-10179
BEAMS (RADIATION)
Optical models of the molecular atmosphere N87-10306
Tropospheric turbulence parameters measured by using the MU radar N87-10436
Phased-array design for MST and ST radars N87-10499
BEAMS (SUPPORTS)
Dynamics and control of orbiting grid and the synchronously deployable beam [NASA-CR-179808] N87-10410
BED REST
Metabolic changes during prolonged antiorthostatic hypokinesia — weightlessness simulation N87-10698
BENDING
Aeroelastic stability of composite rotor blades in hover N87-10060
BERYL
Alexandrite laser source for atmospheric lidar measurements N87-10373
BERYLLIUM OXIDES
Alexandrite laser source for atmospheric lidar measurements N87-10373
BIBLIOGRAPHIES
Aerospace medicine and biology: A continuing bibliography with indexes (supplement 287) [NASA-SP-7011(287)] N87-10001
Nonreacting turbulent mixing flows: A literature survey and data base [DE86-010864] N87-10253
Aerospace medicine and biology: A continuing bibliography with indexes [NASA-SP-7011(289)] N87-10674
A summary of the Foundation Research Program, fiscal year 1985 [AD-A168009] N87-10780
Lawrence Berkeley Laboratory recent papers submitted and reports issued, February 1986 [DE86-011319] N87-10782
BINARY MIXTURES
Constitutive relations for flow of a non-Newtonian fluid through saturated porous media [DE86-702035] N87-10261
BIOCHEMICAL OXYGEN DEMAND
Upper and lower body anaerobic power comparison between biathletes and control subjects [AD-A167636] N87-10710
BIOCHEMISTRY
Lawrence Berkeley Laboratory recent papers submitted and reports issued, February 1986 [DE86-011319] N87-10782
BIOCONVERSION
Bicconversion: A New Technology for Waste and Sludge Disposal. Workshop proceedings [DE86-009668] N87-10539
BIODEGRADATION
The fungal resistance or susceptibility of resins, plasticizers, and other constituents of adhesive formulations [AD-A168930] N87-10207
BIOLOGICAL EFFECTS
Aerospace medicine and biology: A continuing bibliography with indexes (supplement 287) [NASA-SP-7011(287)] N87-10001
Aerospace medicine and biology: A continuing bibliography with indexes [NASA-SP-7011(289)] N87-10674
BIOLOGICAL MODELS (MATHEMATICS)
Math modelling as a complement to the scientific inquiry of physiological adaptation to space flight: Fluid, endocrine and circulatory regulation N87-10709
BIOMASS
Bioconversion: A New Technology for Waste and Sludge Disposal. Workshop proceedings [DE86-009668] N87-10539
BIT SYNCHRONIZATION
Investigations on a digital bit synchronizer for a detailed flight data recovery N87-10099
BLACK AND WHITE PHOTOGRAPHY
Black-and-white photographic chemistry: A reference [NASA-TM-87296] N87-10177
BLACK BODY RADIATION
Intense soft X-rays from RS Ophiuchi during the 1985 outburst [DE86-010175] N87-10820
BLACK HOLES (ASTRONOMY)
On the stability of accretion disks around black holes N87-10805
BODY FLUIDS
The regulation of fluid and electrolyte metabolism in weightlessness N87-10679
Relationship between cardiovascular functions and fluid-electrolyte metabolism during antiorthostatic hypokinesia — weightlessness simulation N87-10701
BODY VOLUME (BIOLOGY)
Volume regulating hormones during a 5 hour head-down tilt at -10 deg. Part 1: Epinephrine, norepinephrine and dopamine N87-10700
BOLTZMANN TRANSPORT EQUATION
Diffusion approximation for modeling of 3-D radiation distributions [DE86-000810] N87-10228
BOMB CALORIMETERS
A trial on performance test method for Cu-water heat pipe N87-10026
BONE DEMINERALIZATION
Bone examination by noninvasive techniques in a 120-day head-down tilt test N87-10688
Histomorphometric study of bone cell mass and activity in man caused by a 120 day decubitus. Test of preventive protocols N87-10689
BONES
Bones and weightlessness N87-10681
Weightlessness effects on the bone tissue of rats after a 5 day space flight (Cosmos 1514) N87-10684
Bone tissue and muscular performance in a population of elderly men as a function of physical exercise N87-10685
Bone examination by noninvasive techniques in a 120-day head-down tilt test N87-10688
The state of bones of pregnant rats during an acute stage of adaptation to weightlessness N87-10708
BOOMS (EQUIPMENT)
Flight service evaluation of composite helicopter components [NASA-CR-178149] N87-10182
BORIDES
Boron-containing organosilane polymers and ceramic materials thereof [NASA-CASE-ARC-11649-1-SB] N87-10205
BORON
Deformation behavior of powder metallurgy Ni Al-Hf-B [DE86-011508] N87-10201
BORON COMPOUNDS
Boron-containing organosilane polymers and ceramic materials thereof [NASA-CASE-ARC-11649-1-SB] N87-10205
BOUNDARY LAYER CONTROL
Wind tunnel test of the modified goldschmied model with propulsion and empennage: Analysis of test results [AD-A167360] N87-10045
BOUNDARY LAYER EQUATIONS
Numerical solution of the 3-dimensional boundary layer equations in the inverse mode using finite differences N87-10005
Finite volume solution of the compressible boundary-layer equations [NASA-CR-4013] N87-10744
BOUNDARY LAYER FLOW
Images of three dimensional flows in computer graphics N87-10017
On accurate numerical solutions of Falkner-Skan equation N87-10018
Numerical modeling of spatial flows on the basis of splitting up method N87-10031
BOUNDARY LAYER PLASMAS
Plasma sheet boundary electric fields during substorms N87-10548
The hot ion composition in the magnetosphere N87-10552
BOUNDARY LAYER SEPARATION
Acta Aeronautica et Astronautica Sinica (selected articles) [AD-A167918] N87-10004
Experimental study of the boundary layer on a low Reynolds number airfoil in steady and unsteady flow N87-10052
BOUNDARY LAYERS
An experimental investigation of end-wall flowfield of a compressor rotor N87-10244
Using a laser aureole to invert lidar return N87-10292
BOUNDARY VALUE PROBLEMS
An asymptotic theory of supersonic turbulent interactions in a compression corner N87-10010
Correction of Doppler-broadened Rayleigh backscattering effects in H2O dial measurements N87-10288
Effect of backscatter-to-extinction ratio on lidar inversions N87-10294
Seminar on Finite Elements in Unsteady Problems [ETN-86-97824] N87-10736
Hierarchical bases for the solution of plane elliptic boundary value problems N87-10742
A study of hierarchical clustering of galaxies in an expanding universe N87-10806
BOW WAVES
The onset of alfvenic turbulence N87-10762
BRAZIL
Some aspects of the urban climates of tropical South America: The Brazilian contribution N87-10644
BREMSSTRAHLUNG
Bright galactic X-ray binary sources: Temporal and spectral studies N87-10804

BRIGHTNESS TEMPERATURE
Observations of molecular clouds in the direction of galactic and extragalactiv radio sources N87-10794
BROADBAND
Nonlinear optics with broad-band lasers [DE86-011286] N87-10382
BROADCASTING
Review of VHF Band 1 field strength prediction [BBC-RD-1986/4] N87-10223
BRUNT-VAISALA FREQUENCY
Evidence of atmospheric gravity wave perturbations of the Brunt-Vaisala frequency in the atmosphere N87-10438
Determination of the Brunt-Vaisala frequency from vertical velocity spectra N87-10449
The use of the experimentally deduced Brunt-Vaisala frequency and turbulent velocity fluctuations to estimate the eddy diffusion coefficient N87-10450
BUCKLING
Short-wavelength buckling and shear failures for compression-loaded composite laminates N87-10403
BUILDINGS
Terrestrial evaluation of the Global Positioning System (GPS) Standard Positioning Service (SPS) [PB86-219599] N87-10059
BUNDLES
Experimental procedure for lifetime testing of graphite bundles under constant load [AD-A167714] N87-10186
BUOYANCY
Atmospheric waves and the nature of buoyancy turbulence in the context of the waves VS 2D-turbulence debate N87-10439
A proposed experimental test to distinguish waves from 2-D turbulence N87-10440
BURNING TIME
Targeting multiburn, long duration apogee burst maneuvers N87-10146

C

CALCIUM
Lidar detection of metallic species at the mesopause level N87-10346
CALCIUM FLUORIDES
Carbide/fluoride/silver self-lubricating composite [NASA-CASE-LEW-14196-1] N87-10179
CALCIUM METABOLISM
Bone examination by noninvasive techniques in a 120-day head-down tilt test N87-10688
Weightlessness effects on the phosphorus-calcium balance and its hormonal regulation in man during STS flight 51-G N87-10691
Metabolic changes during prolonged antiorthostatic hypokinesia — weightlessness simulation N87-10698
CALIBRATING
Orbit geometry for calibration and launch operations of a three-axis controlled satellite with inertial reference N87-10116
Intercomparison and calibration of wind and wave measurements at various frequencies N87-10468
Measurements of antenna polar diagrams and efficiencies using a phase-switched interferometer N87-10507
In-flight absolute radiometric calibration of the LANDSAT thematic mapper N87-10530
CALIFORNIA
Development of worst case meteorology criteria [PB86-215993] N87-10540
CAMBERED WINGS
Supersonic, nonlinear, attached-flow wing design for high lift with experimental validation [NASA-TP-2336] N87-10042
CAMERAS
Research relative to high resolution camera on the advanced X-ray astrophysics facility [NASA-CR-179757] N87-10376
CANARD CONFIGURATIONS
Wind-tunnel investigation of the flight characteristics of a canard general-aviation airplane configuration [NASA-TP-2623] N87-10039
CARBON
Synthetic carbon precursor materials [DE86-011584] N87-10210
CARBON DIOXIDE LASERS
Correction function in the Lidar equation and the solution techniques for CO2 Lidar date reduction N87-10280
Remote express analysis of ground-layer aerosol based on laser-induced spark spectra N87-10303
The effect of turbulence on lidar backscattered signal fluctuations N87-10328
Backscatter and extinction measurements in cloud and drizzle at CO2 laser wavelengths N87-10352
MAPM: A coherent dual CO2 laser DIAL system N87-10358
Atmospheric correlation time measurements using coherent CO2 lidar N87-10363
CO2 lidar system for atmospheric studies N87-10366
CARBON FIBER REINFORCED PLASTICS
Investigation into the attenuation and velocity of acoustic emissions in carbon fiber composite aircraft structures [BAE-KGT-R-GEN-01349] N87-10180
CARBON FIBERS
Effects of thermal cycling on graphie-fiber-reinforced 6061 aluminum [NASA-TP-2612] N87-10184
CARBON MONOXIDE
Laboratory evaluation of three passive CO concentration monitors [PML-1985-13] N87-10538
Development of worst case meteorology criteria [PB86-215993] N87-10540
CARDIOGRAPHY
Cardiovascular measurements in microgravity N87-10676
CARDIOVASCULAR SYSTEM
Cardiovascular measurements in microgravity N87-10676
Cardiovascular examination during STS 51 G mission June (1985) N87-10677
Ground based simulation techniques for cardiovascular and hormonal changes observed in man in weightlessness N87-10696
Levels of plasma atrial natriuretic factor (alpha h ANF) during acute simulated weightlessness N87-10699
Relationship between cardiovascular functions and fluid-electrolyte metabolism during antiorthostatic hypokinesia — weightlessness simulation N87-10701
CARTESIAN COORDINATES
Determination of U, V, and W from single station Doppler radar radial velocities N87-10502
CAST ALLOYS
Castable hot corrosion resistant alloy [NASA-CASE-LEW-14134-1] N87-10192
CATALYSTS
Polymer systems for rapid sealing of aircraft structures at low temperature [AD-A167667] N87-10209
CATECHOLAMINE
Volume regulating hormones during a 5 hour head-down tilt at -10 deg. Part 1: Epinephrine, norepinephrine and dopamine N87-10700
CATHODES
Design, construction and long life endurance testing of cathode assemblies for use in microwave high-power transmitting tubes [NASA-CR-175116] N87-10237
CEILINGS (METEOROLOGY)
Cloud detection by lidar extinction calculations N87-10353
Laser heterodyne system for obtaining height profiles of minor species in the atmosphere N87-10359
CENTRAL PROCESSING UNITS
A single-board preprocessor and pulse generator N87-10517
CENTRIFUGING STRESS
The interest of centrifuge tests for the selection of French cosmonauts N87-10678
CERAMICS
Boron-containing organosilane polymers and ceramic materials thereof [NASA-CASE-ARC-11649-1-SB] N87-10205
CERTIFICATION
Summary of artificial and natural icing tests conducted on US Army aircraft from 1974 to 1985 [FAA/CT-85/26] N87-10064
CHANNEL FLOW
Study of three-dimensional separation on a spheroid at incidence N87-10016
CHANNELS (DATA TRANSMISSION)
The air/ground transfer of aircraft integrated data systems (AIDS) for Air Traffic Control (ATC) purposes: Present experiments and possible future intentions N87-10091
VSB 2-PSK: A modulation system for digital sound with television [BBC-RD-1986/7] N87-10222
CHARGE COUPLED DEVICES
High resolution CCD spectra of stars in globular clusters. Part 2: Metals and CNO in M71 [NASA-CR-179853] N87-10789
Surface photometry of early-type galaxies N87-10795
CHECKOUT
Experience with the Onboard Checkout And Monitoring System (OCAMS) of a military aircraft resulting improvements and the consequence for future design N87-10079
CHEMICAL ANALYSIS
Research and development activities of the Spectroscopy Division of the Bhabha Atomic Research Centre [DE86-702154] N87-10781
CHEMICAL COMPOSITION
Compositional and microstructural effects on hydrogen embrittlement of ASTM grade 12 titanium (Ti 0.3 Mo - 0.8 Ni) [DE86-011379] N87-10197
Millimeter-wave spectrometry of ozone in the middle atmosphere N87-10629
CHEMICAL EXPLOSIONS
Percussion primer/DDT detonator [DE86-010477] N87-10217
Very low frequency and ELF effects in the upper ionosphere caused by large-scale acoustic waves in the lower ionosphere observed from AUREOL-3 satellite N87-10587
CHEMICAL REACTIONS
Black-and-white photographic chemistry: A reference [NASA-TM-87296] N87-10177
Numerical study of hydrogen-air supersonic combustion by using elliptic and parabolized equations [NASA-CR-179800] N87-10187
RLE progress report [MIT-PR-128] N87-10778
CHEMISORPTION
Chemisorption mechanism and effect of polyacrylic acid on the improvement in bond durability of zinc phosphate-to-polymer adhesive joints [DE86-011535] N87-10213
CHEMOTHERAPY
Histomorphometric study of bone cell mass and activity in man caused by a 120 day decubitus. Test of preventive protocols N87-10689
CHINA
Some aspects of the urban climate of Shanghai N87-10641
CHROMIUM ALLOYS
Modification of the grain boundary microstructure of the austenitic PCA stainless steel to improve helium embrittlement resistance [DE86-010396] N87-10202
CHROMIUM CARBIDES
Carbide/fluoride/silver self-lubricating composite [NASA-CASE-LEW-14196-1] N87-10179
CIRCUIT RELIABILITY
Cross-contact chain [NASA-CASE-NPO-16784-1] N87-10231
CIRCUITS
Electrical circuit modeling of conductors with skin effect [DE86-011085] N87-10240
Electronics Engineering Department technical review [DE86-011371] N87-10241
CIRCULAR CYLINDERS
A description of a turbulent flow past a circular cylinder by a discrete vortex method N87-10014
Acoustic waves emitted by vortex-body interaction N87-10015
CIRCULAR POLARIZATION
Polarization of electromagnetic waves recorded on board the AUREOL-3 satellite N87-10571
CITIES
Terrestrial evaluation of the Global Positioning System (GPS) Standard Positioning Service (SPS) [PB86-219599] N87-10059
Proceedings of the Technical Conference on Urban Climatology and its Applications with Special Regard to Tropical Areas [WMO-652] N87-10636
Urban climatology and the tropical city: An introduction N87-10637
Tropical urban climates: Review and assessment N87-10638
Air quality in tropical cities N87-10639
The urban climate of Mexico City N87-10640
Some aspects of the urban climate of Shanghai N87-10641
Some aspects of the urban climates of tropical Africa N87-10642
Some aspects of the urban climates of India N87-10643
Some aspects of the urban climates of tropical South America: The Brazilian contribution N87-10644
Urban climatological methods and data N87-10645
Urban climate models: Nature, limitations and applications N87-10646
The planning and maintenance of urban settlements to resist extreme climatic forces N87-10647
Life expectancy in tropical climates and urbanization N87-10648
Human comfort in the urban tropics N87-10649
Urban hydrology in the tropics: Problems, solutions, data collection and analysis N87-10650

Energy related issues — urban climatology N87-10651
The introduction of climatology into the administration and development of planning in the city of Stuttgart N87-10652
Problems of design for cities in the tropics N87-10653
Climatic factors in the siting of new towns and specialized urban facilities N87-10654
Design for climate in hot, dry cities N87-10655
Design for climate in hot, humid cities N87-10656

CIVIL AVIATION
Aircraft accident reports: Brief format US civil and foreign aviation, issue number 2 of 1985 accidents [PB86-916916] N87-10056

CLADDING
Investigations on the parameters for laser surface treatment by cladding and alloying [BMFT-FB-T-85-183] N87-10203

CLIMATE
The GSFC gound-based lidar for the measurement of stratospheric ozone N87-10371
Vertical modes and energetics of gravitational and rotational modes in a multilevel global spectral model N87-10633
The assessment of climatological impacts on agricultural production and residential energy demand N87-10666

CLIMATOLOGY
Climatology of gravity waves over Poker Flat, Alaska for 1983 N87-10454
Climatology of tropospheric vertical velocity spectra N87-10455
Mesospheric gravity-wave climatology at Adelaide N87-10456
The Adelaide MF partial-reflection radar and VHF ST radar N87-10490
Proceedings of the Technical Conference on Urban Climatology and its Applications with Special Regard to Tropical Areas [WMO-652] N87-10636
Urban climatology and the tropical city: An introduction N87-10637
Tropical urban climates: Review and assessment N87-10638
Air quality in tropical cities N87-10639
The urban climate of Mexico City N87-10640
Some aspects of the urban climate of Shanghai N87-10641
Some aspects of the urban climates of tropical Africa N87-10642
Some aspects of the urban climates of India N87-10643
Some aspects of the urban climates of tropical South America: The Brazilian contribution N87-10644
Urban climatological methods and data N87-10645
Urban climate models: Nature, limitations and applications N87-10646
The planning and maintenance of urban settlements to resist extreme climatic forces N87-10647
Urban hydrology in the tropics: Problems, solutions, data collection and analysis N87-10650
Energy related issues — urban climatology N87-10651
The introduction of climatology into the administration and development of planning in the city of Stuttgart N87-10652
Problems of design for cities in the tropics N87-10653
Climatic factors in the siting of new towns and specialized urban facilities N87-10654
Design for climate in hot, dry cities N87-10655
The assessment of climatological impacts on agricultural production and residential energy demand N87-10666

CLOUD COVER
The Lidar In-Space Technology Experiment (LITE) N87-10270

CLOUD HEIGHT INDICATORS
Cloud detection by lidar extinction calculations N87-10353

CLOUD PHYSICS
The NCAR Airborne Infrared Lidar System (NAILS) N87-10362
A modeling analysis program for the JPL Table Mountain Io sodium cloud data [NASA-CR-179671] N87-10811

CLOUDS
Airborne lidar observations of Arctic polar stratospheric clouds N87-10341
Investigation of clouds spatial distribution using ground-based lidar N87-10349
Near-IR extinction and backscatter coefficient measurements in low- and mid-altitude clouds N87-10351
Backscatter and extinction measurements in cloud and drizzle at CO2 laser wavelengths N87-10352
Radiation doses from flying through nuclear debris clouds [AD-A167959] N87-10711
A modeling analysis program for the JPL Table Mountain Io sodium cloud data [NASA-CR-179671] N87-10811

CLOUDS (METEOROLOGY)
Inversion of 2 wavelength Lidar data for cloud properties N87-10273
Determination of cloud microphysical properties by laser backscattering and extinction measurements N87-10293
Laboratory measurements of forward and backward scattering of laser beams in water droplet clouds N87-10295
Examples of mesoscale structures and short-term wind variations detected by VHF Doppler radar N87-10422
Observational studies of wave disturbances in the tropical Pacific and their relationship with deep cloud activity N87-10634
An observational study of tropical cloud cluster evolution and cyclogenesis in the Western North Pacific [CSU-ASP-403] N87-10661
Clouds and methane photochemical hazes on the outer planets N87-10815

CMOS
Factors contributing to static RAM cell transient upset [DE86-007710] N87-10715

COAXIAL CABLES
Coaxial tube tether/transmission line for manned nuclear space power [NASA-CASE-LEW-14338-1] N87-10174
High speed digital signal transmission over coaxial pairs between network termination and several terminals without variable equilization [FI-44-TBR-101] N87-10230

CODING
Methods and standards for encryption of spacecraft telemetry and telecommand links [RPT/ENC/62359/BO] N87-10112
Composite load spectra for select space propulsion structural components [NASA-CR-179496] N87-10176
Application of a potential code to general steady flows in three dimensions N87-10262
Adaptation of TSFOIL for Univac 1100/60H computer at NAL, Bangalore [AE-TB-9-83] N87-10718
ANL/RBC: A computer code for the analysis of Rankine bottoming cycles, including system cost evaluation and off-design performance [NASA-CR-179462] N87-10777

COEFFICIENTS
The use of the experimentally deduced Brunt-Vaisala frequency and turbulent velocity fluctuations to estimate the eddy diffusion coefficient N87-10450

COGNITION
Intelligent Computer Assisted Instruction (ICAI): Formative evaluation of two systems [NASA-CR-176873] N87-10716

COHERENT RADAR
Progress in coherent laser radar N87-10326
Remote sensing of atmospheric winds using a coherent, CW lidar and speckle-turbulence interaction N87-10329
Coherent lidar signal fluctuation reduction by means of frequency diversity technique N87-10360
Wavelength dependence of coherent and incoherent satellite-based lidar measurements of wind velocity and aerosol backscatter N87-10361
Atmospheric correlation time measurements using coherent CO2 lidar N87-10363
The Tukey algorithm for enhancing MST radar data N87-10521
The ARCAD 3-SAFARI coordinated study of auroral and polar F-region ionospheric irregularities N87-10600
Comparative magnetospheric/ionospheric studies using Dynamics Explorer spacecraft and ground-based radars N87-10602

COHERENT RADIATION
Coherent lidars based on intracavity heterodyning of echo signals N87-10308
Possibility of obtaining coherent short wave radiation from a solid state free electron laser [DE86-010525] N87-10381

COLD FRONTS
Convective structure of the planetary boundary layer of the ocean during gale N87-10300
Lidar observations and modeling of cold air outbreaks during MASEX and GALE N87-10336

COLD WORKING
Ultrasonic determination of recrystallization [NASA-TM-88855] N87-10399

COLLIMATION
The NOAA TOGA antenna array N87-10500

COLLISION RATES
Rotationally resolved collisional transfer rates in OH N87-10323

COLLISIONAL PLASMAS
Two dimensional analysis of high voltage solar array interfering with ionospheric plasma N87-10022

COLOR TELEVISION
An algorithm for the detection of signals by colour contrast on the screen of a colour cathode ray tube (colour display) — radarscopes [DRIC-T-7655] N87-10233

COLOR VISION
An algorithm for the detection of signals by colour contrast on the screen of a colour cathode ray tube (colour display) — radarscopes [DRIC-T-7655] N87-10233

COLUMBIA (ORBITER)
Summary of longitudinal stability and control parameters as determined from space shuttle Columbia flight test data [NASA-TM-87768] N87-10101

COMBUSTIBLE FLOW
Acta Aeronautica et Astronautica Sinica (selected articles) [AD-A167918] N87-10004

COMBUSTION CHAMBERS
Main chamber combustion and cooling technology study [NASA-CR-178853] N87-10175
Demonstration of laser speckle system on burner liner cyclic rig [NASA-CR-179509] N87-10377

COMBUSTION CHEMISTRY
Developing simplified models of combustion chemistry by simulation with detailed chemical kinetics models [DE86-006381] N87-10188

COMBUSTION STABILITY
Main chamber combustion and cooling technology study [NASA-CR-178853] N87-10175

COMFORT
Human comfort in the urban tropics N87-10649
Design for climate in hot, humid cities N87-10656

COMMERCIAL AIRCRAFT
Aircraft accident reports: Brief format US civil and foreign aviation, issue number 2 of 1985 accidents [PB86-916916] N87-10056

COMMUNICATION EQUIPMENT
The new space network: The tracking and data relay satellite system [NASA-EP-251] N87-10171

COMMUNICATION NETWORKS
Data communications and monitor for the Penn State University profiler network N87-10523

COMMUNICATION SATELLITES
Very first orbit determination after launch or main maneuvers. Applications to geostationary Telecom 1A and 1B N87-10135
Olympus: Apogee engine firing N87-10143
Optimal injection of TV SAT with multi-impulse apogee maneuvers with mission constraints and thrust uncertainties N87-10144
Stationkeeping for DFS-Kopernikus N87-10152
Stationkeeping strategy for TDF 1 satellite N87-10154
Eccentricity control strategy for geosynchronous communications satellites N87-10155
Geostationary satellites: Their market, their evolution in the 1990s N87-10165

COMPONENT RELIABILITY
Engine-transmission-structural airframe members compatibility N87-10069
Engine-airframe integration for rotorcraft: Component specifications and qualification N87-10071

COMPOSITE FUNCTIONS
Composite load spectra for select space propulsion structural components [NASA-CR-179496] N87-10176

COMPOSITE MATERIALS
Carbide/fluoride/silver self-lubricating composite [NASA-CASE-LEW-14196-1] N87-10179

COMPOSITE STRUCTURES
Investigation into the attenuation and velocity of acoustic emissions in carbon fiber composite aircraft structures [BAE-KGT-R-GEN-01349] N87-10180
Flight service evaluation of composite helicopter components [NASA-CR-178149] N87-10182

COMPRESSIBILITY
An asymptotic theory of supersonic turbulent interactions in a compression corner N87-10010

COMPRESSIBLE FLOW
Finite volume solution of the compressible boundary-layer equations [NASA-CR-4013] N87-10744

COMPRESSION LOADS
Fatigue response of notched laminates subjected to tension-compression cyclic loads
[NASA-CR-179804] N87-10183
Short-wavelength buckling and shear failures for compression-loaded composite laminates N87-10403
Growth of cracks under far-field cyclic compressive loads: Numerical and experimental results
[DE86-010279] N87-10416
COMPRESSOR ROTORS
An experimental investigation of end-wall flowfield of a compressor rotor N87-10244
COMPRESSORS
Response of a small-turboshaft-engine compression system to inlet temperature distortion
[NASA-TM-83765] N87-10100
COMPUTATION
Parallel logic programming for numeric applications
[DE86-011004] N87-10726
COMPUTATIONAL FLUID DYNAMICS
Numerical solution of the 3-dimensional boundary layer equations in the inverse mode using finite differences
N87-10005
Proceedings of the Symposium on Mechanics for Space Flight, 1985
[ISAS-SP-4] N87-10011
Report of the International Symposium on Computational Fluid Dynamics, Tokyo N87-10029
Computational aerodynamics of supersonic lifting vehicles N87-10030
Computational fluid mechanics utilizing the variational principle of modeling damping seals
[NASA-CR-178902] N87-10248
Mixed finite element methods in flow mechanics
N87-10741
Computational hydrodynamics in astrophysical studies: Highly shocked flows in 3 dimensions N87-10796
COMPUTER AIDED DESIGN
A rule based computer aided design system
[NASA-TM-86241] N87-10721
Pulse forming network design program for linear and time-varying loads for the IBM personal computer
[DE86-011209] N87-10727
COMPUTER AIDED MAPPING
Digital mapping: Fact or fiction
[AD-A167571] N87-10528
COMPUTER ASSISTED INSTRUCTION
Orbitography course for ground operators
N87-10157
Intelligent Computer Assisted Instruction (ICAI): Formative evaluation of two systems
[NASA-CR-176873] N87-10716
COMPUTER GRAPHICS
Images of three dimensional flows in computer graphics N87-10017
GRAPH 3: A digitizing and graph plotting program
[DE86-010628] N87-10722
Integrated testing and analysis of mathematical software tools. Summary of research activities, 1 August 1985-1 May 1986
[DE86-010662] N87-10723
PLOT 3D: A multipurpose, interactive program for plotting three dimensional graphs
[DE86-702101] N87-10730
COMPUTER NETWORKS
Proceedings of the 5th Annual Users' Conference
[NASA-CP-2399] N87-10720
Remote capabilities in computer networks
[RSRE-3947] N87-10732
COMPUTER PROGRAMMING
Programming of sensor based assembly robots
[KFK-PFT-120] N87-10396
Intelligent Computer Assisted Instruction (ICAI): Formative evaluation of two systems
[NASA-CR-176873] N87-10716
COMPUTER PROGRAMS
Computer simulation in engineering hydrodynamics
N87-10038
Composite load spectra for select space propulsion structural components
[NASA-CR-179496] N87-10176
A statistical model to estimate refractivity turbulence structure constant C sub n sup 2 in the free atmosphere
N87-10448
Adaptation of TSFOIL for Univac 1100/60H computer at NAL, Bangalore
[AE-TB-9-83] N87-10718
GRAPH 3: A digitizing and graph plotting program
[DE86-010628] N87-10722
Software process interpretation and software environments
[DE86-010881] N87-10725
Implementation and optimization of portable standard LISP for the CRAY
[DE86-008717] N87-10729
PLOT 3D: A multipurpose, interactive program for plotting three dimensional graphs
[DE86-702101] N87-10730
Issues in expert system aids for a large engineering simulation code
[DE86-009098] N87-10735
Mathematical model for the Bridgman-Stockbarger crystal growing system
[NASA-CR-178921] N87-10766
The ultraviolet spectra of DA white dwarfs
N87-10783
COMPUTER SYSTEMS DESIGN
Choosing Aircraft Integrated Data Systems (AIDS) architecture suitable for Engine Health Monitoring (EHM) on future generation engines N87-10083
Dynamic remapping decisions in multi-phase parallel computations
[NASA-CR-178174] N87-10719
Fault and error latency under real workload: An experimental study
[NASA-CR-179802] N87-10733
Study of UNIX and its suitability for the Air Force's WWMCCS Information System
[DE86-011293] N87-10771
COMPUTER SYSTEMS PERFORMANCE
Parallel logic programming for numeric applications
[DE86-011004] N87-10726
COMPUTER SYSTEMS PROGRAMS
Software for flight recorder data processing developed by Lufthansa N87-10090
Extension of the electromagnetic method of moments code CHAOS to treat configurations of dielectric-coated wires
[AWRE-O-18/85] N87-10234
Software process interpretation and software environments
[DE86-010881] N87-10725
Computational methods and software for differential equations and their applications
[DE86-010231] N87-10746
Computer software evaluation methodology and data base management system selection
[DE86-011343] N87-10772
COMPUTER TECHNIQUES
Computer assisted gas chromatography for thermodynamic measurements of polymer surfaces
[AD-A167450] N87-10206
Generation of attenuation corrected images from lidar data N87-10367
An accelerated forth data-acquisition system
N87-10516
Data communications and monitor for the Penn State University profiler network N87-10523
Digital mapping: Fact or fiction
[AD-A167571] N87-10528
COMPUTERIZED SIMULATION
Computer simulation in engineering hydrodynamics
N87-10038
Stationkeeping strategy test, design and optimization by computer simulation — geostationary satellites
N87-10153
Developing simplified models of combustion chemistry by simulation with detailed chemical kinetics models
[DE86-008381] N87-10188
Review of VHF Band 1 field strength prediction
[BBC-RD-1986/4] N87-10223
MODTEQ (Modulation Techniques), AN/FRC-170(V), equalization, and channel medium simulations
[AD-A167965] N87-10226
Electronics Engineering Department technical review
[DE86-011371] N87-10241
Absorption heat pump simulation and studies: a modular computer simulation of absorption systems
[DE86-011206] N87-10256
Detailed transient model of a liquid-metal heat pipe
[DE86-011212] N87-10257
Influence of Rayleigh-Doppler broadening on the selection of H2O dial system parameters N87-10287
An all-purpose computer program for lidar simulations and reduction of lidar data N87-10299
Optimal filtration of the atmospheric parameters profiles N87-10305
Overtone production of soft x-rays with free-electron lasers
[DE86-011248] N87-10383
WEST-3 wind turbine simulator development. Volume 2: Verification
[NASA-CR-174982] N87-10531
Radiation doses from flying through nuclear debris clouds
[AD-A167959] N87-10711
Factors contributing to static RAM cell transient upset
[DE86-007710] N87-10715
Pulse forming network design program for linear and time-varying loads for the IBM personal computer
[DE86-011209] N87-10727
Issues in expert system aids for a large engineering simulation code
[DE86-009098] N87-10735
Physical processes in collapse driven supernova
N87-10808
COMPUTERS
Design guidelines for human-computer dialogues
[DE86-011543] N87-10728
CONCENTRATION (COMPOSITION)
Laboratory evaluation of three passive CO concentration monitors
[PML-1985-13] N87-10538
CONDUCTIVE HEAT TRANSFER
An analysis of the performance of a vertically oriented, gas loaded, variable conductance heat pipe
[AD-A167874] N87-10250
CONFERENCES
Report of the International Symposium on Computational Fluid Dynamics, Tokyo N87-10029
Doppler Radar Detection of Wind Shear
[NASA-CP-2435] N87-10054
Proceedings of the 13th Symposium on Aircraft Integrated Data Systems
[DFVLR-MITT-86-04] N87-10075
Proceedings of an International Conference on Space Dynamics for Geostationary Satellites
[ISBN-2-85428-149-7] N87-10113
Thirteenth International Laser Radar Conference
[NASA-CP-2431] N87-10263
Assessment of dial data collection and analysis techniques N87-10281
Results of the ARCAD 3 Project and of Recent Programs in Magnetospheric and Ionospheric Physics — conferences
[ISBN-2-85428-126-8] N87-10541
Proceedings of the Technical Conference on Urban Climatology and its Applications with Special Regard to Tropical Areas
[WMO-652] N87-10636
Proceedings of 2nd International Conference on Space Physiology
[ESA-SP-237] N87-10675
CONGRESSIONAL REPORTS
Department of Housing and Urban Development-Independent Agencies Appropriation Bill, 1987
[S-REPT-99-487] N87-10773
National Aeronautics and Space Administration Authorization Act, 1987 N87-10775
CONICAL FLOW
Technical overview of plume radiation from a solid rocket motor N87-10021
Supersonic flow around tip sides of wings
N87-10033
CONICAL NOZZLES
Far field noise studies of contoured and solid/porous conical plug-nozzle jet flows N87-10049
CONICS
Artificial ion beam interaction with the auroral plasma
N87-10591
CONSTRAINTS
Guidebook for analysis of tether applications
[NASA-CR-178904] N87-10169
CONTAMINATION
Response of a small-turboshaft-engine compression system to inlet temperature distortion
[NASA-TM-83765] N87-10100
CONTINENTAL SHELVES
The internal tide off southern California
[AD-A167722] N87-10672
CONTINUITY (MATHEMATICS)
Numerical study of hydrogen-air supersonic combustion by using elliptic and parabolized equations
[NASA-CR-179800] N87-10187
CONTINUOUS RADIATION
Nonthermal continuum-terrestrial myriametric radiation narrowband electromagnetic emission N87-10579
CONTINUOUS SPECTRA
Periodic amplitude variations in Jovian continuum radiatior:
[NASA-CR-177070] N87-10813
CONTINUUM MECHANICS
Periodic amplitude variations in Jovian continuum radiation
[NASA-CR-177070] N87-10813
CONTINUUM MODELING
Constitutive relations for flow of a non-Newtonian fluid through saturated porous media
[DE86-702035] N87-10261
CONTRACTION
Functions of skeletal muscles of rats and monkeys after 5-day space flight (on Cosmos 1514) N87-10686
CONTRAST
A system for controlled presentation of the Arden contrast sensitivity test
[AD-A167969] N87-10712

CONTROL EQUIPMENT
A single-board preprocessor and pulse generator N87-10517
A microprogrammable radar controller N87-10518
CONTROL SURFACES
The effect of free stream disturbances and control surface deflections on the performance of the Wortmann airfoil at low Reynolds numbers N87-10007
Prediction of gust loadings and alleviation at transonic speeds
[AD-A167748] N87-10047
Tunnel interference from pressure measurements on control surfaces
[AE-TM-8-83] N87-10104
CONTROL SYSTEMS DESIGN
Performance monitoring of sensors in high reliable flight control systems using deterministic observers N87-10087
Technology review of flight crucial flight control systems (application of optical technology)
[NASA-CR-172332] N87-10102
A new three-axis control system for a geosynchronous satellite in transfer orbit N87-10139
Reliability issues in active control of large flexible space structures
[NASA-CR-179785] N87-10167
Control of large flexible space structures
[NASA-CR-177063] N87-10168
Electronics Engineering Department technical review
[DE86-011371] N87-10241
Dynamic modeling and control of robotic manipulators N87-10390
Fault tolerant control laws
[NASA-CR-178094] N87-10400
Controller design via structural reduced modeling by FETM
[NASA-CR-179838] N87-10408
CONTROLLERS
Experimental identification and control of the tip position of a flexible, single link manipulator N87-10397
Controller design via structural reduced modeling by FETM
[NASA-CR-179838] N87-10408
FORPS: A FORTH-based production system and its application to a real-time robot control problem
[DE86-005426] N87-10734
CONVECTION
Hardware requirements: A new generation partial reflection radar for studies of the equatorial mesosphere N87-10431
Case studies of the structure of the atmospheric boundary layer entrainment zone N87-10627
Observational studies of wave disturbances in the tropical Pacific and their relationship with deep cloud activity N87-10634
CONVERGENCE
The local convergence of Ritz and Galerkin methods for nonlinear problems N87-10737
COOLING
Operating characteristics of cooling underground power cables using up sloped long heat pipes in conduit N87-10028
COOLING SYSTEMS
Advanced desiccant materials research
[DE86-010695] N87-10536
COPOLYMERS
Synthesis of energetic materials
[AD-A167787] N87-10214
CORRELATION
Transverse correlations in start-up of a free electron laser from noise
[DE86-009917] N87-10380
Comparison of medium frequency pulsed radar interferometer and correlation analysis winds, part 1 N87-10474
CORROSION RESISTANCE
Pressure-resistant plane disc viewports from allyl diglycol carbonate plastic for hyperbaric chambers
[AD-A168007] N87-10105
Castable hot corrosion resistant alloy
[NASA-CASE-LEW-14134-1] N87-10192
CORROSION TESTS
Pressure-resistant plane disc viewports from allyl diglycol carbonate plastic for hyperbaric chambers
[AD-A168007] N87-10105
Surface attack on metals in the presence of liquid metals
[AD-A167403] N87-10193
CORTISONE
Anticortisol monoclonal antibodies: Characterization of their specificity N87-10680
COSMIC DUST
The effect of a quasi-stellar object on its host galaxy: Dynamical and physical processes in the interstellar medium around a QSO N87-10797
Gas and dust in regions of recent star formation N87-10800
COSMIC RAYS
Solar-geophysical data number 501, May 1986. Part 1: (Prompt reports). Data for April 1986, March 1986 and late data
[PB86-218039] N87-10623
Amplitude distribution of cosmic ray events in extrinsic IR detectors
[AD-A167692] N87-10819
Cosmic-ray hadrons underground
[DE86-011334] N87-10822
COSMOLOGY
Possible significance of a new dimensionless ratio in cosmology
[DE86-011026] N87-10801
Particle theory and cosmology
[DE86-010366] N87-10802
COSMONAUTS
The interest of centrifuge tests for the selection of French cosmonauts N87-10678
COSMOS SATELLITES
Cosmos 1514 flight: Study of rhesus monkey ECG N87-10707
The state of bones of pregnant rats during an acute stage of adaptation to weightlessness N87-10708
COST EFFECTIVENESS
Influence of engine variables on future helicopter systems N87-10072
COST ESTIMATES
Review of storage battery system cost estimates
[DE86-011182] N87-10537
COUNTERMEASURES
Flash/crazing effects on simulator pursuit tracking performance
[AD-A167689] N87-10759
COUPLING
New solution of the problem of EMP coupling on cables over ground of finite conductivity
[DE86-006078] N87-10229
Consequences of imperfect magnetosphere-ionosphere coupling N87-10549
Magnetospheric-ionospheric coupling deduced from measurements above a discrete auroral arc N87-10550
CRACK CLOSURE
Growth of cracks under far-field cyclic compressive loads: Numerical and experimental results
[DE86-010279] N87-10416
CRACK INITIATION
Fatigue response of notched laminates subjected to tension-compression cyclic loads
[NASA-CR-179804] N87-10183
CRACK PROPAGATION
Grain boundary segregation and environmentally-induced fracture of materials
[DE86-010219] N87-10195
Dynamic delamination crack propagation in a graphite/epoxy laminate N87-10402
The effects of temperature and loading rate on R-curves using the CLWL techniques — crack growth resistance curve (R curve); crack line wedge load (CLWL)
[BAE-MSM-R-GEN-0544] N87-10405
Further results on the initiation and growth of adiabatic shear bands
[AD-A168012] N87-10412
Growth of cracks under far-field cyclic compressive loads: Numerical and experimental results
[DE86-010279] N87-10416
CRACK TIPS
Crack-tip fields in a viscoplastic material
[AD-A168014] N87-10413
CRASH LANDING
Aircraft accident reeport, Delta Air Lines, Inc., Lockheed L-1011-385-1, N726DA, Dallas/Fort Worth International Airport, Texas, August 2, 1985
[PB86-910406] N87-10053
The Boeing B 720 aircraft Controlled Impact Demonstration (CID): Flight data recorder/cockpit voice recorder experiment N87-10096
United States Navy - Canadian Forces solid state flight data recorder/crash position locator experiment on the B-720 controlled impact demonstration N87-10097
CRASHWORTHINESS
Crashworthiness experiment summary full-scale transport controlled impact demonstration program
[DOT/FAA/CT-85/20] N87-10055
Aircraft accident reports: Brief format US civil and foreign aviation, issue number 2 of 1985 accidents
[PB86-916916] N87-10056
The Boeing B 720 aircraft Controlled Impact Demonstration (CID): Flight data recorder/cockpit voice recorder experiment N87-10096
CRAY COMPUTERS
Implementation and optimization of portable standard LISP for the CRAY
[DE86-008717] N87-10729
CREEP PROPERTIES
Experimental procedure for lifetime testing of graphite bundles under constant load
[AD-A167714] N87-10186
CREW STATIONS
Human factors research in aircrew performance and training
[AD-A167950] N87-10714
CRITICAL LOADING
The effects of temperature and loading rate on R-curves using the CLWL techniques — crack growth resistance curve (R curve); crack line wedge load (CLWL)
[BAE-MSM-R-GEN-0544] N87-10405
CROP GROWTH
The assessment of climatological impacts on agricultural production and residential energy demand N87-10666
CROSS CORRELATION
Investigations on a digital bit synchronizer for a detailed flight data recovery N87-10099
Atmospheric contributions to the column variance in direct-detection dial N87-10289
Nonlinear optics with broad-band lasers
[DE86-011286] N87-10382
CROSS FLOW
Numerical studies of a tubulent jet in crossflow N87-10243
Transient behavior of liquid jets injected normal to a high velocity gas stream N87-10246
CRYOGENIC EQUIPMENT
Cryogenic resonant-mass gravitational wave detectors N87-10609
CRYPTOGRAPHY
Methods and standards for encryption of spacecraft telemetry and telecommand links
[RPT/ENC/62359/BO] N87-10112
CRYSTAL DEFECTS
Workshop on the Physics and Chemistry of Solar-Flux Effects on Condensed Phase/Gas Interfaces
[DE86-004460] N87-10817
CRYSTAL GROWTH
Mathematical model for the Bridgman-Stockbarger crystal growing system
[NASA-CR-178921] N87-10766
Interface properties and crystal-growth mechanisms
[DE86-010646] N87-10767
CRYSTAL LATTICES
Possibility of obtaining coherent short wave radiation from a solid state free electron laser
[DE86-010525] N87-10381
CRYSTAL OSCILLATORS
A variable-frequency local oscillator for the frequency-hopping technique N87-10515
CRYSTAL STRUCTURE
A method of estimating the molecular weight of polymeric materials
[NASA-CASE-LAR-13212-1] N87-10206
Sulfur-based synthetic metal superconductors
[DE86-010512] N87-10768
CUMULUS CLOUDS
Turbulent mixing, droplet spectral evolution and dynamics of warm cumulus clouds N87-10667
CURING
Polymer systems for rapid sealing of aircraft structures at low temperature
[AD-A167667] N87-10209
CURRENT DENSITY
Relationship between critical current and microstructure of internal tin wire
[DE86-009922] N87-10238
Transverse correlations in start-up of a free electron laser from noise
[DE86-009917] N87-10380
Fine structure of fields and plasma in the field-aligned current region on the Intercosmos-Bulgaria-1300 satellite data N87-10568
A study of disturbed solar wind and magnetotail based on ISEE-3 data
[NASA-CR-177060] N87-10816
CURRENT DISTRIBUTION
Models of electric potential and current distribution in stable discrete auroral forms N87-10551
CURVE FITTING
Modeling and analysis of spacecraft power systems N87-10173
CYCLIC LOADS
Growth of cracks under far-field cyclic compressive loads: Numerical and experimental results
[DE86-010279] N87-10416
CYCLONES
An observational study of tropical cloud cluster evolution and cyclogenesis in the Western North Pacific
[CSU-ASP-403] N87-10661
Relationships between available potential energy, kinetic energy and extratropical cyclones within limited regions of the Northern Hemisphere during the FGGE Year N87-10668

CYCLOTRON RADIATION
The cyclotron maser theory of AKR and Z-mode radiation — Auroral Kilometric Radiation (AKR) N87-10578
Plasma wave observations at Uranus from Voyager 2 [NASA-CR-177069] N87-10814
CYLINDRICAL BODIES
Vortex shedding of a square cylinder in front of a slender airfoil at high Reynolds numbers. Part 1: Spacing effect [MPIS-23/1985] N87-10048
CYLINDRICAL SHELLS
Concentrations of plastic strains in the clamping region of cylindrical shells under excessive loading [KFK-3915] N87-10417

D

D REGION
Interference detection and correction applied to incoherent-scatter radar power spectrum measurement N87-10520
DATA ACQUISITION
Experimental study of the boundary layer on a low Reynolds number airfoil in steady and unsteady flow N87-10052
Airline data acquisition in an ACARS environment N87-10092
Assesment of dial data collection and analysis techniques N87-10281
Recent progress in the Urbana MST radar N87-10485
Colorado wind profilers N87-10486
The first operation and results of the Chung-Li VHF radar N87-10495
An overview of data acquisition, signal coding and data analysis techniques for MST radars N87-10512
An accelerated forth data-acquisition system N87-10516
In-flight absolute radiometric calibration of the LANDSAT thematic mapper N87-10530
DATA BASE MANAGEMENT SYSTEMS
Database algorithms for multiprocessor and very large memory systems [DE86-009406] N87-10724
Computer software evaluation methodology and data base management system selection [DE86-011343] N87-10772
DATA BASES
Archival of Poker Flat MST radar data N87-10524
MST data exchange through the NCAR incoherent-scatter radar data base N87-10525
Database algorithms for multiprocessor and very large memory systems [DE86-009406] N87-10724
DATA COMPRESSION
Data compression techniques for multifunction flight data recorders N87-10094
DATA LINKS
The air/ground transfer of aircraft integrated data systems (AIDS) for Air Traffic Control (ATC) purposes: Present experiments and possible future intentions N87-10091
DATA PROCESSING
Data recovery techniques, an update — flight data N87-10089
Software for flight recorder data processing developed by Lufthansa N87-10090
Observations of vertical velocity power spectra with the SOUSY VHF radar N87-10465
The PROUST radar N87-10491
An example of scaling MST Doppler spectra using median spectra, spectral smoothing, and velocity tracing N87-10519
Remote capabilities in computer networks [RSRE-3947] N87-10732
Study of UNIX and its suitability for the Air Force's WWMCCS Information System [DE86-011293] N87-10771
DATA RECORDING
Data compression techniques for multifunction flight data recorders N87-10094
DATA REDUCTION
Correction function in the Lidar equation and the solution techniques for CO2 Lidar date reduction N87-10280
Assesment of dial data collection and analysis techniques N87-10281
An overview of data acquisition, signal coding and data analysis techniques for MST radars N87-10512
DATA SMOOTHING
An example of scaling MST Doppler spectra using median spectra, spectral smoothing, and velocity tracing N87-10519
The Tukey algorithm for enhancing MST radar data N87-10521
DATA STORAGE
Archival of Poker Flat MST radar data N87-10524
DATA SYSTEMS
Study of UNIX and its suitability for the Air Force's WWMCCS Information System [DE86-011293] N87-10771
DATA TRANSMISSION
The new space network: The tracking and data relay satellite system [NASA-EP-251] N87-10171
Plasma wave observations at Uranus from Voyager 2 [NASA-CR-177069] N87-10814
DECISION MAKING
Use of fuzzy sets mathematics to assist pavement evaluation and management (revised March 18, 1986) [PB86-214798] N87-10747
DEFENSE PROGRAM
Air Force technical objective document fiscal year 1987 [AD-A167324] N87-10779
Aeronautics and space report of the President [NASA-TM-89239] N87-10827
DEFLAGRATION
Percussion primer/DDT detonator [DE86-010477] N87-10217
DEFLECTION
High precision absolute laser power measurements using a magnetically suspended rotor [DE86-011585] N87-10389
DEFLECTORS
Experimental and theoretical investigations of the flow field of an airfoil with a deflected spoiler N87-10050
DEFORMATION
Deformation behavior of powder metallurgy Ni Al-Hf-B [DE86-011506] N87-10201
DELAMINATING
Dynamic delamination crack propagation in a graphite/epoxy laminate N87-10402
Mode 1 delamination growth in adhesively bonded joints under static and fatigue loads [NASA-CR-179812] N87-10409
DELTA WINGS
Analysis of the vortical flow around a 60 deg Delta wing with vortex flap N87-10006
DENSITY MEASUREMENT
The Lidar In-Space Technology Experiment (LITE) N87-10270
DESALINIZATION
Thermopervaporation device [DE86-011151] N87-10255
DESICCANTS
Advanced desiccant materials research [DE86-010695] N87-10536
DESIGN ANALYSIS
Development of a turbomachinery design optimization procedure using a multiple-parameter nonlinear perturbation method [NASA-CR-3831] N87-10003
Main chamber combustion and cooling technology study [NASA-CR-178853] N87-10175
Problems of design for cities in the tropics N87-10653
Design for climate in hot, dry cities N87-10655
Design for climate in hot, humid cities N87-10656
DETECTION
Cryogenic resonant-mass gravitational wave detectors N87-10609
DETONATION
Simple blast model for structural design [DE86-000802] N87-10414
DETONATORS
Numerical model of the thermal processes leading to ignition in a pyrotechnic device [DE86-009626] N87-10189
Percussion primer/DDT detonator [DE86-010477] N87-10217
CP DDT detonators. 5: Output performance and analysis of multiple-out devices [DE86-010995] N87-10219
DIELECTRICS
The study of microstrip antenna arrays and related problems [NASA-CR-179714] N87-10225
Extension of the electromagnetic method of moments code CHAOS to treat configurations of dielectric-coated wires [AWRE-O-18/85] N87-10234
Wire dipoles and antennas with dielectric or magnetic coatings [AWRE-O-19/85] N87-10235
Linewidth characteristics of Raman-shifted dye laser output at 720 and 940 nm N87-10372
DIESEL ENGINES
Cold-start tests with speed diesel engines using alcohol as main fuel [DE86-751651] N87-10392
DIFFERENCE EQUATIONS
The third order compact schemes for fluid dynamic problems N87-10032
DIFFERENTIAL EQUATIONS
Aeroelastic stability of composite rotor blades in hover N87-10060
DIFFUSION
Diffusion approximation for modeling of 3-D radiation distributions [DE86-000810] N87-10228
Multiple scattering of laser beams in dense hydrosols N87-10316
DIFFUSION ELECTRODES
Surface attack on metals in the presence of liquid metals [AD-A167403] N87-10193
DIGITAL DATA
Airline data acquisition in an ACARS environment N87-10092
DIGITAL SYSTEMS
Computer assisted gas chromatography for thermodynamic measurements of polymer surfaces [AD-A16745[illegible] N87-10208
Digital mapping: Fact or fiction [AD-A167571] N87-10528
DIMENSIONLESS NUMBERS
Possible significance of a new dimensionless ratio in cosmology [DE86-011026] N87-10601
DIODES
The TFP and a pulsed LD: New lidar components N87-10374
DIPOLE ANTENNAS
Wire dipoles and antennas with dielectric or magnetic coatings [AWRE-O-19/85] N87-10235
Method to determine the optimal parameters of the Arecibo 46.8-MHz antenna system N87-10510
DIRECTIONAL ANTENNAS
Measurements of antenna polar diagrams and efficiencies using a phase-switched interferometer N87-10507
Use of the Sun to determine pointing of ST radar beams N87-10508
DISCRETE FUNCTIONS
A description of a turbulent flow past a circular cylinder by a discrete vortex method N87-10014
DISPERSION
Possibility of measuring gravity-wave momentum flux by single beam observation of MST radar N87-10458
DISPLACEMENT
Current enhancement for hose-unstable electron beams [AD-A167804] N87-10755
DISPLAY DEVICES
Design guidelines for human-computer dialogues [DE86-011543] N87-10728
DISTILLATION
Permeation membrane-type distiller [DE86-011153] N87-10254
DISTRIBUTION (PROPERTY)
Emission-line galaxies toward the Bootes void N87-10607
DOPPLER EFFECT
Influence of Rayleigh-Doppler broadening on the selection of H2O dial system parameters N87-10287
Correction of Doppler-broadened Rayleigh backscattering effects in H2O dial measurements N87-10288
Doppler effects on velocity spectra observed by MST radars N87-10464
Mesospheric wind measurements using a medium-frequency imaging Doppler interferometer N87-10476
DOPPLER RADAR
Doppler Radar Detection of Wind Shear [NASA-CP-2435] N87-10054
State/orbit estimation from real Doppler data for solid apogee motor burning phase of geostationary satellite N87-10129
Experimental and theoretical Doppler-lidar signatures of aircraft wake vortices N87-10330
Calibration and analysis for a 0.53 micron incoherent Doppler lidar N87-10365
A theory for the retrieval of virtual temperature from winds, radiances and the equations of fluid dynamics N87-10421
Examples of mesoscale structures and short-term wind variations detected by VHF Doppler radar N87-10422
Measurements of precipitating atmosphere by the MU radar N87-10426
Performance characteristics of wind profiling radars N87-10429
A look at profiler performance N87-10430
A model for gravity-wave spectra observed by Doppler sounding systems N87-10434

Tropospheric turbulence parameters measured by using the MU radar N87-10436

Observations of thunder with the Arecibo VHF radar N87-10444

Possibility of measuring gravity-wave momentum flux by single beam observation of MST radar N87-10458

Methods for verifying the accuracy of wind profiles N87-10471

Scientific reasons for a network of ST radars and cooperative campaigns N87-10480

Progress in existing and planned MST radars N87-10481

The proposed flatland radar N87-10482

Current status of the Poker Flat MST radar N87-10483

Recent progress in the Urbana MST radar N87-10485

Colorado wind profilers N87-10486

Wind profiler demonstration system N87-10487

The Penn State Doppler network progress report N87-10489

The Adelaide MF partial-reflection radar and VHF ST radar N87-10490

The PROUST radar N87-10491

The Provence ST radar N87-10492

The INSU and DMN network of ST radars N87-10493

Investigations of the lower and middle atmosphere at the Arecibo Observatory and a description of the new VHF radar project N87-10494

The first operation and results of the Chung-Li VHF radar N87-10495

Progress in the MF radar system at Saskatoon N87-10496

System aspects of the Indian MST radar facility N87-10497

HISCAT: A proposed new scatter facility in Northern Scandinavia N87-10498

Phased-array design for MST and ST radars N87-10499

Determination of U, V, and W from single station Doppler radar radial velocities N87-10502

The elimination of a class of pseudo echoes by an improved T/R switch technique N87-10511

An overview of data acquisition, signal coding and data analysis techniques for MST radars N87-10512

Optimum coding techniques for MST radars N87-10513

An example of scaling MST Doppler spectra using median spectra, spectral smoothing, and velocity tracing N87-10519

The Tukey algorithm for enhancing MST radar data N87-10521

Data communications and monitor for the Penn State University profiler network N87-10523

NASA and FAA launch wind shear research project [NASA-NEWS-REL-86-143] N87-10659

Further studies with data collected by NASA's airborne Doppler lidar in Oklahoma in 1981 [NASA-CR-179779] N87-10660

DOSAGE

Anticortisol monoclonal antibodies: Characterization of their specificity N87-10680

DRAG

Observations and a model of gravity-wave variability in the middle atmosphere N87-10453

DRAINAGE

Urban hydrology in the tropics: Problems, solutions, data collection and analysis N87-10650

DROP SIZE

Transient behavior of liquid jets injected normal to a high velocity gas stream N87-10246

DUCTS

Experimental evidence of field-aligned ELF plasma ducts in the ionospheric trough and in the auroral zone N87-10574

Fundamental investigations of the finite element solutions for acoustic propagation in ducts [NASA-CR-179845] N87-10751

DYE LASERS

Pulsed mononode dye laser developed for a geophysical application N87-10364

Linewidth characteristics of Raman-shifted dye laser output at 720 and 940 nm N87-10370

Linewidth characteristics of Raman-shifted dye laser output at 720 and 940 nm N87-10372

Nonlinear optics with broad-band lasers [DE86-011286] N87-10382

DYNAMIC CONTROL

A space station Structures and Assembly Verification Experiment, SAVE [NASA-TM-89004] N87-10170

Structural optimization for control of stiffened laminated composite plates using nonlinear mixed integer programming N87-10181

Dynamic modeling and control of robotic manipulators N87-10390

DYNAMIC LOADS

Response of a 3-layered ring to an axisymmetric impulse [DE86-011016] N87-10415

DYNAMIC MODELS

Telecom-1 dynamic simulator N87-10160

Reliability issues in active control of large flexible space structures [NASA-CR-179785] N87-10167

Dynamic modeling and control of robotic manipulators N87-10390

DYNAMIC RESPONSE

Free vibration and dynamic response analysis of spinning structures [NASA-CR-179672] N87-10717

DYNAMIC STRUCTURAL ANALYSIS

Study about the structural behavior of WStE-36N steel [DE86-702011] N87-10394

A Taylor-Galerkin finite element algorithm for transient nonlinear thermal-structural analysis [NASA-CR-177064] N87-10406

Dynamics and control of orbiting grid and the synchronously deployable beam [NASA-CR-179808] N87-10410

Free vibration and dynamic response analysis of spinning structures [NASA-CR-179672] N87-10717

DYNAMICAL SYSTEMS

Dynamic delamination crack propagation in a graphite/epoxy laminate N87-10402

Flow dynamics and stability in severe rainbands N87-10669

Null surface dynamics N87-10770

Pulse timing and neutron star structure N87-10799

DYNAMICS EXPLORER 1 SATELLITE

De-1/Siple VLF wave-injection experiments N87-10586

Comparative magnetospheric/ionospheric studies using Dynamics Explorer spacecraft and ground-based radars N87-10602

DYNAMICS EXPLORER 2 SATELLITE

Comparative magnetospheric/ionospheric studies using Dynamics Explorer spacecraft and ground-based radars N87-10602

E

E REGION

The E region instabilities in the polar ionosphere N87-10599

Comparative magnetospheric/ionospheric studies using Dynamics Explorer spacecraft and ground-based radars N87-10602

Self-consistent analysis of high drift velocity measurements with the Scandinavian Twin Auroral Radar Experiment (STARE) system N87-10606

EARTH ATMOSPHERE

A statistical model to estimate refractivity turbulence structure constant C sub n sup 2 in the free atmosphere N87-10448

Possibility of measuring gravity-wave momentum flux by single beam observation of MST radar N87-10458

EARTH OBSERVATIONS (FROM SPACE)

Lidar remote sensing from space: NASA's plans in the Earth sciences N87-10265

Tunable solid-state laser technology for applications to scientific and technological experiments from space N87-10266

Coherent lidar technology for global wind profiling N87-10267

Development of a high-altitude airborne dial system: The Lidar Atmospheric Sensing Experiment (LASE) N87-10268

MIE Lidar proposed for the German Space Shuttle Mission D2 N87-10269

Space imaging radar for remote sensing of the Earth: An evaluation [BMFT-FB-W-85-024] N87-10529

EARTH ORBITS

DMA (Defense Mapping Agency) orbit determination for transit satellites: 1985 [AD-A167567] N87-10108

EARTH PLANETARY STRUCTURE

World geodetic system 1984 [AD-A167570] N87-10527

EARTHQUAKES

Earthquake effects in the ionosphere according to Intercosmos-19 and AUREOL-3 satellite data N87-10588

Study of VLF emissions apparently associated with earthquakes from ground-based and GEOS satellites data N87-10589

ECCENTRICITY

Efficiency eccentricity control using continuous, vectored thrusting for satellites with large area/mass ratios N87-10151

Eccentricity control strategy for geosynchronous communications satellites N87-10155

ECHO SUPPRESSORS

The elimination of a class of pseudo echoes by an improved T/R switch technique N87-10511

ECONOMIC ANALYSIS

Review of storage battery system cost estimates [DE86-011182] N87-10537

ECONOMICS

The assessment of climatological impacts on agricultural production and residential energy demand N87-10666

EDDY CURRENTS

An eddy-current model for three-dimensional nondestructive evaluation of advanced composites [AD-A167688] N87-10185

EDITING ROUTINES (COMPUTERS)

Computational methods and software for differential equations and their applications [DE86-010231] N87-10746

EDUCATION

Human factors research in aircrew performance and training [AD-A167950] N87-10714

Intelligent Computer Assisted Instruction (ICAI): Formative evaluation of two systems [NASA-CR-176873] N87-10716

EFFICIENCY

Methods of testing to determine the thermal performance of solar collectors [DE86-009311] N87-10533

EINSTEIN EQUATIONS

Null surface dynamics N87-10770

EISCAT RADAR SYSTEM (EUROPE)

Energy spectra of electrons precipitating above the EISCAT area. Comparison with ARCAD measurements N87-10598

ELASTIC PROPERTIES

Foundation interaction problems involving an elastic half-plane [AD-A167925] N87-10411

Crack-tip fields in a viscoplastic material [AD-A168014] N87-10413

Simple blast model for structural design [DE86-000802] N87-10414

ELECTRIC CONDUCTORS

Electrical circuit modeling of conductors with skin effect [DE86-011085] N87-10240

ELECTRIC CONTACTS

Cross-contact chain [NASA-CASE-NPO-16784-1] N87-10231

ELECTRIC CURRENT

Electrical circuit modeling of conductors with skin effect [DE86-011085] N87-10240

ELECTRIC FIELDS

Plasma sheet boundary electric fields during substorms N87-10548

Fine structure of fields and plasma in the field-aligned current region on the Intercosmos-Bulgaria-1300 satellite data N87-10568

Small scale structures of electric field variations and particle precipitations as observed onboard AUREOL-3 satellite N87-10569

Simultaneous observations of Pc4 and Pc5 electric fields in the noon sector with GEOS-1 and GEOS-2 N87-10597

Comparison of the coupling of grounded and ungrounded humans to vertical 60-Hz electric fields [DE86-011140] N87-10713

ELECTRIC MOTOR VEHICLES

Evaluation of a new type stable nickel-zinc battery for electric vehicle application [DE86-010895] N87-10534

ELECTRIC MOTORS

Process control in arc welding [KFK-PFT-105] N87-10395

ELECTRIC POTENTIAL

Models of electric potential and current distribution in stable discrete auroral forms N87-10551

ELECTRIC POWER SUPPLIES

Experience with the application of photovoltaics devices [DE86-010472] N87-10535

ELECTRIC PULSES

Pulse forming network design program for linear and time-varying loads for the IBM personal computer [DE86-011209] N87-10727

ELECTRIC WIRE
Extension of the electromagnetic method of moments code CHAOS to treat configurations of dielectric-coated wires
[AWRE-O-18/85] N87-10234
Wire dipoles and antennas with dielectric or magnetic coatings
[AWRE-O-19/85] N87-10235
ELECTRICAL ENGINEERING
Electronics Engineering Department technical review
[DE86-011371] N87-10241
A summary of the Foundation Research Program, fiscal year 1985
[AD-A168009] N87-10780
ELECTRICAL GROUNDING
Comparison of the coupling of grounded and ungrounded humans to vertical 60-Hz electric fields
[DE86-011140] N87-10713
ELECTRICAL IMPEDANCE
Electrical circuit modeling of conductors with skin effect
[DE86-011085] N87-10240
ELECTRICAL MEASUREMENT
Electrical circuit modeling of conductors with skin effect
[DE86-011085] N87-10240
Electrical measurement techniques for pulsed high current electron beams
[DE86-010980] N87-10756
ELECTRICAL PROPERTIES
Theoretical studies on the structures of insulating and metallic glasses
[DE86-011484] N87-10212
Current enhancement for hose-unstable electron beams
[AD-A167804] N87-10755
Sulfur-based synthetic metal superconductors
[DE86-010512] N87-10768
ELECTRICAL RESISTIVITY
New solution of the problem of EMP coupling on cables over ground of finite conductivity
[DE86-006078] N87-10229
Comparison of the coupling of grounded and ungrounded humans to vertical 60-Hz electric fields
[DE86-011140] N87-10713
ELECTRO-OPTICS
Technology review of flight crucial flight control systems (application of optical technology)
[NASA-CR-172332] N87-10102
ELECTROCARDIOGRAPHY
Cosmos 1514 flight: Study of rhesus monkey ECG
N87-10707
ELECTRODES
Process for preparing nickel coatings in conducting, porous bodies, especially for battery electrodes
[DE86-901439] N87-10200
ELECTRODYNAMICS
Guidebook for analysis of tether applications
[NASA-CR-178904] N87-10169
ELECTROHYDRODYNAMICS
The numerical method of calculation of two-dimensional stationary electro-gasdynamic internal flows N87-10037
Coordinated data on auroral electrodynamics from ground based radar diagnostics and AUREOL-3 satellite
N87-10607
ELECTROJETS
A study of disturbed solar wind and magnetotail based on ISEE-3 data
[NASA-CR-177060] N87-10816
ELECTROLYTE METABOLISM
The regulation of fluid and electrolyte metabolism in weightlessness N87-10679
Relationship between cardiovascular functions and fluid-electrolyte metabolism during antiorthostatic hypokinesia — weightlessness simulation N87-10701
ELECTROMAGNETIC FIELDS
Extension of the electromagnetic method of moments code CHAOS to treat configurations of dielectric-coated wires
[AWRE-O-18/85] N87-10234
ELECTROMAGNETIC INTERFERENCE
Interference detection and correction applied to incoherent-scatter radar power spectrum measurement
N87-10520
ELECTROMAGNETIC MEASUREMENT
Review of measurements of the RF spectrum of radiation from lightning
[NASA-TM-87788] N87-10658
ELECTROMAGNETIC NOISE MEASUREMENT
Earthquake effects in the ionosphere according to Intercosmos-19 and AUREOL-3 satellite data
N87-10588
ELECTROMAGNETIC PROPERTIES
An eddy-current model for three-dimensional nondestructive evaluation of advanced composites
[AD-A167688] N87-10185
ELECTROMAGNETIC PULSES
New solution of the problem of EMP coupling on cables over ground of finite conductivity
[DE86-006078] N87-10229
ELECTROMAGNETIC RADIATION
Periodic amplitude variations in Jovian continuum radiation
[NASA-CR-177070] N87-10813
Plasma wave observations at Uranus from Voyager 2
[NASA-CR-177069] N87-10814
ELECTROMAGNETIC SCATTERING
Theory of wire-grid modelling: Criteria for highly conducting surfaces — plane wave scattering
[AWRE-O-20/85] N87-10224
ELECTROMAGNETISM
The Provence ST radar N87-10492
ELECTRON ACCELERATORS
Electrical measurement techniques for pulsed high current electron beams
[DE86-010980] N87-10756
ELECTRON BEAM WELDING
Weldability of an NiAl alloy
[DE86-011510] N87-10199
ELECTRON BEAMS
Transverse correlations in start-up of a free electron laser from noise
[DE86-009917] N87-10380
Objectives and design of the ECHO 6 electron beam experiment: Large ionospheric perturbations and energetic particle patterns — rocket sounding N87-10590
Current enhancement for hose-unstable electron beams
[AD-A167804] N87-10755
Electrical measurement techniques for pulsed high current electron beams
[DE86-010980] N87-10756
ELECTRON DENSITY (CONCENTRATION)
Simultaneous VHF and UHF radar observation of the mesosphere at Arecibo during a solar flare: A check on the gradient-mixing hypothesis N87-10437
Simultaneous rocket and MST radar observation of an internal gravity wave breaking in the mesosphere
N87-10443
An analysis at mesospheric coherent-scatter power enhancements during solar flare events N87-10479
ELECTRON DENSITY PROFILES
Statistical study of auroral electron precipitation structures detected by the AUREOL-3 Satellite
N87-10543
Observations of low intensity particle fluxes inside the region of the ionospheric main trough and their variability
N87-10556
Density gradient instability in the high latitude ionosphere. Relation with the electrostatic turbulence and convection N87-10573
Instabilities associated with the equatorial spread-F phenomenon and their north-south asymmetry
N87-10576
Two-dimensional snapshots of electron density in the main trough and diffuse auroral zone from a close network of ionosondes: Comparison with measurements from AUREOL-3 satellite N87-10601
Step-like profiles of electron density in the subauroral lower F-region in the morning sector and possible mechanisms of their formation during substorms: The comparison of data of ground-based ionosondes with the AUREOL-3 satellite measurements N87-10603
ELECTRON EMISSION
Design, construction and long life endurance testing of cathode assemblies for use in microwave high-power transmitting tubes
[NASA-CR-175116] N87-10237
ELECTRON ENERGY
Simultaneous measurements of thermal electron density-temperature and low energy precipitating electron fluxes in topside ionosphere N87-10544
Energy spectra of electrons precipitating above the EISCAT area. Comparison with ARCAD measurements
N87-10598
Infrared emission lines from planetary nebulae
N87-10791
Electron-positron pair production by ultrarelativistic electrons in a soft photon field N87-10798
ELECTRON PLASMA
Self-consistent analysis of high drift velocity measurements with the Scandinavian Twin Auroral Radar Experiment (STARE) system N87-10606
ELECTRON PRECIPITATION
Magnetic field-aligned particle precipitation
N87-10542
Statistical study of auroral electron precipitation structures detected by the AUREOL-3 Satellite
N87-10543
Simultaneous measurements of thermal electron density-temperature and low energy precipitating electron fluxes in topside ionosphere N87-10544
Observations of low intensity particle fluxes inside the region of the ionospheric main trough and their variability
N87-10556
Dynamic variations of the auroral precipitation and the polar cap N87-10559
Precipitation of electrons and protons in the subauroral zone stimulated by ground-based VLF emitter
N87-10585
Energy spectra of electrons precipitating above the EISCAT area. Comparison with ARCAD measurements
N87-10598
ELECTRONIC EQUIPMENT
Research and development activities of the Spectroscopy Division of the Bhabha Atomic Research Centre
[DE86-702154] N87-10781
ELECTRONIC EQUIPMENT TESTS
Cross-contact chain
[NASA-CASE-NPO-16784-1] N87-10231
ELECTROSTATIC WAVES
Growing electrostatic waves with a wavelength of 67 cm in the upper ionosphere N87-10604
ELECTROSTATICS
Magnetic field-aligned potential drops N87-10545
ELEMENTARY PARTICLE INTERACTIONS
Prompt neutrino production in 400 GeV proton copper interactions
[USIP-86-02] N87-10754
ELLIPTIC DIFFERENTIAL EQUATIONS
Hierarchical bases for the solution of plane elliptic boundary value problems N87-10742
ELLIPTICAL CYLINDERS
Numerical and experimental study of dynamics of two-dimensional body
[ISAS-619] N87-10748
ELONGATION
Deformation behavior of powder metallurgy Ni Al-Hf-B
[DE86-011508] N87-10201
EMBRITTLEMENT
Review of embrittlement mechanisms in tungsten heavy alloys
[DE86-011114] N87-10196
Modification of the grain boundary microstructure of the austenitic PCA stainless steel to improve helium embrittlement resistance
[DE86-010396] N87-10202
EMISSION SPECTRA
Differential optical absorption techniques for diagnostics of fossil fuel combustion
[DE86-010084] N87-10190
Emission-line galaxies toward the Bootes void
N87-10807
ENERGY CONSUMPTION
Upper and lower body anaerobic power comparison between biathletes and control subjects
[AD-A167636] N87-10710
ENERGY CONVERSION EFFICIENCY
Laser-powered MHD generators for space application
[NASA-TP-2621] N87-10764
ENERGY DISSIPATION
A statistical model to estimate refractivity turbulence structure constant C sub n sup 2 in the free atmosphere
N87-10448
ENERGY DISTRIBUTION
Energy spectra of electrons precipitating above the EISCAT area. Comparison with ARCAD measurements
N87-10598
Electron-positron pair production by ultrarelativistic electrons in a soft photon field N87-10798
ENERGY REQUIREMENTS
Energy related issues — urban climatology
N87-10651
ENERGY SPECTRA
A model for gravity-wave spectra observed by Doppler sounding systems N87-10434
Energy spectra of electrons precipitating above the EISCAT area. Comparison with ARCAD measurements
N87-10598
Amplitude distribution of cosmic ray events in extrinsic IR detectors
[AD-A167692] N87-10819
ENERGY TRANSFER
Energy delivery processes in shock tubes
N87-10106
Observational and theoretical investigation of stable auroral red arcs and their magnetospheric energy source, volumes 1 and 2 N87-10632
ENGINE MONITORING INSTRUMENTS
Experience with the Onboard Checkout And Monitoring System (OCAMS) of a military aircraft resulting improvements and the consequence for future design
N87-10079
The Airborne Integrated Data System (AIDS) for the Airbus A-310 engine condition monitoring N87-10082

Choosing Aircraft Integrated Data Systems (AIDS) architecture suitable for Engine Health Monitoring (EHM) on future generation engines N87-10083
Lufthansa's Aircraft Integrated Data Systems (AIDS) based A-310 engine condition monitoring system: Progress achieved between the 12th and 13th AIDS Symposiums N87-10084

ENGINE TESTS
Response of a small-turboshaft-engine compression system to inlet temperature distortion
[NASA-TM-83765] N87-10100

ENTHALPY
Computer assisted gas chromatography for thermodynamic measurements of polymer surfaces
[AD-A167450] N87-10208
Re-examination of the neptunium-hydrogen system
[DE86-010197] N87-10216

ENTRAINMENT
A high resolution entrainment model for the convective planetary boundary layer N87-10611
Case studies of the structure of the atmospheric boundary layer entrainment zone N87-10627

ENTROPY
Computer assisted gas chromatography for thermodynamic measurements of polymer surfaces
[AD-A167450] N87-10208
Re-examination of the neptunium-hydrogen system
[DE86-010197] N87-10216

ENVIRONMENT PROTECTION
Impact of IPS and IRS configurations on engine installation design N87-10070

ENVIRONMENTAL ENGINEERING
Climatic factors in the siting of new towns and specialized urban facilities N87-10654

ENVIRONMENTAL TESTS
Vertical junction solar cells
[AD-A167757] N87-10532

EPHEMERIDES
DMAHTC (Defense Mapping Agency Hydrographic/Topographic Center) GPS point positioning software: Initial results
[AD-A167566] N87-10058

EPOXY RESINS
Polymer systems for rapid sealing of aircraft structures at low temperature
[AD-A167667] N87-10209

EQUALIZERS (CIRCUITS)
MODTEQ (Modulation Techniques), AN/FRC-170(V), equalization, and channel medium simulations
[AD-A167965] N87-10226
High speed digital signal transmission over coaxial pairs between network termination and several terminals without variable equilization
[FI-44-TBR-101] N87-10230

EQUATORIAL ATMOSPHERE
Hardware requirements: A new generation partial reflection radar for studies of the equatorial mesosphere N87-10431
Equatorial magnetospheric particles and auroral precipitations N87-10557

EQUIPMENT SPECIFICATIONS
Engine-airframe integration for rotorcraft: Component specifications and qualification N87-10071
Orbital transfer vehicle launch operations study. Volume 2: Detailed summary
[NASA-CR-179791] N87-10111
Development of a high-altitude airborne dial system: The Lidar Atmospheric Sensing Experiment (LASE) N87-10268
A Meteorological (humidity, temperature, aerosols)) mobile dial system: Concepts and design N87-10266
Time-resolved lidar fluorosensor for sea pollution detection N87-10317
Investigations of the lower and middle atmosphere at the Arecibo Observatory and a description of the new VHF radar project N87-10494
The first operation and results of the Chung-Li VHF radar N87-10495
System aspects of the Indian MST radar facility N87-10497
The NOAA TOGA antenna array N87-10500
Design support of the Burst and Transient Source Experiment (BATSE) of the Gamma Ray Observatory (GRO) mission
[NASA-CR-178920] N87-10758

ERROR ANALYSIS
Fault and error latency under real workload: An experimental study
[NASA-CR-179802] N87-10733
Asymptotic error expansions of finite element solutions of parabolic equations N87-10738
Adaptive finite element methods — error estimates N87-10740

ERRORS
High spectral purity, narrow linewidth laser transmitter for dial measurements N87-10290
Intercomparison and calibration of wind and wave measurements at various frequencies N87-10468
An evaluation of errors observed in the measurement of low wind velocities N87-10469

ESA SATELLITES
Application of simplified spin axis attitude determination techniques to ESA telecom satellites N87-10126

ESTIMATES
The use of the experimentally deduced Brunt-Vaisala frequency and turbulent velocity fluctuations to estimate the eddy diffusion coefficient N87-10450

ESTIMATING
A decentralized fault-tolerant approach to estimation in multi-sensor navigation systems N87-10057

EULER EQUATIONS OF MOTION
Report of the International Symposium on Computational Fluid Dynamics, Tokyo N87-10029
The numerical method of calculation of two-dimensional stationary electro-gasdynamic internal flows N87-10037
Global pressure relaxation procedure with application to viscous and inviscid flows N87-10247

EUROPEAN SPACE PROGRAMS
ESA activities in space laser sounding and ranging N87-10264

EVALUATION
Summary and evaluation of field performance data on unitary heat pumps
[DE86-011289] N87-10258
Computer software evaluation methodology and data base management system selection
[DE86-011343] N87-10772

EVOLUTION (DEVELOPMENT)
An observational study of tropical cloud cluster evolution and cyclogenesis in the Western North Pacific
[CSU-ASP-403] N87-10661
Turbulent mixing, droplet spectral evolution and dynamics of warm cumulus clouds N87-10667

EXCIMER LASERS
The GSFC gound-based lidar for the measurement of stratospheric ozone N87-10371
Long-pulse excimer lasers for materials processing and medical applications
[DE86-011267] N87-10384

EXERCISE PHYSIOLOGY
Bone tissue and muscular performance in a population of elderly men as a function of physical exercise N87-10685
Histomorphometric study of bone cell mass and activity in man caused by a 120 day decubitus. Test of preventive protocols N87-10689
Exercise-induced myocardial ischemia at high altitude simulated in a negative pressure chamber N87-10702
Upper and lower body anaerobic power comparison between biathletes and control subjects
[AD-A167636] N87-10710

EXHAUST EMISSION
Technical overview of plume radiation from a solid rocket motor N87-10021

EXOBIOLOGY
Aerospace medicine and biology: A continuing bibliography with indexes (supplement 287)
[NASA-SP-7011(287)] N87-10001
Aerospace medicine and biology: A continuing bibliography with indexes
[NASA-SP-7011(289)] N87-10674

EXOS-C SATELLITE
Monitoring of the MU radar antenna pattern by Satellite Ohzora (EXOS-C) N87-10509

EXOTHERMIC REACTIONS
Chemistry and shock initiation of intermetallic reactions
[DE86-010549] N87-10221

EXPERIMENT DESIGN
MIE Lidar proposed for the German Space Shuttle Mission D2 N87-10269
Numerical and experimental study of dynamics of two-dimensional body
[ISAS-619] N87-10748

EXPERT SYSTEMS
SEAGOS: A prototype expert system to aid ground operators in satellite command and control tasks N87-10161
Issues in expert system aids for a large engineering simulation code
[DE86-009098] N87-10735

EXPLOSIONS
Simple blast model for structural design
[DE86-000802] N87-10414

EXTINCTION
Aerosol studies in mid-latitude coastal environments in Australia N87-10271
Extinction and visibility measurements in the lower atmosphere with UV-YAG-lidar N87-10276
Determination of cloud microphysical properties by laser backscattering and extinction measurements N87-10293
Effect of backscatter-to-extinction ratio on lidar inversions N87-10294
Laboratory measurements of forward and backward scattering of laser beams in water droplet clouds N87-10295
Improved solution of the lidar equation utilizing particle counter measurements N87-10310
Multiple scattering measurements in laboratory and foggy atmosphere N87-10315
Lidar method of measurement of atmospheric extinction and ozone profiles N87-10334
Near-IR extinction and backscatter coefficient measurements in low- and mid-altitude clouds N87-10351
Backscatter and extinction measurements in cloud and drizzle at CO2 laser wavelengths N87-10352
Cloud detection by lidar extinction calculations N87-10353

EXTRAGALACTIC RADIO SOURCES
Observations of molecular clouds in the direction of galactic and extragalactiv radio sources N87-10794
Interpretation of extragalactic jets
[DE86-011211] N87-10823
Investigations of radio jets in M87, 3C273 and 3C345 N87-10824

EXTRAVEHICULAR ACTIVITY
A space station Structures and Assembly Verification Experiment, SAVE
[NASA-TM-89004] N87-10170
The use of decompression to simulate the effect of extravehicular activity on human lymphocyte transformation N87-10697

EXTREME ULTRAVIOLET EXPLORER SATELLITE
Extreme ultraviolet explorer: Mirror optical tests and results
[DE86-010560] N87-10760

EXTREMELY LOW FREQUENCIES
Attenuation bands and cut-off frequencies for ELF electromagnetic waves — high latitudes N87-10570
The direction finding aboard AUREOL-3 of ELF waves at frequency above and below the proton gyrofrequency N87-10572
Experimental evidence of field-aligned ELF plasma ducts in the ionospheric trough and in the auroral zone N87-10574
Very low frequency and ELF effects in the upper ionosphere caused by large-scale acoustic waves in the lower ionosphere observed from AUREOL-3 satellite N87-10587

F

F REGION
Observations of low intensity particle fluxes inside the region of the ionospheric main trough and their variability N87-10556
Experimental evidence of field-aligned ELF plasma ducts in the ionospheric trough and in the auroral zone N87-10574
The ARCAD 3-SAFARI coordinated study of auroral and polar F-region ionospheric irregularities N87-10600
Two-dimensional snapshots of electron density in the main trough and diffuse auroral zone from a close network of ionosondes: Comparison with measurements from AUREOL-3 satellite N87-10601
Step-like profiles of electron density in the subauroral lower F-region in the morning sector and possible mechanisms of their formation during substorms: The comparison of data of ground-based ionosondes with the AUREOL-3 satellite measurements N87-10603
Observational and theoretical investigation of stable auroral red arcs and their magnetospheric energy source, volumes 1 and 2 N87-10632

FABRICATION
Long-pulse excimer lasers for materials processing and medical applications
[DE86-011267] N87-10384

FAILURE
Short-wavelength buckling and shear failures for compression-loaded composite laminates N87-10403

FAILURE ANALYSIS
A system theoretical based method for module failure diagnostic of turbine engines N87-10085
Reliability issues in active control of large flexible space structures
[NASA-CR-179785] N87-10167

FAILURE MODES
Fault and error latency under real workload: An experimental study
[NASA-CR-179802] N87-10733

FALKNER-SKAN EQUATION
On accurate numerical solutions of Falkner-Skan equation N87-10018

FALLOUT
Radiation doses from flying through nuclear debris clouds
[AD-A167959] N87-10711
FAR FIELDS
Growth of cracks under far-field cyclic compressive loads: Numerical and experimental results
[DE86-010279] N87-10416
FATIGUE (MATERIALS)
Fatigue response of notched laminates subjected to tension-compression cyclic loads
[NASA-CR-179804] N87-10183
Mode 1 delamination growth in adhesively bonded joints under static and fatigue loads
[NASA-CR-178812] N87-10409
FATIGUE LIFE
Experimental procedure for lifetime testing of graphite bundles under constant load
[AD-A167714] N87-10186
FATIGUE TESTS
Design rule for fatigue of welded joints in elevated-temperature nuclear components
[DE86-007569] N87-10393
FAULT TOLERANCE
A decentralized fault-tolerant approach to estimation in multi-sensor navigation systems N87-10057
Reliability issues in active control of large flexible space structures
[NASA-CR-179785] N87-10167
Control of large flexible space structures
[NASA-CR-177063] N87-10168
Fault tolerant control laws
[NASA-CR-178094] N87-10400
FTMP (Fault Tolerant Multiprocessor) programmer's manual
[NASA-TM-89015] N87-10731
FEDERAL BUDGETS
Microelectronics research and development background paper
[PB86-205200] N87-10242
Department of Housing and Urban Development-Independent Agencies Appropriation Bill, 1987
[S-REPT-99-487] N87-10773
National Aeronautics and Space Administration
N87-10774
National Aeronautics and Space Administration Authorization Act, 1987 N87-10775
FEEDBACK CONTROL
Dynamic modeling and control of robotic manipulators
N87-10390
Experimental identification and control of the tip position of a flexible, single link manipulator N87-10397
Rapid precise end point control of a wrist carried by a flexible manipulator N87-10398
Fault tolerant control laws
[NASA-CR-178094] N87-10400
FIBER OPTICS
Technology review of flight crucial flight control systems (application of optical technology)
[NASA-CR-172332] N87-10102
CP DDT detonators. 5: Output performance and analysis of multiple-out devices
[DE86-010995] N87-10219
Wide-area remote-sensing system of pollution and gas dispersal by near-infrared absorption based on low-loss optical fiber network N87-10354
Integrated-optical components for fiber gyroscopes
[AD-A167624] N87-10376
Attempts to characterize microballoon sensors for shock velocity and material motion studies
[DE86-011210] N87-10379
FIBER REINFORCED COMPOSITES
An eddy-current model for three-dimensional nondestructive evaluation of advanced composites
[AD-A167688] N87-10185
Experimental procedure for lifetime testing of graphite bundles under constant load
[AD-A167714] N87-10186
Computer assisted gas chromatography for thermodynamic measurements of polymer surfaces
[AD-A167450] N87-10208
FIBER STRENGTH
Experimental procedure for lifetime testing of graphite bundles under constant load
[AD-A167714] N87-10186
FIELD EFFECT TRANSISTORS
Optically controlled GaAs dual-gate MESFET and permeable base transistors
[NASA-TM-88823] N87-10232
FIELD STRENGTH
Review of VHF Band 1 field strength prediction
[BBC-RD-1986/4] N87-10223
FILM BOILING
Dynamic heat transfer mechanism of two-phase closed thermosyphon N87-10025
FINANCIAL MANAGEMENT
Department of Housing and Urban Development-Independent Agencies Appropriation Bill, 1987
[S-REPT-99-487] N87-10773
National Aeronautics and Space Administration
N87-10774
FINE STRUCTURE
Fine structure of fields and plasma in the field-aligned current region on the Intercosmos-Bulgaria-1300 satellite data N87-10568
Infrared emission lines from planetary nebulae
N87-10791
FINITE DIFFERENCE THEORY
Numerical solution of the 3-dimensional boundary layer equations in the inverse mode using finite differences
N87-10005
Images of three dimensional flows in computer graphics N87-10017
Supersonic flow around tip sides of wings
N87-10033
FINITE ELEMENT METHOD
A Taylor-Galerkin finite element algorithm for transient nonlinear thermal-structural analysis
[NASA-CR-177064] N87-10406
Controller design via structural reduced modeling by FETM
[NASA-CR-179838] N87-10408
Foundation interaction problems involving an elastic half-plane
[AD-A167925] N87-10411
Further results on the initiation and growth of adiabatic shear bands
[AD-A168012] N87-10412
Free vibration and dynamic response analysis of spinning structures
[NASA-CR-179672] N87-10717
Seminar on Finite Elements in Unsteady Problems
[ETN-86-97824] N87-10736
The local convergence of Ritz and Galerkin methods for nonlinear problems N87-10737
Asymptotic error expansions of finite element solutions of parabolic equations N87-10738
Unsteady calculations of ground water problems — finite element method N87-10739
Adaptive finite element methods — error estimates
N87-10740
Mixed finite element methods in flow mechanics
N87-10741
Fundamental investigations of the finite element solutions for acoustic propagation in ducts
[NASA-CR-179645] N87-10751
FINITE VOLUME METHOD
Finite volume solution of the compressible boundary-layer equations
[NASA-CR-4013] N87-10744
FIRES
Vulnerability methodology and protective measures for aircraft fire and explosion hazards. Volume 3: On-Board Inert Gas Generator System (OBIGGS) studies. Part 1: OBIGGS ground performance tests
[AD-A167357] N87-10066
FIZEAU EFFECT
Pulsed mononode dye laser developed for a geophysical application N87-10364
FLAPS (CONTROL SURFACES)
Effects of flap position on longitudinal parameters of HFB-320
[NAL-TM-SE-8602] N87-10062
Toward comparing experiment and theory for corroborative research on hingeless rotor stability in forward flight (an experimental and analytical investigation of isolated rotor-flap-lag stability in forward flight)
[NASA-CR-179711] N87-10063
FLASH BLINDNESS
Flash/crazing effects on simulator pursuit tracking performance
[AD-A167689] N87-10759
FLAT PLATES
Acoustic waves emitted by vortex-body interaction
N87-10015
On accurate numerical solutions of Falkner-Skan equation N87-10018
FLEXIBLE SPACECRAFT
Parameter optimization and attitude stabilization of a flexible spacecraft N87-10138
Maneuver and control of flexible spacecraft
N87-10166
Control of large flexible space structures
[NASA-CR-177063] N87-10168
Identification and control of structures in space
[NASA-CR-179811] N87-10172
FLEXING
Rapid precise end point control of a wrist carried by a flexible manipulator N87-10398
FLIGHT CHARACTERISTICS
Wind-tunnel investigation of the flight characteristics of a canard general-aviation airplane configuration
[NASA-TP-2623] N87-10039
FLIGHT CONTROL
Spin-tunnel investigation of a 1/25-scale model of the General Dynamics F-16XL airplane
[NASA-TM-85660] N87-10041
Performance monitoring of sensors in high reliable flight control systems using deterministic observers
N87-10087
Technology review of flight crucial flight control systems (application of optical technology)
[NASA-CR-172332] N87-10102
FLIGHT CREWS
Radiation doses from flying through nuclear debris clouds
[AD-A167959] N87-10711
Human factors research in aircrew performance and training
[AD-A167950] N87-10714
FLIGHT MECHANICS
Proceedings of the Symposium on Mechanics for Space Flight, 1985
[ISAS-SP-4] N87-10011
Application of bifurcation and catastrophe theories to near stall flight mechanics
[AD-A167697] N87-10046
FLIGHT OPTIMIZATION
Wind tunnel test of the modified goldschmied model with propulsion and empennage: Analysis of test results
[AD-A167360] N87-10045
FLIGHT RECORDERS
Crashworthiness experiment summary full-scale transport controlled impact demonstration program
[DOT/FAA/CT-85/20] N87-10055
Proceedings of the 13th Symposium on Aircraft Integrated Data Systems
[DFVLR-MITT-86-04] N87-10075
Integrated monitoring systems for tactical aircraft
N87-10080
Application of operational flight recording to helicopters N87-10081
The Airborne Integrated Data System (AIDS) for the Airbus A-310 engine condition monitoring N87-10082
The impact of flight data on an airline: A case study
N87-10088
Data recovery techniques, an update — flight data
N87-10089
Software for flight recorder data processing developed by Lufthansa N87-10090
Airline data acquisition in an ACARS environment
N87-10092
Flight recorders: New US regulations and new International Civil Aviation Organization (ICAO) standards N87-10093
Data compression techniques for multifunction flight data recorders N87-10094
The Fairchild CVDR: A new combination voice and data recorder — Cockpit Voice and Data Recorder (CVDR)
N87-10095
The Boeing B 720 aircraft Controlled Impact Demonstration (CID): Flight data recorder/cockpit voice recorder experiment N87-10096
United States Navy - Canadian Forces solid state flight data recorder/crash position locator experiment on the B-720 controlled impact demonstration N87-10097
Comparative evaluation of redundant flight data recorded by a digital aircraft integrated data system recorder (DAR) on board an Airbus A-310 aircraft
N87-10098
Investigations on a digital bit synchronizer for a detailed flight data recovery N87-10099
FLIGHT SIMULATORS
Human factors research in aircrew performance and training
[AD-A167950] N87-10714
FLIGHT TESTS
Design and fabrication of the NASA decoupler pylon for the F-16 aircraft
[NASA-CR-172354] N87-10065
Application of operational flight recording to helicopters N87-10081
Wind shear measurement on board a MORANE 893
N87-10086
Comparative evaluation of redundant flight data recorded by a digital aircraft integrated data system recorder (DAR) on board an Airbus A-310 aircraft
N87-10098
Response of a small-turboshaft-engine compression system to inlet temperature distortion
[NASA-TM-83765] N87-10100
Summary of longitudinal stability and control parameters as determined from space shuttle Columbia flight test data
[NASA-TM-87768] N87-10101

In-flight total forces, moments and static aeroelastic characteristics of an oblique-wing research airplane
[NASA-TP-2224] N87-10103

Flight service evaluation of composite helicopter components
[NASA-CR-178149] N87-10182

Shuttle derived atmospheric density model. Part 1: Comparisons of the various ambient atmospheric source data with derived parameters from the first twelve STS entry flights, a data package for AOTV atmospheric development
[NASA-CR-171824] N87-10662

FLOOD CONTROL

Urban hydrology in the tropics: Problems, solutions, data collection and analysis N87-10650

FLOW DISTORTION

Studies on vortex motion based on the dividing vorton model N87-10013

FLOW DISTRIBUTION

A study of the flow field about an upper surface blown wing and its effects on longitudinal static stability of a small jet airplane N87-10009

Theoretical study of strong interaction of vortex filaments N87-10012

Numerical simulation of two-dimensional freejet flow-fields N87-10020

Technical overview of plume radiation from a solid rocket motor N87-10021

Computational aerodynamics of supersonic lifting vehicles N87-10030

Numerical modeling of spatial flows on the basis of splitting up method N87-10031

Supersonic flow around tip sides of wings N87-10033

Experimental and theoretical investigations of the flow field of an airfoil with a deflected spoiler N87-10050

Unsteady flow over an airfoil inside a wind tunnel with and without transpiration N87-10051

An experimental investigation of end-wall flowfield of a compressor rotor N87-10244

Ordered and random structures in pulsatile flow through constricted tubes N87-10245

Flow dynamics and stability in severe rainbands N87-10669

FLOW STABILITY

Linearized model for the hydrodynamic stability investigation of molten fuel jets into the coolant of a Liquid Metal Fast Breeder Reactor (LMFBR)
[KFK-3978] N87-10757

FLOW THEORY

Modelling of the filling up of a porous plate
[DE86-702033] N87-10260

Mixed finite element methods in flow mechanics N87-10741

FLOW VELOCITY

Free surface turbulence
[AD-A168013] N87-10251

FLOW VISUALIZATION

Development of a turbomachinery design optimization procedure using a multiple-parameter nonlinear perturbation method
[NASA-CR-3831] N87-10003

Analysis of the vortical flow around a 60 deg Delta wing with vortex flap N87-10006

Separation and wakes over 3-dimensional bodies N87-10008

Study of three-dimensional separation on a spheroid at incidence N87-10016

FLUID DYNAMICS

A theory for the retrieval of virtual temperature from winds, radiances and the equations of fluid dynamics N87-10421

Numerical and experimental study of dynamics of two-dimensional body
[ISAS-619] N87-10748

FLUID FLOW

Computer simulation in engineering hydrodynamics N87-10038

Detailed transient model of a liquid-metal heat pipe
[DE86-011212] N87-10257

FLUID JETS

Transient behavior of liquid jets injected normal to a high velocity gas stream N87-10246

FLUID-SOLID INTERACTIONS

Hydrodynamic and thermal interaction between two spheres in a steady viscous flow N87-10035

Constitutive relations for flow of a non-Newtonian fluid through saturated porous media
[DE86-702035] N87-10261

FLUOROHYDROCARBONS

Synthesis of energetic materials
[AD-A167787] N87-10214

FLUOROPOLYMERS

Synthesis of energetic materials
[AD-A167787] N87-10214

FLUTTER

Design and fabrication of the NASA decoupler pylon for the F-16 aircraft
[NASA-CR-172354] N87-10065

FOG

Multiple scattering measurements in laboratory and foggy atmosphere N87-10315

FOG DISPERSAL

Three atmospheric dispersion experiments involving oil fog plumes measured by lidar N87-10321

FORGING

Development of iron aluminides
[AD-A168576] N87-10194

Deformation behavior of powder metallurgy Ni Al-Hf-B
[DE86-011506] N87-10201

FORMAT

Proceedings of the 5th Annual Users' Conference
[NASA-CP-2399] N87-10720

FORMULATIONS

Foundation interaction problems involving an elastic half-plane
[AD-A167925] N87-10411

FOSSIL FUELS

Differential optical absorption techniques for diagnostics of fossil fuel combustion
[DE86-010084] N87-10190

FOUNDATIONS

Foundation interaction problems involving an elastic half-plane
[AD-A167925] N87-10411

FOURIER ANALYSIS

Propagating tides in the mesosphere N87-10441

FOURIER SERIES

Gauge invariant perturbation theory prediction of the sensitivity required for experimental measurement of quadrupole and higher moments of the cosmic microwave background radiation N87-10825

FOURIER TRANSFORMATION

Review of measurements of the RF spectrum of radiation from lightning
[NASA-TM-87788] N87-10658

FRACTURE STRENGTH

Review of embrittlement mechanisms in tungsten heavy alloys
[DE86-011114] N87-10196

FRACTURING

Grain boundary segregation and environmentally-induced fracture of materials
[DE86-010219] N87-10195

FREE ELECTRON LASERS

Transverse correlations in start-up of a free electron laser from noise
[DE86-009917] N87-10380

Overtone production of soft x-rays with free-electron lasers
[DE86-011248] N87-10383

FREE FLOW

The effect of free stream disturbances and control surface deflections on the performance of the Wortmann airfoil at low Reynolds numbers N87-10007

Adaptation of TSFOIL for Univac 1100/60H computer at NAL, Bangalore
[AE-TB-9-83] N87-10718

FREE JETS

Numerical simulation of two-dimensional freejet flow-fields N87-10020

Free jet feasibility study of a thermal acoustic shield concept for AST/VCE application: Dual stream nozzles
[NASA-CR-3867] N87-10752

FREE VIBRATION

Free vibration and dynamic response analysis of spinning structures
[NASA-CR-179672] N87-10717

FRENCH SPACE PROGRAMS

The interest of centrifuge tests for the selection of French cosmonauts N87-10678

FREQUENCIES

Propagating tides in the mesosphere N87-10441

Effects of anisotropy on the frequency spectrum of gravity waves observed by MST radar N87-10460

Intercomparison and calibration of wind and wave measurements at various frequencies N87-10468

FREQUENCY DISTRIBUTION

Cramer-Rao bound analysis for frequency estimation of sinusoids in noise
[AD-A167992] N87-10227

The frequency spectrum of C sub n sup 2 from MST radar data N87-10461

FREQUENCY HOPPING

Improving range resolution with a frequency-hopping technique N87-10514

A variable-frequency local oscillator for the frequency-hopping technique N87-10515

FREQUENCY MODULATION

An intensity-modulated dual-wavelength He-Ne laser for remote sensing of methane N87-10319

FREQUENCY RANGES

Review of VHF Band 1 field strength prediction
[BBC-RD-1986/4] N87-10223

Improving range resolution with a frequency-hopping technique N87-10514

FREQUENCY SHIFT

The elimination of a class of pseudo echoes by an improved T/R switch technique N87-10511

FRONTS (METEOROLOGY)

Observations of mesoscale vertical velocities around frontal zones N87-10424

The PROUST radar: First results N87-10445

Flow dynamics and stability in severe rainbands N87-10669

FUEL COMBUSTION

Developing simplified models of combustion chemistry by simulation with detailed chemical kinetics models
[DE86-008381] N87-10188

Differential optical absorption techniques for diagnostics of fossil fuel combustion
[DE86-010084] N87-10190

FUEL CONSUMPTION

Influence of engine variables on future helicopter systems N87-10072

The assessment of climatological impacts on agricultural production and residential energy demand N57-10666

FUEL PRODUCTION

Laser-initiated chain reactions in the partial oxidation of methane
[DE86-011272] N87-10388

FUEL TANKS

Vulnerability methodology and protective measures for aircraft fire and explosion hazards. Volume 3: On-Board Inert Gas Generator System (OBIGGS) studies. Part 1: OBIGGS ground performance tests
[AD-A167357] N87-10066

FUELS

Cold-start tests with speed diesel engines using alcohol as main fuel
[DE86-751651] N87-10392

FUNGI

The fungal resistance or susceptibility of resins, plasticizers, and other constituents of adhesive formulations
[AD-A166930] N87-10207

FUNGICIDES

The fungal resistance or susceptibility of resins, plasticizers, and other constituents of adhesive formulations
[AD-A166930] N87-10207

FUSION REACTORS

Plasma confinement by a radio frequency plugging potential in an axisymmetric mirror-cusp device
[IPPJ-784] N87-10763

FUZZY SETS

Use of fuzzy sets mathematics to assist pavement evaluation and management (revised March 18, 1986)
[PB86-214798] N87-10747

G

GALACTIC CLUSTERS

A study of hierarchical clustering of galaxies in an expanding universe N87-10806

Emission-line galaxies toward the Bootes void N87-10807

On the tidal interaction between spherical galaxies N87-10810

GALACTIC EVOLUTION

On the tidal interaction between spherical galaxies N87-10810

GALACTIC RADIO WAVES

Observations of molecular clouds in the direction of galactic and extragalactiv radio sources N87-10794

GALACTIC STRUCTURE

Molecular clouds in the Carina arm
[NASA-TM-87798] N87-10786

On the tidal interaction between spherical galaxies N87-10810

GALAXIES

Surface photometry of early-type galaxies N87-10795

The effect of a quasi-stellar object on its host galaxy: Dynamical and physical processes in the interstellar medium around a QSO N87-10797

Emission-line galaxies toward the Bootes void N87-10807

GALERKIN METHOD

A Taylor-Galerkin finite element algorithm for transient nonlinear thermal-structural analysis
[NASA-CR-177064] N87-10406

The local convergence of Ritz and Galerkin methods for nonlinear problems N87-10737

GALLIUM ARSENIDES
Optically controlled GaAs dual-gate MESFET and permeable base transistors [NASA-TM-88823] N87-10232
GAMMA RAY BURSTS
Design support of the Burst and Transient Source Experiment (BATSE) of the Gamma Ray Observatory (GRO) mission [NASA-CR-178920] N87-10758
GAMMA RAY OBSERVATORY
Design support of the Burst and Transient Source Experiment (BATSE) of the Gamma Ray Observatory (GRO) mission [NASA-CR-178920] N87-10758
GAMMA RAYS
Radiation doses from flying through nuclear debris clouds [AD-A167959] N87-10711
GAS ANALYSIS
Time-domain sensitivity enhancement in pulsed Pb-TDL gas monitors N87-10324
GAS CHROMATOGRAPHY
Computer assisted gas chromatography for thermodynamic measurements of polymer surfaces [AD-A167450] N87-10208
GAS COMPOSITION
Spectroscopic aspects of differential method for sounding gas composition of the atmosphere N87-10369
GAS DETECTORS
Wide-area remote-sensing system of pollution and gas dispersal by near-infrared absorption based on low-loss optical fiber network N87-10354
Gas correlation lidar for methane detection N87-10356
Detection of NO sub x,C2H4 concentrations by using CO and CO2 lasers N87-10357
MAPM: A coherent dual CO2 laser DIAL system N87-10358
Gas dispersion measurements using a mobile Raman lidar system N87-10368
GAS DYNAMICS
The numerical method of calculation of two-dimensional stationary electro-gasdynamic internal flows N87-10037
Computational hydrodynamics in astrophysical studies: Highly shocked flows in 3 dimensions N87-10796
GAS EXPLOSIONS
Vulnerability methodology and protective measures for aircraft fire and explosion hazards. Volume 3: On-Board Inert Gas Generator System (OBIGGS) studies. Part 1: OBIGGS ground performance tests [AD-A167357] N87-10066
GAS FLOW
An improved PSI-cell method for turbulent multi-phase flows N87-10034
Gas dispersion measurements using a mobile Raman lidar system N87-10368
GAS LASERS
Detection of NO sub x,C2H4 concentrations by using CO and CO2 lasers N87-10357
GAS TUNGSTEN ARC WELDING
Weldability of an NiAl alloy [DE86-011510] N87-10199
GAS TURBINE ENGINES
A system theoretical based method for module failure diagnostic of turbine engines N87-10085
GASEOUS DIFFUSION
Gas dispersion measurements using a mobile Raman lidar system N87-10368
GASEOUS FUELS
Vulnerability methodology and protective measures for aircraft fire and explosion hazards. Volume 3: On-Board Inert Gas Generator System (OBIGGS) studies. Part 1: OBIGGS ground performance tests [AD-A167357] N87-10066
Photosynthetic water splitting [DE86-010269] N87-10215
GASES
Energy delivery processes in shock tubes N87-10106
Tropospheric trace gases N87-10614
GATES (CIRCUITS)
Optically controlled GaAs dual-gate MESFET and permeable base transistors [NASA-TM-88823] N87-10232
Factors contributing to static RAM cell transient upset [DE86-007710] N87-10715
GAUGE THEORY
Gauge invariant perturbation theory prediction of the sensitivity required for experimental measurement of quadrupole and higher moments of the cosmic microwave background radiation N87-10825
GEARS
Analysis of the vibration of the input bevel pinion in RAN Wessex helicopter main rotor gearbox WAK143 prior to failure [ARL-AERO-PROP-R-169] N87-10061
Engine-Airframe Integration for Rotorcraft [AGARD-LS-148] N87-10067
GENERAL AVIATION AIRCRAFT
Wind-tunnel investigation of the flight characteristics of a canard general-aviation airplane configuration [NASA-TP-2623] N87-10039
GEODESIC LINES
Trajectory scoring in geodetic coordinates using transponder-interrogator range data [DE86-009554] N87-10109
GEODESY
DMAHTC (Defense Mapping Agency Hydrographic/Topographic Center) GPS point positioning software: Initial results [AD-A167566] N87-10058
World geodetic system 1984 [AD-A167570] N87-10527
Science opportunities from the Topex/Poseidon mission [NASA-CR-179752] N87-10671
GEODETIC COORDINATES
Trajectory scoring in geodetic coordinates using transponder-interrogator range data [DE86-009554] N87-10109
GEOLOGY
Lawrence Berkeley Laboratory recent papers submitted and reports issued, February 1986 [DE86-011319] N87-10782
GEOMAGNETIC PULSATIONS
Simultaneous observations of Pc4 and Pc5 electric fields in the noon sector with GEOS-1 and GEOS-2 N87-10597
Generation of Pc2 pulsations by energetic O(+) ions N87-10605
GEOMAGNETIC TAIL
The distant magnetotail — magnetic substorms N87-10558
A multipoint study of a substorm on 4 March 1979 — magnetosphere N87-10595
GEOMAGNETISM
Magnetic field-aligned particle precipitation N87-10542
Solar-geophysical data number 499, March 1986. Part 1: (Prompt reports). Data for February 1986, January 1986 and late data [NASA-CR-179795] N87-10626
GEOMETRY
Geometric and material nonlinear dynamic analysis of complex shells N87-10401
GEOPHYSICS
ESA activities in space laser sounding and ranging N87-10264
Pulsed mononode dye laser developed for a geophysical application N87-10364
Solar-geophysical data number 501, May 1986. Part 2: (Comprehensive reports). Data for November 1985 and miscellanea [PB86-218047] N87-10622
Solar-geophysical data number 501, May 1986. Part 1: (Prompt reports). Data for April 1986, March 1986 and late data [PB86-218039] N87-10623
Solar-geophysical data number 499, March 1986, supplement [NASA-CR-179797] N87-10624
Solar-geophysical data number 499, March 1986. Part 2: (Comprehensive reports). Data for September 1986 and miscellanea [NASA-CR-179796] N87-10625
Solar-geophysical data number 499, March 1986. Part 1: (Prompt reports). Data for February 1986, January 1986 and late data [NASA-CR-179795] N87-10626
GEOS SATELLITES (ESA)
Study of VLF emissions apparently associated with earthquakes from ground-based and GEOS satellites data N87-10589
Simultaneous observations of Pc4 and Pc5 electric fields in the noon sector with GEOS-1 and GEOS-2 N87-10597
GEOS 2 SATELLITE
Operational implementation of deorbiting maneuvers — GEOS-2 N87-10148
Observations of auroral electrons with sounding rockets and the GEOS-2 geostationary satellite N87-10596
GEOSYNCHRONOUS ORBITS
Transfer orbit optimization for dual launches N87-10114
An investigation on passively controlled geosynchronous orbits N87-10118
Geostationary Operational Environmental Satellite (GOES) mission profile N87-10123
Coverage transition times of IR pencil beam sensors — satellite attitude sensors N87-10125
Initial orbit determination for geostationary satellites N87-10131
Geostationary satellite positioning with a restartable motor N87-10142
Definition of a structure for the apogee thrusts for geostationary satellite positioning: Application to TDF-1 N87-10145
Longitudinal orbit control from INTELSAT 5 inclination stationkeeping maneuvers N87-10156
GEOTHERMAL RESOURCES
Lawrence Berkeley Laboratory recent papers submitted and reports issued, February 1986 [DE86-011319] N87-10782
GERONTOLOGY
Bone tissue and muscular performance in a population of elderly men as a function of physical exercise N87-10685
GIANT STARS
Conditions for the formation of massive stars N87-10803
GLASS FIBERS
Transient heat transfer analysis and radiative properties measurements of porous thermal insulation [DE86-011296] N87-10259
GLASS LASERS
Remote express analysis of ground-layer aerosol based on laser-induced spark spectra N87-10303
GLOBAL ATMOSPHERIC RESEARCH PROGRAM
An observational study of tropical cloud cluster evolution and cyclogenesis in the Western North Pacific [CSU-ASP-403] N87-10661
GLOBAL POSITIONING SYSTEM
DMAHTC (Defense Mapping Agency Hydrographic/Topographic Center) GPS point positioning software: Initial results [AD-A167566] N87-10058
Terrestrial evaluation of the Global Positioning System (GPS) Standard Positioning Service (SPS) [PB86-219599] N87-10059
Orbit determination of geostationary satellites using the global positioning system N87-10133
GLOBULAR CLUSTERS
High resolution CCD spectra of stars in globular clusters. Part 2: Metals and CNO in M71 [NASA-CR-179853] N87-10789
Spectroscopy of the globular clusters in M87 [NASA-CR-179854] N87-10790
GOES SATELLITES
Geostationary Operational Environmental Satellite (GOES) mission profile N87-10123
GOVERNMENT PROCUREMENT
Microelectronics research and development background paper [PB86-205200] N87-10242
GOVERNMENTS
Aeronautics and space report of the President [NASA-TM-89239] N87-10827
GRAIN BOUNDARIES
Grain boundary segregation and environmentally-induced fracture of materials [DE86-010219] N87-10195
Modification of the grain boundary microstructure of the austenitic PCA stainless steel to improve helium embrittlement resistance [DE86-010396] N87-10202
Interface properties and crystal-growth mechanisms [DE86-010846] N87-10767
Microstructure, grain boundaries and properties of sintered and isotatically hot pressed SiC materials [KFK-4063] N87-10769
GRAPH THEORY
Application of graph theory to the nonlinear analysis of large space structures N87-10418
GRAPHITE
Experimental procedure for lifetime testing of graphite bundles under constant load [AD-A167714] N87-10186
GRAPHITE-EPOXY COMPOSITES
Fatigue response of notched laminates subjected to tension-compression cyclic loads [NASA-CR-179804] N87-10183
An eddy-current model for three-dimensional nondestructive evaluation of advanced composites [AD-A167688] N87-10185
Dynamic delamination crack propagation in a graphite/epoxy laminate N87-10402
GRAVITATION
An analysis of the performance of a vertically oriented, gas loaded, variable conductance heat pipe [AD-A167874] N87-10250
GRAVITATION THEORY
Null surface dynamics N87-10770

Particle theory and cosmology
[DE86-010366] N87-10802

GRAVITATIONAL EFFECTS
Analysis on gravitational effect to nonlinear diffusion system of vapor molecules in a heat pipe N87-10023
The interest of centrifuge tests for the selection of French cosmonauts N87-10678
Preliminary results on the equilibrium and vertigo experiment performed during STS 51-G shuttle flight N87-10692

GRAVITATIONAL PHYSIOLOGY
Proceedings of 2nd International Conference on Space Physiology
[ESA-SP-237] N87-10675
Cardiovascular measurements in microgravity N87-10676
Cardiovascular examination during STS 51 G mission June (1985) N87-10677
The interest of centrifuge tests for the selection of French cosmonauts N87-10678
The regulation of fluid and electrolyte metabolism in weightlessness N87-10679
Bones and weightlessness N87-10681
The muscular system in weightlessness N87-10682
Microgravity effects on the contractile proteins of rat muscles N87-10683
Weightlessness effects on the bone tissue of rats after a 5 day space flight (Cosmos 1514) N87-10684
Functions of skeletal muscles of rats and monkeys after 5-day space flight (on Cosmos 1514) N87-10686
Hindlimb suspension effects on rat skeletal muscle response N87-10687
Bone examination by noninvasive techniques in a 120-day head-down tilt test N87-10688
Weightlessness effects on the phosphorus-calcium balance and its hormonal regulation in man during STS flight 51-G N87-10691
Ground based simulation techniques for cardiovascular and hormonal changes observed in man in weightlessness N87-10696
The use of decompression to simulate the effect of extravehicular activity on human lymphocyte transformation N87-10697
Metabolic changes during prolonged antiorthostatic hypokinesia — weightlessness simulation N87-10698
Levels of plasma atrial natriuretic factor (alpha h ANF) during acute simulated weightlessness N87-10699
Volume regulating hormones during a 5 hour head-down tilt at -10 deg. Part 1: Epinephrine, norepinephrine and dopamine N87-10700
Relationship between cardiovascular functions and fluid-electrolyte metabolism during antiorthostatic hypokinesia — weightlessness simulation N87-10701
Animal studies on Spacelab-3 N87-10704
Animal models in space physiology N87-10705
Contribution of animal models to the investigation of bone changes in weightlessness N87-10706
Cosmos 1514 flight: Study of rhesus monkey ECG N87-10707
Math modelling as a complement to the scientific inquiry of physiological adaptation to space flight: Fluid, endocrine and circulatory regulation N87-10709

GRAVITATIONAL WAVES
Cryogenic resonant-mass gravitational wave detectors N87-10609

GRAVITY ANOMALIES
World geodetic system 1984
[AD-A167570] N87-10527

GRAVITY WAVES
Daytime lidar measurements of tidal winds in the mesospheric sodium layer at Urbana, Illinois N87-10347
Middle Atmosphere Program. Handbook for MAP, volume 20
[NASA-CR-176882] N87-10419
Gravity waves in the middle atmosphere: Recent progress and needed studies N87-10433
A model for gravity-wave spectra observed by Doppler sounding systems N87-10434
Evidence of atmospheric gravity wave perturbations of the Brunt-Vaisala frequency in the atmosphere N87-10438
Atmospheric waves and the nature of buoyancy turbulence in the context of the waves VS 2D-turbulence debate N87-10439
A proposed experimental test to distinguish waves from 2-D turbulence N87-10440
Gravity waves in severe weather N87-10442
Simultaneous rocket and MST radar observation of an internal gravity wave breaking in the mesosphere N87-10443
The PROUST radar: First results N87-10445
Simultaneous fine structure observation of wind and temperature profiles by the Arecibo 430-MHz radar and in situ measurements N87-10446
A statistical model to estimate refractivity turbulence structure constant C sub n sup 2 in the free atmosphere N87-10448
Determination of the Brunt-Vaisala frequency from vertical velocity spectra N87-10449
The relation of gravity waves and turbulence in the mesosphere N87-10451
Can stochastic, dissipative wave fields be treated as random walk generators N87-10452
Observations and a model of gravity-wave variability in the middle atmosphere N87-10453
Climatology of gravity waves over Poker Flat, Alaska for 1983 N87-10454
Climatology of tropospheric vertical velocity spectra N87-10455
Mesospheric gravity-wave climatology at Adelaide N87-10456
Horizontal wind perturbations and their relation to transient internal gravity waves N87-10457
Possibility of measuring gravity-wave momentum flux by single beam observation of MST radar N87-10458
Preliminary estimates of vertical momentum flux N87-10459
Effects of anisotropy on the frequency spectrum of gravity waves observed by MST radar N87-10460
A study of gravity-wave spectra in the troposphere and stratosphere at 5-min to 5-day periods with the Poker Flat MST radar N87-10462
Doppler effects on velocity spectra observed by MST radars N87-10464
Observations of vertical velocity power spectra with the SOUSY VHF radar N87-10465
Mesospheric wave number spectra from Poker Flat MST radar measurements compared with gravity-wave model N87-10466
Evidence of a saturated gravity-wave spectrum throughout the atmosphere N87-10467
A comparison of vertical velocities measured from specular and nonspecular echoes by a VHF radar N87-10470
Current status of the Poker Flat MST radar N87-10483
The Adelaide MF partial-reflection radar and VHF ST radar N87-10490
Gravity wave dynamics near the mesopause over Poker Flat, Alaska N87-10631

GREEN'S FUNCTIONS
Crack-tip fields in a viscoplastic material
[AD-A168014] N87-10413

GRIDS
Dynamics and control of orbiting grid and the synchronously deployable beam
[NASA-CR-179808] N87-10410

GROOVES
High capacity heat pipe with axial grooves N87-10027

GROUND BASED CONTROL
Orbit and attitude operations during the Telecom 1B transfer phase N87-10147
Orbitography course for ground operators N87-10157

GROUND CREWS
Orbitography course for ground operators N87-10157
SEAGOS: A prototype expert system to aid ground operators in satellite command and control tasks N87-10161

GROUND STATIONS
Study of VLF emissions apparently associated with earthquakes from ground-based and GEOS satellites data N87-10589

GROUND TRUTH
Terrestrial evaluation of the Global Positioning System (GPS) Standard Positioning Service (SPS)
[PB86-219599] N87-10059
In-flight absolute radiometric calibration of the LANDSAT thematic mapper N87-10530

GROUND WATER
Unsteady calculations of ground water problems — finite element method N87-10739

GUIDANCE SENSORS
A decentralized fault-tolerant approach to estimation in multi-sensor navigation systems N87-10057

GUST LOADS
Acta Aeronautica et Astronautica Sinica (selected articles)
[AD-A167918] N87-10004
Prediction of gust loadings and alleviation at transonic speeds
[AD-A167748] N87-10047

GYROFREQUENCY
The direction finding aboard AUREOL-3 of ELF waves at frequency above and below the proton gyrofrequency N87-10572

GYROSCOPES
Integrated-optical components for fiber gyroscopes
[AD-A167624] N87-10378

H

HADRONS
Cosmic-ray hadrons underground
[DE86-011334] N87-10822

HAFNIUM
Chemistry and shock initiation of intermetallic reactions
[DE86-009694] N87-10220

HAFNIUM ALLOYS
Deformation behavior of powder metallurgy Ni Al-Hf-B
[DE86-011508] N87-10201
Chemistry and shock initiation of intermetallic reactions
[DE86-010549] N87-10221

HALOCARBONS
Lidar stratospheric ozone measurements at the observatoire de Haute Provence (France) N87-10344
Tropospheric trace gases N87-10614

HARDNESS TESTS
Study about the structural behavior of WStE-36N steel
[DE86-702011] N87-10394

HARMONIC ANALYSIS
World geodetic system 1984
[AD-A167570] N87-10527

HARMONIC GENERATIONS
Overtone production of soft x-rays with free-electron lasers
[DE86-011248] N87-10383

HARMONICS
The internal tide off southern California
[AD-A167722] N87-10672

HASTELLOY (TRADEMARK)
Transformations and new PHACOMP analysis in weld metal of Hastelloy C-type alloys
[DE86-011422] N87-10198

HAWAII
Features of stratospheric aerosol lidar observations at Mauna Loa, 1974 - 1985 N87-10312

HAZE
Methods for estimating the optical constants of atmospheric hazes based on complex optical measurements N87-10301
Vertical structure of Arctic haze observed by lidar N87-10335

HEAT ISLANDS
Proceedings of the Technical Conference on Urban Climatology and its Applications with Special Regard to Tropical Areas
[WMO-652] N87-10636
Tropical urban climates: Review and assessment N87-10638
Some aspects of the urban climates of India N87-10643

HEAT MEASUREMENT
High capacity heat pipe with axial grooves N87-10027

HEAT PIPES
Analysis on gravitational effect to nonlinear diffusion system of vapor molecules in a heat pipe N87-10023
Effect of surplus standing liquid on heat transfer resistance in the heat pipe (with mesh wick in a horizontal mode) N87-10024
A trial on performance test method for Cu-water heat pipe N87-10026
High capacity heat pipe with axial grooves N87-10027
Operating characteristics of cooling underground power cables using up sloped long heat pipes in conduit N87-10028
An analysis of the performance of a vertically oriented, gas loaded, variable conductance heat pipe
[AD-A167874] N87-10250
Analysis of heat-pipe absorbers in evacuated-tube solar collectors
[DE86-010764] N87-10252
Detailed transient model of a liquid-metal heat pipe
[DE86-011212] N87-10257

HEAT PUMPS
Absorption heat pump simulation and studies: a modular computer simulation of absorption systems
[DE86-011206] N87-10256
Summary and evaluation of field performance data on unitary heat pumps
[DE86-011289] N87-10258

HEAT RESISTANT ALLOYS
Castable hot corrosion resistant alloy
[NASA-CASE-LEW-14134-1] N87-10192
Development of iron aluminides
[AD-A168578] N87-10194

HEAT SHIELDING
Free jet feasibility study of a thermal acoustic shield concept for AST/VCE application: Dual stream nozzles [NASA-CR-3867] N87-10752
HEAT TRANSFER
Technical overview of plume radiation from a solid rocket motor N87-10021
Dynamic heat transfer mechanism of two-phase closed thermosyphon N87-10025
A trial on performance test method for Cu-water heat pipe N87-10026
High capacity heat pipe with axial grooves N87-10027
Hydrodynamic and thermal interaction between two spheres in a steady viscous flow N87-10035
Computer simulation in engineering hydrodynamics N87-10038
Analysis of heat-pipe absorbers in evacuated-tube solar collectors [DE86-010764] N87-10252
Transient heat transfer analysis and radiative properties measurements of porous thermal insulation [DE86-011296] N87-10259
Convective structure of the planetary boundary layer of the ocean during gale N87-10300
Methods of testing to determine the thermal performance of solar collectors [DE86-009311] N87-10533
HEAT TRANSMISSION
Effect of surplus standing liquid on heat transfer resistance in the heat pipe (with mesh wick in a horizontal mode) N87-10024
HEAT TREATMENT
Development of iron aluminides [AD-A168578] N87-10194
Study about the structural behavior of WStE-36N steel [DE86-702011] N87-10394
HEATING
Interface properties and crystal-growth mechanisms [DE86-010846] N87-10767
HELICOPTER DESIGN
Impact of IPS and IRS configurations on engine installation design N87-10070
Influence of engine variables on future helicopter systems N87-10072
Helicopter air intake protection systems N87-10073
HELICOPTERS
Helicopter MLS Flight Inspection Project [DOT/FAA/CT-86/14] N87-10002
Analysis of the vibration of the input bevel pinion in RAN Wessex helicopter main rotor gearbox WAK143 prior to failure [ARL-AERO-PROP-R-169] N87-10061
Engine-Airframe Integration for Rotorcraft [AGARD-LS-148] N87-10067
Engine-airframe integration considerations for preliminary air vehicle performance analysis N87-10068
Engine-transmission-structural airframe members compatibility N87-10069
Engine-airframe integration for rotorcraft: System specifications and qualification N87-10074
Application of operational flight recording to helicopters N87-10081
Flight service evaluation of composite helicopter components [NASA-CR-178149] N87-10182
Testing of UH-60A helicopter transmission in NASA Lewis 2240-kW (3000-hp) facility [NASA-TP-2626] N87-10391
Human factors research in aircrew performance and training [AD-A167950] N87-10714
HELIOSPHERE
Three-dimensional structure of the heliosphere: Quiet-time and disturbed periods N87-10818
HELIUM
Modification of the grain boundary microstructure of the austenitic PCA stainless steel to improve helium embrittlement resistance [DE86-010396] N87-10202
HELIUM-NEON LASERS
An intensity-modulated dual-wavelength He-Ne laser for remote sensing of methane N87-10319
HELMHOLTZ RESONATORS
The Helmholtz resonance behavior of single and multiple rooms [NASA-CR-178173] N87-10749
HFB-320 AIRCRAFT
Effects of flap position on longitudinal parameters of HFB-320 [NAL-TM-SE-8602] N87-10062
HIERARCHIES
Hierarchical bases for the solution of plane elliptic boundary value problems N87-10742
A study of hierarchical clustering of galaxies in an expanding universe N87-10806
HIGH ALTITUDE TESTS
Exercise-induced myocardial ischemia at high altitude simulated in a negative pressure chamber N87-10702
HIGH LEVEL LANGUAGES
Programming of sensor based assembly robots [KFK-PFT-120] N87-10396
HIGH RESOLUTION
Research relative to high resolution camera on the advanced X-ray astrophysics facility [NASA-CR-179757] N87-10376
A high resolution entrainment model for the convective planetary boundary layer N87-10611
HIGH REYNOLDS NUMBER
Vortex shedding of a square cylinder in front of a slender airfoil at high Reynolds numbers. Part 1: Spacing effect [MPIS-23/1985] N87-10048
HIGH SPEED
Computational fluid mechanics utilizing the variational principle of modeling damping seals [NASA-CR-178902] N87-10248
HIGH STRENGTH ALLOYS
Development of iron aluminides [AD-A168578] N87-10194
HIGH STRENGTH STEELS
Study about the structural behavior of WStE-36N steel [DE86-702011] N87-10394
HIGH TEMPERATURE PLASMAS
The hot ion composition in the magnetosphere N87-10552
HIGH VOLTAGES
Coaxial tube tether/transmission line for manned nuclear space power [NASA-CASE-LEW-14338-1] N87-10174
HISS
Experimental evidence of field-aligned ELF plasma ducts in the ionospheric trough and in the auroral zone N87-10574
HISTOCHEMICAL ANALYSIS
Hindlimb suspension effects on rat skeletal muscle response N87-10687
HISTOGRAMS
PLOT 3D: A multipurpose, interactive program for plotting three dimensional graphs [DE86-702101] N87-10730
HOLOGRAPHY
Optical systems for synchrotron radiation. Lecture 4: Soft X-ray imaging systems [DE86-011567] N87-10761
HORIZONTAL ORIENTATION
Horizontal wind perturbations and their relation to transient internal gravity waves N87-10457
HORMONE METABOLISMS
Weightlessness effects on the phosphorus-calcium balance and its hormonal regulation in man during STS flight 51-G N87-10691
Ground based simulation techniques for cardiovascular and hormonal changes observed in man in weightlessness N87-10696
Levels of plasma atrial natriuretic factor (alpha h ANF) during acute simulated weightlessness N87-10699
Volume regulating hormones during a 5 hour head-down tilt at -10 deg. Part 1: Epinephrine, norepinephrine and dopamine N87-10700
Volume regulating hormones during a 5-hour head-down tilt at -10 deg. Part 2: Plasma renin activity and aldosterone N87-10703
HOT CORROSION
Castable hot corrosion resistant alloy [NASA-CASE-LEW-14134-1] N87-10192
HUMAN BEINGS
Comparison of the coupling of grounded and ungrounded humans to vertical 60-Hz electric fields [DE86-011140] N87-10713
HUMAN BODY
Upper and lower body anaerobic power comparison between biathletes and control subjects [AD-A167636] N87-10710
HUMAN CENTRIFUGES
The interest of centrifuge tests for the selection of French cosmonauts N87-10678
HUMAN FACTORS ENGINEERING
Life expectancy in tropical climates and urbanization N87-10648
Human comfort in the urban tropics N87-10649
Human factors research in aircrew performance and training [AD-A167950] N87-10714
Design guidelines for human-computer dialogues [DE86-011543] N87-10728
HUMIDITY
Aerosol studies in mid-latitude coastal environments in Australia N87-10271
Case studies of the structure of the atmospheric boundary layer entrainment zone N87-10627
Design for climate in hot, humid cities N87-10656
HURRICANES
Environmental influences on hurricane intensification N87-10635
HYDRAULIC EQUIPMENT
Process control in arc welding [KFK-PFT-105] N87-10395
HYDRODYNAMICS
Hydrodynamic and thermal interaction between two spheres in a steady viscous flow N87-10035
Computer simulation in engineering hydrodynamics N87-10038
Wind tunnel test of the modified goldschmied model with propulsion and empennage: Analysis of test results [AD-A167360] N87-10045
HYDROGEN EMBRITTLEMENT
Grain boundary segregation and environmentally-induced fracture of materials [DE86-010219] N87-10195
Review of embrittlement mechanisms in tungsten heavy alloys [DE86-011114] N87-10196
Compositional and microstructural effects on hydrogen embrittlement of ASTM grade 12 titanium (Ti 0.3 Mo - 0.8 Ni) [DE86-011379] N87-10197
HYDROGEN IONS
Nonstationary field-aligned fluxes of thermal ions O(+) and H(+) outside the plasmapause: Refinement of the polar wind theory N87-10566
Field-aligned motions of O(+) and H(+) thermal ions in a magnetic field tube convected across the dayside polar cusp: Model calculations N87-10567
HYDROGEN MASERS
A study of the ground state hydroxyl maser emissions associated with eleven regions of star formation N87-10826
HYDROGEN PRODUCTION
Photosynthetic water splitting [DE86-010269] N87-10215
HYDROLOGY MODELS
Unsteady calculations of ground water problems — finite element method N87-10739
HYDROLYSIS
Photosynthetic water splitting [DE86-010269] N87-10215
HYDROXYL RADICALS
Differential optical absorption techniques for diagnostics of fossil fuel combustion [DE86-010084] N87-10190
Improvements in the Goddard balloon-borne lidar N87-10311
Rotationally resolved collisional transfer rates in OH N87-10323
Atmospheric Ozone 1985. Assessment of our understanding of the processes controlling its present distribution and change, volume 1 [NASA-TM-89237] N87-10612
A study of the ground state hydroxyl maser emissions associated with eleven regions of star formation N87-10826
HYPERBARIC CHAMBERS
Pressure-resistant plane disc viewports from allyl diglycol carbonate plastic for hyperbaric chambers [AD-A168007] N87-10105
HYPERFINE STRUCTURE
Research and development activities of the Spectroscopy Division of the Bhabha Atomic Research Centre [DE86-702154] N87-10781
HYPOBARIC ATMOSPHERES
Exercise-induced myocardial ischemia at high altitude simulated in a negative pressure chamber N87-10702
HYPOKINESIA
Metabolic changes during prolonged antiorthostatic hypokinesia — weightlessness simulation N87-10698
Relationship between cardiovascular functions and fluid-electrolyte metabolism during antiorthostatic hypokinesia — weightlessness simulation N87-10701
HYPOXIA
Exercise-induced myocardial ischemia at high altitude simulated in a negative pressure chamber N87-10702

I

ICE FORMATION
Summary of artificial and natural icing tests conducted on US Army aircraft from 1974 to 1985 [FAA/CT-85/26] N87-10064
ICE PREVENTION
Summary of artificial and natural icing tests conducted on US Army aircraft from 1974 to 1985 [FAA/CT-85/26] N87-10064
IGNEOUS ROCKS
Cosmic-ray hadrons underground [DE86-011334] N87-10822

IGNITION
Numerical model of the thermal processes leading to ignition in a pyrotechnic device
[DE86-009626] N87-10189
Titanium oxidation kinetics and the mechanism for thermal ignition of titanium-based pyrotechnics
[DE86-010987] N87-10218
Cold-start tests with speed diesel engines using alcohol as main fuel
[DE86-751651] N87-10392

IGNITION SYSTEMS
Cold-start tests with speed diesel engines using alcohol as main fuel
[DE86-751651] N87-10392

IMAGE CONTRAST
An algorithm for the detection of signals by colour contrast on the screen of a colour cathode ray tube (colour display) — radarscopes
[DRIC-T-7655] N87-10233

IMAGE PROCESSING
Proceedings of the 5th Annual Users' Conference
[NASA-CP-2399] N87-10720

IMAGES
Optical systems for synchrotron radiation. Lecture 4: Soft X-ray imaging systems
[DE86-011567] N87-10761

IMAGING TECHNIQUES
Images of three dimensional flows in computer graphics N87-10017
Generation of attenuation corrected images from lidar data N87-10367

IMMOBILIZATION
Histomorphometric study of bone cell mass and activity in man caused by a 120 day decubitus. Test of preventive protocols N87-10689

IMMUNOASSAY
Volume regulating hormones during a 5-hour head-down tilt at -10 deg. Part 2: Plasma renin activity and aldosterone N87-10703

IMPACT DAMAGE
Crashworthiness experiment summary full-scale transport controlled impact demonstration program
[DOT/FAA/CT-85/20] N87-10055

IMPULSES
Response of a 3-layered ring to an axisymmetric impulse
[DE86-011016] N87-10415

IMPURITIES
Grain boundary segregation and environmentally-induced fracture of materials
[DE86-010219] N87-10195

INCIDENCE
Study of three-dimensional separation on a spheroid at incidence N87-10016

INCOHERENT SCATTER RADAR
Wavelength dependence of coherent and incoherent satellite-based lidar measurements of wind velocity and aerosol backscatter N87-10361
Calibration and analysis for a 0.53 micron incoherent Doppler lidar N87-10365
Interference detection and correction applied to incoherent-scatter radar power spectrum measurement N87-10520
Polar cap/polar cusp studies using incoherent scatter radar facilities — ionosphere N87-10562

INCOMPRESSIBLE FLOW
Analysis of two-dimensional incompressible flow past airfoils using unsteady Navier-Stokes equations
[NASA-CR-179823] N87-10040
Experimental study of the boundary layer on a low Reynolds number airfoil in steady and unsteady flow N87-10052
Modelling of the filling up of a porous plate
[DE86-702033] N87-10260
Constitutive relations for flow of a non-Newtonian fluid through saturated porous media
[DE86-702035] N87-10261
Application of a potential code to general steady flows in three dimensions N87-10262

INCOMPRESSIBLE FLUIDS
Theoretical study of strong interaction of vortex filaments N87-10012
Studies on vortex motion based on the dividing vorton model N87-10013

INDIA
System aspects of the Indian MST radar facility N87-10497
Some aspects of the urban climates of India N87-10643

INDUCTION HEATING
A method of estimating the molecular weight of polymeric materials
[NASA-CASE-LAR-13212-1] N87-10206

INDUSTRIES
Aeronautics and space report of the President
[NASA-TM-89239] N87-10827

INEQUALITIES
Cramer-Rao bound analysis for frequency estimation of sinusoids in noise
[AD-A167992] N87-10227

INERTIAL GUIDANCE
Trajectory scoring in geodetic coordinates using transponder-interrogator range data
[DE86-009554] N87-10109

INERTIAL NAVIGATION
A decentralized fault-tolerant approach to estimation in multi-sensor navigation systems N87-10057

INERTIAL REFERENCE SYSTEMS
Orbit geometry for calibration and launch operations of a three-axis controlled satellite with inertial reference N87-10116

INFORMATION MANAGEMENT
MST data exchange through the NCAR incoherent-scatter radar data base N87-10525

INFORMATION RETRIEVAL
MST data exchange through the NCAR incoherent-scatter radar data base N87-10525

INFORMATION SYSTEMS
Study of UNIX and its suitability for the Air Force's WWMCCS Information System
[DE86-011293] N87-10771

INFORMATION TRANSFER
MST data exchange through the NCAR incoherent-scatter radar data base N87-10525

INFRARED DETECTORS
Time-domain sensitivity enhancement in pulsed Pb-TDL gas monitors N87-10324
Amplitude distribution of cosmic ray events in extrinsic IR detectors
[AD-A167692] N87-10819

INFRARED LASERS
Laser heterodyne system for obtaining height profiles of minor species in the atmosphere N87-10359

INFRARED PHOTOGRAPHY
Infrared measurement of eye movement. Presentation of the Eye Movement in Infrared and Angular Torsion (EMIRAT) experiment — Spacelab payload N87-10695

INFRARED RADAR
The NCAR Airborne Infrared Lidar System (NAILS) N87-10362

INFRARED RADIATION
Near-IR extinction and backscatter coefficient measurements in low- and mid-altitude clouds N87-10351
Wide-area remote-sensing system of pollution and gas dispersal by near-infrared absorption based on low-loss optical fiber network N87-10354

INFRARED RADIOMETERS
On the potential use of radar-derived information in operational numerical weather prediction N87-10420

INFRARED SCANNERS
Coverage transition times of IR pencil beam sensors — satellite attitude sensors N87-10125

INFRARED SPECTRA
Infrared emission lines from planetary nebulae N87-10791

INGESTION (ENGINES)
Impact of IPS and IRS configurations on engine installation design N87-10070

INITIATION
Chemistry and shock initiation of intermetallic reactions
[DE86-009694] N87-10220
Chemistry and shock initiation of intermetallic reactions
[DE86-010549] N87-10221

INJECTION
Active experiments from ground — magnetosphere; ionosphere N87-10581
Detection from AUREOL-3 of the modulation of auroral electrojet by HF-heating from ELF signals in the upper ionosphere above Tromsoe (Norway) N87-10582
Study of the middle latitude broadening of the spectrum of the waves emitted from ground N87-10583
On the spectral broadening of the ground-based VLF transmitter signals in the high-latitude ionosphere observed from Intercosmos-19 and AUREOL-3 satellites N87-10584
Precipitation of electrons and protons in the subauroral zone stimulated by ground-based VLF emitter N87-10585
De-1/Siple VLF wave-injection experiments N87-10586

INLET FLOW
Numerical study of the entrance flow and its transition of a circular pipe N87-10019

INLET TEMPERATURE
Response of a small-turboshaft-engine compression system to inlet temperature distortion
[NASA-TM-83765] N87-10100

INSERTION LOSS
Integrated-optical components for fiber gyroscopes
[AD-A167624] N87-10378

INSTRUMENT APPROACH
Aircraft accident reeport, Delta Air Lines, Inc., Lockheed L-1011-385-1, N726DA, Dallas/Fort Worth International Airport, Texas, August 2, 1985
[PB86-910406] N87-10053

INSULATION
Theoretical studies on the structures of insulating and metallic glasses
[DE86-011484] N87-10212

INTAKE SYSTEMS
Impact of IPS and IRS configurations on engine installation design N87-10070
Helicopter air intake protection systems N87-10073

INTEGRALS
Crack-tip fields in a viscoplastic material
[AD-A168014] N87-10413

INTEGRATED CIRCUITS
Cross-contact chain
[NASA-CASE-NPO-16784-1] N87-10231
Thermionic integrated circuits
[DE86-005849] N87-10239
Integrated-optical components for fiber gyroscopes
[AD-A167624] N87-10378
RLE progress report
[MIT-PR-128] N87-10778

INTELSAT SATELLITES
Longitudinal orbit control from INTELSAT 5 inclination stationkeeping maneuvers N87-10156
Operational performance of the INTELSAT 5 attitude determination and control system N87-10158

INTERCOSMOS SATELLITES
On the spectral broadening of the ground-based VLF transmitter signals in the high-latitude ionosphere observed from Intercosmos-19 and AUREOL-3 satellites N87-10584
Intercosmos-Bulgaria-1300 satellite: Large-scale structure and dynamics of the polar ionosphere during geomagnetic storms N87-10592
Some results of scanner spectrophotometric measurements of aurora and airglow from IK-Bulgaria-1300 satellite and prospects of similar measurements N87-10593

INTERFEROMETERS
Comparison of medium frequency pulsed radar interferometer and correlation analysis winds, part 2 N87-10475

INTERFEROMETRY
Mesospheric wind measurements using a medium-frequency imaging Doppler interferometer N87-10476
Progress in the MF radar system at Saskatoon N87-10496

INTERMETALLICS
Chemistry and shock initiation of intermetallic reactions
[DE86-009694] N87-10220
Chemistry and shock initiation of intermetallic reactions
[DE86-010549] N87-10221

INTERNAL WAVES
Horizontal wind perturbations and their relation to transient internal gravity waves N87-10457
Observations of vertical velocity power spectra with the SOUSY VHF radar N87-10465
The internal tide off southern California
[AD-A167722] N87-10672

INTERNATIONAL COOPERATION
Scientific reasons for a network of ST radars and cooperative campaigns N87-10480
The planning and maintenance of urban settlements to resist extreme climatic forces N87-10647

INTERPLANETARY MAGNETIC FIELDS
The distant magnetotail — magnetic substorms N87-10558
Evidence for ion energy dispersion in the polar cusp related to a northward directed Interplanetary Magnetic Field (IMF) N87-10561
A multipoint study of a substorm on 4 March 1979 — magnetosphere N87-10595

INTERPLANETARY SPACE
Plasma wave observations at Uranus from Voyager 2
[NASA-CR-177069] N87-10614

INTERSTELLAR EXTINCTION
Gas and dust in regions of recent star formation N87-10800

INTERSTELLAR GAS
Gas and dust in regions of recent star formation N87-10800

INTERSTELLAR MATTER
The effect of a quasi-stellar object on its host galaxy: Dynamical and physical processes in the interstellar medium around a QSO N87-10797

Gas and dust in regions of recent star formation N87-10800

INTERSTELLAR SPACE
Nuclide production by primary cosmic-ray protons [DE86-011268] N87-10821

INVERSIONS
Inversion of 2 wavelength Lidar data for cloud properties N87-10273
The usefulness of Klett's inversion algorthms to simulated satellite Lidar returns N87-10274
Sensitivity of the Lidar ratio to changes in size distribution and index of refraction N87-10277
Lidar measurements of slant visual range N87-10278
Using a laser aureole to invert lidar return N87-10292
Methods for estimating the optical constants of atmospheric hazes based on complex optical measurements N87-10301
Multifrequency dial sensing of the atmospheric gaseous constituents using the first and second harmonics of a tunable CO2 laser radiation N87-10302
Variation of the urban NO2 concentration during a ground inversion situation N87-10318

INVESTIGATION
Fundamental investigations of the finite element solutions for acoustic propagation in ducts [NASA-CR-179845] N87-10751

INVISCID FLOW
Studies on vortex motion based on the dividing vorton model N87-10013
Viscous wing theory development. Volume 1: Analysis, method and results [NASA-CR-178156] N87-10043
Global pressure relaxation procedure with application to viscous and inviscid flows N87-10247
Application of a potential code to general steady flows in three dimensions N87-10262

IO
A modeling analysis program for the JPL Table Mountain Io sodium cloud data [NASA-CR-179671] N87-10811

ION BEAMS
Artificial ion beam interaction with the auroral plasma N87-10591

ION CURRENTS
Evidence for high latitude ionospheric ion acceleration N87-10564

ION DISTRIBUTION
Two dimensional analysis of high voltage solar array interfering with ionospheric plasma N87-10022
Positive ion distributions in the morning auroral zone: Local acceleration and drift effects N87-10547

ION INJECTION
Injection of low-energy ions during geomagnetic storms N87-10553
Equatorial magnetospheric particles and auroral precipitations N87-10557

ION MOTION
Vertical transport of O(+) ions at high latitudes N87-10565
Field-aligned motions of O(+) and H(+) thermal ions in a magnetic field tube convected across the dayside polar cusp: Model calculations N87-10567

ION PROPULSION
NASA studying concept to measure distance between stars, galaxies [NASA-NEWS-REL-86-133] N87-10787

IONIZATION
Laser induced chemical reactions and laser-collision processes [DE86-011459] N87-10385

IONOSONDES
Two-dimensional snapshots of electron density in the main trough and diffuse auroral zone from a close network of ionosondes: Comparison with measurements from AUREOL-3 satellite N87-10601

IONOSPHERE
HISCAT: A proposed new scatter facility in Northern Scandinavia N87-10498
Consequences of imperfect magnetosphere-ionosphere coupling N87-10549
Magnetospheric-ionospheric coupling deduced from measurements above a discrete auroral arc N87-10550
A photometric and in situ study of stable auroral red arcs N87-10628
A study of disturbed solar wind and magnetotail based on ISEE-3 data [NASA-CR-177060] N87-10816

IONOSPHERIC CURRENTS
Small scale and intense field-aligned currents detected by their magnetic signature N87-10546

IONOSPHERIC DISTURBANCES
Observations of low intensity particle fluxes inside the region of the ionospheric main trough and their variability N87-10556
Objectives and design of the ECHO 6 electron beam experiment: Large ionospheric perturbations and energetic particle patterns — rocket sounding N87-10590
The E region instabilities in the polar ionosphere N87-10599

IONOSPHERIC DRIFT
Positive ion distributions in the morning auroral zone: Local acceleration and drift effects N87-10547

IONOSPHERIC ELECTRON DENSITY
Simultaneous measurements of thermal electron density-temperature and low energy precipitating electron fluxes in topside ionosphere N87-10544
Density gradient instability in the high latitude ionosphere. Relation with the electrostatic turbulence and convection N87-10573
Two-dimensional snapshots of electron density in the main trough and diffuse auroral zone from a close network of ionosondes: Comparison with measurements from AUREOL-3 satellite N87-10601
Step-like profiles of electron density in the subauroral lower F-region in the morning sector and possible mechanisms of their formation during substorms: The comparison of data of ground-based ionosondes with the AUREOL-3 satellite measurements N87-10603

IONOSPHERIC ION DENSITY
Injection of low-energy ions during geomagnetic storms N87-10553
Evidence for ion energy dispersion in the polar cusp related to a northward directed Interplanetary Magnetic Field (IMF) N87-10561
Nonstationary field-aligned fluxes of thermal ions O(+) and H(+) outside the plasmapause: Refinement of the polar wind theory N87-10566

IONOSPHERIC PROPAGATION
Experimental evidence of field-aligned ELF plasma ducts in the ionospheric trough and in the auroral zone N87-10574
On the spectral broadening of the ground-based VLF transmitter signals in the high-latitude ionosphere observed from Intercosmos-19 and AUREOL-3 satellites N87-10584

IONOSPHERIC SOUNDING
Results of the ARCAD 3 Project and of Recent Programs in Magnetospheric and Ionospheric Physics — conferences [ISBN-2-85428-126-8] N87-10541
Polar cap/polar cusp studies using incoherent scatter radar facilities — ionosphere N87-10562
Observations of polar-cap ionospheric signatures of polar wind/magnetosphere coupling N87-10563
Evidence for high latitude ionospheric ion acceleration N87-10564
Vertical transport of O(+) ions at high latitudes N87-10565
Active experiments from ground — magnetosphere; ionosphere N87-10581
Objectives and design of the ECHO 6 electron beam experiment: Large ionospheric perturbations and energetic particle patterns — rocket sounding N87-10590
Artificial ion beam interaction with the auroral plasma N87-10591
Intercosmos-Bulgaria-1300 satellite: Large-scale structure and dynamics of the polar ionosphere during geomagnetic storms N87-10592
A multipoint study of a substorm on 4 March 1979 — magnetosphere N87-10595
The ARCAD 3-SAFARI coordinated study of auroral and polar F-region ionospheric irregularities N87-10600
Comparative magnetospheric/ionospheric studies using Dynamics Explorer spacecraft and ground-based radars N87-10602
Self-consistent analysis of high drift velocity measurements with the Scandinavian Twin Auroral Radar Experiment (STARE) system N87-10606
Coordinated data on auroral electrodynamics from ground based radar diagnostics and AUREOL-3 satellite N87-10607

IONOSPHERICS
Two dimensional analysis of high voltage solar array interfering with ionospheric plasma N87-10022

IRON ALLOYS
Castable hot corrosion resistant alloy [NASA-CASE-LEW-14134-1] N87-10192
Review of embrittlement mechanisms in tungsten heavy alloys [DE86-011114] N87-10196

IRON COMPOUNDS
Development of iron aluminides [AD-A168578] N87-10194

ISCHEMIA
Exercise-induced myocardial ischemia at high altitude simulated in a negative pressure chamber N87-10702

ISOTHERMS
Computer assisted gas chromatography for thermodynamic measurements of polymer surfaces [AD-A167450] N87-10208

J

JAPANESE SPACECRAFT
Operational criteria for geostationary satellites in National Space Development Agency (NASDA) N87-10119
Attitude determinations for geostationary satellites of the National Space Development Agency (NASDA) N87-10124

JET AIRCRAFT
A study of the flow field about an upper surface blown wing and its effects on longitudinal static stability of a small jet airplane N87-10009

JET AIRCRAFT NOISE
Free jet feasibility study of a thermal acoustic shield concept for AST/VCE application: Dual stream nozzles [NASA-CR-3867] N87-10752
Free-jet acoustic investigation of high-radius-ratio coannular plug nozzles [NASA-CR-3818] N87-10753

JET FLAPS
A study of the flow field about an upper surface blown wing and its effects on longitudinal static stability of a small jet airplane N87-10009

JET FLOW
Far field noise studies of contoured and solid/porous conical plug-nozzle jet flows N87-10049
Near field pressure fluctuations in a circular jet [NASA-CR-179847] N87-10249
Free surface turbulence [AD-A168013] N87-10251

JET PROPULSION
Wind tunnel test of the modified goldschmied model with propulsion and empennage: Analysis of test results [AD-A167360] N87-10045

JET STREAMS (METEOROLOGY)
Examples of mesoscale structures and short-term wind variations detected by VHF Doppler radar N87-10422
Preliminary estimates of vertical momentum flux N87-10459

JOINTS (JUNCTIONS)
Control of large flexible space structures [NASA-CR-177063] N87-10168
Chemisorption mechanism and effect of polyacrylic acid on the improvement in bond durability of zinc phosphate-to-polymer adhesive joints [DE86-011535] N87-10213
Mode 1 delamination growth in adhesively bonded joints under static and fatigue loads [NASA-CR-178812] N87-10409

JUPITER (PLANET)
Periodic amplitude variations in Jovian continuum radiation [NASA-CR-177070] N87-10813
Clouds and methane photochemical hazes on the outer planets N87-10815

K

KILOMETRIC WAVES
Scenarios for the generation of auroral kilometric radiation N87-10577
The cyclotron maser theory of AKR and Z-mode radiation — Auroral Kilometric Radiation (AKR) N87-10578

KINEMATICS
Three-dimensional structure of the heliosphere: Quiet-time and disturbed periods N87-10818

KINETIC ENERGY
A study of gravity-wave spectra in the troposphere and stratosphere at 5-min to 5-day periods with the Poker Flat MST radar N87-10462
A model for the evolving stably stratified nocturnal boundary layer based on the turbulent kinetic energy equation N87-10608
Relationships between available potential energy, kinetic energy and extratropical cyclones within limited regions of the Northern Hemisphere during the FGGE Year N87-10668

KINETIC EQUATIONS
A high resolution entrainment model for the convective planetary boundary layer N87-10611

KINETICS
Titanium oxidation kinetics and the mechanism for thermal ignition of titanium-based pyrotechnics [DE86-010987] N87-10218

KRYPTON FLUORIDE LASERS
Subpicosecond high-brightness UV laser system [DE86-011271] N87-10387

L

LAMINAR BOUNDARY LAYER

Experimental study of the boundary layer on a low Reynolds number airfoil in steady and unsteady flow N87-10052

LAMINATES

Short-wavelength buckling and shear failures for compression-loaded composite laminates N87-10403

LAND USE

Space imaging radar for remote sensing of the Earth: An evaluation [BMFT-FB-W-85-024] N87-10529

LANDAU DAMPING

Observational and theoretical investigation of stable auroral red arcs and their magnetospheric energy source, volumes 1 and 2 N87-10632

LANDSAT SATELLITES

LANDSAT imagery of the Central Andes [NASA-CR-179852] N87-10526

LARGE SPACE STRUCTURES

Reliability issues in active control of large flexible space structures [NASA-CR-179785] N87-10167

Control of large flexible space structures [NASA-CR-177063] N87-10168

A space station Structures and Assembly Verification Experiment, SAVE [NASA-TM-89004] N87-10170

Application of graph theory to the nonlinear analysis of large space structures N87-10418

LASER ALTIMETERS

World geodetic system 1984 [AD-A167570] N87-10527

LASER APPLICATIONS

Investigations on the parameters for laser surface treatment by cladding and alloying [BMFT-FB-T-85-183] N87-10203

Thirteenth International Laser Radar Conference [NASA-CP-2431] N87-10263

Lidar remote sensing from space: NASA's plans in the Earth sciences N87-10265

Tunable solid-state laser technology for applications to scientific and technological experiments from space N87-10266

Development of a high-altitude airborne dial system: The Lidar Atmospheric Sensing Experiment (LASE) N87-10268

Methods for estimating the optical constants of atmospheric hazes based on complex optical measurements N87-10301

Progress in coherent laser radar N87-10326

Lower atmospheric temperature profile measurements using a Raman lidar N87-10331

Chemical contamination remote sensing N87-10375

Laser-initiated chain reactions in the partial oxidation of methane [DE86-011272] N87-10388

High precision absolute laser power measurements using a magnetically suspended rotor [DE86-011585] N87-10389

LASER CAVITIES

Pulsed mononode dye laser developed for a geophysical application N87-10364

Possibility of obtaining coherent short wave radiation from a solid state free electron laser [DE86-010525] N87-10381

LASER DAMAGE

Flash/crazing effects on simulator pursuit tracking performance [AD-A167680] N87-10759

Workshop on the Physics and Chemistry of Solar-Flux Effects on Condensed Phase/Gas Interfaces [DE86-004460] N87-10817

LASER INDUCED FLUORESCENCE

Feasibility experiments on time-resolved fluorosensing applied to oil slicks N87-10322

Rotationally resolved collisional transfer rates in OH N87-10323

LASER OUTPUTS

Optical models of the molecular atmosphere N87-10306

Multiple scattering of laser beams in dense hydrosols N87-10316

An intensity-modulated dual-wavelength He-Ne laser for remote sensing of methane N87-10319

Linewidth characteristics of Raman-shifted dye laser output at 720 and 940 nm N87-10370

Scattered radiation field of a laser beam propagating through turbid media [DE86-010188] N87-10386

High precision absolute laser power measurements using a magnetically suspended rotor [DE86-011585] N87-10389

LASER PLASMA INTERACTIONS

Laser-powered MHD generators for space application [NASA-TP-2621] N87-10764

LASER RANGE FINDERS

ESA activities in space laser sounding and ranging N87-10264

LASER SPECTROSCOPY

A combined Raman lidar for low tropospheric studies N87-10332

Spectroscopic aspects of differential method for sounding gas composition of the atmosphere N87-10369

LASER TARGETS

Feasibility experiments on time-resolved fluorosensing applied to oil slicks N87-10322

LASERS

Thirteenth International Laser Radar Conference [NASA-CP-2431] N87-10263

Visibility related to backscatter at 1.54 micron N87-10272

Laser induced chemical reactions and laser-collision processes [DE86-011459] N87-10385

LATE STARS

Observations of non-thermal radiation from late-type stars N87-10793

LAUNCH WINDOWS

Analysis of the problem of satellite launch windows for Ariane dual launches N87-10115

LAUNCHING SITES

Orbital transfer vehicle launch operations study. Volume 1: Executive summary [NASA-CR-179701] N87-10110

LEADING EDGE FLAPS

Analysis of the vortical flow around a 60 deg Delta wing with vortex flap N87-10006

LEADING EDGE THRUST

Wind tunnel test of the modified goldschmied model with propulsion and empennage: Analysis of test results [AD-A167360] N87-10045

LEAST SQUARES METHOD

New solution of the problem of EMP coupling on cables over ground of finite conductivity [DE86-006078] N87-10229

Strength, width, and pressure shift measurements of 54 lines in the oxygen A-band N87-10298

LIFE (DURABILITY)

Fatigue response of notched laminates subjected to tension-compression cyclic loads [NASA-CR-179604] N87-10183

Design, construction and long life endurance testing of cathode assemblies for use in microwave high-power transmitting tubes [NASA-CR-175116] N87-10237

LIFE SPAN

Life expectancy in tropical climates and urbanization N87-10648

LIFT

A study of the flow field about an upper surface blown wing and its effects on longitudinal static stability of a small jet airplane N87-10009

Computational aerodynamics of supersonic lifting vehicles N87-10030

LIFT DEVICES

A study of the flow field about an upper surface blown wing and its effects on longitudinal static stability of a small jet airplane N87-10009

LIGHT BEAMS

Multiple scattering measurements in laboratory and foggy atmosphere N87-10315

Scattered radiation field of a laser beam propagating through turbid media [DE86-010188] N87-10386

LIGHT SCATTERING

The influence of scattering particles morphology on the characteristics of lidar signals N87-10309

Multiple scattering measurements in laboratory and foggy atmosphere N87-10315

Multiple scattering of laser beams in dense hydrosols N87-10316

Lidar mapping of a mixture of aerosol concentrations in a varying atmosphere N87-10320

Vertical structure of Arctic haze observed by lidar N87-10335

Scattered radiation field of a laser beam propagating through turbid media [DE86-010188] N87-10386

Light scattering in resonance region from polydisperse non-spherical particles N87-10792

LIGHT TRANSMISSION

Scattered radiation field of a laser beam propagating through turbid media [DE86-010188] N87-10386

LIGHTNING

Observations of thunder with the Arecibo VHF radar N87-10444

UHF and VHF radar observations of thunderstorms N87-10473

Review of measurements of the RF spectrum of radiation from lightning [NASA-TM-87788] N87-10658

LINE SPECTRA

Linewidth characteristics of Raman-shifted dye laser output at 720 and 940 nm N87-10370

High resolution spectroscopy of quasar absorption lines N87-10785

LINEAR ACCELERATORS

Progress made during 1985 in the scientific and technical program of National Physical Laboratory's Division of Radiation Science and Acoustics N87-10776

LINEAR EQUATIONS

Nonlinear rotordynamics analysis [NASA-CR-178931] N87-10407

Novel parallel architectures and algorithms for linear algebra processing [NASA-CR-179826] N87-10743

LINEAR PROGRAMMING

Application of linear programming to final positioning (drift orbit) of a geostationary satellite N87-10149

TV-SAT final orbit acquisition optimization strategy N87-10150

LININGS

Demonstration of laser speckle system on burner liner cyclic rig [NASA-CR-179509] N87-10377

LIQUID METAL COOLED REACTORS

Design rule for fatigue of welded joints in elevated-temperature nuclear components [DE86-007569] N87-10393

LIQUID METAL FAST BREEDER REACTORS

Linearized model for the hydrodynamic stability investigation of molten fuel jets into the coolant of a Liquid Metal Fast Breeder Reactor (LMFBR) [KFK-3978] N87-10757

LIQUID METALS

Surface attack on metals in the presence of liquid metals [AD-A167403] N87-10193

Detailed transient model of a liquid-metal heat pipe [DE86-011212] N87-10257

LIQUID SLOSHING

Spin dynamics with sloshing effects for solid motor burning phase — satellite dynamics N87-10140

LIQUID-VAPOR INTERFACES

Interface properties and crystal-growth mechanisms [DE86-010846] N87-10767

LOAD TESTS

Experimental procedure for lifetime testing of graphite bundles under constant load [AD-A167714] N87-10186

The effects of temperature and loading rate on R-curves using the CLWL techniques — crack growth resistance curve (R curve); crack line wedge load (CLWL) [BAE-MSM-R-GEN-0544] N87-10405

LOADS (FORCES)

Composite load spectra for select space propulsion structural components [NASA-CR-179496] N87-10176

LOGIC CIRCUITS

The NOAA TOGA antenna array N87-10500

LOGIC PROGRAMMING

A rule based computer aided design system [NASA-TM-86241] N87-10721

Parallel logic programming for numeric applications [DE86-011004] N87-10726

LONG TERM EFFECTS

An investigation on passively controlled geosynchronous orbits N87-10118

LONG WAVE RADIATION

Observational studies of wave disturbances in the tropical Pacific and their relationship with deep cloud activity N87-10634

LONGITUDINAL CONTROL

Effects of flap position on longitudinal parameters of HFB-320 [NAL-TM-SE-8602] N87-10062

Longitudinal orbit control from INTELSAT 5 inclination stationkeeping maneuvers N87-10156

LONGITUDINAL STABILITY

Summary of longitudinal stability and control parameters as determined from space shuttle Columbia flight test data [NASA-TM-87768] N87-10101

LOW GRAVITY MANUFACTURING

Microgravity Science and Applications [NASA-CR-179793] N87-10204

LOW PASS FILTERS

MODTEQ (Modulation Techniques), AN/FRC-170(V), equalization, and channel medium simulations [AD-A167965] N87-10226

LOW REYNOLDS NUMBER

The effect of free stream disturbances and control surface deflections on the performance of the Wortmann airfoil at low Reynolds numbers N87-10007

LOW TEMPERATURE TESTS

Surface attack on metals in the presence of liquid metals [AD-A167403] N87-10193

LOWER ATMOSPHERE

Extinction and visibility measurements in the lower atmosphere with UV-YAG-lidar N87-10276

Lower atmospheric temperature profile measurements using a Raman lidar N87-10331

LOWER IONOSPHERE

Very low frequency and ELF effects in the upper ionosphere caused by large-scale acoustic waves in the lower ionosphere observed from AUREOL-3 satellite N87-10587

LYMPHOCYTES

The use of decompression to simulate the effect of extravehicular activity on human lymphocyte transformation N87-10697

M

MAGNETIC ANOMALIES

Scenarios for the generation of auroral kilometric radiation N87-10577

MAGNETIC DISTURBANCES

Solar-geophysical data number 501, May 1986. Part 2: (Comprehensive reports). Data for November 1985 and miscellanea [PB86-218047] N87-10622

MAGNETIC EFFECTS

The distant magnetotail — magnetic substorms N87-10558

Field-aligned motions of O(+) and H(+) thermal ions in a magnetic field tube convected across the dayside polar cusp: Model calculations N87-10567

MAGNETIC FIELD CONFIGURATIONS

Magnetic field-aligned potential drops N87-10545

Fine structure of fields and plasma in the field-aligned current region on the Intercosmos-Bulgaria-1300 satellite data N87-10568

MAGNETIC FIELDS

Mathematical and computational models of plasma flows N87-10036

Solar-geophysical data number 501, May 1986. Part 1: (Prompt reports). Data for April 1986, March 1986 and late data [PB86-218039] N87-10623

MAGNETIC FILMS

Wire dipoles and antennas with dielectric or magnetic coatings [AWRE-O-19/85] N87-10235

MAGNETIC PROPERTIES

Theoretical studies on the structures of insulating and metallic glasses [DE86-011484] N87-10212

Sulfur-based synthetic metal superconductors [DE86-010512] N87-10768

MAGNETIC SIGNATURES

Small scale and intense field-aligned currents detected by their magnetic signature N87-10546

MAGNETIC STORMS

Plasma sheet boundary electric fields during substorms N87-10548

Consequences of imperfect magnetosphere-ionosphere coupling N87-10549

Injection of low-energy ions during geomagnetic storms N87-10553

Formation and deformation of the plasmapause during a substorm event N87-10555

The distant magnetotail — magnetic substorms N87-10558

Fine structure of fields and plasma in the field-aligned current region on the Intercosmos-Bulgaria-1300 satellite data N87-10568

Intercosmos-Bulgaria-1300 satellite: Large-scale structure and dynamics of the polar ionosphere during geomagnetic storms N87-10592

Connection between particle precipitations and the plasma sheet during substorms N87-10594

A multipoint study of a substorm on 4 March 1979 — magnetosphere N87-10595

Step-like profiles of electron density in the subauroral lower F-region in the morning sector and possible mechanisms of their formation during substorms: The comparison of data of ground-based ionosondes with the AUREOL-3 satellite measurements N87-10603

A study of disturbed solar wind and magnetotail based on ISEE-3 data [NASA-CR-177060] N87-10816

MAGNETIC SUSPENSION

High precision absolute laser power measurements using a magnetically suspended rotor [DE86-011585] N87-10389

MAGNETIZATION

The onset of alfvenic turbulence N87-10762

MAGNETOHYDRODYNAMIC FLOW

Mathematical and computational models of plasma flows N87-10036

The hot ion composition in the magnetosphere N87-10552

MAGNETOHYDRODYNAMIC GENERATORS

Laser-powered MHD generators for space application [NASA-TP-2621] N87-10764

MAGNETOHYDRODYNAMIC STABILITY

Plasma confinement by a radio frequency plugging potential in an axisymmetric mirror-cusp device [IPPJ-784] N87-10763

MAGNETOHYDRODYNAMIC WAVES

The onset of alfvenic turbulence N87-10762

MAGNETOSPHERE

Results of the ARCAD 3 Project and of Recent Programs in Magnetospheric and Ionospheric Physics — conferences [ISBN-2-85428-126-6] N87-10541

Consequences of imperfect magnetosphere-ionosphere coupling N87-10549

Magnetospheric-ionospheric coupling deduced from measurements above a discrete auroral arc N87-10550

Observations of polar-cap ionospheric signatures of polar wind/magnetosphere coupling N87-10563

Mechanism of low-frequency wave propagation in the magnetosphere N87-10580

Active experiments from ground — magnetosphere; ionosphere N87-10581

Comparative magnetospheric/ionospheric studies using Dynamics Explorer spacecraft and ground-based radars N87-10602

Generation of Pc2 pulsations by energetic O(+) ions N87-10605

A photometric and in situ study of stable auroral red arcs N87-10626

Periodic amplitude variations in Jovian continuum radiation [NASA-CR-177070] N87-10813

Plasma wave observations at Uranus from Voyager 2 [NASA-CR-177069] N87-10814

MAGNETOSPHERIC ION DENSITY

The hot ion composition in the magnetosphere N87-10552

Equatorial magnetospheric particles and auroral precipitations N87-10557

MAINTENANCE

Wind profiler demonstration system N87-10487

Integrated testing and analysis of mathematical software tools. Summary of research activities, 1 August 1985-1 May 1986 [DE86-010882] N87-10723

Use of fuzzy sets mathematics to assist pavement evaluation and management (revised March 18, 1986) [PB86-214798] N87-10747

MAN MACHINE SYSTEMS

Design guidelines for human-computer dialogues [DE86-011543] N87-10728

MAN-COMPUTER INTERFACE

Integrated testing and analysis of mathematical software tools. Summary of research activities, 1 August 1985-1 May 1986 [DE86-010882] N87-10723

MANAGEMENT

Use of fuzzy sets mathematics to assist pavement evaluation and management (revised March 18, 1986) [PB86-214798] N87-10747

A summary of the Foundation Research Program, fiscal year 1985 [AD-A168009] N87-10780

MANAGEMENT PLANNING

Engine-airframe integration for rotorcraft: System specifications and qualification N87-10074

MANIPULATORS

Dynamic modeling and control of robotic manipulators N87-10390

Experimental identification and control of the tip position of a flexible, single link manipulator N87-10397

Rapid precise end point control of a wrist carried by a flexible manipulator N87-10398

FORPS: A FORTH-based production system and its application to a real-time robot control problem [DE86-005426] N87-10734

MANNED SPACE FLIGHT

Space motion sickness N87-10693

MAPPING

DMAHTC (Defense Mapping Agency Hydrographic/Topographic Center) GPS point positioning software: Initial results [AD-A167586] N87-10058

Dynamic remapping decisions in multi-phase parallel computations [NASA-CR-178174] N87-10719

MAPS

Digital mapping: Fact or fiction [AD-A167571] N87-10528

MARINE ENVIRONMENTS

Modeling the effects of the spatially varying sea surface temperature on the marine atmospheric boundary layer N87-10673

MARINE METEOROLOGY

Using a laser aureole to invert lidar return N87-10292

Lidar observations and modeling of cold air outbreaks during MASEX and GALE N87-10336

Multiple scattering depolarization in marine stratus clouds: Lidar experiments N87-10350

MARKET RESEARCH

Geostationary satellites: Their market, their evolution in the 1990s N87-10165

MARS (MANNED REUSABLE SPACECRAFT)

The case for Mars: Concept development for a Mars research station [NASA-CR-179753] N87-10812

MARS SURFACE

The case for Mars: Concept development for a Mars research station [NASA-CR-179753] N87-10812

MASER OUTPUTS

A study of the ground state hydroxyl maser emissions associated with eleven regions of star formation N87-10826

MASERS

The cyclotron maser theory of AKR and Z-mode radiation — Auroral Kilometric Radiation (AKR) N87-10578

MASS TRANSFER

Computer simulation in engineering hydrodynamics N87-10038

MATHEMATICAL MODELS

Computational aerodynamics of supersonic lifting vehicles N87-10030

Mathematical and computational models of plasma flows N87-10036

An eddy-current model for three-dimensional nondestructive evaluation of advanced composites [AD-A167688] N87-10185

The study of microstrip antenna arrays and related problems [NASA-CR-179714] N87-10225

Electrical circuit modeling of conductors with skin effect [DE86-011085] N87-10240

Detailed transient model of a liquid-metal heat pipe [DE86-011212] N87-10257

Nonlinear rotordynamics analysis [NASA-CR-178931] N87-10407

Gravity wave dynamics near the mesopause over Poker Flat, Alaska N87-10631

Advective influences on steady and transient forced tropical motions N87-10670

Free vibration and dynamic response analysis of spinning structures [NASA-CR-179672] N87-10717

Numerical and experimental study of dynamics of two-dimensional body [ISAS-619] N87-10748

Mathematical model for the Bridgman-Stockbarger crystal growing system [NASA-CR-178921] N87-10766

On the tidal interaction between spherical galaxies N87-10810

Three-dimensional structure of the heliosphere: Quiet-time and disturbed periods N87-10818

MATRICES (MATHEMATICS)

Optimal filtration of the atmospheric parameters profiles N87-10305

MATTER (PHYSICS)

Possible significance of a new dimensionless ratio in cosmology [DE86-011026] N87-10801

MAXIMUM LIKELIHOOD ESTIMATES

Cramer-Rao bound analysis for frequency estimation of sinusoids in noise [AD-A167992] N87-10227

MEASURING INSTRUMENTS

Attempts to characterize microballoon sensors for shock velocity and material motion studies [DE86-011210] N87-10379

MST radar networks and campaigns session summary and recommendations N87-10478

MECHANICAL DRIVES

Engine-Airframe Integration for Rotorcraft [AGARD-LS-148] N87-10067

MECHANICAL ENGINEERING
A summary of the Foundation Research Program, fiscal year 1985 [AD-A168009] N87-10780
MECHANICAL PROPERTIES
Chemistry research resource [DE86-009891] N87-10178
Development of iron aluminides [AD-A168578] N87-10194
MELTS (CRYSTAL GROWTH)
Interface properties and crystal-growth mechanisms [DE86-010846] N87-10767
MEMBRANES
Permeation membrane-type distiller [DE86-011153] N87-10254
Thermopervaporation device [DE86-011151] N87-10255
MESH
Theory of wire-grid modelling: Criteria for highly conducting surfaces — plane wave scattering [AWRE-O-20/85] N87-10224
MESOMETEOROLOGY
On the potential use of radar-derived information in operational numerical weather prediction N87-10420
MESOPAUSE
Lidar detection of metallic species at the mesopause level N87-10346
Investigations of the lower and middle atmosphere at the Arecibo Observatory and a description of the new VHF radar project N87-10494
MESOSCALE PHENOMENA
Examples of mesoscale structures and short-term wind variations detected by VHF Doppler radar N87-10422
Observations of mesoscale vertical velocities around frontal zones N87-10424
Comparison of vertical velocities analyzed by a numerical model and measured by a VHF wind profiler N87-10425
Hardware requirements: A new generation partial reflection radar for studies of the equatorial mesosphere N87-10431
A model for gravity-wave spectra observed by Doppler sounding systems N87-10434
Evidence of a saturated gravity-wave spectrum throughout the atmosphere N87-10467
MESOSPHERE
Lidar observation of the mesospheric sodium layer in Antarctica N87-10345
Daytime lidar measurements of tidal winds in the mesospheric sodium layer at Urbana, Illinois N87-10347
Mesospheric wind measurements using a medium-frequency imaging Doppler interferometer N87-10476
An analysis at mesospheric coherent-scatter power enhancements during solar flare events N87-10479
Progress in existing and planned MST radars N87-10481
Current status of the Poker Flat MST radar N87-10483
Recent progress in the Urbana MST radar N87-10485
The Penn State Doppler network progress report N87-10489
System aspects of the Indian MST radar facility N87-10497
Gravity wave dynamics near the mesopause over Poker Flat, Alaska N87-10631
METABOLISM
Upper and lower body anaerobic power comparison between biathletes and control subjects [AD-A167636] N87-10710
METAL FATIGUE
Design rule for fatigue of welded joints in elevated-temperature nuclear components [DE86-007569] N87-10393
METAL HYDRIDES
Re-examination of the neptunium-hydrogen system [DE86-010197] N87-10216
METAL MATRIX COMPOSITES
Effects of thermal cycling on graphie-fiber-reinforced 6061 aluminum [NASA-TP-2612] N87-10184
METAL SURFACES
Investigations on the parameters for laser surface treatment by cladding and alloying [BMFT-FB-T-85-183] N87-10203
METALLIC GLASSES
Theoretical studies on the structures of insulating and metallic glasses [DE86-011484] N87-10212
METALLICITY
High resolution CCD spectra of stars in globular clusters. Part 2: Metals and CNO in M71 [NASA-CR-179653] N87-10789
METALS
Surface attack on metals in the presence of liquid metals [AD-A167403] N87-10193
METEOROID PROTECTION
Coaxial tube tether/transmission line for manned nuclear space power [NASA-CASE-LEW-14338-1] N87-10174
METEOROLOGICAL CHARTS
Monthly and seasonal weather outlook for mid-May to mid-June 1986, volume 40, number 10, May 14, 1986 [PB86-199825] N87-10664
METEOROLOGICAL PARAMETERS
Thirteenth International Laser Radar Conference [NASA-CP-2431] N87-10263
ESA activities in space laser sounding and ranging N87-10264
Lidar remote sensing from space: NASA's plans in the Earth sciences N87-10265
Tunable solid-state laser technology for applications to scientific and technological experiments from space N87-10266
MIE Lidar proposed for the German Space Shuttle Mission D2 N87-10269
Correction function in the Lidar equation and the solution techniques for CO2 Lidar date reduction N87-10280
A Meteorological (humidity, temperature, aerosols)) mobile dial system: Concepts and design N87-10286
Optical models of the molecular atmosphere N87-10306
A combined Raman lidar for low tropospheric studies N87-10332
Alexandrite laser source for atmospheric lidar measurements N87-10373
Development of worst case meteorology criteria [PB86-215993] N87-10540
The urban climate of Mexico City N87-10640
Some aspects of the urban climate of Shanghai N87-10641
Some aspects of the urban climates of India N87-10643
Shuttle derived atmospheric density model. Part 1: Comparisons of the various ambient atmospheric source data with derived parameters from the first twelve STS entry flights, a data package for AOTV atmospheric development [NASA-CR-171824] N87-10662
METEOROLOGICAL RADAR
Middle Atmosphere Program. Handbook for MAP, volume 20 [NASA-CR-176882] N87-10419
A theory for the retrieval of virtual temperature from winds, radiances and the equations of fluid dynamics N87-10421
Examples of mesoscale structures and short-term wind variations detected by VHF Doppler radar N87-10422
Wind profiler data in a mesoscale experiment from a meteorological perspective N87-10423
Observations of mesoscale vertical velocities around frontal zones N87-10424
Comparison of vertical velocities analyzed by a numerical model and measured by a VHF wind profiler N87-10425
Measurements of precipitating atmosphere by the MU radar N87-10426
The influence of velocity variability on the determination of wind profiles N87-10428
A look at profiler performance N87-10430
Simultaneous VHF and UHF radar observation of the mesosphere at Arecibo during a solar flare: A check on the gradient-mixing hypothesis N87-10437
Gravity waves in severe weather N87-10442
Simultaneous rocket and MST radar observation of an internal gravity wave breaking in the mesosphere N87-10443
The PROUST radar: First results N87-10445
Simultaneous fine structure observation of wind and temperature profiles by the Arecibo 430-MHz radar and in situ measurements N87-10446
Comparison between S. T. radar and in situ balloon measurements N87-10447
A statistical model to estimate refractivity turbulence structure constant C sub n sup 2 in the free atmosphere N87-10448
Determination of the Brunt-Vaisala frequency from vertical velocity spectra N87-10449
The use of the experimentally deduced Brunt-Vaisala frequency and turbulent velocity fluctuations to estimate the eddy diffusion coefficient N87-10450
Mesospheric gravity-wave climatology at Adelaide N87-10456
Possibility of measuring gravity-wave momentum flux by single beam observation of MST radar N87-10458
Preliminary estimates of vertical momentum flux N87-10459
The frequency spectrum of C sub n sup 2 from MST radar data N87-10461
On the varying slope of velocity spectra N87-10463
Doppler effects on velocity spectra observed by MST radars N87-10464
Observations of vertical velocity power spectra with the SOUSY VHF radar N87-10465
Mesospheric wave number spectra from Poker Flat MST radar measurements compared with gravity-wave model N87-10466
Intercomparison and calibration of wind and wave measurements at various frequencies N87-10468
An evaluation of errors observed in the measurement of low wind velocities N87-10469
A comparison of vertical velocities measured from specular and nonspecular echoes by a VHF radar N87-10470
Methods for verifying the accuracy of wind profiles N87-10471
A comparison of thunderstorm reflectivities measured at the VHF and UHF N87-10472
UHF and VHF radar observations of thunderstorms N87-10473
Comparison of medium frequency pulsed radar interferometer and correlation analysis winds, part 1 N87-10474
Colorado wind profilers N87-10486
METEOROLOGY
A theory for the retrieval of virtual temperature from winds, radiances and the equations of fluid dynamics N87-10421
Examples of mesoscale structures and short-term wind variations detected by VHF Doppler radar N87-10422
Gravity waves in the middle atmosphere: Recent progress and needed studies N87-10433
A summary of the Foundation Research Program, fiscal year 1985 [AD-A168009] N87-10780
METHANE
Developing simplified models of combustion chemistry by simulation with detailed chemical kinetics models [DE86-008381] N87-10188
An intensity-modulated dual-wavelength He-Ne laser for remote sensing of methane N87-10319
Gas correlation lidar for methane detection N87-10356
Laser-initiated chain reactions in the partial oxidation of methane [DE86-011272] N87-10388
Bioconversion: A New Technology for Waste and Sludge Disposal. Workshop proceedings [DE86-009668] N87-10539
METHOD OF MOMENTS
Extension of the electromagnetic method of moments code CHAOS to treat configurations of dielectric-coated wires [AWRE-O-18/85] N87-10234
METHYL COMPOUNDS
Synthesis of energetic materials [AD-A167787] N87-10214
MEXICO
The urban climate of Mexico City N87-10640
MICROANALYSIS
Micro-tomography using synchrotron radiation [DE86-010982] N87-10191
MICROBALANCES
Advanced desiccant materials research [DE86-010695] N87-10536
MICROBALLOONS
Attempts to characterize microballoon sensors for shock velocity and material motion studies [DE86-011210] N87-10379
MICROBURSTS
Aircraft accident reeport, Delta Air Lines, Inc., Lockheed L-1011-385-1, N726DA, Dallas/Fort Worth International Airport, Texas, August 2, 1985 [PB86-910406] N87-10053
Doppler Radar Detection of Wind Shear [NASA-CP-2435] N87-10054
MICROCHANNEL PLATES
The development and test of multi-anode microchannel array detector systems. Part 2: Soft X-ray detectors [NASA-CR-177066] N87-10236
MICROCOMPUTERS
An accelerated forth data-acquisition system N87-10516
MICROELECTRONICS
Electronics Engineering Department technical review [DE86-011371] N87-10241
Microelectronics research and development background paper [PB86-205200] N87-10242

MICROORGANISMS
The fungal resistance or susceptibility of resins, plasticizers, and other constituents of adhesive formulations
[AD-A166930] N87-10207
MICROPROGRAMMING
A microprogrammable radar controller N87-10516
MICROSCOPY
RLE progress report
[MIT-PR-128] N87-10778
MICROSTRIP TRANSMISSION LINES
The study of microstrip antenna arrays and related problems
[NASA-CR-179714] N87-10225
MICROSTRUCTURE
Review of embrittlement mechanisms in tungsten heavy alloys
[DE86-011114] N87-10196
Compositional and microstructural effects on hydrogen embrittlement of ASTM grade 12 titanium (Ti 0.3 Mo - 0.8 Ni)
[DE86-011379] N87-10197
Modification of the grain boundary microstructure of the austenitic PCA stainless steel to improve helium embrittlement resistance
[DE86-010396] N87-10202
Synthetic carbon precursor materials
[DE86-011584] N87-10210
Relationship between critical current and microstructure of internal tin wire
[DE86-009922] N87-10238
Methods for estimating the optical constants of atmospheric hazes based on complex optical measurements N87-10301
Microstructure, grain boundaries and properties of sintered and isotatically hot pressed SiC materials
[KFK-4063] N87-10769
MICROWAVE EQUIPMENT
Optically controlled GaAs dual-gate MESFET and permeable base transistors
[NASA-TM-88823] N87-10232
MICROWAVE LANDING SYSTEMS
Helicopter MLS Flight Inspection Project
[DOT/FAA/CT-86/14] N87-10002
MICROWAVES
Measurements of precipitating atmosphere by the MU radar N87-10426
MIDDLE ATMOSPHERE
Thirteenth International Laser Radar Conference
[NASA-CP-2431] N87-10263
XeF lidar measurements of density and temperature in the middle atmosphere N87-10342
On the potential use of radar-derived information in operational numerical weather prediction N87-10420
Examples of mesoscale structures and short-term wind variations detected by VHF Doppler radar N87-10422
Wind profiler data in a mesoscale experiment from a meteorological perspective N87-10423
Observations of mesoscale vertical velocities around frontal zones N87-10424
Comparison of vertical velocities analyzed by a numerical model and measured by a VHF wind profiler N87-10425
Measurements of precipitating atmosphere by the MU radar N87-10426
Hardware requirements: A new generation partial reflection radar for studies of the equatorial mesosphere N87-10431
Gravity waves in the middle atmosphere: Recent progress and needed studies N87-10433
Simultaneous VHF and UHF radar observation of the mesosphere at Arecibo during a solar flare: A check on the gradient-mixing hypothesis N87-10437
Propagating tides in the mesosphere N87-10441
Gravity waves in severe weather N87-10442
Simultaneous rocket and MST radar observation of an internal gravity wave breaking in the mesosphere N87-10443
The relation of gravity waves and turbulence in the mesosphere N87-10451
Can stochastic, dissipative wave fields be treated as random walk generators N87-10452
Observations and a model of gravity-wave variability in the middle atmosphere N87-10453
Mesospheric gravity-wave climatology at Adelaide N87-10456
Mesospheric wave number spectra from Poker Flat MST radar measurements compared with gravity-wave model N87-10466
Evidence of a saturated gravity-wave spectrum throughout the atmosphere N87-10467
Dynamical processes N87-10617
Millimeter-wave spectrometry of ozone in the middle atmosphere N87-10629
MIDLATITUDE ATMOSPHERE
Study of the middle latitude broadening of the spectrum of the waves emitted from ground N87-10583
MIE SCATTERING
Light scattering in resonance region from polydisperse non-spherical particles N87-10792
MILITARY AIRCRAFT
Experience with the Onboard Checkout And Monitoring System (OCAMS) of a military aircraft resulting improvements and the consequence for future design N87-10079
Integrated monitoring systems for tactical aircraft N87-10080
MILITARY TECHNOLOGY
Summary of artificial and natural icing tests conducted on US Army aircraft from 1974 to 1985
[FAA/CT-85/26] N87-10064
Intelligent Computer Assisted Instruction (ICAI): Formative evaluation of two systems
[NASA-CR-176873] N87-10716
MILKY WAY GALAXY
Molecular clouds in the Carina arm
[NASA-TM-87798] N87-10786
MILLIMETER WAVES
Millimeter-wave spectrometry of ozone in the middle atmosphere N87-10629
MINIMUM VARIANCE ORBIT DETERMINATION
Orbit achievement of RCA communication satellites N87-10122
MIRRORS
Polymer reflectors research during Fiscal Year 1985
[DE86-010697] N87-10211
Extreme ultraviolet explorer: Mirror optical tests and results
[DE86-010560] N87-10760
Plasma confinement by a radio frequency plugging potential in an axisymmetric mirror-cusp device
[IPPJ-784] N87-10763
MISSILE DEFENSE
Strategic Defense Initiative Program: Status of airborne optical adjunct and terminal imaging radar
[P86-221132] N87-10107
MISSION PLANNING
Orbital transfer vehicle launch operations study. Volume 2: Detailed summary
[NASA-CR-179791] N87-10111
ESA activities in space laser sounding and ranging N87-10264
Direct computation of orbital sunrise or sunset event parameters
[NASA-TM-87717] N87-10620
MODAL RESPONSE
Response of a 3-layered ring to an axisymmetric impulse
[DE86-011016] N87-10415
MODELS
Spin-tunnel investigation of a 1/25-scale model of the General Dynamics F-16XL airplane
[NASA-TM-85660] N87-10041
Computational fluid mechanics utilizing the variational principle of modeling damping seals
[NASA-CR-178902] N87-10246
MODULES
Vertical junction solar cells
[AD-A167757] N87-10532
MOLECULAR ABSORPTION
Vulnerability methodology and protective measures for aircraft fire and explosion hazards. Volume 3: On-Board Inert Gas Generatur System (OBIGGS) studies. Part 1: OBIGGS ground performance tests
[AD-A167357] N87-10066
MOLECULAR CLOUDS
Molecular clouds in the Carina arm
[NASA-TM-87798] N87-10786
Observations of molecular clouds in the direction of galactic and extragalactiv radio sources N87-10794
Gas and dust in regions of recent star formation N87-10800
Molecular clouds in Orion and Monoceros N87-10809
MOLECULAR DIFFUSION
Analysis on gravitational effect to nonlinear diffusion system of vapor molecules in a heat pipe N87-10023
MOLECULAR GASES
Molecular clouds in Orion and Monoceros N87-10809
MOLECULAR WEIGHT
A method of estimating the molecular weight of polymeric materials
[NASA-CASE-LAR-13212-1] N87-10206
Synthesis of energetic materials
[AD-A167787] N87-10214
An analysis of the performance of a vertically oriented, gas loaded, variable conductance heat pipe
[AD-A167874] N87-10250
MOMENTUM
Observations and a model of gravity-wave variability in the middle atmosphere N87-10453
Possibility of measuring gravity-wave momentum flux by single beam observation of MST radar N87-10458
Preliminary estimates of vertical momentum flux N87-10459
MOMENTUM TRANSFER
Guidebook for analysis of tether applications
[NASA-CR-178904] N87-10169
MONITORS
Monitoring of the MU radar antenna pattern by Satellite Ohzora (EXOS-C) N87-10509
Laboratory evaluation of three passive CO concentration monitors
[PML-1985-13] N87-10538
MONKEYS
Functions of skeletal muscles of rats and monkeys after 5-day space flight (on Cosmos 1514) N87-10686
Animal studies on Spacelab-3 N87-10704
Contribution of animal models to the investigation of bone changes in weightlessness N87-10706
Cosmos 1514 flight: Study of rhesus monkey ECG N87-10707
MONOMERS
Synthesis of energetic materials
[AD-A167787] N87-10214
MONTE CARLO METHOD
Using a laser aureole to invert lidar return N87-10292
MONTH
Monthly and seasonal weather outlook for mid-May to mid-June 1986, volume 40, number 10, May 14, 1986
[PB86-199825] N87-10684
MORNING
Positive ion distributions in the morning auroral zone: Local acceleration and drift effects N87-10547
Step-like profiles of electron density in the subauroral lower F-region in the morning sector and possible mechanisms of their formation during substorms: The comparison of data of ground-based ionosondes with the AUREOL-3 satellite measurements N87-10603
MORPHOLOGY
Bright galactic X-ray binary sources: Temporal and spectral studies N87-10804
MOTION SICKNESS
Space motion sickness N87-10693
MULTIBEAM ANTENNAS
Simultaneous multibeam sounding of wind and turbulence N87-10506
MULTIPHASE FLOW
An improved PSI-cell method for turbulent multi-phase flows N87-10034
MULTIPROCESSING (COMPUTERS)
Dynamic remapping decisions in multi-phase parallel computations
[NASA-CR-178174] N87-10719
Database algorithms for multiprocessor and very large memory systems
[DE86-009406] N87-10724
Parallel logic programming for numeric applications
[DE86-011004] N87-10726
FTMP (Fault Tolerant Multiprocessor) programmer's manual
[NASA-TM-89015] N87-10731
MULTISENSOR APPLICATIONS
A decentralized fault-tolerant approach to estimation in multi-sensor navigation systems N87-10057
MULTISTATIC RADAR
The PROUST radar: First results N87-10445
MULTIVARIATE STATISTICAL ANALYSIS
Preliminary orbit determination by static multivariate search N87-10127
MUSCLES
The muscular system in weightlessness N87-10682
Microgravity effects on the contractile proteins of rat muscles N87-10683
MUSCULAR FUNCTION
Hindlimb suspension effects on rat skeletal muscle response N87-10687
MUSCULAR TONUS
Bone tissue and muscular performance in a population of elderly men as a function of physical exercise N87-10685
MUSCULOSKELETAL SYSTEM
Functions of skeletal muscles of rats and monkeys after 5-day space flight (on Cosmos 1514) N87-10686

N

NARROWBAND
Nonthermal continuum-terrestrial myriametric radiation narrowband electromagnetic emission N87-10579

NASA PROGRAMS
Department of Housing and Urban Development-Independent Agencies Appropriation Bill, 1987 [S-REPT-99-487] N87-10773
National Aeronautics and Space Administration N87-10774
National Aeronautics and Space Administration Authorization Act, 1987 N87-10775
Aeronautics and space report of the President [NASA-TM-89239] N87-10827

NASA SPACE PROGRAMS
Total-dose radiation effects data for semiconductor devices. 1985 Supplement. Volume 2, part B [NASA-CR-179741] N87-10765

NAVIER-STOKES EQUATION
Report of the International Symposium on Computational Fluid Dynamics, Tokyo N87-10029
Numerical modeling of spatial flows on the basis of splitting up method N87-10031
Analysis of two-dimensional incompressible flow past airfoils using unsteady Navier-Stokes equations [NASA-CR-179823] N87-10040
Numerical study of hydrogen-air supersonic combustion by using elliptic and parabolized equations [NASA-CR-179600] N87-10187
Global pressure relaxation procedure with application to viscous and inviscid flows N87-10247

NAVIGATION
Trajectory scoring in geodetic coordinates using transponder-interrogator range data [DE86-009554] N87-10109

NAVIGATION AIDS
A decentralized fault-tolerant approach to estimation in multi-sensor navigation systems N87-10057
Terrestrial evaluation of the Global Positioning System (GPS) Standard Positioning Service (SPS) [PB86-219599] N87-10059

NAVIGATION SATELLITES
DMA (Defense Mapping Agency) orbit determination for transit satellites: 1985 [AD-A167567] N87-10108

NAVSTAR SATELLITES
Orbit determination of geostationary satellites using the global positioning system N87-10133

NEAR FIELDS
Near field pressure fluctuations in a circular jet [NASA-CR-179647] N87-10249

NEODYMIUM LASERS
Remote express analysis of ground-layer aerosol based on laser-induced spark spectra N87-10303

NEPTUNE (PLANET)
Clouds and methane photochemical hazes on the outer planets N87-10815

NEPTUNIUM COMPOUNDS
Re-examination of the neptunium-hydrogen system [DE86-010197] N87-10216

NETWORK CONTROL
Data communications and monitor for the Penn State University profiler network N87-10523

NEUTRINOS
Prompt neutrino production in 400 GeV proton copper interactions [USIP-86-02] N87-10754

NEUTRON STARS
Pulse timing and neutron star structure N87-10799
Physical processes in collapse driven supernova N87-10808

NEUTRONS
Progress made during 1985 in the scientific and technical program of National Physical Laboratory's Division of Radiation Science and Acoustics N87-10776

NICKEL ALLOYS
Castable hot corrosion resistant alloy [NASA-CASE-LEW-14134-1] N87-10192
Review of embrittlement mechanisms in tungsten heavy alloys [DE86-011114] N87-10196
Weldability of an NiAl alloy [DE86-011510] N87-10199
Ultrasonic determination of recrystallization [NASA-TM-88855] N87-10399

NICKEL COATINGS
Process for preparing nickel coatings in conducting, porous bodies, especially for battery electrodes [DE86-901439] N87-10200

NICKEL HYDROGEN BATTERIES
Process for preparing nickel coatings in conducting, porous bodies, especially for battery electrodes [DE86-901439] N87-10200

NICKEL ZINC BATTERIES
Evaluation of a new type stable nickel-zinc battery for electric vehicle application [DE86-010895] N87-10534

NIGHT
A model for the evolving stably stratified nocturnal boundary layer based on the turbulent kinetic energy equation N87-10608

NIGHT SKY
Instabilities associated with the equatorial spread-F phenomenon and their north-south asymmetry N87-10576

NIOBIUM ALLOYS
Study about the structural behavior of WStE-36N steel [DE86-702011] N87-10394

NITROGEN DIOXIDE
Variation of the urban NO2 concentration during a ground inversion situation N87-10318

NITROGEN OXIDES
Linewidth characteristics of Raman-shifted dye laser output at 720 and 940 nm N87-10372
Tropospheric trace gases N87-10614

NOCTURNAL VARIATIONS
A model for the evolving stably stratified nocturnal boundary layer based on the turbulent kinetic energy equation N87-10608

NOISE PREDICTION (AIRCRAFT)
Prediction of helicopter rotor discrete frequency noise: A computer program incorporating realistic blade motions and advanced acoustic formulation [NASA-TM-87721] N87-10750

NOISE PROPAGATION
Far field noise studies of contoured and solid/porous conical plug-nozzle jet flows N87-10049

NOISE REDUCTION
An all-purpose computer program for lidar simulations and reduction of lidar data N87-10299
Free jet feasibility study of a thermal acoustic shield concept for AST/VCE application: Dual stream nozzles [NASA-CR-3867] N87-10752
Free-jet acoustic investigation of high-radius-ratio coannular plug nozzles [NASA-CR-3818] N87-10753

NOISE SPECTRA
An example of scaling MST Doppler spectra using median spectra, spectral smoothing, and velocity tracing N87-10519

NONDESTRUCTIVE TESTS
An eddy-current model for three-dimensional nondestructive evaluation of advanced composites [AD-A167688] N87-10185
Ultrasonic determination of recrystallization [NASA-TM-88855] N87-10399

NONLINEAR EQUATIONS
Analysis on gravitational effect to nonlinear diffusion system of vapor molecules in a heat pipe N87-10023

NONLINEAR FEEDBACK
Dynamic modeling and control of robotic manipulators N87-10390

NONLINEAR OPTICS
Nonlinear optics with broad-band lasers [DE86-011286] N87-10382

NONLINEAR SYSTEMS
Application of bifurcation and catastrophe theories to near stall flight mechanics [AD-A167697] N87-10046
Application of graph theory to the nonlinear analysis of large space structures N87-10418

NONLINEARITY
Geometric and material nonlinear dynamic analysis of complex shells N87-10401
Advective influences on steady and transient forced tropical motions N87-10670
The local convergence of Ritz and Galerkin methods for nonlinear problems N87-10737
A study of hierarchical clustering of galaxies in an expanding universe N87-10806

NORMALIZING (STATISTICS)
Improved solution of the lidar equation utilizing particle counter measurements N87-10310

NORTHERN HEMISPHERE
Relationships between available potential energy, kinetic energy and extratropical cyclones within limited regions of the Northern Hemisphere during the FGGE Year N87-10668

NOVAE
Intense soft X-rays from RS Ophiuchi during the 1985 outburst [DE86-010175] N87-10820

NOZZLE FLOW
Far field noise studies of contoured and solid/porous conical plug-nozzle jet flows N87-10049

NOZZLES
Castable hot corrosion resistant alloy [NASA-CASE-LEW-14134-1] N87-10192

NUCLEAR ELECTRIC POWER GENERATION
Research and development activities of the Spectroscopy Division of the Bhabha Atomic Research Centre [DE86-702154] N87-10781

NUCLEAR EXPLOSION EFFECT
Radiation doses from flying through nuclear debris clouds [AD-A167959] N87-10711

NUCLEAR EXPLOSIONS
Some seismic results of an underground explosion at the Mururoa Test Site (Shot Report no. 6) [AWRE-O-17/85] N87-10619

NUCLEAR FUELS
Linearized model for the hydrodynamic stability investigation of molten fuel jets into the coolant of a Liquid Metal Fast Breeder Reactor (LMFBR) [KFK-3978] N87-10757

NUCLEAR PHYSICS
Lawrence Berkeley Laboratory recent papers submitted and reports issued, February 1986 [DE86-011319] N87-10782

NUCLIDES
Nuclide production by primary cosmic-ray protons [DE86-011268] N87-10821

NULL HYPOTHESIS
Null surface dynamics N87-10770

NUMERICAL ANALYSIS
Numerical study of hydrogen-air supersonic combustion by using elliptic and parabolized equations [NASA-CR-179600] N87-10187
Numerical studies of a tubulent jet in crossflow N87-10243
Global pressure relaxation procedure with application to viscous and inviscid flows N87-10247
Correction function in the Lidar equation and the solution techniques for CO2 Lidar date reduction N87-10280
Geometric and material nonlinear dynamic analysis of complex shells N87-10401
Nonlinear rotordynamics analysis [NASA-CR-176931] N87-10407
Numerical studies of thermally and mechanically forced circulations over complex terrain N87-10630
Current enhancement for hose-unstable electron beams [AD-A167804] N87-10755

NUMERICAL INTEGRATION
An all-purpose computer program for lidar simulations and reduction of lidar data N87-10299
Electron-positron pair production by ultrarelativistic electrons in a soft photon field N87-10798

NUMERICAL WEATHER FORECASTING
Middle Atmosphere Program. Handbook for MAP, volume 20 [NASA-CR-176882] N87-10419
On the potential use of radar-derived information in operational numerical weather prediction N87-10420
The real-time use of wind profilers in nowcasting N87-10427
The influence of velocity variability on the determination of wind profiles N87-10428

O

OBLIQUE WINGS
In-flight total forces, moments and static aeroelastic characteristics of an oblique-wing research airplane [NASA-TP-2224] N87-10103

OBSERVABILITY (SYSTEMS)
Performance monitoring of sensors in high reliable flight control systems using deterministic observers N87-10087

OBSERVATION
Plasma wave observations at Uranus from Voyager 2 [NASA-CR-177069] N87-10614

OCCULTATION
Direct computation of orbital sunrise or sunset event parameters [NASA-TM-87717] N87-10620

OCEAN BOTTOM
The internal tide off southern California [AD-A167722] N87-10672

OCEANOGRAPHY
Science opportunities from the Topex/Poseidon mission [NASA-CR-179752] N87-10671
A summary of the Foundation Research Program, fiscal year 1985 [AD-A168009] N87-10780

OCEANS
Time-resolved lidar fluorosensor for sea pollution detection N87-10317

OHMIC DISSIPATION
Energy delivery processes in shock tubes N87-10106

OIL SLICKS
Feasibility experiments on time-resolved fluorosensing applied to oil slicks N87-10322

ON-LINE SYSTEMS
Real-time atmospheric absorption spectra for in-flight tuning of an airborne dial system N87-10296
ONBOARD DATA PROCESSING
Proceedings of the 13th Symposium on Aircraft Integrated Data Systems
[DFVLR-MITT-86-04] N87-10075
OPACITY
Diffusion approximation for modeling of 3-D radiation distributions
[DE86-000610] N87-10228
OPERATING SYSTEMS (COMPUTERS)
Study of UNIX and its suitability for the Air Force's WWMCCS Information System
[DE86-011293] N87-10771
OPERATIONAL AMPLIFIERS
Electrical circuit modeling of conductors with skin effect
[DE86-011085] N87-10240
OPERATIONS RESEARCH
A summary of the Foundation Research Program, fiscal year 1985
[AD-A168009] N87-10780
OPERATOR PERFORMANCE
An algorithm for the detection of signals by colour contrast on the screen of a colour cathode ray tube (colour display) — raderscopes
[DRIC-T-7655] N87-10233
Flash/crazing effects on simulator pursuit tracking performance
[AD-A167689] N87-10759
OPTICAL DEPOLARIZATION
Multiple scattering depolarization in marine stratus clouds: Lidar experiments N87-10350
OPTICAL EQUIPMENT
Optically controlled GaAs dual-gate MESFET and permeable base transistors
[NASA-TM-88823] N87-10232
Integrated-optical components for fiber gyroscopes
[AD-A167624] N87-10378
Flash/crazing effects on simulator pursuit tracking performance
[AD-A167689] N87-10759
OPTICAL HETERODYNING
Laser heterodyne system for obtaining height profiles of minor species in the atmosphere N87-10359
OPTICAL PATHS
Integrated-optical components for fiber gyroscopes
[AD-A167624] N87-10378
OPTICAL PROPERTIES
Lidar measurements of slant visual range N87-10278
Optical models of the molecular atmosphere N87-10306
OPTICAL RADAR
Thirteenth International Laser Radar Conference
[NASA-CP-2431] N87-10263
ESA activities in space laser sounding and ranging N87-10264
Lidar remote sensing from space: NASA's plans in the Earth sciences N87-10265
Tunable solid-state laser technology for applications to scientific and technological experiments from space N87-10266
Coherent lidar technology for global wind profiling N87-10267
Development of a high-altitude airborne dial system: The Lidar Atmospheric Sensing Experiment (LASE) N87-10268
MIE Lidar proposed for the German Space Shuttle Mission D2 N87-10269
The Lidar In-Space Technology Experiment (LITE) N87-10270
Aerosol studies in mid-latitude coastal environments in Australia N87-10271
Visibility related to backscatter at 1.54 micron N87-10272
Inversion of 2 wavelength Lidar data for cloud properties N87-10273
The usefulness of Klett's inversion algorithms to simulated satellite Lidar returns N87-10274
Wavelength dependence of aerosol backscatter coefficients obtained by multiple wavelength Lidar measurements N87-10275
Extinction and visibility measurements in the lower atmosphere with UV-YAG-lidar N87-10276
Sensitivity of the Lidar ratio to changes in size distribution and index of refraction N87-10277
Lidar measurements of slant visual range N87-10278
Visibility and aerosol measurement by diode-laser random-modulation CW lidar N87-10279
Correction function in the Lidar equation and the solution techniques for CO2 Lidar date reduction N87-10280
Assesment of dial data collection and analysis techniques N87-10281
Airborne Lidar measurements of the atmospheric pressure profile with tunable Alexandrite lasers N87-10282
Measurements of the effect of horizontal variability of atmospheric backscatter on dial measurements N87-10283
Flight tests of a range-resolved airborne dial with two min-tea CO2 lasers N87-10284
Nd:Glass-Raman laser for water vapor dial N87-10285
A Meteorological (humidity, temperature, aerosols)) mobile dial system: Concepts and design N87-10286
Influence of Rayleigh-Doppler broadening on the selection of H2O dial system parameters N87-10287
Correction of Doppler-broadened Rayleigh backscattering effects in H2O dial measurements N87-10288
Atmospheric contributions to the column variance in direct-detection dial N87-10289
High spectral purity, narrow linewidth laser transmitter for dial measurements N87-10290
On the measurement of atmospheric density using dial in the O2 A-band (770 nm) N87-10291
Using a laser aurecle to invert lidar return N87-10292
Determination of cloud microphysical properties by laser backscattering and extinction measurements N87-10293
Effect of backscatter-to-extinction ratio on lidar inversions N87-10294
Laboratory measurements of forward and backward scattering of laser beams in water droplet clouds N87-10295
Real-time atmospheric absorption spectra for in-flight tuning of an airborne dial system N87-10296
Observation of atmospheric ozone by dial with Raman lasers pumped by a KrF laser N87-10297
Strength, width, and pressure shift measurements of 54 lines in the oxygen A-band N87-10298
An all-purpose computer program for lidar simulations and reduction of lidar data N87-10299
Convective structure of the planetary boundary layer of the ocean during gale N87-10300
Multifrequency dial sensing of the atmospheric gaseous constituents using the first and second harmonics of a tunable CO2 laser radiation N87-10302
Remote express analysis of ground-layer aerosol based on laser-induced spark spectra N87-10303
Laser sounding of instantaneous and mean speed of wind using correlation method N87-10304
Optimal filtration of the atmospheric parameters profiles N87-10305
The influrence of an optical receiving system on statistical characteristics of a lidar signal N87-10307
Coherent lidars based on intracavity heterodyning of echo signals N87-10308
The influence of scattering particles morphology on the characteristics of lidar signals N87-10309
Improved solution of the lidar equation utilizing particle counter measurements N87-10310
Improvements in the Goddard balloon-borne lidar N87-10311
Features of stratospheric aerosol lidar observations at Mauna Loa, 1974 - 1985 N87-10312
El Chichon aerosols in the stratosphere: Analyses of lidar data and calculations of radiation budget N87-10313
Lidar measurement of stratospheric aerosol at Syowa Station, Antarctica N87-10314
Time-resolved lidar fluorosensor for sea pollution detection N87-10317
Variation of the urban NO2 concentration during a ground inversion situation N87-10318
Lidar mapping of a mixture of aerosol concentrations in a varying atmosphere N87-10320
Three atmospheric dispersion experiments involving oil fog plumes measured by lidar N87-10321
Rotationally resolved collisional transfer rates in OH N87-10323
Performance testing of lidar receivers N87-10325
Progress in coherent laser radar N87-10326
Doppler lidar studies of atmospheric wind field dynamics N87-10327
The effect of turbulence on lidar backscattered signal fluctuations N87-10328
Remote sensing of atmospheric winds using a coherent, CW lidar and speckle-turbulence interaction N87-10329
Experimental and theoretical Doppler-lidar signatures of aircraft wake vortices N87-10330
Lower atmospheric temperature profile measurements using a Raman lidar N87-10331
A combined Raman lidar for low tropospheric studies N87-10332
Intercomparisons of high-resolution solar blind Raman lidar atmospheric profiles of water vapor with radiosondes and kytoon N87-10333
Lidar method of measurement of atmospheric extinction and ozone profiles N87-10334
Vertical structure of Arctic haze observed by lidar N87-10335
Lidar observations and modeling of cold air outbreaks during MASEX and GALE N87-10336
The application of lidar to stratospheric aerosol studies N87-10337
Volcanic eruptions and the increases in the stratospheric aerosol content: Lidar measurements from 1982 to 1986 N87-10338
Observations of stratospheric aerosols associated with the El Chichon eruption N87-10339
Lidar observations of the decline of the El Chichon stratospheric load N87-10340
Airborne lidar observations of Arctic polar stratospheric clouds N87-10341
XeF lidar measurements of density and temperature in the middle atmosphere N87-10342
Lidar measurements of thermal structure N87-10343
Lidar stratospheric ozone measurements at the observatoire de Haute Provence (France) N87-10344
Lidar observation of the mesospheric sodium layer in Antarctica N87-10345
Lidar detection of metallic species at the mesopause level N87-10346
Daytime lidar measurements of tidal winds in the mesospheric sodium layer at Urbana, Illinois N87-10347
Lidar study of storm tops N87-10348
Investigation of clouds spatial distribution using ground-based lidar N87-10349
Multiple scattering depolarization in marine stratus clouds: Lidar experiments N87-10350
Near-IR extinction and backscatter coefficient measurements in low- and mid-altitude clouds N87-10351
Backscatter and extinction measurements in cloud and drizzle at CO2 laser wavelengths N87-10352
Cloud detection by lidar extinction calculations N87-10353
Wide-area remote-sensing system of pollution and gas dispersal by near-infrared absorption based on low-loss optical fiber network N87-10354
A mobile system for active otpical pollution monitoring N87-10355
Gas correlation lidar for methane detection N87-10356
Coherent lidar signal fluctuation reduction by means of frequency diversity technique N87-10360
Wavelength dependence of coherent and incoherent satellite-based lidar measurements of wind velocity and aerosol backscatter N87-10361
The NCAR Airborne Infrared Lidar System (NAILS) N87-10362
Atmospheric correlation time measurements using coherent CO2 lidar N87-10363
Calibration and analysis for a 0.53 micron incoherent Doppler lidar N87-10365
CO2 lidar system for atmospheric studies N87-10366
Generation of attenuation corrected images from lidar data N87-10367
Gas dispersion measurements using a mobile Raman lidar system N87-10368
Spectroscopic aspects of differential method for sounding gas composition of the atmosphere N87-10369
The GSFC gound-based lidar for the measurement of stratospheric ozone N87-10371
Alexandrite laser source for atmospheric lidar measurements N87-10373
The TFP and a pulsed LD: New lidar components N87-10374
Chemical contamination remote sensing N87-10375
A theory for the retrieval of virtual temperature from winds, radiances and the equations of fluid dynamics N87-10421
Methods for verifying the accuracy of wind profiles N87-10471
Further studies with data collected by NASA's airborne Doppler lidar in Oklahoma in 1981
[NASA-CR-179779] N87-10660
OPTICAL RESONANCE
Lidar detection of metallic species at the mesopause level N87-10346
OPTICAL TRACKING
Optical tracking of the SIRIO satellite N87-10134
Flash/crazing effects on simulator pursuit tracking performance
[AD-A167689] N87-10759
OPTIMIZATION
Development of a turbomachinery design optimization procedure using a multiple-parameter nonlinear perturbation method
[NASA-CR-3831] N87-10003

Parameter optimization and attitude stabilization of a flexible spacecraft N87-10138
Structural optimization for control of stiffened laminated composite plates using nonlinear mixed integer programming N87-10161

ORBIT CALCULATION
DMA (Defense Mapping Agency) orbit determination for transit satellites: 1985
[AD-A167567] N87-10108
Optimal transfer to inclined geosynchronous orbits N87-10117
Optimal tracking strategy determination — satellite tracking N87-10120
Accuracy of goestationary orbit determination N87-10121
Application of simplified spin axis attitude determination techniques to ESA telecom satellites N87-10126
Preliminary orbit determination by static multivariate search N87-10127
Early orbit determination — satellite orbits N87-10128
Real time orbit determination during apogee maneuvers — satellite orbits N87-10130
Initial orbit determination for geostationary satellites N87-10131
Real time orbit and dynamic search zone computations to aid satellite acquisition in S-band during the launch phase of Geosynchronous Transfer Orbit (GTO) N87-10132
Orbit determination of geostationary satellites using the global positioning system N87-10133
Very first orbit determination after launch or main maneuvers. Applications to geostationary Telecom 1A and 1B N87-10135
Tracking and Data Relay Satellite (TDRS) tracking and orbit determination N87-10136
Operational implementation of deorbiting maneuvers — GEOS-2 N87-10148
Application of linear programming to final positioning (drift orbit) of a geostationary satellite N87-10149
TV-SAT final orbit acquisition optimization strategy N87-10150
Comparison of different autonomous stationkeeping systems for geostationary satellites N87-10163

ORBIT PERTURBATION
Efficiency eccentricity control using continuous, vectored thrusting for satellites with large area/mass ratios N87-10151

ORBIT TRANSFER VEHICLES
Orbital transfer vehicle launch operations study. Volume 1: Executive summary
[NASA-CR-179701] N87-10110
Orbital transfer vehicle launch operations study. Volume 2: Detailed summary
[NASA-CR-179791] N87-10111
Shuttle derived atmospheric density model. Part 2: STS atmospheric implications for AOTV trajectory analysis, a proposed GRAM perturbation density model
[NASA-CR-171824] N87-10663

ORBITAL ASSEMBLY
A space station Structures and Assembly Verification Experiment, SAVE
[NASA-TM-89004] N87-10170

ORBITAL LAUNCHING
Transfer orbit optimization for dual launches N87-10114
Real time orbit and dynamic search zone computations to aid satellite acquisition in S-band during the launch phase of Geosynchronous Transfer Orbit (GTO) N87-10132

ORBITAL LIFETIME
Operational implementation of deorbiting maneuvers — GEOS-2 N87-10148

ORBITAL MANEUVERING VEHICLES
Orbital transfer vehicle launch operations study. Volume 2: Detailed summary
[NASA-CR-179791] N87-10111

ORBITAL MANEUVERS
Operational criteria for geostationary satellites in National Space Development Agency (NASDA) N87-10119
Geostationary Operational Environmental Satellite (GOES) mission profile N87-10123
Real time orbit determination during apogee maneuvers — satellite orbits N87-10130
Very first orbit determination after launch or main maneuvers. Applications to geostationary Telecom 1A and 1B N87-10135
Synchronous transfer orbit operation under three-axis control N87-10137
Operational strategies for multi-burn apogee maneuvers of geostationary spacecraft N87-10141
Optimal injection of TV SAT with multi-impulse apogee maneuvers with mission constraints and thrust uncertainties N87-10144
Targeting multiburn, long duration apogee burst maneuvers N87-10146
Stationkeeping for DFS-Kopernikus N87-10152
Updates to operational procedures as a result of in-orbit experience with SYMPHONIE spacecraft N87-10159

ORBITAL MECHANICS
Proceedings of an International Conference on Space Dynamics for Geostationary Satellites
[ISBN-2-85428-149-7] N87-10113
Transfer orbit optimization for dual launches N87-10114
Orbit geometry for calibration and launch operations of a three-axis controlled satellite with inertial reference N87-10116
Optimal transfer to inclined geosynchronous orbits N87-10117
An investigation on passively controlled geosynchronous orbits N87-10118
Optimal tracking strategy determination — satellite tracking N87-10120
Efficiency eccentricity control using continuous, vectored thrusting for satellites with large area/mass ratios N87-10151
Guidebook for analysis of tether applications
[NASA-CR-178904] N87-10169
Direct computation of orbital sunrise or sunset event parameters
[NASA-TM-87717] N87-10620

ORBITAL POSITION ESTIMATION
Optimal tracking strategy determination — satellite tracking N87-10120
Accuracy of goestationary orbit determination N87-10121
State/orbit estimation from real Doppler data for solid apogee motor burning phase of geostationary satellite N87-10129

ORBITAL SPACE STATIONS
Orbital transfer vehicle launch operations study. Volume 2: Detailed summary
[NASA-CR-179791] N87-10111
A space station Structures and Assembly Verification Experiment, SAVE
[NASA-TM-89004] N87-10170
Lidar remote sensing from space: NASA's plans in the Earth sciences N87-10265
Proceedings of the 5th Annual Users' Conference
[NASA-CP-2399] N87-10720
National Aeronautics and Space Administration N87-10774
National Aeronautics and Space Administration Authorization Act, 1987 N87-10775

ORGANIC SILICON COMPOUNDS
Boron-containing organosilane polymers and ceramic materials thereof
[NASA-CASE-ARC-11649-1-SB] N87-10205

ORION CONSTELLATION
Molecular clouds in Orion and Monoceros N87-10809

ORTHOSTATIC TOLERANCE
Metabolic changes during prolonged antiorthostatic hypokinesia — weightlessness simulation N87-10698
Relationship between cardiovascular functions and fluid-electrolyte metabolism during antiorthostatic hypokinesia — weightlessness simulation N87-10701

OSCILLATIONS
Cramer-Rao bound analysis for frequency estimation of sinusoids in noise
[AD-A167992] N87-10227

OSTEOPOROSIS
Amputation-induced osteoporosis: A new model to explore the effects of weightlessness on the human skeleton N87-10690

OUTPUT
CP DDT detonators. 5: Output performance and analysis of multiple-out devices
[DE86-010995] N87-10219

OXIDATION
Developing simplified models of combustion chemistry by simulation with detailed chemical kinetics models
[DE86-008381] N87-10188
Titanium oxidation kinetics and the mechanism for thermal ignition of titanium-based pyrotechnics
[DE86-010987] N87-10218

OXIDATION RESISTANCE
Castable hot corrosion resistant alloy
[NASA-CASE-LEW-14134-1] N87-10192

OXYGEN
Radiative processes N87-10618

OXYGEN IONS
Detection of suprathermal O(+) ions inside the plasmasphere N87-10554
Vertical transport of O(+) ions at high latitudes N87-10565
Nonstationary field-aligned fluxes of thermal ions O(+) and H(+) outside the plasmapause: Refinement of the polar wind theory N87-10566
Field-aligned motions of O(+) and H(+) thermal ions in a magnetic field tube convected across the dayside polar cusp: Model calculations N87-10567
Generation of Pc2 pulsations by energetic O(+) ions N87-10605

OZONE
Wavelength dependence of aerosol backscatter coefficients obtained by multiple wavelength Lidar measurements N87-10275
Flight tests of a range-resolved airborne dial with two min-tea CO2 lasers N87-10284
Observation of atmospheric ozone by dial with Raman lasers pumped by a KrF laser N87-10297
Improvements in the Goddard balloon-borne lidar N87-10311
Lidar method of measurement of atmospheric extinction and ozone profiles N87-10334
Lidar stratospheric ozone measurements at the observatoire de Haute Provence (France) N87-10344
The GSFC gound-based lidar for the measurement of stratospheric ozone N87-10371
Atmospheric Ozone 1985. Assessment of our understanding of the processes controlling its present distribution and change, volume 1
[NASA-TM-89237] N87-10612
Stratospheric chemistry N87-10613
Tropospheric chemistry N87-10615
Strat-trop exchange N87-10616
Radiative processes N87-10618
Millimeter-wave spectrometry of ozone in the middle atmosphere N87-10629

P

P-N JUNCTIONS
Factors contributing to static RAM cell transient upset
[DE86-007710] N87-10715

PACIFIC OCEAN
Continuous wind measurement in the tropical Pacific using VHF raders N87-10484
Some seismic results of an underground explosion at the Mururoa Test Site (Shot Report no. 6)
[AWRE-O-17/85] N87-10619
Observational studies of wave disturbances in the tropical Pacific and their relationship with deep cloud activity N87-10634
An observational study of tropical cloud cluster evolution and cyclogenesis in the Western North Pacific
[CSU-ASP-403] N87-10661
The internal tide off southern California
[AD-A167722] N87-10672

PAIR PRODUCTION
Electron-positron pair production by ultrarelativistic electrons in a soft photon field N87-10798

PANEL FLUTTER
Effect of static inplane loads and boundary conditions on the flutter of flat rectangular panels
[NAL-TM-ST-8604] N87-10404

PANEL METHOD (FLUID DYNAMICS)
Application of a potential code to general steady flows in three dimensions N87-10262

PARABOLIC DIFFERENTIAL EQUATIONS
Asymptotic error expansions of finite element solutions of parabolic equations N87-10738

PARABOLIC REFLECTORS
The TFP and a pulsed LD: New lidar components N87-10374

PARALLEL PROCESSING (COMPUTERS)
WEST-3 wind turbine simulator development. Volume 2: Verification
[NASA-CR-174962] N87-10531
Dynamic remapping decisions in multi-phase parallel computations
[NASA-CR-178174] N87-10719
Database algorithms for multiprocessor and very large memory systems
[DE86-009406] N87-10724
Parallel logic programming for numeric applications
[DE86-011004] N87-10726
Novel parallel architectures and algorithms for linear algebra processing
[NASA-CR-179626] N87-10743
Computational methods and software for differential equations and their applications
[DE86-010231] N87-10746

PARALLEL PROGRAMMING
Parallel logic programming for numeric applications
[DE86-011004] N87-10726

PARAMETER IDENTIFICATION
Effects of flap position on longitudinal parameters of HFB-320
[NAL-TM-SE-8602] N87-10062

Summary of longitudinal stability and control parameters as determined from space shuttle Columbia flight test data [NASA-TM-87768] N87-10101
The usefulness of Klett's inversion algorithms to simulated satellite Lidar returns N87-10274

PARAMETERIZATION
Parameter optimization and attitude stabilization of a flexible spacecraft N87-10138

PARTIAL DIFFERENTIAL EQUATIONS
Global collocation methods for approximation and the solution of partial differential equations [NASA-CR-178179] N87-10745
Computational methods and software for differential equations and their applications [DE86-010231] N87-10746

PARTICLE ACCELERATION
Positive ion distributions in the morning auroral zone: Local acceleration and drift effects N87-10547
Evidence for high latitude ionospheric ion acceleration N87-10564

PARTICLE ACCELERATORS
Lawrence Berkeley Laboratory recent papers submitted and reports issued, February 1986 [DE86-011319] N87-10782

PARTICLE BEAMS
Current enhancement for hose-unstable electron beams [AD-A167604] N87-10755

PARTICLE DENSITY (CONCENTRATION)
Atmospheric correlation time measurements using coherent CO2 lidar N87-10363
Models of electric potential and current distribution in stable discrete auroral forms N87-10551

PARTICLE IN CELL TECHNIQUE
An improved PSI-cell method for turbulent multi-phase flows N87-10034

PARTICLE PRECIPITATION
Positive ion distributions in the morning auroral zone: Local acceleration and drift effects N87-10547
Equatorial magnetospheric particles and auroral precipitations N87-10557
Polar cap particle precipitation as measured by the AUREOL-3 and Intercosmos-19 satellites N87-10560
Fine structure of fields and plasma in the field-aligned current region on the Intercosmos-Bulgaria-1300 satellite data N87-10568
Small scale structures of electric field variations and particle precipitations as observed onboard AUREOL-3 satellite N87-10569
Connection between particle precipitations and the plasma sheet during substorms N87-10594

PARTICLE PRODUCTION
Prompt neutrino production in 400 GeV proton copper interactions [USIP-86-02] N87-10754
Nuclide production by primary cosmic-ray protons [DE86-011268] N87-10821

PARTICLE THEORY
Particle theory and cosmology [DE86-010366] N87-10802

PARTICLE TRAJECTORIES
An improved PSI-cell method for turbulent multi-phase flows N87-10034

PARTICLES
The influence of scattering particles morphology on the characteristics of lidar signals N87-10309
Light scattering in resonance region from polydisperse non-spherical particles N87-10792

PATIENTS
Exercise-induced myocardial ischemia at high altitude simulated in a negative pressure chamber N87-10702

PAVEMENTS
Use of fuzzy sets mathematics to assist pavement evaluation and management (revised March 18, 1986) [PB86-214798] N87-10747

PAYLOADS
Orbital transfer vehicle launch operations study. Volume 2: Detailed summary [NASA-CR-179791] N87-10111

PELVIS
Amputation-induced osteoporosis: A new model to explore the effects of weightlessness on the human skeleton N87-10690

PERFORMANCE TESTS
A trial on performance test method for Cu-water heat pipe N87-10026
Engine-airframe integration considerations for preliminary air vehicle performance analysis N87-10068
Comparative evaluation of redundant flight data recorded by a digital aircraft integrated data system recorder (DAR) on board an Airbus A-310 aircraft N87-10098
Strategic Defense Initiative Program: Status of airborne optical adjunct and terminal imaging radar [P86-221132] N87-10107
Performance testing of lidar receivers N87-10325
Chemical contamination remote sensing N87-10375
The first operation and results of the Chung-Li VHF radar N87-10495
Methods of testing to determine the thermal performance of solar collectors [DE86-009311] N87-10533
Evaluation of a new type stable nickel-zinc battery for electric vehicle application [DE86-010895] N87-10534
Laboratory evaluation of three passive CO concentration monitors [PML-1985-13] N87-10538
Extreme ultraviolet explorer: Mirror optical tests and results [DE86-010560] N87-10760

PERIODIC VARIATIONS
Periodic amplitude variations in Jovian continuum radiation [NASA-CR-177070] N87-10813

PERMEABILITY
Permeation membrane-type distiller [DE86-011153] N87-10254
Thermopervaporation device [DE86-011151] N87-10255
Modelling of the filling up of a porous plate [DE86-702033] N87-10260

PERSONAL COMPUTERS
Pulse forming network design program for linear and time-varying loads for the IBM personal computer [DE86-011209] N87-10727

PERSONNEL
Human factors research in aircrew performance and training [AD-A167950] N87-10714

PERSONNEL SELECTION
The interest of centrifuge tests for the selection of French cosmonauts N87-10678
Vestibular tests in cosmonaut selection and training N87-10694

PERTURBATION
Evidence of atmospheric gravity wave perturbations of the Brunt-Vaisala frequency in the atmosphere N87-10436
Horizontal wind perturbations and their relation to transient internal gravity waves N87-10457

PERTURBATION THEORY
Development of a turbomachinery design optimization procedure using a multiple-parameter nonlinear perturbation method [NASA-CR-3831] N87-10003
Gauge invariant perturbation theory prediction of the sensitivity required for experimental measurement of quadrupole and higher moments of the cosmic microwave background radiation N87-10825

PHASE CHANGE MATERIALS
Chemistry research resource [DE86-009891] N87-10178

PHASE SHIFT KEYING
MODTEQ (Modulation Techniques), AN/FRC-170(V), equalization, and channel medium simulations [AD-A167965] N87-10226

PHASE SWITCHING INTERFEROMETERS
Measurements of antenna polar diagrams and efficiencies using a phase-switched interferometer N87-10507

PHASE TRANSFORMATIONS
Transformations and new PHACOMP analysis in weld metal of Hastelloy C-type alloys [DE86-011422] N87-10198

PHASE-SPACE INTEGRAL
Electron-positron pair production by ultrarelativistic electrons in a soft photon field N87-10798

PHASED ARRAYS
Phased-array design for MST and ST radars N87-10499
Beam steering system N87-10501
A 405-MHz, 5-beam phased array antenna N87-10503
Monitoring of the MU radar antenna pattern by Satellite Ohzora (EXOS-C) N87-10509

PHOSPHORUS METABOLISM
Weightlessness effects on the phosphorus-calcium balance and its hormonal regulation in man during STS flight 51-G N87-10691

PHOTOCHEMICAL REACTIONS
Atmospheric Ozone 1985. Assessment of our understanding of the processes controlling its present distribution and change, volume 1 [NASA-TM-89237] N87-10612
Stratospheric chemistry N87-10613
Strat-trop exchange N87-10616
Radiative processes N87-10618
Workshop on the Physics and Chemistry of Solar-Flux Effects on Condensed Phase/Gas Interfaces [DE86-004460] N87-10817

PHOTODISSOCIATION
Laser induced chemical reactions and laser-collision processes [DE86-011459] N87-10385

PHOTOGRAMMETRY
Demonstration of laser speckle system on burner liner cyclic rig [NASA-CR-179509] N87-10377

PHOTOGRAPHIC PROCESSING
Black-and-white photographic chemistry: A reference [NASA-TM-87296] N87-10177

PHOTOIONIZATION
The ultraviolet spectra of DA white dwarfs N87-10783

PHOTOLYSIS
Laser induced chemical reactions and laser-collision processes [DE86-011459] N87-10385
Laser-initiated chain reactions in the partial oxidation of methane [DE86-011272] N87-10388

PHOTOMETRY
Surface photometry of early-type galaxies N87-10795

PHOTOMULTIPLIER TUBES
The development and test of multi-anode microchannel array detector systems. Part 2: Soft X-ray detectors [NASA-CR-177068] N87-10236

PHOTONS
Research relative to high resolution camera on the advanced X-ray astrophysics facility [NASA-CR-179757] N87-10376

PHOTOSYNTHESIS
Photosynthetic water splitting [DE86-010269] N87-10215

PHOTOVOLTAIC CONVERSION
Experience with the application of photovoltaics devices [DE86-010472] N87-10535

PHYSICAL FITNESS
Upper and lower body anaerobic power comparison between biathletes and control subjects [AD-A167636] N87-10710

PHYSIOLOGICAL EFFECTS
Proceedings of 2nd International Conference on Space Physiology [ESA-SP-237] N87-10675
Cardiovascular measurements in microgravity N87-10676
Bones and weightlessness N87-10681
The muscular system in weightlessness N87-10682
Microgravity effects on the contractile proteins of rat muscles N87-10683
Weightlessness effects on the bone tissue of rats after a 5 day space flight (Cosmos 1514) N87-10684
Functions of skeletal muscles of rats and monkeys after 5-day space flight (on Cosmos 1514) N87-10686
Ground based simulation techniques for cardiovascular and hormonal changes observed in man in weightlessness N87-10696

PHYSIOLOGICAL RESPONSES
The regulation of fluid and electrolyte metabolism in weightlessness N87-10679

PICTURE TUBES
An algorithm for the detection of signals by colour contrast on the screen of a colour cathode ray tube (colour display) — radarscopes [DRIC-T-7655] N87-10233

PILOT PERFORMANCE
Human factors research in aircrew performance and training [AD-A167950] N87-10714

PILOT TRAINING
Human factors research in aircrew performance and training [AD-A167950] N87-10714

PIPE FLOW
Numerical study of the entrance flow and its transition of a circular pipe N87-10019
Operating characteristics of cooling underground power cables using up sloped long heat pipes in conduit N87-10028
The numerical method of calculation of two-dimensional stationary electro-gasdynamic internal flows N87-10037

PIPES (TUBES)
Analysis of heat-pipe absorbers in evacuated-tube solar collectors [DE86-010764] N87-10252
Design rule for fatigue of welded joints in elevated-temperature nuclear components [DE86-007569] N87-10393
Concentrations of plastic strains in the clamping region of cylindrical shells under excessive loading [KFK-3915] N87-10417

PITCH (INCLINATION)
Acta Aeronautica et Astronautica Sinica (selected articles) [AD-A167918] N87-10004
PIXELS
A component decomposition model for evaluating atmospheric effects in remote sensing N87-10610
PLANE WAVES
Theory of wire-grid modelling: Criteria for highly conducting surfaces — plane wave scattering [AWRE-O-20/85] N87-10224
PLANETARY BOUNDARY LAYER
The Lidar In-Space Technology Experiment (LITE) N87-10270
Convective structure of the planetary boundary layer of the ocean during gale N87-10300
A high resolution entrainment model for the convective planetary boundary layer N87-10611
PLANETARY MAGNETIC FIELDS
A modeling analysis program for the JPL Table Mountain Io sodium cloud data [NASA-CR-179671] N87-10811
PLANETARY NEBULAE
Infrared emission lines from planetary nebulae N87-10791
PLANETARY WAVES
Half-day and four-day waves in the statosphere N87-10435
Atmospheric waves and the nature of buoyancy turbulence in the context of the waves VS 2D-turbulence debate N87-10439
A proposed experimental test to distinguish waves from 2-D turbulence N87-10440
Propagating tides in the mesosphere N87-10441
PLANNING
Air Force technical objective document fiscal year 1987 [AD-A167324] N87-10779
PLASMA CONDUCTIVITY
Current enhancement for hose-unstable electron beams [AD-A167804] N87-10755
PLASMA CONTROL
Plasma confinement by a radio frequency plugging potential in an axisymmetric mirror-cusp device [IPPJ-784] N87-10763
PLASMA DENSITY
Models of electric potential and current distribution in stable discrete auroral forms N87-10551
Formation and deformation of the plasmapause during a substorm event N87-10555
Fine structure of fields and plasma in the field-aligned current region on the Intercosmos-Bulgaria-1300 satellite data N87-10568
PLASMA DIAGNOSTICS
The hot ion composition in the magnetosphere N87-10552
Injection of low-energy ions during geomagnetic storms N87-10553
Detection of suprathermal O(+) ions inside the plasmasphere N87-10554
Observations of polar-cap ionospheric signatures of polar wind/magnetosphere coupling N87-10563
Intercosmos-Bulgaria-1300 satellite: Large-scale structure and dynamics of the polar ionosphere during geomagnetic storms N87-10592
Coordinated data on auroral electrodynamics from ground based radar diagnostics and AUREOL-3 satellite N87-10607
RLE progress report [MIT-PR-128] N87-10778
PLASMA DRIFT
Vertical transport of O(+) ions at high latitudes N87-10565
Self-consistent analysis of high drift velocity measurements with the Scandinavian Twin Auroral Radar Experiment (STARE) system N87-10606
PLASMA DYNAMICS
Mathematical and computational models of plasma flows N87-10036
PLASMA LAYERS
Plasma sheet boundary electric fields during substorms N87-10548
Connection between particle precipitations and the plasma sheet during substorms N87-10594
PLASMA LOSS
Plasma confinement by a radio frequency plugging potential in an axisymmetric mirror-cusp device [IPPJ-784] N87-10763
PLASMA WAVES
Polarization of electromagnetic waves recorded on board the AUREOL-3 satellite N87-10571
Plasma wave observations at Uranus from Voyager 2 [NASA-CR-177069] N87-10814
PLASMA-ELECTROMAGNETIC INTERACTION
Artificial ion beam interaction with the auroral plasma N87-10591
PLASMAPAUSE
Formation and deformation of the plasmapause during a substorm event N87-10555
PLASMAS (PHYSICS)
The onset of alfvenic turbulence N87-10762
PLASMASPHERE
Detection of suprathermal O(+) ions inside the plasmasphere N87-10554
Observational and theoretical investigation of stable auroral red arcs and their magnetospheric energy source, volumes 1 and 2 N87-10632
PLASTIC AIRCRAFT STRUCTURES
Investigation into the attenuation and velocity of acoustic emissions in carbon fiber composite aircraft structures [BAE-KGT-R-GEN-01349] N87-10180
PLASTIC DEFORMATION
Further results on the initiation and growth of adiabatic shear bands [AD-A168012] N87-10412
PLASTICIZERS
The fungal resistance or susceptibility of resins, plasticizers, and other constituents of adhesive formulations [AD-A166930] N87-10207
PLASTICS
Further results on the initiation and growth of adiabatic shear bands [AD-A168012] N87-10412
PLATINUM
Chemistry and shock initiation of intermetallic reactions [DE86-009694] N87-10220
PLATINUM ALLOYS
Chemistry and shock initiation of intermetallic reactions [DE86-010549] N87-10221
PLOTTERS
GRAPH 3: A digitizing and graph plotting program [DE86-010626] N87-10722
PLOT 3D: A multipurpose, interactive program for plotting three dimensional graphs [DE86-702101] N87-10730
PLUG NOZZLES
Far field noise studies of contoured and solid/porous conical plug-nozzle jet flows N87-10049
Free-jet acoustic investigation of high-radius-ratio coannular plug nozzles [NASA-CR-3818] N87-10753
PLUMES
Transient behavior of liquid jets injected normal to a high velocity gas stream N87-10246
POLAR CAP ABSORPTION
Evidence for ion energy dispersion in the polar cusp related to a northward directed Interplanetary Magnetic Field (IMF) N87-10561
POLAR CAPS
Dynamic variations of the auroral precipitation and the polar cap N87-10559
Polar cap particle precipitation as measured by the AUREOL-3 and Intercosmos-19 satellites N87-10560
Polar cap/polar cusp studies using incoherent scatter radar facilities — ionosphere N87-10562
Observations of polar-cap ionospheric signatures of polar wind/magnetosphere coupling N87-10563
POLAR CUSPS
Evidence for ion energy dispersion in the polar cusp related to a northward directed Interplanetary Magnetic Field (IMF) N87-10561
Polar cap/polar cusp studies using incoherent scatter radar facilities — ionosphere N87-10562
Field-aligned motions of O(+) and H(+) thermal ions in a magnetic field tube convected across the dayside polar cusp: Model calculations N87-10567
POLAR REGIONS
Evidence for high latitude ionospheric ion acceleration N87-10564
Vertical transport of O(+) ions at high latitudes N87-10565
Nonstationary field-aligned fluxes of thermal ions O(+) and H(+) outside the plasmapause: Refinement of the polar wind theory N87-10566
Field-aligned motions of O(+) and H(+) thermal ions in a magnetic field tube convected across the dayside polar cusp: Model calculations N87-10567
Attenuation bands and cut-off frequencies for ELF electromagnetic waves — high latitudes N87-10570
Density gradient instability in the high latitude ionosphere. Relation with the electrostatic turbulence and convection N87-10573
On the spectral broadening of the ground-based VLF transmitter signals in the high-latitude ionosphere observed from Intercosmos-19 and AUREOL-3 satellites N87-10584
Intercosmos-Bulgaria-1300 satellite: Large-scale structure and dynamics of the polar ionosphere during geomagnetic storms N87-10592
The E region instabilities in the polar ionosphere N87-10599
The ARCAD 3-SAFARI coordinated study of auroral and polar F-region ionospheric irregularities N87-10600
POLARIZATION (WAVES)
Mesospheric gravity-wave climatology at Adelaide N87-10456
Possibility of measuring gravity-wave momentum flux by single beam observation of MST radar N87-10458
POLICIES
Microelectronics research and development background paper [PB86-205200] N87-10242
POLLUTION MONITORING
A mobile system for active otpical pollution monitoring N87-10355
MAPM: A coherent dual CO2 laser DIAL system N87-10358
CO2 lidar system for atmospheric studies N87-10366
POLLUTION TRANSPORT
Lidar measurement of stratospheric aerosol at Syowa Station, Antarctica N87-10314
Variation of the urban NO2 concentration during a ground inversion situation N87-10318
Vertical structure of Arctic haze observed by lidar N87-10335
Lidar observations of the decline of the El Chichon stratospheric load N87-10340
Tropospheric chemistry N87-10615
POLYMER CHEMISTRY
Chemistry research resource [DE86-009891] N87-10178
Synthesis of energetic materials [AD-A167787] N87-10214
POLYMERIC FILMS
A method of estimating the molecular weight of polymeric materials [NASA-CASE-LAR-13212-1] N87-10206
Polymer reflectors research during Fiscal Year 1985 [DE86-010697] N87-10211
POLYMERS
A method of estimating the molecular weight of polymeric materials [NASA-CASE-LAR-13212-1] N87-10206
POLYSULFIDES
Polymer systems for rapid sealing of aircraft structures at low temperature [AD-A167667] N87-10209
POROUS MATERIALS
Process for preparing nickel coatings in conducting, porous bodies, especially for battery electrodes [DE86-901439] N87-10200
Transient heat transfer analysis and radiative properties measurements of porous thermal insulation [DE86-011296] N87-10259
POROUS PLATES
Modelling of the filling up of a porous plate [DE86-702033] N87-10260
Constitutive relations for flow of a non-Newtonian fluid through saturated porous media [DE86-702035] N87-10261
PORTABLE EQUIPMENT
Chemical contamination remote sensing N87-10375
PORTS (OPENINGS)
Pressure-resistant plane disc viewports from allyl diglycol carbonate plastic for hyperbaric chambers [AD-A168007] N87-10105
POSEIDON SATELLITE
Science opportunities from the Topex/Poseidon mission [NASA-CR-179752] N87-10671
POSITION (LOCATION)
Periodic amplitude variations in Jovian continuum radiation [NASA-CR-177070] N87-10813
POSITION INDICATORS
United States Navy - Canadian Forces solid state flight data recorder/crash position locator experiment on the B-720 controlled impact demonstration N87-10097
POSITIONING
Geostationary satellite positioning with a restartable motor N87-10142
Definition of a structure for the apogee thrusts for geostationary satellite positioning: Application to TDF-1 N87-10145
Application of linear programming to final positioning (drift orbit) of a geostationary satellite N87-10149
POSTURE
Metabolic changes during prolonged antiorthostatic hypokinesia — weightlessness simulation N87-10698

POTENTIAL ENERGY
Relationships between available potential energy, kinetic energy and extratropical cyclones within limited regions of the Northern Hemisphere during the FGGE Year N87-10668

POTENTIAL FLOW
Application of a potential code to general steady flows in three dimensions N87-10262

POTENTIAL GRADIENTS
Magnetic field-aligned potential drops N87-10545

POWDER METALLURGY
Deformation behavior of powder metallurgy Ni Al-Hf-B
[DE86-011508] N87-10201

POWER CONDITIONING
Pulse forming network design program for linear and time-varying loads for the IBM personal computer
[DE86-011209] N87-10727

POWER LINES
Operating characteristics of cooling underground power cables using up sloped long heat pipes in conduit N87-10028
Coaxial tube tether/transmission line for manned nuclear space power
[NASA-CASE-LEW-14338-1] N87-10174

POWER SPECTRA
Determination of the Brunt-Vaisala frequency from vertical velocity spectra N87-10449
Climatology of tropospheric vertical velocity spectra N87-10455
Interference detection and correction applied to incoherent-scatter radar power spectrum measurement N87-10520

PRECIPITATION (METEOROLOGY)
Measurements of precipitating atmosphere by the MU radar N87-10426

PREDICTION ANALYSIS TECHNIQUES
Prediction of gust loadings and alleviation at transonic speeds
[AD-A167748] N87-10047
Toward comparing experiment and theory for corroborative research on hingeless rotor stability in forward flight (an experimental and analytical investigation of isolated rotor-flap-lag stability in forward flight)
[NASA-CR-179711] N87-10063
Review of VHF Band 1 field strength prediction
[BBC-RD-1986/4] N87-10223
Development of worst case meteorology criteria
[PB86-215993] N87-10540
A high resolution entrainment model for the convective planetary boundary layer N87-10611
Fault and error latency under real workload: An experimental study
[NASA-CR-179802] N87-10733
The Helmholtz resonance behavior of single and multiple rooms
[NASA-CR-178173] N87-10749
Gauge invariant perturbation theory prediction of the sensitivity required for experimental measurement of quadrupole and higher moments of the cosmic microwave background radiation N87-10825

PREDICTIONS
Earthquake effects in the ionosphere according to Intercosmos-19 and AUREOL-3 satellite data N87-10588
Surface measurements of gust fronts and microbursts during the JAWS (Joint Airport Weather Studies) Project: Statistical results and implications for wind shear detection, prediction and modeling
[PB86-200847] N87-10665

PREPROCESSING
A single-board preprocessor and pulse generator N87-10517

PRESIDENTIAL REPORTS
Aeronautics and space report of the President
[NASA-TM-89239] N87-10827

PRESSURE DISTRIBUTION
Experimental study of the boundary layer on a low Reynolds number airfoil in steady and unsteady flow N87-10052

PRESSURE EFFECTS
Stratospheric chemistry N87-10613

PRESSURE GRADIENTS
On accurate numerical solutions of Falkner-Skan equation N87-10018
Global pressure relaxation procedure with application to viscous and inviscid flows N87-10247
Near field pressure fluctuations in a circular jet
[NASA-CR-179847] N87-10249

PRESSURE MEASUREMENT
Tunnel interference from pressure measurements on control surfaces
[AE-TM-8-83] N87-10104
Airborne Lidar measurements of the atmospheric pressure profile with tunable Alexandrite lasers N87-10282
Real-time atmospheric absorption spectra for in-flight tuning of an airborne dial system N87-10296
Strength, width, and pressure shift measurements of 54 lines in the oxygen A-band N87-10298

PRESSURE REDUCTION
Numerical study of the entrance flow and its transition of a circular pipe N87-10019
The use of decompression to simulate the effect of extravehicular activity on human lymphocyte transformation N87-10697

PRESSURE VESSELS
Pressure-resistant plane disc viewports from allyl diglycol carbonate plastic for hyperbaric chambers
[AD-A168007] N87-10105
Simple blast model for structural design
[DE86-000802] N87-10414

PRESSURIZED WATER REACTORS
Concentrations of plastic strains in the clamping region of cylindrical shells under excessive loading
[KFK-3915] N87-10417

PREVENTION
Histomorphometric study of bone cell mass and activity in man caused by a 120 day decubitus. Test of preventive protocols N87-10689

PRIMERS (EXPLOSIVES)
Percussion primer/DDT detonator
[DE86-010477] N87-10217

PROBABILITY THEORY
Composite load spectra for select space propulsion structural components
[NASA-CR-179496] N87-10176

PROBLEM SOLVING
Engine-transmission-structural airframe members compatibility N87-10069
Global collocation methods for approximation and the solution of partial differential equations
[NASA-CR-178179] N87-10745

PROCEDURES
Remote capabilities in computer networks
[RSRE-3947] N87-10732

PROCESS CONTROL (INDUSTRY)
Synthetic carbon precursor materials
[DE86-011584] N87-10210
Process control in arc welding
[KFK-PFT-105] N87-10395

PRODUCT DEVELOPMENT
Aircraft Integrated Data Systems (AIDS): Evolution and revolution N87-10077
Lufthansa's Aircraft Integrated Data Systems (AIDS) based A-310 engine condition monitoring system: Progress achieved between the 12th and 13th AIDS Symposiums N87-10084

PRODUCTION COSTS
Digital mapping: Fact or fiction
[AD-A167571] N87-10528

PROGRAM VERIFICATION (COMPUTERS)
Intelligent Computer Assisted Instruction (ICAI): Formative evaluation of two systems
[NASA-CR-176873] N87-10716

PROGRAMMING LANGUAGES
A rule based computer aided design system
[NASA-TM-86241] N87-10721
Software process interpretation and software environments
[DE86-010881] N87-10725

PROJECT MANAGEMENT
Main chamber combustion and cooling technology study
[NASA-CR-178853] N87-10175

PROPULSION
Wind tunnel test of the modified goldschmied model with propulsion and empennage: Analysis of test results
[AD-A167360] N87-10045

PROTECTION
Helicopter air intake protection systems N87-10073

PROTECTIVE COATINGS
Carbide/fluoride/silver self-lubricating composite
[NASA-CASE-LEW-14196-1] N87-10179

PROTEINS
Microgravity effects on the contractile proteins of rat muscles N87-10683

PROTON BEAMS
Prompt neutrino production in 400 GeV proton copper interactions
[USIP-86-02] N87-10754

PROTON PRECIPITATION
Precipitation of electrons and protons in the subauroral zone stimulated by ground-based VLF emitter N87-10585

PROTONS
The direction finding aboard AUREOL-3 of ELF waves at frequency above and below the proton gyrofrequency N87-10572
Nuclide production by primary cosmic-ray protons
[DE86-011268] N87-10821

PROTOSTARS
Conditions for the formation of massive stars N87-10803

PROVING
Human factors research in aircrew performance and training
[AD-A167950] N87-10714

PULSARS
Pulse timing and neutron star structure N87-10799

PULSE AMPLITUDE
Performance testing of lidar receivers N87-10325

PULSE COMMUNICATION
High speed digital signal transmission over coaxial pairs between network termination and several terminals without variable equilization
[FI-44-TBR-101] N87-10230

PULSE DOPPLER RADAR
Doppler lidar studies of atmospheric wind field dynamics N87-10327
A variable-frequency local oscillator for the frequency-hopping technique N87-10515
A single-board preprocessor and pulse generator N87-10517

PULSE DURATION
Performance characteristics of wind profiling radars N87-10429
Improving range resolution with a frequency-hopping technique N87-10514

PULSE GENERATORS
Subpicosecond high-brightness UV laser system
[DE86-011271] N87-10387
A single-board preprocessor and pulse generator N87-10517
Pulse forming network design program for linear and time-varying loads for the IBM personal computer
[DE86-011209] N87-10727

PULSE RADAR
Comparison of medium frequency pulsed radar interferometer and correlation analysis winds, part 2 N87-10475

PULSED LASERS
Pulsed mononode dye laser developed for a geophysical application N87-10364
The TFP and a pulsed LD: New lidar components N87-10374

PUPILLOMETRY
Infrared measurement of eye movement. Presentation of the Eye Movement in Infrared and Angular Torsion (EMIRAT) experiment — Spacelab payload N87-10695

PURITY
High spectral purity, narrow linewidth laser transmitter for dial measurements N87-10290

PURSUIT TRACKING
Flash/crazing effects on simulator pursuit tracking performance
[AD-A167689] N87-10759

PYLONS
Design and fabrication of the NASA decoupler pylon for the F-16 aircraft
[NASA-CR-172354] N87-10065

PYROTECHNICS
Numerical model of the thermal processes leading to ignition in a pyrotechnic device
[DE86-009626] N87-10189
Titanium oxidation kinetics and the mechanism for thermal ignition of titanium-based pyrotechnics
[DE86-010987] N87-10218
CP DDT detonators. 5: Output performance and analysis of multiple-out devices
[DE86-010995] N87-10219
Chemistry and shock initiation of intermetallic reactions
[DE86-010549] N87-10221

Q

QUALITY CONTROL
Engine-airframe integration for rotorcraft: Component specifications and qualification N87-10071

QUANTUM ELECTRONICS
RLE progress report
[MIT-PR-128] N87-10778

QUASARS
The X-ray properties of high redshift, optically selected QSOs N87-10784
High resolution spectroscopy of quasar absorption lines N87-10785
The effect of a quasi-stellar object on its host galaxy: Dynamical and physical processes in the interstellar medium around a QSO N87-10797

R

RADAR
On the potential use of radar-derived information in operational numerical weather prediction N87-10420
Hardware requirements: A new generation partial reflection radar for studies of the equatorial mesosphere N87-10431
Observations of thunder with the Arecibo VHF radar N87-10444
Effects of anisotropy on the frequency spectrum of gravity waves observed by MST radar N87-10460
A study of gravity-wave spectra in the troposphere and stratosphere at 5-min to 5-day periods with the Poker Flat MST radar N87-10462

RADAR ANTENNAS
Performance characteristics of wind profiling radars N87-10429
Propagating tides in the mesosphere N87-10441
Beam steering system N87-10501
Low-altitude coverage of ST radars N87-10504
The grid array antenna N87-10505
Use of the Sun to determine pointing of ST radar beams N87-10508
Monitoring of the MU radar antenna pattern by Satellite Ohzora (EXOS-C) N87-10509
A variable-frequency local oscillator for the frequency-hopping technique N87-10515

RADAR BEAMS
Possibility of measuring gravity-wave momentum flux by single beam observation of MST radar N87-10458
On the use of colour reflectivity plots to monitor the structure of the troposphere and stratosphere N87-10522

RADAR DATA
Archival of Poker Flat MST radar data N87-10524

RADAR DETECTION
Gas correlation lidar for methane detection N87-10356
Detection of NO sub x,C2H4 concentrations by using CO and CO2 lasers N87-10357
MAPM: A coherent dual CO2 laser DIAL system N87-10358
Calibration and analysis for a 0.53 micron incoherent Doppler lidar N87-10365
Interference detection and correction applied to incoherent-scatter radar power spectrum measurement N87-10520

RADAR ECHOES
Coherent lidars based on intracavity heterodyning of echo signals N87-10308
Measurements of precipitating atmosphere by the MU radar N87-10426
Tropospheric turbulence parameters measured by using the MU radar N87-10436
Observations of thunder with the Arecibo VHF radar N87-10444
Comparison between S. T. radar and in situ balloon measurements N87-10447
The use of the experimentally deduced Brunt-Vaisala frequency and turbulent velocity fluctuations to estimate the eddy diffusion coefficient N87-10450
A comparison of vertical velocities measured from specular and nonspecular echoes by a VHF radar N87-10470
A comparison of thunderstorm reflectivities measured at the VHF and UHF N87-10472
UHF and VHF radar observations of thunderstorms N87-10473
Comparison of reflectivity and wind profiles measured on 46.8 MHz and 430 MHz at the Arecibo Observatory N87-10477
The Adelaide MF partial-reflection radar and VHF ST radar N87-10490
Simultaneous multibeam sounding of wind and turbulence N87-10506
The elimination of a class of pseudo echoes by an improved T/R switch technique N87-10511
On the use of colour reflectivity plots to monitor the structure of the troposphere and stratosphere N87-10522
Archival of Poker Flat MST radar data N87-10524

RADAR EQUIPMENT
Thirteenth International Laser Radar Conference [NASA-CP-2431] N87-10263

RADAR FILTERS
Linewidth characteristics of Raman-shifted dye laser output at 720 and 940 nm N87-10372
Optimum coding techniques for MST radars N87-10513
Archival of Poker Flat MST radar data N87-10524

RADAR IMAGERY
Space imaging radar for remote sensing of the Earth: An evaluation [BMFT-FB-W-85-024] N87-10529

RADAR MEASUREMENT
Doppler Radar Detection of Wind Shear [NASA-CP-2435] N87-10054
Lidar measurements of slant visual range N87-10278
Visibility and aerosol measurement by diode-laser random-modulation CW lidar N87-10279
Assesment of dial data collection and analysis techniques N87-10281
Airborne Lidar measurements of the atmospheric pressure profile with tunable Alexandrite lasers N87-10282
Flight tests of a range-resolved airborne dial with two min-tea CO2 lasers N87-10284
Nd:Glass-Raman laser for water vapor dial N87-10285
A Meteorological (humidity, temperature, aerosols)) mobile dial system: Concepts and design N87-10286
Influence of Rayleigh-Doppler broadening on the selection of H2O dial system parameters N87-10287
Correction of Doppler-broadened Rayleigh backscattering effects in H2O dial measurements N87-10288
Atmospheric contributions to the column variance in direct-detection dial N87-10289
High spectral purity, narrow linewidth laser transmitter for dial measurements N87-10290
On the measurement of atmospheric density using dial in the O2 A-band (770 nm) N87-10291
Determination of cloud microphysical properties by laser backscattering and extinction measurements N87-10293
Effect of backscatter-to-extinction ratio on lidar inversions N87-10294
Laboratory measurements of forward and backward scattering of laser beams in water droplet clouds N87-10295
Observation of atmospheric ozone by dial with Raman lasers pumped by a KrF laser N87-10297
Strength, width, and pressure shift measurements of 54 lines in the oxygen A-band N87-10298
Convective structure of the planetary boundary layer of the ocean during gale N87-10300
Multifrequency dial sensing of the atmospheric gaseous constituents using the first and second harmonics of a tunable CO2 laser radiation N87-10302
Improved solution of the lidar equation utilizing particle counter measurements N87-10310
Improvements in the Goddard balloon-borne lidar N87-10311
Features of stratospheric aerosol lidar observations at Mauna Loa, 1974 - 1985 N87-10312
El Chichon aerosols in the stratosphere: Analyses of lidar data and calculations of radiation budget N87-10313
Lidar measurement of stratospheric aerosol at Syowa Station, Antarctica N87-10314
Three atmospheric dispersion experiments involving oil fog plumes measured by lidar N87-10321
Rotationally resolved collisional transfer rates in OH N87-10323
Daytime lidar measurements of tidal winds in the mesospheric sodium layer at Urbana, Illinois N87-10347
Remote temperature profiling in the troposphere and stratosphere by the radio-acoustic sounding technique N87-10488
Self-consistent analysis of high drift velocity measurements with the Scandinavian Twin Auroral Radar Experiment (STARE) system N87-10606
Further studies with data collected by NASA's airborne Doppler lidar in Oklahoma in 1981 [NASA-CR-179779] N87-10660

RADAR NETWORKS
Determination of U, V, and W from single station Doppler radar radial velocities N87-10502

RADAR RECEIVERS
Performance testing of lidar receivers N87-10325

RADAR SCANNING
Low-altitude coverage of ST radars N87-10504

RADAR SCATTERING
Simultaneous VHF and UHF radar observation of the mesosphere at Arecibo during a solar flare: A check on the gradient-mixing hypothesis N87-10437
Observations of thunder with the Arecibo VHF radar N87-10444
Comparison between S. T. radar and in situ balloon measurements N87-10447
A comparison of vertical velocities measured from specular and nonspecular echoes by a VHF radar N87-10470
A comparison of thunderstorm reflectivities measured at the VHF and UHF N87-10472
UHF and VHF radar observations of thunderstorms N87-10473
Comparison of medium frequency pulsed radar interferometer and correlation analysis winds, part 1 N87-10474

RADAR SIGNATURES
Experimental and theoretical Doppler-lidar signatures of aircraft wake vortices N87-10330

RADAR TRACKING
Lidar study of storm tops N87-10348

RADAR TRANSMITTERS
Hardware requirements: A new generation partial reflection radar for studies of the equatorial mesosphere N87-10431

RADARSCOPES
An algorithm for the detection of signals by colour contrast on the screen of a colour cathode ray tube (colour display) — radarscopes [DRIC-T-7655] N87-10233

RADIAL VELOCITY
Determination of U, V, and W from single station Doppler radar radial velocities N87-10502

RADIANCE
A theory for the retrieval of virtual temperature from winds, radiances and the equations of fluid dynamics N87-10421
A component decomposition model for evaluating atmospheric effects in remote sensing N87-10610

RADIATION ABSORPTION
An intensity-modulated dual-wavelength He-Ne laser for remote sensing of methane N87-10319

RADIATION DETECTORS
The development and test of multi-anode microchannel array detector systems. Part 2: Soft X-ray detectors [NASA-CR-177066] N87-10236
Research relative to high resolution camera on the advanced X-ray astrophysics facility [NASA-CR-179757] N87-10376

RADIATION DOSAGE
Radiation doses from flying through nuclear debris clouds [AD-A167959] N87-10711
Total-dose radiation effects data for semiconductor devices. 1985 Supplement. Volume 2, part B [NASA-CR-179741] N87-10765

RADIATION EFFECTS
Thermionic integrated circuits [DE86-005849] N87-10239
Vertical junction solar cells [AD-A167757] N87-10532
Total-dose radiation effects data for semiconductor devices. 1985 Supplement. Volume 2, part B [NASA-CR-179741] N87-10765
Amplitude distribution of cosmic ray events in extrinsic IR detectors [AD-A167692] N87-10819

RADIATION HAZARDS
Radiation doses from flying through nuclear debris clouds [AD-A167959] N87-10711

RADIATION MEASUREMENT
A preliminary cloudless standard atmosphere for radiation computation [WCP-112] N87-10657
Progress made during 1985 in the scientific and technical program of National Physical Laboratory's Division of Radiation Science and Acoustics N87-10776

RADIATIVE TRANSFER
Diffusion approximation for modeling of 3-D radiation distributions [DE86-000810] N87-10226
A component decomposition model for evaluating atmospheric effects in remote sensing N87-10610
Modeling the effects of the spatially varying sea surface temperature on the marine atmospheric boundary layer N87-10673

RADIO ASTRONOMY
RLE progress report [MIT-PR-128] N87-10778
Molecular clouds in the Carina arm [NASA-TM-87798] N87-10786
New space astronomy technique developed to study celestial bodies [NASA-NEWS-REL-86-140] N87-10788
Investigations of radio jets in M87, 3C273 and 3C345 N87-10824

RADIO BEACONS
United States Navy - Canadian Forces solid state flight data recorder/crash position locator experiment on the B-720 controlled impact demonstration N87-10097

RADIO DIRECTION FINDERS
The direction finding aboard AUREOL-3 of ELF waves at frequency above and below the proton gyrofrequency N87-10572

RADIO EMISSION
Observations of non-thermal radiation from late-type stars N87-10793

RADIO FREQUENCY HEATING
Detection from AUREOL-3 of the modulation of auroral electrojet by HF-heating from ELF signals in the upper ionosphere above Tromsoe (Norway) N87-10582
Plasma confinement by a radio frequency plugging potential in an axisymmetric mirror-cusp device [IPPJ-784] N87-10783

RADIO INTERFEROMETERS
Comparison of medium frequency pulsed radar interferometer and correlation analysis winds, part 1 N87-10474

RADIO JETS (ASTRONOMY)
Interpretation of extragalactic jets [DE86-011211] N87-10623
Investigations of radio jets in M87, 3C273 and 3C345 N87-10624

RADIO NAVIGATION
Terrestrial evaluation of the Global Positioning System (GPS) Standard Positioning Service (SPS) [PB86-219599] N87-10059

RADIO SOURCES (ASTRONOMY)
Plasma wave observations at Uranus from Voyager 2 [NASA-CR-177069] N87-10814

RADIO SPECTRA
On the spectral broadening of the ground-based VLF transmitter signals in the high-latitude ionosphere observed from Intercosmos-19 and AUREOL-3 satellites N87-10584
Review of measurements of the RF spectrum of radiation from lightning [NASA-TM-87788] N87-10658

RADIO TELESCOPES
New space astronomy technique developed to study celestial bodies [NASA-NEWS-REL-86-140] N87-10788

RADIO WAVES
Periodic amplitude variations in Jovian continuum radiation [NASA-CR-177070] N87-10813

RADIOIMMUNOASSAY
Anticortisol monoclonal antibodies: Characterization of their specificity N87-10680

RADIOMETERS
In-flight absolute radiometric calibration of the LANDSAT thematic mapper N87-10530

RADIOSONDES
Aerosol studies in mid-latitude coastal environments in Australia N87-10271
Intercomparisons of high-resolution solar blind Raman lidar atmospheric profiles of water vapor with radiosondes and kytoon N87-10333
Observations of mesoscale vertical velocities around frontal zones N87-10424
Methods for verifying the accuracy of wind profiles N87-10471

RAINSTORMS
Flow dynamics and stability in severe rainbands N87-10669

RAMAN SPECTRA
Gas dispersion measurements using a mobile Raman lidar system N87-10368
Linewidth characteristics of Raman-shifted dye laser output at 720 and 940 nm N87-10370

RAMAN SPECTROSCOPY
Lower atmospheric temperature profile measurements using a Raman lidar N87-10331
A combined Raman lidar for low tropospheric studies N87-10332
Intercomparisons of high-resolution solar blind Raman lidar atmospheric profiles of water vapor with radiosondes and kytoon N87-10333
Lidar method of measurement of atmospheric extinction and ozone profiles N87-10334

RANDOM ACCESS MEMORY
Factors contributing to static RAM cell transient upset [DE86-007710] N87-10715

RANDOM NOISE
Cramer-Rao bound analysis for frequency estimation of sinusoids in noise [AD-A167992] N87-10227

RANDOM WALK
Can stochastic, dissipative wave fields be treated as random walk generators N87-10452

RANGEFINDING
Trajectory scoring in geodetic coordinates using transponder-interrogator range data [DE86-009554] N87-10109
A mobile system for active otpical pollution monitoring N87-10355

RANKINE CYCLE
ANL/RBC: A computer code for the analysis of Rankine bottoming cycles, including system cost evaluation and off-design performance [NASA-CR-179462] N87-10777

RATINGS
Use of fuzzy sets mathematics to assist pavement evaluation and management (revised March 18, 1986) [PB86-214796] N87-10747

RATS
Microgravity effects on the contractile proteins of rat muscles N87-10683
Weightlessness effects on the bone tissue of rats after a 5 day space flight (Cosmos 1514) N87-10684
Functions of skeletal muscles of rats and monkeys after 5-day space flight (on Cosmos 1514) N87-10686
Hindlimb suspension effects on rat skeletal muscle response N87-10687
Animal studies on Spacelab-3 N87-10704
Contribution of animal models to the investigation of bone changes in weightlessness N87-10706
The state of bones of pregnant rats during an acute stage of adaptation to weightlessness N87-10708

RAYLEIGH SCATTERING
Influence of Rayleigh-Doppler broadening on the selection of H2O dial system parameters N87-10287
Correction of Doppler-broadened Rayleigh backscattering effects in H2O dial measurements N87-10288
Lidar measurements of thermal structure N87-10343

RCA SATCOM SATELLITES
Orbit achievement of RCA communication satellites N87-10122

REACTION KINETICS
Developing simplified models of combustion chemistry by simulation with detailed chemical kinetics models [DE86-008381] N87-10188

REACTOR MATERIALS
Design rule for fatigue of welded joints in elevated-temperature nuclear components [DE86-007569] N87-10393
Research and development activities of the Spectroscopy Division of the Bhabha Atomic Research Centre [DE86-702154] N87-10781

REAL TIME OPERATION
Real-time atmospheric absorption spectra for in-flight tuning of an airborne dial system N87-10296
The real-time use of wind profilers in nowcasting N87-10427
Colorado wind profilers N87-10486

REATTACHED FLOW
Supersonic, nonlinear, attached-flow wing design for high lift with experimental validation [NASA-TP-2336] N87-10042

RECRYSTALLIZATION
Ultrasonic determination of recrystallization [NASA-TM-88855] N87-10399

RED ARCS
Observational and theoretical investigation of stable auroral red arcs and their magnetospheric energy source, volumes 1 and 2 N87-10632

RED SHIFT
The X-ray properties of high redshift, optically selected QSOs N87-10784
Gauge invariant perturbation theory prediction of the sensitivity required for experimental measurement of quadrupole and higher moments of the cosmic microwave background radiation N87-10825

REDUCED GRAVITY
Microgravity Science and Applications [NASA-CR-179793] N87-10204
Cardiovascular measurements in microgravity N87-10676
The regulation of fluid and electrolyte metabolism in weightlessness N87-10679
Microgravity effects on the contractile proteins of rat muscles N87-10683
Preliminary results on the equilibrium and vertigo experiment performed during STS 51-G shuttle flight N87-10692

REDUNDANCY
Reliability issues in active control of large flexible space structures [NASA-CR-179785] N87-10167

REFLECTANCE
Polymer reflectors research during Fiscal Year 1985 [DE86-010697] N87-10211
Observations of mesoscale vertical velocities around frontal zones N87-10424
Comparison between S. T. radar and in situ balloon measurements N87-10447
Comparison of reflectivity and wind profiles measured on 46.8 MHz and 430 MHz at the Arecibo Observatory N87-10477
On the use of colour reflectivity plots to monitor the structure of the troposphere and stratosphere N87-10522
In-flight absolute radiometric calibration of the LANDSAT thematic mapper N87-10530

REFLECTING TELESCOPES
The TFP and a pulsed LD: New lidar components N87-10374

REFLECTOR ANTENNAS
Method to determine the optimal parameters of the Arecibo 46.8-MHz antenna system N87-10510

REFRACTIVITY
Sensitivity of the Lidar ratio to changes in size distribution and index of refraction N87-10277
Measurements of precipitating atmosphere by the MU radar N87-10426
Simultaneous VHF and UHF radar observation of the mesosphere at Arecibo during a solar flare: A check on the gradient-mixing hypothesis N87-10437
A statistical model to estimate refractivity turbulence structure constant C sub n sup 2 in the free atmosphere N87-10448
The use of the experimentally deduced Brunt-Vaisala frequency and turbulent velocity fluctuations to estimate the eddy diffusion coefficient N87-10450
The frequency spectrum of C sub n sup 2 from MST radar data N87-10461
A comparison of thunderstorm reflectivities measured at the VHF and UHF N87-10472
UHF and VHF radar observations of thunderstorms N87-10473

REFRACTORY MATERIALS
Development of iron aluminides [AD-A168578] N87-10194

REGIONAL PLANNING
The planning and maintenance of urban settlements to resist extreme climatic forces N87-10647

REGRESSION ANALYSIS
Ordered and random structures in pulsatile flow through constricted tubes N87-10245

REGULATIONS
Flight recorders: New US regulations and new International Civil Aviation Organization (ICAO) standards N87-10093

REINFORCING FIBERS
Effects of thermal cycling on graphie-fiber-reinforced 6061 aluminum [NASA-TP-2612] N87-10184
Experimental procedure for lifetime testing of graphite bundles under constant load [AD-A167714] N87-10186

RELAXATION (MECHANICS)
Global pressure relaxation procedure with application to viscous and inviscid flows N87-10247

RELIABILITY
Fault and error latency under real workload: An experimental study [NASA-CR-179802] N87-10733

REMOTE CONTROL
Methods and standards for encryption of spacecraft telemetry and telecommand links [RPT/ENC/62359/BO] N87-10112

REMOTE HANDLING
Remote capabilities in computer networks [RSRE-3947] N87-10732

REMOTE SENSING
Wide-area remote-sensing system of pollution and gas dispersal by near-infrared absorption based on low-loss optical fiber network N87-10354
LANDSAT imagery of the Central Andes [NASA-CR-179852] N87-10526
Space imaging radar for remote sensing of the Earth: An evaluation [BMFT-FB-W-85-024] N87-10529
A component decomposition model for evaluating atmospheric effects in remote sensing N87-10610

REMOTE SENSORS
Coverage transition times of IR pencil beam sensors — satellite attitude sensors N87-10125

RESEARCH AIRCRAFT
In-flight total forces, moments and static aeroelastic characteristics of an oblique-wing research airplane [NASA-TP-2224] N87-10103

RESEARCH AND DEVELOPMENT
Microelectronics research and development background paper [PB86-205200] N87-10242
Scientific reasons for a network of ST radars and cooperative campaigns N87-10480
Research and development activities of the Spectroscopy Division of the Bhabha Atomic Research Centre [DE86-702154] N87-10781

RESEARCH MANAGEMENT
Solar-geophysical data number 499, March 1986, supplement [NASA-CR-179797] N87-10624
Air Force technical objective document fiscal year 1987 [AD-A167324] N87-10779

RESIDENTIAL ENERGY
The assessment of climatological impacts on agricultural production and residential energy demand N87-10686
RESIN BONDING
Chemisorption mechanism and effect of polyacrylic acid on the improvement in bond durability of zinc phosphate-to-polymer adhesive joints
[DE86-011535] N87-10213
RESINS
The fungal resistance or susceptibility of resins, plasticizers, and other constituents of adhesive formulations
[AD-A166930] N87-10207
RESISTANCE HEATING
Energy delivery processes in shock tubes
N87-10106
RESONANCE SCATTERING
Light scattering in resonance region from polydisperse non-spherical particles N87-10792
RESONANT FREQUENCIES
The Helmholtz resonance behavior of single and multiple rooms
[NASA-CR-178173] N87-10749
RESOURCES
Chemistry research resource
[DE86-009891] N87-10178
REVERSED FLOW
Numerical solution of the 3-dimensional boundary layer equations in the inverse mode using finite differences
N87-10005
REVERSING
Current enhancement for hose-unstable electron beams
[AD-A167804] N87-10755
REVISIONS
The PROUST radar N87-10491
Design support of the Burst and Transient Source Experiment (BATSE) of the Gamma Ray Observatory (GRO) mission
[NASA-CR-178920] N87-10758
RING CURRENTS
The hot ion composition in the magnetosphere
N87-10552
RITZ AVERAGING METHOD
The local convergence of Ritz and Galerkin methods for nonlinear problems N87-10737
ROBOTICS
Dynamic modeling and control of robotic manipulators
N87-10390
Rapid precise end point control of a wrist carried by a flexible manipulator N87-10398
ROBOTS
Dynamic modeling and control of robotic manipulators
N87-10390
Programming of sensor based assembly robots
[KFK-PFT-120] N87-10396
Experimental identification and control of the tip position of a flexible, single link manipulator N87-10397
Rapid precise end point control of a wrist carried by a flexible manipulator N87-10398
FORPS: A FORTH-based production system and its application to a real-time robot control problem
[DE86-005426] N87-10734
ROBUSTNESS (MATHEMATICS)
Reliability issues in active control of large flexible space structures
[NASA-CR-179785] N87-10167
Control of large flexible space structures
[NASA-CR-177063] N87-10168
ROCKET EXHAUST
Technical overview of plume radiation from a solid rocket motor N87-10021
ROCKET FIRING
Operational strategies for multi-burn apogee maneuvers of geostationary spacecraft N87-10141
Optimal injection of TV SAT with multi-impulse apogee maneuvers with mission constraints and thrust uncertainties N87-10144
Targeting multiburn, long duration apogee burst maneuvers N87-10146
ROCKET SOUNDING
Objectives and design of the ECHO 6 electron beam experiment: Large ionospheric perturbations and energetic particle patterns --- rocket sounding N87-10590
Observations of auroral electrons with sounding rockets and the GEOS-2 geostationary satellite N87-10596
ROOMS
The Helmholtz resonance behavior of single and multiple rooms
[NASA-CR-178173] N87-10749
ROTARY WINGS
Engine-airframe integration considerations for preliminary air vehicle performance analysis N87-10068
Response of a small-turboshaft-engine compression system to inlet temperature distortion
[NASA-TM-83765] N87-10100
ROTATING BODIES
Free vibration and dynamic response analysis of spinning structures
[NASA-CR-179672] N87-10717
ROTOR AERODYNAMICS
Toward comparing experiment and theory for corroborative research on hingeless rotor stability in forward flight (an experimental and analytical investigation of isolated rotor-flap-lag stability in forward flight)
[NASA-CR-179711] N87-10063
ROTOR BLADES (TURBOMACHINERY)
Aeroelastic stability of composite rotor blades in hover
N87-10060
Toward comparing experiment and theory for corroborative research on hingeless rotor stability in forward flight (an experimental and analytical investigation of isolated rotor-flap-lag stability in forward flight)
[NASA-CR-179711] N87-10063
ROTORS
Analysis of the vibration of the input bevel pinion in RAN Wessex helicopter main rotor gearbox WAK143 prior to failure
[ARL-AERO-PROP-R-169] N87-10061
High precision absolute laser power measurements using a magnetically suspended rotor
[DE86-011585] N87-10389
Prediction of helicopter rotor discrete frequency noise: A computer program incorporating realistic blade motions and advanced acoustic formulation
[NASA-TM-87721] N87-10750

S

SACCADIC EYE MOVEMENTS
Infrared measurement of eye movement. Presentation of the Eye Movement in Infrared and Angular Torsion (EMIRAT) experiment — Spacelab payload N87-10695
SAFETY DEVICES
Electronics Engineering Department technical review
[DE86-011371] N87-10241
SAFETY FACTORS
Crashworthiness experiment summary full-scale transport controlled impact demonstration program
[DOT/FAA/CT-85/20] N87-10055
SATELLITE ATMOSPHERES
A modeling analysis program for the JPL Table Mountain Io sodium cloud data
[NASA-CR-179671] N87-10811
SATELLITE ATTITUDE CONTROL
Operational criteria for geostationary satellites in National Space Development Agency (NASDA)
N87-10119
Orbit achievement of RCA communication satellites
N87-10122
Attitude determinations for geostationary satellites of the National Space Development Agency (NASDA)
N87-10124
Coverage transition times of IR pencil beam sensors — satellite attitude sensors N87-10125
Application of simplified spin axis attitude determination techniques to ESA telecom satellites N87-10126
Synchronous transfer orbit operation under three-axis control N87-10137
Parameter optimization and attitude stabilization of a flexible spacecraft N87-10138
A new three-axis control system for a geosynchronous satellite in transfer orbit N87-10139
Orbit and attitude operations during the Telecom 1B transfer phase N87-10147
Longitudinal orbit control from INTELSAT 5 inclination stationkeeping maneuvers N87-10156
Operational performance of the INTELSAT 5 attitude determination and control system N87-10158
Updates to operational procedures as a result of in-orbit experience with SYMPHONIE spacecraft N87-10159
SATELLITE CONTROL
An investigation on passively controlled geosynchronous orbits N87-10118
Efficiency eccentricity control using continuous, vectored thrusting for satellites with large area/mass ratios N87-10151
Stationkeeping strategy for TDF 1 satellite
N87-10154
Eccentricity control strategy for geosynchronous communications satellites N87-10155
Orbitography course for ground operators
N87-10157
SEAGOS: A prototype expert system to aid ground operators in satellite command and control tasks
N87-10161
Geostationary satellites autonomous stationkeeping
N87-10164
SATELLITE DESIGN
Telecom-1 dynamic simulator N87-10160
SATELLITE DRAG
Two dimensional analysis of high voltage solar array interfering with ionospheric plasma N87-10022
SATELLITE IMAGERY
LANDSAT imagery of the Central Andes
[NASA-CR-179852] N87-10526
Some results of scanner spectrophotometric measurements of aurora and airglow from IK-Bulgaria-1300 satellite and prospects of similar measurements N87-10593
SATELLITE NETWORKS
Constraints imposed by an intersatellite communication link upon stationkeeping of two close geostationary satellites N87-10162
SATELLITE OBSERVATION
An observational study of tropical cloud cluster evolution and cyclogenesis in the Western North Pacific
[CSU-ASP-403] N87-10661
SATELLITE ORBITS
DMA (Defense Mapping Agency) orbit determination for transit satellites: 1985
[AD-A167567] N87-10108
Optimal transfer to inclined geosynchronous orbits
N87-10117
Early orbit determination --- satellite orbits
N87-10128
Real time orbit determination during apogee maneuvers — satellite orbits N87-10130
Eccentricity control strategy for geosynchronous communications satellites N87-10155
Operational performance of the INTELSAT 5 attitude determination and control system N87-10158
SATELLITE ORIENTATION
A new three-axis control system for a geosynchronous satellite in transfer orbit N87-10139
World geodetic system 1984
[AD-A167570] N87-10527
SATELLITE SOUNDING
On the potential use of radar-derived information in operational numerical weather prediction N87-10420
Statistical study of auroral electron precipitation structures detected by the AUREOL-3 Satellite
N87-10543
Small scale and intense field-aligned currents detected by their magnetic signature N87-10546
The hot ion composition in the magnetosphere
N87-10552
Dynamic variations of the auroral precipitation and the polar cap N87-10559
Polar cap particle precipitation as measured by the AUREOL-3 and Intercosmos-19 satellites N87-10560
Small scale structures of electric field variations and particle precipitations as observed onboard AUREOL-3 satellite N87-10569
Polarization of electromagnetic waves recorded on board the AUREOL-3 satellite N87-10571
Intercosmos-Bulgaria-1300 satellite: Large-scale structure and dynamics of the polar ionosphere during geomagnetic storms N87-10592
A multipoint study of a substorm on 4 March 1979 — magnetosphere N87-10595
Observations of auroral electrons with sounding rockets and the GEOS-2 geostationary satellite N87-10596
Energy spectra of electrons precipitating above the EISCAT area. Comparison with ARCAD measurements
N87-10598
The ARCAD 3-SAFARI coordinated study of auroral and polar F-region ionospheric irregularities N87-10600
Two-dimensional snapshots of electron density in the main trough and diffuse auroral zone from a close network of ionosondes: Comparison with measurements from AUREOL-3 satellite N87-10601
SATELLITE TRACKING
Optimal tracking strategy determination --- satellite tracking N87-10120
Accuracy of goestationary orbit determination
N87-10121
Preliminary orbit determination by static multivariate search N87-10127
Early orbit determination — satellite orbits
N87-10128
Optical tracking of the SIRIO satellite N87-10134
Tracking and Data Relay Satellite (TDRS) tracking and orbit determination N87-10136
World geodetic system 1984
[AD-A167570] N87-10527
SATELLITE-BORNE INSTRUMENTS
Space Environment Laboratory, FY 1985
[PB86-218567] N87-10621
SATURN (PLANET)
Clouds and methane photochemical hazes on the outer planets N87-10815
SCALING LAWS
An example of scaling MST Doppler spectra using median spectra, spectral smoothing, and velocity tracing
N87-10519

SCATTER PROPAGATION
Mechanism of low-frequency wave propagation in the magnetosphere N87-10580
SCATTERING
Comparison of medium frequency pulsed radar interferometer and correlation analysis winds, part 2 N87-10475
Mesospheric wind measurements using a medium-frequency imaging Doppler interferometer N87-10476
SCATTERING COEFFICIENTS
Vertical structure of Arctic haze observed by lidar N87-10335
Investigation of clouds spatial distribution using ground-based lidar N87-10349
Near-IR extinction and backscatter coefficient measurements in low- and mid-altitude clouds N87-10351
SEA SURFACE TEMPERATURE
Modeling the effects of the spatially varying sea surface temperature on the marine atmospheric boundary layer N87-10673
SEALERS
Polymer systems for rapid sealing of aircraft structures at low temperature
[AD-A167667] N87-10209
SEALS (STOPPERS)
Computational fluid mechanics utilizing the variational principle of modeling damping seals
[NASA-CR-178902] N87-10248
SECURITY
A summary of the Foundation Research Program, fiscal year 1985
[AD-A168009] N87-10780
SEISMIC WAVES
Some seismic results of an underground explosion at the Mururoa Test Site (Shot Report no. 6)
[AWRE-O-17/85] N87-10619
SEISMOGRAMS
Some seismic results of an underground explosion at the Mururoa Test Site (Shot Report no. 6)
[AWRE-O-17/85] N87-10619
SEISMOLOGY
Earthquake effects in the ionosphere according to Intercosmos-19 and AUREOL-3 satellite data N87-10588
SELECTIVE FADING
MODTEQ (Modulation Techniques), AN/FRC-170(V), equalization, and channel medium simulations
[AD-A167965] N87-10226
SELF LUBRICATING MATERIALS
Carbide/fluoride/silver self-lubricating composite
[NASA-CASE-LEW-14196-1] N87-10179
SEMICONDUCTOR DEVICES
Total-dose radiation effects data for semiconductor devices. 1985 Supplement. Volume 2, part B
[NASA-CR-179741] N87-10765
SENSITIVITY
A system for controlled presentation of the Arden contrast sensitivity test
[AD-A167969] N87-10712
SENSORIMOTOR PERFORMANCE
Preliminary results on the equilibrium and vertigo experiment performed during STS 51-G shuttle flight N87-10692
SEPARATED FLOW
Acta Aeronautica et Astronautica Sinica (selected articles)
[AD-A167918] N87-10004
Numerical solution of the 3-dimensional boundary layer equations in the inverse mode using finite differences N87-10005
Separation and wakes over 3-dimensional bodies N87-10008
Study of three-dimensional separation on a spheroid at incidence N87-10016
Numerical modeling of spatial flows on the basis of splitting up method N87-10031
SEPARATORS
Impact of IPS and IRS configurations on engine installation design N87-10070
SERVICE LIFE
Flight service evaluation of composite helicopter components
[NASA-CR-178149] N87-10182
Polymer reflectors research during Fiscal Year 1985
[DE86-010697] N87-10211
SHEAR PROPERTIES
Foundation interaction problems involving an elastic half-plane
[AD-A167925] N87-10411
Further results on the initiation and growth of adiabatic shear bands
[AD-A168012] N87-10412
SHEAR STRESS
Ordered and random structures in pulsatile flow through constricted tubes N87-10245
Short-wavelength buckling and shear failures for compression-loaded composite laminates N87-10403
SHELLS (STRUCTURAL FORMS)
Geometric and material nonlinear dynamic analysis of complex shells N87-10401
Response of a 3-layered ring to an axisymmetric impulse
[DE86-011016] N87-10415
SHOCK LAYERS
An asymptotic theory of supersonic turbulent interactions in a compression corner N87-10010
SHOCK TUBES
Energy delivery processes in shock tubes N87-10106
SHOCK WAVES
Numerical modeling of spatial flows on the basis of splitting up method N87-10031
Supersonic flow around tip sides of wings N87-10033
Chemistry and shock initiation of intermetallic reactions
[DE86-009694] N87-10220
Chemistry and shock initiation of intermetallic reactions
[DE86-010549] N87-10221
Attempts to characterize microballoon sensors for shock velocity and material motion studies
[DE86-011210] N87-10379
The onset of alfvenic turbulence N87-10762
Computational hydrodynamics in astrophysical studies: Highly shocked flows in 3 dimensions N87-10796
The effect of a quasi-stellar object on its host galaxy: Dynamical and physical processes in the interstellar medium around a QSO N87-10797
Physical processes in collapse driven supernova N87-10808
SHOT NOISE
Transverse correlations in start-up of a free electron laser from noise
[DE86-009917] N87-10380
SHUTTLE IMAGING RADAR
Space imaging radar for remote sensing of the Earth: An evaluation
[BMFT-FB-W-85-024] N87-10529
SIDELOBES
Phased-array design for MST and ST radars N87-10499
Optimum coding techniques for MST radars N87-10513
SIEVES
Vulnerability methodology and protective measures for aircraft fire and explosion hazards. Volume 3: On-Board Inert Gas Generator System (OBIGGS) studies. Part 1: OBIGGS ground performance tests
[AD-A167357] N87-10066
SIGNAL ANALYSIS
Propagating tides in the mesosphere N87-10441
SIGNAL DETECTION
An algorithm for the detection of signals by colour contrast on the screen of a colour cathode ray tube (colour display) — radarscopes
[DRIC-T-7655] N87-10233
SIGNAL ENCODING
An overview of data acquisition, signal coding and data analysis techniques for MST radars N87-10512
Optimum coding techniques for MST radars N87-10513
SIGNAL PROCESSING
Strategic Defense Initiative Program: Status of airborne optical adjunct and terminal imaging radar
[P86-221132] N87-10107
Sensitivity of the Lidar ratio to changes in size distribution and index of refraction N87-10277
Using a laser aureole to invert lidar return N87-10292
An all-purpose computer program for lidar simulations and reduction of lidar data N87-10299
Laser sounding of instantaneous and mean speed of wind using correlation method N87-10304
The influrence of an optical receiving system on statistical characteristics of a lidar signal N87-10307
The influence of scattering particles morphology on the characteristics of lidar signals N87-10309
Time-resolved lidar fluorosensor for sea pollution detection N87-10317
Coherent lidar signal fluctuation reduction by means of frequency diversity technique N87-10360
Wind profiler demonstration system N87-10487
Progress in the MF radar system at Saskatoon N87-10496
An overview of data acquisition, signal coding and data analysis techniques for MST radars N87-10512
A microprogrammable radar controller N87-10518
RLE progress report
[MIT-PR-128] N87-10778
SIGNAL RECEPTION
Coherent lidar signal fluctuation reduction by means of frequency diversity technique N87-10360
Comparison of reflectivity and wind profiles measured on 46.8 MHz and 430 MHz at the Arecibo Observatory N87-10477
SIGNAL REFLECTION
Progress in existing and planned MST radars N87-10481
SIGNAL TO NOISE RATIOS
Cramer-Rao bound analysis for frequency estimation of sinusoids in noise
[AD-A167992] N87-10227
Improving range resolution with a frequency-hopping technique N87-10514
An example of scaling MST Doppler spectra using median spectra, spectral smoothing, and velocity tracing N87-10519
SIGNAL TRANSMISSION
High speed digital signal transmission over coaxial pairs between network termination and several terminals without variable equilization
[FI-44-TBR-101] N87-10230
The effect of turbulence on lidar backscattered signal fluctuations N87-10328
SILANES
Boron-containing organosilane polymers and ceramic materials thereof
[NASA-CASE-ARC-11649-1-SB] N87-10205
SILICON
Interface properties and crystal-growth mechanisms
[DE86-010846] N87-10767
SILICON CARBIDES
Boron-containing organosilane polymers and ceramic materials thereof
[NASA-CASE-ARC-11649-1-SB] N87-10205
Microstructure, grain boundaries and properties of sintered and isotatically hot pressed SiC materials
[KFK-4063] N87-10769
SILICON POLYMERS
Boron-containing organosilane polymers and ceramic materials thereof
[NASA-CASE-ARC-11649-1-SB] N87-10205
SILVER
Carbide/fluoride/silver self-lubricating composite
[NASA-CASE-LEW-14196-1] N87-10179
SIMULATION
Developing simplified models of combustion chemistry by simulation with detailed chemical kinetics models
[DE86-008381] N87-10188
Effect of backscatter-to-extinction ratio on lidar inversions N87-10294
Numerical studies of thermally and mechanically forced circulations over complex terrain N87-10630
SINE WAVES
Cramer-Rao bound analysis for frequency estimation of sinusoids in noise
[AD-A167992] N87-10227
SINTERING
Microstructure, grain boundaries and properties of sintered and isotatically hot pressed SiC materials
[KFK-4063] N87-10769
SIRIO SATELLITE
Optical tracking of the SIRIO satellite N87-10134
SITE SELECTION
Accuracy of goestationary orbit determination N87-10121
Climatic factors in the siting of new towns and specialized urban facilities N87-10654
SIZE DISTRIBUTION
Sensitivity of the Lidar ratio to changes in size distribution and index of refraction N87-10277
SLENDER BODIES
Vortex shedding of a square cylinder in front of a slender airfoil at high Reynolds numbers. Part 1: Spacing effect
[MPIS-23/1985] N87-10048
SLEWING
Maneuver and control of flexible spacecraft N87-10166
SLOPES
On the varying slope of velocity spectra N87-10463
SODIUM
Lidar observation of the mesospheric sodium layer in Antarctica N87-10345
A modeling analysis program for the JPL Table Mountain Io sodium cloud data
[NASA-CR-179671] N87-10811
SOFTWARE ENGINEERING
The Penn State Doppler network progress report N87-10489
Progress in the MF radar system at Saskatoon N87-10496
Proceedings of the 5th Annual Users' Conference
[NASA-CP-2399] N87-10720

Software process interpretation and software environments
[DE86-010881] N87-10725

SOFTWARE TOOLS
Proceedings of the 5th Annual Users' Conference
[NASA-CP-2399] N87-10720
Integrated testing and analysis of mathematical software tools. Summary of research activities, 1 August 1985-1 May 1986
[DE86-010882] N87-10723
Computer software evaluation methodology and data base management system selection
[DE86-011343] N87-10772

SOLAR ACTIVITY
Solar-geophysical data number 499, March 1986, supplement
[NASA-CR-179797] N87-10624
Solar-geophysical data number 499, March 1986. Part 2: (Comprehensive reports). Data for September 1986 and miscellanea
[NASA-CR-179796] N87-10625
Solar-geophysical data number 499, March 1986. Part 1: (Prompt reports). Data for February 1986, January 1986 and late data
[NASA-CR-179795] N87-10626

SOLAR ACTIVITY EFFECTS
Simultaneous VHF and UHF radar observation of the mesosphere at Arecibo during a solar flare: A check on the gradient-mixing hypothesis N87-10437

SOLAR ARRAYS
Two dimensional analysis of high voltage solar array interfering with ionospheric plasma N87-10022
Modeling and analysis of spacecraft power systems
N87-10173

SOLAR COLLECTORS
Analysis of heat-pipe absorbers in evacuated-tube solar collectors
[DE86-010764] N87-10252
Methods of testing to determine the thermal performance of solar collectors
[DE86-009311] N87-10533
Workshop on the Physics and Chemistry of Solar-Flux Effects on Condensed Phase/Gas Interfaces
[DE86-004460] N87-10817

SOLAR COSMIC RAYS
Nuclide production by primary cosmic-ray protons
[DE86-011268] N87-10821

SOLAR CYCLES
A photometric and in situ study of stable auroral red arcs N87-10628

SOLAR ENERGY CONVERSION
Experience with the application of photovoltaics devices
[DE86-010472] N87-10535

SOLAR FLARES
Simultaneous VHF and UHF radar observation of the mesosphere at Arecibo during a solar flare: A check on the gradient-mixing hypothesis N87-10437
Solar-geophysical data number 501, May 1986. Part 2: (Comprehensive reports). Data for November 1985 and miscellanea
[PB86-218047] N87-10622
Solar-geophysical data number 501, May 1986. Part 1: (Prompt reports). Data for April 1986, March 1986 and late data
[PB86-218039] N87-10623
Three-dimensional structure of the heliosphere: Quiet-time and disturbed periods N87-10818

SOLAR FLUX
Workshop on the Physics and Chemistry of Solar-Flux Effects on Condensed Phase/Gas Interfaces
[DE86-004460] N87-10817

SOLAR PHYSICS
Space Environment Laboratory, FY 1985
[PB86-218567] N87-10621

SOLAR PROMINENCES
Solar-geophysical data number 501, May 1986. Part 2: (Comprehensive reports). Data for November 1985 and miscellanea
[PB86-218047] N87-10622

SOLAR RADIATION
Radiative processes N87-10618
Solar-geophysical data number 499, March 1986. Part 2: (Comprehensive reports). Data for September 1986 and miscellanea
[NASA-CR-179796] N87-10625

SOLAR RADIO BURSTS
Solar-geophysical data number 501, May 1986. Part 2: (Comprehensive reports). Data for November 1985 and miscellanea
[PB86-218047] N87-10622
Solar-geophysical data number 501, May 1986. Part 1: (Prompt reports). Data for April 1986, March 1986 and late data
[PB86-218039] N87-10623

SOLAR REFLECTORS
Polymer reflectors research during Fiscal Year 1985
[DE86-010697] N87-10211

SOLAR TERRESTRIAL INTERACTIONS
Evidence for ion energy dispersion in the polar cusp related to a northward directed Interplanetary Magnetic Field (IMF) N87-10561
Observations of polar-cap ionospheric signatures of polar wind/magnetosphere coupling N87-10563

SOLAR WIND
Observations of polar-cap ionospheric signatures of polar wind/magnetosphere coupling N87-10563
A multipoint study of a substorm on 4 March 1979 — magnetosphere N87-10595
Three-dimensional structure of the heliosphere: Quiet-time and disturbed periods N87-10818

SOLID ELECTRODES
Surface attack on metals in the presence of liquid metals
[AD-A167403] N87-10193

SOLID LUBRICANTS
Carbide/fluoride/silver self-lubricating composite
[NASA-CASE-LEW-14196-1] N87-10179

SOLID STATE
Hardware requirements: A new generation partial reflection radar for studies of the equatorial mesosphere
N87-10431

SOLIDIFICATION
Transformations and new PHACOMP analysis in weld metal of Hastelloy C-type alloys
[DE86-011422] N87-10198

SORPTION
Advanced desiccant materials research
[DE86-010695] N87-10536

SOUND WAVES
Acoustic waves emitted by vortex-body interaction
N87-10015
Observations of thunder with the Arecibo VHF radar
N87-10444
Very low frequency and ELF effects in the upper ionosphere caused by large-scale acoustic waves in the lower ionosphere observed from AUREOL-3 satellite
N87-10587

SOUNDING ROCKETS
Simultaneous rocket and MST radar observation of an internal gravity wave breaking in the mesosphere
N87-10443

SOUTHERN CALIFORNIA
The internal tide off southern California
[AD-A167722] N87-10672

SPACE COLONIES
The case for Mars: Concept development for a Mars research station
[NASA-CR-179753] N87-10812

SPACE COMMERCIALIZATION
Microgravity Science and Applications
[NASA-CR-179793] N87-10204
National Aeronautics and Space Administration
N87-10774

SPACE ERECTABLE STRUCTURES
A space station Structures and Assembly Verification Experiment, SAVE
[NASA-TM-89004] N87-10170

SPACE EXPLORATION
The case for Mars: Concept development for a Mars research station
[NASA-CR-179753] N87-10812
Aeronautics and space report of the President
[NASA-TM-89239] N87-10827

SPACE FLIGHT
Proceedings of the Symposium on Mechanics for Space Flight, 1985
[ISAS-SP-4] N87-10011
Proceedings of 2nd International Conference on Space Physiology
[ESA-SP-237] N87-10675
Animal models in space physiology N87-10705
Cosmos 1514 flight: Study of rhesus monkey ECG
N87-10707
The state of bones of pregnant rats during an acute stage of adaptation to weightlessness N87-10708
Math modelling as a complement to the scientific inquiry of physiological adaptation to space flight: Fluid, endocrine and circulatory regulation N87-10709

SPACE HABITATS
The case for Mars: Concept development for a Mars research station
[NASA-CR-179753] N87-10812

SPACE PLASMAS
Plasma sheet boundary electric fields during substorms N87-10548

SPACE PLATFORMS
Coherent lidar technology for global wind profiling
N87-10267

SPACE POWER REACTORS
Coaxial tube tether/transmission line for manned nuclear space power
[NASA-CASE-LEW-14338-1] N87-10174

SPACE PROCESSING
Microgravity Science and Applications
[NASA-CR-179793] N87-10204

SPACE SHUTTLE MAIN ENGINE
Main chamber combustion and cooling technology study
[NASA-CR-178853] N87-10175
Composite load spectra for select space propulsion structural components
[NASA-CR-179496] N87-10176
Nonlinear rotordynamics analysis
[NASA-CR-178931] N87-10407

SPACE SHUTTLE MISSION 51-G
Cardiovascular examination during STS 51 G mission June (1985) N87-10677
Weightlessness effects on the phosphorus-calcium balance and its hormonal regulation in man during STS flight 51-G N87-10691
Preliminary results on the equilibrium and vertigo experiment performed during STS 51-G shuttle flight
N87-10692

SPACE SHUTTLE MISSIONS
Shuttle derived atmospheric density model. Part 1: Comparisons of the various ambient atmospheric source data with derived parameters from the first twelve STS entry flights, a data package for AOTV atmospheric development
[NASA-CR-171824] N87-10662
Shuttle derived atmospheric density model. Part 2: STS atmospheric implications for AOTV trajectory analysis, a proposed GRAM perturbation density model
[NASA-CR-171824] N87-10663

SPACE SHUTTLE PAYLOADS
The Lidar In-Space Technology Experiment (LITE)
N87-10270

SPACE SHUTTLES
Summary of longitudinal stability and control parameters as determined from space shuttle Columbia flight test data
[NASA-TM-87768] N87-10101
Nonlinear rotordynamics analysis
[NASA-CR-178931] N87-10407

SPACE STATION POWER SUPPLIES
Coaxial tube tether/transmission line for manned nuclear space power
[NASA-CASE-LEW-14338-1] N87-10174

SPACE STATIONS
Orbital transfer vehicle launch operations study. Volume 1: Executive summary
[NASA-CR-179701] N87-10110

SPACE TRANSPORTATION SYSTEM
National Aeronautics and Space Administration
N87-10774
National Aeronautics and Space Administration Authorization Act, 1987 N87-10775

SPACEBORNE ASTRONOMY
New space astronomy technique developed to study celestial bodies
[NASA-NEWS-REL-86-140] N87-10788

SPACEBORNE EXPERIMENTS
Cardiovascular examination during STS 51 G mission June (1985) N87-10677

SPACEBORNE TELESCOPES
Extreme ultraviolet explorer: Mirror optical tests and results
[DE86-010560] N87-10760
NASA studying concept to measure distance between stars, galaxies
[NASA-NEWS-REL-86-133] N87-10787

SPACECRAFT COMMUNICATION
Constraints imposed by an intersatellite communication link upon stationkeeping of two close geostationary satellites N87-10162
Study of the middle latitude broadening of the spectrum of the waves emitted from ground N87-10583

SPACECRAFT CONFIGURATIONS
Orbital transfer vehicle launch operations study. Volume 1: Executive summary
[NASA-CR-179701] N87-10110

SPACECRAFT CONTROL
Summary of longitudinal stability and control parameters as determined from space shuttle Columbia flight test data
[NASA-TM-87768] N87-10101
Methods and standards for encryption of spacecraft telemetry and telecommand links
[RPT/ENC/62359/BO] N87-10112
Maneuver and control of flexible spacecraft
N87-10166

SPACECRAFT DESIGN
Modeling and analysis of spacecraft power systems
N87-10173

SPACECRAFT INSTRUMENTS

Plasma wave observations at Uranus from Voyager 2 [NASA-CR-177069] N87-10614

SPACECRAFT LAUNCHING

Orbital transfer vehicle launch operations study. Volume 1: Executive summary [NASA-CR-179701] N87-10110

Analysis of the problem of satellite launch windows for Ariane dual launches N87-10115

Orbit geometry for calibration and launch operations of a three-axis controlled satellite with inertial reference N87-10116

SPACECRAFT LUBRICATION

Carbide/fluoride/silver self-lubricating composite [NASA-CASE-LEW-14196-1] N87-10179

SPACECRAFT MANEUVERS

Maneuver and control of flexible spacecraft N87-10166

Identification and control of structures in space [NASA-CR-179811] N87-10172

SPACECRAFT MODELS

Telecom-1 dynamic simulator N87-10160

SPACECRAFT POWER SUPPLIES

Modeling and analysis of spacecraft power systems N87-10173

Coaxial tube tether/transmission line for manned nuclear space power [NASA-CASE-LEW-14338-1] N87-10174

SPACECRAFT PROPULSION

Composite load spectra for select space propulsion structural components [NASA-CR-179496] N87-10176

SPACECRAFT STABILITY

Spin dynamics with sloshing effects for solid motor burning phase — satellite dynamics N87-10140

SPACECRAFT STRUCTURES

Effects of thermal cycling on graphie-fiber-reinforced 6061 aluminum [NASA-TP-2612] N87-10184

SPACECREWS

Vestibular tests in cosmonaut selection and training N87-10694

SPACELAB PAYLOADS

MIE Lidar proposed for the German Space Shuttle Mission D2 N87-10269

Infrared measurement of eye movement. Presentation of the Eye Movement in Infrared and Angular Torsion (EMIRAT) experiment — Spacelab payload N87-10695

Animal studies on Spacelab-3 N87-10704

SPACING

Vortex shedding of a square cylinder in front of a slender airfoil at high Reynolds numbers. Part 1: Spacing effect [MPIS-23/1985] N87-10048

SPATIAL DISTRIBUTION

Numerical modeling of spatial flows on the basis of splitting up method N87-10031

Investigation of clouds spatial distribution using ground-based lidar N87-10349

Molecular clouds in the Carina arm [NASA-TM-87798] N87-10786

SPATIAL RESOLUTION

Simultaneous multibeam sounding of wind and turbulence N87-10506

Improving range resolution with a frequency-hopping technique N87-10514

SPECIFICATIONS

Engine-airframe integration for rotorcraft: System specifications and qualification N87-10074

SPECKLE PATTERNS

Remote sensing of atmospheric winds using a coherent, CW lidar and speckle-turbulence interaction N87-10329

Demonstration of laser speckle system on burner liner cyclic rig [NASA-CR-179509] N87-10377

SPECTRA

Observations and a model of gravity-wave variability in the middle atmosphere N87-10453

Effects of anisotropy on the frequency spectrum of gravity waves observed by MST radar N87-10460

A study of gravity-wave spectra in the troposphere and stratosphere at 5-min to 5-day periods with the Poker Flat MST radar N87-10462

On the varying slope of velocity spectra N87-10463

Doppler effects on velocity spectra observed by MST radars N87-10464

Observations of vertical velocity power spectra with the SOUSY VHF radar N87-10465

Mesospheric wave number spectra from Poker Flat MST radar measurements compared with gravity-wave model N87-10466

Evidence of a saturated gravity-wave spectrum throughout the atmosphere N87-10467

SPECTRAL EMISSION

High spectral purity, narrow linewidth laser transmitter for dial measurements N87-10290

Feasibility experiments on time-resolved fluorosensing applied to oil slicks N87-10322

SPECTRAL LINE WIDTH

Linewidth characteristics of Raman-shifted dye laser output at 720 and 940 nm N87-10370

SPECTROGRAPHS

The development and test of multi-anode microchannel array detector systems. Part 2: Soft X-ray detectors [NASA-CR-177066] N87-10236

SPECTROPHOTOMETRY

Some results of scanner spectrophotometric measurements of aurora and airglow from IK-Bulgaria-1300 satellite and prospects of similar measurements N87-10593

SPECTROSCOPIC TELESCOPES

Spectroscopy of the globular clusters in M87 [NASA-CR-179854] N87-10790

SPECTRUM ANALYSIS

Remote express analysis of ground-layer aerosol based on laser-induced spark spectra N87-10303

Effects of anisotropy on the frequency spectrum of gravity waves observed by MST radar N87-10460

The frequency spectrum of C sub n sup 2 from MST radar data N87-10461

Mesospheric wave number spectra from Poker Flat MST radar measurements compared with gravity-wave model N87-10466

An evaluation of errors observed in the measurement of low wind velocities N87-10469

Global collocation methods for approximation and the solution of partial differential equations [NASA-CR-178179] N87-10745

Bright galactic X-ray binary sources: Temporal and spectral studies N87-10804

SPECULAR REFLECTION

Polymer reflectors research during Fiscal Year 1985 [DE86-010697] N87-10211

SPHERES

Light scattering in resonance region from polydisperse non-spherical particles N87-10792

SPHERICAL COORDINATES

Analysis of two-dimensional incompressible flow past airfoils using unsteady Navier-Stokes equations [NASA-CR-179823] N87-10040

SPHEROIDS

Study of three-dimensional separation on a spheroid at incidence N87-10016

SPIN DYNAMICS

Spin-tunnel investigation of a 1/25-scale model of the General Dynamics F-16XL airplane [NASA-TM-85660] N87-10041

Spin dynamics with sloshing effects for solid motor burning phase — satellite dynamics N87-10140

Free vibration and dynamic response analysis of spinning structures [NASA-CR-179672] N87-10717

SPIN STABILIZATION

Application of simplified spin axis attitude determination techniques to ESA telecom satellites N87-10126

SPIN TESTS

Spin-tunnel investigation of a 1/25-scale model of the General Dynamics F-16XL airplane [NASA-TM-85660] N87-10041

SPOILERS

Experimental and theoretical investigations of the flow field of an airfoil with a deflected spoiler N87-10050

SPORTS MEDICINE

Upper and lower body anaerobic power comparison between biathletes and control subjects [AD-A167636] N87-10710

SPRAYING

Transient behavior of liquid jets injected normal to a high velocity gas stream N87-10246

SPREAD F

Instabilities associated with the equatorial spread-F phenomenon and their north-south asymmetry N87-10576

SQUALLS

Flow dynamics and stability in severe rainbands N87-10669

STABILITY

Acta Aeronautica et Astronautica Sinica (selected articles) [AD-A167918] N87-10004

Flow dynamics and stability in severe rainbands N87-10669

On the stability of accretion disks around black holes N87-10805

STABILITY AUGMENTATION

Fault tolerant control laws [NASA-CR-178094] N87-10400

STABILIZATION

Long-pulse excimer lasers for materials processing and medical applications [DE86-011267] N87-10384

STAINLESS STEELS

Design rule for fatigue of welded joints in elevated-temperature nuclear components [DE86-007569] N87-10393

STANDARDS

Flight recorders: New US regulations and new International Civil Aviation Organization (ICAO) standards N87-10093

Methods of testing to determine the thermal performance of solar collectors [DE86-009311] N87-10533

Development of worst case meteorology criteria [PB86-215993] N87-10540

Progress made during 1985 in the scientific and technical program of National Physical Laboratory's Division of Radiation Science and Acoustics N87-10776

STAR FORMATION

Gas and dust in regions of recent star formation N87-10800

A study of the ground state hydroxyl maser emissions associated with eleven regions of star formation N87-10826

STARS

NASA studying concept to measure distance between stars, galaxies [NASA-NEWS-REL-86-133] N87-10787

STATIC LOADS

Mode 1 delamination growth in adhesively bonded joints under static and fatigue loads [NASA-CR-179612] N87-10409

STATIC STABILITY

Wind tunnel test of the modified goldschmied model with propulsion and empennage: Analysis of test results [AD-A167360] N87-10045

STATIONKEEPING

Stationkeeping for DFS-Kopernikus N87-10152

Stationkeeping strategy test, design and optimization by computer simulation — geostationary satellites N87-10153

Stationkeeping strategy for TDF 1 satellite N87-10154

Longitudinal orbit control from INTELSAT 5 inclination stationkeeping maneuvers N87-10156

Constraints imposed by an intersatellite communication link upon stationkeeping of two close geostationary satellites N87-10162

Comparison of different autonomous stationkeeping systems for geostationary satellites N87-10163

Geostationary satellites autonomous stationkeeping N87-10164

STATISTICAL ANALYSIS

A statistical model to estimate refractivity turbulence structure constant C sub n sup 2 in the free atmosphere N87-10448

The Tukey algorithm for enhancing MST radar data N87-10521

Gravity wave dynamics near the mesopause over Poker Flat, Alaska N87-10631

STEADY STATE

Wind tunnel test of the modified goldschmied model with propulsion and empennage: Analysis of test results [AD-A167360] N87-10045

An analysis of the performance of a vertically oriented, gas loaded, variable conductance heat pipe [AD-A167874] N87-10250

STEERABLE ANTENNAS

Beam steering system N87-10501

Determination of U, V, and W from single station Doppler radar radial velocities N87-10502

Method to determine the optimal parameters of the Arecibo 46.8-MHz antenna system N87-10510

STELLAR ACTIVITY

Observations of non-thermal radiation from late-type stars N87-10793

STELLAR COMPOSITION

Pulse timing and neutron star structure N87-10799

STELLAR EVOLUTION

Conditions for the formation of massive stars N87-10803

STELLAR FLARES

Intense soft X-rays from RS Ophiuchi during the 1985 outburst [DE86-010175] N87-10820

STELLAR LUMINOSITY

The X-ray properties of high redshift, optically selected QSOs N87-10784

STELLAR MASS ACCRETION

Conditions for the formation of massive stars N87-10803

STELLAR RADIATION

The X-ray properties of high redshift, optically selected QSOs N87-10784

Observations of non-thermal radiation from late-type stars N87-10793

STELLAR SPECTROPHOTOMETRY
Spectroscopy of the globular clusters in M87
[NASA-CR-179854] N87-10790
STELLAR STRUCTURE
Pulse timing and neutron star structure N87-10799
Physical processes in collapse driven supernova
N87-10808
STELLAR WINDS
Intense soft X-rays from RS Ophiuchi during the 1985 outburst
[DE86-010175] N87-10820
STIFFNESS MATRIX
Foundation interaction problems involving an elastic half-plane
[AD-A167925] N87-10411
STOCHASTIC PROCESSES
Analysis on gravitational effect to nonlinear diffusion system of vapor molecules in a heat pipe N87-10023
STORAGE BATTERIES
Review of storage battery system cost estimates
[DE86-011162] N87-10537
STORMS
Convective structure of the planetary boundary layer of the ocean during gale N87-10300
Lidar study of storm tops N87-10348
Gravity waves in severe weather N87-10442
STRAIN MEASUREMENT
Demonstration of laser speckle system on burner liner cyclic rig
[NASA-CR-179509] N87-10377
STRATEGY
Strategic Defense Initiative Program: Status of airborne optical adjunct and terminal imaging radar
[P86-221132] N87-10107
STRATOSPHERE
Improvements in the Goddard balloon-borne lidar
N87-10311
Features of stratospheric aerosol lidar observations at Mauna Loa, 1974 - 1985 N87-10312
El Chichon aerosols in the stratosphere: Analyses of lidar data and calculations of radiation budget
N87-10313
Lidar measurement of stratospheric aerosol at Syowa Station, Antarctica N87-10314
The application of lidar to stratospheric aerosol studies N87-10337
Volcanic eruptions and the increases in the stratospheric aerosol content: Lidar measurements from 1982 to 1986
N87-10338
Observations of stratospheric aerosols associated with the El Chichon eruption N87-10339
Lidar observations of the decline of the El Chichon stratospheric load N87-10340
Airborne lidar observations of Arctic polar stratospheric clouds N87-10341
Lidar stratospheric ozone measurements at the observatoire de Haute Provence (France) N87-10344
The GSFC gound-based lidar for the measurement of stratospheric ozone N87-10371
Performance characteristics of wind profiling radars
N87-10429
Need for a subtropical wind profiling system
N87-10432
Half-day and four-day waves in the statosphere
N87-10435
Evidence of atmospheric gravity wave perturbations of the Brunt-Vaisala frequency in the atmosphere
N87-10438
Simultaneous fine structure observation of wind and temperature profiles by the Arecibo 430-MHz radar and in situ measurements N87-10446
Comparison between S. T. radar and in situ balloon measurements N87-10447
Determination of the Brunt-Vaisala frequency from vertical velocity spectra N87-10449
Climatology of gravity waves over Poker Flat, Alaska for 1983 N87-10454
A study of gravity-wave spectra in the troposphere and stratosphere at 5-min to 5-day periods with the Poker Flat MST radar N87-10462
Observations of vertical velocity power spectra with the SOUSY VHF radar N87-10465
Evidence of a saturated gravity-wave spectrum throughout the atmosphere N87-10467
Comparison of reflectivity and wind profiles measured on 46.8 MHz and 430 MHz at the Arecibo Observatory
N87-10477
Scientific reasons for a network of ST radars and cooperative campaigns N87-10480
Progress in existing and planned MST radars
N87-10481
The proposed flatland radar N87-10482
Current status of the Poker Flat MST radar
N87-10483
Recent progress in the Urbana MST radar
N87-10485
Remote temperature profiling in the troposphere and stratosphere by the radio-acoustic sounding technique
N87-10488
The Penn State Doppler network progress report
N87-10489
The PROUST radar N87-10491
The Provence ST radar N87-10492
The INSU and DMN network of ST radars
N87-10493
Investigations of the lower and middle atmosphere at the Arecibo Observatory and a description of the new VHF radar project N87-10494
System aspects of the Indian MST radar facility
N87-10497
On the use of colour reflectivity plots to monitor the structure of the troposphere and stratosphere
N87-10522
Atmospheric Ozone 1985. Assessment of our understanding of the processes controlling its present distribution and change, volume 1
[NASA-TM-89237] N87-10612
Stratospheric chemistry N87-10613
Tropospheric trace gases N87-10614
Strat-trop exchange N87-10616
STRATUS CLOUDS
Multiple scattering depolarization in marine stratus clouds: Lidar experiments N87-10350
STREAMLINING
Wind tunnel test of the modified goldschmied model with propulsion and empennage: Analysis of test results
[AD-A167380] N87-10045
STRESS ANALYSIS
Foundation interaction problems involving an elastic half-plane
[AD-A167925] N87-10411
Response of a 3-layered ring to an axisymmetric impulse
[DE86-011016] N87-10415
STRESS CONCENTRATION
Concentrations of plastic strains in the clamping region of cylindrical shells under excessive loading
[KFK-3915] N87-10417
STRESS CORROSION
Grain boundary segregation and environmentally-induced fracture of materials
[DE86-010219] N87-10195
STRESS-STRAIN RELATIONSHIPS
Crack-tip fields in a viscoplastic material
[AD-A168014] N87-10413
STRESSES
Further results on the initiation and growth of adiabatic shear bands
[AD-A168012] N87-10412
STRING THEORY
Particle theory and cosmology
[DE86-010366] N87-10802
STRUCTURAL ANALYSIS
Guidebook for analysis of tether applications
[NASA-CR-178904] N87-10169
Main chamber combustion and cooling technology study
[NASA-CR-178853] N87-10175
Controller design via structural reduced modeling by FETM
[NASA-CR-179838] N87-10408
Application of graph theory to the nonlinear analysis of large space structures N87-10418
STRUCTURAL DESIGN
In-flight total forces, moments and static aeroelastic characteristics of an oblique-wing research airplane
[NASA-TP-2224] N87-10103
The new space network: The tracking and data relay satellite system
[NASA-EP-251] N87-10171
Permeation membrane-type distiller
[DE86-011153] N87-10254
Experimental identification and control of the tip position of a flexible, single link manipulator N87-10397
Simple blast model for structural design
[DE86-000802] N87-10414
Vertical junction solar cells
[AD-A167757] N87-10532
Design support of the Burst and Transient Source Experiment (BATSE) of the Gamma Ray Observatory (GRO) mission
[NASA-CR-178920] N87-10758
STRUCTURAL DESIGN CRITERIA
Design and fabrication of the NASA decoupler pylon for the F-16 aircraft
[NASA-CR-172354] N87-10065
Engine-transmission-structural airframe members compatibility N87-10069
Helicopter air intake protection systems N87-10073
Engine-airframe integration for rotorcraft: System specifications and qualification N87-10074
Control of large flexible space structures
[NASA-CR-177063] N87-10168
STRUCTURAL RELIABILITY
Structural optimization for control of stiffened laminated composite plates using nonlinear mixed integer programming N87-10181
STRUCTURAL STABILITY
Structural optimization for control of stiffened laminated composite plates using nonlinear mixed integer programming N87-10181
STRUCTURAL VIBRATION
Effect of static inplane loads and boundary conditions on the flutter of flat rectangular panels
[NAL-TM-ST-8604] N87-10404
SUBSONIC FLOW
The numerical method of calculation of two-dimensional stationary electro-gasdynamic internal flows N87-10037
SUCTION
Wind tunnel test of the modified goldschmied model with propulsion and empennage: Analysis of test results
[AD-A167360] N87-10045
SUDDEN IONOSPHERIC DISTURBANCES
Solar-geophysical data number 501, May 1986. Part 1: (Prompt reports). Data for April 1986, March 1986 and late data
[PB86-218039] N87-10623
SUMMER
Evidence for ion energy dispersion in the polar cusp related to a northward directed Interplanetary Magnetic Field (IMF) N87-10561
SUN
Direct computation of orbital sunrise or sunset event parameters
[NASA-TM-87717] N87-10620
SUPERCONDUCTORS
Sulfur-based synthetic metal superconductors
[DE86-010512] N87-10768
SUPERCRITICAL FLOW
Supersonic, nonlinear, attached-flow wing design for high lift with experimental validation
[NASA-TP-2336] N87-10042
SUPERNOVAE
Physical processes in collapse driven supernova
N87-10808
Molecular clouds in Orion and Monoceros
N87-10809
SUPERSONIC AIRCRAFT
Computational aerodynamics of supersonic lifting vehicles N87-10030
SUPERSONIC AIRFOILS
Supersonic, nonlinear, attached-flow wing design for high lift with experimental validation
[NASA-TP-2336] N87-10042
SUPERSONIC COMBUSTION RAMJET ENGINES
Numerical study of hydrogen-air supersonic combustion by using elliptic and parabolized equations
[NASA-CR-179600] N87-10187
SUPERSONIC FLOW
Acta Aeronautica et Astronautica Sinica (selected articles)
[AD-A167918] N87-10004
An asymptotic theory of supersonic turbulent interactions in a compression corner N87-10010
Supersonic flow around tip sides of wings
N87-10033
Supersonic, nonlinear, attached-flow wing design for high lift with experimental validation
[NASA-TP-2336] N87-10042
Computational hydrodynamics in astrophysical studies: Highly shocked flows in 3 dimensions N87-10796
SUPERSONIC JET FLOW
Numerical simulation of two-dimensional freejet flow-fields N87-10020
SUPPRESSORS
Free jet feasibility study of a thermal acoustic shield concept for AST/VCE application: Dual stream nozzles
[NASA-CR-3867] N87-10752
SURFACE FINISHING
Investigations on the parameters for laser surface treatment by cladding and alloying
[BMFT-FB-T-85-183] N87-10203
SURFACE PROPERTIES
Surface photometry of early-type galaxies
N87-10795
SURFACE REACTIONS
Computer assisted gas chromatography for thermodynamic measurements of polymer surfaces
[AD-A167450] N87-10208
SURGES
Factors contributing to static RAM cell transient upset
[DE86-007710] N87-10715
SURVEYS
Technology review of flight crucial flight control systems (application of optical technology)
[NASA-CR-172332] N87-10102

Summary and evaluation of field performance data on unitary heat pumps
[DE86-011289] N87-10258

SWEDEN
Variation of the urban NO2 concentration during a ground inversion situation N87-10318

SWITCHING CIRCUITS
The elimination of a class of pseudo echoes by an improved T/R switch technique N87-10511

SYMPHONIE SATELLITES
Updates to operational procedures as a result of in-orbit experience with SYMPHONIE spacecraft N87-10159

SYNCHRONOUS SATELLITES
Proceedings of an International Conference on Space Dynamics for Geostationary Satellites
[ISBN-2-85428-149-7] N87-10113
Operational criteria for geostationary satellites in National Space Development Agency (NASDA) N87-10119
Attitude determinations for geostationary satellites of the National Space Development Agency (NASDA) N87-10124
State/orbit estimation from real Doppler data for solid apogee motor burning phase of geostationary satellite N87-10129
Initial orbit determination for geostationary satellites N87-10131
Real time orbit and dynamic search zone computations to aid satellite acquisition in S-band during the launch phase of Geosynchronous Transfer Orbit (GTO) N87-10132
Orbit determination of geostationary satellites using the global positioning system N87-10133
A new three-axis control system for a geosynchronous satellite in transfer orbit N87-10139
Operational strategies for multi-burn apogee maneuvers of geostationary spacecraft N87-10141
Geostationary satellite positioning with a restartable motor N87-10142
Definition of a structure for the apogee thrusts for geostationary satellite positioning: Application to TDF-1 N87-10145
Application of linear programming to final positioning (drift orbit) of a geostationary satellite N87-10149
TV-SAT final orbit acquisition optimization strategy N87-10150
Stationkeeping strategy test, design and optimization by computer simulation — geostationary satellites N87-10153
Eccentricity control strategy for geosynchronous communications satellites N87-10155
Constraints imposed by an intersatellite communication link upon stationkeeping of two close geostationary satellites N87-10162
Comparison of different autonomous stationkeeping systems for geostationary satellites N87-10163
Geostationary satellites autonomous stationkeeping N87-10164
Geostationary satellites: Their market, their evolution in the 1990s N87-10165

SYNCHROTRON RADIATION
Micro-tomography using synchrotron radiation
[DE86-010982] N87-10191
Optical systems for synchrotron radiation. Lecture 4: Soft X-ray imaging systems
[DE86-011567] N87-10761

SYNOPTIC METEOROLOGY
Half-day and four-day waves in the statosphere N87-10435
The proposed flatland radar N87-10482

SYNTHESIS (CHEMISTRY)
Boron-containing organosilane polymers and ceramic materials thereof
[NASA-CASE-ARC-11649-1-SB] N87-10205
Synthesis of energetic materials
[AD-A167787] N87-10214
Laser-initiated chain reactions in the partial oxidation of methane
[DE86-011272] N87-10388

SYNTHETIC METALS
Sulfur-based synthetic metal superconductors
[DE86-010512] N87-10768

SYSTEMS ANALYSIS
A system theoretical based method for module failure diagnostic of turbine engines N87-10085
Dynamic remapping decisions in multi-phase parallel computations
[NASA-CR-178174] N87-10719

SYSTEMS ENGINEERING
Modeling and analysis of spacecraft power systems N87-10173

SYSTEMS INTEGRATION
Engine-Airframe Integration for Rotorcraft
[AGARD-LS-148] N87-10067
Engine-airframe integration for rotorcraft: System specifications and qualification N87-10074

T

TABLES (DATA)
Monthly and seasonal weather outlook for mid-May to mid-June 1986, volume 40, number 10, May 14, 1986
[PB86-199825] N87-10664

TAIL ASSEMBLIES
Wind tunnel test of the modified goldschmied model with propulsion and empennage: Analysis of test results
[AD-A167360] N87-10045

TAIL ROTORS
Flight service evaluation of composite helicopter components
[NASA-CR-178149] N87-10182

TAPE RECORDERS
The Fairchild CVDR: A new combination voice and data recorder — Cockpit Voice and Data Recorder (CVDR) N87-10095

TARGET ACQUISITION
Optimal tracking strategy determination — satellite tracking N87-10120

TAYLOR SERIES
A Taylor-Galerkin finite element algorithm for transient nonlinear thermal-structural analysis
[NASA-CR-177064] N87-10406

TDR SATELLITES
Tracking and Data Relay Satellite (TDRS) tracking and orbit determination N87-10136
The new space network: The tracking and data relay satellite system
[NASA-EP-251] N87-10171
New space astronomy technique developed to study celestial bodies
[NASA-NEWS-REL-86-140] N87-10788

TEA LASERS
CO2 lidar system for atmospheric studies N87-10366

TECHNOLOGICAL FORECASTING
Aircraft Integrated Data Systems (AIDS): Evolution and revolution N87-10077
Geostationary satellites: Their market, their evolution in the 1990s N87-10165
Air Force technical objective document fiscal year 1987
[AD-A167324] N87-10779

TECHNOLOGY ASSESSMENT
Technology review of flight crucial flight control systems (application of optical technology)
[NASA-CR-172332] N87-10102
Energy delivery processes in shock tubes N87-10106
Digital mapping: Fact or fiction
[AD-A167571] N87-10528

TECHNOLOGY UTILIZATION
Influence of engine variables on future helicopter systems N87-10072
Modern Aircraft Integrated Data Systems (AIDS) technology exemplified on the A-320 N87-10078
The impact of flight data on an airline: A case study N87-10088
Experience with the application of photovoltaics devices
[DE86-010472] N87-10535

TELEMETRY
Methods and standards for encryption of spacecraft telemetry and telecommand links
[RPT/ENC/62359/BO] N87-10112

TELESCOPES
The development and test of multi-anode microchannel array detector systems. Part 2: Soft X-ray detectors
[NASA-CR-177066] N87-10236
The influrence of an optical receiving system on statistical characteristics of a lidar signal N87-10307

TELEVISION SYSTEMS
VSB 2-PSK: A modulation system for digital sound with television
[BBC-RD-1986/7] N87-10222

TELEVISION TRANSMISSION
VSB 2-PSK: A modulation system for digital sound with television
[BBC-RD-1986/7] N87-10222

TEMPERATURE DISTRIBUTION
Effect of surplus standing liquid on heat transfer resistance in the heat pipe (with mesh wick in a horizontal mode) N87-10024

TEMPERATURE EFFECTS
The effects of temperature and loading rate on R-curves using the CLWL techniques — crack growth resistance curve (R curve); crack line wedge load (CLWL)
[BAE-MSM-R-GEN-0544] N87-10405
Methods of testing to determine the thermal performance of solar collectors
[DE86-009311] N87-10533
Stratospheric chemistry N87-10613
Human comfort in the urban tropics N87-10649
Modeling the effects of the spatially varying sea surface temperature on the marine atmospheric boundary layer N87-10673
Workshop on the Physics and Chemistry of Solar-Flux Effects on Condensed Phase/Gas Interfaces
[DE86-004460] N87-10817

TEMPERATURE GRADIENTS
A theory for the retrieval of virtual temperature from winds, radiances and the equations of fluid dynamics N87-10421

TEMPERATURE MEASUREMENT
The Lidar In-Space Technology Experiment (LITE) N87-10270
Aerosol studies in mid-latitude coastal environments in Australia N87-10271
Real-time atmospheric absorption spectra for in-flight tuning of an airborne dial system N87-10296
Comparison between S. T. radar and in situ balloon measurements N87-10447
Millimeter-wave spectrometry of ozone in the middle atmosphere N87-10629
Observations of molecular clouds in the direction of galactic and extragalactiv radio sources N87-10794

TEMPERATURE PROFILES
A trial on performance test method for Cu-water heat pipe N87-10026
Nd:Glass-Raman laser for water vapor dial N87-10285
Lower atmospheric temperature profile measurements using a Raman lidar N87-10331
Simultaneous rocket and MST radar observation of an internal gravity wave breaking in the mesosphere N87-10443
Simultaneous fine structure observation of wind and temperature profiles by the Arecibo 430-MHz radar and in situ measurements N87-10446
Remote temperature profiling in the troposphere and stratosphere by the radio-acoustic sounding technique N87-10488
Vertical modes and energetics of gravitational and rotational modes in a multilevel global spectral model N87-10633

TEMPORAL RESOLUTION
Time-resolved lidar fluorosensor for sea pollution detection N87-10317

TENSILE DEFORMATION
Deformation behavior of powder metallurgy Ni Al-Hf-B
[DE86-011508] N87-10201

TENSILE PROPERTIES
Fatigue response of notched laminates subjected to tension-compression cyclic loads
[NASA-CR-179804] N87-10183
Review of embrittlement mechanisms in tungsten heavy alloys
[DE86-011114] N87-10196
Modification of the grain boundary microstructure of the austenitic PCA stainless steel to improve helium embrittlement resistance
[DE86-010396] N87-10202

TERRAIN
The proposed flatland radar N87-10482
Numerical studies of thermally and mechanically forced circulations over complex terrain N87-10630

TERRESTRIAL RADIATION
Nonthermal continuum-terrestrial myriametric radiation narrowband electromagnetic emission N87-10579
Radiative processes N87-10618

TETHERING
Guidebook for analysis of tether applications
[NASA-CR-178904] N87-10169

TETHERLINES
Guidebook for analysis of tether applications
[NASA-CR-178904] N87-10169
Coaxial tube tether/transmission line for manned nuclear space power
[NASA-CASE-LEW-14338-1] N87-10174

THEMATIC MAPPING
In-flight absolute radiometric calibration of the LANDSAT thematic mapper N87-10530

THERMAL ANALYSIS
Titanium oxidation kinetics and the mechanism for thermal ignition of titanium-based pyrotechnics
[DE86-010987] N87-10218
A Taylor-Galerkin finite element algorithm for transient nonlinear thermal-structural analysis
[NASA-CR-177064] N87-10406

THERMAL CONDUCTIVITY
Effect of surplus standing liquid on heat transfer resistance in the heat pipe (with mesh wick in a horizontal mode) N87-10024
Hydrodynamic and thermal interaction between two spheres in a steady viscous flow N87-10035
Mathematical model for the Bridgman-Stockbarger crystal growing system
[NASA-CR-178921] N87-10766

THERMAL CYCLING TESTS
Effects of thermal cycling on graphie-fiber-reinforced 6061 aluminum
[NASA-TP-2612] N87-10184
Vertical junction solar cells
[AD-A167757] N87-10532
THERMAL DIFFUSION
Numerical model of the thermal processes leading to ignition in a pyrotechnic device
[DE86-009626] N87-10189
THERMAL ENERGY
Issues in expert system aids for a large engineering simulation code
[DE86-009098] N87-10735
THERMAL INSULATION
Transient heat transfer analysis and radiative properties measurements of porous thermal insulation
[DE86-011296] N87-10259
THERMAL RADIATION
Technical overview of plume radiation from a solid rocket motor N87-10021
THERMAL RESISTANCE
Effect of surplus standing liquid on heat transfer resistance in the heat pipe (with mesh wick in a horizontal mode) N87-10024
THERMIONIC DIODES
Thermionic integrated circuits
[DE86-005849] N87-10239
THERMIONICS
Thermionic integrated circuits
[DE86-005849] N87-10239
THERMODYNAMIC CYCLES
ANL/RBC: A computer code for the analysis of Rankine bottoming cycles, including system cost evaluation and off-design performance
[NASA-CR-179462] N87-10777
THERMODYNAMIC EFFICIENCY
Photosynthetic water splitting
[DE86-010269] N87-10215
THERMODYNAMIC PROPERTIES
Re-examination of the neptunium-hydrogen system
[DE86-010197] N87-10216
Vertical junction solar cells
[AD-A167757] N87-10532
Physical processes in collapse driven supernova
N87-10808
THERMODYNAMICS
An observational study of tropical cloud cluster evolution and cyclogenesis in the Western North Pacific
[CSU-ASP-403] N87-10661
THERMOSIPHONS
Dynamic heat transfer mechanism of two-phase closed thermosyphon N87-10025
THERMOSPHERE
Gravity waves in the middle atmosphere: Recent progress and needed studies N87-10433
Climatology of gravity waves over Poker Flat, Alaska for 1983 N87-10454
THIN FILMS
The TFP and a pulsed LD: New lidar components
N87-10374
THIOLS
Polymer systems for rapid sealing of aircraft structures at low temperature
[AD-A167667] N87-10209
THIOPLASTICS
Polymer systems for rapid sealing of aircraft structures at low temperature
[AD-A167667] N87-10209
THREAT EVALUATION
The planning and maintenance of urban settlements to resist extreme climatic forces N87-10647
THREE AXIS STABILIZATION
Orbit geometry for calibration and launch operations of a three-axis controlled satellite with inertial reference
N87-10116
Synchronous transfer orbit operation under three-axis control N87-10137
A new three-axis control system for a geosynchronous satellite in transfer orbit N87-10139
THREE DIMENSIONAL BODIES
Acta Aeronautica et Astronautica Sinica (selected articles)
[AD-A167918] N87-10004
Separation and wakes over 3-dimensional bodies
N87-10006
Viscous wing theory development. Volume 2: GRUMWING computer program user's manual
[NASA-CR-178157] N87-10044
THREE DIMENSIONAL BOUNDARY LAYER
Numerical solution of the 3-dimensional boundary layer equations in the inverse mode using finite differences
N87-10005
THREE DIMENSIONAL FLOW
Study of three-dimensional separation on a spheroid at incidence N87-10016
Images of three dimensional flows in computer graphics N87-10017
Application of a potential code to general steady flows in three dimensions N87-10262
THRUST VECTOR CONTROL
Olympus: Apogee engine firing N87-10143
Definition of a structure for the apogee thrusts for geostationary satellite positioning: Application to TDF-1
N87-10145
Targeting multiburn, long duration apogee burst maneuvers N87-10146
Efficiency eccentricity control using continuous, vectored thrusting for satellites with large area/mass ratios N87-10151
THUNDERSTORMS
Aircraft accident reeport, Delta Air Lines, Inc., Lockheed L-1011-385-1, N726DA, Dallas/Fort Worth International Airport, Texas, August 2, 1985
[PB86-910406] N87-10053
Wind profiler data in a mesoscale experiment from a meteorological perspective N87-10423
Observations of thunder with the Arecibo VHF radar
N87-10444
A comparison of thunderstorm reflectivities measured at the VHF and UHF N87-10472
UHF and VHF radar observations of thunderstorms
N87-10473
Further studies with data collected by NASA's airborne Doppler lidar in Oklahoma in 1981
[NASA-CR-179779] N87-10660
TIDES
The internal tide off southern California
[AD-A167722] N87-10672
On the tidal interaction between spherical galaxies
N87-10810
TIME DEPENDENCE
Mathematical and computational models of plasma flows N87-10036
New solution of the problem of EMP coupling on cables over ground of finite conductivity
[DE86-006078] N87-10229
TIME LAG
Atmospheric contributions to the column variance in direct-detection dial N87-10289
Fault and error latency under real workload: An experimental study
[NASA-CR-179602] N87-10733
TIME MEASUREMENT
Atmospheric correlation time measurements using coherent CO2 lidar N87-10363
Pulse timing and neutron star structure N87-10799
TIME SERIES ANALYSIS
Climatology of tropospheric vertical velocity spectra
N87-10455
TIN ALLOYS
Relationship between critical current and microstructure of internal tin wire
[DE86-009922] N87-10238
TIRES
Geometric and material nonlinear dynamic analysis of complex shells N87-10401
TITANIUM
Titanium oxidation kinetics and the mechanism for thermal ignition of titanium-based pyrotechnics
[DE86-010867] N87-10218
TITANIUM ALLOYS
Compositional and microstructural effects on hydrogen embrittlement of ASTM grade 12 titanium (Ti 0.3 Mo - 0.8 Ni)
[DE86-011379] N87-10197
TOMOGRAPHY
Micro-tomography using synchrotron radiation
[DE86-010982] N87-10191
TOPEX
Science opportunities from the Topex/Poseidon mission
[NASA-CR-179752] N87-10671
TOUGHNESS
Review of embrittlement mechanisms in tungsten heavy alloys
[DE86-011114] N87-10196
TRACE CONTAMINANTS
CO2 lidar system for atmospheric studies N87-10366
TRACKING STATIONS
Accuracy of goestationary orbit determination
N87-10121
TRAILING EDGES
Viscous wing theory development. Volume 1: Analysis, method and results
[NASA-CR-178156] N87-10043
TRAINING ANALYSIS
Vestibular tests in cosmonaut selection and training
N87-10694
TRAJECTORIES
Trajectory scoring in geodetic coordinates using transponder-interrogator range data
[DE86-009554] N87-10109
TRAJECTORY ANALYSIS
Shuttle derived atmospheric density model. Part 2: STS atmospheric implications for AOTV trajectory analysis, a proposed GRAM perturbation density model
[NASA-CR-171824] N87-10663
TRANSFER ORBITS
Transfer orbit optimization for dual launches
N87-10114
Optimal transfer to inclined geosynchronous orbits
N87-10117
Orbit achievement of RCA communication satellites
N87-10122
Real time orbit and dynamic search zone computations to aid satellite acquisition in S-band during the launch phase of Geosynchronous Transfer Orbit (GTO)
N87-10132
Synchronous transfer orbit operation under three-axis control N87-10137
A new three-axis control system for a geosynchronous satellite in transfer orbit N87-10139
Optimal injection of TV SAT with multi-impulse apogee maneuvers with mission constraints and thrust uncertainties N87-10144
Orbit and attitude operations during the Telecom 1B transfer phase N87-10147
Operational implementation of deorbiting maneuvers — GEOS-2 N87-10148
TRANSIENT HEATING
A Taylor-Galerkin finite element algorithm for transient nonlinear thermal-structural analysis
[NASA-CR-177064] N87-10406
TRANSITION FLOW
Numerical study of the entrance flow and its transition of a circular pipe N87-10019
TRANSMISSIONS (MACHINE ELEMENTS)
Analysis of the vibration of the input bevel pinion in RAN Wessex helicopter main rotor gearbox WAK143 prior to failure
[ARL-AERO-PROP-R-169] N87-10061
Testing of UH-60A helicopter transmission in NASA Lewis 2240-kW (3000-hp) facility
[NASA-TP-2626] N87-10391
TRANSONIC FLOW
The numerical method of calculation of two-dimensional stationary electro-gasdynamic internal flows N87-10037
Viscous wing theory development. Volume 1: Analysis, method and results
[NASA-CR-178156] N87-10043
Viscous wing theory development. Volume 2: GRUMWING computer program user's manual
[NASA-CR-178157] N87-10044
TRANSPORT AIRCRAFT
Crashworthiness experiment summary full-scale transport controlled impact demonstration program
[DOT/FAA/CT-85/20] N87-10055
TRANSPORT THEORY
Can stochastic, dissipative wave fields be treated as random walk generators N87-10452
Dynamical processes N87-10617
TROPICAL METEOROLOGY
Need for a subtropical wind profiling system
N87-10432
TROPICAL REGIONS
Continuous wind measurement in the tropical Pacific using VHF radars N87-10484
Observational studies of wave disturbances in the tropical Pacific and their relationship with deep cloud activity N87-10634
Proceedings of the Technical Conference on Urban Climatology and its Applications with Special Regard to Tropical Areas
[WMO-652] N87-10636
Urban climatology and the tropical city: An introduction N87-10637
Tropical urban climates: Review and assessment
N87-10638
Air quality in tropical cities N87-10639
The urban climate of Mexico City N87-10640
Some aspects of the urban climates of tropical Africa
N87-10642
Some aspects of the urban climates of tropical South America: The Brazilian contribution N87-10644
Urban climatological methods and data N87-10645
Life expectancy in tropical climates and urbanization
N87-10648
Human comfort in the urban tropics N87-10649
Urban hydrology in the tropics: Problems, solutions, data collection and analysis N87-10650
Problems of design for cities in the tropics
N87-10653
Design for climate in hot, humid cities N87-10656

TROPOSPHERE
On the measurement of atmospheric density using dial in the O2 A-band (770 nm) N87-10291
Observation of atmospheric ozone by dial with Raman lasers pumped by a KrF laser N87-10297
A combined Raman lidar for low tropospheric studies N87-10332
The real-time use of wind profilers in nowcasting N87-10427
A look at profiler performance N87-10430
Half-day and four-day waves in the statosphere N87-10435
Tropospheric turbulence parameters measured by using the MU radar N87-10436
Evidence of atmospheric gravity wave perturbations of the Brunt-Vaisala frequency in the atmosphere N87-10438
Simultaneous fine structure observation of wind and temperature profiles by the Arecibo 430-MHz radar and in situ measurements N87-10446
Comparison between S. T. radar and in situ balloon measurements N87-10447
Determination of the Brunt-Vaisala frequency from vertical velocity spectra N87-10449
Climatology of gravity waves over Poker Flat, Alaska for 1983 N87-10454
Climatology of tropospheric vertical velocity spectra N87-10455
The frequency spectrum of C sub n sup 2 from MST radar data N87-10461
A study of gravity-wave spectra in the troposphere and stratosphere at 5-min to 5-day periods with the Poker Flat MST radar N87-10462
Observations of vertical velocity power spectra with the SOUSY VHF radar N87-10465
Comparison of reflectivity and wind profiles measured on 46.8 MHz and 430 MHz at the Arecibo Observatory N87-10477
Scientific reasons for a network of ST radars and cooperative campaigns N87-10480
Progress in existing and planned MST radars N87-10481
The proposed flatland radar N87-10482
Current status of the Poker Flat MST radar N87-10483
Recent progress in the Urbana MST radar N87-10485
Remote temperature profiling in the troposphere and stratosphere by the radio-acoustic sounding technique N87-10488
The Penn State Doppler network progress report N87-10489
The PROUST radar N87-10491
The Provence ST radar N87-10492
The INSU and DMN network of ST radars N87-10493
Investigations of the lower and middle atmosphere at the Arecibo Observatory and a description of the new VHF radar project N87-10494
System aspects of the Indian MST radar facility N87-10497
On the use of colour reflectivity plots to monitor the structure of the troposphere and stratosphere N87-10522
Atmospheric Ozone 1985. Assessment of our understanding of the processes controlling its present distribution and change, volume 1
[NASA-TM-89237] N87-10612
Tropospheric chemistry N87-10615
Strat-trop exchange N87-10616
Environmental influences on hurricane intensification N87-10635

TROPOSPHERIC SCATTERING
Lidar mapping of a mixture of aerosol concentrations in a varying atmosphere N87-10320

TUNABLE LASERS
Time-domain sensitivity enhancement in pulsed Pb-TDL gas monitors N87-10324

TUNGSTEN ALLOYS
Review of embrittlement mechanisms in tungsten heavy alloys
[DE86-011114] N87-10196

TURBIDITY
Scattered radiation field of a laser beam propagating through turbid media
[DE86-010188] N87-10386

TURBINE BLADES
WEST-3 wind turbine simulator development. Volume 2: Verification
[NASA-CR-174982] N87-10531

TURBOFAN ENGINES
Acta Aeronautica et Astronautica Sinica (selected articles)
[AD-A167918] N87-10004

TURBOMACHINE BLADES
Development of a turbomachinery design optimization procedure using a multiple-parameter nonlinear perturbation method
[NASA-CR-3831] N87-10003

TURBOMACHINERY
Computational fluid mechanics utilizing the variational principle of modeling damping seals
[NASA-CR-178902] N87-10248

TURBULENCE
The frequency spectrum of C sub n sup 2 from MST radar data N87-10461
The onset of alfvenic turbulence N87-10762

TURBULENCE EFFECTS
The effect of turbulence on lidar backscattered signal fluctuations N87-10328

TURBULENT BOUNDARY LAYER
Viscous wing theory development. Volume 1: Analysis, method and results
[NASA-CR-178156] N87-10043

TURBULENT DIFFUSION
The use of the experimentally deduced Brunt-Vaisala frequency and turbulent velocity fluctuations to estimate the eddy diffusion coefficient N87-10450
Can stochastic, dissipative wave fields be treated as random walk generators N87-10452

TURBULENT FLOW
Numerical solution of the 3-dimensional boundary layer equations in the inverse mode using finite differences N87-10005
An asymptotic theory of supersonic turbulent interactions in a compression corner N87-10010
A description of a turbulent flow past a circular cylinder by a discrete vortex method N87-10014
Report of the International Symposium on Computational Fluid Dynamics, Tokyo N87-10029
An improved PSI-cell method for turbulent multi-phase flows N87-10034
Unsteady flow over an airfoil inside a wind tunnel with and without transpiration N87-10051
Nonreacting turbulent mixing flows: A literature survey and data base
[DE86-010664] N87-10253

TURBULENT JETS
Numerical studies of a tubulent jet in crossflow N87-10243

TURBULENT MIXING
Nonreacting turbulent mixing flows: A literature survey and data base
[DE86-010664] N87-10253
Turbulent mixing, droplet spectral evolution and dynamics of warm cumulus clouds N87-10667

TURBULENT WAKES
A description of a turbulent flow past a circular cylinder by a discrete vortex method N87-10014
Free surface turbulence
[AD-A168013] N87-10251

TWO DIMENSIONAL BODIES
Numerical and experimental study of dynamics of two-dimensional body
[ISAS-619] N87-10748

TWO DIMENSIONAL FLOW
Numerical simulation of two-dimensional freejet flow-fields N87-10020

TWO PHASE FLOW
Dynamic heat transfer mechanism of two-phase closed thermosyphon N87-10025

U

ULTRAHIGH FREQUENCIES
A comparison of thunderstorm reflectivities measured at the VHF and UHF N87-10472
UHF and VHF radar observations of thunderstorms N87-10473

ULTRASHORT PULSED LASERS
Subpicosecond high-brightness UV laser system
[DE86-011271] N87-10367

ULTRASONIC FLAW DETECTION
Ultrasonic determination of recrystallization
[NASA-TM-88855] N87-10399

ULTRASONIC RADIATION
Ultrasonic determination of recrystallization
[NASA-TM-88855] N87-10399

ULTRAVIOLET LASERS
Subpicosecond high-brightness UV laser system
[DE86-011271] N87-10367

ULTRAVIOLET RADIATION
Long-pulse excimer lasers for materials processing and medical applications
[DE86-011267] N87-10384

ULTRAVIOLET SPECTRA
The ultraviolet spectra of DA white dwarfs N87-10783
Gas and dust in regions of recent star formation N87-10800

ULTRAVIOLET TELESCOPES
Extreme ultraviolet explorer: Mirror optical tests and results
[DE86-010560] N87-10780

UNDERGROUND EXPLOSIONS
Some seismic results of an underground explosion at the Mururoa Test Site (Shot Report no. 6)
[AWRE-O-17/85] N87-10619

UNDERGROUND TRANSMISSION LINES
Operating characteristics of cooling underground power cables using up sloped long heat pipes in conduit N87-10028

UNIFIED FIELD THEORY
Particle theory and cosmology
[DE86-010366] N87-10802

UNIFORM FLOW
Numerical and experimental study of dynamics of two-dimensional body
[ISAS-619] N87-10748

UNITED KINGDOM
Progress made during 1985 in the scientific and technical program of National Physical Laboratory's Division of Radiation Science and Acoustics N87-10778

UNITED STATES
Microelectronics research and development background paper
[PB86-205200] N87-10242
Aeronautics and space report of the President
[NASA-TM-89239] N87-10827

UNSTEADY FLOW
Analysis of two-dimensional incompressible flow past airfoils using unsteady Navier-Stokes equations
[NASA-CR-179823] N87-10040
Unsteady flow over an airfoil inside a wind tunnel with and without transpiration N87-10051
Application of a potential code to general steady flows in three dimensions N87-10262
Seminar on Finite Elements in Unsteady Problems
[ETN-86-97824] N87-10736
Unsteady calculations of ground water problems — finite element method N87-10739

UNSTEADY STATE
Seminar on Finite Elements in Unsteady Problems
[ETN-86-97824] N87-10736

UPPER IONOSPHERE
Detection from AUREOL-3 of the modulation of auroral electrojet by HF-heating from ELF signals in the upper ionosphere above Tromsoe (Norway) N87-10582
Very low frequency and ELF effects in the upper ionosphere caused by large-scale acoustic waves in the lower ionosphere observed from AUREOL-3 satellite N87-10587
Growing electrostatic waves with a wavelength of 67 cm in the upper ionosphere N87-10604

URANUS (PLANET)
Plasma wave observations at Uranus from Voyager 2
[NASA-CR-177069] N87-10814
Clouds and methane photochemical hazes on the outer planets N87-10815

URBAN DEVELOPMENT
Department of Housing and Urban Development-Independent Agencies Appropriation Bill, 1987
[S-REPT-99-487] N87-10773

URBAN PLANNING
Proceedings of the Technical Conference on Urban Climatology and its Applications with Special Regard to Tropical Areas
[WMO-652] N87-10636
Urban climatology and the tropical city: An introduction N87-10637
Some aspects of the urban climates of tropical South America: The Brazilian contribution N87-10644
Urban climate models: Nature, limitations and applications N87-10646
Human comfort in the urban tropics N87-10649
Urban hydrology in the tropics: Problems, solutions, data collection and analysis N87-10650
Energy related issues — urban climatology N87-10651
The introduction of climatology into the administration and development of planning in the city of Stuttgart N87-10652
Problems of design for cities in the tropics N87-10653
Climatic factors in the siting of new towns and specialized urban facilities N87-10654
Design for climate in hot, dry cities N87-10655

URBAN RESEARCH
Tropical urban climates: Review and assessment N87-10638

UREAS
Levels of plasma atrial natriuretic factor (alpha h ANF) during acute simulated weightlessness N87-10699

USER MANUALS (COMPUTER PROGRAMS)
Viscous wing theory development. Volume 2: GRUMWING computer program user's manual
[NASA-CR-178157] N87-10044
FTMP (Fault Tolerant Multiprocessor) programmer's manual
[NASA-TM-89015] N87-10731
ANL/RBC: A computer code for the analysis of Rankine bottoming cycles, including system cost evaluation and off-design performance
[NASA-CR-179482] N87-10777
USER REQUIREMENTS
Engine-airframe integration for rotorcraft: Component specifications and qualification N87-10071
Helicopter air intake protection systems N87-10073
Engine-airframe integration for rotorcraft: System specifications and qualification N87-10074
A-310 Aircraft Integrated Data SystemS (AIDS) design philosophy N87-10076
The new space network: The tracking and data relay satellite system
[NASA-EP-251] N87-10171
Digital mapping: Fact or fiction
[AD-A167571] N87-10528

V

VAPOR PHASES
Analysis on gravitational effect to nonlinear diffusion system of vapor molecules in a heat pipe N87-10023
Workshop on the Physics and Chemistry of Solar-Flux Effects on Condensed Phase/Gas Interfaces
[DE86-004460] N87-10817
VARIABLE MASS SYSTEMS
An analysis of the performance of a vertically oriented, gas loaded, variable conductance heat pipe
[AD-A167874] N87-10250
VECTOR ANALYSIS
Propagating tides in the mesosphere N87-10441
VELOCITY
Doppler effects on velocity spectra observed by MST radars N87-10464
VELOCITY DISTRIBUTION
Numerical study of the entrance flow and its transition of a circular pipe N87-10019
VELOCITY MEASUREMENT
Attempts to characterize microballoon sensors for shock velocity and material motion studies
[DE86-011210] N87-10379
Comparison between S. T. radar and in situ balloon measurements N87-10447
Self-consistent analysis of high drift velocity measurements with the Scandinavian Twin Auroral Radar Experiment (STARE) system N87-10606
VERTICAL AIR CURRENTS
Wind profiler data in a mesoscale experiment from a meteorological perspective N87-10423
Observations of mesoscale vertical velocities around frontal zones N87-10424
Comparison of vertical velocities analyzed by a numerical model and measured by a VHF wind profiler
N87-10425
The real-time use of wind profilers in nowcasting
N87-10427
Performance characteristics of wind profiling radars
N87-10429
Hardware requirements: A new generation partial reflection radar for studies of the equatorial mesosphere
N87-10431
The PROUST radar: First results N87-10445
A comparison of vertical velocities measured from specular and nonspecular echoes by a VHF radar
N87-10470
Turbulent mixing, droplet spectral evolution and dynamics of warm cumulus clouds N87-10667
VERTICAL DISTRIBUTION
Vertical structure of Arctic haze observed by lidar
N87-10335
VERTICAL JUNCTION SOLAR CELLS
Vertical junction solar cells
[AD-A167757] N87-10532
VERTICAL MOTION
Vertical transport of O(+) ions at high latitudes
N87-10565
VERTICAL ORIENTATION
An analysis of the performance of a vertically oriented, gas loaded, variable conductance heat pipe
[AD-A167874] N87-10250
VERTIGO
Preliminary results on the equilibrium and vertigo experiment performed during STS 51-G shuttle flight
N87-10692
VERY HIGH FREQUENCIES
Observations of vertical velocity power spectra with the SOUSY VHF radar N87-10465
A comparison of thunderstorm reflectivities measured at the VHF and UHF N87-10472
UHF and VHF radar observations of thunderstorms
N87-10473
The proposed flatland radar N87-10482
Continuous wind measurement in the tropical Pacific using VHF radars N87-10484
The first operation and results of the Chung-Li VHF radar N87-10495
VERY LONG BASE INTERFEROMETRY
New space astronomy technique developed to study celestial bodies
[NASA-NEWS-REL-86-140] N87-10788
VERY LOW FREQUENCIES
Small scale structures of electric field variations and particle precipitations as observed onboard AUREOL-3 satellite N87-10569
Very low frequency saucers with attenuation bands
N87-10575
Mechanism of low-frequency wave propagation in the magnetosphere N87-10580
Study of the middle latitude broadening of the spectrum of the waves emitted from ground N87-10583
On the spectral broadening of the ground-based VLF transmitter signals in the high-latitude ionosphere observed from Intercosmos-19 and AUREOL-3 satellites
N87-10584
Precipitation of electrons and protons in the subauroral zone stimulated by ground-based VLF emitter
N87-10585
De-1/Siple VLF wave-injection experiments
N87-10586
Very low frequency and ELF effects in the upper ionosphere caused by large-scale acoustic waves in the lower ionosphere observed from AUREOL-3 satellite
N87-10587
Study of VLF emissions apparently associated with earthquakes from ground-based and GEOS satellites data N87-10589
VESTIBULAR TESTS
Vestibular tests in cosmonaut selection and training
N87-10694
VIBRATION
Nonlinear rotordynamics analysis
[NASA-CR-178931] N87-10407
VIBRATION DAMPING
Maneuver and control of flexible spacecraft
N87-10166
Identification and control of structures in space
[NASA-CR-179811] N87-10172
Computational fluid mechanics utilizing the variational principle of modeling damping seals
[NASA-CR-178902] N87-10248
Experimental identification and control of the tip position of a flexible, single link manipulator N87-10397
VIBRATION MEASUREMENT
Analysis of the vibration of the input bevel pinion in RAN Wessex helicopter main rotor gearbox WAK143 prior to failure
[ARL-AERO-PROP-R-169] N87-10061
Testing of UH-60A helicopter transmission in NASA Lewis 2240-kW (3000-hp) facility
[NASA-TP-2626] N87-10391
VIBRATIONAL SPECTRA
Detection of NO sub x,C2H4 concentrations by using CO and CO2 lasers N87-10357
VISCOPLASTICITY
Crack-tip fields in a viscoplastic material
[AD-A168014] N87-10413
VISCOUS FLOW
Theoretical study of strong interaction of vortex filaments N87-10012
The third order compact schemes for fluid dynamic problems N87-10032
Hydrodynamic and thermal interaction between two spheres in a steady viscous flow N87-10035
Viscous wing theory development. Volume 1: Analysis, method and results
[NASA-CR-178156] N87-10043
Viscous wing theory development. Volume 2: GRUMWING computer program user's manual
[NASA-CR-178157] N87-10044
Unsteady flow over an airfoil inside a wind tunnel with and without transpiration N87-10051
VISIBILITY
Visibility related to backscatter at 1.54 micron
N87-10272
Extinction and visibility measurements in the lower atmosphere with UV-YAG-lidar N87-10276
Visibility and aerosol measurement by diode-laser random-modulation CW lidar N87-10279
VISION
A system for controlled presentation of the Arden contrast sensitivity test
[AD-A167969] N87-10712
VISUAL ACUITY
A system for controlled presentation of the Arden contrast sensitivity test
[AD-A167969] N87-10712
VISUAL PERCEPTION
A system for controlled presentation of the Arden contrast sensitivity test
[AD-A167969] N87-10712
VOICE
The Fairchild CVDR: A new combination voice and data recorder — Cockpit Voice and Data Recorder (CVDR)
N87-10095
VOICE COMMUNICATION
RLE progress report
[MIT-PR-128] N87-10778
VOLCANOES
El Chichon aerosols in the stratosphere: Analyses of lidar data and calculations of radiation budget
N87-10313
The application of lidar to stratospheric aerosol studies N87-10337
Volcanic eruptions and the increases in the stratospheric aerosol content: Lidar measurements from 1982 to 1986
N87-10338
Observations of stratospheric aerosols associated with the El Chichon eruption N87-10339
Lidar observations of the decline of the El Chichon stratospheric load N87-10340
VORTEX FILAMENTS
Theoretical study of strong interaction of vortex filaments N87-10012
Studies on vortex motion based on the dividing vorton model N87-10013
VORTEX RINGS
Studies on vortex motion based on the dividing vorton model N87-10013
Acoustic waves emitted by vortex-body interaction
N87-10015
VORTEX SHEDDING
Vortex shedding of a square cylinder in front of a slender airfoil at high Reynolds numbers. Part 1: Spacing effect
[MPIS-23/1985] N87-10048
VORTICES
Analysis of the vortical flow around a 60 deg Delta wing with vortex flap N87-10006
Proceedings of the Symposium on Mechanics for Space Flight, 1985
[ISAS-SP-4] N87-10011
Viscous wing theory development. Volume 1: Analysis, method and results
[NASA-CR-178156] N87-10043
An experimental investigation of end-wall flowfield of a compressor rotor N87-10244
Free surface turbulence
[AD-A168013] N87-10251
Experimental and theoretical Doppler-lidar signatures of aircraft wake vortices N87-10330
VORTICITY EQUATIONS
Theoretical study of strong interaction of vortex filaments N87-10012
A description of a turbulent flow past a circular cylinder by a discrete vortex method N87-10014
Numerical study of the entrance flow and its transition of a circular pipe N87-10019
VULNERABILITY
Vulnerability methodology and protective measures for aircraft fire and explosion hazards. Volume 3: On-Board Inert Gas Generator System (OBIGGS) studies. Part 1: OBIGGS ground performance tests
[AD-A167357] N87-10066

W

WAFERS
Cross-contact chain
[NASA-CASE-NPO-16784-1] N87-10231
WAKES
Separation and wakes over 3-dimensional bodies
N87-10008
WALLS
An experimental investigation of end-wall flowfield of a compressor rotor N87-10244
WARNING SYSTEMS
NASA and FAA launch wind shear research project
[NASA-NEWS-REL-86-143] N87-10659
WASTE TREATMENT
Bioconversion: A New Technology for Waste and Sludge Disposal. Workshop proceedings
[DE86-009668] N87-10539
WATER POLLUTION
Time-resolved lidar fluorosensor for sea pollution detection N87-10317
WATER VAPOR
Nd:Glass-Raman laser for water vapor dial
N87-10285

Intercomparisons of high-resolution solar blind Raman lidar atmospheric profiles of water vapor with radiosondes and kytoon N87-10333
Backscatter and extinction measurements in cloud and drizzle at CO2 laser wavelengths N87-10352
Linewidth characteristics of Raman-shifted dye laser output at 720 and 940 nm N87-10370

WAVE ATTENUATION
Ultrasonic determination of recrystallization [NASA-TM-88855] N87-10399

WAVE FRONTS
The direction finding aboard AUREOL-3 of ELF waves at frequency above and below the proton gyrofrequency N87-10572

WAVE GENERATION
Scenarios for the generation of auroral kilometric radiation N87-10577
Study of VLF emissions apparently associated with earthquakes from ground-based and GEOS satellites data N87-10589

WAVE INTERACTION
Simultaneous fine structure observation of wind and temperature profiles by the Arecibo 430-MHz radar and in situ measurements N87-10446
Active experiments from ground — magnetosphere; ionosphere N87-10581
Study of the middle latitude broadening of the spectrum of the waves emitted from ground N87-10583
Precipitation of electrons and protons in the subauroral zone stimulated by ground-based VLF emitter N87-10585
De-1/Siple VLF wave-injection experiments N87-10586

WAVE PROPAGATION
The influrence of an optical receiving system on statistical characteristics of a lidar signal N87-10307
Multiple scattering measurements in laboratory and foggy atmosphere N87-10315
Middle Atmosphere Program. Handbook for MAP, volume 20 [NASA-CR-176882] N87-10419
Half-day and four-day waves in the statosphere N87-10435
Atmospheric waves and the nature of buoyancy turbulence in the context of the waves VS 2D-turbulence debate N87-10439
A proposed experimental test to distinguish waves from 2-D turbulence N87-10440
Propagating tides in the mesosphere N87-10441
Gravity waves in severe weather N87-10442
Simultaneous rocket and MST radar observation of an internal gravity wave breaking in the mesosphere N87-10443
Observations and a model of gravity-wave variability in the middle atmosphere N87-10453
Mesospheric gravity-wave climatology at Adelaide N87-10456
MST radar networks and campaigns session summary and recommendations N87-10478
Attenuation bands and cut-off frequencies for ELF electromagnetic waves — high latitudes N87-10570
Growing electrostatic waves with a wavelength of 67 cm in the upper ionosphere N87-10604
Observational studies of wave disturbances in the tropical Pacific and their relationship with deep cloud activity N87-10634
Advective influences on steady and transient forced tropical motions N87-10670

WAVELENGTHS
Wavelength dependence of aerosol backscatter coefficients obtained by multiple wavelength Lidar measurements N87-10275

WEAR RESISTANCE
Carbide/fluoride/silver self-lubricating composite [NASA-CASE-LEW-14196-1] N87-10179

WEATHER
Gravity waves in severe weather N87-10442

WEATHER FORECASTING
Lidar study of storm tops N87-10348
Comparison of vertical velocities analyzed by a numerical model and measured by a VHF wind profiler N87-10425
Scientific reasons for a network of ST radars and cooperative campaigns N87-10480
Wind profiler demonstration system N87-10487
The INSU and DMN network of ST radars N87-10493
Space Environment Laboratory, FY 1985 [PB86-216567] N87-10621
Environmental influences on hurricane intensification N87-10635
Monthly and seasonal weather outlook for mid-May to mid-June 1986, volume 40, number 10, May 14, 1986 [PB86-199825] N87-10664

WEATHER STATIONS
Need for a subtropical wind profiling system N87-10432

WEDGES
The effects of temperature and loading rate on R-curves using the CLWL techniques — crack growth resistance curve (R curve); crack line wedge load (CLWL) [BAE-MSM-R-GEN-0544] N87-10405

WEIGHT REDUCTION
Engine-transmission-structural airframe members compatibility N87-10069
Influence of engine variables on future helicopter systems N87-10072

WEIGHTLESSNESS
Proceedings of 2nd International Conference on Space Physiology [ESA-SP-237] N87-10675
Bones and weightlessness N87-10681
The muscular system in weightlessness N87-10682
Weightlessness effects on the bone tissue of rats after a 5 day space flight (Cosmos 1514) N87-10684
Functions of skeletal muscles of rats and monkeys after 5-day space flight (on Cosmos 1514) N87-10686
Weightlessness effects on the phosphorus-calcium balance and its hormonal regulation in man during STS flight 51-G N87-10691
Contribution of animal models to the investigation of bone changes in weightlessness N87-10706
The state of bones of pregnant rats during an acute stage of adaptation to weightlessness N87-10708
Math modelling as a complement to the scientific inquiry of physiological adaptation to space flight: Fluid, endocrine and circulatory regulation N87-10709

WEIGHTLESSNESS SIMULATION
Hindlimb suspension effects on rat skeletal muscle response N87-10687
Bone examination by noninvasive techniques in a 120-day head-down tilt test N87-10688
Histomorphometric study of bone cell mass and activity in man caused by a 120 day decubitus. Test of preventive protocols N87-10689
Amputation-induced osteoporosis: A new model to explore the effects of weightlessness on the human skeleton N87-10690
Ground based simulation techniques for cardiovascular and hormonal changes observed in man in weightlessness N87-10696
The use of decompression to simulate the effect of extravehicular activity on human lymphocyte transformation N87-10697
Metabolic changes during prolonged antiorthostatic hypokinesia — weightlessness simulation N87-10698
Levels of plasma atrial natriuretic factor (alpha h ANF) during acute simulated weightlessness N87-10699
Volume regulating hormones during a 5 hour head-down tilt at -10 deg. Part 1: Epinephrine, norepinephrine and dopamine N87-10700
Relationship between cardiovascular functions and fluid-electrolyte metabolism during antiorthostatic hypokinesia — weightlessness simulation N87-10701
Volume regulating hormones during a 5-hour head-down tilt at -10 deg. Part 2: Plasma renin activity and aldosterone N87-10703

WELDABILITY
Weldability of an NiAl alloy [DE86-011510] N87-10199

WELDED JOINTS
Design rule for fatigue of welded joints in elevated-temperature nuclear components [DE86-007569] N87-10393

WELDING
Transformations and new PHACOMP analysis in weld metal of Hastelloy C-type alloys [DE86-011422] N87-10198

WEST GERMANY
The introduction of climatology into the administration and development of planning in the city of Stuttgart N87-10652

WHITE DWARF STARS
The ultraviolet spectra of DA white dwarfs N87-10783

WHITE NOISE
Cramer-Rao bound analysis for frequency estimation of sinusoids in noise [AD-A167992] N87-10227

WIND (METEOROLOGY)
Middle Atmosphere Program. Handbook for MAP, volume 20 [NASA-CR-176882] N87-10419
A theory for the retrieval of virtual temperature from winds, radiances and the equations of fluid dynamics N87-10421
Wind profiler data in a mesoscale experiment from a meteorological perspective N87-10423
Observations of mesoscale vertical velocities around frontal zones N87-10424
The influence of velocity variability on the determination of wind profiles N87-10428
A look at profiler performance N87-10430
Need for a subtropical wind profiling system N87-10432
A model for gravity-wave spectra observed by Doppler sounding systems N87-10434
Gravity waves in severe weather N87-10442
Simultaneous rocket and MST radar observation of an internal gravity wave breaking in the mesosphere N87-10443
The PROUST radar: First results N87-10445
Simultaneous fine structure observation of wind and temperature profiles by the Arecibo 430-MHz radar and in situ measurements N87-10446
Determination of the Brunt-Vaisala frequency from vertical velocity spectra N87-10449
Can stochastic, dissipative wave fields be treated as random walk generators N87-10452
Climatology of gravity waves over Poker Flat, Alaska for 1983 N87-10454
A study of gravity-wave spectra in the troposphere and stratosphere at 5-min to 5-day periods with the Poker Flat MST radar N87-10462
Doppler effects on velocity spectra observed by MST radars N87-10464
Evidence of a saturated gravity-wave spectrum throughout the atmosphere N87-10467
Comparison of medium frequency pulsed radar interferometer and correlation analysis winds, part 1 N87-10474
Mesospheric wind measurements using a medium-frequency imaging Doppler interferometer N87-10476
Numerical studies of thermally and mechanically forced circulations over complex terrain N87-10630
Surface measurements of gust fronts and microbursts during the JAWS (Joint Airport Weather Studies) Project: Statistical results and implications for wind shear detection, prediction and modeling [PB86-200847] N87-10665

WIND DIRECTION
Comparison of medium frequency pulsed radar interferometer and correlation analysis winds, part 1 N87-10474
Use of the Sun to determine pointing of ST radar beams N87-10508

WIND MEASUREMENT
Wind shear measurement on board a MORANE 893 N87-10066
Doppler lidar studies of atmospheric wind field dynamics N87-10327
Remote sensing of atmospheric winds using a coherent, CW lidar and speckle-turbulence interaction N87-10329
The NCAR Airborne Infrared Lidar System (NAILS) N87-10362
Calibration and analysis for a 0.53 micron incoherent Doppler lidar N87-10365
A theory for the retrieval of virtual temperature from winds, radiances and the equations of fluid dynamics N87-10421
A look at profiler performance N87-10430
Simultaneous fine structure observation of wind and temperature profiles by the Arecibo 430-MHz radar and in situ measurements N87-10446
Simultaneous multibeam sounding of wind and turbulence N87-10506
Further studies with data collected by NASA's airborne Doppler lidar in Oklahoma in 1981 [NASA-CR-179779] N87-10660

WIND PROFILES
Coherent lidar technology for global wind profiling N87-10267
Examples of mesoscale structures and short-term wind variations detected by VHF Doppler radar N87-10422
Wind profiler data in a mesoscale experiment from a meteorological perspective N87-10423
Comparison of vertical velocities analyzed by a numerical model and measured by a VHF wind profiler N87-10425
The real-time use of wind profilers in nowcasting N87-10427
The influence of velocity variability on the determination of wind profiles N87-10428
Performance characteristics of wind profiling radars N87-10429
A look at profiler performance N87-10430
Need for a subtropical wind profiling system N87-10432
The PROUST radar: First results N87-10445
Simultaneous fine structure observation of wind and temperature profiles by the Arecibo 430-MHz radar and in situ measurements N87-10446
An evaluation of errors observed in the measurement of low wind velocities N87-10469

Methods for verifying the accuracy of wind profiles N87-10471
Comparison of reflectivity and wind profiles measured on 46.8 MHz and 430 MHz at the Arecibo Observatory N87-10477
Progress in existing and planned MST radars N87-10481
The proposed flatland radar N87-10482
Continuous wind measurement in the tropical Pacific using VHF radars N87-10484
Colorado wind profilers N87-10486
Wind profiler demonstration system N87-10487
The Penn State Doppler network progress report N87-10489
The Adelaide MF partial-reflection radar and VHF ST radar N87-10490
The PROUST radar N87-10491
The Provence ST radar N87-10492
The INSU and DMN network of ST radars N87-10493
Progress in the MF radar system at Saskatoon N87-10496
Determination of U, V, and W from single station Doppler radar radial velocities N87-10502
Low-altitude coverage of ST radars N87-10504
A microprogrammable radar controller N87-10518
Data communications and monitor for the Penn State University profiler network N87-10523

WIND SHEAR
Aircraft accident reeport, Delta Air Lines, Inc., Lockheed L-1011-385-1, N726DA, Dallas/Fort Worth International Airport, Texas, August 2, 1985
[PB86-910406] N87-10053
Doppler Radar Detection of Wind Shear
[NASA-CP-2435] N87-10054
Wind shear measurement on board a MORANE 893 N87-10086
The real-time use of wind profilers in nowcasting N87-10427
NASA and FAA launch wind shear research project
[NASA-NEWS-REL-86-143] N87-10659

WIND TUNNEL TESTS
The effect of free stream disturbances and control surface deflections on the performance of the Wortmann airfoil at low Reynolds numbers N87-10007
Wind-tunnel investigation of the flight characteristics of a canard general-aviation airplane configuration
[NASA-TP-2623] N87-10039
Experimental and theoretical investigations of the flow field of an airfoil with a deflected spoiler N87-10050
Unsteady flow over an airfoil inside a wind tunnel with and without transpiration N87-10051
Design and fabrication of the NASA decoupler pylon for the F-16 aircraft
[NASA-CR-172354] N87-10065
In-flight total forces, moments and static aeroelastic characteristics of an oblique-wing research airplane
[NASA-TP-2224] N87-10103
Tunnel interference from pressure measurements on control surfaces
[AE-TM-8-83] N87-10104
Adaptation of TSFOIL for Univac 1100/60H computer at NAL, Bangalore
[AE-TB-9-83] N87-10718

WIND TUNNEL WALLS
Unsteady flow over an airfoil inside a wind tunnel with and without transpiration N87-10051
Tunnel interference from pressure measurements on control surfaces
[AE-TM-8-83] N87-10104

WIND TURBINES
WEST-3 wind turbine simulator development. Volume 2: Verification
[NASA-CR-174982] N87-10531

WIND VELOCITY
Laser sounding of instantaneous and mean speed of wind using correlation method N87-10304
Climatology of gravity waves over Poker Flat, Alaska for 1983 N87-10454
On the varying slope of velocity spectra N87-10463
Mesospheric wave number spectra from Poker Flat MST radar measurements compared with gravity-wave model N87-10466
Comparison of medium frequency pulsed radar interferometer and correlation analysis winds, part 2 N87-10475
Gravity wave dynamics near the mesopause over Poker Flat, Alaska N87-10631
Three-dimensional structure of the heliosphere: Quiet-time and disturbed periods N87-10818

WIND VELOCITY MEASUREMENT
Experimental and theoretical Doppler-lidar signatures of aircraft wake vortices N87-10330
Wavelength dependence of coherent and incoherent satellite-based lidar measurements of wind velocity and aerosol backscatter N87-10361
CO2 lidar system for atmospheric studies N87-10366
Observations of mesoscale vertical velocities around frontal zones N87-10424
Comparison of vertical velocities analyzed by a numerical model and measured by a VHF wind profiler N87-10425
The real-time use of wind profilers in nowcasting N87-10427
The influence of velocity variability on the determination of wind profiles N87-10428
Simultaneous rocket and MST radar observation of an internal gravity wave breaking in the mesosphere N87-10443
Intercomparison and calibration of wind and wave measurements at various frequencies N87-10468
An evaluation of errors observed in the measurement of low wind velocities N87-10469
A comparison of vertical velocities measured from specular and nonspecular echoes by a VHF radar N87-10470
Methods for verifying the accuracy of wind profiles N87-10471
Comparison of medium frequency pulsed radar interferometer and correlation analysis winds, part 1 N87-10474
Beam steering system N87-10501
Use of the Sun to determine pointing of ST radar beams N87-10508
The Tukey algorithm for enhancing MST radar data N87-10521

WINDS ALOFT
Horizontal wind perturbations and their relation to transient internal gravity waves N87-10457

WING TIPS
Supersonic flow around tip sides of wings N87-10033

WING-FUSELAGE STORES
Design and fabrication of the NASA decoupler pylon for the F-16 aircraft
[NASA-CR-172354] N87-10065

WINGS
Acta Aeronautica et Astronautica Sinica (selected articles)
[AD-A167918] N87-10004
A study of the flow field about an upper surface blown wing and its effects on longitudinal static stability of a small jet airplane N87-10009
Viscous wing theory development. Volume 1: Analysis, method and results
[NASA-CR-178156] N87-10043
Viscous wing theory development. Volume 2: GRUMWING computer program user's manual
[NASA-CR-178157] N87-10044

WIRE
Relationship between critical current and microstructure of internal tin wire
[DE86-009922] N87-10238
Dynamics and control of orbiting grid and the synchronously deployable beam
[NASA-CR-179808] N87-10410

WORK CAPACITY
Upper and lower body anaerobic power comparison between biathletes and control subjects
[AD-A167636] N87-10710

WORKSTATIONS
Integrated testing and analysis of mathematical software tools. Summary of research activities, 1 August 1985-1 May 1986
[DE86-010882] N87-10723

X

X RAY ANALYSIS
Micro-tomography using synchrotron radiation
[DE86-010962] N87-10191

X RAY ASTRONOMY
The X-ray properties of high redshift, optically selected QSOs N87-10784

X RAY ASTROPHYSICS FACILITY
Research relative to high resolution camera on the advanced X-ray astrophysics facility
[NASA-CR-179757] N87-10376

X RAY SOURCES
Bright galactic X-ray binary sources: Temporal and spectral studies N87-10804

X RAY SPECTRA
Observations of non-thermal radiation from late-type stars N87-10793

X RAYS
The development and test of multi-anode microchannel array detector systems. Part 2: Soft X-ray detectors
[NASA-CR-177066] N87-10236
Overtone production of soft x-rays with free-electron lasers
[DE86-011248] N87-10383
An analysis at mesospheric coherent-scatter power enhancements during solar flare events N87-10479
Solar-geophysical data number 501, May 1986. Part 2: (Comprehensive reports). Data for November 1985 and miscellanea
[PB86-218047] N87-10622
Optical systems for synchrotron radiation. Lecture 4: Soft X-ray imaging systems
[DE86-011587] N87-10761
Progress made during 1985 in the scientific and technical program of National Physical Laboratory's Division of Radiation Science and Acoustics N87-10776
The X-ray properties of high redshift, optically selected QSOs N87-10784
Intense soft X-rays from RS Ophiuchi during the 1985 outburst
[DE86-010175] N87-10820

XENON FLUORIDE LASERS
XeF lidar measurements of density and temperature in the middle atmosphere N87-10342

Z

ZINC
Chemisorption mechanism and effect of polyacrylic acid on the improvement in bond durability of zinc phosphate-to-polymer adhesive joints
[DE86-011535] N87-10213

ZIRCONIUM ALLOYS
Castable hot corrosion resistant alloy
[NASA-CASE-LEW-14134-1] N87-10192

PERSONAL AUTHOR INDEX

SCIENTIFIC AND TECHNICAL AEROSPACE REPORTS VOLUME 25 NUMBER 1

Typical Personal Author Index Listing

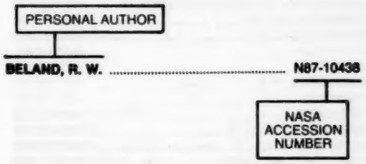

Listings in this index are arranged alphabetically by personal author. The NASA accession number denotes the number by which the citation is identified.

A

ABE, Y.	N87-10590
ABERNATHY, J. MICHAEL	N87-10248
ABU-SABA, ELIAS G.	N87-10410
ACHENBACH, J. D.	N87-10413
ACKERMANN, M. R.	N87-10715
ADAMS, G. W.	N87-10476
ADAMS, JOHN Y.	N87-10064
ADATI, K.	N87-10763
ADOLPH, H. G.	N87-10214
AGIN, B.	N87-10678
AGNENI, A.	N87-10118
AGOURIDIS, D. C.	N87-10229
AGUILAR-CHIU, LUIS ALBERTO	N87-10810
AINBUND, M. R.	N87-10556
AKASOFU, S.-I.	N87-10816
AKIYAMA, SATOSHI	N87-10017
AKIYOSHI, H.	N87-10313
ALBY, FERNAND	N87-10154
ALCAYDE, D.	N87-10598
ALEXANDRE, C.	N87-10681 N87-10684 N87-10685 N87-10689 N87-10690 N87-10691
ALLARIO, F.	N87-10266
ALLEN, J.	N87-10778
ALLEN, J. W.	N87-10252
ALLEVARD, A. M.	N87-10700 N87-10703
ALLISON, S. W.	N87-10389
ALTSCHAEFFL, A. G.	N87-10747
AMENDE, WELF	N87-10203
AMZAJERDIAN, FARZIN	N87-10329
ANANDA, M. P.	N87-10133
ANCELLET, G. M.	N87-10363
ANDERSON, C. L.	N87-10066
ANDERSON, D. E., JR.	N87-10618
ANDERSON, G. P.	N87-10618
ANDERSON, J. W.	N87-10729
ANDERSON, SCOTT FREDERICK	N87-10784
ANDONYADIS, M.	N87-10747
ANDREEV, YU. M.	N87-10302
ANDREWS, D. G.	N87-10617
ANNAT, G.	N87-10700 N87-10703
ANSELMO, L.	N87-10134
ANSMANN, A.	N87-10288
AOKI, T.	N87-10763
ARBEILLE, PH.	N87-10677 N87-10696
ARLUK, M. P.	N87-10156
ARNOLD, CLIFFORD NICHOLAS	N87-10796
ARNOLD, S.	N87-10159
ARRITT, RAYMOND W.	N87-10630
ARSHINOV, YU. F.	N87-10332
ARUGA, T.	N87-10284
ASAI, K.	N87-10284
ASAI, KAZUHIRO	N87-10374
AUGUSTINE, JOHN	N87-10423
AUKERMAN, L.	N87-10819
AVDIUCHINE, S. I.	N87-10599
AVERILL, R. D.	N87-10268
AYERS, A. E.	N87-10517

B

BABA, H.	N87-10279
BACA, G. T.	N87-10379
BACHMAIER, C.	N87-10120
BACHMANN, K.	N87-10702
BADER, H. P.	N87-10112
BAKIS, C. E.	N87-10183
BAKULIN, A. V.	N87-10708
BALAKRISHNA, S.	N87-10062
BALEBANOV, V. M.	N87-10568 N87-10593
BALIN, YU. S.	N87-10278
BALLARD, J. R.	N87-10070
BALSLEY, B. B.	N87-10455 N87-10462 N87-10483 N87-10484 N87-10500 N87-10524
BALSLEY, BEN B.	N87-10443 N87-10454
BANAKH, V. A.	N87-10307
BARAT, J.	N87-10447
BARBER, T. L.	N87-10272
BARBINI, R.	N87-10366
BARR, P.	N87-10820
BARRETT, CHARLES A.	N87-10192
BARTSCHER, W.	N87-10216
BASCANDS, J. L.	N87-10700
BASSAN, MASSIMO	N87-10609
BATRA, R.	N87-10237
BATRA, ROMESH C.	N87-10412
BATTISTELLI, E.	N87-10315
BAUDIN, F.	N87-10493
BAUER, O. H.	N87-10591
BAUGHCUM, S. L.	N87-10388
BAUMGART, J. S.	N87-10379
BAUMUELLER, J.	N87-10652
BEAL, ROY E.	N87-10193
BEAUDET, M. F.	N87-10157
BECHTOLD, JILL ELEANOR	N87-10785
BEDARD, A. J.	N87-10665
BEGHIN, C.	N87-10544 N87-10553 N87-10554 N87-10573 N87-10574 N87-10576 N87-10600 N87-10601 N87-10603
BELAND, R. W.	N87-10438
BELON, B.	N87-10130 N87-10147
BEMRA, R. S.	N87-10462
BENARD, J.	N87-10286
BENKOVA, N. P.	N87-10601
BENN, G. S. L.	N87-10069
BENO, M. A.	N87-10768
BENOIT, A.	N87-10139
BENSON, P. E.	N87-10540
BENTS, DAVID J.	N87-10174
BERGES, J. C.	N87-10147
BERNER, WILLIAM E.	N87-10779
BERRY, W.	N87-10704
BERSON, M.	N87-10677
BERTELSMEIER, MANFRED	N87-10230
BERTHELIER, A.	N87-10546 N87-10547
BERTHELIER, J. J.	N87-10546 N87-10547 N87-10553 N87-10565 N87-10570 N87-10573 N87-10574 N87-10607
BERTHOZ, A.	N87-10692
BERTIN, F.	N87-10445 N87-10446 N87-10447 N87-10491
BES, A.	N87-10696 N87-10700
BEST, PAUL	N87-10759
BHASIN, K. B.	N87-10232
BHAT, R. S.	N87-10127
BHUTIANI, P. K.	N87-10753
BIESIADNY, THOMAS J.	N87-10100
BILLMANN, BARRY R.	N87-10002
BIRD, A. G.	N87-10114
BIRETTA, JOHN ANTHONY	N87-10824
BIRGENEAU, R.	N87-10778
BIRKUI, P. J.	N87-10680
BISWAS, SUBODH C.	N87-10409
BIZOLLON, C. A.	N87-10703
BLOM, A. F.	N87-10416
BLOSTIN, R.	N87-10707
BLUESTEIN, HOWARD B.	N87-10660
BLUME, C.	N87-10396
BLUMSTEIN, D.	N87-10149
BOBROVNIKOV, S. M.	N87-10332
BODE, M. F.	N87-10820
BOERS, R.	N87-10300 N87-10336
BOGACZ, S. A.	N87-10381
BOGAN, JAMES R.	N87-10358
BOISSIERES, J.	N87-10142
BOLAND, PHILIPPE	N87-10115
BOLJUNOVA, A. D.	N87-10560
BONDE-PETERSEN, F.	N87-10676
BONSE, U.	N87-10191
BOOKBINDER, JAY AARON	N87-10793
BORNSTEIN, R. D.	N87-10646
BOSENBERG, J.	N87-10288
BOSQUED, J. M.	N87-10543 N87-10544 N87-10547 N87-10553 N87-10554 N87-10560 N87-10561 N87-10564 N87-10585 N87-10598 N87-10603 N87-10607
BOSTROM, R.	N87-10498
BOUDKO, N.	N87-10570
BOWHILL, S. A.	N87-10419 N87-10441 N87-10442 N87-10479 N87-10485 N87-10501 N87-10514 N87-10516 N87-10521
BRASE, J. M.	N87-10191
BRASKI, D. N.	N87-10202
BRAUN, CHARLES	N87-10299
BRAUSCH, J. F.	N87-10752
BRENDEL, MICHAEL	N87-10052
BRENTNER, KENNETH S.	N87-10750
BRIGGS, B. H.	N87-10507
BRISTOW, FRANK	N87-10787
BRISTOWE, P. J. D.	N87-10080
BRITTINGER, P.	N87-10159
BROCA, P.	N87-10135
BROENING, K.	N87-10550
BROOKS, C.	N87-10539
BROSNAHAN, J. W.	N87-10476
BROUGHTON, J. Q.	N87-10767
BROWELL, E. V.	N87-10268 N87-10281 N87-10370 N87-10372 N87-10616
BROWELL, EDWARD V.	N87-10275 N87-10287

BROWN, D. R. N87-10239
N87-10368
N87-10537
BROWN, DAVID R. N87-10116
BROWN, J. H. N87-10438
BROWN, JOHN V. N87-10137
BRUMBACK, BRIAN DAVID N87-10057
BRUN, E. N87-10447
N87-10506
BRUSCAGLIONI, P. N87-10315
BRUSHLINSKY, K. V. N87-10036
BRYANT, WILLIAM C. N87-10123
BUCKLEY, E. C. N87-10102
BUGLIA, JAMES J. N87-10620
BUKOWSKI, C. F. N87-10077
BURAKOV, S. D. N87-10308
BURKE, J. C. N87-10258
BURRIS, JOHN N87-10323
BUTLER, JAMES N87-10323
BUTLER, R. N87-10726

C

CABRIT, P. N87-10073
CAHEN, CL. N87-10286
CAILLER, B. N87-10707
CALLAHAN, P. N87-10704
CALLOW, R. A. N87-10735
CAMAGNI, P. N87-10322
CAMPAN, G. N87-10147
CAMUS, A. L. N87-10695
CANDY, B. N87-10507
CANTIN, M. N87-10698
CARCIELLO, N. N87-10213
CARDELLI, JASON A. N87-10800
CARLSON, CHARLES W. N87-10542
CARLSON, K. D. N87-10768
CARNUTH, W. N87-10340
CAROZZO, FRED D., JR. N87-10186
CARR, B. J. N87-10601
CARRICO, JOHN P. N87-10375
CARROLL, JOSEPH A. N87-10169
CARSWELL, A. I. N87-10273
N87-10293
N87-10295
CARTER, D. A. N87-10455
N87-10484
N87-10500
N87-10517
CASASENT, DAVID N87-10743
CEBALLOS, DECIO CASTILHO N87-10138
CERISIER, J. C. N87-10546
N87-10570
N87-10573
N87-10574
CHADWICK, R. B. N87-10487
CHAMBERS, HARRY W. N87-10064
CHAMEAU, J. L. N87-10747
CHAMEIDES, W. N87-10615
CHAMPLIN, NICHOLAS N87-10209
CHAN, TIMOTHY S. N87-10205
CHANDLER, M. O. N87-10602
CHANG, CHONG-AN N87-10797
CHAO, B. P. N87-10728
CHAO, J. K. N87-10495
N87-10522
CHAPPARD, D. N87-10684
N87-10685
N87-10689
N87-10690
CHAPPELL, C. R. N87-10602
CHAPPELL, P. J. C. N87-10208
CHAPUY, C. N87-10691
CHATARD, J. C. N87-10685
CHAYKOVSKY, M. N87-10214
CHEN, SHILU N87-10004
CHEN, XINGJIAN N87-10004
CHERNY, S. G. N87-10031
CHETVERSUSHKIN, B. I. N87-10038
CHIANG, WEN-WEI N87-10398
CHILLAREGE, RAM N87-10733
CHING, W. Y. N87-10212
CHITANVIS, S. M. N87-10386
CHITSOMBOON, TAWIT N87-10187
CHO, BO HYUNG N87-10173
CHOEN, A. N87-10328
CHOW, R. R. N87-10043
N87-10044
CHOW, SHU DJEN N87-10641
CHU, Y. S. N87-10495
CHURBANOV, A. G. N87-10038
CHUSHKIN, P. I. N87-10030
CICERONE, R. J. N87-10614
CIESLAK, M. J. N87-10198
CINTRON, N. M. N87-10679
CLARK, W. L. N87-10470
N87-10502
CLAUTRIER, M. N87-10165
CLAYTON, J. D. N87-10065
CLEMENT, G. N87-10692
CLERE, J. M. N87-10678
COE, HAROLD H. N87-10391
COFFEY, H. E. N87-10622
N87-10623
N87-10625
N87-10626
COHEN, ARIEL N87-10320
COLOMBO, G. N87-10322
CONNOR, BRIAN JOSEPH N87-10629
COONEY, J. N87-10333
COONEY, JOHN A. N87-10334
COOPER-SARKAR, A. M. N87-10754
COOTER, ELLEN JEAN N87-10666
CORCUFF, Y. N87-10575
CORDOVA, F. A. N87-10820
CORNILLEAU-WEHRLIN, N. N87-10598
CORUM, J. M. N87-10393
COSS, JAMES R. N87-10765
COSTANZA, VINCE N87-10226
COSTELLO, FREDERICK A. N87-10257
COSTIS, CHRISTOPHER E. N87-10008
COTNOIR, L. J. N87-10291
N87-10370
N87-10372
COUTO, I. N87-10131
COX, M. E. N87-10091
COX, R. A. N87-10613
CRASNIER, J. N87-10561
CREIGHTON, J. R. N87-10188
CREMIEU, A. N87-10445
CROCHET, M. N87-10447
N87-10480
N87-10492
N87-10493
N87-10506
CROSS, KENNETH D. N87-10714
CRUM, TIMOTHY D. N87-10627
CULBERTSON, G. C. N87-10194
CUNDY, D. C. N87-10754
CUNNIIG, JOHN N87-10423
CUQ, F. N87-10447
CURRAN, ROBERT J. N87-10265
CURRIE, I. F. N87-10732
CURRY, ROBERT E. N87-10103
CUSIC, RODNEY LEE N87-10010
CUTTEN, D. N87-10271
CUVILO, J. N87-10560
CVIJIN, P. VUJKOVIC N87-10360
CZANDERNA, A. W. N87-10211
N87-10536

D

DAGAMA, R. M. S. N87-10261
DALAUDIER, F. N87-10447
DANDOURAS, J. N87-10595
DANEN, W. C. N87-10388
DANIELSEN, E. F. N87-10616
DANTAS, ARMANDO R. V. N87-10765
DARROY, J. M. N87-10161
DAS, INDU SHEKHER N87-10049
DAVID, S. A. N87-10199
DAVIES, J. E. N87-10271
DAVIS, IAN R. N87-10647
DAVIS, J. R. N87-10693
DAY, WILLIAM B. N87-10407
DEBRIE, R. N87-10544
N87-10574
DECHAUMPHAI, PRAMOTE N87-10406
DECKER, B. L. N87-10527
DEE, V. I. N87-10582
DEFAZIO, ROBERT L. N87-10123
DEFIGUEIREDOMONTEIRO, CARLOS AUGUSTOS
N87-10644
DEFOOR, T. N87-10312
DEGNAN, J. J. N87-10268
DEGNER, TODD R. N87-10092
DEKINDER, R. E., JR. N87-10228
DELABEUJARDIERE, O. N87-10563
DELANY, A. C. N87-10614
DELASERVETTE, X. N87-10073
DELCOURT, D. N87-10553
N87-10554
DELMAS, P. N87-10691
DELNORE, V. E. N87-10054
DELUSI, J. J. N87-10312
DEMERJIAN, K. L. N87-10615
DEMORE, W. B. N87-10613
DENNIS, T. S. N87-10424
N87-10425
DENOYER, BARBARA J. N87-10058
DEPAOLIS, R. N87-10059
DERYDER, L. J. N87-10170
DESPLANCHES, D. N87-10687
DEUBER, H. J. N87-10702
DEWAN, E. M. N87-10438
DEWAN, EDMOND M. N87-10439
N87-10440
DIAS, P. DASILVA N87-10615
DIBBLE, R. W. N87-10253
DICKINSON, R. E. N87-10618
DIENGER, G. N87-10064
DIETDERICH, D. R. N87-10238
DINI, DINO N87-10069
DIXIT, R. M. N87-10781
DJORGOVSKI, STANISLAV BRATISLAV N87-10795
DOBROWOLSKI, B. N87-10034
DOMBROWSKI, M. N87-10282
N87-10283
N87-10296
DOMINGUEZ, D. E. N87-10379
DONAT, H. N87-10147
DOOLEY, R. N87-10239
DOSSANTOSPINTO, M. N87-10394
DRAGHI, S. N87-10356
DRAYSON, S. R. N87-10618
DREWS, P. N87-10395
DRIES, GREGORY A. N87-10184
DROEGE, W. N87-10754
DUBININ, E. M. N87-10568
DUBINSKY, R. N. N87-10293
DUGGAN, A. N87-10710
DUNCAN, U. N87-10697
DUNNE, THOMAS N87-10650
DURRANT, P. R. N87-10222
DZENIS, V. V. N87-10688

E

EARLY, MICHAEL L. N87-10072
EBEL, A. N87-10457
EBERHARD, W. L. N87-10321
ECKLUND, W. L. N87-10455
N87-10484
N87-10499
N87-10500
N87-10504
N87-10505
N87-10506
N87-10511
ECKSTEIN, M. C. N87-10153
EDNER, H. N87-10355
EDWARDS, BELVA N87-10419
EDWARDS, D. F. N87-10760
EGERT, SMADAR N87-10320
EILTS, MICHAEL N87-10430
ELIASSON, LARS N87-10596
ELIZAROVA, T. G. N87-10038
ELLIOTT, C. J. N87-10383
ELLIOTT, NORMAN E. N87-10316
ELORANTA, EDWIN W. N87-10367
EMGE, T. J. N87-10768
ENDEMANN, M. N87-10269
ERICKSON, K. L. N87-10218
ERICKSON, K. N. N87-10590
ESCUDIER, PH. N87-10145
ETORI, KANJI N87-10023
EVANS, B. T. N. N87-10277
EVERSMAN, W. N87-10751
EZZO, MAUREEN B. N87-10182

F

FABER, P. N87-10200
FAGG, A. S. N87-10126
FARRINGTON, M. N87-10339
FASTIG, S. N87-10328
FEATHER, FRANK E. N87-10731
FELL, PATRICK J. N87-10108
FELS, S. N87-10618
FERGUSON, E. E. N87-10613
FERNSLER, R. F. N87-10755
FERRARIO, A. N87-10317
FILIPPOV, V. M. N87-10603
FINDLAY, JOHN T. N87-10662
N87-10663
FINK, R. K. N87-10735
FINLEY, D. S. N87-10760
FIRSOV, K. M. N87-10306
FITZGERALD, K. F. N87-10258
FLAMANT, P. N87-10373
FLAMANT, P. H. N87-10290
FLANDROIS, R. N87-10687
FLURY, W. N87-10143

FOETH, H. N87-10754
FOLIARD, J. N87-10147
FONI, A. N87-10118
FONTAINE, D. N87-10596
FORBES, G. S. N87-10422
FORREST, DANIEL K. N87-10367
FOSTER, J. M. N87-10732
FOX, ROBERT L. N87-10206
FOX, S. N87-10122
FOXLEY, DONALD E. N87-10083
FRAITURE, L. N87-10125
FRAME, B. J. N87-10210
FRANKLIN, DENNIS P. N87-10528
FRANTZIS, L. N87-10258
FRAWLEY, R. C. N87-10068
FREDERICK, J. E. N87-10618
FREDRIKSSON, K. N87-10355
FRISCH, A. S. N87-10429
FRITTS, DAVID C. N87-10433
N87-10443
N87-10453
N87-10466
N87-10467
FROEHLICH, WALTER N87-10171
FROMMHERZ, B. N87-10396
FROST, A. D. N87-10059
FRUTOSO, J. N87-10687
FRY, CRAIG DANIEL N87-10818
FU, I. J. N87-10495
N87-10522
FU, L.-L. N87-10671
FUJITA, H. N87-10763
FUJITA, K. N87-10254
FUJIWARA, M. N87-10313
FUKAO, SHOICHIRO N87-10426
N87-10436
N87-10509
FUKUNISHI, H. N87-10314
N87-10345
FUNK, G. N87-10704

G

GAGE, K. S. N87-10455
N87-10482
N87-10524
GALEEV, A. A. N87-10569
GALLE, B. N87-10318
GALLETTI, E. N87-10356
GALPERIN, Y. I. N87-10546
GALPERIN, YU. I. N87-10543
N87-10547
N87-10551
N87-10561
N87-10566
N87-10567
N87-10569
N87-10584
N87-10585
N87-10587
N87-10588
N87-10601
N87-10607
GALWAY, W. F. N87-10729
GAMA, R. M. S. DA N87-10260
GAMMON, R. N87-10614
GANTOUS, DALE J. N87-10155
GAONKAR, G. N87-10063
GARBI, M. N87-10356
GARDNER, C. R. N87-10226
GARDNER, C. S. N87-10347
GARELLO, RENE N87-10454
GARN, J. N87-10773
GARODZ, L. N87-10055
GARODZ, LEO J. N87-10096
GAUME, RALPH A., JR. N87-10826
GAUQUELIN, G. N87-10699
N87-10700
N87-10703
GAUTHIER, MICHAEL K. N87-10765
GEELEN, G. N87-10700
N87-10703
GEELIN, G. N87-10699
GEISER, U. N87-10768
GEISS, M. N87-10417
GELLER, M. A. N87-10617
GENERAZIO, EDWARD R. N87-10399
GENGCHEN, WANG N87-10357
GERASIMOV, B. P. N87-10038
GERBER, H. N87-10292
GERSTL, S. A. W. N87-10316
N87-10386
GERSTL, S. A.W. N87-10228
GHAEMMAGHAMI, F. N87-10699
GHARIB, C. N87-10677
N87-10699
N87-10703
GHARIB, CL. N87-10696
GHIA, K. N. N87-10040
GHIA, U. N87-10040
GHIGO, A. N87-10366
GHOSH, SANJOY N87-10762
GIBSON, R. B. N87-10387
GILLESPIE, C. H. N87-10760
GILLIES, G. T. N87-10389
GIORGI, M. N87-10366
GIVONI, BARUCH N87-10655
GLADYSHEV, V. A. N87-10561
N87-10565
N87-10587
GLASS, M. N87-10445
N87-10491
GLAZOV, G. N. N87-10305
GLOVER, GREY A., SR. N87-10250
GNANALINGAM, S. N87-10442
GOAD, J. H. N87-10268
GOBLET, C. N87-10683
GODIN, S. N87-10344
GODLEVSKII, A. P. N87-10308
GOERTZ, C. K. N87-10550
GOGOSHEV, M. M. N87-10593
GOGOSHEVA, TS. N. N87-10593
GOKHBERG, M. B. N87-10588
GOLDBERG, BRUCE A. N87-10811
GOLDSCHMIED, FABIO R. N87-10045
GOLDWASSER, J. M. N87-10214
GOOD, R. E. N87-10438
GOPINATH, N. S. N87-10127
GOPINATH, R. N87-10104
N87-10718
GOULDIN, F. C. N87-10253
GRABELSKY, DAVID ANDREW N87-10786
GRADY, JOSEPH EDWARD N87-10402
GRAESSLER, H. N87-10754
GRANDMONTAGNE, M. N87-10687
GRANGE, CH. N87-10699
GRANIER, C. N87-10346
GRANT, A. N87-10754
GRANT, WILLIAM B. N87-10358
GRARD, REJEAN N87-10597
GRAY, WILLIAM M. N87-10661
GREEN, J. L. N87-10459
N87-10470
N87-10482
N87-10502
N87-10511
N87-10519
GREEN, JAMES L. N87-10602
GREENBAUM, E. N87-10215
GRIBENYUKOV, A. I. N87-10302
GRIGORIEV, A. I. N87-10684
N87-10688
N87-10701
GRIGORIEV, S. A. N87-10566
GRINDELAND, R. N87-10704
GROSE, W. L. N87-10617
GROSS, G. E. N87-10617
GROSSI, D. R. N87-10093
GROSSMAN, G. N87-10256
GROSSMANN, B. E. N87-10370
N87-10372
GUDIMETLA, V. S. RAO N87-10329
GUELL, A. N87-10677
N87-10696
N87-10699
N87-10700
N87-10703
GUERMONPREZ, V. N87-10162
GUEZENNEC, Y. N87-10678
GUITART, A. N87-10135
GURNETT, D. A. N87-10813
N87-10814
GURWELL, W. E. N87-10196
GUTKOVSKA, J. N87-10699

H

HAGARD, ARNE N87-10276
HAGEN, J. N87-10494
HAGEN, J. B. N87-10510
HAGFORS, T. N87-10432
HALL, F. F., JR. N87-10327
HALL, L. A. N87-10618
HALL, R. F. C. N87-10180
HALL, W. M. N87-10268
HALLER, R. L. N87-10065
HAMMINGER, RAINER N87-10769
HANUISE, C. N87-10600
HARDESTY, R. M. N87-10327
HARDT, A. P. N87-10220
N87-10221
HARRIS, ELFRIEDA N87-10720
HARRIS, H. N87-10617
HARRISS, R. T. N87-10614
HART, W. D. N87-10348
HARTEL, KAREL N87-10757
HASEGAWA, M. N87-10119
HASSENZAHL, W. V. N87-10238
HASSLER, J. M., JR. N87-10065
HATTORI, K. N87-10763
HAWKINS, BARRY J. N87-10095
HAWKINS, CARL A. N87-10046
HAYAKAWA, M. N87-10572
N87-10583
HAYASHIDA, S. N87-10338
HEADLEY, T. J. N87-10198
HEAMES, L. E. N87-10219
HEAPS, WILLIAM N87-10323
HEAPS, WILLIAM S. N87-10311
HEIKKILA, WALTER J. N87-10558
HELFRICH, HANS-PETER N87-10738
HELLIWELL, R. A. N87-10581
HIDEKUMA, S. N87-10763
HIGDON, N. S. N87-10370
N87-10372
HINDAWY, MAGDY IBRAHIM N87-10418
HINTON, D. E. N87-10268
HIRASAWA, T. N87-10314
N87-10345
HO, CHIH-MING N87-10249
HO, H. N87-10176
HO, JOHN K. N87-10400
HOERMANN, K. N87-10396
HOFF, R. M. N87-10335
HOFMANN, D. J. N87-10310
HOLDEN, D. N. N87-10444
N87-10465
N87-10473
HOLM, D. K. N87-10416
HOLMES, J. FRED N87-10329
HOLT, WILLIAM H. N87-10192
HOLTON, J. R. N87-10616
HOLY, X. N87-10683
HONG, CHANG HO N87-10060
HOOPER, WILLIAM P. N87-10292
HORII, M. N87-10124
HORTON, J. A. N87-10199
HOSKINS, B. J. N87-10616
HOUSTON, J. D. N87-10295
N87-10368
HOWARD, G. T. N87-10780
HOWELLS, M. R. N87-10761
HSU, MING-TA S. N87-10205
HUBBARD, D. W. N87-10251
HUBBARD, HARVEY H. N87-10749
HUBBARD, R. F. N87-10755
HUFFAKER, R. MILTON N87-10267
N87-10361
HUGHES, R. L. N87-10219
HUI, B. N87-10755
HULL, J. R. N87-10252
HULTQVIST, BENGT N87-10552
N87-10604
HUNT, J. J. N87-10675
HUNT, JOHN M. N87-10329
HUNTLEY, A. F. N87-10772
HUO, XIUFANG N87-10004
HUSSAIN, A. K. M. F. N87-10012

I

IDO, YUJI N87-10027
IDSCHOK, U. N87-10754
IERKIC, H. M. N87-10432
N87-10473
N87-10494
N87-10510
IGARASHI, T. N87-10284
IGONIN, G. M. N87-10305
IIKURA, Y. N87-10338
IKEDA, YOSHIO N87-10024
IKUSHIMA, Y. N87-10015
ILEV, I. K. N87-10349
ILYAN, E. A. N87-10708
INABA, HUMIO N87-10354
INAN, U. S. N87-10581
N87-10586
INHESTER, B. N87-10605
INOOKA, YASUHIRO N87-10509
INUKI, HISAO N87-10488
IPPOLITOV, I. I. N87-10369
ISHIKAWA, N. N87-10279
ISHIZU, M. N87-10284
ISHU, YOSHIO N87-10016
ISMAIL, SYED N87-10267
ITABE, T. N87-10284

IWASAKA, Y. N87-10314
N87-10345
IYENGAR, V. S. N87-10132
IYER, K. N. N87-10366
IZUTSU, NAOKI N87-10748

J

JAEGER, H. N87-10310
N87-10340
JAIN, S. L. N87-10359
JALUFKA, N. W. N87-10764
JANARDAN, B. A. N87-10752
N87-10753
JANSON, H. A. N87-10688
JATEGAONKAR, R. V. N87-10062
JAUREGUI, ERNESTO N87-10638
N87-10640
JAYASWAL, B. N87-10730
JEELANI, SHAIK N87-10409
JEGOU, J. P. N87-10346
N87-10364
JENKINS, D. B. N87-10339
N87-10343
JENNINGS, S. G. N87-10352
JENSEN, BRIAN J. N87-10206
JENSEN, JORGEN BJORNEVAD N87-10667
JOERGENSEN, T. S. N87-10562
JOHNSON, D. N87-10055
JOHNSON, L. J. N87-10515
JOHNSON, LEONARD M. N87-10378
JOHNSON, P. C. N87-10679
JOHNSON, Q. C. N87-10191
JOHNSTON, S. C. N87-10253
JONES, DYFRIG N87-10579
JONES, G. J. N87-10535
JONES, R. H. N87-10195
JORGENSEN, P. S. N87-10133
JORJIO, N. V. N87-10544
N87-10554
N87-10556
N87-10569
N87-10585
N87-10587
N87-10588
N87-10607
JOSHI, A. N87-10404
JOUVENOT, C. N87-10082
JOYCE, G. N87-10755

K

KAAIJK, A. N87-10538
KABZA, Z. N57-10034
KAGANN, R. H. N87-10285
KAISER, HANS-ARMIN N87-10090
KALACHINSKAYA, I. S. N87-10038
KALBE, H. N87-10076
KALLOS, GEORGE BASIL N87-10669
KAMADA, RAY FRANCIS N87-10611
KAMATA, MAKOTO N87-10024
KAMBE, T. N87-10015
KAMMEYER, PETER C. N87-10146
KAN, J. R. N87-10549
KANAGARAJAN, V. N87-10718
KANDA, H. N87-10019
KANEKO, KEN-ICHI N87-10025
KANO, T. N87-10345
KAPITANOV, V. A. N87-10302
KAPLAN, A. M. N87-10207
KAPLAN, D. L. N87-10207
KAPRIELOV, B. K. N87-10349
KAPUSTINA, O. N87-10570
KARAGICHEV, A. B. N87-10038
KASTNER, CAROL JANE N87-10530
KASTNER, M. N87-10274
KATAGIRI, MASAKAZU N87-10018
KATO, SUSUMU N87-10426
N87-10436
N87-10509
KATZ, CASIMIR N87-10739
KAUNE, W. T. N87-10713
KAVAYA, MICHAEL J. N87-10361
KAVKYANOV, S. I. N87-10278
KAWAGUCHI, S. N87-10345
KAWAMOTO, T. N87-10763
KAWAMURA, T. N87-10639
KELLY, G. MEL N87-10662
N87-10663
KELLY, J. D. N87-10563
KENT, G. S. N87-10341
KERGUELEN, M. N97-10694
KERST, D. W. N87-10240
KESSLER, EDWIN N87-10430
KESSLER, R. R. N87-10729
KETTERSON, J. B. N87-10381
KHALIL, M. A. K. N87-10614
KHALIPOV, V. L. N87-10553
N87-10603
KHMELNITSKII, G. S. N87-10302
KIEHL, J. N87-10618
KIMURA, HIROSHI N87-10021
KIMURA, TAKASHI N87-10255
KINEV, K. N87-10593
KINNEY, J. H. N87-10191
KISTLER, L. M. N87-10713
KLANN, GARY A. N87-10100
KLAUS, V. N87-10493
KLEIMAN, MOSHE N87-10320
KLEY, D. N87-10616
KLOTZ, H. N87-10152
KNOTT, P. R. N87-10753
KO, SHUN DER N87-10633
KOBRICK, JOHN L. N87-10712
KOECHLER, C. N87-10322
KOEPP, F. N87-10330
KOFMAN, W. N87-10596
KOGA, R. N87-10324
KOLEV, I. N. N87-10304
N87-10349
KOLLMANN, W. N87-10253
KOMER, CATHERINE A. N87-10526
KOPCZEWSKI, M. R. N87-10217
KOPKA, H. N87-10582
KOPPES, W. M. N87-10214
KOPYTIN, YU. D. N87-10303
N87-10306
KORB, C. L. N87-10282
N87-10283
N87-10296
KOROLKOV, V. A. N87-10303
KORTH, A. N87-10595
N87-10598
N87-10605
KORTOVICH, C. S. N87-10194
KOSAKA, M. N87-10324
KOSTIN, B. S. N87-10301
KOVENYA, V. M. N87-10031
KOVRAZHKIN, R. A. N87-10543
N87-10544
N87-10547
N87-10553
N87-10554
N87-10564
N87-10569
N87-10585
N87-10587
N87-10598
KOZLOV, E. F. N87-10601
KOZYRA, JANET URBANSKI N87-10632
KRASNOSELSKIKH, V. V. N87-10569
KREKOV, G. M. N87-10278
KREMSER, G. N87-10594
N87-10595
N87-10596
KREUTZMANN, H. N87-10754
KRICHBAUMER, W. A. N87-10330
KRINSKY, S. N87-10380
KRONBERG, PETER N87-10529
KRUEGER, A. J. N87-10616
KRUSE, H. W. N87-10379
KUKACKA, L. E. N87-10213
KUKOWSKI, JIM N87-10757
KULAEV, B. N87-10707
KUMAZAWA, R. N87-10763
KUNINAKA, HITOSHI N87-10022
KUO, F. S. N87-10495
N87-10522
KURIKI, KYOICHI N87-10022
KURTH, R. E. N87-10176
KURTH, W. S. N87-10613
N87-10614
KUSUMOTO, FUSAO N87-10025
KUTIEV, I. N87-10592
KUWABARA, SINZI N87-10013
KUZMIN, A. K. N87-10593
KWON, K. H. N87-10347

L

LACOUR, J. R. N87-10685
LACSER, AVRAHAM N87-10608
LAGOUTTE, D. N87-10583
LAI, HIEN THE N87-10247
LAMPE, M. N87-10755
LANDSBERG, H. E. N87-10653
LARKINA, V. I. N87-10588
LARSEN, M. F. N87-10424
N87-10425
N87-10432
N87-10444
N87-10465
N87-10472
N87-10473
LARSON, D. R. N87-10272
LATYSHEV, K. S. N87-10566
N87-10567
LAURIKKO, J. N87-10392
LAW, DANIEL C. N87-10503
N87-10518
LAWRENCE, T. R. N87-10327
LAZAREV, S. V. N57-10306
LEA, TING KAUNG N87-10280
LEACH, C. S. N87-10679
LEBEDEV, V. I. N87-10708
LEBRETON, J. P. N87-10591
LEE, CHENG SHANG N87-10661
LEE, CHYANG SHENG JOHNSON N87-10050
LEE, K. N87-10383
LEE, R. W. N87-10223
LEEP, E. MYCKKY N87-10789
LEFEBVRE, J. N87-10665
LEFEBVRE, M. N87-10671
LEFEUVRE, F. N87-10570
N87-10571
N87-10572
N87-10574
N87-10582
N87-10583
N87-10588
N87-10589
LEGENDRE, P. N87-10147
LEGER, A. N87-10694
LEIBOLD, A. F. N87-10144
LEINBACH, H. N87-10621
LEITH, J. R. N87-10189
LEJEUNE, D. N87-10694
LEMAIRE, J. N87-10555
LEMONS, R. N87-10239
LENCKI, W. N87-10704
LENSCHOW, D. H. N87-10615
LENT, HANS-M. N87-10048
LENTZ, W. J. N87-10353
LEONARD, J. I. N87-10709
LEOVY, C. N87-10618
LEQUEAU, D. N87-10577
LEROY, GRAHAM G. N87-10096
LEROY, M. N87-10680
LESCLAUX, R. N87-10613
LESNE, J. L. N87-10286
LESS, DAVID MATTHEW N87-10246
LESTIENNE, F. N87-10692
LESUNOVSKY, A. V. N87-10038
LETOULLEC, CH. N87-10677
LEVINE, DAVID M. N87-10658
LEVINE, RICHARD R. N87-10759
LEVITSKII, M. E. N87-10303
LI, SHUSUN N87-10610
LICEAGA, CARLOS A. N87-10731
LIEBER, BARUCH BARRY N87-10245
LIEBERMAN, M. L. N87-10219
LIENEWEG, UDO N87-10231
LIGHT, J. C. N87-10385
LIGHTSEY, P. A. N87-10362
LISAKOV, YU. V. N87-10585
LISSAKOV, YU. V. N87-10556
N87-10587
LITTFASS, M. N87-10310
LITTLE, JEFFERY K. N87-10100
LIU, C. H. N87-10458
N87-10460
N87-10464
N87-10495
N87-10522
LO, Y. T. N87-10225
LOFFMAN, R. S. N87-10771
LOGAN, J. A. N87-10614
N87-10615
LONGENECKER, D. U. N87-10312
LOONEY, L. D. N87-10379
LORIA, E. A. N87-10201
LOTH, C. N87-10373
LOYD, BERNARD N87-10744
LUND, DAVID J. N87-10759
LUNDIN, B. N87-10571
LUNDIN, RICKARD N87-10596
LUSK, E. N87-10726
LUTZ, H. N87-10264
LY, UY-LOI N87-10400
LYCHKINA, I. V. N87-10584
LYNCH, M. J. N87-10271
LYNN, D. N87-10239
LYONS, T. J. N87-10654

M

MACE, G. N87-10160
MACHARD, C. N87-10546
MACKAY, RAYMOND A. N87-10375
MACROBERTS, M. N87-10239
MADDALENA, RONALD JOSEPH N87-10809
MAEDA, M. N87-10297
N87-10342
MAGEDOC, V. N87-10707
MAGEDOV, V. S. N87-10686
MAGES, K. N87-10395
MAJJIGI, R. K. N87-10752
N87-10753
MAKUSHKIN, YU. S. N87-10306
MALCOLM-COE, J. N87-10223
MALCOLM, P. R. N87-10590
MALTSEVA, O. A. N87-10574
N87-10580
N87-10582
MALTSEVE, O. A. N87-10584
MANSON, A. H. N87-10457
N87-10474
N87-10475
N87-10496
MARCONI, F. N87-10043
MARDOIAN, GEORGE H. N87-10182
MARINO, D. N87-10237
MARTIN, H. L. N87-10734
MARTIN, KEITH E. N87-10765
MARTINEZ-GARCIA, J. J. N87-10120
MASHIKO, KOICHI N87-10028
MASLOV, V. D. N87-10553
N87-10554
N87-10565
N87-10587
MASON, K. O. N87-10820
MASON, WILLIAM H. N87-10042
MASSEBEUF, M. N87-10445
MASSEVITCH, N. I. N87-10574
MASTICHIADIS, APOSTOLOS N87-10798
MASUDA, YOSHIHISA N87-10488
MATHEUS, C. J. N87-10734
MATHEWS, J. D. N87-10437
N87-10520
MATOSDEMEDEIROS, VALDER N87-10150
MATSUI, I. N87-10338
MATSUI, ICHIRO N87-10374
MATSUMOTO, HIROMASA N87-10436
MATTHEWS, JOHN N87-10597
MATUURA, NOBUO N87-10488
MATVIENKO, G. G. N87-10304
MAUREL, C. N87-10543
N87-10544
MAUROUX, J. L. N87-10696
N87-10703
MAUTE, P. N87-10164
MAYET, M. H. N87-10687
MAYLE, RONALD WILLIAM N87-10808
MAZIASZ, P. J. N87-10202
MCCAUL, EUGENE W., JR. N87-10660
MCCLELLAN, V. A. N87-10054
MCCORMICK, B. N87-10239
MCCORMICK, M. P. N87-10270
N87-10337
MCCUNE, W. N87-10726
MCDUFF, G. G. N87-10727
MCFADDEN, P. D. N87-10061
MCGEE, THOMAS J. N87-10323
N87-10371
MCHUGH, S. L. N87-10220
N87-10221
MCILWAIN, C. E. N87-10557
MCKEE, M. RANDALL N87-10805
MCLENNAN, G. A. N87-10777
MCNEAL, R. J. N87-10615
MCNICE, G. T. N87-10321
MCPHERSON, RONALD D. N87-10420
MCVEY, B. D. N87-10383
MEASURE, EDWARD M. N87-10294
MEDINA, R. S. N87-10379
MEEHAN, R. T. N87-10697
MEEK, C. E. N87-10457
N87-10474
N87-10475
N87-10496
MEGIE, G. N87-10344
N87-10346
N87-10364
N87-10373
N87-10616
MEIER, GERD E. A. N87-10048
MEIROVITCH, LEONARD N87-10172
MELFI, S. H. N87-10300
N87-10331
N87-10336
MELNIK, R. E. N87-10043
MELNITCHENKO, V. N87-10707
MENG, CHING-I. N87-10559
MENTALL, J. E. N87-10618
MENTEK, JOSEPH STANLEY N87-10792
MENZIES, R. T. N87-10363
MEREWETHER, K. O. N87-10441
N87-10501
MERRIGAN, M. A. N87-10257
MERRILL, ROBERT T. N87-10635
MESNARD, R. N87-10135
MESQUITA, LUIS CLEMENTE N87-10181
MEYER, THEODORE E. N87-10058
MEYER, W. N87-10125
MICHAILOVA, G. N87-10570
MICHELSON, E. N87-10256
MIDGLEY, P. N87-10614
MIDY, F. N87-10694
MIGULIN, V. V. N87-10588
MIKAWA, R. E. N87-10715
MIKKAILOV, V. M. N87-10701
MILHAUD, C. N87-10706
N87-10707
MILHAUD, C. L. N87-10705
MILLER, DAVID S. N87-10042
MILLER, M. C. N87-10713
MILROD, J. N87-10282
N87-10296
MILTON, M. J. T. N87-10289
MINAIRE, P. N87-10684
N87-10689
MINOTA, T. N87-10015
MIRONOV, V. L. N87-10307
MITCHELL, ANDREW M. N87-10391
MITSEL, A. A. N87-10306
MIYAZAKI, YOSHIRO N87-10027
MOCHIZUKI, MASATAKA N87-10028
MOGILEVSKY, M. M. N87-10546
N87-10554
N87-10569
N87-10582
N87-10585
N87-10587
N87-10588
MOHNEN, V. A. N87-10615
MOHTAI, TSUNEAKI N87-10028
MOLCHANOV, O. A. N87-10569
N87-10580
N87-10582
N87-10584
N87-10585
N87-10587
N87-10588
MOLCHANY, JEROME W. N87-10759
MOMBOURQUETTE, C. N87-10239
MONCHANT, M. N87-10554
MONTAGUE, A. F. N87-10257
MOODY, JOSEPH WARD N87-10807
MOODY, N. R. N87-10197
MOONEY, F. W. N87-10059
MOORE, J. N87-10224
N87-10234
N87-10235
MORGAN, PAUL N87-10526
MORRIS, J. W., JR. N87-10238
MORRIS, LESTER N87-10209
MORUKOV, B. V. N87-10668
N87-10698
MOULD, J. R. N87-10790
MOUNIER, Y. N87-10663
MOUNIER, YVONNE N87-10662
MUGELLESI, R. N87-10143
MULIARCHIK, T. M. N87-10561
MULLEN, STEPHEN N87-10712
MURMAN, EARLL M. N87-10744
MURPHY, JESSE K. N87-10106
MURRAY, E. R. N87-10375

N

NAATS, I. E. N87-10301
N87-10309
NADEEV, A. I. N87-10332
NAKAGAWA, TAKEO N87-10048
NAKAI, Y. N87-10136
NAKAJIMA, HIROSHI N87-10014
NAKANE, H. N87-10338
NAKATSUJI, HIROYUKI N87-10020
NANDKUMAR, RADHA N87-10799
NAPFEL, HANS F. N87-10095
NASH, ANA GOMES N87-10794
NASTROM, G. D. N87-10459
N87-10461
N87-10470
N87-10482
NEAL, T. R. N87-10414
NEALE, L. N87-10667
NEBOLSIN, M. F. N87-10303
NEGISHI, KANJI N87-10025
NEIDLINGER, H. H. N87-10211
NELAN, EDMUND PAUL N87-10783
NELLEN, B. N87-10754
NELLES, H. N87-10086
NELSON, B. D. N87-10727
NEMEC, J. M. N87-10790
NEWELL, J. F. N87-10176
NEWELL, R. E. N87-10616
NEY, R. N87-10491
NICHOLS, M. A. N87-10760
NICHOLS, M. C. N87-10191
NICOL, DAVID M. N87-10719
NIELSEN, E. N87-10606
NIEUWOLT, S. N87-10656
NIKOLAENKO, L. M. N87-10556
N87-10587
N87-10603
NISHIKAWA, NOBUHIDE N87-10017
NISHIMURA, N. N87-10413
NISHIMURA, YOICHI N87-10028
NITSCHE, J. A. N87-10737
NIXON, DAVID N87-10047
NOGUES, C. N87-10706
NOKES, W. A. N87-10540
NOMURA, A. N87-10314
N87-10345
NOMURA, TAKESHI N87-10255
NORMAN, M. L. N87-10823
NORRIS, CONSTANCE N87-10226
NORSK, P. N87-10676
NOUEL, F. N87-10135
NOWAK, S. N87-10405
NUMBERGER, K. N87-10079
NUSSHARDT, R. N87-10191

O

OBRIEN, K. N87-10822
OCONNOR, D. G. N87-10393
ODA, MINORU N87-10011
ODONNELL, FRANKLIN N87-10788
OGANOV, V. S. N87-10684
N87-10686
N87-10688
N87-10706
N87-10708
OGILVIE, P. L. N87-10044
OGUNTOYINBO, J. S. N87-10642
OKA, KEISUKE N87-10028
OKAMURA, S. N87-10763
OKE, J. B. N87-10789
N87-10790
OKE, T. R. N87-10636
N87-10637
OKUBO, Y. N87-10763
OLDENBORG, R. C. N87-10388
OMENETTO, N. N87-10322
OMRY, DAN N87-10106
ONEILL, A. N87-10617
ONO, SHUJI N87-10129
N87-10140
ONO, T. N87-10314
OSHIMA, K. N87-10019
OSHIMA, KOICHI N87-10029
OSHIMA, YUKO N87-10016
OSORIO, J. N87-10131
OSSWALD, G. A. N87-10040
OSTANIN, S. A. N87-10308
OSTERWEIL, L. N87-10723
N87-10725
OSWALD, FRED B. N87-10391
OTSUKA, N. N87-10313
OVERBEEK, R. N87-10726
OWEN, T. E. N87-10109

P

PADILLA, PETER A. N87-10731
PADMANABHAMURTY, B. N87-10643
PAGE, JOHN K. N87-10651
PAIN, T. N87-10364
PAL, S. R. N87-10273
N87-10293
PALLASCHKE, S. N87-10120
N87-10128
PALLE, S. N87-10684
N87-10685
N87-10689
N87-10690
PALUCCI, A. N87-10366

PANDEY, R. N57-10576
PARKER, J. N87-10479
PARKS, G. K. N87-10595
PARROT, M. N87-10589
PARVANOV, O. P. N87-10349
PARVEZ, S. N87-10122
PATAT, L. N87-10677
PATTON, J. F. N87-10710
PEDERSEN, ARNE N87-10548
PEDRINI, A. N87-10322
PELLAT, R. N87-10577
PELLINEN, R. J. N87-10607
PELON, J. N87-10344
N87-10373
PENAZZI, G. N87-10493
PENKETT, S. A. N87-10615
PEQUIGNOT, J. M. N87-10700
PERLIKOV, A. M. N87-10584
PERRAUT, S. N87-10586
N87-10605
PERRY, LEON N87-10788
PESQUIES, P. N87-10706
N87-10707
PETERHAENSEL, W. N87-10120
PETERS, R. N87-10489
PETERS, ROBERT M. N87-10523
PETHERAM, J. C. N87-10285
PETITDIDIER, M. N87-10445
N87-10446
N87-10480
N87-10491
N87-10493
PETKOV, N. P. N87-10593
PETRI, K. N87-10333
PETRILLA, RICHARD L. N87-10350
PETRONI, R. N87-10356
PETROV, V. N87-10595
PEYRIN, L. N87-10700
PHELPS, KIRKMAN R. N87-10375
PHILBRICK, C. RUSSELL N87-10443
PIERCE, K. G. N87-10189
PILI, P. N87-10315
PILONCHERY, G. N87-10691
PITKAENEN, J. N87-10392
PITTMAN, JAMES L. N87-10042
PIVOVAROV N87-10565
PIZZOLATI, P. L. N87-10317
PLATT, U. N87-10615
PLUMB, R. A. N87-10617
PLUMMER, D. N87-10114
POCHA, J. J. N87-10141
PODGORNY, I. M. N87-10566
POIRIER, J. L. N87-10678
POKHUNKOV, A. A. N87-10599
POKRAS, V. M. N87-10554
PONOMAREV, YU. N. N87-10306
N87-10369
PONSARDIN, P. N87-10286
POOLE, L. R. N87-10341
POPOV, A. A. N87-10309
POPOVA, I. A. N87-10698
PORTE, F. N87-10164
PORTER, DAVID HENRY N87-10806
POST, M. J. N87-10327
POTTELETTE, R. N87-10591
POTTIER, J. M. N87-10698
POTTIER, J.-M. N87-10677
POULETTY, PH. N87-10680
POURCELOT, L. N87-10677
N87-10696
N87-10700
POYNTER, R. L. N87-10814
POZDNYAK, S. I. N87-10233
POZIN, P. A. N87-10233
PRATHER, M. N87-10614
PREMACK, TIMOTHY N87-10721
PRICE, WILLIAM E. N87-10765
PRIETO, T. N87-10120
PRIGGE, R. N87-10152
PROBST, K. N87-10079
PRVANOV, O. P. N87-10304

Q

QINXIN, KONG N87-10357
QUENZEL, H. N87-10269
N87-10274
QUINN, ROGER DENNIS N87-10166
QUINTY, P. N87-10493

R

RADWAN, SAMIR FARID N87-10005
RAHN, DEBRA J. N87-10659
RAJASINGH, C. K. N87-10144
RAJENDRAPRASAD, P. N87-10127
RAKHMANOV, A. S. N87-10686
N87-10688
RAMAKRISHNAN, SRINIVASAN N87-10397
RANEY, J. P. N87-10170
RANGWALLA, AKIL ABBAS N87-10262
RANK, ERNST N87-10740
RANSOM, V. H. N87-10735
RASPOPOV, O. M. N87-10584
RASTOGI, P. K. N87-10437
N87-10462
N87-10512
N87-10520
RAUCH, J. L. N87-10570
N87-10571
N87-10572
N87-10574
N87-10582
RAVISHANKARA, A. R. N87-10613
RAY, JAMES A. N87-10071
N87-10074
RAYMER, M. G. N87-10382
RAZENKOV, I. A. N87-10278
REBIZANT, J. N87-10216
REBOLLO, CH. N87-10680
REDIESS, H. A. N87-10102
REEDY, R. C. N87-10621
REID, I. M. N87-10474
N87-10475
REINLEITNER, L. A. N87-10606
REME, H. N87-10553
N87-10560
N87-10561
N87-10564
N87-10585
N87-10595
RENARD, CL. N87-10599
RENGER, W. N87-10269
RENNIER, A. D. N87-10516
REYNOLDS, PAUL F., JR. N87-10719
RIANT, P. N87-10163
RIBEZZO, S. N87-10366
RICCITIELLO, SALVATORE R. N87-10205
RICHMOND, A. D. N87-10525
RIDDLE, A. C. N87-10508
N87-10524
RIFFAT, G. N87-10684
N87-10685
N87-10689
N87-10690
RITCHIE, R. P. N87-10222
RITTER, K. J. N87-10298
ROBERTS, C. A. N87-10093
ROBERTS, GLYN O. N87-10766
ROBERTS, THOMAS M. N87-10185
ROBINSON, A. P. N87-10222
ROBINSON, S. L. N87-10197
ROESLER, F. L. N87-10347
ROESNICK, M. N87-10085
ROFER, C. N87-10388
ROGERS, J. W., JR. N87-10218
ROMANI, PAUL NICHOLS N87-10815
ROMIG, A. D., JR. N87-10198
RONCIN, A. N87-10677
ROSEN, J. M. N87-10310
ROSENAU, G. N87-10098
ROSENBERG, A. N87-10285
N87-10365
ROSSI, G. N87-10322
ROTTGER, J. N87-10424
N87-10425
N87-10432
N87-10437
N87-10465
N87-10472
N87-10473
N87-10494
N87-10495
N87-10510
N87-10522
ROTTGER, JURGEN N87-10428
N87-10435
N87-10449
N87-10450
N87-10451
N87-10463
N87-10477
N87-10478
ROUX, A. N87-10577
ROUX, D. N87-10561
N87-10564
N87-10565
N87-10573
N87-10576
RUBEN, H. D. N87-10081
RUDENKO, V. P. N87-10306
RUEPPEL, R. A. N87-10112
RUMMEL, J. A. N87-10709
RUSSELL, J. A. N87-10537
RUSSELL, RICHARD A. N87-10170

S

SABBAGH, HAROLD A. N87-10185
SABBAGH, L. DAVID N87-10185
SACHIDANANDAMURTHY, K. N. N87-10244
SAGARTZ, M. J. N87-10415
SAGDEEV, R. Z. N87-10587
SAGGIO, F., III N87-10094
SAHA, A. K. N87-10359
SAIGAL, SUNIL N87-10401
SAINT-MARC, A. N87-10595
SAKURAI, K. N87-10279
SAKURAI, YASUSHI N87-10021
SALBY, M. N87-10617
SALIK, A. N87-10333
SALUS, ALAN M. N87-10779
SAMARSKH, A. A. N87-10038
SAMII, M. N87-10136
SAMOKHVALOV, I. V. N87-10304
SAMOROKIN, N. I. N87-10601
SAMPAIO, R. N87-10260
N87-10261
SANCHEZDECARMONA, LUIS N87-10649
SANDAHL, INGRID N87-10596
SANDELL, R. S. N87-10223
SANDER, S. P. N87-10613
SANO, H. N87-10324
SANTELLA, M. L. N87-10199
SASANO, Y. N87-10338
SASANO, YASUHIRO N87-10275
SASSEN, KENNETH N87-10350
SASSOLAS, A. N87-10703
SATO, T. N87-10763
SATO, TORU N87-10436
N87-10509
SATRAN, DALE R. N87-10039
SAUTER, JUDITH A. N87-10123
SAUVAUD, J. A. N87-10543
N87-10544
N87-10547
N87-10554
N87-10561
N87-10564
N87-10595
SAVILOV, A. A. N87-10701
SCARF, F. L. N87-10813
N87-10814
SCHATTE, C. N87-10704
SCHEFER, R. W. N87-10253
SCHEFFLER, A. O. N87-10464
SCHERTZ, W. W. N87-10252
SCHISSEL, P. N87-10211
SCHLATTER, THOMAS W. N87-10427
SCHMITT, M. J. N87-10383
SCHNEIDER, R. P. N87-10517
SCHOTLAND, R. M. N87-10360
SCHOTLAND, RICHARD M. N87-10280
SCHULTZ, A. J. N87-10768
SCHURATH, U. N87-10615
SCHWEMMER, G. K. N87-10282
N87-10283
N87-10291
N87-10296
SCHWENZFEGER, K. J. N87-10736
SCHWIESOW, R. L. N87-10362
SCRIMGEOUR, ALISON C. N87-10235
SECHRIST, C. F., JR. N87-10347
SELLECK, C. B. N87-10722
SEMPORE, B. N87-10687
SEMUSHIN, S. A. N87-10038
SENATOROV, A. K. N87-10233
SENFT, D. C. N87-10347
SERAFIMOV, K. N87-10592
SHAFI, Q. N87-10602
SHAMS, M. Y. N87-10325
SHARIN, P. O. N87-10308
SHELEVOY, K. D. N87-10332
SHELSWELL, P. N87-10222
SHEPHERD, KEVIN P. N87-10749
SHIBAEV, I. G. N87-10569
SHIBATA, T. N87-10297
N87-10342
SHIMATANI, SHUNICHI N87-10255
SHIMIZU, H. N87-10338
SHIMIZU, HIROSHI N87-10374
SHIPILIN, A. V. N87-10037
SHIRVINSKAYA, M. A. N87-10686
SHOHET, H. N. N87-10068
SHOLLENBERGER, SCOTT B. N87-10002

SHUART, MARK JAMES N87-10403
SHUISKAYA, F. K. N87-10560
N87-10564
SHURE, MARK ALAN N87-10791
SIDOROV, B. G. N87-10303
SIKKA, V. K. N87-10201
SIM, ALEX G. N87-10103
SIMONS, R. N. N87-10232
SINAH, D. N87-10239
SINGH, U. N. N87-10290
N87-10291
N87-10370
N87-10372
SIVTSEVA, L. D. N87-10603
SKIPPER, J. KERRY N87-10117
SKON, JOY M. N87-10227
SKURATOVA, S. A. N87-10686
SLABINSKI, VICTOR J. N87-10151
SLATER, DONALD WAYNE N87-10628
SLATER, JAMES A. N87-10058
SLINEY, HAROLD E. N87-10179
SMALLEY, M. J. N87-10114
SMITH, R. B. N87-10295
SMITH, STEVEN A. N87-10443
N87-10466
N87-10467
SMITH, STEVEN ANDREWS N87-10631
SMITH, TRACY LORRAINE N87-10427
SMYSHLIAEV, V. M. N87-10607
SMYTH, WILLIAM H. N87-10811
SOLDATKIN, N. P. N87-10303
SOLIES, UWE PETER N87-10009
SOLOMONOFF, A. N87-10745
SOMA, P. N87-10132
SOMASHEKAR, B. R. N87-10404
SOSNIN, A. V. N87-10302
SPINHIRNE, J. D. N87-10348
SPROTT, J. C. N87-10240
SRIDHAR, S. N87-10531
SROGA, J. N87-10365
STACHIW, J. D. N87-10105
STAHARA, STEPHEN S. N87-10003
STAMPER, DAVID A. N87-10759
STEFFEN, J. E. N87-10590
STEINHOFF, J. N87-10043
STEPANOV, A. E. N87-10603
STEPHAN, EDWIN A., JR. N87-10758
STETSON, KARL A. N87-10377
STEWART, D. F. N87-10693
STEWART, R. N87-10671
STEWART, R. C. N87-10619
STICKLER, J. A. N87-10059
STINCHCOMB, W. W. N87-10183
STITT, G. R. N87-10514
N87-10515
STOKER, C. R. N87-10812
STOKES, GRANT H. N87-10316
STOKHOLM, M. N87-10605
STRAUCH, R. C. N87-10471
STRAUCH, R. G. N87-10429
N87-10486
STREIT, G. E. N87-10388
STRUVE, K. W. N87-10756
STUCHEBROV, G. A. N87-10302
STUCKENBERG, NORBERT N87-10067
STUPIN, DAVID M. N87-10316
SUGAMA, T. N87-10213
SUGIMOTO, N. N87-10338
SUIT, WILLIAM T. N87-10101
SULZER, MICHAEL P. N87-10513
SUMANTRAN, V. N87-10007
SUNESSON, A. N87-10318
N87-10355
SUNG, BONGZOO N87-10006
SUNG, J. C. N87-10413
SURESH, S. N87-10416
SUZUKI, AKIRA N87-10017
SVANBERG, S. N87-10355
SWANSON, R. L. N87-10590
SWARTZ, W. N87-10473
SZCZUR, MARTHA N87-10720
SZE, N. D. N87-10613
SZE, ROBERT CHIA-TING N87-10384
SZTANKAY, Z. G. N87-10351

T

TAESLER, ROGER N87-10645
TAGUCHI, FUJITAKA N87-10319
TAI, KING-SHENG N87-10634
TAKAKI, RYUJI N87-10012
TAKEUCHI, N. N87-10279
N87-10338
TANAKA, A. N87-10119
TANAKA, Y. N87-10583
TANAKA, YOSHIO N87-10026
TARNAVSKY, G. A. N87-10031
TAYLOR, G. R. N87-10697
TAYLOR, L. V. N87-10266
TAYLOR, R. C. N87-10379
TCHAMURLIEV, G. N87-10707
TEDESCHI, WILLIAM JOHN N87-10051
TEITELBAUM, H. N87-10446
TELES, J. N87-10136
TEMERIN, MICHAEL A. N87-10545
TENNIS, GEORGE T. N87-10058
TESHIMA, KOJI N87-10020
TESSIER, C. N87-10161
THEILEN-WILLIGE, BARBARA N87-10529
THIDE, B. N87-10498
THOMAS, D. N87-10446
THOMAS, KEVIN N87-10430
THOMAS, L. N87-10339
N87-10343
THOMAS, T. M. N87-10536
THOMPSON, R. L. N87-10080
THOMPSON, W. C., III N87-10724
THOMSON, D. W. N87-10469
THORNTON, EARL A. N87-10406
TIMM, RAINER N87-10048
TIMOFEEV, E. E. N87-10551
N87-10607
TIMOTHY, J. G. N87-10236
TITOVA, E. E. N87-10569
N87-10580
N87-10582
N87-10584
TIWARI, SURENDRA N. N87-10187
TIXIER, M. N87-10575
TOLSTYKH, A. I. N87-10032
TOMPKINS, STEPHEN S. N87-10184
TONG, T. W. N87-10259
TORRE, CHARLES GREGORY N87-10770
TOSHEV, E. T. N87-10035
TOURASSIS, VASSILIOS DIMITRIOS N87-10390
TRAKHTENGERTZ, V. YU. N87-10584
TREILHOU, J. P. N87-10595
TREILHOU, J.-P. N87-10558
TREUMANN, R. N87-10591
TREVINO, G. N87-10251
TRINDADE, M. B. N87-10394
TROUTMAN, PATRICK A. N87-10662
N87-10663
TROXEL, S. W. N87-10321
TRUMPY, S. N87-10118
N87-10134
TSUCHIHASHI, HACHIRO N87-10028
TUCK, A. F. N87-10616
TURCOTTE, LOUIS H. N87-10411
TURKEL, E. N87-10745
TURNER, M. S. N87-10801
TYERYAR, JAMES R. N87-10206
TZENG, PEI YUAN N87-10243
TZUOO, KEH L. N87-10047
TZVI, GAL-CHEN N87-10421

U

UEHARA, KIYOJI N87-10319
UENO, T. N87-10279
ULBRICH, C. W. N87-10473
ULITSKY, A. N87-10295
ULIVIERI, C. N87-10118
UNEUS, L. N87-10355
UNRUH, WESLEY P. N87-10316
USHAKOV, A. S. N87-10698
UTASHIMA, M. N87-10119

V

VALLINKOSKI, M. K. N87-10607
VANDENBOSCH, PETER M. N87-10711
VANDERHA, JOZEF N87-10148
VANDERPLOEG, J. M. N87-10693
VANDERVELDE, W. E. N87-10167
N87-10168
VANHOLTZ, L. N87-10126
VANKLEECK, J. N87-10175
VANTUYL, ANDREW HUGH N87-10670
VANZANDT, T. E. N87-10434
N87-10448
N87-10481
N87-10482
VANZANDT, THOMAS E. N87-10466
VAUGHAN, G. N87-10339
N87-10343
N87-10616
VAUGHAN, J. M. N87-10326
VAUGHAN, W. R. N87-10268
VERFUERTH, R. N87-10741
VICO, L. N87-10684
N87-10685
N87-10689
N87-10690
VIEILLEFOND, H. N87-10678
VIEVILLE, T. N87-10692
VILLAIN, J. P. N87-10600
VINCENT, M. N87-10699
N87-10703
VINCENT, R. A. N87-10431
N87-10458
N87-10468
N87-10490
N87-10507
N87-10617
VINCENT, ROBERT A. N87-10453
VIRDEE, L. N87-10156
N87-10158
VISWANATHAN, G. N87-10497
VIVIANO, JEROME J. N87-10228
VOELZ, D. G. N87-10347
VOEVODIN, V. G. N87-10302
VOGT, P. G. N87-10753
VOLKOMISKAYA, L. V. N87-10571
VOLKOV, M. A. N87-10551
VOLOSEVICH, A. V. N87-10551
VONLAUE, H.-D. N87-10099
VOSKRESENSKY, G. P. N87-10030
N87-10033
VRTILEK, SAEQA DIL N87-10804

W

WAI, MICKEY MAN-KUI N87-10673
WAKASUGI, KOICHIRO N87-10426
WALDEN, H. N87-10282
N87-10296
WALDMANN, D. N87-10078
WALIGORA, J. N87-10697
WALKER, ERNIE D. N87-10177
WALKER, RANDALL N87-10226
WALKINGTON, N. J. N87-10751
WALLER, P. N87-10068
WALLERSTEIN, GEORGE N87-10789
WANG, H. H. N87-10768
WARBURTON, PENELOPE J. N87-10619
WARD, J. W. N87-10216
WARD, S. J. N87-10218
WAREING, D. N87-10339
WAREING, D. P. N87-10343
WARNOCK, J. M. N87-10448
N87-10470
N87-10502
WARREN, J. B. N87-10213
WATTERS, D. M. N87-10097
WEBB, ERNEST N. N87-10375
WEBBER, M. C. N87-10141
WEBER, B. L. N87-10429
WEBER, O. N87-10098
WEDEKEN, U. N87-10605
WEIHE, W. H. N87-10648
WEINLAND, S. L. N87-10220
N87-10221
WEINMAN, J. A. N87-10316
WEINMASTER, R. R. N87-10217
WEINSTOCK, J. N87-10452
WELCH, S. M. N87-10812
WELLS, J. G. N87-10268
WENDT, W. N87-10318
N87-10355
WENG, C. Y. N87-10283
WERNER, CH. N87-10269
WHANGBO, M. H. N87-10768
WHIPPLE, RAYMOND D. N87-10041
WHITE, R. J. N87-10709
WHITE, WILLIAM L. N87-10041
WHITEMAN, D. N87-10331
WICKS, T. W. N87-10751
WICKWAR, V. B. N87-10563
WIENGARN, N. N87-10125
WILEY, B. J. N87-10207
WILKERSON, T. D. N87-10291
N87-10298
N87-10370
N87-10372
WILLIAMS, J. M. N87-10768
WILLIAMS, MORRIS N87-10209
WILLIAMS, ROBIN G. N87-10672
WILLIAMS, S. R. N87-10469
N87-10489
WILSON, HOWARD B. N87-10411
WILSON, KENNETH EARL N87-10825
WINCKLER, J. R. N87-10590
WNUK, K. N87-10078

WOBBE, H. N87-10159
WOFSY, S. C. N87-10614
WOLFIRE, MARK GUY N87-10803
WOODMAN, R. F. N87-10446
WOODMAN, RONALD F. N87-10513
WOODRUM, ARTHUR N87-10711
WOODS, P. T. N87-10261
N87-10289
WORTMAN, A. N87-10702
WRIGHT, THOMAS W. N87-10412
WU, C. S. N87-10578
WUENSCH, B. N87-10754

Y

YAMAMOTO, TADASHI N87-10026
YAMANOUCHI, HIROSHI N87-10028
YAMBE, M. N87-10119
YAN, HENGYUAN N87-10004
YING, W. P. N87-10520
YOSHIMURA, ATSUNARI N87-10255
YOSHIZAWA, YOSHIMASA N87-10014
YOUNG, S. A. N87-10271
YOUSUFF, AJMAL N87-10408
YSERENTANT, HARRY N87-10742
YU, L. H. N87-10380
YUROV, V. E. N87-10569
N87-10582
N87-10584

Z

ZACCANTI, C. N87-10315
ZAICHICK, V. E. N87-10688
ZAITZEV, A. N. N87-10595
ZALIK, RICHARD A. N87-10407
ZANZOTTERA, E. N87-10317
N87-10356
ZAPOTOCNY, JOHN VICTOR N87-10668
ZAPRYANOV, Z. D. N87-10035
ZARDECKI, A. N87-10228
N87-10316
N87-10386
ZARROUATI, O. N87-10121
ZEINER, PETER K. N87-10072
ZELLNER, R. N87-10613
ZELTZER, HARRY I. N87-10712
ZHANG, HANXIN N87-10004
ZHAO, YAN-ZENG N87-10360
ZHAO, YANZENG N87-10280
ZHURIN, V. V. N87-10037
ZIMMERMAN, R. K. N87-10494
N87-10510
ZININ, L. V. N87-10566
N87-10567
N87-10582
ZINNIE, L. V. N87-10565
ZIPSER, EDWARD J. N87-10423
ZOBLER, D. N87-10135
ZUEV, A. E. N87-10307
ZUEV, V. E. N87-10301
N87-10302
N87-10303
N87-10304
N87-10305
N87-10306
N87-10308
N87-10309
N87-10332
ZUEV, V. V. N87-10369

CORPORATE SOURCE INDEX

Typical Corporate Source Index Listing

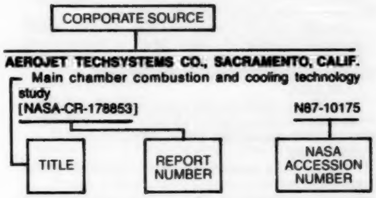
CORPORATE SOURCE
AEROJET TECHSYSTEMS CO., SACRAMENTO, CALIF.
Main chamber combustion and cooling technology study
[NASA-CR-178853]
N87-10175
TITLE
REPORT NUMBER
NASA ACCESSION NUMBER

Listings in this index are arranged alphabetically by corporate source. The title of the document provides the user with a brief description of the subject matter. The report number helps to indicate the type of document cited (e.g., NASA report, translation, NASA contractor report). The NASA accession number denotes the number by which the citation is identified. The titles are arranged under each corporate source in ascending accession number order.

A

ACADEMIA SINICA, BEIJING (CHINA).

Detection of NO sub x, C2H4 concentrations by using CO and CO2 lasers N87-10357

ACADEMY OF SCIENCES, SOFIA (BULGARIA).

Investigation of clouds spatial distribution using ground-based lidar N87-10349

ACADEMY OF SCIENCES (USSR), APATITY.

Small scale structures of electric field variations and particle precipitations as observed onboard AUREOL-3 satellite N87-10569

On the spectral broadening of the ground-based VLF transmitter signals in the high-latitude ionosphere observed from Intercosmos-19 and AUREOL-3 satellites N87-10584

ACADEMY OF SCIENCES (USSR), MOSCOW.

Computational aerodynamics of supersonic lifting vehicles N87-10030

The third order compact schemes for fluid dynamic problems N87-10032

Supersonic flow around tip sides of wings N87-10033

Mathematical and computational models of plasma flows N87-10036

The numerical method of calculation of two-dimensional stationary electro-gasdynamic internal flows N87-10037

Computer simulation in engineering hydrodynamics N87-10038

Models of electric potential and current distribution in stable discrete auroral forms N87-10551

Detection of suprathermal O(+) ions inside the plasmasphere N87-10554

Observations of low intensity particle fluxes inside the region of the ionospheric main trough and their variability N87-10556

Polar cap particle precipitation as measured by the AUREOL-3 and Intercosmos-19 satellites N87-10560

Nonstationary field-aligned fluxes of thermal ions O(+) and H(+) outside the plasmapause: Refinement of the polar wind theory N87-10566

Field-aligned motions of O(+) and H(+) thermal ions in a magnetic field tube convected across the dayside polar cusp: Model calculations N87-10567

Fine structure of fields and plasma in the field-aligned current region on the Intercosmos-Bulgaria-1300 satellite data N87-10568

Polarization of electromagnetic waves recorded on board the AUREOL-3 satellite N87-10571

Precipitation of electrons and protons in the subauroral zone stimulated by ground-based VLF emitter N87-10585

Very low frequency and ELF effects in the upper ionosphere caused by large-scale acoustic waves in the lower ionosphere observed from AUREOL-3 satellite N87-10587

Earthquake effects in the ionosphere according to Intercosmos-19 and AUREOL-3 satellite data N87-10588

Some results of scanner spectrophotometric measurements of aurora and airglow from IK-Bulgaria-1300 satellite and prospects of similar measurements N87-10593

Two-dimensional snapshots of electron density in the main trough and diffuse auroral zone from a close network of ionosondes: Comparison with measurements from AUREOL-3 satellite N87-10601

Coordinated data on auroral electrodynamics from ground based radar diagnostics and AUREOL-3 satellite N87-10607

ACADEMY OF SCIENCES (USSR), TOMSK.

Lidar measurements of slant visual range N87-10278

Methods for estimating the optical constants of atmospheric hazes based on complex optical measurements N87-10301

Multifrequency dial sensing of the atmospheric gaseous constituents using the first and second harmonics of a tunable CO2 laser radiation N87-10302

Remote express analysis of ground-layer aerosol based on laser-induced spark spectra N87-10303

Laser sounding of instantaneous and mean speed of wind using correlation method N87-10304

Optimal filtration of the atmospheric parameters profiles N87-10305

Optical models of the molecular atmosphere N87-10306

The influrence of an optical receiving system on statistical characteristics of a lidar signal N87-10307

Coherent lidars based on intracavity heterodyning of echo signals N87-10308

The influence of scattering particles morphology on the characteristics of lidar signals N87-10309

A combined Raman lidar for low tropospheric studies N87-10332

Spectroscopic aspects of differential method for sounding gas composition of the atmosphere N87-10369

ACADEMY OF SCIENCES (USSR), TROITSK.

Mechanism of low-frequency wave propagation in the magnetosphere N87-10580

ACADEMY OF SCIENCES (USSR), YAKUTSK.

Step-like profiles of electron density in the subauroral lower F-region in the morning sector and possible mechanisms of their formation during substorms: The comparison of data of ground-based ionosondes with the AUREOL-3 satellite measurements N87-10603

ADELAIDE UNIV. (AUSTRALIA).

Hardware requirements: A new generation partial reflection radar for studies of the equatorial mesosphere N87-10431

Mesospheric gravity-wave climatology at Adelaide N87-10456

Intercomparison and calibration of wind and wave measurements at various frequencies N87-10468

The Adelaide MF partial-reflection radar and VHF ST radar N87-10490

Measurements of antenna polar diagrams and efficiencies using a phase-switched interferometer N87-10507

ADVISORY GROUP FOR AEROSPACE RESEARCH AND DEVELOPMENT, NEUILLY-SUR-SEINE (FRANCE).

Engine-Airframe Integration for Rotorcraft
[AGARD-LS-148] N87-10067

AEROFORMATION BLAGNAC (FRANCE).

Orbitography course for ground operators N87-10157

AEROJET TECHSYSTEMS CO., SACRAMENTO, CALIF.

Main chamber combustion and cooling technology study
[NASA-CR-178853] N87-10175

AERONAUTICAL RESEARCH INST. OF SWEDEN, BROMMA.

Growth of cracks under far-field cyclic compressive loads: Numerical and experimental results
[DE86-010279] N87-10416

AERONAUTICAL RESEARCH LABS., MELBOURNE (AUSTRALIA).

Analysis of the vibration of the input bevel pinion in RAN Wessex helicopter main rotor gearbox WAK143 prior to failure
[ARL-AERO-PROP-R-169] N87-10061

AEROSPACE CORP., EL SEGUNDO, CALIF.

Orbit determination of geostationary satellites using the global positioning system N87-10133

Amplitude distribution of cosmic ray events in extrinsic IR detectors
[AD-A167692] N87-10619

AIR FORCE GEOPHYSICS LAB., HANSCOM AFB, MASS.

Evidence of atmospheric gravity wave perturbations of the Brunt-Vaisala frequency in the atmosphere N87-10438

Atmospheric waves and the nature of buoyancy turbulence in the context of the waves VS 2D-turbulence debate N87-10439

A proposed experimental test to distinguish waves from 2-D turbulence N87-10440

AIR FORCE INST. OF TECH., WRIGHT-PATTERSON AFB, OHIO.

Application of bifurcation and catastrophe theories to near stall flight mechanics
[AD-A167697] N87-10046

AIR FORCE SYSTEMS COMMAND, WRIGHT-PATTERSON AFB, OHIO.

Acta Aeronautica et Astronautica Sinica (selected articles)
[AD-A167916] N87-10004

AIR FORCE WRIGHT AERONAUTICAL LABS., WRIGHT-PATTERSON AFB, OHIO.

Air Force technical objective document fiscal year 1987
[AD-A167324] N87-10779

AKADEMIYA NAUK SSSR, NOVOSIBIRSK.

Numerical modeling of spatial flows on the basis of splitting up method N87-10031

ALABAMA UNIV., UNIVERSITY.

Foundation interaction problems involving an elastic half-plane
[AD-A167925] N87-10411

ALASKA UNIV., FAIRBANKS.

Gravity waves in the middle atmosphere: Recent progress and needed studies N87-10433

Simultaneous rocket and MST radar observation of an internal gravity wave breaking in the mesosphere N87-10443

Observations and a model of gravity-wave variability in the middle atmosphere N87-10453

Mesospheric wave number spectra from Poker Flat MST radar measurements compared with gravity-wave model N87-10466

Evidence of a saturated gravity-wave spectrum throughout the atmosphere N87-10467

Consequences of imperfect magnetosphere-ionosphere coupling N87-10549

Gravity wave dynamics near the mesopause over Poker Flat, Alaska N87-10631

A study of disturbed solar wind and magnetotail based on ISEE-3 data
[NASA-CR-177060] N87-10816

Three-dimensional structure of the heliosphere: Quiet-time and disturbed periods N87-10818

AMALGAMATED TECHNOLOGIES, INC., SCOTTSDALE, ARIZ.

Surface attack on metals in the presence of liquid metals
[AD-A167403] N87-10193

ANACAPA SCIENCES, INC., FORT RUCKER, ALA.

Human factors research in aircrew performance and training
[AD-A167950] N87-10714

ANALYTICAL MECHANICS ASSOCIATES, INC., HAMPTON, VA.
Shuttle derived atmospheric density model. Part 1: Comparisons of the various ambient atmospheric source data with derived parameters from the first twelve STS entry flights, a data package for AOTV atmospheric development
[NASA-CR-171824] N87-10662
Shuttle derived atmospheric density model. Part 2: STS atmospheric implications for AOTV trajectory analysis, a proposed GRAM perturbation density model
[NASA-CR-171824] N87-10663

ARECIBO IONOSPHERIC OBSERVATORY, PUERTO RICO.
The influence of velocity variability on the determination of wind profiles N87-10428
Need for a subtropical wind profiling system N87-10432
Half-day and four-day waves in the statosphere N87-10435
Determination of the Brunt-Vaisala frequency from vertical velocity spectra N87-10449
The use of the experimentally deduced Brunt-Vaisala frequency and turbulent velocity fluctuations to estimate the eddy diffusion coefficient N87-10450
The relation of gravity waves and turbulence in the mesosphere N87-10451
On the varying slope of velocity spectra N87-10463
Comparison of reflectivity and wind profiles measured on 46.8 MHz and 430 MHz at the Arecibo Observatory N87-10477
MST radar networks and campaigns session summary and recommendations N87-10478
Investigations of the lower and middle atmosphere at the Arecibo Observatory and a description of the new VHF radar project N87-10494
Method to determine the optimal parameters of the Arecibo 46.8-MHz antenna system N87-10510
Optimum coding techniques for MST radars N87-10513
On the use of colour reflectivity plots to monitor the structure of the troposphere and stratosphere N87-10522

ARGONNE NATIONAL LAB., ILL.
Analysis of heat-pipe absorbers in evacuated-tube solar collectors
[DE86-010764] N87-10252
Possibility of obtaining coherent short wave radiation from a solid state free electron laser
[DE86-010525] N87-10381
Bioconversion: A New Technology for Waste and Sludge Disposal. Workshop proceedings
[DE86-009668] N87-10539
Parallel logic programming for numeric applications
[DE86-011004] N87-10726
Sulfur-based synthetic metal superconductors
[DE86-010512] N87-10768
ANL/RBC: A computer code for the analysis of Rankine bottoming cycles, including system cost evaluation and off-design performance
[NASA-CR-179462] N87-10777

ARIANESPACE, EVRY (FRANCE).
Analysis of the problem of satellite launch windows for Ariane dual launches N87-10115

ARIZONA UNIV., TUCSON.
Correction function in the Lidar equation and the solution techniques for CO2 Lidar date reduction N87-10280
Coherent lidar signal fluctuation reduction by means of frequency diversity technique N87-10360
In-flight absolute radiometric calibration of the LANDSAT thematic mapper N87-10530
High resolution spectroscopy of quasar absorption lines N87-10785

ARMY AVIATION SYSTEMS COMMAND, ST. LOUIS, MO.
Summary of artificial and natural icing tests conducted on US Army aircraft from 1974 to 1985
[FAA/CT-85/26] N87-10064
Engine-airframe integration for rotorcraft: Component specifications and qualification N87-10071
Engine-airframe integration for rotorcraft: System specifications and qualification N87-10074

ARMY CHEMICAL RESEARCH AND DEVELOPMENT CENTER, ABERDEEN PROVING GROUND, MD.
Chemical contamination remote sensing N87-10375

ARMY NATICK LABS., MASS.
The fungal resistance or susceptibility of resins, plasticizers, and other constituents of adhesive formulations
[AD-A166930] N87-10207

ARMY RESEARCH INST. OF ENVIRONMENTAL MEDICINE, NATICK, MASS.
Upper and lower body anaerobic power comparison between biathletes and control subjects
[AD-A167636] N87-10710
A system for controlled presentation of the Arden contrast sensitivity test
[AD-A167969] N87-10712

ASHRAE, INC., ATLANTA, GA.
Methods of testing to determine the thermal performance of solar collectors
[DE86-009311] N87-10533

ATMOSPHERIC AND ENVIRONMENTAL RESEARCH, INC., CAMBRIDGE, MASS.
A modeling analysis program for the JPL Table Mountain Io sodium cloud data
[NASA-CR-179671] N87-10611

ATMOSPHERIC ENVIRONMENT SERVICE, DOWNSVIEW (ONTARIO).
Vertical structure of Arctic haze observed by lidar N87-10335

ATMOSPHERIC SCIENCES LAB., WHITE SANDS MISSILE RANGE, N. MEX.
Visibility related to backscatter at 1.54 micron N87-10272
Effect of backscatter-to-extinction ratio on lidar inversions N87-10294

ATOMIC WEAPONS RESEARCH ESTABLISHMENT, ALDERMASTON (ENGLAND).
Theory of wire-grid modelling: Criteria for highly conducting surfaces
[AWRE-O-20/85] N87-10224
Extension of the electromagnetic method of moments code CHAOS to treat configurations of dielectric-coated wires
[AWRE-O-18/85] N87-10234
Wire dipoles and antennas with dielectric or magnetic coatings
[AWRE-O-19/85] N87-10235
Some seismic results of an underground explosion at the Mururoa Test Site (Shot Report no. 6)
[AWRE-O-17/85] N87-10619

AUBURN UNIV., ALA.
Nonlinear rotordynamics analysis
[NASA-CR-178931] N87-10407

B

BALLISTIC RESEARCH LABS., ABERDEEN PROVING GROUND, MD.
Further results on the initiation and growth of adiabatic shear bands
[AD-A168012] N87-10412

BEN GURION UNIV. OF THE NEGEV, SEDE BOQER (ISRAEL).
Design for climate in hot, dry cities N87-10655

BHABHA ATOMIC RESEARCH CENTRE, BOMBAY (INDIA).
PLOT 3D: A multipurpose, interactive program for plotting three dimensional graphs
[DE86-702101] N87-10730
Research and development activities of the Spectroscopy Division of the Bhabha Atomic Research Centre
[DE86-702154] N87-10781

BIONETICS CORP., HAMPTON, VA.
The Helmholtz resonance behavior of single and multiple rooms
[NASA-CR-178173] N87-10749

BOEING AEROSPACE CO., KENNEDY SPACE CENTER, FLA.
Orbital transfer vehicle launch operations study. Volume 1: Executive summary
[NASA-CR-179701] N87-10110
Orbital transfer vehicle launch operations study. Volume 2: Detailed summary
[NASA-CR-179791] N87-10111

BOEING COMMERCIAL AIRPLANE CO., SEATTLE, WASH.
Fault tolerant control laws
[NASA-CR-178094] N87-10400

BOEING MILITARY AIRPLANE DEVELOPMENT, SEATTLE, WASH.
Vulnerability methodology and protective measures for aircraft fire and explosion hazards. Volume 3: On-Board Inert Gas Generator System (OBIGGS) studies. Part 1: OBIGGS ground performance tests
[AD-A167357] N87-10066

BONN UNIV. (WEST GERMANY).
Asymptotic error expansions of finite element solutions of parabolic equations N87-10738

BORER ELECTRONICS A.G., SOLOTHURN (SWITZERLAND).
Methods and standards for encryption of spacecraft telemetry and telecommand links
[RPT/ENC/62359/BO] N87-10112

BOSTON UNIV., MASS.
Electron-positron pair production by ultrarelativistic electrons in a soft photon field N87-10798

BRITISH AEROSPACE AIRCRAFT GROUP, WEYBRIDGE (ENGLAND).
Investigation into the attenuation and velocity of acoustic emissions in carbon fiber composite aircraft structures
[BAE-KGT-R-GEN-01349] N87-10180
The effects of temperature and loading rate on R-curves using the CLWL techniques
[BAE-MSM-R-GEN-0544] N87-10405

BRITISH AEROSPACE DYNAMICS GROUP, STEVENAGE (ENGLAND).
Operational strategies for multi-burn apogee maneuvers of geostationary spacecraft N87-10141

BRITISH AIRWAYS, HEATHROW (ENGLAND).
Choosing Aircraft Integrated Data Systems (AIDS) architecture suitable for Engine Health Monitoring (EHM) on future generation engines N87-10063

BRITISH ANTARCTIC SURVEY, CAMBRIDGE (ENGLAND).
Nonthermal continuum-terrestrial myriametric radiation narrowband electromagnetic emission N87-10579

BRITISH BROADCASTING CORP., KINGSWOOD (ENGLAND).
VSB 2-PSK: A modulation system for digital sound with television
[BBC-RD-1986/7] N87-10222
Review of VHF Band 1 field strength prediction
[BBC-RD-1986/4] N87-10223

BRITISH COLUMBIA UNIV., VANCOUVER.
Urban climatology and the tropical city: An introduction N87-10637

BROOKHAVEN NATIONAL LAB., UPTON, N. Y.
Chemisorption mechanism and effect of polyacrylic acid on the improvement in bond durability of zinc phosphate-to-polymer adhesive joints
[DE86-011535] N87-10213
Transverse correlations in start-up of a free electron laser from noise
[DE86-009917] N87-10380

BROWN UNIV., PROVIDENCE, R. I.
Growth of cracks under far-field cyclic compressive loads: Numerical and experimental results
[DE86-010279] N87-10416

BULGARIAN ACADEMY OF SCIENCE, SOFIA.
Hydrodynamic and thermal interaction between two spheres in a steady viscous flow N87-10035
Intercosmos-Bulgaria-1300 satellite: Large-scale structure and dynamics of the polar ionosphere during geomagnetic storms N87-10592

BUNDESMINISTERIUM FUER FORSCHUNG UND TECHNOLOGIE, BONN (WEST GERMANY).
Atmospheric Ozone 1985. Assessment of our understanding of the processes controlling its present distribution and change, volume 1
[NASA-TM-89237] N87-10612

C

CALIFORNIA INST. OF TECH., PASADENA.
Spectroscopy of the globular clusters in M87
[NASA-CR-179854] N87-10790
Investigations of radio jets in M87, 3C273 and 3C345 N87-10824

CALIFORNIA STATE DEPT. OF TRANSPORTATION, SACRAMENTO.
Development of worst case meteorology criteria
[PB86-215993] N87-10540

CALIFORNIA UNIV., BERKELEY.
Experimental identification and control of the tip position of a flexible, single link manipulator N87-10397
Magnetic field-aligned particle precipitation N87-10542
Magnetic field-aligned potential drops N87-10545
Surface photometry of early-type galaxies N87-10795
A study of hierarchical clustering of galaxies in an expanding universe N87-10806
Physical processes in collapse driven supernova N87-10808
On the tidal interaction between spherical galaxies N87-10810

CALIFORNIA UNIV., BERKELEY. LAWRENCE BERKELEY LAB.
Relationship between critical current and microstructure of internal tin wire
[DE86-009922] N87-10238
Optical systems for synchrotron radiation. Lecture 4: Soft X-ray imaging systems
[DE86-011567] N87-10761
Lawrence Berkeley Laboratory recent papers submitted and reports issued, February 1986
[DE86-011319] N87-10782

CALIFORNIA UNIV., DAVIS.
Nonreacting turbulent mixing flows: A literature survey and data base
[DE86-010864] N87-10253

A high resolution entrainment model for the convective planetary boundary layer N87-10611

CALIFORNIA UNIV., SAN DIEGO.
Equatorial magnetospheric particles and auroral precipitations N87-10557
Design support of the Burst and Transient Source Experiment (BATSE) of the Gamma Ray Observatory (GRO) mission
[NASA-CR-178920] N87-10758

CALIFORNIA UNIV., SANTA BARBARA.
A component decomposition model for evaluating atmospheric effects in remote sensing N87-10610

CARNEGIE-MELLON UNIV., PITTSBURGH, PA.
Dynamic modeling and control of robotic manipulators N87-10390
Novel parallel architectures and algorithms for linear algebra processing
[NASA-CR-179626] N87-10743

CASE WESTERN RESERVE UNIV., CLEVELAND, OHIO.
Simultaneous VHF and UHF radar observation of the mesosphere at Arecibo during a solar flare: A check on the gradient-mixing hypothesis N87-10437
A study of gravity-wave spectra in the troposphere and stratosphere at 5-min to 5-day periods with the Poker Flat MST radar N87-10462
An overview of data acquisition, signal coding and data analysis techniques for MST radars N87-10512
Interference detection and correction applied to incoherent-scatter radar power spectrum measurement N87-10520

CENTRE D'ESSAIS EN VOL, BRETIGNY-SUR-ORGE (FRANCE).
The interest of centrifuge tests for the selection of French cosmonauts N87-10678
Vestibular tests in cosmonaut selection and training N87-10694

CENTRE D'ETUDE SPATIALE DES RAYONNEMENTS, TOULOUSE (FRANCE).
Statistical study of auroral electron precipitation structures detected by the AUREOL-3 Satellite N87-10543
Positive ion distributions in the morning auroral zone: Local acceleration and drift effects N87-10547
Injection of low-energy ions during geomagnetic storms N87-10553
Evidence for ion energy dispersion in the polar cusp related to a northward directed Interplanetary Magnetic Field (IMF) N87-10561
Evidence for high latitude ionospheric ion acceleration N87-10564
A multipoint study of a substorm on 4 March 1979 N87-10595

CENTRE D'ETUDES ET DE RECHERCHES DE MEDECINE AERONAUTIQUE, PARIS (FRANCE).
Animal models in space physiology N87-10705
Contribution of animal models to the investigation of bone changes in weightlessness N87-10706
Cosmos 1514 flight: Study of rhesus monkey ECG N87-10707

CENTRE D'ETUDES ET DE RECHERCHES GEODYNAMIQUES ET ASTRONOMIQUES, GRASSE (FRANCE).
Constraints imposed by an intersatellite communication link upon stationkeeping of two close geostationary satellites N87-10162

CENTRE DE RECHERCHES EN PHYSIQUE DE L'ENVIRONNEMENT, ISSY-LES-MOULINEAUX (FRANCE).
Energy spectra of electrons precipitating above the EISCAT area. Comparison with ARCAD measurements N87-10598

CENTRE DE RECHERCHES EN PHYSIQUE DE L'ENVIRONNEMENT, SAINT MAUR DES FOSSES (FRANCE).
The PROUST radar N87-10491
Small scale and intense field-aligned currents detected by their magnetic signature N87-10546
Vertical transport of O(+) ions at high latitudes N87-10565
Density gradient instability in the high latitude ionosphere. Relation with the electrostatic turbulence and convection N87-10573
Artificial ion beam interaction with the auroral plasma N87-10591

CENTRE HOSPITALIER UNIV. RANGUEIL, TOULOUSE (FRANCE).
Cardiovascular examination during STS 51 G mission June (1985) N87-10677

CENTRE NATIONAL D'ETUDES DES TELECOMMUNICATIONS, SAINT MAUR DES FOSSES (FRANCE).
The PROUST radar: First results N87-10445
Simultaneous fine structure observation of wind and temperature profiles by the Arecibo 430-MHz radar and in situ measurements N87-10446
Scientific reasons for a network of ST radars and cooperative campaigns N87-10480

CENTRE NATIONAL D'ETUDES SPATIALES, TOULOUSE (FRANCE).
Proceedings of an International Conference on Space Dynamics for Geostationary Satellites
[ISBN-2-85428-149-7] N87-10113
Accuracy of geostationary orbit determination N87-10121
Real time orbit determination during apogee maneuvers N87-10130
Very first orbit determination after launch or main maneuvers. Applications to geostationary Telecom 1A and 1B N87-10135
Synchronous transfer orbit operation under three-axis control N87-10137
Definition of a structure for the apogee thrusts for geostationary satellite positioning: Application to TDF-1 N87-10145
Orbit and attitude operations during the Telecom 1B transfer phase N87-10147
Application of linear programming to final positioning (drift orbit) of a geostationary satellite N87-10149
Stationkeeping strategy for TDF 1 satellite N87-10154
Operational performance of the INTELSAT 5 attitude determination and control system N87-10158
Geostationary satellites: Their market, their evolution in the 1990s N87-10165
Results of the ARCAD 3 Project and of Recent Programs in Magnetospheric and Ionospheric Physics
[ISBN-2-85428-126-8] N87-10541
Infrared measurement of eye movement. Presentation of the Eye Movement in Infrared and Angular Torsion (EMIRAT) experiment N87-10695

CENTRE NATIONAL DE LA RECHERCHE SCIENTIFIQUE, LYON (FRANCE).
Hindlimb suspension effects on rat skeletal muscle response N87-10687

CENTRE NATIONAL DE LA RECHERCHE SCIENTIFIQUE, ORLEANS (FRANCE).
Simultaneous measurements of thermal electron density-temperature and low energy precipitating electron fluxes in topside ionosphere N87-10544
Attenuation bands and cut-off frequencies for ELF electromagnetic waves N87-10570
Experimental evidence of field-aligned ELF plasma ducts in the ionospheric trough and in the auroral zone N87-10574
Instabilities associated with the equatorial spread-F phenomenon and their north-south asymmetry N87-10576
Detection from AUREOL-3 of the modulation of auroral electrojet by HF-heating from ELF signals in the upper ionosphere above Tromsoe (Norway) N87-10582
Study of VLF emissions apparently associated with earthquakes from ground-based and GEOS satellites data N87-10589

CENTRE NATIONAL DE LA RECHERCHE SCIENTIFIQUE, PARIS (FRANCE).
Preliminary results on the equilibrium and vertigo experiment performed during STS 51-G shuttle flight N87-10692

CENTRE NATIONAL DE LA RECHERCHE SCIENTIFIQUE, VERRIERES-LE BUISSON (FRANCE).
Lidar stratospheric ozone measurements at the observatoire de Haute Provence (France) N87-10344
Lidar detection of metallic species at the mesopause level N87-10346
Pulsed mononode dye laser developed for a geophysical application N87-10364
Alexandrite laser source for atmospheric lidar measurements N87-10373
Comparison between S. T. radar and in situ balloon measurements N87-10447

CENTRO INFORMAZIONI STUDI ESPERIENZE, MILAN (ITALY).
Time-resolved lidar fluorosensor for sea pollution detection N87-10317
Gas correlation lidar for methane detection N87-10356

CHIBA UNIV. (JAPAN).
Images of three dimensional flows in computer graphics N87-10017

CHICAGO UNIV., ILL.
Laser induced chemical reactions and laser-collision processes
[DE86-011459] N87-10385
Possible significance of a new dimensionless ratio in cosmology
[DE86-011026] N87-10801

CINCINNATI UNIV., OHIO.
Analysis of two-dimensional incompressible flow past airfoils using unsteady Navier-Stokes equations
[NASA-CR-179823] N87-10040
Global pressure relaxation procedure with application to viscous and inviscid flows N87-10247

CIVIL AVIATION AUTHORITY, REDHILL (ENGLAND).
Application of operational flight recording to helicopters N87-10081

CLEMSON UNIV., S.C.
Observations of mesoscale vertical velocities around frontal zones N87-10424
Comparison of vertical velocities analyzed by a numerical model and measured by a VHF wind profiler N87-10425
Observations of thunder with the Arecibo VHF radar N87-10444
Observations of vertical velocity power spectra with the SOUSY VHF radar N87-10465
A comparison of thunderstorm reflectivities measured at the VHF and UHF N87-10472
UHF and VHF radar observations of thunderstorms N87-10473

CNRM, TOULOUSE (FRANCE).
The INSU and DMN network of ST radars N87-10493

COHERENT TECHNOLOGIES, INC., BOULDER, COLO.
Coherent lidar technology for global wind profiling N87-10267
Wavelength dependence of coherent and incoherent satellite-based lidar measurements of wind velocity and aerosol backscatter N87-10361

COLOGNE UNIV. (WEST GERMANY).
Horizontal wind perturbations and their relation to transient internal gravity waves N87-10457

COLORADO STATE UNIV., FORT COLLINS.
Numerical studies of thermally and mechanically forced circulations over complex terrain N87-10630
Environmental influences on hurricane intensification N87-10635
An observational study of tropical cloud cluster evolution and cyclogenesis in the Western North Pacific
[CSU-ASP-403] N87-10661

COLORADO UNIV., BOULDER.
An asymptotic theory of supersonic turbulent interactions in a compression corner N87-10010
Use of the Sun to determine pointing of ST radar beams N87-10506
Archival of Poker Flat MST radar data N87-10524
Integrated testing and analysis of mathematical software tools. Summary of research activities, 1 August 1985-1 May 1986
[DE86-010882] N87-10723
Software process interpretation and software environments
[DE86-010881] N87-10725

COLUMBIA UNIV., NEW YORK.
Bright galactic X-ray binary sources: Temporal and spectral studies N87-10804
Molecular clouds in Orion and Monoceros N87-10809

COMISSAO NACIONAL DE ENERGIA NUCLEAR DE BRASIL, RIO DE JANEIRO.
Study about the structural behavior of WStE-36N steel
[DE86-702011] N87-10394

COMMISSION OF THE EUROPEAN COMMUNITIES, BRUSSELS (BELGIUM).
Atmospheric Ozone 1985. Assessment of our understanding of the processes controlling its present distribution and change, volume 1
[NASA-TM-89237] N87-10612

COMMISSION OF THE EUROPEAN COMMUNITIES, KARLSRUHE (WEST GERMANY).
Re-examination of the neptunium-hydrogen system
[DE86-010197] N87-10216

COMMITTEE ON APPROPRIATIONS (U. S. SENATE).
Department of Housing and Urban Development-Independent Agencies Appropriation Bill, 1987
[S-REPT-99-487] N87-10773
National Aeronautics and Space Administration N87-10774

COMMITTEE ON SCIENCE AND TECHNOLOGY (U. S. HOUSE).
National Aeronautics and Space Administration Authorization Act, 1987 N87-10775

COMMUNICATIONS SATELLITE CORP., WASHINGTON, D.C.
Orbit geometry for calibration and launch operations of a three-axis controlled satellite with inertial reference N87-10116
Targeting multiburn, long duration apogee burst maneuvers N87-10146
Efficiency eccentricity control using continuous, vectored thrusting for satellites with large area/mass ratios N87-10151
Longitudinal orbit control from INTELSAT 5 inclination stationkeeping maneuvers N87-10156

CONSIGLIO NAZIONALE DELLE RICERCHE, PISA (ITALY).
Optical tracking of the SIRIO satellite N87-10134
CONTINUUM, INC., HUNTSVILLE, ALA.
Computational fluid mechanics utilizing the variational principle of modeling damping seals
[NASA-CR-178902] N87-10248
CONTROL DATA CORP., MINNEAPOLIS, MINN.
Preliminary estimates of vertical momentum flux N87-10459
The frequency spectrum of C sub n sup 2 from MST radar data N87-10461
COPENHAGEN UNIV. (DENMARK).
Cardiovascular measurements in microgravity N87-10676
CORNELL UNIV., ITHACA, N.Y.
Nonreacting turbulent mixing flows: A literature survey and data base
[DE86-010864] N87-10253
Infrared emission lines from planetary nebulae N87-10791
COSTELLO (FREDERICK A.), INC., HERNDON, VA.
Detailed transient model of a liquid-metal heat pipe
[DE86-011212] N87-10257

D

DANISH METEOROLOGICAL INST., COPENHAGEN.
Polar cap/polar cusp studies using incoherent scatter radar facilities N87-10562
DARTMOUTH COLL., HANOVER, N.H.
The ultraviolet spectra of DA white dwarfs N87-10783
DEFENCE RESEARCH ESTABLISHMENT VALCARTIER (QUEBEC).
Sensitivity of the Lidar ratio to changes in size distribution and index of refraction N87-10277
DEFENCE RESEARCH INFORMATION CENTRE, ORPINGTON (ENGLAND).
An algorithm for the detection of signals by colour contrast on the screen of a colour cathode ray tube (colour display)
[DRIC-T-7655] N87-10233
DEFENSE MAPPING AGENCY, WASHINGTON, D.C.
Digital mapping: Fact or fiction
[AD-A167571] N87-10528
DEFENSE MAPPING AGENCY AEROSPACE CENTER, ST. LOUIS, MO.
World geodetic system 1984
[AD-A167570] N87-10527
DEFENSE MAPPING AGENCY HYDROGRAPHIC AND TOPOGRAPHIC CENTER, WASHINGTON, D.C.
DMAHTC (Defense Mapping Agency Hydrographic/Topographic Center) GPS point positioning software: Initial results
[AD-A167566] N87-10058
DMA (Defense Mapping Agency) orbit determination for transit satellites: 1985
[AD-A167567] N87-10108
DELAWARE UNIV., NEWARK.
Short-wavelength buckling and shear failures for compression-loaded composite laminates N87-10403
Particle theory and cosmology
[DE86-010366] N87-10802
DEPARTMENT OF ENERGY, NEW YORK.
Cosmic-ray hadrons underground
[DE86-011334] N87-10822
DEUTSCHE FORSCHUNGS- UND VERSUCHSANSTALT FUER LUFT- UND RAUMFAHRT, BRUNSWICK (WEST GERMANY).
Proceedings of the 13th Symposium on Aircraft Integrated Data Systems
[DFVLR-MITT-86-04] N87-10075
Performance monitoring of sensors in high reliable flight control systems using deterministic observers N87-10087
Comparative evaluation of redundant flight data recorded by a digital aircraft integrated data system recorder (DAR) on board an Airbus A-310 aircraft N87-10098
DEUTSCHE FORSCHUNGS- UND VERSUCHSANSTALT FUER LUFT- UND RAUMFAHRT, OBERPFAFFENHOFEN (WEST GERMANY).
Optimal injection of TV SAT with multi-impulse apogee maneuvers with mission constraints and thrust uncertainties N87-10144
Stationkeeping strategy test, design and optimization by computer simulation N87-10153
Updates to operational procedures as a result of in-orbit experience with SYMPHONIE spacecraft N87-10159
DEUTSCHE FORSCHUNGS- UND VERSUCHSANSTALT FUER LUFT- UND RAUMFAHRT, WESSELING (WEST GERMANY).
MIE Lidar proposed for the German Space Shuttle Mission D2 N87-10269
Experimental and theoretical Doppler-lidar signatures of aircraft wake vortices N87-10330
DEUTSCHE LUFTHANSA AKTIENGESELLSCHAFT, FRANKFURT AM MAIN (WEST GERMANY).
Software for flight recorder data processing developed by Lufthansa N87-10090
DEUTSCHE LUFTHANSA A.G., HAMBURG (WEST GERMANY).
Lufthansa's Aircraft Integrated Data Systems (AIDS) based A-310 engine condition monitoring system: Progress achieved between the 12th and 13th AIDS Symposiums N87-10084
DORTMUND UNIV. (WEST GERMANY).
Micro-tomography using synchrotron radiation
[DE86-010982] N87-10191
DREXEL UNIV., PHILADELPHIA, PA.
Lidar method of measurement of atmospheric extinction and ozone profiles N87-10334
Controller design via structural reduced modeling by FETM
[NASA-CR-179838] N87-10408

E

ECOLE POLYTECHNIQUE, PALAISEAU (FRANCE).
Scenarios for the generation of auroral kilometric radiation N87-10577
EDGERTON, GERMESHAUSEN AND GRIER, INC., IDAHO FALLS, IDAHO.
Issues in expert system aids for a large engineering simulation code
[DE86-009098] N87-10735
EIDGENOESSISCHE TECHNISCHE HOCHSCHULE, ZURICH (SWITZERLAND).
Methods and standards for encryption of spacecraft telemetry and telecommand links
[RPT/ENC/62359/BO] N87-10112
ELECTRICITE DE FRANCE, CHATOU.
A Meteorological (humidity, temperature, aerosols)) mobile dial system: Concepts and design N87-10286
ENERGY SCIENCE LABS., INC., SAN DIEGO, CALIF.
Guidebook for analysis of tether applications
[NASA-CR-178904] N87-10169
ERLANGEN-NUREMBERG UNIV. (WEST GERMANY).
Exercise-induced myocardial ischemia at high altitude simulated in a negative pressure chamber N87-10702
ESCUELA TECNICA SUPERIOR DE INGENIEROS AERONAUTICOS, MADRID (SPAIN).
Optimal tracking strategy determination N87-10120
EUROCONTROL AGENCY, BRUSSELS (BELGIUM).
The air/ground transfer of aircraft integrated data systems (AIDS) for Air Traffic Control (ATC) purposes: Present experiments and possible future intentions N87-10091
EUROPEAN NUCLEAR ENERGY AGENCY, FRASCATI (ITALY).
CO2 lidar system for atmospheric studies N87-10366
EUROPEAN SPACE AGENCY, PARIS (FRANCE).
Proceedings of 2nd International Conference on Space Physiology
[ESA-SP-237] N87-10675
The muscular system in weightlessness N87-10682
EUROPEAN SPACE AGENCY. EUROPEAN SPACE OPERATIONS CENTER, DARMSTADT (WEST GERMANY).
Coverage transition times of IR pencil beam sensors N87-10125
Early orbit determination N87-10128
Olympus: Apogee engine firing N87-10143
Operational implementation of deorbiting maneuvers N87-10148
Intense soft X-rays from RS Ophiuchi during the 1985 outburst
[DE86-010175] N87-10820
EUROPEAN SPACE AGENCY. EUROPEAN SPACE RESEARCH AND TECHNOLOGY CENTER, ESTEC, NOORDWIJK (NETHERLANDS).
Transfer orbit optimization for dual launches N87-10114
ESA activities in space laser sounding and ranging N87-10264
Plasma sheet boundary electric fields during substorms N87-10546
Simultaneous observations of Pc4 and Pc5 electric fields in the noon sector with GEOS-1 and GEOS-2 N87-10597

F

FAIRCHILD WESTON SYSTEMS, INC., SARASOTA, FLA.
The Fairchild CVDR: A new combination voice and data recorder N87-10095
FEDERAL AVIATION ADMINISTRATION, ATLANTIC CITY, N.J.
Helicopter MLS Flight Inspection Project
[DOT/FAA/CT-86/14] N87-10002
Crashworthiness experiment summary full-scale transport controlled impact demonstration program
[DOT/FAA/CT-85/20] N87-10055
The Boeing B 720 aircraft Controlled Impact Demonstration (CID): Flight data recorder/cockpit voice recorder experiment N87-10096
FEDERAL AVIATION ADMINISTRATION, WASHINGTON, D.C.
Atmospheric Ozone 1985. Assessment of our understanding of the processes controlling its present distribution and change, volume 1
[NASA-TM-89237] N87-10612
FERMI NATIONAL ACCELERATOR LAB., BATAVIA, ILL.
Possible significance of a new dimensionless ratio in cosmology
[DE86-011026] N87-10801
FLIGHT DATA CO., LONDON (ENGLAND).
The impact of flight data on an airline: A case study N87-10088
FLORENCE UNIV. (ITALY).
Multiple scattering measurements in laboratory and foggy atmosphere N87-10315
FLORIDA ATLANTIC UNIV., BOCA RATON.
Toward comparing experiment and theory for corroborative research on hingeless rotor stability in forward flight (an experimental and analytical investigation of isolated rotor-flap-lag stability in forward flight)
[NASA-CR-179711] N87-10063
FORSCHUNGSINSTITUT DER DEUTSCHEN BUNDESPOST, DARMSTADT (WEST GERMANY).
High speed digital signal transmission over coaxial pairs between network termination and several terminals without variable equilization
[FI-44-TBR-101] N87-10230
FRAUNHOFER-INST. FUER ATMOSPHAERISCHE UMWELTFORSCHUNG, GARMISCH-PARTENKIRCHEN (WEST GERMANY).
Improved solution of the lidar equation utilizing particle counter measurements N87-10310
Lidar observations of the decline of the El Chichon stratospheric load N87-10340

G

GARRETT TURBINE ENGINE CO., PHOENIX, ARIZ.
Influence of engine variables on future helicopter systems N87-10072
GENERAL ACCOUNTING OFFICE, WASHINGTON, D. C.
Strategic Defense Initiative Program: Status of airborne optical adjunct and terminal imaging radar
[PB6-221132] N87-10107
GENERAL DYNAMICS CORP., FORT WORTH, TEX.
Design and fabrication of the NASA decoupler pylon for the F-16 aircraft
[NASA-CR-172354] N87-10065
GENERAL ELECTRIC CO., CINCINNATI, OHIO.
Free jet feasibility study of a thermal acoustic shield concept for AST/VCE application: Dual stream nozzles
[NASA-CR-3867] N87-10752
Free-jet acoustic investigation of high-radius-ratio coannular plug nozzles
[NASA-CR-3818] N87-10753
GENERAL ELECTRIC CO., PHILADELPHIA, PA.
Detailed transient model of a liquid-metal heat pipe
[DE86-011212] N87-10257
GEORGIA INST. OF TECH., ATLANTA.
Numerical solution of the 3-dimensional boundary layer equations in the inverse mode using finite differences N87-10005
Ordered and random structures in pulsatile flow through constricted tubes N87-10245
Flow dynamics and stability in severe rainbands N87-10669
GOETTINGEN UNIV. (WEST GERMANY).
Generation of Pc2 pulsations by energetic O(+) ions N87-10605
GOLDSCHMIED (FABIO R.), MONROEVILLE, PA.
Wind tunnel test of the modified goldschmied model with propulsion and empennage: Analysis of test results
[AD-A167360] N87-10045
GROUPE D'ETUDE EN MEDECINE ET PHYSIOLOGIE SPATIALES, TOULOUSE (FRANCE).
Ground based simulation techniques for cardiovascular and hormonal changes observed in man in weightlessness N87-10696
GRUMMAN AEROSPACE CORP., BETHPAGE, N.Y.
Viscous wing theory development. Volume 1: Analysis, method and results
[NASA-CR-178156] N87-10043

Viscous wing theory development. Volume 2: GRUMWING computer program user's manual [NASA-CR-178157] N87-10044

H

HAMILTON STANDARD, FARMINGTON, CONN.

Aircraft Integrated Data Systems (AIDS): Evolution and revolution N87-10077

HARRY DIAMOND LABS., ADELPHI, MD.

Near-IR extinction and backscatter coefficient measurements in low- and mid-altitude clouds N87-10351

HARVARD UNIV., CAMBRIDGE, MASS.

Millimeter-wave spectrometry of ozone in the middle atmosphere N87-10629

Observations of non-thermal radiation from late-type stars N87-10793

HARVEY MUDD COLL., CLAREMONT, CALIF.

Free vibration and dynamic response analysis of spinning structures [NASA-CR-179672] N87-10717

HELSINKI UNIV. TECHNOLOGY, OTANIEMI (FINLAND).

Cold-start tests with speed diesel engines using alcohol as main fuel [DE86-751651] N87-10392

HOPITAL LARIBOISIERE, PARIS (FRANCE).

Anticortisol monoclonal antibodies: Characterization of their specificity N87-10680

HOPITAL NORD, SAINT-PRIEST-EN-JAREZ (FRANCE).

Bones and weightlessness N87-10681

Weightlessness effects on the bone tissue of rats after a 5 day space flight (Cosmos 1514) N87-10684

Bone tissue and muscular performance in a population of elderly men as a function of physical exercise N87-10685

Histomorphometric study of bone cell mass and activity in man caused by a 120 day decubitus. Test of preventive protocols N87-10689

Amputation-induced osteoporosis: A new model to explore the effects of weightlessness on the human skeleton N87-10690

Weightlessness effects on the phosphorus-calcium balance and its hormonal regulation in man during STS flight 51-G N87-10691

HYDROMETEOROLOGICAL SERVICE OF THE USSR.

The E region instabilities in the polar ionosphere N87-10599

I

IBADAN UNIV. (NIGERIA).

Some aspects of the urban climates of tropical Africa N87-10642

IBM JAPAN.

Numerical study of the entrance flow and its transition of a circular pipe N87-10019

ILLINOIS UNIV., URBANA.

Daytime lidar measurements of tidal winds in the mesospheric sodium layer at Urbana, Illinois N87-10347

Propagating tides in the mesosphere N87-10441

Gravity waves in severe weather N87-10442

Doppler effects on velocity spectra observed by MST radars N87-10464

An analysis at mesospheric coherent-scatter power enhancements during solar flare events N87-10479

Recent progress in the Urbana MST radar N87-10485

Beam steering system N87-10501

Improving range resolution with a frequency-hopping technique N87-10514

A variable-frequency local oscillator for the frequency-hopping technique N87-10515

An accelerated forth data-acquisition system N87-10516

The Tukey algorithm for enhancing MST radar data N87-10521

FORPS: A FORTH-based production system and its application to a real-time robot control problem [DE86-005426] N87-10734

Computational methods and software for differential equations and their applications [DE86-010231] N87-10746

ILLINOIS UNIV., URBANA-CHAMPAIGN.

The study of microstrip antenna arrays and related problems [NASA-CR-179714] N87-10225

Possibility of measuring gravity-wave momentum flux by single beam observation of MST radar N87-10458

Effects of anisotropy on the frequency spectrum of gravity waves observed by MST radar N87-10460

Observational studies of wave disturbances in the tropical Pacific and their relationship with deep cloud activity N87-10634

Fault and error latency under real workload: An experimental study [NASA-CR-179802] N87-10733

Pulse timing and neutron star structure N87-10799

INDIAN METEOROLOGICAL DEPT., NEW DELHI.

Some aspects of the urban climates of India N87-10643

INDIAN SPACE RESEARCH ORGANIZATION, BANGALORE.

Preliminary orbit determination by static multivariate search N87-10127

Real time orbit and dynamic search zone computations to aid satellite acquisition in S-band during the launch phase of Geosynchronous Transfer Orbit (GTO) N87-10132

System aspects of the Indian MST radar facility N87-10497

INSTITUT D'AERONOMIE SPATIALE DE BELGIQUE, BRUSSELS.

Formation and deformation of the plasmapause during a substorm event N87-10555

INSTITUTE OF BIOMEDICAL PROBLEMS, MOSCOW (USSR).

Functions of skeletal muscles of rats and monkeys after 5-day space flight (on Cosmos 1514) N87-10686

Bone examination by noninvasive techniques in a 120-day head-down tilt test N87-10688

Metabolic changes during prolonged antiorthostatic hypokinesia N87-10698

Relationship between cardiovascular functions and fluid-electrolyte metabolism during antiorthostatic hypokinesia N87-10701

The state of bones of pregnant rats during an acute stage of adaptation to weightlessness N87-10708

INSTITUTO DE PESQUISAS ESPACIAIS, SAO JOSE DOS CAMPOS (BRAZIL).

Parameter optimization and attitude stabilization of a flexible spacecraft N87-10138

TV-SAT final orbit acquisition optimization strategy N87-10150

INTERNATIONAL COUNCIL OF SCIENTIFIC UNIONS, URBANA, ILL.

Middle Atmosphere Program. Handbook for MAP, volume 20 [NASA-CR-176882] N87-10419

IOWA STATE UNIV. OF SCIENCE AND TECHNOLOGY, AMES.

Application of a potential code to general steady flows in three dimensions N87-10262

Application of graph theory to the nonlinear analysis of large space structures N87-10418

IOWA UNIV., IOWA CITY.

Periodic amplitude variations in Jovian continuum radiation [NASA-CR-177070] N87-10813

A study of the ground state hydroxyl maser emissions associated with eleven regions of star formation N87-10826

ISRAEL ATOMIC ENERGY COMMISSION, YAVNEH.

The effect of turbulence on lidar backscattered signal fluctuations N87-10328

ISRAEL INST. FOR BIOLOGICAL RESEARCH, NESS-ZIONA.

Lidar mapping of a mixture of aerosol concentrations in a varying atmosphere N87-10320

J

JET PROPULSION LAB., CALIFORNIA INST. OF TECH., PASADENA.

MAPM: A coherent dual CO2 laser DIAL system N87-10358

Atmospheric correlation time measurements using coherent CO2 lidar N87-10363

Science opportunities from the Topex/Poseidon mission [NASA-CR-179752] N87-10671

Intelligent Computer Assisted Instruction (ICAI): Formative evaluation of two systems [NASA-CR-176873] N87-10716

Total-dose radiation effects data for semiconductor devices. 1985 Supplement. Volume 2, part B [NASA-CR-179741] N87-10765

The case for Mars: Concept development for a Mars research station [NASA-CR-179753] N87-10812

Periodic amplitude variations in Jovian continuum radiation [NASA-CR-177070] N87-10813

Plasma wave observations at Uranus from Voyager 2 [NASA-CR-177069] N87-10814

JOHNS HOPKINS UNIV., LAUREL, MD.

Dynamic variations of the auroral precipitation and the polar cap N87-10559

JOINT RESEARCH CENTRE OF THE EUROPEAN COMMUNITIES, ISPRA (ITALY).

Feasibility experiments on time-resolved fluorosensing applied to oil slicks N87-10322

K

KEIO UNIV., YOKAHAMA (JAPAN).

An intensity-modulated dual-wavelength He-Ne laser for remote sensing of methane N87-10319

KENTUCKY UNIV., LEXINGTON.

Transient heat transfer analysis and radiative properties measurements of porous thermal insulation [DE86-011296] N87-10259

KERNFORSCHUNGSZENTRUM, KARLSRUHE (WEST GERMANY).

Process control in arc welding [KFK-PFT-105] N87-10395

Programming of sensor based assembly robots [KFK-PFT-120] N87-10396

Concentrations of plastic strains in the clamping region of cylindrical shells under excessive loading [KFK-3915] N87-10417

Linearized model for the hydrodynamic stability investigation of molten fuel jets into the coolant of a Liquid Metal Fast Breeder Reactor (LMFBR) [KFK-3978] N87-10757

Microstructure, grain boundaries and properties of sintered and isotatically hot pressed SiC materials [KFK-4063] N87-10769

KIRUNA GEOPHYSICAL INST. (SWEDEN).

The hot ion composition in the magnetosphere N87-10552

Observations of auroral electrons with sounding rockets and the GEOS-2 geostationary satellite N87-10596

Growing electrostatic waves with a wavelength of 67 cm in the upper ionosphere N87-10604

KYOTO INST. OF TECH. (JAPAN).

Measurements of precipitating atmosphere by the MU radar N87-10426

KYOTO UNIV. (JAPAN).

Numerical simulation of two-dimensional freejet flow-fields N87-10020

KYOTO UNIV., UJI (JAPAN).

Tropospheric turbulence parameters measured by using the MU radar N87-10436

Monitoring of the MU radar antenna pattern by Satellite Ohzora (EXOS-C) N87-10509

KYUSHU UNIV., FUKUOKA (JAPAN).

Observation of atmospheric ozone by dial with Raman lasers pumped by a KrF laser N87-10297

El Chichon aerosols in the stratosphere: Analyses of lidar data and calculations of radiation budget N87-10313

XeF lidar measurements of density and temperature in the middle atmosphere N87-10342

L

LABORATORIO DE COMPUTACAO CIENTIFICA, RIO DE JANEIRO (BRAZIL).

Modelling of the filling up of a porous plate [DE86-702033] N87-10260

Constitutive relations for flow of a non-Newtonian fluid through saturated porous media [DE86-702035] N87-10261

LAWRENCE LIVERMORE NATIONAL LAB., CALIF.

Chemistry research resource [DE86-009891] N87-10178

Micro-tomography using synchrotron radiation [DE86-010982] N87-10191

Chemistry and shock initiation of intermetallic reactions [DE86-009694] N87-10220

Chemistry and shock initiation of intermetallic reactions [DE86-010549] N87-10221

Electronics Engineering Department technical review [DE86-011371] N87-10241

Electrical measurement techniques for pulsed high current electron beams [DE86-010960] N87-10756

Extreme ultraviolet explorer: Mirror optical tests and results [DE86-010560] N87-10760

LEAR SIEGLER, INC., GRAND RAPIDS, MICH.

Data compression techniques for multifunction flight data recorders N87-10094

LETTERMAN ARMY INST. OF RESEARCH, SAN FRANCISCO, CALIF.
Flash/crazing effects on simulator pursuit tracking performance
[AD-A167689] N87-10759
LITTLE (ARTHUR D.), INC., CAMBRIDGE, MASS.
Summary and evaluation of field performance data on unitary heat pumps
[DE86-011289] N87-10258
LONDON UNIV. (ENGLAND).
Possible significance of a new dimensionless ratio in cosmology
[DE86-011026] N87-10801
LOS ALAMOS NATIONAL LAB., N. MEX.
Developing simplified models of combustion chemistry by simulation with detailed chemical kinetics models
[DE86-008381] N87-10188
Re-examination of the neptunium-hydrogen system
[DE86-010197] N87-10216
Diffusion approximation for modeling of 3-D radiation distributions
[DE86-000810] N87-10228
Thermionic integrated circuits
[DE86-005849] N87-10239
Detailed transient model of a liquid-metal heat pipe
[DE86-011212] N87-10257
Multiple scattering of laser beams in dense hydrosols N87-10316
Attempts to characterize microballoon sensors for shock velocity and material motion studies
[DE86-011210] N87-10379
Overtone production of soft x-rays with free-electron lasers
[DE86-011248] N87-10383
Long-pulse excimer lasers for materials processing and medical applications
[DE86-011267] N87-10384
Scattered radiation field of a laser beam propagating through turbid media
[DE86-010188] N87-10386
Subpicosecond high-brightness UV laser system
[DE86-011271] N87-10387
Laser-initiated chain reactions in the partial oxidation of methane
[DE86-011272] N87-10388
Simple blast model for structural design
[DE86-000802] N87-10414
Database algorithms for multiprocessor and very large memory systems
[DE86-009406] N87-10724
Pulse forming network design program for linear and time-varying loads for the IBM personal computer
[DE86-011209] N87-10727
Implementation and optimization of portable standard LISP for the CRAY
[DE86-008717] N87-10729
Intense soft X-rays from RS Ophiuchi during the 1985 outburst
[DE86-010175] N87-10820
Nuclide production by primary cosmic-ray protons
[DE86-011268] N87-10821
Interpretation of extragalactic jets
[DE86-011211] N87-10823
LUDWIG-MAXIMILIANS-UNIVERSITAET, MUNICH (WEST GERMANY).
The usefulness of Klett's inversion algorithms to simulated satellite Lidar returns N87-10274
LUNAR AND PLANETARY INST., HOUSTON, TEX.
LANDSAT imagery of the Central Andes
[NASA-CR-179852] N87-10526
LUND INST. OF TECH. (SWEDEN).
Variation of the urban NO2 concentration during a ground inversion situation N87-10318
A mobile system for active otpical pollution monitoring N87-10355
LYON-1 UNIV. (FRANCE).
Levels of plasma atrial natriuretic factor (alpha h ANF) during acute simulated weightlessness N87-10699
Volume regulating hormones during a 5 hour head-down tilt at -10 deg. Part 1: Epinephrine, norepinephrine and dopamine N87-10700
Volume regulating hormones during a 5-hour head-down tilt at -10 deg. Part 2: Plasma renin activity and aldosterone N87-10703

M

MARTIN MARIETTA AEROSPACE, ORLANDO, FLA.
MODTEQ (Modulation Techniques), AN/FRC-170(V), equalization, and channel medium simulations
[AD-A167965] N87-10226
MARYLAND UNIV., COLLEGE PARK.
Aeroelastic stability of composite rotor blades in hover N87-10060
High spectral purity, narrow linewidth laser transmitter for dial measurements N87-10290
Strength, width, and pressure shift measurements of 54 lines in the oxygen A-band N87-10298
The cyclotron maser theory of AKR and Z-mode radiation N87-10578
Problems of design for cities in the tropics N87-10653
The onset of alfvenic turbulence N87-10762
MASCHINENFABRIK AUGSBURG-NUERNBERG A.G., MUNICH (WEST GERMANY).
Investigations on the parameters for laser surface treatment by cladding and alloying
[BMFT-FB-T-85-183] N87-10203
MASSACHUSETTS INST. OF TECH., CAMBRIDGE.
Reliability issues in active control of large flexible space structures
[NASA-CR-179785] N87-10167
Control of large flexible space structures
[NASA-CR-177063] N87-10168
Finite volume solution of the compressible boundary-layer equations
[NASA-CR-4013] N87-10744
RLE progress report
[MIT-PR-128] N87-10778
MASSACHUSETTS INST. OF TECH., LEXINGTON.
Cramer-Rao bound analysis for frequency estimation of sinusoids in noise
[AD-A167992] N87-10227
Integrated-optical components for fiber gyroscopes
[AD-A167624] N87-10378
MATERIALS RESEARCH LABS., ASCOT VALE (AUSTRALIA).
Computer assisted gas chromatography for thermodynamic measurements of polymer surfaces
[AD-A167450] N87-10208
MATRA ESPACE, PARIS-VELIZY (FRANCE).
A new three-axis control system for a geosynchronous satellite in transfer orbit N87-10139
Comparison of different autonomous stationkeeping systems for geostationary satellites N87-10163
MATRA ESPACE, TOULOUSE (FRANCE).
Geostationary satellite positioning with a restartable motor N87-10142
Telecom-1 dynamic simulator N87-10160
SEAGOS: A prototype expert system to aid ground operators in satellite command and control tasks N87-10161
MAX-PLANCK-INST. FUER AERONOMIE, KATLENBURG-LINDAU (WEST GERMANY).
Magnetospheric-ionospheric coupling deduced from measurements above a discrete auroral arc N87-10550
Connection between particle precipitations and the plasma sheet during substorms N87-10594
Self-consistent analysis of high drift velocity measurements with the Scandinavian Twin Auroral Radar Experiment (STARE) system N87-10606
MAX-PLANCK-INST. FUER METEOROLOGIE, HAMBURG (WEST GERMANY).
Correction of Doppler-broadened Rayleigh backscattering effects in H2O dial measurements N87-10288
MAX-PLANCK-INSTITUT FUER STROEMUNGSFORSCHUNG, GOETTINGEN (WEST GERMANY).
Vortex shedding of a square cylinder in front of a slender airfoil at high Reynolds numbers. Part 1: Spacing effect
[MPIS-23/1985] N87-10048
MESSERSCHMITT-BOELKOW-BLOHM G.M.B.H., BREMEN (WEST GERMANY).
Stationkeeping for DFS-Kopernikus N87-10152
MESSERSCHMITT-BOELKOW-BLOHM G.M.B.H., HAMBURG (WEST GERMANY).
A-310 Aircraft Integrated Data SystemS (AIDS) design philosophy N87-10076
MESSERSCHMITT-BOELKOW-BLOHM G.M.B.H., OTTOBRUNN (WEST GERMANY).
Experience with the Onboard Checkout And Monitoring System (OCAMS) of a military aircraft resulting improvements and the consequence for future design N87-10079
MICHIGAN TECHNOLOGICAL UNIV., HOUGHTON.
Free surface turbulence
[AD-A168013] N87-10251
MICHIGAN UNIV., ANN ARBOR.
Numerical studies of a tubulent jet in crossflow N87-10243
Observational and theoretical investigation of stable auroral red arcs and their magnetospheric energy source, volumes 1 and 2 N87-10632
Vertical modes and energetics of gravitational and rotational modes in a multilevel global spectral model N87-10633
Computational hydrodynamics in astrophysical studies: Highly shocked flows in 3 dimensions N87-10796
Emission-line galaxies toward the Bootes void N87-10807
Clouds and methane photochemical hazes on the outer planets N87-10815
MIDWEST RESEARCH INST., GOLDEN, COLO.
Polymer reflectors research during Fiscal Year 1985
[DE86-010697] N87-10211
Advanced desiccant materials research
[DE86-010695] N87-10536
Workshop on the Physics and Chemistry of Solar-Flux Effects on Condensed Phase/Gas Interfaces
[DE86-004460] N87-10817
MINNESOTA UNIV., MINNEAPOLIS.
Objectives and design of the ECHO 6 electron beam experiment: Large ionospheric perturbations and energetic particle patterns N87-10590
MISSISSIPPI STATE UNIV., MISSISSIPPI STATE.
Differential optical absorption techniques for diagnostics of fossil fuel combustion
[DE86-010084] N87-10190
MISSOURI UNIV., KANSAS CITY.
Theoretical studies on the structures of insulating and metallic glasses
[DE86-011484] N87-10212
MISSOURI UNIV., ROLLA.
Fundamental investigations of the finite element solutions for acoustic propagation in ducts
[NASA-CR-179845] N87-10751
MITSUBISHI HEAVY-INDUSTRIES LTD., TOKYO (JAPAN).
A description of a turbulent flow past a circular cylinder by a discrete vortex method N87-10014
MIYAZAKI UNIV. (JAPAN).
Analysis on gravitational effect to nonlinear diffusion system of vapor molecules in a heat pipe N87-10023
MULLARD SPACE SCIENCE LAB., DORKING (ENGLAND).
Intense soft X-rays from RS Ophiuchi during the 1985 outburst
[DE86-010175] N87-10820
MURDOCH UNIV. (AUSTRALIA).
Climatic factors in the siting of new towns and specialized urban facilities N87-10654

N

NAGOYA UNIV. (JAPAN).
Lidar measurement of stratospheric aerosol at Syowa Station, Antarctica N87-10314
Plasma confinement by a radio frequency plugging potential in an axisymmetric mirror-cusp device
[IPPJ-784] N87-10763
NAGOYA UNIV., TOYOKAWA (JAPAN).
The direction finding aboard AUREOL-3 of ELF waves at frequency above and below the proton gyrofrequency N87-10572
Study of the middle latitude broadening of the spectrum of the waves emitted from ground N87-10583
NATIONAL ACADEMY OF SCIENCES - NATIONAL RESEARCH COUNCIL, WASHINGTON, D. C.
Microgravity Science and Applications
[NASA-CR-179793] N87-10204
NATIONAL AERONAUTICAL LAB., BANGALORE (INDIA).
Effects of flap position on longitudinal parameters of HFB-320
[NAL-TM-SE-8602] N87-10062
Tunnel interference from pressure measurements on control surfaces
[AE-TM-6-83] N87-10104
Effect of static inplane loads and boundary conditions on the flutter of flat rectangular panels
[NAL-TM-ST-8604] N87-10404
Adaptation of TSFOIL for Univac 1100/60H computer at NAL, Bangalore
[AE-TB-9-83] N87-10718
NATIONAL AERONAUTICS AND SPACE ADMINISTRATION, WASHINGTON, D.C.
Aerospace medicine and biology: A continuing bibliography with indexes (supplement 287)
[NASA-SP-7011(287)] N87-10001
The new space network: The tracking and data relay satellite system
[NASA-EP-251] N87-10171
Lidar remote sensing from space: NASA's plans in the Earth sciences N87-10265
Atmospheric Ozone 1985. Assessment of our understanding of the processes controlling its present distribution and change, volume 1
[NASA-TM-89237] N87-10612
Stratospheric chemistry N87-10613
Tropospheric trace gases N87-10614
Tropospheric chemistry N87-10615
Strat-trop exchange N87-10616
Dynamical processes N87-10617

Radiative processes N87-10618

NASA and FAA launch wind shear research project
[NASA-NEWS-REL-86-143] N87-10659

Aerospace medicine and biology: A continuing bibliography with indexes
[NASA-SP-7011(289)] N87-10674

Animal studies on Spacelab-3 N87-10704

Math modelling as a complement to the scientific inquiry of physiological adaptation to space flight: Fluid, endocrine and circulatory regulation N87-10709

NASA studying concept to measure distance between stars, galaxies
[NASA-NEWS-REL-86-133] N87-10787

New space astronomy technique developed to study celestial bodies
[NASA-NEWS-REL-86-140] N87-10788

Aeronautics and space report of the President
[NASA-TM-89239] N87-10827

NATIONAL AERONAUTICS AND SPACE ADMINISTRATION. AMES RESEARCH CENTER, MOFFETT FIELD, CALIF.

In-flight total forces, moments and static aeroelastic characteristics of an oblique-wing research airplane
[NASA-TP-2224] N87-10103

Boron-containing organosilane polymers and ceramic materials thereof
[NASA-CASE-ARC-11649-1-SB] N87-10205

NATIONAL AERONAUTICS AND SPACE ADMINISTRATION. GODDARD INST. FOR SPACE STUDIES, NEW YORK.

Molecular clouds in the Carina arm
[NASA-TM-87798] N87-10786

NATIONAL AERONAUTICS AND SPACE ADMINISTRATION. GODDARD SPACE FLIGHT CENTER, GREENBELT, MD.

Geostationary Operational Environmental Satellite (GOES) mission profile N87-10123

Tracking and Data Relay Satellite (TDRS) tracking and orbit determination N87-10136

Airborne Lidar measurements of the atmospheric pressure profile with tunable Alexandrite lasers N87-10282

On the measurement of atmospheric density using dial in the O2 A-band (770 nm) N87-10291

Real-time atmospheric absorption spectra for in-flight tuning of an airborne dial system N87-10296

Convective structure of the planetary boundary layer of the ocean during gale N87-10300

Improvements in the Goddard balloon-borne lidar N87-10311

Rotationally resolved collisional transfer rates in OH N87-10323

Lower atmospheric temperature profile measurements using a Raman lidar N87-10331

Lidar observations and modeling of cold air outbreaks during MASEX and GALE N87-10336

Lidar study of storm tops N87-10348

The GSFC gound-based lidar for the measurement of stratospheric ozone N87-10371

Review of measurements of the RF spectrum of radiation from lightning
[NASA-TM-87788] N87-10658

Proceedings of the 5th Annual Users' Conference
[NASA-CP-2399] N87-10720

A rule based computer aided design system
[NASA-TM-86241] N87-10721

NATIONAL AERONAUTICS AND SPACE ADMINISTRATION. LYNDON B. JOHNSON SPACE CENTER, HOUSTON, TEX.

The regulation of fluid and electrolyte metabolism in weightlessness N87-10679

Space motion sickness N87-10693

The use of decompression to simulate the effect of extravehicular activity on human lymphocyte transformation N87-10697

NATIONAL AERONAUTICS AND SPACE ADMINISTRATION. LANGLEY RESEARCH CENTER, HAMPTON, VA.

Wind-tunnel investigation of the flight characteristics of a canard general-aviation airplane configuration
[NASA-TP-2623] N87-10039

Spin-tunnel investigation of a 1/25-scale model of the General Dynamics F-16XL airplane
[NASA-TM-85660] N87-10041

Supersonic, nonlinear, attached-flow wing design for high lift with experimental validation
[NASA-TP-2336] N87-10042

Doppler Radar Detection of Wind Shear
[NASA-CP-2435] N87-10054

Summary of longitudinal stability and control parameters as determined from space shuttle Columbia flight test data
[NASA-TM-87768] N87-10101

A space station Structures and Assembly Verification Experiment, SAVE
[NASA-TM-89004] N87-10170

Effects of thermal cycling on graphie-fiber-reinforced 6061 aluminum
[NASA-TP-2612] N87-10184

A method of estimating the molecular weight of polymeric materials
[NASA-CASE-LAR-13212-1] N87-10206

Thirteenth International Laser Radar Conference
[NASA-CP-2431] N87-10263

Tunable solid-state laser technology for applications to scientific and technological experiments from space N87-10266

Development of a high-altitude airborne dial system: The Lidar Atmospheric Sensing Experiment (LASE) N87-10268

The Lidar In-Space Technology Experiment (LITE) N87-10270

Wavelength dependence of aerosol backscatter coefficients obtained by multiple wavelength Lidar measurements N87-10275

Assessment of dial data collection and analysis techniques N87-10281

Measurements of the effect of horizontal variability of atmospheric backscatter on dial measurements N87-10283

Influence of Rayleigh-Doppler broadening on the selection of H2O dial system parameters N87-10287

The application of lidar to stratospheric aerosol studies N67-10337

Airborne lidar observations of Arctic polar stratospheric clouds N87-10341

Linewidth characteristics of Raman-shifted dye laser output at 720 and 940 nm N87-10370

Linewidth characteristics of Raman-shifted dye laser output at 720 and 940 nm N87-10372

Direct computation of orbital sunrise or sunset event parameters
[NASA-TM-87717] N87-10620

Dynamic remapping decisions in multi-phase parallel computations
[NASA-CR-178174] N87-10719

FTMP (Fault Tolerant Multiprocessor) programmer's manual
[NASA-TM-89015] N87-10731

Global collocation methods for approximation and the solution of partial differential equations
[NASA-CR-178179] N87-10745

Prediction of helicopter rotor discrete frequency noise: A computer program incorporating realistic blade motions and advanced acoustic formulation
[NASA-TM-87721] N87-10750

Laser-powered MHD generators for space application
[NASA-TP-2621] N87-10764

NATIONAL AERONAUTICS AND SPACE ADMINISTRATION. LEWIS RESEARCH CENTER, CLEVELAND, OHIO.

Response of a small-turboshaft-engine compression system to inlet temperature distortion
[NASA-TM-83765] N87-10100

Coaxial tube tether/transmission line for manned nuclear space power
[NASA-CASE-LEW-14338-1] N87-10174

Black-and-white photographic chemistry: A reference
[NASA-TM-87296] N87-10177

Carbide/fluoride/silver self-lubricating composite
[NASA-CASE-LEW-14196-1] N87-10179

Castable hot corrosion resistant alloy
[NASA-CASE-LEW-14134-1] N87-10192

Optically controlled GaAs dual-gate MESFET and permeable base transistors
[NASA-TM-88823] N87-10232

Testing of UH-60A helicopter transmission in NASA Lewis 2240-kW (3000-hp) facility
[NASA-TP-2626] N87-10391

Ultrasonic determination of recrystallization
[NASA-TM-88855] N87-10399

NATIONAL AERONAUTICS AND SPACE ADMINISTRATION. MARSHALL SPACE FLIGHT CENTER, HUNTSVILLE, ALA.

Comparative magnetospheric/ionospheric studies using Dynamics Explorer spacecraft and ground-based radars N87-10602

NATIONAL AERONAUTICS AND SPACE ADMINISTRATION. PASADENA OFFICE, CALIF.

Cross-contact chain
[NASA-CASE-NPO-16784-1] N87-10231

NATIONAL CENTER FOR ATMOSPHERIC RESEARCH, BOULDER, COLO.

The NCAR Airborne Infrared Lidar System (NAILS) N87-10362

Wind profiler data in a mesoscale experiment from a meteorological perspective N87-10423

MST data exchange through the NCAR incoherent-scatter radar data base N87-10525

NATIONAL CENTRAL UNIV., CHUNG-LI (TAIWAN).

The first operation and results of the Chung-Li VHF radar N87-10495

NATIONAL GEOPHYSICAL DATA CENTER, BOULDER, COLO.

Solar-geophysical data number 501, May 1986. Part 2: (Comprehensive reports). Data for November 1985 and miscellanea
[PB86-218047] N87-10622

Solar-geophysical data number 501, May 1986. Part 1: (Prompt reports). Data for April 1986, March 1986 and late data
[PB86-218039] N87-10623

Solar-geophysical data number 499, March 1986, supplement
[NASA-CR-179797] N87-10624

Solar-geophysical data number 499, March 1986. Part 2: (Comprehensive reports). Data for September 1986 and miscellanea
[NASA-CR-179796] N87-10625

Solar-geophysical data number 499, March 1986. Part 1: (Prompt reports). Data for February 1986, January 1986 and late data
[NASA-CR-179795] N87-10626

NATIONAL INST. FOR ENVIRONMENTAL STUDIES, TSUKUBA (JAPAN).

Visibility and aerosol measurement by diode-laser random-modulation CW lidar N87-10279

Volcanic eruptions and the increases in the stratospheric aerosol content: Lidar measurements from 1982 to 1986 N87-10338

The TFP and a pulsed LD: New lidar components N87-10374

NATIONAL METEOROLOGICAL CENTER, WASHINGTON, D.C.

On the potential use of radar-derived information in operational numerical weather prediction N87-10420

NATIONAL OCEANIC AND ATMOSPHERIC ADMINISTRATION, BOULDER, COLO.

Features of stratospheric aerosol lidar observations at Mauna Loa, 1974 - 1985 N87-10312

Three atmospheric dispersion experiments involving oil fog plumes measured by lidar N87-10321

Doppler lidar studies of atmospheric wind field dynamics N87-10327

The real-time use of wind profilers in nowcasting N87-10427

Performance characteristics of wind profiling radars N87-10429

A model for gravity-wave spectra observed by Doppler sounding systems N87-10434

A statistical model to estimate refractivity turbulence structure constant C sub n sup 2 in the free atmosphere N87-10448

Can stochastic, dissipative wave fields be treated as random walk generators N87-10452

Climatology of gravity waves over Poker Flat, Alaska for 1983 N87-10454

Climatology of tropospheric vertical velocity spectra N87-10455

A comparison of vertical velocities measured from specular and nonspecular echoes by a VHF radar N87-10470

Methods for verifying the accuracy of wind profiles N87-10471

Progress in existing and planned MST radars N87-10481

The proposed flatland radar N87-10482

Current status of the Poker Flat MST radar N87-10483

Continuous wind measurement in the tropical Pacific using VHF radars N87-10484

Colorado wind profilers N87-10486

Wind profiler demonstration system N87-10487

Phased-array design for MST and ST radars N87-10499

The NOAA TOGA antenna array N87-10500

Determination of U, V, and W from single station Doppler radar radial velocities N87-10502

A 405-MHz, 5-beam phased array antenna N87-10503

Low-altitude coverage of ST radars N87-10504

The grid array antenna N87-10505

The elimination of a class of pseudo echoes by an improved T/R switch technique N87-10511

A single-board preprocessor and pulse generator N87-10517

A microprogrammable radar controller N87-10518

An example of scaling MST Doppler spectra using median spectra, spectral smoothing, and velocity tracing N87-10519

Space Environment Laboratory, FY 1985
[PB86-218567] N87-10621

Surface measurements of gust fronts and microbursts during the JAWS (Joint Airport Weather Studies) Project: Statistical results and implications for wind shear detection, prediction and modeling
[PB86-200647] N87-10665

NATIONAL OCEANIC AND ATMOSPHERIC ADMINISTRATION, WASHINGTON, D. C.
An all-purpose computer program for lidar simulations and reduction of lidar data N87-10299
Atmospheric Ozone 1985. Assessment of our understanding of the processes controlling its present distribution and change, volume 1 [NASA-TM-89237] N87-10612

NATIONAL PHYSICAL LAB., NEW DELHI (INDIA).
Laser heterodyne system for obtaining height profiles of minor species in the atmosphere N87-10359

NATIONAL PHYSICAL LAB., TEDDINGTON (ENGLAND).
Atmospheric contributions to the column variance in direct-detection dial N87-10289
Progress made during 1985 in the scientific and technical program of National Physical Laboratory's Division of Radiation Science and Acoustics N87-10776

NATIONAL RESEARCH INST. FOR POLLUTION AND RESOURCES, TOKYO (JAPAN).
A trial on performance test method for Cu-water heat pipe N87-10026

NATIONAL SEVERE STORMS LAB., NORMAN, OKLA.
A look at profiler performance N87-10430

NATIONAL SPACE DEVELOPMENT AGENCY, IBARAKI (JAPAN).
Operational criteria for geostationary satellites in National Space Development Agency (NASDA) N87-10119
Attitude determinations for geostationary satellites of the National Space Development Agency (NASDA) N87-10124

NATIONAL SPACE DEVELOPMENT AGENCY, TOKYO (JAPAN).
State/orbit estimation from real Doppler data for solid apogee motor burning phase of geostationary satellite N87-10129
Spin dynamics with sloshing effects for solid motor burning phase N87-10140

NATIONAL TRANSPORTATION SAFETY BOARD, WASHINGTON, D. C.
Aircraft accident reaport, Delta Air Lines, Inc., Lockheed L-1011-385-1, N726DA, Dallas/Fort Worth International Airport, Texas, August 2, 1985 [PB86-910406] N87-10053
Aircraft accident reports: Brief format US civil and foreign aviation, issue number 2 of 1985 accidents [PB86-916916] N87-10056
Flight recorders: New US regulations and new International Civil Aviation Organization (ICAO) standards N87-10093

NATIONAL WEATHER SERVICE, WASHINGTON, D.C.
Monthly and seasonal weather outlook for mid-May to mid-June 1986, volume 40, number 10, May 14, 1986 [PB86-199825] N87-10664

NAVAL AIR DEVELOPMENT CENTER, WARMINSTER, PA.
Intercomparisons of high-resolution solar blind Raman lidar atmospheric profiles of water vapor with radiosondes and kytoon N87-10333

NAVAL AIR TEST CENTER, PATUXENT RIVER, MD.
United States Navy - Canadian Forces solid state flight data recorder/crash position locator experiment on the B-720 controlled impact demonstration N87-10097

NAVAL OCEAN SYSTEMS CENTER, SAN DIEGO, CALIF.
Pressure-resistant plane disc viewports from allyl diglycol carbonate plastic for hyperbaric chambers [AD-A168007] N87-10105

NAVAL POSTGRADUATE SCHOOL, MONTEREY, CALIF.
Experimental procedure for lifetime testing of graphite bundles under constant load [AD-A167714] N87-10186
An analysis of the performance of a vertically oriented, gas loaded, variable conductance heat pipe [AD-A167874] N87-10250
Cloud detection by lidar extinction calculations N87-10353
A summary of the Foundation Research Program, fiscal year 1985 [AD-A168009] N87-10780

NAVAL RESEARCH LAB., WASHINGTON, D. C.
Using a laser aureole to invert lidar return N87-10292
Current enhancement for hose-unstable electron beams [AD-A167804] N87-10755

NAVAL SURFACE WEAPONS CENTER, SILVER SPRING, MD.
Synthesis of energetic materials [AD-A167787] N87-10214

NAVAL WEAPONS SUPPORT CENTER, CRANE, IND.
Evaluation of a new type stable nickel-zinc battery for electric vehicle application [DE86-010895] N87-10534

NEW MEXICO UNIV., ALBUQUERQUE.
Numerical model of the thermal processes leading to ignition in a pyrotechnic device [DE86-009626] N87-10189

NIELSEN ENGINEERING AND RESEARCH, INC., MOUNTAIN VIEW, CALIF.
Development of a turbomachinery design optimization procedure using a multiple-parameter nonlinear perturbation method [NASA-CR-3831] N87-10003
Prediction of gust loadings and alleviation at transonic speeds [AD-A167748] N87-10047

NIPPON INST. OF TECH. (JAPAN).
Effect of surplus standing liquid on heat transfer resistance in the heat pipe (with mesh wick in a horizontal mode) N87-10024

NITTO ELECTRIC INDUSTRIAL CO. LTD., IBARAKI (JAPAN).
Thermopervaporation device [DE86-011151] N87-10255

NORD-MICRO ELEKTRONIC FEINMECHANIK G.M.B.H., FRANKFORT (WEST GERMANY).
Modern Aircraft Integrated Data Systems (AIDS) technology exemplified on the A-320 N87-10078

NORTH CAROLINA AGRICULTURAL AND TECHNICAL STATE UNIV., GREENSBORO.
Dynamics and control of orbiting grid and the synchronously deployable beam [NASA-CR-179808] N87-10410

NORTH CAROLINA STATE UNIV., RALEIGH.
A model for the evolving stably stratified nocturnal boundary layer based on the turbulent kinetic energy equation N87-10606
Modeling the effects of the spatially varying sea surface temperature on the marine atmospheric boundary layer N87-10673
Sulfur-based synthetic metal superconductors [DE86-010512] N87-10768

NORTH CAROLINA UNIV., CHAPEL HILL.
Null surface dynamics N87-10770

NORTHWESTERN UNIV., EVANSTON, ILL.
Possibility of obtaining coherent short wave radiation from a solid state free electron laser [DE86-010525] N87-10381
Crack-tip fields in a viscoplastic material [AD-A168014] N87-10413

NOTRE DAME UNIV., IND.
Experimental study of the boundary layer on a low Reynolds number airfoil in steady and unsteady flow N87-10052

O

OAK RIDGE GASEOUS DIFFUSION PLANT, TENN.
Synthetic carbon precursor materials [DE86-011584] N87-10210
Thermopervaporation device [DE86-011151] N87-10255
High precision absolute laser power measurements using a magnetically suspended rotor [DE86-011585] N87-10389

OAK RIDGE NATIONAL LAB., TENN.
Weldability of an NiAl alloy [DE86-011510] N87-10199
Deformation behavior of powder metallurgy Ni Al-Hf-B [DE86-011508] N87-10201
Modification of the grain boundary microstructure of the austenitic PCA stainless steel to improve helium embrittlement resistance [DE86-010396] N87-10202
Photosynthetic water splitting [DE86-010269] N87-10215
New solution of the problem of EMP coupling on cables over ground of finite conductivity [DE86-006078] N87-10229
Design rule for fatigue of welded joints in elevated-temperature nuclear components [DE86-007569] N87-10393
Study of UNIX and its suitability for the Air Force's WWMCCS Information System [DE86-011293] N87-10771
Computer software evaluation methodology and data base management system selection [DE86-011343] N87-10772

OAK RIDGE Y-12 PLANT, TENN.
Permeation membrane-type distiller [DE86-011153] N87-10254

OFFICE FOR CHEMICAL ANALYSES, STUTTGART (WEST GERMANY).
The introduction of climatology into the administration and development of planning in the city of Stuttgart N87-10652

OFFICE OF TECHNOLOGY ASSESSMENT, WASHINGTON, D.C.
Microelectronics research and development background paper [PB86-205200] N87-10242

OKAYAMA UNIV. (JAPAN).
Time-domain sensitivity enhancement in pulsed Pb-TDL gas monitors N87-10324

OKLAHOMA UNIV., NORMAN.
A theory for the retrieval of virtual temperature from winds, radiances and the equations of fluid dynamics N87-10421
Further studies with data collected by NASA's airborne Doppler lidar in Oklahoma in 1981 [NASA-CR-179779] N87-10660
The assessment of climatological impacts on agricultural production and residential energy demand N87-10666

OLD DOMINION UNIV., NORFOLK, VA.
Numerical study of hydrogen-air supersonic combustion by using elliptic and parabolized equations [NASA-CR-179800] N87-10187
A Taylor-Galerkin finite element algorithm for transient nonlinear thermal-structural analysis [NASA-CR-177064] N87-10406

OPTECH, INC., DOWNSVIEW (ONTARIO).
Laboratory measurements of forward and backward scattering of laser beams in water droplet clouds N87-10295
Gas dispersion measurements using a mobile Raman lidar system N87-10368

OREGON GRADUATE CENTER FOR STUDY AND RESEARCH, BEAVERTON.
Remote sensing of atmospheric winds using a coherent, CW lidar and speckle-turbulence interaction N87-10329

OSAKA UNIV. (JAPAN).
Dynamic heat transfer mechanism of two-phase closed thermosyphon N87-10025

OXFORD POLYTECHNIC (ENGLAND).
The planning and maintenance of urban settlements to resist extreme climatic forces N87-10647

P

PACIFIC NORTHWEST LABS., RICHLAND, WASH.
Grain boundary segregation and environmentally-induced fracture of materials [DE86-010219] N87-10195
Review of embrittlement mechanisms in tungsten heavy alloys [DE86-011114] N87-10196
Review of storage battery system cost estimates [DE86-011182] N87-10537
Comparison of the coupling of grounded and ungrounded humans to vertical 60-Hz electric fields [DE86-011140] N87-10713

PARAGON PACIFIC, INC., TORRANCE, CALIF.
WEST-3 wind turbine simulator development. Volume 2: Verification [NASA-CR-174982] N87-10531

PENNSYLVANIA STATE UNIV., UNIVERSITY PARK.
An experimental investigation of end-wall flowfield of a compressor rotor N87-10244
Examples of mesoscale structures and short-term wind variations detected by VHF Doppler radar N87-10422
An evaluation of errors observed in the measurement of low wind velocities N87-10469
The Penn State Doppler network progress report N87-10489
Data communications and monitor for the Penn State University profiler network N87-10523
On the stability of accretion disks around black holes N87-10805

PHILIPS ZENTRALLABORATORIUM G.M.B.H., HAMBURG (WEST GERMANY).
A system theoretical based method for module failure diagnostic of turbine engines N87-10085

PISA UNIV. (ITALY).
Engine-transmission-structural airframe members compatibility N87-10069

PITTSBURGH UNIV., PA.
The effect of a quasi-stellar object on its host galaxy: Dynamical and physical processes in the interstellar medium around a QSO N87-10797

PLESSEY CO. LTD., HAVANT (ENGLAND).
Integrated monitoring systems for tactical aircraft N87-10080

POITIERS UNIV. (FRANCE).
Very low frequency saucers with attenuation bands N87-10575

PORTO UNIV. (PORTUGAL).
Initial orbit determination for geostationary satellites N87-10131

PRESTON POLYTECHNIC (ENGLAND).
Intense soft X-rays from RS Ophiuchi during the 1985 outburst [DE86-010175] N87-10820

PRINS MAURITS LAB. TNO, RIJSWIJK (NETHERLANDS).
Laboratory evaluation of three passive CO concentration monitors [PML-1985-13] N87-10538

PRODUCTS RESEARCH AND CHEMICAL CORP., GLENDALE, CALIF.
Polymer systems for rapid sealing of aircraft structures at low temperature [AD-A167667] N87-10209

PURDUE UNIV., WEST LAFAYETTE, IND.
Geometric and material nonlinear dynamic analysis of complex shells N87-10401
Dynamic delamination crack propagation in a graphite/epoxy laminate N87-10402
Use of fuzzy sets mathematics to assist pavement evaluation and management (revised March 18, 1986) [PB86-214796] N87-10747

R

RADIO RESEARCH LABS., TOKYO (JAPAN).
Flight tests of a range-resolved airborne dial with two min-tea CO2 lasers N87-10284
Remote temperature profiling in the troposphere and stratosphere by the radio-acoustic sounding technique N87-10488

RCA ASTRO-ELECTRONICS DIV., PRINCETON, N. J.
Orbit achievement of RCA communication satellites N87-10122
Nd:Glass-Raman laser for water vapor dial N87-10285
Calibration and analysis for a 0.53 micron incoherent Doppler lidar N87-10365

RESEARCH INST. OF NATIONAL DEFENCE, LINKOEPING (SWEDEN).
Extinction and visibility measurements in the lower atmosphere with UV-YAG-lidar N87-10276

RHEINISCH WESTFAELISCHE ELEKTRIZITAETSWERKE A.G., ESSEN (WEST GERMANY).
Process for preparing nickel coatings in conducting, porous bodies, especially for battery electrodes [DE86-901439] N87-10200

ROBERTS ASSOCIATES, INC., VIENNA, VA.
Mathematical model for the Bridgman-Stockbarger crystal growing system [NASA-CR-178921] N87-10766

ROCHESTER UNIV., N. Y.
Nonlinear optics with broad-band lasers [DE86-011286] N87-10382

ROCKWELL INTERNATIONAL CORP., CANOGA PARK, CALIF.
Composite load spectra for select space propulsion structural components [NASA-CR-179496] N87-10176

ROLLS-ROYCE LTD., WATFORD (ENGLAND).
Impact of IPS and IRS configurations on engine installation design N87-10070

ROME UNIV. (ITALY).
An investigation on passively controlled geosynchronous orbits N87-10118

ROYAL INST. OF TECH., STOCKHOLM (SWEDEN).
Growth of cracks under far-field cyclic compressive loads: Numerical and experimental results [DE86-010279] N87-10416

ROYAL SIGNALS AND RADAR ESTABLISHMENT, MALVERN (ENGLAND).
Progress in coherent laser radar N87-10326
Remote capabilities in computer networks [RSRE-3947] N87-10732

S

SABBAGH ASSOCIATES, INC., BLOOMINGTON, IND.
An eddy-current model for three-dimensional nondestructive evaluation of advanced composites [AD-A167688] N87-10185

SAN JOSE STATE UNIV., CALIF.
Urban climate models: Nature, limitations and applications N87-10646

SANDIA NATIONAL LABS., ALBUQUERQUE, N. MEX.
Trajectory scoring in geodetic coordinates using transponder-interrogator range data [DE86-009554] N87-10109
Numerical model of the thermal processes leading to ignition in a pyrotechnic device [DE86-009626] N87-10189
Transformations and new PHACOMP analysis in weld metal of Hastelloy C-type alloys [DE86-011422] N87-10196
Percussion primer/DDT detonator [DE86-010477] N87-10217
Titanium oxidation kinetics and the mechanism for thermal ignition of titanium-based pyrotechnics [DE86-010987] N87-10218
CP DDT detonators. 5: Output performance and analysis of multiple-out devices [DE86-010895] N87-10219
Nonreacting turbulent mixing flows: A literature survey and data base [DE86-010864] N87-10253
Response of a 3-layered ring to an axisymmetric impulse [DE86-011016] N87-10415
Experience with the application of photovoltaics devices [DE86-010472] N87-10535
Factors contributing to static RAM cell transient upset [DE86-007710] N87-10715
GRAPH 3: A digitizing and graph plotting program [DE86-010628] N87-10722
Design guidelines for human-computer dialogues [DE86-011543] N87-10728

SANDIA NATIONAL LABS., LIVERMORE, CALIF.
Micro-tomography using synchrotron radiation [DE86-010982] N87-10191
Compositional and microstructural effects on hydrogen embrittlement of ASTM grade 12 titanium (Ti 0.3 Mo - 0.8 Ni) [DE86-011379] N87-10197

SAO PAULO UNIV. (BRAZIL).
Some aspects of the urban climates of tropical South America: The Brazilian contribution N87-10644

SASKATCHEWAN UNIV., SASKATOON.
Comparison of medium frequency pulsed radar interferometer and correlation analysis winds, part 1 N87-10474
Comparison of medium frequency pulsed radar interferometer and correlation analysis winds, part 2 N87-10475
Progress in the MF radar system at Saskatoon N87-10496

SCHOOL OF AEROSPACE MEDICINE, BROOKS AFB, TEX.
Radiation doses from flying through nuclear debris clouds [AD-A167959] N87-10711

SCRIPPS INSTITUTION OF OCEANOGRAPHY, LA JOLLA, CALIF.
The internal tide off southern California [AD-A167722] N87-10672

SHANGHAI NORMAL UNIV. (CHINA).
Some aspects of the urban climate of Shanghai N87-10641

SHEFFIELD UNIV. (ENGLAND).
Energy related issues N87-10651

SHINSHU UNIV., NAGANO (JAPAN).
Lidar observation of the mesospheric sodium layer in Antarctica N87-10345

SIKORSKY AIRCRAFT, STRATFORD, CONN.
Engine-airframe integration considerations for preliminary air vehicle performance analysis N87-10068
Flight service evaluation of composite helicopter components [NASA-CR-178149] N87-10182

SMITHSONIAN ASTROPHYSICAL OBSERVATORY, CAMBRIDGE, MASS.
Research relative to high resolution camera on the advanced X-ray astrophysics facility [NASA-CR-179757] N87-10376

SOCIETE DE FABRICATION D'INSTRUMENTS DE MESURE, MASSY (FRANCE).
The Airborne Integrated Data System (AIDS) for the Airbus A-310 engine condition monitoring N87-10082

SOCIETE NATIONALE INDUSTRIELLE AEROSPATIALE, CANNES (FRANCE).
Geostationary satellites autonomous stationkeeping N87-10164

SOCIETE NATIONALE INDUSTRIELLE AEROSPATIALE, MARIGNANE (FRANCE).
Helicopter air intake protection systems N87-10073

SOLAREX CORP., GAITHERSBURG, MD.
Vertical junction solar cells [AD-A167757] N87-10532

SOUTHERN METHODIST UNIV., DALLAS, TEX.
A decentralized fault-tolerant approach to estimation in multi-sensor navigation systems N87-10057

SRI INTERNATIONAL CORP., MENLO PARK, CALIF.
Observations of polar-cap ionospheric signatures of polar wind/magnetosphere coupling N87-10563

STANFORD UNIV., CALIF.
Experimental and theoretical investigations of the flow field of an airfoil with a deflected spoiler N87-10050
Energy delivery processes in shock tubes N87-10106
The development and test of multi-anode microchannel array detector systems. Part 2: Soft X-ray detectors [NASA-CR-177066] N87-10236
Rapid precise end point control of a wrist carried by a flexible manipulator N87-10396
Cryogenic resonant-mass gravitational wave detectors N87-10609

STANFORD UNIV., PALO ALTO, CALIF.
Active experiments from ground N87-10581
De-1/Siple VLF wave-injection experiments N87-10586

STATE UNIV. OF NEW YORK, STONY BROOK.
Interface properties and crystal-growth mechanisms [DE86-010846] N87-10767

SUNDSTRAND DATA CONTROL, INC., REDMOND, WASH.
Data recovery techniques, an update N87-10089

SWEDISH METEOROLOGICAL AND HYDROLOGICAL INST., NORKOEPING.
Urban climatological methods and data N87-10645

SYRACUSE UNIV., N. Y.
Far field noise studies of contoured and solid/porous conical plug-nozzle jet flows N87-10049

SYSTEMS RESEARCH LABS., INC., DAYTON, OHIO.
Development of iron aluminides [AD-A168578] N87-10194

T

TECHNICAL UNIV. OF OPOLE (POLAND).
An improved PSI-cell method for turbulent multi-phase flows N87-10034

TECHNION - ISRAEL INST. OF TECH., HAIFA.
Absorption heat pump simulation and studies: a modular computer simulation of absorption systems [DE86-011206] N87-10256

TECHNISCHE HOCHSCHULE, AACHEN (WEST GERMANY).
Wind shear measurement on board a MORANE 893 N87-10086
Hierarchical bases for the solution of plane elliptic boundary value problems N87-10742
Prompt neutrino production in 400 GeV proton copper interactions [USIP-86-02] N87-10754

TECHNISCHE UNIV., BRUNSWICK (WEST GERMANY).
Investigations on a digital bit synchronizer for a detailed flight data recovery N87-10099

TECHNISCHE UNIV., CLAUSTHAL-ZELLERFELD (WEST GERMANY).
Space imaging radar for remote sensing of the Earth: An evaluation [BMFT-FB-W-85-024] N87-10529

TECHNISCHE UNIV., MUNICH (WEST GERMANY).
Adaptive finite element methods N87-10740

TELESAT CANADA, OTTAWA (ONTARIO).
Optimal transfer to inclined geosynchronous orbits N87-10117
Eccentricity control strategy for geosynchronous communications satellites N87-10155

TENNESSEE UNIV., KNOXVILLE.
A study of the flow field about an upper surface blown wing and its effects on longitudinal static stability of a small jet airplane N87-10009

TEXAS UNIV., AUSTIN.
Unsteady flow over an airfoil inside a wind tunnel with and without transpiration N87-10051
Gauge invariant perturbation theory prediction of the sensitivity required for experimental measurement of quadrupole and higher moments of the cosmic microwave background radiation N87-10625

TEXAS UNIV. AT DALLAS, RICHARDSON.
The distant magnetotail N87-10558

TEXTRON, INC., IRVINE, CALIF.
Technology review of flight crucial flight control systems (application of optical technology) [NASA-CR-172332] N87-10102

TOHOKU UNIV., SENDAI (JAPAN).
Wide-area remote-sensing system of pollution and gas dispersal by near-infrared absorption based on low-loss optical fiber network N87-10354

TOKYO ELECTRIC POWER CO., INC. (JAPAN).
Operating characteristics of cooling underground power cables using up sloped long heat pipes in conduit N87-10026

TOKYO UNIV. (JAPAN).
Proceedings of the Symposium on Mechanics for Space Flight, 1985 [ISAS-SP-4] N87-10011
Theoretical study of strong interaction of vortex filaments N87-10012
Studies on vortex motion based on the dividing vorton model N87-10013

Acoustic waves emitted by vortex-body interaction N87-10015
Study of three-dimensional separation on a spheroid at incidence N87-10016
Technical overview of plume radiation from a solid rocket motor N87-10021
Two dimensional analysis of high voltage solar array interfering with ionospheric plasma N87-10022
Report of the International Symposium on Computational Fluid Dynamics, Tokyo N87-10029
Numerical and experimental study of dynamics of two-dimensional body
[ISAS-619] N87-10748

TOSHIBA CORP., TOKYO (JAPAN).
High capacity heat pipe with axial grooves N87-10027

TOULON UNIV. (FRANCE).
The Provence ST radar N87-10492
Simultaneous multibeam sounding of wind and turbulence N87-10506

TOULON UNIV., LA GARDE (FRANCE).
The ARCAD 3-SAFARI coordinated study of auroral and polar F-region ionospheric irregularities N87-10600

TRANS WORLD AIRLINES, INC., KANSAS CITY, MO.
Airline data acquisition in an ACARS environment N87-10092

TRANSPORTATION SYSTEMS CENTER, CAMBRIDGE, MASS.
Terrestrial evaluation of the Global Positioning System (GPS) Standard Positioning Service (SPS)
[PB86-219599] N87-10059

TRW MATERIALS AND MFG. CENTER, EUCLID, OHIO.
Development of iron aluminides
[AD-A168578] N87-10194

TSUKUBA UNIV. (JAPAN).
Air quality in tropical cities N87-10639

TUSKEGEE INST., ALA.
Mode 1 delamination growth in adhesively bonded joints under static and fatigue loads
[NASA-CR-179812] N87-10409

U

UNITED NATIONS ENVIRONMENT PROGRAM, NAIROBI (KENYA).
Atmospheric Ozone 1985. Assessment of our understanding of the processes controlling its present distribution and change, volume 1
[NASA-TM-89237] N87-10612

UNITED TECHNOLOGIES CORP., EAST HARTFORD, CONN.
Demonstration of laser speckle system on burner liner cyclic rig
[NASA-CR-179509] N87-10377

UNIVERSIDAD NACIONAL DE MEXICO, MEXICO CITY.
Tropical urban climates: Review and assessment N87-10638
The urban climate of Mexico City N87-10640

UNIVERSITAET DER BUNDESWEHR, NEUBIBERG (WEST GERMANY).
Seminar on Finite Elements in Unsteady Problems
[ETN-86-97824] N87-10736
The local convergence of Ritz and Galerkin methods for nonlinear problems N87-10737
Unsteady calculations of ground water problems N87-10739
Mixed finite element methods in flow mechanics N87-10741

UNIVERSITE DES SCIENCES ET TECHNIQUES DE LILLE (FRANCE).
Microgravity effects on the contractile proteins of rat muscles N87-10683

UNIVERSITY COLL., GALWAY (IRELAND).
Backscatter and extinction measurements in cloud and drizzle at CO2 laser wavelengths N87-10352

UNIVERSITY COLL. OF WALES, ABERYSTWYTH.
Observations of stratospheric aerosols associated with the El Chichon eruption N87-10339
Lidar measurements of thermal structure N87-10343

UNIVERSITY OF SOUTHERN CALIFORNIA, LOS ANGELES.
Near field pressure fluctuations in a circular jet
[NASA-CR-179647] N87-10249

UNIVERSITY OF THE WEST INDIES, MONA (JAMAICA).
Performance testing of lidar receivers N87-10325

UNIVERSITY OF WESTERN AUSTRALIA, PERTH.
Aerosol studies in mid-latitude coastal environments in Australia N87-10271

UPPSALA IONOSPHERIC OBSERVATORY (SWEDEN).
HISCAT: A proposed new scatter facility in Northern Scandinavia N87-10498

UTAH STATE UNIV., LOGAN.
Mesospheric wind measurements using a medium-frequency imaging Doppler interferometer N87-10476

UTAH UNIV., SALT LAKE CITY.
Multiple scattering depolarization in marine stratus clouds: Lidar experiments N87-10350

V

VEGA SPACE SYSTEMS ENGINEERING, SAINT-ALBANS (ENGLAND).
Application of simplified spin axis attitude determination techniques to ESA telecom satellites N87-10126

VIRGINIA POLYTECHNIC INST. AND STATE UNIV., BLACKSBURG.
Analysis of the vortical flow around a 60 deg Delta wing with vortex flap N87-10006
The effect of free stream disturbances and control surface deflections on the performance of the Wortmann airfoil at low Reynolds numbers N87-10007
Separation and wakes over 3-dimensional bodies N87-10008
Maneuver and control of flexible spacecraft N87-10166
Identification and control of structures in space
[NASA-CR-179811] N87-10172
Modeling and analysis of spacecraft power systems N87-10173
Structural optimization for control of stiffened laminated composite plates using nonlinear mixed integer programming N87-10181
Fatigue response of notched laminates subjected to tension-compression cyclic loads
[NASA-CR-179804] N87-10183
Transient behavior of liquid jets injected normal to a high velocity gas stream N87-10246

VIRGINIA UNIV., CHARLOTTESVILLE.
High precision absolute laser power measurements using a magnetically suspended rotor
[DE86-011585] N87-10389

W

WASHINGTON UNIV., SEATTLE.
A photometric and in situ study of stable auroral red arcs N87-10628
Urban hydrology in the tropics: Problems, solutions, data collection and analysis N87-10650
Turbulent mixing, droplet spectral evolution and dynamics of warm cumulus clouds N87-10667
The X-ray properties of high redshift, optically selected QSOs N87-10784
High resolution CCD spectra of stars in globular clusters. Part 2: Metals and CNO in M71
[NASA-CR-179853] N87-10789
Gas and dust in regions of recent star formation N87-10800

WATKINS-JOHNSON CO., PALO ALTO, CALIF.
Design, construction and long life endurance testing of cathode assemblies for use in microwave high-power transmitting tubes
[NASA-CR-175116] N87-10237

WISCONSIN UNIV., MADISON.
Electrical circuit modeling of conductors with skin effect
[DE86-011085] N87-10240
Generation of attenuation corrected images from lidar data N87-10367
Case studies of the structure of the atmospheric boundary layer entrainment zone N87-10627
Relationships between available potential energy, kinetic energy and extratropical cyclones within limited regions of the Northern Hemisphere during the FGGE Year N87-10668
Advective influences on steady and transient forced tropical motions N87-10670
Observations of molecular clouds in the direction of galactic and extragalactiv radio sources N87-10794
Conditions for the formation of massive stars N87-10803

WORLD CLIMATE PROGRAMME, GENEVA (SWITZERLAND).
A preliminary cloudless standard atmosphere for radiation computation
[WCP-112] N87-10657

WORLD METEOROLOGICAL ORGANIZATION, GENEVA (SWITZERLAND).
Atmospheric Ozone 1985. Assessment of our understanding of the processes controlling its present distribution and change, volume 1
[NASA-TM-89237] N87-10612
Proceedings of the Technical Conference on Urban Climatology and its Applications with Special Regard to Tropical Areas
[WMO-652] N87-10636
Human comfort in the urban tropics N87-10649
Design for climate in hot, humid cities N87-10656

WYOMING UNIV., LARAMIE.
Light scattering in resonance region from polydisperse non-spherical particles N87-10792

Y

YAMAGATA UNIV. (JAPAN).
On accurate numerical solutions of Falkner-Skan equation N87-10018

YORK UNIV., DOWNSVIEW (ONTARIO).
Inversion of 2 wavelength Lidar data for cloud properties N87-10273
Determination of cloud microphysical properties by laser backscattering and extinction measurements N87-10293

Z

ZURICH UNIV. (SWITZERLAND).
Life expectancy in tropical climates and urbanization N87-10648

CONTRACT NUMBER INDEX

Typical Contract Number Index Listing

N00014-81-C-0006
N87-10545
CONTRACT NUMBER
NASA ACCESSION NUMBER

Listings in this index are arranged alphanumerically by contract number. Under each contract number the NASA accession numbers denoting documents that have been produced as a result of research done under that contract are arranged in ascending order. The NASA accession number denotes the number by which the citation is identified.

AF-AFOSR-0160-80 .... N87-10040
A82/KL/118 .... N87-10538
A93B/1362 .... N87-10180
A93B/1391 .... N87-10405
CNES-73-212 .... N87-10558
CNES-84-1212 .... N87-10553
CNES-212 .... N87-10561
CNRS-ERA-668 .... N87-10600
DA PROJ. 2Q2-63731-A-792 .... N87-10714
DA PROJ. 2Q2-63731-A-793 .... N87-10714
DA PROJ. 2Q2-63743-A-794 .... N87-10716
DAAG29-81-D-0100 .... N87-10291
DACW39-83-M-2630 .... N87-10411
DCA100-81-G-0001 .... N87-10226
DE-AC02-76CH-00016 .... N87-10213
N87-10380
DE-AC02-76CH-03000 .... N87-10801
DE-AC02-76ER-02383 .... N87-10746
DE-AC02-78ER-04908 .... N87-10385
DE-AC02-81ER-10979 .... N87-10382
DE-AC02-83CH-10093 .... N87-10211
N87-10536
N87-10817
DE-AC03-76SF-00098 .... N87-10238
N87-10761
N87-10782
DE-AC04-76DP-00789 .... N87-10109
N87-10189
N87-10198
N87-10217
N87-10218
N87-10219
N87-10415
N87-10535
N87-10715
N87-10722
N87-10728
DE-AC04-76DR-00789 .... N87-10197
N87-10253
DE-AC05-84OR-21400 .... N87-10199
N87-10201
N87-10202
N87-10215
N87-10229
N87-10256
N87-10258
N87-10259
N87-10393
N87-10734
N87-10771
N87-10772
DE-AC05-84OS-21400 .... N87-10254
N87-10255
DE-AC05-84OT-21400 .... N87-10210
N87-10389
DE-AC06-76RL-01830 .... N87-10195
N87-10196
N87-10537
N87-10713
DE-AC07-76ID-01570 .... N87-10735
DE-AC21-82MC-19314 .... N87-10190
DE-AI01-76ET-20320 .... N87-10531
DE-AI01-83CE-90038 .... N87-10534
DE-AI01-86CE-50162 .... N87-10777
DE-FG02-84ER-13283 .... N87-10723
N87-10725
DE-FG02-84ER-40176 .... N87-10802
DE-FG02-84ER-45167 .... N87-10416
DE-FG02-84ER-45170 .... N87-10212
DE-FG02-85ER-45218 .... N87-10767
DE-FG02-85ER-53198 .... N87-10240
DE-FG03-81SF-08392 .... N87-10533
DEN3-247 .... N87-10531
DOT/FAA/CT-85/28P N87-10096
DPP80-22282 .... N87-10581
N87-10586
DPP80-22540 .... N87-10581
N87-10586
DRET-50-85-26 .... N87-10699
N87-10700
N87-10703
DTFA03-80-A-00199 .... N87-10064
ESTEC-5815/84-NL-BI(SC) N87-10112
F61-542 .... N87-10209
F04701-85-C-0086 .... N87-10819
F19628-80-C-0002 .... N87-10378
F19628-85-C-0002 .... N87-10227
F33615-78-C-2063 .... N87-10066
F33615-81-C-5155 .... N87-10194
MDA903-81-C-0504 .... N87-10714
NAG1-126 .... N87-10167
N87-10168
NAG1-198 .... N87-10751
NAG1-225 .... N87-10172
NAG1-343 .... N87-10183
NAG1-405 .... N87-10410
NAG1-420 .... N87-10249
NAG1-423 .... N87-10187
NAG1-447 .... N87-10409
NAG1-465 .... N87-10040
NAG1-507 .... N87-10744
NAG1-575 .... N87-10743
NAG1-613 .... N87-10733
NAG1-622 .... N87-10408
NAG3-418 .... N87-10225
NAG5-571 .... N87-10816
NAG5-622 .... N87-10236
NAG6-10 .... N87-10542
NAG8-527 .... N87-10376
NASA ORDER C-80002-E N87-10777
NASA ORDER H-78746B N87-10660
NASA ORDER W-15519 .... N87-10624
N87-10625
N87-10626
NASW-3949 .... N87-10811
NASW-4066 .... N87-10526
NAS1-16858 .... N87-10043
N87-10044
NAS1-16879 .... N87-10065
NAS1-16978 .... N87-10749
NAS1-17070 .... N87-10719
N87-10745
NAS1-17403 .... N87-10102
NAS1-17635 .... N87-10400
NAS1-18107 .... N87-10719
N87-10745
NAS3-20619 .... N87-10753
NAS3-20836 .... N87-10003
NAS3-22137 .... N87-10752
NAS3-23346 .... N87-10237
NAS3-24382 .... N87-10176
NAS3-24615 .... N87-10377
NAS5-25688 .... N87-10581
N87-10586
NAS7-100 .... N87-10765
NAS7-918 .... N87-10231
N87-10671
N87-10716
N87-10812
NAS8-35012 .... N87-10758
NAS8-35499 .... N87-10169
NAS8-35506 .... N87-10248
NAS8-36167 .... N87-10175
NAS8-36190 .... N87-10766
NAS8-36475 .... N87-10407
NAS9-15487 .... N87-10709
NAS9-15850 .... N87-10709
NAS9-16328 .... N87-10709
NAS9-17151 .... N87-10709
NAS9-17158 .... N87-10662
N87-10663
NAS10-11165 .... N87-10110
N87-10111
NA83-AA-A-00036 .... N87-10291
NCCI-32 .... N87-10372
NCC1-25 .... N87-10291
NCC2-361 .... N87-10063
NGL-05-005-007 .... N87-10557
NGL-05-020-008 .... N87-10581
NGL-21-002-005 .... N87-10578
NGL05-002-134 .... N87-10789
N87-10790
NSF ATM-80-24889 .... N87-10563
NSF ATM-81-21671 .... N87-10563
NSF ATM-83-17456 .... N87-10549
NSF ATM-83-18491 .... N87-10624
N87-10625
N87-10626
NSF ATM-84-19116 .... N87-10661
NSF DMR-81-19500 .... N87-10204
NSF INT-8119963 .... N87-10557
NSF 84-15353 .... N87-10789
NSG-1321 .... N87-10406
NSG-5085 .... N87-10558
NSG-5088 .... N87-10590
N00014-76-C-0063 .... N87-10413
N00014-79-C-0472 .... N87-10672
N00014-81-C-0006 .... N87-10545
N00014-82-K-0183 .... N87-10613
N00014-82-K-0489 .... N87-10581
N00014-83-C-2340 .... N87-10532
N00014-84-C-0149 .... N87-10733
N00014-85-C-0848 .... N87-10193
N00014-85-K-0236 .... N87-10251
N00014-85-K-0404 .... N87-10814
N00167-81-C-0075 .... N87-10045
N00167-83-C-0114 .... N87-10047
N60921-85-C-0046 .... N87-10185
N62269-81-C-0741 .... N87-10209
RP-1630-13 .... N87-10646
W-31-109-ENG-38 .... N87-10252
N87-10381
N87-10539
N87-10726
N87-10768
W-7405-ENG-36 .... N87-10216
N87-10228
N87-10239
N87-10257
N87-10379
N87-10383
N87-10384
N87-10386
N87-10387
N87-10388
N87-10414
N87-10727
N87-10729
N87-10820
N87-10821
N87-10823
W-7405-ENG-48 .... N87-10178
N87-10188
N87-10191
N87-10220
N87-10221
N87-10241
N87-10724
N87-10756
N87-10760
323-51-43-00-11 .... N87-10765
480-51-13-01 .... N87-10170
505-31-3B N87-10753
505-32-6A N87-10100
505-33-43-07 .... N87-10065
505-40-74 .... N87-10752
505-43-13-01 .... N87-10041

505-43-23-02 .... N87-10042
505-43-44 .... N87-10103
505-45-43-01 .... N87-10039
505-45-73-01 .... N87-10102
505-60-01-01 .... N87-10043
N87-10044
505-62-51 .... N87-10391
505-66-21-02 .... N87-10731
505-66-41-31 .... N87-10054
505-90-11-01 .... N87-10744
505-90-21-01 .... N87-10719
N87-10745
506-41-41-01 .... N87-10764
506-43-11 .... N87-10399
506-43-21-02 .... N87-10184
506-44-21 .... N87-10232
506-46-21-01 .... N87-10101
533-04-11 .... N87-10377
533-13-00 .... N87-10176
535-03-11-01 .... N87-10750
618-32-33-07 .... N87-10263
665-45-20-21 .... N87-10620
776-33-41-02 .... N87-10749
936-15-01-01 .... N87-10662
N87-10663

REPORT/ACCESSION NUMBER INDEX

SCIENTIFIC AND TECHNICAL AEROSPACE REPORTS VOLUME 25 NUMBER 1

Typical Report Number Index Listing

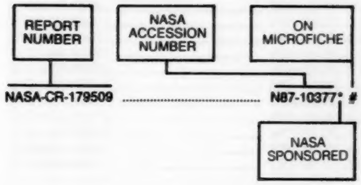

Listings in this index are arranged alphanumerically by report number. The NASA accession number denotes the number by which the citation is identified. An asterisk (*) indicates that the item is a NASA report. A pound sign (#) indicates that the item is available on microfiche.

AD-A166930 ..... N87-10207 #
AD-A167324 ..... N87-10779 #
AD-A167357 ..... N87-10066 #
AD-A167360 ..... N87-10045 #
AD-A167403 ..... N87-10193 #
AD-A167450 ..... N87-10208 #
AD-A167566 ..... N87-10058 #
AD-A167567 ..... N87-10108 #
AD-A167570 ..... N87-10527 #
AD-A167571 ..... N87-10528 #
AD-A167624 ..... N87-10378 #
AD-A167636 ..... N87-10710 #
AD-A167667 ..... N87-10209 #
AD-A167688 ..... N87-10185 #
AD-A167689 ..... N87-10759 #
AD-A167692 ..... N87-10819 #
AD-A167697 ..... N87-10046 #
AD-A167714 ..... N87-10186 #
AD-A167722 ..... N87-10672 #
AD-A167748 ..... N87-10047 #
AD-A167757 ..... N87-10532 #
AD-A167787 ..... N87-10214 #
AD-A167804 ..... N87-10755 #
AD-A167874 ..... N87-10250 #
AD-A167910 ..... N87-10716* #
AD-A167918 ..... N87-10004 #
AD-A167923 ..... N87-10613* #
AD-A167924 ..... N87-10614* #
AD-A167925 ..... N87-10411 #
AD-A167950 ..... N87-10714 #
AD-A167959 ..... N87-10711 #
AD-A167965 ..... N87-10226 #
AD-A167969 ..... N87-10712 #
AD-A167992 ..... N87-10227 #
AD-A168007 ..... N87-10105 #
AD-A168009 ..... N87-10780 #
AD-A168012 ..... N87-10412 #
AD-A168013 ..... N87-10251 #
AD-A168014 ..... N87-10413 #
AD-A168578 ..... N87-10194 #

AE-TB-9-83 ..... N87-10718 #

AE-TM-8-83 ..... N87-10104 #

AFIT/CI/NR-86-54T ..... N87-10046 #

AFWAL-TR-84-4000 ..... N87-10779 #
AFWAL-TR-85-2060-V-3-PT-1 ..... N87-10066 #
AFWAL-TR-85-4000 ..... N87-10779 #
AFWAL-TR-85-4155 ..... N87-10194 #

AGARD-LS-148 ..... N87-10067 #

AMA-84-16 ..... N87-10662* #

ANL-86-16 ..... N87-10252 #

ANL/CNSV-TM-174 ..... N87-10539 #

ANL/CT-86-3 ..... N87-10777* #

ANL/MCS-TM-72 ..... N87-10726 #

AR-1 ..... N87-10176* #
AR-3 ..... N87-10182* #
AR-004-049 ..... N87-10061 #

ARI-RN-85-104 ..... N87-10714 #
ARI-RN-86-29 ..... N87-10716* #

ARL-AERO-PROP-R-169 ..... N87-10061 #

ASI-479-19-1 ..... N87-10714 #

AWRE-O-17/85 ..... N87-10619 #
AWRE-O-18/85 ..... N87-10234 #
AWRE-O-19/85 ..... N87-10235 #
AWRE-O-20/85 ..... N87-10224 #

B-223094 ..... N87-10107 #

BAE-KGT-R-GEN-01349 ..... N87-10180 #

BAE-MSM-R-GEN-0544 ..... N87-10405 #

BARC-1269 ..... N87-10781 #
BARC-1274 ..... N87-10730 #

BBC-RD-1986/4 ..... N87-10223
BBC-RD-1986/7 ..... N87-10222

BER-319-241 ..... N87-10411 #

BMFT-FB-T-85-183 ..... N87-10203 #

BMFT-FB-W-85-024 ..... N87-10529 #

BNL-37808 ..... N87-10213 #
BNL-37898 ..... N87-10380 #

BRL-MR-3508 ..... N87-10412 #

BR97093 ..... N87-10405 #
BR97643 ..... N87-10180 #
BR98864 ..... N87-10234 #
BR99171 ..... N87-10235 #
BR99172 ..... N87-10224 #
BR99175 ..... N87-10619 #
BR99447 ..... N87-10233
BR100129 ..... N87-10732 #

CCMS-86-04 ..... N87-10183* #

CFDL-TR-86-1 ..... N87-10744* #

CI-FR-0088 ..... N87-10246* #

CNEN-DR-130/85 ..... N87-10394 #

CONF-850539 ..... N87-10539 #
CONF-850614-39 ..... N87-10238 #
CONF-851027-11 ..... N87-10713 #
CONF-851185-20 ..... N87-10389 #
CONF-851272-2 ..... N87-10820 #
CONF-860316-4 ..... N87-10380 #
CONF-860316-7 ..... N87-10381 #
CONF-860316-8 ..... N87-10383 #
CONF-860340-4 ..... N87-10195 #
CONF-860366-8 ..... N87-10760 #
CONF-860375-2 ..... N87-10821 #
CONF-860384-8 ..... N87-10756 #
CONF-860421-31 ..... N87-10202 #
CONF-860445-13 ..... N87-10191 #
CONF-860594-4 ..... N87-10199 #
CONF-860594-5 ..... N87-10198 #
CONF-860612-7 ..... N87-10257 #
CONF-860616-3 ..... N87-10414 #
CONF-860620-3 ..... N87-10387 #
CONF-860620-4 ..... N87-10388 #
CONF-860655-10 ..... N87-10535 #
CONF-860674-2 ..... N87-10727 #
CONF-860706-1 ..... N87-10239 #
CONF-860706-2 ..... N87-10229 #
CONF-860706-9 ..... N87-10715 #
CONF-860722-6 ..... N87-10393 #
CONF-860722-14 ..... N87-10734 #
CONF-860729-2 ..... N87-10188 #
CONF-860729-5 ..... N87-10735 #
CONF-860733-1 ..... N87-10729 #
CONF-860739-2 ..... N87-10189 #
CONF-860739-3 ..... N87-10220 #
CONF-860739-3-REV-1 ..... N87-10221 #
CONF-860739-4 ..... N87-10217 #
CONF-860739-6 ..... N87-10218 #
CONF-860739-7 ..... N87-10219 #
CONF-860739-12 ..... N87-10379 #
CONF-860740-1 ..... N87-10724 #
CONF-860876-1 ..... N87-10201 #
CONF-8506205-4 ..... N87-10823 #
CONF-8506217-2 ..... N87-10228 #
CONF-8507124-SUMM ..... N87-10817 #
CONF-8509255-4 ..... N87-10761 #
CONF-8604181-1 ..... N87-10386 #
CONF-8604192-1 ..... N87-10768 #
CONF-8605110-2 ..... N87-10384 #
CONF-8605114-1 ..... N87-10216 #
CONF-8605116-1 ..... N87-10196 #

COO-2383-0122 ..... N87-10746 #

CSG-55 ..... N87-10733* #

CSU-ASP-403 ..... N87-10661 #

CU-CS-324-86 ..... N87-10725 #

DE86-000802 ..... N87-10414 #
DE86-000810 ..... N87-10228 #
DE86-004460 ..... N87-10817 #
DE86-005426 ..... N87-10734 #
DE86-005849 ..... N87-10239 #
DE86-006078 ..... N87-10229 #
DE86-007569 ..... N87-10393 #
DE86-007710 ..... N87-10715 #
DE86-008381 ..... N87-10188 #
DE86-008717 ..... N87-10729 #
DE86-009096 ..... N87-10735 #
DE86-009311 ..... N87-10533 #
DE86-009406 ..... N87-10724 #
DE86-009554 ..... N87-10109 #
DE86-009626 ..... N87-10189 #
DE86-009668 ..... N87-10536 #
DE86-009694 ..... N87-10220 #
DE86-009891 ..... N87-10178 #
DE86-009917 ..... N87-10380 #
DE86-009922 ..... N87-10238 #
DE86-010064 ..... N87-10190 #
DE86-010175 ..... N87-10820 #
DE86-010188 ..... N87-10386 #
DE86-010197 ..... N87-10216 #
DE86-010219 ..... N87-10195 #
DE86-010231 ..... N87-10746 #
DE86-010269 ..... N87-10215 #
DE86-010279 ..... N87-10416 #
DE86-010366 ..... N87-10802 #
DE86-010396 ..... N87-10202 #
DE86-010472 ..... N87-10535 #
DE86-010477 ..... N87-10217 #
DE86-010512 ..... N87-10768 #
DE86-010525 ..... N87-10381 #
DE86-010549 ..... N87-10221 #
DE86-010560 ..... N87-10760 #
DE86-010626 ..... N87-10722 #
DE86-010695 ..... N87-10536 #
DE86-010697 ..... N87-10211 #
DE86-010764 ..... N87-10252 #
DE86-010846 ..... N87-10767 #
DE86-010864 ..... N87-10253 #
DE86-010881 ..... N87-10725 #
DE86-010882 ..... N87-10723 #
DE86-010895 ..... N87-10534 #
DE86-010960 ..... N87-10756 #
DE86-010962 ..... N87-10191 #
DE86-010967 ..... N87-10218 #
DE86-010995 ..... N87-10219 #
DE86-011004 ..... N87-10726 #
DE86-011016 ..... N87-10415 #

DE86-011026 N87-10801 #
DE86-011065 N87-10240 #
DE86-011114 N87-10196 #
DE86-011140 N87-10713 #
DE86-011151 N87-10255 #
DE86-011153 N87-10254 #
DE86-011162 N87-10537 #
DE86-011206 N87-10256 #
DE86-011209 N87-10727 #
DE86-011210 N87-10379 #
DE86-011211 N87-10823 #
DE86-011212 N87-10257 #
DE86-011248 N87-10383 #
DE86-011267 N87-10384 #
DE86-011268 N87-10821 #
DE86-011271 N87-10387 #
DE86-011272 N87-10386 #
DE86-011286 N87-10382 #
DE86-011289 N87-10258 #
DE86-011293 N87-10771 #
DE86-011296 N87-10259 #
DE86-011319 N87-10782 #
DE86-011334 N87-10822 #
DE86-011343 N87-10772 #
DE86-011371 N87-10241 #
DE86-011379 N87-10197 #
DE86-011422 N87-10198 #
DE86-011459 N87-10385 #
DE86-011484 N87-10212 #
DE86-011508 N87-10201 #
DE86-011510 N87-10199 #
DE86-011535 N87-10213 #
DE86-011543 N87-10728 #
DE86-011567 N87-10761 #
DE86-011584 N87-10210 #
DE86-011585 N87-10389 #
DE86-702011 N87-10394 #
DE86-702033 N87-10260 #
DE86-702035 N87-10261 #
DE86-702101 N87-10730 #
DE86-702154 N87-10781 #
DE86-751651 N87-10392 #
DE86-901439 N87-10200 #

DFVLR-MITT-86-04 N87-10075 #

DOE/CE-90038/T1 N87-10534 #

DOE/ER-02383/0122 N87-10746 #
DOE/ER-04908/T1 N87-10385 #
DOE/ER-10979/12 N87-10382 #
DOE/ER-13283/4 N87-10723 #
DOE/ER-13283/5 N87-10725 #
DOE/ER-40176/02 N87-10802 #
DOE/ER-45167/3 N87-10416 #
DOE/ER-45170/T1 N87-10212 #
DOE/ER-45218/1 N87-10767 #
DOE/ER-53198/90 N87-10240 #

DOE/MC-19314/2046 N87-10190 #

DOE/NASA-0247/2 N87-10531* #

DOE/NASA/80002-1 N87-10777* #

DOE/SF-08392/T1 N87-10533 #

DOT-TSC-RSPA-86-1 N87-10059 #

DOT/FAA/CT-85/20 N87-10055 #
DOT/FAA/CT-86/14 N87-10002 #

DRIC-T-7655 N87-10233

DTNSRDC/ASED-CR-01-86 N87-10047 #
DTNSRDC/ASED-CR-02-86 N87-10045 #

D180-28862-VOL-3-PT-1 N87-10066 #

E-2177 N87-10753* #
E-2198 N87-10100* #
E-2392 N87-10752* #
E-2941 N87-10391* #
E-3006 N87-10177* #
E-3183-1 N87-10232* #
E-3248 N87-10399* #

EGG-M-29685 N87-10735 #

EML-447 N87-10822 #

ER-8215-6 N87-10194 #

ESA-CR(P)-2194 N87-10112 #

ESA-SP-237 N87-10675 #

ESD-TR-85-323 N87-10227 #
ESD-TR-86-011 N87-10378 #

ETN-86-94737 N87-10541
ETN-86-97232 N87-10754 #
ETN-86-97561 N87-10675 #
ETN-86-97658 N87-10636 #
ETN-86-97794 N87-10112 #
ETN-86-97807 N87-10657 #
ETN-86-97824 N87-10736 #
ETN-86-97825 N87-10230 #
ETN-86-97833 N87-10417 #
ETN-86-97834 N87-10757 #
ETN-86-97837 N87-10769 #
ETN-86-97838 N87-10395 #
ETN-86-97840 N87-10396 #
ETN-86-97842 N87-10203 #
ETN-86-97843 N87-10529 #
ETN-86-97946 N87-10405 #
ETN-86-97947 N87-10180 #
ETN-86-97992 N87-10233
ETN-86-97994 N87-10619 #
ETN-86-97995 N87-10234 #
ETN-86-97996 N87-10235 #
ETN-86-97997 N87-10224 #
ETN-86-98044 N87-10538
ETN-86-98079 N87-10113
ETN-86-98176 N87-10075 #
ETN-86-98221 N87-10048 #

FAA/CT-85/26 N87-10064 #

FAA/PM-86/31 N87-10054* #

FHWA/CA/TL-85/14 N87-10540 #

FHWA/IN/JHRP-85/14-REV N87-10747 #

FI-44-TBR-101 N87-10230 #

FNAL/PUB-86/66-A N87-10801 #

FRG-82-1 N87-10045 #

FTD-ID(RS)T-0109-86 N87-10004 #

GAO/NSIAD-86-153 N87-10107 #

GPO-495-812 N87-10827* #

GRI-86/0087 N87-10215 #

H-1181 N87-10103* #

ICASE-86-58 N87-10719* #
ICASE-86-60 N87-10745* #

IPPJ-784 N87-10763 #

ISAS-SP-4 N87-10011 #

ISAS-619 N87-10748 #

ISBN-2-85428-126-8 N87-10541
ISBN-2-85428-149-7 N87-10113
ISBN-92-835-1529-3 N87-10067 #

ISSN-0170-1339 N87-10529 #
ISSN-0176-7739 N87-10075 #
ISSN-0285-6808 N87-10748 #
ISSN-0303-4003 N87-10417 #
ISSN-0303-4003 N87-10757 #
ISSN-0303-4003 N87-10769 #
ISSN-0340-7608 N87-10203 #
ISSN-0379-6566 N87-10675 #
ISSN-0436-1199 N87-10048 #
ISSN-0469-4732 N87-10763 #

JHRP-85-14-REV N87-10747 #

JPL-PUB-85-43-VOL-2-PT-B N87-10765* #
JPL-PUB-86-18 N87-10671* #
JPL-PUB-86-28 N87-10812* #

K/TS-11-704 N87-10389 #
K/TS-11-796 N87-10210 #

KFK-PFT-105 N87-10395 #
KFK-PFT-120 N87-10396 #

KFK-3915 N87-10417 #
KFK-3978 N87-10757 #
KFK-4063 N87-10769 #

L-15616 N87-10041* #
L-15787 N87-10042* #
L-15929 N87-10039* #
L-16130 N87-10750* #
L-16139 N87-10184* #
L-16155 N87-10620* #
L-16201 N87-10263* #

LA-UR-85-3347 N87-10228 #
LA-UR-85-3420 N87-10414 #
LA-UR-86-428 N87-10239 #
LA-UR-86-831 N87-10729 #
LA-UR-86-1216 N87-10820 #
LA-UR-86-1332 N87-10386 #
LA-UR-86-1401 N87-10216 #
LA-UR-86-1483 N87-10388 #
LA-UR-86-1499 N87-10387 #
LA-UR-86-1524 N87-10821 #
LA-UR-86-1525 N87-10384 #
LA-UR-86-1682 N87-10383 #
LA-UR-86-1703 N87-10727 #
LA-UR-86-1704 N87-10379 #
LA-UR-86-1705 N87-10823 #
LA-UR-86-1707 N87-10257 #

LAIR-214 N87-10759 #

LBL-PUB-445 N87-10782 #

LBL-19406 N87-10238 #
LBL-21365 N87-10761 #

LCC-021/85 N87-10260 #
LCC-023/85 N87-10261 #

MAP-HANDBOOK-20 N87-10419* #

MIT-PR-128 N87-10778 #

MPIS-23/1985 N87-10048 #

MPL-U-34/85 N87-10672 #

MPR-1370-M-9 N87-10175* #

MRL-R-982 N87-10208 #

MS-6890 N87-10378 #

NADC-85158-60 N87-10209 #

NAL-TM-SE-8602 N87-10062 #

NAL-TM-ST-8604 N87-10404 #

NAS 1.15:85660 N87-10041* #
NAS 1.15:86241 N87-10721* #
NAS 1.15:87296 N87-10177* #
NAS 1.15:87717 N87-10620* #
NAS 1.15:87721 N87-10750* #
NAS 1.15:87768 N87-10101* #
NAS 1.15:87788 N87-10658* #
NAS 1.15:87798 N87-10786* #
NAS 1.15:88823 N87-10232* #
NAS 1.15:88855 N87-10399* #
NAS 1.15:89004 N87-10170* #
NAS 1.15:89015 N87-10731* #
NAS 1.15:89237 N87-10612* #
NAS 1.15:89239 N87-10827* #
NAS 1.19:251 N87-10171* #
NAS 1.21:7011(287) N87-10001*
NAS 1.21:7011(289) N87-10674*
NAS 1.26:3818 N87-10753* #
NAS 1.26:3831 N87-10003* #
NAS 1.26:3867 N87-10752* #
NAS 1.26:4013 N87-10744* #
NAS 1.26:83765 N87-10100* #
NAS 1.26:171824 N87-10662* #
NAS 1.26:171824 N87-10663* #
NAS 1.26:172332 N87-10102* #
NAS 1.26:172354 N87-10065* #
NAS 1.26:174962 N87-10531* #
NAS 1.26:175116 N87-10237* #
NAS 1.26:176873 N87-10716* #
NAS 1.26:176882 N87-10419* #
NAS 1.26:177060 N87-10616* #
NAS 1.26:177063 N87-10168* #
NAS 1.26:177064 N87-10406* #
NAS 1.26:177066 N87-10236* #
NAS 1.26:177069 N87-10814* #
NAS 1.26:177070 N87-10813* #
NAS 1.26:178094 N87-10400* #
NAS 1.26:178149 N87-10182* #
NAS 1.26:178156 N87-10043* #
NAS 1.26:178157 N87-10044* #
NAS 1.26:178173 N87-10749* #
NAS 1.26:178174 N87-10719* #
NAS 1.26:178179 N87-10745* #

NAS 1.26:178853 N87-10175* #
NAS 1.26:178902 N87-10248* #
NAS 1.26:178904 N87-10169* #
NAS 1.26:178920 N87-10758* #
NAS 1.26:178921 N87-10766* #
NAS 1.26:178931 N87-10407* #
NAS 1.26:179462 N87-10777* #
NAS 1.26:179496 N87-10176* #
NAS 1.26:179509 N87-10377* #
NAS 1.26:179671 N87-10811* #
NAS 1.26:179672 N87-10717* #
NAS 1.26:179701 N87-10110* #
NAS 1.26:179711 N87-10063* #
NAS 1.26:179714 N87-10225* #
NAS 1.26:179741 N87-10765* #
NAS 1.26:179752 N87-10671* #
NAS 1.26:179753 N87-10812* #
NAS 1.26:179757 N87-10376* #
NAS 1.26:179779 N87-10660* #
NAS 1.26:179785 N87-10167* #
NAS 1.26:179791 N87-10111* #
NAS 1.26:179793 N87-10204* #
NAS 1.26:179795 N87-10626* #
NAS 1.26:179796 N87-10625* #
NAS 1.26:179797 N87-10624* #
NAS 1.26:179800 N87-10187* #
NAS 1.26:179802 N87-10733* #
NAS 1.26:179804 N87-10183* #
NAS 1.26:179808 N87-10410* #
NAS 1.26:179811 N87-10172* #
NAS 1.26:179812 N87-10409* #
NAS 1.26:179823 N87-10040* #
NAS 1.26:179826 N87-10743* #
NAS 1.26:179838 N87-10408* #
NAS 1.26:179845 N87-10751* #
NAS 1.26:179847 N87-10249* #
NAS 1.26:179852 N87-10526* #
NAS 1.26:179853 N87-10789* #
NAS 1.26:179854 N87-10790* #
NAS 1.55:2399 N87-10720* #
NAS 1.55:2431 N87-10263* #
NAS 1.55:2435 N87-10054* #
NAS 1.60:2224 N87-10103* #
NAS 1.60:2336 N87-10042* #
NAS 1.60:2612 N87-10184* #
NAS 1.60:2621 N87-10764* #
NAS 1.60:2623 N87-10039* #
NAS 1.60:2626 N87-10391* #

NASA-CASE-ARC-11649-1-SB N87-10205* #

NASA-CASE-LAR-13212-1 N87-10206* #

NASA-CASE-LEW-14134-1 N87-10192* #
NASA-CASE-LEW-14196-1 N87-10179* #
NASA-CASE-LEW-14338-1 N87-10174* #

NASA-CASE-NPO-16784-1 N87-10231* #

NASA-CP-2399 N87-10720* #
NASA-CP-2431 N87-10263* #
NASA-CP-2435 N87-10054* #

NASA-CR-3818 N87-10753* #
NASA-CR-3831 N87-10003* #
NASA-CR-3867 N87-10752* #
NASA-CR-4013 N87-10744* #
NASA-CR-171824 N87-10662* #
NASA-CR-171824 N87-10663* #
NASA-CR-172332 N87-10102* #
NASA-CR-172354 N87-10065* #
NASA-CR-174982 N87-10531* #
NASA-CR-175116 N87-10237* #
NASA-CR-176873 N87-10716* #
NASA-CR-176882 N87-10419* #
NASA-CR-177060 N87-10816* #
NASA-CR-177063 N87-10168* #
NASA-CR-177064 N87-10406* #
NASA-CR-177066 N87-10236* #
NASA-CR-177069 N87-10814* #
NASA-CR-177070 N87-10813* #
NASA-CR-178094 N87-10400* #
NASA-CR-178149 N87-10182* #
NASA-CR-178156 N87-10043* #
NASA-CR-178157 N87-10044* #
NASA-CR-178173 N87-10749* #
NASA-CR-178174 N87-10719* #
NASA-CR-178179 N87-10745* #
NASA-CR-178853 N87-10175* #
NASA-CR-178902 N87-10248* #
NASA-CR-178904 N87-10169* #
NASA-CR-178920 N87-10758* #
NASA-CR-178921 N87-10766* #
NASA-CR-178931 N87-10407* #
NASA-CR-179462 N87-10777* #
NASA-CR-179496 N87-10176* #
NASA-CR-179509 N87-10377* #
NASA-CR-179671 N87-10811* #
NASA-CR-179672 N87-10717* #
NASA-CR-179701 N87-10110* #
NASA-CR-179711 N87-10063* #
NASA-CR-179714 N87-10225* #
NASA-CR-179741 N87-10765* #
NASA-CR-179752 N87-10671* #
NASA-CR-179753 N87-10812* #
NASA-CR-179757 N87-10376* #
NASA-CR-179779 N87-10660* #
NASA-CR-179785 N87-10167* #
NASA-CR-179791 N87-10111* #
NASA-CR-179793 N87-10204* #
NASA-CR-179795 N87-10626* #
NASA-CR-179796 N87-10625* #
NASA-CR-179797 N87-10624* #
NASA-CR-179800 N87-10187* #
NASA-CR-179802 N87-10733* #
NASA-CR-179804 N87-10183* #
NASA-CR-179808 N87-10410* #
NASA-CR-179811 N87-10172* #
NASA-CR-179812 N87-10409* #
NASA-CR-179823 N87-10040* #
NASA-CR-179826 N87-10743* #
NASA-CR-179838 N87-10408* #
NASA-CR-179845 N87-10751* #
NASA-CR-179847 N87-10249* #
NASA-CR-179852 N87-10526* #
NASA-CR-179853 N87-10789* #
NASA-CR-179854 N87-10790* #

NASA-EP-251 N87-10171* #

NASA-NEWS-REL-86-133 N87-10787* #
NASA-NEWS-REL-86-140 N87-10788* #
NASA-NEWS-REL-86-143 N87-10659* #

NASA-SP-7011(287) N87-10001*
NASA-SP-7011(289) N87-10374*

NASA-TM-83765 N87-10100* #
NASA-TM-85660 N87-10041* #
NASA-TM-86241 N87-10721* #
NASA-TM-87296 N87-10177* #
NASA-TM-87717 N87-10620* #
NASA-TM-87721 N87-10750* #
NASA-TM-87768 N87-10101* #
NASA-TM-87788 N87-10658* #
NASA-TM-87798 N87-10786* #
NASA-TM-88823 N87-10232* #
NASA-TM-88855 N87-10399* #
NASA-TM-89004 N87-10170* #
NASA-TM-89015 N87-10731* #
NASA-TM-89237 N87-10612* #
NASA-TM-89239 N87-10827* #

NASA-TP-2224 N87-10103* #
NASA-TP-2336 N87-10042* #
NASA-TP-2612 N87-10184* #
NASA-TP-2621 N87-10764* #
NASA-TP-2623 N87-10039* #
NASA-TP-2626 N87-10391* #

NATICK/TR-86/023 N87-10207 #

NEAR-TR-295 N87-10003* #
NEAR-TR-352 N87-10047 #

NOAA-TM-ERL-WPL-135 N87-10665 #

NOSC/TR-1080 N87-10105 #

NP-TR-6901439 N87-10200 #

NPS-012-86-002PR N87-10780 #

NRL-MR-5769 N87-10755 #

NSWC-TR-85-304 N87-10185 #

NTSB/AAB-86/16 N87-10056 #

NTSB/AAR-86/05 N87-10053 #

NU-SML-TR-86-1 N87-10413 #

ORNL-6260 N87-10772 #

ORNL/SUB-83-43337/2 N87-10256 #
ORNL/SUB-84-43366/2 N87-10259 #
ORNL/SUB-85-00219/1 N87-10258 #

ORNL/TM-9901 N87-10771 #
ORNL/TM-10018 N87-10215 #

OTA-BP-CIT-40 N87-10242 #

PB86-196086 N87-10626* #
PB86-196094 N87-10625* #
PB86-196102 N87-10624* #
PB86-199625 N87-10064 #
PB86-200847 N87-10665 #
PB86-202736 N87-10204* #
PB86-205200 N87-10242 #
PB86-214798 N87-10747 #
PB86-215993 N87-10540 #
PB86-218039 N87-10623 #
PB86-218047 N87-10622 #
PB86-218567 N87-10621 #
PB86-219599 N87-10059 #
PB86-910406 N87-10053 #
PB86-916916 N87-10056 #

PML-1985-13 N87-10536

PNL-SA-13067 N87-10195 #
PNL-SA-13600 N87-10713 #
PNL-SA-13645 N87-10196 #

PNL-5741 N87-10537 #

PPI-FID-300102-VOL-2 N87-10531* #

P86-221132 N87-10107 #

RAI-86-B-1 N87-10766* #

RE-725-VOL-1 N87-10043* #
RE-726-VOL-2 N87-10044* #

REPT-86B0078 N87-10721* #

RI/RD86-123 N87-10176* #

RPT/ENC/62359/BO N87-10112 #

RSRE-3947 N87-10732 #

R83AEB574 N87-10753* #
R86-927298-10 N87-10377* #

S-REPT-99-487 N87-10773 #

SA/TR-1/85 N87-10185 #

SAND-85-1586C N87-10198 #
SAND-85-2360 N87-10109 #
SAND-85-2403 N87-10415 #
SAND-85-2798C N87-10189 #
SAND-85-2814C N87-10219 #
SAND-85-2864C N87-10217 #
SAND-85-2872C N87-10218 #
SAND-85-8247 N87-10197 #
SAND-86-0259 N87-10728 #
SAND-86-0341C N87-10715 #
SAND-86-0525 N87-10722 #
SAND-86-2034C N87-10535 #
SAND-86-8217 N87-10253 #

SD-TR-86-17 N87-10819 #

SER-510237 N87-10182* #

SERI/CP-255-2908 N37-10817 #

SERI/PR-255-2835 N87-10211 #
SERI/PR-255-2887 N87-10536 #

SGD-499-PT-1 N87-10626* #
SGD-499-PT-2 N87-10625* #
SGD-499-SUPPL N87-10624* #
SGD-501-PT-1 N87-10623 #
SGD-501-PT-2 N87-10622 #

S10-REF-86-1 N87-10672 #

TDCK-93539 N87-10538

TKK-KO/PM-49 N87-10392 #

TL-604196 N87-10540 #

TR-85-F-11 N87-10064 #
TR-727 N87-10227 #
TR-0086(6427-01)-1 N87-10819 #

U-OF-IOWA-86-16 N87-10814* #
U-OF-IOWA-86-17 N87-10813* #

UCID-20622-86-3 N87-10178 #

UCRL-50025-86-1 .... N87-10241 #
UCRL-93261 .... N87-10756 #
UCRL-93538 .... N87-10191 #
UCRL-93614 .... N87-10188 #
UCRL-94333 .... N87-10724 #
UCRL-94351 .... N87-10220 #
UCRL-94351-REV-1 .... N87-10221 #
UCRL-94362 .... N87-10760 #

UILU-ENG-86-2230 .... N87-10733* #

US-PATENT-APPL-SN-859688 .... N87-10179* #
US-PATENT-APPL-SN-879757 .... N87-10231* #
US-PATENT-APPL-SN-890577 .... N87-10205* #
US-PATENT-APPL-SN-890504 .... N87-10192* #
US-PATENT-APPL-SN-897239 .... N87-10174* #
US-PATENT-APPL-SN-898986 .... N87-10206* #

USAAVSCOM-TR-84-C-13 .... N87-10100* #

USAFSAM-TR-85-86 .... N87-10711 #

USARIEM-M25/86 .... N87-10710 #

USARIEM-T-3/86 .... N87-10712 #

USIP-86-02 .... N87-10754 #

WCP-112 .... N87-10657 #

WES/TR/ATC-86-1 .... N87-10411 #

WMO-REPT-16-VOL-1 .... N87-10612* #

WMO-652 .... N87-10636 #

WMO/TD-24 .... N87-10657 #

Y/TR-86/3 .... N87-10254 #
Y/TR-86/4 .... N87-10255 #

☆ U.S. GOVERNMENT PRINTING OFFICE: 1986-181-546/40023

FEDERAL DEPOSITORY LIBRARIES

ALABAMA

AUBURN UNIV. AT MONTGOMERY LIBRARY
Documents Department
Montgomery, AL 36193
(205) 279-9110, ext. 253

UNIV. OF ALABAMA LIBRARY
Documents Dept.-Box S
University, AL 35486
(205) 348-7369

ARIZONA

DEPT. OF LIBRARY, ARCHIVES AND PUBLIC RECORDS
Third Floor—State Cap.
1700 West Washington
Phoenix, AZ 85007
(602) 255-4121

UNIVERSITY OF ARIZONA LIB.
Government Documents Dept.
Tucson, AZ 85721
(602) 626-5233

ARKANSAS

ARKANSAS STATE LIBRARY
One Capitol Mall
Little Rock, AR 72201
(501) 371-2326

CALIFORNIA

CALIFORNIA STATE LIBRARY
Govt. Publications Section
P.O. Box 2037
Sacramento, CA 95809
(916) 322-4572

COLORADO

UNIV OF COLORADO LIB.
Government Pub. Division
Campus Box 184
Boulder, CO 80309
(303) 492-8834

DENVER PUBLIC LIBRARY
Govt. Pub. Department
1357 Broadway
Denver, CO 80203
(303) 571-2131

CONNECTICUT

CONNECTICUT STATE LIBRARY
Government Documents Unit
231 Capitol Avenue
Hartford, CT 06106
(203) 566-4971

FLORIDA

UNIV. OF FLORIDA LIBRARIES
Library West
Documents Department
Gainesville, FL 32611
(904) 392-0367

GEORGIA

UNIV. OF GEORGIA LIBRARIES
Government Reference Dept.
Athens, GA 30602
(404) 542-8951

HAWAII

UNIV. OF HAWAII LIBRARY
Govt. Documents Collection
2550 The Mall
Honolulu, HI 96822
(808) 948-8230

IDAHO

UNIV. OF IDAHO LIBRARY
Documents Section
Moscow, ID 83843
(208) 885-6344

ILLINOIS

ILLINOIS STATE LIBRARY
Information Services Branch
Centennial Building
Springfield, IL 62706
(217) 782-5185

INDIANA

INDIANA STATE LIBRARY
Serials Documents Section
140 North Senate Avenue
Indianapolis, IN 46204
(317) 232-3686

IOWA

UNIV. OF IOWA LIBRARIES
Govt. Documents Department
Iowa City, IA 52242
(319) 353-3318

KANSAS

UNIVERSITY OF KANSAS
Doc. Collect—Spencer Lib.
Lawrence, KS 66045
(913) 864-4662

KENTUCKY

UNIV. OF KENTUCKY LIBRARIES
Govt. Pub. Department
Lexington, KY 40506
(606) 257-3139

LOUISIANA

LOUISIANA STATE UNIVERSITY
Middleton Library
Govt. Docs. Dept.
Baton Rouge, LA 70803
(504) 388-2570

LOUISIANA TECHNICAL UNIV. LIBRARY
Documents Department
Ruston, LA 71272
(318) 257-4962

MAINE

UNIVERSITY OF MAINE
Raymond H. Fogler Library
Tri-State Regional Documents Depository
Orono, ME 04469
(207) 581-1680

MARYLAND

UNIVERSITY OF MARYLAND
McKeldin Lib.—Doc. Div.
College Park, MD 20742
(301) 454-3034

MASSACHUSETTS

BOSTON PUBLIC LIBRARY
Government Docs. Dept.
Boston, MA 02117
(617) 536-5400 ext.226

MICHIGAN

DETROIT PUBLIC LIBRARY
Sociology Department
5201 Woodard Avenue
Detroit, MI 48202
(313) 833-1409

MICHIGAN STATE LIBRARY
P.O. Box 30007
Lansing, MI 48909
(517) 373-0640

MINNESOTA

UNIVERSITY OF MINNESOTA
Government Pubs. Division
409 Wilson Library
309 19th Avenue South
Minneapolis, MN 55455
(612) 373-7813

MISSISSIPPI

UNIV. OF MISSISSIPPI LIB.
Documents Department
University, MS 38677
(601) 232-5857

MONTANA

UNIV. OF MONTANA
Mansfield Library
Documents Division
Missoula, MT 59812
(406) 243-6700

NEBRASKA

NEBRASKA LIBRARY COMM.
Federal Documents
1420 P Street
Lincoln, NE 68508
(402) 471-2045
In cooperation with University of Nebraska-Lincoln

NEVADA

UNIVERSITY OF NEVADA LIB.
Govt. Pub. Department
Reno, NV 89557
(702) 784-6579

NEW JERSEY

NEWARK PUBLIC LIBRARY
5 Washington Street
Newark, NJ 07101
(201) 733-7812

NEW MEXICO

UNIVERSITY OF NEW MEXICO
Zimmerman Library
Government Pub. Dept.
Albuquerque, NM 87131
(505) 277-5441

NEW MEXICO STATE LIBRARY
Reference Department
325 Don Gaspar Avenue
Santa Fe, NM 87501
(505) 827-2033, ext. 22

NEW YORK

NEW YORK STATE LIBRARY
Empire State Plaza
Albany, NY 12230
(518) 474-5563

NORTH CAROLINA

UNIVERSITY OF NORTH CAROLINA AT CHAPEL HILL
Wilson Library
BA/SS Documents Division
Chapel Hill, NC 27515
(919) 962-1321

NORTH DAKOTA

UNIVERSITY OF NORTH DAKOTA
Chester Fritz Library
Documents Department
Grand Forks, ND 58202
(701) 777-2617, ext. 27
In cooperation with North Dakota State Univ. Library

OHIO

STATE LIBRARY OF OHIO
Documents Department
65 South Front Street
Columbus, OH 43215
(614) 462-7051

OKLAHOMA

OKLAHOMA DEPT. OF LIB.
Government Documents
200 NE 18th Street
Oklahoma City, OK 73105
(405) 521-2502

OKLAHOMA STATE UNIV. LIB.
Documents Department
Stillwater, OK 74078
(405) 624-6546

OREGON

PORTLAND STATE UNIV. LIB.
Documents Department
P.O. Box 1151
Portland, OR 97207
(503) 229-3673

PENNSYLVANIA

STATE LIBRARY OF PENN.
Government Pub. Section
P.O. Box 1601
Harrisburg, PA 17105
(717) 787-3752

TEXAS

TEXAS STATE LIBRARY
Public Services Department
P.O. Box 12927—Cap. Sta.
Austin, TX 78753
(512) 471-2996

TEXAS TECH. UNIV. LIBRARY
Govt. Documents Department
Lubbock, TX 79409
(806) 742-2268

UTAH

UTAH STATE UNIVERSITY
Merrill Library, U.M.C. 30
Logan, UT 84322
(801) 750-2682

VIRGINIA

UNIVERSITY OF VIRGINIA
Alderman Lib.—Public Doc.
Charlottesville, VA 22901
(804) 924-3133

WASHINGTON

WASHINGTON STATE LIBRARY
Documents Section
Olympia, WA 98504
(206) 753-4027

WEST VIRGINIA

WEST VIRGINIA UNIV. LIB.
Documents Department
Morgantown, WV 26506
(304) 293-3640

WISCONSIN

MILWAUKEE PUBLIC LIBRARY
814 West Wisconsin Avenue
Milwaukee, WI 53233
(414) 278-3000

ST. HIST LIB. OF WISCONSIN
Government Pub. Section
816 State Street
Madison, WI 53706
(608) 262-4347

WYOMING

WYOMING STATE LIBRARY
Supreme Ct. & Library Bld.
Cheyenne, WY 82002
(307) 777-6344

National Aeronautics and
Space Administration
Code NTT-4
Washington, D.C.
20546

Official Business
Penalty for Private Use, $300

SPECIAL FOURTH-CLASS RATE
POSTAGE & FEES PAID
NASA
PERMIT No. G 27

NASA

POSTMASTER: If Undeliverable (Section 158
Postal Manual) Do Not Return